U.S. Particle Accelerator School

Education in Beam Physics and Accelerator Technology

FERMILAB-SLIDES-22-004-AD

Colliders

for High Energy and Nuclear Physics

by Valery Lebedev (FNAL/JINR), Nikolai Mokhov (FNAL), Vladimir Shiltsev (FNAL) and Chuyu Liu (BNL. asst.)

US Particle Accelerator School, Jan 24 – Feb 4, 2022

This manuscript has been authored by Fermi Research Alliance, LLC under Contract No. DE-AC02-07CH11359 with the U.S. Department of Energy, Office of Science, Office of High Energy Physics.

Purpose and Audience

Since the middle of the 20th century, charged particle colliders have been at the forefront of scientific discoveries in high-energy and nuclear physics. Collider accelerator technology and beam physics have progressed immensely and modern facilities now operate at energies and luminosities many orders of magnitude greater than the pioneering colliders of the early 1960s. In addition, the field of colliders remains extremely dynamic and continues to develop many innovative approaches. A number of novel concepts are currently being considered for designing and constructing even more powerful colliders. This course will review colliding-beam method and the history of colliders, survey the fundamental accelerator physics phenomena, present the major achievements of operational machines and the key features of near-term collider projects that are currently under development in both high-energy and nuclear physics. We will also briefly overview future project directions in High Energy Physics (HEP) and Nuclear Physics (NP). This course is designed for graduate students and researchers in physics or engineering who want to learn in more detail about the basic concepts and beam physics of particle colliders.

Prerequisites, Objectives, Credit Requirements

- Courses in classical mechanics, electrodynamics, special relativity and physical or engineering mathematics, all at entrance graduate level; and the USPAS course *Fundamentals of Accelerator Physics and Technology with Simulations and Measurements Lab* or equivalent familiarity with accelerators at undergraduate or graduate level are required. It is recommended that students have general familiarity with the following topics: spin dynamics, RF focusing, impedances, instabilities for mono-energetic continuous beam and point-like bunches, Landau damping for a continuous beam, and particle passage through a medium (energy loss, multiple scattering, nuclear scattering).
It is the responsibility of the student to ensure that they meet the course prerequisites or have equivalent experience.

- **Objectives**
On completion of this course, the students are expected to understand the physical principles that make high energy particle colliders function, become familiar with: leading operational and near-future colliders (LHC, SuperKEKB, EIC, etc); the limits of present colliding beam technologies and the promise of future ones, and the issues presented by forefront applications.

- **Credit Requirements**
Students will be evaluated based on the following performances: Homework assignments (60% course grade), Final exam (40% course grade)

Useful Readings and Materials

(Supposed to be provided by the USPAS) *Particle Accelerator Physics* (Fourth Edition) by Helmut Wiedemann, Springer, 2015. A pdf of this book is available for free at https://www.springer.com/gp/book/9783319183169.

Perspective students can prepare for the course in advance and/or evaluate the fit of the course to their goals, by studying the following comprehensive review of high energy physics colliders:

V. Shiltsev, F. Zimmermann, "Modern and Future Colliders," Rev. Mod. Phys. 93, 015006 (2021)
https://journals.aps.org/rmp/abstract/10.1103/RevModPhys.93.015006

and/or the following freely distributed books:

"Accelerator Physics at the Tevatron Collider," V. Lebedev and V. Shiltsev, editors, Springer (2014)
https://link.springer.com/book/10.1007/978-1-4939-0885-1

"Elementary Particles · Accelerators and Colliders", S. Myers, H. Schopper, editors Springer (2013)
https://materials.springer.com/bp/docs/978-3-642-23053-0

CERN Accelerator Schools, including the latest on Colliders (2018)
https://cas.web.cern.ch/schools/zurich-2018

Lectures and Assistants

Valery Lebedev

Vladimir Shiltsev

Nikolai Mokhov

Chuyu Liu (BNL)

Class Roster

	Colliders for High Energy and Nuclear Physics					
	Name	**Education**	**Institution name**	**Residence**	**Status**	**email address**
1	Anderson, Kelly	gs	Michigan State University	United States	grade	kjanderson248@gmail.com
2	Cao, Jiawei	gs	University of Oslo	Norway	grade	jiawei.cao@fys.uio.no
3	Deitrick, Kirsten	phd	Jefferson Lab	United States	audit	kirsten.deitrick@gmail.com
4	Gamage, Randika	phd	Jefferson Lab	United States	audit	randika@jlab.org
5	Gilanliogullari, Onur	gs	Illinois Institute of Technology	United States	grade	ogilanli@hawk.iit.edu
6	Gonzalez-Ortiz, Cristhian	gs	Michigan State University	United States	grade	gonza839@msu.edu
7	Kicsiny, Peter	gs	EPFL and CERN	France	grade	peter.kicsiny@cern.ch
8	Kriske, Richard	phd	MIT	United States	grade	kriskerichard@gmail.com
9	Lobach, Ihar	phd	Argonne National Lab	United States	audit	lobachihor1994@gmail.com
10	Marx, Daniel	phd	Brookhaven National Lab	United States	audit	dmarx@bnl.gov
11	Terzani, Davide	phd	Lawrence Berkeley National Lab	United States	audit	dterzani@lbl.gov
12	Unger, Jonathan	gs	Cornell University	United States	grade	jeu8@cornell.edu

Week 1 : January 24 – January 28, 2022

	Mon 01/24	Tue 01/25	Wed 01/26	Thur 01/27	Fri 01/28
10:00-10:30	Intro All	Homewrk reports	Homewrk reports	Homewrk reports	Homewrk reports
10:30-11:15	Lect VS1 Energy & Lumi	Lect VS3 Beam-beam 1	Lect VS5 Other effects	Lect VS7 Tevatron	Lect VL9 IBS in Plasma
11:15-12:00	Lect VS2 Technology, Hist	Lect VS4 Beam-beam 2	Lect VS6 Circular ee	Lect VS8 LHC	Lect VL10 IBS in a ring
12:00-12:30	lunch	lunch	lunch	Lunch	Lunch
12:30-13:15	Lect VL1 Linear Optics	Lect VL3 Linear Optics: x&s coupling	Lect VL5 Intrinsic non-linearity in FF	Lect VL7 L. emit. Growth due to Noise	Lect VS9 EIC
13:15-14:00	Lect VL2 Linear Optics	Lect VL4 chromaticity of FF and its compens. .	Lect VL6 Motion in RF well, action-phase var.	Lect VL8 Tr. emit. Growth due to Noise	Lect VS10 Large Hadron Colliders
14:00-14:30	Recit VL	Recit VL	Recit VL	Recit VL	Recit VS
14:30-18:00	self-work w.TA	self-work w.TA	self-work w.TA	self-work w.TA	self-work w.TA

Week 2 : January 31 – February 4, 2022

	Mon 01/31	Tue 02/01	Wed 02/02	Thur 02/03	Fri 02/04
10:00-10:30	Homewrk reports	Homewrk reports	Homewrk reports	Homewrk reports	Exams
10:30-11:15	Lect VS11 Muon Colliders	Lect VL13 electron cooling	Lect VS13 Limits of Colliders	Lect NM3	Exams
11:15-12:00	Lect VS12 Linear ee colliders	Lect VL14 Stoch. cooling	Lect VS14 Advanced Colliders	Lect NM4	Exams
12:00-12:30	lunch	lunch	Lunch	lunch	lunch
12:30-13:15	Lect VL11 Lum. Evol. model	Lect VL15 OSC	Lect NM1	Lect NM5	Exams
13:15-14:00	Lect VL12 Lum. Evol. model	Lect VL16 CEC, microbunch EC	Lect NM2	Lect NM6	Exams
14:00-14:30	Recit VL	Recit VL	Recit NM	Recit NM	Exams
14:30-18:00	self-work w.TA	self-work w.TA	self-work w.TA	self-work w.TA	Exams

U.S. Particle Accelerator School

Education in Beam Physics and Accelerator Technology

Fermilab

Managed by Fermi Research Alliance, LLC for the U.S. Department of Energy Office of Science

Colliders: Introduction Technologies and History

Vladimir Shiltsev, Fermilab

part of the "Colliders" class by V.Lebedev, N.Mokhov and V.Shiltsev

US Particle Accelerator School, Jan 24 – Feb 4, 2022

Kinematics of collisions

Two particles ($E_{1,2}$, $m_{1,2}$) collide at angle θ_c

$$E_{cme} = \left(2E_1 E_2 + (m_1^2 + m_2^2)c^4 + +2\cos\theta_c \sqrt{E_1^2 - m_1^2 c^4}\sqrt{E_2^2 - m_2^2 c^4} \right)^{1/2}$$

One particle stationary ($E_2 = m_2 c^2$) $\quad E_{cme} \approx \sqrt{2Emc^2}$

Both particles move ($E_{1,2} >> m_{1,2} c^2$) $\quad E_{cme} \approx 2\sqrt{E_1 E_2}$

Gain for (E= *6500 GeV*, m=*0.936 GeV*) is *~120 times* (0.11 vs 13 TeV)

Lorentz-Invariant Mandelstam Variables

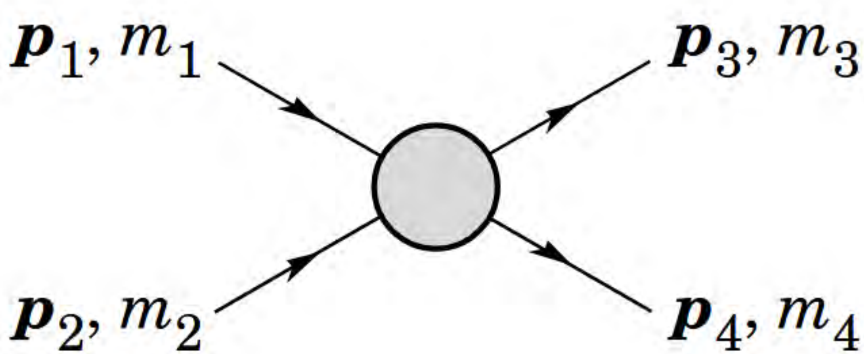

$$
\left.\begin{aligned}
s &= (p_1 + p_2)^2 = (p_3 + p_4)^2 \\
&= m_1^2 + 2E_1E_2 - 2\boldsymbol{p}_1 \cdot \boldsymbol{p}_2 + m_2^2
\end{aligned}\right\} \quad s = E^2_{cme}
$$

$$
\begin{aligned}
t &= (p_1 - p_3)^2 = (p_2 - p_4)^2 \\
&= m_1^2 - 2E_1E_3 + 2\boldsymbol{p}_1 \cdot \boldsymbol{p}_3 + m_3^2 \\
u &= (p_1 - p_4)^2 = (p_2 - p_3)^2 \\
&= m_1^2 - 2E_1E_4 + 2\boldsymbol{p}_1 \cdot \boldsymbol{p}_4 + m_4^2
\end{aligned}
$$

Types of colliding beam facilities

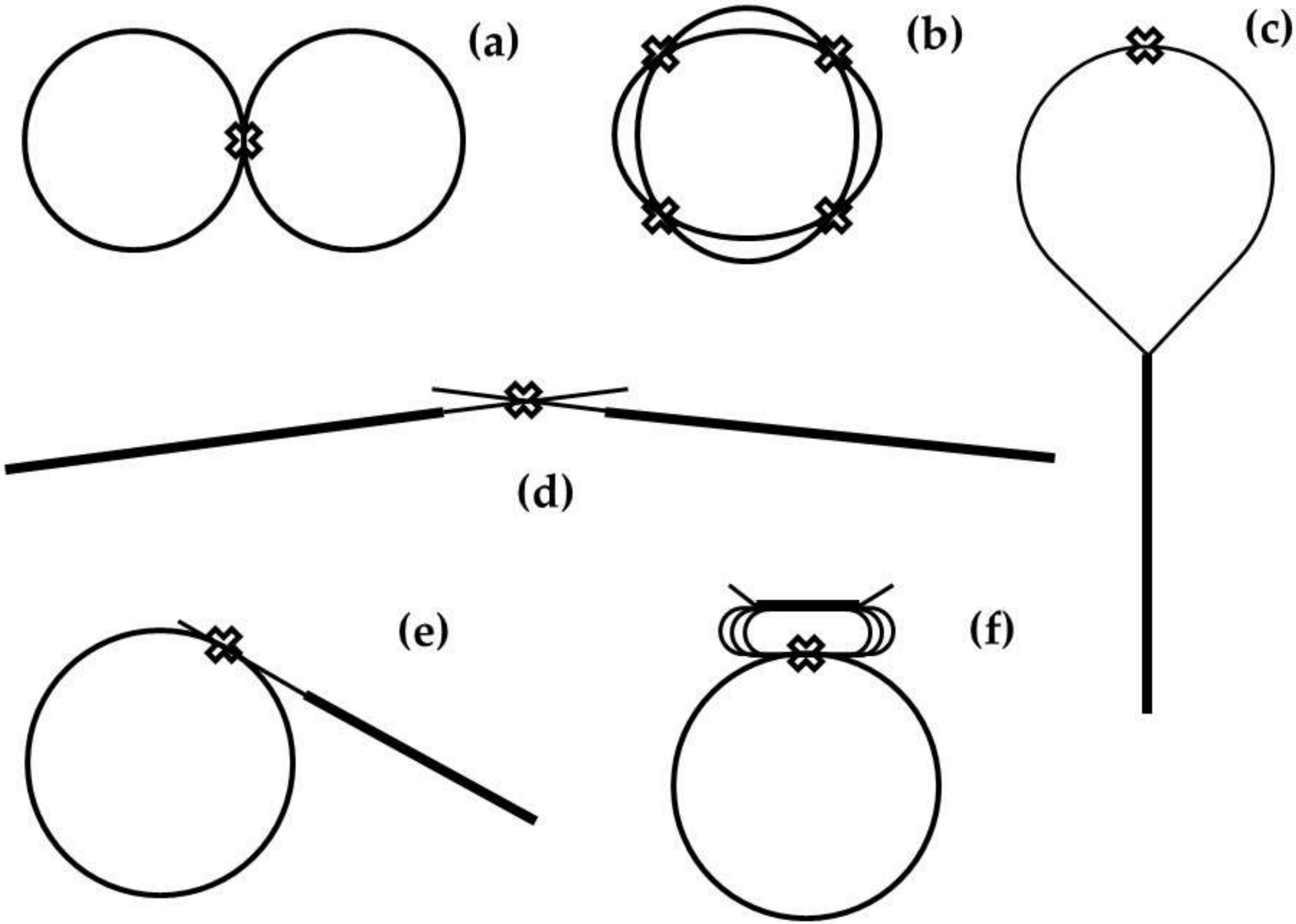

Colliders Landscape

58 years since 1st collisions

- Spring 1964 AdA and VEP-1

31 operated since

- (see RMP review)

7 in operation now

- see next slides

2 under construction

- NICA and EIC

At least 2 more types needed

- Higgs/Electroweak factories
- Frontier *E* >> LHC

V. Shiltsev and F. Zimmermann: Modern and future colliders

	Species	E_b, GeV	C, m	$\mathcal{L}^{max}_{peak}$	Years
AdA	e^+e^-	0.25	4.1	10^{25}	1964
VEP-1	e^-e^-	0.16	2.7	5×10^{27}	1964-68
CBX	e^-e^-	0.5	11.8	2×10^{28}	1965-68
VEPP-2	e^+e^-	0.67	11.5	4×10^{28}	1966-70
ACO	e^+e^-	0.54	22	10^{29}	1967-72
ADONE	e^+e^-	1.5	105	6×10^{29}	1969-93
CEA	e^+e^-	3.0	226	0.8×10^{28}	1971-73
ISR	pp	31.4	943	1.4×10^{32}	1971-80
SPEAR	e^+e^-	4.2	234	1.2×10^{31}	1972-90
DORIS	e^+e^-	5.6	289	3.3×10^{31}	1973-93
VEPP-2M	e^+e^-	0.7	18	5×10^{30}	1974-2000
VEPP-3	e^+e^-	1.55	74	2×10^{27}	1974-75
DCI	e^+e^-	1.8	94.6	2×10^{30}	1977-84
PETRA	e^+e^-	23.4	2304	2.4×10^{31}	1978-86
CESR	e^+e^-	6	768	1.3×10^{33}	1979-2008
PEP	e^+e^-	15	2200	6×10^{31}	1980-90
S$p\bar{p}$S	$p\bar{p}$	455	6911	6×10^{30}	1981-90
TRISTAN	e^+e^-	32	3018	4×10^{31}	1987-95
Tevatron	$p\bar{p}$	980	6283	4.3×10^{32}	1987-2011
SLC	e^+e^-	50	2920	2.5×10^{30}	1989-98
LEP	e^+e^-	104.6	26659	10^{32}	1989-2000
HERA	ep	30+920	6336	7.5×10^{31}	1992-2007
PEP-II	e^+e^-	3.1+9	2200	1.2×10^{34}	1999-2008
KEKB	e^+e^-	3.5+8.0	3016	2.1×10^{34}	1999-2010
VEPP-4M	e^+e^-	6	366	2×10^{31}	1979-
BEPC-I/II	e^+e^-	2.3	238	10^{33}	1989-
DAΦNE	e^+e^-	0.51	98	4.5×10^{32}	1997-
RHIC	p, i	255	3834	2.5×10^{32}	2000-
LHC	p, i	6500	26659	2.1×10^{34}	2009-
VEPP2000	e^+e^-	1.0	24	4×10^{31}	2010-
S-KEKB	e^+e^-	7+4	3016	8×10^{35} *	2018-

Colliders: Energy

FIG. 2. Center of mass energy reach of particle colliders vs their start of operation. Solid and dashed lines indicate a ten-fold increase per decade for hadron (circles) and lepton (triangles) colliders (adapted from [37]).

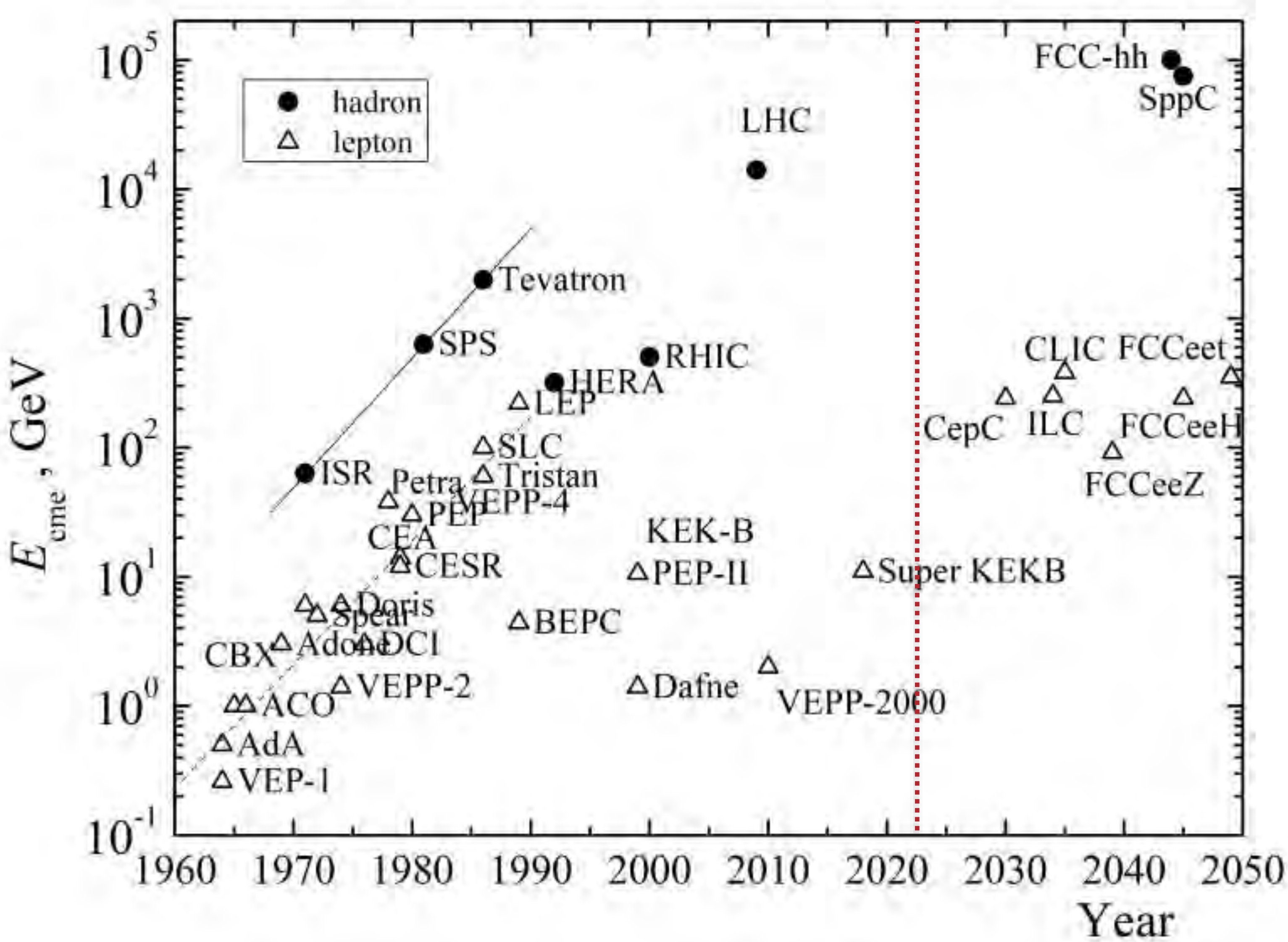

Only Electric Field Boosts Energy

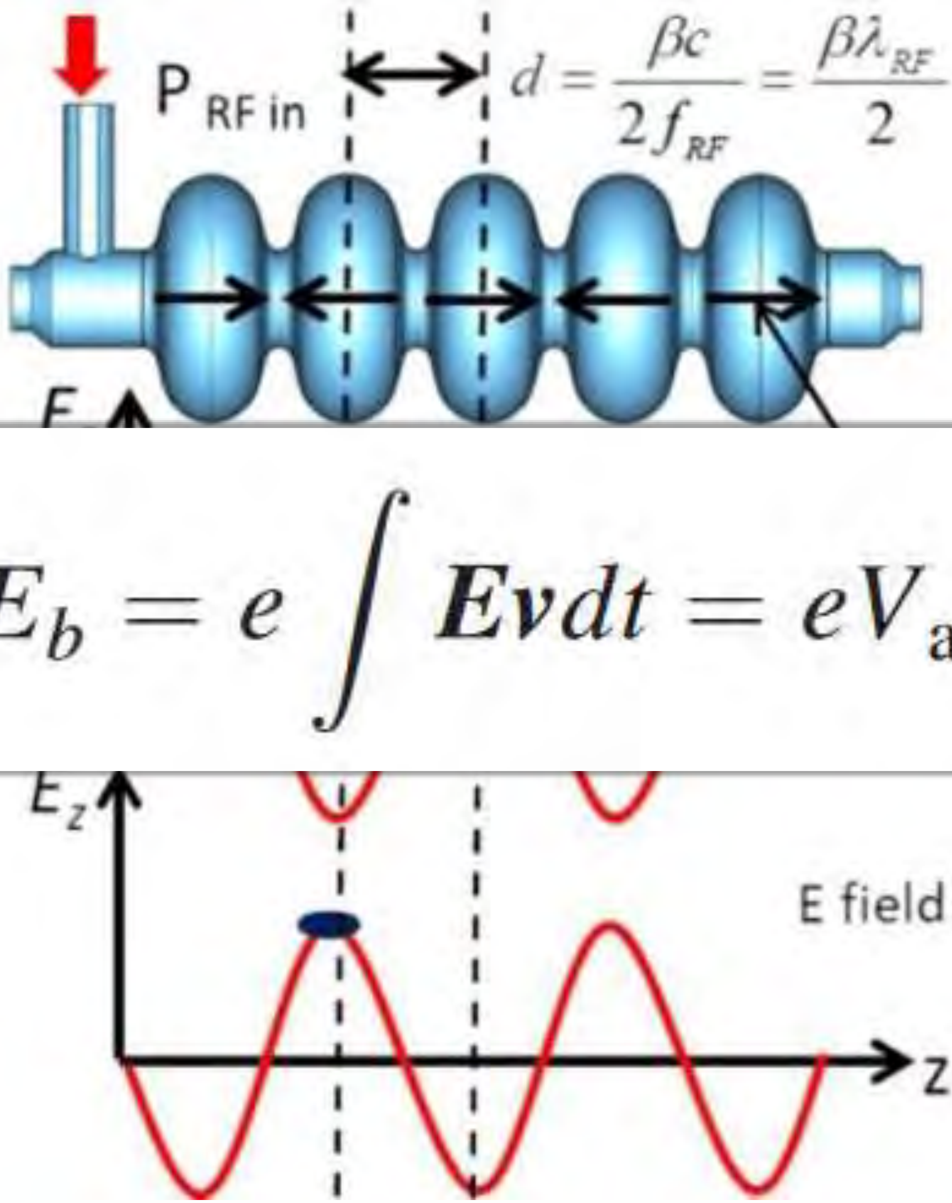

$$\omega_{\mathrm{rf}} = 2\pi f_{\mathrm{rf}}$$

$$\Delta E_b = e \int \boldsymbol{E} v dt = e V_{\mathrm{acc}} \cos\left(\omega_{\mathrm{rf}} t + \phi\right)$$

How much power is needed

$$P_{\text{rf}} = P_b + P_{\text{loss}} = I_b \Delta E_b + \frac{V_{\text{acc}}^2}{2R_s}$$

Where "*shunt impedance*": $R_s = Q(R/Q)$

"Quality factor"

~10^4 for Copper 300K

10^(9-10) for SC Nb cavities

"R/Q" cavity geometry factor

~100 for "open" elliptic cavities

196 Ohm for "pillbox" cvavity

RF Cavities

Resonant cavity, eg "pill-box":

$$\omega_c = \frac{2.405\, c}{R_c}$$

R=10cm at f_{RF}=1.14 GHz

Max gradient/voltage per cavity:

- *Is determined by RF power and shunt impedance*
- *Is limited by breakdown or dark current radiation or loss of superconductivity*
    - depends on frequency, CW or pulse duration, geometry, material, temperature, etc
- *Max ~100 MV/m in normal-conducting cavities at 12 GHz*
- *Max ~31.5 MV/m SRF cavities 1.3GHz*

LEP-I 352 MHz

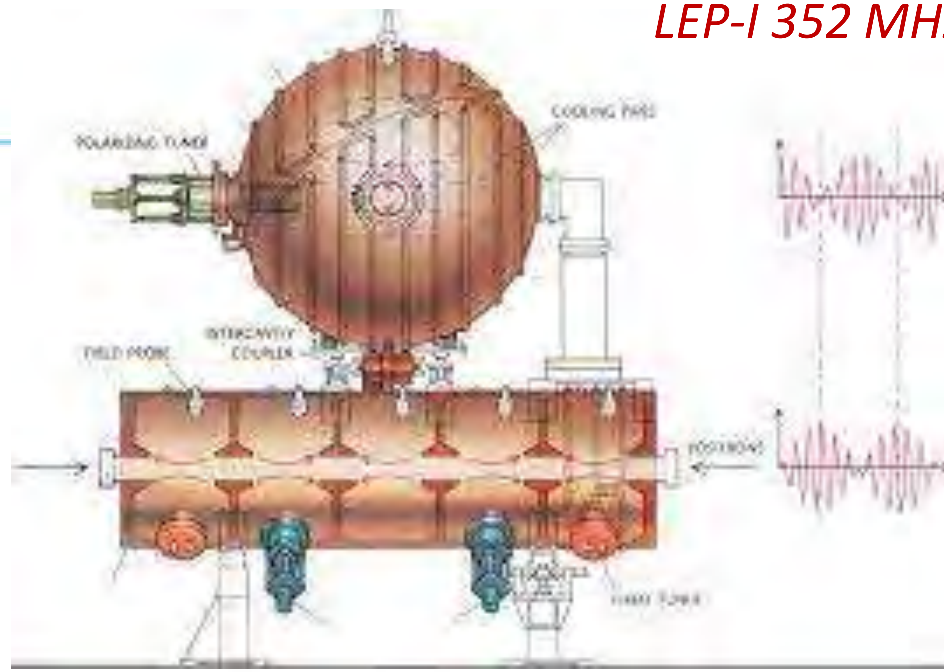

ILC 1300 MHz

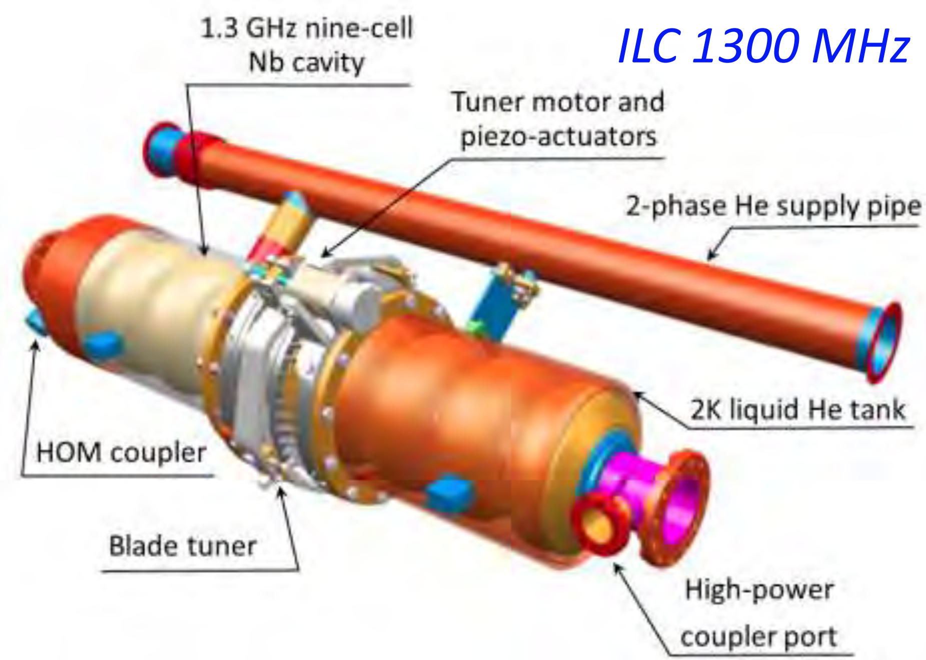

Rings vs Linacs

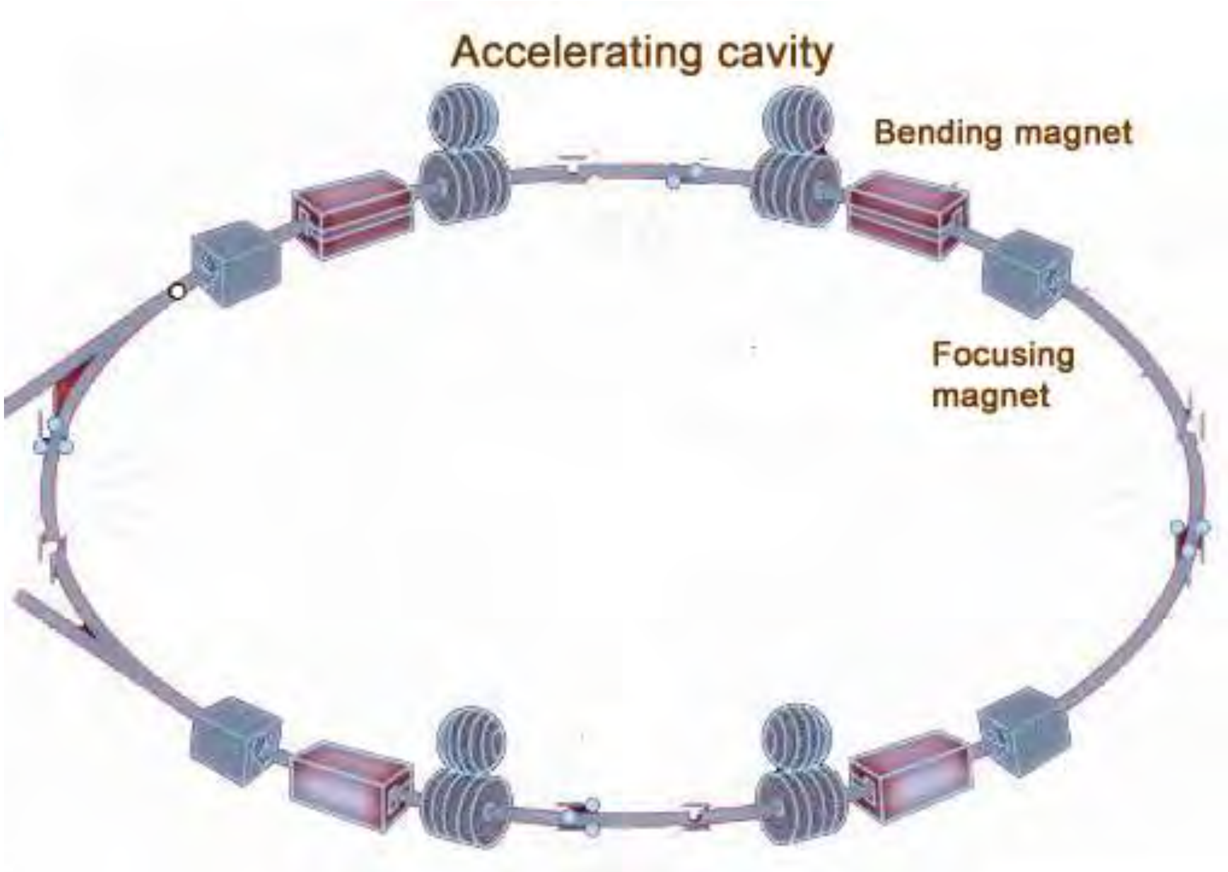

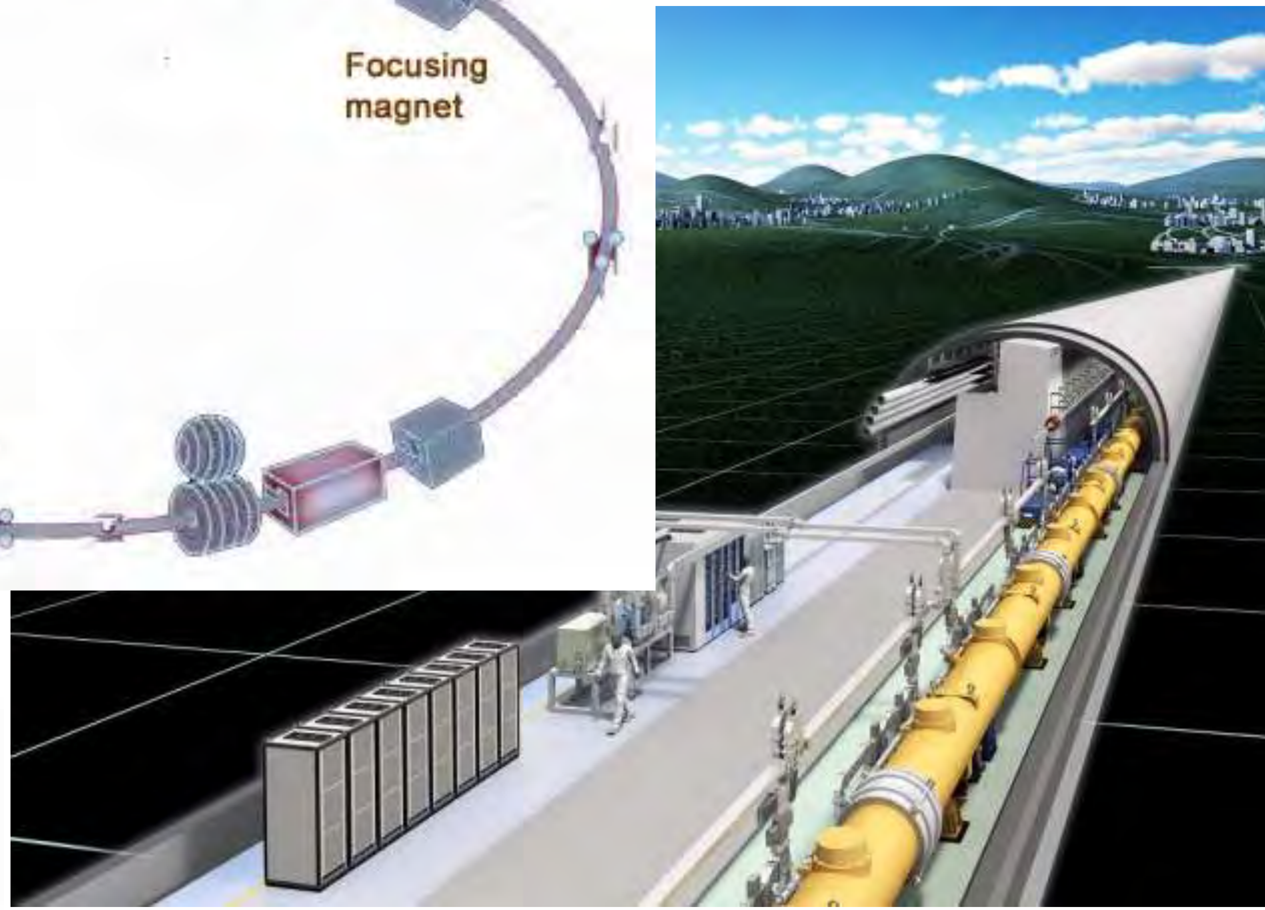

$$I_b \Delta E_b + \frac{V_{\rm acc}^2}{2R_s}$$

lower V_{acc} if you can

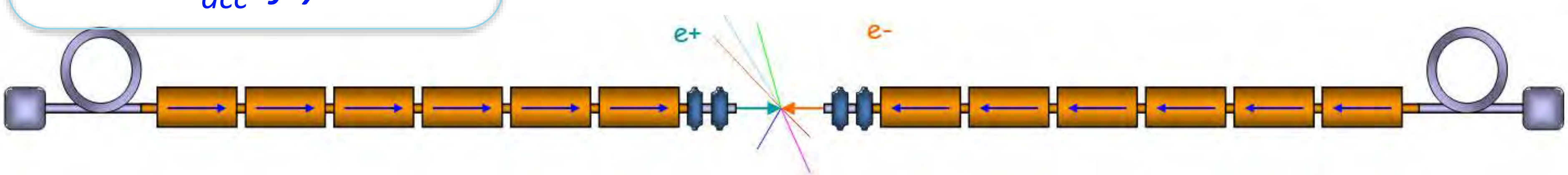

Types of Circular Accelerators

- **Cyclotrons – 1930-40's**
  - **E.O.Lawrence (UCB)**

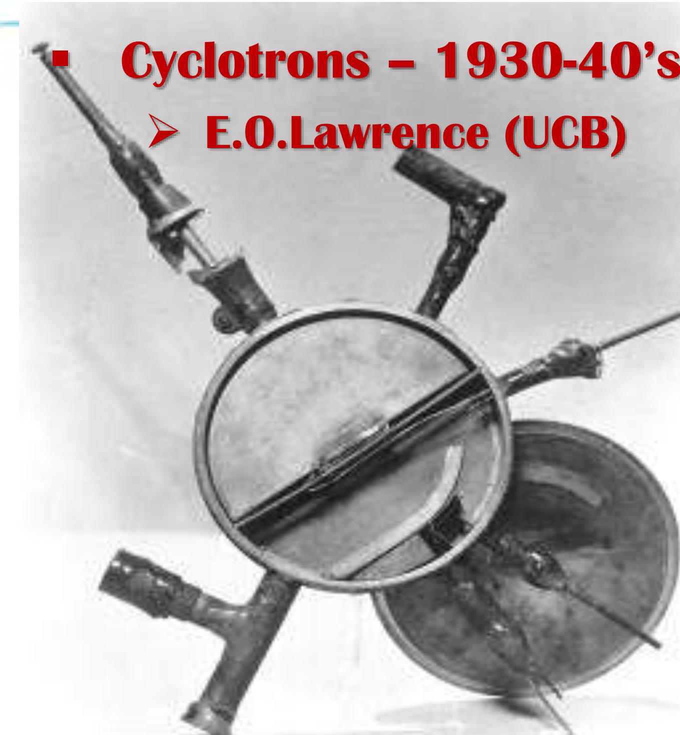

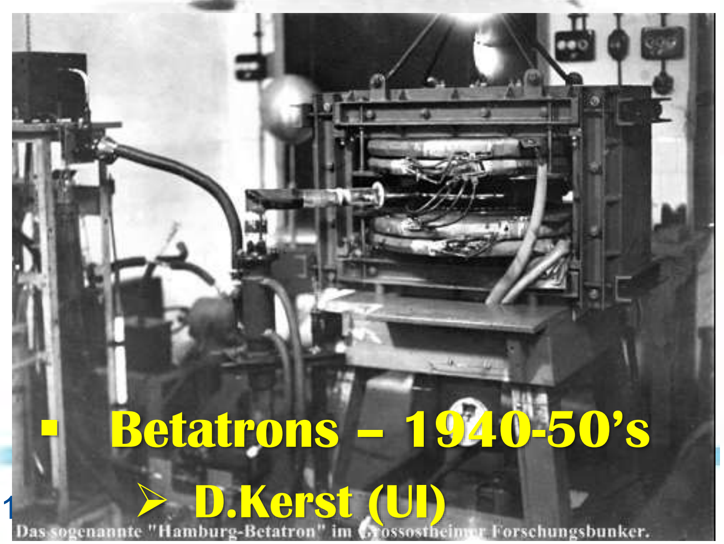

- **Betatrons – 1940-50's**
  - **D.Kerst (UI)**

Synchrotrons (Tevatron, LHC)

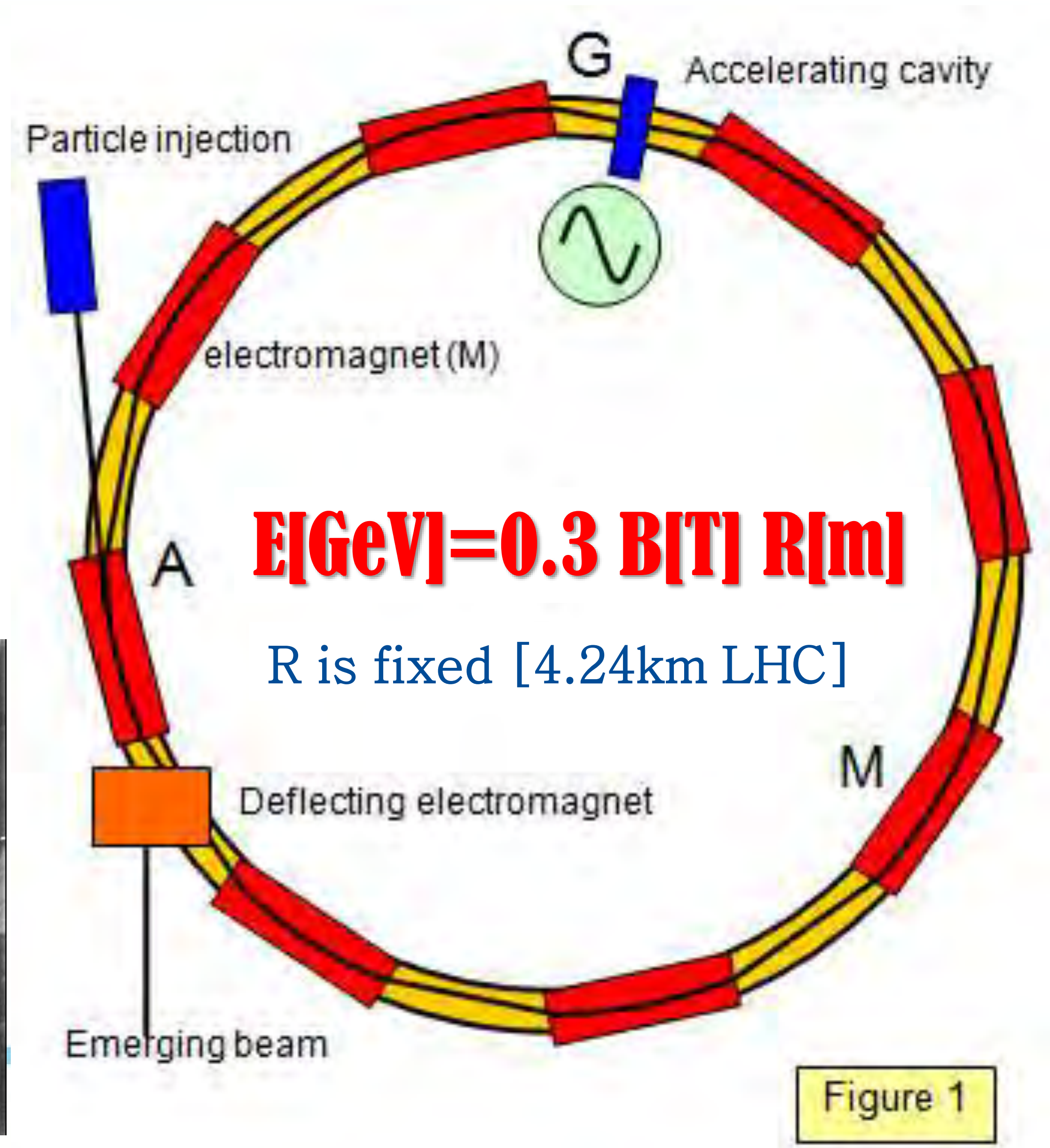

E[GeV]=0.3 B[T] R[m]

R is fixed [4.24km LHC]

Highest Energy = Highest Field SC Magnets

4.5T

Tevatron,
6 m, 76 mm
774 dipoles

4.5 K He, NbTi
+ warm iron
small He-plant

5.3T

HERA,
9 m, 75 mm
416 dipoles

NbTi cable
cold iron
Al collar

3.5T

RHIC,
9 m, 80 mm
264 dipoles

NbTi cable
simple &
cheap

8.3T

LHC,
15 m, 56 mm
1276 dipoles

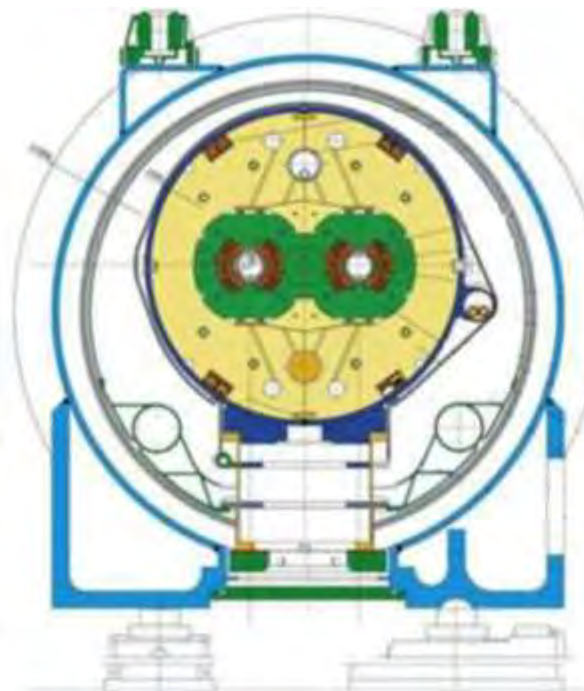

NbTi cable
2K He
two bores

Key for Magnets: Current Density

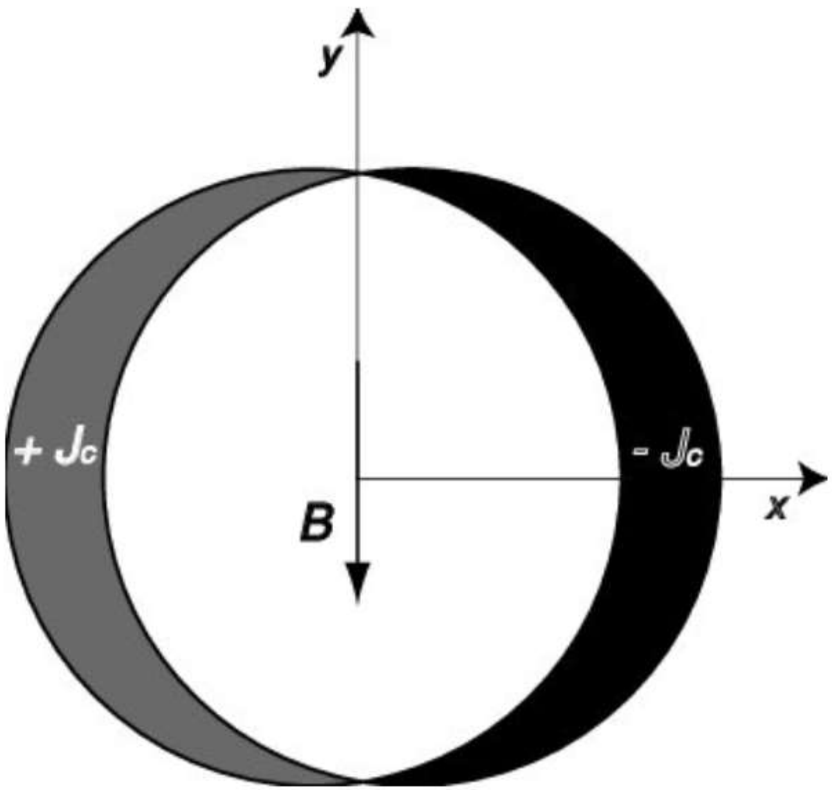

Generation of a pure dipole by a *cos θ* current distribution

Scaling: B_{max}~ *J/Aperture*
(assume all *A* is filled by conductor)

J~j(current density) x A^2

B_{max}*~j x A*

but Cost ~*A^2* (cost of needed conductor) x length ~ *A^2/B* ~ *~A/j*

Therefore, high(est) current density is needed to maxizmize B-field and minimize Cost

- For room temperature copper *j~(*1-10) A/mm^2
- For superconductors → kA/mm^2

SC Magnets: Fields and Current Densities

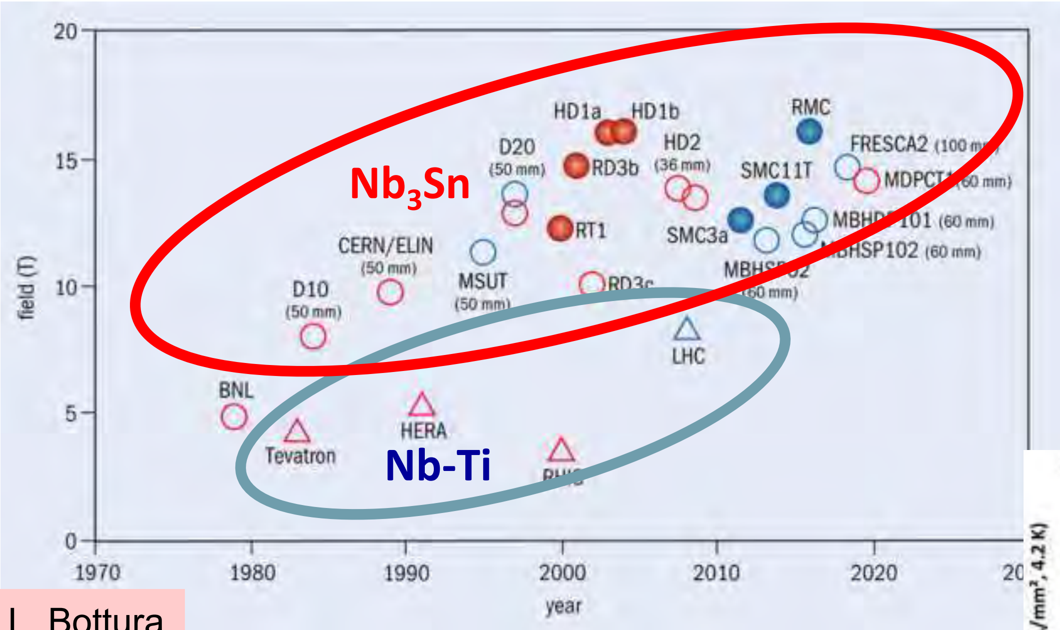

L. Bottura

Superconducting wire critical current density versus magnetic field: three main materials Nb-Ti, Nb$_3$Sn, HTS

P. Lee

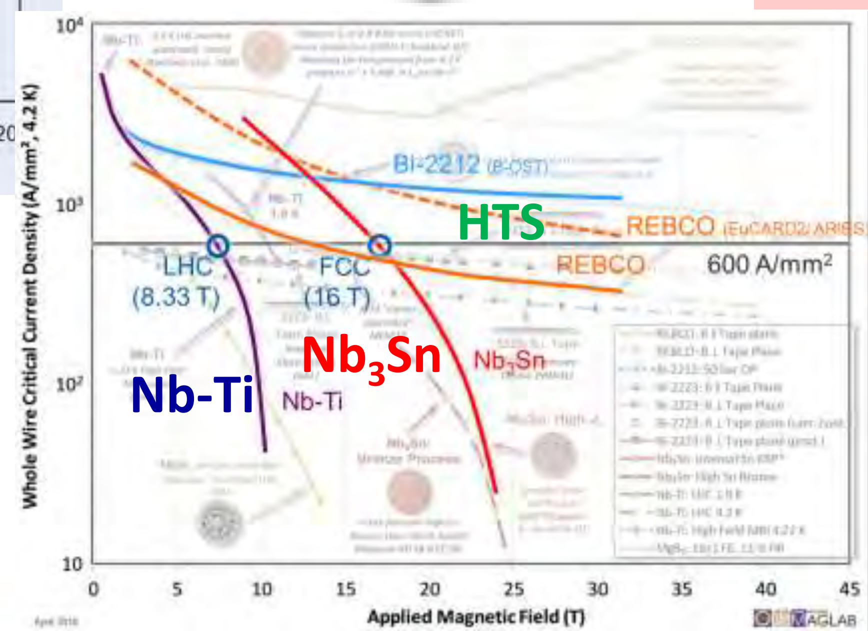

Record fields attained with dipole magnets of various configurations and dimensions, and either at liquid (4.2 K, red) or superfluid (1.9 K, blue) helium temperature.

SC Accelerator Magnets: Current Record 14.5T

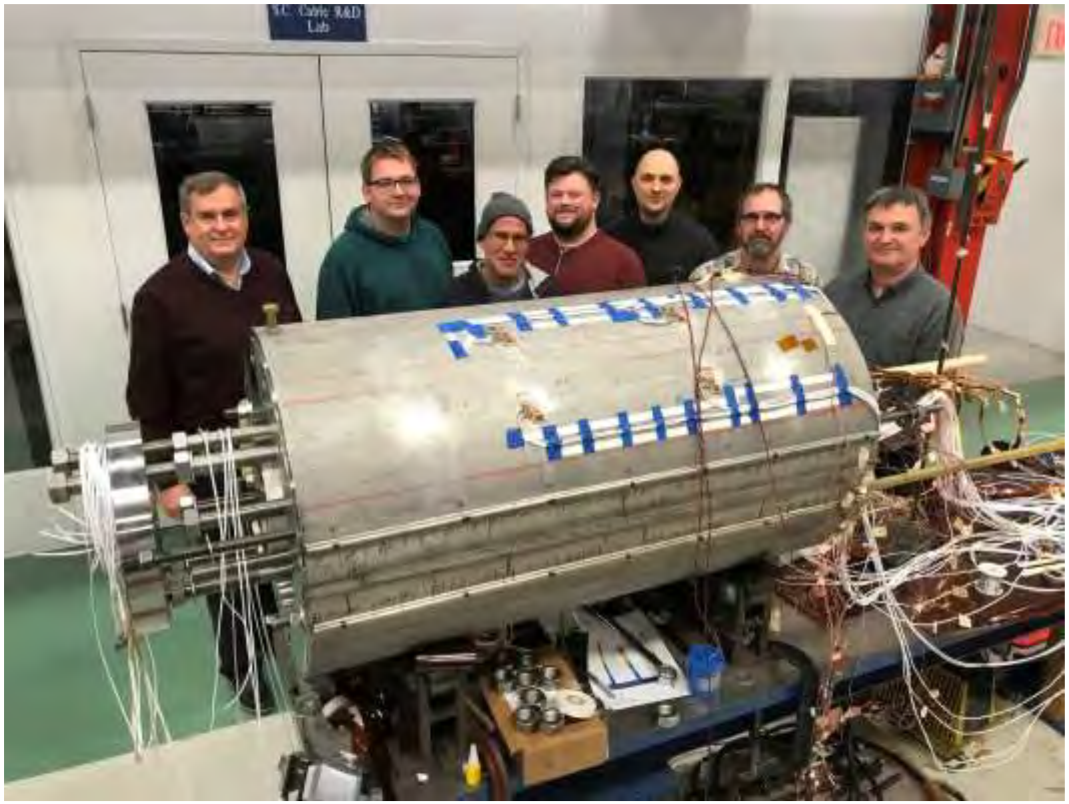

cosθ dipole

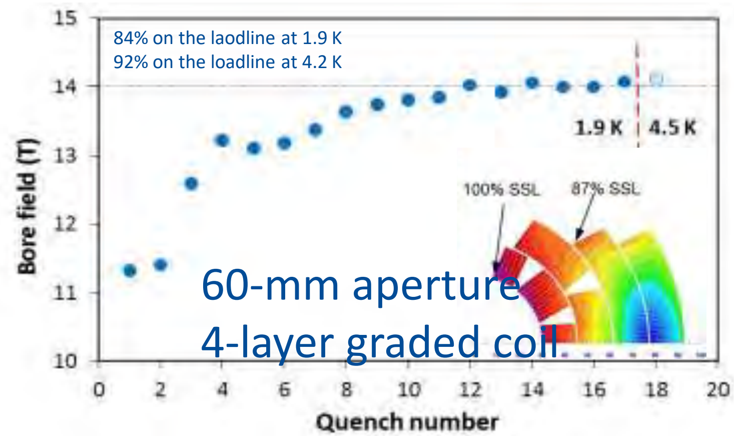

- 15 T dipole demonstrator
- Staged approach: In first step pre-stressed for 14 T
- Second test in June 2020 with additional pre-stress reached 14.5 T

Fermilab

Focusing Beams with Quadrupole Magnets

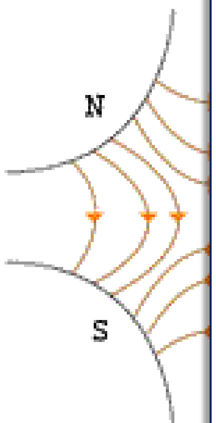

Luckily.

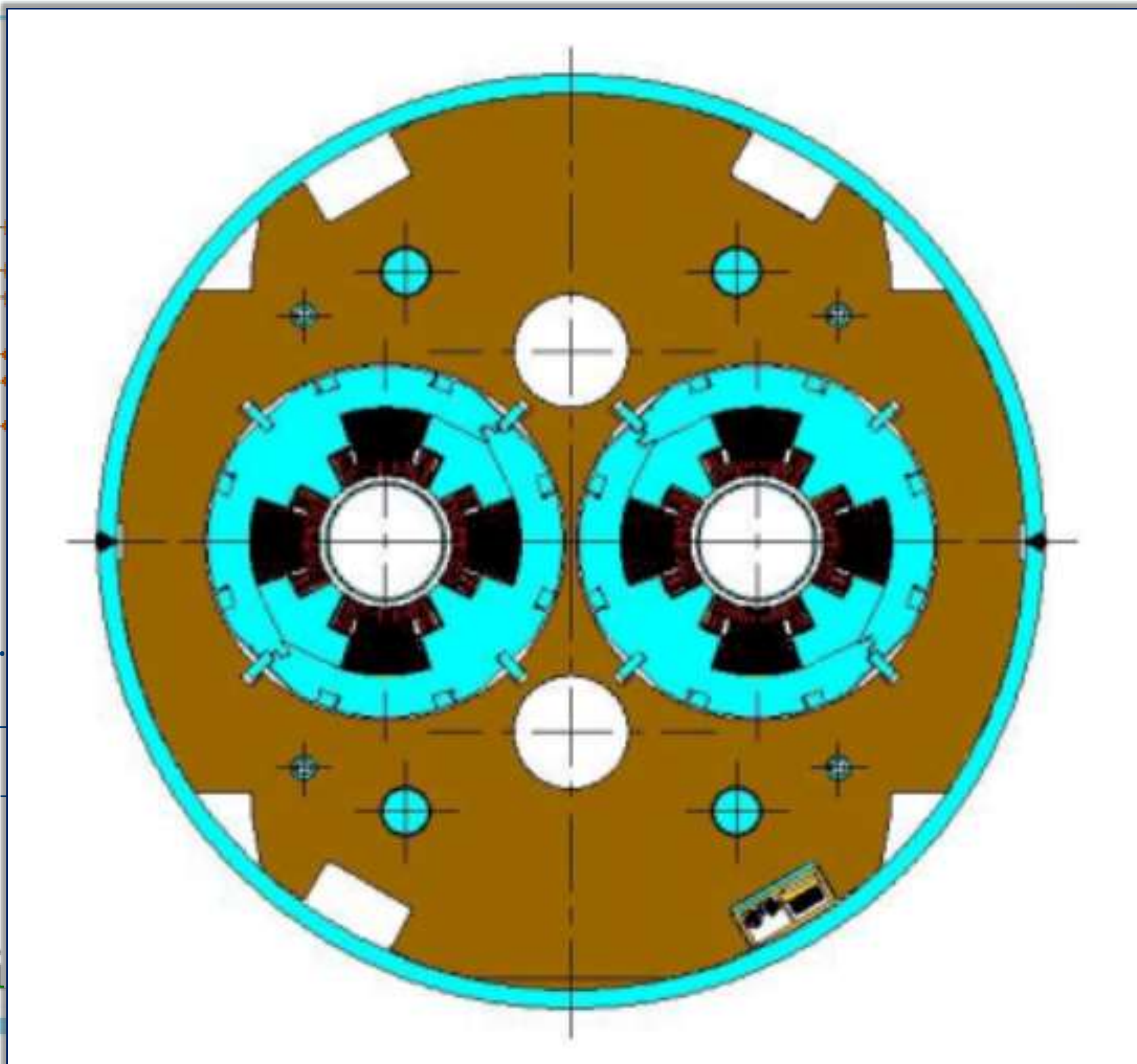

...pai

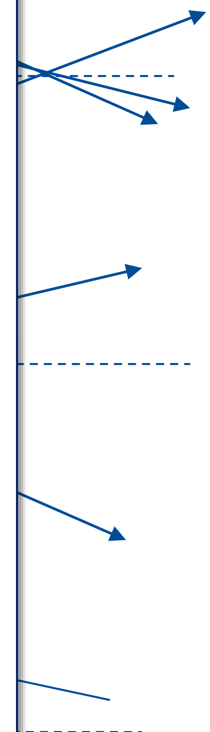

) cell"

Betatron Oscillations, Tune

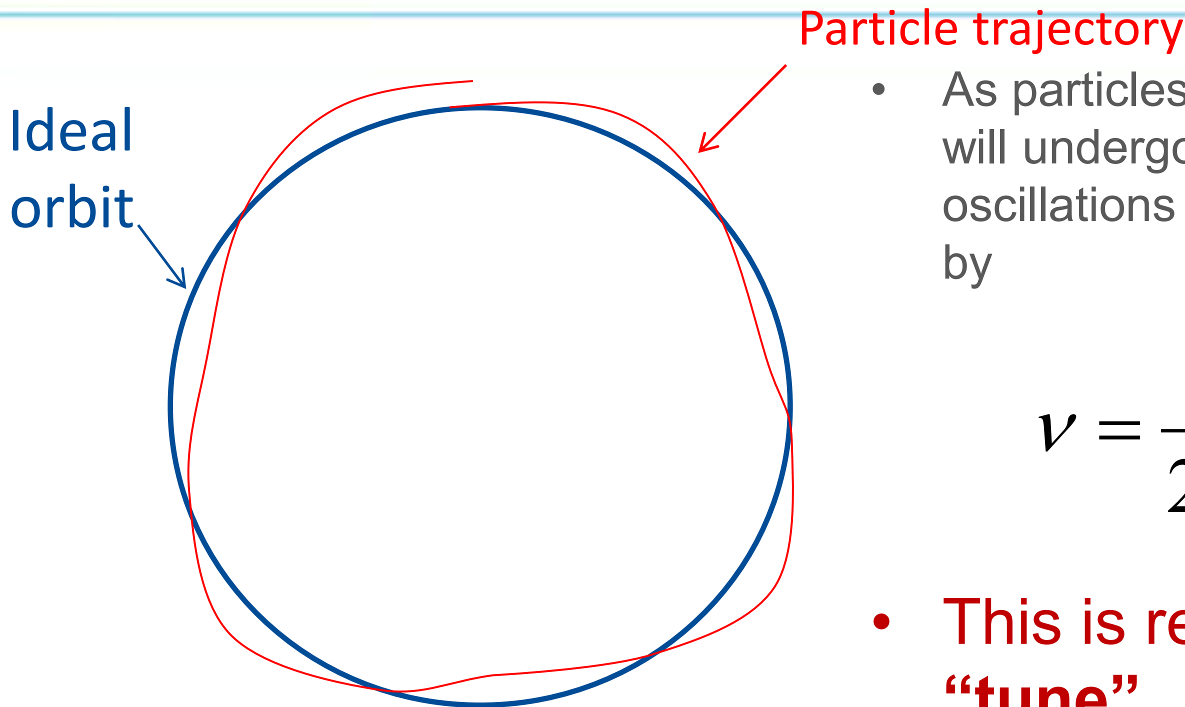

- As particles go around a ring, they will undergo a number of betatron oscillations *ν* (sometimes *Q*) given by

$$\nu = \frac{1}{2\pi}\oint \frac{ds}{\beta(s)}$$

- This is referred to as the **<u>"tune"</u>**

- We can generally think of the tune in two parts:

64.31

Integer : magnet/aperture optimization

Fraction: Beam Stability

see lectures VL1-2

Fermilab

Particle Equations of Motion (1)

$$x'' + K_x x = 0, \quad \text{with} \quad K_x \equiv \frac{e}{p}\frac{\partial B_y}{\partial x} + \frac{1}{\rho^2},$$

$$y'' + K_y y = 0, \quad \text{with} \quad K_y \equiv -\frac{e}{p}\frac{\partial B_y}{\partial x},$$

$$z' = -x/\rho,$$

Solution:

$$x(s) = \sqrt{2J_x\beta_x}\cos\psi_x, \qquad d\psi_x/ds = 1/\beta_x$$

$$x'(s) = -\sqrt{\frac{2J_x}{\beta_x}}[\alpha\cos\psi_x + \sin\psi_x],$$

So, tune: $Q_x = \frac{1}{2\pi}\oint d\psi_x = \frac{1}{2\pi}\oint \frac{ds}{\beta_x(s)}$ b

Key beam parameter: Emittance

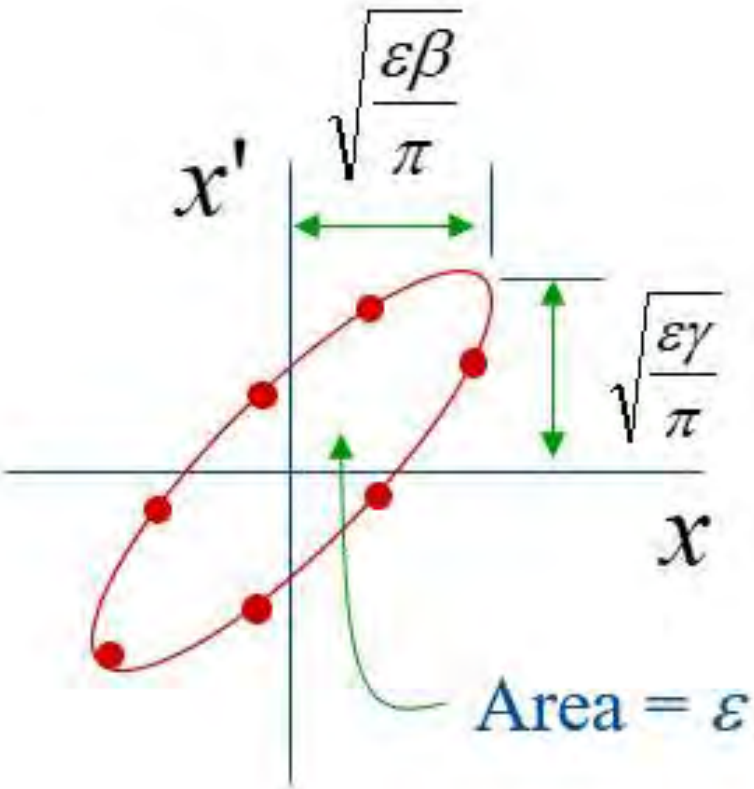

$$\gamma_T x^2 + 2\alpha_T x x' + \beta_T x'^2 = \frac{\varepsilon}{\pi}$$

Twiss
Parameters

- Product *size x angle* *X_rms x X'_rms* is called emittance
- *Emittance x gamma* is adiabatic invariant
- Luminosity (tbd) ~ *1/ε*

As a particle returns to the same point on subsequent revolutions, it will map out an ellipse in phase space – see lectures VL1-2

Most Important Equations

normalized emittance

$$\varepsilon_{n\ (x,y)} = \gamma \cdot \sigma_{x,y} \sigma'_{x,y}$$

$$\sigma_{x,y} = \sqrt{\frac{\varepsilon_n \cdot \beta_{x,y}}{\gamma}}$$

rms beam size

$$\sigma'_{x,y} = \sqrt{\frac{\varepsilon_n}{\gamma \cdot \beta_{x,y}}} = \frac{\sigma_{x,y}}{\beta_{x,y}}$$

rms beam angular spread

10^{-6}

Particle Equations of Motion (2)

Beta-functions are defined by

$$2\beta_x\beta_x'' - \beta_x'^2 + 4\beta_x^2 K_x = 4$$

Eg symmetric solution in free space (K=0):

$$\boxed{\beta_x(s) = \beta_x^* + \frac{s^2}{\beta_x^*}}$$

Also, note that nonlinear fields on beam orbit add complexity:

$$B_y + iB_x = \sum_{n=1}^{\infty}(B_n + iA_n)(x+iy)^{n-1}$$

n=1 dipole
n=2 quadrupole
n=3 octupole
n=4,5,6…

especially at resonant frequencies

$$kQ_x + lQ_y = m, \text{ where } k,\ l, \text{ and } m \text{ are integers}$$

see lectures VL1-2, 5

Collider Spot Size

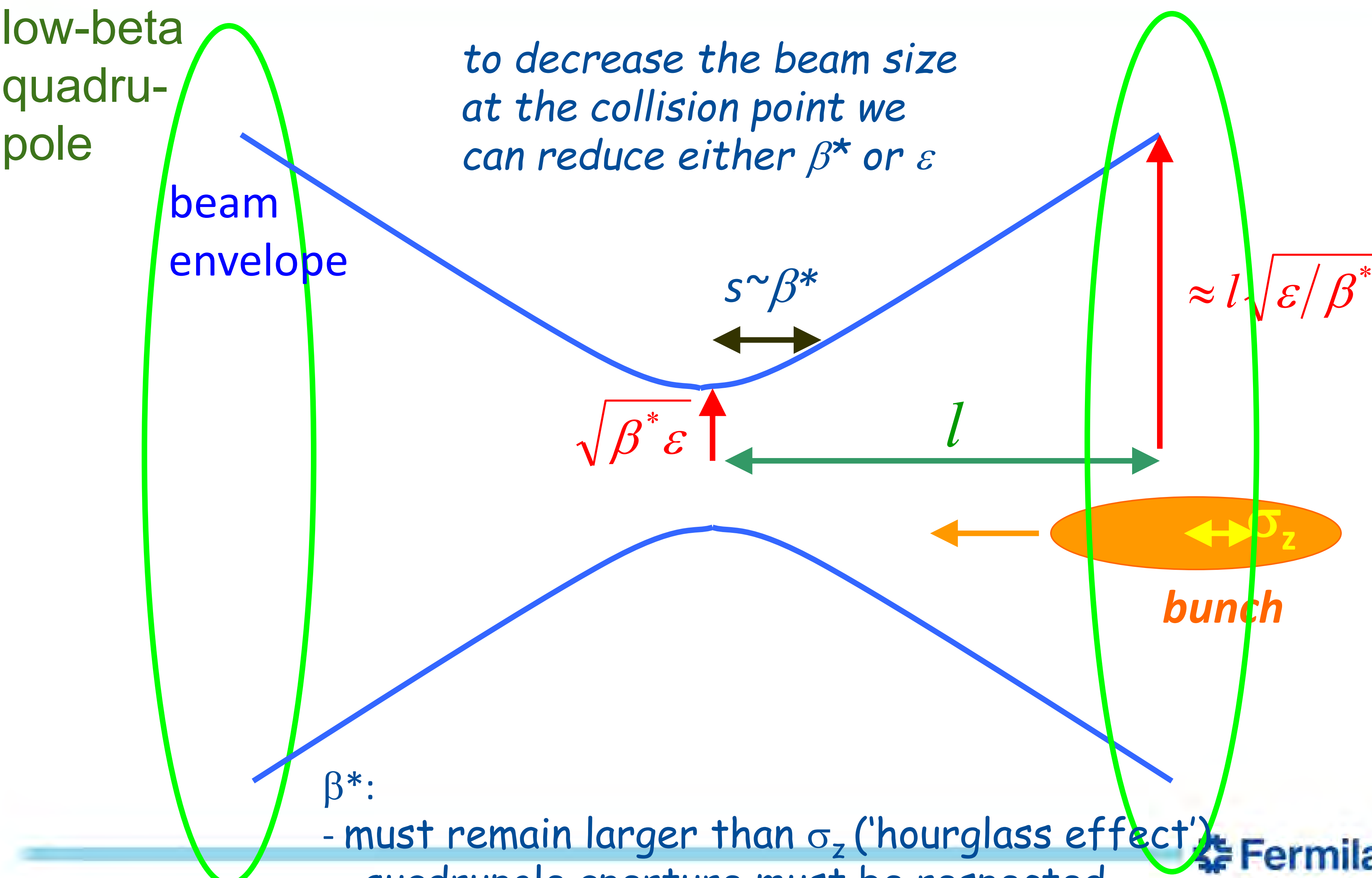

β*:
- must remain larger than σ_z ('hourglass effect')
- quadrupole aperture must be respected

Longitudinal Motion: Phase Stability

Particles are typically accelerated by radiofrequency ("RF") structures. Stability depends on particle arrival time relative to the RF phase. Note: the speed is fixed = speed of light , so time of arrival depends only on the energy (in the bunch – energy deviation wrt "reference central particle")

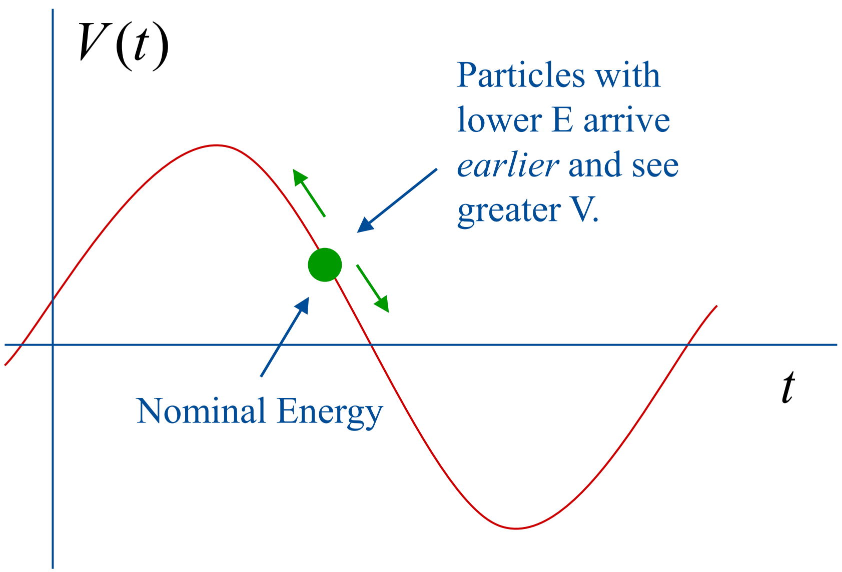

see lecture VL6

Example: LHC

RF Frequency 400 MHz
(35640 times revolution frequency)

- RF Voltage = 8 cavities x 2 MV = 16 MV / turn (max)

In collisions dE/dn= 0 V/turn (synchronouse phase ~0)

Slow energy-position oscillations (23 Hz or ~500 turns)

rms energy spread 1.3e-4 (1GeV) rms bunch length ~ 8cm

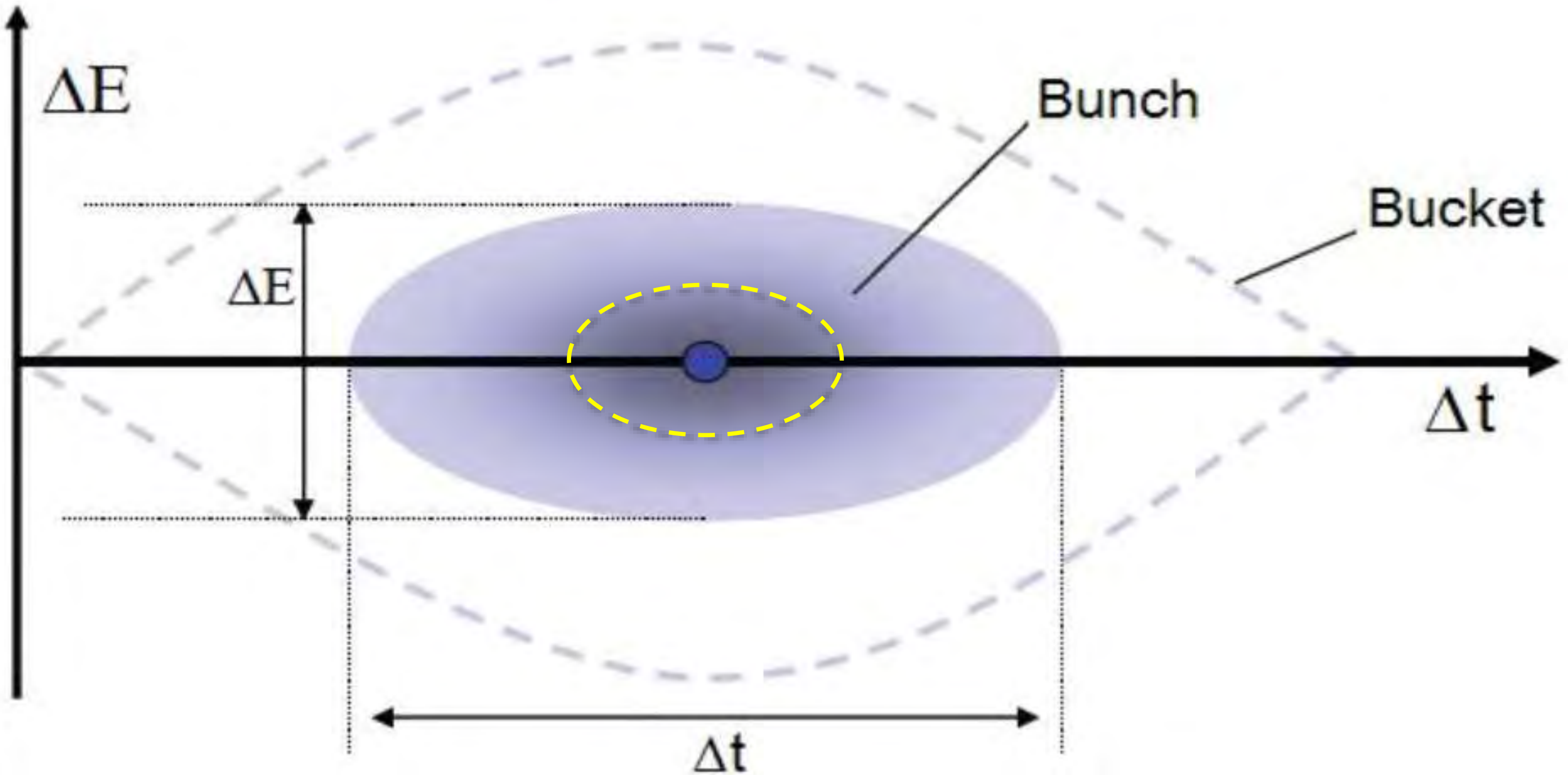

Scales of Time-scales/Frequencies

Longitudinal oscillations are the slowest of all the periodic processes that take place in the accelerators. For example, in the LHC, the frequency of synchrotron oscillations at the top energy of 7 TeV is about $f_s = 23$ Hz, the revolution frequency is $f_{\text{rev}} = 11.3$ kHz, the frequency of betatron oscillations is about $Q_{x,y} f_{\text{rev}} = 680$ kHz, and the rf frequency is $f_{\text{rf}} = 400.8$ MHz ($h = 35\,640$).

…even slower might be operational processes :

- injection/extraction (1/sec… 1/min… 1/hr … 1/day)
- beam cooling (sometimes - hours)
- luminosity decay (min… days)

Luminosity

$$N_{\exp} = \sigma_{\exp} \cdot \int \mathcal{L}(t)dt.$$

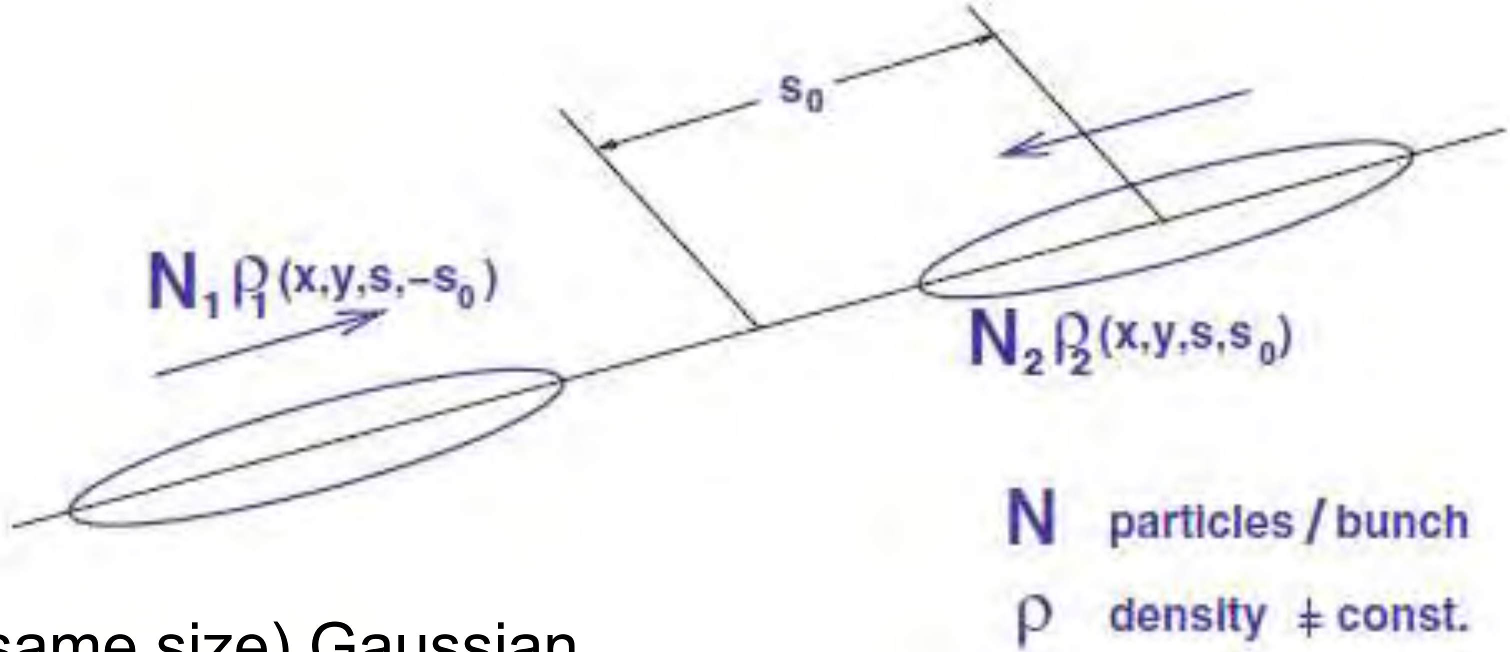

For (same size) Gaussian bunches:

$$\mathcal{L} = f_{\text{coll}} \frac{N_1 N_2}{4\pi\sigma_x^* \sigma_y^*}$$

Luminosity: Unequal Bunches

$$\rho_{iz}(z) = \frac{1}{\sigma_z\sqrt{2\pi}} \exp\left(-\frac{z^2}{2\sigma_z^2}\right) \quad \text{where} \quad i = 1, 2, \quad z = x, y$$

$$\rho_s(s \pm s_0) = \frac{1}{\sigma_s\sqrt{2\pi}} \exp\left(-\frac{(s \pm s_0)^2}{2\sigma_s^2}\right)$$

$$K = \sqrt{(\vec{v}_1 - \vec{v}_2)^2 - (\vec{v}_1 \times \vec{v}_2)^2/c^2}$$

$$\mathcal{L} \propto K N_1 N_2 \cdot \iiiint_{-\infty}^{+\infty} \rho_1(x, y, s, -s_0)\, \rho_2(x, y, s, s_0)\, \mathrm{d}x\mathrm{d}y\mathrm{d}s\mathrm{d}s_0$$

yields:

$$\boxed{\mathcal{L} = \frac{N_1 N_2 f_c}{2\pi\sqrt{\sigma_{1x}^2 + \sigma_{2x}^2}\sqrt{\sigma_{2y}^2 + \sigma_{2y}^2}}}$$

Correction for Crossing Angle and Offset

Offset d_1-$d_2 \neq 0$

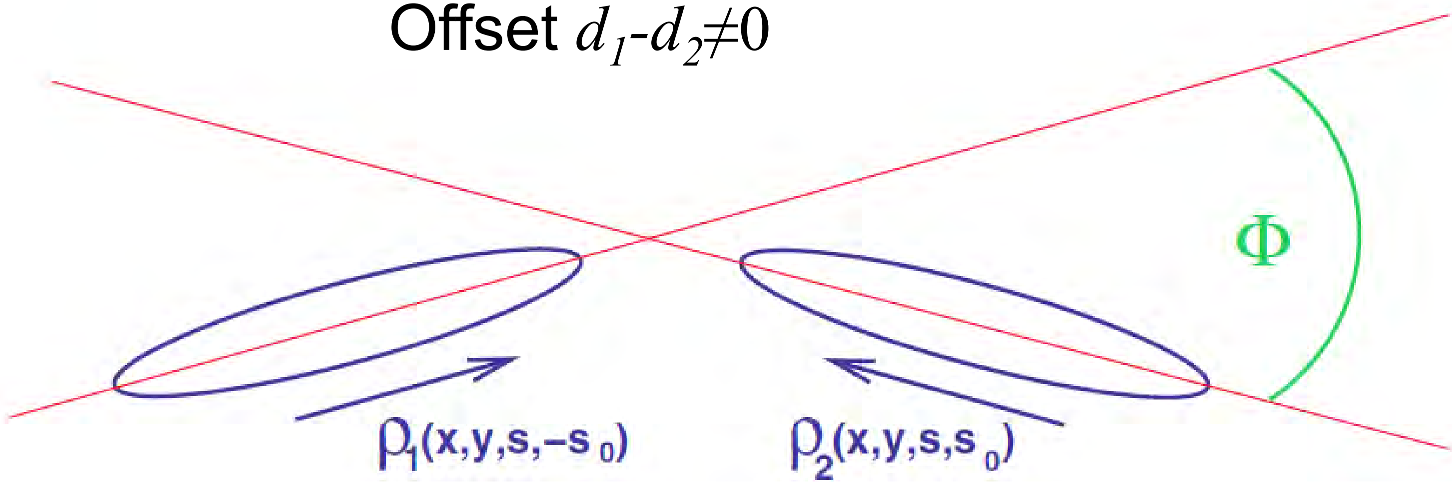

$$\mathcal{L} = \frac{N_1 N_2 f N_b}{4\pi \sigma_x \sigma_y} \cdot W \cdot e^{\frac{B^2}{A}} \cdot S$$

≈ 1

where:

$$A = \frac{\sin^2 \frac{\phi}{2}}{\sigma_x^2} + \frac{\cos^2 \frac{\phi}{2}}{\sigma_s^2}$$

$$B = \frac{(d_2 - d_1)\sin(\phi/2)}{2\sigma_x^2}$$

$$W = e^{-\frac{1}{4\sigma_x^2}(d_2 - d_1)^2}$$

$$S = \frac{1}{\sqrt{1 + \left(\frac{\sigma_s}{\sigma_x} \tan \frac{\phi}{2}\right)^2}} \approx \frac{1}{\sqrt{1 + \left(\frac{\sigma_s}{\sigma_x} \frac{\phi}{2}\right)^2}}$$

"Crab Crossing" Collisions

Head-tail rotation by RF dipole deflectors

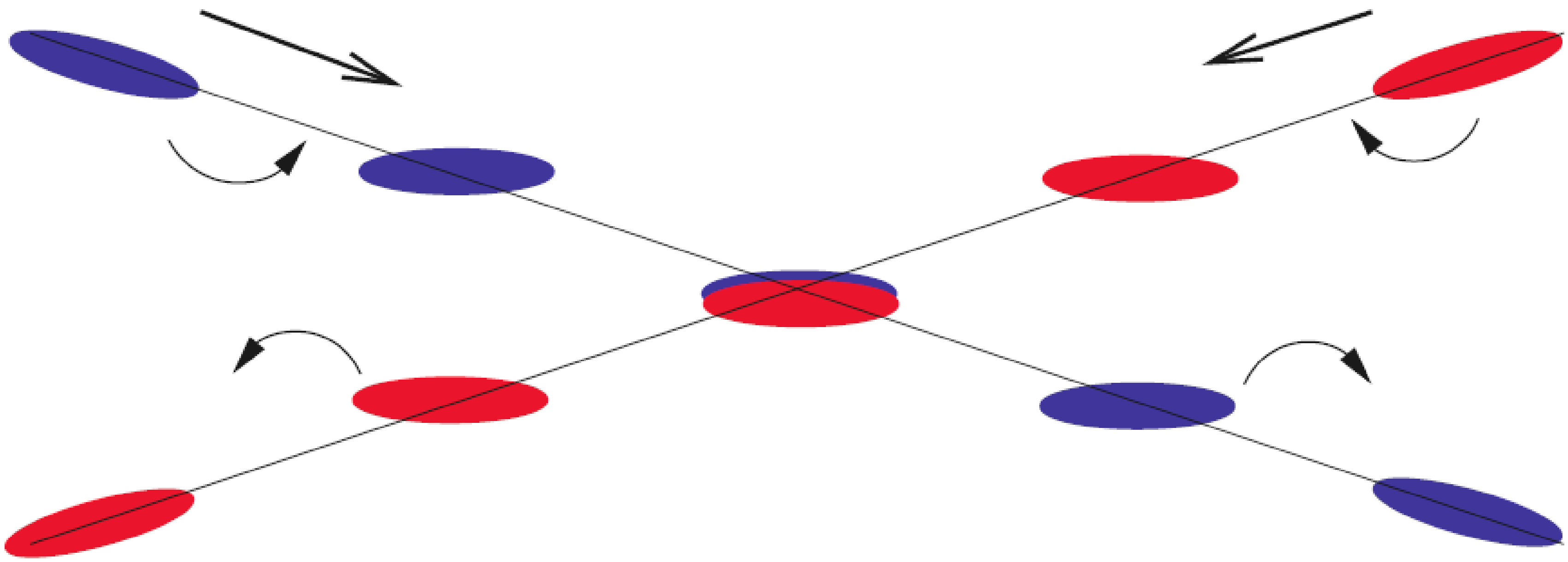

Note: either the crossing angle or amplitude of the crabbing affect instantaneous luminosity → can be used for "luminosity leveling"

Hour-Glass Effect

$$\beta(s) = \beta^* \left(1 + \left(\frac{s}{\beta^*}\right)^2\right)$$

Same for beam size

$\sqrt{\beta\ \varepsilon}$

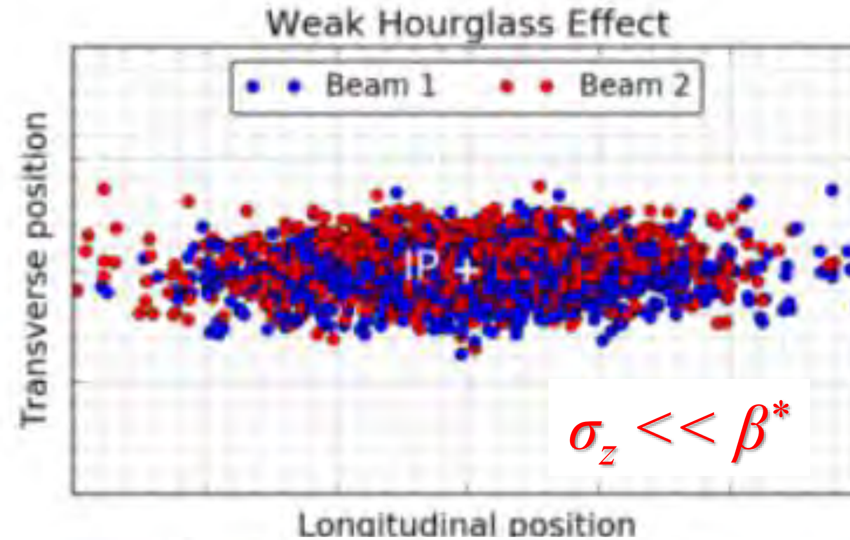

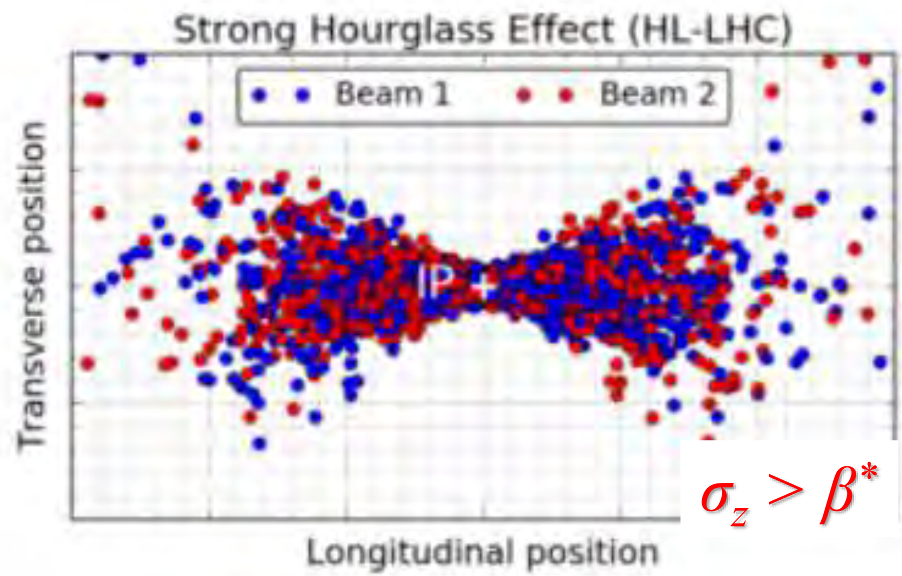

$$\frac{\mathcal{L}(\sigma_s)}{\mathcal{L}(0)} = \int_{-\infty}^{+\infty} \frac{1}{\sqrt{\pi}} \frac{e^{-u^2}}{\sqrt{\left[1 + \left(\frac{u}{u_x}\right)^2\right] \cdot \left[1 + \left(\frac{u}{u_y}\right)^2\right]}} \mathrm{d}u$$

$u_x = \beta_x^* / \sigma_s$

$u_y = \beta_y^* / \sigma_s$

Fermilab

Luminosity Reduction Due to Hourglass

For round beams, equal beta's and no crossing angle, *H*-factor

$$\frac{\mathcal{L}(\sigma_s)}{\mathcal{L}(0)} = H\left(\frac{\sigma_z}{\beta^*}, \theta_c = 0\right) = \sqrt{\pi} A \exp(A^2) \mathrm{erfc}(A)$$

$$A = \beta^* / \sigma_z$$

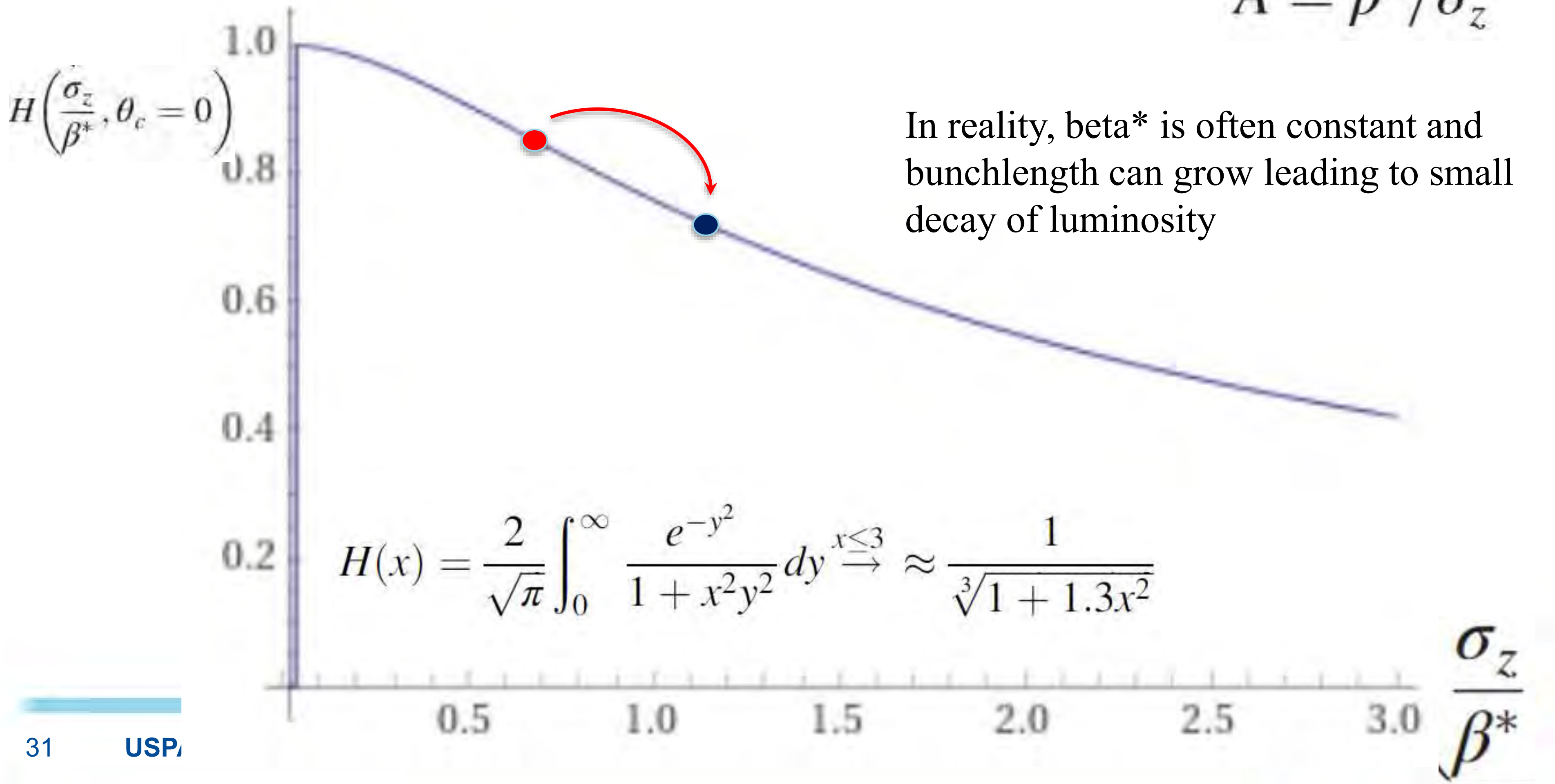

In reality, beta* is often constant and bunchlength can grow leading to small decay of luminosity

$$H(x) = \frac{2}{\sqrt{\pi}} \int_0^\infty \frac{e^{-y^2}}{1 + x^2 y^2} dy \overset{x \leq 3}{\rightarrow} \approx \frac{1}{\sqrt[3]{1 + 1.3x^2}}$$

Luminosity Summary : Key Factors

Want it higher
either smaller rings = higher B
or high rep linear collider (= power)

High *E* helps
This factor comes from adiabatic reduction of the rms beam size for the same emittance

Higher intensity drives *L* *note that N(bunch) comes squared while # of bunches linear; sometimes N is limited by beam-beam, often $n_b N$ is limited → try to put all charge in one bunch*

$$\mathcal{L} = f_0 \gamma n_b \frac{N^2}{4\pi\varepsilon_n \beta^*} H\left(\frac{\sigma_z}{\beta^*}, \theta_c\right)$$

Smallest *emittance*
that's where most of beam physics goes to – cooling to stop heating, noises, dyna-mics in injectors, etc etc etc

Minimize *beta*
need stronger focusing = larger aperture and stronger LB quads

Keep *H* under control
keep bunch length and beta more or less matched, be aware of the crossing angle (sometimes need it → crabs)*

Colliders: Luminosity

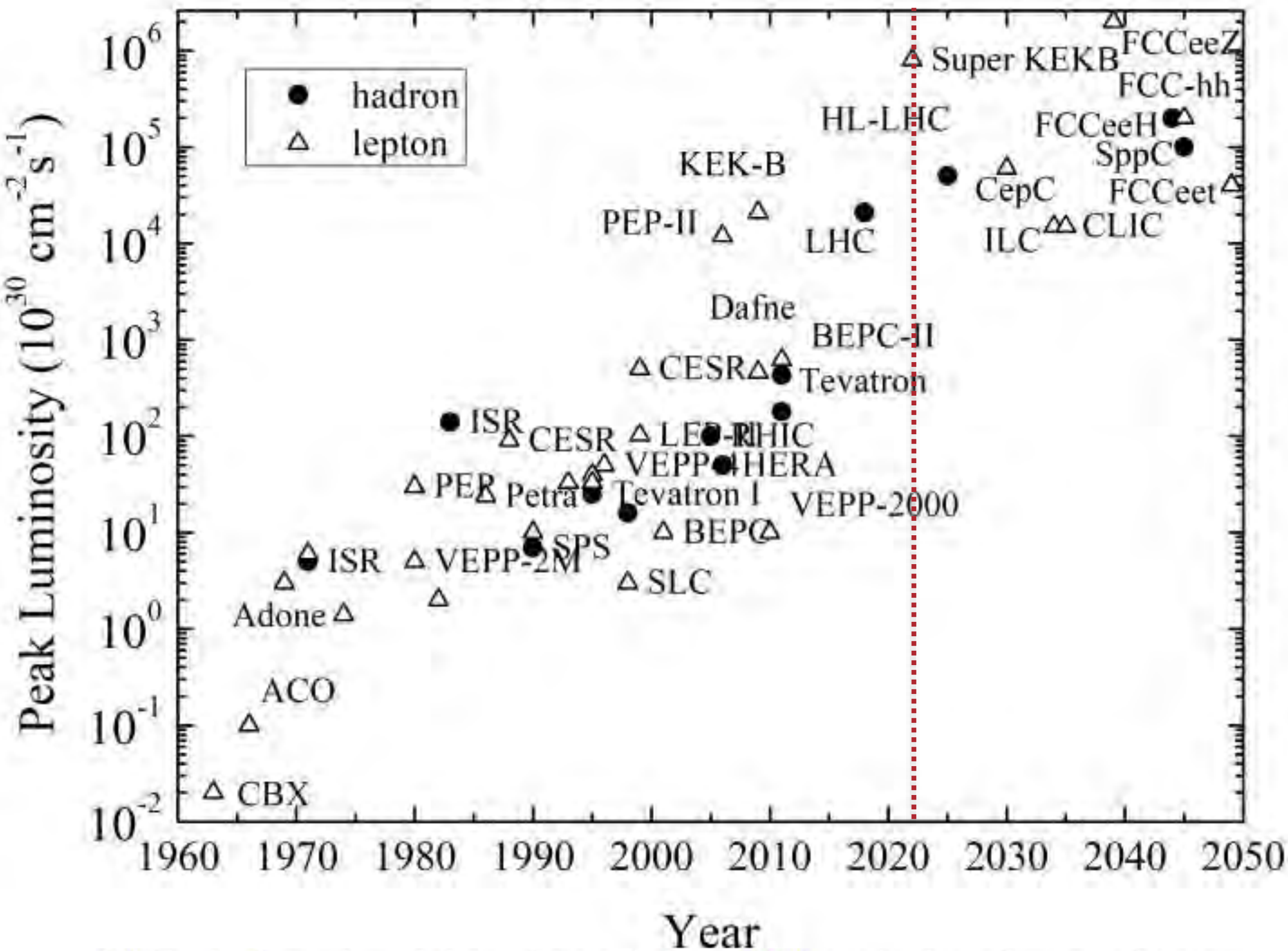

FIG. 3. Luminosities of particle colliders (triangles are lepton colliders and full circles are hadron colliders, adapted from [37]). Values are per collision point.

Luminosity Demand : Leptons

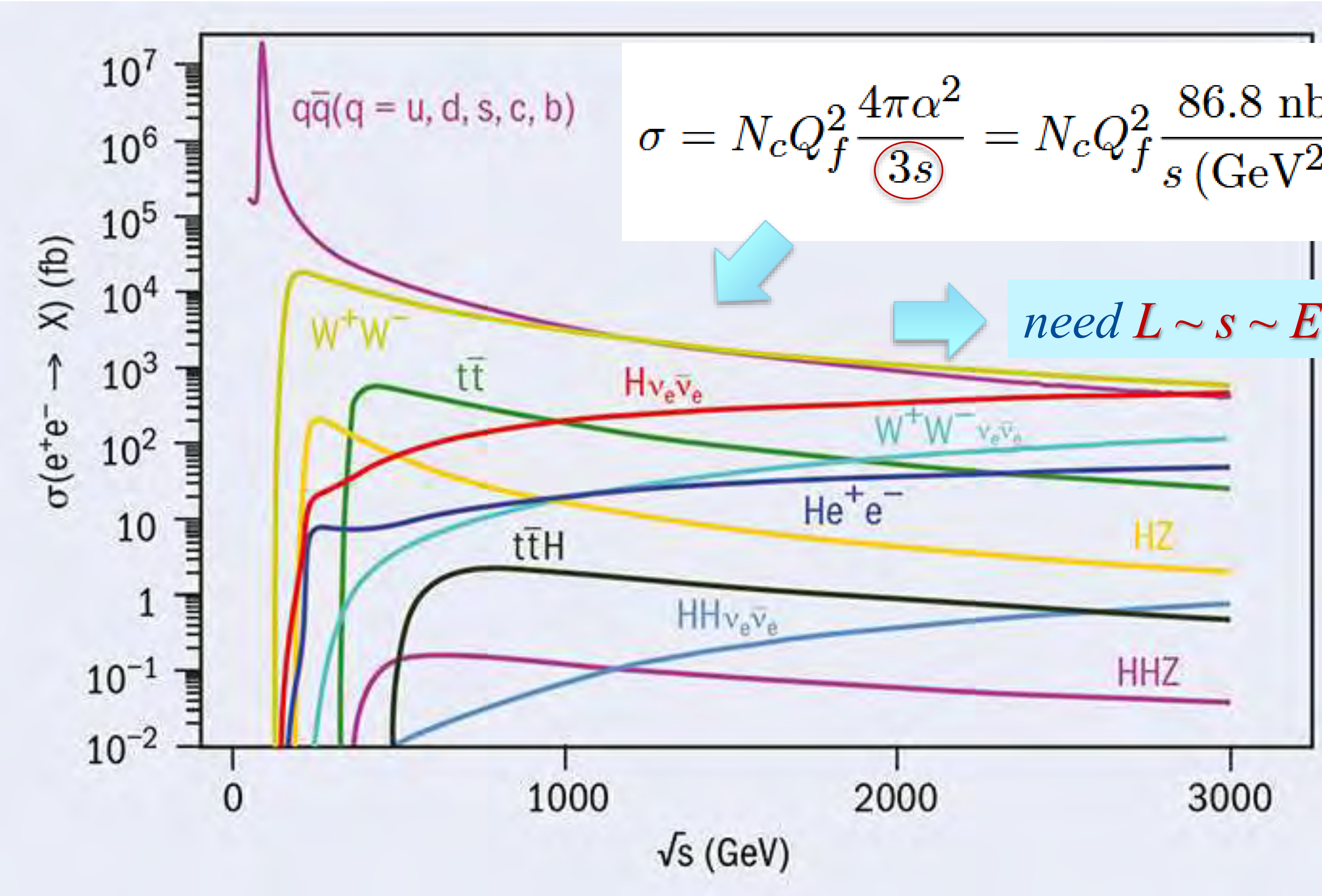

$$\sigma = N_c Q_f^2 \frac{4\pi\alpha^2}{3s} = N_c Q_f^2 \frac{86.8\ \text{nb}}{s\,(\text{GeV}^2)}$$

need $L \sim s \sim E^2$

Hadron Cross Sections – Inclusive vs Parton

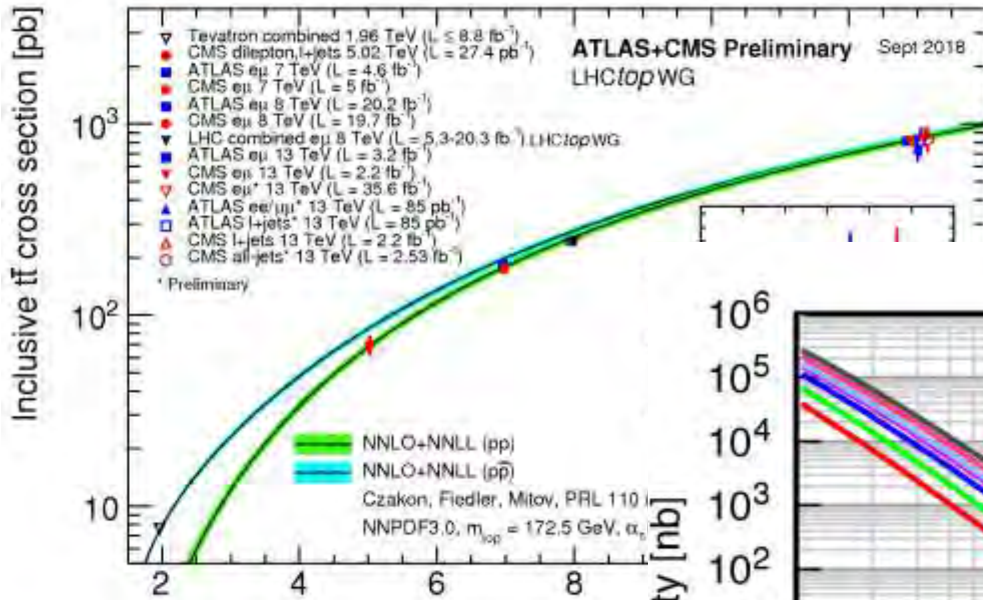

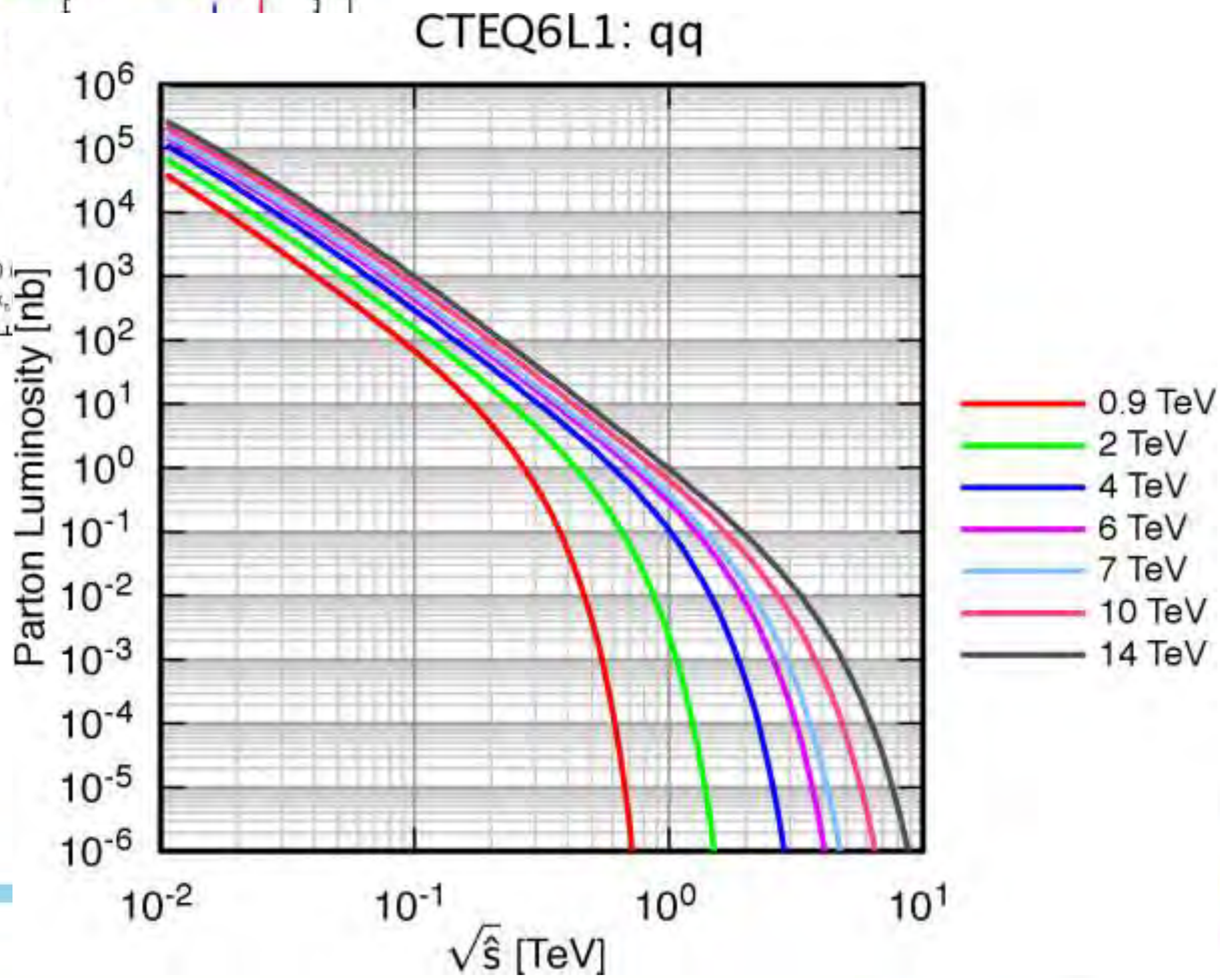

Colliders: Luminosity vs Energy

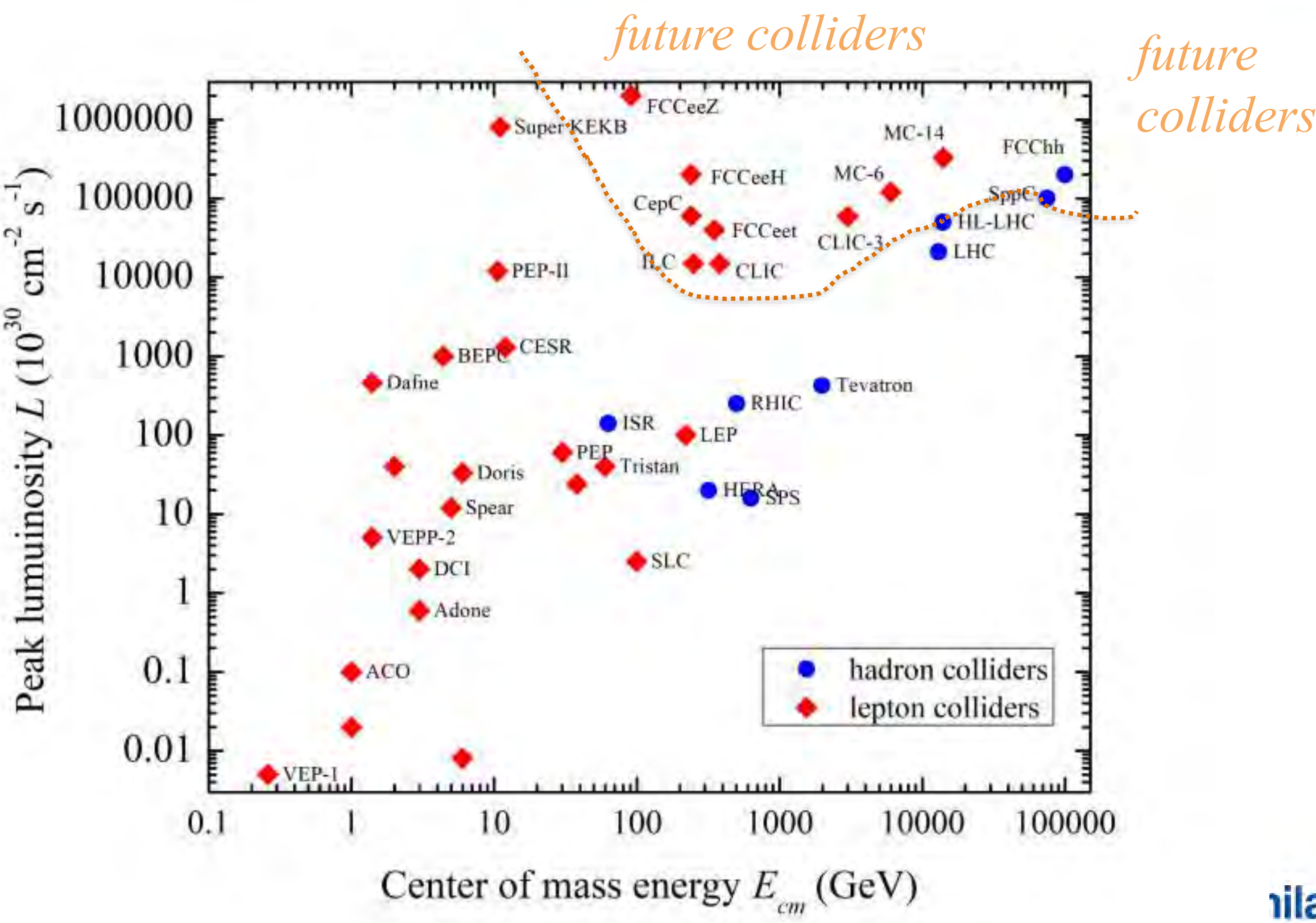

Luminosity evolution

$$L = \gamma f_B \frac{N_1 N_2}{4\pi\beta^* \varepsilon} H(\sigma_s / \beta^*)$$

- Factors change in time

$$L(t) = C\frac{N_1(t)N_2(t)}{\varepsilon(t)} H(t)$$

- Therefore, the lifetime

$$\tau_L^{-1} = \frac{dL(t)}{L(t)dt} = \tau_{N1}^{-1} + \tau_{N2}^{-1} - \tau_{\varepsilon}^{-1} + \tau_H^{-1}$$

LHC Lumi Lifetime (~7 hrs) and Integral

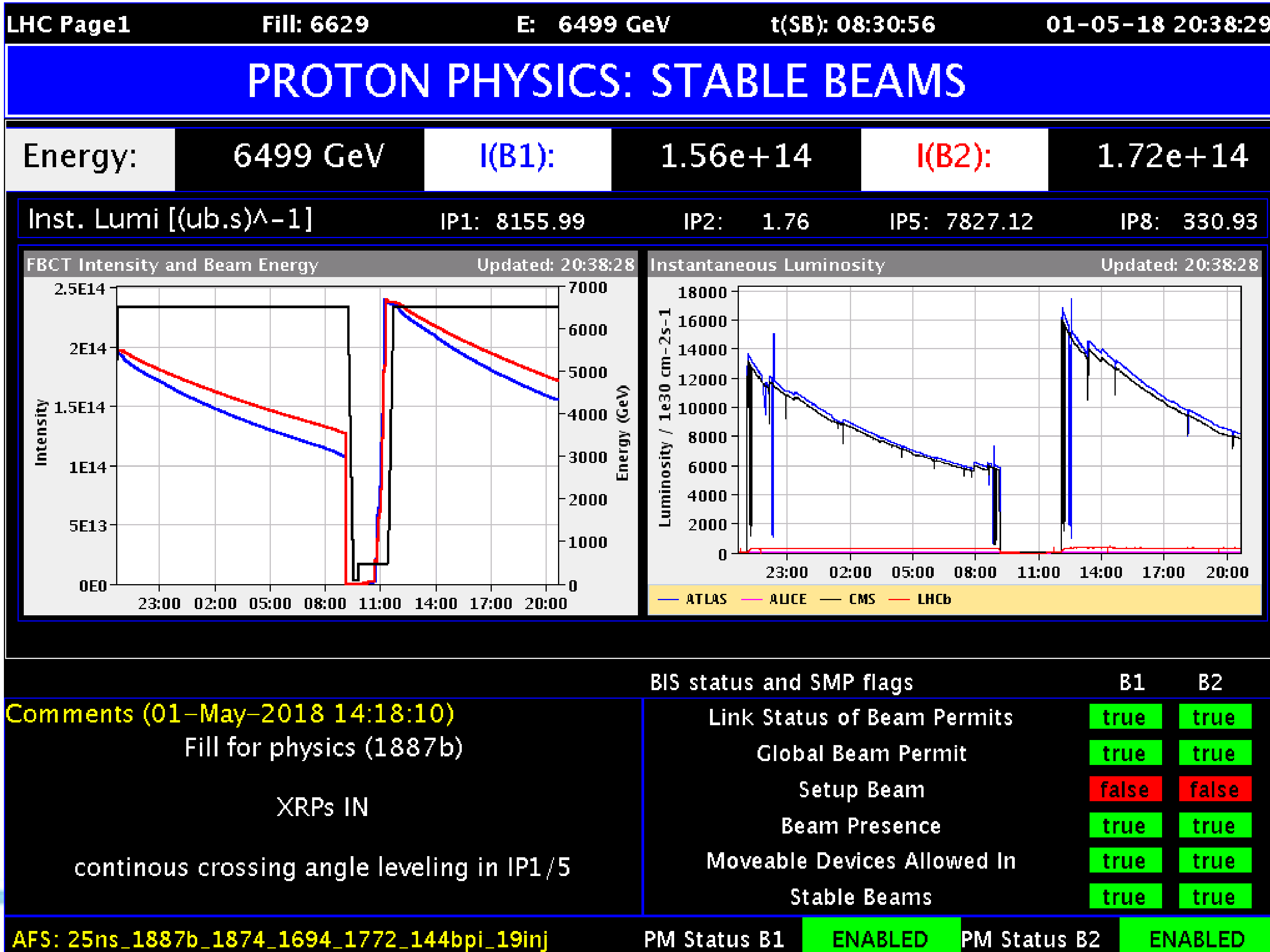

Colliders : Most Important Topics/Effects

- Engineering of magnets, RF, PSs, vacuum, sources, targets, diagnostics, collimators, etc
  - Exciting science: new acceleration techniques/plasma
- Beam physics
  - One particle: beam optics, long-term stability, resonances, losses, noises, diffusion/emittance growth, etc
  - One beam: instabilities, synchrotron radiation, beam-induced radiation deposition, intrabeam scattering, cooling, space-charge effects and compensation
  - Two-beams: beam-beam effects and compensation, beamstrahlung, machine-detector interface, etc
- Assuming particle physics interest → choice of accelerator scheme depends on
  - Readiness, cost and power consumption vs *E, L* reach

(Very) Brief History of Colliders

- Notable machines and most notable effects/discoveries/breakthroughs
- Note that we later will consider in detail:
  - LEP, KEK-B and Super-KEKB (lecture VS6)
  - Tevatron (lecture VS7)
  - LHC and HL-LHC (lecture VS8)
  - RHIC and EIC (lecture VS9)
  - SLC and linear colliders (lecture VS12)

Collider Patent R.Wideroe Sept. 8, 1943

Erteilt auf Grund des Ersten Überleitungsgesetzes vom 8. Juli 1949
(WiGBl. S. 175)

BUNDESREPUBLIK DEUTSCHLAND

AUSGEGEBEN AM
11. MAI 1953

DEUTSCHES PATENTAMT

PATENTSCHRIFT

№ 876 279

KLASSE 21g GRUPPE 36

W 687 VIIIc / 21g

Dr.-Ing. Rolf Wideröe, Oslo
ist als Erfinder genannt worden

Aktiengesellschaft Brown, Boveri & Cie, Baden (Schweiz)

Anordnung zur Herbeiführung von Kernreaktionen

Patentiert im Gebiet der Bundesrepublik Deutschland vom 8. September 1943 an
Patentanmeldung bekanntgemacht am 18. September 1952
Patenterteilung bekanntgemacht am 26. März 1953

Kernreaktionen können dadurch herbeigeführt werden, daß geladene Teilchen von hoher Geschwindigkeit und Energie, in Elektronenvolt gemessen, auf die zu untersuchenden Kerne geschossen werden. Wenn die geladenen Teilchen in einen gewissen Mindestabstand von den Kernen gelangen, werden die Kernreaktionen eingeleitet. Da aber neben den zu untersuchenden Kernen noch die gesamten Elektronen der Atomhülle vorhanden sind und auch der Wirkungsquerschnitt des Kernes sehr klein ist, wird der größte Teil der geladenen Teilchen von den Hüllenelektronen abgebremst, während nur ein sehr kleiner Teil die gewünschten Kernreaktionen herbeiführt.

Erfindungsgemäß wird der Wirkungsgrad der Kernreaktionen dadurch wesentlich erhöht, daß die Reaktion in einem Vakuumgefäß (Reaktionsröhre) durchgeführt wird, in welchem die geladenen Teilchen hoher Geschwindigkeit gegen einen Strahl von den zu untersuchenden und sich entgegengesetzt bewegenden Kernen auf einer sehr langen Strecke laufen müssen. Dies kann in der Weise durchgeführt werden, daß die geladenen Teilchen zum mehrmaligen Umlauf in einer Kreisröhre gezwungen werden, wobei die zu untersuchenden Kerne auf derselben Kreisbahn, aber in entgegengesetzter Richtung umlaufen. Da die geladenen Teilchen dabei nicht von bei der Reaktion unwirksamen Elektronen abgebremst werden und andererseits auf einer sehr langen Wegstrecke gegen die Kerne sich bewegen können, wird die Wahrscheinlichkeit für das Eintreten der Kernreaktionen wesentlich größer und der Wirkungsgrad der Reaktion sehr stark erhöht.

Um die bei der Kreisbewegung entstehenden Zentrifugalkräfte aufzuheben, müssen die umlaufenden Teilchen von nach innen gerichteten Ablenkkräften gesteuert werden, während eine Diffusion der Teile mittels stabilisierender, von allen Seiten auf den Bahnkreis gerichteter Kräfte verhindert wird. Falls die gegen-

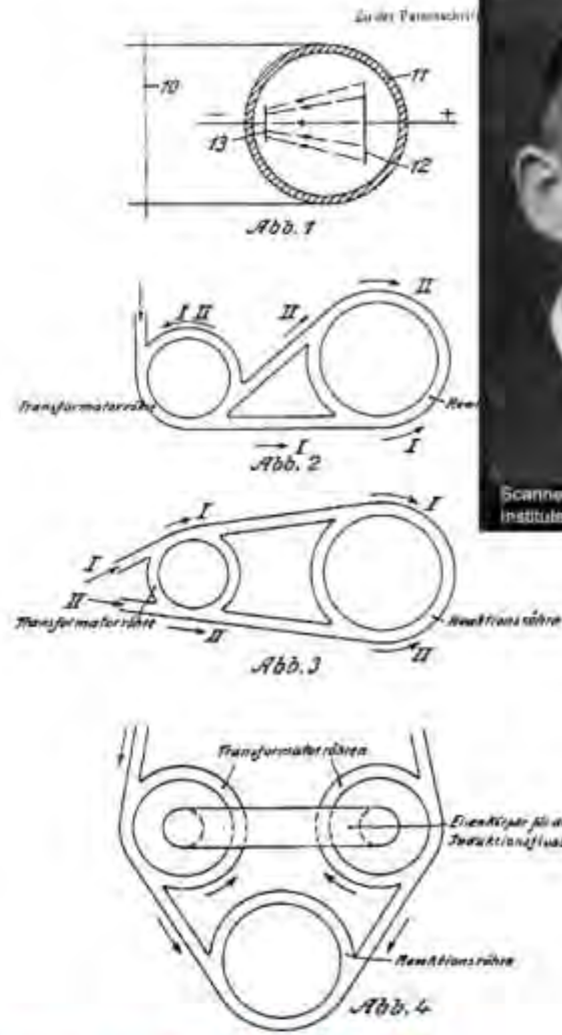

During rough war times, a patent was the only way to communicate the notion !

First Colliders

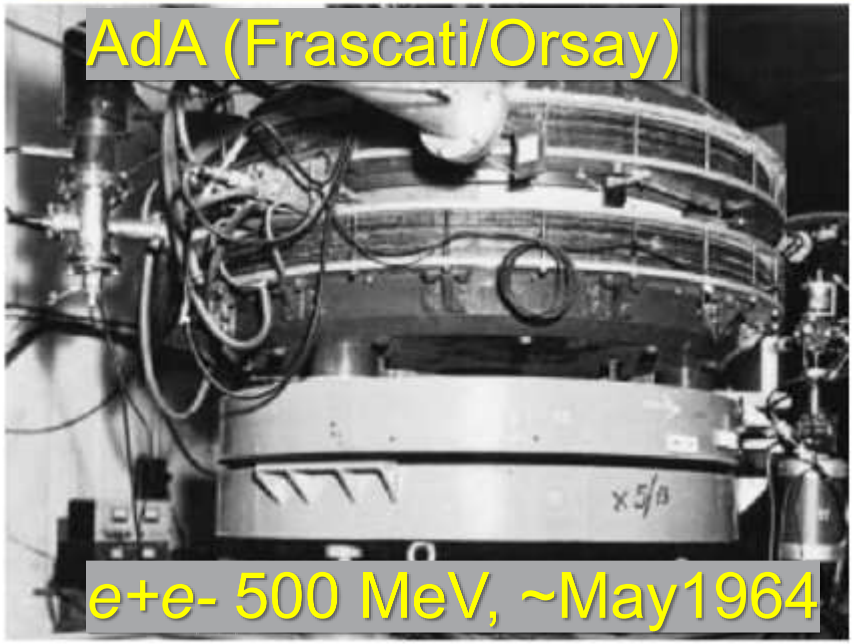

The First "Trio" of Colliders

- Technological challenges addressed:
  - development of nano-second-fast injector kickers
  - attainment of an ultrahigh vacuum of about a micropascal or better
  - reliable luminosity monitoring and other beam diagnostics
- Beam physics advances:
  - Touschek effect (low energy beam losses due to particle scattering inside beam leading to e+e- gettinbg out of RF buckets)
  - luminosity degradation due to beam-beam effects at $\xi_{x;y} \sim 0.02–0.04$
  - complex beam dynamics at non-linear high-order resonances
  - coherent instabilities due to resistive vacuum pipe walls

1970s-80s “small” e+e- (*C*=20…200 m)

ADONE (INFN, Frascati)

SPEAR (SLAC, Stanford)

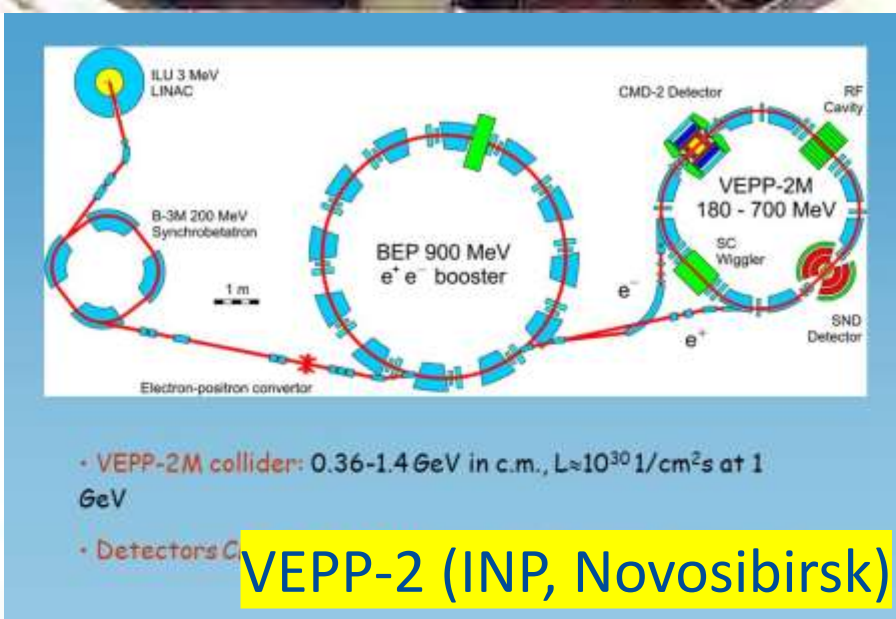

VEPP-2 (INP, Novosibirsk)

DORIS (DESY, Hamburg)

1970s-80s "small" e+e-

- Technological challenges addressed:
  - longitudinal phase feedback system developed and installed (ADONE)
  - 7.5 T SC wiggler to decrease the damping time (VEPP-2M)
- Beam physics advances:
  - Luminosity scaling in SR dominated beams $\mathcal{L} \propto \gamma^4$ (ADONE)
  - Sokolov-Ternov effect: the buildup of electron spin polarization through synchrotroton radiation (VEPP-2 and ACO)
  - CEA: first time a low-beta insertion optics with a small $\beta_y \approx 2.5$ cm
  - SPEAR: Transverse horizontal and vertical head-tail instabilities were observed and suppressed a positive chromaticity Q'>0
  - DCI: first four-beam compensation attempt (limited success)
  - dE/E~10^{-5} resolution via resonant depolarization method (VEPP-2M)
  - Multibunch, e.g. 480 bunches in each ring in DORIS

1980s-90s “large” e+e- (*C*=2…27 km)

1980s-90s "large" e+e-

- Technological challenges addressed:
  - SLC: first ever (and only) linear collider – many subsystems
  - pioneer SRF technology - TRISTAN: 508 MHz 0.4 GV/turn; LEP 352 MHz SC niobium-on-copper cavities, 3.5 GV/turn
  - High current positron sources, incl. 80% polarized e- (SLC)
- Beam physics advances:
  - LEP: losses via e+/e- scattering off thermal photons in RT beampipe
  - LEP single-bunch current limited by TMCI at injection energy
  - LEP: beam-beam record tune shift $4x\xi y=0.33$
  - SLC : BNS (Balakin-Novokhatsky-Smirnov) damping of BBI
  - SLC: ~x2 increase of luminosity due to disruption enhancement @IP

2000s-now "factories" e+e- (Φ-, Charm-, B-meson)

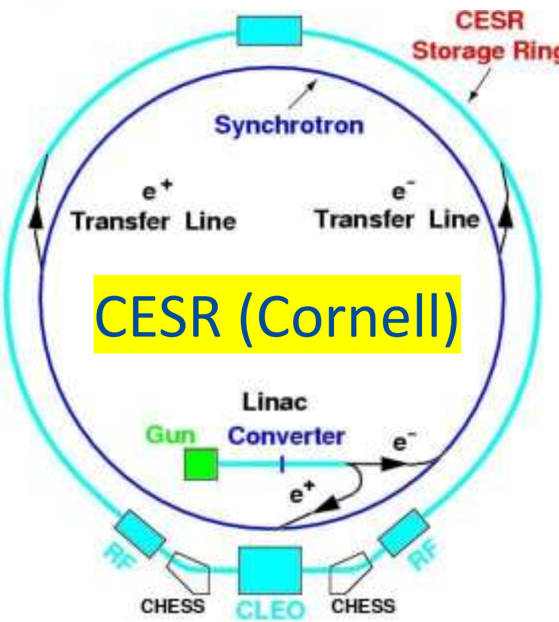

CESR (Cornell)

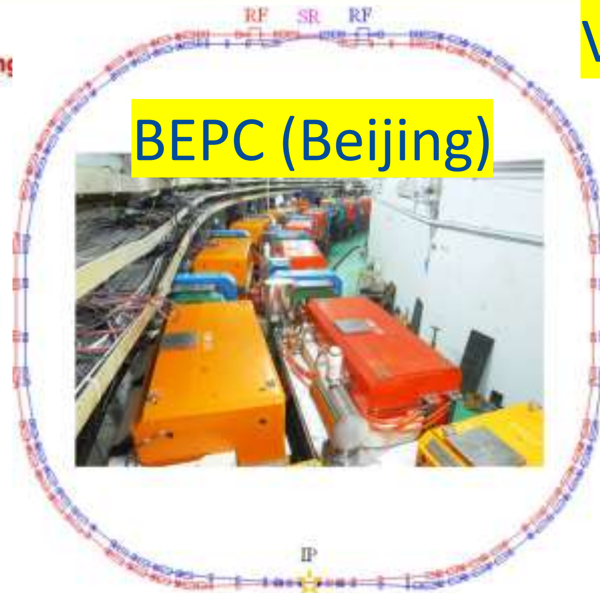

BEPC (Beijing)

VEPP-2000 (BINP, Novosibirsk)

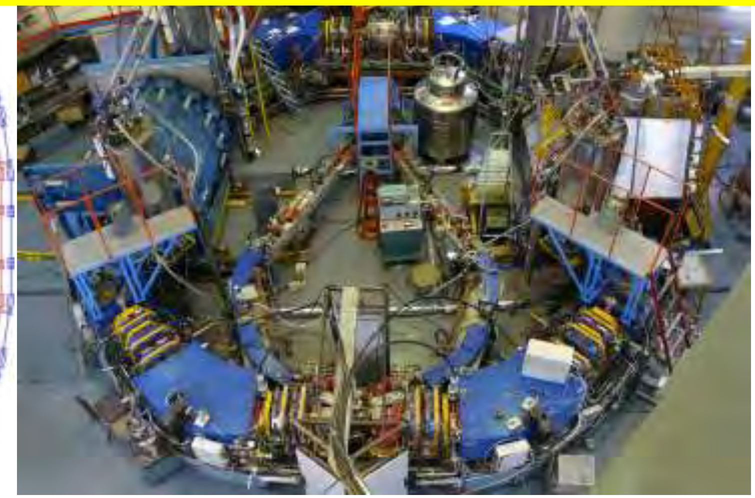

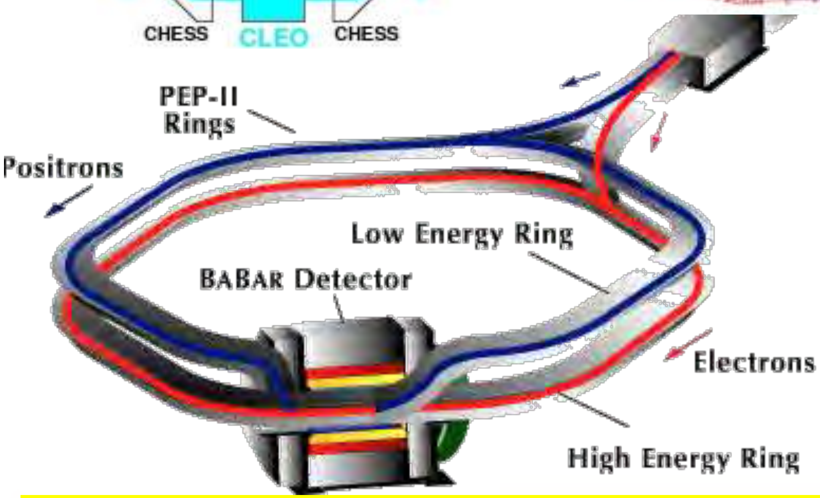

KEK-B → SuperKEKB (KEK, Japan)

PEP-II (SLAC, Stanford)

DAΦNE (INFN, Frascati)

2000s-now “factories” e+e-

- Technological challenges addressed:
  - HV electrostatic orbit separation for e+e- (CESR)
  - Efficient SRF for *Ampere*-class currents, HOM damping
  - Asymmetric rings – KEK-B, PEP-II, Super-KEKB
  - Tight detector background control - vacuum and collimation
  - Since PEP-II/KEKB: top-up injection mode of operation
- Beam physics advances:
  - Advanced optics for tight vertical focusing with β_y ~1cm – few mm
  - VEPP2000 : “round beams” concept $\xi \sim 0.25$
  - (less successful) CESR “Moebius ring” collider scheme (x-y flips)
  - DAΦNE : “crab waist” focusing optics, demo “wire b-b compensation”
  - KEK-B: crab crossing (limited success) → nonobeams (Super-KEKB)

1970s-2010s Hadron Colliders (*C*=1…7 km)

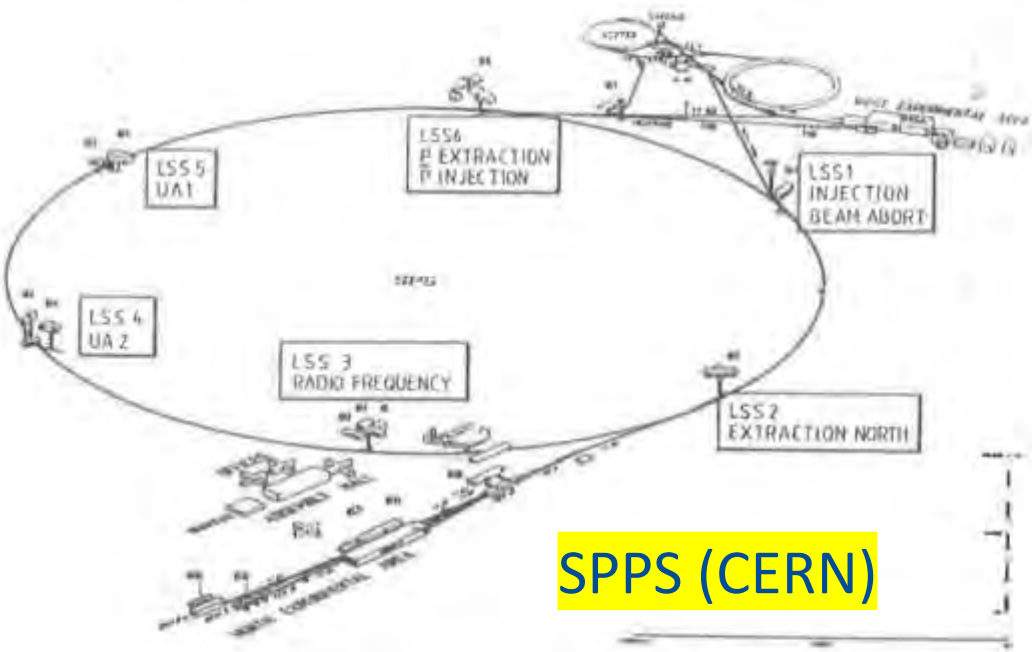

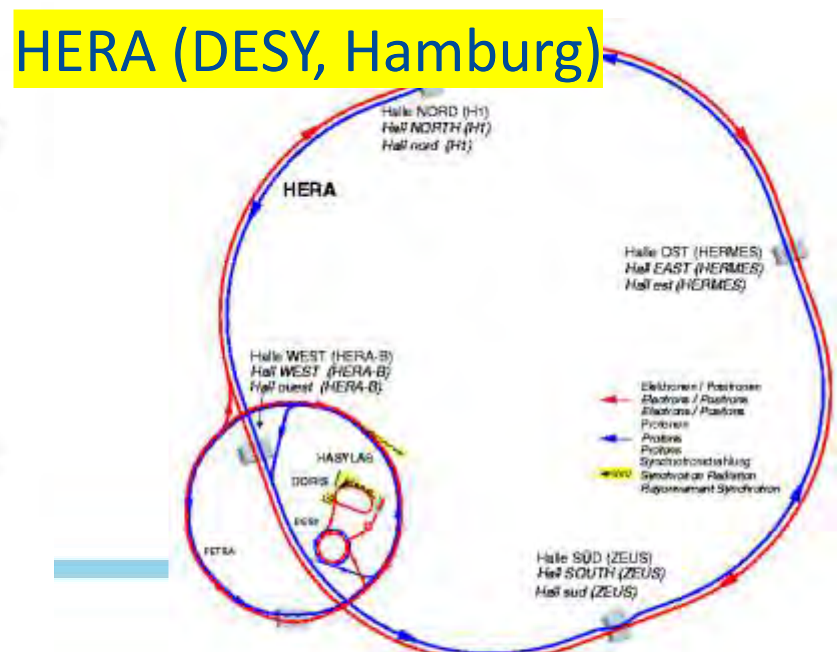

1970s-2000's Hadron Colliders (1)

- Technological challenges addressed:
  - ISR: world's first pp collider (and pp Lumi record holder for >20 yrs)
  - SC NbTi magnets 4-8 T (Tevatron → HERA→ RHIC → LHC)
  - SPPS, &Tevatron: technology of antiproton production & scienc of stochastic (Nobel prize) and electron cooling (up to 4 MeV e-)
  - Tevatron: permanent magnets (3.3 km 8 GeV Recycler)
  - Two-stage collimation systems (HERA, Tevatron)
- Beam physics advances:
  - Longitudinal manipulations : momentum stacking (ISR), slip-stacking and momentum mining (Tevatron)
  - Tevatron: beam-beam record at $\xi_{x;y} \sim 0.025$, first successful demo b-b compensation by electron lenses, hollow e-lens collimation
  - HERA: first e-p collider, transversely polarized e- & spin rotators to 1

2000s-now Hadron Colliders (C=4…27 km)

RHIC (BNL, Brookhaven)

LHC (CERN)

2000s-now Hadron Colliders (2)

- Technological challenges addressed:
  - First use of Nb3Sn SC magnets (HL-LHC)
  - Three (4) stage 99.99% efficient collimation system (LHC)
  - Ions sources and ion-ion, ion-p collisions (RHIC, LHC)
  - Sophisticated polarization control along the chain (55% in RHIC)
- Beam physics advances:
  - RHIC: bunched beam stochastic cooling, bunched beam electron cooling
  - RHIC: head-on beam-beam compensation with electron lenses
  - LHC: sophisticated control of electron-cloud and other instabilities
  - LHC: novel achromatic telescopic squeeze optics to lower beta*
  - LHC: demo wire compensation of long-range beam-beam effects

Super-Colliders That Were Not (1990's)

SSC (Waxahachie, TX)

UNK (IHEP, Protvino)

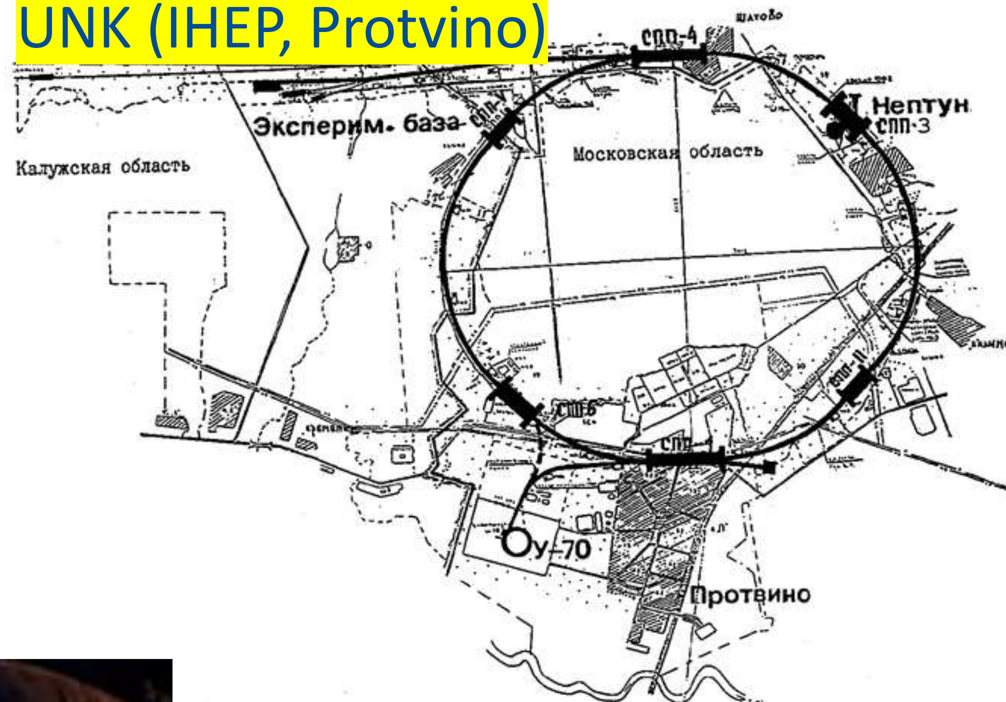

Colliders That Will Be

NICA (JINR, Dubna)

Circumference, m	503,04		
Bunch number per ring	22		
Mean-square bunch size, m	0.6		
Min. beta-function (β*), m	0.6		
Ion energy, GeV/u	1.0	3.0	4.5
Ion number per bunch, 1e9	0.275	2.4	2.2
Peak luminosity, cm^{-2}·s^{-1}	0.9e25	0.9e27	6.3e27

EIC (BNL, Brookhaven)

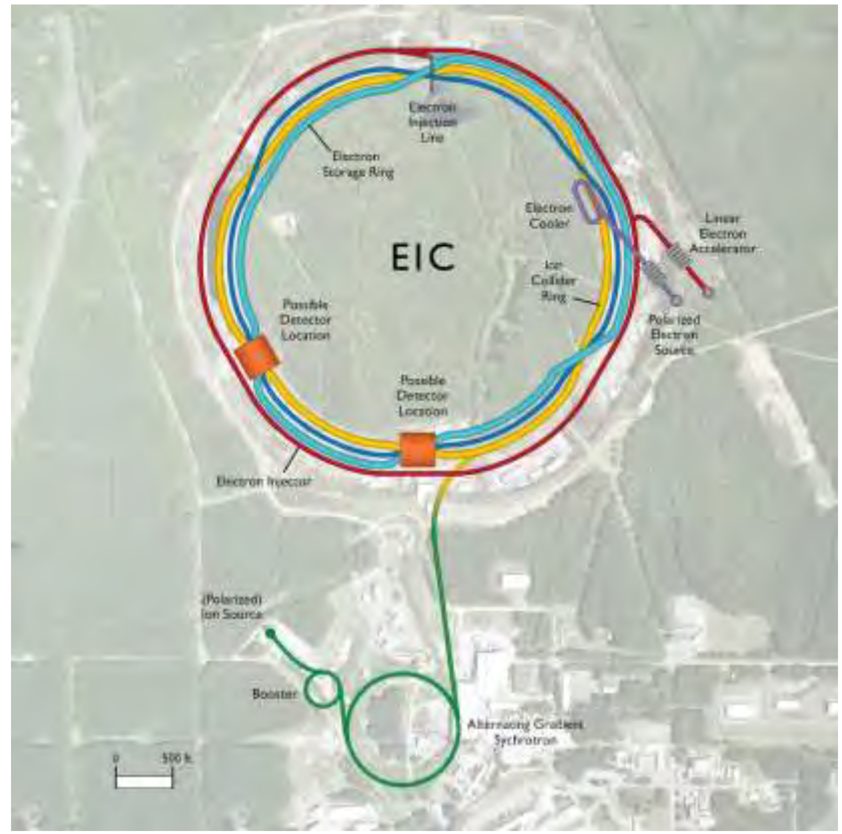

BINP C/Tau-Factory (Novosibirsk)

Fermilab

Colliders That Might Be :

Higgs factories proposals

Name	Details
CepC	e+e-, $\sqrt{s} = 0.24$ TeV, L= 3.0 $\times 10^{34}$
CLIC (Higgs factory)	e+e-, $\sqrt{s} = 0.38$ TeV, L= 1.5 $\times 10^{34}$
ERL ee collider	e+e-, $\sqrt{s} = 0.24$ TeV, L= 73 $\times 10^{34}$
FCC-ee	e+e-, $\sqrt{s} = 0.24$ TeV, L= 17 $\times 10^{34}$
gamma gamma	X-ray FEL-based $\gamma\gamma$ collider
ILC (Higgs factory)	e+e-, $\sqrt{s} = 0.25$ TeV, L= 1.4 $\times 10^{34}$
LHeC	ep, $\sqrt{s} = 1.3$ TeV, L= 0.1 $\times 10^{34}$
MC (Higgs factory)	$\mu\mu$, $\sqrt{s} = 0.13$ TeV, L= 0.01 $\times 10^{34}$

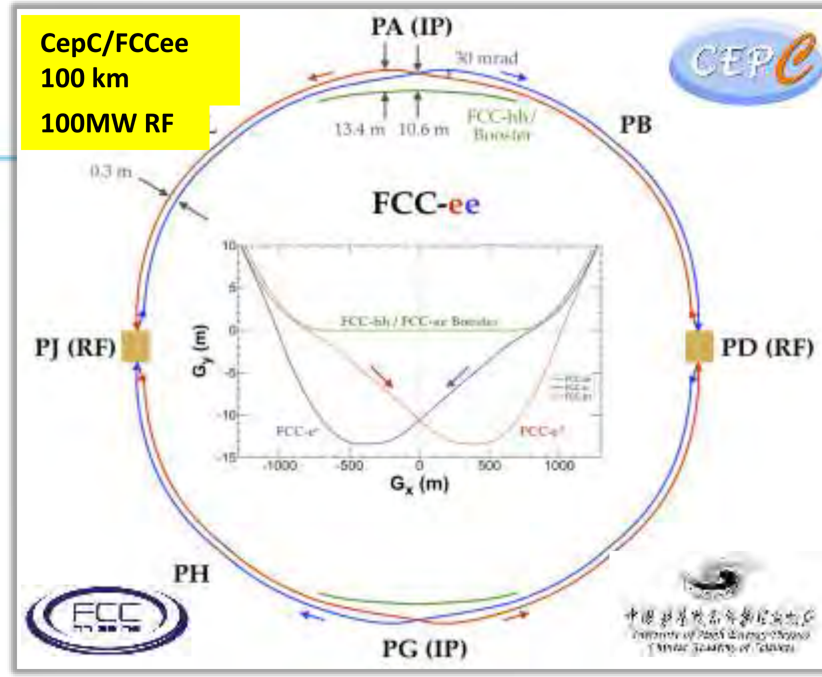

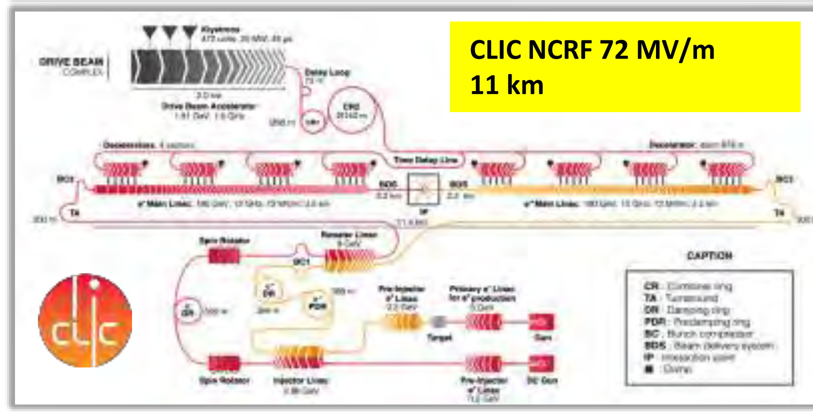

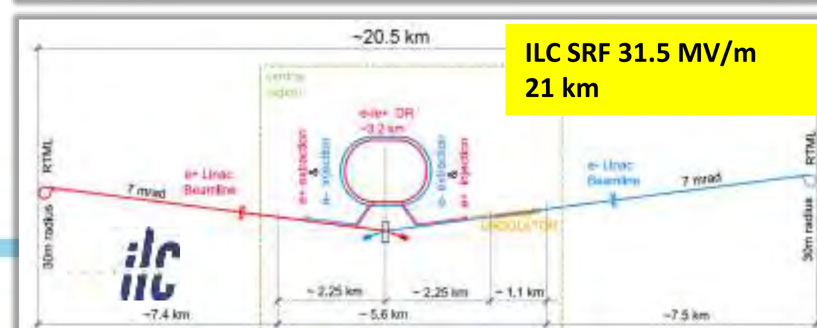

Far-Future High Energy Collider Concepts/Proposals

Name	Details
Cryo-Cooled Copper linac	e+e-, $\sqrt{s} = 2$ TeV, L= 4.5 $\times 10^{34}$
High Energy CLIC	e+e-, $\sqrt{s} = 1.5 - 3$ TeV, L= 5.9 $\times 10^{34}$
High Energy ILC	e+e-, $\sqrt{s} = 1 - 3$ TeV
FCC-hh	pp, $\sqrt{s} = 100$ TeV, L= 30 $\times 10^{34}$
SPPC	pp, $\sqrt{s} = 75/150$ TeV, L= 10 $\times 10^{34}$
Collider-in-Sea	pp, $\sqrt{s} = 500$ TeV, L= 50 $\times 10^{34}$
LHeC	ep, $\sqrt{s} = 1.3$ TeV, L= 1 $\times 10^{34}$
FCC-eh	ep, $\sqrt{s} = 3.5$ TeV, L= 1 $\times 10^{34}$
CEPC-SPPpC-eh	ep, $\sqrt{s} = 6$ TeV, L= 4.5 $\times 10^{33}$
VHE-ep	ep, $\sqrt{s} = 9$ TeV
MC – Proton Driver 1	$\mu\mu$, $\sqrt{s} = 1.5$ TeV, L= 1 $\times 10^{34}$
MC – Proton Driver 2	$\mu\mu$, $\sqrt{s} = 3$ TeV, L= 2 $\times 10^{34}$
MC – Proton Driver 3	$\mu\mu$, $\sqrt{s} = 10 - 14$ TeV, L= 20 $\times 10^{34}$
MC – Positron Driver	$\mu\mu$, $\sqrt{s} = 10 - 14$ TeV, L= 20 $\times 10^{34}$
LWFA-LC (e+e- and $\gamma\gamma$)	Laser driven; e+e-, $\sqrt{s} = 1 - 30$ TeV
PWFA-LC (e+e- and $\gamma\gamma$)	Beam driven; e+e-, $\sqrt{s} = 1 - 30$ TeV
SWFA-LC	Structure wakefields; e+e-, $\sqrt{s} = 1 - 30$ TeV

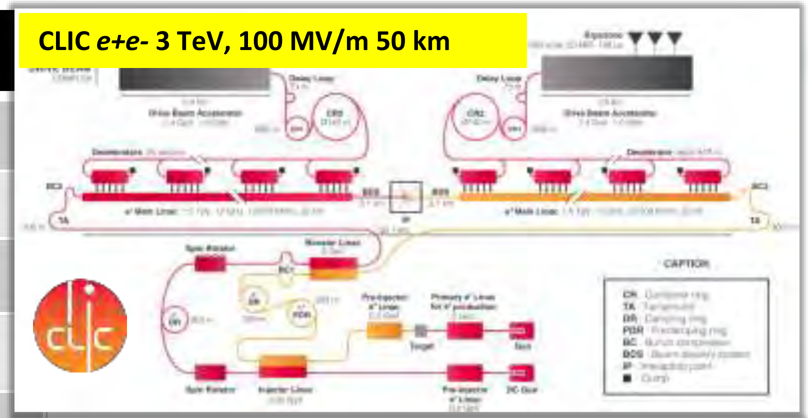

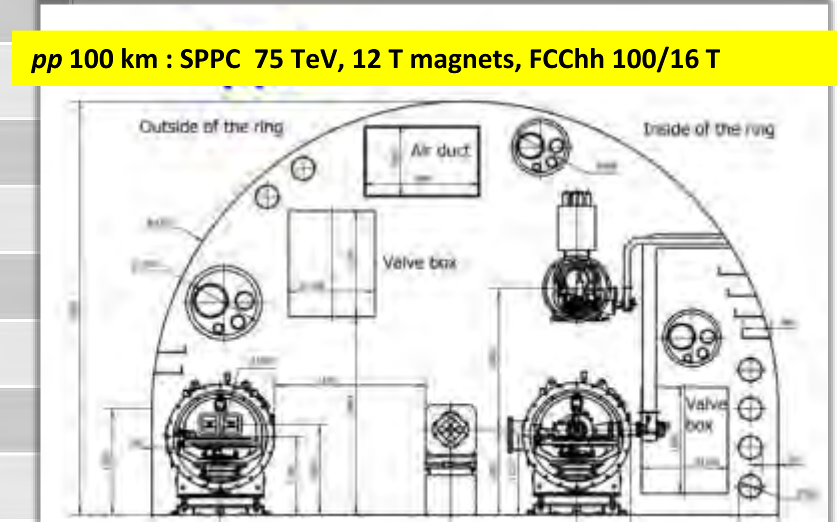

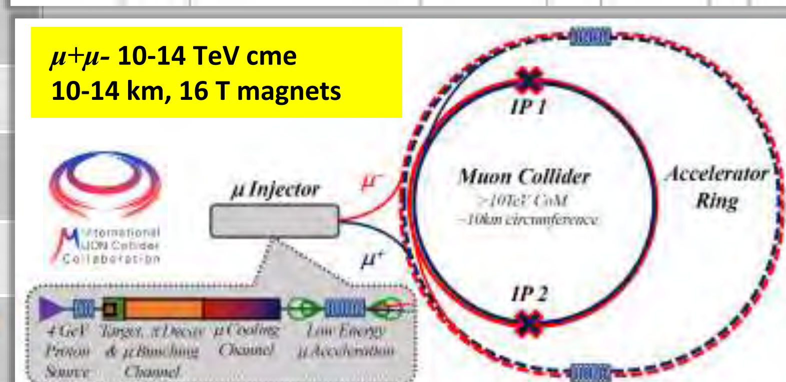

Thanks for Your Attention !

Questions !?

Literature

- V.Shiltsev, F.Zimmermann, Modern and Future Colliders (Rev.Mod.Phys., 2021)

https://journals.aps.org/rmp/abstract/10.1103/RevModPhys.93.015006

- V.Lebedev, V.Shiltsev, Tevatron Book

https://indico.cern.ch/event/774280/attachments/1758668/2915590/2014_Book_AcceleratorPhysicsAtTheTevatro.pdf

U.S. Particle Accelerator School
Education in Beam Physics and Accelerator Technology

Fermilab

Colliders: Beam-Beam Effects

Vladimir Shiltsev, Fermilab

part of the "Colliders" class by V.Lebedev, N.Mokhov and V.Shiltsev

US Particle Accelerator School, Jan 24 – Feb 4, 2022

Beams as moving charges

- Beam is a collection of charges
- Represent electromagnetic potential for other
- charges
- Forces on itself (space-charge) and opposing
- beam (beam-beam effects)
  - Main limit for present and future colliders
  - Important for high density beams, i.e. high intensity and/or small beams = for high luminosity !

Beam-Beam Effects

- Remember:

$$\Longrightarrow \quad \mathcal{L} = \frac{N_1 N_2 f B}{4\pi\sigma_x\sigma_y} \quad = \quad \frac{N_1 N_2 f B}{4\pi \cdot \ \sigma_x\sigma_y}$$

- Overview: which effects are important for
- present and future machines (LEP, PEP,
- Tevatron, RHIC, LHC, ...)
- Qualitative and physical picture of the eects
- Mathematical derivations in:
- Proceedings, Zeuthen 2003

Beam-Beam Effects

- A beam acts on particles like an electromagnetic lens, but:
  - Does not represent simple form, i.e. well-defined multipoles
  - Very non-linear form of the forces, depending on distribution
  - Can change distribution as result of interaction (time dependent forces ..)
- Results in many different effects and problems

Fields and Forces (1)

- Start with a point charge q and integrate over the particle distribution.
- In rest frame only electrostatic field: $E \neq 0$ while B=0
- Transform into moving frame and calculate
- Lorentz force

$$E_{||} = E'_{||}, \qquad E_{\perp} = \gamma \cdot E'_{\perp} \quad \text{with :} \quad \vec{B} \;=\; \vec{\beta} \times \vec{E}/c$$

$$\vec{F} = q(\vec{E} + \vec{\beta} \times \vec{B})$$

- Note that *F≈0* if velocities are collinear

Fields and Forces (2)

- Derive potential *U(x, y, z)* from Poisson equation:

$$\Delta U(x,y,z) = -\frac{1}{\epsilon_0}\rho(x,y,z)$$

- The fields become:

$$\vec{E} \;=\; -\nabla U(x,y,z)$$

- Example Gaussian distribution:

$$\rho(x,y,z) = \frac{Ne}{\sigma_x\sigma_y\sigma_z\sqrt{2\pi}^3}\exp\left(-\frac{x^2}{2\sigma_x^2}-\frac{y^2}{2\sigma_y^2}-\frac{z^2}{2\sigma_z^2}\right)$$

A Common Example: Gaussian

- For 2D case the potential becomes:

$$U(x,y,\sigma_x,\sigma_y) = \frac{ne}{4\pi\epsilon_0}\int_0^\infty \frac{\exp(-\frac{x^2}{2\sigma_x^2+q} - \frac{y^2}{2\sigma_y^2+q})}{\sqrt{(2\sigma_x^2+q)(2\sigma_y^2+q)}}dq$$

- Can derive *E* and *B* fields and therefore forces
- Also easy for uniform distribution: *E* and *B* scale linear with *r* for *r<a*, and *1/r* for *r>a…* easy for simple easily integrable axisymmetric distributions
- For arbitrary distribution (non-Gaussian):
  – difficult (or impossible, numerical solution required)

Further Simplification: Round Gaussian

- Round beams: $\sigma_x = \sigma_y = \sigma$

- Only components Er and B are non-zero

- Force has only radial component, i.e. depends only on distance r from bunch center, i.e. $r^2 = x^2 + y^2$

$$F_r(r) = -\frac{ne^2(1+\beta^2)}{2\pi\epsilon_0 \cdot r}\left[1 - \exp(-\frac{r^2}{2\sigma^2})\right]$$

Bean-Beam Kick

- Kick $\Delta r'$ - angle by which the particle is deflected during the passage
- Derived from force by integration over the collision assume: $\mathbf{m_1 = m_2}$ **and** $\beta_1 = \beta_2$

$$\Delta r'$$

$$F_r(r, s, t) = -\frac{Ne^2(1+\beta^2)}{\sqrt{(2\pi)^3}\epsilon_0 r \sigma_s}\left[1 - \exp(-\frac{r^2}{2\sigma^2})\right] \cdot \left[\exp(-\frac{(s+vt)^2}{2\sigma_s^2})\right]$$

→ Newton's law

$$\Delta r' = \frac{1}{mc\beta\gamma}\int_{\infty}^{\infty} F_r(r, s, t)dt$$

Beam-Beam Kick

- Using the classical particle radius: $r_0 = e^2/4\pi\epsilon_0 mc^2$

- we get radial kick and in Cartesian coordinates:

$$\Delta r' = -\frac{2Nr_0}{\gamma} \cdot \frac{r}{r^2} \cdot \left[1 - \exp(-\frac{r^2}{2\sigma^2})\right]$$

$$\Delta x' = -\frac{2Nr_0}{\gamma} \cdot \frac{x}{r^2} \cdot \left[1 - \exp(-\frac{r^2}{2\sigma^2})\right]$$

$$\Delta y' = -\frac{2Nr_0}{\gamma} \cdot \frac{y}{r^2} \cdot \left[1 - \exp(-\frac{r^2}{2\sigma^2})\right]$$

Beam-Beam Kick

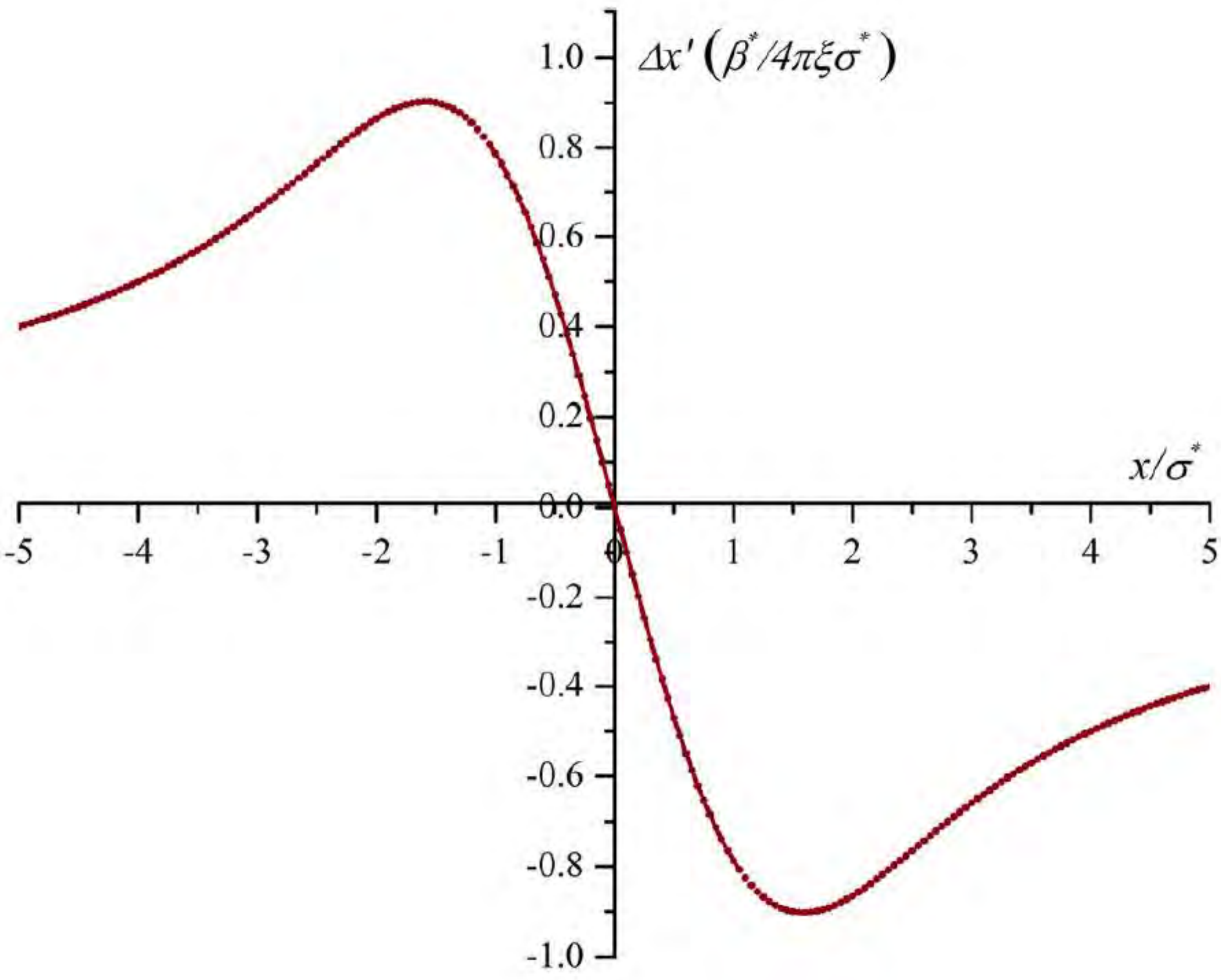

Kick(force) varies strongly with amplitude:

- linear inside → like quadrupole → tune shift amplitude independent at << sigma
- 1/r outside the beam core → amplitude dependent tune shift

Highly nonlinear btw 1 and 3 sigma:

- contains many high order multipoles

What if the beams are not round?

Deflection scan (LEP measurement)

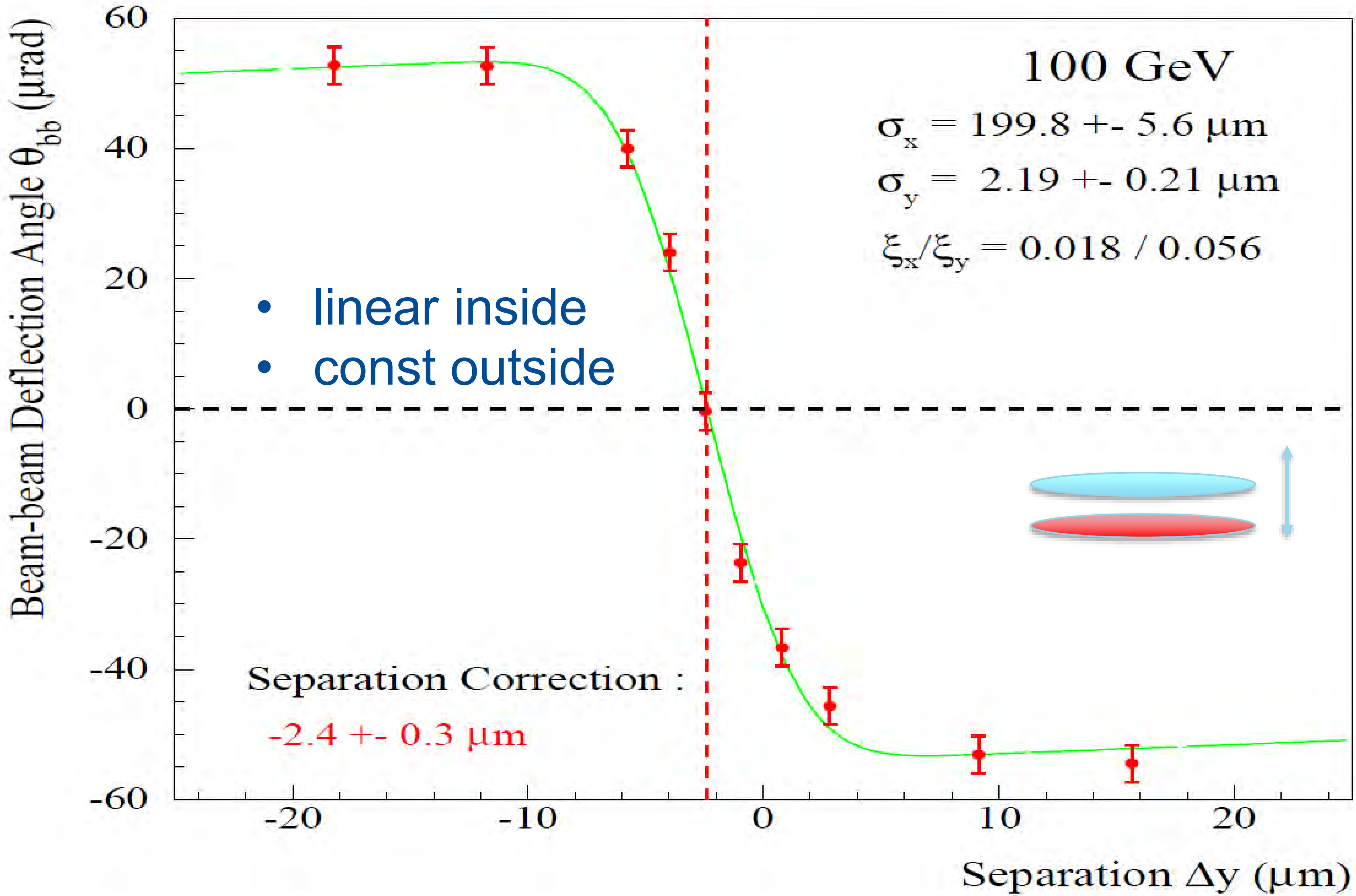

Beam-beam strength parameter → tuneshift

- Slope of force at zero amplitude → proportional to (linear) tune shift $\Delta\ \mathbf{Q}_{bb}$ from beam-beam interaction
- This defines: *beam-beam parameter* ξ
- For head-on interactions we get:

$$\boxed{\xi_{x,y} = \frac{N \cdot r_0 \cdot \beta_{x,y}}{2\pi\gamma\sigma_{x,y}(\sigma_x + \sigma_y)}}$$

- so far: only an additional "quasi-quadrupole" BUT non-linear part of beam-beam force scales with ξ

Note that for flat beams $\sigma_x >> \sigma_y$ $\xi_y >> \xi_x$

Tune Spectra: with/w.o. Beam-Beam

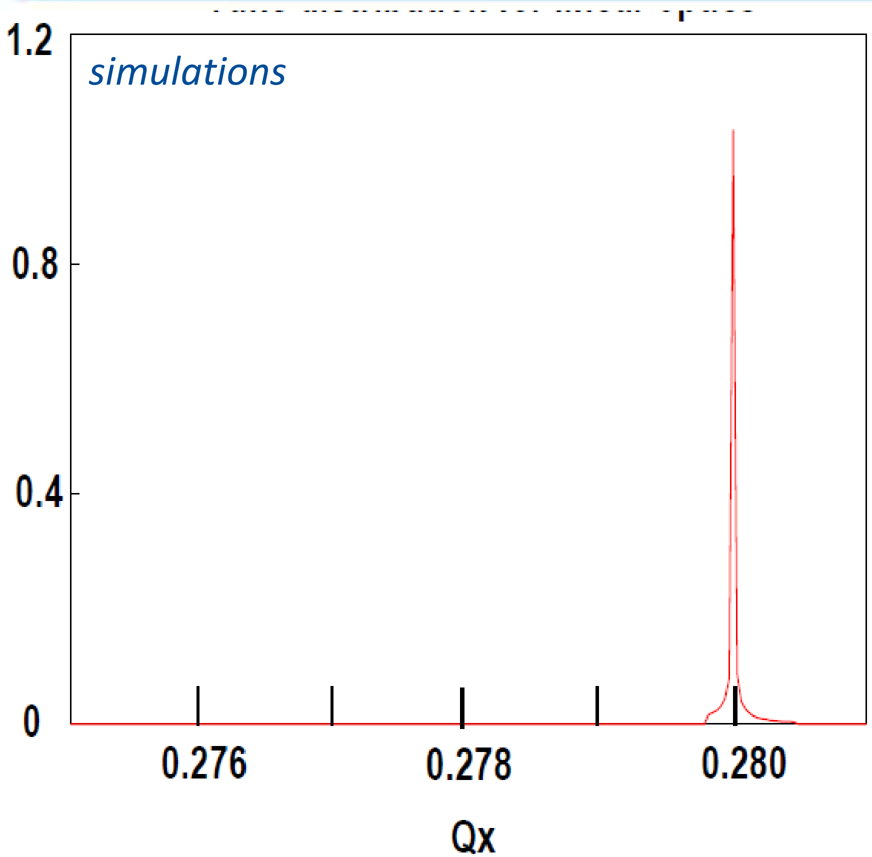

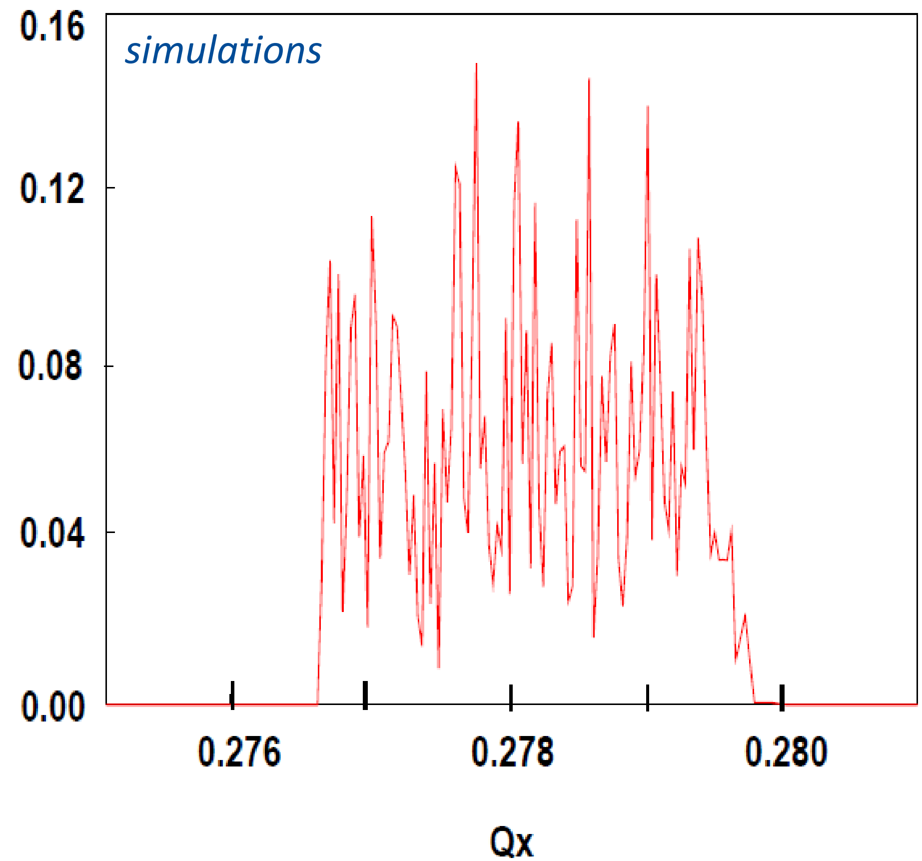

Linear force →
all particles have same tune
→ one line in the spectrum of transverse oscillations

Non−linear force →
particles with different amplitudes have different frequencies (tunes)
We get frequency (tune) spectra
Width of the spectra: ~ξ

Fermilab

In Reality – Even More Complex

Tevatron 980 GeV p and

980 GeV antiprotons (pbars)

Colliding with ***ξ~0.028***

Force is focusing → tuneshift is positive

Measured with 21MHz Schottky monitors

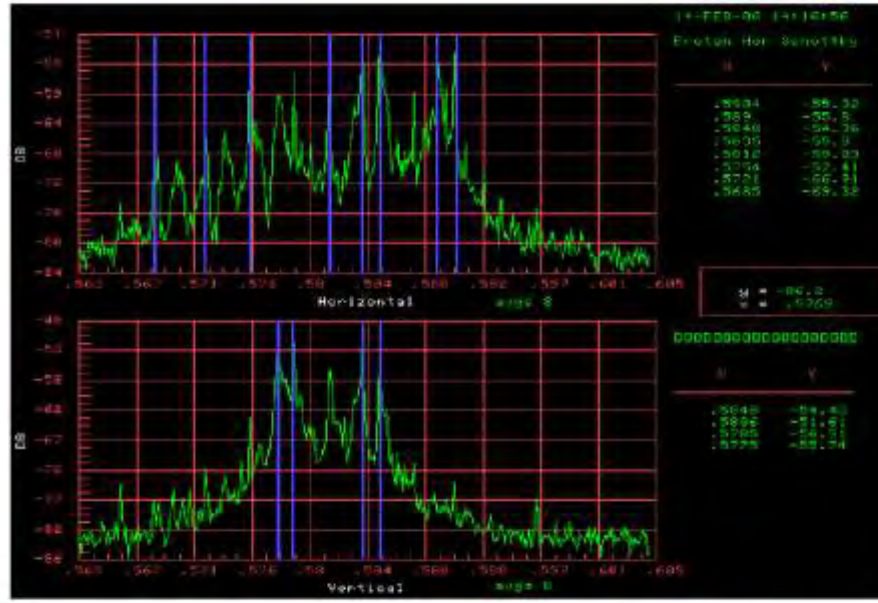

RHIC 100 GeV p + 100 GeV p

Colliding with ***ξ~0.020***

Force is de-focusing → tuneshift is negative

Measured with BTF (beam transfer function) monitor

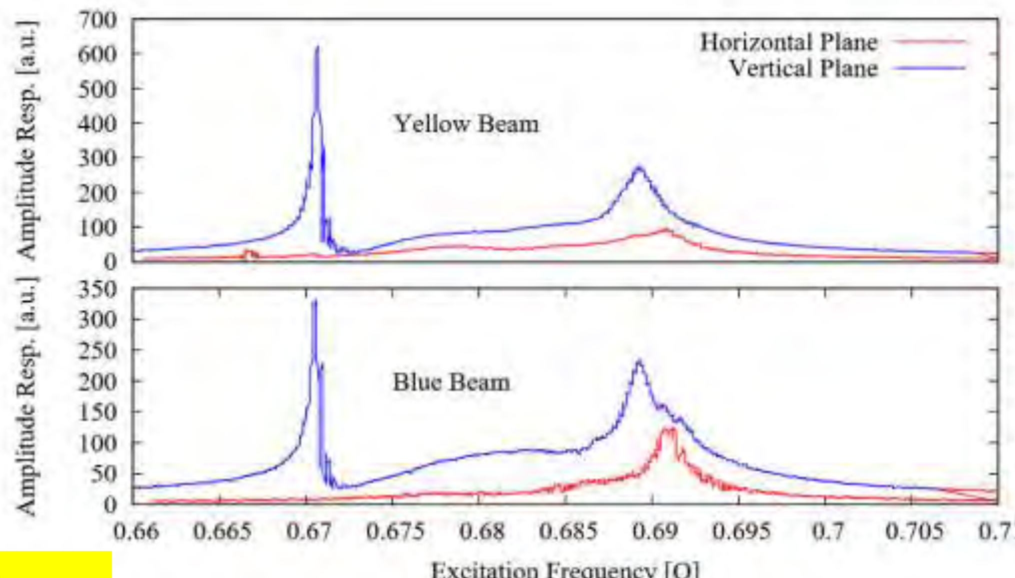

…more on that later

Beam-beam Detuning with Amplitude

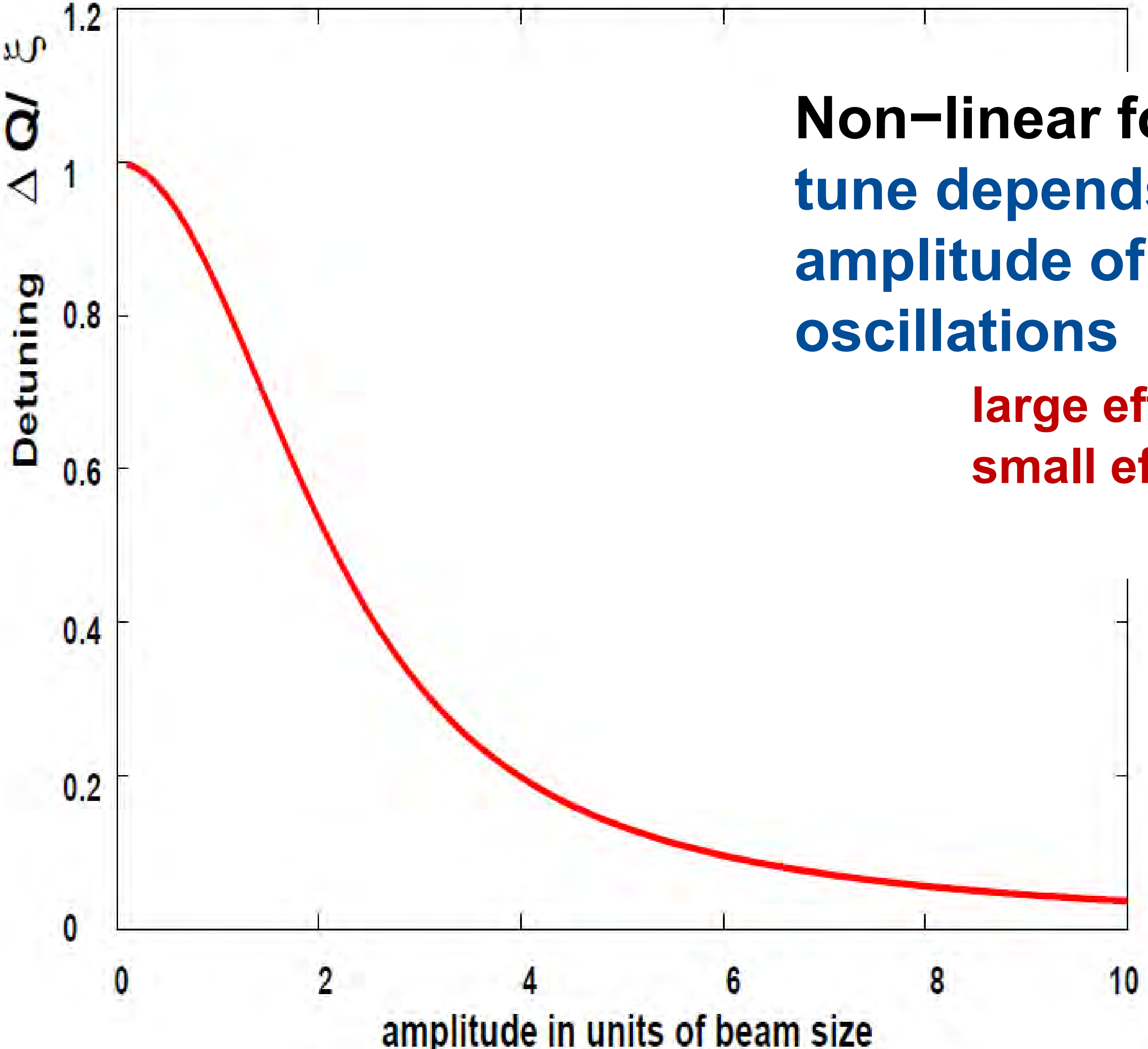

Non−linear force →
tune depends on the amplitude of betatron oscillations

large effect for A<sigma
small effect for A>>sigma

Fermilab

Linear tune shift - two dimensions

"bare lattice" tune

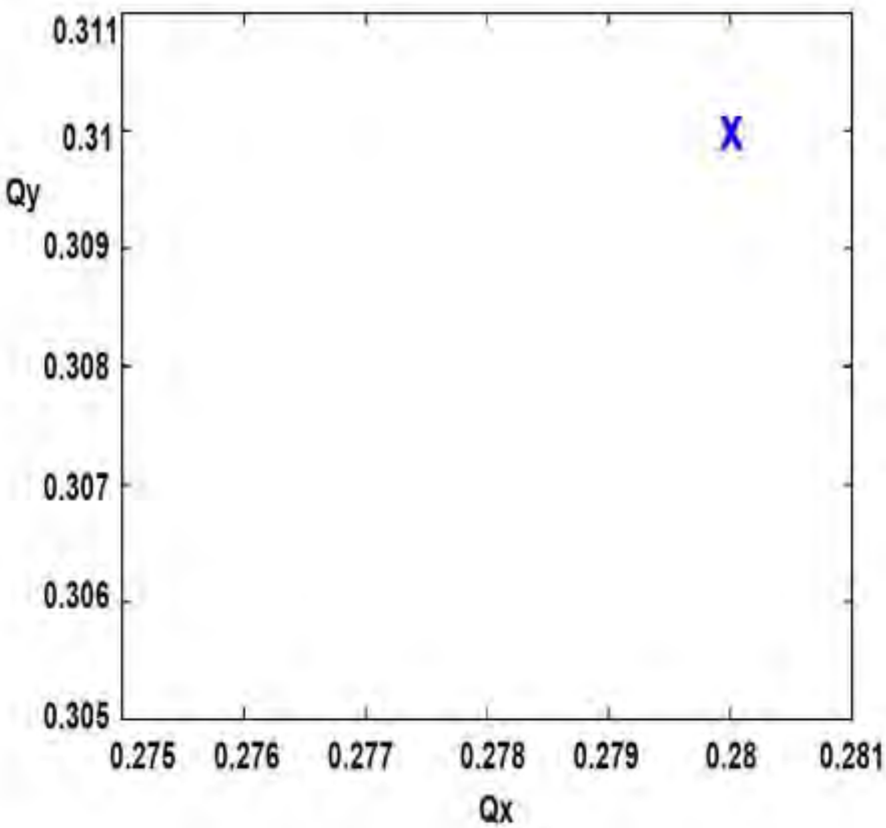

"bare lattice" tune + linear shift due to beam-beam (=core particles)

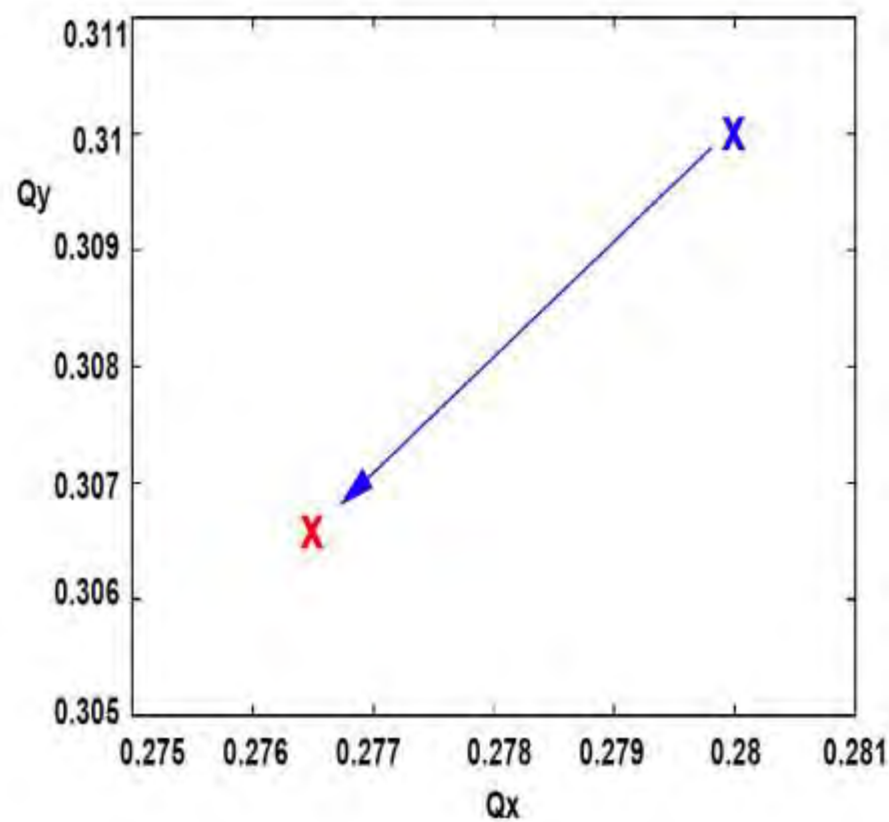

Non-linear tune shift in two dimensions

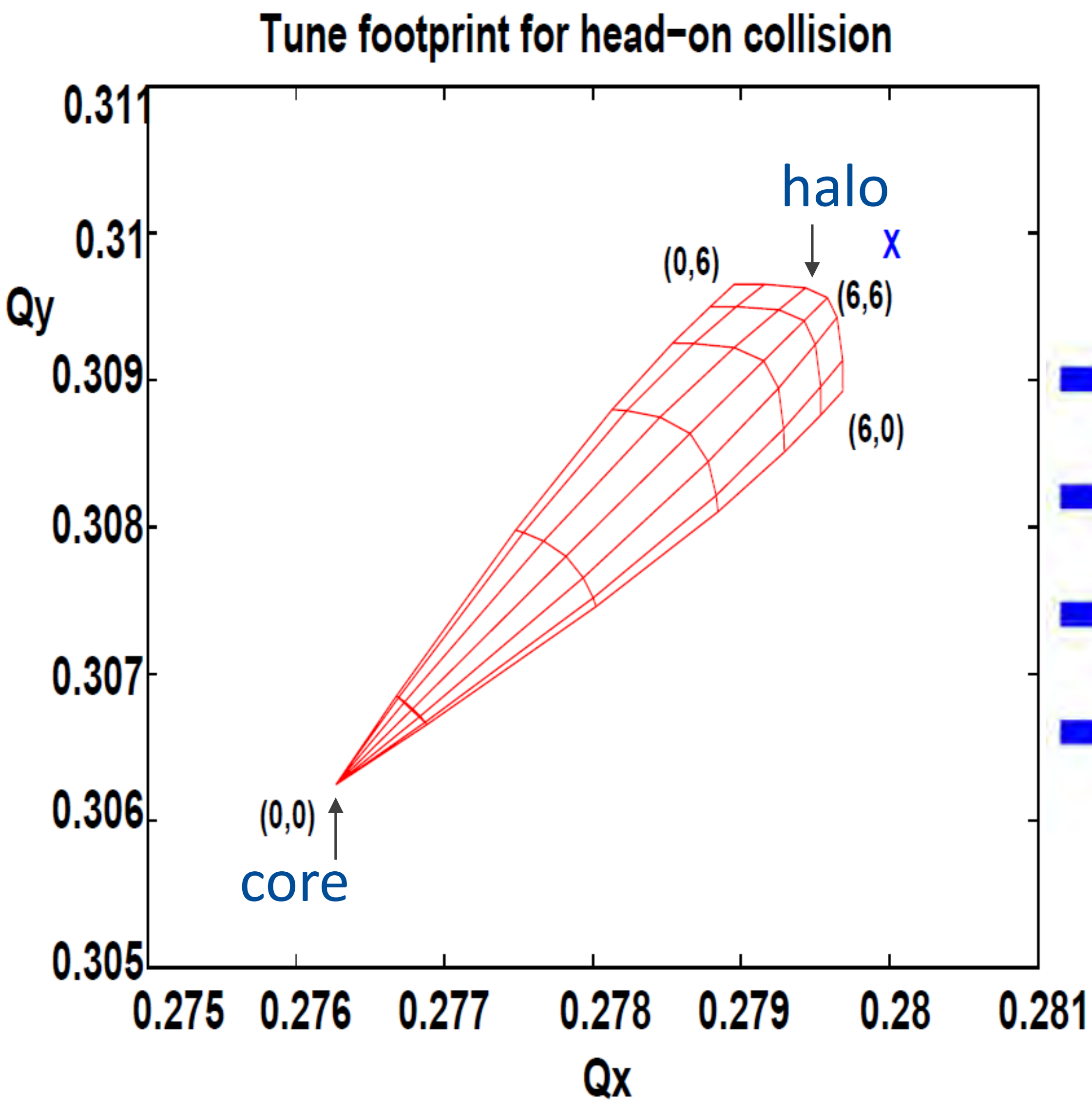

- Tunes depend on x **and** y amplitudes
- No single tune in the beam
- Compute and plot for every amplitude (pair) the tunes in both planes
- In 2 dimensions: plotted as **footprint**

e+e- LEP vs p-pbar collider Tevatron

	LEP	Tevatron
Beam sizes	160 - 200 μm · 2 - 4 μm	30 μm · 30 μm
Intensity N	4.0 · 10^{11}/bunch	3 · 10^{11}/bunch
Energy	100 GeV	980 GeV
$\beta_x^* \cdot \beta_y^*$	1.25 m · 0.05 m	0.28 · 0.28 m
Beam-beam parameter(ξ)	0.0700	0.012 x2 IPs

Observations (Reality of Beam-Beam)

- Remember:

$$\mathcal{L} = \frac{N_1 N_2 f B}{4\pi\sigma_x\sigma_y}$$

- Luminosity should increase $\propto \quad N_1 N_2$

  for:

$$N_1 = N_2 = N \quad \rightarrow \quad \propto \quad N^2$$

- Beam-beam parameter should increase $\propto \quad N$
- But:

Beam-Beam Limits : e+e- Colliders

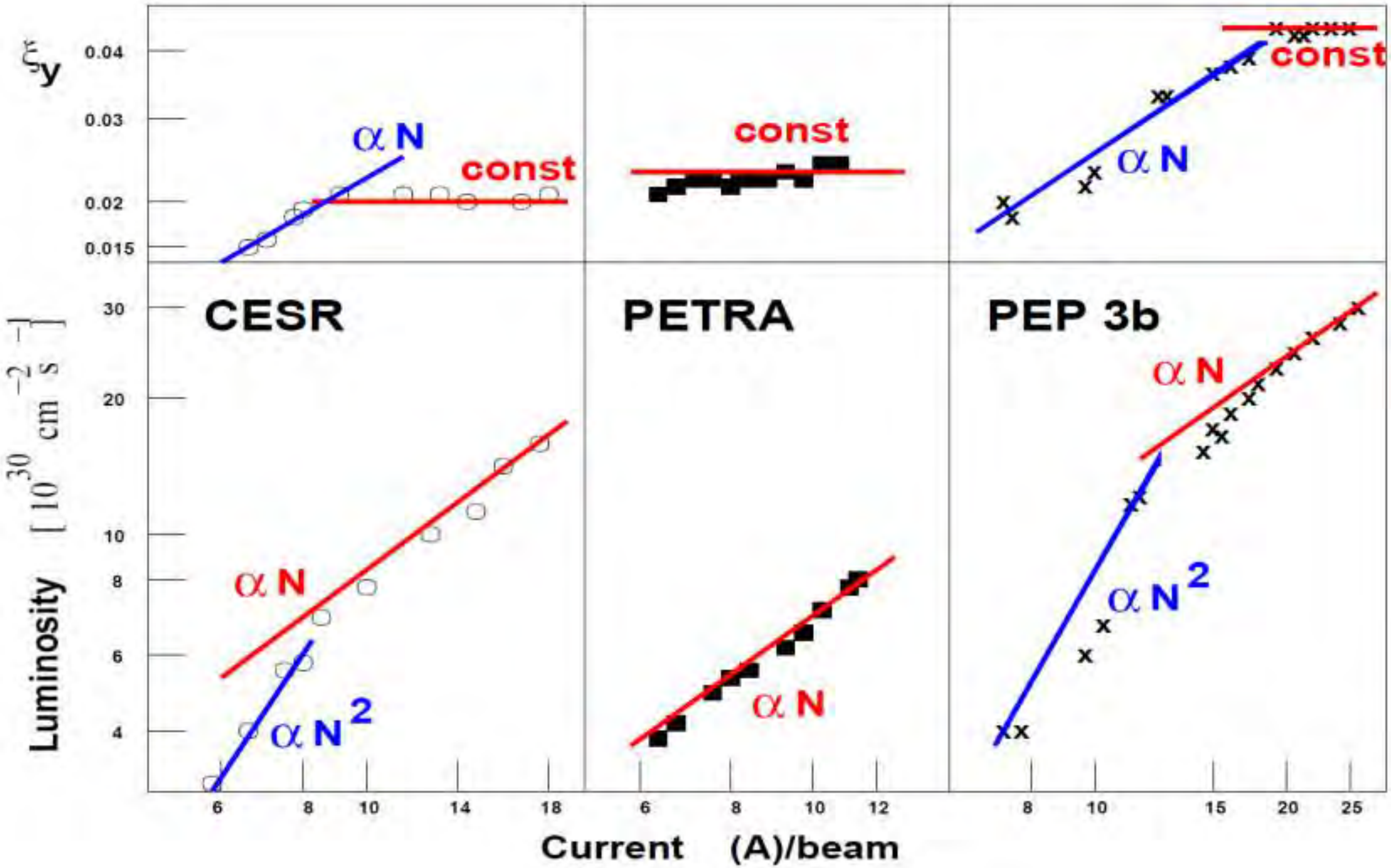

Beam-beam Limit on Luminosity

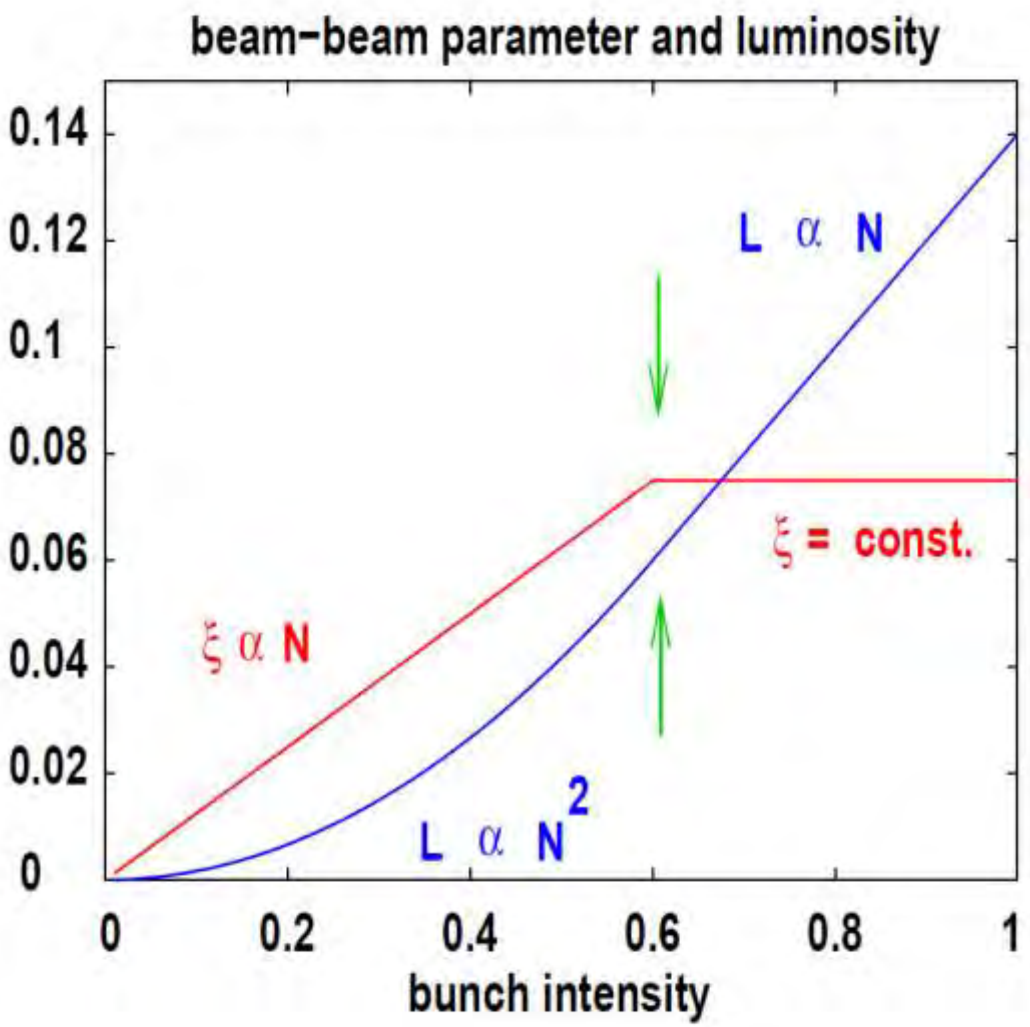

First - Beam−beam parameter increases linearly with intensity
Saturation above some intensity

Then – luminosity increases only linearly with N above the so−called
beam−beam limit

What's happening?

$$\xi_y = \frac{N r_0 \beta_y}{2\pi\gamma\sigma_y(\sigma_x + \sigma_y)} \overset{(\sigma_x \gg \sigma_y)}{\approx} \frac{r_0 \beta_y}{2\pi\gamma(\sigma_x)} \cdot \frac{N}{\sigma_y}$$

and $$\mathcal{L} = \frac{N^2 f B}{4\pi\sigma_x\sigma_y} = \frac{N f B}{4\pi\sigma_x} \cdot \frac{N}{\sigma_y}$$

- Above beam-beam limit: σ_y increases when *N* increase
  - to keep constant → equilibrium emittance !
- Therefore:
- is NOT a universal constant !
  - depends on tunes/WPs, damping rates, etc
  - difficult to predict exactly for hadron machines

Beam-Beam Limits: pp/pbar Colliders

Tevatron Collider Run II

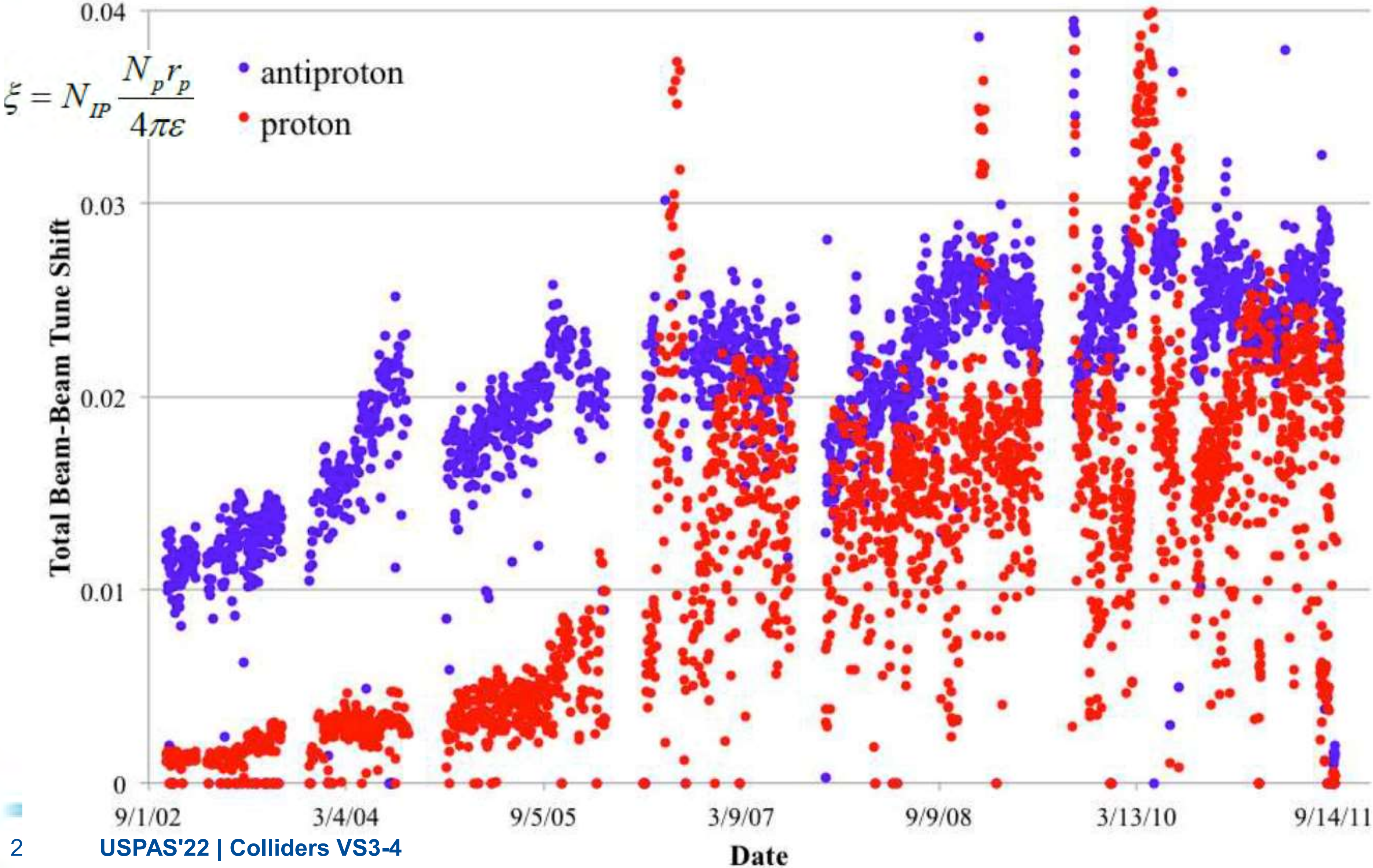

Teavtron Tune Footprint "Confinement"

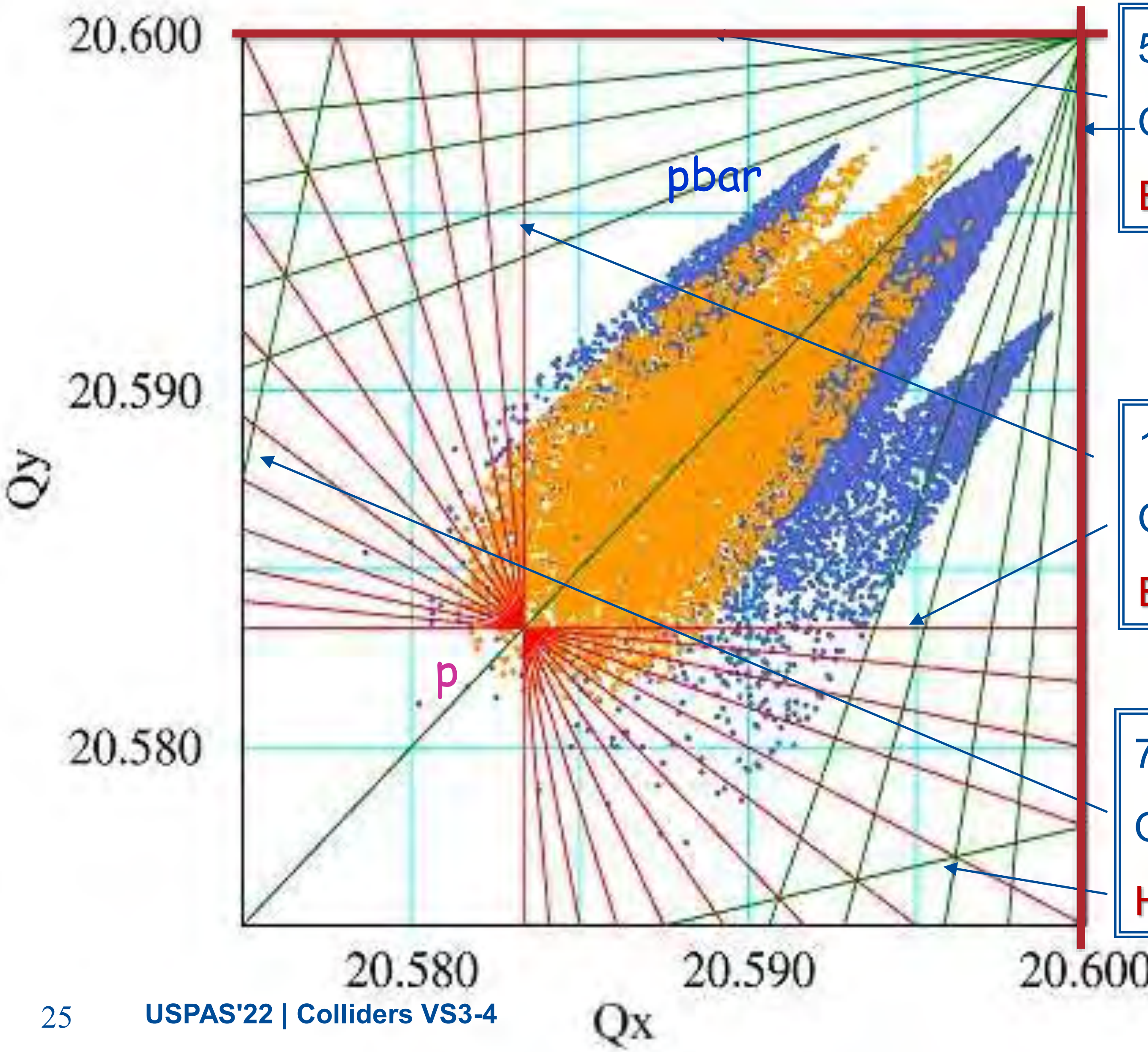

5th order resonances:
Q=3/5=0.600 –
EMITTANCE BLOWUP

protons
antiprotons

12th order resonances:
Q=7/12=0.583 -
BAD BEAM LIFETIME

7th order resonances:
Q=4/7=0.571 -
HIGH LOSSES

Resonances matter! … Diffusion

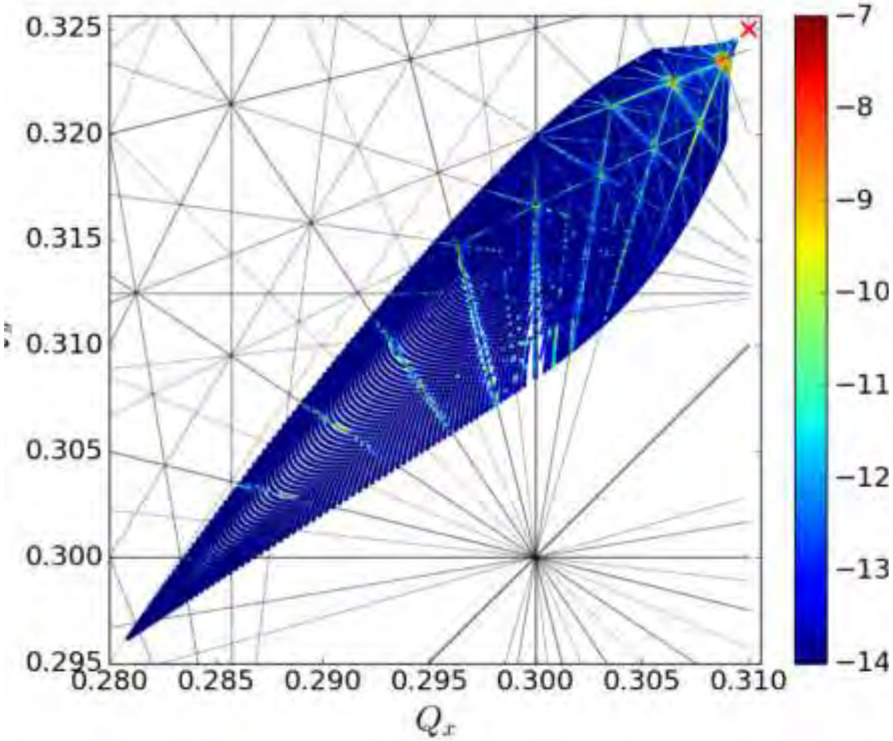

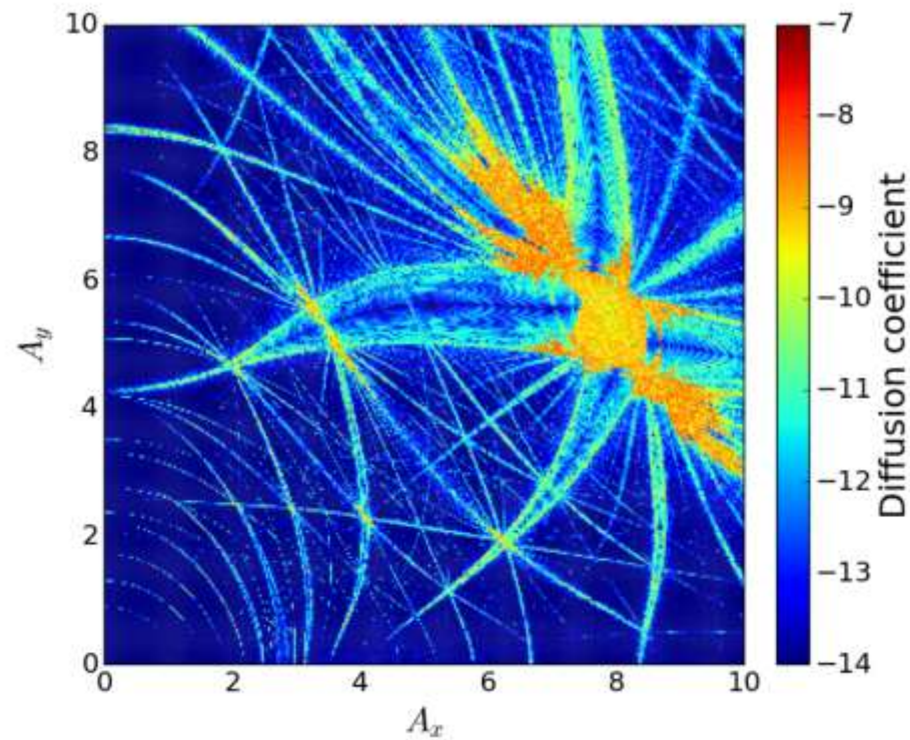

Tune map: LHC (simul)

Shown resonances up to order 20

- $\xi_{tot} = 0.03$, $Q_x = 0.31$, $Q_y = 0.325$
  $N_{mp} = 1e5$, 4D BB , $Q' = 0$
- IC: Grid in 2D (x,y)

Amplitude map: LHC (simul)

Shown diffusion rates vs Ax/Ay

$$D_i = \log_{10}\sqrt{\frac{dQ_{x,i}}{dturn}^2 + \frac{dQ_{y,i}}{dturn}^2}$$

Measure tune of a particle based on (here) 4096 turns -Calculate linear change over 10 measurements, separated by 10k turns

Non-linear Resonances

harmonics of

ω_x ω_y ω_0

- Nonlinear terms in the force *$F(x,y,t) \sim x^{\wedge}l\ y^{\wedge}p\ \delta(t-kT)$* lead to appearance of driving terms oscillating with frequencies mQ_x+nQ_y, and therefore open opportunities for nonlinear resonances if

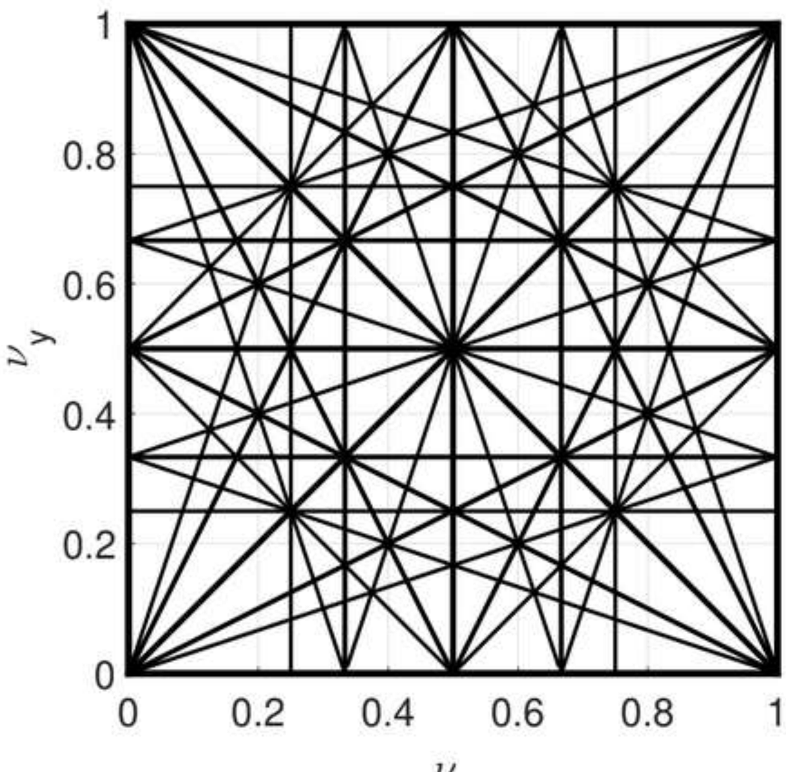

$$mQ_x+nQ_y=p$$

$|m|+|n|$ *is order of the resonance*

i.e. resonance diagram up to fourth order; importance of the resonance depends on the force shape and order (low order = more serious; often longitudinal deviations matter if $mQ_x+nQ_y+lQ_s=p$

Complications : Strong-Strong vs Weak-Strong

- Both beams are very strong (strong-strong):
  - Both beam are affected and change due to beam-beam interaction
  - Examples: LHC, LEP, RHIC, ...
- One beam much stronger (weak-strong):
  - Only the weak beam is affected and changed due to beam-beam interaction
  - Examples: SPS collider, Tevatron (early in Run II) , ...

Incoherent vs Coherent Beam-Beam Effects

- Incoherent (single particle effects):
  - Single particle dynamics - treat as a particle passing through a static electromagnetic lens
  - Basically, non-linear dynamics effects:
    - unstable and/or irregular motion ("chaos")
    - beam size blow up or bad lifetime
    - Very bad: unequal beam sizes (studied at SPS, HERA, Tevatron)
- Coherent (bunches affected as a whole):
  - Collective modes
  - Bunch-by-bunch differences in:
    - Orbits
    - Tunes
    - Chromaticities

Coherent Beam-Beam: Modes

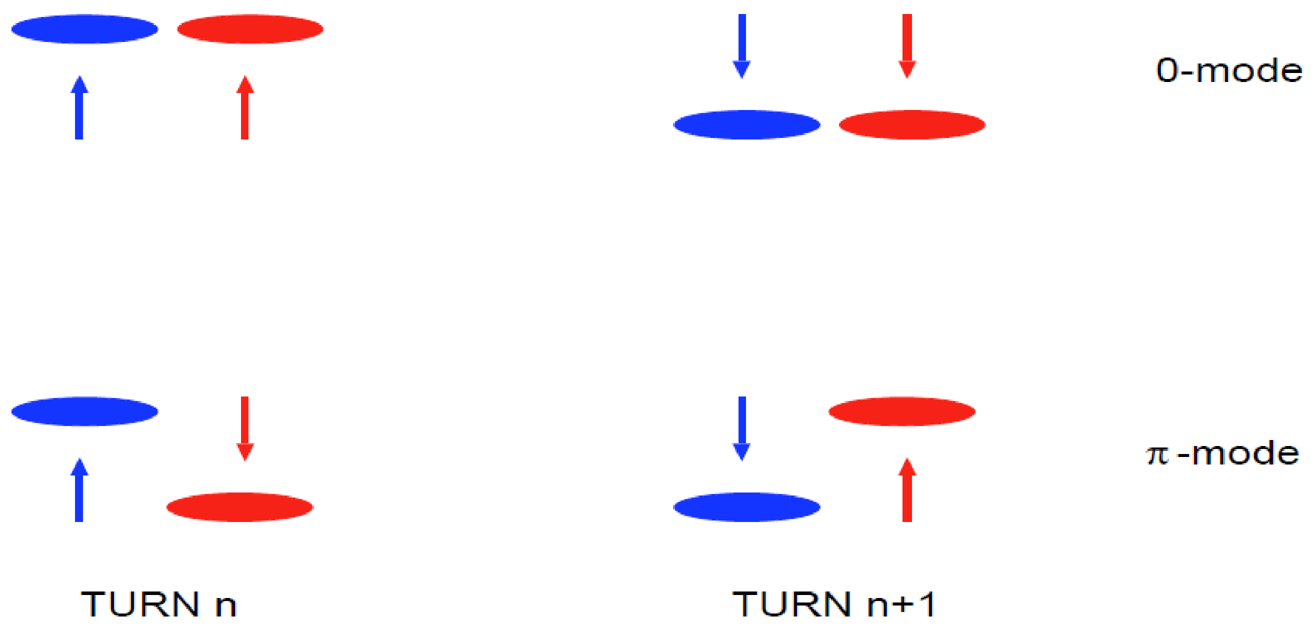

- Coherent mode: two bunches are "locked" in a coherent oscillations
  - 0-mode is stable (Mode with NO tune shift)
  - π-mode can become unstable (Mode with LARGEST tune shift)

Coherent Beam-Beam: Modes

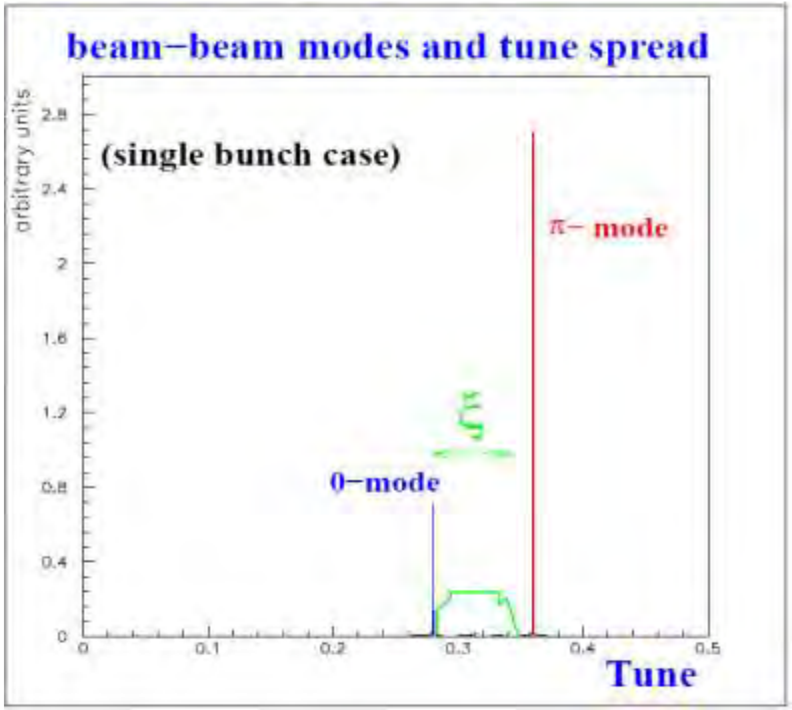

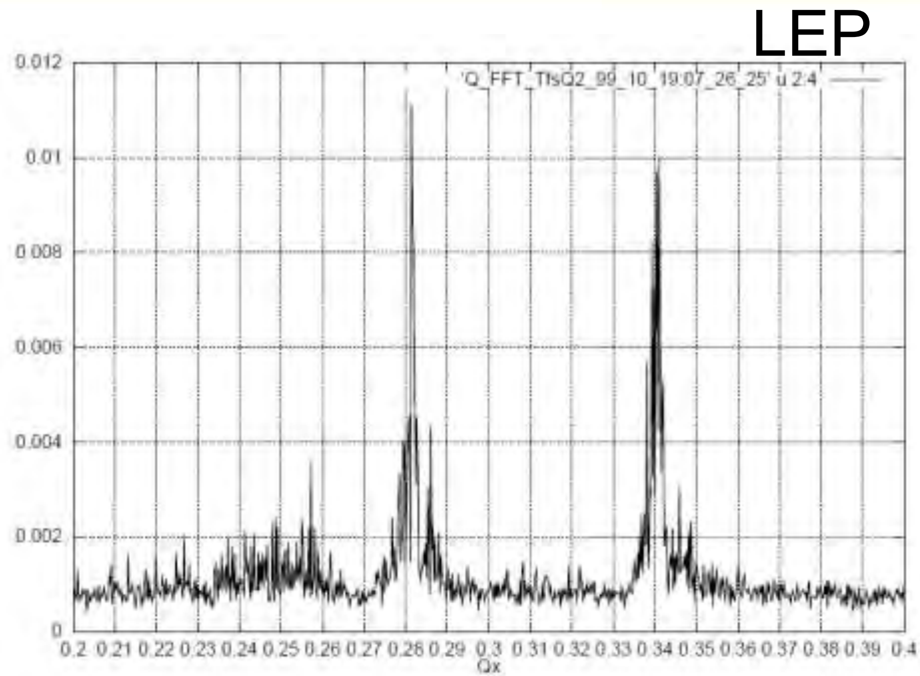

- 0−mode is at unperturbed tune
- π−mode is shifted by 1.1 − 1.3 · ξ
- Incoherent spread between [0.0,1.0] · ξ

Two modes clearly visible
Can be distinguished by phase relation, i.e.
sum and dierence signals

Fermilab

Coherent Beam-Beam: Flip-Flop

Bunch sizes get bigger or smaller out of phase

(PEP-II, VEPP-2000, etc)

The intensity threshold for the flip-flop depends on:

- asymmetry in beam intensities
- x-y coupling

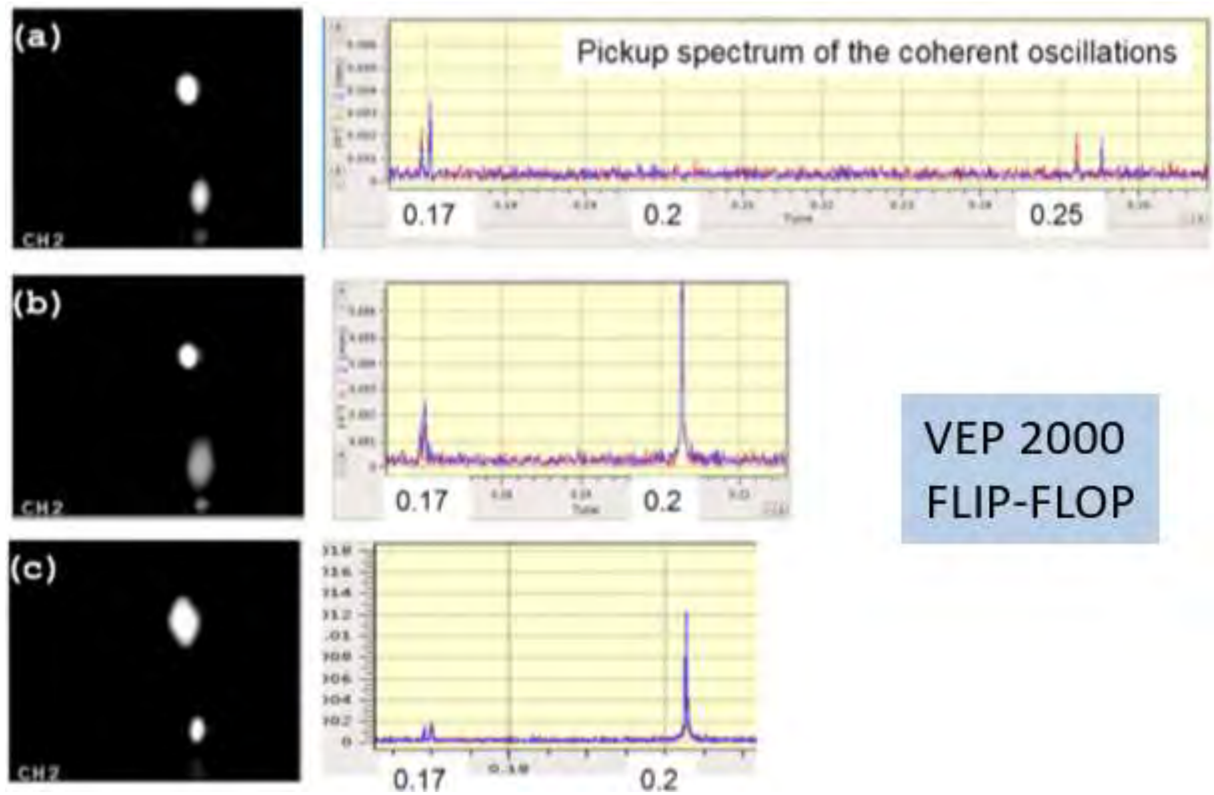

3D Flip-Flop effects triggered by non-linearities of lattice. π-mode on 1/5 resonance. The effect have shown a strong sensitivity to X-Y coupling, beta unbalance and bunch length → main limitation in VEPP 2000.

Multi-Bunch Operation: Need and Issues

$$\mathcal{L} = \frac{N_1 N_2 f \cdot B}{4\pi\sigma_x\sigma_y}$$

- How to collide many bunches (for high *L*) ??
- Must avoid unwanted collisions !! Otherwise $\xi \rightarrow 2B\xi$
- Separation of the beams:
  – Pretzel/helix scheme (SPS,LEP,Tevatron)
  – Bunch trains (LEP, PEP)
  – Crossing angle (LHC)

Tevatron: 36 proton x 36 antiproton

Same beam pipe and magnetic fields → same orbits → 72 IPs

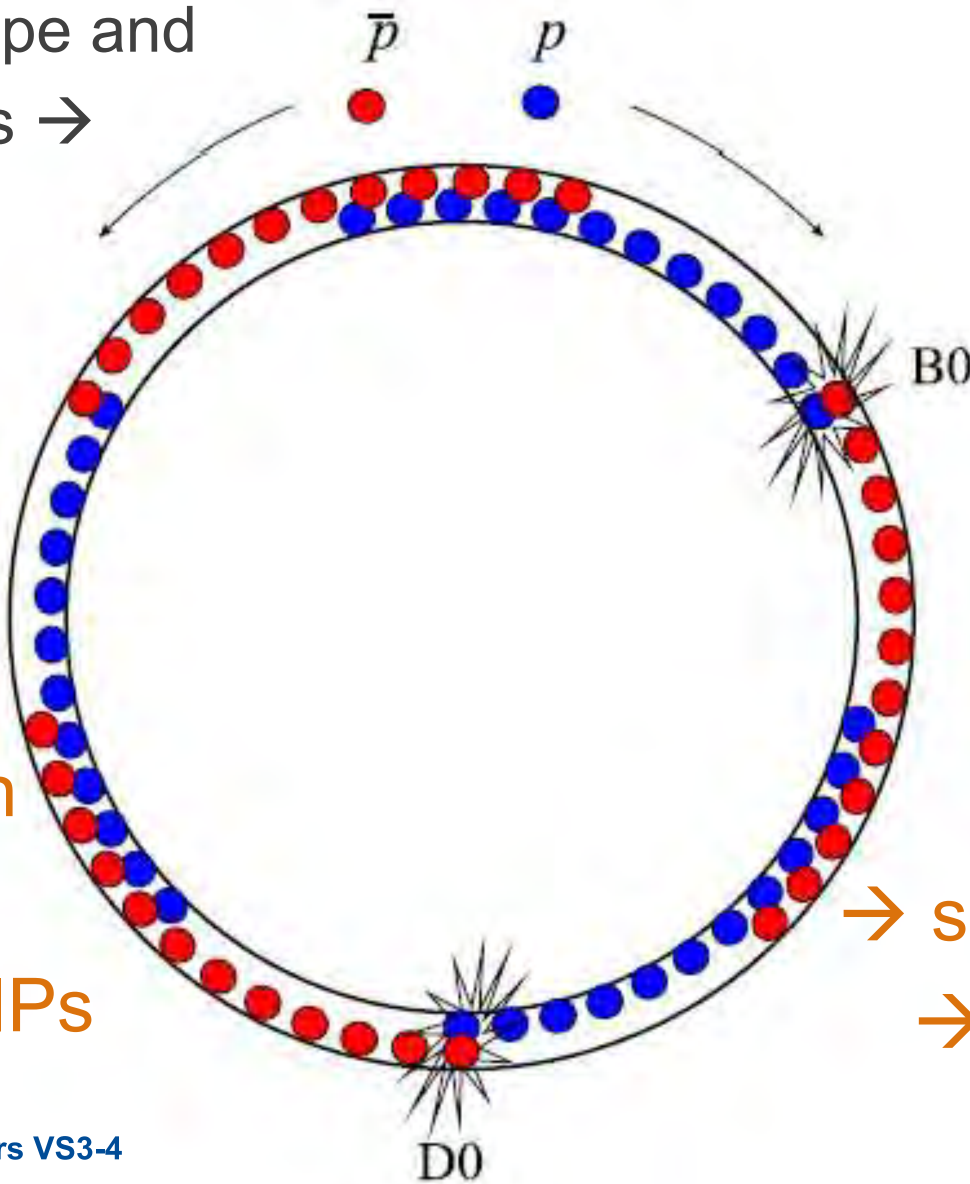

396 ns bunch separation → 59 m btw IPs

Need only 2 → separate at 70 → Electric field

Tevatron High Voltage Electrostatic Separators

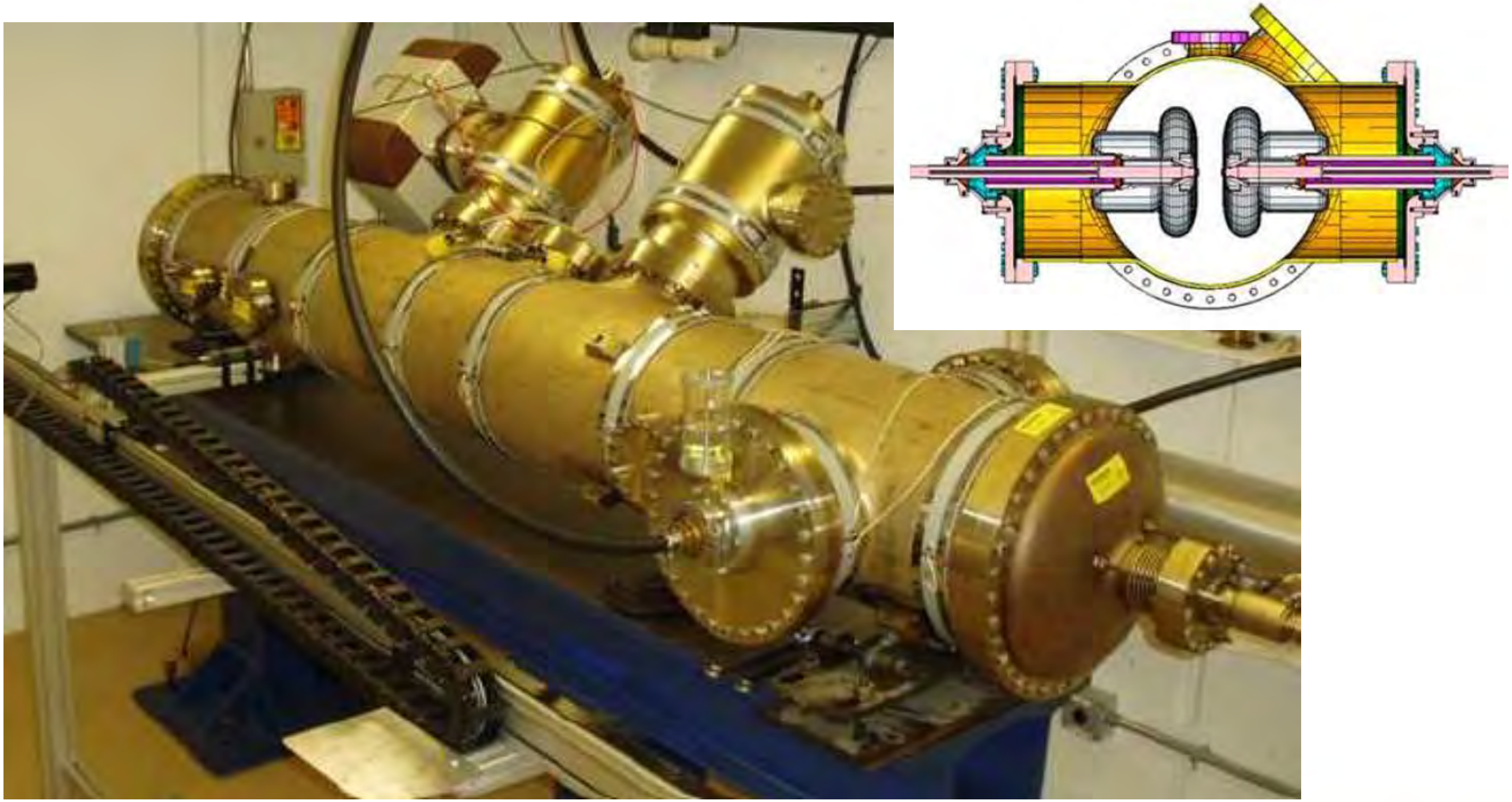

300 kV over 50 mm gap; 3 m ; 24 of them (H/V)

Fermilab

Tevatron Helix

24 electrostatic separators are used

size 12-15 mm
at 150 GeV

6-8 mm
at collisions

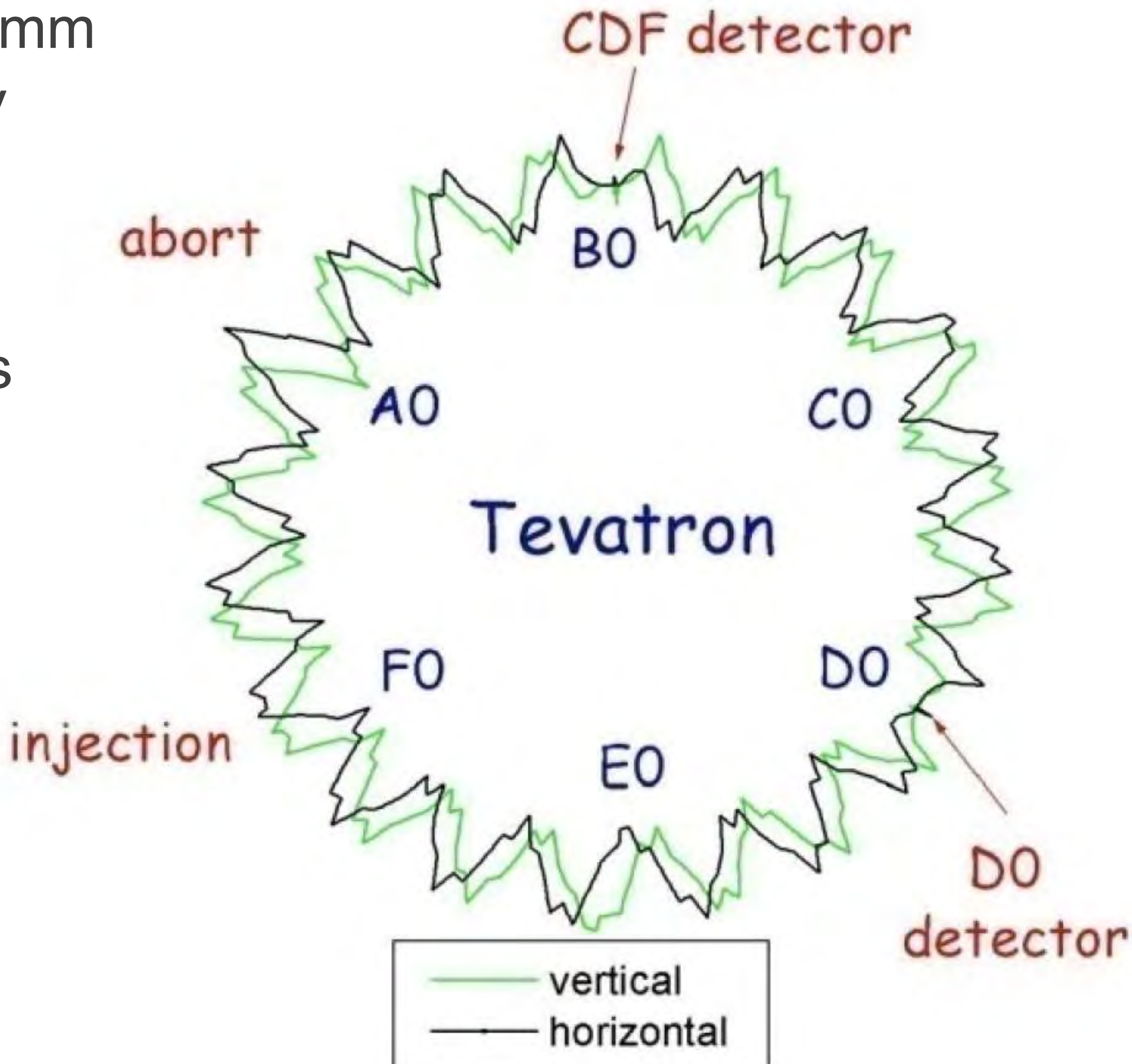

All beam indicators become bunch dependent due to long-range beam-beam effects

$$\Delta x' = \frac{const}{d}[1 - \frac{x}{d} + O(\frac{x^2}{d^2}) + \ldots]$$

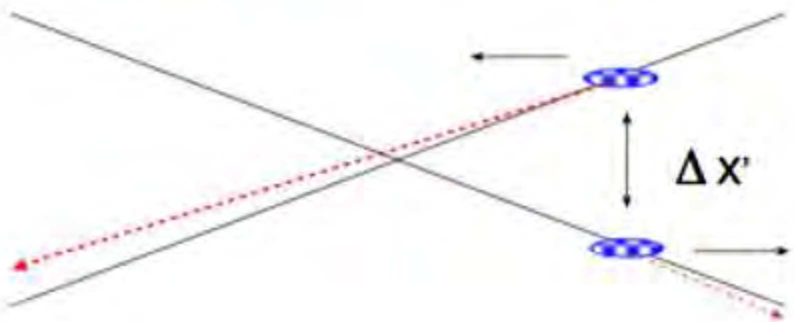

- Orbits
- Tunes, couplings
- Chromaticities
- In both – protons and pbars
- Have 3-fold symmetry (trains of 12)

Long-range B-B Seen at Low-Beta (980 GeV)

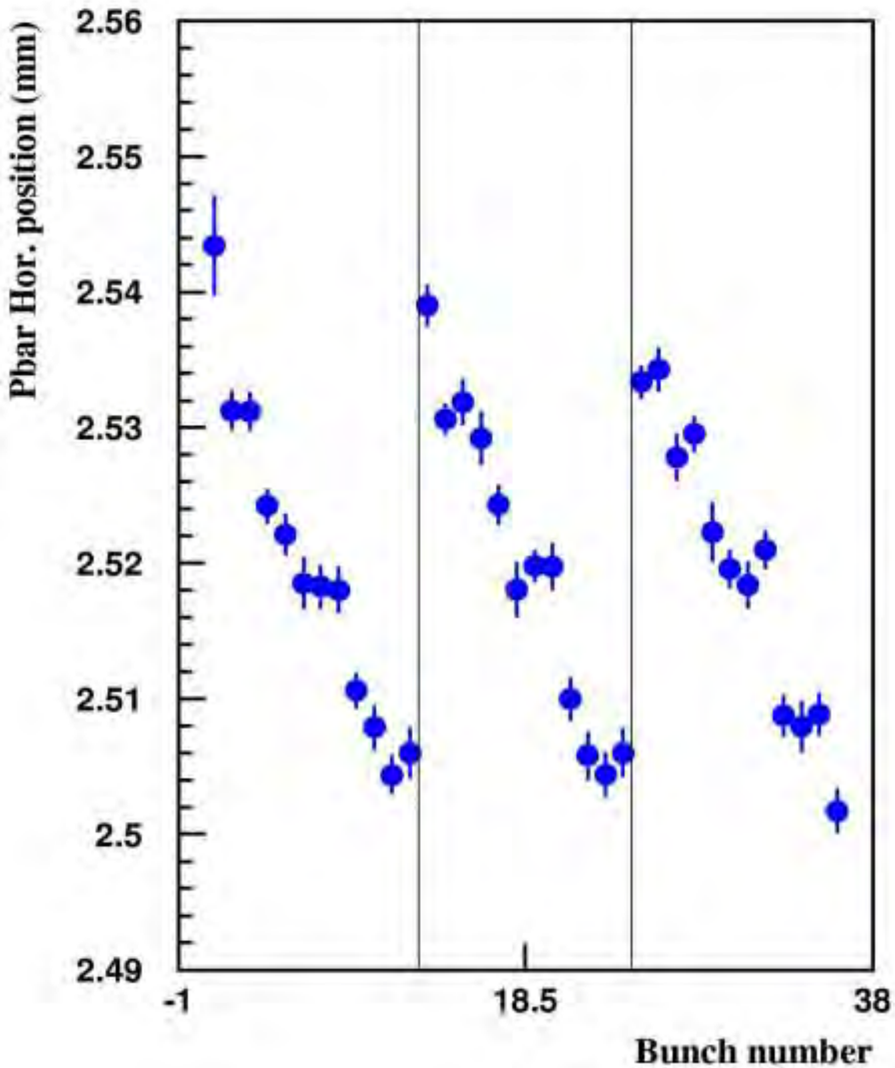

- Synchrotron light monitors show 40 micron b-by-bunch hor pbar orbit variation along the bunch train with 3-train symmetry (4 microns for protons)
- Also indicate coupling differences →

Bunch #1

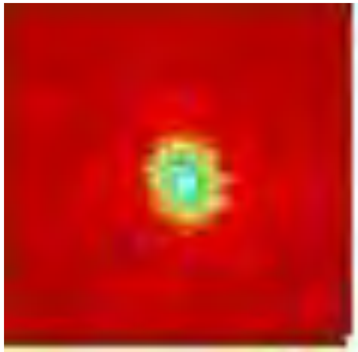

Bunch #8

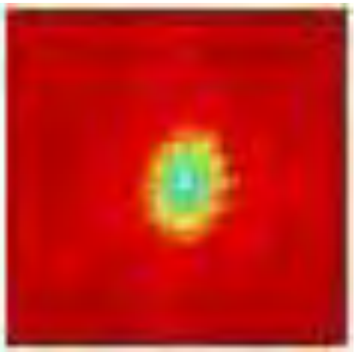

Antiproton Vertical Orbit

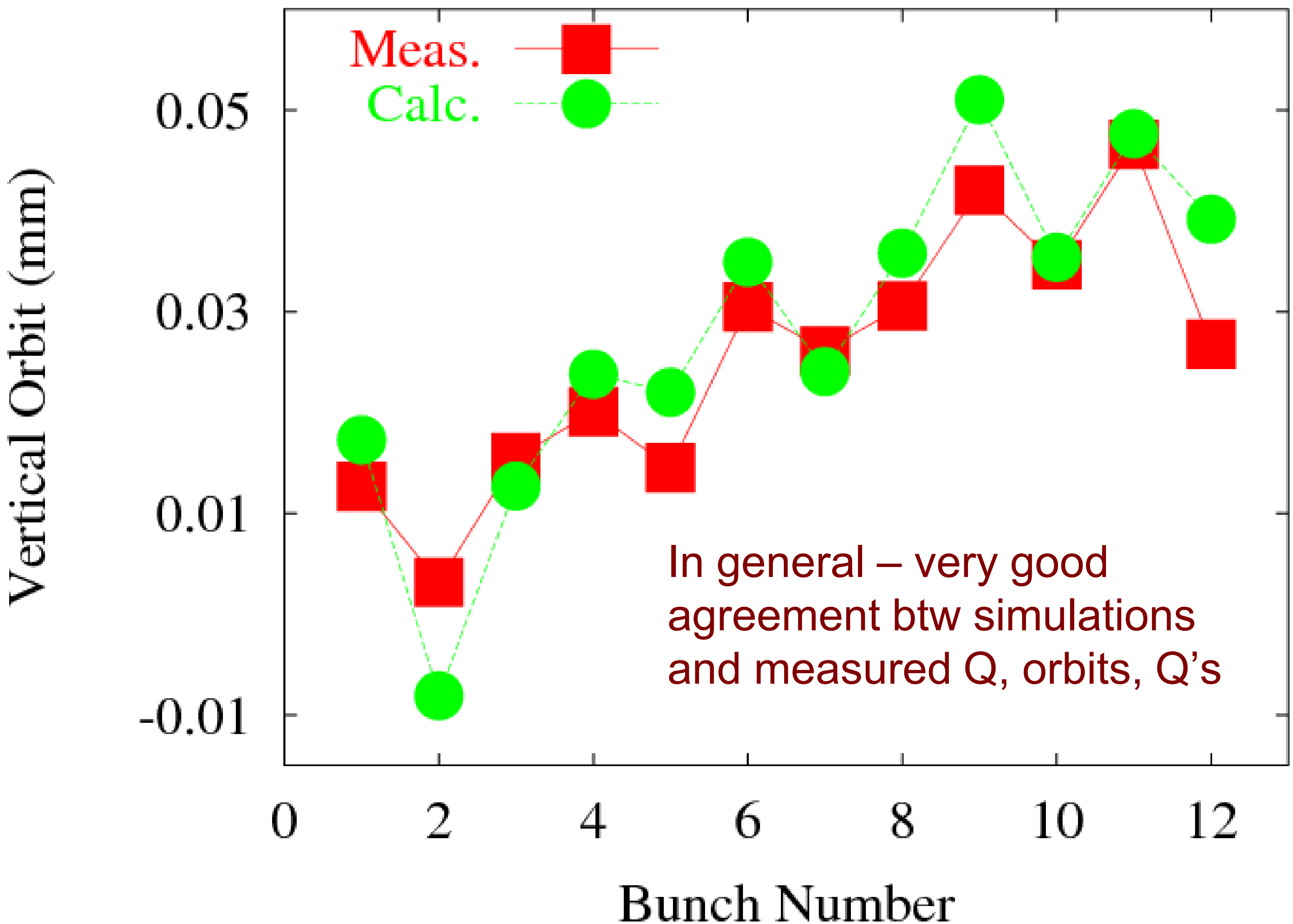

In general – very good agreement btw simulations and measured Q, orbits, Q's

Pbar Bunch Tunes in Collisions

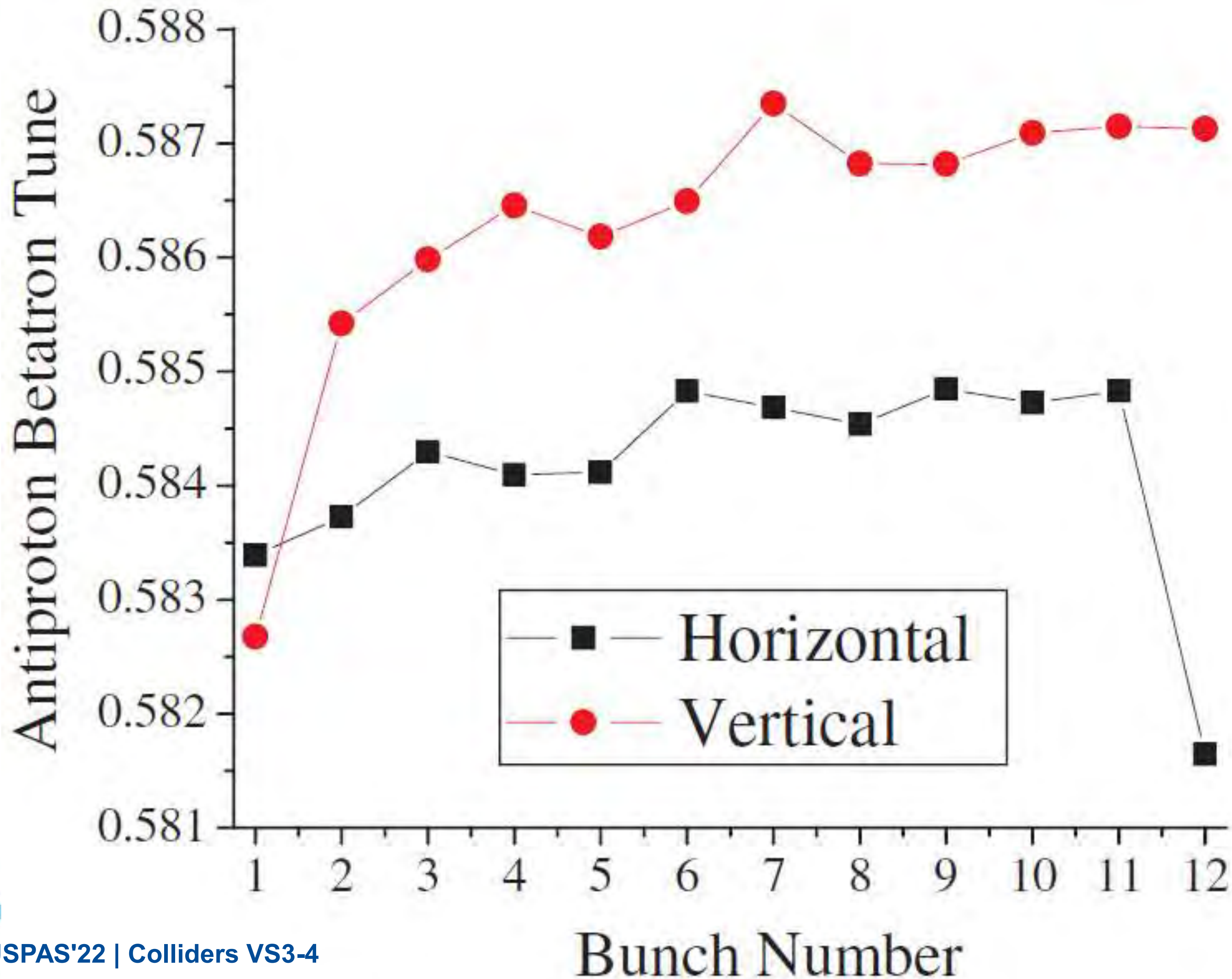

Pbar Bunch Chromaticity in Collisions

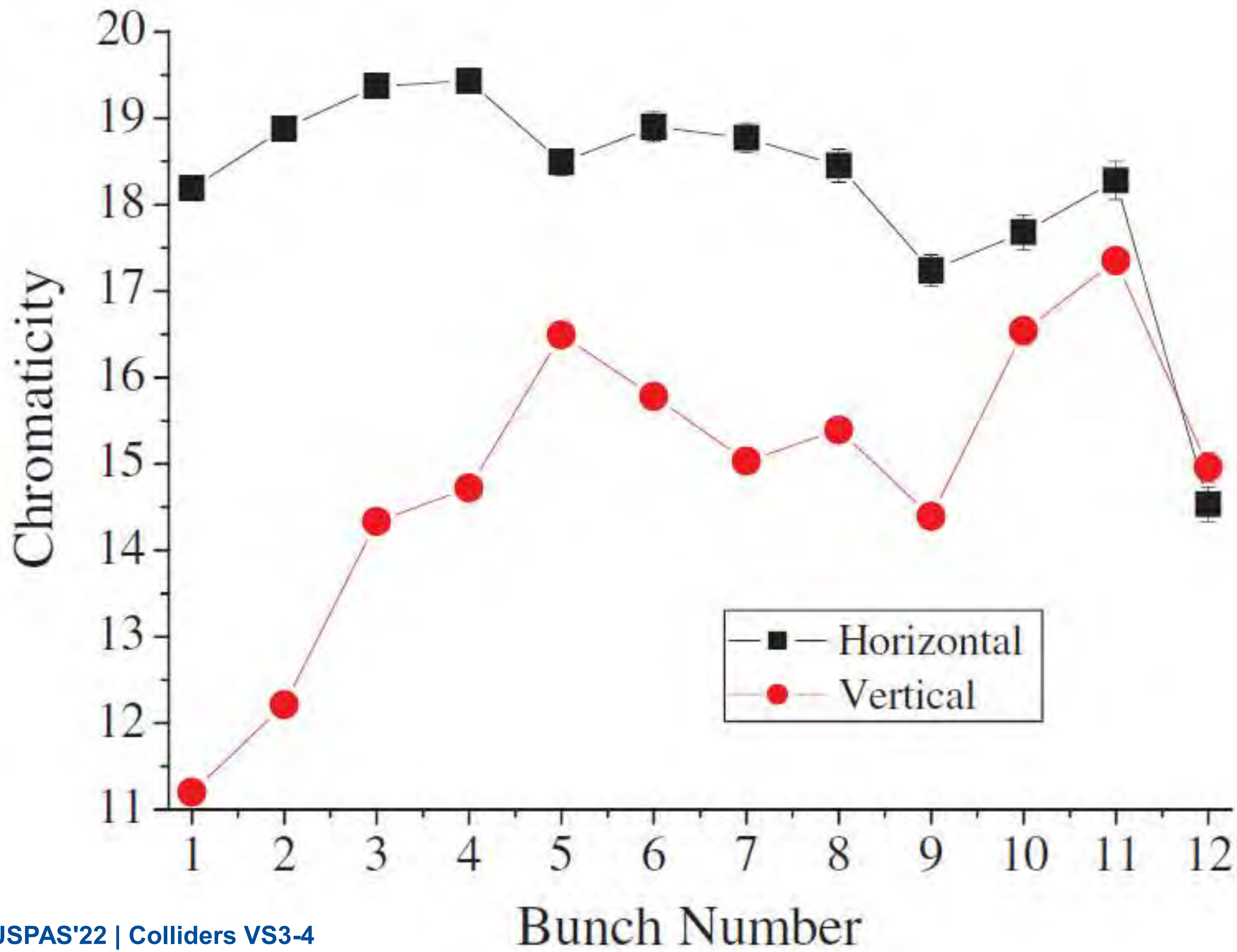

lab

In the LHC

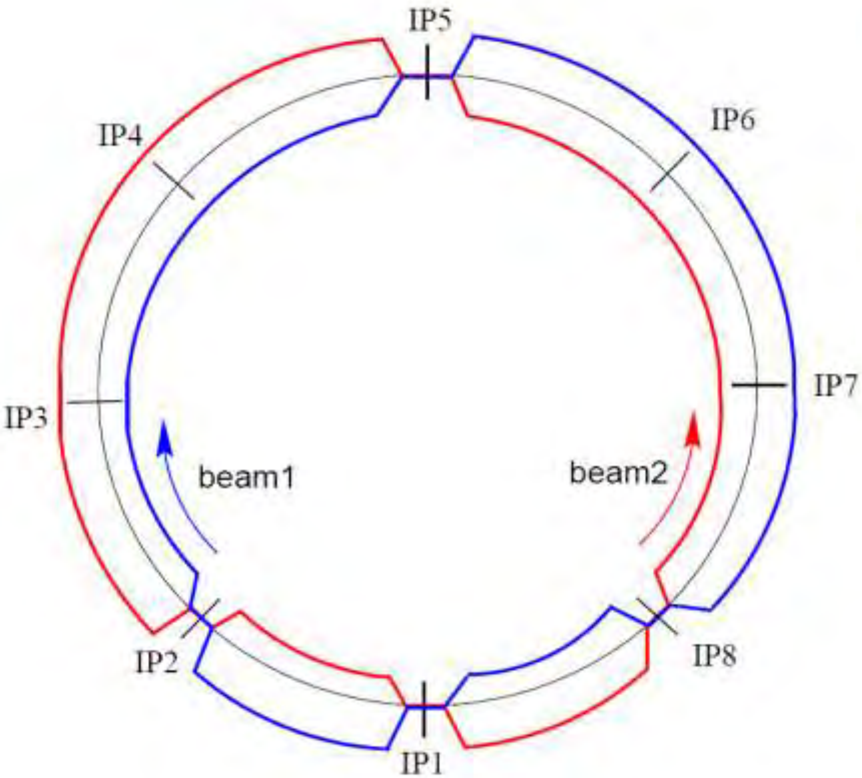

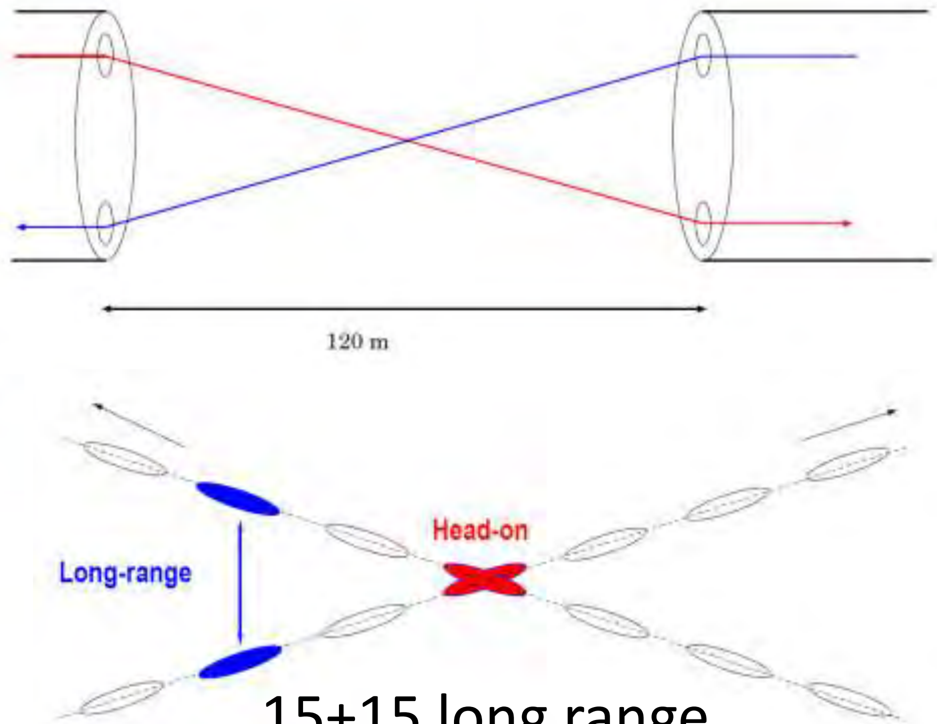

15+15 long range interactions (6-12 σ)

- 2808 p bunches in each beam, every 25 ns
- Two beams in separate beam pipes except in common chamber around 4 experiments
- Local separation via two horizontal and two vertical crossing angles

Parasitic Beam-beam Kicks

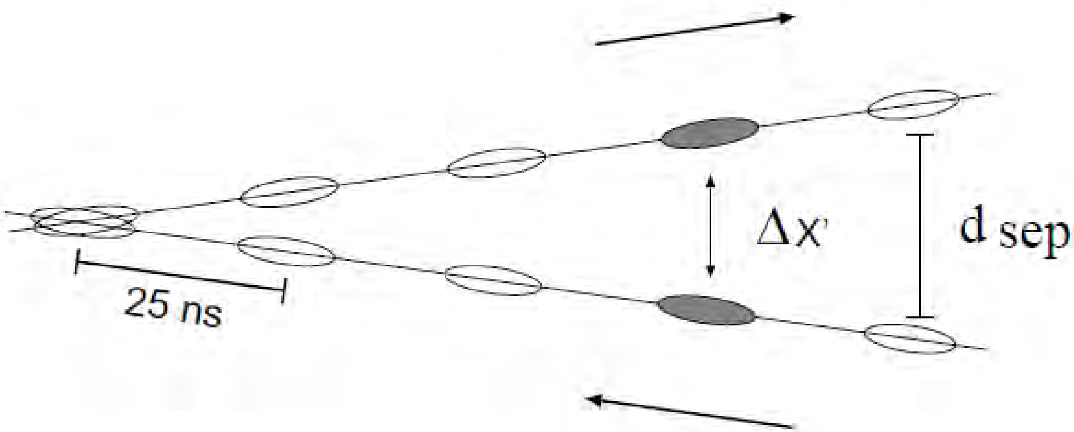

For horizontal separation d:

$$\Delta x'(x+d,y,r) = -\frac{2Nr_0}{\gamma} \cdot \frac{(x+d)}{r^2}\left[1-\exp(-\frac{r^2}{2\sigma^2})\right]$$

$$(with: \quad r^2 = (x+d)^2 + y^2)$$

In LHC 15 collisions on each side, 120 in total!
Effects depend on separation, eg tuneshift

$$\Delta Q \propto -\frac{N}{d^2}$$

PAMCMAN bunches due to gaps

- Average orbit and tune variations can be corrected, but:

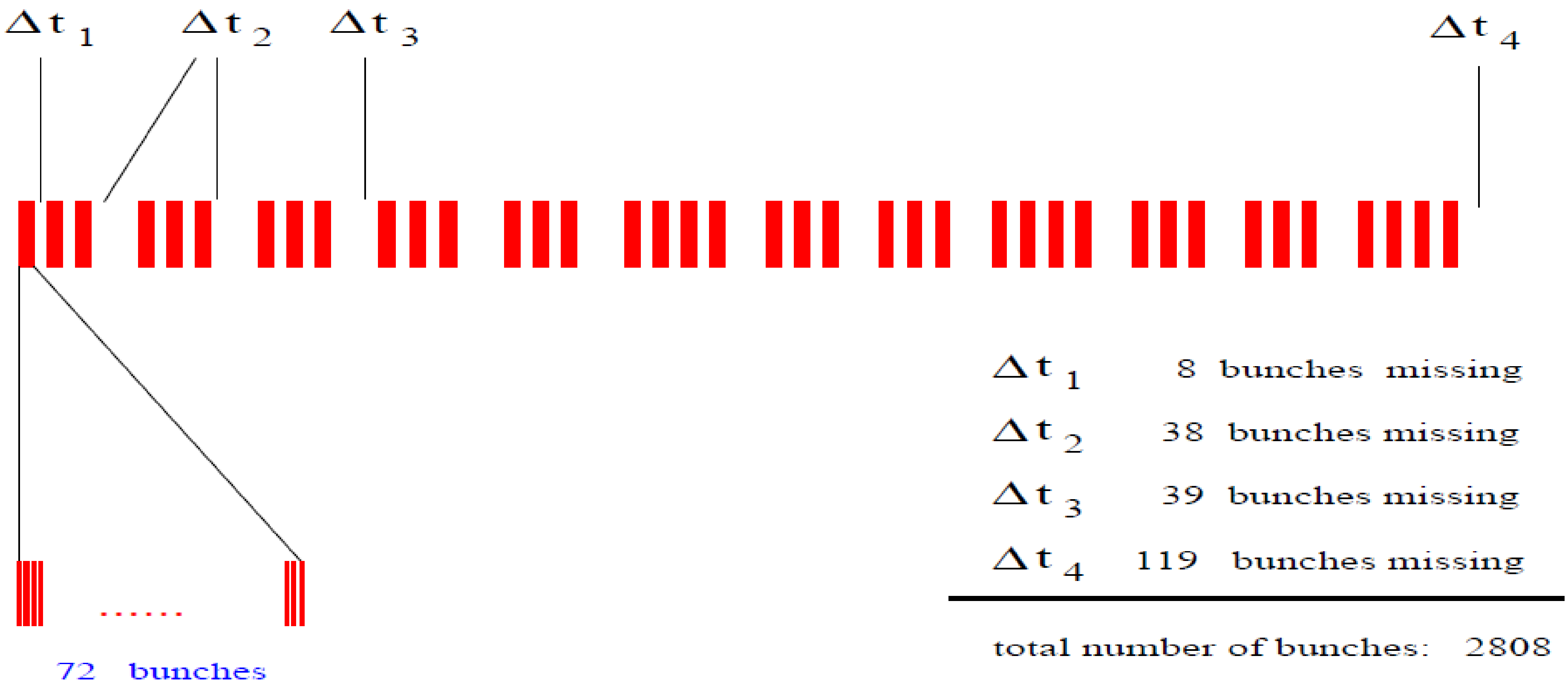

LHC bunch filling not continuous: holes for injection, extraction, dump ..

"Only" 2808 of 3564 possible bunches circulate ! 1756 "holes"

"Holes" meet "holes" at the interaction point - But not always ...

Effect of PACMAN bunches (end of train)

- Some bunches can meet a hole/holes (at beginning and end of bunch train) →
- They see fewer unwanted interactions in total: between 120 (max) and 40 (min) long range collisions → Different integrated beam-beam effect for different bunches

LHC

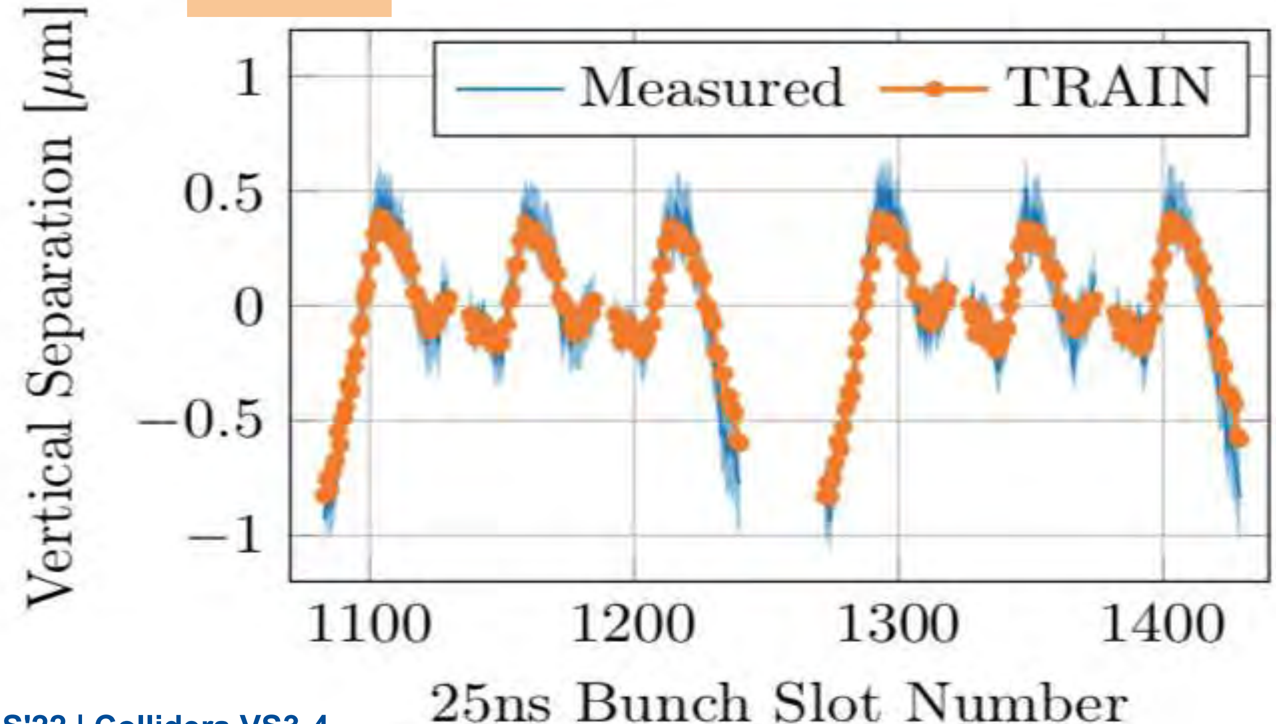

Tune Spread - too large for safe operation

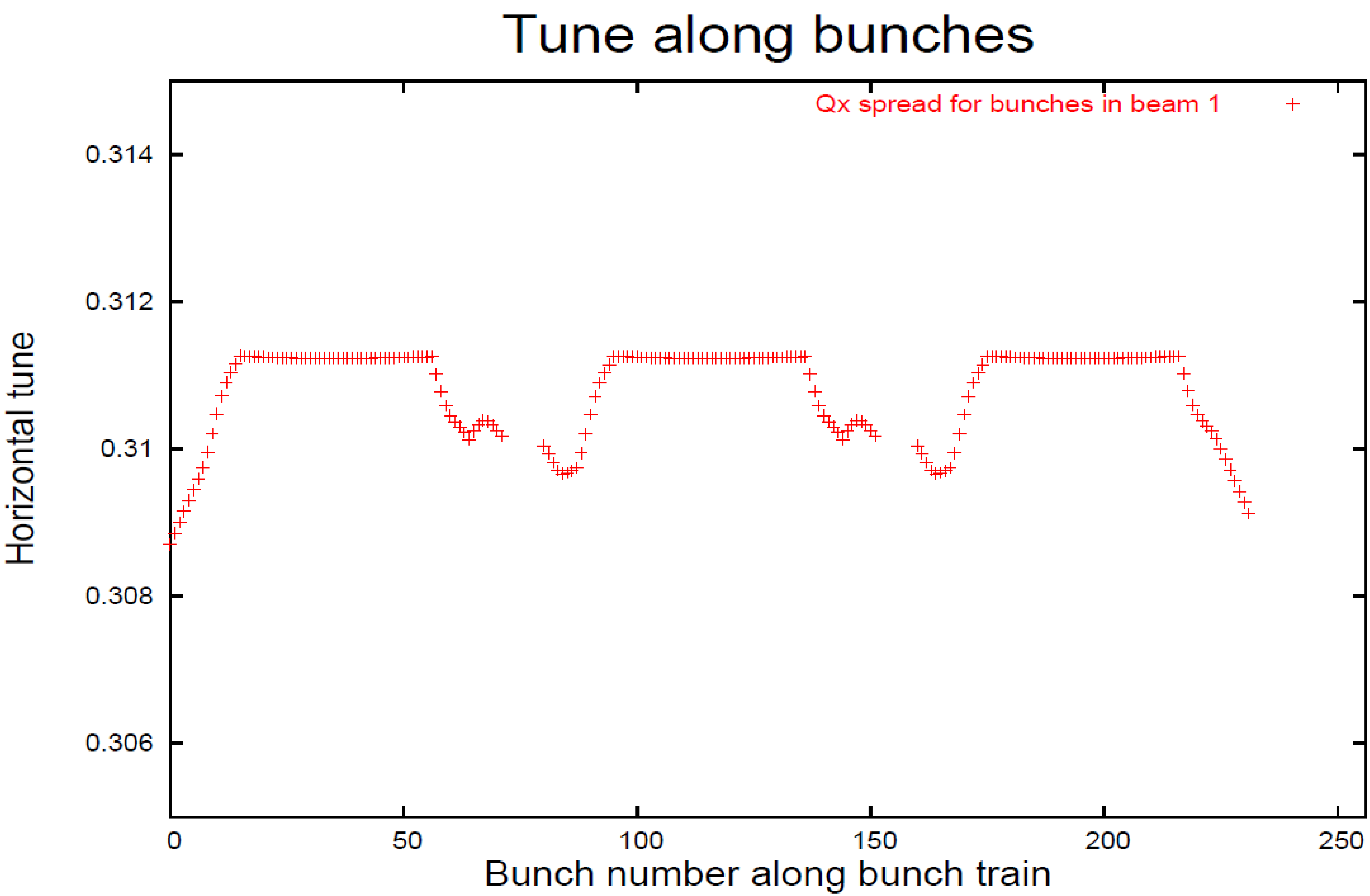

How to control beam-beam effects?

- Find 'lenses' to correct beam-beam effects
- Head on effects:
  - Linear "electron lens" to shift tunes
  - Non-linear "electron lens" to reduce spread
  - Successful e-lenses at FNAL and RHIC
- Long range effects:
  - At very large distance: force is *1/r*
  - Same force as a wire !
- Overall - success with active compensation

Attempt #1: Four beams e-e+ e-e+

four-beam collider *Dispositif de Collisions dans l'Igloo* (DCI, 1970s) at Orsay with two 0.8 GeV electron beams and two positron beams of the same energy, all meeting at the same interaction point *(J.LeDuff et al)*

Q1+Q2+Q3+Q4=0   *J1+J2+J3+J4=0*

E=B=0

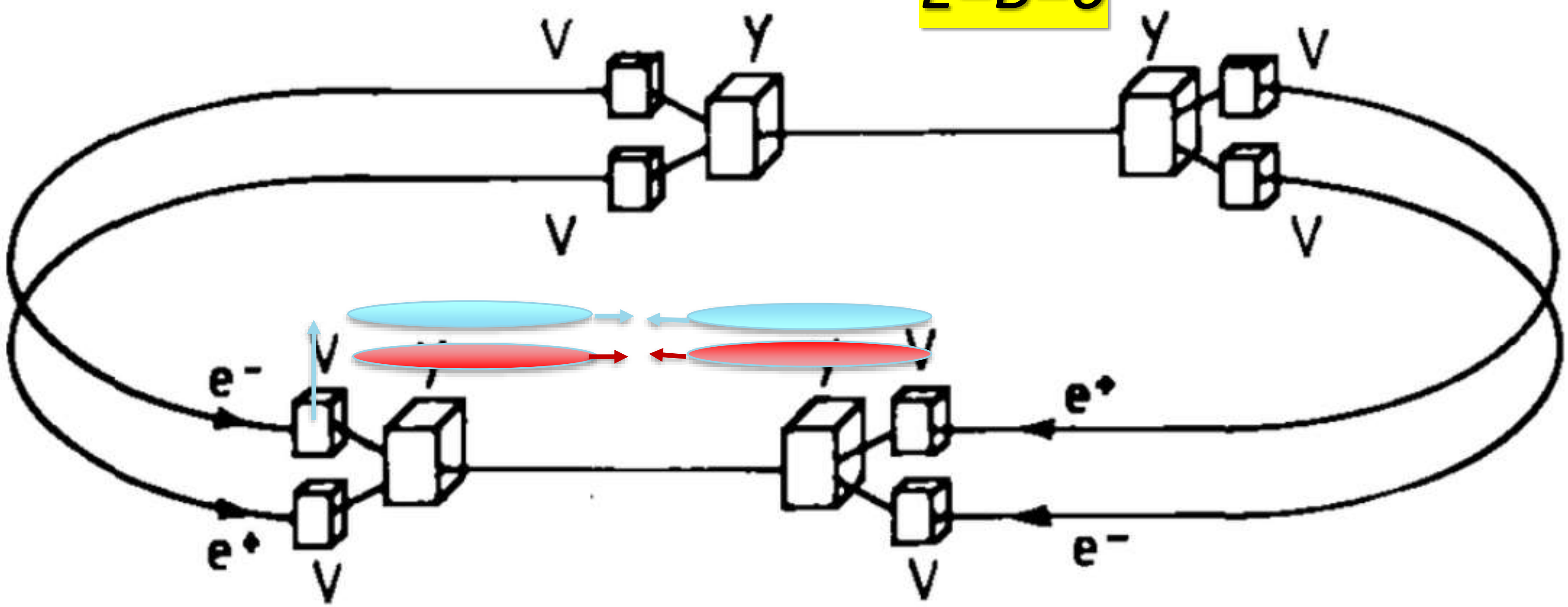

Attempt #1: Four beams compensation

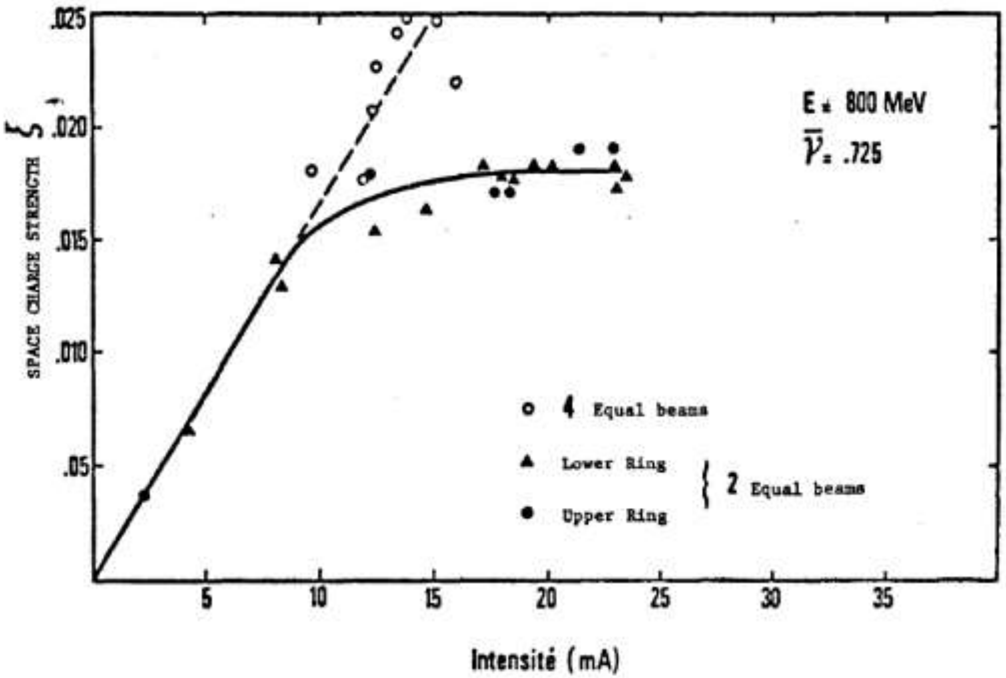

Fig. 12. Comparison between four beams and two beams: ξ versus current at E = 800 MeV and $\bar{\nu}$ = .725

No improvement of performance was obtained in the four-beam configuration compared to collisions of just two beams of electrons and positrons.

A transverse dipole feedback as well as a detuning of the two rings did not help.

The compensation is believed to be unsuccessful due to the loss of beam stability, both for dipole and higher order modes of coherent motion.

Approach #2: Electron lens

e- profile same as ***p+*** $N_e = N_{\mathrm{IP}} N_p / (1 + \beta_e)\,.$

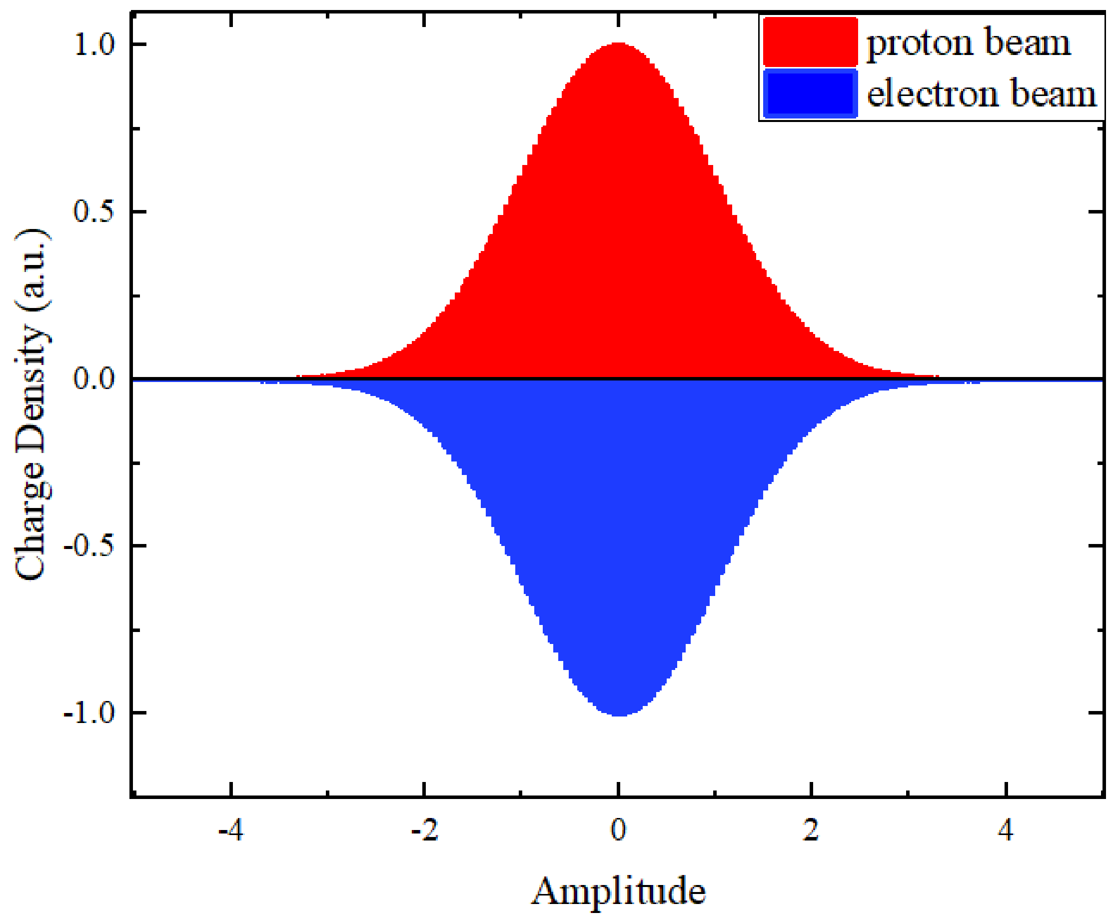

Protons focus pbars +
Electrons defocus

Net effect = zero

Footprint compressed

PHYSICAL REVIEW SPECIAL TOPICS - ACCELERATORS AND BEAMS, VOLUME 2, 071001 (1999)

Considerations on compensation of beam-beam effects in the Tevatron with electron beams

V. Shiltsev, V. Danilov,* D. Finley, and A. Sery†
Fermi National Accelerator Laboratory, Batavia, Illinois 60510
(Received 8 October 1998; published 28 July 1999)

The beam-beam interaction in the Tevatron collider sets limits on bunch intensity and luminosity. These limits are caused by a tune spread in each bunch which is mostly due to head-on collisions, but there is also a bunch-to-bunch tune spread due to parasitic collisions in multibunch operation. We propose to compensate these effects with the use of a countertraveling electron beam, and we present general considerations and physics limitations of this technique.

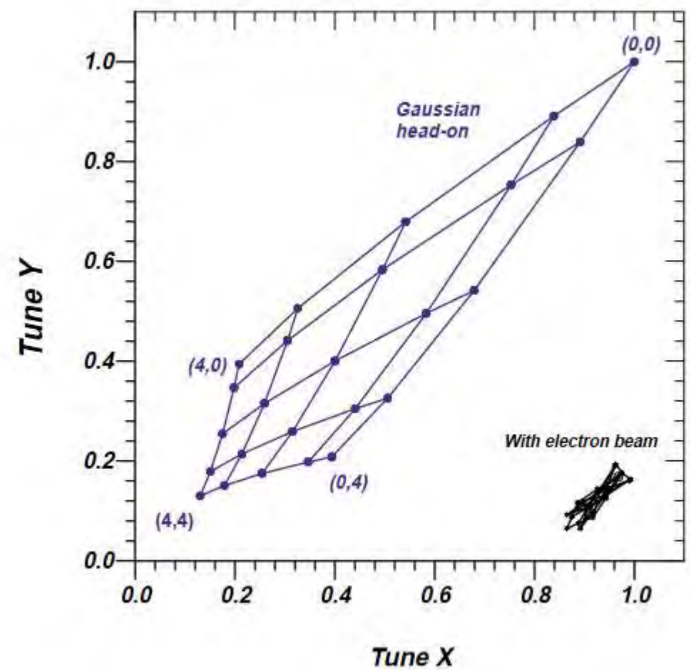

(V.Shiltsev et al)

Electron Lens Compensation

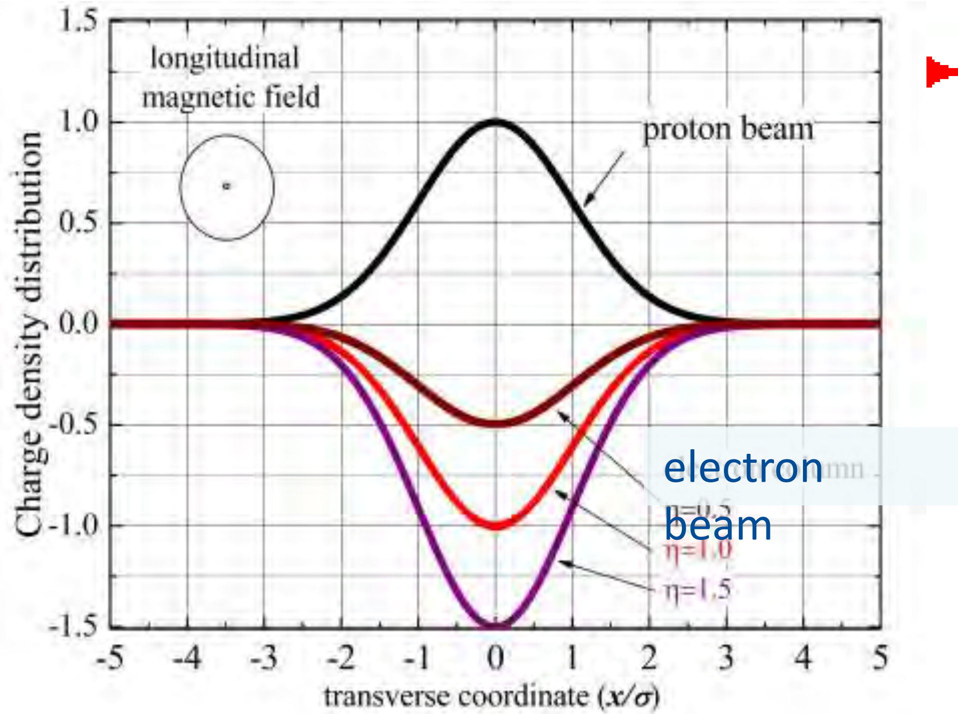

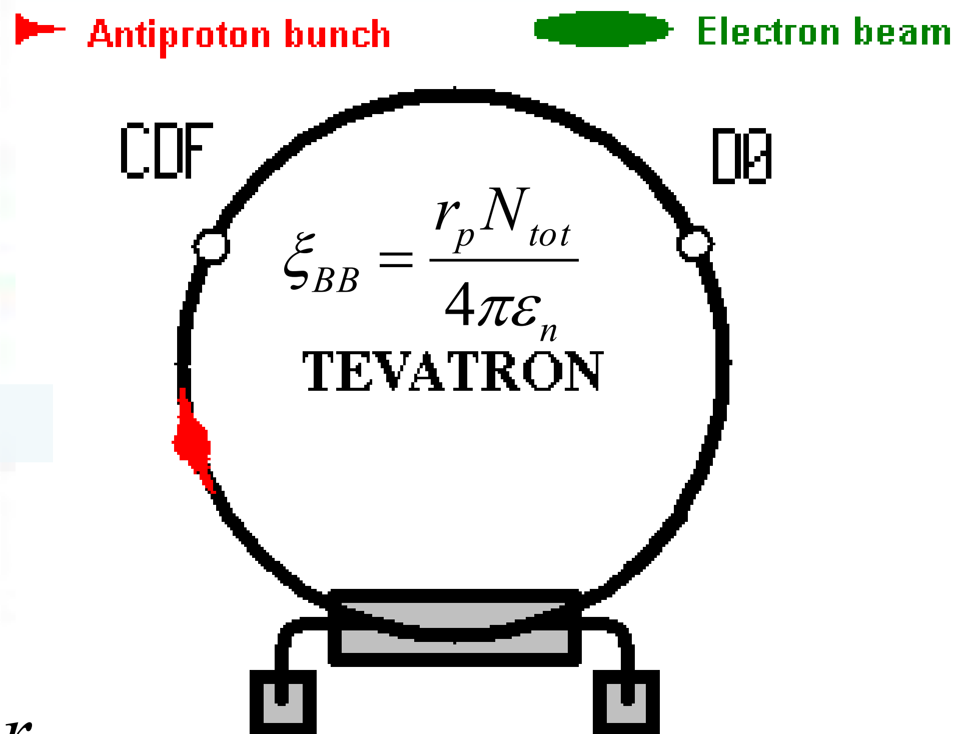

$$dQ_{x,y} = \mp \frac{\beta_{x,y}}{2\pi} \cdot \frac{1 \pm \beta_e}{\beta_e} \cdot \frac{J_e \cdot L_e \cdot r_p}{e \cdot c \cdot a_e^2 \cdot \gamma_p}$$

"…to compensate (in average) space charge forces of positively charged protons acting on antiprotons in the Tevatron by interaction with a negative charge of a low energy high-current electron beam "
(V.Shiltsev, 1997)

Some Facts on Electron Lenses

~4 mm dia 2 m long very straight beam of ~10kV

~1A electrons (~10^{12}) immersed in 3T solenoid

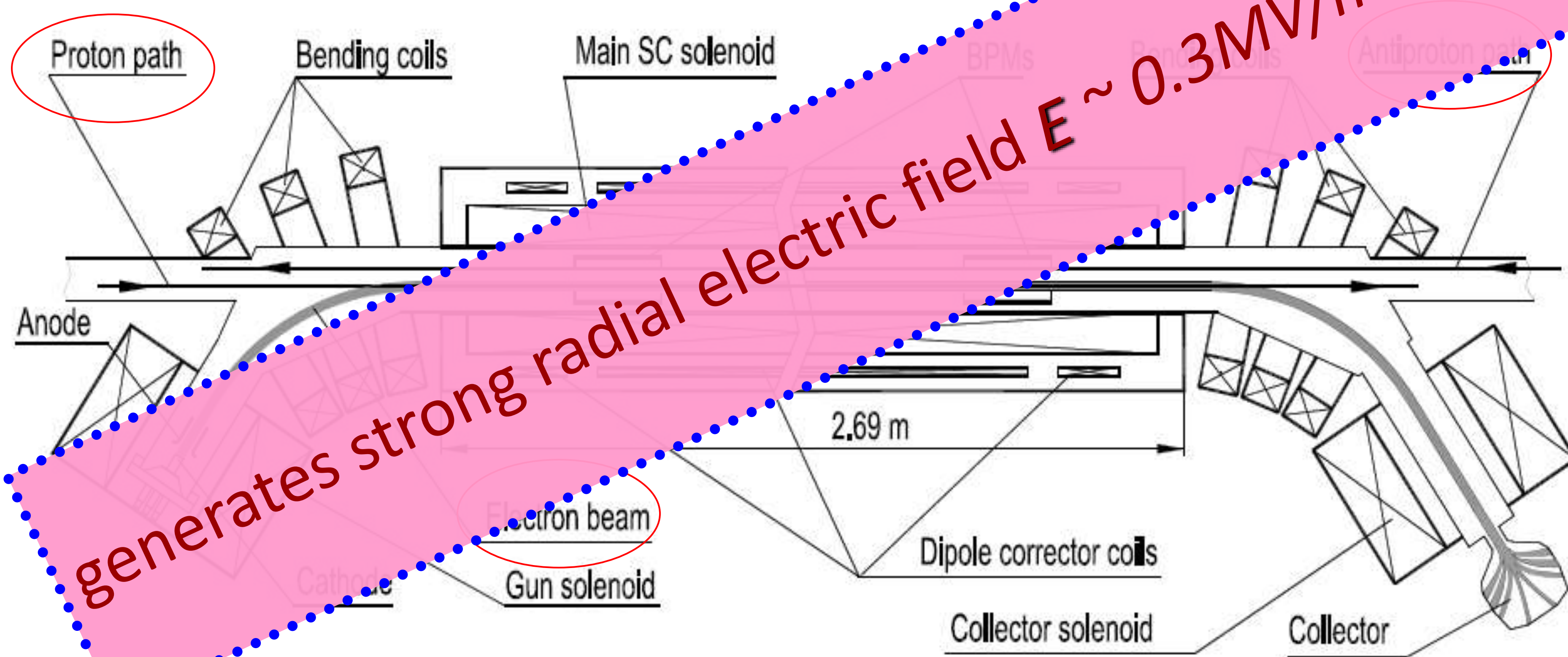

generates strong radial electric field E ~ 0.3MV/m

Tevatron Electron Lens #1 (F48)

TEL2 in the Tevatron Tunnel (A11)

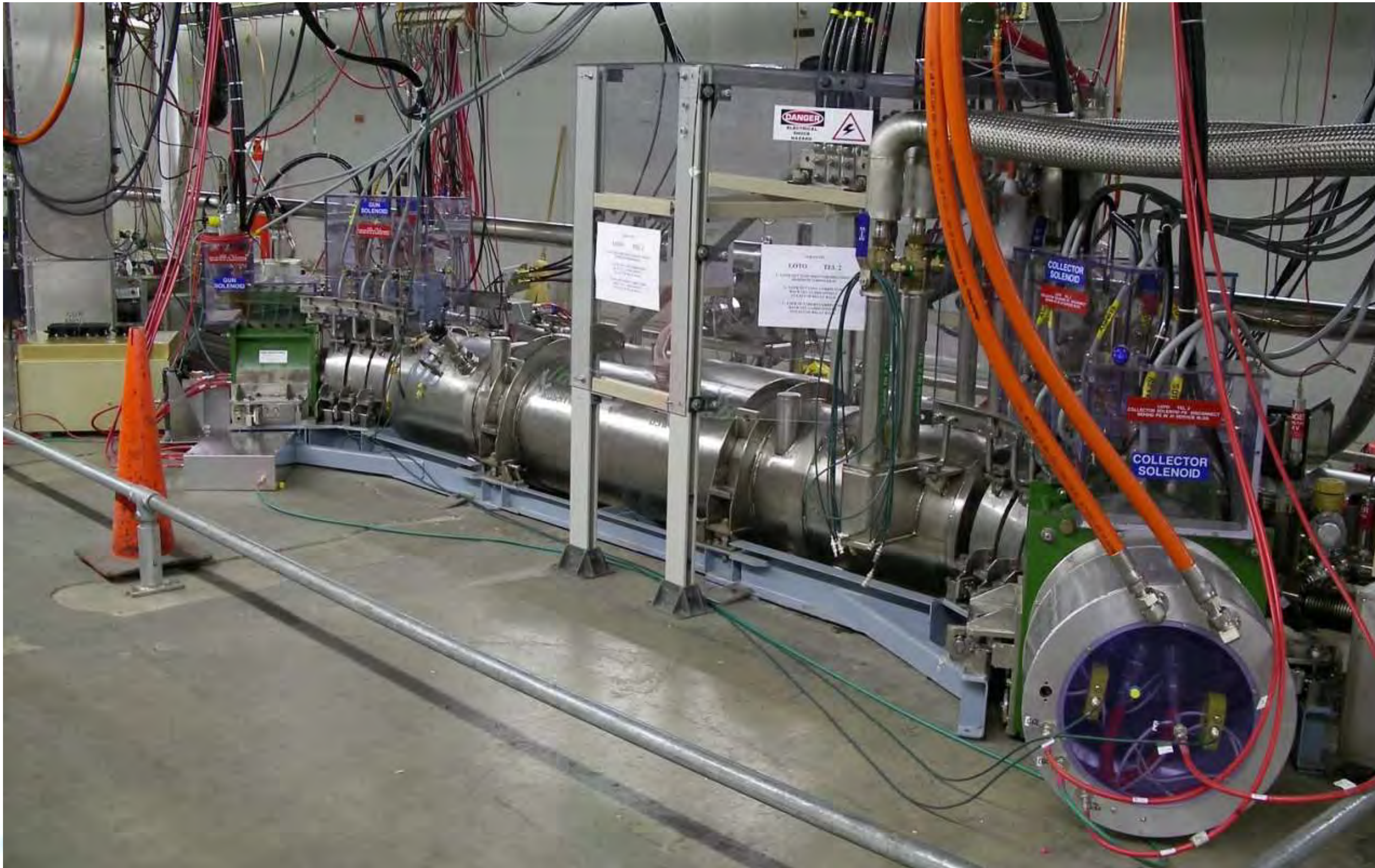

Compensation with Two TELs

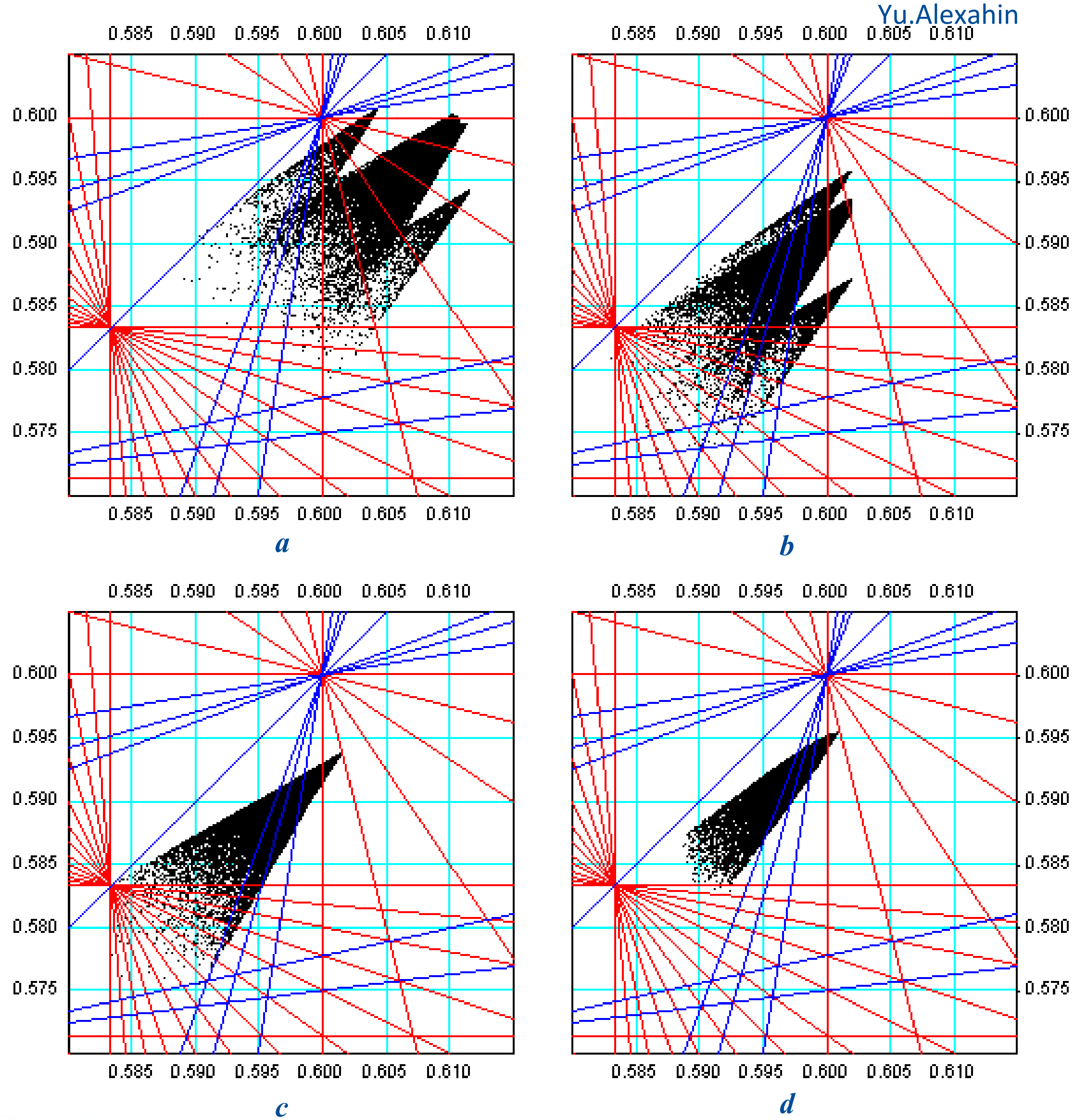

- Tev Run II: 36x36 bunches in 3 trains
- compensate beam-beam tune shifts
  - a) Run II Goal
  - b) one TEL
  - c) two TELs
  - d) 2 nonlinear TELs
- requires
  - 1-3A electron current
  - stability dJ/J<0.1%
  - e-pbar centering
  - e-beam shaping

Electron Charge Distribution

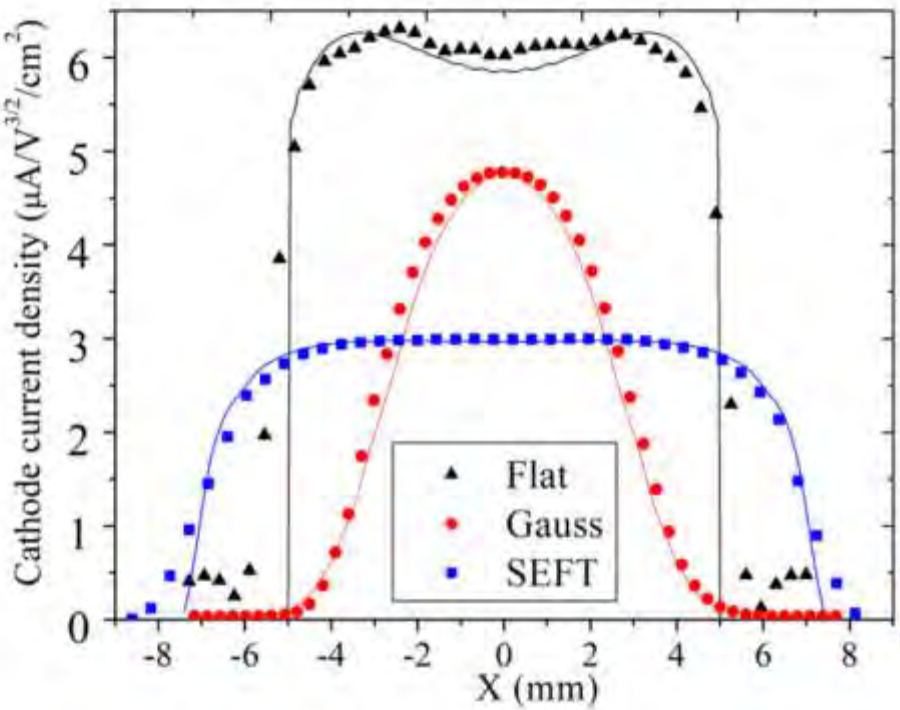

Figure 2. Three profiles of the electron current density at the electron gun cathode: black, flattop profile; red, Gaussian profile; blue, SEFT profile. Symbols represent the measured data and the solid lines are simulation results. All data refer to an anode–cathode voltage of 10 kV.

Shiltsev et al., *PRL* 99, 244801 (2007).
Shiltsev et al., NJP 10, 043042 (2008).

Electron gun

Copper anode

side view

top view

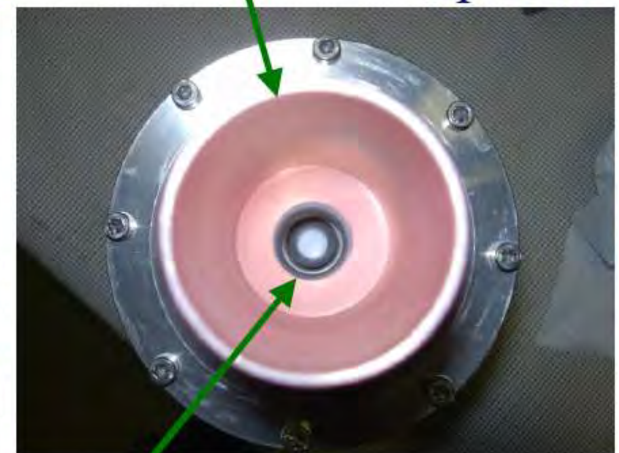

Tungsten dispenser cathode with convex surface

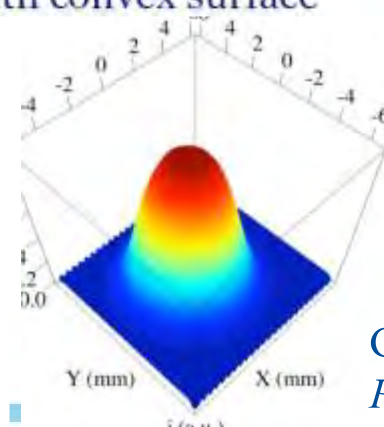

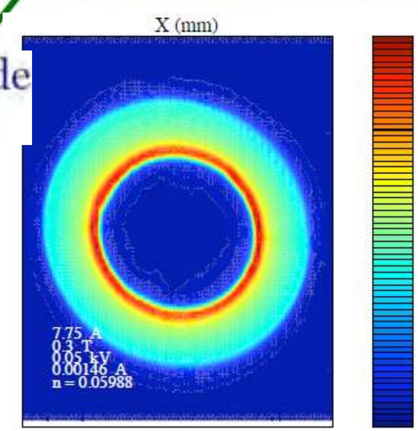

G. *Stancari*, et al., (2011)
Phys. Rev. Lett. 107, 084802

TEL e-beam aligned and timed on protons

in space

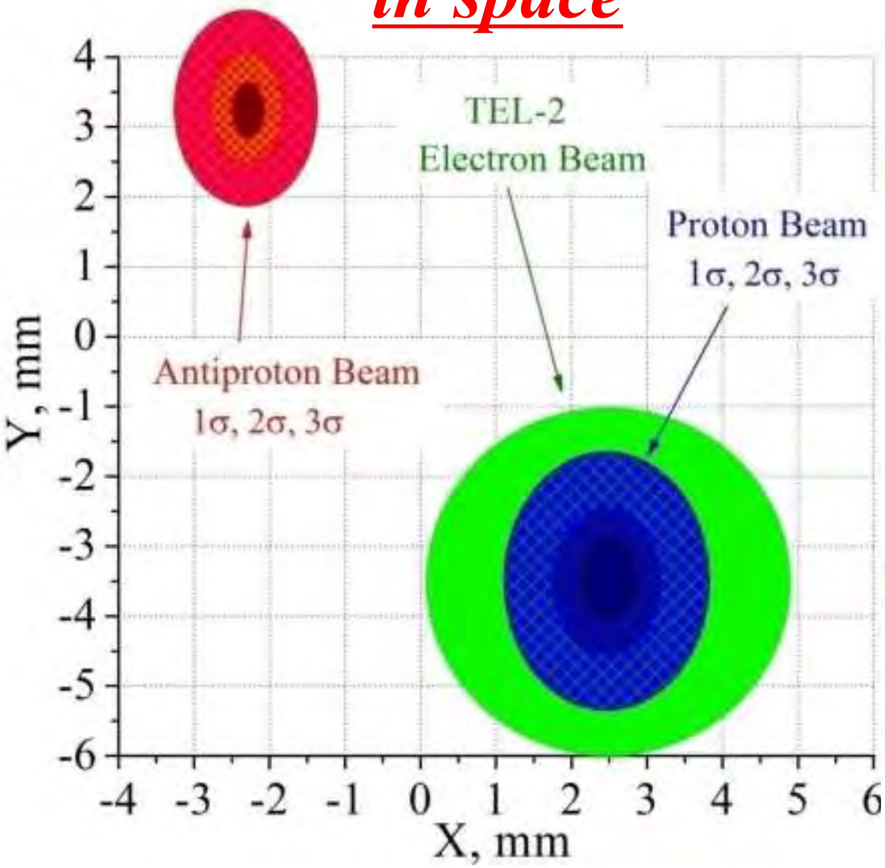

in time

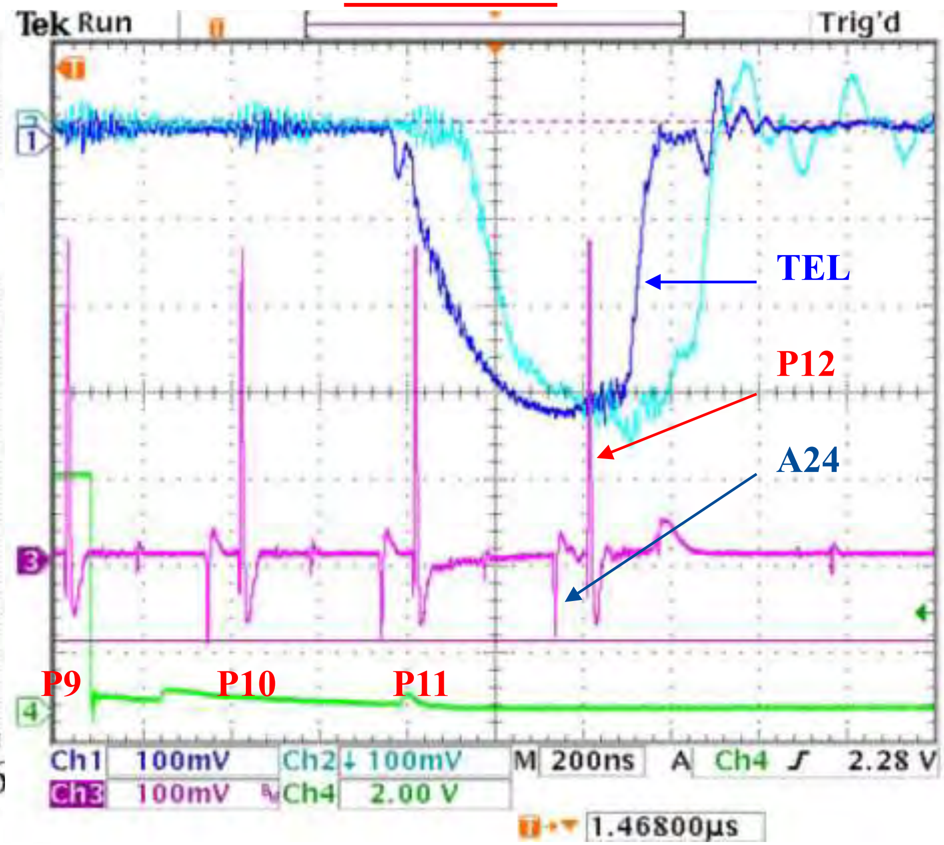

Transverse e-p alignment is very important for minimization of noise effects and optimization of positive effects due to e-beam. _Timing_ is important to keep protons on flat top of e-pulse – to minimize noise and maximize tune shift.

Tevatron Electron Lenses (2001-2011)

- Technology proven, tune shift ~0.01 demo'd
- First successful active compensation
- *Head on effects compensation:*
  - Reduced emittance growth of a PACMAN antiproton bunch ("scallops" effect)
- *Long range effects compensation:*
  - Significant (x2) improvement of the lifetime of most affected proton bunches
    - By shifting tunes of otherwise unfavorable bunch away from resonances

Tuneshift dQ_{hor}=+0.009 by TEL

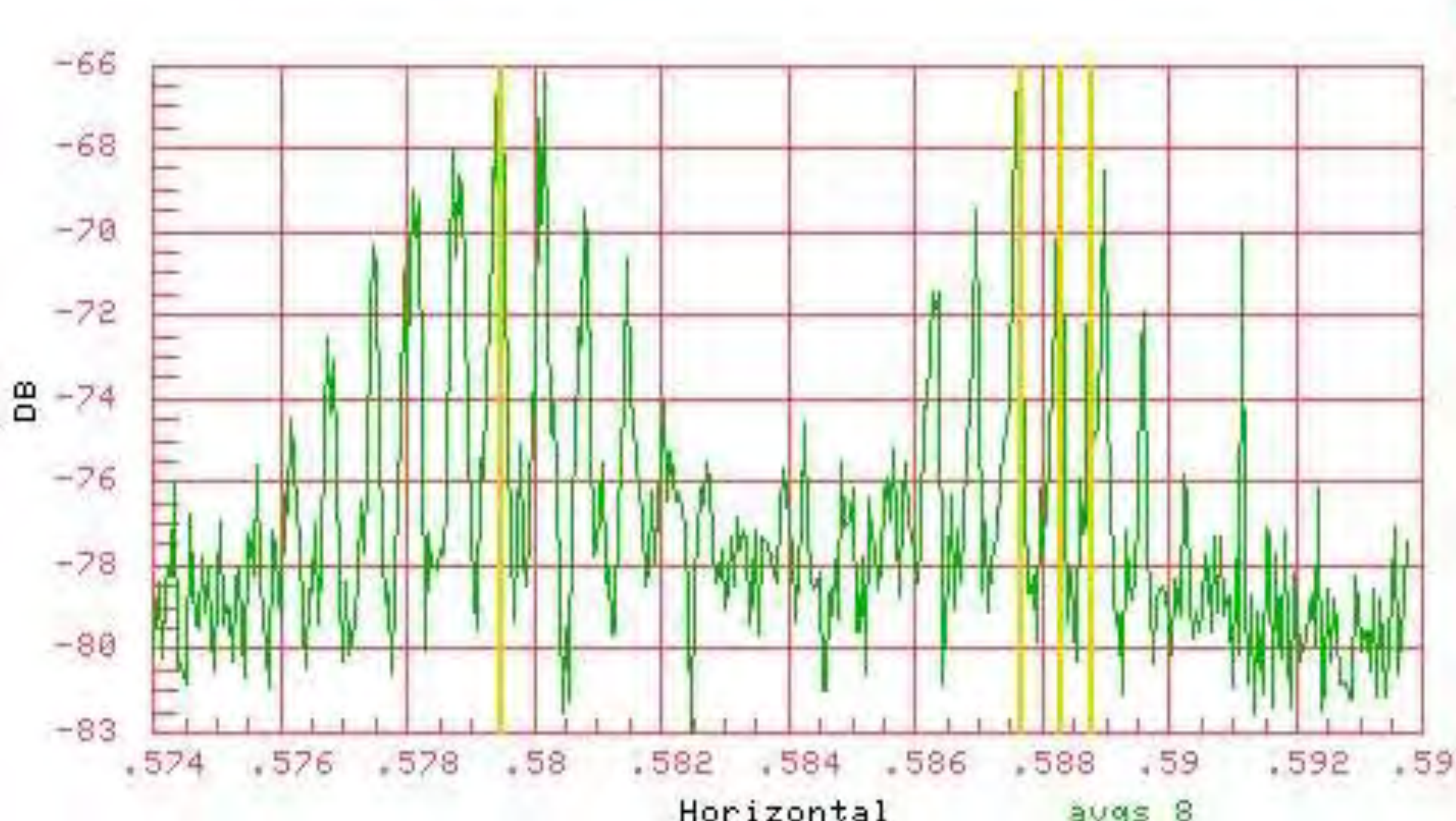

Three bunches in the Tevatron, the TEL acts on one of them

"Scallops" in Pbar Bunch Emittances

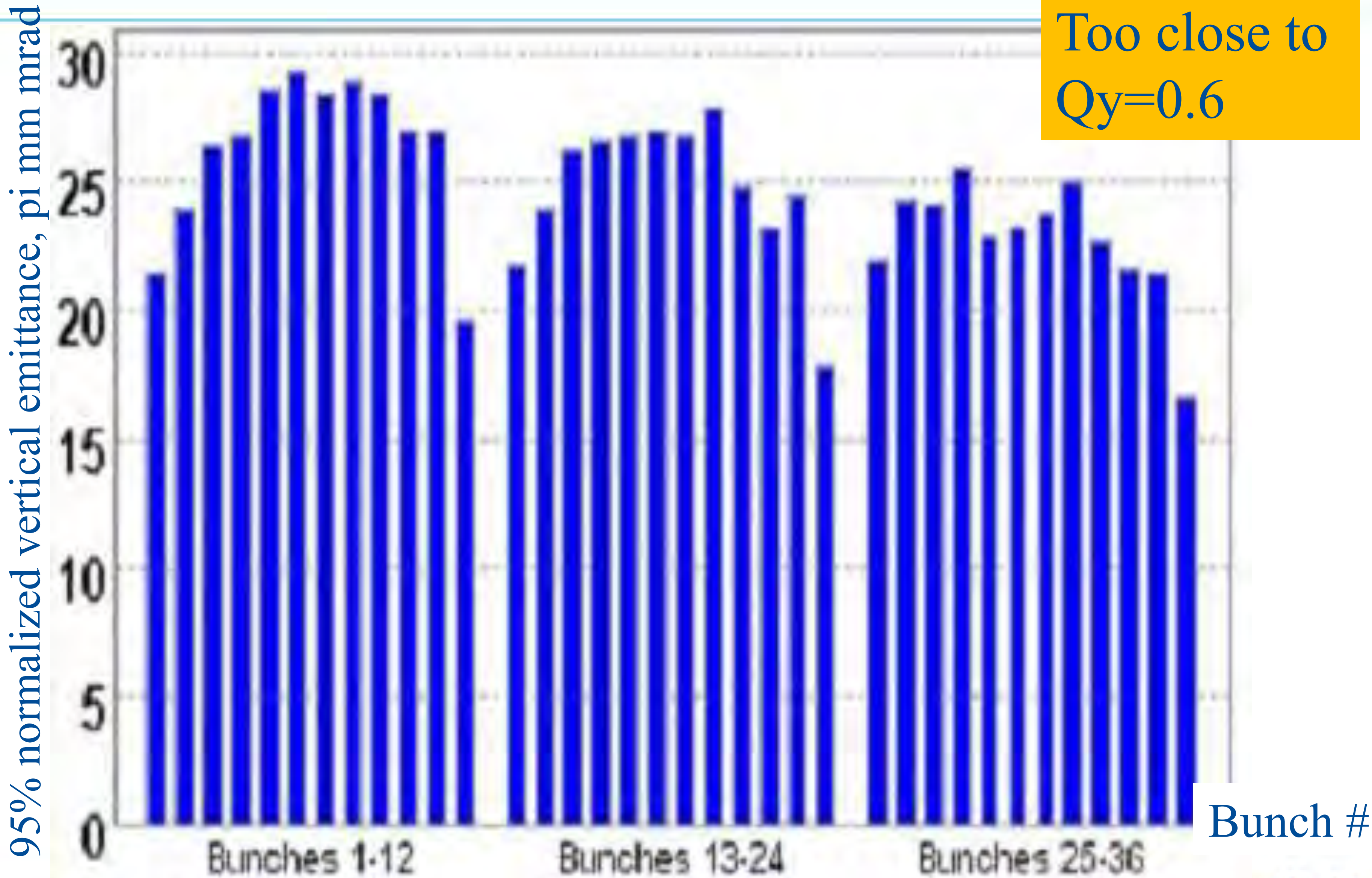

Too close to Qy=0.6

ittance Growth of A33 Suppresed by TEL

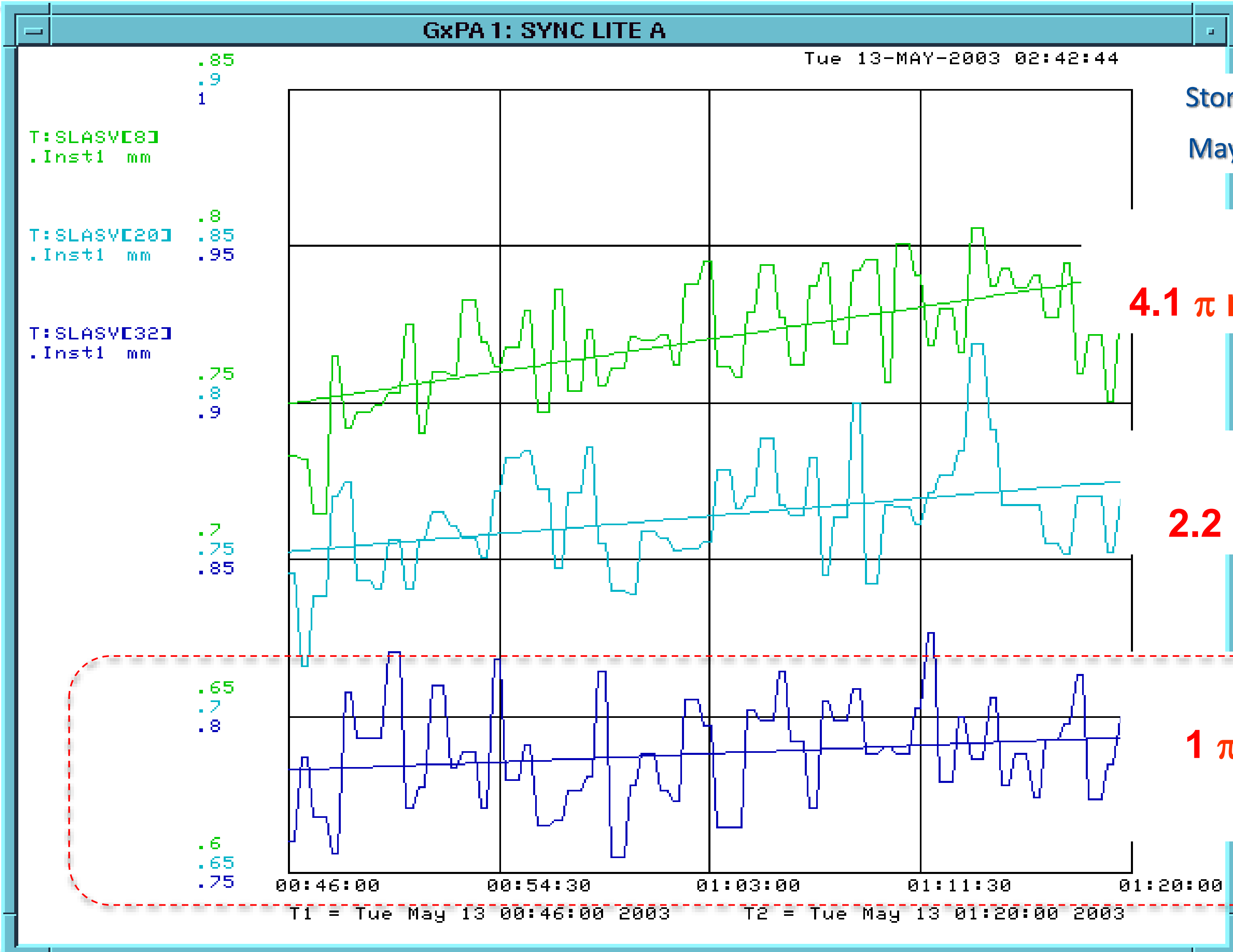

Store #2540

May 12, '03

A9

4.1 π mm mrad/hr

A21

2.2 π mm mrad/hr

A33

1 π mm mrad/hr

-TEL on it

TEL2 on One Proton Bunch P12

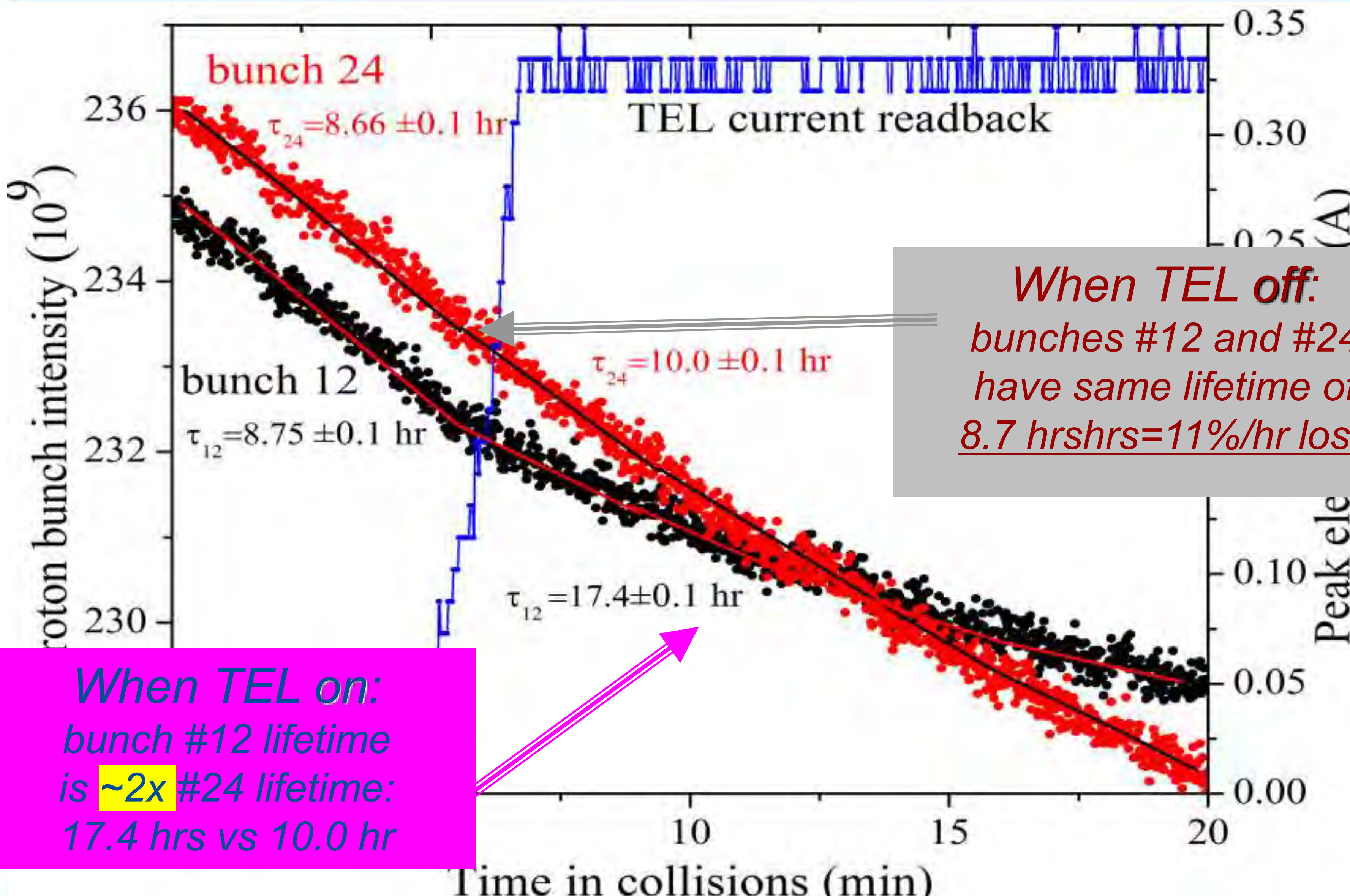

When TEL off:
bunches #12 and #24
have same lifetime of
8.7 hrshrs=11%/hr loss

When TEL on:
bunch #12 lifetime
is ~2x #24 lifetime:
17.4 hrs vs 10.0 hr

Approach #3: Head-On Comp'n in RHIC

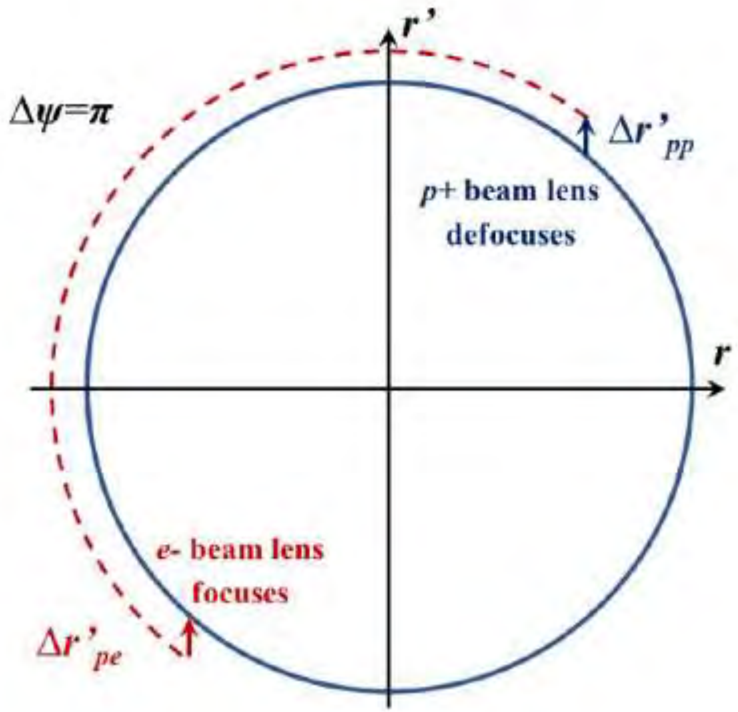

(W.Fischer et al)

With e-lens, one can compensate Head-On effect: not only the tune footprint, but also the *resonant driving terms* if elens is placed 180 degrees (betatron phase) away from the main IP (one IP compensation)

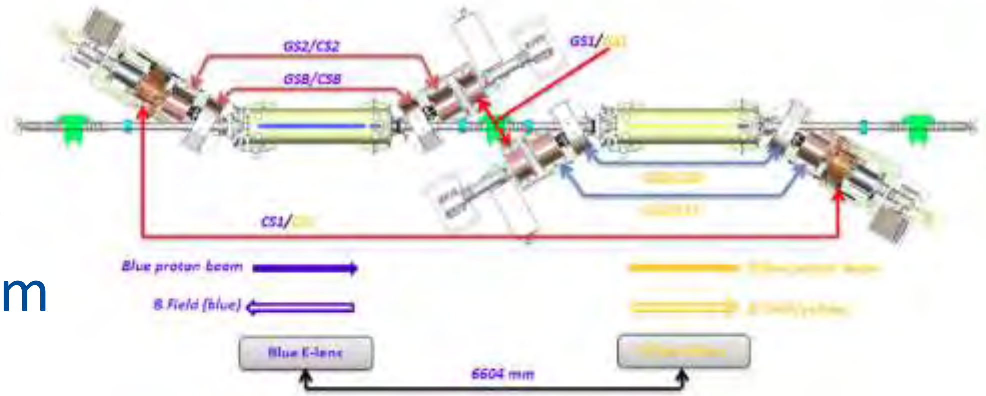

RHIC pp 2015 elens Success

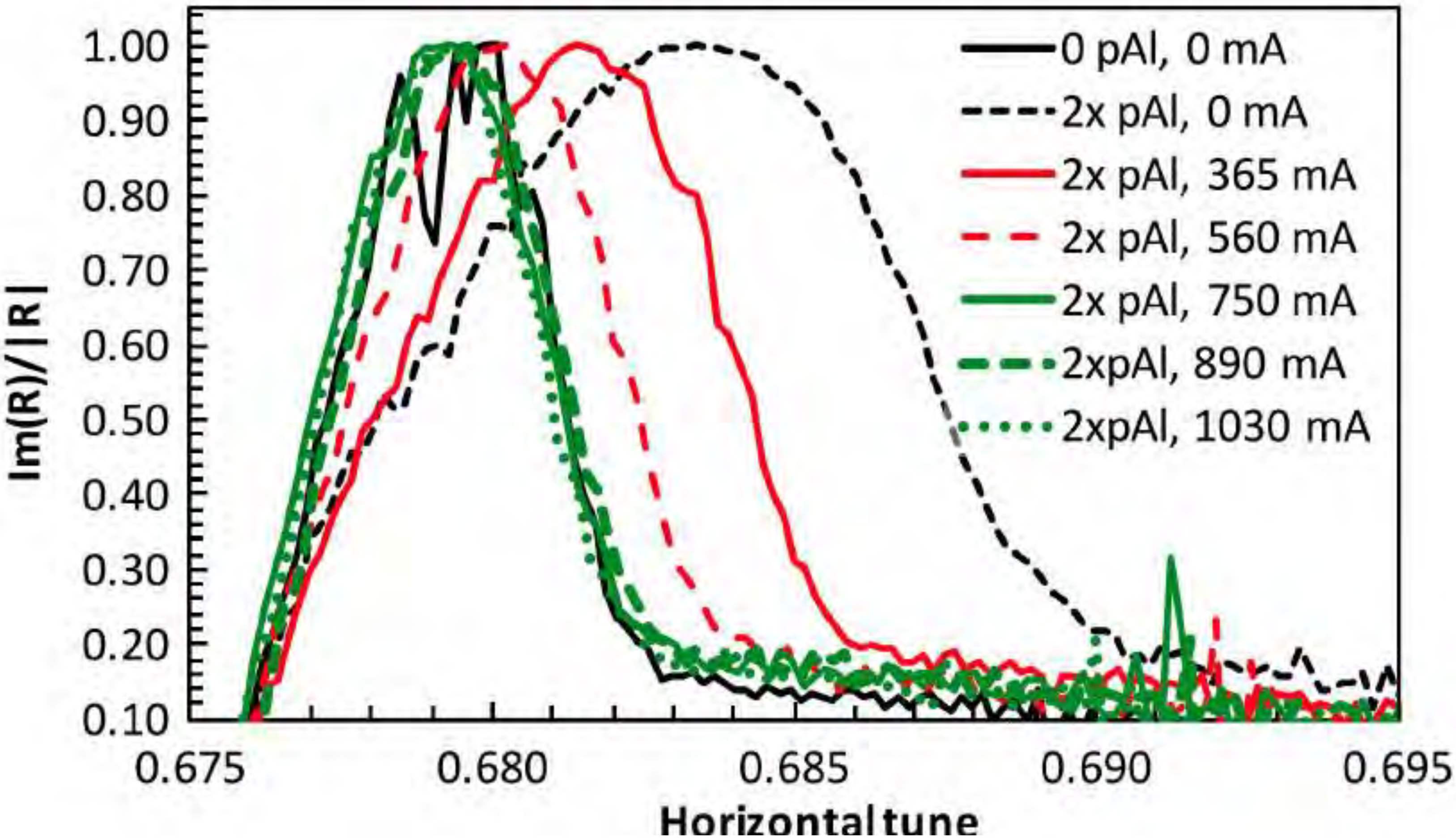

Figure 7: Tune distribution width reduction with the RHIC electron lens, measured in the proton beam with $p+Al$ collisions. The distribution widens due to two beam-beam interactions, and narrows again with increase of the electron lens current to 1.03 A [9].

RHIC pp 2015 elens in Ops

Electron lens parameters

Distance of center from IP	m	1.5	1.5
Effective length L_e	m	2.1	2.1
Kinetic energy E_e	kV	5	5
Relativistic factor β_e		0.14	0.14
Relativistic factor γ_e		1.0002	1.0002
Current I_e	A	1.0	0.43/0.60
Electron beam size at interaction	μm	350	650
Linear tune shift		0.0147	0.01

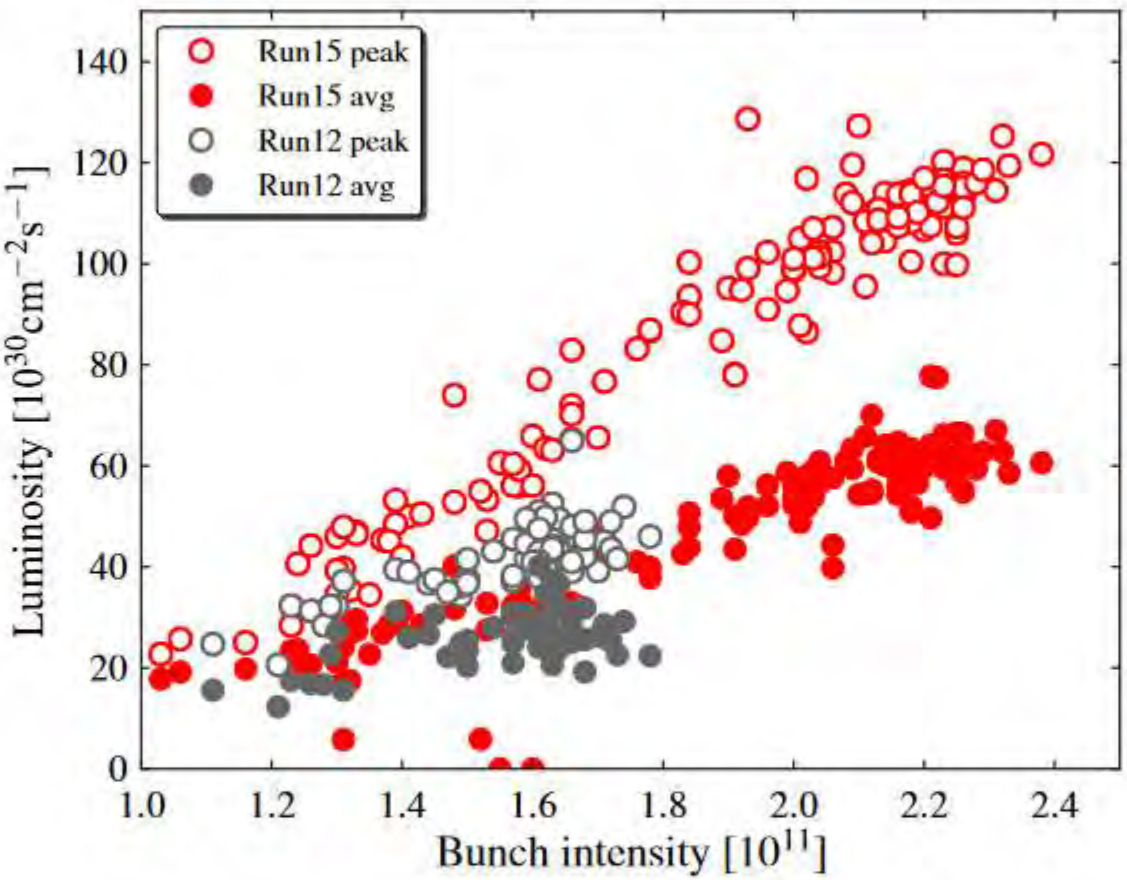

With 0.6A, 2.1m long, 5 kV e-beam, essentially:
- one out of 2 IP head-on effect cancelled,
- max allowed beam intensity increased by ~40%,
- peak average lumi ~tripled, averaged lumi ~ doubled

FIG. 3. Peak and average store luminosity in polarized proton operation at 100 GeV beam energy in 2012 and 2015.

Fermilab

Approach #4 : Wire Compensation of Long Range Beam-Beam Interactions

Fields of separated p+ beam:

$E \sim N_{IPs} N_p / d$

$B = E$

Field of separated conductor (wire):

$E = 0$

$B \sim 2 J_e / d$

Combined effects of p+ beam + e- beam will cancel out if

wire is placed at the same d

wire kick Jxlength matches $N_{IPs} N_p$

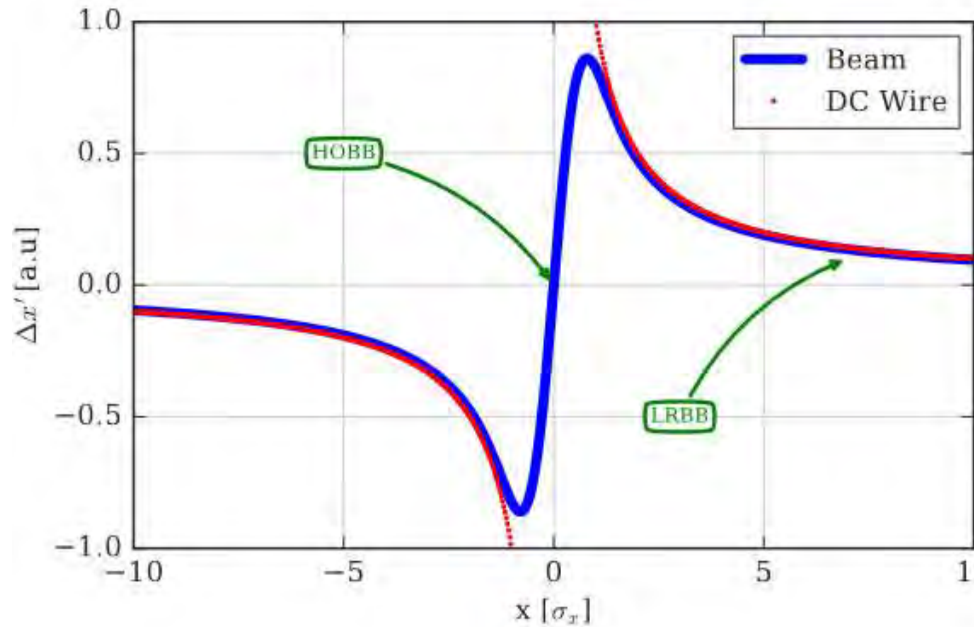

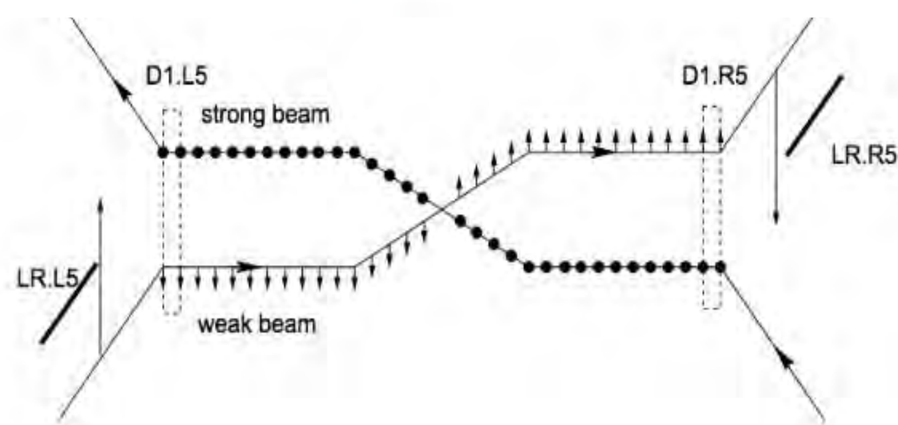

(J.P.Koutchouk, G.Sterbini et al)

Wire Compensation in the LHC (2018)

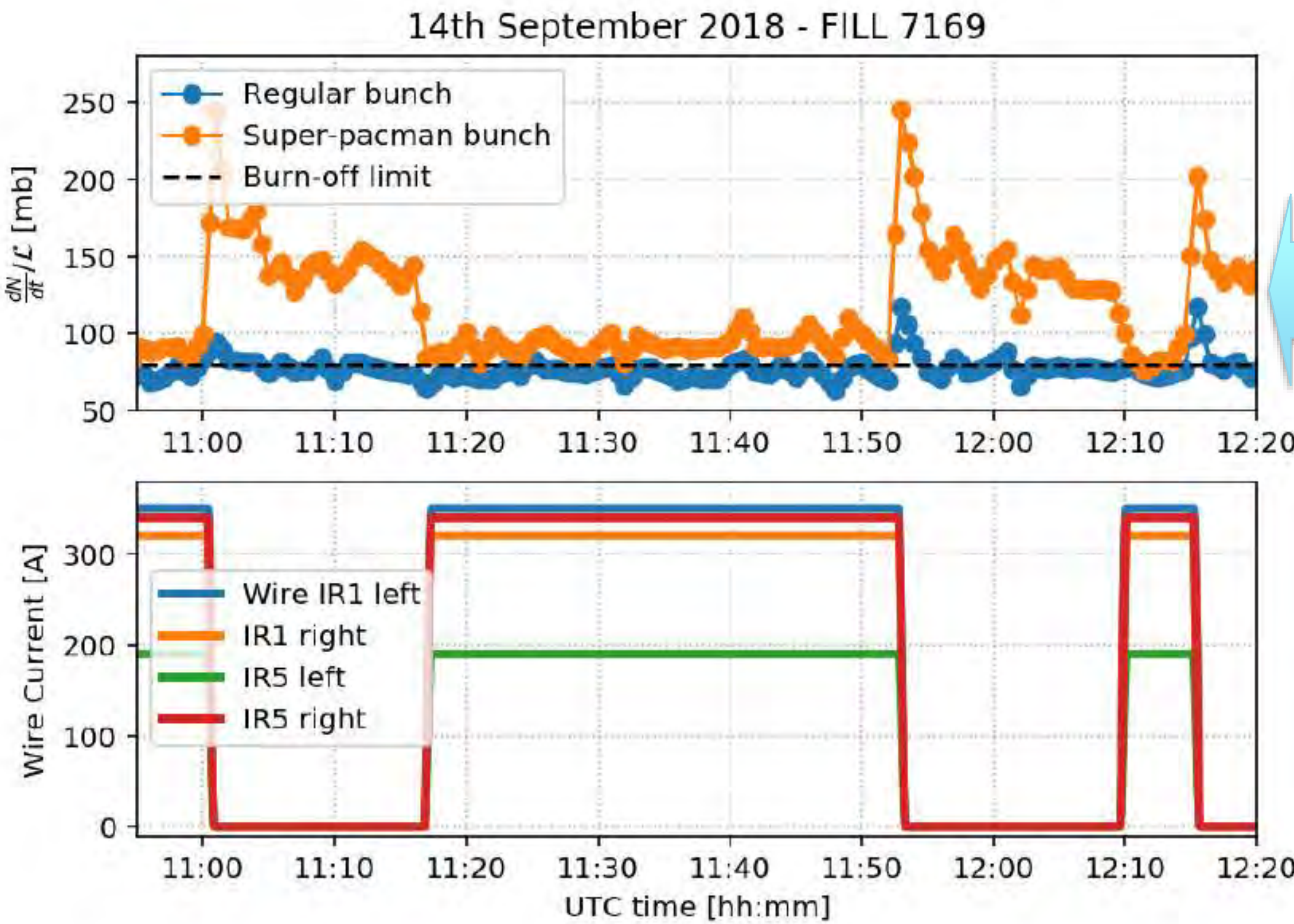

Proton losses in collisons are due to: Luminosity burn up *dN/dt=-L*x80 mbarn

and beam-beam effects - different for regular and PACMAN bunches

So, plotted is *dN/dt/Lumi* for regular and PACMAN bunches

Not mentioned here (but will be later)

- Beam-beam effects in linear colliders
- Beamstrahlung
- Asymmetric beams
- Synchrobetatron coupling
- Crabbed and crab-waist schemes
- Monochromatization
- Beam-beam simulation codes

... etc.

Thanks for Your Attention !

Questions !?

Literature

- W.Herr, CAS school

https://cds.cern.ch/record/941319/files/p379.pdf

- V.Lebedev, V.Shiltsev, Tevatron Book Ch.8

https://indico.cern.ch/event/774280/attachments/1758668/2915590/2014_Book_AcceleratorPhysicsAtTheTevatro.pdf

- Proc. 2013 ICFA mini-workshop on "Beam-Beam Effects in Hadron Colliders"

https://indico.cern.ch/event/189544/

- Past schools :
  - A. Chao, The beam-beam instability, SLAC-PUB-3179 (1983).
  - L. Evans, The beam-beam interaction, CAS Course on proton-antiproton
  - colliders, in CERN 84-15 (1984).
  - L. Evans and J. Gareyte, Beam-beam effects, CERN Accelerator School, Oxford
  - 1985, in: CERN 87-03 (1987).
  - A. Zholents, Beam-beam effects in electron-positron storage rings, Joint
  - US-CERN School on Particle Accelerators, in Springer, Lecture Notes in
  - Physics, 400 (1992).

U.S. Particle Accelerator School

Education in Beam Physics and Accelerator Technology

Fermilab

Managed by Fermi Research Alliance, LLC for the U.S. Department of Energy Office of Science

Colliders: a) Important Effects and Phenomena b) circular e+e- colliders

Vladimir Shiltsev, Fermilab

part of the "Colliders" class by V.Lebedev, N.Mokhov and V.Shiltsev

US Particle Accelerator School, Jan 24 – Feb 4, 2022

Important Effects (besides Beam-beam)

- Space-charge effects
- Instabilities
- Diffusion and Intrabeam scattering
- Cooling
- Collimation
- Synchrotron radiation
- Beamstrahlung
- Polarization (see lecture VS9)

Intense Beams : Forces and Losses (1)

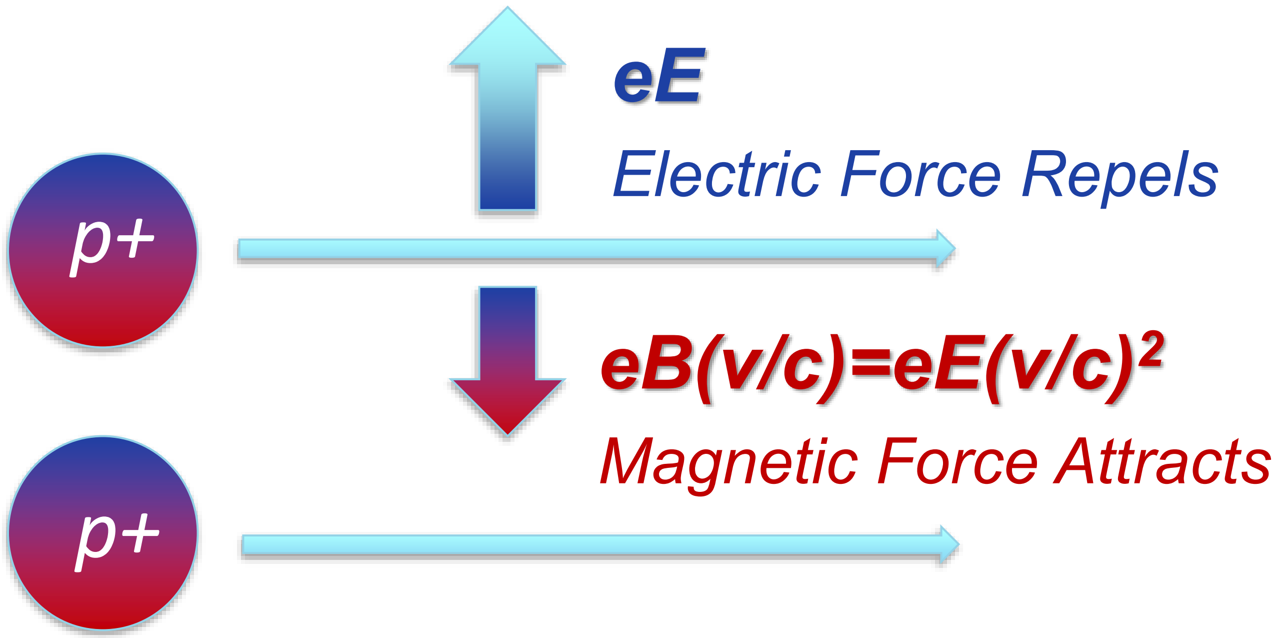

Net Force: Repels

$$eE - eE(v/c)^2 = eE\,(1-\beta^2) = eE/\gamma^2$$

Intense Beams : Forces and Losses (2)

Defocusing Force is Non-linear

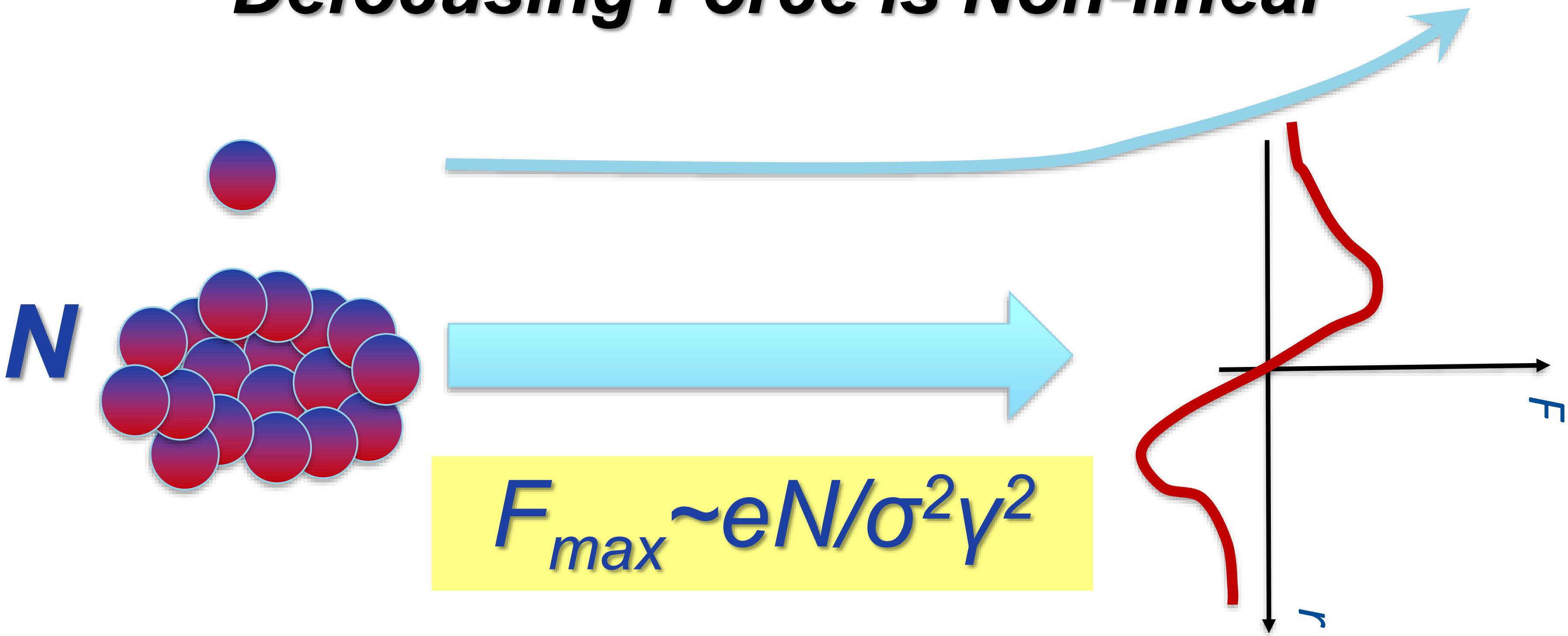

$$F_{max} \sim eN/\sigma^2\gamma^2$$

Space-charge effects (emittance growth, losses):

a) proportional to current (N)

b) scale inversely with beam size (σ)

c) scale with time at low energies (γ)

Linacs 5-20 MeV/m
Rings 0.002-0.01 MeV/m

Space-charge effects: Proton Rings

- SC tune shift

$$\Delta Q_{SC} = -\frac{N_p r_p B_f}{4\pi\varepsilon\beta_p\gamma_p^2}$$

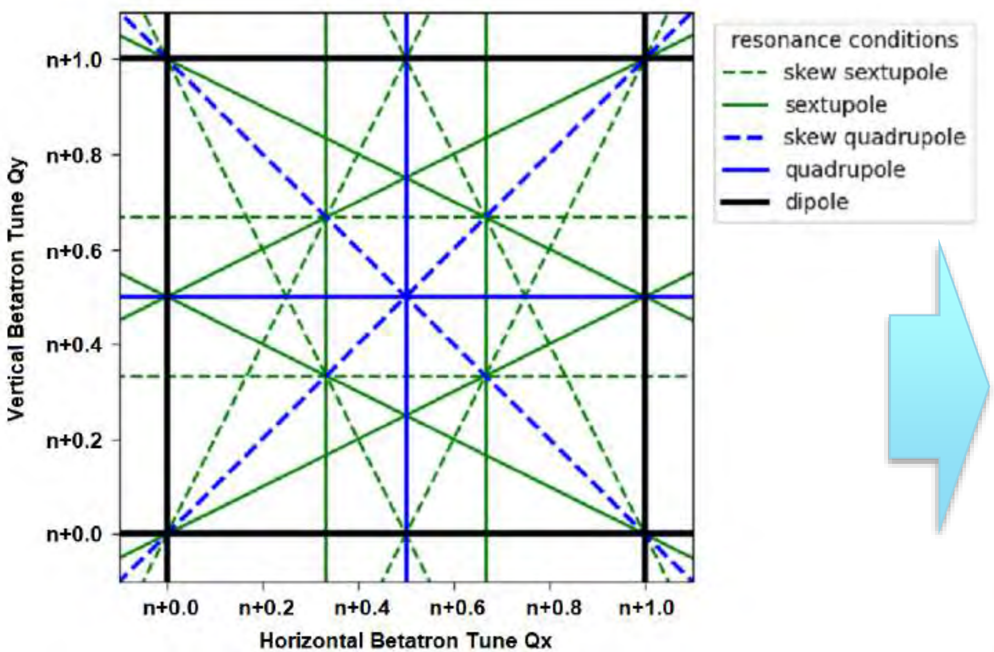

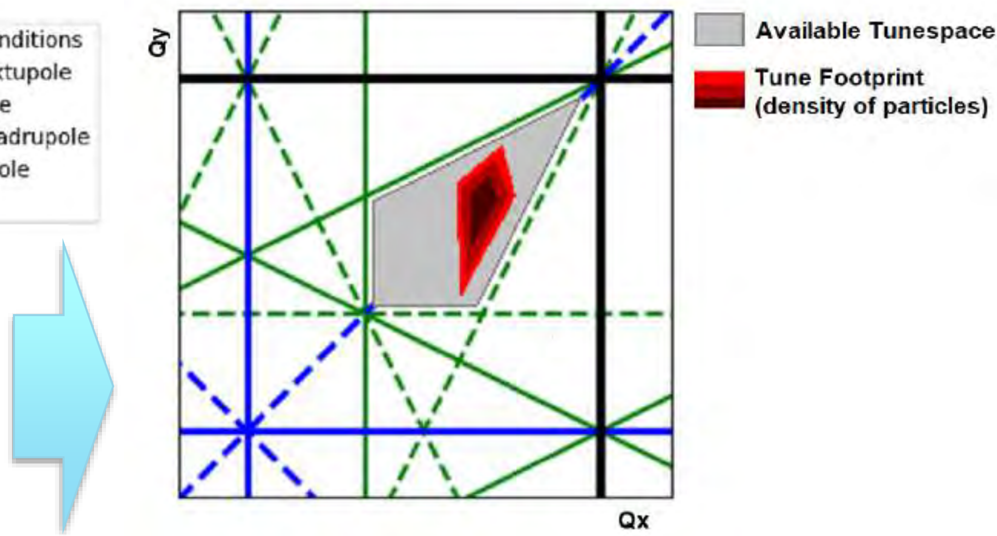

Max SC tuneshift Achieved: -0.2…-0.5

	E_i/E_p	N_p	T	P	ΔQ_{sc}	$\%_{N_p}$	$\%_\epsilon$	C	S	$Q_{h,v}$
ISIS	0.07/0.80	3.1	0.01 s	200	0.4	2		163	10	4.31/3.83
PS-B	0.05/1.4	0.25	1.2	n/a*	0.50	5	20	157	16	4.3/4.45
CSNS	0.08/1.6	1.6	0.02	100	0.28	1	20	228	4	4.86/4.78
J-RCS	0.4/3	4.2	0.02	500	0.35	0.3	10	348	3	6.45/6.32
FNAL-B	0.4/8	0.45	0.03	84	0.60	5	20	474	24	6.78/6.88
CERN-PS	1.4/28	1.5	3.6	n/a*	0.24	3	5	628	50	6.12/6.24
JPARC-MR	3/30	27	1.5	515	0.4	1.5	10	1568	3	21.35/21.43
FNAL-MI	8/120	5.1	0.62	803	0.09	2.5	5	3319	1	26.46/25.38
CERN-SPS	28/450	0.9	19	n/a*	0.21	5	10	6911	6	20.13/20.18
PSR	0.8	3.1	6e-4	80	0.29	0.3		90	10	3.18/2.19
SNS-R	1	14	0.001	1400	0.15	0.01		248	4	6.23/6.20
FNAL-RR	8	5.2	0.84	54	0.09	2.5	10	3319	1	25.44/24.43

Figure 3: Operational high intensity RCSs and accumulator rings: injection/extraction kinetic energies E_i/E_p in GeV, number of protons per pulse N_p in 10^{13}, beam acceleration/storage time T in s, average beam power P in kW, maximum SC tune shift ΔQ_{sc}, fractional intensity loss $\%_{N_p} = \Delta N_p/N_p$ and emittance growth $\%_\epsilon = \Delta\epsilon/\epsilon$ in %, circumference C in m, lattice periodicity S and tunes $Q_{h,v}$. (* For CNGS operation in 2005-2012, the SPS delivered 510 kW average power at 400 GeV). Figure and caption from [10].

Ways to Increase "Protons Per Pulse"

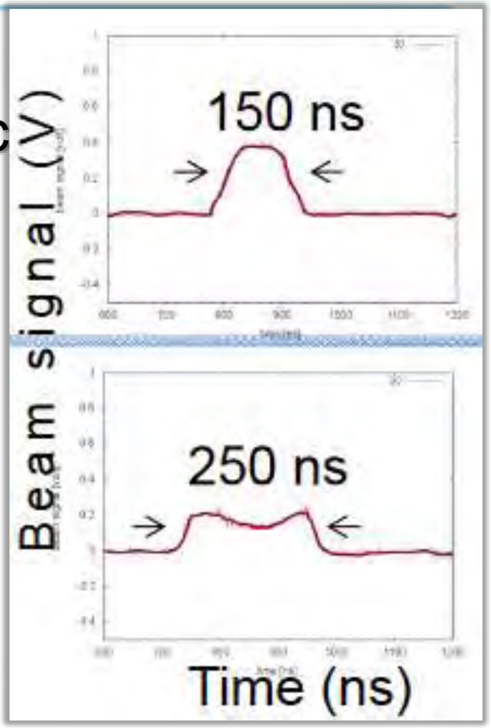

- **Increase the injection energy**:
  - Gain about $N_p \sim \beta\gamma^2$, need (often - costly) linac
- **Flatten the beams** (using 2nd harm, RF) :
  - Makes SC force uniform, $N_p \sim$ x2
- **"Painting" beams** at injection:
  - To linearize SC force across beams $N_p \sim$x1.5
- **Better collimation system beams:**
  - From $\eta \sim 80\%$ to ~95% $N_p \sim$x1.5
- **Make focusing lattice perfectly periodic**:
  - Eg P=24 in Fermilab Booster, P=3 in JPARC MR → $N_p \sim$ x1.5
- **(to be tested) Introduce *Non-linear Integrable Optics*** :
  - May reduce the losses and allow $N_p \sim$ x 1.5-2
- **(tbt) Space-Charge Compensation** by electron lenses :
  - Electrons to focus protons, may allow $N_p \sim$x1.5 - 2

Space-Charge Compensation R&D

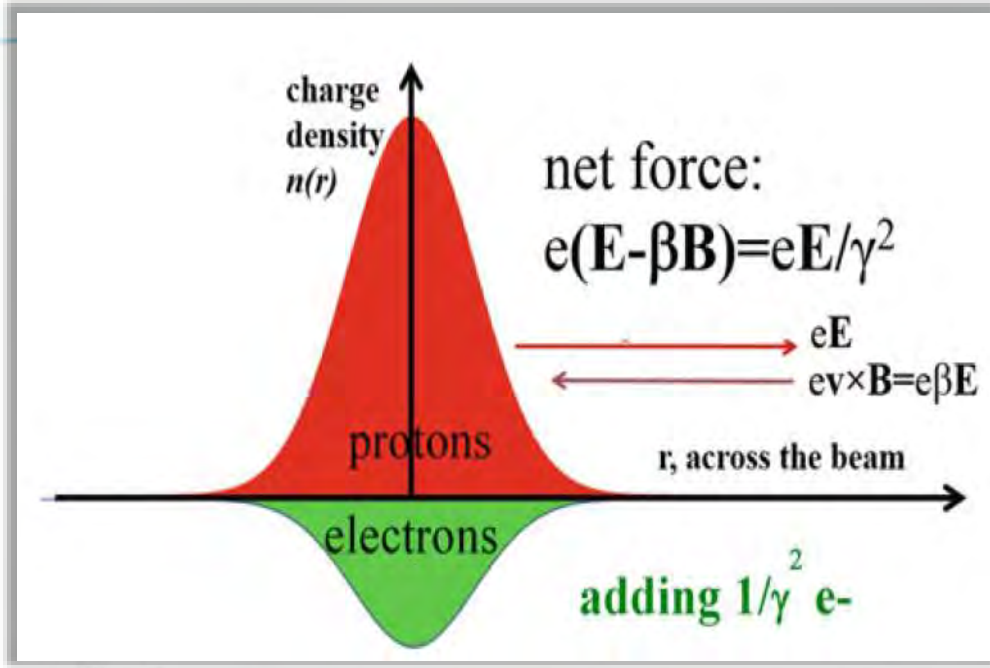

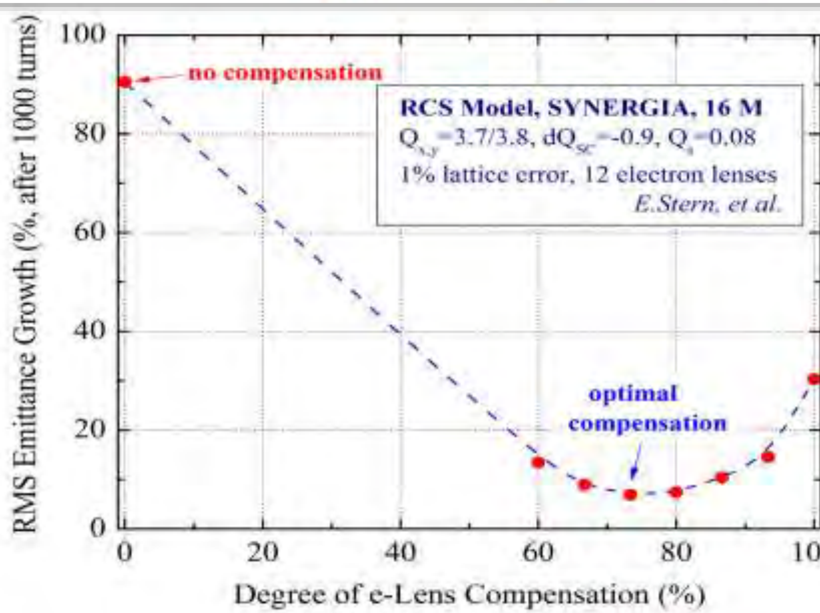

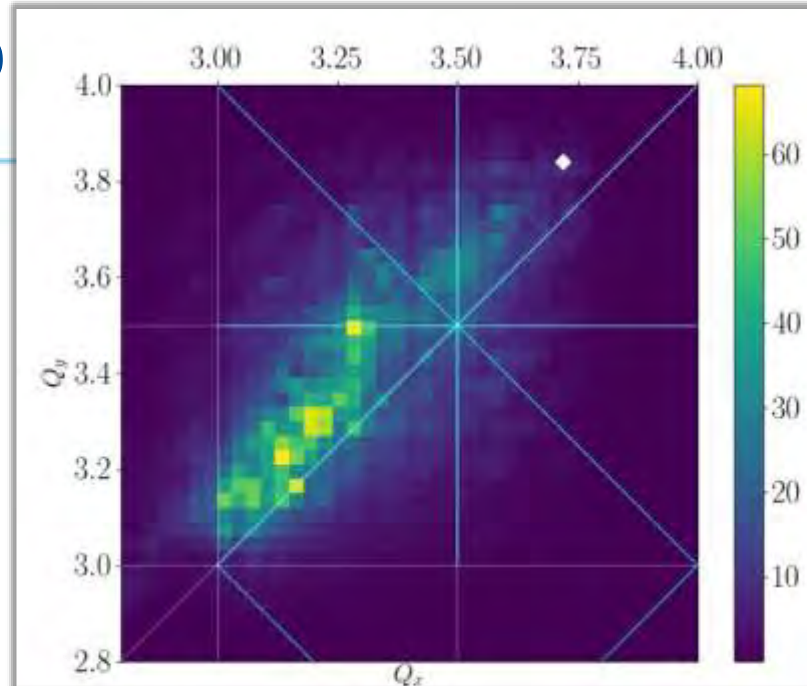

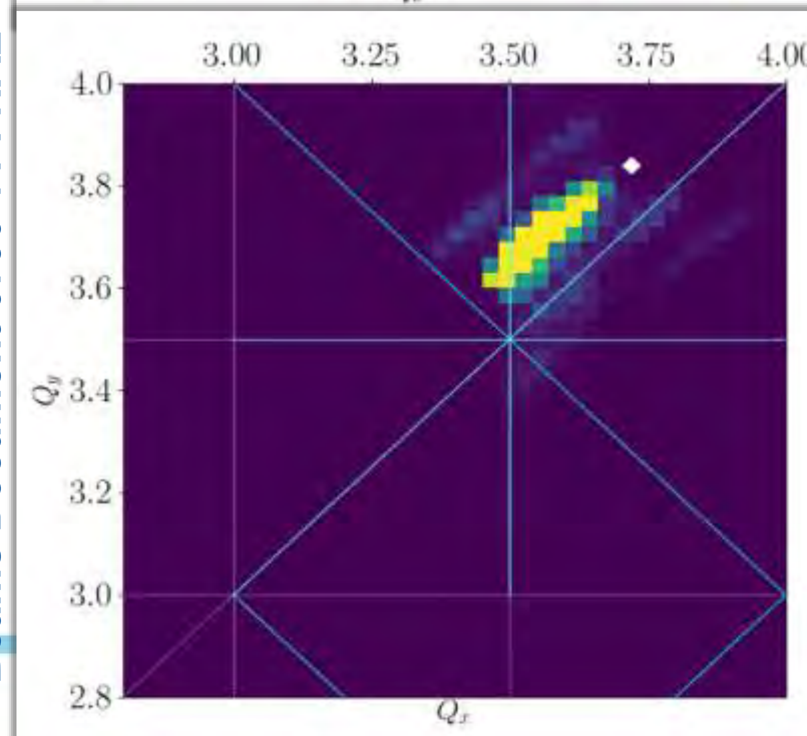

IOTA: *Integrable Optics Test Accelerator @ FNAL*

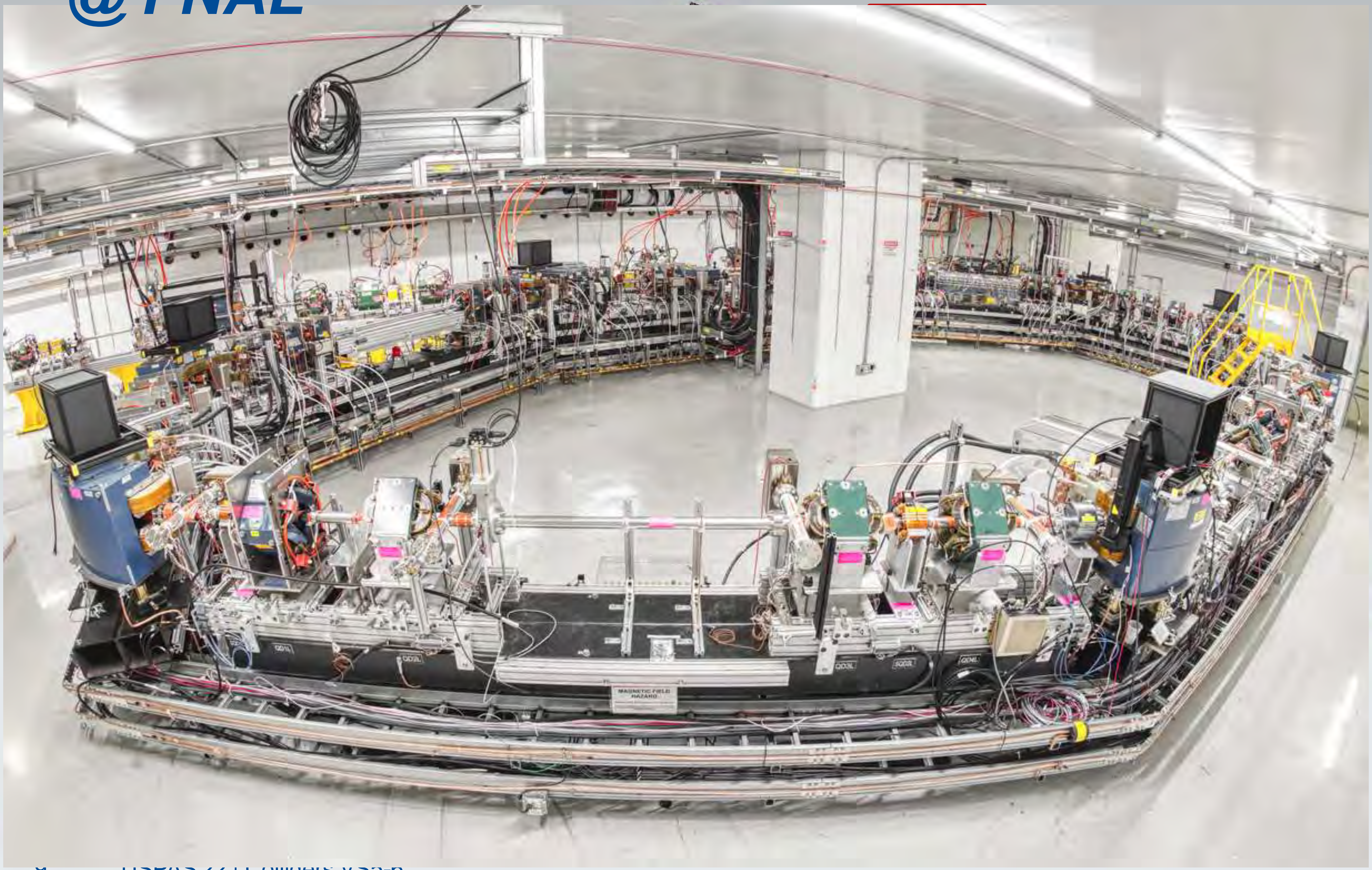

Instabilities

- Beam instabilities are driven by the **electromagnetic interaction with the accelerator environment** (-> **wakefields/impedances**) and by **electron clouds**.
- Above a certain **intensity threshold** the beam's oscillation amplitude increases exponentially and the beam is either **lost at the wall** (transverse instabilities) or from the rfbucket (longitudinal) and/or the **emittance increases**.
- Presently, heat loads and instabilities are one of the **main beam quality and intensity limitation** in particle accelerators for high intensity and brightness !
- Finding "**cures" for instabilities** is one of the major challenges in beam physics and accelerator technology for **future machines**.
- **High energy beams:** Beam instabilities are a 'current effect'. However, synchrotron radiation, photoelectrons or other high energy effects affect instability thresholds.

Maxwell’s equations and Lorentz Force

$$\nabla \cdot \boldsymbol{E} = \frac{\rho}{\varepsilon_0}$$

$$\nabla \cdot \boldsymbol{B} = 0$$

$$\nabla \times \boldsymbol{E} = -\frac{\partial \mathbf{B}}{\partial t}$$

$$\nabla \times \boldsymbol{B} = \mu_0 \mathbf{j} + \frac{1}{c^2}\frac{\partial \boldsymbol{E}}{\partial t}$$

+ boundary conditions at the walls

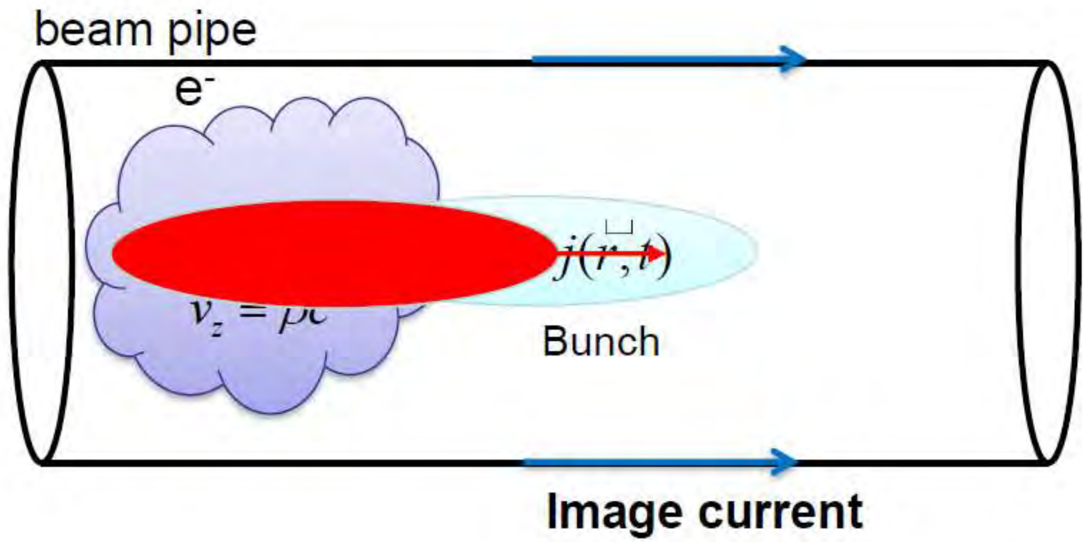

Impulse approximation

$$c\Delta \boldsymbol{p} = q\int_{-\infty}^{\infty} (\boldsymbol{E} + \boldsymbol{v} \times \boldsymbol{B})\, ds$$

The EM force continuously acting on a test charge is lumped in a single kick after the passage through the structure.

Rigid bunch approximation

$$j = \beta_0 c \rho e_z$$

The beam traverses the structure rigidly.

EM forces due to : a) wake fields and impedances, b) electron cloud, c) beam-beam, d) etc

more on b) and c) in later lectures

Wake-fields

$$W(\mathrm{r}_2, \mathrm{r}_1, z) = -\frac{1}{q_1}\int_{-\infty}^{\infty} [\mathrm{E} + \mathrm{v} \times \mathrm{B}]\left(\mathrm{r}_2, z, t = \frac{z+s}{c}\right) ds$$

T. Weiland and R. Wanzenberg, "Wake Fields and Impedances," in CERN Accelerator School (CAS), 1993. 20, 28, 99

L. Palumbo, V. G. Vaccaro, and M. Zobov, "Wake Fields and Impedance," in Cern Accelerator School, 1994. 20

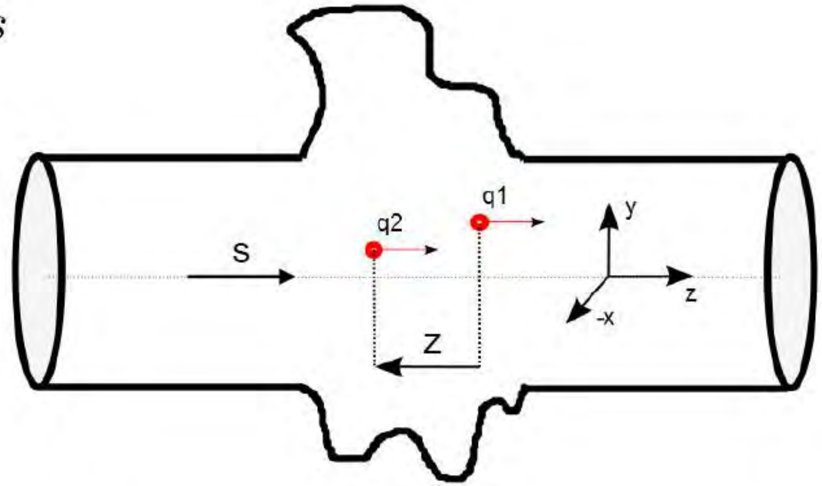

Longitudinal:

$$W_{\parallel}(z) = -\frac{1}{q_1}\int_{-\infty}^{\infty} E_z\left(\mathrm{r}_2 = 0, z, t = \frac{z+s}{c}\right) ds$$

Transverse:

$$W_{\perp}(z) = -\frac{1}{q_1 d_1}\int_{-\infty}^{\infty} [\mathrm{E} + \mathrm{v} \times \mathrm{B}]_{\perp}\left(\mathrm{r}_2 = 0, z, t = \frac{z+s}{c}\right) ds$$

Wake-fields - Examples

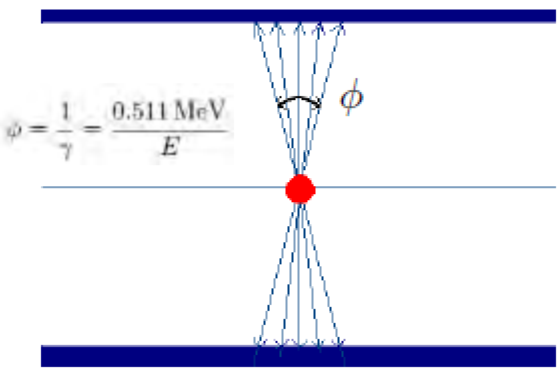

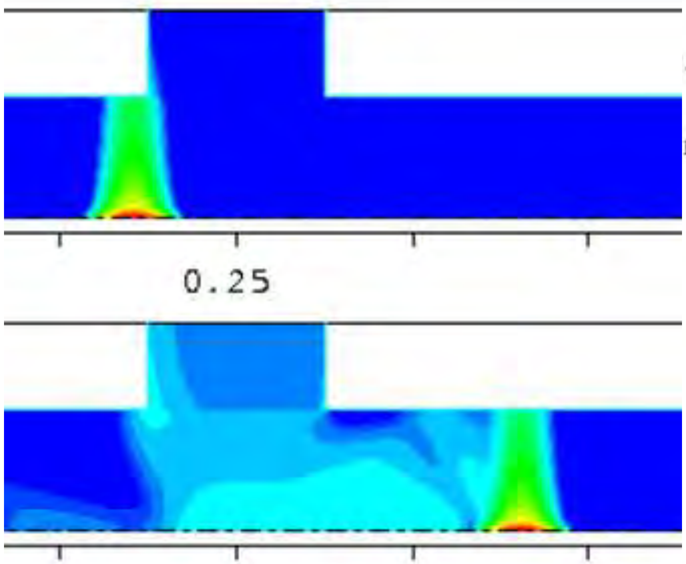

Wake fields in a cavity

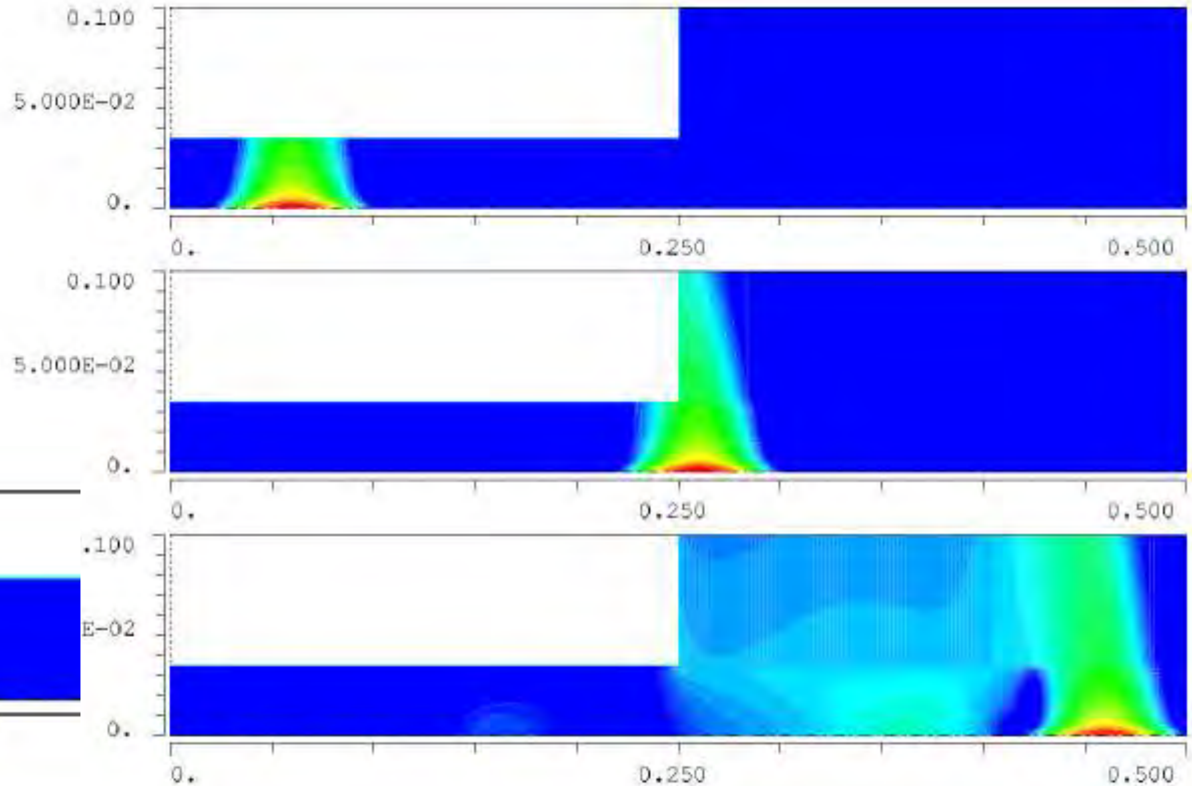

Wake fields behind a bunch generated at a step-out transition from a small to a larger beam pipe

What is you have many particles

- Wake-functions

Longitudinal: $\int_0^L F_z ds = -q^2 W_{\parallel}(z)$

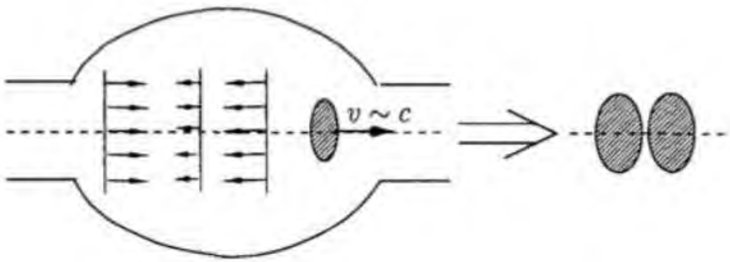

For a test particle in a bunch:

$$\int_0^L F_z ds = qV \qquad V = -q \int W_{\parallel}(z-u)\,\lambda(u)\,du$$

(Voltage kick or Wake potential)

Line density: $\lambda(z) = \dfrac{dN}{dz}$

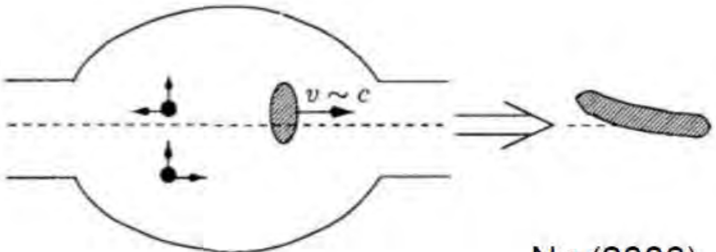

Ng (2006)

Transverse: $\int_0^L F_{\perp} ds = -q^2 r W_{\perp}(z)$

For a test particle in a bunch:

$$\frac{1}{\gamma_0 mc^2}\int_0^L F_x ds = \Delta x' \qquad \Delta x' = -\frac{q^2}{\gamma_0 mc^2}\int W_{\perp}(z-u)\,\lambda(u)\,\bar{x}(u)\,du$$

(horizontal kick)

$\bar{x} = \langle x \rangle$: local bunch offset

Even "simple" resistive wall leaves wakes

Longitudinal: $$W_{\parallel}(z) = \frac{c}{4\pi b}\sqrt{\frac{Z_0}{\pi\sigma}}\frac{L}{|z|^{3/2}}$$

Transverse: $$W_{\perp}(z) = \frac{c}{\pi b^3}\sqrt{\frac{Z_0}{\pi\sigma}}\frac{L}{|z|^{1/2}}$$

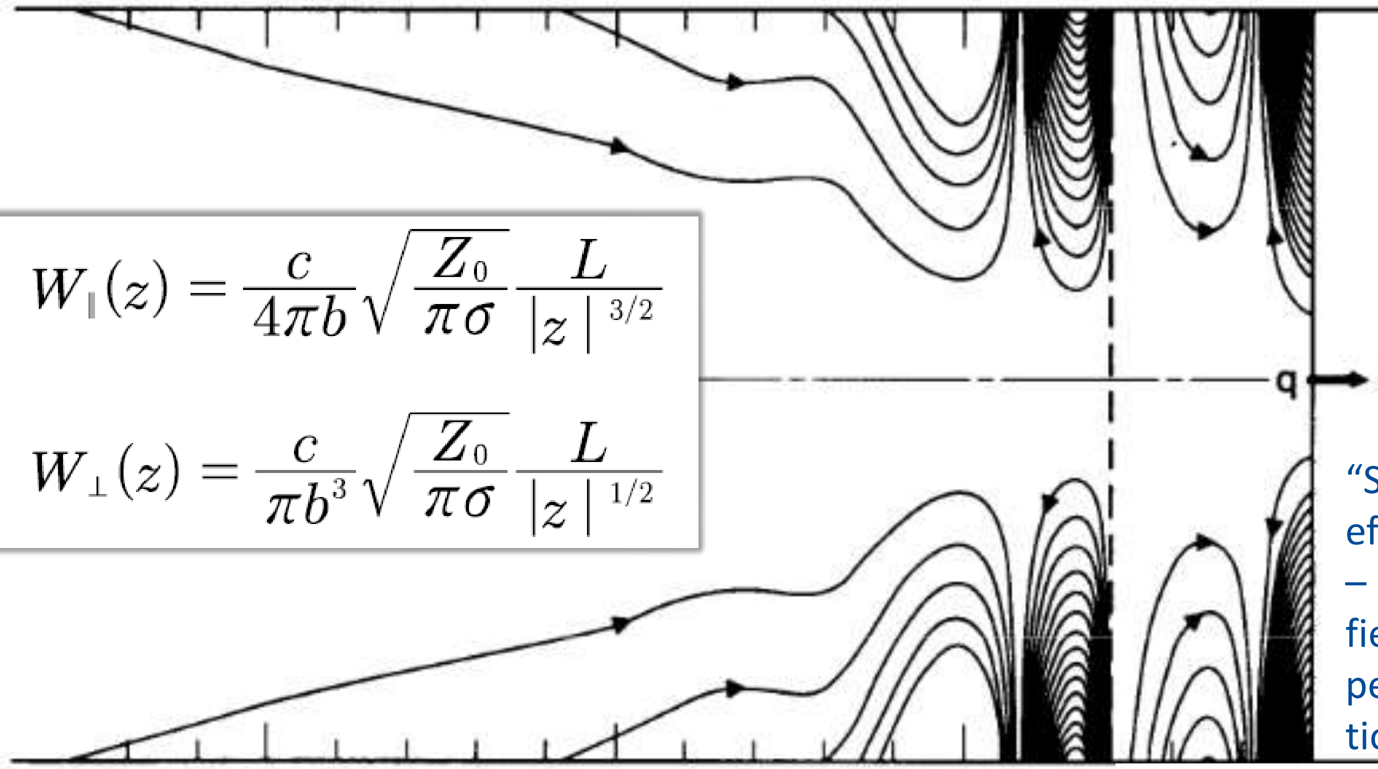

"Skin-effect" – EM field penetration depth

$$\delta r = \sqrt{\frac{c|z|}{\pi\sigma}}$$

Figure 2.3. Wake electric field lines in a resistive wall pipe generated by a point charge q. The field pattern shows oscillatory behavior in the region $|z| \lesssim 5(2\chi)^{1/3}b$ (or $|z| \lesssim 0.35$ mm for an aluminum pipe with $b = 5$ cm). The field line density to the left of the dashed line has been magnified by a factor of 40. (Courtesy Karl Bane, 1991.)

Key points: a) longitudinal wakefield leads to particle energy loss and pipe heating; b) transverse wake is defocusing for vacuum beam pipe (focusing in case of electron cloud)

Consequences: two-particle model

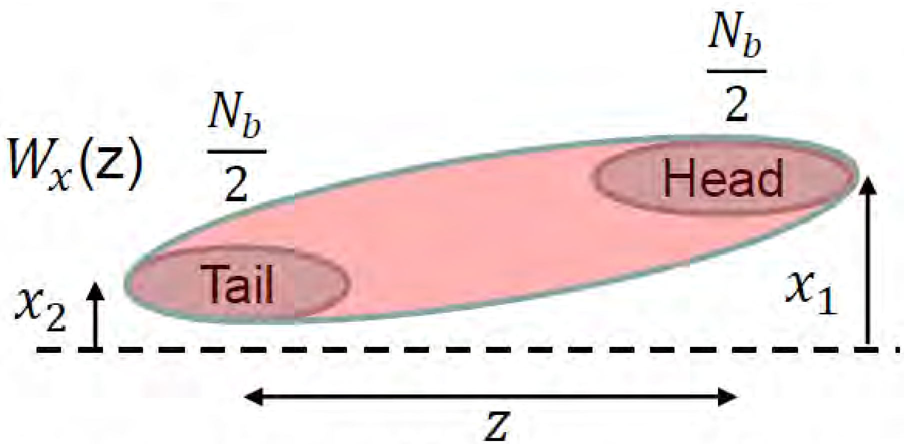

Two-particle coupled betatron oscillations:

$$x_1'' + \varkappa x_1 = 0$$

$$x_2'' + \varkappa x_2 = \frac{q^2 N_b W_x(z)}{2LE_0} x_1 \qquad \varkappa = \frac{Q_x^2}{R^2}$$

New coordinates:

$$\tilde{x}_l = x_l + i\frac{x'_l}{\varkappa} \qquad l = 1,2$$

Solution:

Linear growth !

$$\tilde{x}_1(s) = \tilde{x}_1(0)\, e^{-i\varkappa s}$$

$$\tilde{x}_2(s) = \tilde{x}_2(0)\, e^{-i\varkappa s} - \boxed{i\frac{q^2 N_b W_x(z)}{4E_0 L\varkappa}\tilde{x}_1(0)\, s e^{-i\varkappa s}}$$

In linacs: Beam-break up (BBU) instability

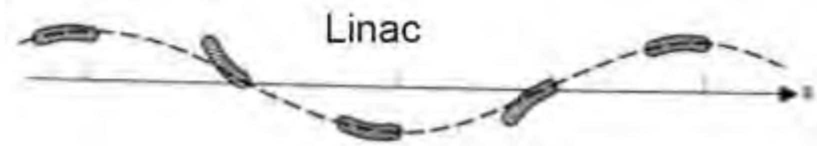

In rings: Head-tail instability (aka TMCI = Transverse Mode Coupling Instability)

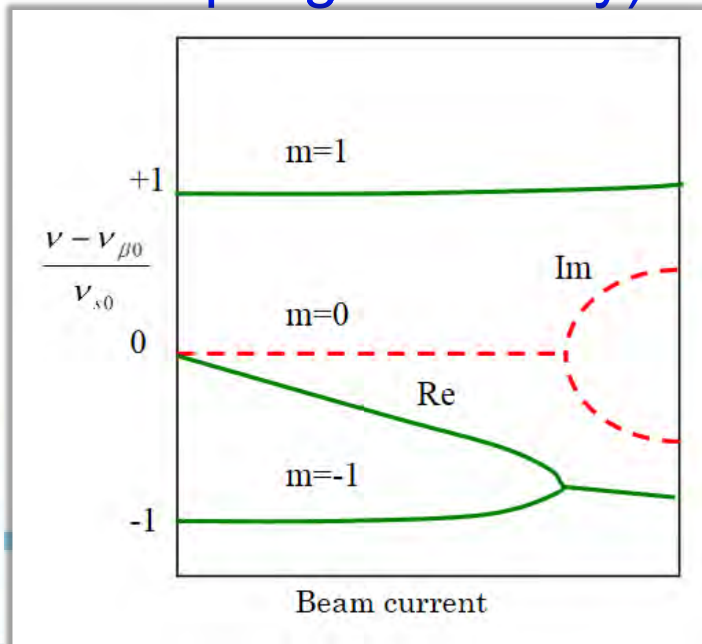

Intensity Limits and Cures

Beampipe heating is important for cryo – may limit on $N_b\ I_b$

Instabilities severely limit either single bunch current I_b or total beam current $N_b\ I_b$

Cures employed so far:

1) Reduce wakes/impedances – no discontinuities in beam pipe, better conducting materials, etc
2) In linacs – *BNS damping*= introduce energy difference btw head and tail of the bunch (RF phase choice) leading to slight difference in the betatron oscillation frequencies
3) In rings
   1) Feedback dampers (might not work for single bunch instabilities)
   2) introduce betatron frequency spread via chromaticity $dQ=Q'(dP/P)$ (does not always work) or octupoles $dQ\sim Oct^*\sigma^2$ (mostly worked so far) or electron beams for Landau damping (next gen colliders)

Intensity Limits and Cures

168 LHC octupoles for Landau Damping

Tune shifts (integrated):

$$\Delta Q_x = a_x J_x - b_{xy} J_y$$
$$\Delta Q_y = a_y J_y - b_{xy} J_x$$

Concern is that these octupolse are so nonlinear that they reduce *Dynamic Aperture* of the collider
→ affect lifetime

Landay Damping by Electron Lenses

Matched transverse beam radii.

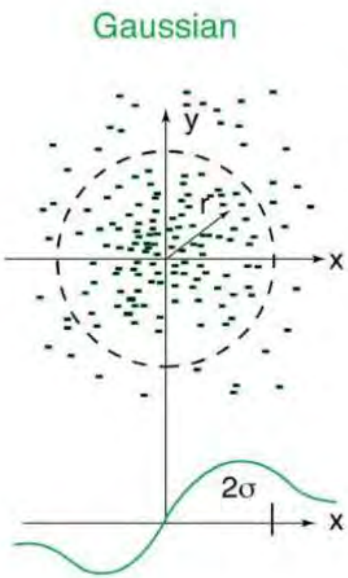

Gaussian electron beam provides a nonlinear tune shift.

Similar to the beam-beam force !

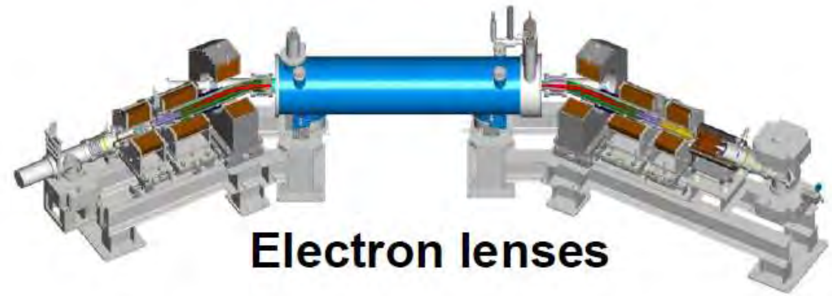

Tune shift induced by a counter-propagating electron beam:

$$\Delta Q_x^e = \frac{1+\beta_e}{\beta_e} \frac{I_e l r_p}{2\pi e c \varepsilon_x}$$

V. Shiltsev et al., PRL (2017)

Example: One e-lens (l=2 m, I_e=1 A) in LHC would provide a tune spread similar to the 168 octupoles.

Collimation

- To protect from enormous beam power (and power density) of high energy accelerators and colliders – events and processes:
  - Injection errors
  - Instabilities
  - Losses due to beam-beam, beam-gas, intrabeam scattering, etc
  - Synchrotron radiation photons
- Protect magnets, RF and detectors !

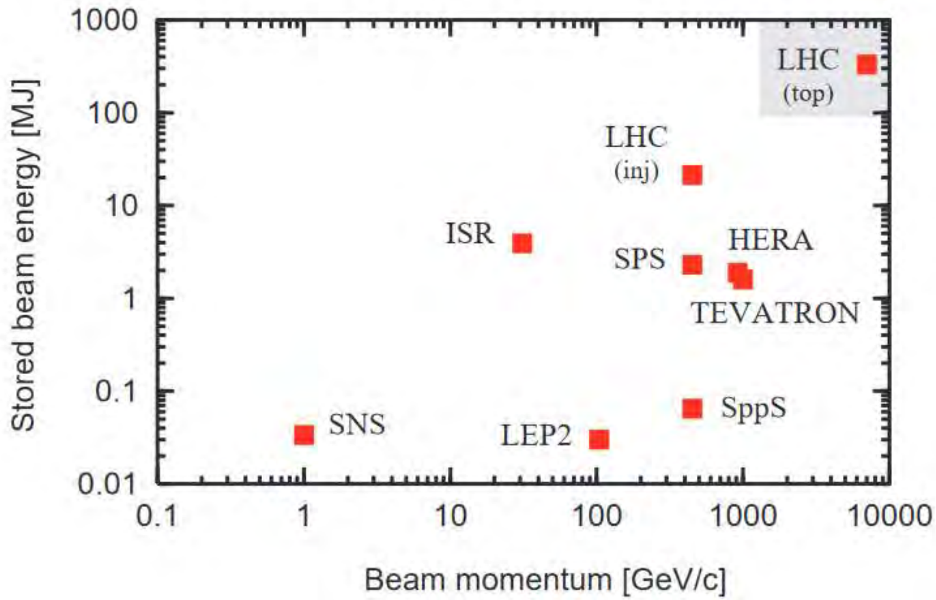

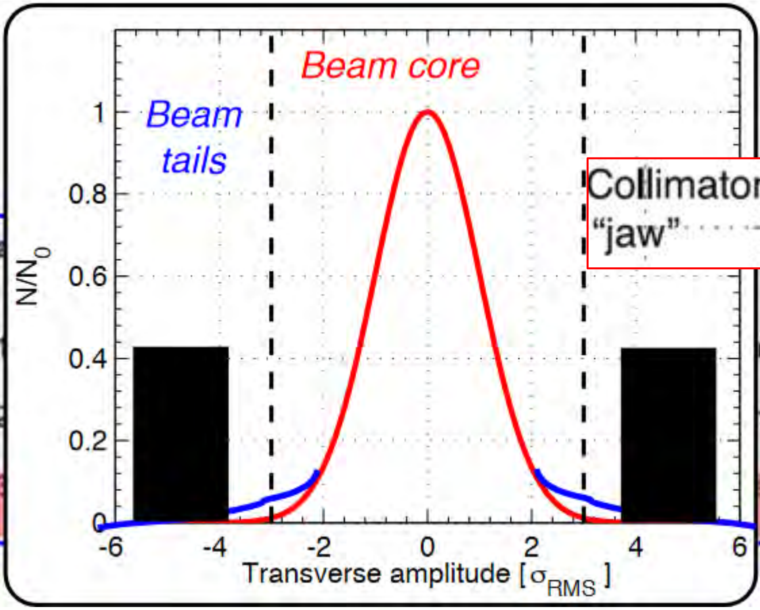

Collimators

- Tevatron 12 collimators:
  - Hor and Vert
  - Proton and antiproton
  - 4 primaries
    - 5 mm W
  - 8 secondaries
    - 1.5 m stainless steel
    - Flat to <25 micron
    - As close as few mm to the
- Efficiency 95-99%
  - reduction of background in CDF and D0 detectors x20-100

Damage to E03 1.5m Collimator

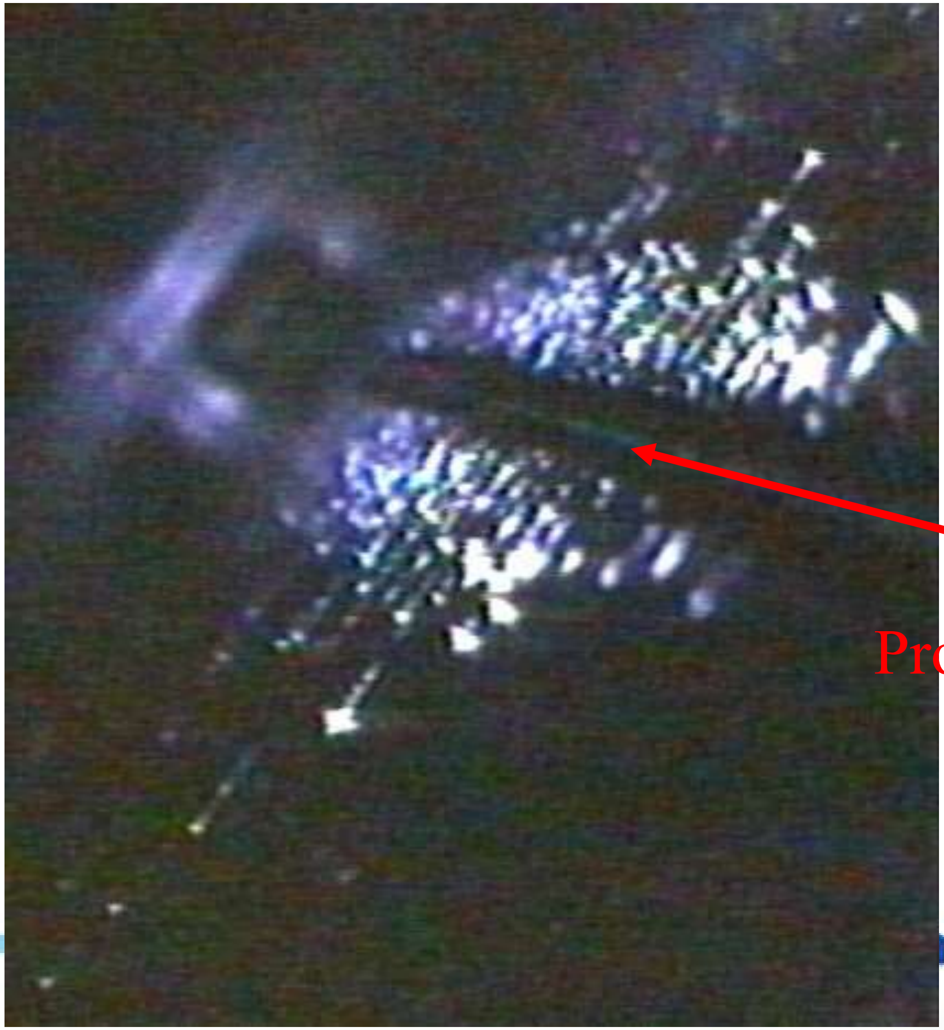

Protons

 see lectures NM1-4

nilab

(Most Sophisticated) LHC Collimation

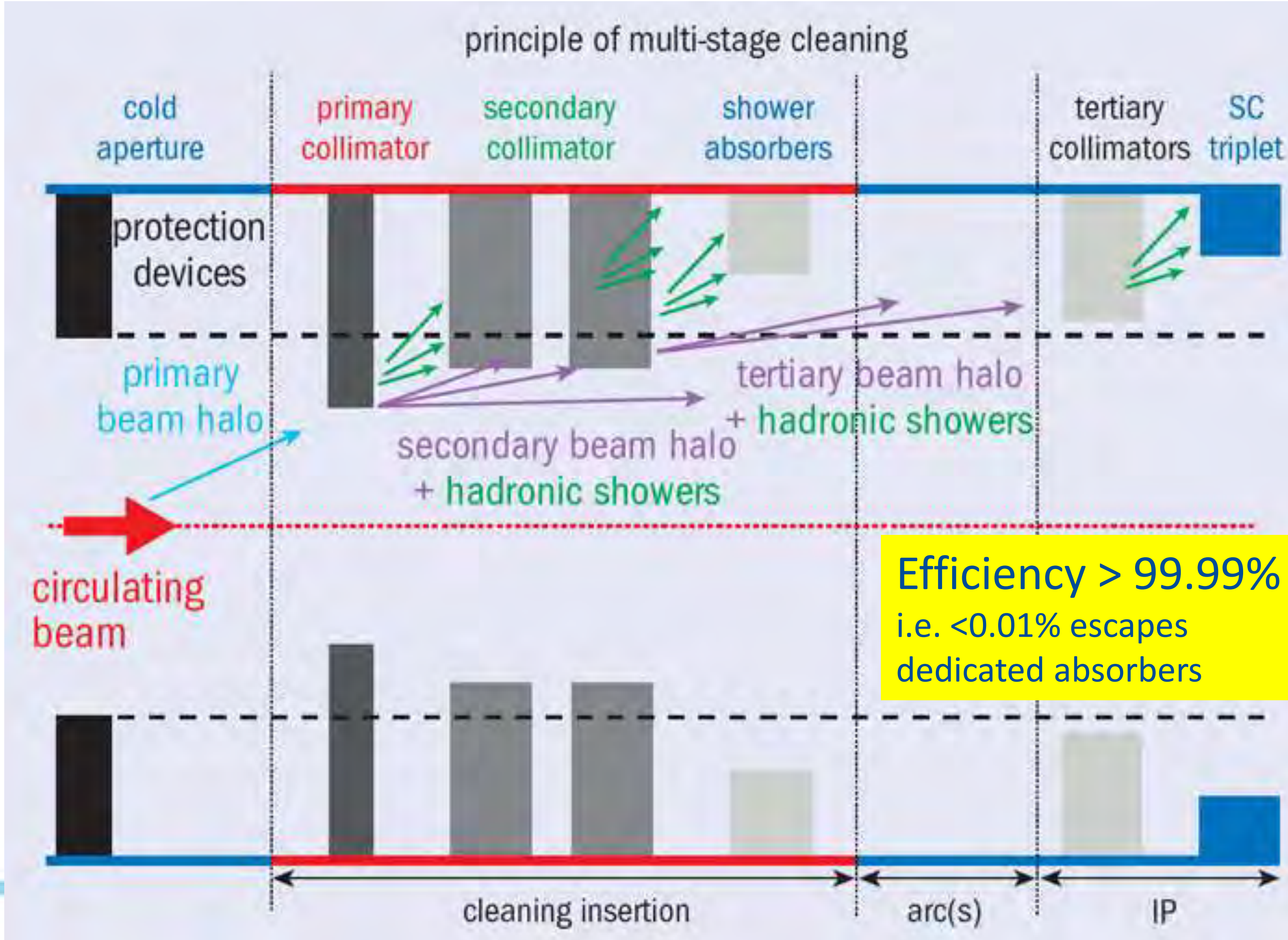

Efficiency > 99.99%
i.e. <0.01% escapes dedicated absorbers

Collimation Challenges and Cures

- Too many, too close to beams → large wakefields/impedance
- Can be damaged/destroyed …. NEW METHODS

Bent crystal collimation

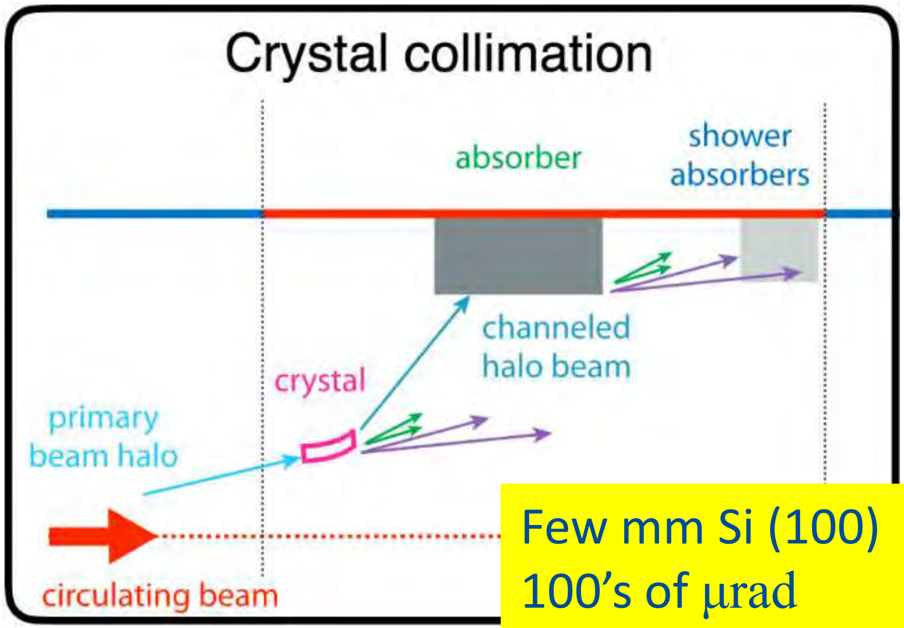

Few mm Si (100)
100's of μrad

Makes bigger deflection → better interception of scattered particles

Tested at the Tevatron and LHC

Hollow e-beam collimation

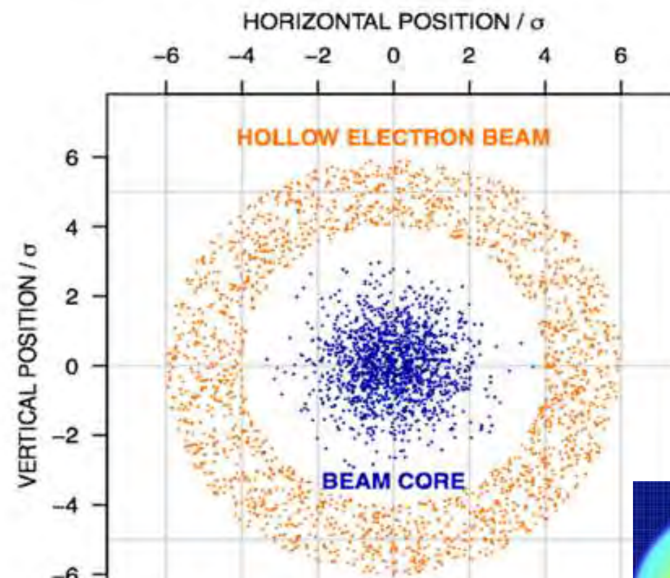

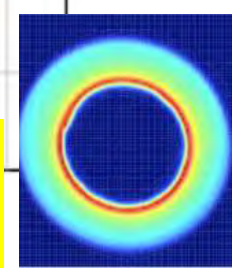

Few Amperes, few mm dia, few m long e-beam

Soft "penetrable" & fast diffusor → undamageable. Tested at the Tevatron and being built for LHC

Beam Cooling

$$\mathcal{L} = f_{\text{coll}} \frac{N_1 N_2}{4\pi\sigma_x^* \sigma_y^*}$$

Beam Phase Space Density Increase

- As needed for a collider
- Forbidden by the *Liouville theorem* in non-dissipative systems

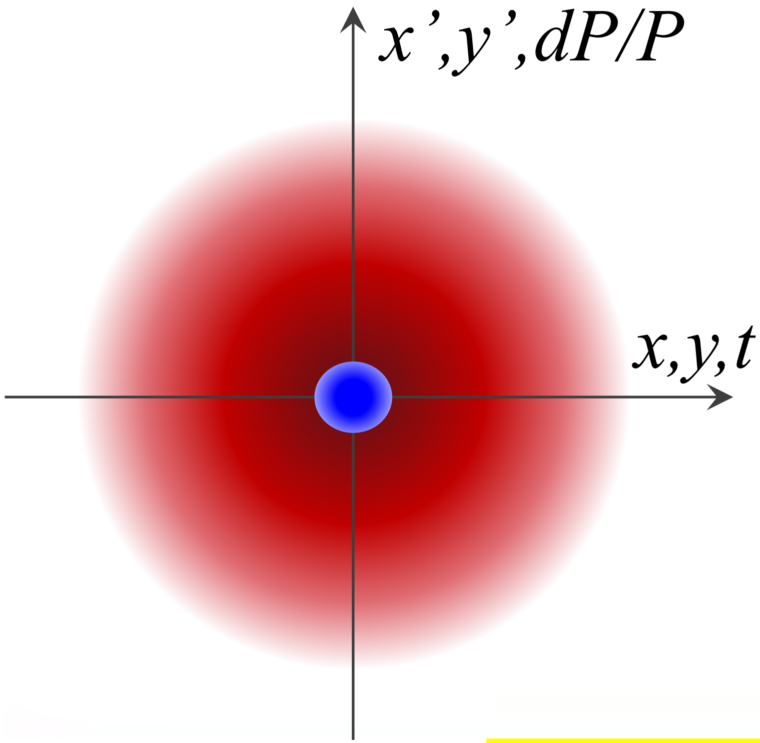

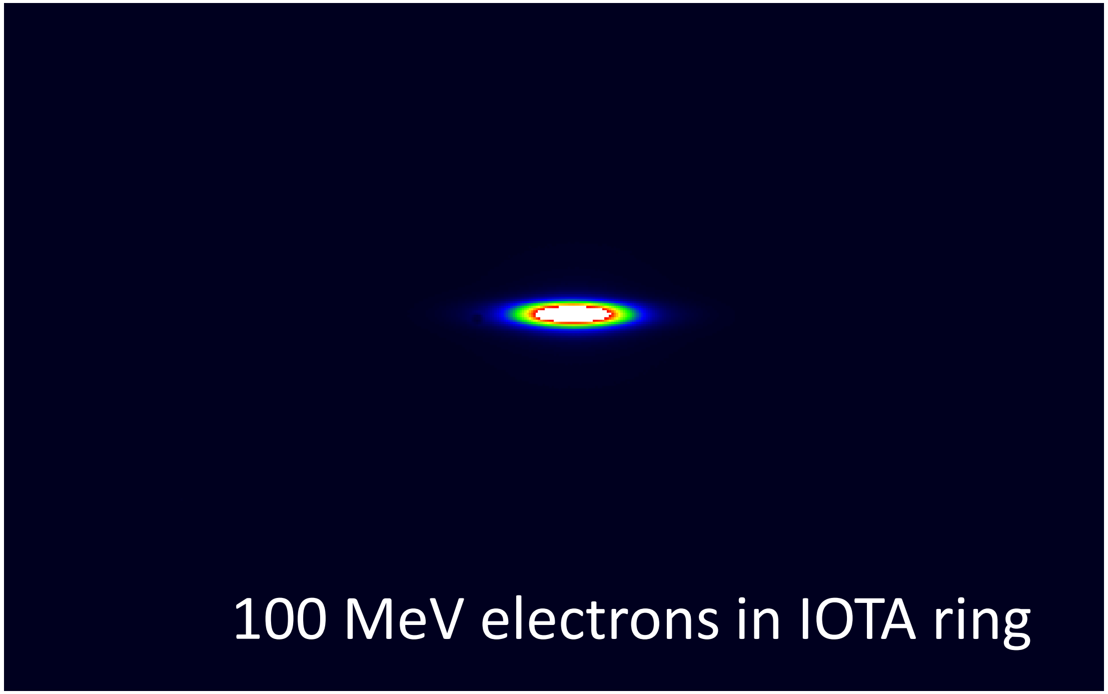

Ideally - "6D-Cooling"

Diffusion and Cooling (1)

Diffusion equation for beam distribution function *f(J,t)*, *J*- action variable

$$\frac{\partial f}{\partial t} = \frac{\partial}{\partial t}\left(D(J) \frac{\partial f}{\partial J} \right)$$

Lectures VL7-10

In the presence of cooling:

$$\frac{d\varepsilon_n}{dt} = \beta\gamma \frac{dD(J)}{dJ} - \frac{\varepsilon_n}{\tau_{\text{cool}}}$$

where for example:

Dipole noise For a single dipole steering error randomly fluctuating each revolution of the accelerator with rms value θ_{rms}, the emittance growth rate is

$$\frac{d\epsilon_N}{dt} = \frac{1}{2} f_0 (\gamma v/c) \beta_0 \theta^2_{\text{rms}} \qquad (10)$$

where β_0 is the β-function at the location of the error, and f_0 is the revolution frequency.

Coulomb scattering If the scattering is due to small angle Coulomb interactions between the beam particles and other material in the beam chamber, then

$$\frac{d\epsilon_N}{dt} = \frac{1}{2} f_0 \langle \beta \rangle \left(\frac{13.6\,\text{MeV}}{mc^2} \right)^2 \frac{z}{\gamma (v/c)^3} \frac{\ell}{X_0} \qquad (12)$$

where mc^2 is the rest energy of a beam particle, z its charge, and X_0 is the radiation length of the

Beam Cooling Methods to Date

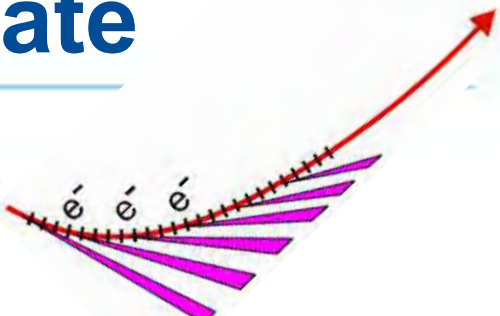

Synchrotron Radiation Damping – since 1960's

- common in all e+/e- rings

Electron Cooling – since 1970's

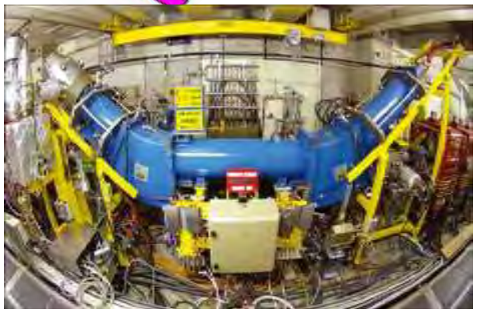

- Widely used to cool ions and antiprotons
- 0.1 - 8 GeV/n (50 keV – 4 MeV electrons DC)

Stochastic Cooling – since 1970's

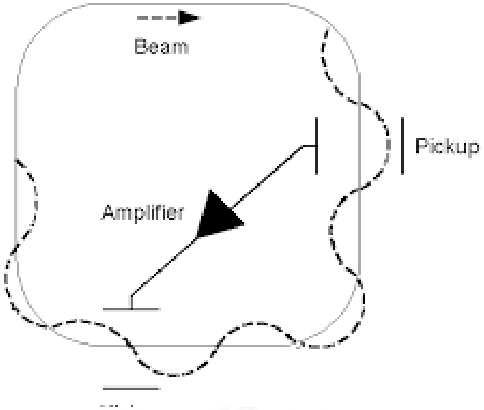

- Widely used to cool ions and antiprotons
- 0.1-100 GeV/n (up to 10 GHz feedback BW)

Laser Cooling – since 1990's

$$\Omega = \gamma\omega_{21}(1 - \beta\cos\theta)$$

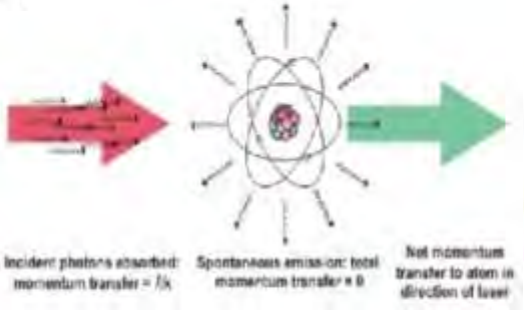

- Works for some highly charged ions
- 0.1-0.5 GeV/n, deep cooling, spectroscopy

Lectures VL13-14

Recent Beam Cooling Breakthroughs

2019 - Ionization cooling of muons (140 MeV/*c*, RAL, UK)

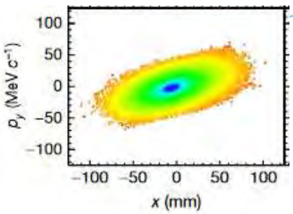

MICE

~10% in one pass

2020 – "Bunched" electron cooling of ions (γ~5, BNL)

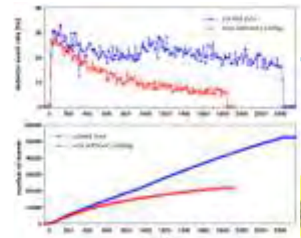

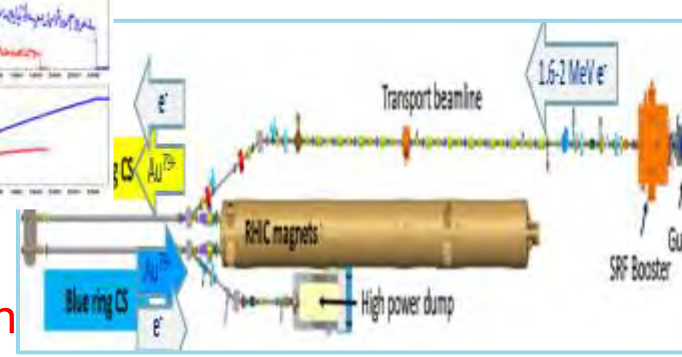

RHIC

RF e-gun

2021 – Coherent Electron cooling of ions (26.5 GeV/*n*, RHIC) – ongoing PoP exp't at BNL

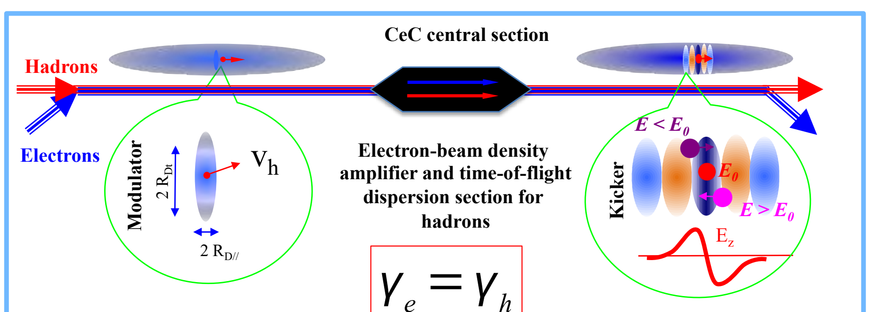

2021 – Optical Stochastic cooling e- (100 MeV, FNAL)

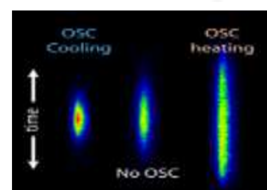

IOTA

THz bandwidth

Synchrotron Radiation (1)

Average radiated power restored by RF

$$U_0 \cong 10^{-3} \text{ of } E_0$$

- Electron loses energy each turn
- RF cavities provide voltage to accelerate electronsback to the nominal energy

$$V_{RF} > U_0$$

Radiation damping

- Average rate of energy loss produces DAMPINGof electron oscillations in all three degrees of freedom (if properly arranged!)

Quantum fluctuations

- Statistical fluctuations in energy loss (from quantised emission of radiation) produce RANDOM EXCITATION of these oscillations

Equilibrium distributions

- The balance between the damping and the excitation of the electron oscillations determines the equilibrium distribution of particles in the beam

Radiation is emitted in a narrow cone

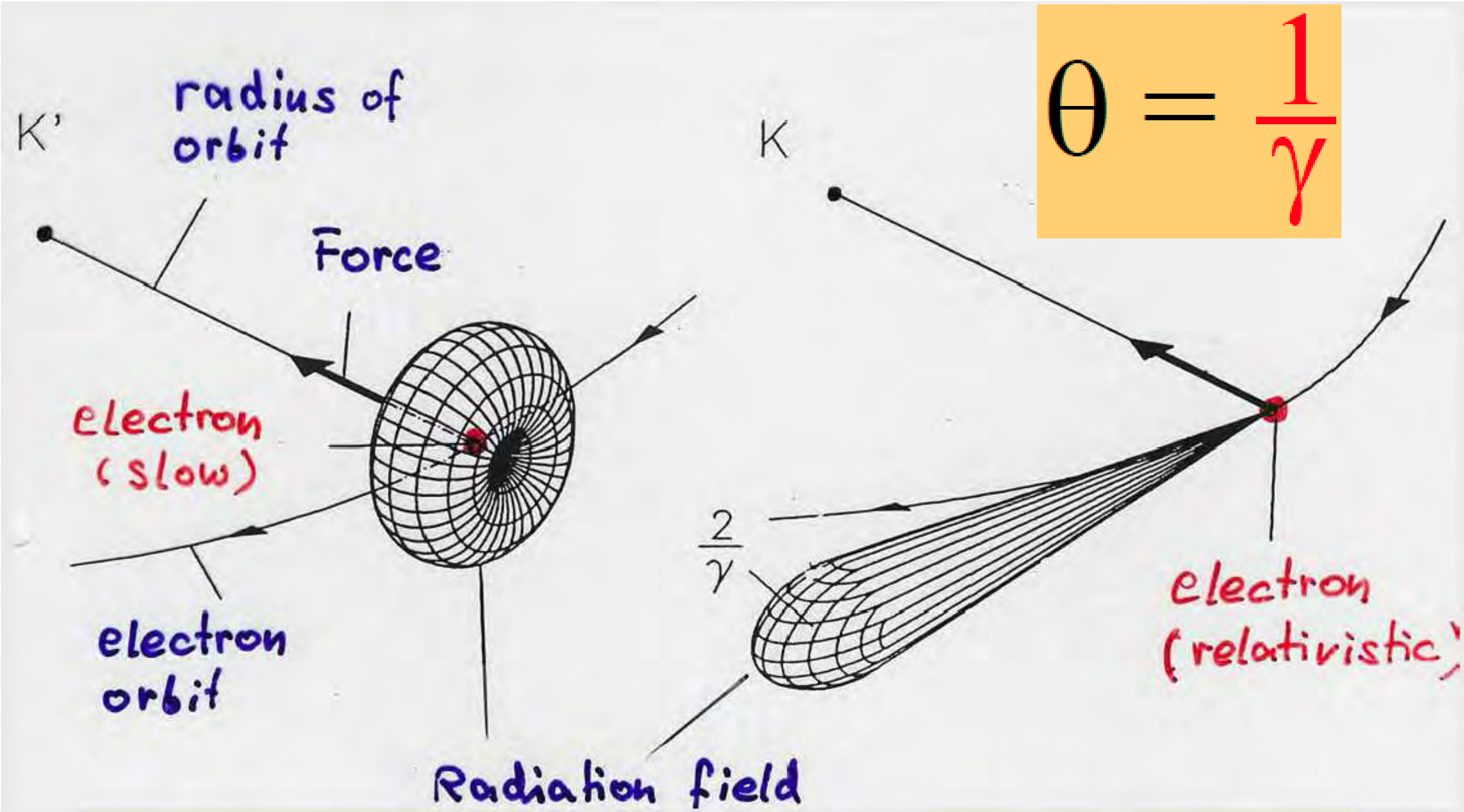

$$\theta = \frac{1}{\gamma}$$

$v << c$

$v \approx c$

Synchrotron radiation power

Power emitted is proportional to:

$$\boxed{P \propto E^2 B^2}$$

$$P_\gamma = \frac{cC_\gamma}{2\pi} \cdot \frac{E^4}{\rho^2}$$

$$P_\gamma = \frac{2}{3} \alpha \hbar c^2 \cdot \frac{\gamma^4}{\rho^2}$$

$$C_\gamma = \frac{4\pi}{3} \frac{r_e}{(m_e c^2)^3} = 8.858 \cdot 10^{-5} \left[\frac{\text{m}}{\text{GeV}^3}\right]$$

$$\alpha = \frac{1}{\ldots}$$

$$\Delta E_{\text{SR}} = 0.089 \text{ MeV}/\text{turn}\, E_b^4 \text{ (GeV)}/\rho \text{ (m)}$$

$$\hbar c = 197 \text{ Mev} \cdot \text{fm}$$

Energy loss per turn:

$$U_0 = C_\gamma \cdot \frac{E^4}{\rho}$$

$$U_0 = \frac{4\pi}{3} \alpha \hbar c \frac{\gamma^4}{\rho}$$

Diffusion and Cooling (2)

Examples proton beam scattering with the residual gas (assumed to be air) gives

$$\frac{d\epsilon_N}{dt} = \langle\beta\rangle \left(1.6 \times 10^{-7}/\mathrm{s}\right) \frac{P[\mu\mathrm{Torr}]}{\gamma} \qquad (13)$$

or Intrabeam Scattering:
(see lectures VL7-8, 9-10)

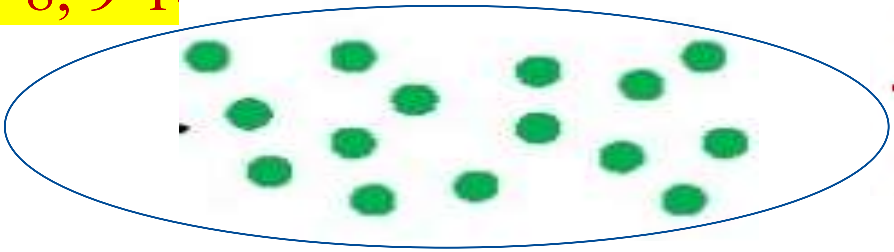

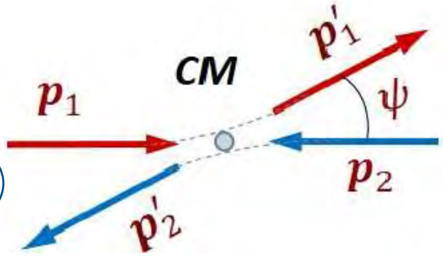

or fluctuations of synchrotron radiation:

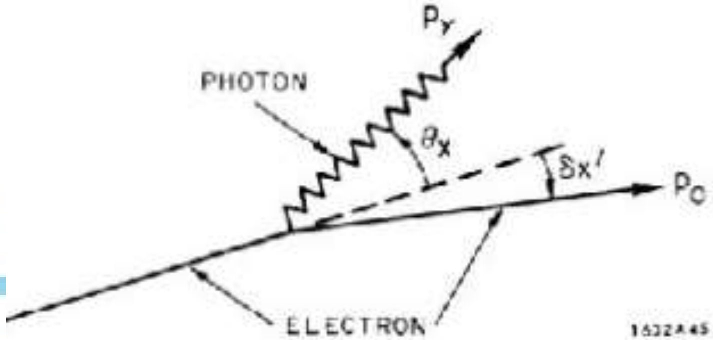

Quantum Nature of Synchrotron Radiation

Damping only: If damping was the whole story, the beam emittance (size) would shrink to microscopic dimensions! Because the radiation is emitted in quanta, radiation itself takes care of the problem! It is sufficient to use quasi-classical picture a) Emission time is very short
b) Emission times are statistically independent (each emission leads to only a small change in electron energy)

→ **Purely stochastic (Poisson) process**

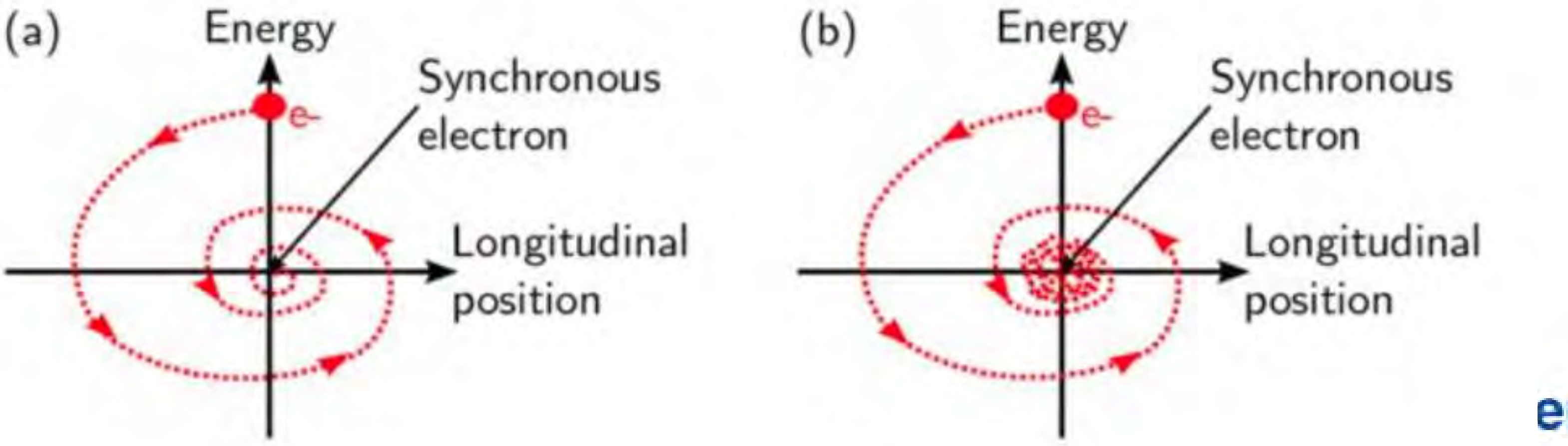

ermilab

Quantum Excitation of Energy Oscillations

Photons are emitted with typical energy $u_{ph} \approx \hbar\omega_{typ} = \hbar c \frac{\gamma^3}{\rho}$

at the rate (photons/second) $\mathcal{N} = \frac{P_\gamma}{u_{ph}}$

Fluctuations in this rate excite oscillations

During a small interval Δt electron emits photons $N = \mathcal{N} \cdot \Delta t$

losing energy of $N \cdot u_{ph}$

Actually, because of fluctuations, the number is $N \pm \sqrt{N}$

resulting in **spread in energy loss** $\pm\sqrt{N} \cdot u_{ph}$

For large time intervals RF compensates the energy loss, providing damping towards the design energy E_0

Steady state: typical deviations from E_0

$\approx$ typical fluctuations in energy during a damping time τ_ε

Equilibrium energy spread

We then expect the rms energy spread to be $\sigma_\varepsilon \approx \sqrt{N \cdot \tau_\varepsilon \cdot u_{ph}}$

and since $\tau_\varepsilon \approx \dfrac{E_0}{P_\gamma}$ and $P_\gamma = N \cdot u_{ph}$

$\sigma_\varepsilon \approx \sqrt{E_0 \cdot u_{ph}}$ geometric mean of the electron and photon energies!

Relative energy spread can be written then as:

$$\frac{\sigma_\varepsilon}{E_0} \approx \gamma \sqrt{\frac{\lambda\!\!\!^{-}_e}{\rho}} \qquad \lambda\!\!\!^{-}_e = \frac{\hbar}{m_e c} \approx 4 \cdot 10^{-13} m$$

it is roughly constant for all rings

$$\boxed{\frac{\sigma_\varepsilon}{E_0} \sim const \sim 10^{-3}}$$

- typically $\rho \propto E^2$

Excitation of Betatron Oscillations

$$x = x_\beta + x_\varepsilon$$

$$x_\varepsilon = D \cdot \frac{\varepsilon}{E}$$

$$x' = x'_\beta + x'_\varepsilon$$

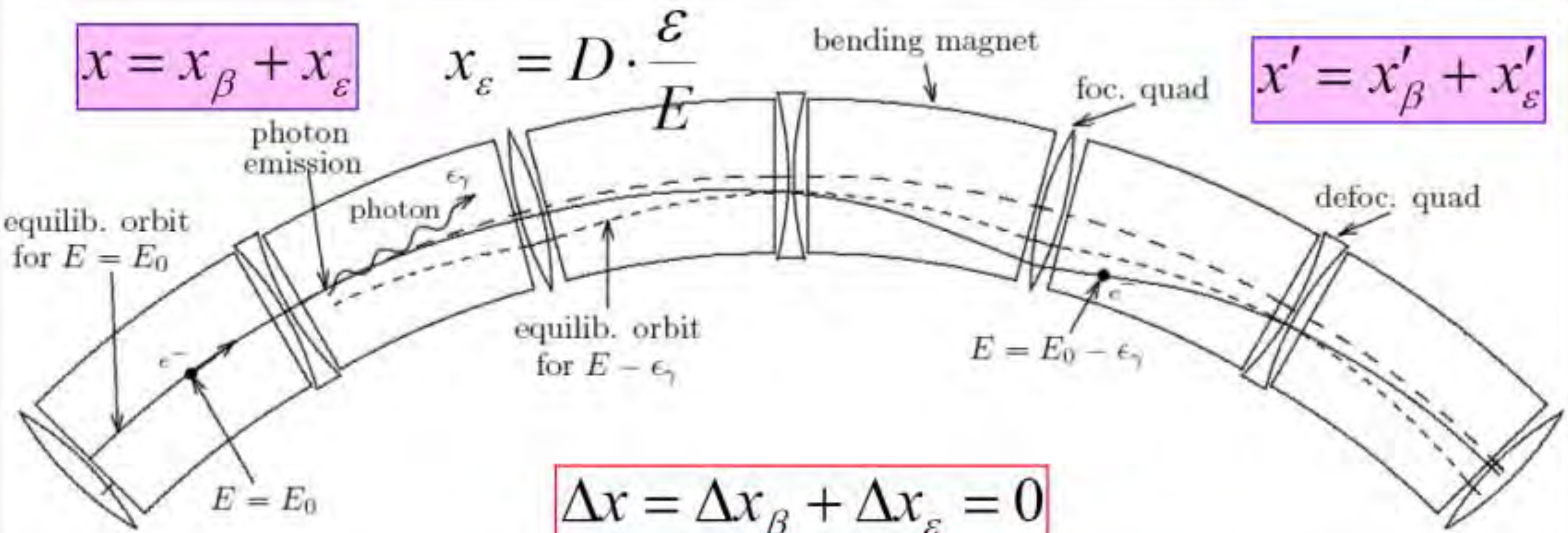

$$\Delta x = \Delta x_\beta + \Delta x_\varepsilon = 0$$

$$\Delta x_\beta = -D \cdot \frac{\varepsilon_\gamma}{E}$$

Courant Snyder invariant

$$\Delta x'_\beta = -D' \cdot \frac{\varepsilon_\gamma}{E}$$

$$\Delta\varepsilon = \gamma \Delta x_\beta^2 + 2\alpha \Delta x_\beta \Delta x'_\beta + \beta \Delta x'^2_\beta = \left[\gamma D^2 + 2\alpha D D' + \beta D'^2\right] \cdot \left(\frac{\varepsilon_\gamma}{E}\right)^2$$

e- Rings are All set By Optical Lattice

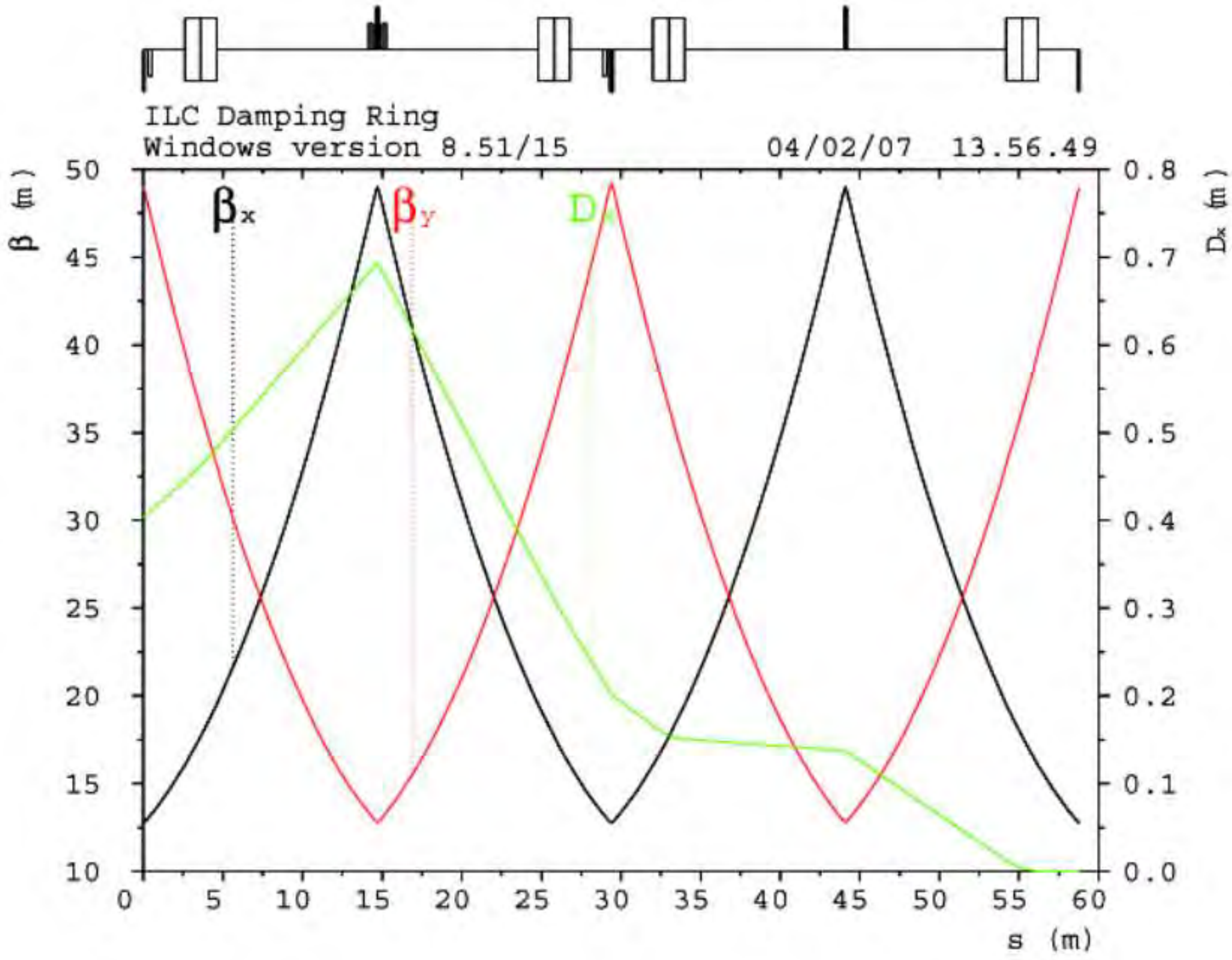

Five Integrals

$$I_1 = \oint \frac{D}{\rho}\, ds$$

$$I_2 = \oint \frac{ds}{\rho^2}$$

$$I_3 = \oint \frac{ds}{|\rho^3|}$$

$$I_4 = \oint \frac{D}{\rho}\left(2k + \frac{1}{\rho^2}\right) ds$$

$$I_5 = \oint \frac{\mathcal{H}}{|\rho^3|}\, ds$$

$$C_\gamma = \frac{4\pi}{3}\frac{r_e}{(m_e c^2)^3} = 8.858 \cdot 10^{-5}\left[\frac{\text{m}}{\text{GeV}^3}\right]$$

Momentum compaction factor

$$\boxed{\alpha = \frac{I_1}{2\pi R}}$$

Energy loss per turn

$$\boxed{U_0 = \frac{1}{2\pi} C_\gamma E^4 \cdot I_2}$$

Summary of SR Integrals

Damping parameter

$$\boxed{\mathcal{D} = \frac{I_4}{I_2}}$$

Damping times, partition numbers

$$\boxed{J_\varepsilon = 2 + \mathcal{D}\,, \quad J_x = 1 - \mathcal{D}\,, \quad J_y = 1}$$

$$\boxed{\tau_i = \frac{\tau_0}{J_i}} \qquad \boxed{\tau_0 = \frac{2ET_0}{U_0}}$$

Equilibrium energy spread

$$\boxed{\left(\frac{\sigma_\varepsilon}{E}\right)^2 = \frac{C_q E^2}{J_\varepsilon} \cdot \frac{I_3}{I_2}}$$

Equilibrium emittance

$$\boxed{\varepsilon_{x0} = \frac{\sigma_{x\beta}^2}{\beta} = \frac{C_q E^2}{J_x} \cdot \frac{I_5}{I_2}}$$

$$I_1 = \oint \frac{D}{\rho}\, ds$$

$$I_2 = \oint \frac{ds}{\rho^2}$$

$$I_3 = \oint \frac{ds}{|\rho^3|}$$

$$I_4 = \oint \frac{D}{\rho}\left(2k + \frac{1}{\rho^2}\right) ds$$

$$I_5 = \oint \frac{\mathcal{H}}{|\rho^3|}\, ds$$

$$C_q = \frac{55}{32\sqrt{3}} \frac{\hbar c}{(m_e c^2)^3} = 1.468 \cdot 10^{-6} \left[\frac{\mathrm{m}}{\mathrm{GeV}^2}\right]$$

$$\mathcal{H} = \gamma D^2 + 2\alpha D D' + \beta D'^2$$

Fermilab

Beamstrahlung – SR due to Opposite Bunch

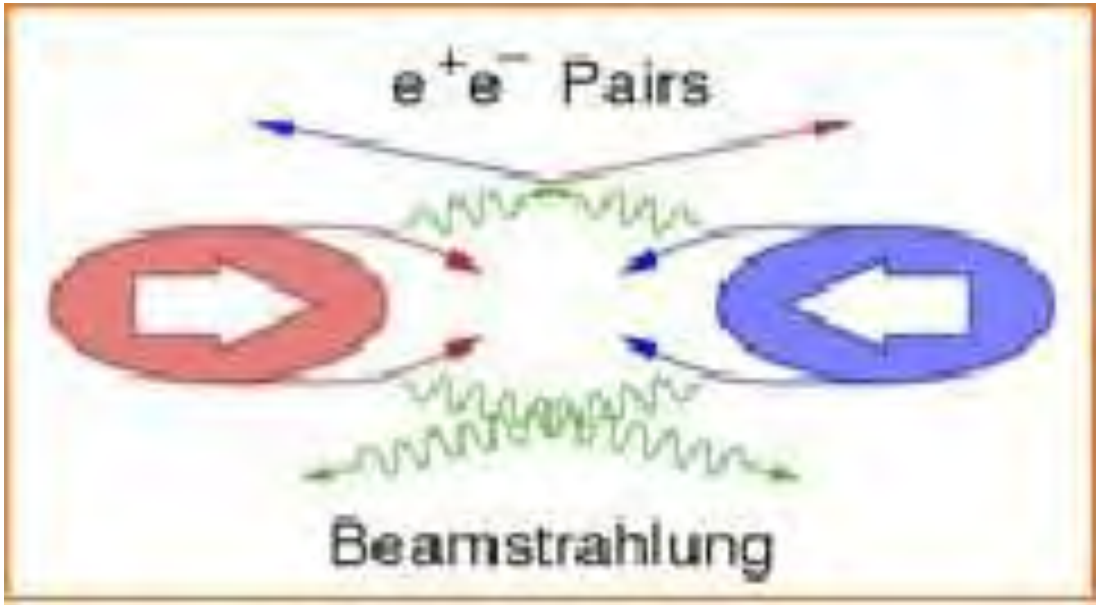

- Effect depends on the energy and field of opposite bunch approx

$$\sim\gamma^2 B^2$$

- Serious for large bunch populations (N), small hor. beam size (σ_x) & short bunches (σ_s)
- Linear colliders: 1% to 100% energy spread after 1 collision
- Circular : particles with 1-2% energy loss lost on Dynamic Aperture

Coherent Synchrotron Radiation

- In the case of short bunches with length comparable with radiation wavelength → SR from tail decelerates head

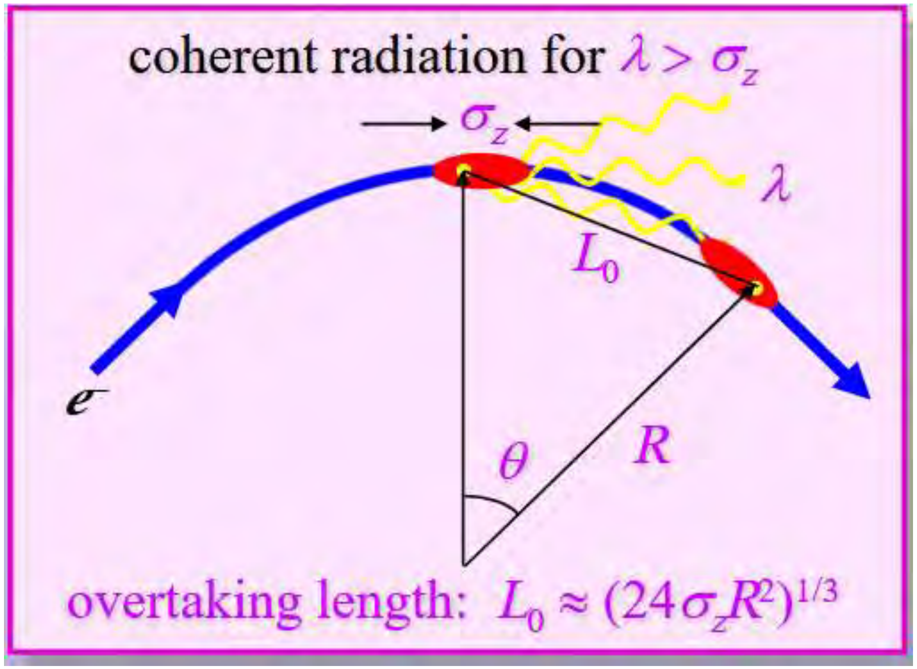

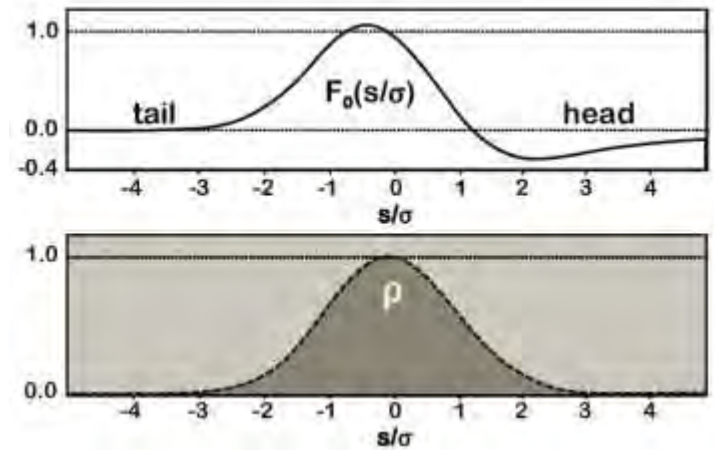

microbunching instability (fast)

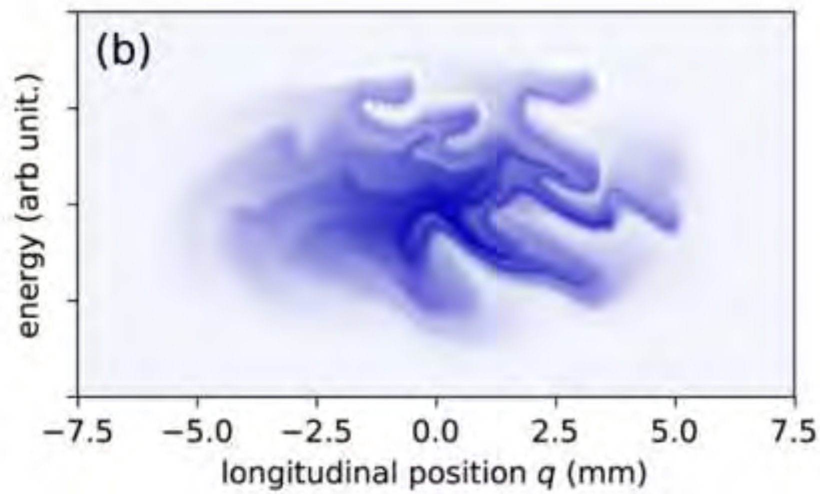

Electron-positron colliders

- Initially, ***e-e+*** was effective way to save as two beams can be bent by the same set of magnets (opposite charges in opposite directions → same direction currents → same force in same B-field ***q*[*vxB*]**)
- Unique need of *B*-physics required relativistic boost of *e+e-* > *B-meson* reaction products (B-mesons to have relativistic velocities to be detected and analyzed → asymmetric energies eg 3.1+9 GeV (*e+e-* PEP-II), 3.5+8 GeV (*e+e-* KEKB)
- Below we consider five *e+e-* colliders: VEPP-2000 (round beams), **DAFNE** (crab waist), **Super-KEKB** (Lumi-record holder) and **FCCee & CEPC** (future giants)

VEPP-2000 Collider in Novosibirsk

e+e- collider at φ-meson energy E_{cm}=0.3-2 GeV

C=24.4 m, 1+1 bunch

L=5e31 at 1 GeV cme

Axially symmetric linear focusing in arcs

Round beams at 2 IPs with four 13 T solenoids

World record beam-beam tune shift!
ξ=0.34

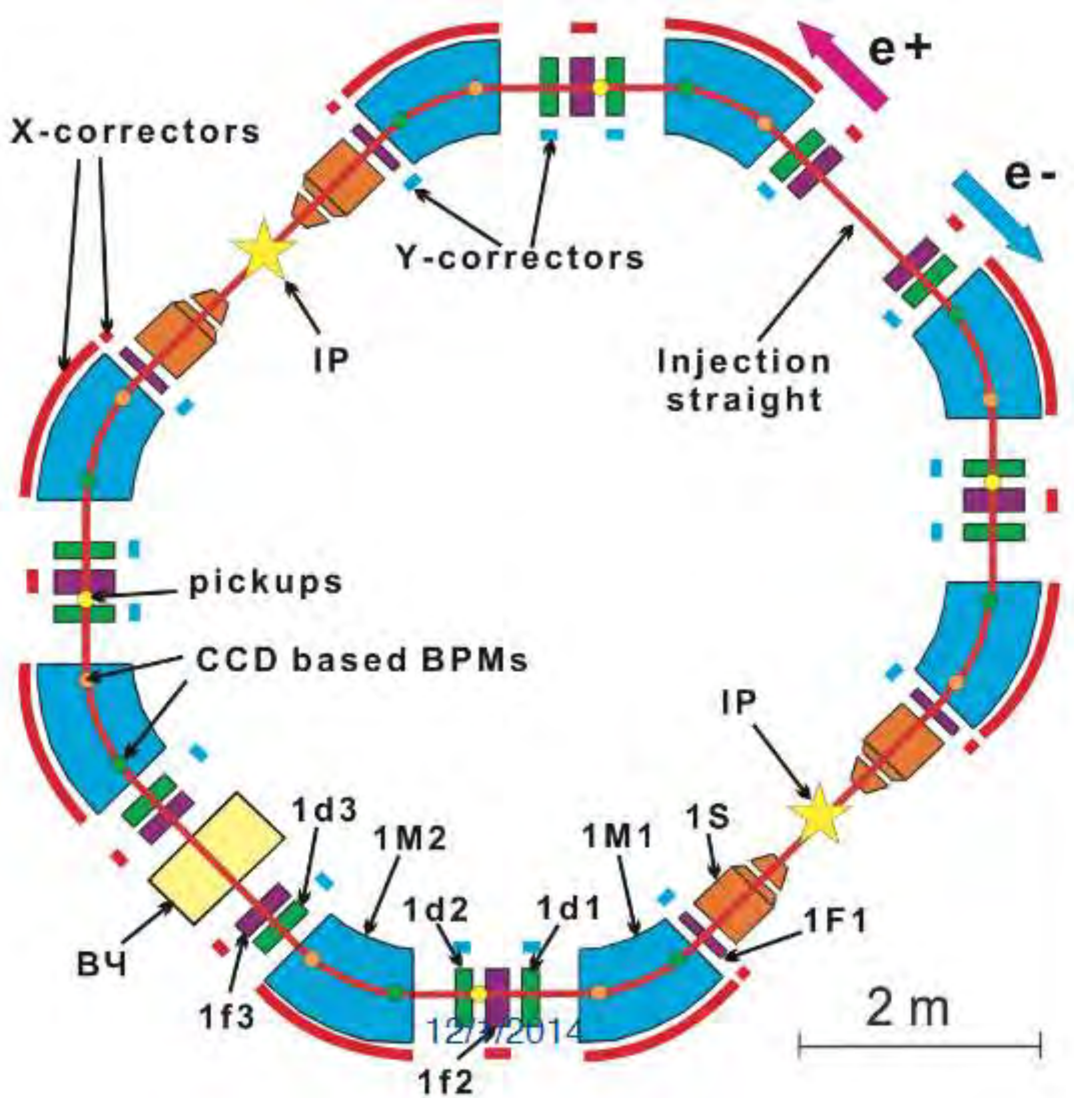

Fermilab

"Round Beams" in practice

- Usually, SR-dominated beams have flat beams – large horizontal emittance and small vertical emittance. The ratio V/H is set by the coupling of x-y degrees of freedom → usually quite small ~1%, that helps to keep vertical beam-beam parameter under b-b limit ~0.05:

$$\xi_{x,y} = \frac{r_0 N \beta^*_{x,y}}{2\pi\gamma\sigma^*_{x,y}(\sigma^*_x + \sigma^*_y)} \qquad \mathcal{L} = f_0\gamma \frac{I_b \xi_y}{2 e r_e \beta^*_y}\left(1 + \frac{\sigma^*_y}{\sigma^*_x}\right)$$

- Round beams boost the b-b parameter via less resonances. For that
  1. Small and equal x and y beta-functions at the IPs, head-on collision
  2. Equal beam emittances in x and y
  3. Equal betatron tunes Qx = Qy

  Axial symmetry of counter beam force together with *x-y* symmetry of transfer matrix provides additional integral of motion (angular momentum *$M_z = x'y - xy'$*). Particle dynamics remains nonlinear, but becomes **1D** (fewer res Q=n/m)

V.V.Danilov et al., EPAC'96, Barcelona, p.1149, (1996)

Operation Modes – Polarity of Solenoids

4 solenoids in total:
2 at each IP
Equal strength:
each rotates x-y oscillations
by 45 degrees ie
$HL=\pi(B_{ring}\rho_{ring})/2$

eg "Mobius" +-++ =
+45-45+45+45=90 degrees
that is *x*→*y* flip per turn

"normal round" ++--=
+45+45-45-45=0 degrees,
x→*y*→*x* per turn

Recall: in solenoid
$Force_x = e\, \mathbf{v}_y \times \mathbf{B}_z$
i.e. coupling **x-y**

$$\frac{1}{f} = \frac{e^2}{4\gamma^2 m^2 v_z^2} \int B^2 dz$$

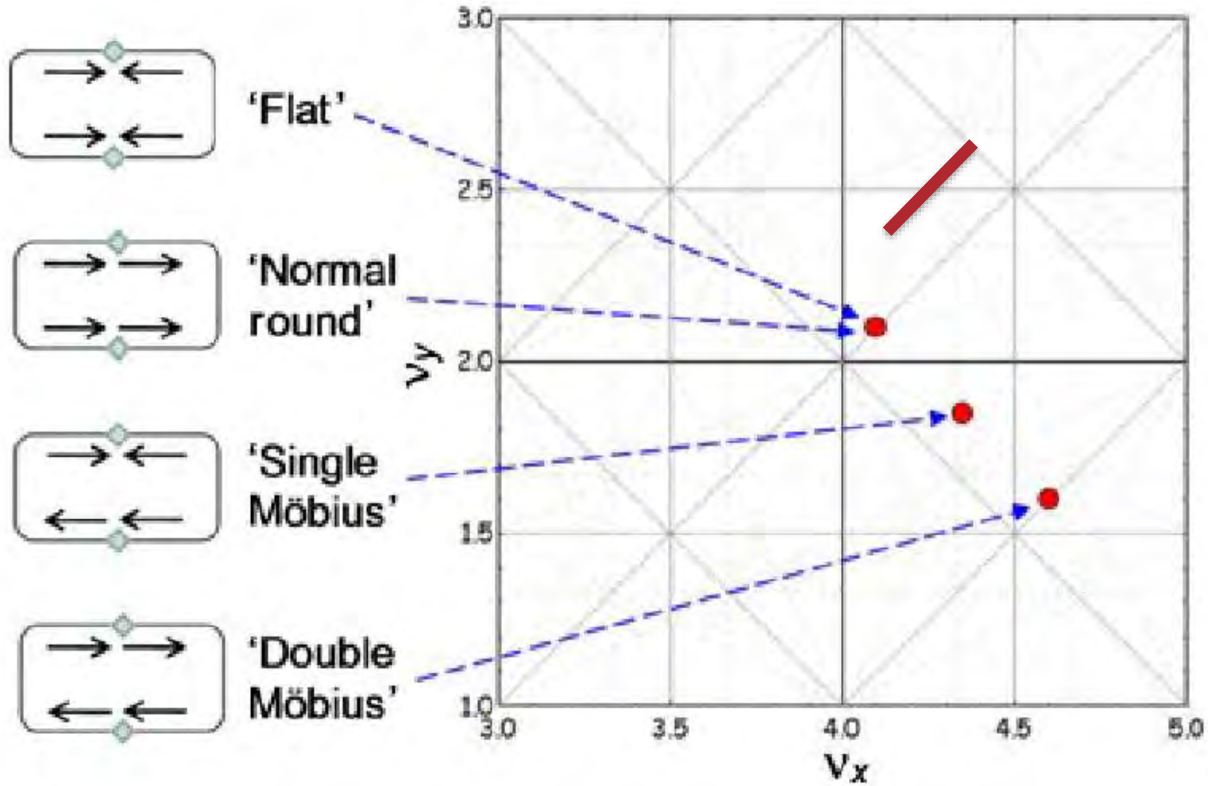

Figure 4: VEPP-2000 round beam options.

DAFNE and Crab-waist

e+e- collider at φ-meson energy E_{cm}=1.02 GeV

110 bunches per beam

L=4.5e32 at 1 GeV cme

Crab waist logics:

a) luminosity demands low β_y; b) hour-glass effect says that β_y smaller than beam longitudinal overlap length ~σ_z reduces lumi; c) let's reduce the overlap length by large crossing angle $\theta \rightarrow$ can lower β_y to ~$2\sigma_x\theta$ → **higher lumi if b-b allows (see next slide how)**

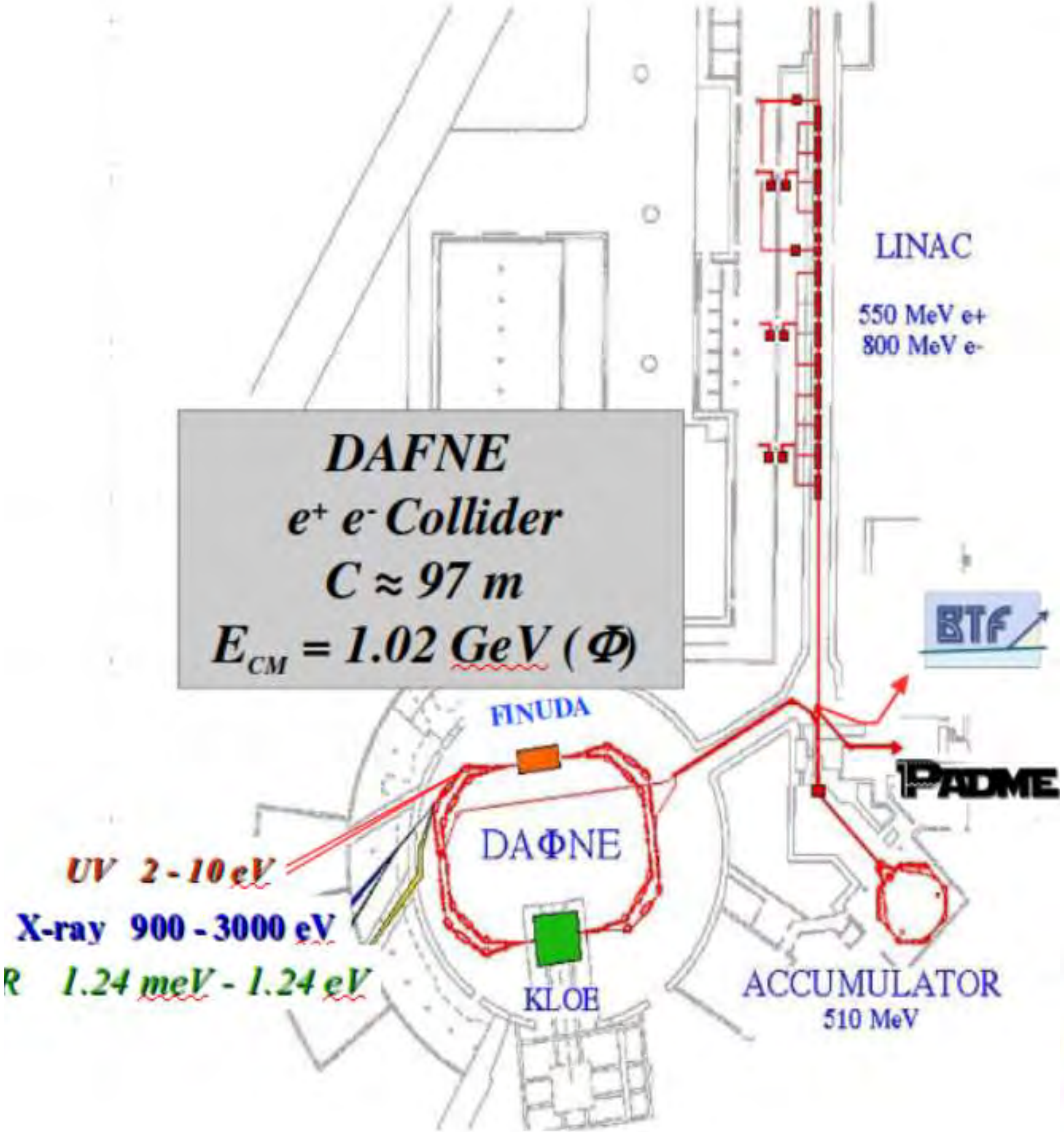

Crab waist (P.Raimondi 2006)

Luminosity $L = \frac{\gamma}{2er_e} \cdot \frac{I_{tot}\xi_y}{\beta_y^*} R_H$

Large Piwinski angle: $\phi = \frac{\sigma_z}{\sigma_x} \tan\left(\frac{\theta}{2}\right)$

1. Transverse beam separation in parasitic IPs helps
   - distance between bunches is not limited by beam-beam
2. Interaction area length $L_i \ll \sigma_z$
   - $\beta_y^* \approx L_i \ll \sigma_z$ no hour-glass
3. CRAB waist (CRAB sextupoles) suppresses betatron and synchro-betatron resonances
   - $\xi_y \sim 0.2$

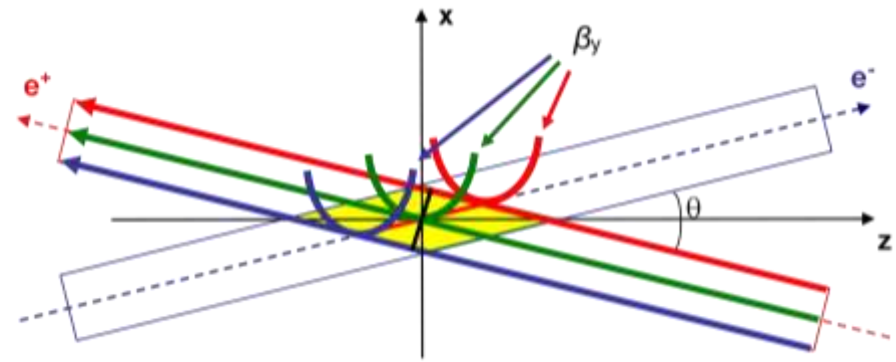

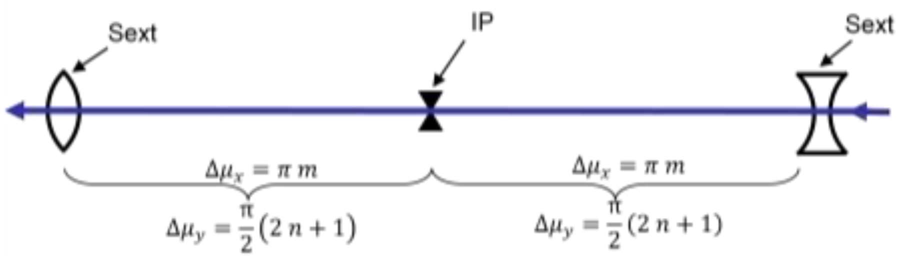

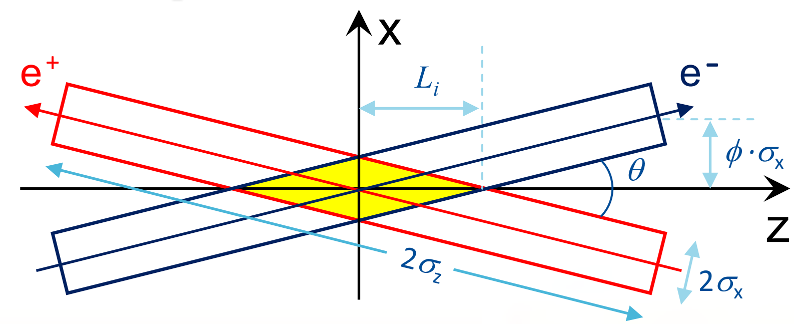

Fermilab

Crab-Waist vs Head-on Collisions

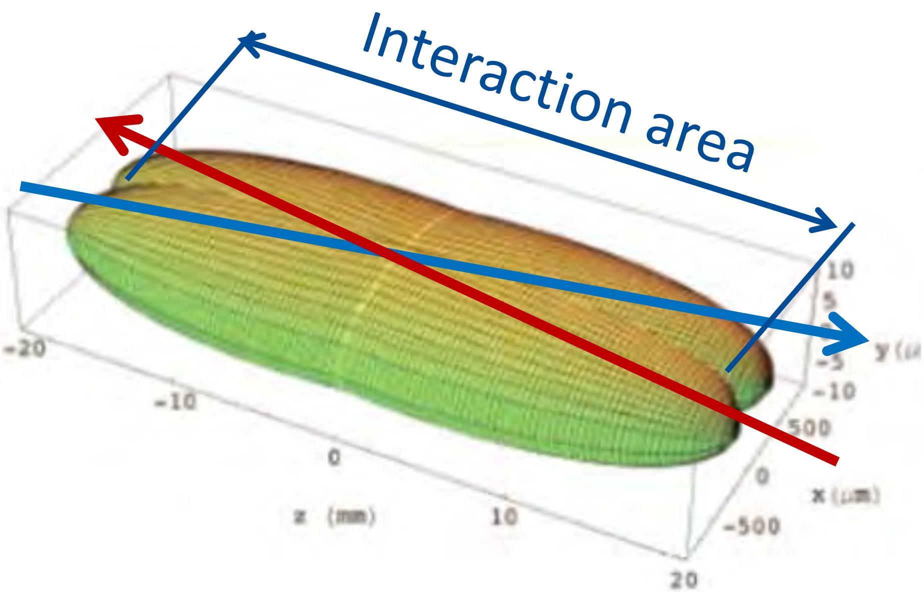

Head-on (almost)

We can not squeeze the beams due to Hour Glass effect

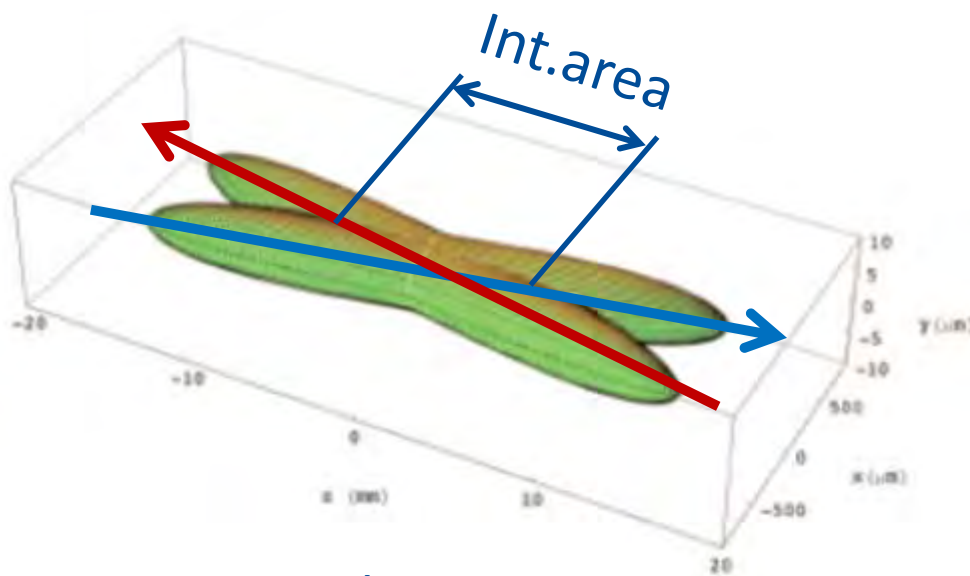

Crab-Waist

We can squeeze the beams, increase particle density and luminosity

Crab-Waist Sextipoles Off

1. P.Raimondi, 2°SuperB Workshop, March 2006

2. P.Raimondi, D.Shatilov, M.Zobov, physics/0702033

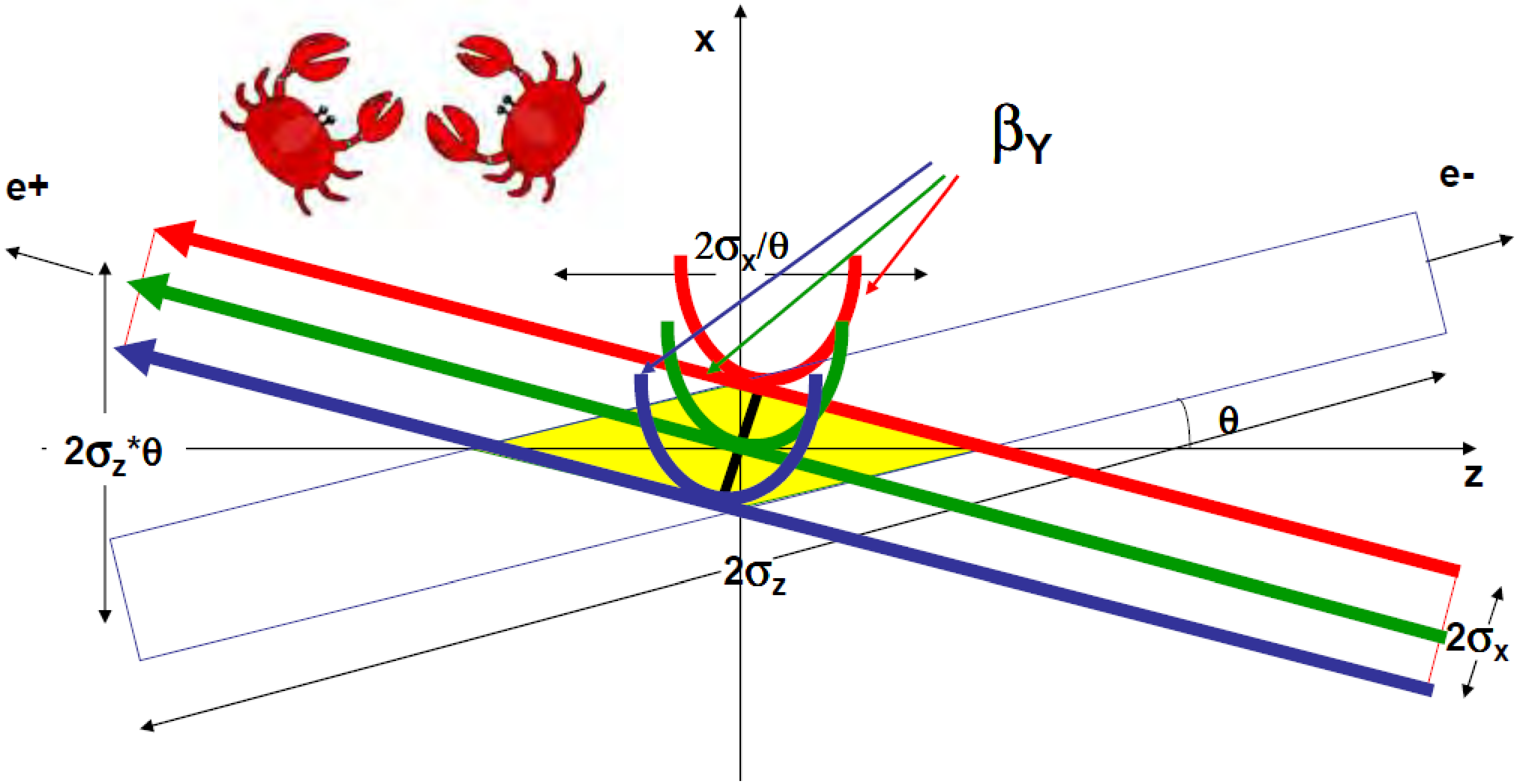

Crab-Waist Sextupoles on

1. P.Raimondi, 2°SuperB Workshop, March 2006

2. P.Raimondi, D.Shatilov, M.Zobov, physics/0702033

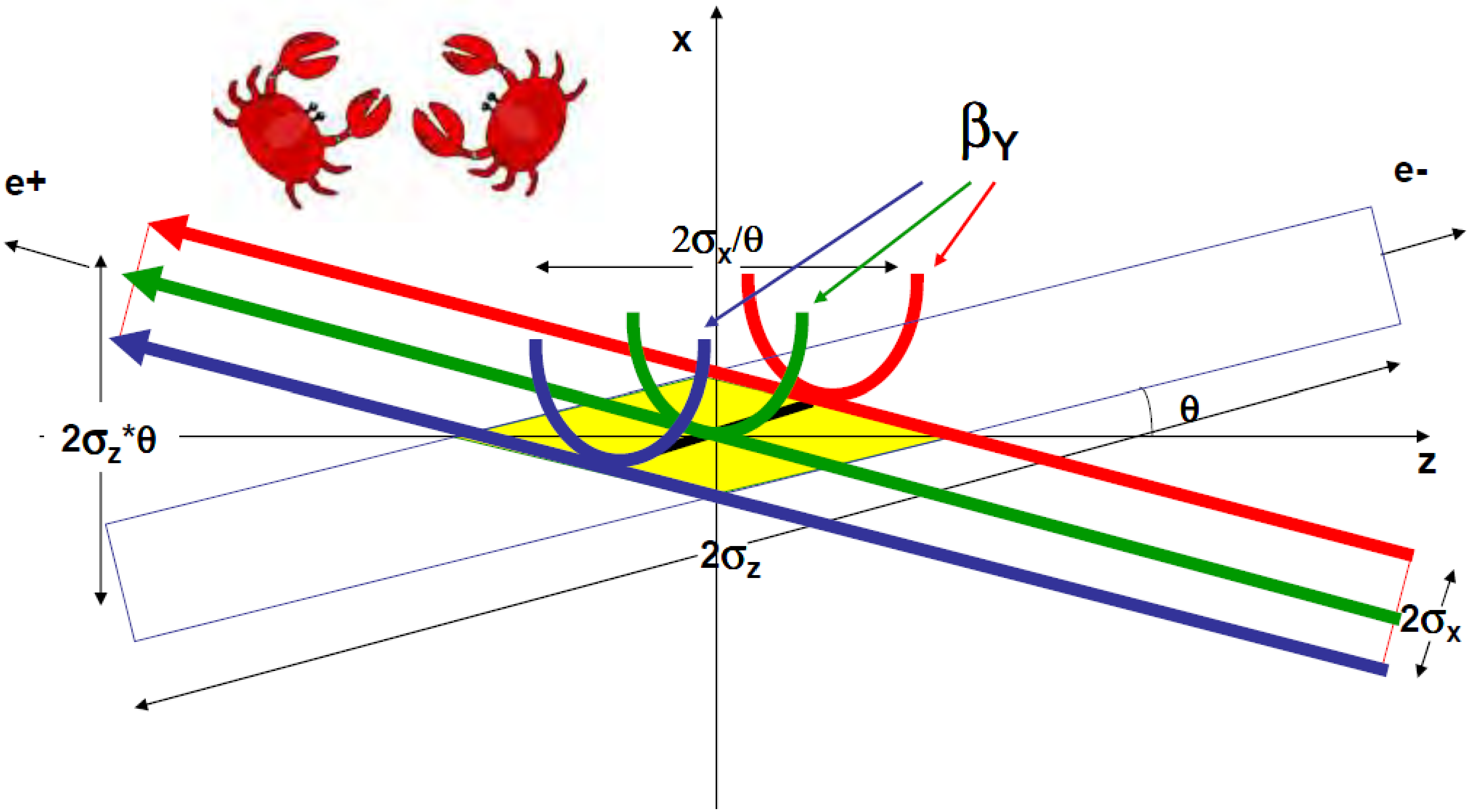

Fermilab

Luminosity vs Betatron Tunes

Red area = high luminosity

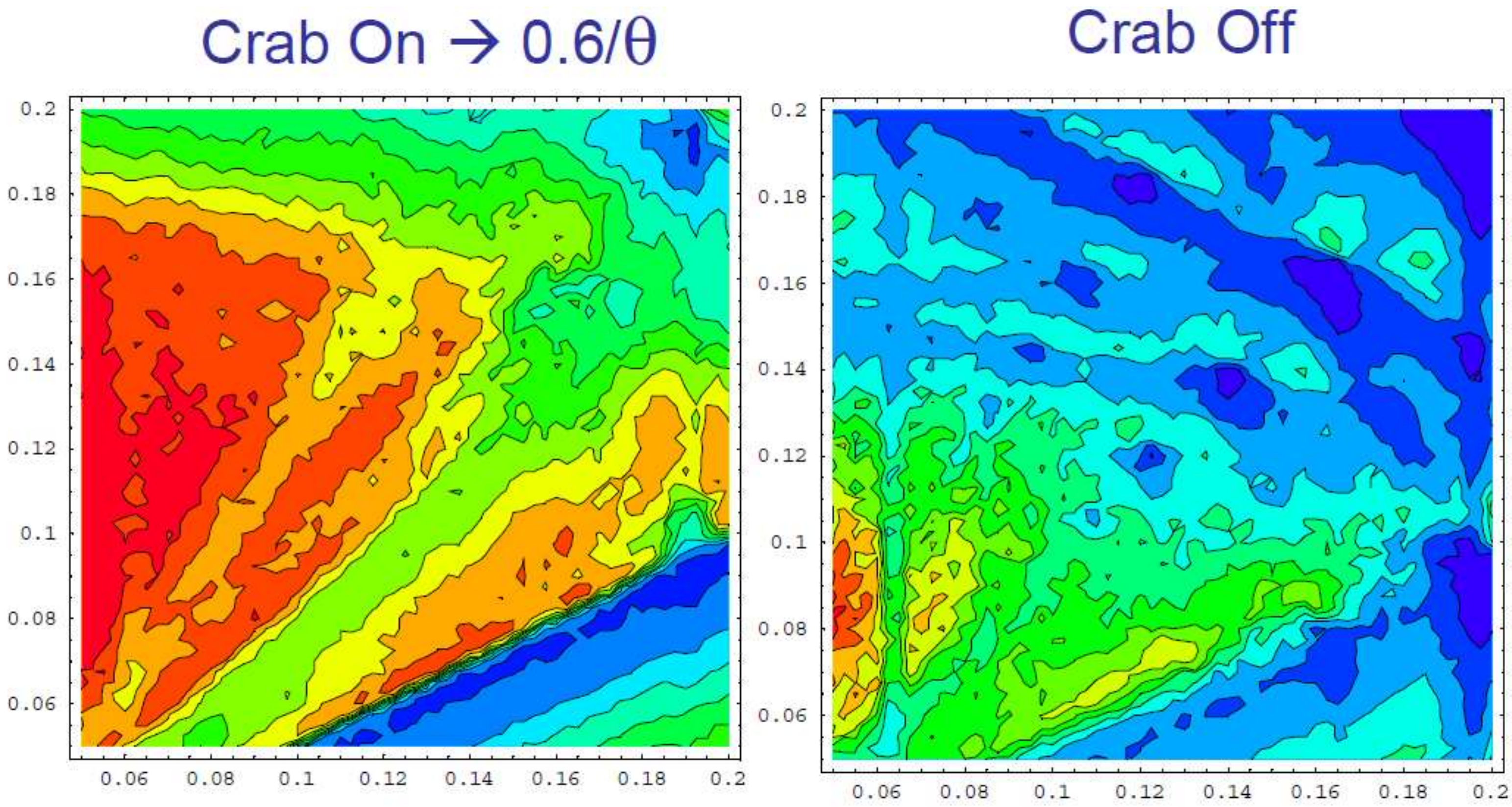

***Crab Waist* helps greatly!**

Crab-waist Condition

- Sextupole acts as a (vertical) focusing element whose strength proportional to ***x***-position $B_x = -6B_3xy$
- To shift only the IP location for different ***x*** one needs two: of certain strength

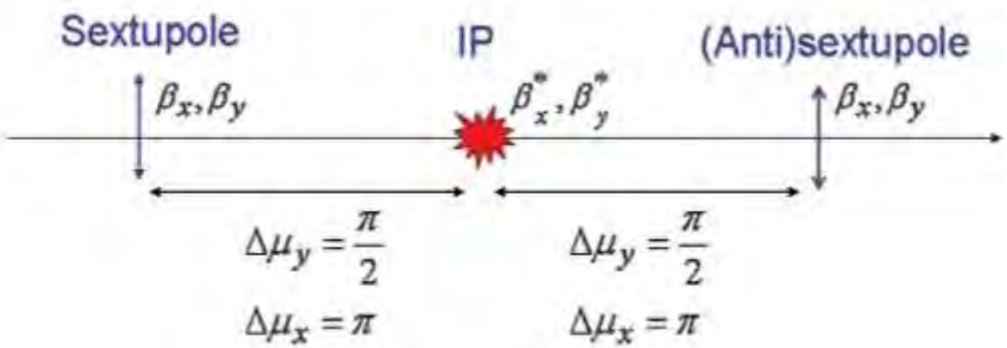

$$K = \frac{1}{\theta}\frac{1}{\beta^*_y\beta_y}\sqrt{\frac{\beta^*_x}{\beta_x}}.$$

- As the result

$$L \propto \frac{N\xi_y}{\beta^*_y}; \qquad \xi_y \propto \frac{N\sqrt{\beta^*_y/\varepsilon_y}}{\sigma_z\theta}; \qquad \xi_x \propto \frac{N}{(\sigma_z\theta)^2},$$

- Factor ~3 increase in the DAFNE luminosity with max ξ=0.2

DAΦNE: “crab waist” collisions

DAΦNE Peak Luminosity

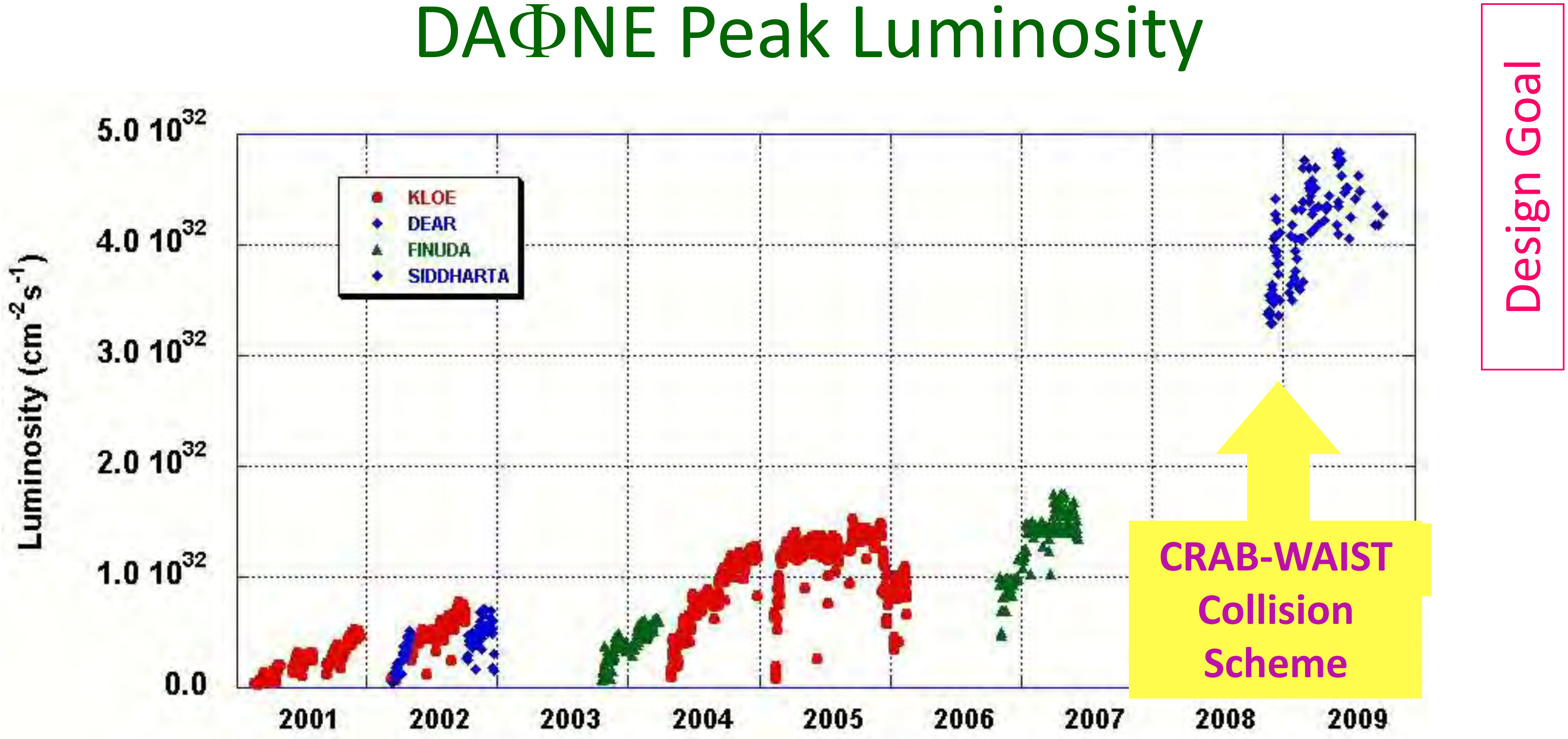

M. Zobov

Super-KEKB – Next Gen Asymmetric B-factory

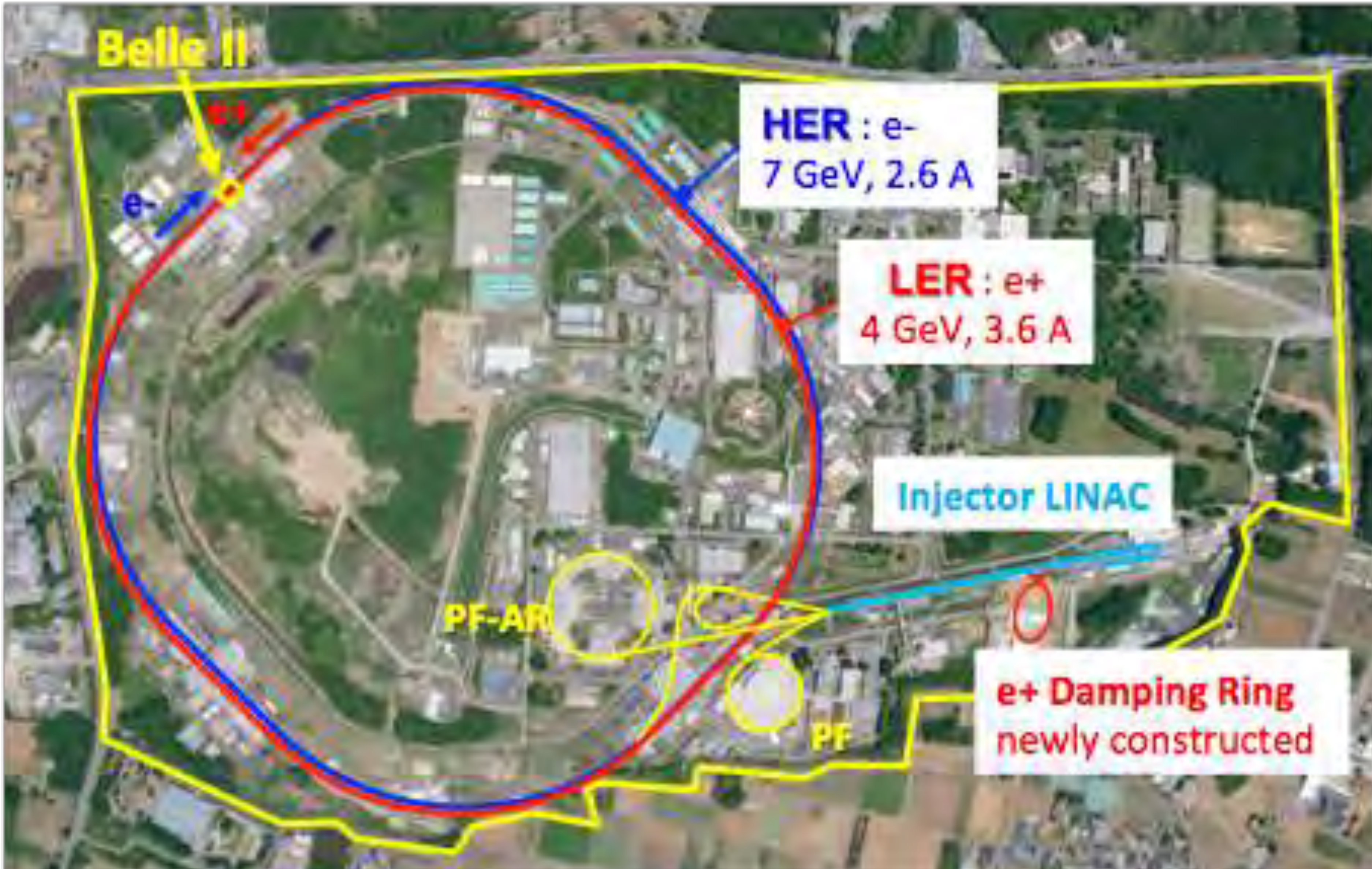

Super-KEKB Nanobeams

40x=20 from beta* and 2 from currents

To get 40x luminosity of KEKB

Reduce beam size to a few 100 atomic layers!

Lorentz factor

Beam current

Beam-Beam parameter

$$L = \frac{\gamma_\pm}{2er_e}\left(1+\frac{\sigma_y^*}{\sigma_x^*}\right)\frac{I_\pm \xi_{y\pm}}{\beta_{y\pm}^*}\left(\frac{R_L}{R_{\xi_y}}\right)$$

Geometrical reduction factors (crossing angle, hourglass effect)

Beam aspect ratio at IP

Vertical beta function at IP

Parameter		KEKB		SuperKEKB		units
		LER	HER	LER	HER	
beam energy	E_b	3.5	8	4	7	GeV
CM boost	$\beta\gamma$	0.425		0.28		
half crossing angle	ϕ	11		41.5		mrad
horizontal emittance	ε_x	18	24	3.2	4.6	nm
beta-function at IP	β_x^*/β_y^*	1200/5.9		32/0.27	25/0.30	mm
beam currents	I_b	1.64	1.19	3.6	2.6	A
beam-beam parameter	ξ_y	0.129	0.090	0.0881	0.0807	nm
beam size at IP	σ_x^*/σ_y^*	100/2		10/0.059		μm
Luminosity	L	2.1×10^{34}		8×10^{35}		$cm^{-2}s^{-1}$

Super-KEKB – Next Gen B-factory

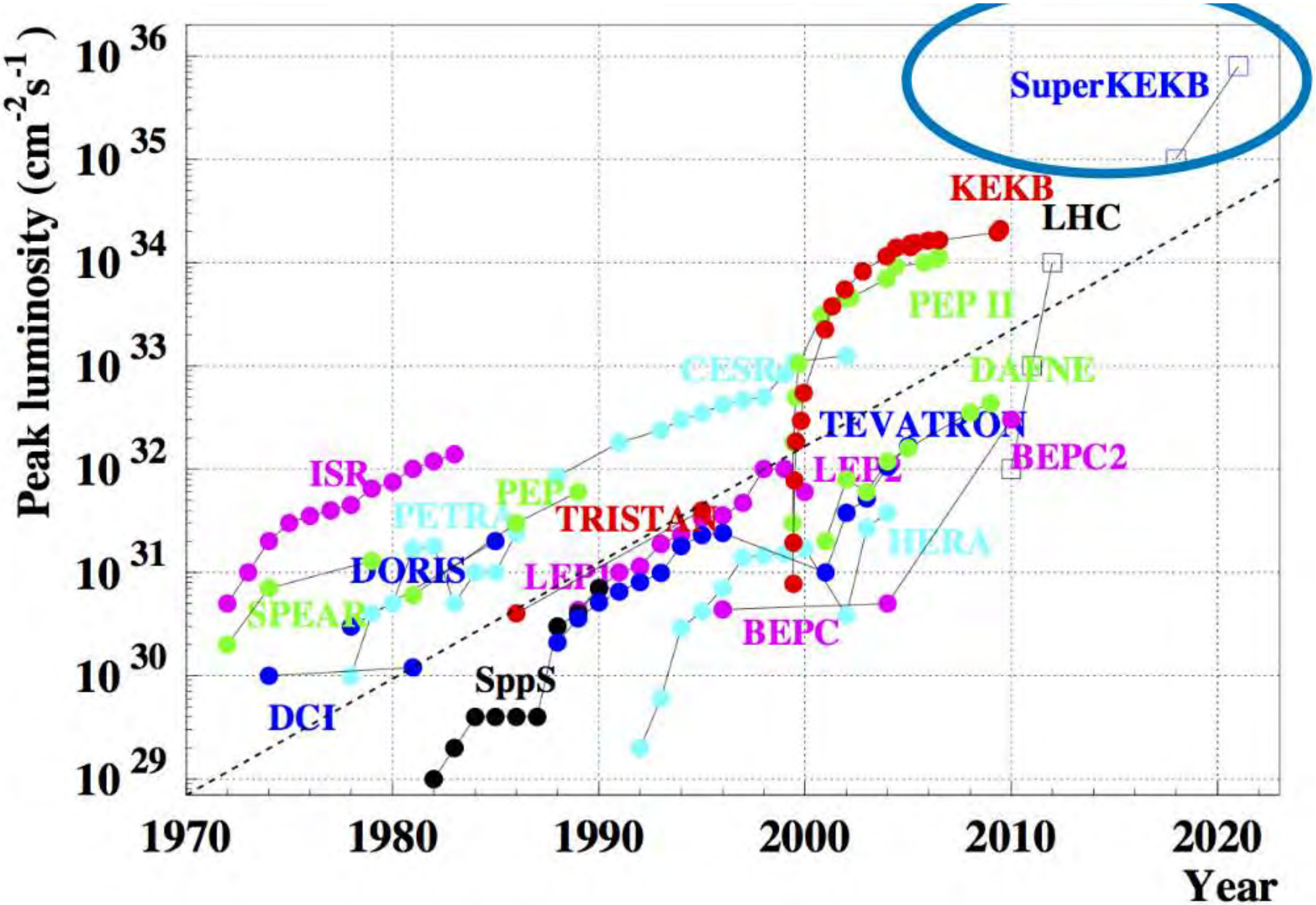

Super-KEKB :Status and Challenges

- Peak luminosity 3.81x10^{34} cm^{-2}s^{-1} – *collider world record*
- Design goal 80 x10^{34} cm^{-2}s^{-1}
- Challenges now :
  - One of the LEP (e+) low-beta quadrupole cryostats have no shielding – fields affect optics
  - Small dynamic aperture in LER(e+) leads to poor lifetime – need to correct optics
  - Beam background and beam aborts due to (extremely fast) beam loss.
    - Serious radiation dose at collimators, severe damage at collimators, damage on Belle II detector.
    - Large risks for increasing beam currents (to achieve higher luminosity).
  - Collimator transverse impedance (TMCI threshold)
  - Beam-beam blowup (in vertical plane)…Chromatic X-Y coupling??
  - Quality and amount of the injection beam from Linac
    - Larger emittance than expected… from CSR in beamline?

Future Circular e+e- Colliders

- Energy of interest – at least Higgs production (ZH, ~240 GeV)
- High luminosity O(1e34-1e35)…(10^4-10^5) Higgses per year
- High beam energy 120 GeV → huge SR loss/turn multi-GeV

$$U_0[\mathrm{keV}] = 88.46 \frac{E[\mathrm{GeV}]^4}{\rho[\mathrm{m}]}$$

120 GeV, 10 km → 2 GeV

- High lumi needs high current → huge RF power = SR power
- As the result – large rings, 100MW power $P_{SR} = 2I \cdot \Delta E_{SR}$

$$\mathcal{L} = \frac{3}{16\pi r_0^2 (m_e c^2)} \frac{P_{\mathrm{SR}} \xi_y \rho}{\beta_y^* \gamma^3}$$

Two Competing Projects

91 km FCCee at CERN, 100 MW

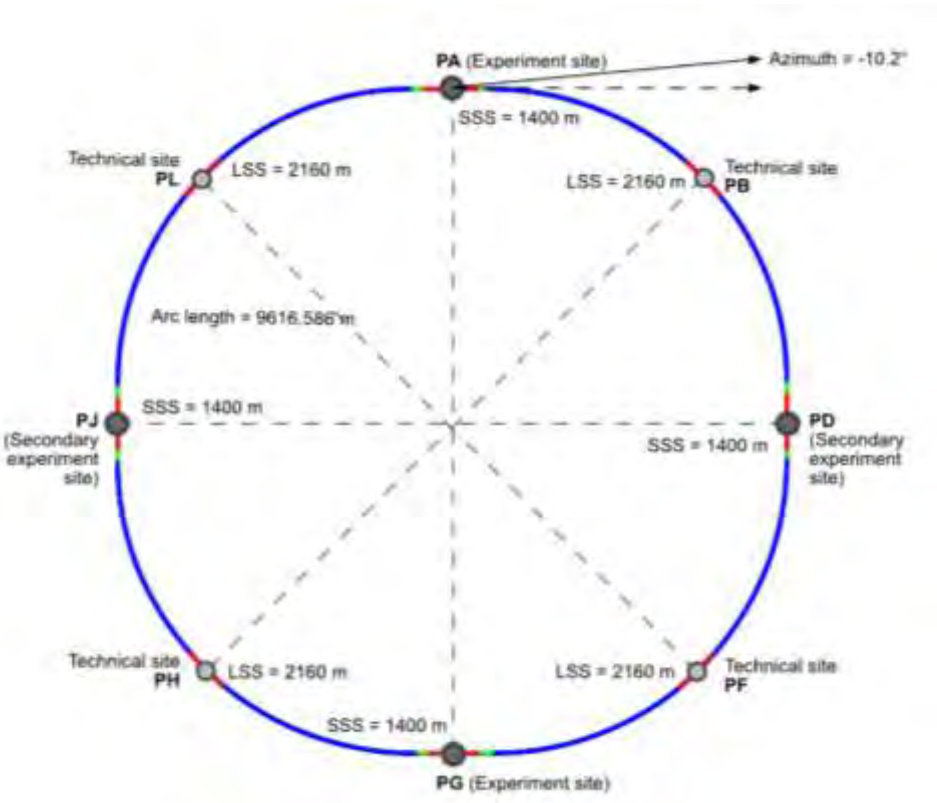

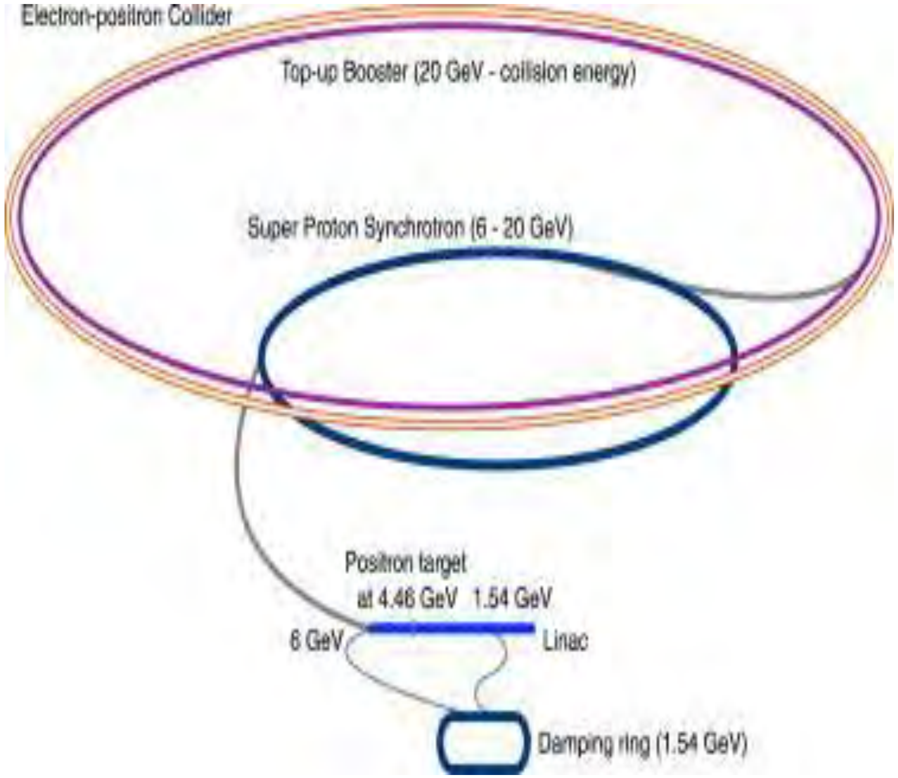

100 km CEPC (IHEP), 60 MW

Two rings for e+ and e-

Two rings for e+ and e-

FCCee& CEPC @ Several Energies of Interest

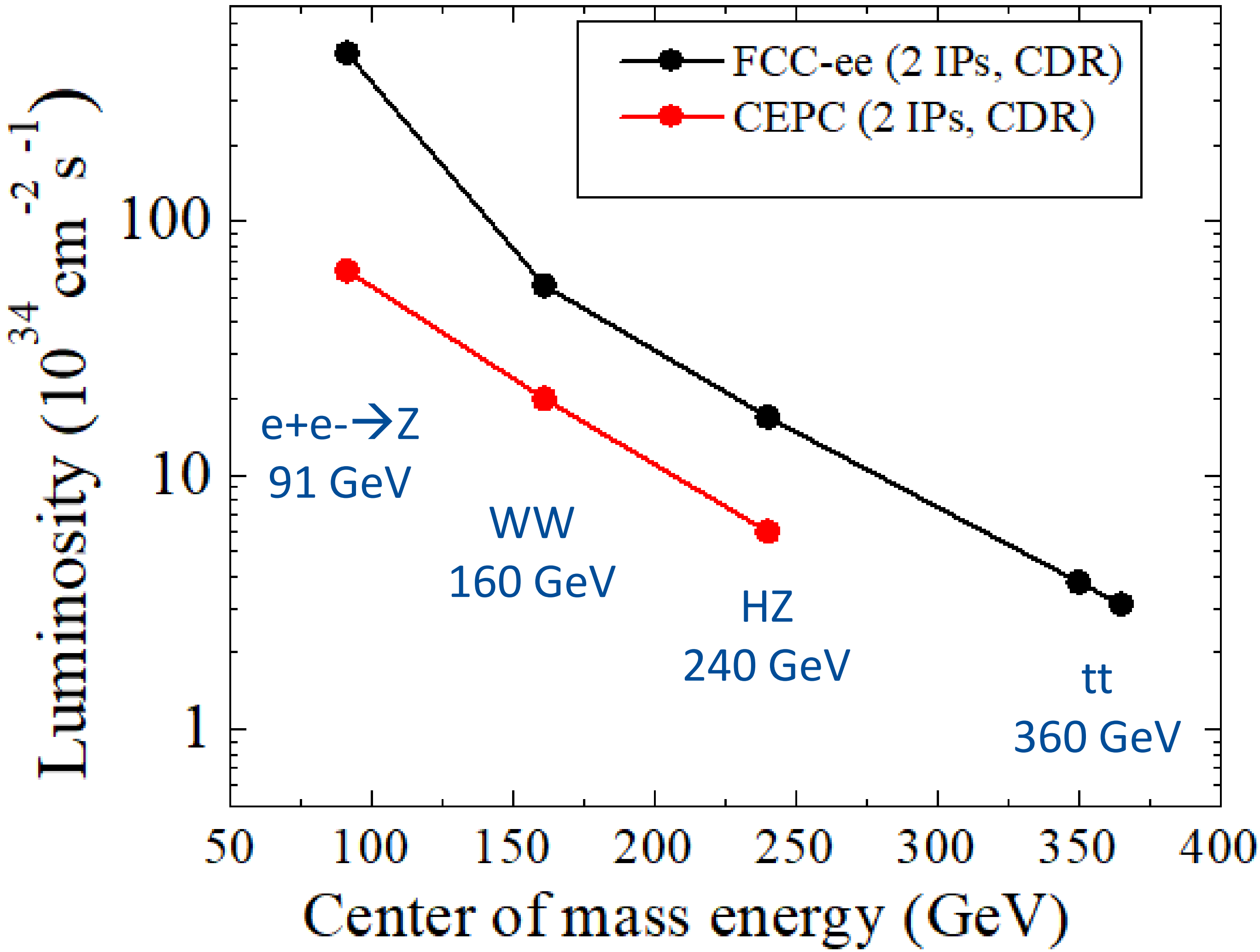

Fermilab

Specific Issues for FCCee and CEPC

- Wall-plug power to RF & beam efficiency (280 MW →100MW)
- Shielding from 1 MeV SR photons
- Cost
- Beamstrahlung – emission of hard photons → beam losses

$$\tau_{bs} \propto \frac{\rho^{3/2}\sqrt{\eta}}{\sigma_s}\exp(A\eta\rho) \qquad \frac{1}{\rho} \approx \frac{N r_e}{\gamma \sigma_x \sigma_s}$$

η : ring energy acceptance

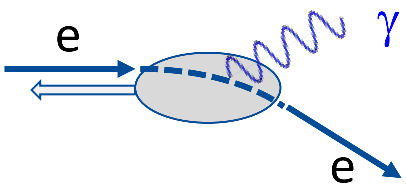

ρ : mean bending radius at the IP (in the field of the opposing bunch)

- ❑ for acceptable lifetime, ρ×η must be sufficiently large
  - o *flat beams (large σ_x) !*
  - o *bunch length !*
  - o *large momentum acceptance: aiming for* ***≥1.5% at 175 GeV***
    - LEP: <1% acceptance, SuperKEKB ~ 1.5%

FUTURE CIRCULAR COLLIDER

FCC-ee collider parameters (stage 1)

K. Oide

Parameter [4 IPs, 91.2 km, T_{rev}=0.3 ms]	Z	WW	H (ZH)	ttbar
beam energy [GeV]	45	80	120	182.5
beam current [mA]	1400	135	26.7	5.0
number bunches/beam	8800	1120	336	42
bunch intensity [10^{11}]	2.76	2.29	1.51	2.26
SR energy loss / turn [GeV]	0.0391	0.37	1.869	10.0
total RF voltage 400/800 MHz [GV]	0.120/0	1.0/0	2.48/0	4.0/7.67
long. damping time [turns]	1170	216	64.5	18.5
horizontal beta* [m]	0.15	0.2	0.3	1
vertical beta* [mm]	0.8	1	1	1.6
horizontal geometric emittance [nm]	0.71	2.17	0.64	1.49
vertical geom. emittance [pm]	1.42	4.34	1.29	2.98
horizontal rms IP spot size [μm]	10	21	14	39
vertical rms IP spot size [nm]	34	66	36	69
beam-beam parameter ξ_x / ξ_y	0.004/ .159	0.011/0.111	0.0187/0.129	0.096/0.138
rms bunch length with SR / BS [mm]	4.32 / 15.2	3.55 / 7.02	2.5 / 4.45	1.67 / 2.54
luminosity per IP [10^{34} cm^{-2}s^{-1}]	181	17.3	7.2	1.25
total integrated luminosity / year [ab^{-1}/yr]	86	8	3.4	0.6
beam lifetime rad Bhabha / BS [min]	19 / ?	20 / ?	10 / 19	12 / 46

Consequence of Low Lifetime →

To keep average luminosity ~ peak luminosity

requires alternating replenishment of the two colliding beams, keeping beam currents stable within a few per cent (aka "top-up injection")

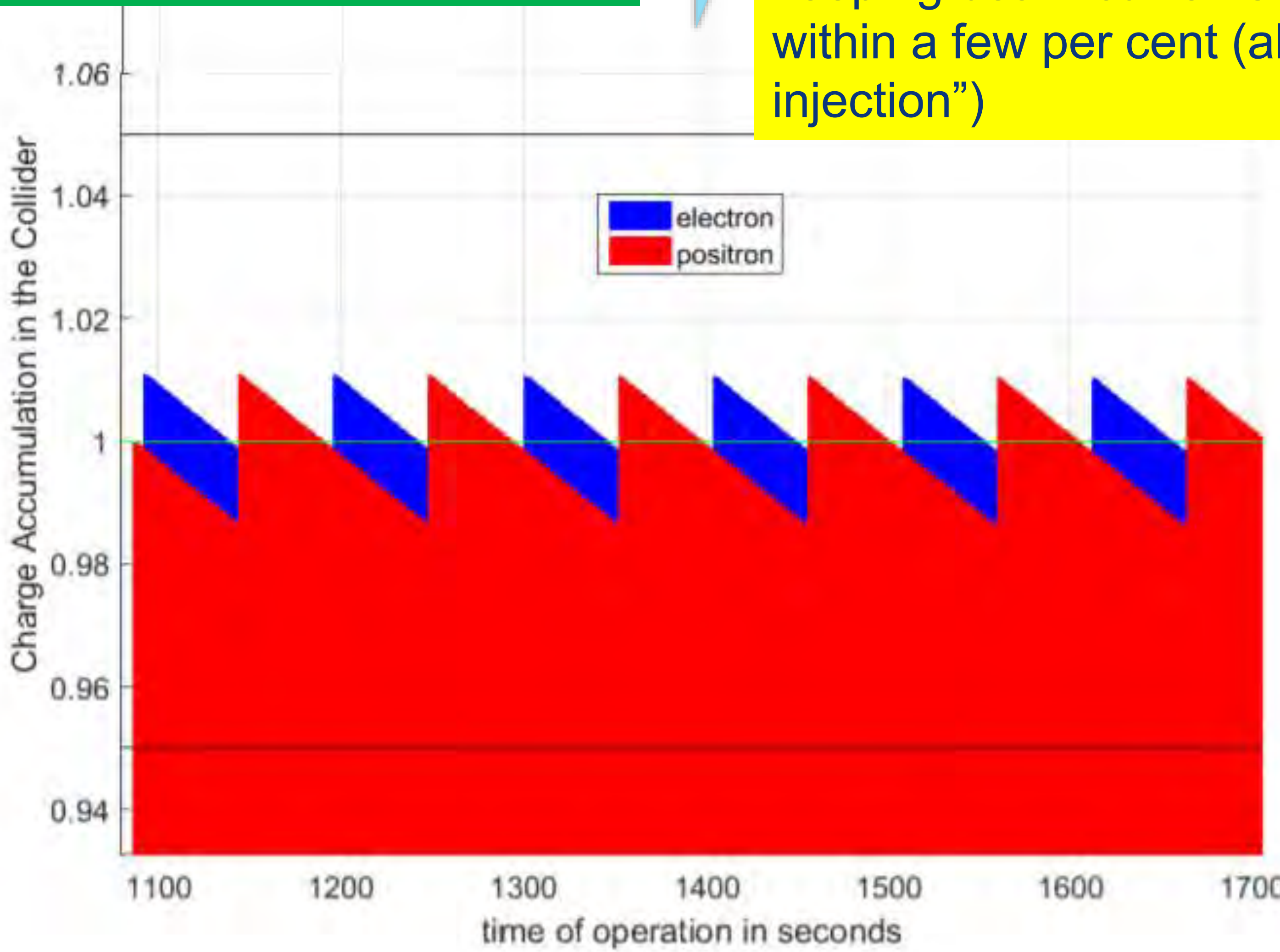

Top-Up Injection in FCCee

beside the collider ring(s), a booster of the same size (same tunnel) must provide beams for top-up injection to sustain the extremely high luminosity

- same size of RF system, but low power (~ MW)
- top up frequency ≈0.1 Hz
- booster injection energy ≈5-20 GeV
- bypass around the experiments

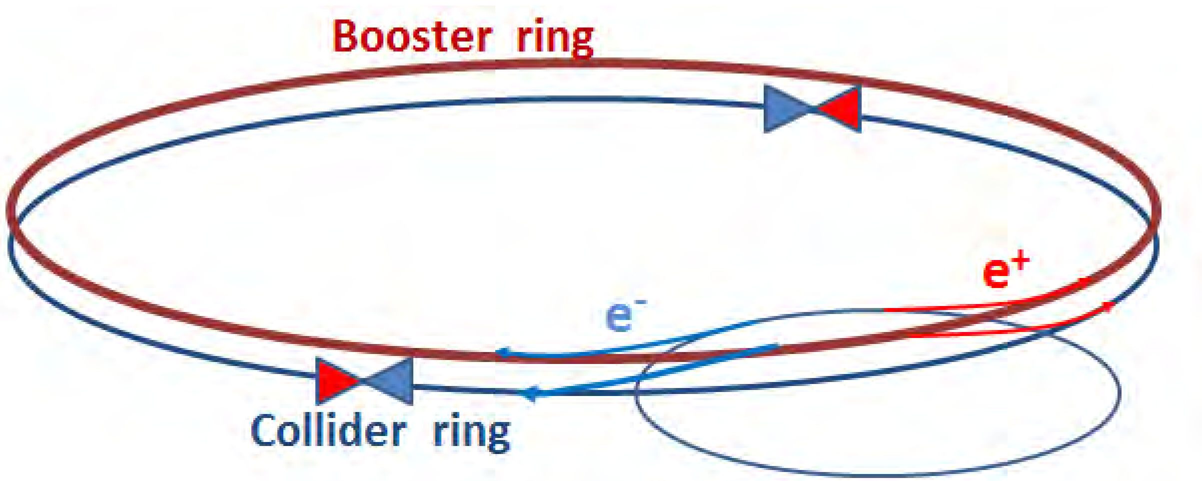

Two separate booster rings for e+ and e- in the CEPC

Cost !!!

Beam Polarization and Spin Dynamics

Sokolov-Ternov effect: SR jumps prefer spin-down

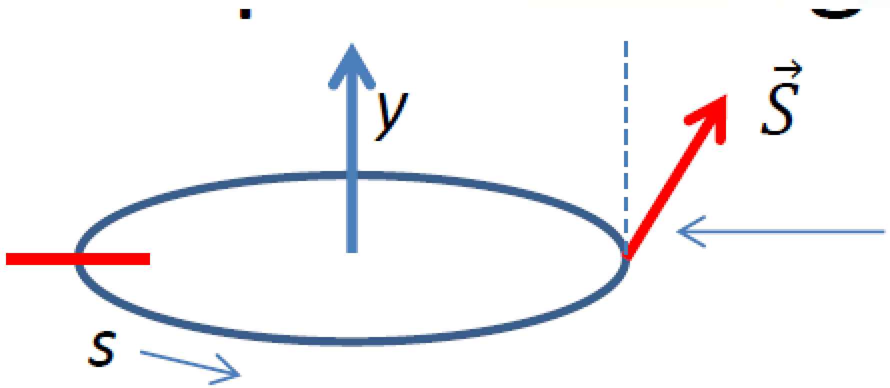

$$\xi(t) = A\left(1 - e^{-t/\tau}\right)$$

$$A = 8\sqrt{3}/15 \approx 0.924$$

$$\tau = \frac{8\hbar^2}{5\sqrt{3}mce^2}\left(\frac{mc^2}{E}\right)^2\left(\frac{H_0}{H}\right)^3$$

$H_0 \approx 4.414 \times 10^{13}$ gauss is the Schwinger field

260 hrs at 45 GeV… at 80 GeV, this time falls as $(45/80)^5$ to 15 hrs.
45 GeV LEP: 5 hours → *P*~6%

$$P = 92.4\,(\%)/(1 + \tau_{ST}/\tau_{dep})$$

Depolarization due to vertical orbit (= B_x field in quads) and B_z in detector solenoids

Resonant spin harmonic amplitudes in orbit distortions can be compensated using special orbit bumps or global correction (in LEP → *P*~40%)…no use in collisions but can be used for non-colliding bunches to do energy calibration to dE/E ~1e-6

Thanks for Your Attention !

Questions !?

Literature

Instabilities:
A.Chao, *Physics of collective beam instabilities in high energy accelerators* (1993)
https://www.slac.stanford.edu/~achao/wileybook.html

Many useful articles:
S.Myers, H.Schopper *Accelerators and Colliders* (2013, open access)
https://link.springer.com/book/10.1007/978-3-030-34245-6

U.S. Particle Accelerator School
Education in Beam Physics and Accelerator Technology

Fermilab

Managed by Fermi Research Alliance, LLC for the U.S. Department of Energy Office of Science

Hadron Colliders: Tevatron and LHC

Vladimir Shiltsev, Fermilab

part of the "Colliders" class by V.Lebedev, N.Mokhov and V.Shiltsev

US Particle Accelerator School, Jan 24 – Feb 4, 2022

Tevatron Collider at Fermilab

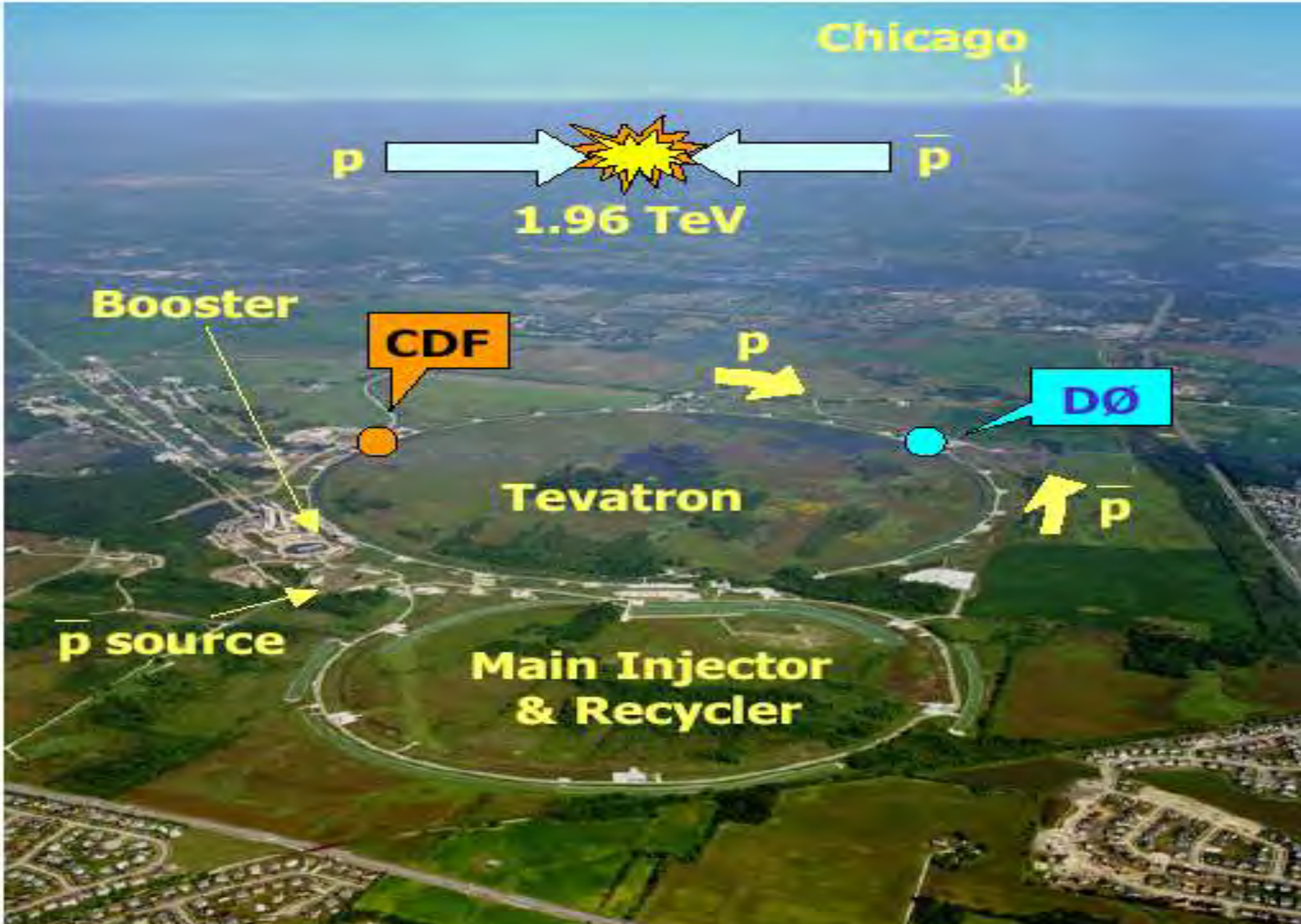

ab

Tevatron

C=6.28km
~800 SC
Magnets (4d+q)
B_max=4.5T
E=980GeV
E_inj=150 GeV
Proton clockws
Pbars counter
36+36 bunches
Same aperture
26 HV separators
2 Low-beta
insertions

<u>*Same magnets = to turn into a COLLIDER = need same direction currents as F=J x B = particles and antiparticles (p and pbars)*</u>

Tevatron Contributions to Science and Technology

- Technology:
  - 1st SC accelerator ring - NbTi magnets 4.5 T
  - 1st ever permanent magnets 3.3 km 8 GeV Recycler Ring
  - Record antiproton production & accumulation with stochastic and electron cooling systems in Debuncher, AA, and Recycler → 90% of the world's total man-made nuclear antimatter ever produced (17 ng)
  - Two-stage collimation systems

- Beam physics advances:
  - Longitudinal manipulations slip-stacking in Main Injector and momentum mining in Recycler
  - Beam-beam record at $\xi_{x;y} \sim 0.025$, first successful demo b-b compensation by electron lenses,
  - New collimation techniques : crystal collimation, hollow e-lens collimation and longitudinal abort gap collimation

Tevatron Accelerator Complex

Protons: Linac→ Booster→Main Injector → Tevatron

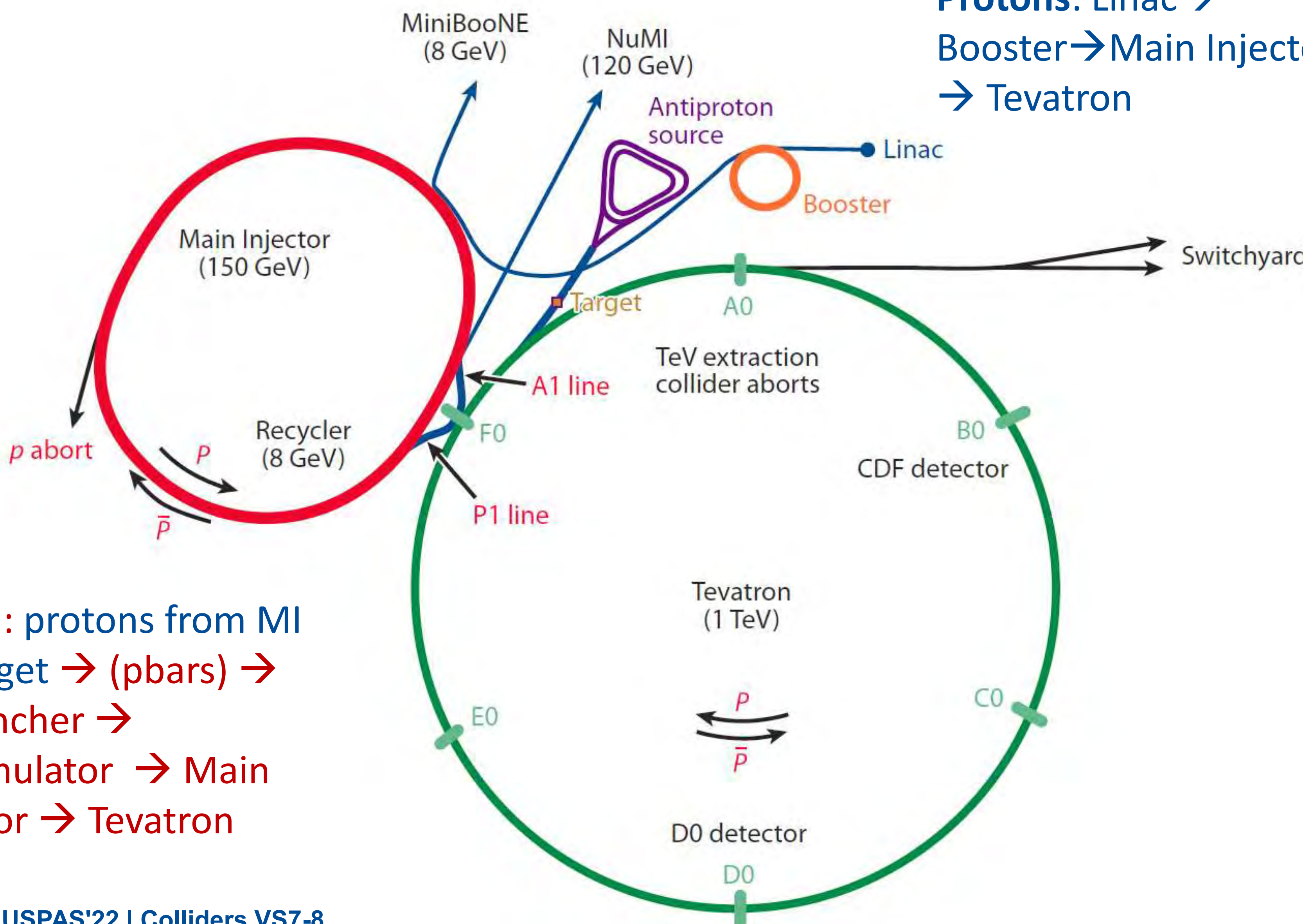

Pbars : protons from MI → target → (pbars) → Debuncher → Accumulator → Main Injector → Tevatron

Tevatron Timeline

Jul 1983 Tevatron SC synchrotron commissioned, reached world record 512 GeV (protons)

1982-1985 Antiproton source construction & commissioning, installation of the B0 low beta insertion magnets

Oct 1985 First 1.6 TeV c.o.m. p-pbar collisions in CDF

1987-1989 Collider Run at 1.8TeV c.o.m., magnet leads fix

1990 -1992 HV separators installed, new low beta insertions at D0 and B0 interaction regions

1992 -1993 Collider Run Ia at 1.8 TeV c.o.m.,both CDF & D0

1992 -1993 400 MeV Linac construction and commissioning

1994 -1996 Collider Run Ib, top quark discovery

1993 -1999 Main Injector construction and commissioning

2001 - 2011 Collider Run II, 1.96 TeV c.o.m.

Detectors: CDF and D0

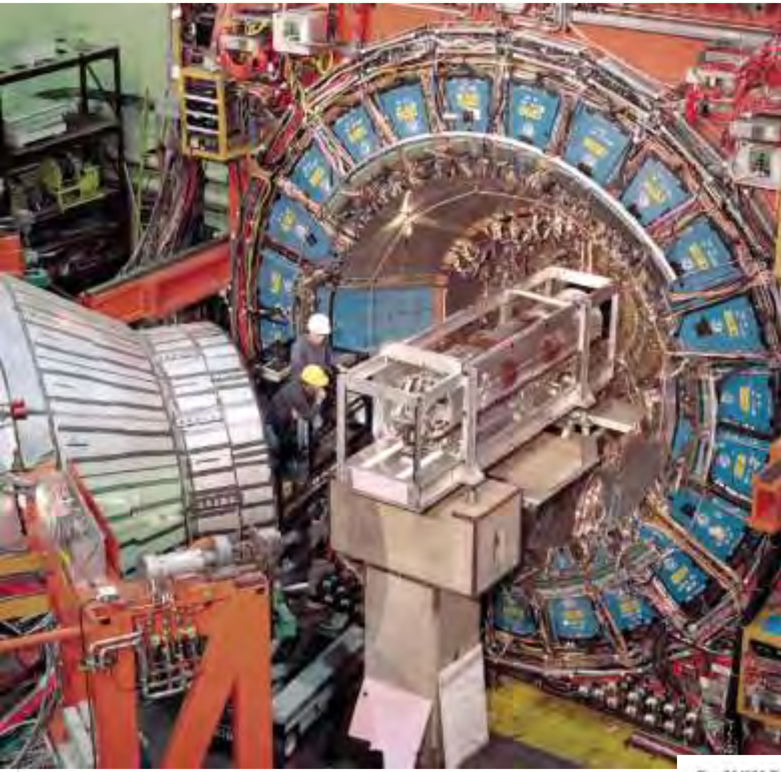

For the purpose of these lectures:

Fascinating apparata

Great people (~700 in each team)

Tons of great results:
top quark discovery 1996, Higgs observation (before LHC)

Have some systems affecting beam: $\beta^{*}=28\text{cm}$

Very instrumental and can be a great beam diagnostics

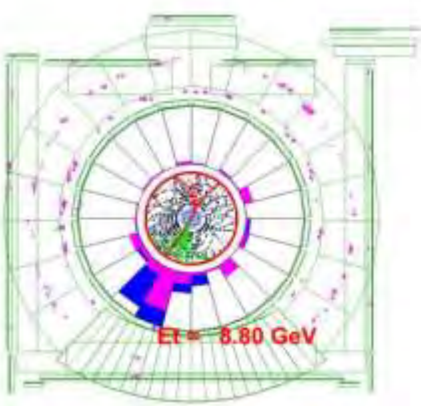

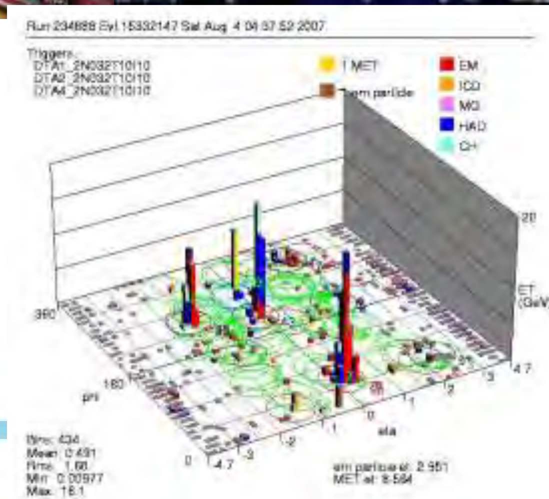

Luminosity, Lifetime and Integral

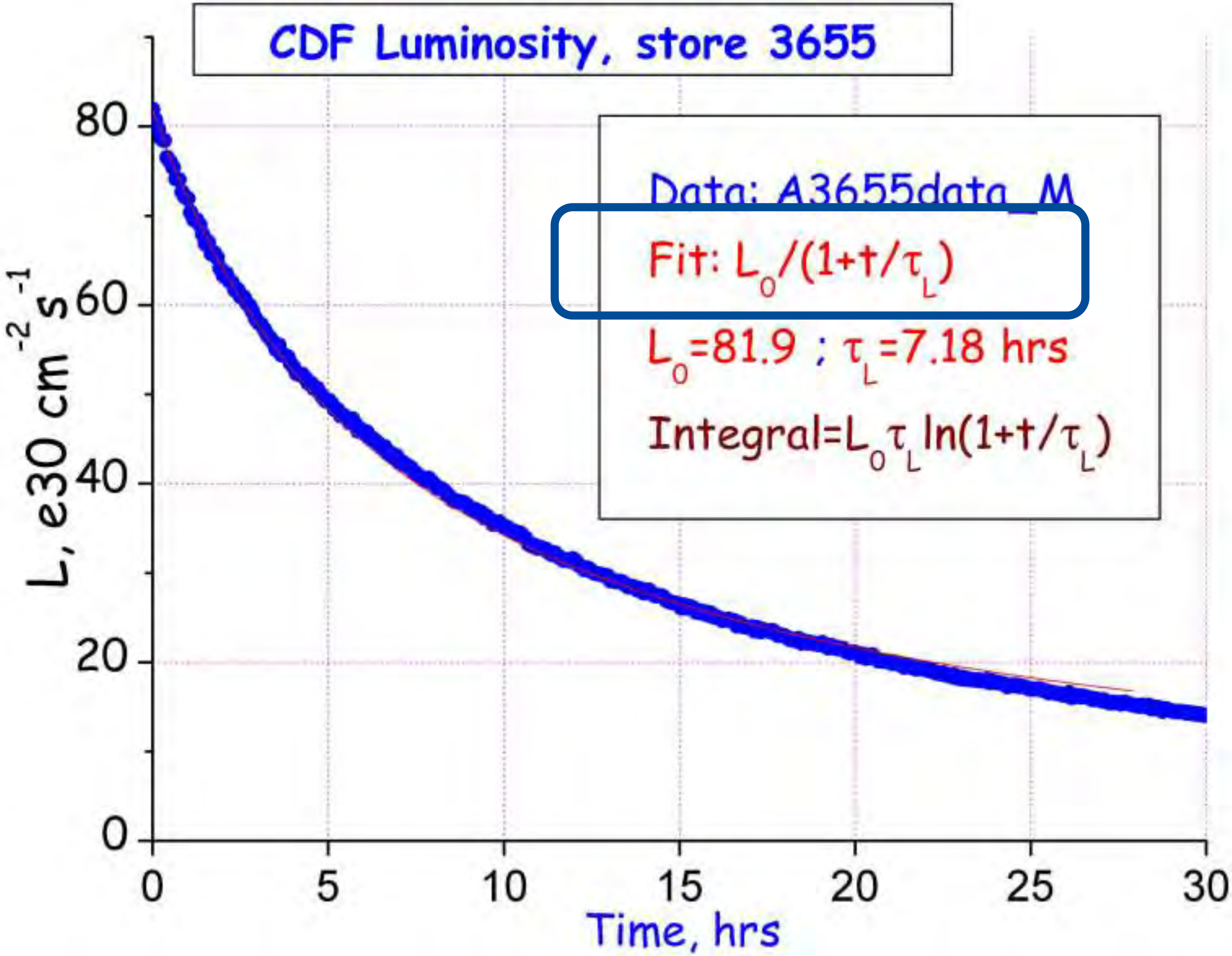

Luminosity and Luminosity Integral

$$L = \gamma f_0 \frac{(B N_{\bar{p}}) N_p}{2\pi\beta^* \left(\varepsilon_p + \varepsilon_{\bar{p}}\right)} H\left(\sigma_l / \beta^*\right)$$

$$I = \int L dt \approx N_{stores} \tau_L L_0 \ln(1 + T / \tau_L)$$

Luminosity Integral: primary factors

- ❑Number of antiprotons: BN_{pbar}
- ❑Number of protons: N_p
- ❑Emittances ε_p ε_{pbar}
- ❑Beta* at IP and bunchlength: H(x)/beta^*
- ❑Lumi-lifetime: τ_L
- ❑Number Stores: N_{stores}

Lifetime Constituents (end of Run II)

$$\tau_L^{-1} = \tau_\varepsilon^{-1} + \tau_a^{-1} + \tau_p^{-1} + \tau_H^{-1}$$

(9-11) + (16-18) +(25-45)+(70-80) =(5-5.5) hrs

- Emittance growth = >90% IBS + <10% Beam-Beam
- Pbar lifetime = (80-85)% burnup + ~15% LR Beam-Beam
- Proton lifetime = >50% Beam-Beam + <50 % burnup
- Hougrlass lifetime = >90% IBS + <10% Beam-Beam

$$\left(\frac{1}{\tau_a}\right)_{BB} = \left(\frac{dN_a}{N_a dt}\right)_{BB} \propto N_p \frac{\varepsilon_a^2}{S^3}$$

IBS determined ~50-55% of lifetime

Burnup due to luminosity – another 30-35

Beam-Beam Interaction reduces lumi- lifetime by 12-17 %

Tevatron Parameters

Table 2. Design and achieved performance parameters for Collider Runs I and II (typical values at the beginning of a store).

	Run Ia	Run Ib	Run II	
Energy (center-of-mass)	1800	1800	1960	GeV
Protons/bunch	1.2	2.3	2.9	$\times 10^{11}$
Antiprotons/bunch	3.1	5.5	8.1	$\times 10^{10}$
Bunches/beam	6	6	36	
Total Antiprotons	19	33	290	$\times 10^{10}$
Proton emittance (rms, normalized)	3.3	3.8	3.0	π mm-mrad
Antiproton emittance (rms, normalized)	2	2.1	1.5	π mm-mrad
β^*	35	35	28	cm
Luminosity (Typical Peak)	5.4	16	340	$\times 10^{30}$ cm^{-2}sec^{-1}
Luminosity (Design Goal)	5	10	200	$\times 10^{30}$ cm^{-2}sec^{-1}

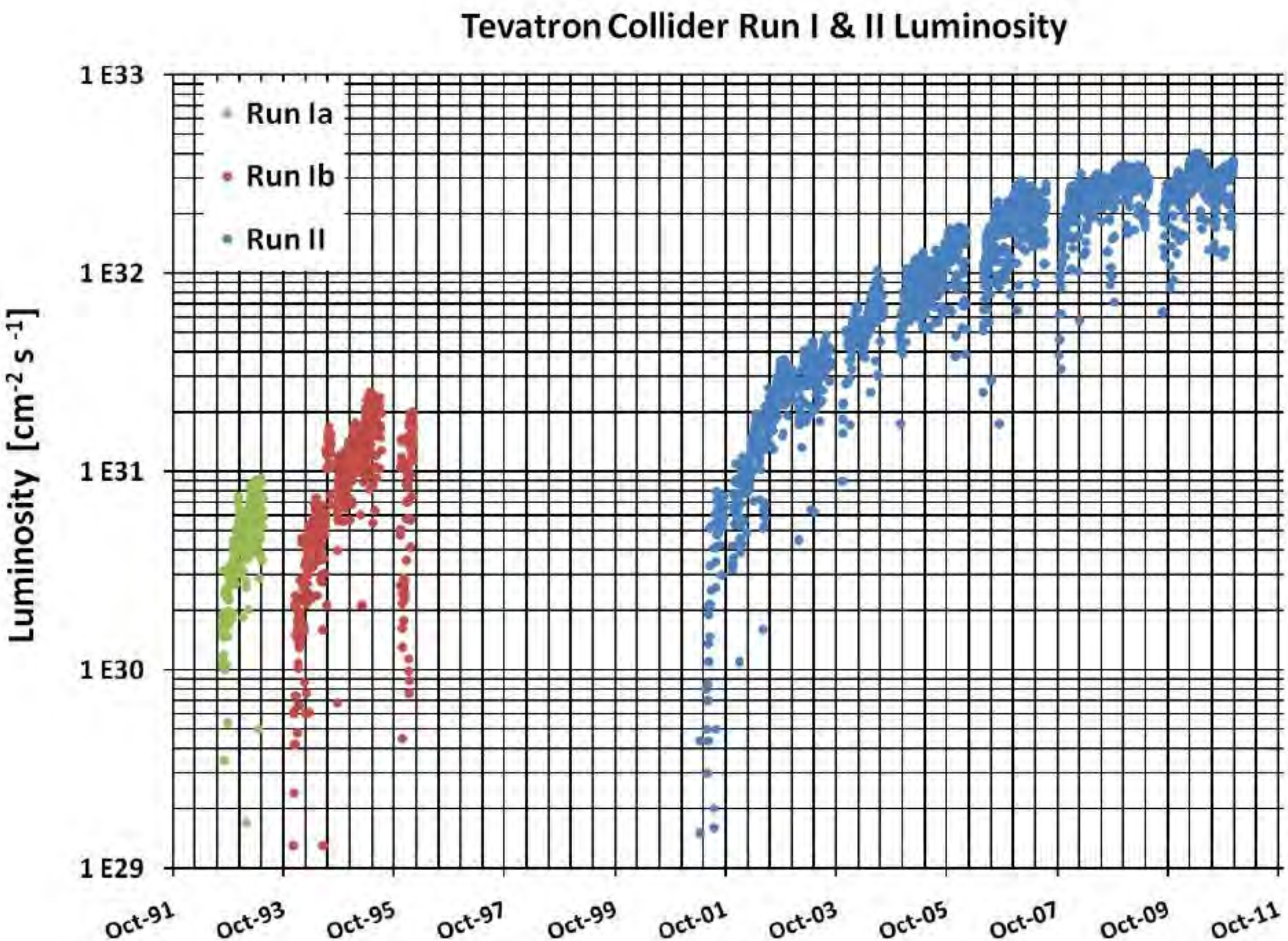

Tevatron Collider Run I & II Luminosity
Run Ia
Run Ib
Run II
Luminosity [cm-2 s-1]
1 E33
1 E32
1 E31
1 E30
1 E29
Oct-91
Oct-93
Oct-95
Oct-97
Oct-99
Oct-01
Oct-03
Oct-05
Oct-07
Oct-09
Oct-11

Tevatron Optics: FODO cells +IPs

	Dipoles	Quads	Spools
Number	772+2	90+90	88+88

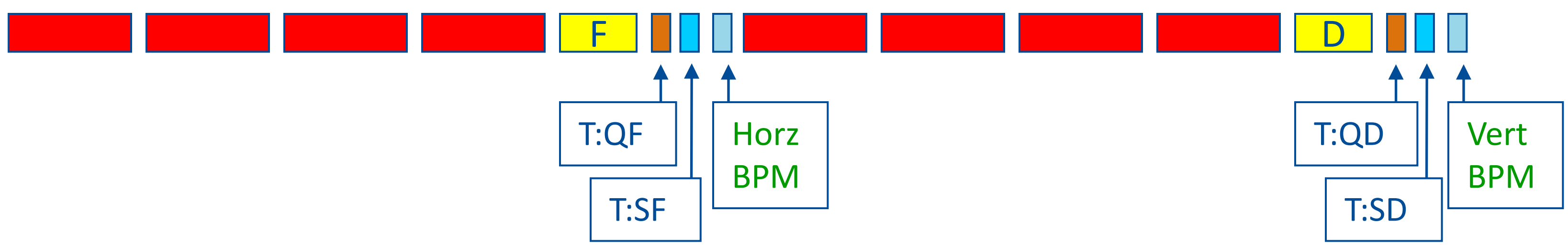

Tevatron Dipole

(There are 772 Tevatron dipoles)

F Tevatron Quadrupole

Tevatron Quad corrector

Tevatron Sextupole corrector

Tevatron Beam Position Monitor

Heart of the Collider – 4.5 T SC magnets

Age Effect: *SC Coils Sank wrt Iron Yoke*

After ~20 years of operation, the coil block sank wrt iron yoke under strong forces of springs in “smart bolts” (smashed G10 spacers)

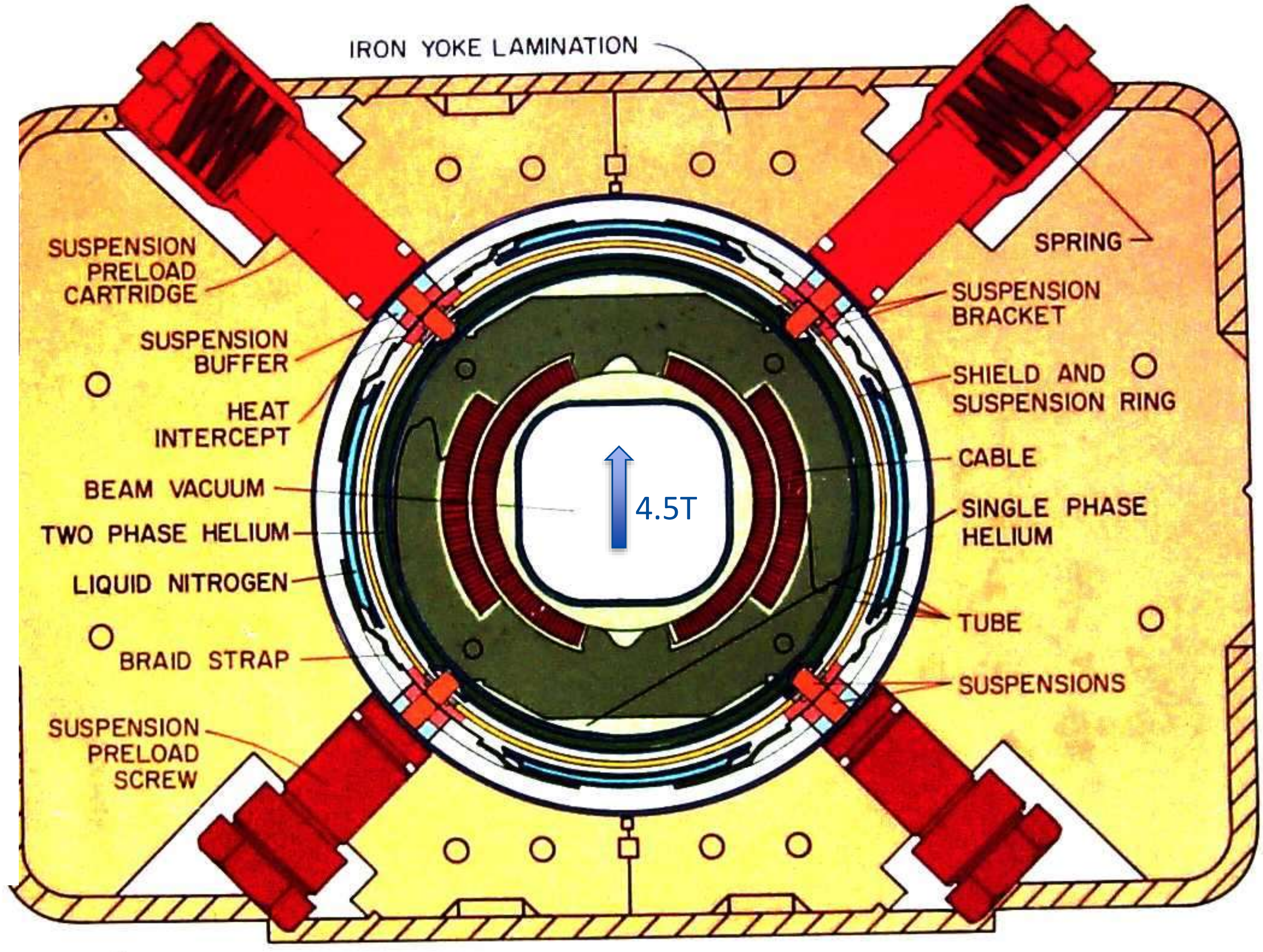

Reshimming=Lifting Up SC Coils

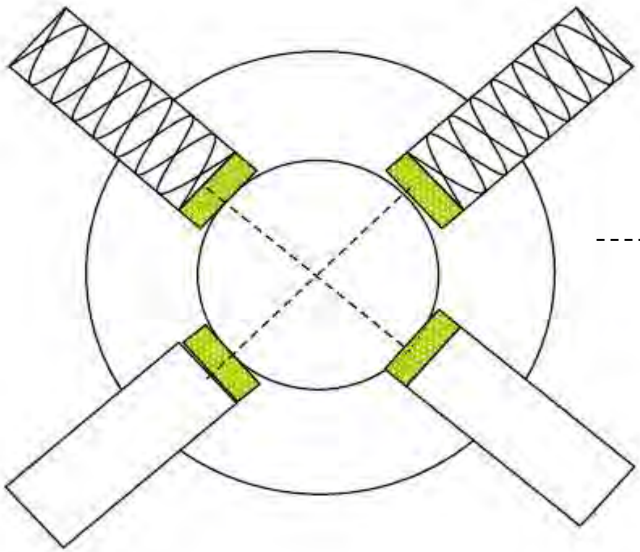

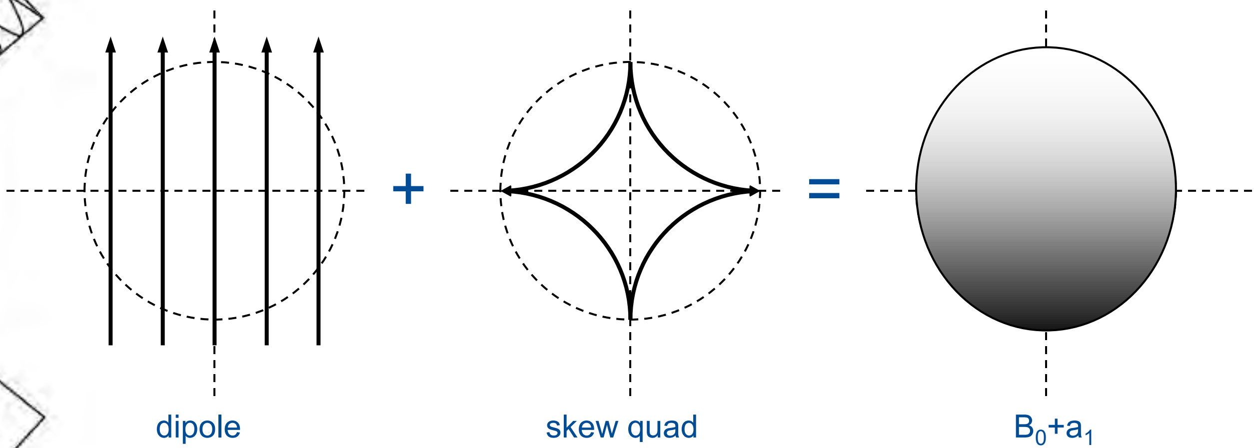

dB_skew/B_dipole=1.4e-4
at 25.4 mm

Solution: add 140 micron shims to the bottom suspensions to raise the coil block. In 3 years we did it for all 774 dipoles (18 “smart” bolts and 18 lower bolts per magnet) → coupling reduced as expected and correspondingly beam size mismatch at injection

Skew quadrupole → x-y coupling

Expected Motion (and as the results – optics functions)

$$X'' + 4\pi^2 Q_x^{\,2}\, x = 0$$
$$Y'' + 4\pi^2 Q_y^{\,2}\, y = 0$$

"Skew" uqadrupole field components add extra forces

$$X'' + 4\pi^2 Q_x^{\,2}\, x = +(Skew)\, y$$
$$Y'' + 4\pi^2 Q_y^{\,2}\, y = -(Skew)\, x$$

(especially if strong and systematic all around the ring)
Messes up with all optics functions, orbit, separations, tunes, chromaticities, etc → lost control over beam dynamics in collider

Fermilab

Persistent Currents Effect

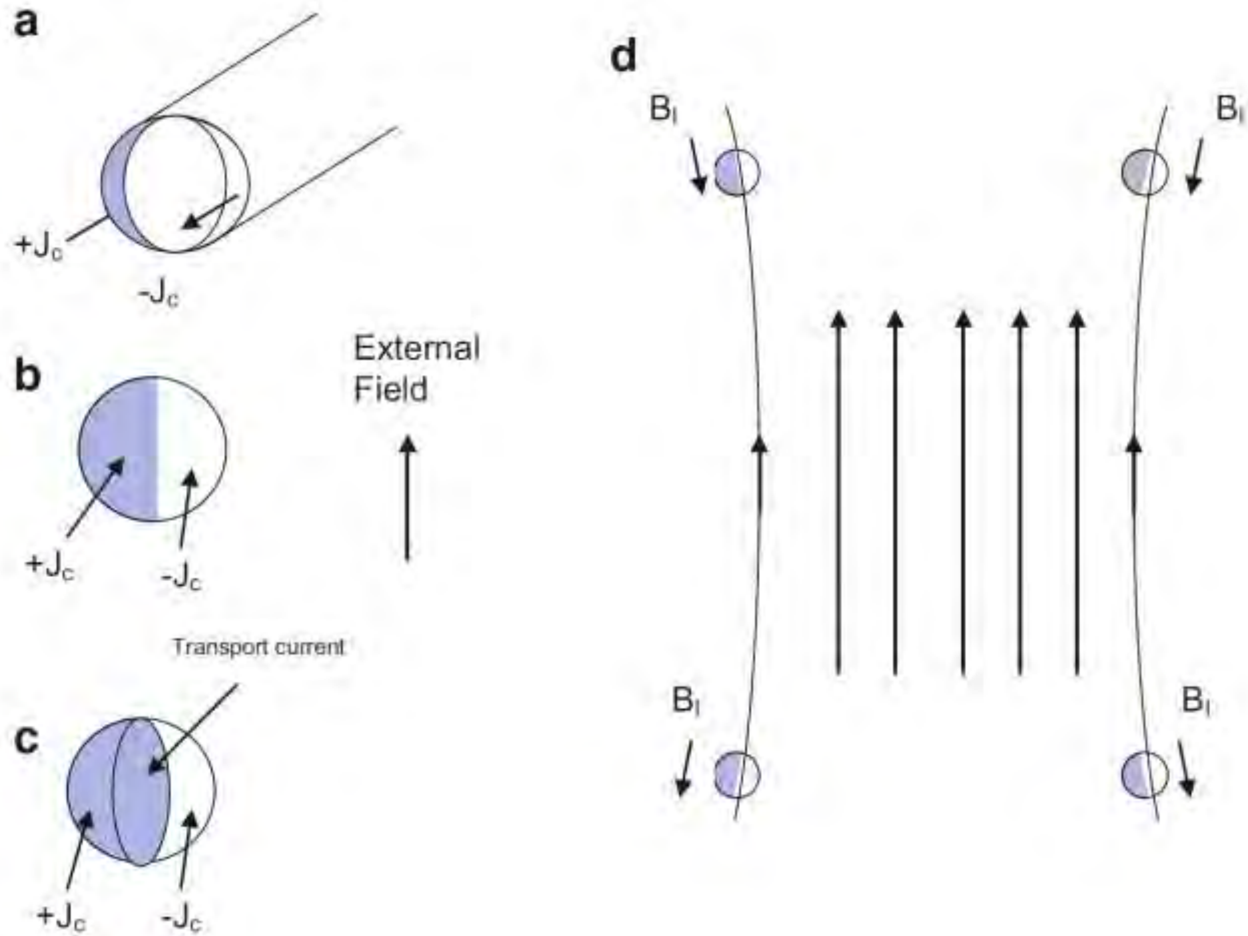

Persistent currents in SC due to Messner effect: a) shielding of external field; b) external field changes → more shielding; c) on top of than – transport current that drived the B-field; d) appearance of sextupole field component for four symmetrical "micro-dipoles"

If the magnets are held at a fixed excitation, say, at the injection field, the persistent currents and thus the sextupole fields decay with a logarithmic dependence of time. The source of the decay is the resistive redistribution of Interstrand Coupling Currents (ISCC). These coupling currents flow through a complicated pattern in the copper strands and splices, and as they change, the magnetization of the cable decays.

Fermilab

Another Peculiarity of SC Magnets - Sextupole component due to so called *persistent currents* in SC

1 unit
=1e-4
dB/B
at r=1”

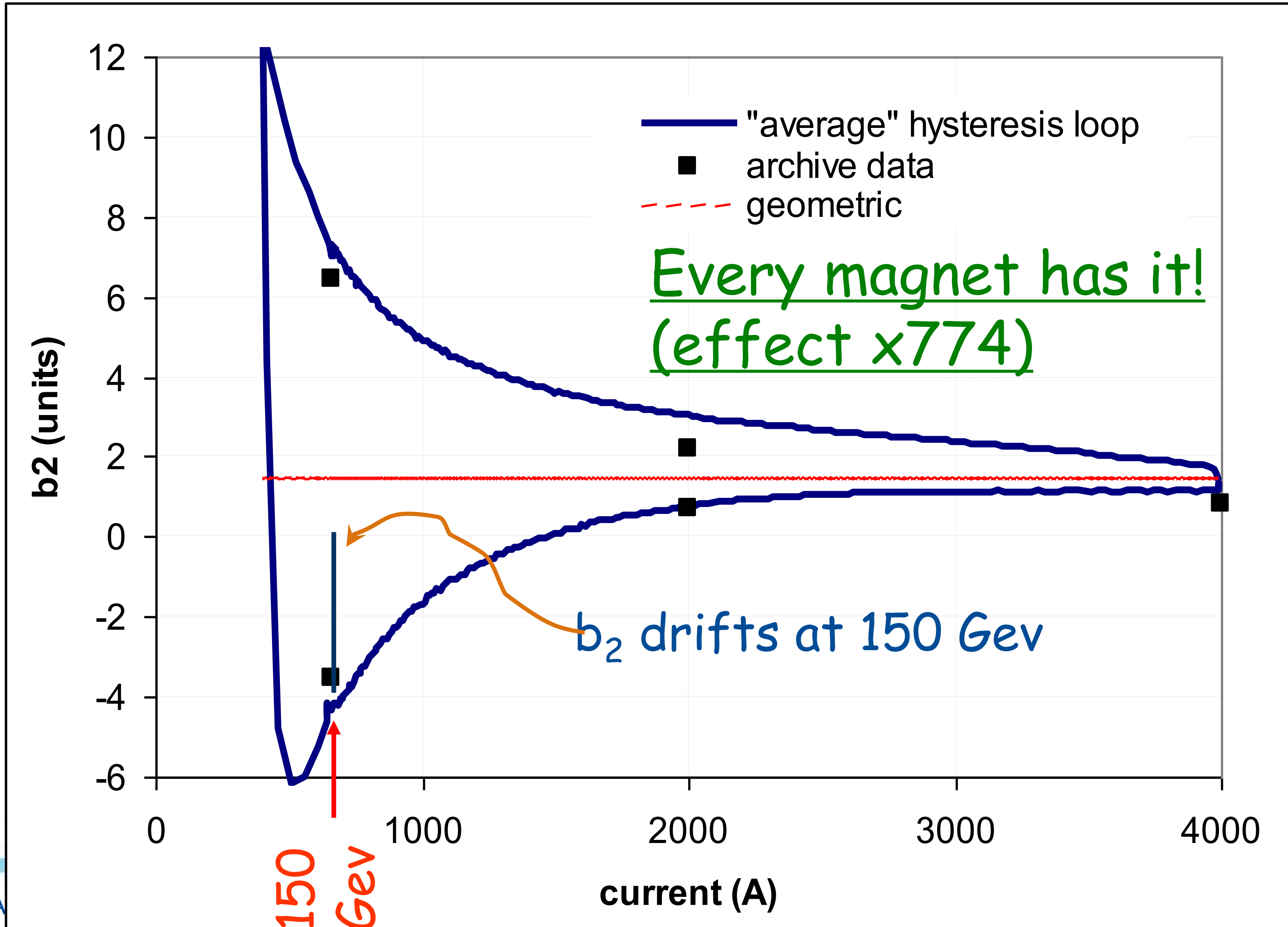

Sextupole Fields → Chromaticity

Expected Motion (and as the results – optics functions)

$$X'' + 4\pi^2 Q_x^{\,2}\, x = 0$$
$$Y'' + 4\pi^2 Q_y^{\,2}\, y = 0$$

Sextupoles result in additional forces $F_x \sim Sxy$ and $F_y \sim S(x^2 - y^2)$
In the arcs where dispersion is non-zero $x = x_\beta + D_x\,(dP/P)$ that leads to additional terms like

$$X'' + 4\pi^2 Q_x^{\,2}\, x = -\,K_x\, S\, D_x\,(dP/P)\, x$$
$$Y'' + 4\pi^2 Q_y^{\,2}\, y = -\,K_y\, S\, D_x\,(dP/P)\, y$$

Which result in tune variation with momentum $Q_{x=}Q_x + Q'_x\,(dP/P)$
Coefficient $Q'_{x,y} = dQ_{x,y}/(dP/P)$ is called chromaticity → critical!
Eg spread $(dP/P)\sim 0.1\%$ and $Q'_{x,y} = 10 \rightarrow dQ_{x,y} = 0.01$

Fermilab

Measured b_2 Drift in Tevatron @150 GeV

Equivalent to ~10 units of chromaticity drift
Scale depends on the history of the Tevatron magnets ramping up and down! → was well understood and carefully corrected
Also, seen and corrected in orbits, tunes and cpoupling

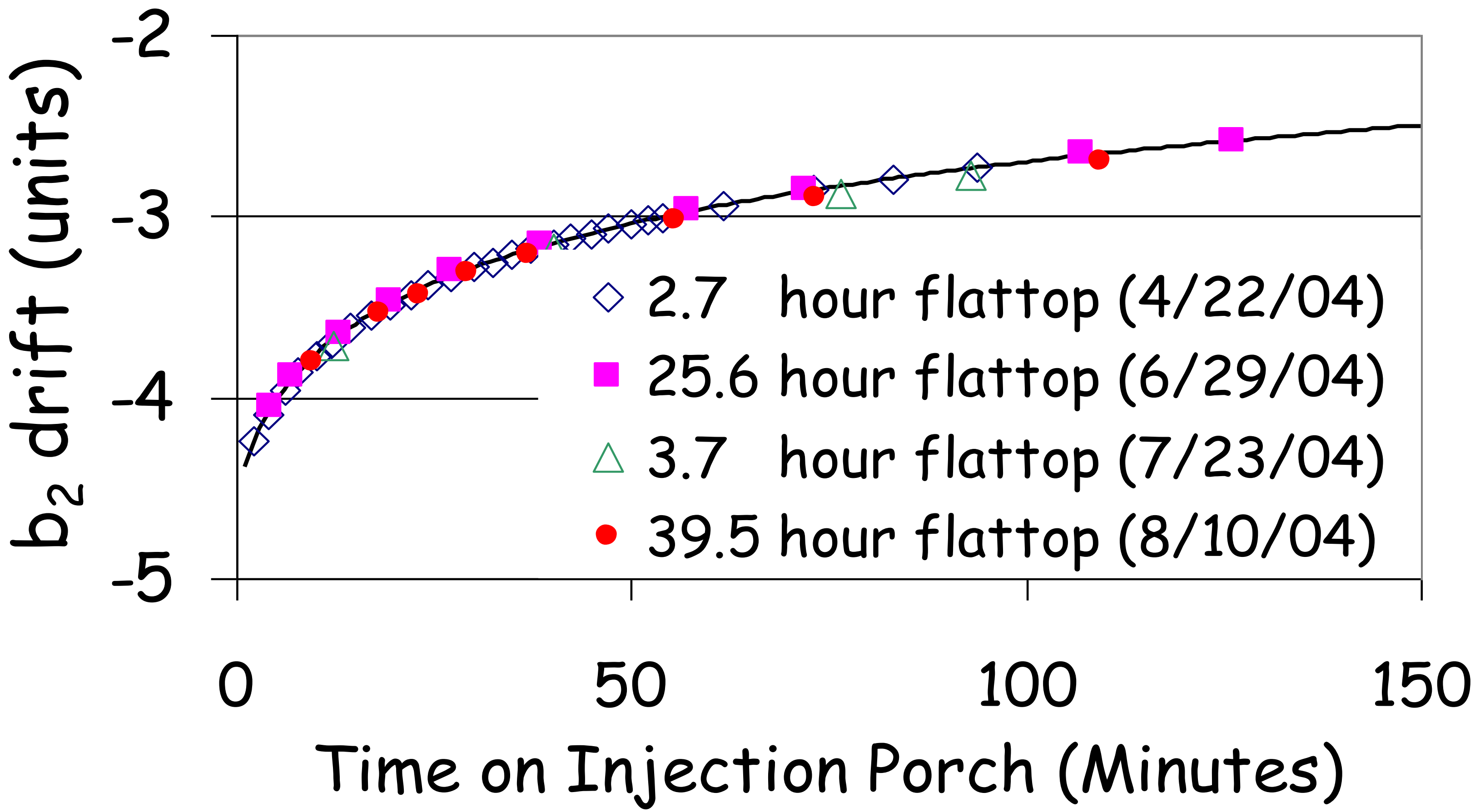

lab

Proton Source

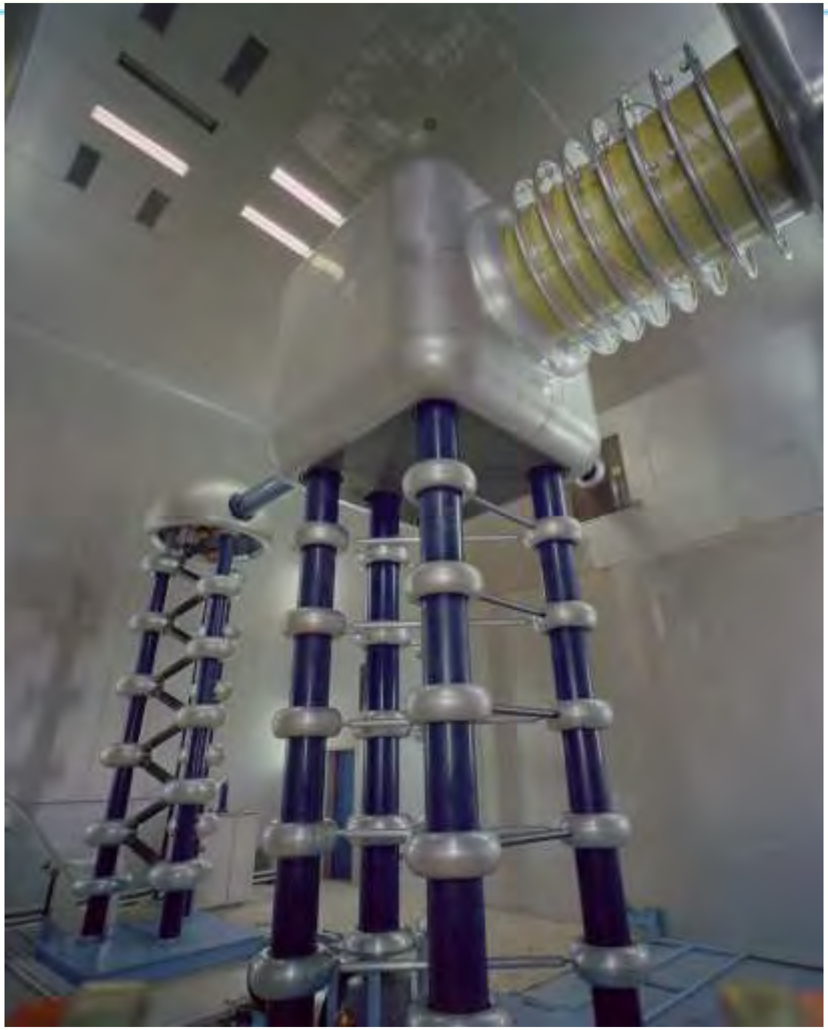

H- ion source and 750keV Cockcroft-Walton accelerator, sends beam to Linac

E_kin=400MeV H- to Booster
room temperature RF linac
400MHz

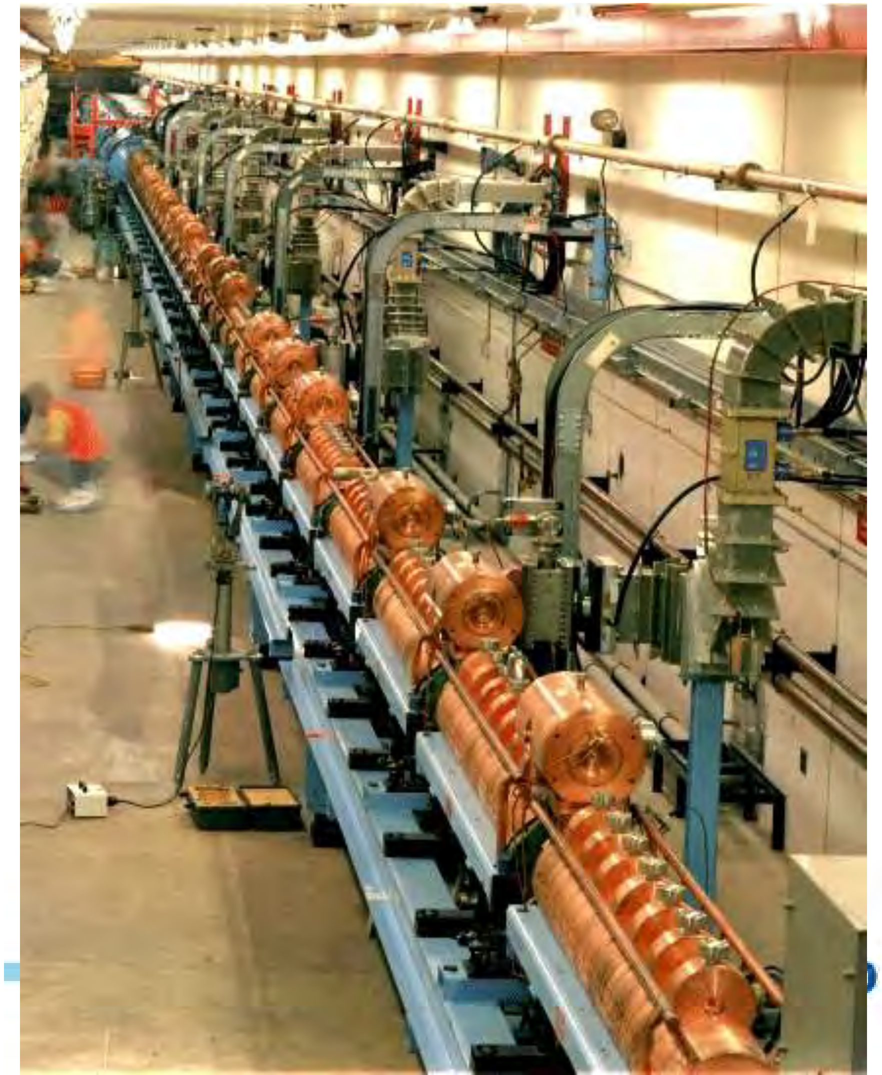

Booster, Debuncher and Antiproton Accumulator

Two 8 GeV pbar rings for stochastic cooling in one Δ-shape tunnel
Debuncher (fast cool)
Accumulator (deep cooling with stacking).. aperture

Booster: C=480m
15 Hz synchtron
E_inj=400 MeV H-
E_max=8GeV protons
~5e12 p/pulse max
Space charge dominated

Main Injector

C=3.32km

Room temperature magnets (<2T)

E_max=150GeV
E_inj=8 GeV

Min cycle time 1.4s

Accelerates protons and Pbars to 150GeV for Tevatron

Accelerates protons to 120 GeV for pbar production and NuMI

Fermilab

Coalescing in Main Injector

Combine 7 proton bunches in one big one to inject to the Tevatron
Requires two RF systems : 53 MHz and 2.5MHz (1/25 of 53 MHz)

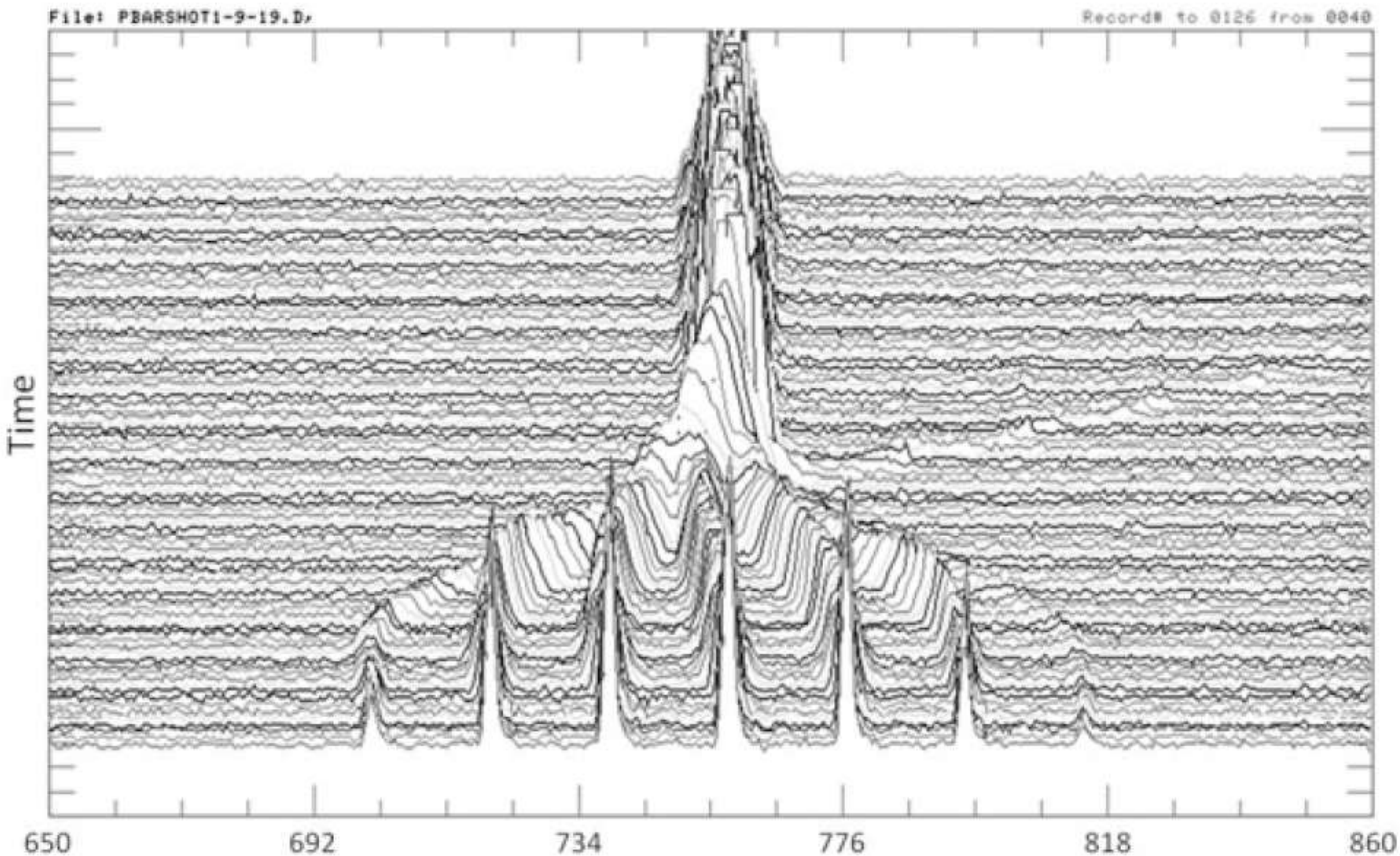

Antiproton Production Target

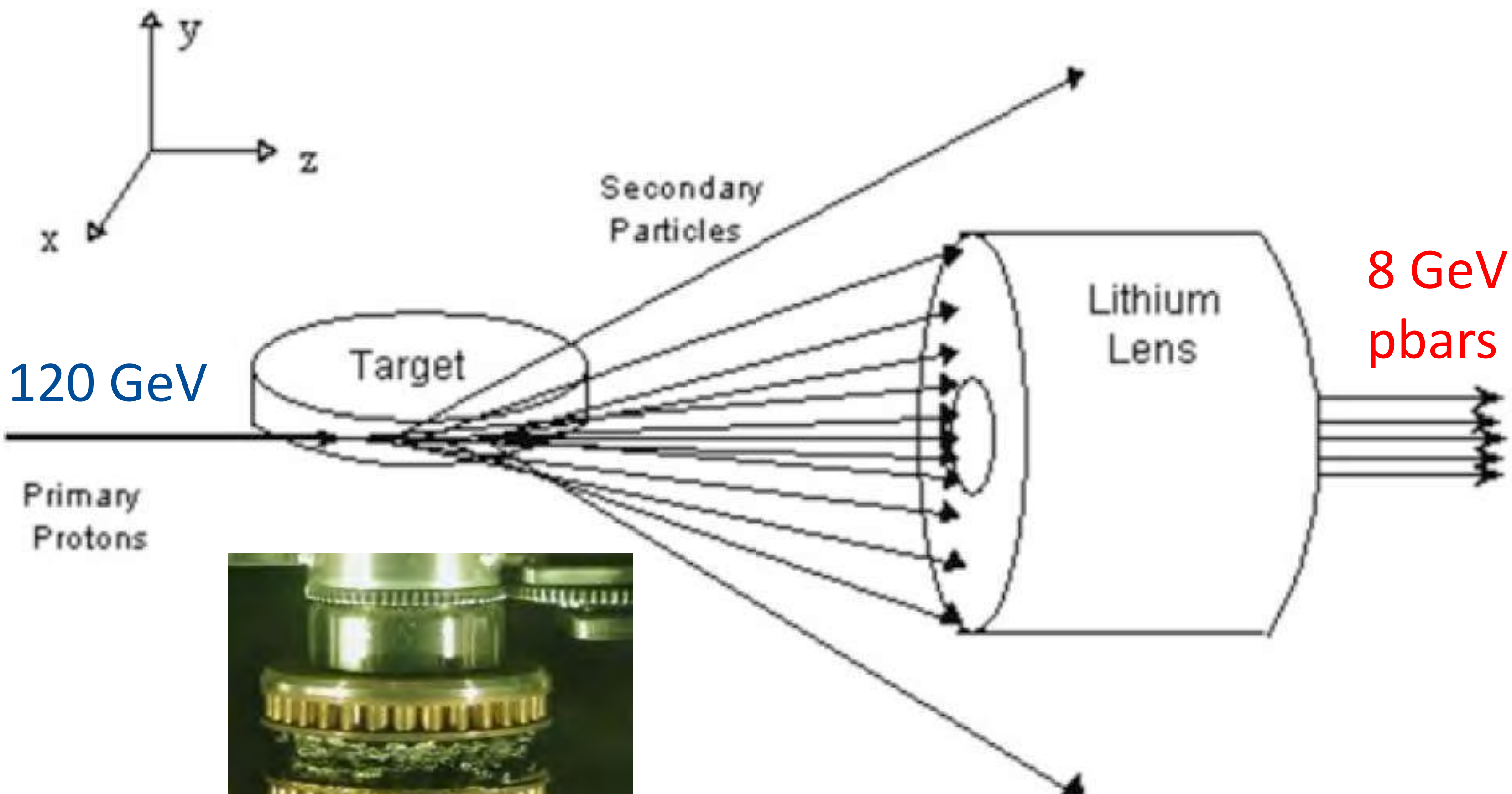

Stochastic Cooling in Accumulator C=474 m, E=8 GeV

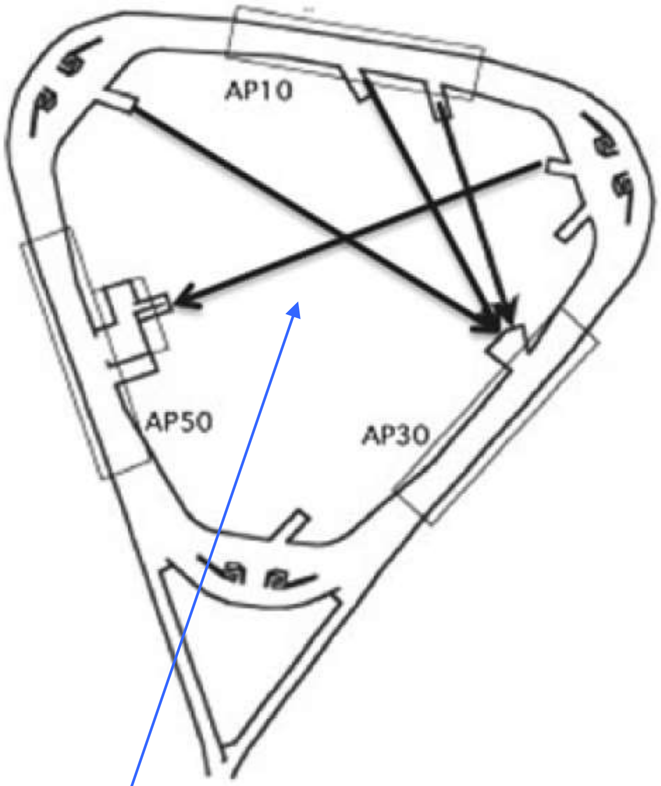

Stochastic Cooling signal paths

Fermilab

see lectures VL13-14

How to Overcome That Transverse Emittance ?

$$\frac{d\varepsilon}{dt} = -\frac{\varepsilon}{\tau_{Stoch.Cooling}} + (IBS\ Heating)$$

$$\varepsilon_{equilibrium} = \tau_{Stoch.Cooling} \times (IBS\ Heating) =$$

$$\propto \tau_{Stoch.Cooling} \times \frac{N_a}{\varepsilon_{Long}^{1/2}\varepsilon_{Transv}^{3/2}} \times \frac{D^2 + (D'\beta - D\beta'/2\beta)^2}{\beta}$$

see lectures VL13-14

Recycler Ring

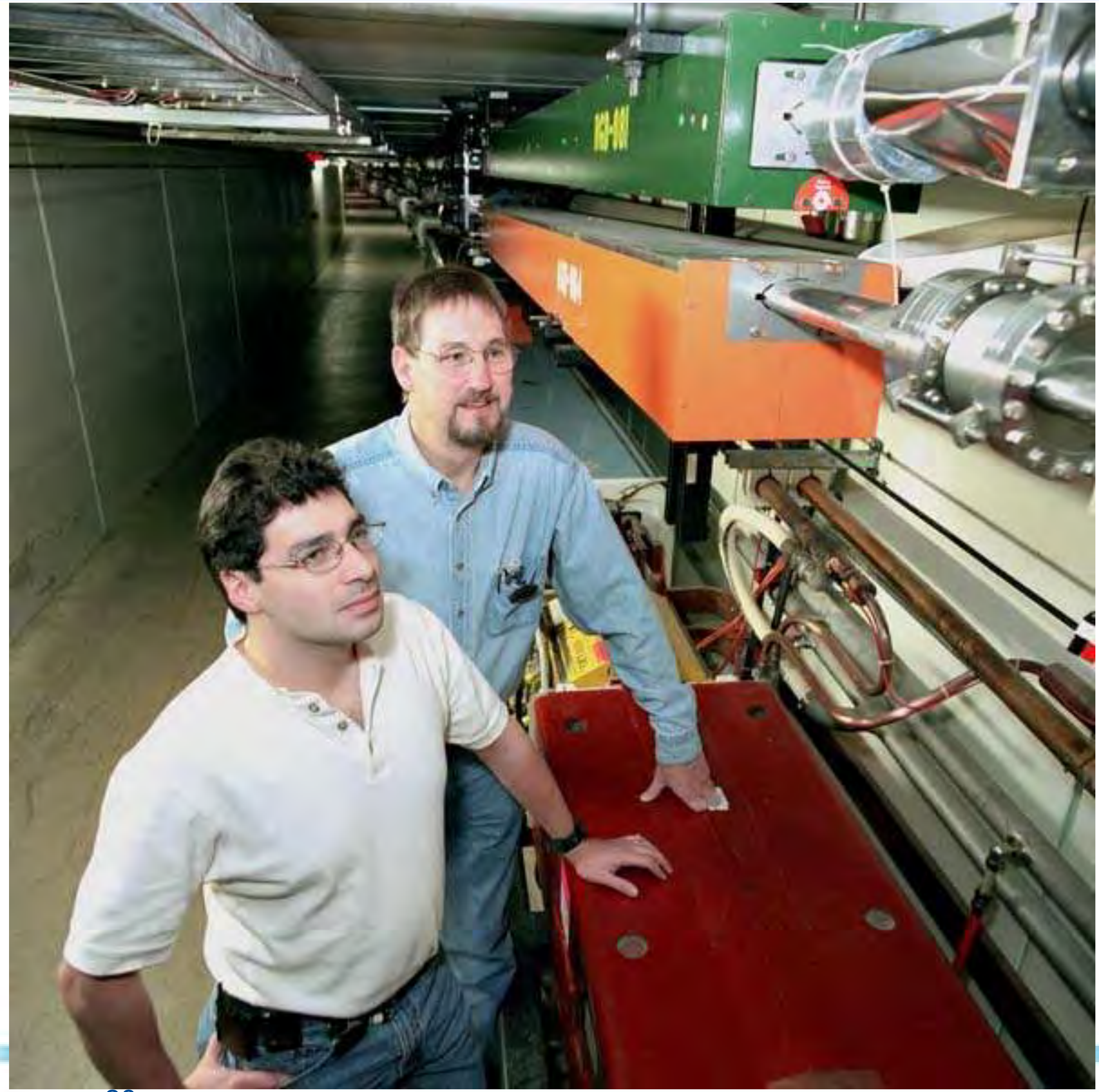

Shares tunnel with Main Injector

C=3.32km

Permanent magnets (344, 1.45T, Sr-Fe combined function)

E_kin=8 GeV fixed

Stores and cools antiprotons From Antiproton Accumulator ring

8 GeV Recycler Ring Magnets (1.4kG)

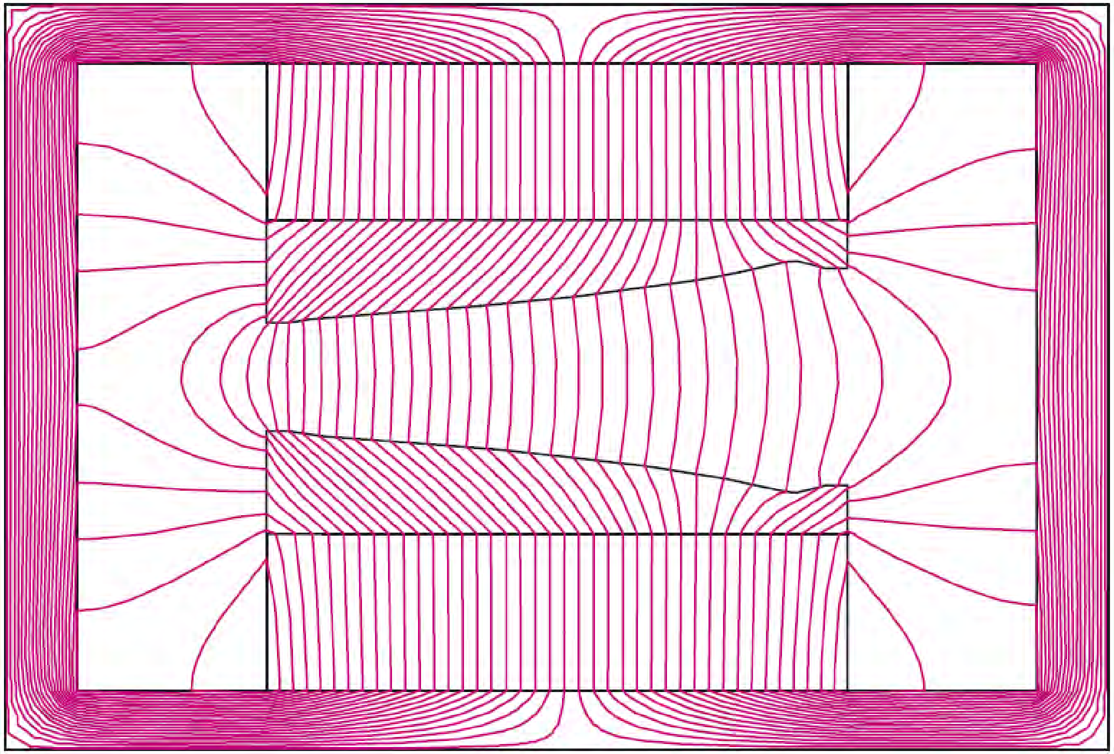

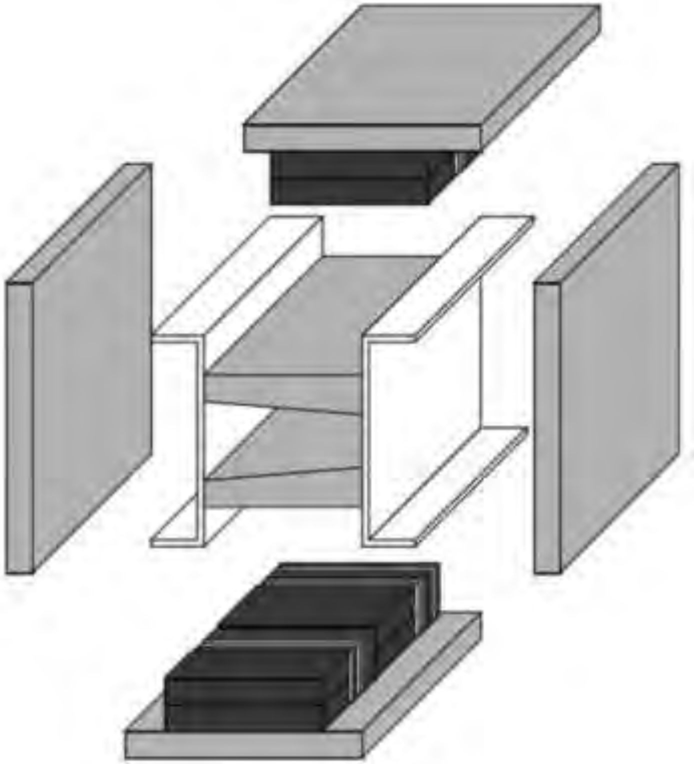

Recycler permanent magnet gradient dipole components shown in an exploded view. For every 4” wide brick there is an 0.5” interval of temperature compensator material composed of 10 strips

Electron Cooling of 8GeV Pbars in Recycler

"Bath" of cold electrons

Condition#1 for effective heat transfer: V_e = V_antiptoton 4.338 MeV e- for 8.89MeV pbar

Other conditions (below)

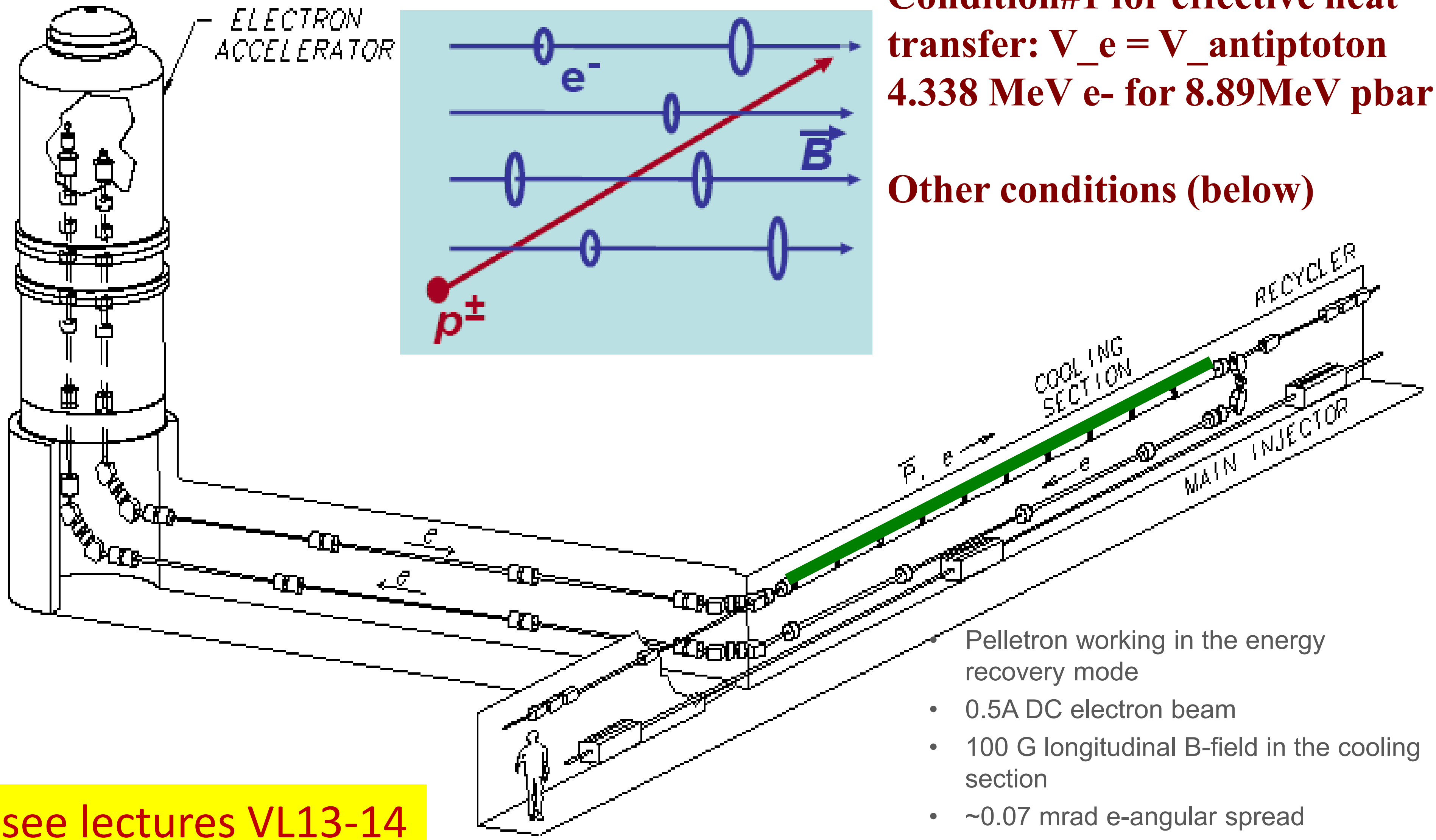

- Pelletron working in the energy recovery mode
- 0.5A DC electron beam
- 100 G longitudinal B-field in the cooling section
- ~0.07 mrad e-angular spread

see lectures VL13-14

Electron Cooling Device

4.5MeV Pelletron=Van der Graaf

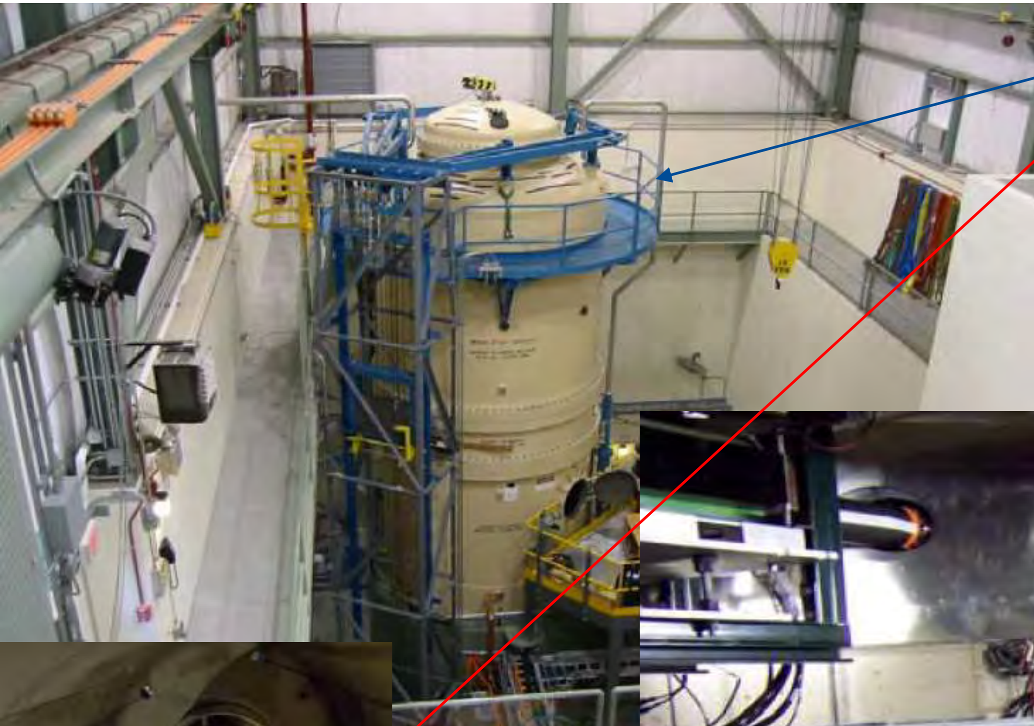

Interaction section in RR/MI tunnel

Antoproton production rate

90% of the world's total man-made nuclear antimatter (17 ng)

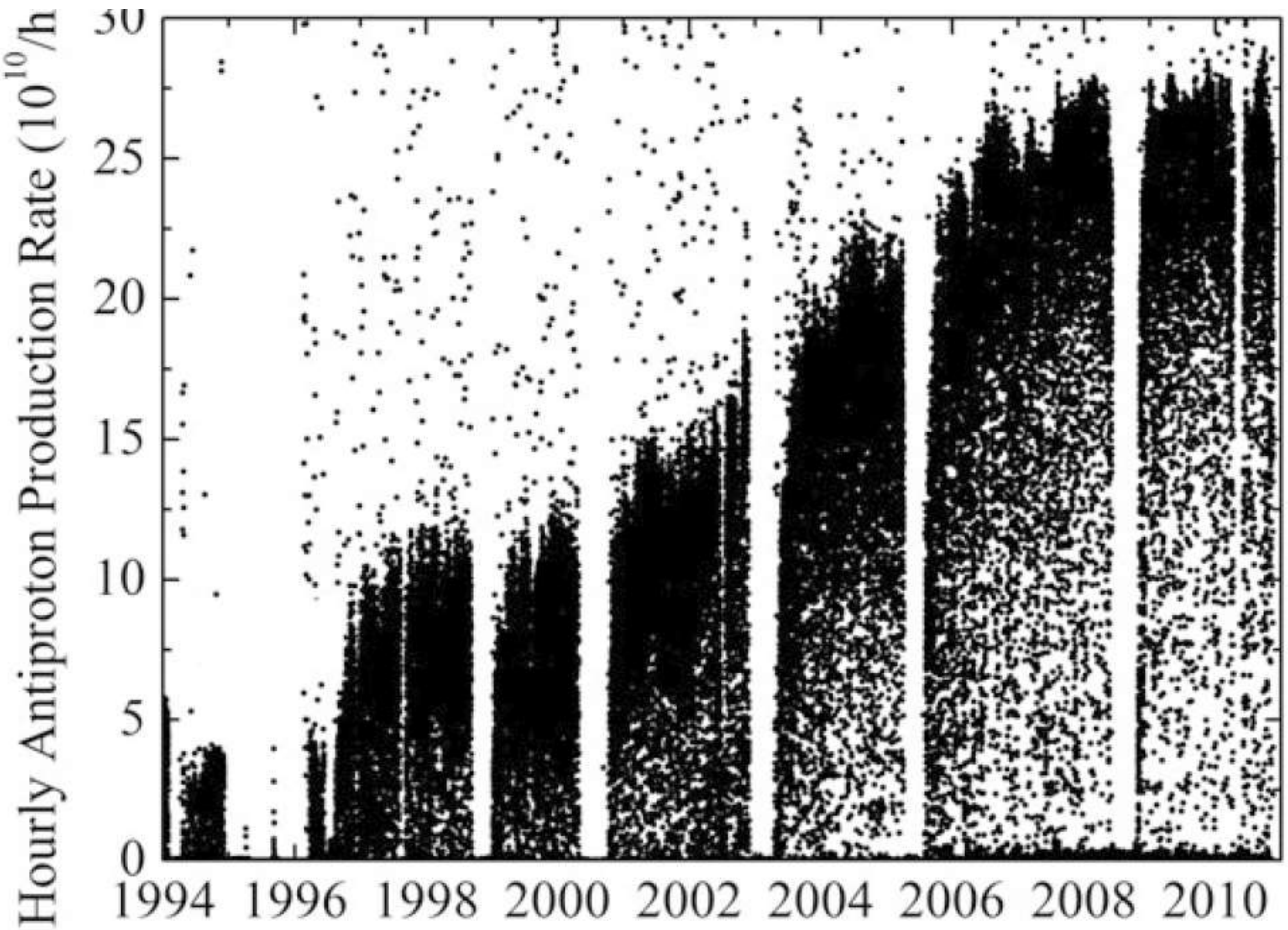

Average antiproton accumulation rate since 1994 and during all of Collider Run II (including production in the Antiproton Source and storage in the Recycler)

Tevatron Inefficiencies: 2001

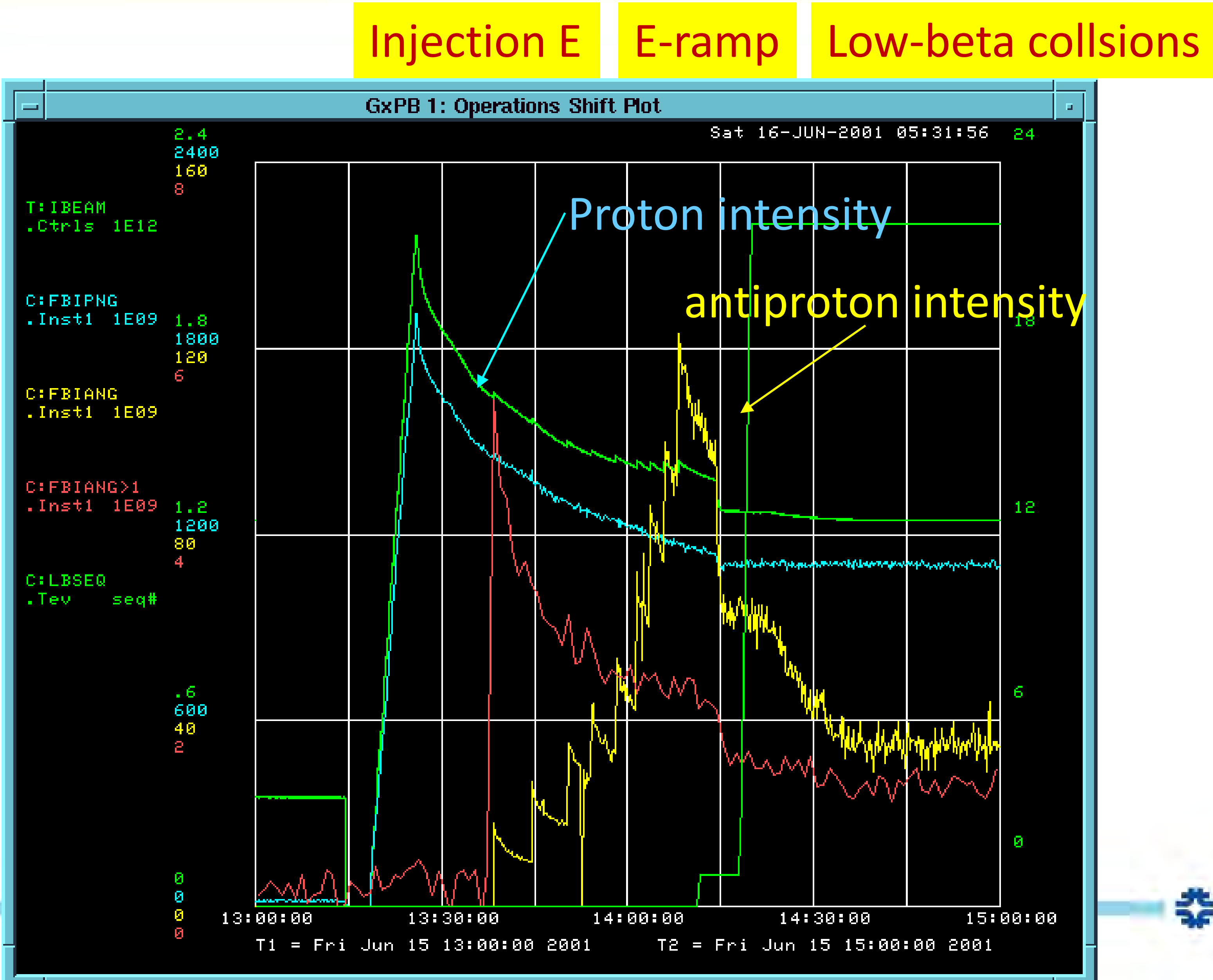

Store #535
Jun 15, 2001

Importance of Helical Orbits

- Beams share beam pipe → be separated
  - Helical separation ~(10-22)mm at 150 GeV
  - ***S*** ~(3-6) mm at 980 GeV
- Lifetime is strong function of ***S***
  - 30 sec at 2σ , 50 hrs at 7σ

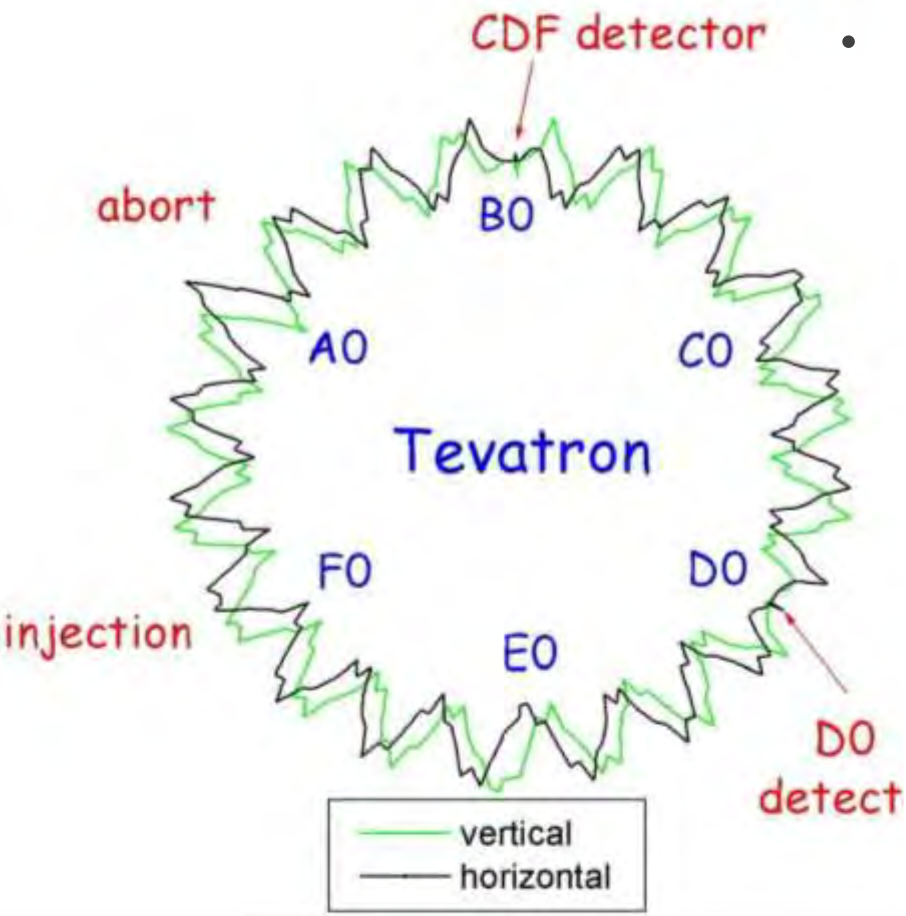

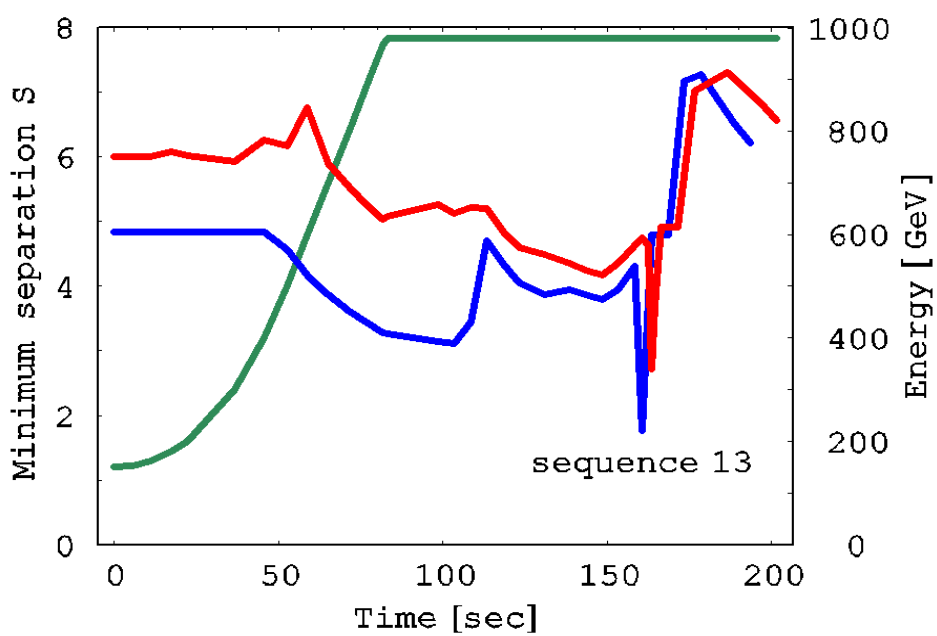

Betatron Tunes of Tev Beams

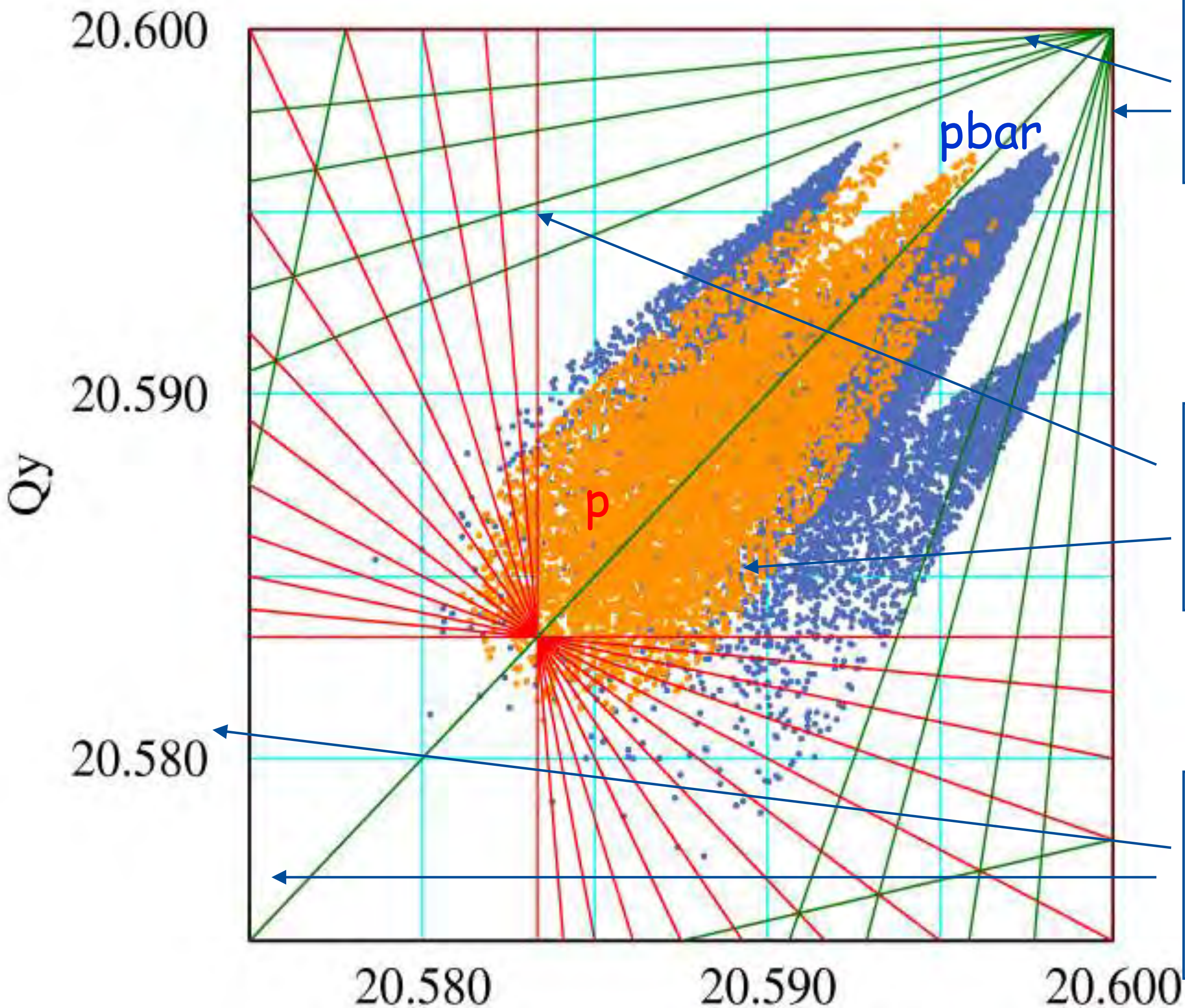

5th order resonances:
Q=3/5=0.600 -
EMITTANCE BLOWUP

12th order resonances:
Q=7/12=0.583 -
Bad lifetime

7th order resonances:
Q=4/7=0.571 -
HIGH LOSSES

Head-On Beam-Beam Collisions

affected mostly protons

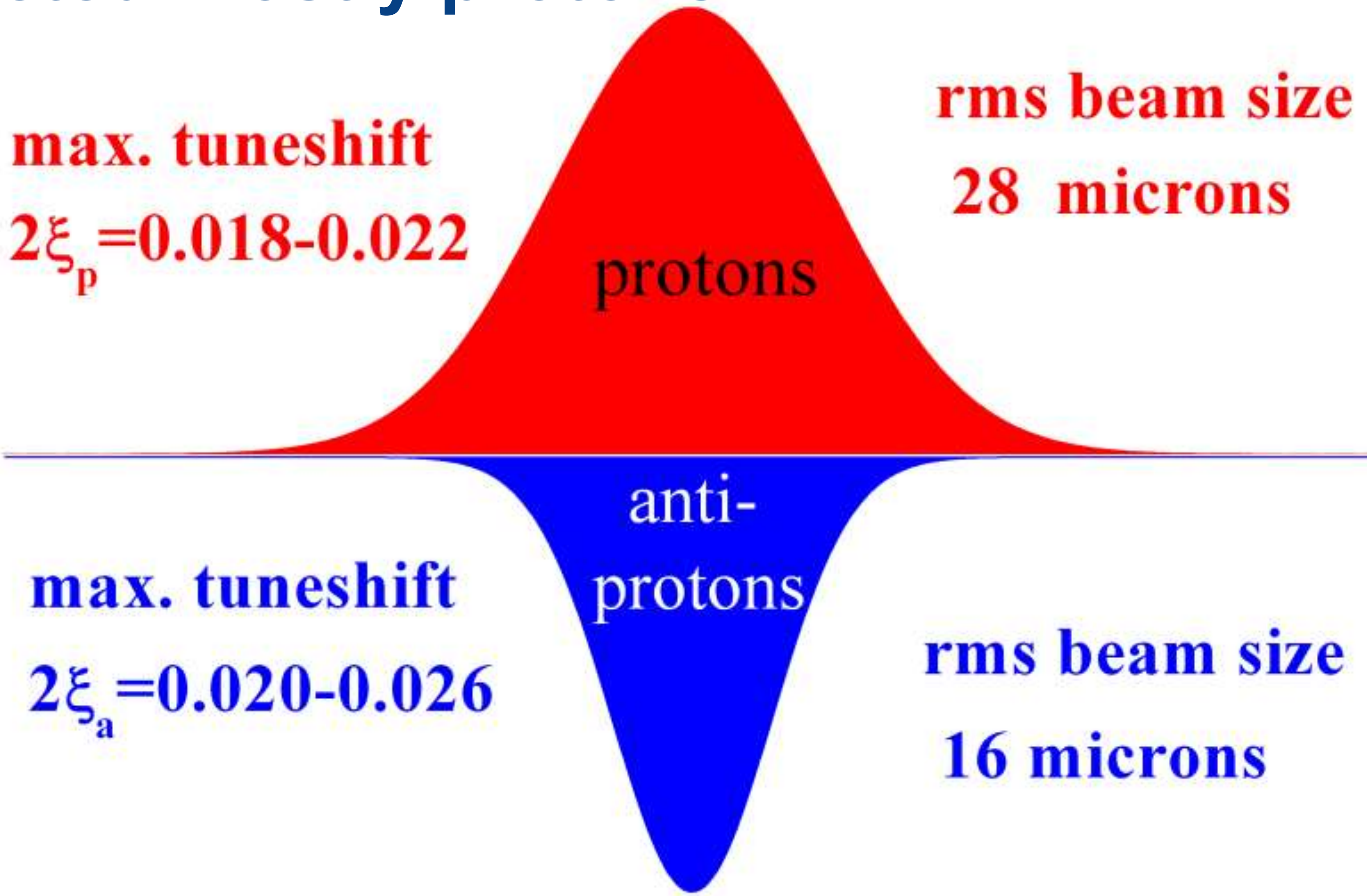

emittance ratio (ε_p/ε_a) ~3

Losses of particles due to beam-beam

***Antiprotons** 980 GeV :*

ξ_{max}=+0.024

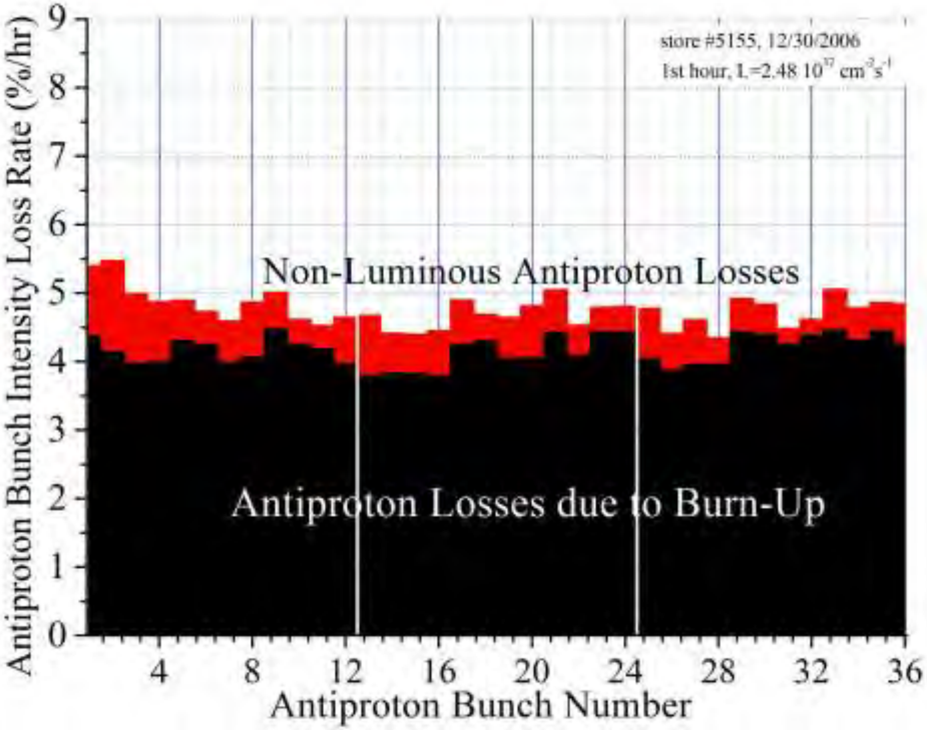

***Protons** 980 GeV :*

ξ_{max}=+0.016

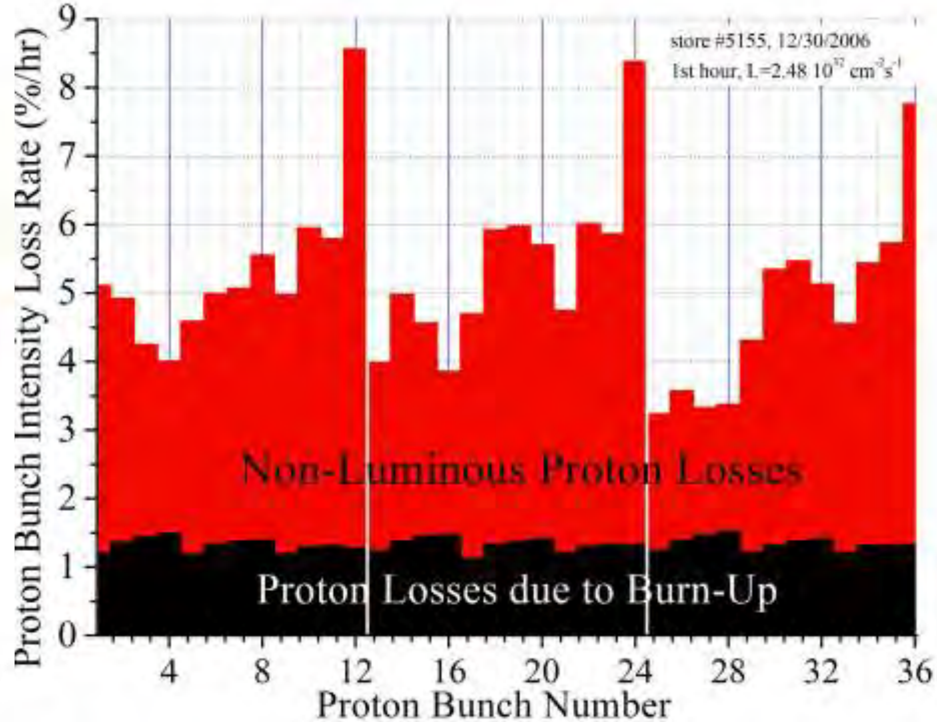

At present, beam-beam effects are relatively stronger on protons, accounting for some 10-15% loss of the integrated luminosity. Proton loss rates vary greatly from bunch to bunch.

Total Beam-Beam Luminosity Loss

At the end of Run II
22-32% hit on Int.Lumi

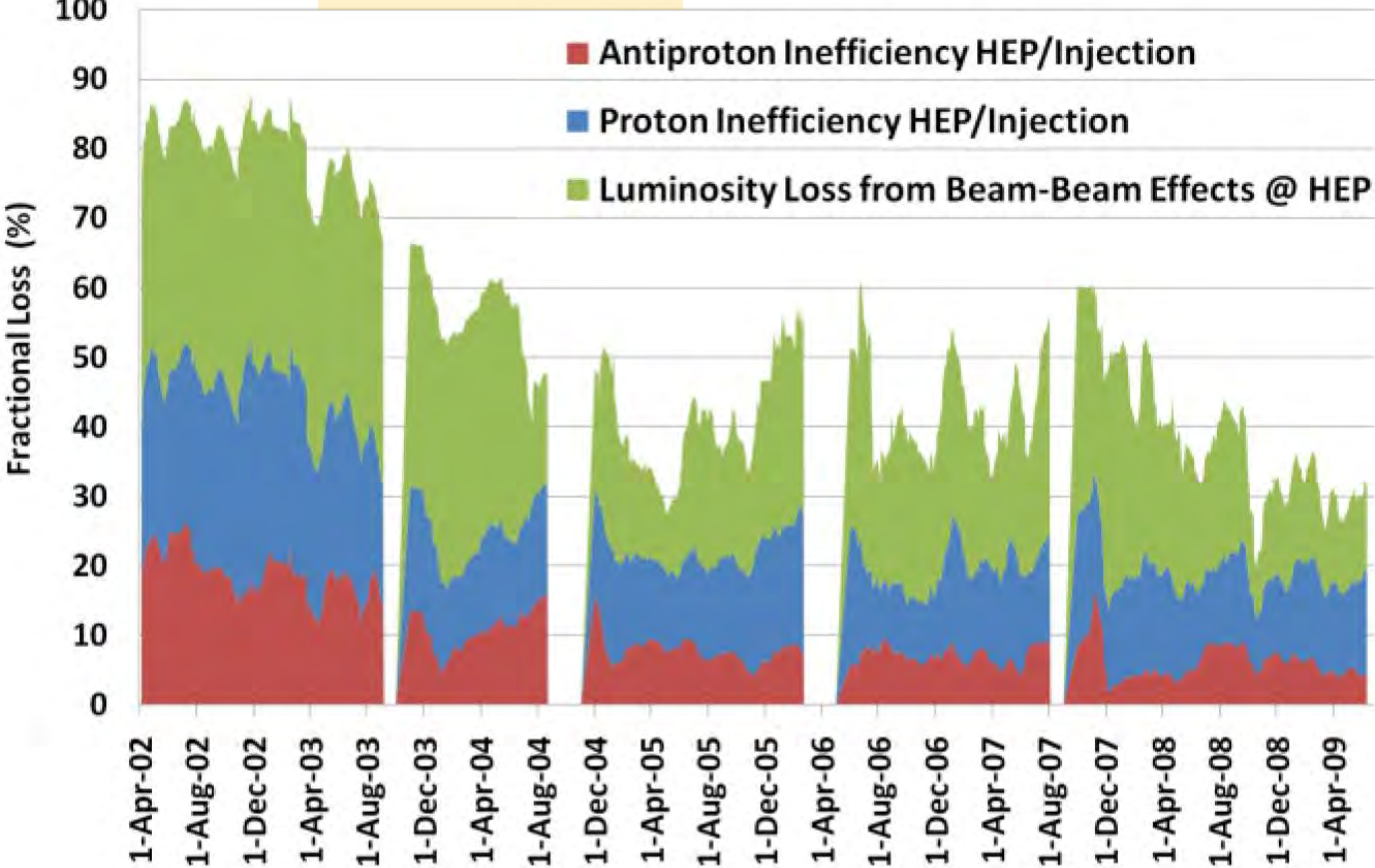

Intrabeam Scattering and Longitudinal Oscillations Lead to Generation of DC beam in Abort Gaps

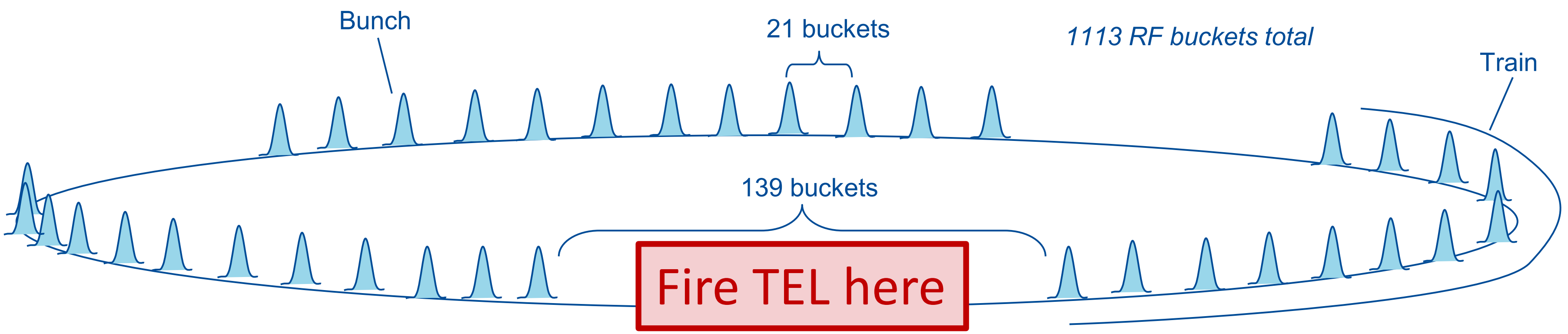

- The Tevatron operates with 36 bunches in 3 groups called trains
- Between each train there is an abort gap that is 139 RF buckets long
  - RF bucket is 18.8 ns → Abort gap is 2.6 μs
- Protons leak out of main bunches to the gaps. Tevatron is sensitive to few x 10^9 particles in the abort gaps (total beam ~ 10^{13}) as they lead to quench on beam abort (kicker sprays them)
- Kill (diffuse) DC beam in gaps by electron lens

e-Lnes for Beam Collimation

Pulsed e-current
in the abort gap
→ Drive out DC beam

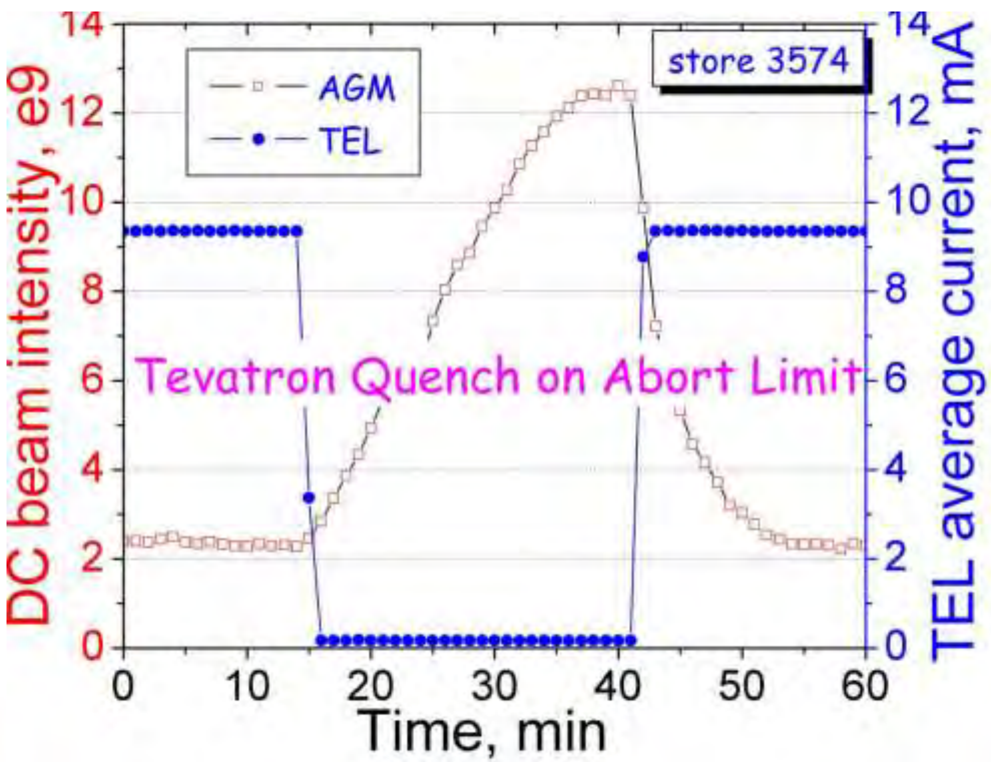

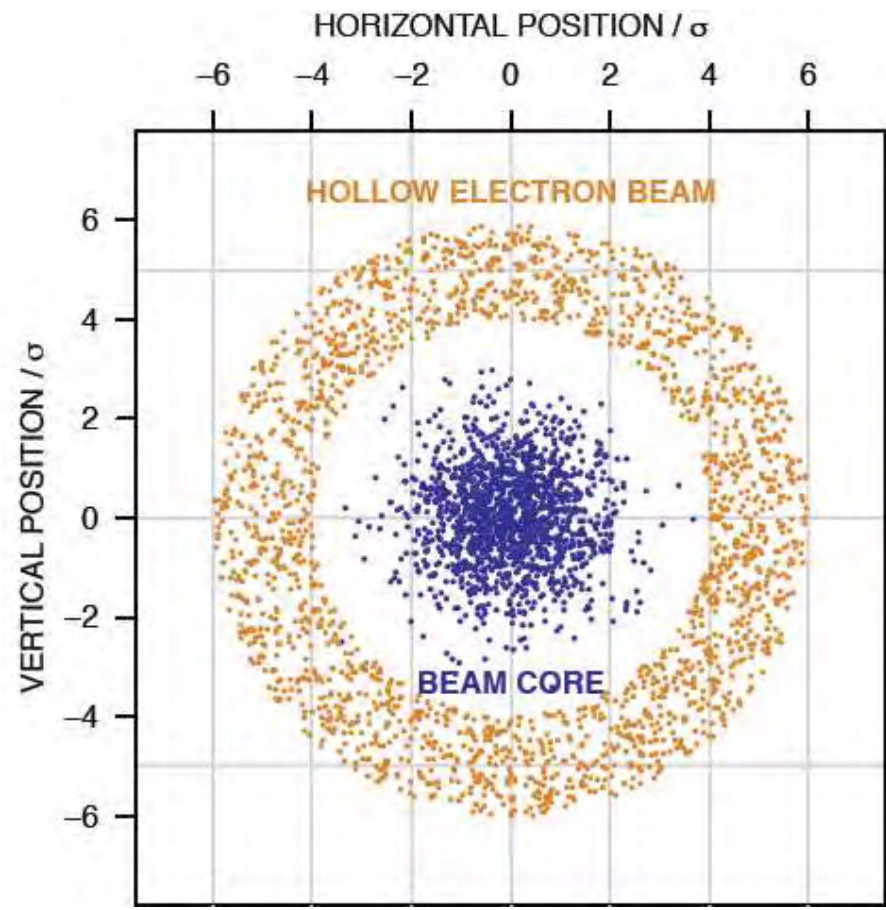

Hollow-e-beam →
no EM field inside
Strong field outside

Table 3. Tevatron Collider Run II major luminosity improvements history.

Improvement		Luminosity gain
Optics correction in Accumulator (AA) to Main Injector (MI) beam line	12/2001	2[illegible]
Tevatron quenches on abort stopped by electron lens	02/2002	[illegible]bility
Antiproton loss at the step #13 of Tevatron low-beta squeeze fixed	04/2002	[illegible]
New Tevatron injection helix implemented	05/20[illegible]	[illegible]
New AA lattice reduces IBS, emittances	07/[illegible]	[illegible]
Beam Line Tuner to reduce emittance dilution at Tevatron injection	[illegible]	[illegible] %
Antiproton multi-bunch coalescing efficiency improved in MI	[illegible]	[illegible] %
Small aperture Lambertson magnets removed from Tevatron C0 sec[illegible]	[illegible]	15 %
Tevatron sextupoles tuned / SEMs taken out of antiproton beam [illegible]	[illegible]	10 %
New Tevatron helix implemented on ramp to reduce beam lo[illegible]	[illegible]03	2 %
Tevatron magnet reshimming (to center coils inside iron y[illegible]	[illegible]/2003	10 %
MI dampers operations / HEP store length increased	02/2004	30 %
Improved efficiency of 2.5 MHz antiproton transfer[illegible]	04/2004	8 %
Reduction of Tevatron β^* to 35 cm	05/2004	20 %
Antiproton injections from both Recycler and[illegible]	07/2004	8 %
Electron cooling system in Recycler opera[illegible]	01–07/2005	~ 25 %
Longitudinal slip-stacking system in M[illegible]ional	03/2005	~ 20 %
Tevatron octupoles optimized at inj[illegible] GeV	04/2005	~ 5 %
Further reduction of the Tevatron[illegible]'s β^* to 28 cm	09/2005	~ 10 %
Antiproton production optimi[illegible]	02/2006	~ 10 %
Tevatron helical separation[illegible]V improved, more protons	06/2006	~ 10 %
Tevatron collision heli[illegible]ne improved, better lifetime	07/2006	~ 15 %
New Recycler work[illegible] smaller antiproton emittances	07/2006	~ 25 %
Faster antiproton[illegible]m AA to RR (1 hour → 1 min)	12/2006	~ 15 %
New antiprot[illegible]r gradient Li lens operational	01/2007	~ 10 %
Tevatron s[illegible]rcuits set up for new working point	2007	~ 10 %
Compe[illegible] chromaticity in Tevatron beam optics	2008	~ 5 %
Sho[illegible]d by multi-bunch proton injection	2008–09	~ 5 %
Bette[illegible]quality by scraping in Main Injector	2008	~ 5 %
Antipro[illegible] size dilution at collisions / B0 aperture opened up	2008	~ 5 %
Booster p[illegible]n emittances reduced / tune up of P1 and A1 transfer lines	04/2010	~ 10 %
Tevatron collimators employed during low-beta squeeze, more protons	04/2011	~ 8 %

x43 in luminosity in 32 steps

Holmes, Moore, Shiltsev 2011 JINST 6 T08001

CPT Theorem for Accelerators

$$C \times P = T$$

C = Complexity of the machine

P = Performance (or Challenge)

= Ln(*Lumi Increase Ratio*)

T = Time to reach *P*

$$\boxed{\textit{i.e.,}\ L(T)=L(0) \times \exp\,(T/C)}$$

Fermilab

Tevatron Luminosity Progress

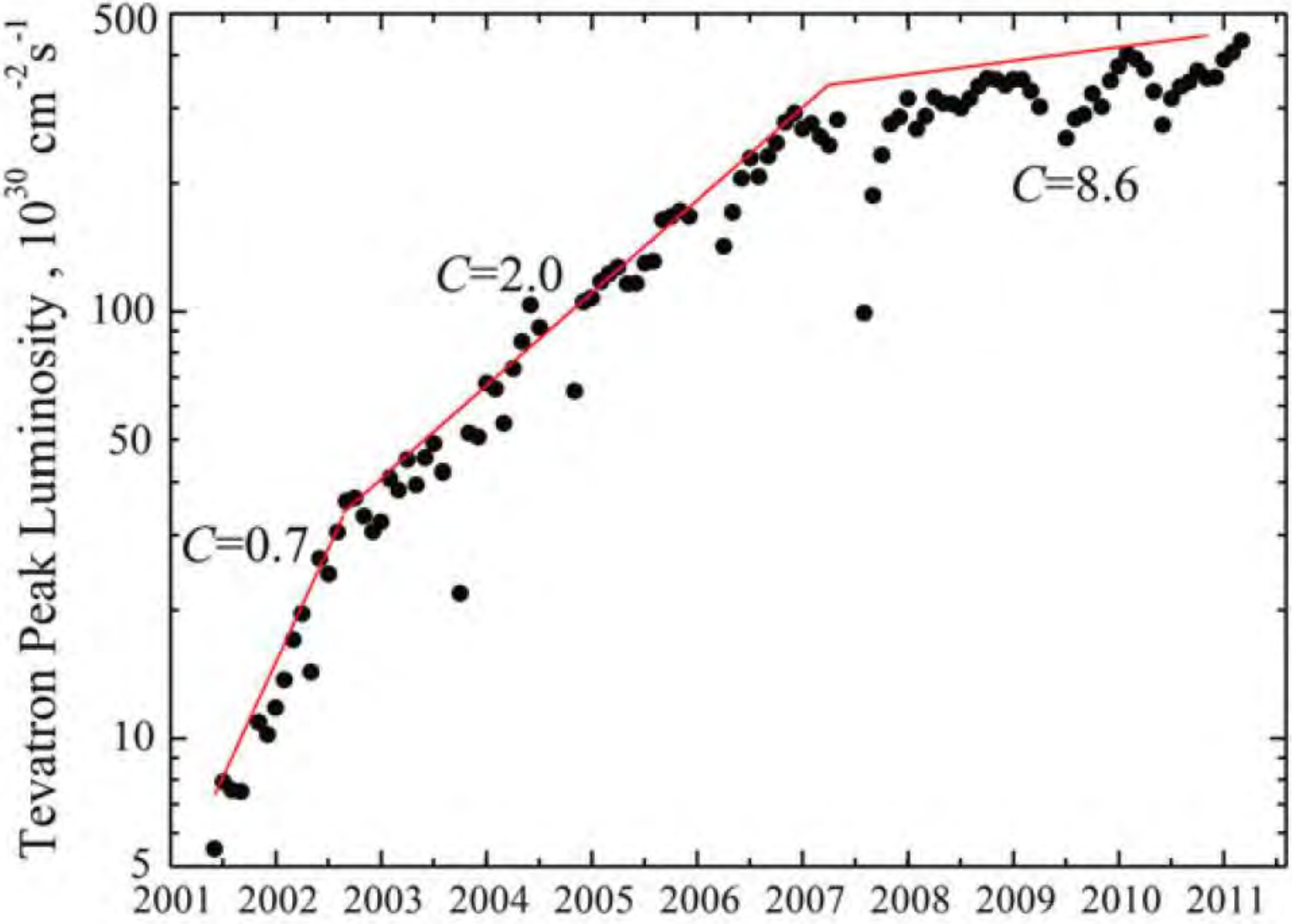

Complexity of Beams in *log*-Scale (TV tube=0)

Complexity 0.5	light sources
Complexity 1	p-synchrotron
Complexity 1	B-factories
Complexity 1.5	eCool,HERA,EIC
Complexity 2	DCI-Orsay,’80
Complexity 2	Tevatron,LHC
Complexity 2.5	Tev+elens BBC

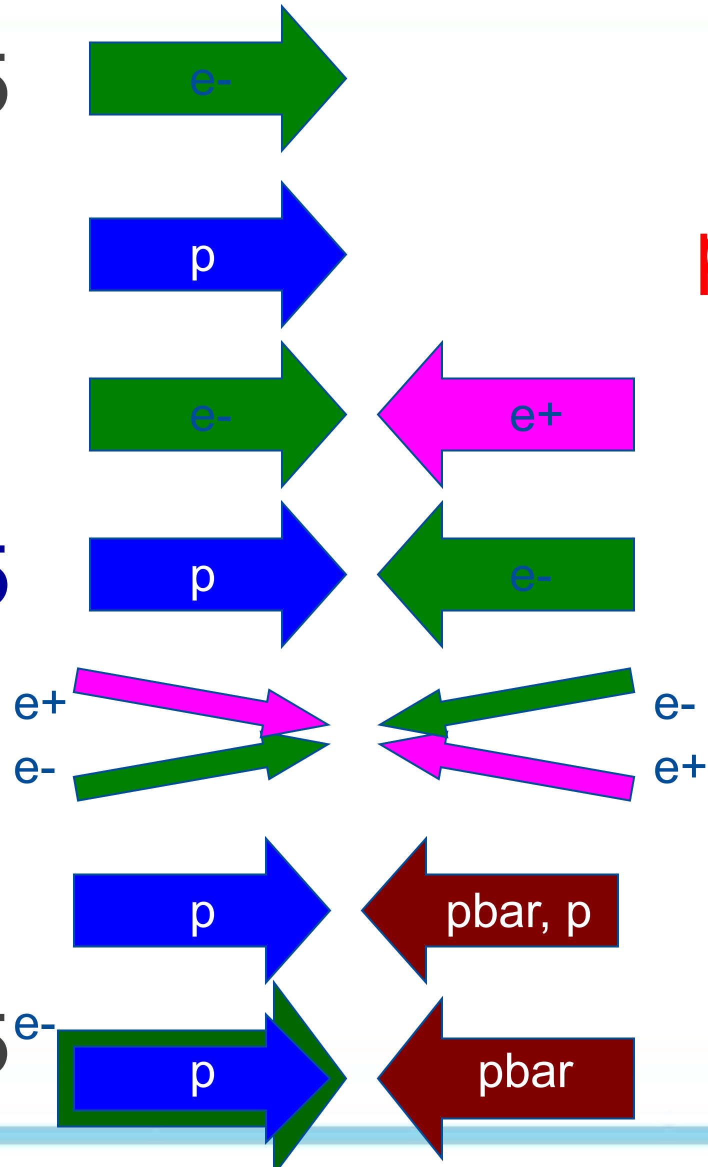

LHC Luminosity Outlook: 2003 Vision

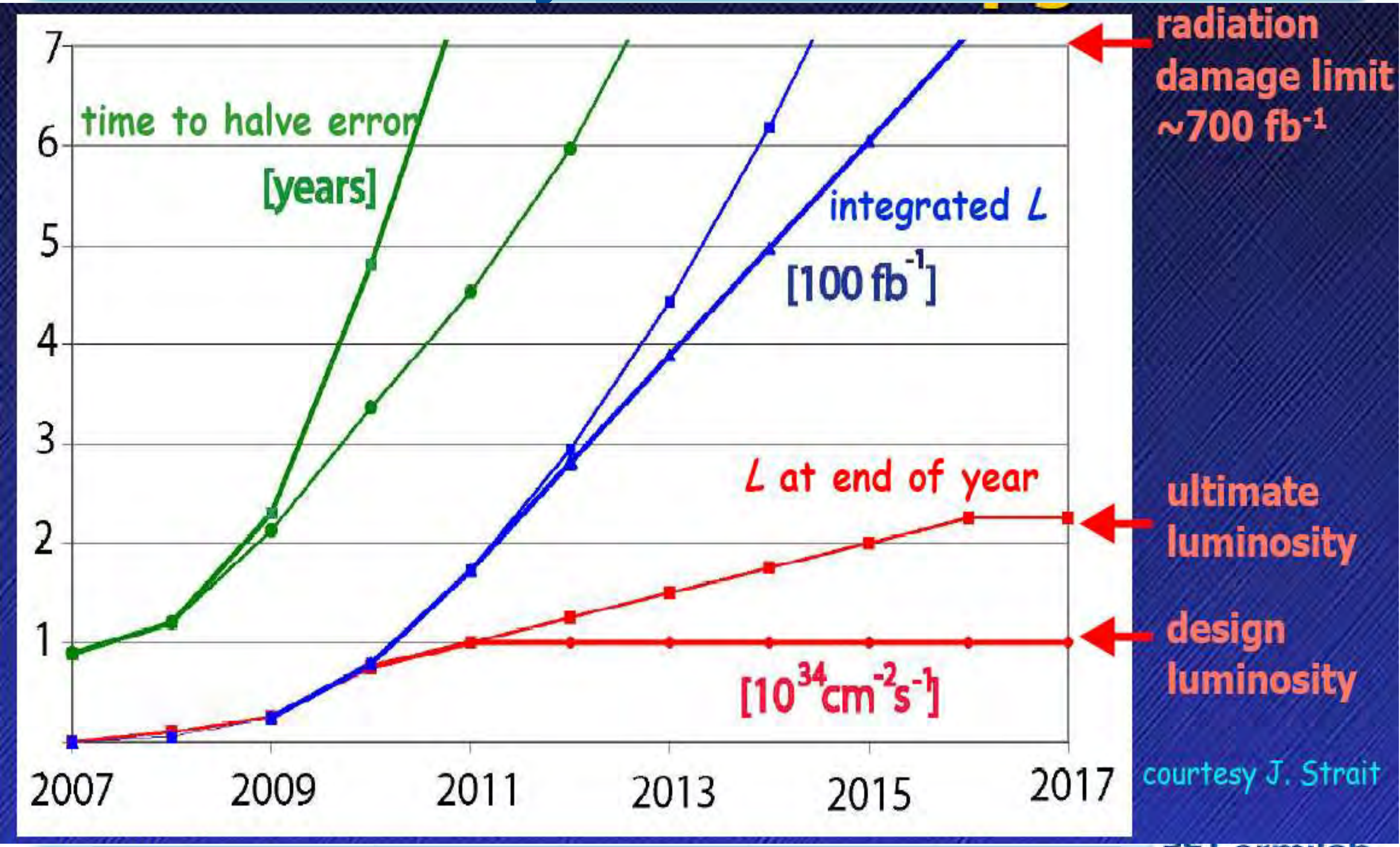

LHC Luminosity CPT-Prediction (2006)

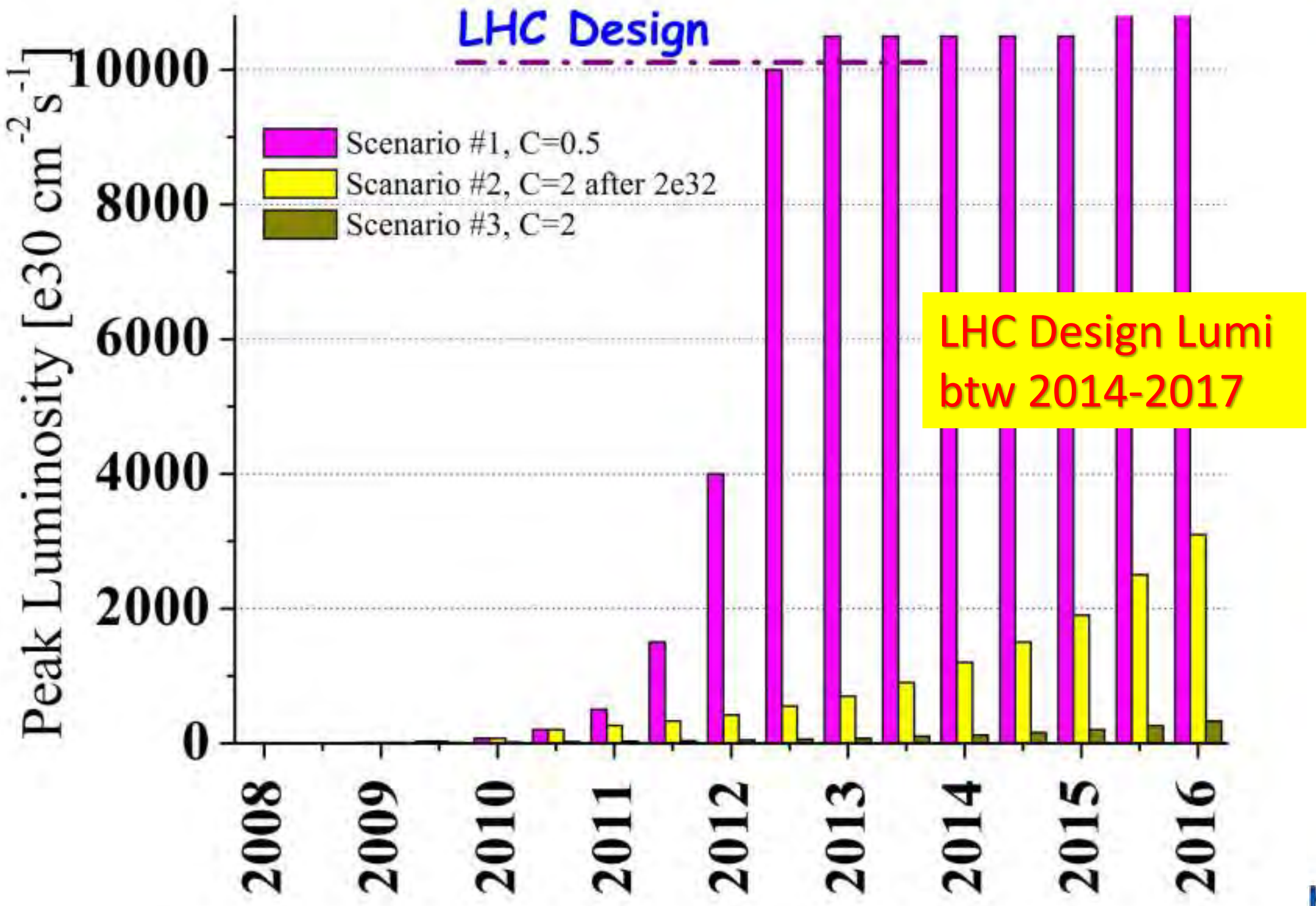

LHC: Design Lumi in July 2016

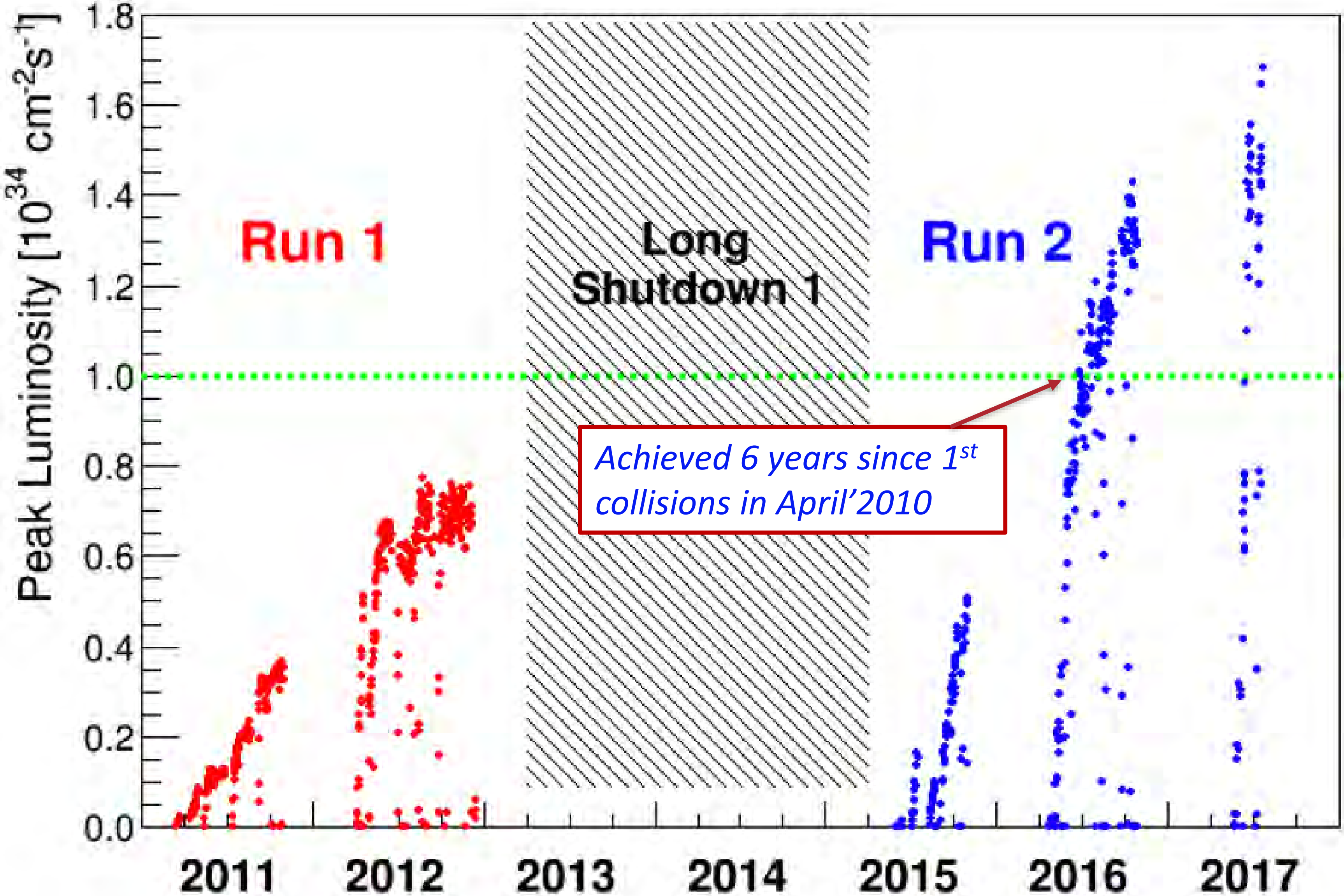

LHC Contributions to Science and Technology

- Technology:
  - Record field NbTi magnets 8 T
  - Record field Nb_3Sn magnets for IR 12T@poles – for HL-LHC
  - >99.99% efficient 4-stage system of 128 collimators
  - Crab-cavities to compensate crossing angle *Lumi* reduction – for HL-LHC

- Beam physics advances:
  - Record pp Luminosity 2.1<u>4</u>E34 $cm^{-2}s^{-1}$ (x2 over LHC design; x50 Tevatron)
  - Effective electron cloud control (scrubbing, etc)
  - Crystal collimation demo
  - Long-range beam-beam wire compensation demo
  - Hollow e-beam collimation – for HL-LHC

- 26 658.883 m
- 6.5 TeV x 2

LHC Page1 | Fill: 6629 | E: 6499 GeV | t(SB): 08:30:56 | 01-05-18 20:38:29

PROTON PHYSICS: STABLE BEAMS

Energy:	6499 GeV	I(B1):	1.56e+14	I(B2):	1.72e+14

Inst. Lumi [(ub.s)^-1] IP1: 8155.99 IP2: 1.76 IP5: 7827.12 IP8: 330.93

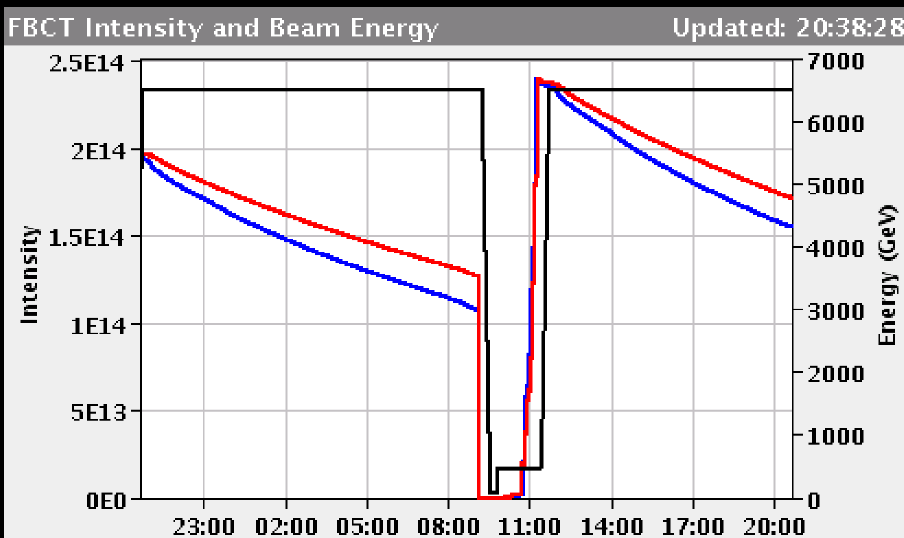

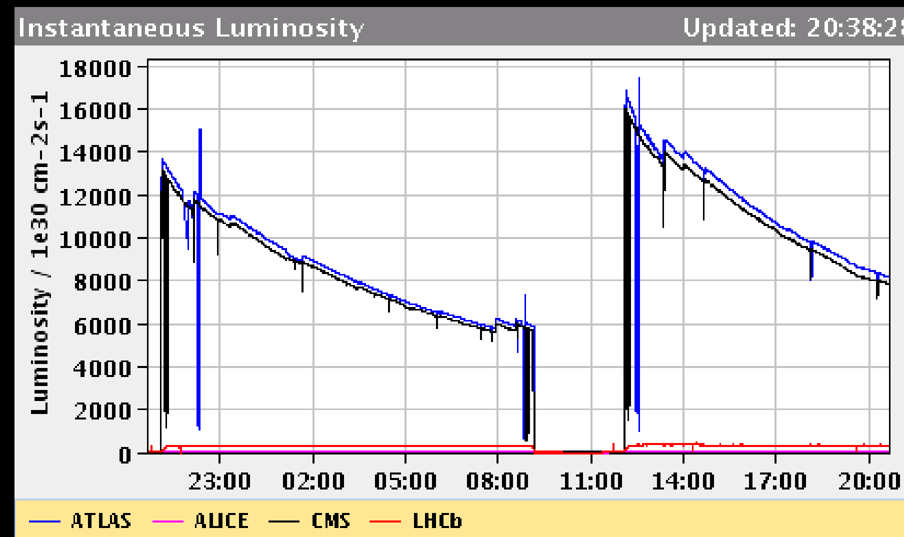

Comments (01-May-2018 14:18:10)

Fill for physics (1887b)

XRPs IN

continous crossing angle leveling in IP1/5

BIS status and SMP flags	B1	B2
Link Status of Beam Permits	true	true
Global Beam Permit	true	true
Setup Beam	false	false
Beam Presence	true	true
Moveable Devices Allowed In	true	true
Stable Beams	true	true

AFS: 25ns_1887b_1874_1694_1772_144bpi_19inj

PM Status B1: ENABLED | PM Status B2: ENABLED

Luminosity and Burn-Up

The relationship of the beam to the rate of observed physics processes is given by the "Luminosity"

Rate → $R = L\sigma$

"Luminosity"

Cross-section ("physics")

Standard unit for Luminosity is $cm^{-2}s^{-1}$

Example: total *p-p* inelastic+elastic cross section at 13 TeV cme is ~*110* mbarn (58 inel+ 12 ssd+40 el not seen)→
~60 interactions per crossing x
40,000,000 collision/sec= 2.4e9 protons leave each beam every second

Beam lifetime due to such "Burn up" *T=N/(dN/dt)=*
2.8e14 protons/(2.4e9/s) =32 hours

LHC Luminosity Evolution

Instantaneous Luminosity: $L = \frac{f_{rev} \cdot n_b \cdot N_1 \cdot N_2}{2\pi\sqrt{(\sigma_{x,1}^2 + \sigma_{x,2}^2)} \cdot \sqrt{(\sigma_{y,1}^2 + \sigma_{y,2}^2)}} \cdot F \cdot H$

$n_b \sim 2800$ $F = 1/\sqrt{1+\left(\frac{\sigma_z \phi}{\sigma_t\, 2}\right)^2} \sim 0.85$

Proton burn-up rate $dN/dt = -\, n_{\mathrm{IP}} L \sigma_{\mathrm{tot}}$

where $L = L_0\,(N(t)/N_0)^2$

Solution $N(t) = N_0/(1+t/\tau)$

$L(t) = L_0/(1+t/\tau)^2$

where $\tau = N_0 / n_{\mathrm{IP}} L_0\, \sigma_{\mathrm{tot}}$

~32 hours

Fermilab

Luminosity lifetime (*eats itself*)

Take into account two IPs (ATLAS, CMS and 3% LHCb) 1/32+1/32 hrs^{-1}

Take into account beam gas 1/110hrs^{-1} and that *Lumi~N^2* → x2

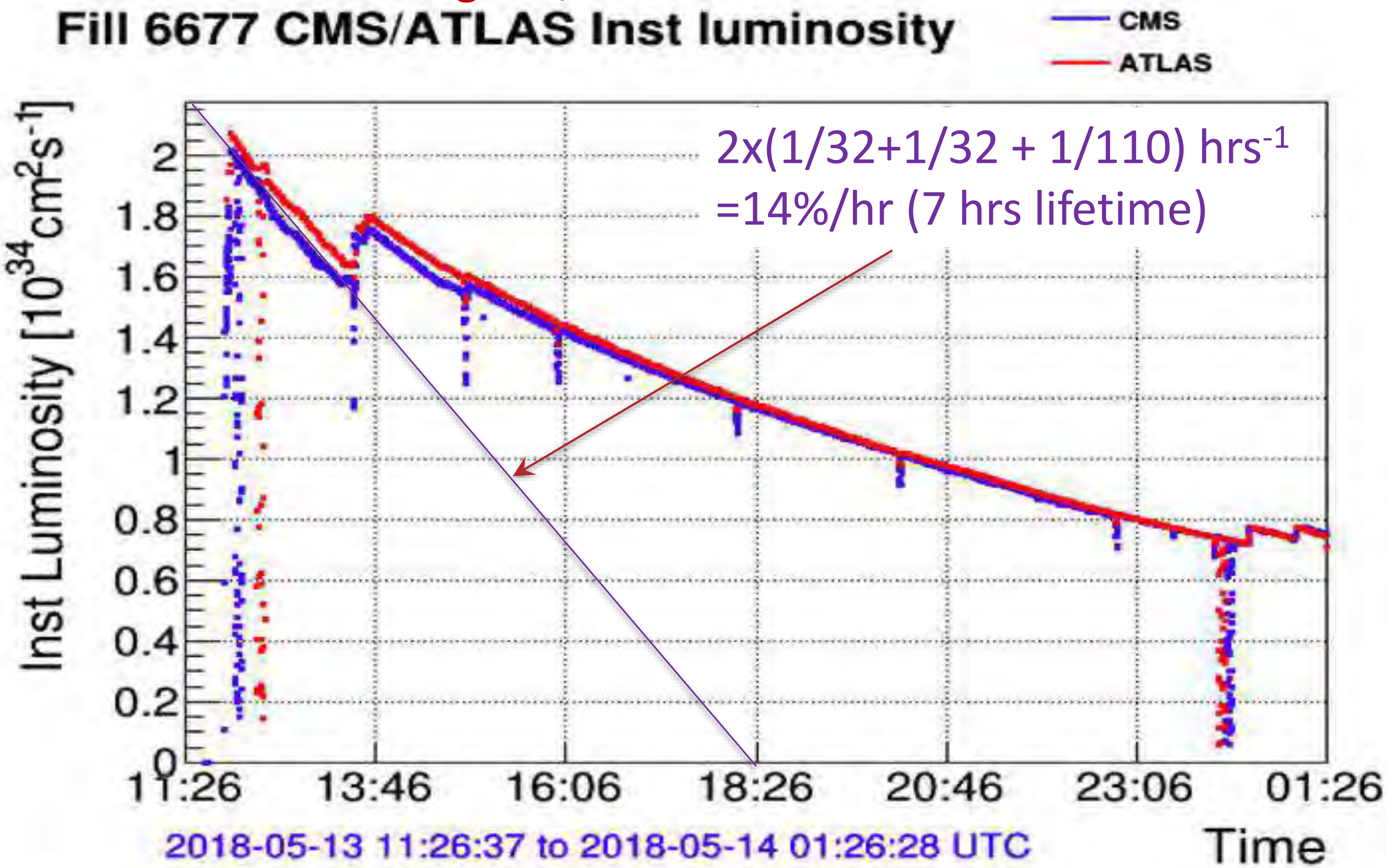

Heart of the LHC: State-of-the-Art SC Magnets

1232 bending magnets 15m
NbTi cables, 13 кA@1.9 K 10 GJ

4.5T

Tevatron,
6 m, 76 mm
774 dipoles

4.5 K He, NbTi
+ warm iron
small He-plant

5.3T

HERA,
9 m, 75 mm
416 dipoles

NbTi cable
cold iron
Al collar

3.5T

RHIC,
9 m, 80 mm
264 dipoles

NbTi cable
simple &
cheap

8.3T

LHC,
15 m, 56 mm
1276 dipoles

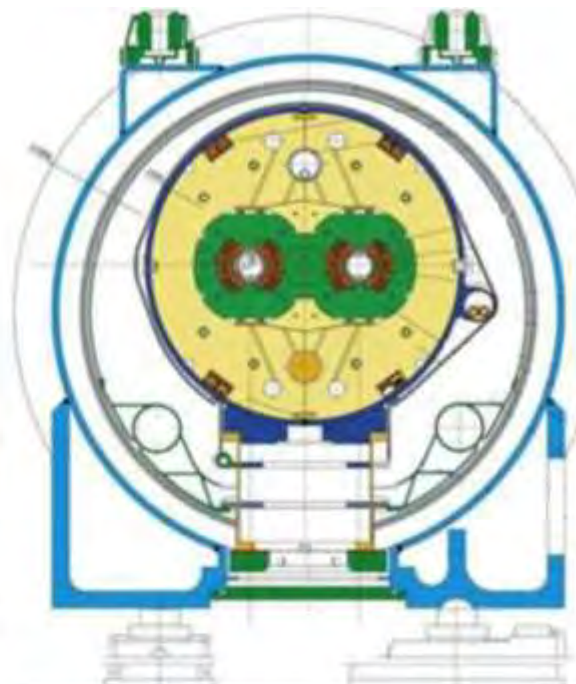

NbTi cable
2K He
two bores

Fermilab

Focusing by 2-Aperture Quadrupole Magnets

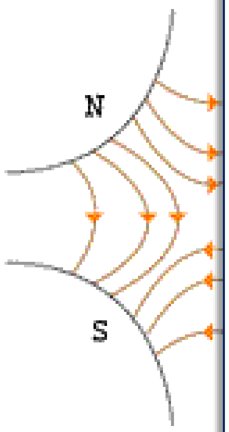

Luckily..

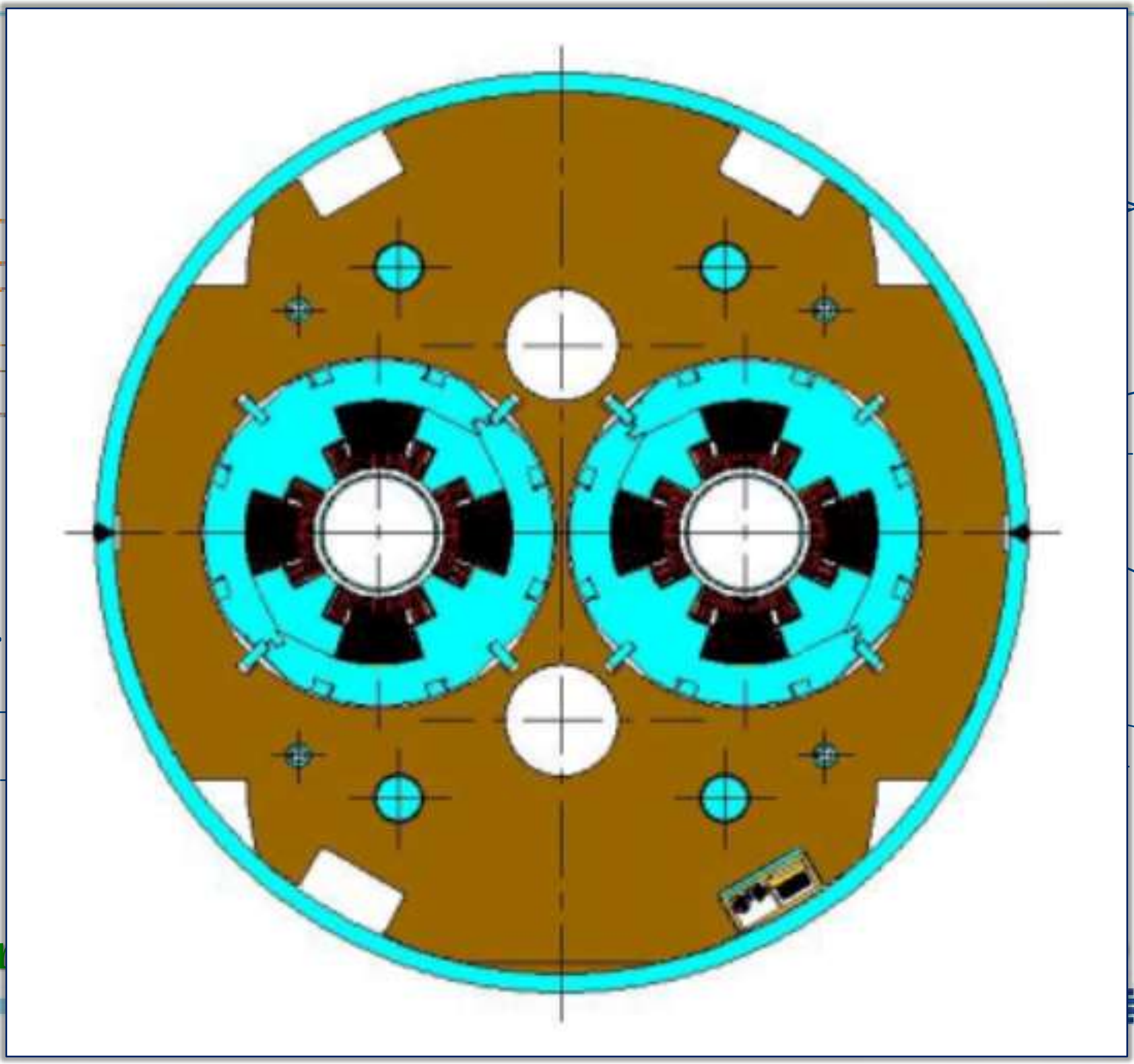

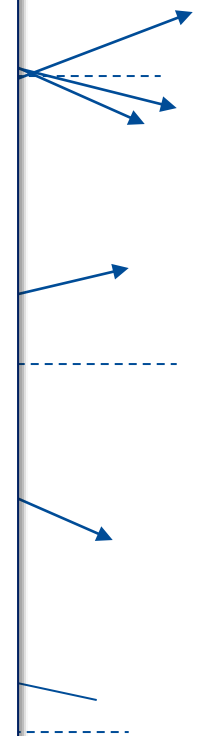

...pai

cell"

CERN Complex

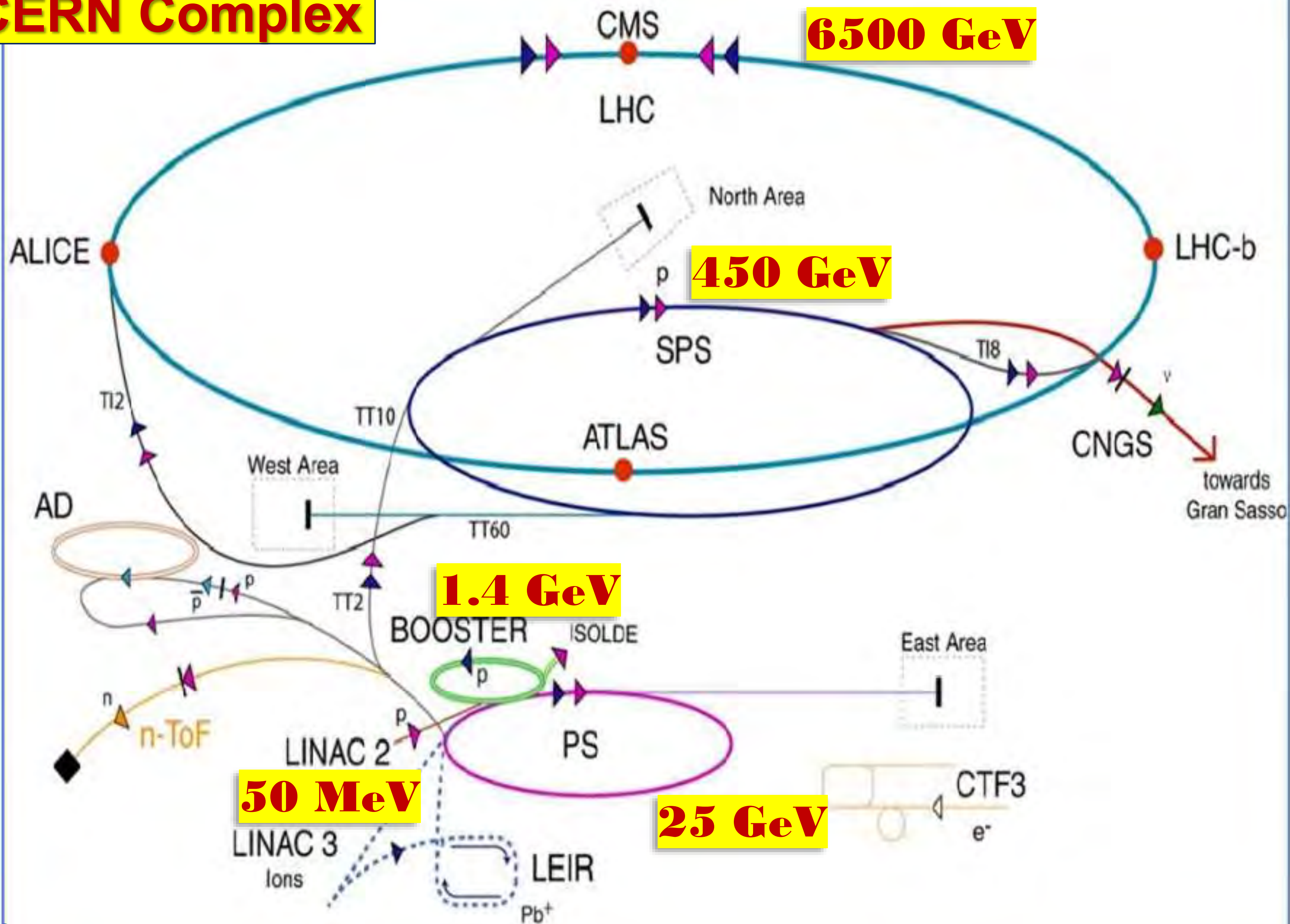

Electron Cloud & Need of *Scrubbing*

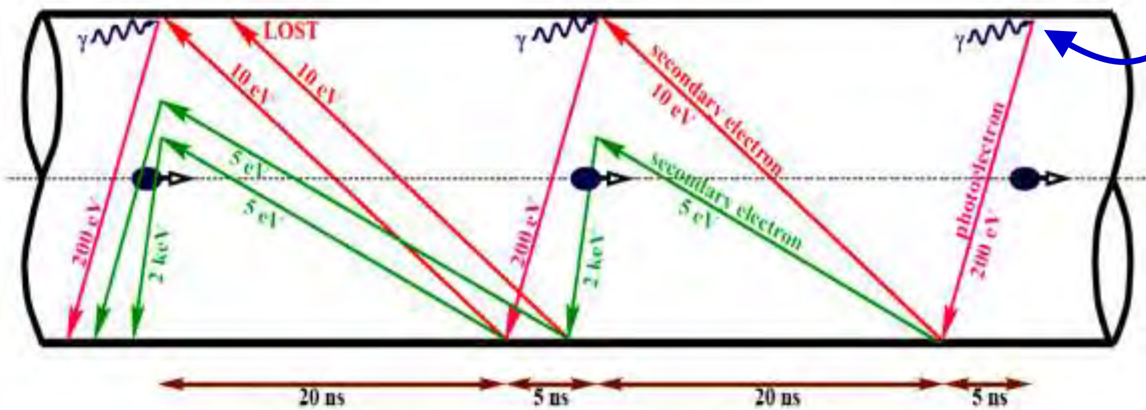

The critical energy of the photons at 7 TeV ~ 44 eV

- Primary sources of electrons in the LHC
  - At Injection (450 GeV) gas ionization
  - At 7 TeV Synchrotron Radiation

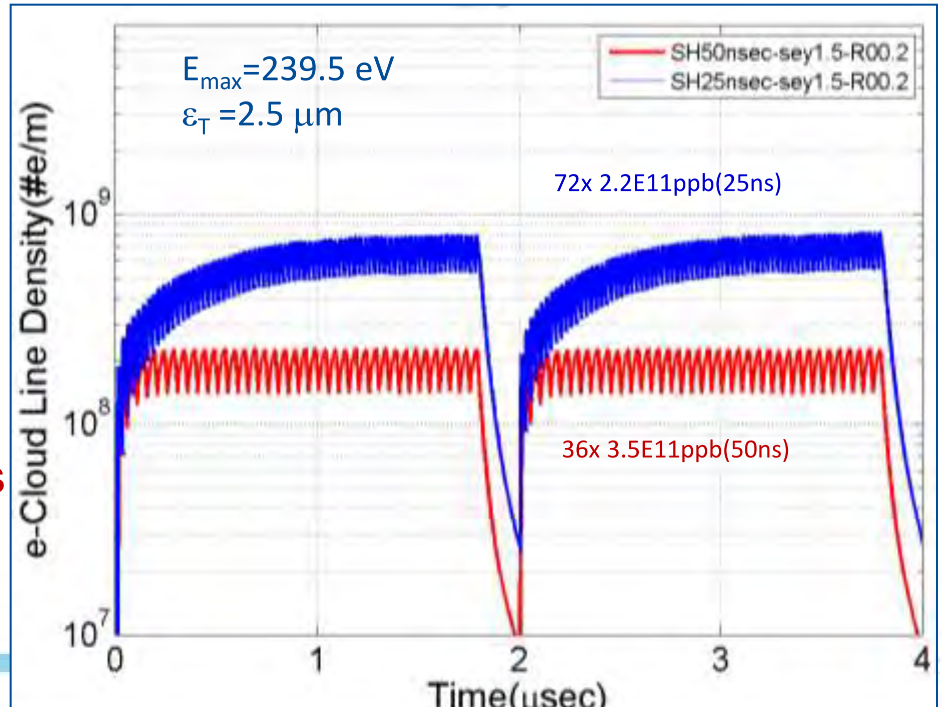

Consequences:

- instabilities, emittance growth, desorption ←bad vacuum, beam loss

- excessive energy deposition in the cold sectors

What e-cloud can do to the Beam?

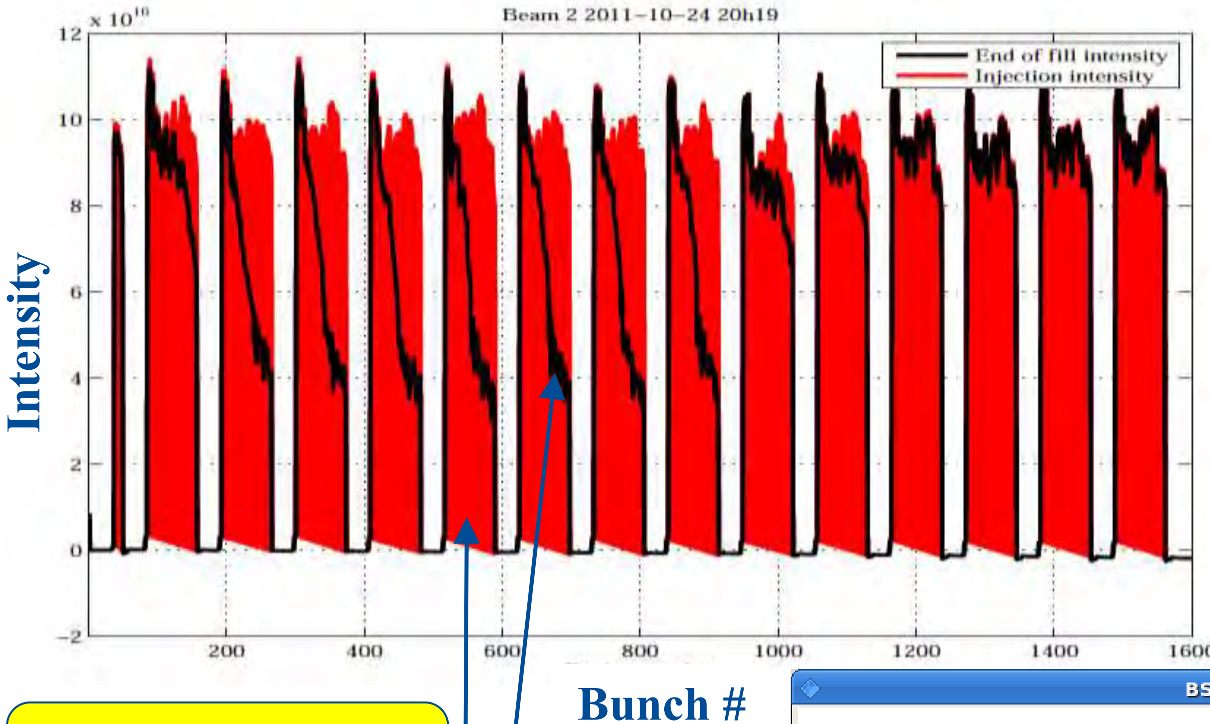

Injection Intensity
End of fill Intensity

- Fill: 2249 (2011)
  25 ns Bunch Spacing
- Energy = 450 GeV
- Time between Injection to End ~10 min
- Dumped by BPM
- 1020 Bunches

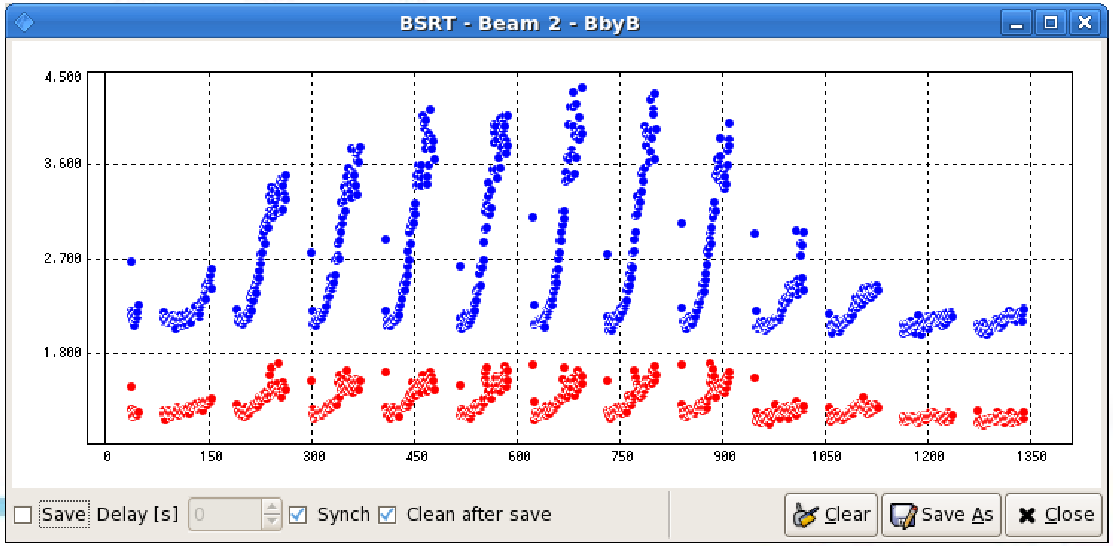

Measured Emittance Growth

~33% Horizontal
~110% Vertical
Associated beam loss

Scrubbing @ 25 ns bunch spacing

So far it is the only cure in the LHC….Takes time to clean the surface and reduce SEY (secondary electron yield) from ~2.2 to ~1.5

Scrubbing "memory" kept while running with 25 ns beams - **deconditioning** was observed after few weeks of low e-cloud operation

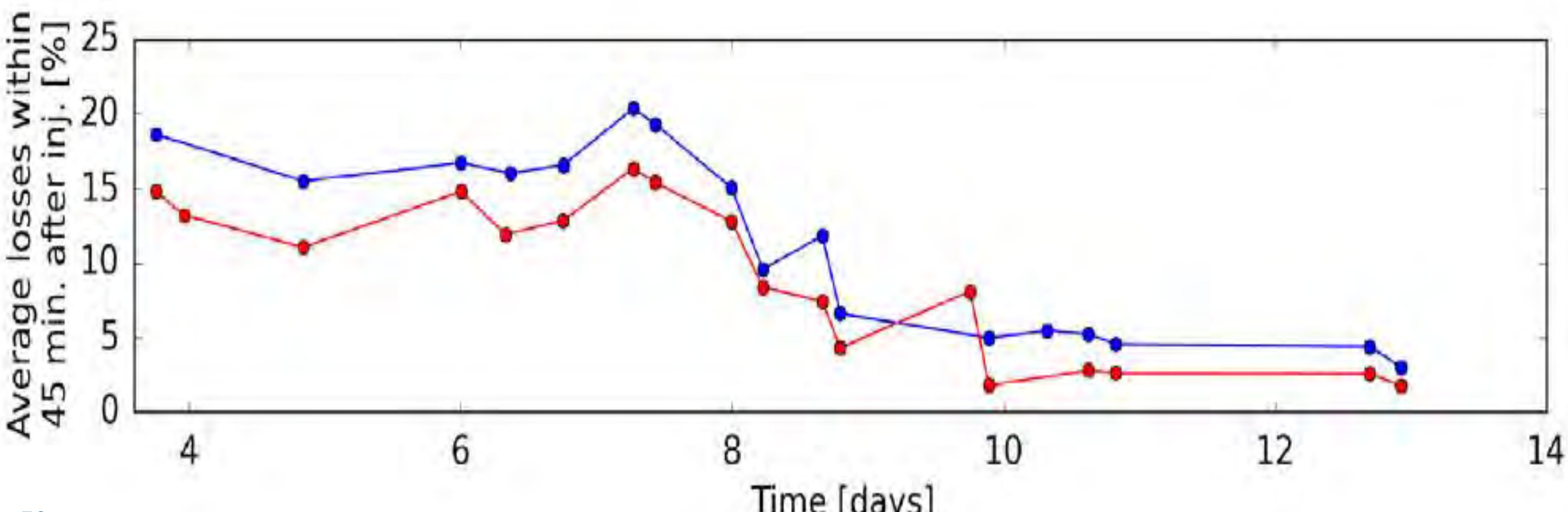

UFOs & 16L2

'Unidentified Falling Objects'

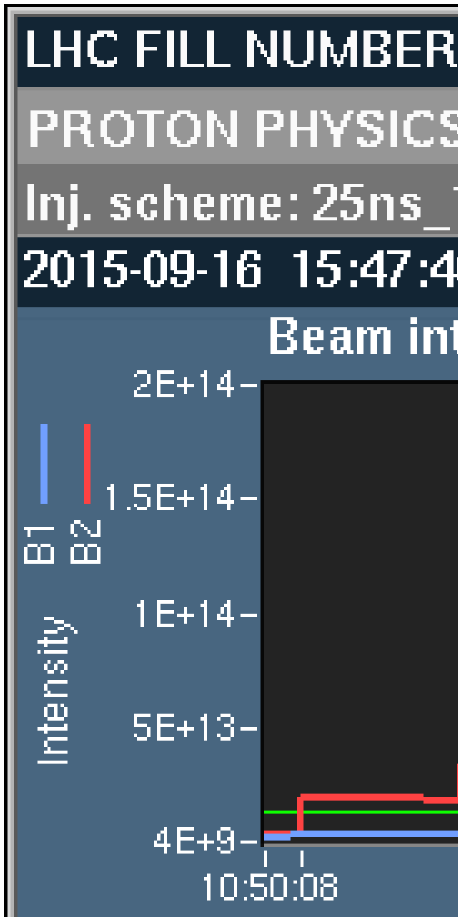

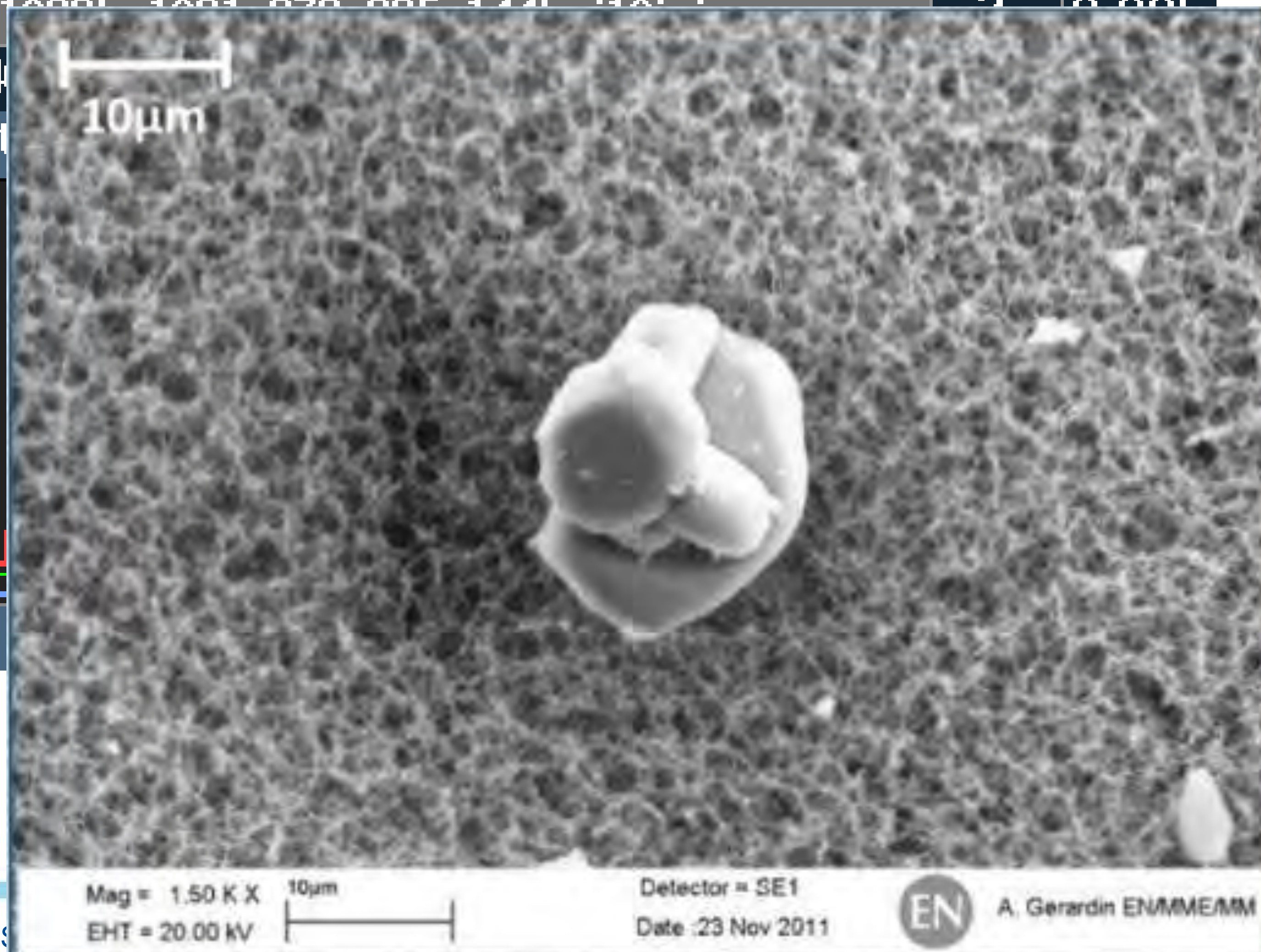

UFOs: there are many of them, they are frequent !

UFO events observed quite often during operation at 6.5 TeV

Conditioning is observed on the UFO rate in spite of the increasing number of bunches

BLM thresholds being optimize to find a **good compromise between availability and quench protection**

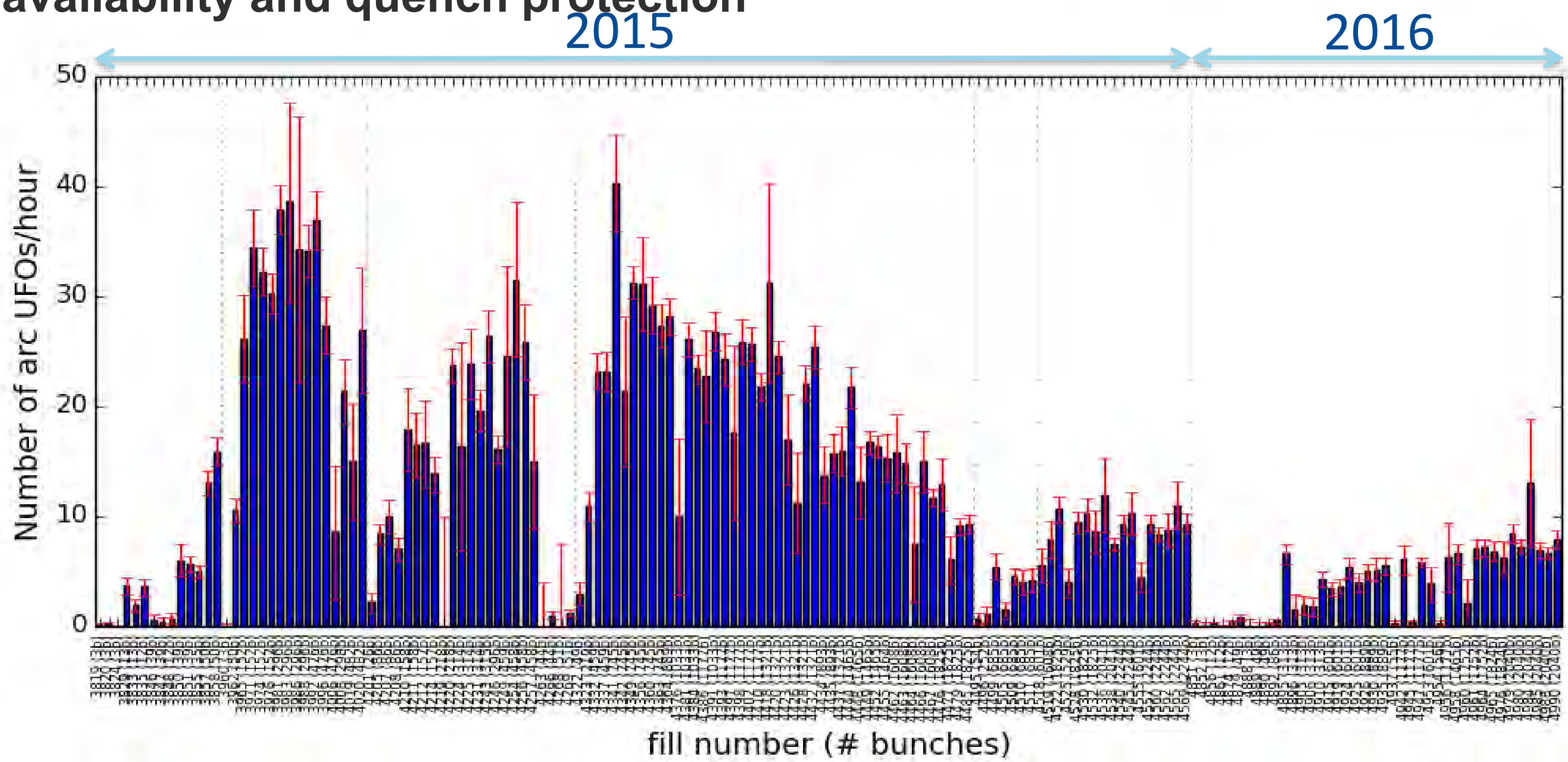

- arc UFOs (cell >11): rates similar to end of 2015
  - did not lose conditioning over the Xmas stop

LHC collimation system

- LHC has **complex** and **distributed collimation** system of >100 collimators
  → *several stages to protects LHC components as well as detectors*

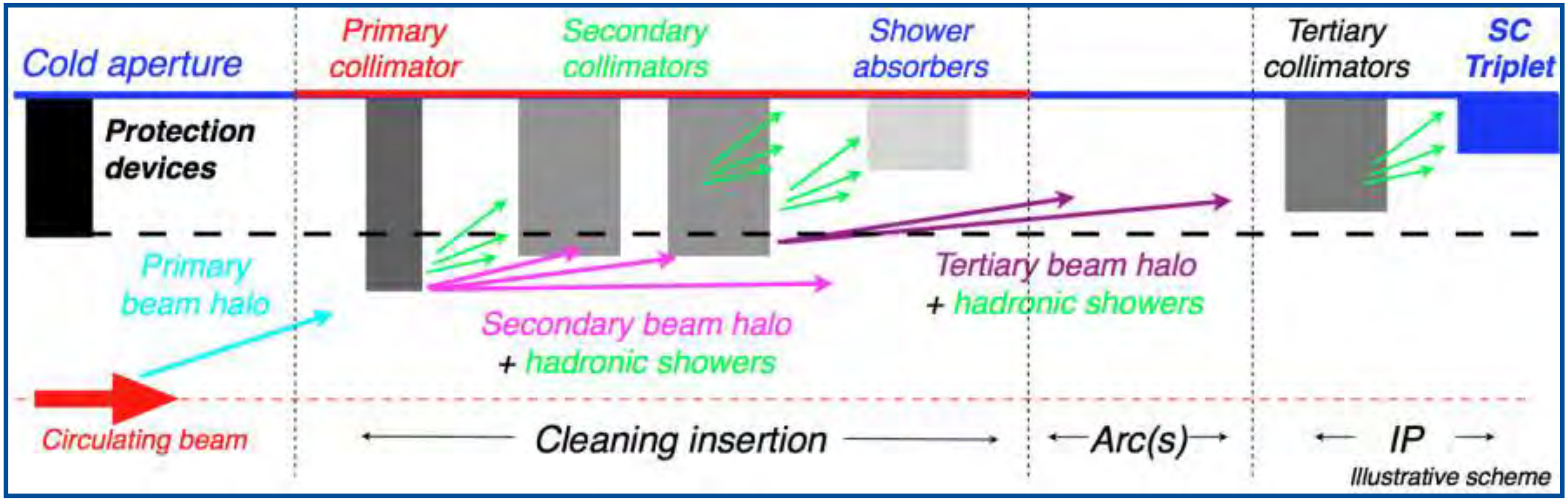

- **Collimation** is designed to provide cleaning efficiencies > 99.99%
  → *need **good statistical accuracy** at limiting loss locations;*
  → *simulate only halo particles that interact with collimators, not the core.*

LHC Collimator

- Two jaws, beam passing in between, most are 1 m long

Carbon fiber composite.

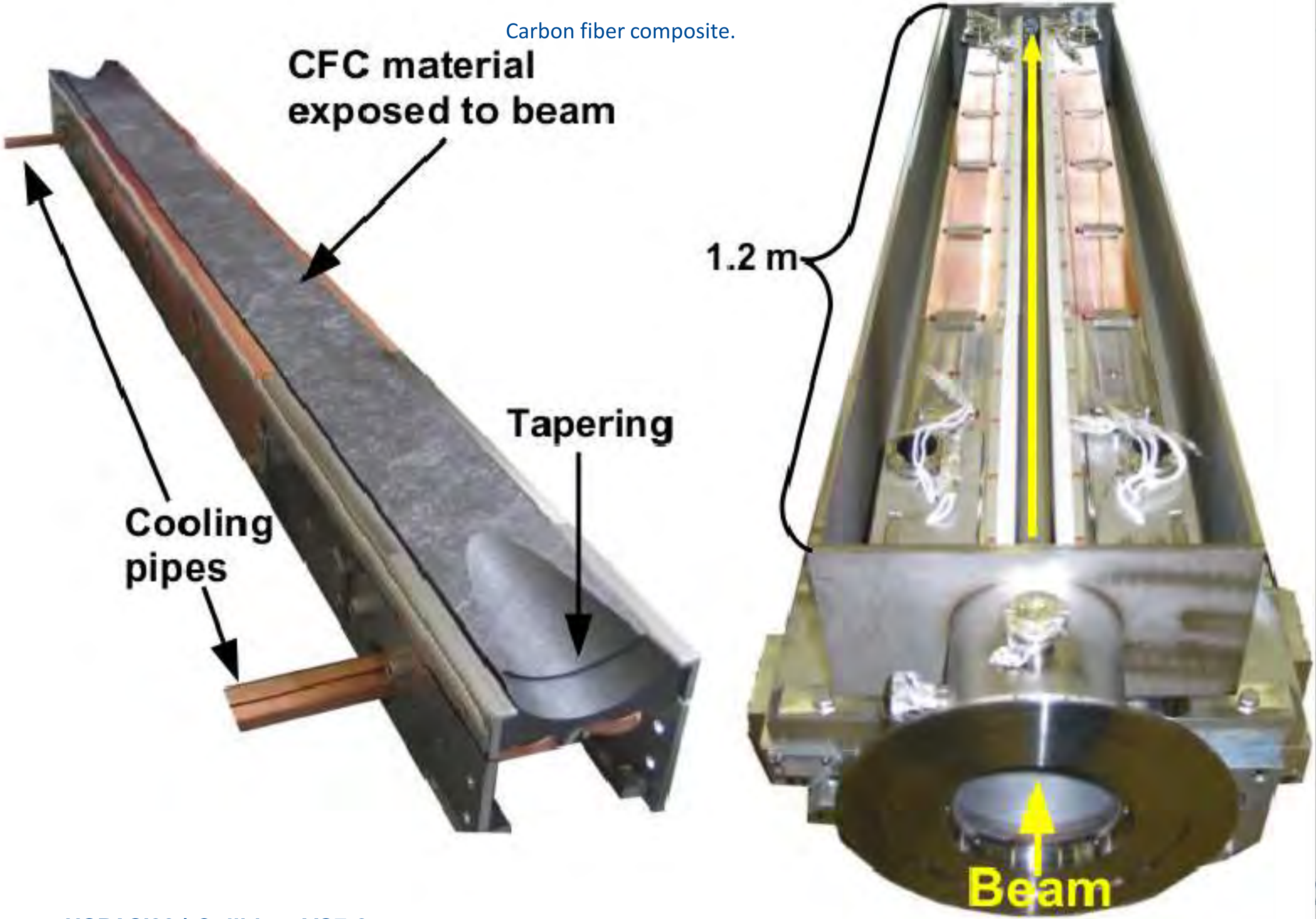

LHC Collimation System Layout

Two warm cleaning insertions, 3 collimation planes

- **IR3: Momentum cleaning**
  - **1 primary (H)**
  - **4 secondary (H)**
  - **4 shower abs. (H,V)**
- **IR7: Betatron cleaning**
  - **3 primary (H,V,S)**
  - **11 secondary (H,V,S)**
  - **5 shower abs. (H,V)**

Local cleaning at triplets

- **8 tertiary (2 per IP)**

Passive absorbers for warm magnets

Physics debris absorbers

Transfer lines (13 collimators)
Injection and dump protection (10)

Total of 108 collimators (100 movable). Two jaws (4 motors) per collimator!

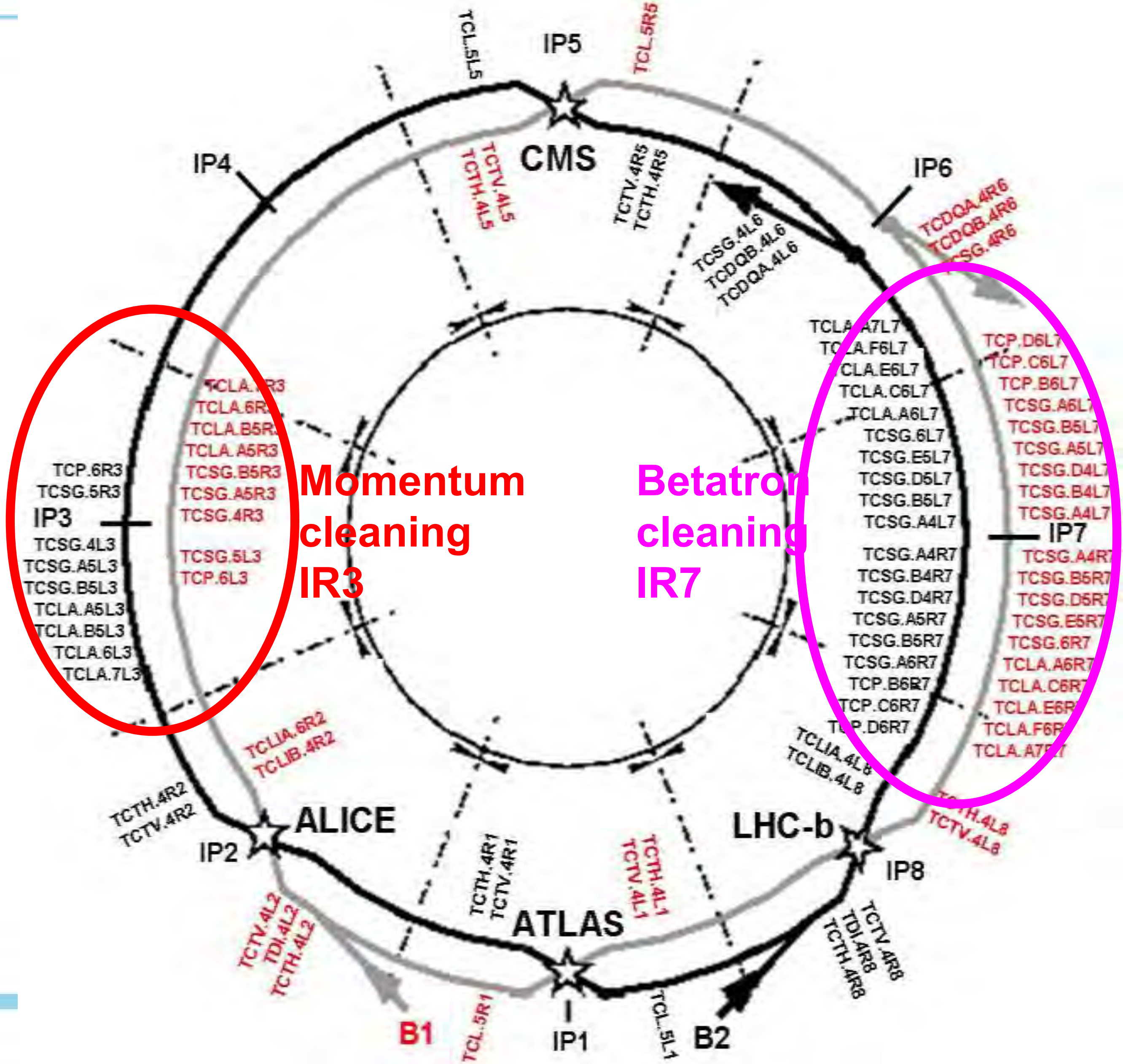

Super-Effective Halo Cleaning in LHC

- 2015

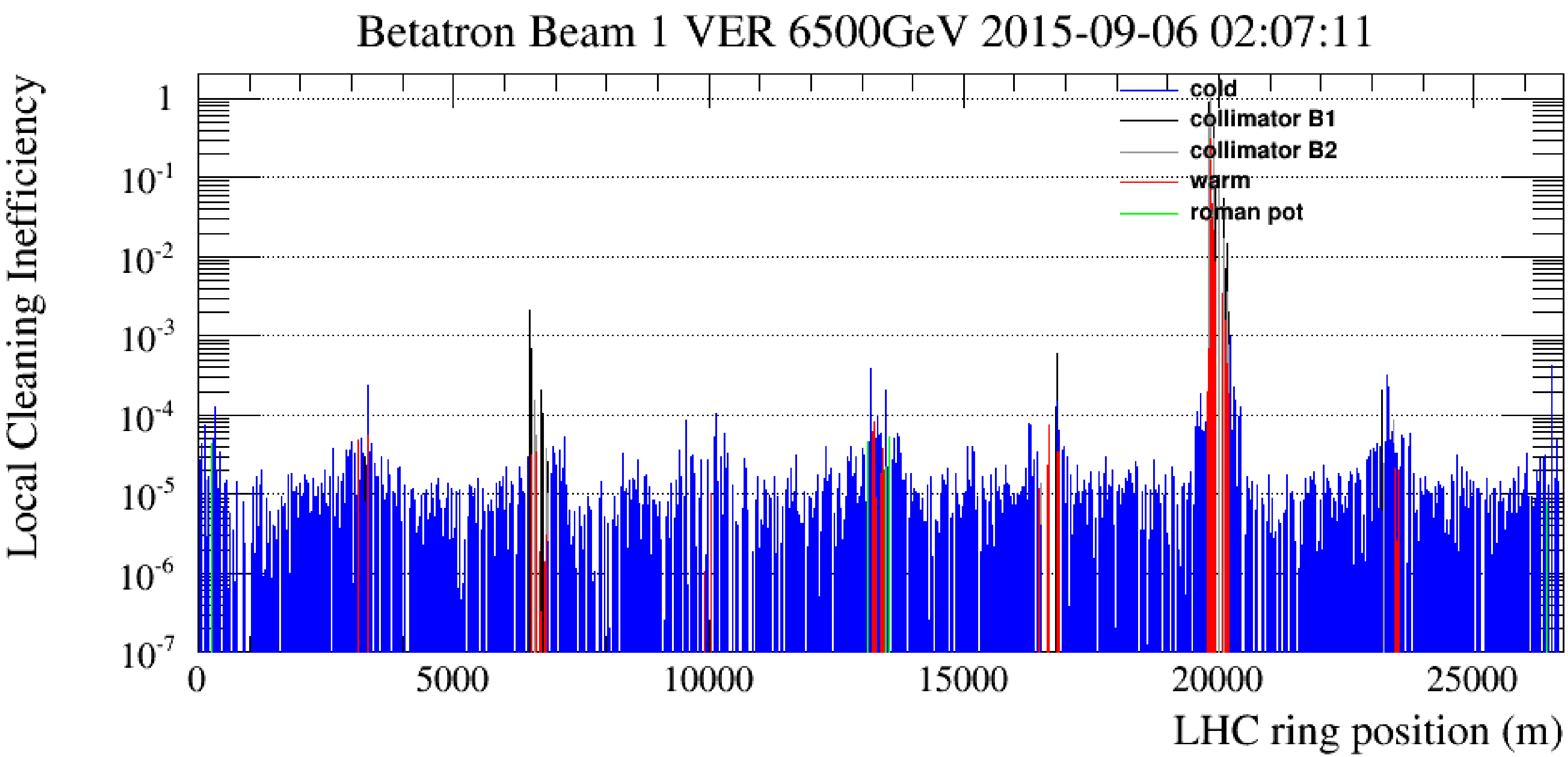

Fermilab

LHC Luminosity Upgrade (ca 2027): Goals

Luminosity recipe :

$$L = \frac{n_b \cdot N_1 \cdot N_2 \cdot \gamma \cdot f_{rev}}{4\pi \cdot \beta^* \cdot \varepsilon_n} \cdot F(\phi, \beta^*, \varepsilon, \sigma_s)$$

→ 1) maximize bunch intensities	→ Injector complex	1.15 → 2.2e11
→ 2) minimize the beam emittance	LIU ⇔ IBS	3.75 → 2.5 μm
→ 3) minimize beam size (constant beam power);	→ triplet aperture	β* 0.3 → 0.15 m
→ 4) maximize number of bunches (beam power);	→ 25ns	
→ 5) compensate for 'F';	→ Crab Cavities	0.3 w/o Crab Cavities 0.83 w. Crab Cavities
→ 6) Improve machine 'Efficiency'	→ minimize number of unscheduled beam aborts	

With all these changes luminosity could peak at **~20e34** → 10x 2018 lumi and 10x pile up, ie μ>540 → luminosity leveling will be done at **~5e34**

integrated luminosity now **150 fb-1** → **3000 fb-1** by 2041

HL-LHC Luminosity Leveling
by change of the Crab-Strength or beta*

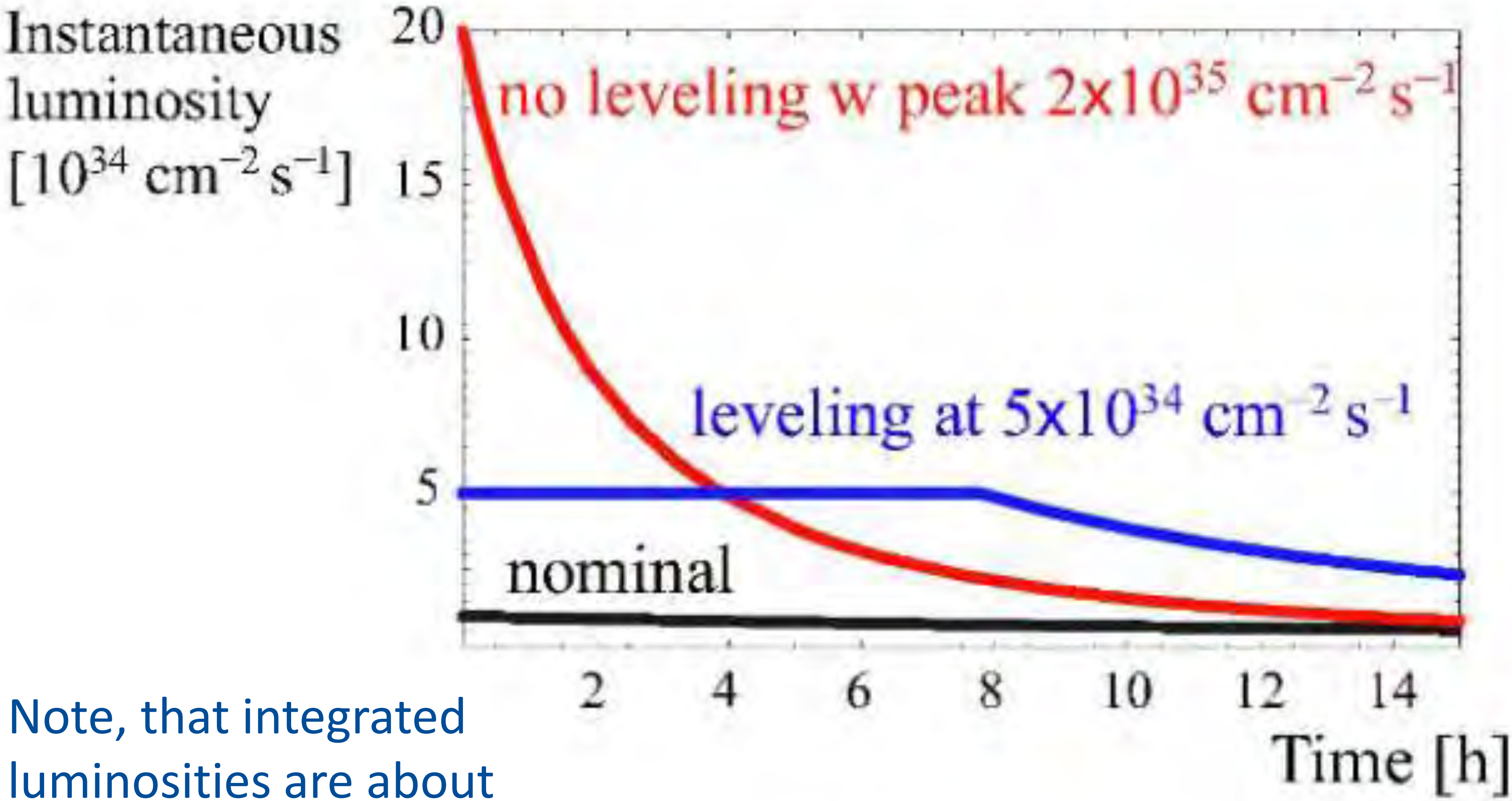

Note, that integrated luminosities are about the same in two cases

HL-LHC Scale: Hardware and Cost

The HL-LHC Project

976MCHF (-142 +208)

~2,500 man-years

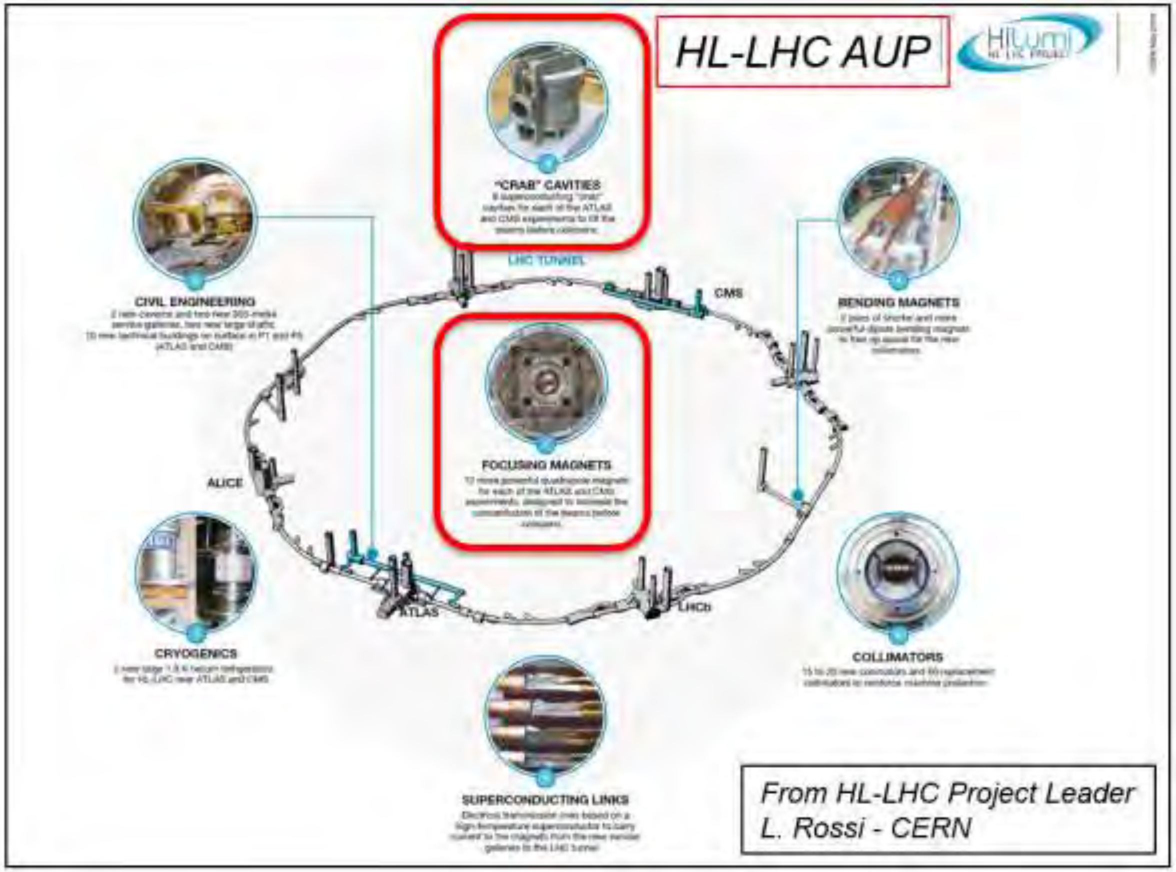

- New IR-quads Nb_3Sn (inner triplets)
- New 11 T Nb_3Sn (short) dipoles
- Collimation upgrade
- Cryogenics upgrade
- Crab Cavities
- Cold powering
- Machine protection
- …

Major intervention on more than 1.2 km of the LHC

Other Ideas and Options for LHC

- (besides/beyond HL-LHC… ie after ~2040)
- High luminosity electron-proton collider LHeC – see lectures VS9-10
- High energy LHC (16T magnets → 28 TeV cme)
- Injector for the future 100km 100 TeV cme FCChh – see see lectures VS9-10

Thanks for Your Attention !

Questions !?

Fermilab

Literature

- V.Shiltsev, F.Zimmermann, Modern and Future Colliders (Rev.Mod.Phys., 2021)

https://journals.aps.org/rmp/abstract/10.1103/RevModPhys.93.015006

- V.Lebedev, V.Shiltsev, Accelerator Physics at the Tevatron Collider (Springer, 2014)

https://indico.cern.ch/event/774280/attachments/1758668/2915590/2014_Book_AcceleratorPhysicsAtTheTevatro.pdf

- S.Myers, H.Schopper, eds. Accelerator and Colliders (Springer, 2013, 2020)

https://link.springer.com/book/10.1007/978-3-030-34245-6

- "Particle accelerator physics - 4th ed." (Springer) by Wiedemann, Helmut.

https://library.oapen.org/handle/20.500.12657/23641

- "Measurement and control of charged particle beams" (Springer) by Minty, Michiko G; Zimmermann, Frank

https://library.oapen.org/handle/20.500.12657/23642

parameter	FCC-hh		HE-LHC	(HL) LHC
collision energy cms [TeV]	100		27	14
dipole field [T]	16		16	8.33
circumference [km]	100		27	27
straight section length [m]	1400		528	528
# IP	2 main & 2		2 & 2	2 & 2
beam current [A]	0.5		1.12	(1.12) 0.58
bunch intensity [10^{11}]	1	1 (0.2)	2.2 (0.44)	(2.2) 1.15
bunch spacing [ns]	25	25 (5)	25 (5)	25
rms bunch length [cm]	7.55		7.55	(8.1) 7.55
peak luminosity [10^{34} cm^{-2}s^{-1}]	5	30	25	(5) 1
events/bunch crossing	170	1k (200)	~800 (160)	(135) 27
stored energy/beam [GJ]	8.4		1.3	(0.7) 0.36
beta* [m]	1.1-0.3		0.25	(0.20) 0.55
norm. emittance [μm]	2.2 (0.4)		2.5 (0.5)	(2.5) 3.75

Challenges FCC:

- Cost of 100 km magnets & civil and new 3.3 TeV injector (24-27 BCHF)
- 16 T magnets
- ~1000 pileup
- Collimation/protection
- x100 LHC radiation power /meter

Challenges HE-LHC:

- Cost of 27 km magnets & new 1.3 TeV inj/beamlines (~ 7 BCHF)
- 16 T magnets, curved
- ~800 pileup
- x15 LHC radiation power /meter

U.S. Particle Accelerator School
Education in Beam Physics and Accelerator Technology

Fermilab

Managed by Fermi Research Alliance, LLC for the U.S. Department of Energy Office of Science

Electron-Ion Colliders
Future Large Hadron Colliders

Vladimir Shiltsev, Fermilab

part of the "Colliders" class by V.Lebedev, N.Mokhov and V.Shiltsev

US Particle Accelerator School, Jan 24 – Feb 4, 2022

Nuclear Physics Requirements for EIC

• Center of Mass Energies	20 GeV – 140 GeV
• Maximum Luminosity	10^{34} cm^{-2}s^{-1}
• Hadron Beam Polarization	>70%
• Electron Beam Polarization	>70%
• Ion Species Range	*p* to Uranium
• Number of interaction regions	up to two

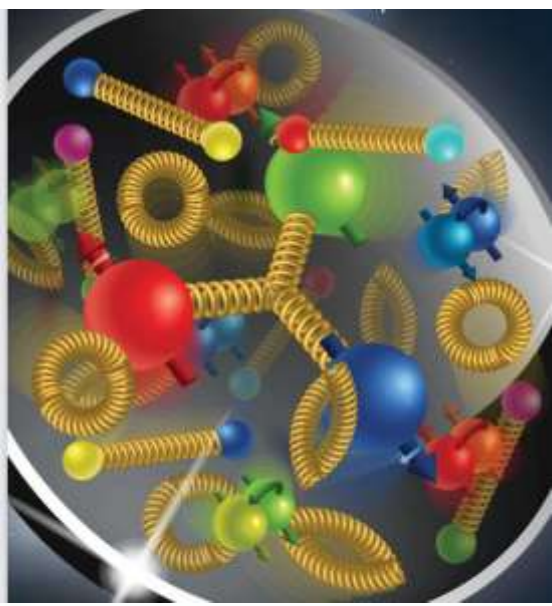

NSAC - Department of Energy Nuclear Science Advisory Committee

NAS - National Academies of Sciences, Engineering, and Medicine

Predecessor: HERA at DESY 30 GeV e- and 920 GeV p , Luminosity 7.5 10^{31} cm^{-2}s^{-1}

EIC Collider Concept

Design based on **existing** RHIC,
RHIC is well maintained, operating at its peak

- **Hadron storage ring 40-275 GeV** (existing)
  - o Many bunches
  - o Bright beam emittance
  - o Need strong cooling **or** frequent injections
- **Electron storage ring (2.5–18 GeV** (new))
  - o Many bunches,
  - o Large beam current (2.5 A) ➔ 10 MW S.R. power
- **Electron rapid cycling synchrotron** (new)
  - o 1-2 Hz
  - o Spin transparent due to high periodicity
- **High luminosity interaction region(s)** (new)
  - o $L = 10^{34} cm^{-2} s^{-1}$
  - o Superconducting magnets
  - o 25 mrad Crossing angle with crab cavities
  - o Spin Rotators (longitudinal spin)
  - o Forward hadron instrumentation

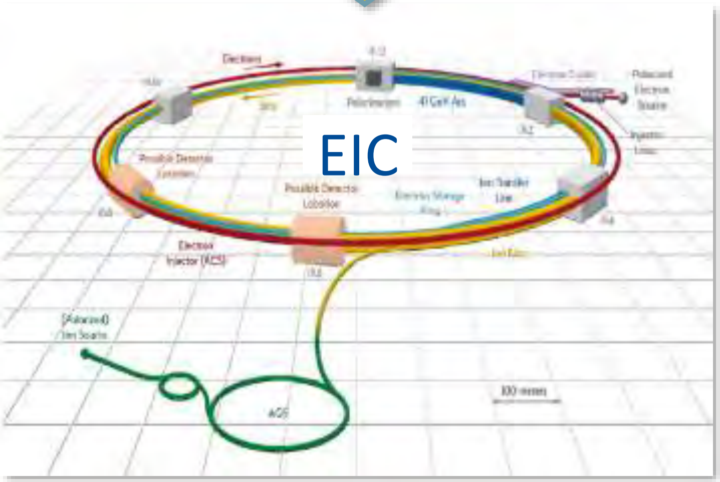

From RHIC to the EIC

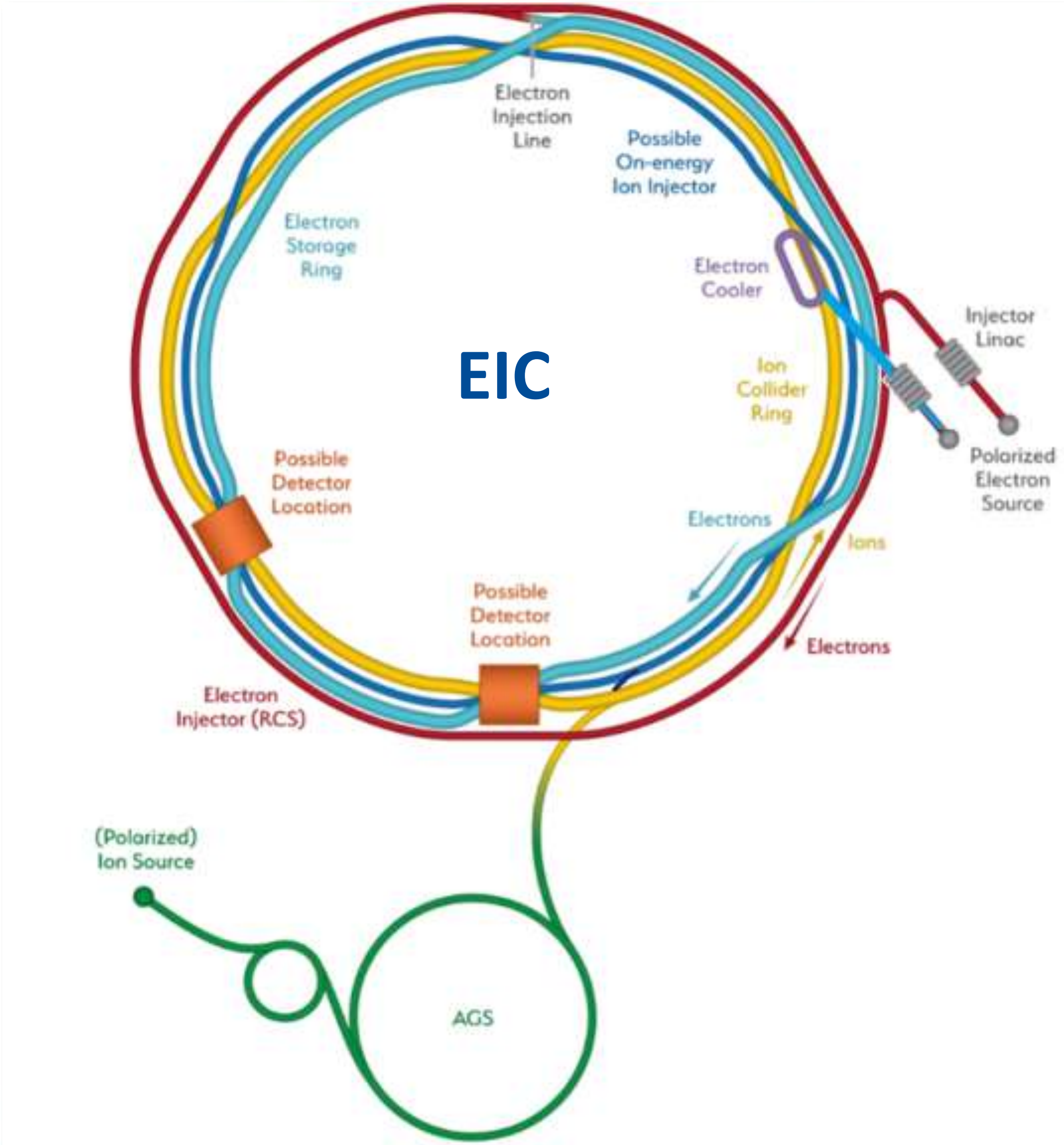

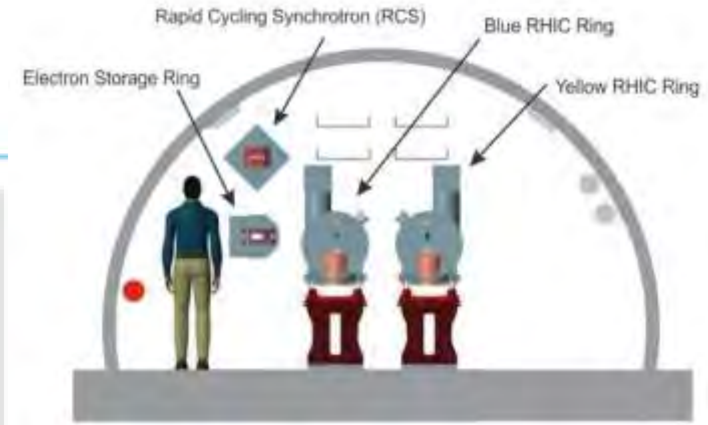

Existing RHIC with Blue and Yellow rings + add electron storage ring which holds the electrons which collide with hadrons + add e- injector complex to deliver full energy e- to the storage ring + strong hadron cooling facility completes the facility

- Hadron Storage Ring
- Electron Storage Ring
- e- Injector Synchrotron
- Possible on-energy Hadron injector ring
- Hadron injector complex

EIC Parameter Table

Parameter	hadron	electron
Center-of-mass energy [GeV]	104.9	
Energy [GeV]	275	10
Number of bunches	1160	
Particles per bunch [10^{10}]	6.9	17.2
Beam current [A]	1.0	2.5
Horizontal emittance [nm]	9.6	20.0
Vertical emittance [nm]	1.5	1.2
Horizontal β-function at IP β_x^* [cm]	90	43
Vertical β-function at IP β_y^* [cm]	4.0	5.0
Horizontal/Vertical fractional betatron tunes	0.305/0.31	0.08/0.06
Horizontal divergence at IP $\sigma_{x'}^*$ [mrad]	0.103	0.215
Vertical divergence at IP $\sigma_{y'}^*$ [mrad]	0.195	0.156
Horizontal beam-beam parameter ξ_x	0.014	0.073
Vertical beam-beam parameter ξ_y	0.007	0.1
IBS growth time longitudinal/horizontal [hr]	3.4/2.0	-
Synchrotron radiation power [MW]	-	9.0
Bunch length [cm]	6	2
Hourglass and crab reduction factor [16]	0.86	
Luminosity [10^{34} cm^{-2} sec^{-1}]	1.0	

EIC covers full center of mass energy range of 20 GeV – 140 GeV

$$E_{cme} \approx 2\sqrt{E_1 E_2}$$

10 e-/e+ and 275 p →
105 GeV cme collisions

Protons up to 275 GeV:

- Existing RHIC with superconducting magnets allow up to $\mathbf{E_p = 275}$ **GeV** and down to $\mathbf{E_p = 41}$ **GeV**
- RHIC beam parameters are close to what is required for EIC

Electrons up to 18 GeV:

Electron storage ring with up to **18 GeV** installed RHIC tunnel, readily achievable with

- large circumference of 3870 m and
- available superconducting RF technology → U_{rf} = 62 MV

low electron energy of **2.5 GeV** is easily obtainable

EIC achieves high luminosity $L = 10^{34}$ cm^{-2}s^{-1}

- **Large bunch charges** $N_e \leq 1.7 \cdot 10^{11}$, $N_p \leq 0.69 \cdot 10^{11}$
- **Many bunches,** n_b=1160 (vs 110 in RHIC)
  - o crossing angle collision geometry
  - o large total beam currents (x3 RHIC)
  - o limited by installed RF power of 10 MW
- **Small beam size** at collision point achieved by
  - o small emittance, requiring either:
    - strong hadron cooling to prevent emittance growth **or**
    - frequent hadron injection
  - o and strong focusing at interaction point (small β_y)
  - o flat beams $\sigma_x/\sigma_y \approx 10$

Strong focusing β_y =5 cm

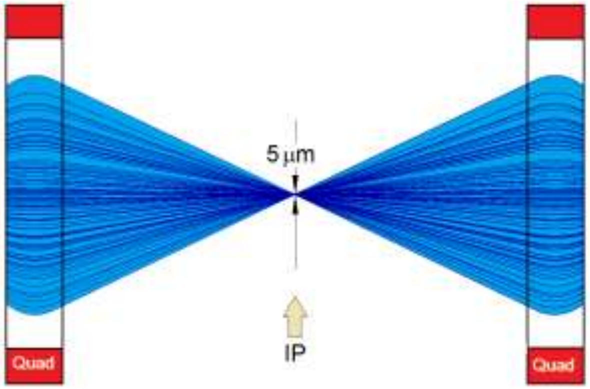

- **Strong, but previously demonstrated beam-beam interaction**

  ξ_p = 0.01 demonstrated in RHIC

  ξ_e = 0.1 demonstrated in HERA, B-factories

EIC High Luminosity with a Crossing Angle

- **Modest crossing angle of 25 mrad**
  - o Avoid parasitic collisions due to short bunch spacing
  - o For machine elements, to improve detection
  - o Reduce detector background

- **However**, crossing angle causes
  - o Low luminosity
  - o Beam dynamics issues
- **avoided by Crab Crossing**

Then :
  - o Effective head-on collision restored
  - o Beam dynamic issues resolved
- RF resonator (crab-cavity) prototypes built and tested with proton beam in the CERN-SPS

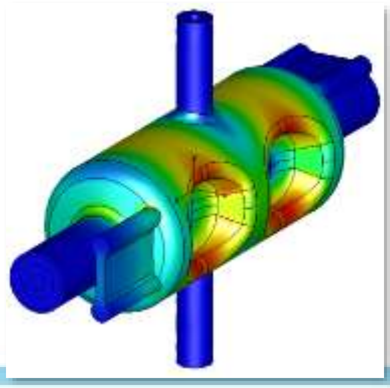

Interaction Region Design

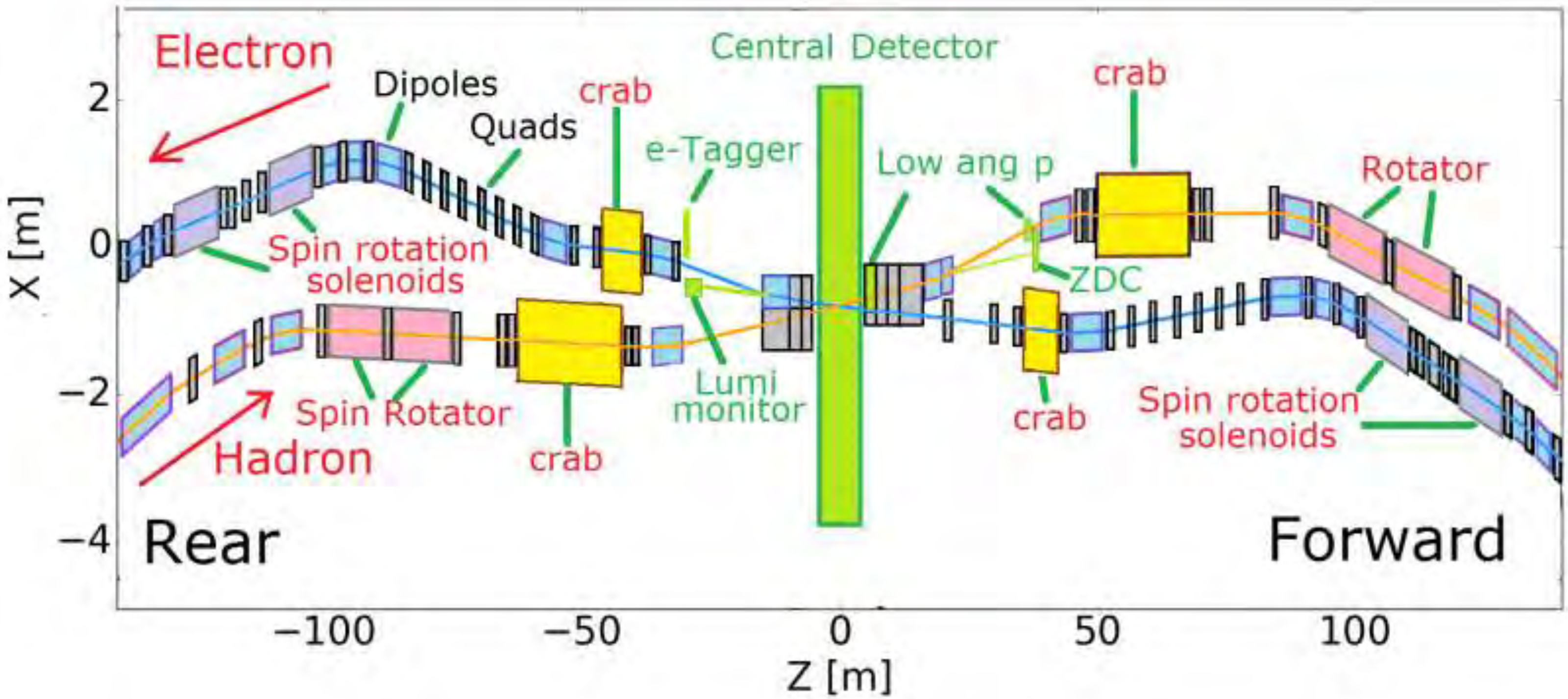

- Interaction Region, the accelerator around the colliding beam detector is the most complex and most constrained section of a collider:
  - $\beta_y \leq 5$ cm @ $\sigma_y = 5$ µm
  - provides sufficient separation of the hadron beam from the 5 mrad forward neutron cone
  - separates the electron beam from the Bethe-Heitler photons used for luminosity measurements,
  - allows for a safe passage of the synchrotron-radiation fan generated upstream of the IP through the detector.

Maintaining high luminosity during a fill

- **Issue:** Dense hadron beam leads to emittance growth due to IBS – causes luminosity decay, would imply reduced average luminosity
- **eA collisions:** existing stochastic cooling system preserves emittance – e-ion luminosity maintained, thus for Ions, **no issue**
- **ep collisions**: need to actively prevent p emittance growth with cooling scheme
- **EIC Strong Hadron Cooling**: extension of established stochastic cooling to higher bandwidth: replacing cables @ amplifiers with electron beam and beam dynamical effects: **Coherent Electron Cooling (CeC)**
- **Establishing CeC will provide**:
  - **Long un-interrupted luminosity runs**
  - **Significant advance in accelerator science**
- Ongioing active R&D on demonstrating CeC
- Has also considered an alternative of frequent on-energy injections using existing Blue Ring that restores average luminosity up to ~ the peak luminosity
- Several alternative options are also being studied – an electron storage ring (single or dual energy) for incoherent electron cooling, use of induction accelerators to produce high power electron beam for cooling, etc.

CeC to Address Lumi Risk ~x(3-10)

Schematic of the layout of the eRHIC strong hadron cooling facility: electron ERL 150 MeV e-, 100mA. Note that the vertical scale has been stretched by a factor of ~50. cooling rate 1 - 2 h is enough to counteract the IBS in EIC

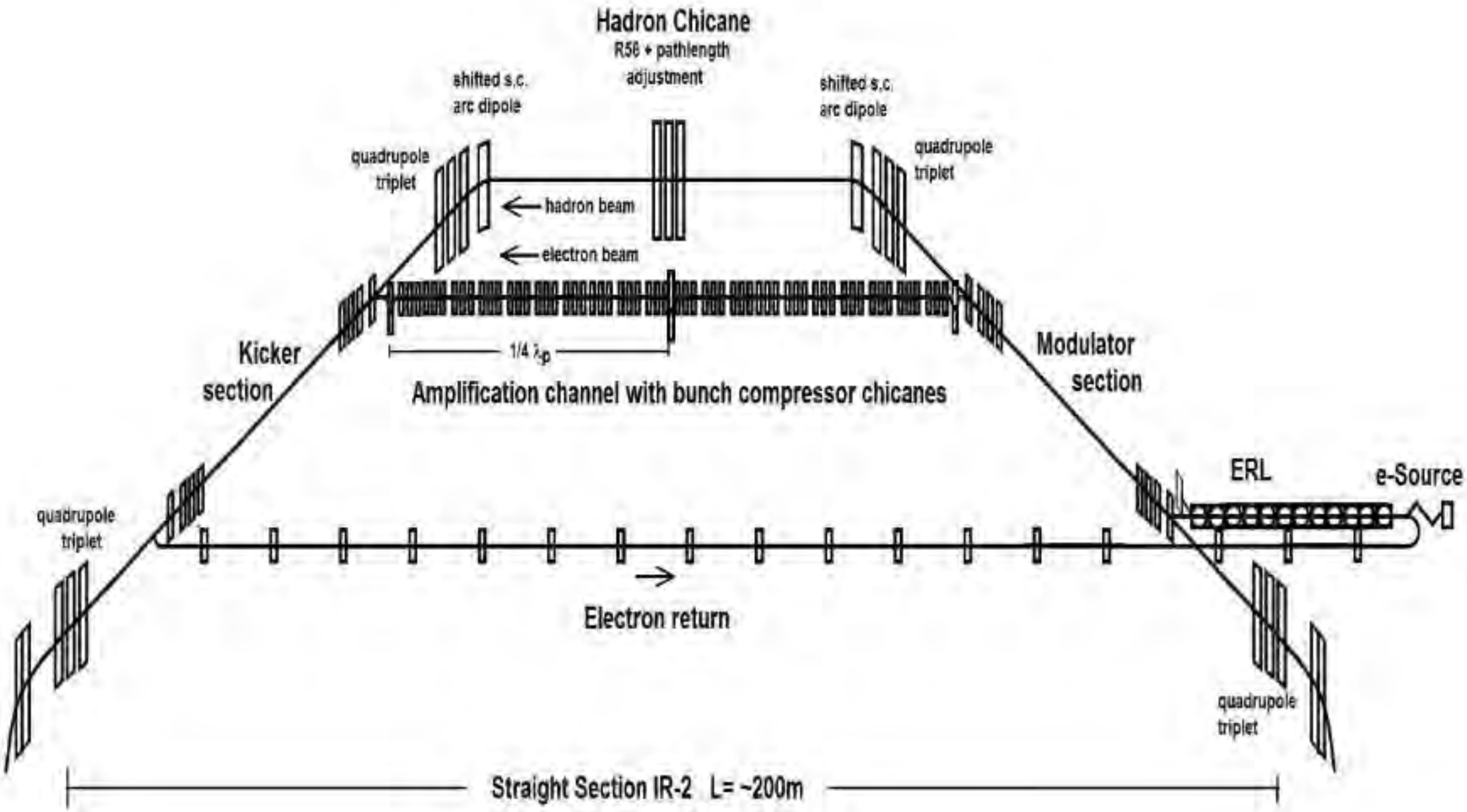

Principle of Coherent Electron Cooling

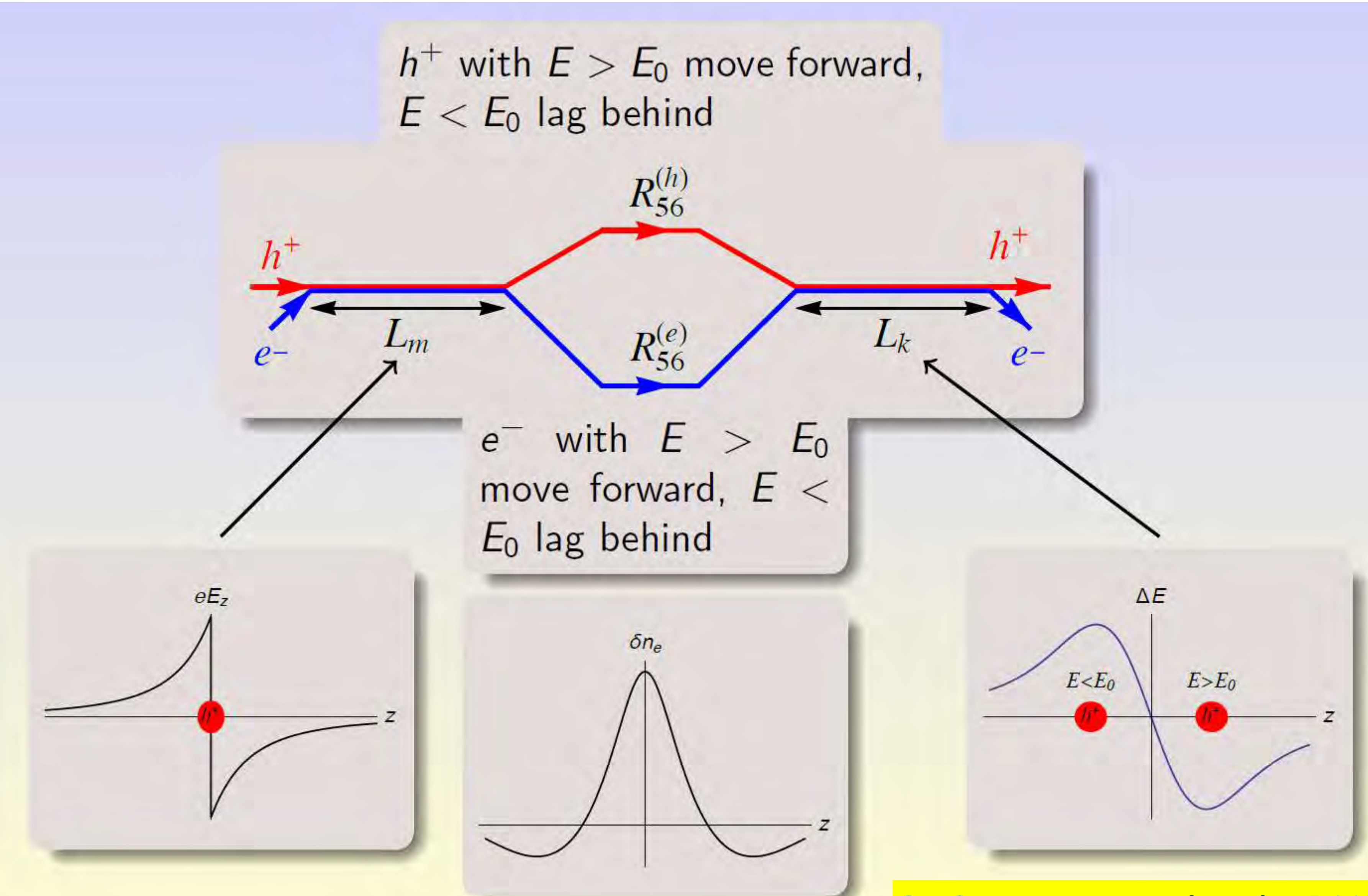

CeC tests ongoing in RHIC

Luminosity Limits

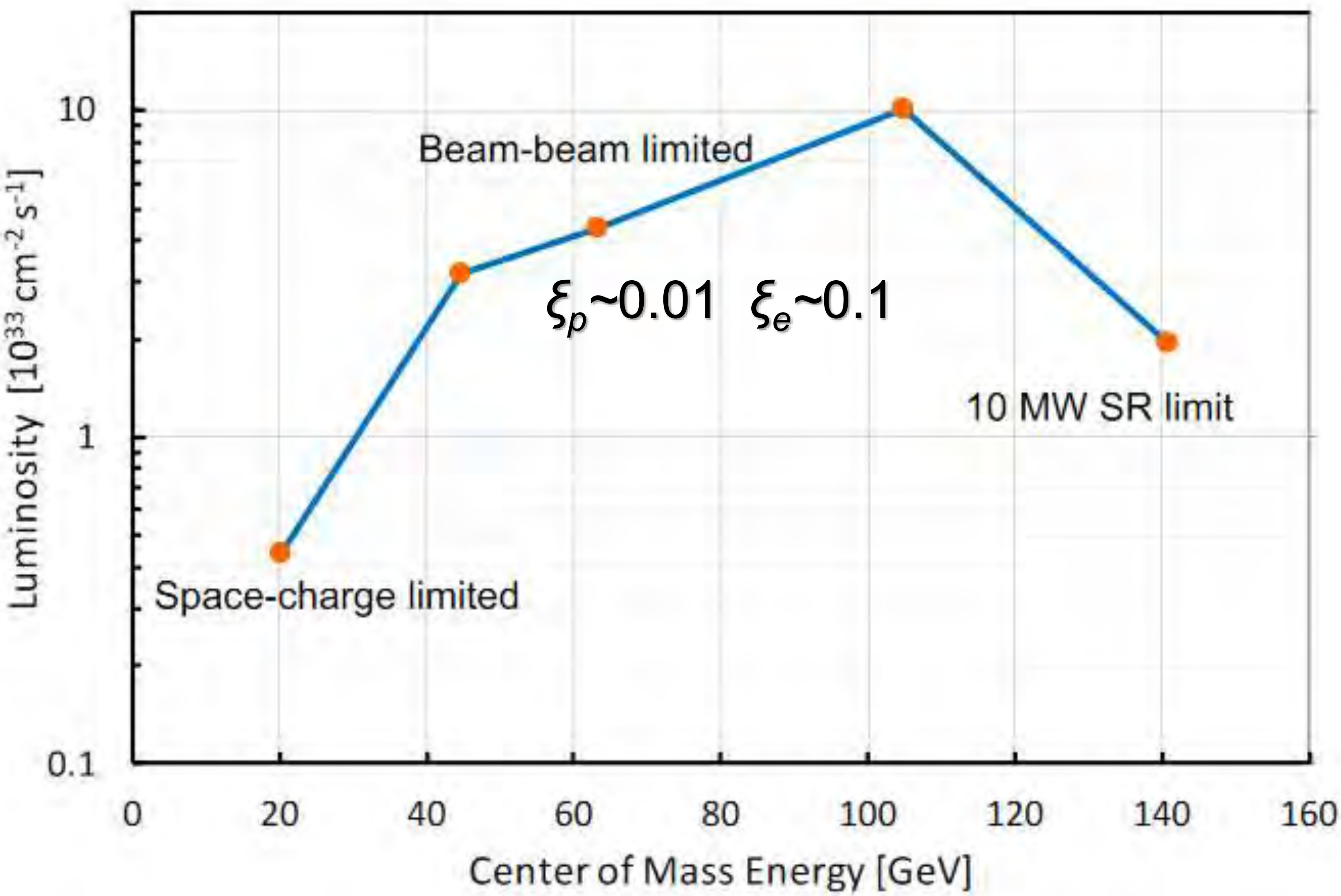

Polarization Challenge : 18 GeV e- RCS

- 85% polarized electrons from a polarized source and a 400 MeV s-band linac get injected into the fast cycling synchrotron in the RHIC tunnel
- Depolarization suppressed by lattice periodicity to E >18 GeV, [Q]=50

intrinsic spin resonances condition $$G\gamma = nP \pm [Q_y]$$

$G = \frac{g-2}{2} = 0.001\ 159\ 65$ is the anomalous gyromagnetic ratio of the electron

- Good orbit control $y_{cl.o.} < 0.05$ mm; good reproducibility suppresses depolarization by imperfection resonances

➔ No depolarizing resonances during acceleration 0.4-18 GeV

no loss of polarization on the entire ramp up to 18 GeV (100 ms ramp time, 2 Hz)

RCS Design

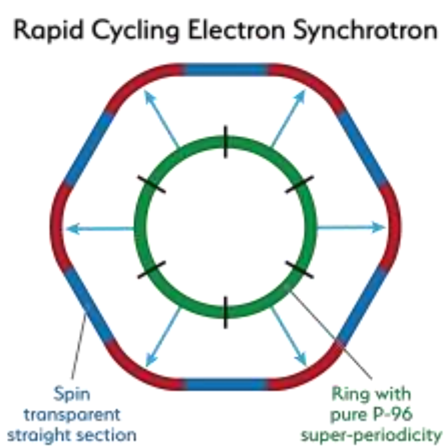

RCS Polarization Performance confirmed by extensive simulations

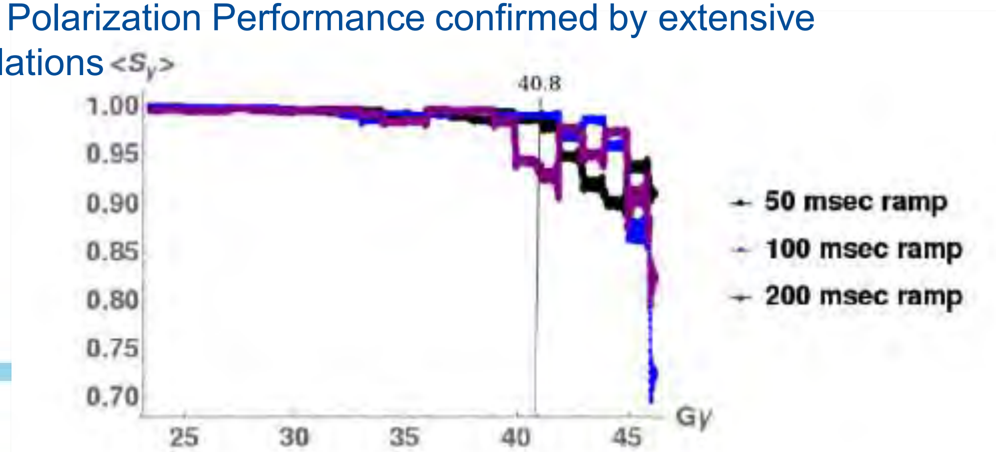

High average polarization in electron storage ring of 80% by

- Frequent injection of bunches on energy with high initial polarization of 85%
- Initial polarization decays towards P_∞ < ~50% (equilibrium of self-polarization and stochastic excitation)
- At 18 GeV, every bunch is refreshed within minutes with RCS cycling rate of 2Hz
- Need both polarization directions present at the same time

B P
Refilled every 1.2 minutes

B P
Refilled every 3.2 minutes

Re-injection

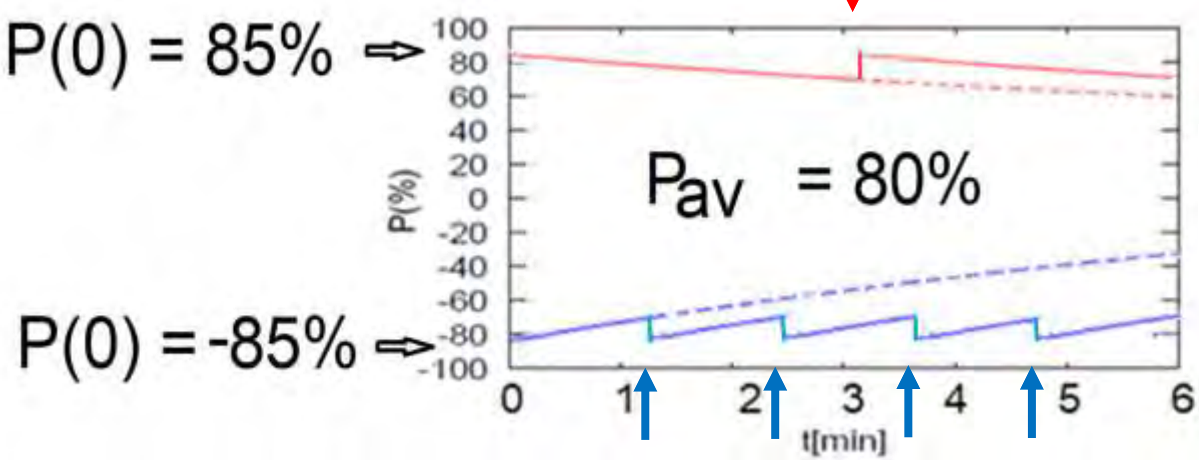

P_∞= 30% (conservative)

Re-injections

Fermilab

EIC Hadron Polarization

- Existing p Polarization in RHIC achieved with “Siberian snakes”
- Near term improvements will increase proton polarization in RHIC from 60% to 80%
- ^{3}He polarization of >80% measured in source
- 80% polarized ^{3}He in EIC will be achieved with six “snakes”,
- Acceleration of polarized Deuterons in EIC 100% spin transparent
- Need tune jumps in the hadron booster synchrotron

Electron beam ion source EBIS with polarized ^{3}He extension

Electron-Proton Collider LHeC

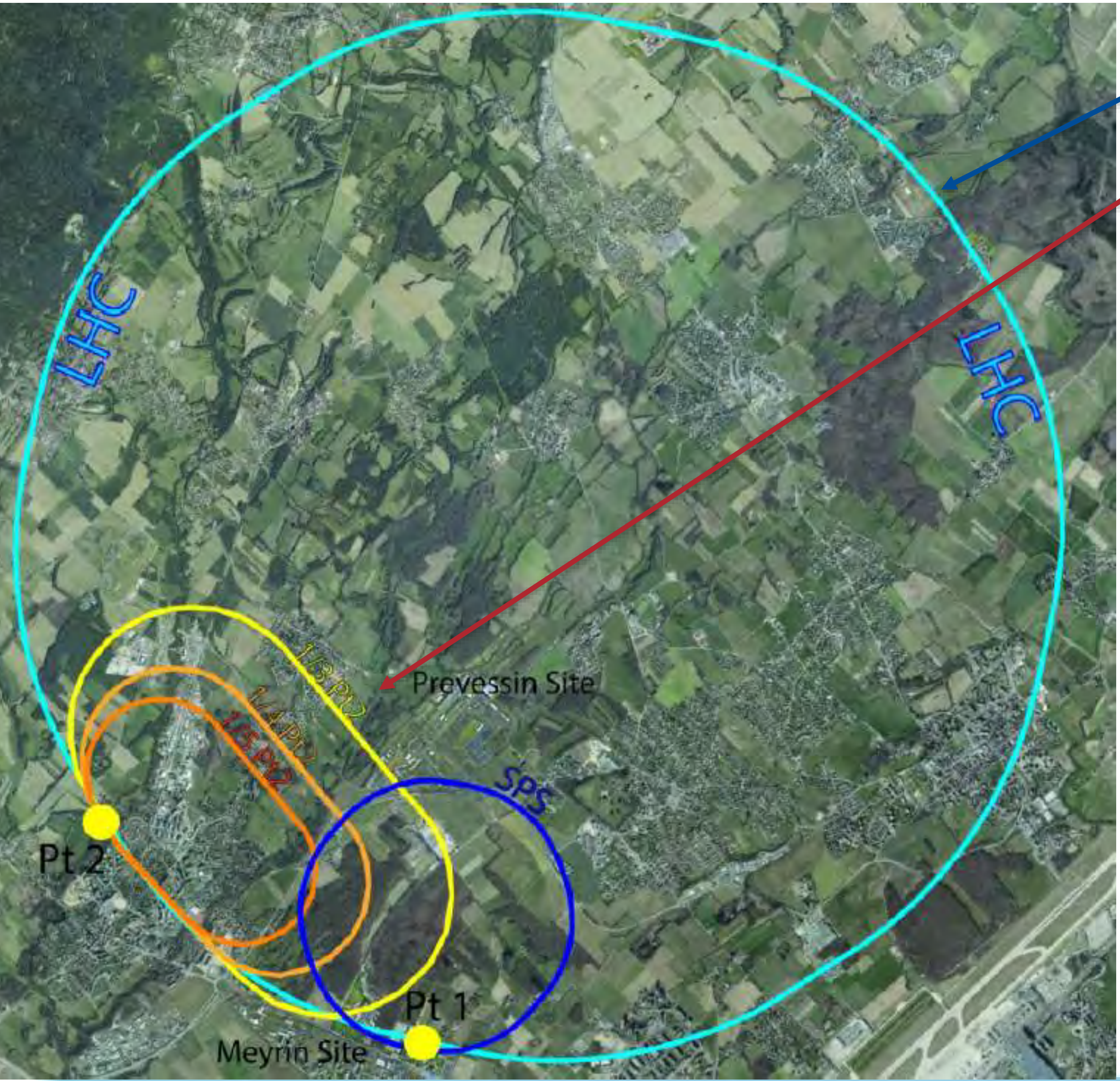

7000 GeV LHC protons

~60 GeV electrons ERL

C=1/3,1/4 or 1/5 LHC

$$E_{cme} \approx 2\sqrt{E_1 E_2}$$

1300 GeV

ERL: Energy Recovery Linac

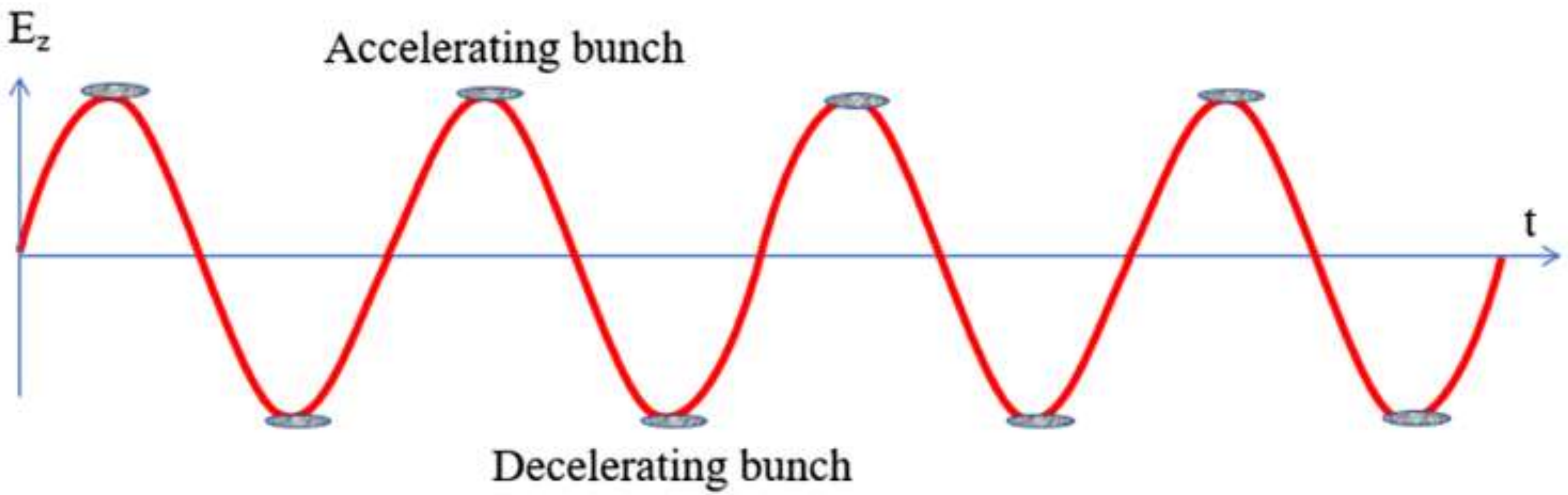

- Basic ERL principle: Accelerating bunches take energy from a srf linac, while decelerating bunches return energy.
- Way to get high current at high energy with lower cost for RF power sources

60 GeV Electron ERL for LHeC

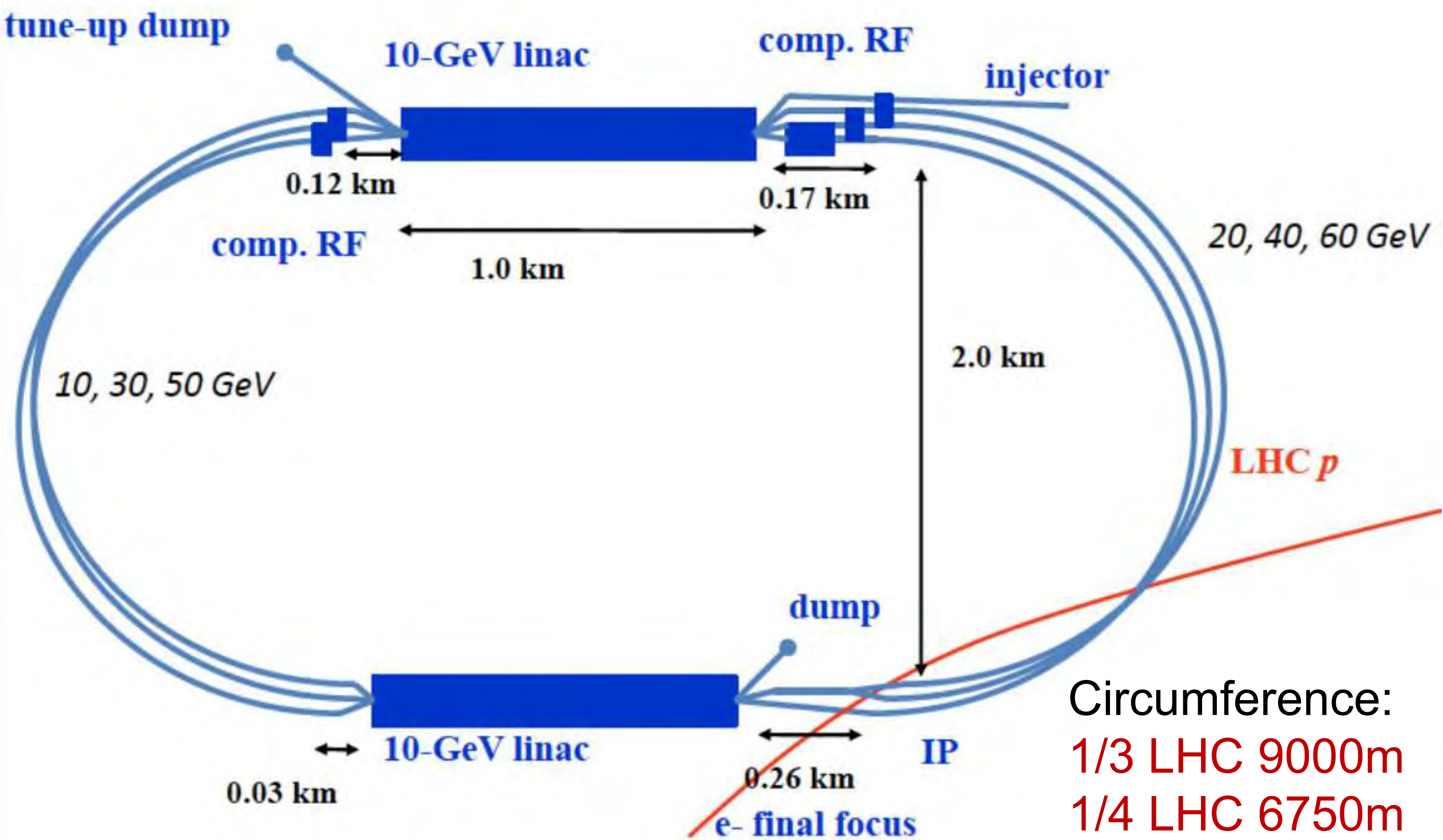

Circumference:
1/3 LHC 9000m
1/4 LHC 6750m
1/5 LHC 5332m

Main Parameters

$$L = \frac{N_e N_p n_p f_{rev} \gamma_p}{4\pi \epsilon_p \beta^*} \cdot \prod_{i=1}^{3} H_i$$

Parameter	Unit	LHeC			
		CDR	Run 5	Run 6	Dedicated
E_e	GeV	60	30	50	50
N_p	10^{11}	1.7	2.2	2.2	2.2
ϵ_p	μm	3.7	2.5	2.5	2.5
I_e	mA	6.4	15	20	50
N_e	10^9	1	2.3	3.1	7.8
β^*	cm	10	10	7	7
Luminosity	10^{33} cm^{-2}s^{-1}	1	5	9	23

With <100 MW facility power, L ~1e34

Major challenge high average current 20-50 mA: $I_e = eN_e f$

f=40 MHz, *eN*=0.5nC

PERLE (Orsay) ERL Demo Facility

- 20mA current goal, 3 turns and a 500MeV beam = ERL facility in the 10MW power range

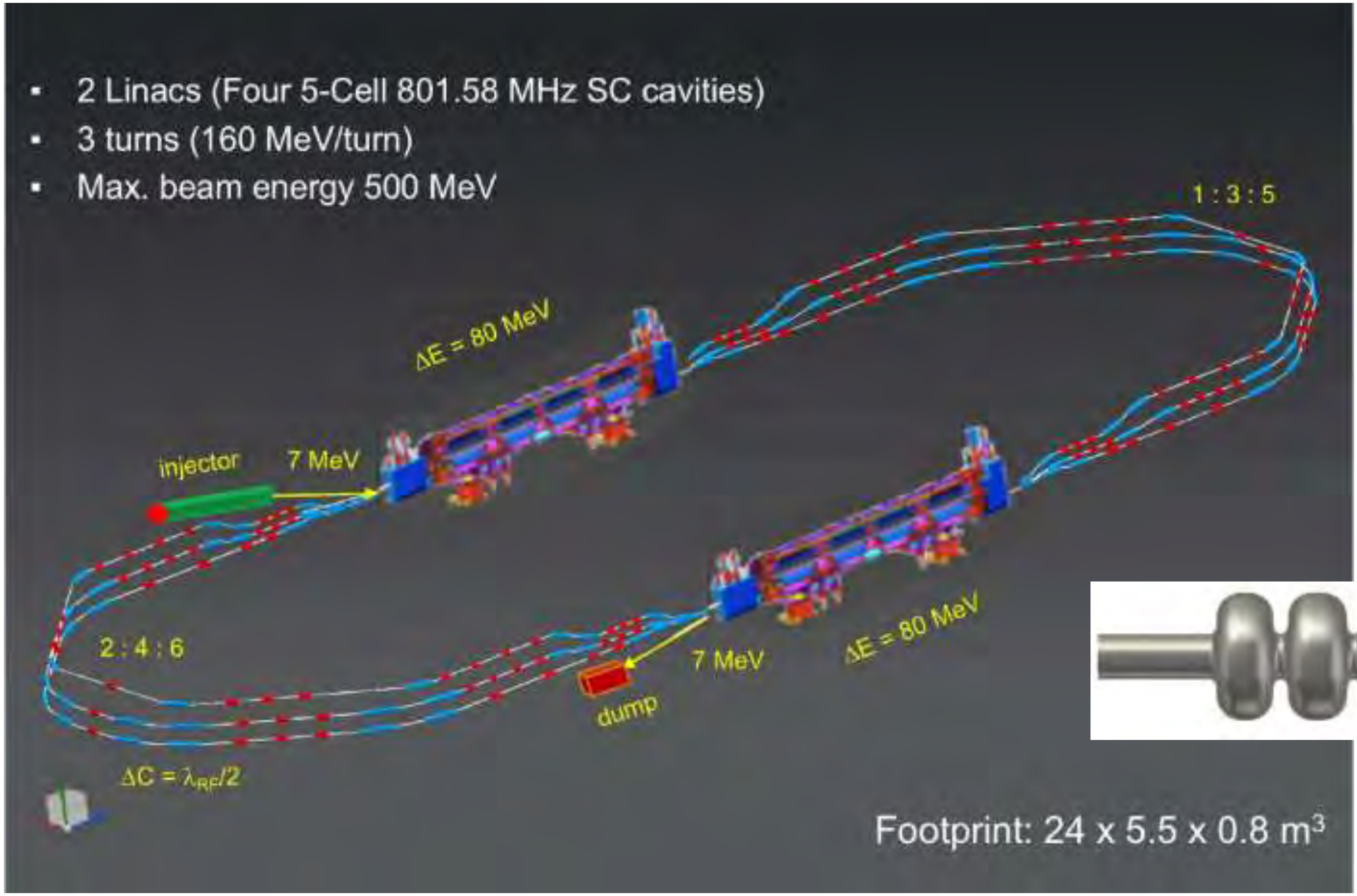

SRF
802 MHz
18 MV/m

<50kW
RF/cavity

PERLE (and any ERL) challenges are collective effects, such as space charge, the multipass beam breakup (BBU) instability, coherent synchrotron radiation (CSR) and the microbunching instability (BI), beam dynamic issues such as halo, the interaction of the beam with the RF system and other environmental impedances.

PERLE 802 MHz RF and Bunches

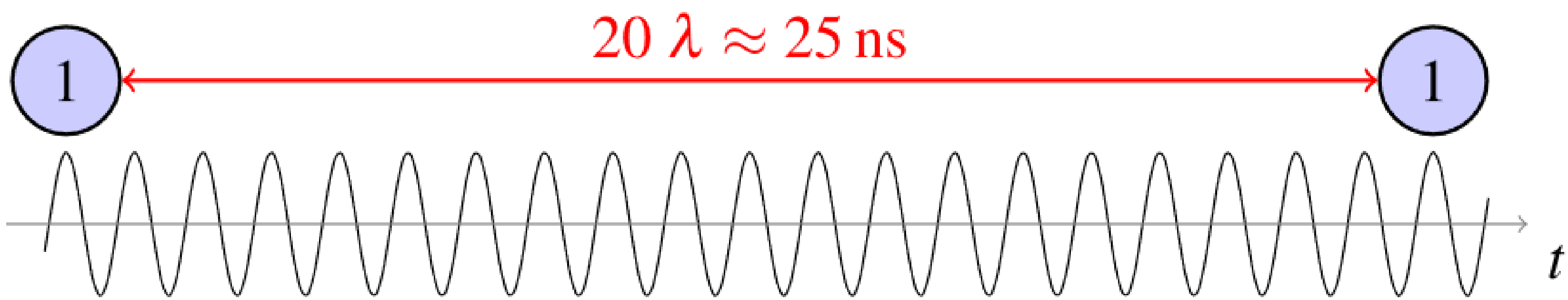

Basic RF structure, without recirculation. Bunches are injected every 25 ns. The waves indicate the RF electromagnetic oscillations.

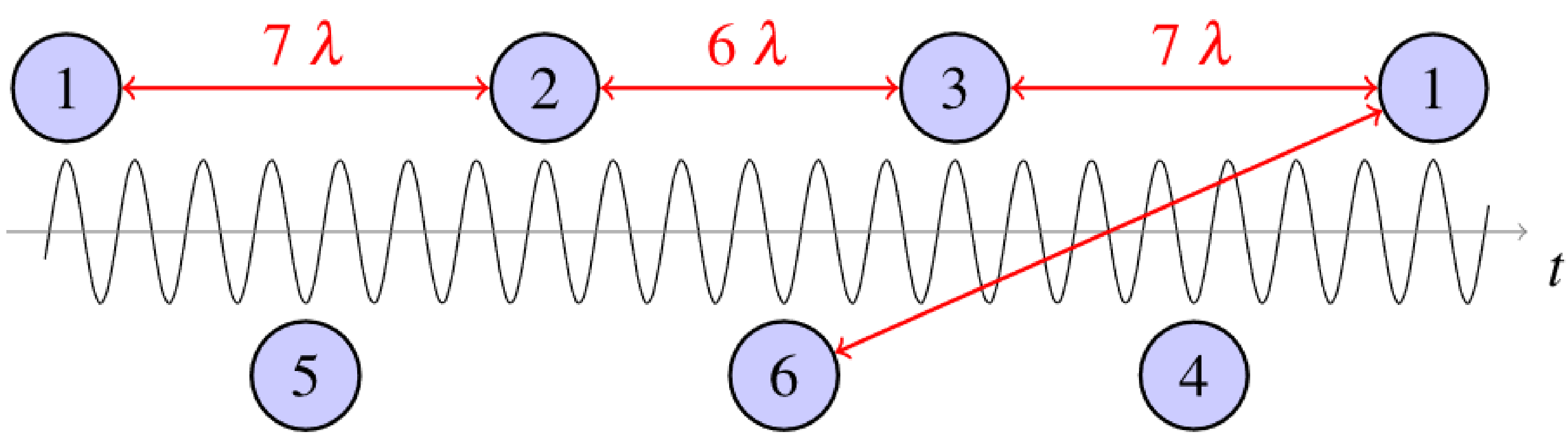

When the recirculation is in place, the linacs are populated with bunches at different turns（the turn number is indicated.

Impedance spectrum for the longitudinal modes

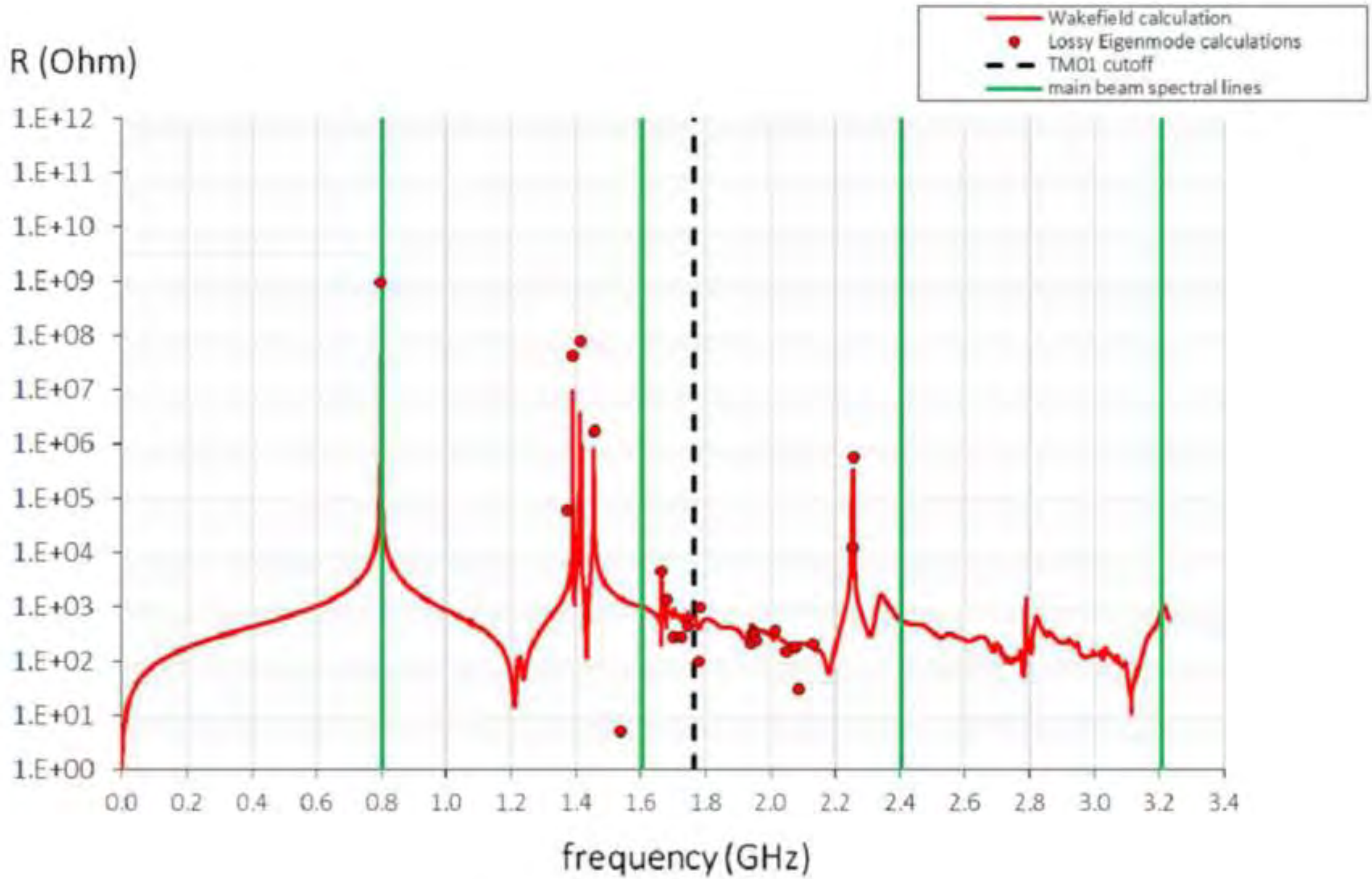

Impedance spectrum for the transverse modes

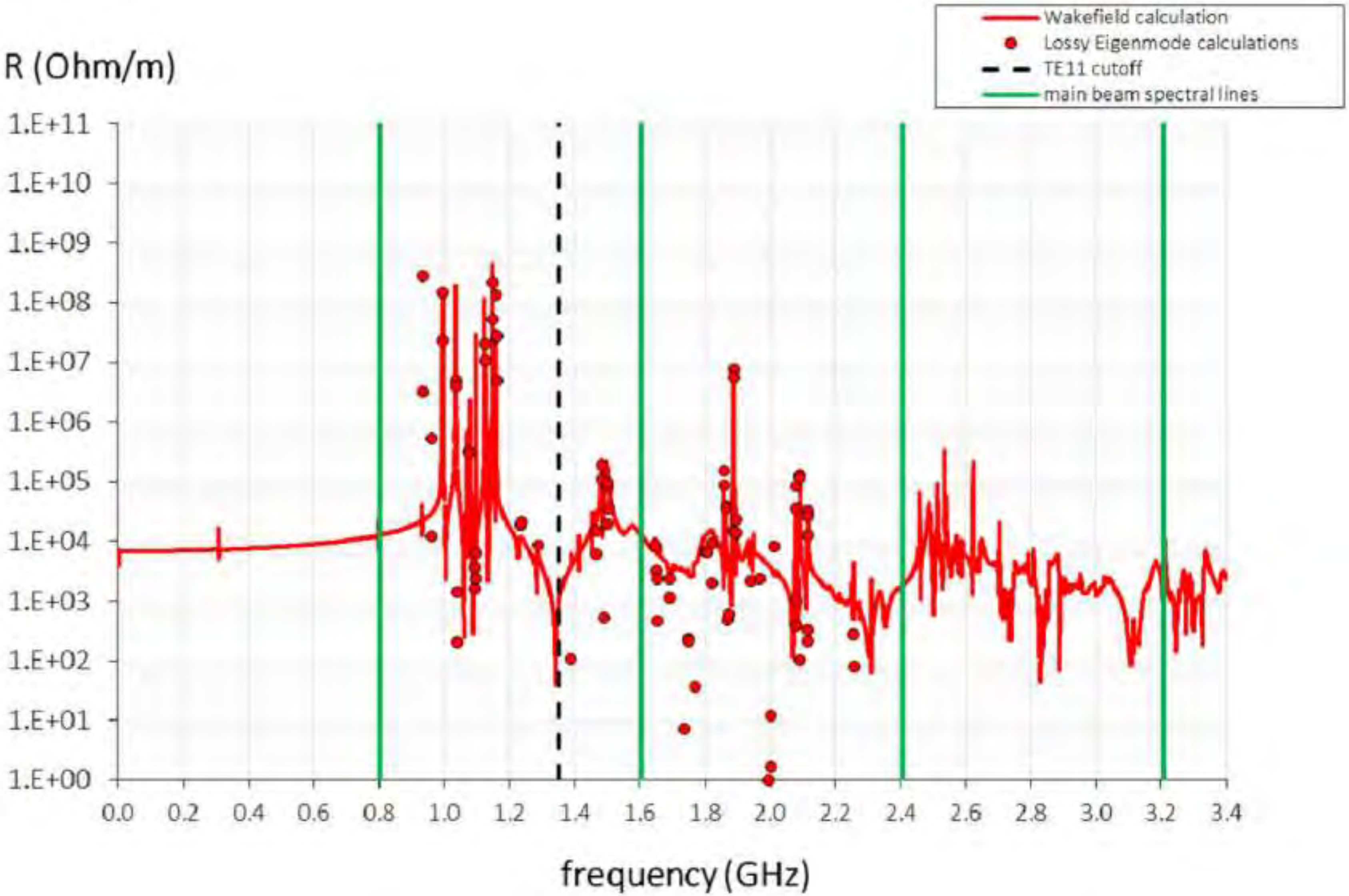

ERL landscape – Beam Power Scales

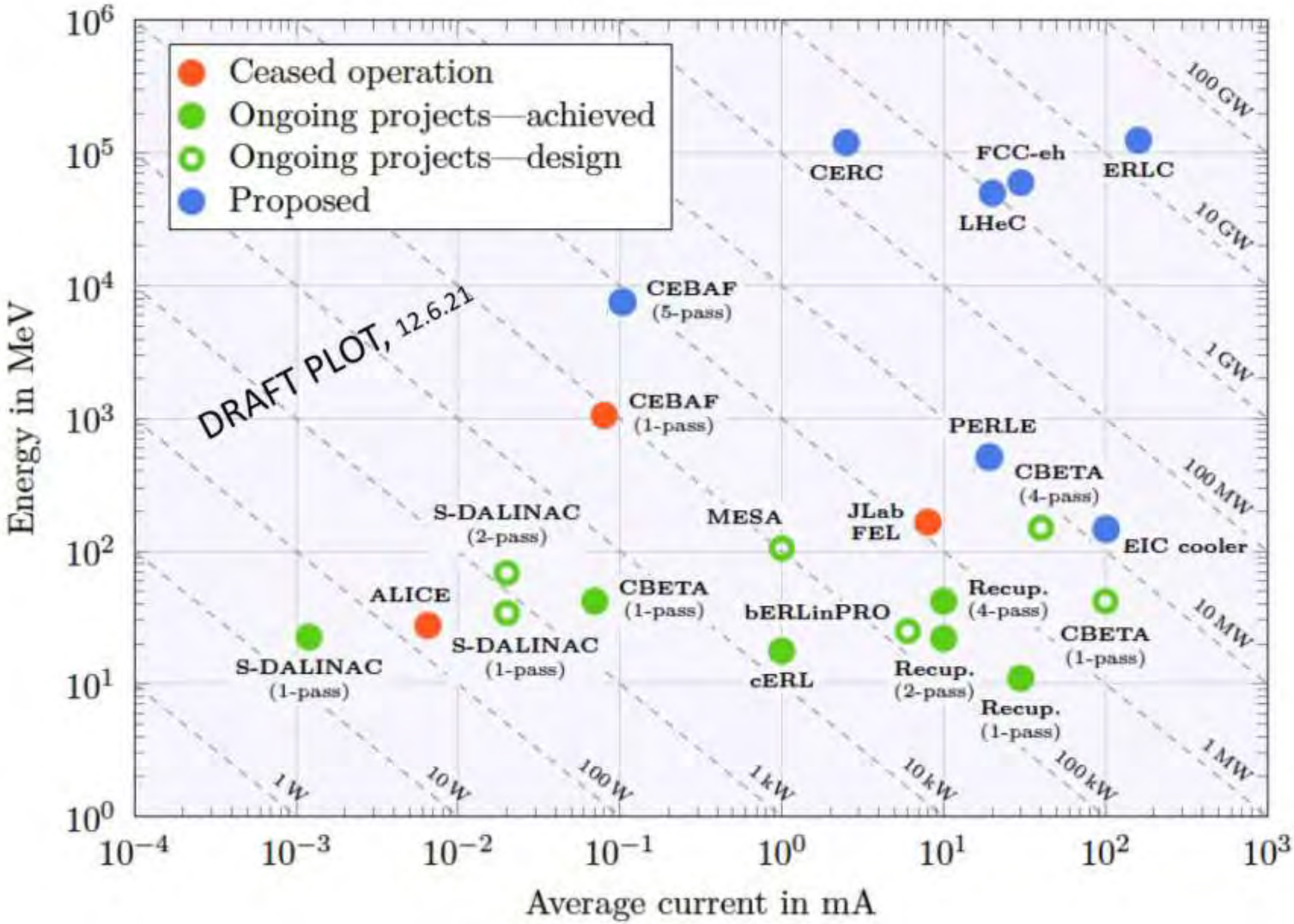

Other EIC Beam Dynamics Challenges

- Proton beam stability (emittance growth, halo forming) in presence of strong, crab-enhanced beam-beam effects, strong chromatics
- Electron cloud in the hadron vacuum (x10 bunches) , suppression of secondary emission yield
- Fast Ion instability for the electron beam
- Multi-bunch stability and feedback: Feedback noise and hadron emittance growth
- Impedance optimization in the IR ($I_{\text{threshold}} \sim 1/\beta$)
- Dynamic aperture with extreme beta in the IR

Fermilab

Energy Frontier *pp* Colliders

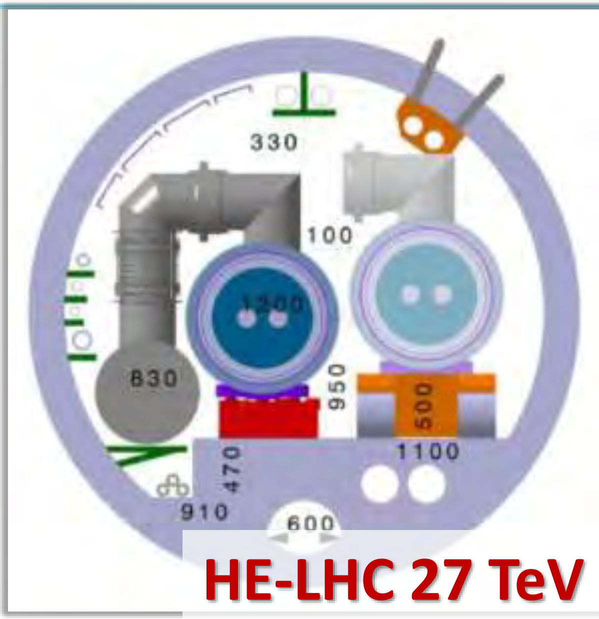

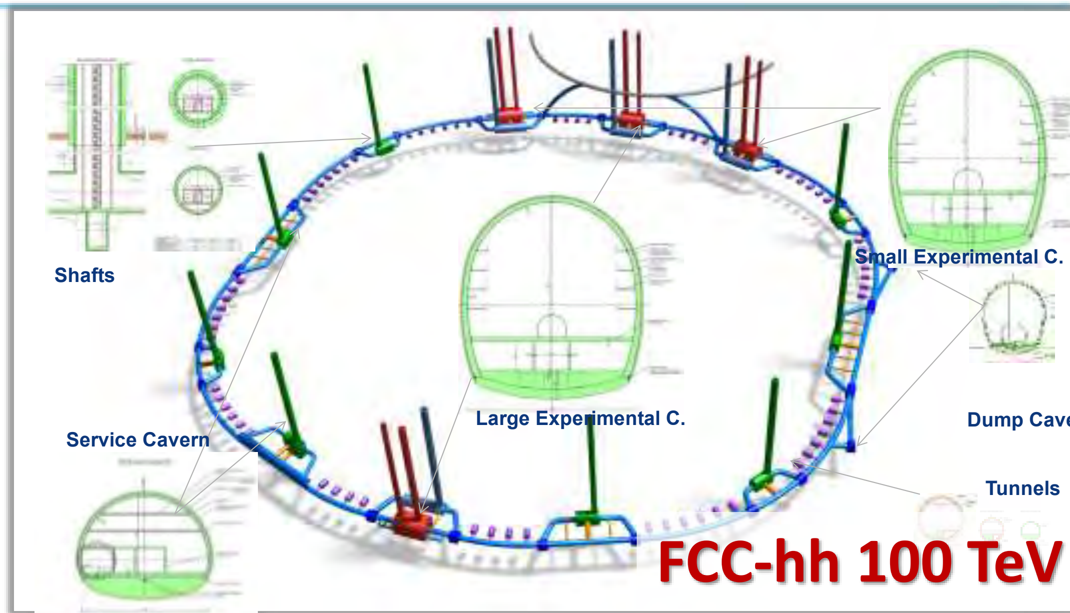

Key facts: *HE-LHC / FCC-hh* / SppC**

Large tunnel – 27 / 100 / 100 km

SC magnets – 16 / 16 / 12 T

High Lumi / pileup $O(10^{35})$ / $O(500)$

Site power (MW) – 200 / 500? / ?

Cost (BCHF) – 7.2 / 17.1 / ?

** follow up after e+e- Higgs factories*

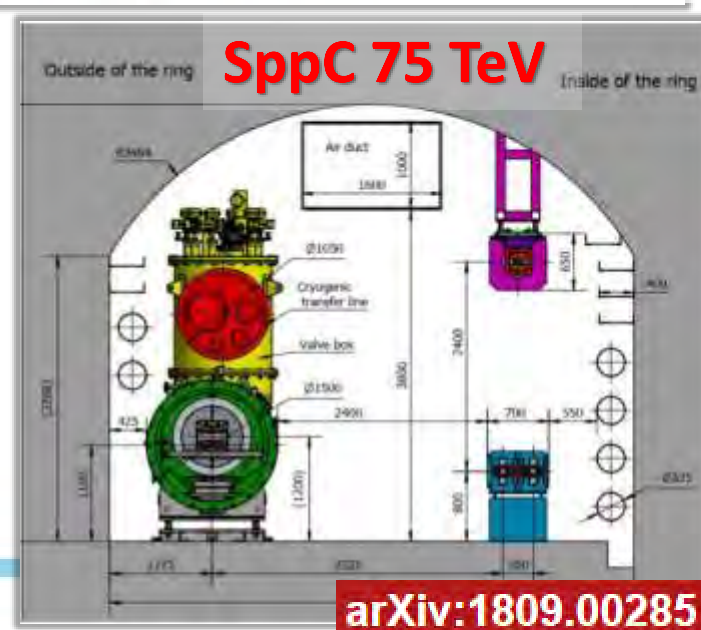

Future pp Colliders: Parameters and Problems (1)

parameter	FCC-hh		SppC	HL-LHC	LHC
collision energy cms [TeV]	100		75	14	14
dipole field [T]	16		12	8.33	8.33
circumference [km]	97.75		100	26.7	26.7
beam current [A]	0.5		0.73	1.1	0.58
bunch intensity [10^{11}]	1	1	1.5	2.2	1.15
bunch spacing [ns]	25	25	25	25	25
synchr. rad. power / ring [kW]	2400		1100	7.3	3.6
SR power / length [W/m/ap.]	28.4		12.8	0.33	0.17
long. emit. damping time [h]	0.54		1.17	12.9	12.9
beta* [m]	1.1	0.3	0.75	0.15 (min.)	0.55
normalized emittance [µm]	2.2		2.4	2.5	3.75
peak luminosity [10^{34} cm^{-2}s^{-1}]	5	30	10	5 (lev.)	1
events/bunch crossing	170	1000	~300	132	27
stored energy/beam [GJ]	8.4		9.1	0.7	0.36

Two Groups: IHEP-CAS and CERN

$$E[GeV] = 0.3 \times B[T] \times \rho[m]$$

High Energy Circular Colliders for next decades	**SPPC** 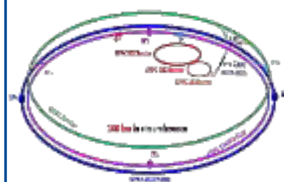 	**FCC** 
Proposed institution	IHEP-CAS, China	CERN, Europe
Proposed dates	2012	2013
Site of the project	China	Europe
Baseline technology	IBS 12~24 T to reach 75-150 TeV, Nb_3Sn etc as options	Nb_3Sn 16 T to reach 100 TeV
Timeline	Construction at 2040s	Construction at 2050-60s
Cost	*	**

Reminder from Lecrture 1: Key is Current *Density*

Scaling:

$$B_{max} \sim J/Aperture$$

Assume all aperture *A* is filled with conductor → max current is

$$J \sim j(current\ density) \cdot A\hat{}2$$

thus :

$$\boxed{B_{max} \sim j \cdot A}$$

but **Cost** *~A/j* (=*A*^2· ***length*** = cost of needed conductor)

Therefore, high(est) current density is needed to maximize *B*-field and minimize *Cost*

- For room temperature copper *j*~(1-10) A/mm^2
- For superconductors → kA/mm^2

Superconductors Current Densities *j(B, T)*

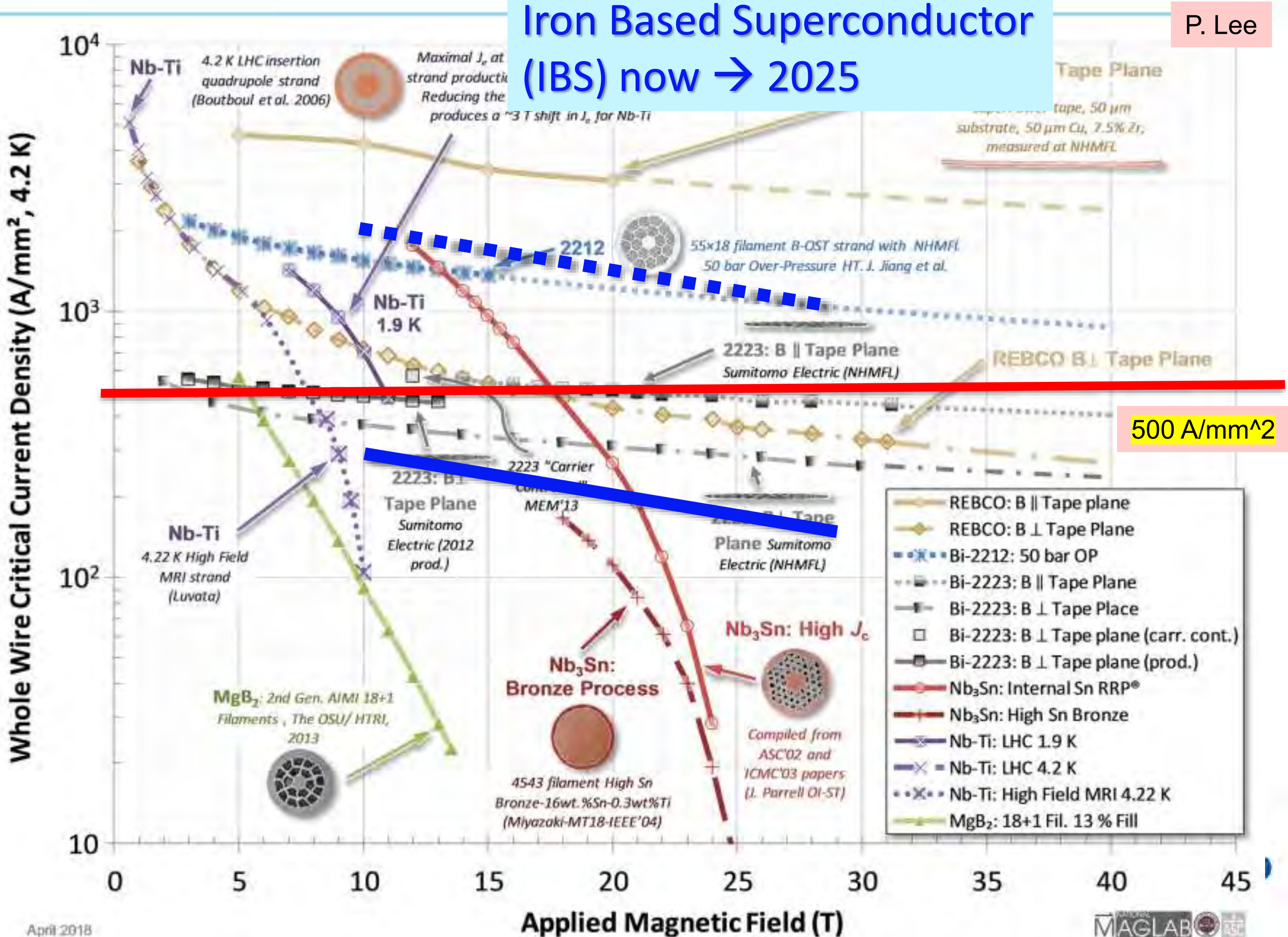

April 2018

Low Temperature Superconductors (LTS)

- Nb-Ti @ 1.8K
  - Plenty of experience
  - May be able to increase practical field a little
  - Large industrial capacity

~10 T

- High Performance Nb_3Sn
  - Fields up to 16T in dipole configuration, but challenging
  - Strain sensitive
  - No significant industrial capacity
  - Not inexpensive

~16 T

But is that a "practical" limit?

- Iron-Based Superconductor (IBS)
  - High field, low cost, better mechanical properties
  - Successful conductor could lead to commercial demand

High risk, high potential payoff
Still much work to be done

Nb3Sn Conductor R&D for FCChh

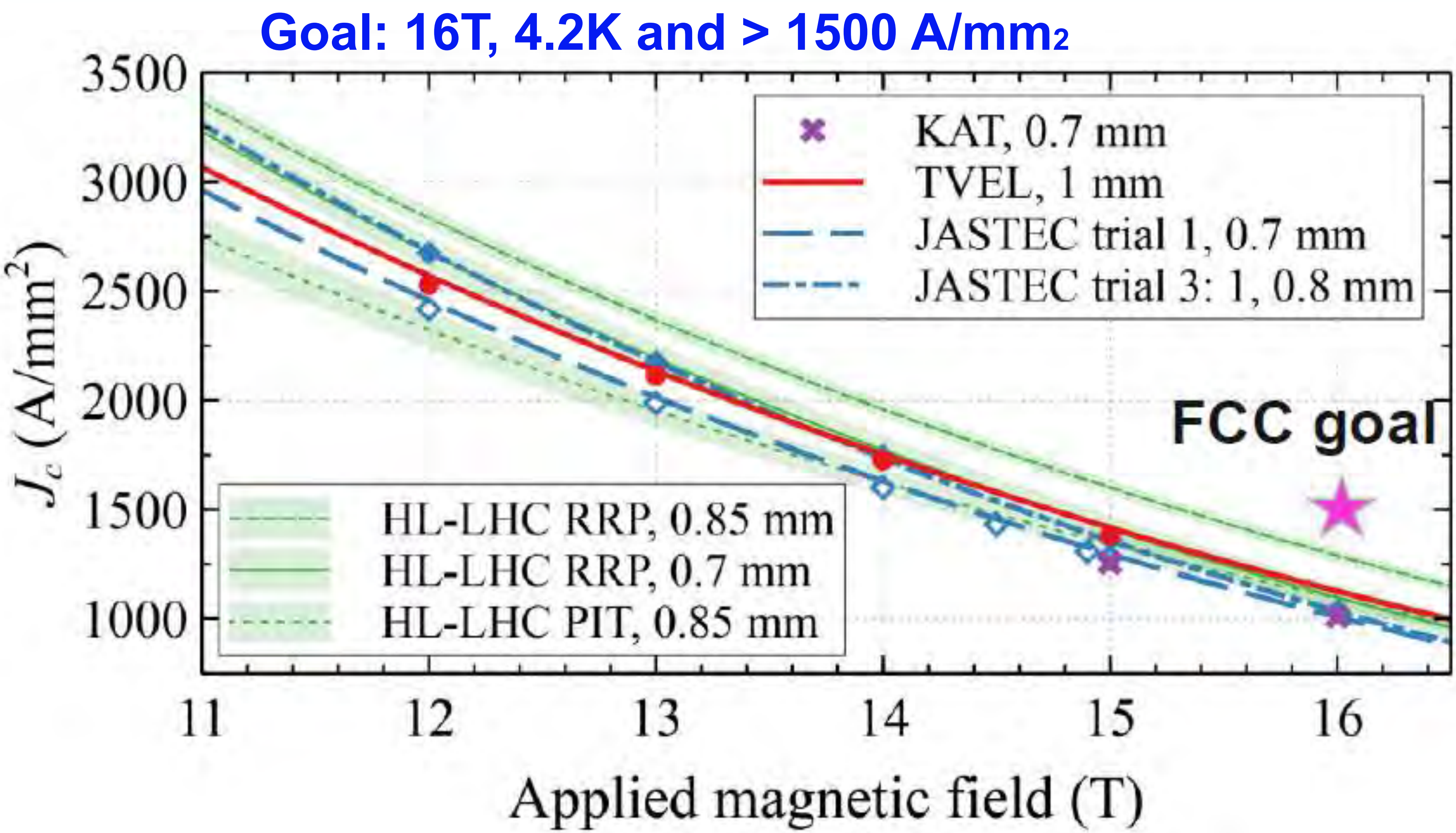

Challenges and lessons of Nb_3Sn (Hint, it's stress!!)

- MDP 15T project
  - MDPCT achieved 14.5 T at 1.9K
  - Degradation on subsequent thermal cycle

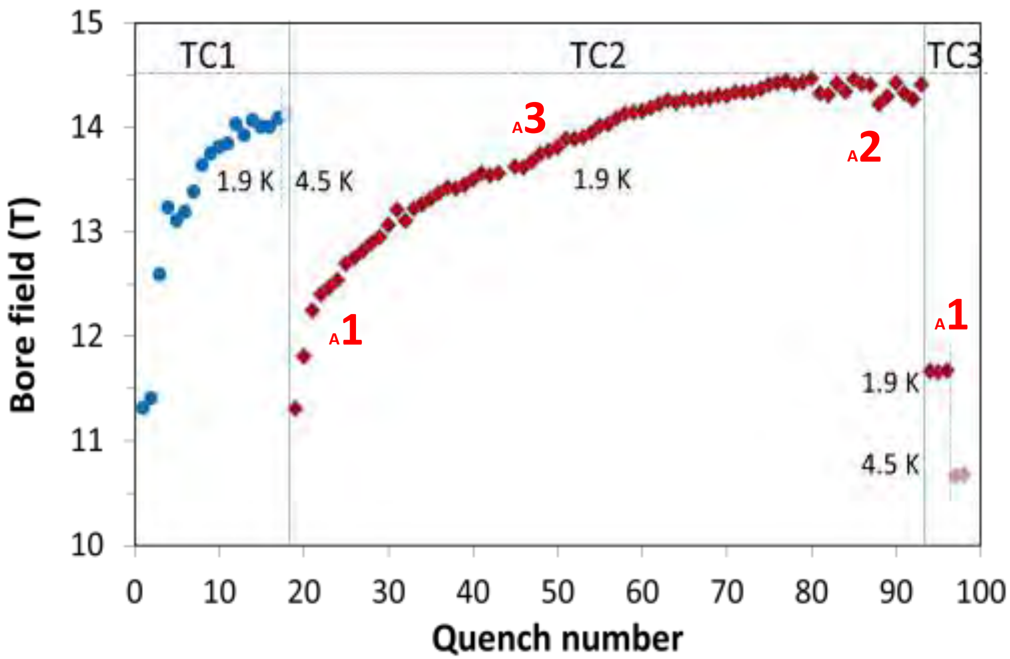

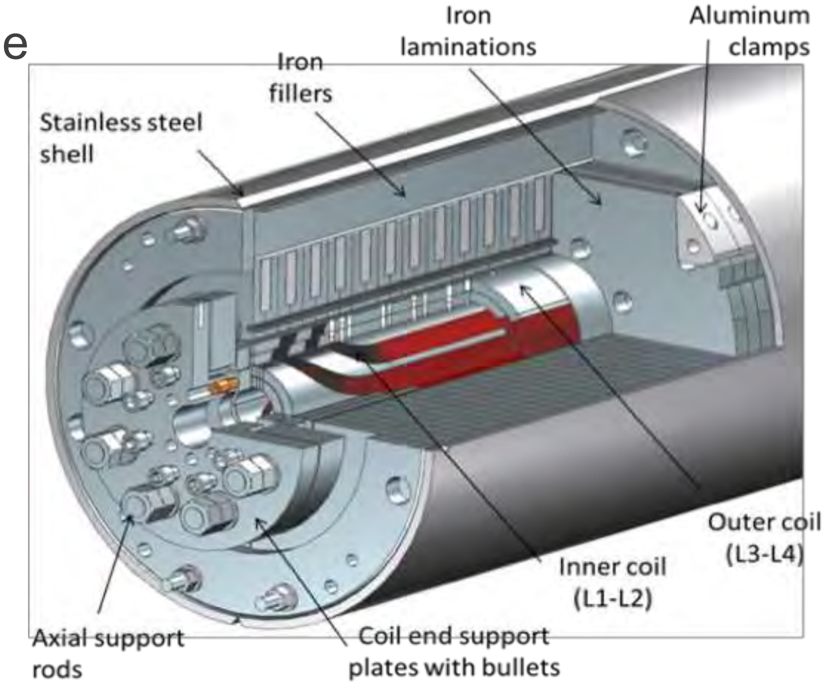

Courtesy, A. Zlobin, FNAL

On Mechanical Stress Limit

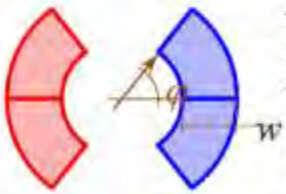

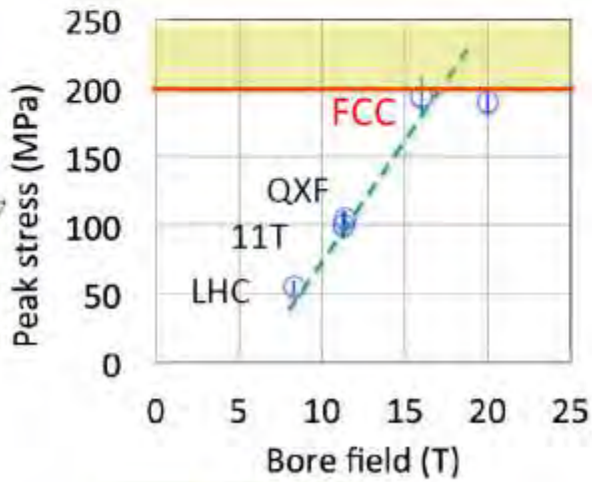

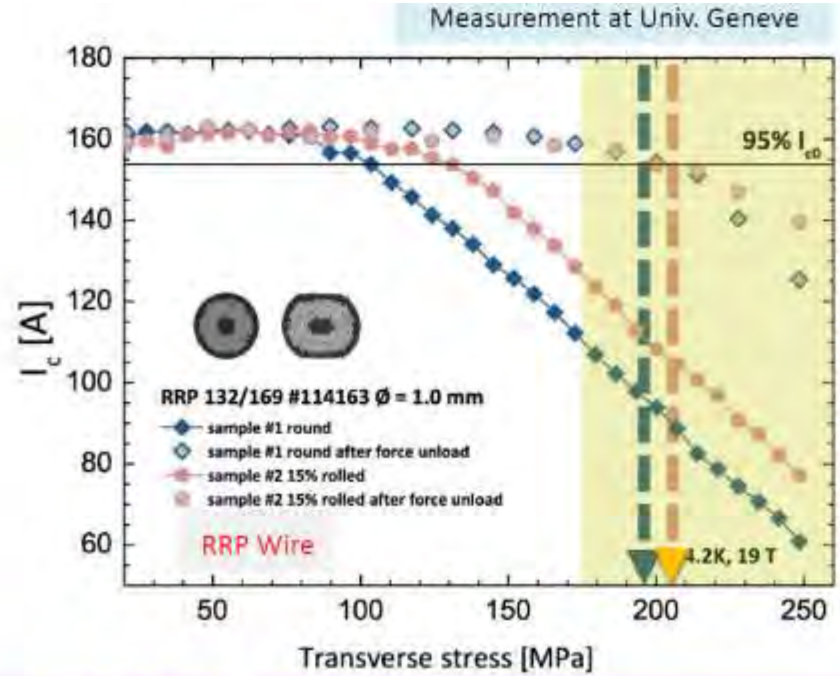

$$\left.\begin{array}{l} F \propto B^2 \\ w \propto \dfrac{B}{J} \end{array}\right\} \rightarrow \sigma \cup \frac{F}{w} \propto JB$$

or

$$p \sim B^2$$

Attention, I_c (J_c) reduction:

- reversible at <150 MPa (~15% at 11.6 T),
- irreversible at >170 MPa.

as a critical constraint because of fundamental mechanical property.

Fermilab

Several Design Approaches: FCChh

Worldwide short model magnet R&D →various coil geometries (2018 –2025)

Cos-theta

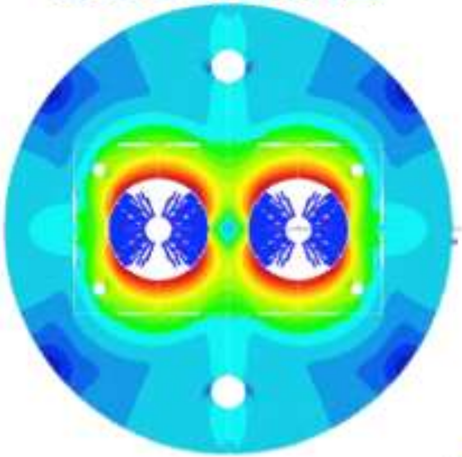

Common coils

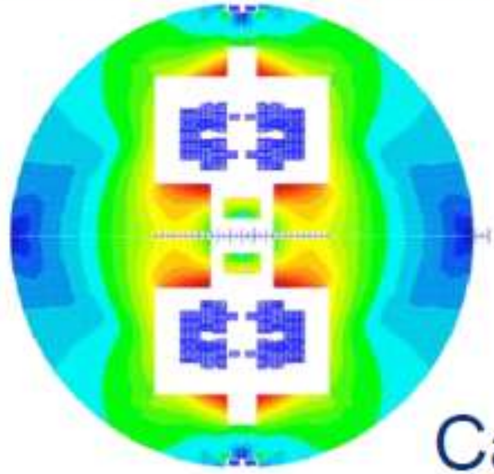

Blocks

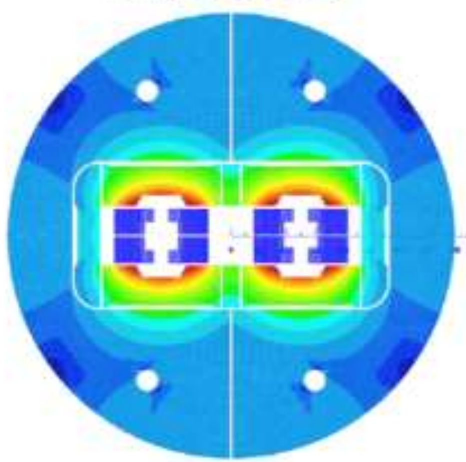

Canted Cos-theta

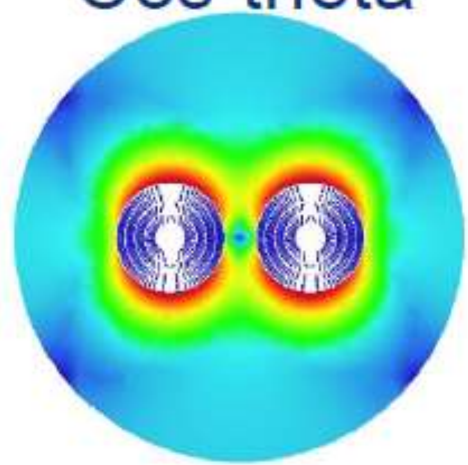

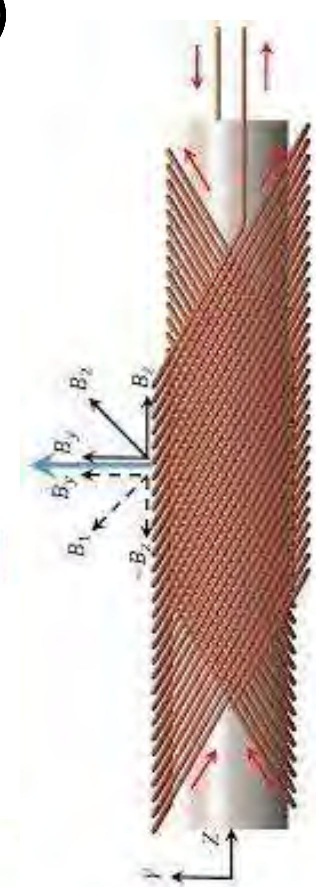

CEA, CIEMAT, INFN, PSI, FNAL, LBNL, BINP

Cost (probably most important)

- Cost of the magnets ~50% or more of the total collider cost (~30B$)
- Three approx. equal components:
- Cost of conductor
- Cost of labor
- Cost of structure

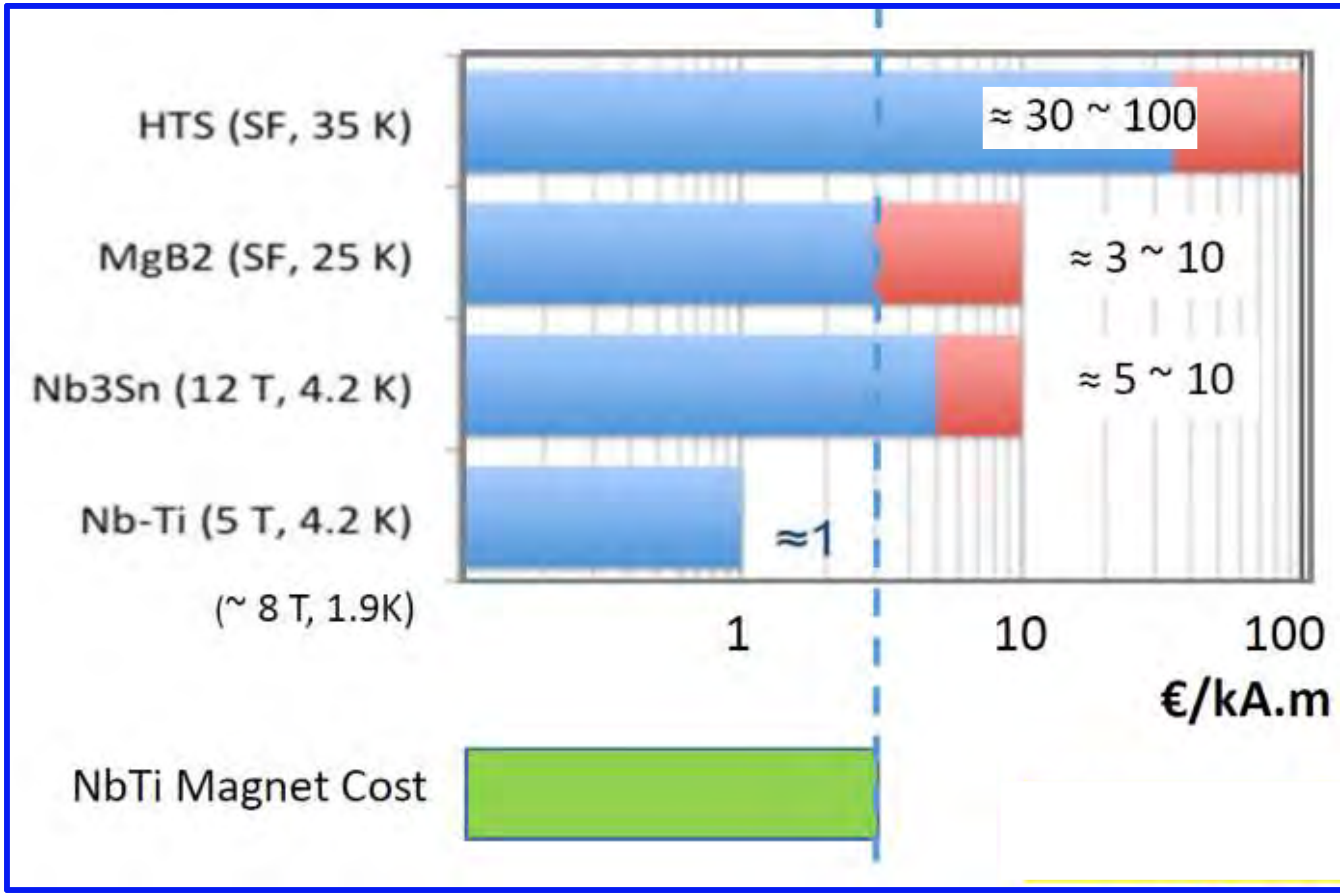

(Rough) cost of conductor per kA·m **IBS : NbTi : Nb3Sn : HTS**

now 0.25(?) : 1 : 5 : 30

Fermilab

IBS Magnet R&D in China

The 12-T Fe-based Dipole Magnet

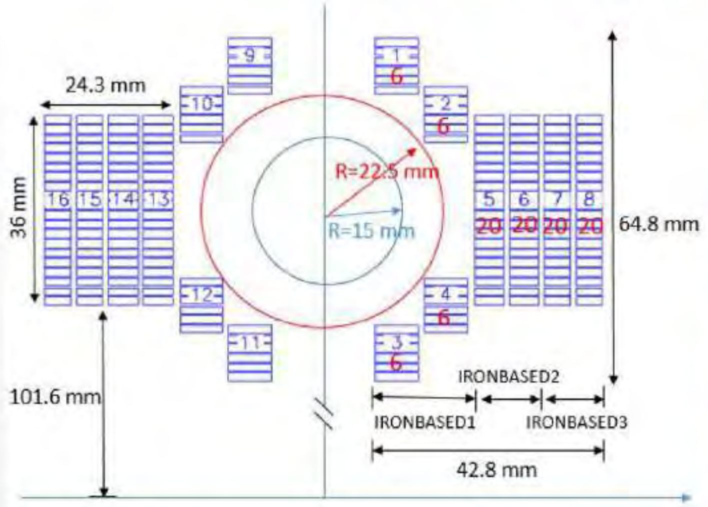

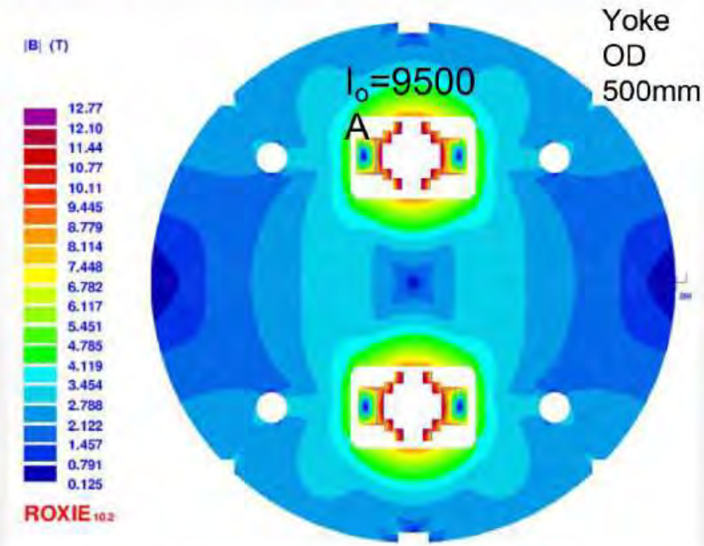

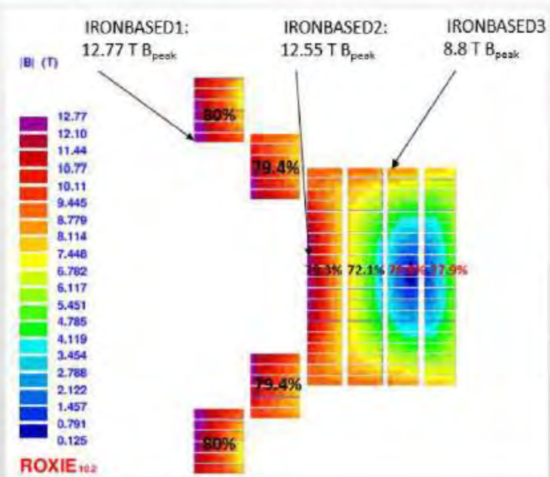

Design with expected J_e of IBS in 2025

Strand	diam.	cu/sc	RRR	Tref	Bref	Jc@ BrTr	dJc/dB
IBS	0.802	1	200	4.2	10	4000	111

- For 100-km SPPC, **3000 tons of IBS** is needed
- Target cost of IBS: **20 RMB /kAm @12 T**
- Total cost for IBS conductors: **~10B RMB**

Future pp Colliders: Parameters and Problems (2)

parameter	FCC-hh		SppC	HL-LHC	LHC
collision energy cms [TeV]	100		75	14	14
dipole field [T]	16		12	8.33	8.33
circumference [km]	97.75		100	26.7	26.7
beam current [A]	0.5		0.73	1.1	0.58
bunch intensity [10^{11}]	1	1	1.5	2.2	1.15
bunch spacing [ns]	25	25	25	25	25
synchr. rad. power / ring [kW]	2400		1100	7.3	3.6
SR power / length [W/m/ap.]	28.4		12.8	0.33	0.17
long. emit. damping time [h]	0.54		1.17	12.9	12.9
beta* [m]	1.1	0.3	0.75	0.15 (min.)	0.55
normalized emittance [μm]	2.2		2.4	2.5	3.75
peak luminosity [10^{34} $cm^{-2}s^{-1}$]	5	30	10	5 (lev.)	1
events/bunch crossing	170	1000	~300	132	27
stored energy/beam [GJ]	8.4		9.1	0.7	0.36

Synchrotron Radiation of Protons

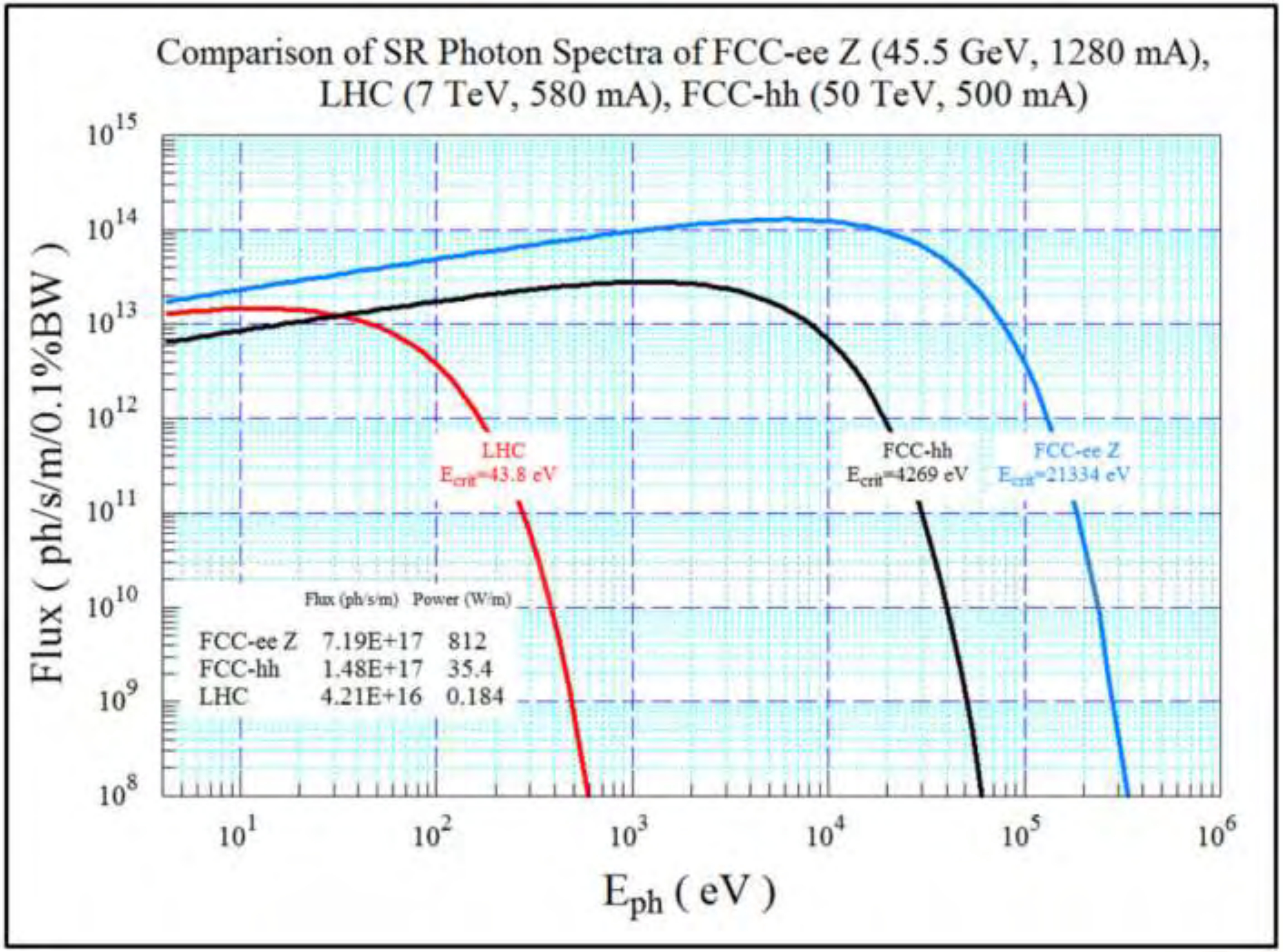

Intercept 5MW of SR

- While the linear photon flux for FCC-hh is only a factor of 3.5 times higher than that of LHC, the linear SR power density at 50 TeV is almost 200 times higher, ruling out a scaled version of the LHC beam-screen.
- Calculations have ruled out the possibility of using LHC-sized capillaries (<4 mm) because the supercritical helium flow rate would not be sufficient. The required number of pumping slots would also affect the impedance budget too much .

- **New type of beam pipe:**
  - Low impedance
  - Good pumping conductivity
  - Intercept SR photons at 50K
  - Avoid build up of e-cloud

  (a-C coating or LASE grooves)
  - Low th-conductivity 50K→2K

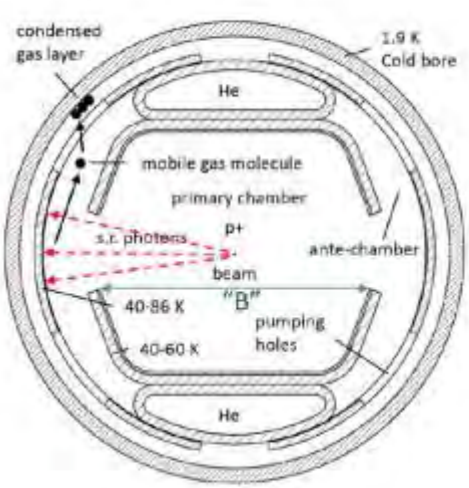

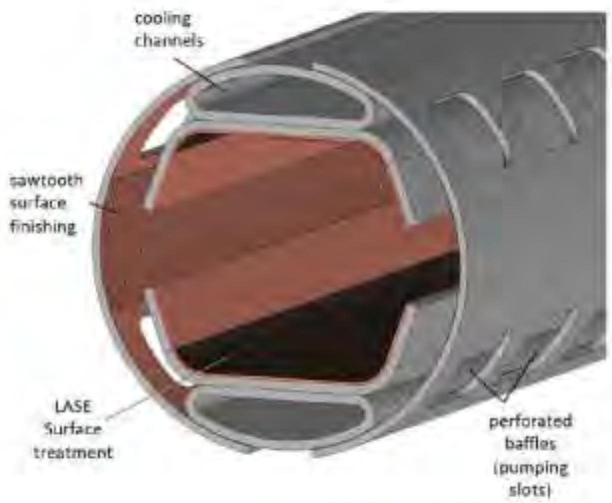

FCChh: 47 mm OD

Synchrotron Radiation of Protons

Overall optimization of cryo-power, vacuum and impedance. Contributions: beam screen (BS) & cold bore (BS heat radiation). Vacuum pumping prefers higher T. Optimum 50-100 K but impedances grow with T → so, 50 K

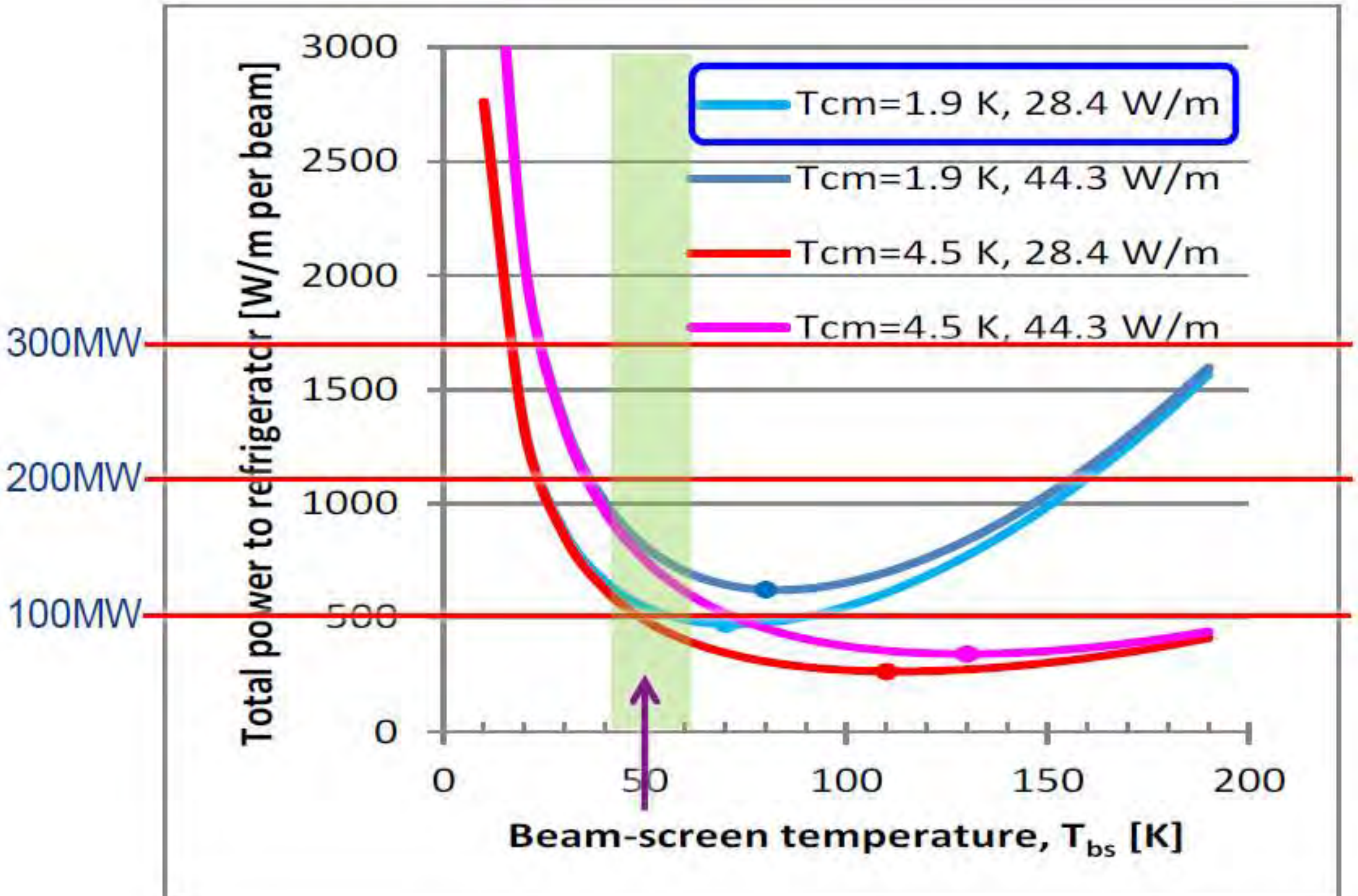

Fermilab

Possible New Phenomena : beam Screen nano-vibrations

In dipoles the (small) magnetic permeability of the beam-screen induces small field imperfections that are linked with shape.

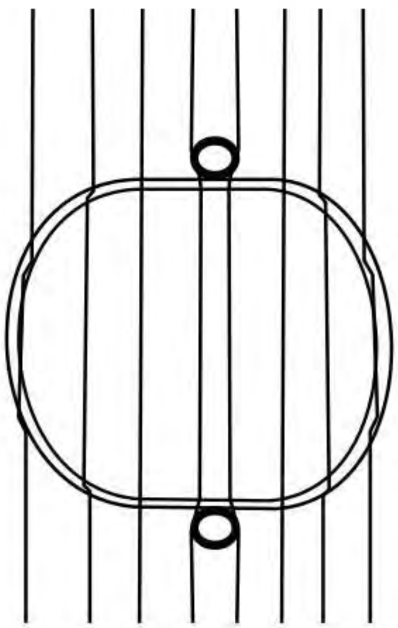

In quadrupoles: fields are in beam-screen apertures follow the beam screen position from a certain frequency ([1])

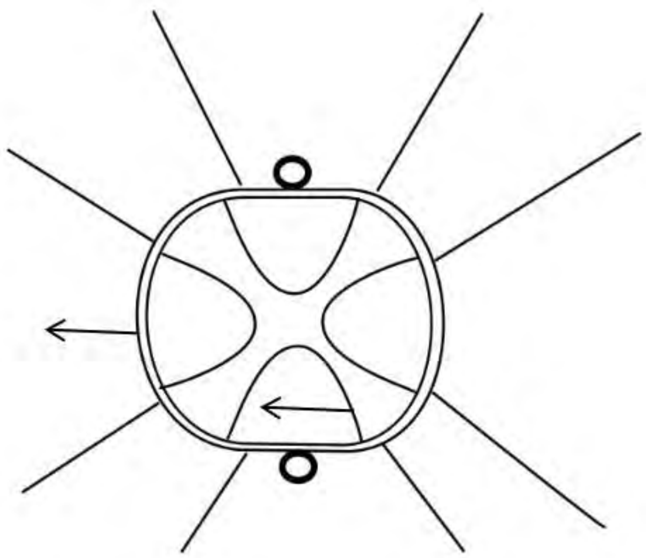

Effects on the Beam: Emm Growth

Emittance growth from a single dipolar noise source [1, 2]

$$\frac{d\epsilon_N}{dt} = \frac{1}{2}\epsilon_N f_0 \frac{\langle \Delta x'^2 \rangle}{\sigma_x'^2} = \frac{1}{2} f_0 \gamma \beta(s) \langle \Delta x'^2(s) \rangle$$

Orbit noise

$$\langle x^2(s') \rangle \le \frac{\beta(s')\beta(s)}{2\sin(\pi Q)} \langle \Delta x'^2(s) \rangle$$

$$\langle \Delta x'^2 \rangle = \left(\frac{el}{Pc}\right)^2 \langle \delta B^2 \rangle \text{ or } \langle \Delta x'^2 \rangle = \left(\frac{el}{Pc}\right)^2 2\pi f_0 \Sigma S_{\delta B}\big(2\pi f_0 (n - Q)\big)$$ if the power spectrum is known

Effect due to the main bends MB

$$\langle \Delta x'^2 \rangle = N \left\langle \left(\frac{2\pi}{N}\frac{\delta B}{B}\right)^2 \right\rangle \rightarrow \frac{d\epsilon_N}{dt} = f_0 \gamma \beta_{ave} \frac{4\pi^2}{2N} \left\langle \left(\frac{\delta B}{B}\right)^2 \right\rangle$$ [$4\pi^2$ missing in ref 2]

Effect in quadrupoles

$$\langle \Delta x'^2 \rangle = \left(\frac{elg}{Pc}\right)^2 \langle \delta x^2 \rangle$$

	$\sqrt{\langle \delta B^2 \rangle}/B$	$1/\epsilon_N\, d\epsilon_N/dt$ [h
All MB	5 10^{-10}	24
	$\sqrt{\langle \delta x^2 \rangle}$	$1/\epsilon_N$ d
Single HL Triplets	1.8 10^{-10}	24

Spectrum of turbulence

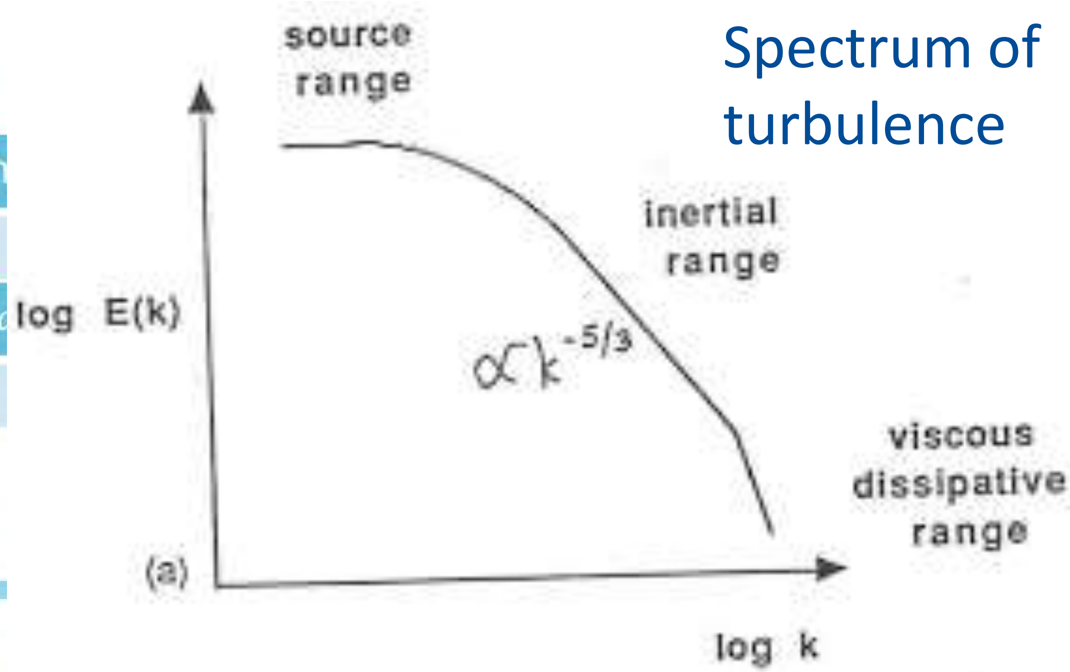

“Good side” of Synchrotron Radiation

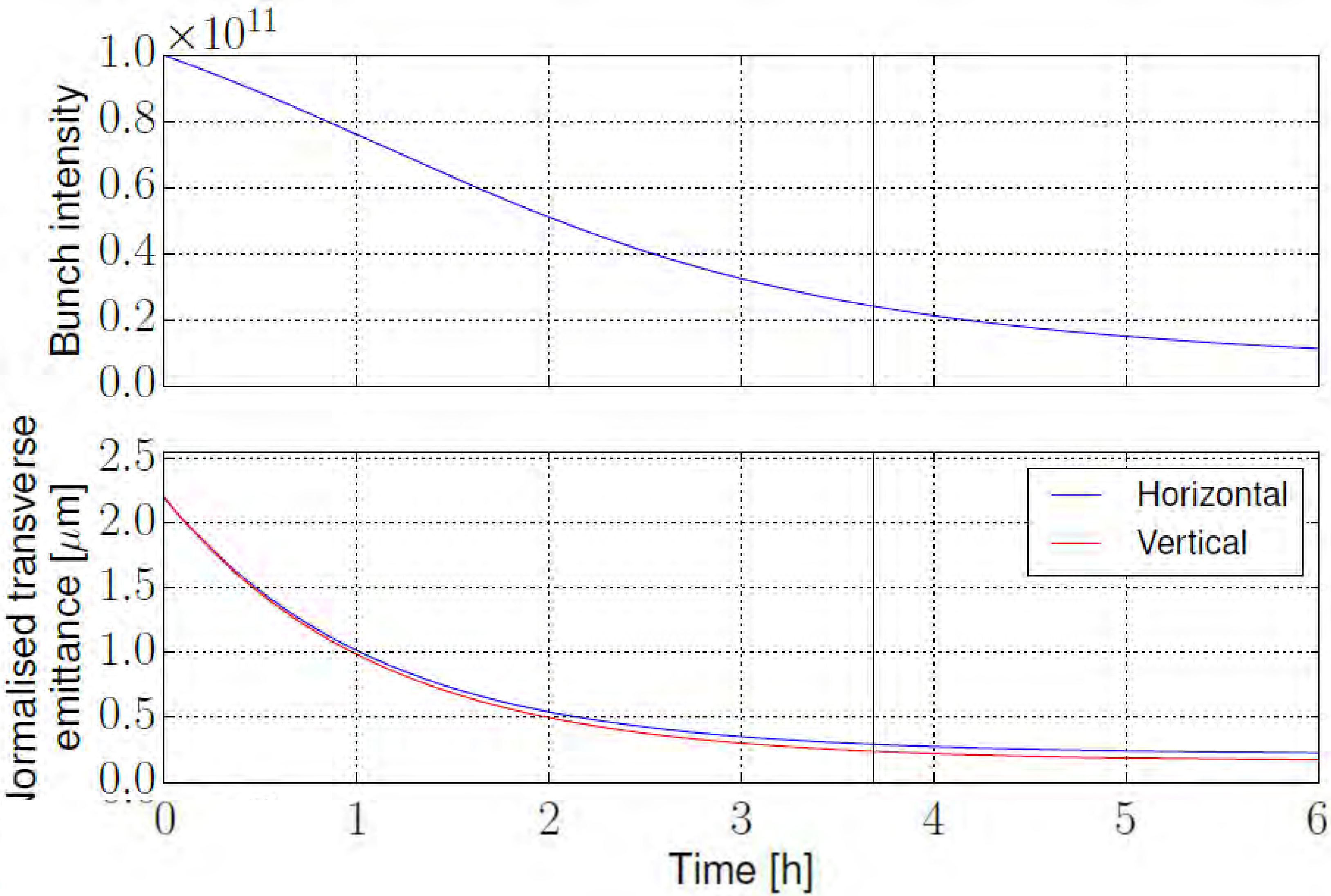

Synchrotron Radiation Cooling

SR Cooling → Luminosity Growth!

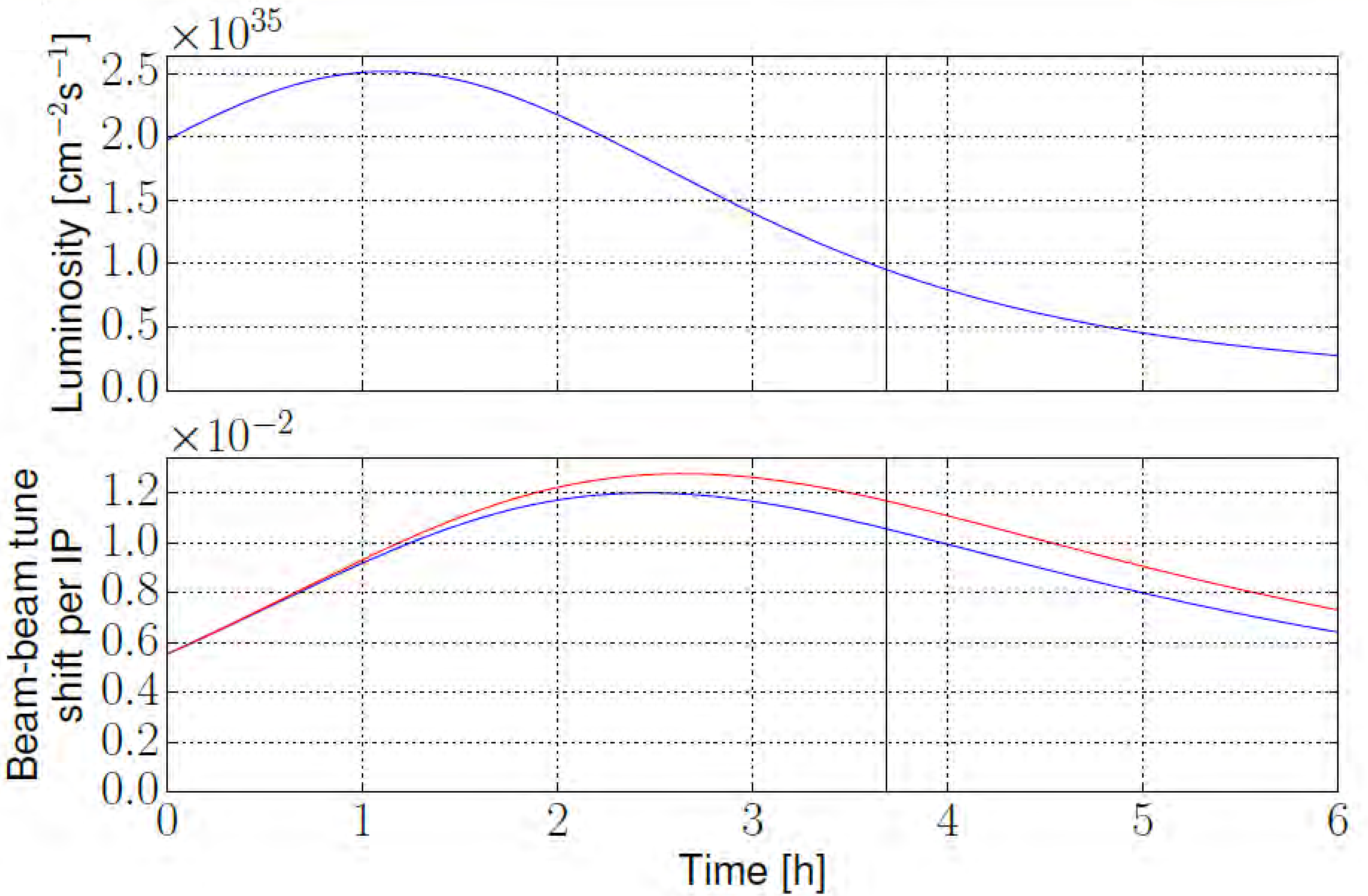

Future pp Colliders: Parameters and Problems (3)

parameter	FCC-hh		SppC	HL-LHC	LHC
collision energy cms [TeV]	100		75	14	14
dipole field [T]	16		12	8.33	8.33
circumference [km]	97.75		100	26.7	26.7
beam current [A]	0.5		0.73	1.1	0.58
bunch intensity [10^{11}]	1	1	1.5	2.2	1.15
bunch spacing [ns]	25	25	25	25	25
synchr. rad. power / ring [kW]	2400		1100	7.3	3.6
SR power / length [W/m/ap.]	28.4		12.8	0.33	0.17
long. emit. damping time [h]	0.54		1.17	12.9	12.9
beta* [m]	1.1	0.3	0.75	0.15 (min.)	0.55
normalized emittance [μm]	2.2		2.4	2.5	3.75
peak luminosity [10^{34} cm^{-2}s^{-1}]	5	30	10	5 (lev.)	1
events/bunch crossing	170	1000	~300	132	27
stored energy/beam [GJ]	8.4		9.1	0.7	0.36

Fermilab

"Pile Up"

Protons break protons

Too many events per crossing (interaction)

Makes it hard to detect and analyze

Rate → $R = L\sigma$ ← Cross-section ("physics")

Luminosity

Example: LHC Luminosity is 2e34 $cm^{-2}s^{-1}$

p-p inelastic cross section at 13 TeV cme is ~*82* mbarn (1mbarn =1e-27 cm^{-2}) → ***R***=1.64 billion per second

in ~2800 bunches crossings per turn, 11000 turns per sec →

Max pile up is 54 interactions per crossing (early in collisions)

LHC : PU=25→250… FCChh PU=1000?

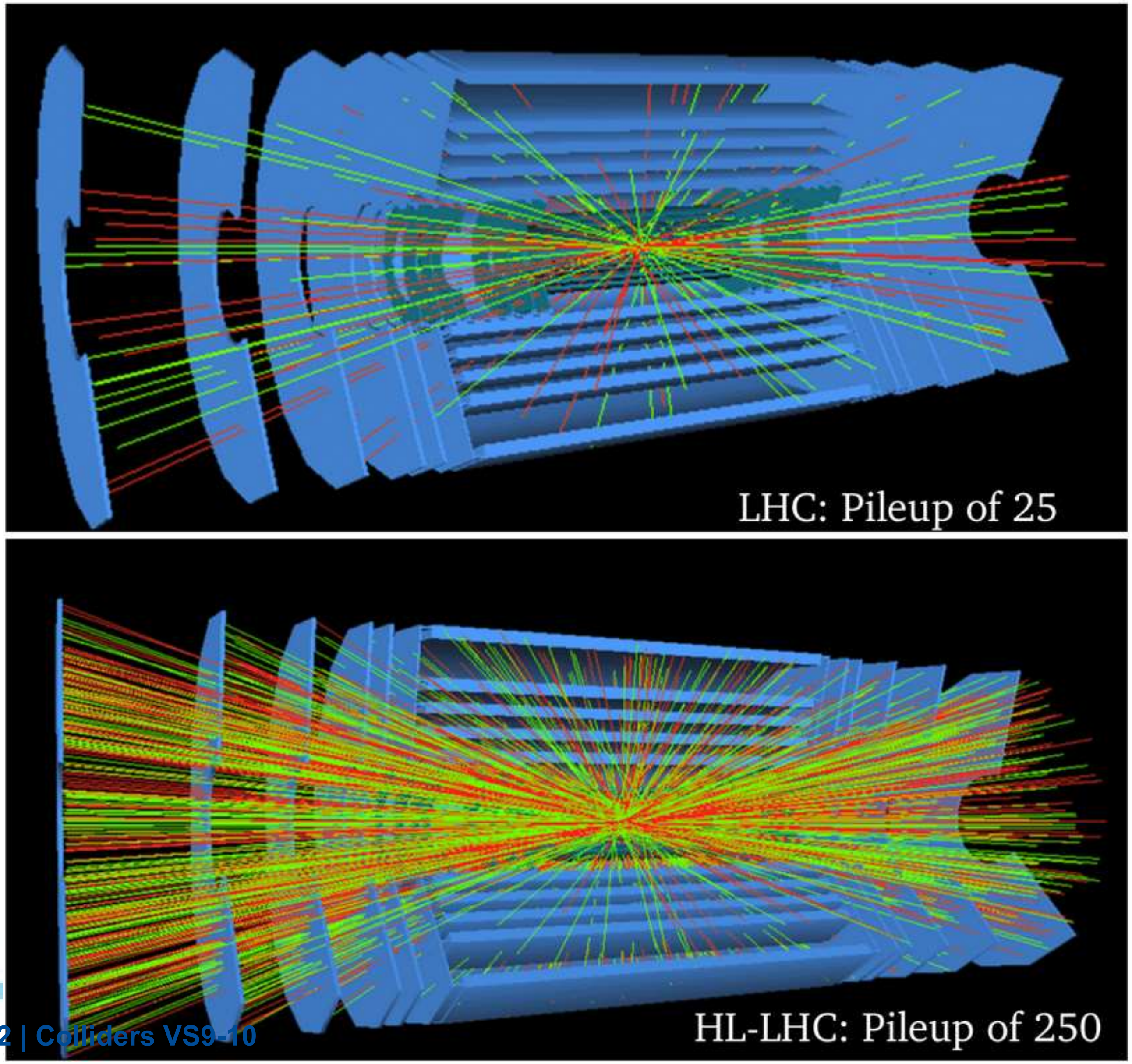

Future pp Colliders: Parameters and Problems (4)

parameter	FCC-hh		SppC	HL-LHC	LHC
collision energy cms [TeV]	100		75	14	14
dipole field [T]	16		12	8.33	8.33
circumference [km]	97.75		100	26.7	26.7
beam current [A]	0.5		0.73	1.1	0.58
bunch intensity [10^{11}]	1	1	1.5	2.2	1.15
bunch spacing [ns]	25	25	25	25	25
synchr. rad. power / ring [kW]	2400		1100	7.3	3.6
SR power / length [W/m/ap.]	28.4		12.8	0.33	0.17
long. emit. damping time [h]	0.54		1.17	12.9	12.9
beta* [m]	1.1	0.3	0.75	0.15 (min.)	0.55
normalized emittance [μm]	2.2		2.4	2.5	3.75
peak luminosity [10^{34} $cm^{-2}s^{-1}$]	5	30	10	5 (lev.)	1
events/bunch crossing	170	1000	~300	132	27
stored energy/beam [GJ]	8.4		9.1	0.7	0.36

Fermilab

8-9 GJ Stored Energy in the Beam

#1 Beam handling
and dumping

8 GJ kinetic energy per beam

- Boing 747 at cruising speed
- 2000 kg TNT
- 400 kg of chocolate
  - Run 25,000 km to spent calories
- O(20) times LHC

Requires careful “rastering” (dilution) to spread deposited energy evenly in the beam dump (not to destroy it)

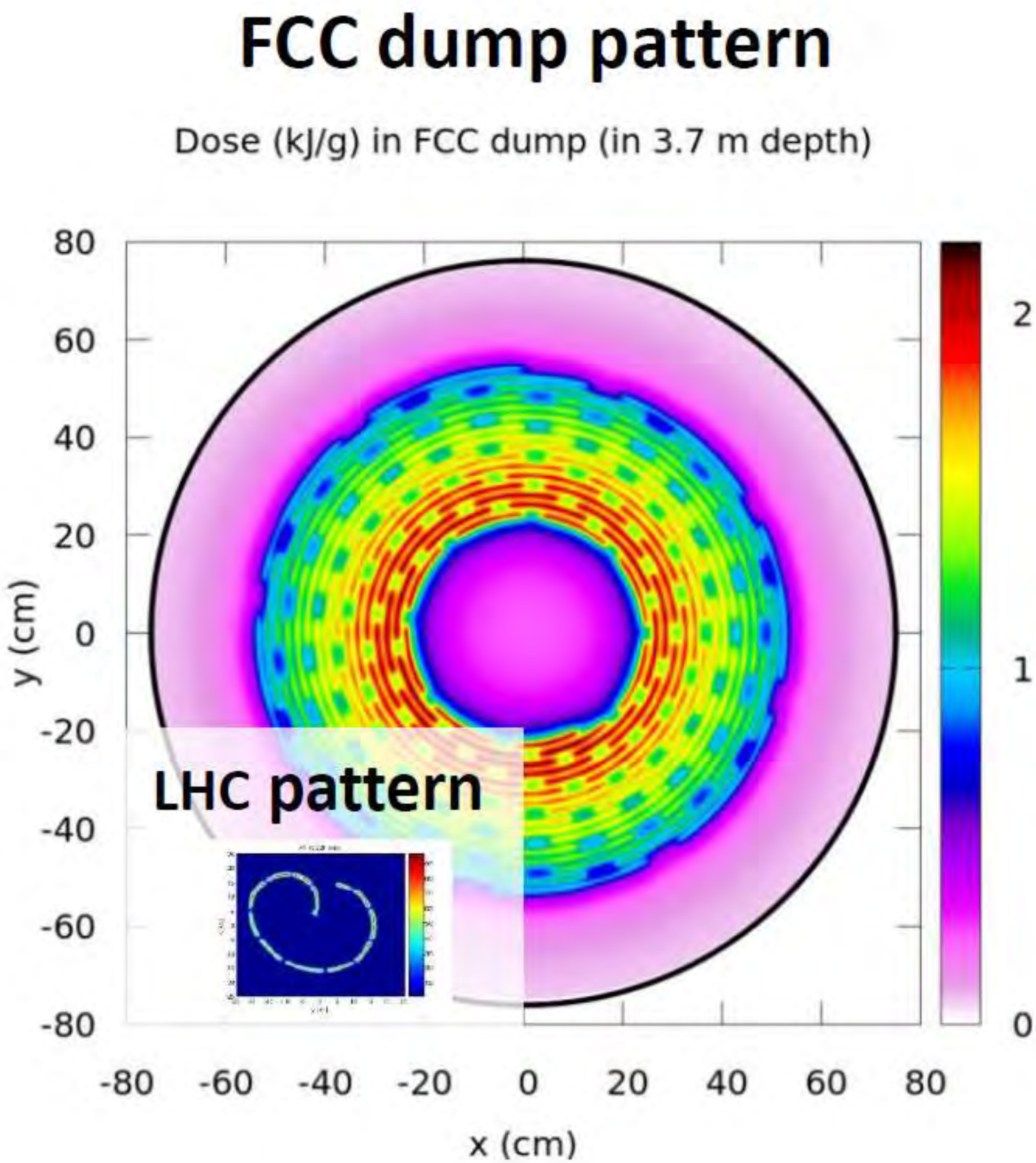

8-9 GJ Stored Energy in the Beam

#2 Efficient collimation -

0.1% of full intensity = 1 MJ can melt 2kg of copper

Collimation system design:

- Must cope with possible losses
- Have small (enough) impedance

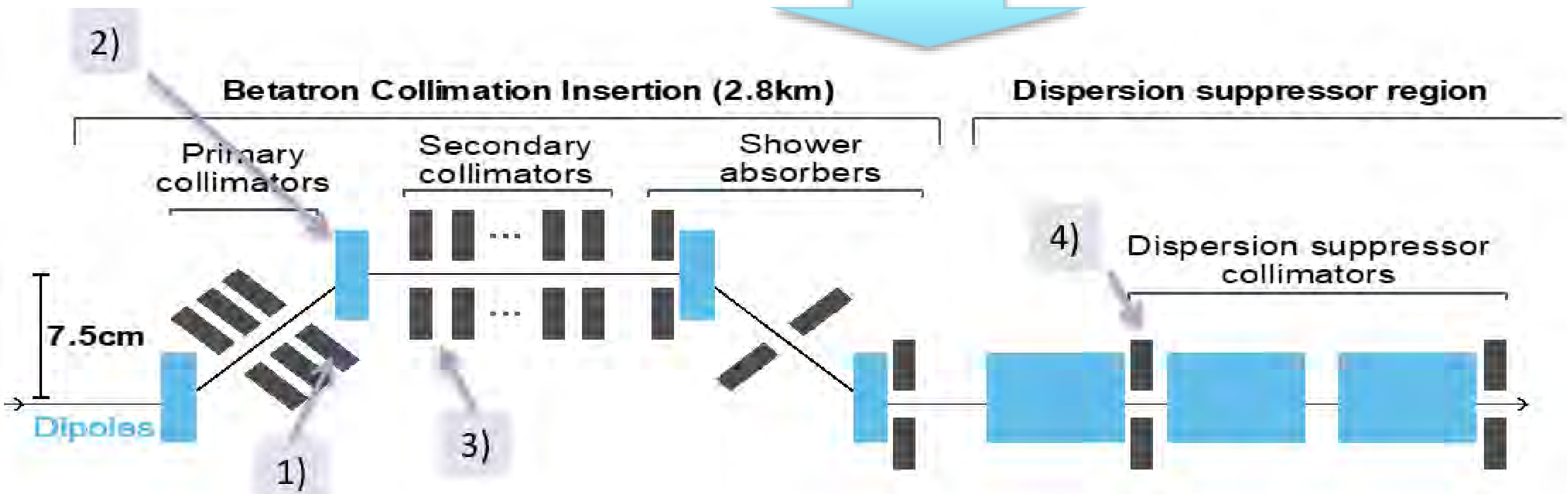

1) Use of thin primaries, no skew collimator
2) Protection of chicane (1 MW)
3) Protection/design of secondaries
4) Protection of arcs (kw)
General collimation performance studies

May need hollow e-lens to diffuse halo

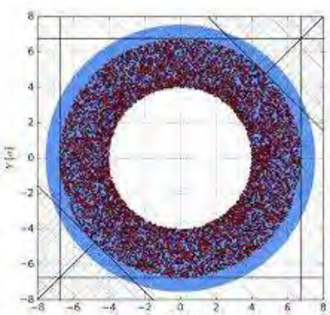

Sumnary on R&D:

- High field dipoles:
  - Nb3Sn 16 T / iron-based 12 T
  - Conductor (wire) development
- Intercept of synchrotron radiation :
  - 5 MW FCC-hh / 1 MW CepC
- Collimation :
  - x7 LHC circulating beam power
- Optimal injector:
  - 1.3TeV scSPS, 3.3 TeV in LHC/FCC
- Overall machine design :
  - IRs, pileup, vacuum, etc
  - Power and cost reduction

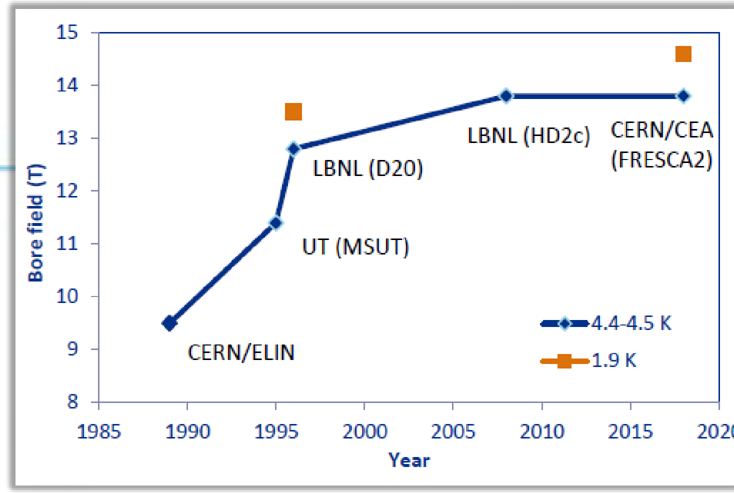

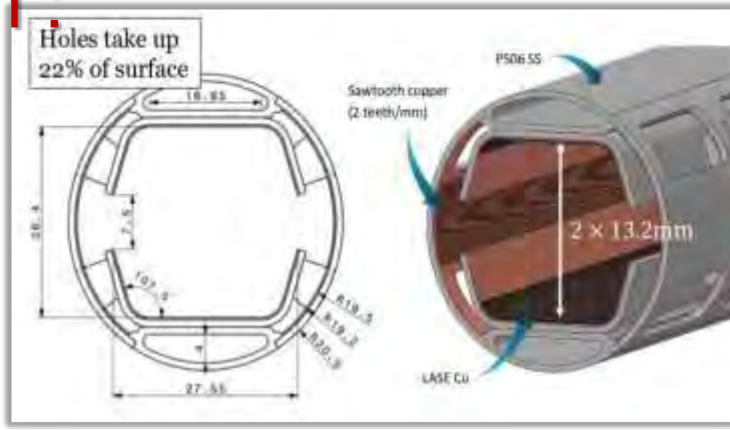

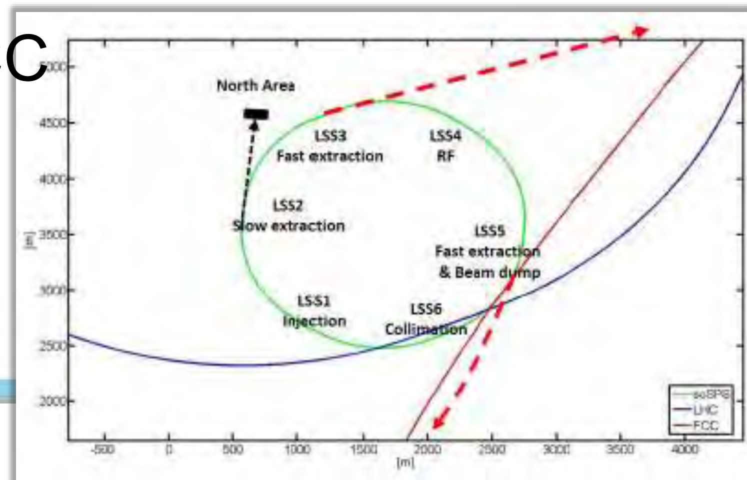

All that might take 12-18 years

Thanks for Your Attention !

Questions !?

Literature

- V.Shiltsev, F.Zimmermann, Modern and Future Colliders (Rev.Mod.Phys., 2021)

https://journals.aps.org/rmp/abstract/10.1103/RevModPhys.93.015006

- V.Lebedev, V.Shiltsev, Accelerator Physics at the Tevatron Collider (Springer, 2014)

https://indico.cern.ch/event/774280/attachments/1758668/2915590/2014_Book_AcceleratorPhysicsAtTheTevatro.pdf

- S.Myers, H.Schopper, eds. Accelerator and Colliders (Springer, 2013, 2020)

https://link.springer.com/book/10.1007/978-3-030-34245-6

- "Particle accelerator physics - 4th ed." (Springer) by Wiedemann, Helmut.

https://library.oapen.org/handle/20.500.12657/23641

- "Measurement and control of charged particle beams" (Springer) by Minty, Michiko G; Zimmermann, Frank

https://library.oapen.org/handle/20.500.12657/23642

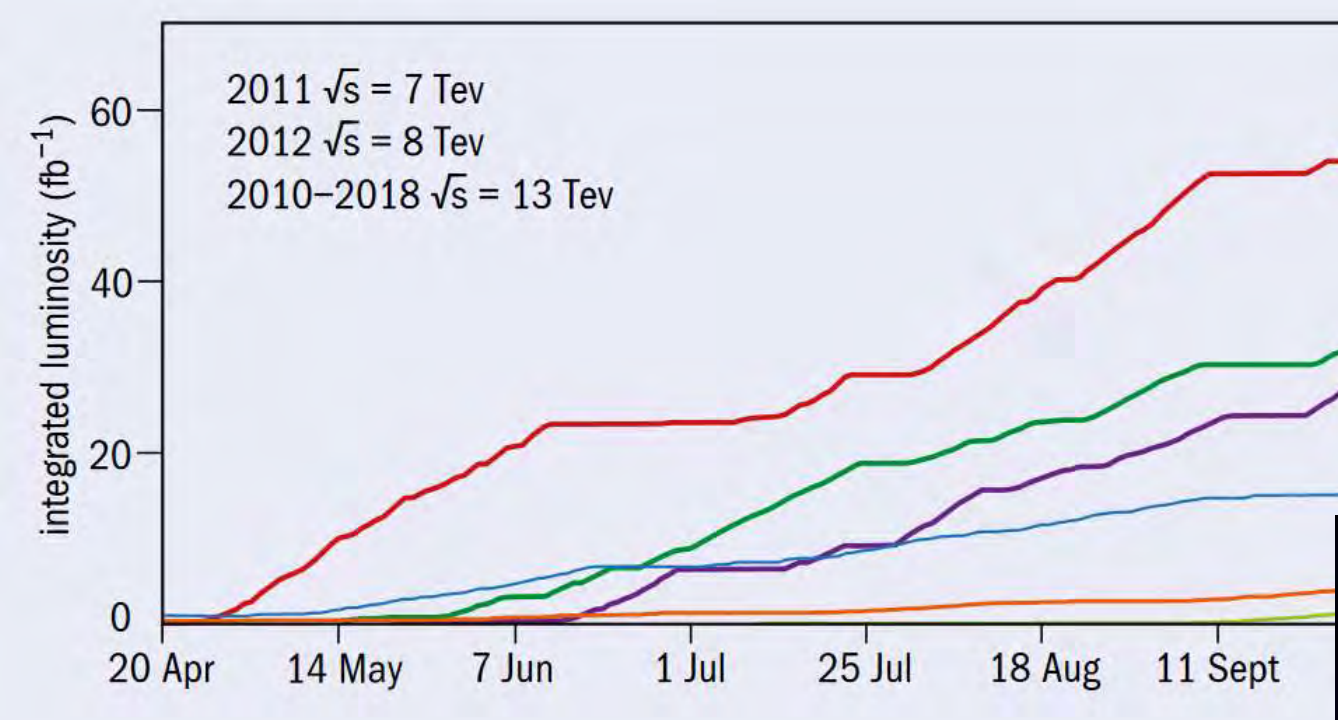

"16L2" refers to a group or "cell" of three dipoles, one quadrupole and some corrector magnets, sitting 16 cells to the left of point 2 of the LHC.

The majority of recent beam dumps can be traced back to this cell and a likely hypothesis is the presence of gas in the vacuum pipes

U.S. Particle Accelerator School
Education in Beam Physics and Accelerator Technology

Fermilab

Managed by Fermi Research Alliance, LLC for the U.S. Department of Energy Office of Science

a) Linear Colliders
b) Muon Colliders

Vladimir Shiltsev, Fermilab

part of the "Colliders" class by V.Lebedev, N.Mokhov and V.Shiltsev

US Particle Accelerator School, Jan 24 – Feb 4, 2022

Linear Collider vs Rings

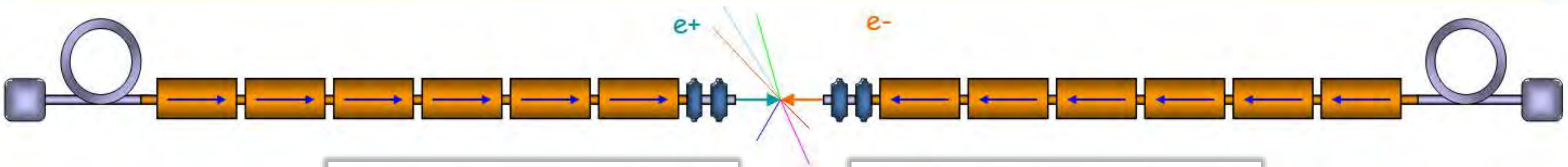

$$E_b = eGL \quad + \quad E_b = eGL$$

Major advantages (wrt e+e- ring-ring colliders):

- No SR losses (no bending magnets… E_{cme} can go up to few TeV)
- More compact if gradient G is high
- (Somewhat) lower cost for Higgs energy E_{cme}=250 GeV
- Polarized beams

Major disadvantages (wrt e+e- ring-ring colliders):

- One IP at a time (vs up to 4 in rings)
- Lower luminosity at E_{cme}< 0.5 TeV (lower *Lumi/Power* ratio)
- Big *Lumi* challenges: ultra low ε, jitters, beamstrahlung, e+ prod'n
- Limited experience (one SLC vs dozens of e+e- rings)

Linear *lepton* Colliders

- Choice of particles :
  - Mostly *e+e-*
  - Muons possible, but μ-sources are expensive (and limited production rate *dN/dt*)
  - Protons possible, but lose factor of 7 in effective cme energy reach in *hh* collisions (ie need to accelerate to 7x the e+e- energy)
  - Interesting option $\gamma\gamma$-colliders
    - Need two *e-* linacs, few mm from IP convert *e-* → γ and collide photons
    - Higgs production via s-channel and requires only ~63GeV electrons! (ie factor of 2 smaller beam energy… in e+e- → ZH need 125 GeV)
    - Allows avoid beamstrahlung but low luminosity and broad cme dE/E
- Choice of RF technology:
  - *Super-Conducting RF → ILC*
  - *Room Temperature Copper NC RF → CLIC*
  - *Liquid Nitrogen Temperature Copper RF → C^3*

International Linear Collider

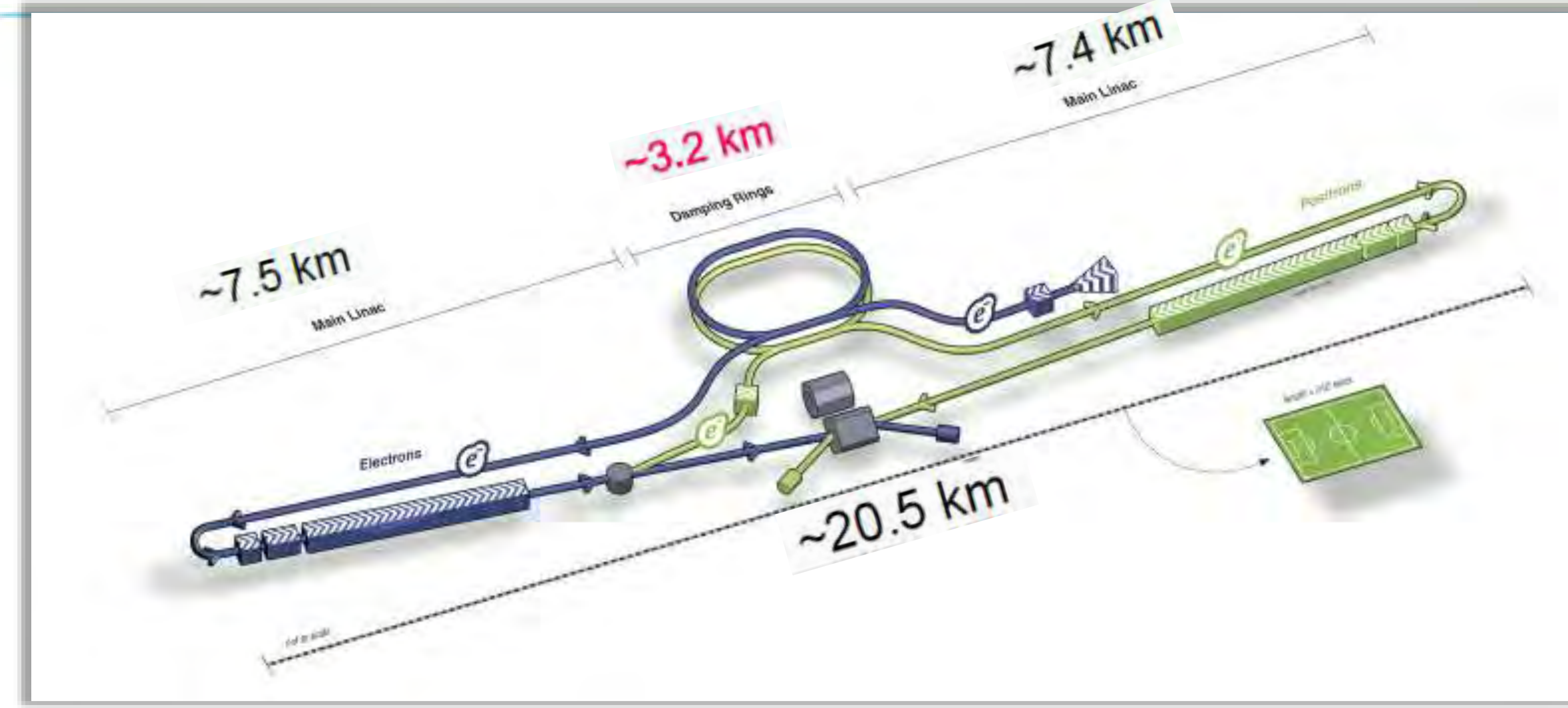

Key facts:

20 km, including 5 km of Final Focus

SRF 1.3 GHz, 31.5 MV/m, 2 K

130 MW site power @ 250 GeV c.m.e.

Cost estimate 700 B JPY*

** ± 25% err, includes labor cost*

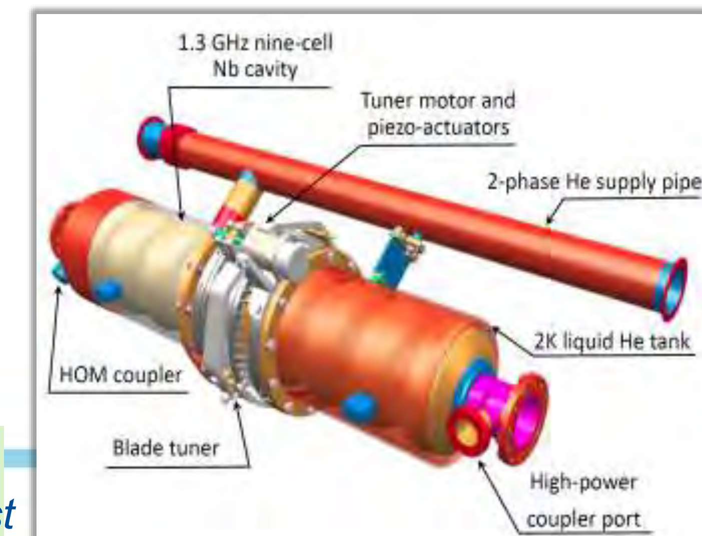

Compact LInear Collider

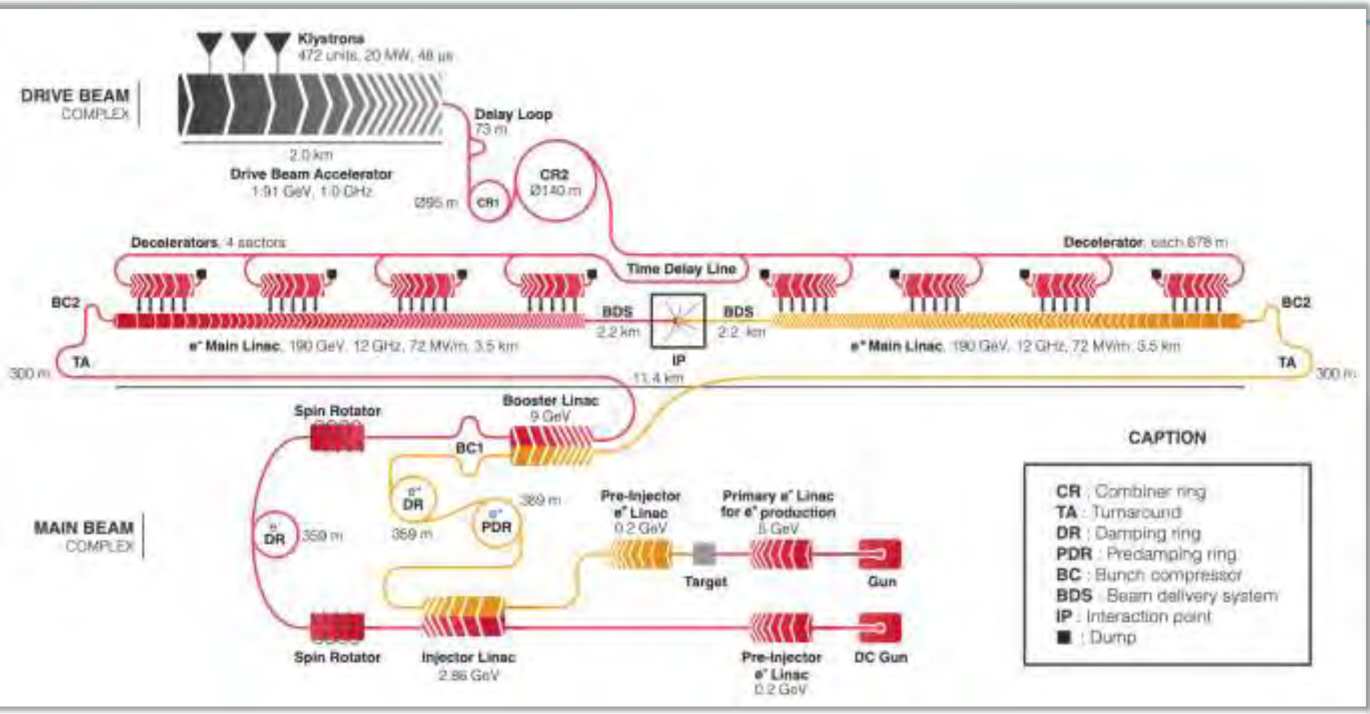

Key facts:

11 km main linac @ 380 GeV c.m.e.

NC RF 72 MV/m, *two-beam* scheme

168 MW site power (~9MW beams)

Cost est. 5.9 BCHF ± 25%

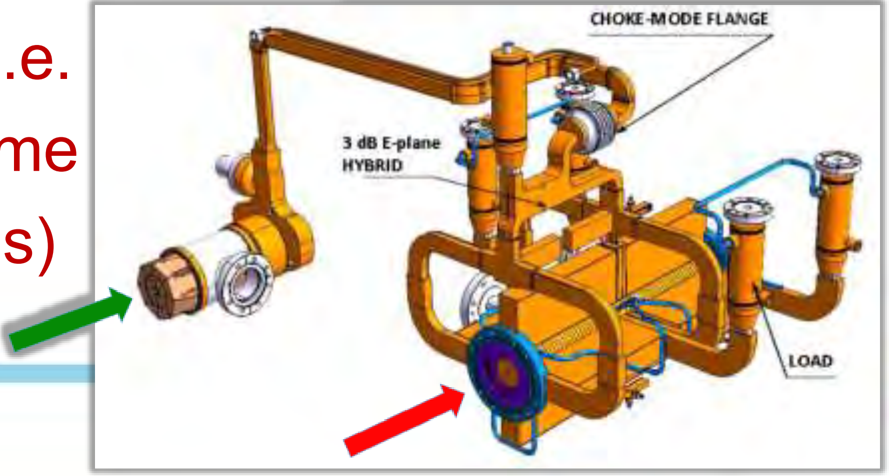

Cool Copper Collider (aka C^3)

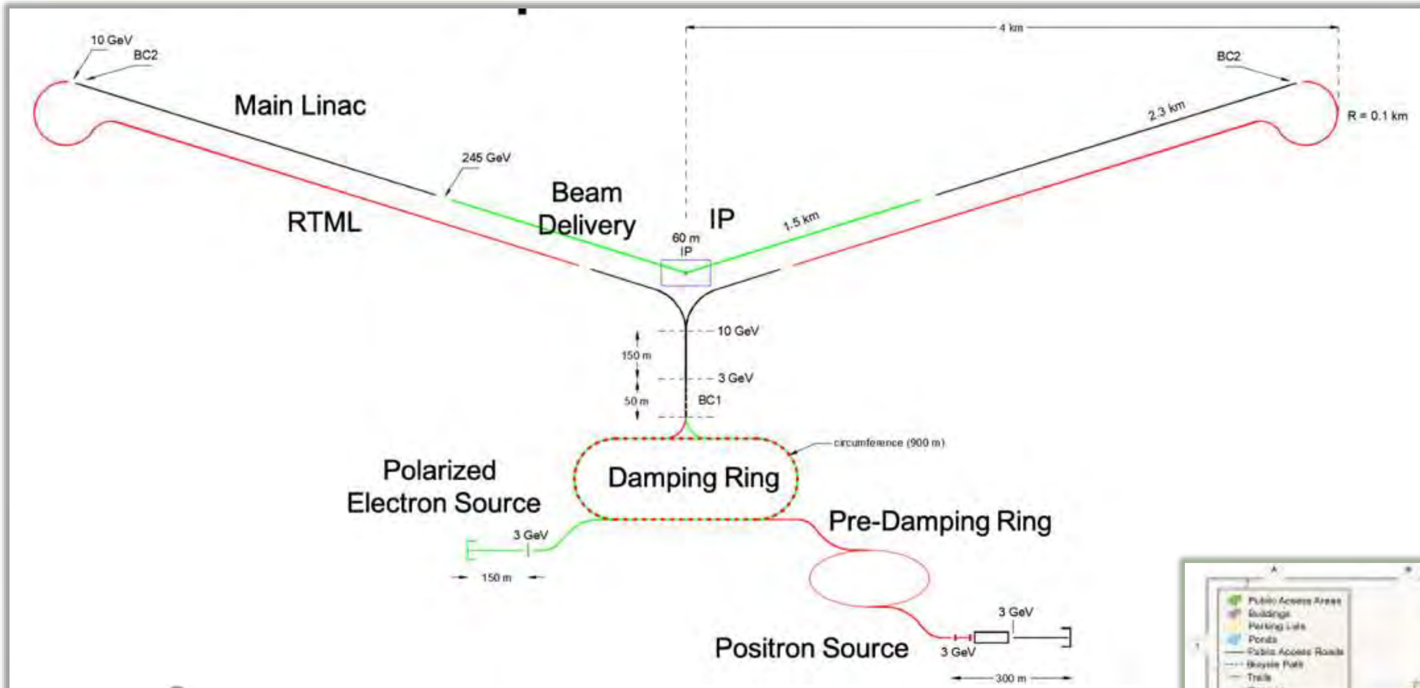

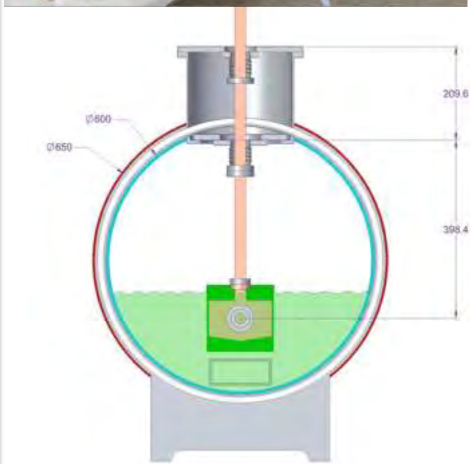

Key facts:

7-8 km, including 3 km of Final Focus

NC RF 5.7 GHz, 120 MV/m, 77 K

150 MW site power @ 250 GeV c.m.e.

Cost estimate ~2/3 of ILC

Linear e+e- Colliders Energy Limits

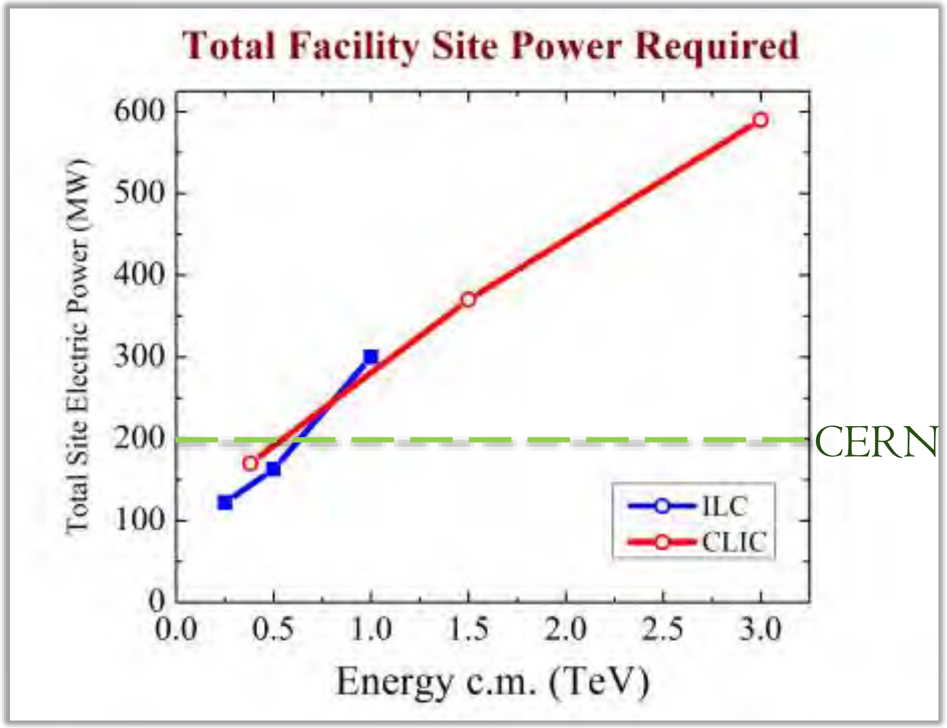

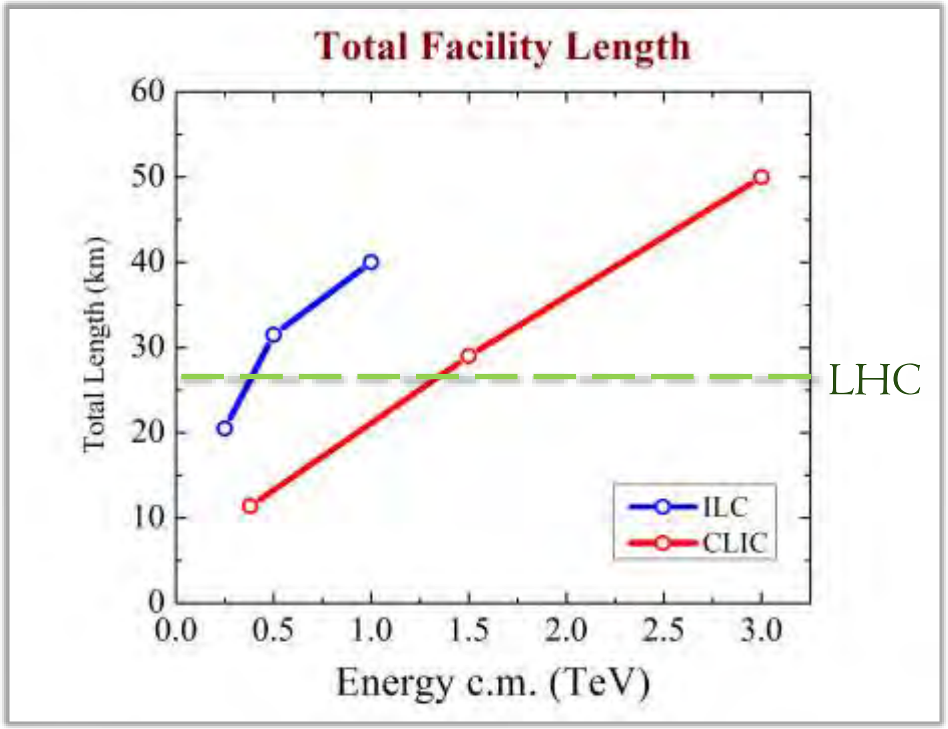

Recent progress: Linear Colliders

- Accelerating gradients demonstrated (in reasonably long RF systems):
  - ILC 31.5 MeV/m with beam – FNAL'17, KEK'19
    - One 12m long SRF cryomodule + 1 klystron
    - ILC needs 1000 of them +300 klystron
  - CLIC ~100 MeV/m with beam – CLEX@CERN
    - Several 0.25 m long structures driven by one low energy very powerful 12 GHz beam
    - CLIC needs ~15,000 structures and two "superbeam" 12 GHz 2 GeV driver beams
  - C^3 150 MeV/m no beam – SLAC'20
    - One ~1m long structure + 1 klystron
    - C^3 needs ~1000 structures and 500 klystrons

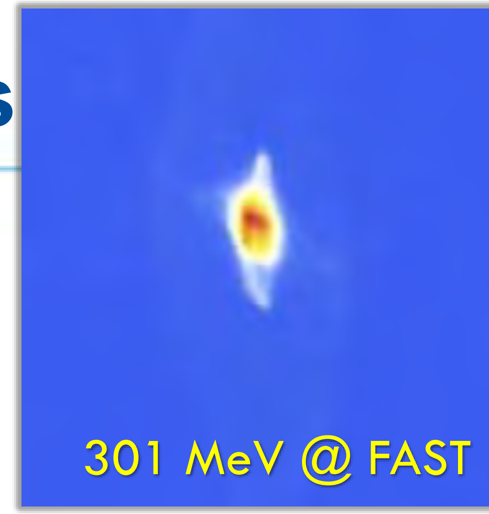

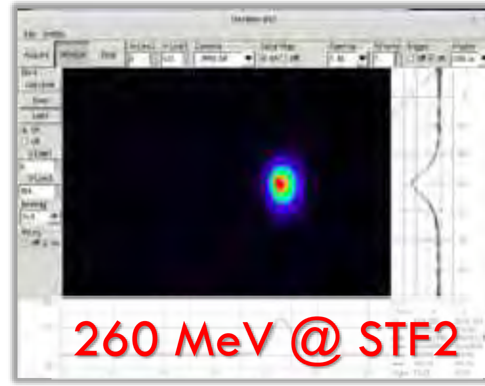

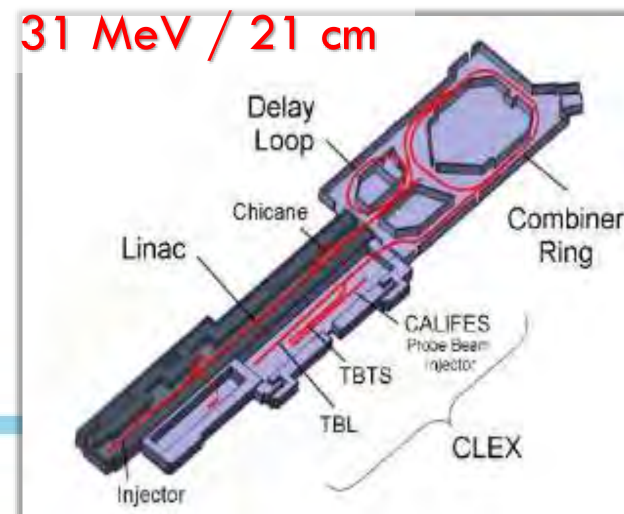

(Besides RF) Most Systems "Common"

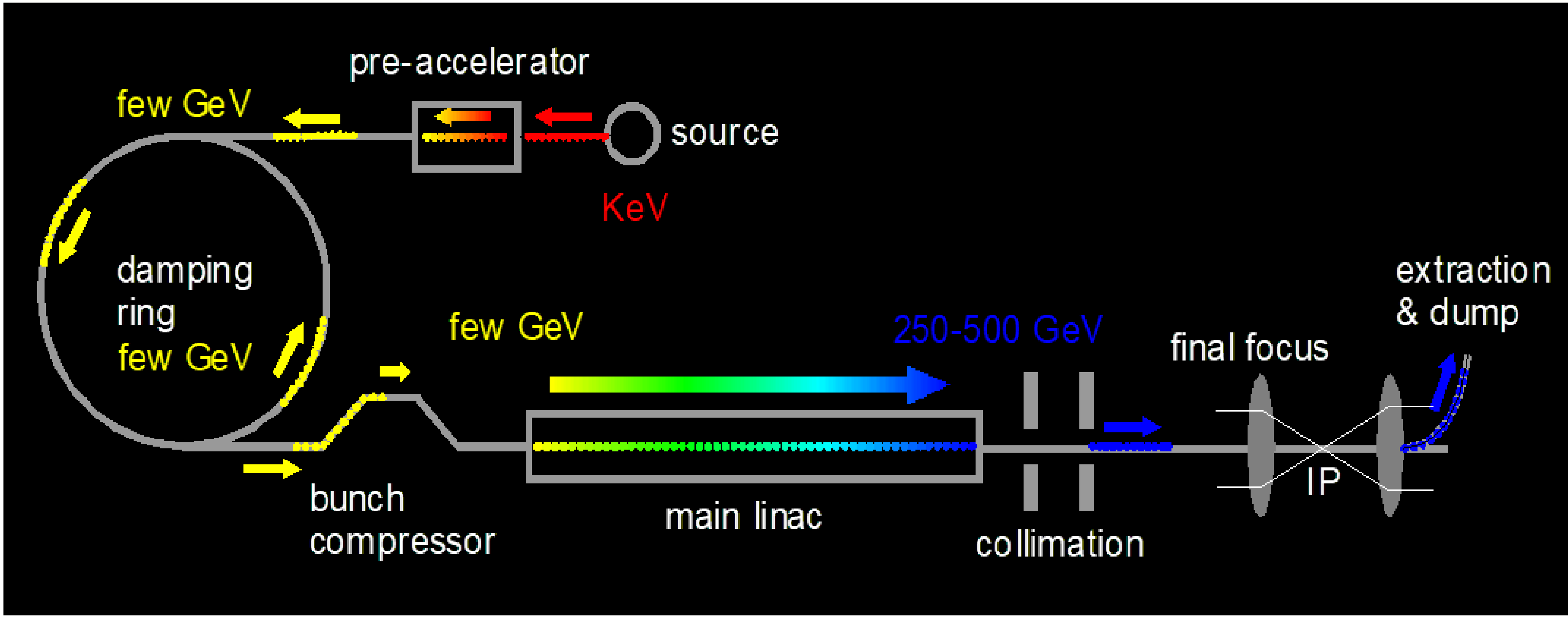

- Electron source → damping ring → bunch compressor
- Positron source → damping ring → bunch compressor
- **Acceleration**
- Final Focus system and beam dumps

e^- Source

- laser-driven photo injector
- circ. polarised photons on GaAs cathode
  $\rightarrow$ long. polarised e^-
- laser pulse modulated to give required time structure
- <u>very</u> high vacuum requirements for GaAs ($<10^{-11}$ mbar)
- beam quality is dominated by <u>*space charge*</u>
  (note $v \sim 0.2c$)

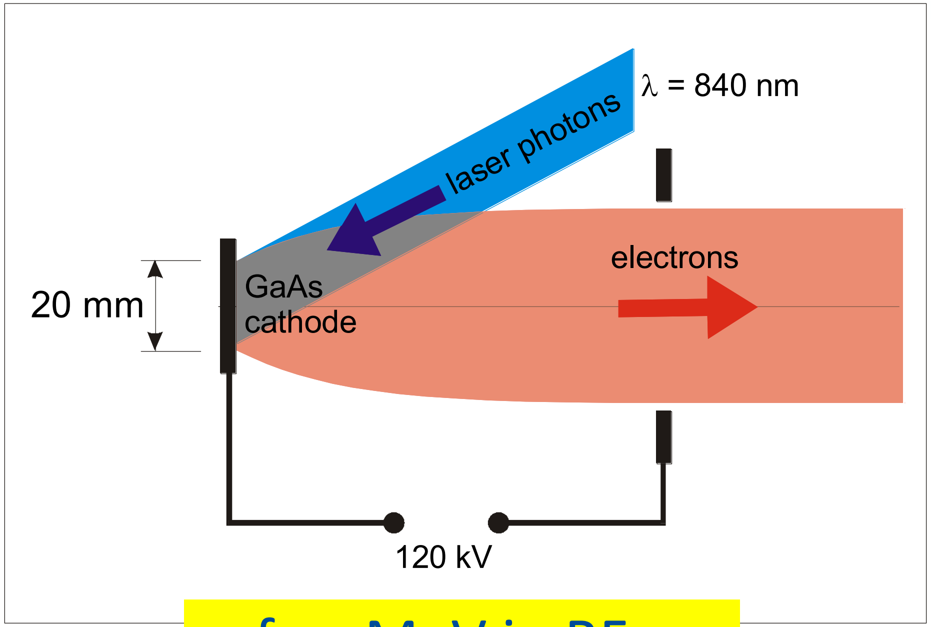

or few MeV in RF gun

$\varepsilon_n \approx 10^{-5} m$

factor 10 in x plane

factor ~500 in y plane

Fermilab

e^+ Source

Photon conversion to $e^{\pm}$ pairs in target material

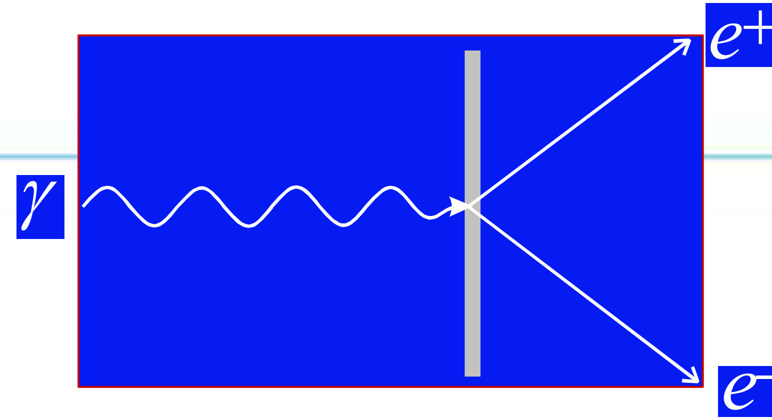

Standard method is e^- beam on ‘thick’ target (em-shower)

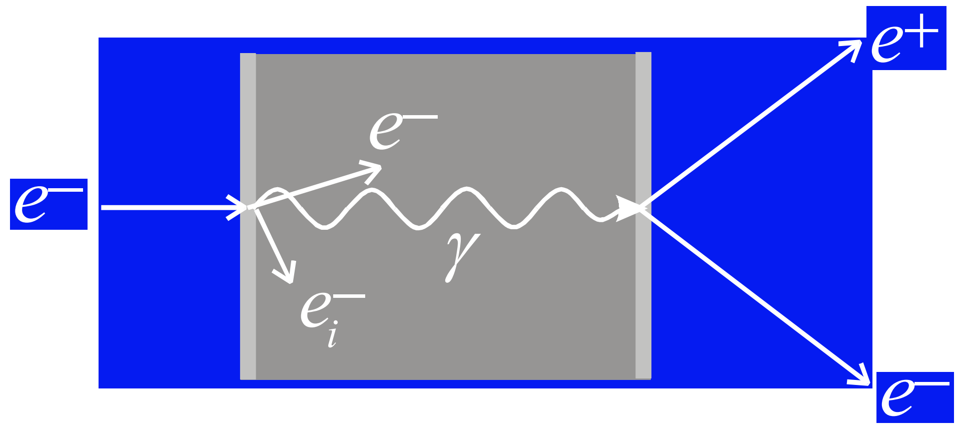

Undulator based

SR radiation from undulator generates photons

no need for ‘thick’ target to generate shower

thin target reduces multiple-Coulomb scattering: hence better emittance (but still much bigger than needed)

less power deposited in target (no need for mult. systems)

Achilles heel: needs initial electron energy > 150 GeV!

$\sim$ 30 MeV

$0.4X_0$

10^{-2} m

5 kW

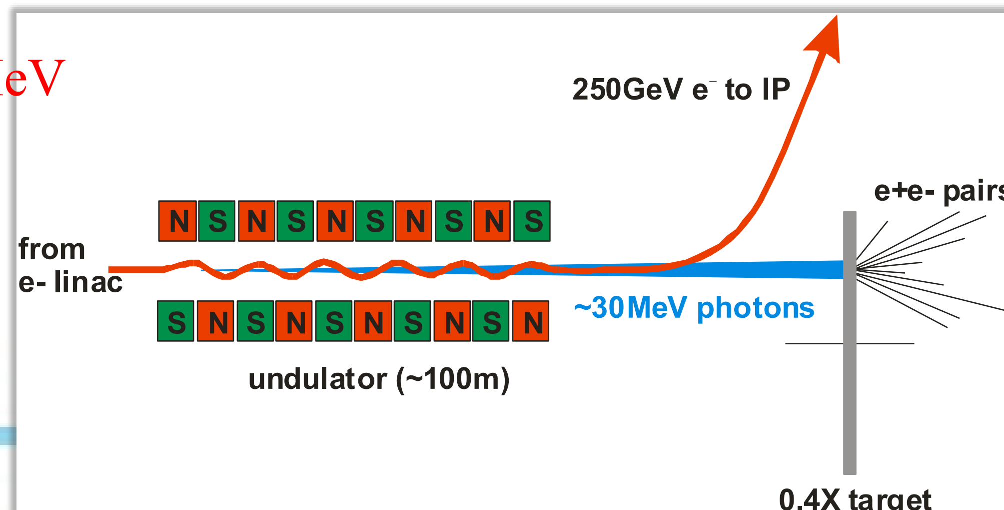

e^+ Source :undulator-based

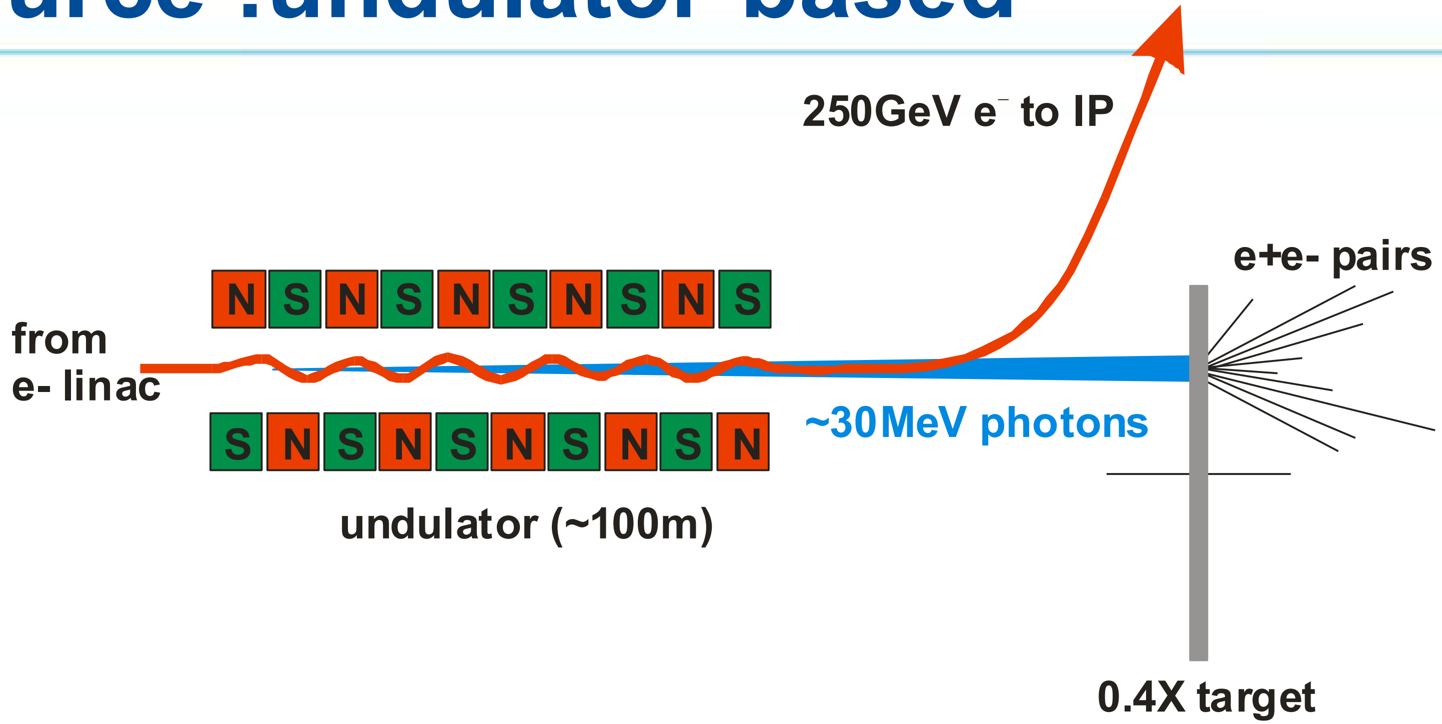

- SR radiation from undulator generates photons ~ 30 MeV
- no need for 'thick' target to generate shower $0.4X_0$
- thin target reduces multiple-Coulomb scattering: hence better emittance (but still much bigger than needed) 10^{-2} m
- less power deposited in target (no need for mult. systems) 5 kW
- Achilles heel: needs initial electron energy > 150 GeV!

Fermilab

(Technology) Challenge of *e+* Production

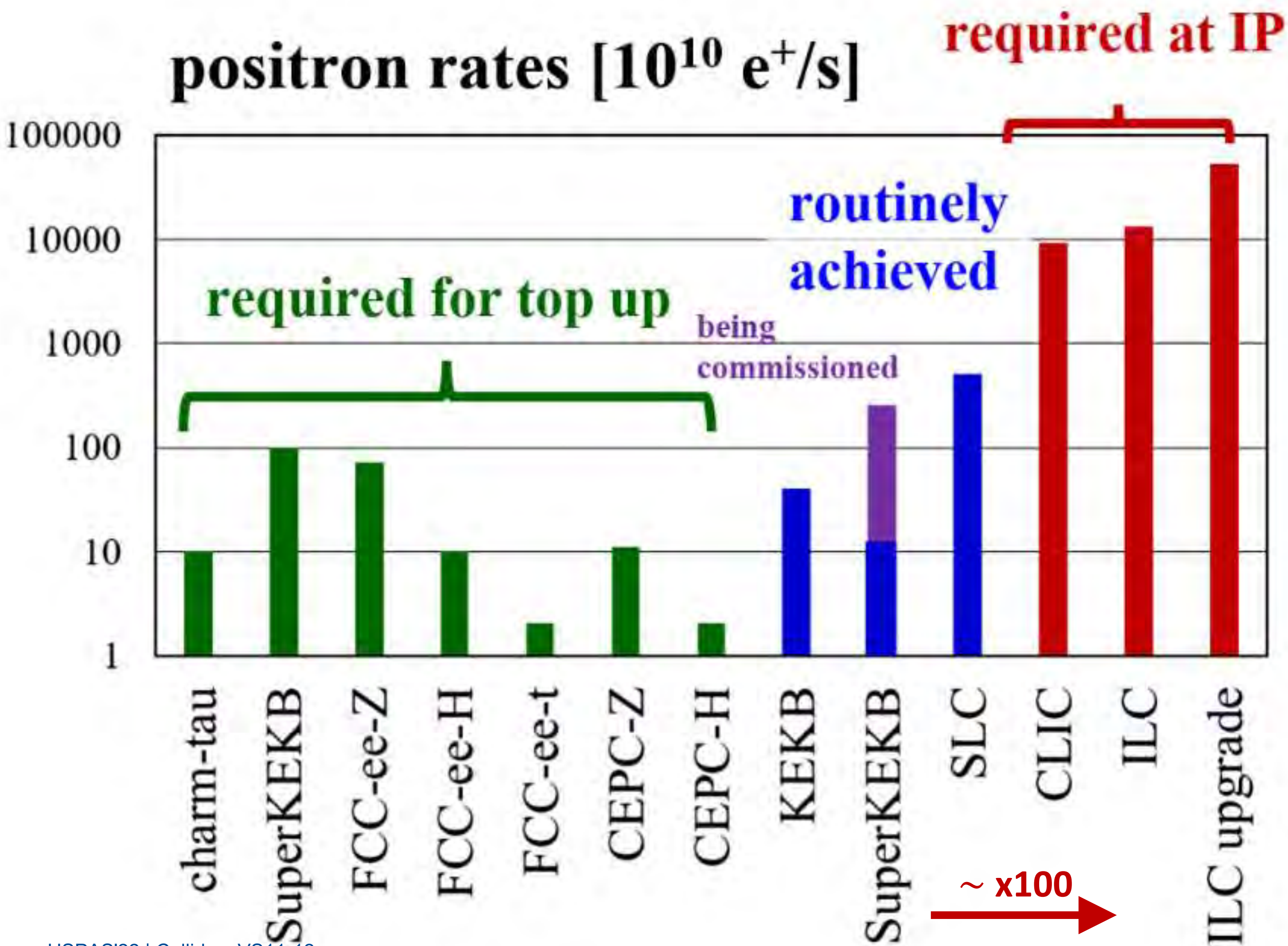

rmilab

Damping Rings

- (storage) ring in which the bunch train is stored for T_{store} ~20-200 ms
- emittances are reduced via the interplay of synchrotron radiation and RF acceleration

initial emittance
(~0.01m for e^+)

$$\varepsilon_f = \varepsilon_{eq} + (\varepsilon_i - \varepsilon_{eq}) e^{-2T/\tau_D}$$

final emittance

equilibrium
emittance

damping time

Damping Rings for Linear Colliders *: ATF at KEK*

- DR emittances demonst'd
  - Wigglers, instabilities, IBS ε growth, coupling
- IP beam focusing methods
  - 40 nm V beam size ATF2@KEK'16
  - ATF2 Goal : 37 nm → 7.7nm@ILC250GeV

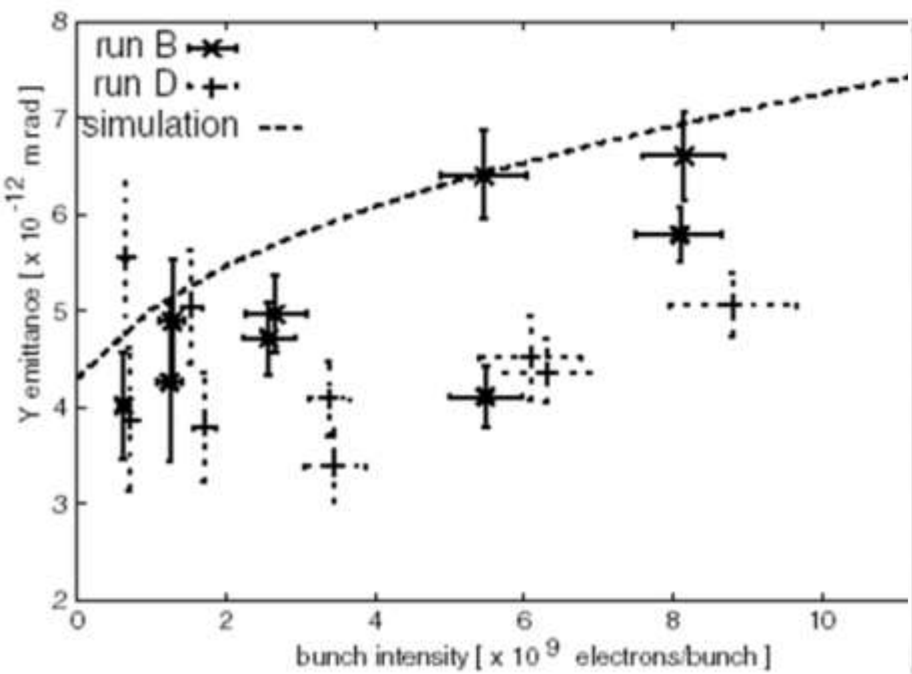

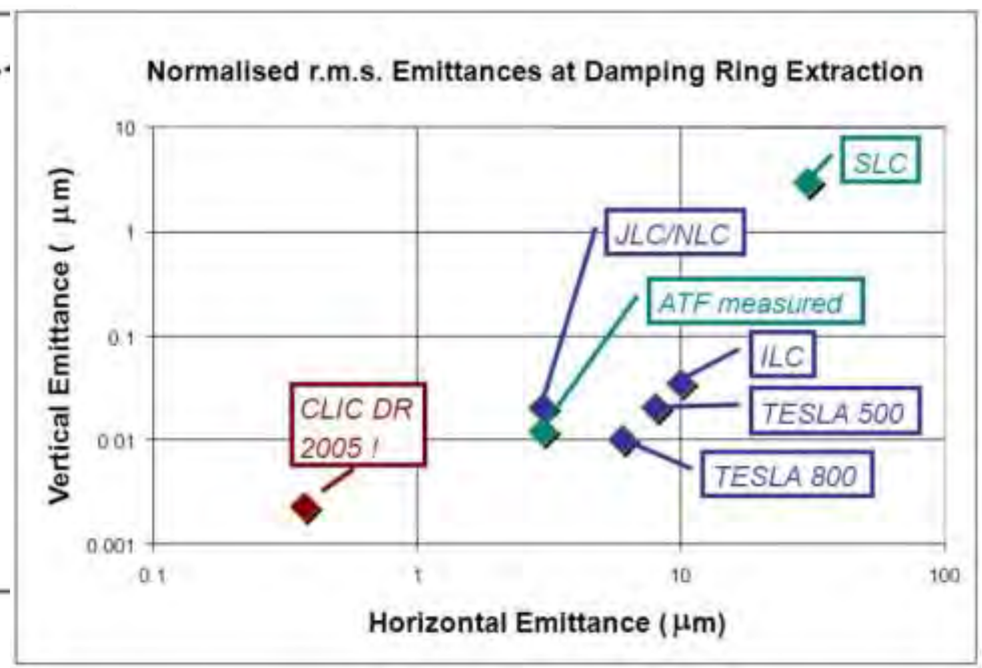

Parameters and Challenges

Collider	NLC[28]	CLIC[29]	ILC[5]	C^3	C^3
CM Energy [GeV]	500	380	250 (500)	250	550
σ_z [μm]	150	70	300	100	100
β_x [mm]	10	8.0	8.0	12	12
β_y [mm]	0.2	0.1	0.41	0.12	0.12
ϵ_x [nm-rad]	4000	900	500	900	900
ϵ_y [nm-rad]	110	20	35	20	20
Num. Bunches per Train	90	352	1312	133	75
Train Rep. Rate [Hz]	180	50	5	120	120
Bunch Spacing [ns]	1.4	0.5	369	5.26	3.5
Bunch Charge [nC]	1.36	0.83	3.2	1	1
Beam Power [MW]	5.5	2.8	2.63	2	2.45
Crossing Angle [rad]	0.020	0.0165	0.014	0.014	0.014
Crab Angle	0.020/2	0.0165/2	0.014/2	0.014/2	0.014/2
Luminosity [x10^{34}]	0.6	1.5	1.35	1.3	2.4
	(w/ IP dil.)	(max is 4)			
Gradient [MeV/m]	37	72	31.5	70	120
Effective Gradient [MeV/m]	29	57	21	63	108
Shunt Impedance [MΩ/m]	98	95		300	300
Effective Shunt Impedance [MΩ/m]	50	39		300	300
Site Power [MW]	121	168	125	~150	~175
Length [km]	23.8	11.4	20.5 (31)	8	8
L* [m]	2	6	4.1	4.3	4.3

Luminosity Challenges of Linear Colliders

$$\mathcal{L} = \frac{H_D}{4\pi} \frac{N}{\sigma_x} N n_b f_r \frac{1}{\sigma_y} \quad \sim 10^{34}$$

Luminosity Spectrum (Physics)

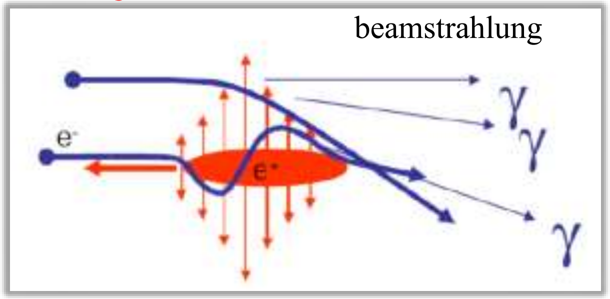

- $\delta E/E$ ~1.5% in ILC
- Grows with E: 40% of CLIC lumi 1% off $\sqrt{s}$

Beam Current (RF power limited, beam stability)

- Challenging $e+$ production (two schemes)
- CLIC high-current drive beam bunched at 12 GHz
- Many high-power klystrons for C^3

Beam Quality (Many systems)

- Record small DR emittances
- 0.1 μm BPMs
- IP beam sizes

ILC 8nm/500nm
CLIC 3nm/150nm
C^3 4nm/180nm

BeamStrahlung at IP

linear colliders

synchrotron radiation in the strong field of the opposing beam (="**beamstrahlung**") degrades the luminosity spectrum

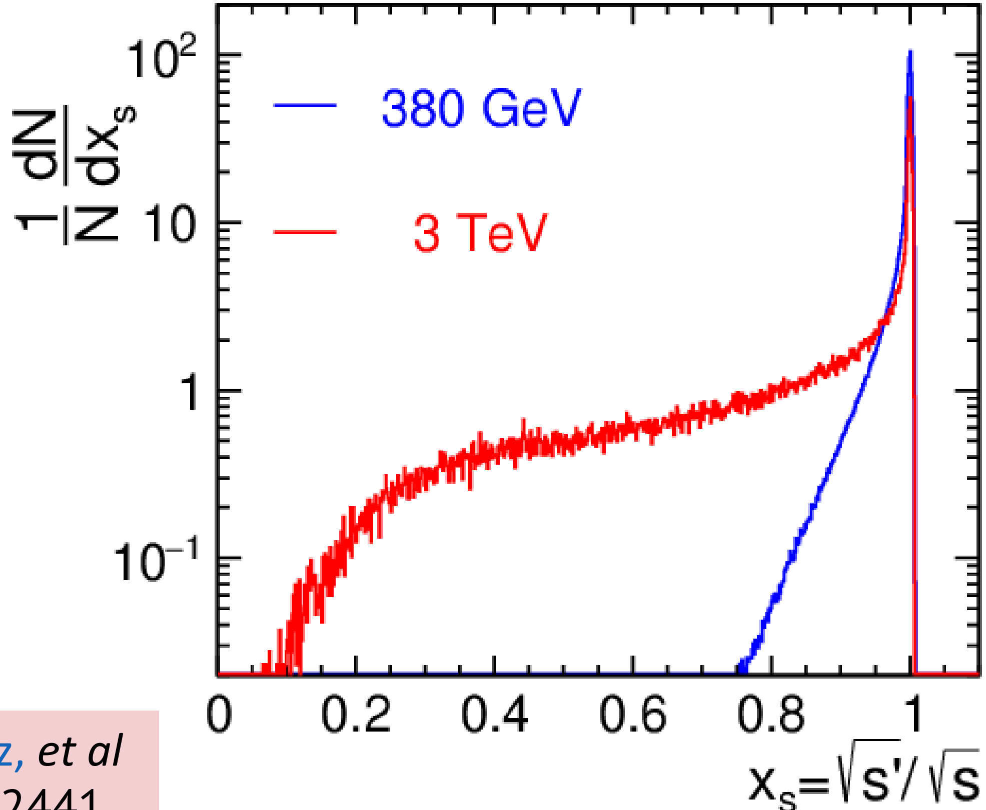

CLIC at 380 GeV: 60% of total luminosity within 1% of target energy

CLIC at 3 TeV: only 33% of total luminosity within 1% of target

e^+e^- collisions in linear colliders lose their distinct energy precision

D. Schulte

H. Abramowicz, *et al* - arXiv:1807.02441

Beamstrahlung Kills high-*E* LCs

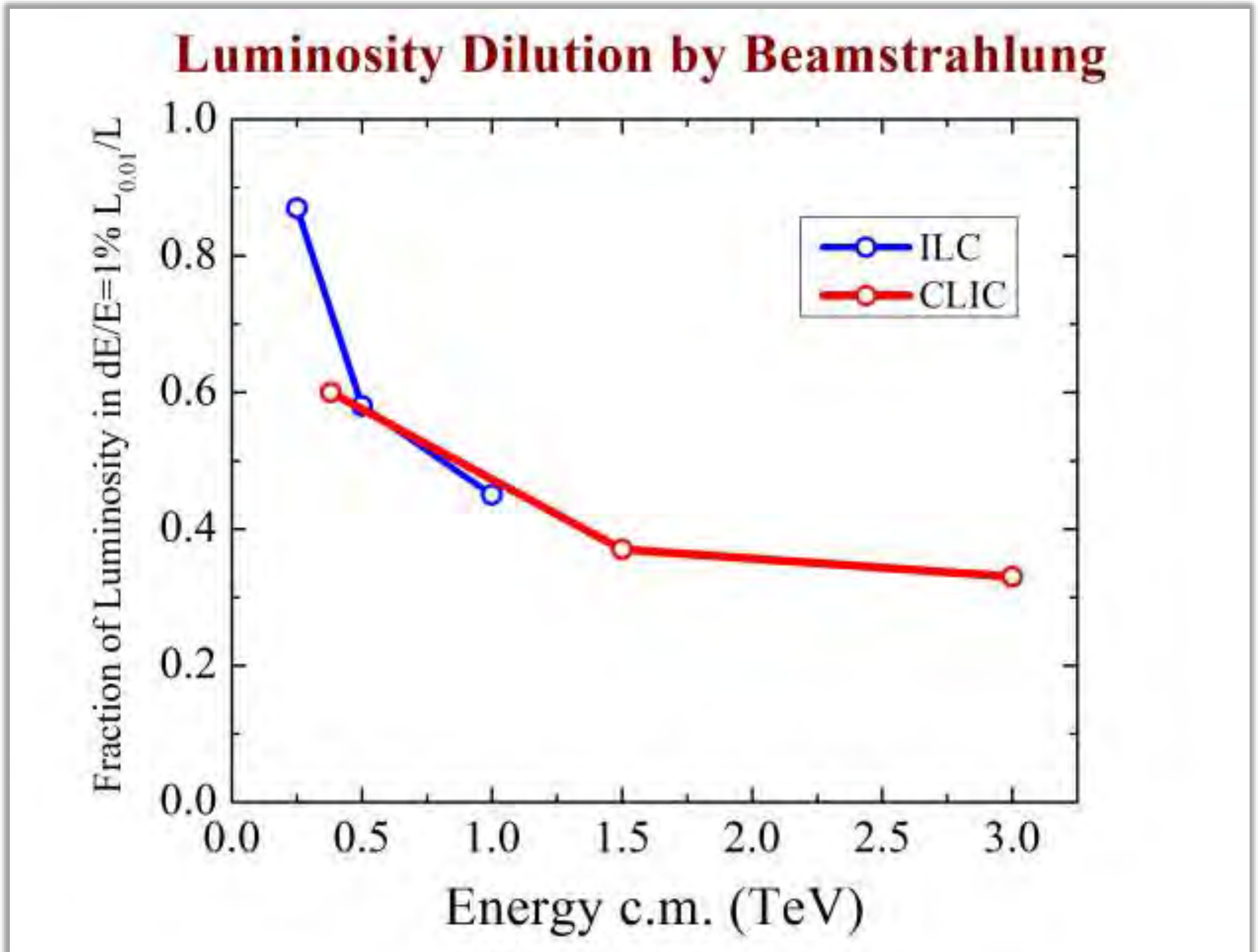

Beamstrahlung rms energy spread :

$$\delta_{BS} \propto \left(\frac{E_{cm}}{\sigma_z}\right)\frac{N^2}{\sigma_x^2}$$

→ Luminosity :

$$L \propto P_{beam}\sqrt{\frac{\delta}{\gamma\varepsilon_y}}H_D$$

How to get Luminosity

- To increase probability of direct e^+e^- collisions (luminosity) and birth of new particles, beam sizes at IP must be very small
- Eexemplary beam sizes just before collision (500GeV CM):
  250 * 3 * 110000 nanometers
  (x y z)

Vertical size is smallest

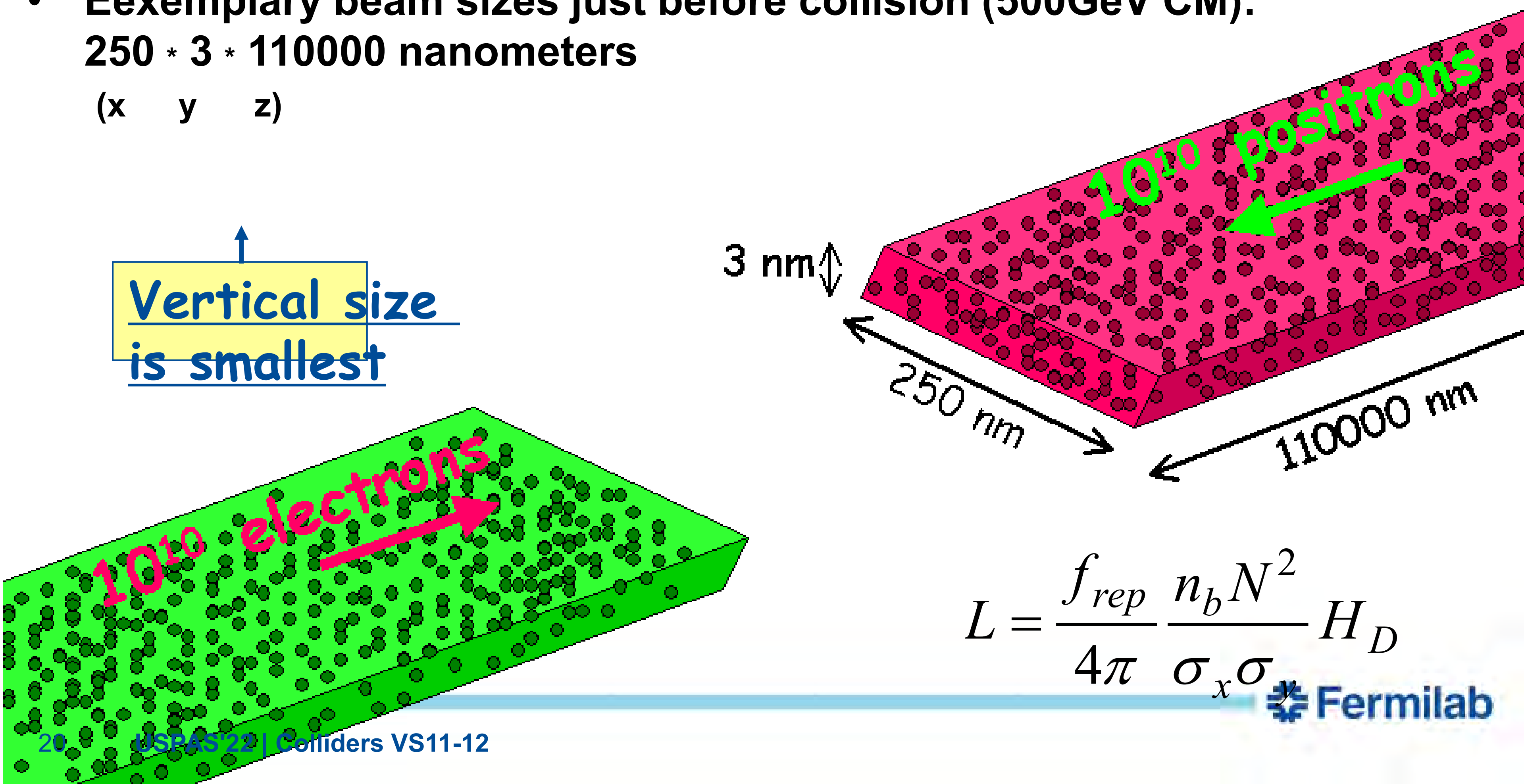

$$L = \frac{f_{rep}}{4\pi} \frac{n_b N^2}{\sigma_x \sigma_y} H_D$$

Smallest size at IP and chromaticity of FF

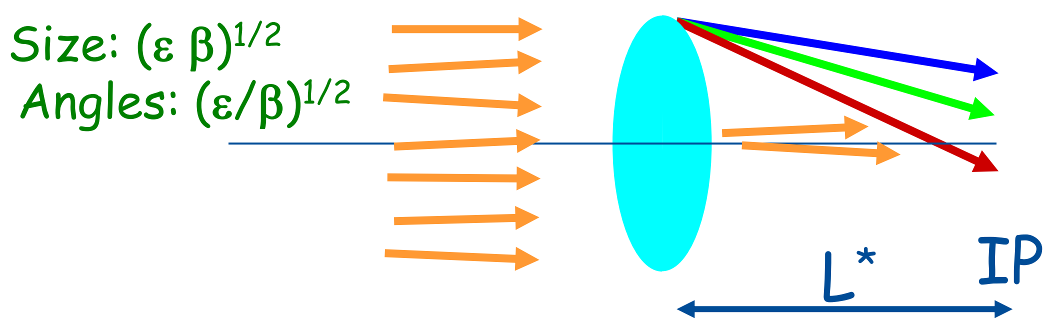

Size at IP:
$L^*\ (\varepsilon/\beta)^{1/2}$
$+\ \ (\varepsilon\ \beta)^{1/2}\ \sigma_E$

Beta at IP:
$L^*\ (\varepsilon/\beta)^{1/2} = (\varepsilon\ \beta^*)^{1/2}$
$\Rightarrow\ \ \beta^* = L^{*2}/\beta$

Chromatic dilution:
$(\varepsilon\ \beta)^{1/2}\ \sigma_E\ /\ (\varepsilon\ \beta^*)^{1/2}$
$= \sigma_E\ L^*/\beta^*$

- **The last (final) lens need to be the strongest**
  - (two lenses for both x and y => "Final Doublet" or FD)
- **FD determines chromaticity of FF**
- **Chromatic dilution of the beam size is $\Delta\sigma/\sigma \sim \sigma_E\ L^*/\beta^*$**

Typical:
σ_E -- energy spread in the beam ~ 0.01
L^* -- distance from FD to IP ~ 3 m
β^* -- beta function in IP ~ 0.1 mm

- **For typical parameters, $\Delta\sigma/\sigma \sim 300$ too big !**
- **=> Chromaticity of FF need to be compensated**

Fermilab

SR in FF magnets

Chromaticity is cancelled **locally** by two sextupoles **interleaved with FD**, a bend upstream generates dispersion across FD

Geometric aberrations of the FD sextupoles are cancelled by two more sextupoles placed in phase with them and upstream of the bend

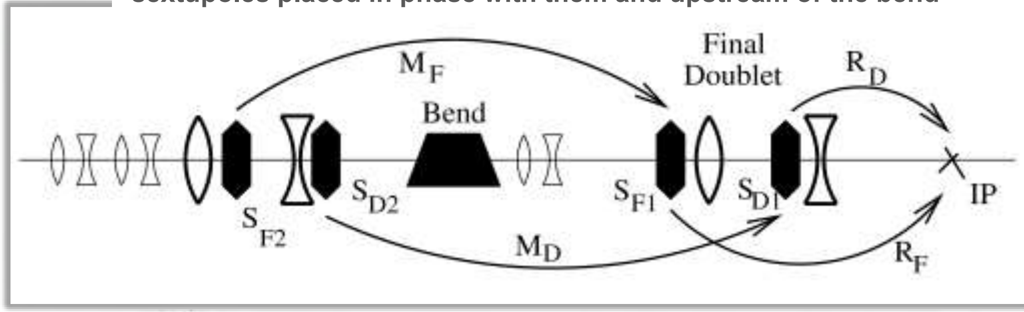

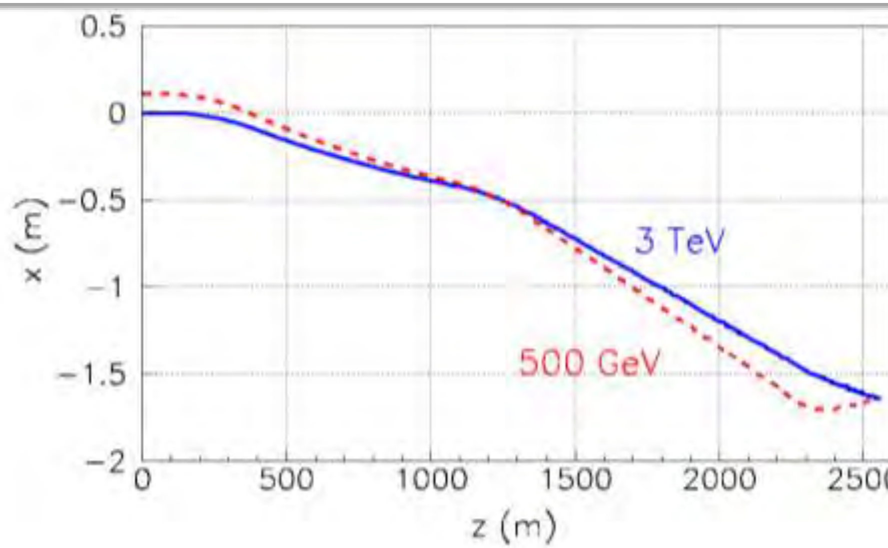

CLIC 3-TeV and 500-GeV BDS (M. Aleksa et al., 2003, CLIC-Note-551

- Bends are needed for compensation of chromaticity
- SR causes increase of energy spread which may perturb compensation of chromaticity
- Bends need to be long and weak, especially at high energy
- SR in FD quads is also harmful (*Oide effect*) and may limit the achievable beam size

K. Oide, Phys. Rev. Lett. 61, 1713 (1988)

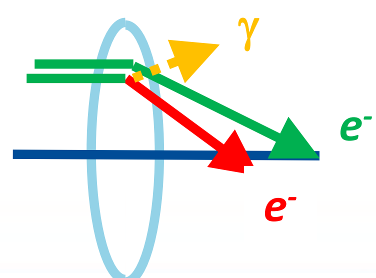

final quadrupole lens

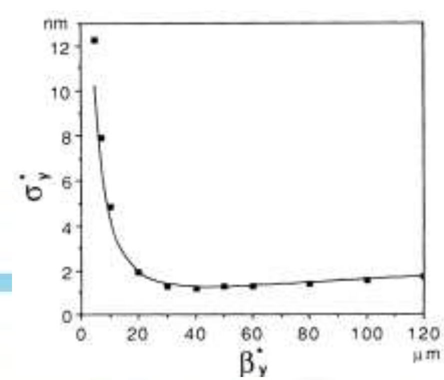

Oide effect (SR in Final Doublet)

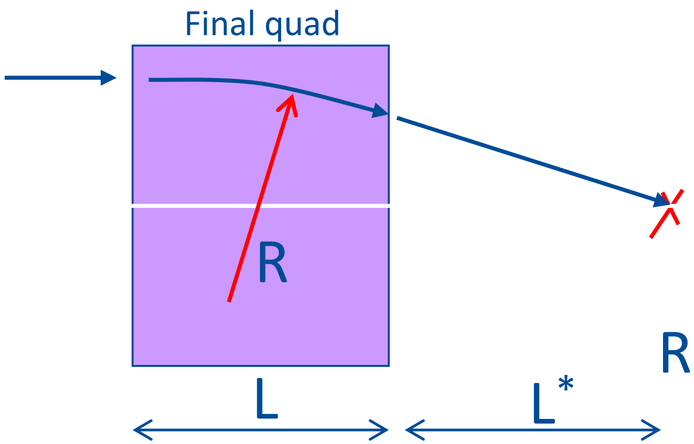

IP divergence:

$$\theta^* = \sqrt{\varepsilon/\beta^*}$$

IP size:

$$\sigma^* = \sqrt{\varepsilon\,\beta^*}$$

Energy spread obtained in the quad:

$$\left(\frac{\Delta E}{E}\right)^2 \approx \frac{r_e\,\lambda_e\,\gamma^5\,L}{R^3}$$

Radius of curvature of the trajectory: $R = L/\theta^*$

Growth of the IP beam size: $\sigma^2 \approx \sigma_0^2 + \left(L^*\,\theta^*\right)^2 \left(\frac{\Delta E}{E}\right)^2$

Which gives $\sigma^2 \approx \varepsilon\beta^* + C_1 \left(\frac{L^*}{L}\right)^2 r_e\,\lambda_e\,\gamma^5 \left(\frac{\varepsilon}{\beta^*}\right)^{5/2}$ (where C_1 is ~ 7 (depend on FD params.))

This achieve minimum possible value:

$$\sigma_{min} \approx 1.35\, C_1^{1/7} \left(\frac{L^*}{L}\right)^{2/7} \left(r_e\,\lambda_e\right)^{1/7} \left(\gamma\varepsilon\right)^{5/7}$$

When beta* is:

$$\beta_{optimal} \approx 1.29\, C_1^{2/7} \left(\frac{L^*}{L}\right)^{4/7} \left(r_e\,\lambda_e\right)^{2/7} \gamma \left(\gamma\varepsilon\right)^{3/7}$$

Note that beam distribution at IP will be non-Gaussian. Usually need to use tracking to estimate impact on luminosity. Note also that optimal β may be smaller than the σ_z (i.e. cannot be used).

All Linear Colliders Assume Crab-Crossing

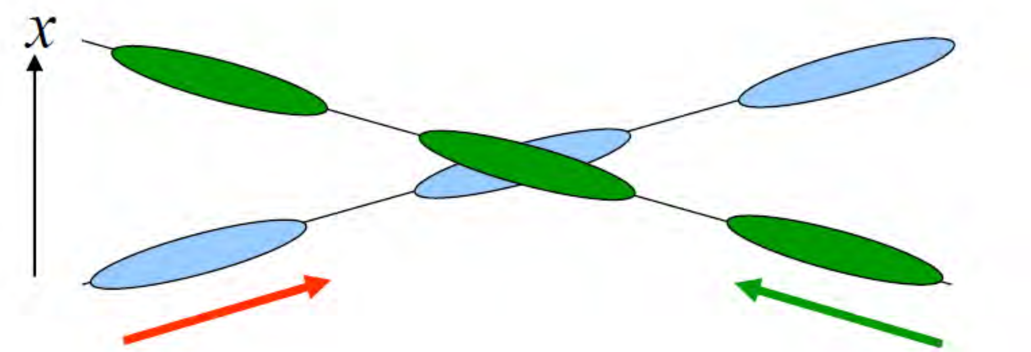

With crossing angle θ_c, the projected x-size is $(\sigma_x^2+\theta_c^2\sigma_z^2)^{0.5} \sim\theta_c\sigma_z \sim 4\mu m$

→ several time reduction in L without corrections

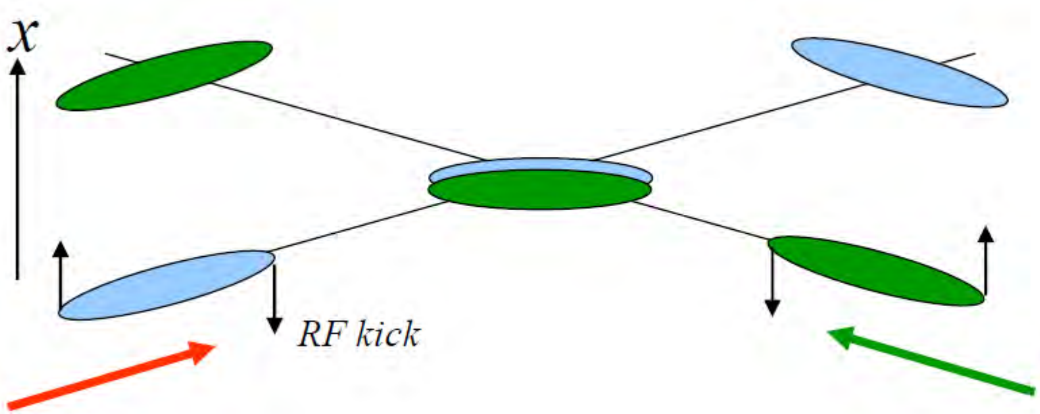

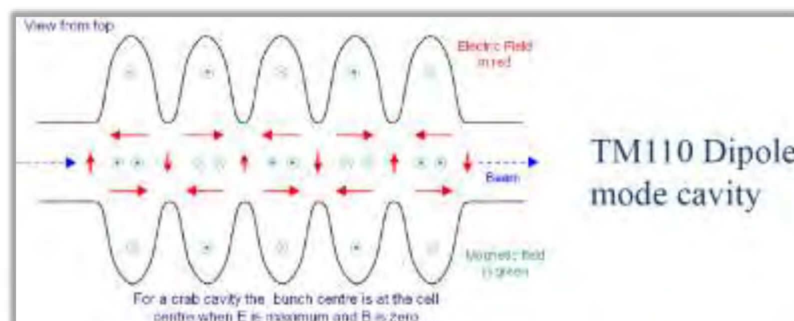

Use transverse (crab) RF cavity to 'tilt' the bunch at IP

Disruption parameter

- Strong fields will distort the opposing beam
- Normalized beam-beam focusing force at the IP:

$$K_{x,y} = \frac{2\lambda r_e}{\gamma\sigma_{x,y}(\sigma_x + \sigma_y)} \qquad x'' + Kx = 0$$

- Disruption parameter defined using thin lens approximation and comparing focal to bunch length

$$D_{x,y} \equiv \frac{\sigma_z}{f_{x,y}} = \frac{2Nr_e\sigma_z}{\gamma\sigma_{x,y}(\sigma_x + \sigma_y)} \quad = 2\pi\xi_y\sigma_z/\beta^*_y$$

- Assume a rectangular distribution → number of oscillations in opposing bunch:

$$n \approx 1.3\frac{\sqrt{D}}{2\pi}$$

Disruption Parameter D_y and "Travelling Focus"

At modest D~3-10 → luminosity enhancement due to "traveling focus"

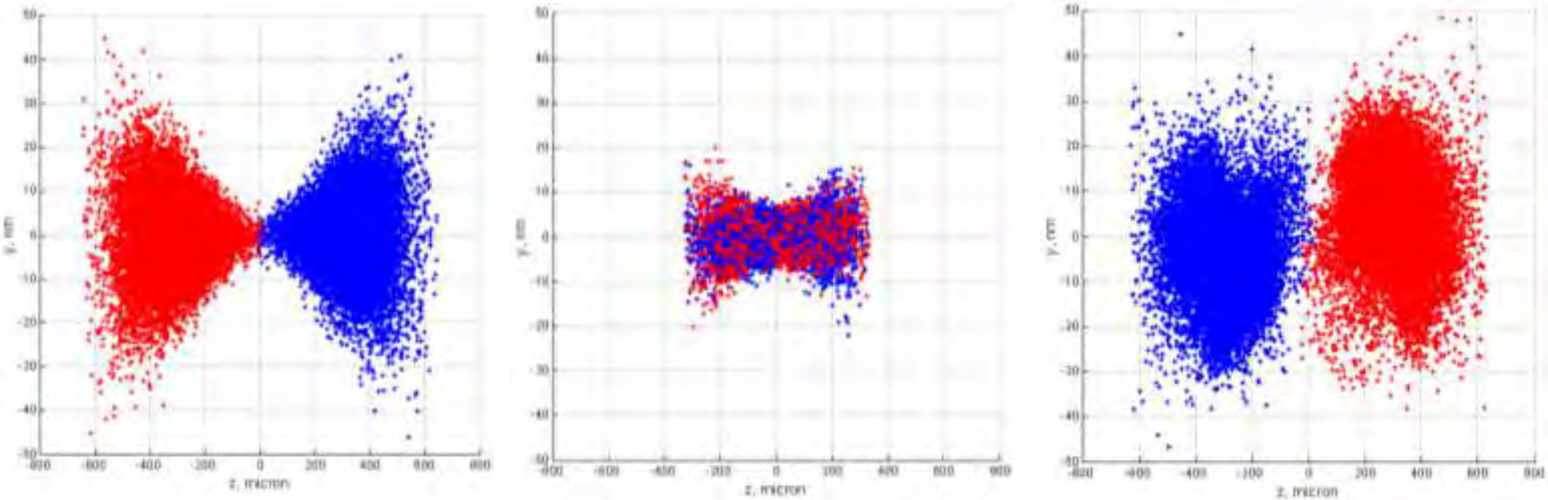

D_y~12

At large D>15 → luminosity destruction by "kink instability"

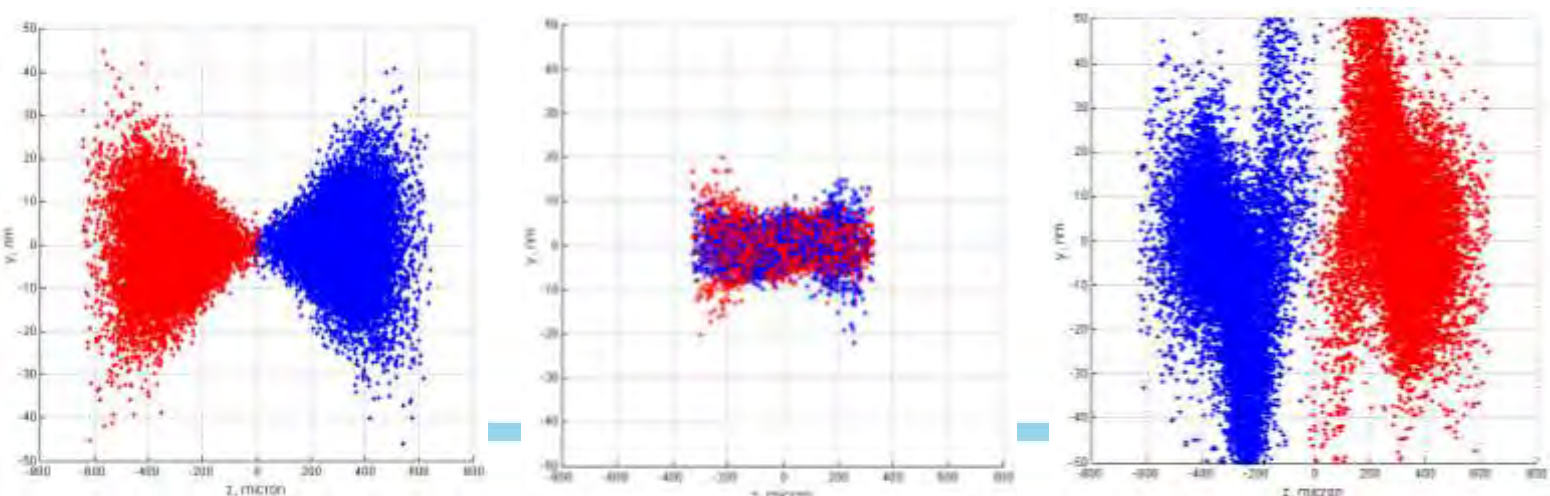

Nx2
D_y~24

Fermilab

Trajectory Stability and Control

- Two effects due to ground motion, vibrations, jitter and other mechanical and EM noises:
  - Two beams get separated at the IP (rms Y size few nm)
  - Each beam goes thru not ideal trajectory along its linac and experiences either dipole kicks due to displacement in quadrupoles Kick ~ B-Gradient x Position or a kick in RF cavity due to a wakefield or (if the cavity is tilted) Kick~E-Gradient x Tilt → ***beam-beam separation @IP and emittance growth***
- Ways to counteract (if necessary) are:
  - Mechanical stabilization of most important elements (eg FF)
  - Beam-based feedback systems acting either from pulse to pulse or (if bunch train is long) from bunch-to-bunch
  - Note that FB systems also introduce “noise” if eg BPMs have position measurement error *O* (1 micron)

Stability – tolerance to Final Doublet motion

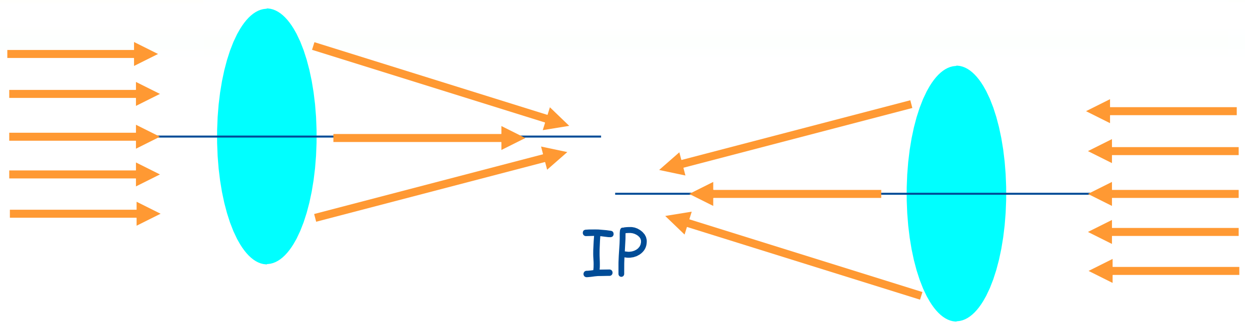

- Displacement of FD by dY cause displacement of the beam at IP by the same amount → Therefore, stability of FD need to be maintained with a fraction of nanometer accuracy
- Such small offsets of FD or beams can be detected using beam-beam deflection
- Linac misalignments affect dY as well:

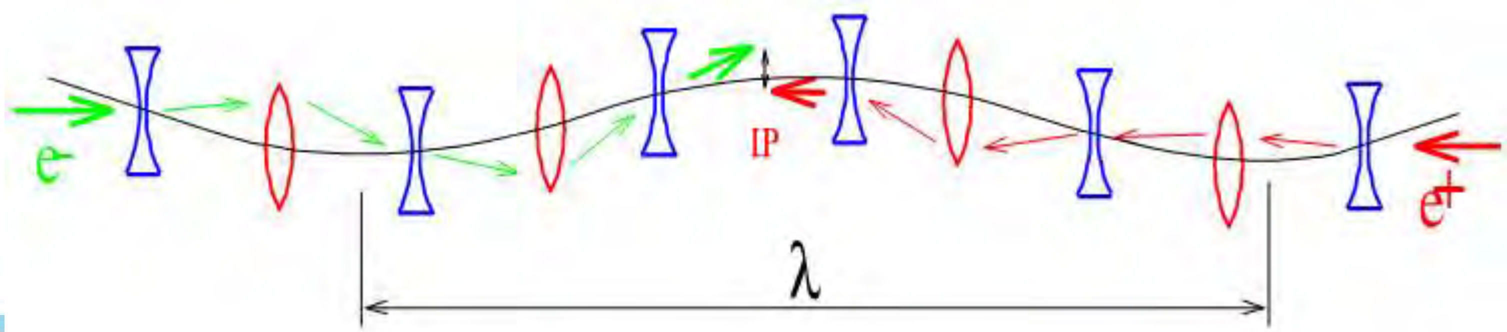

Of course, what matters is differential motion with wavelength < betatron one (i.e. differential quad-to-quad motion)

Fast Vibrations (*f*> *f_rep/6*)

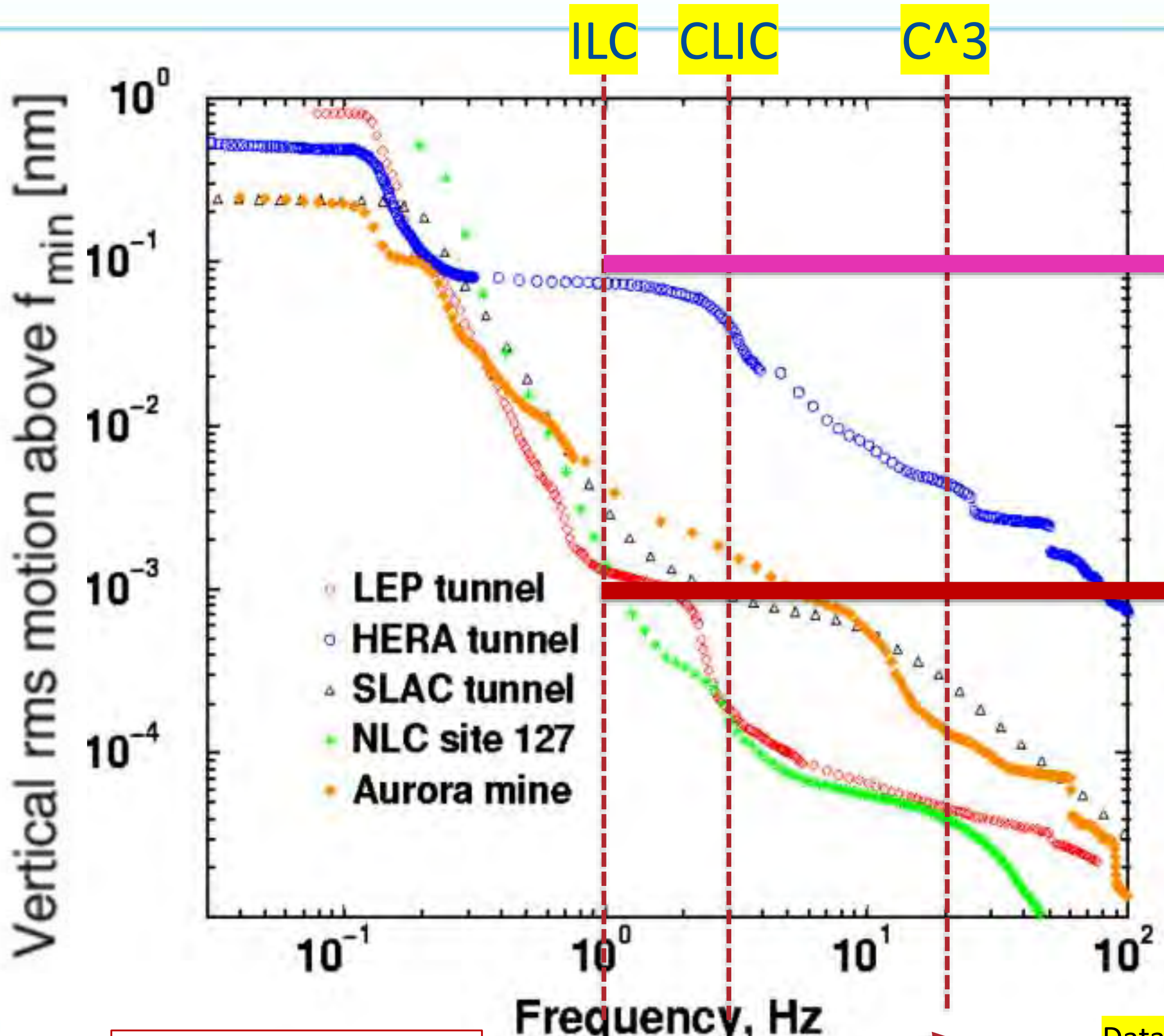

Approx. tolerable level for **linac elements**: depends on machine parameters – see below

Approx. tolerable level for **FF elements**: depends on machine parameters – see below

Below these frequencies FB systems can possibly control GM effects

Data for relatively quiet conditions on tunnel floors ("ground motion")

Example Issue: Ground Motion at CLIC

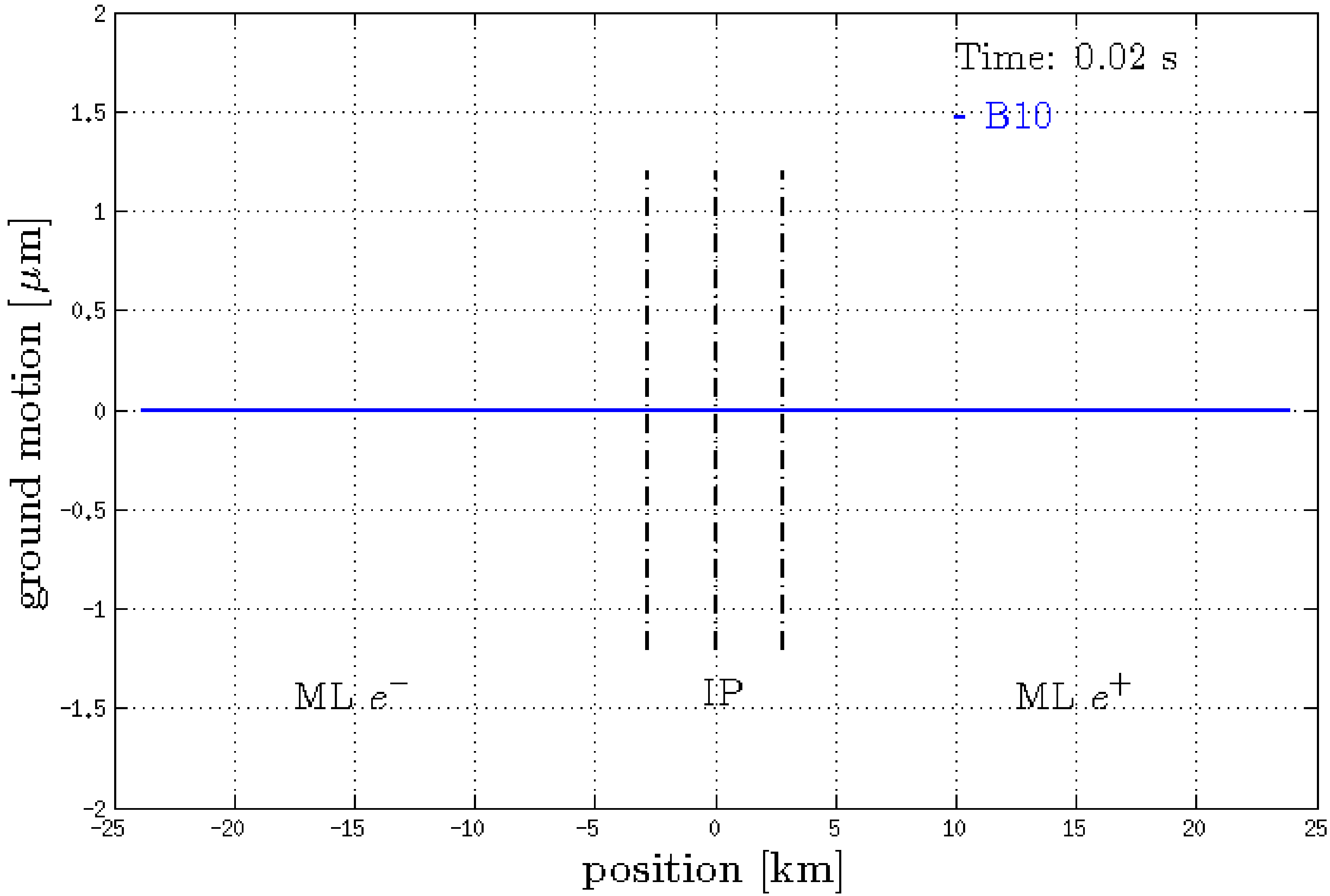

J. Pfingstner

Resulting Beam Jitter (CLIC)

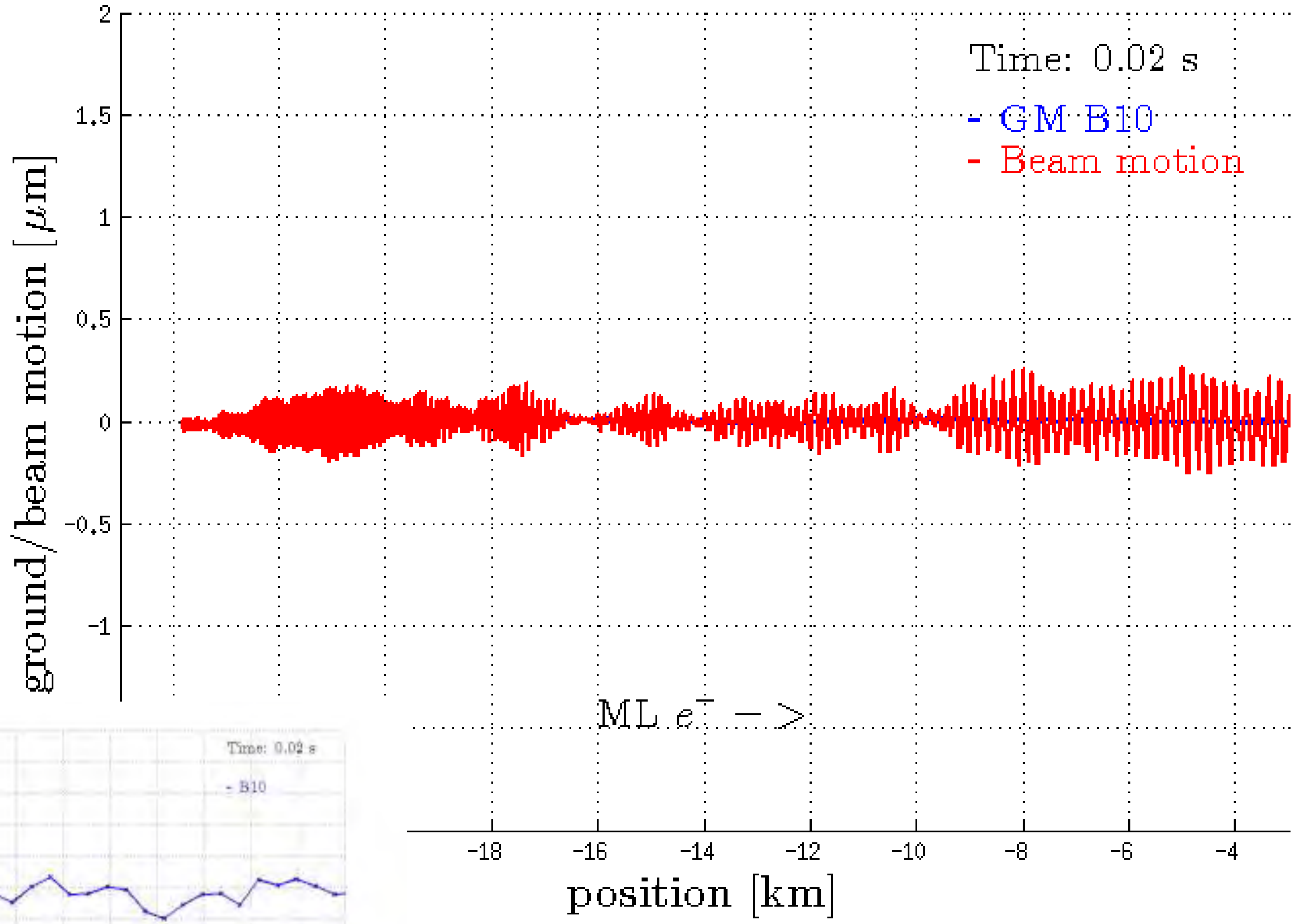

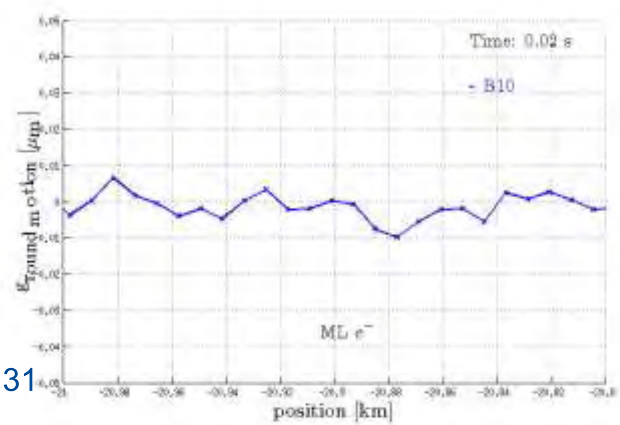

J. Pfingstner

Fermilab

Beams at Collision (CLIC)

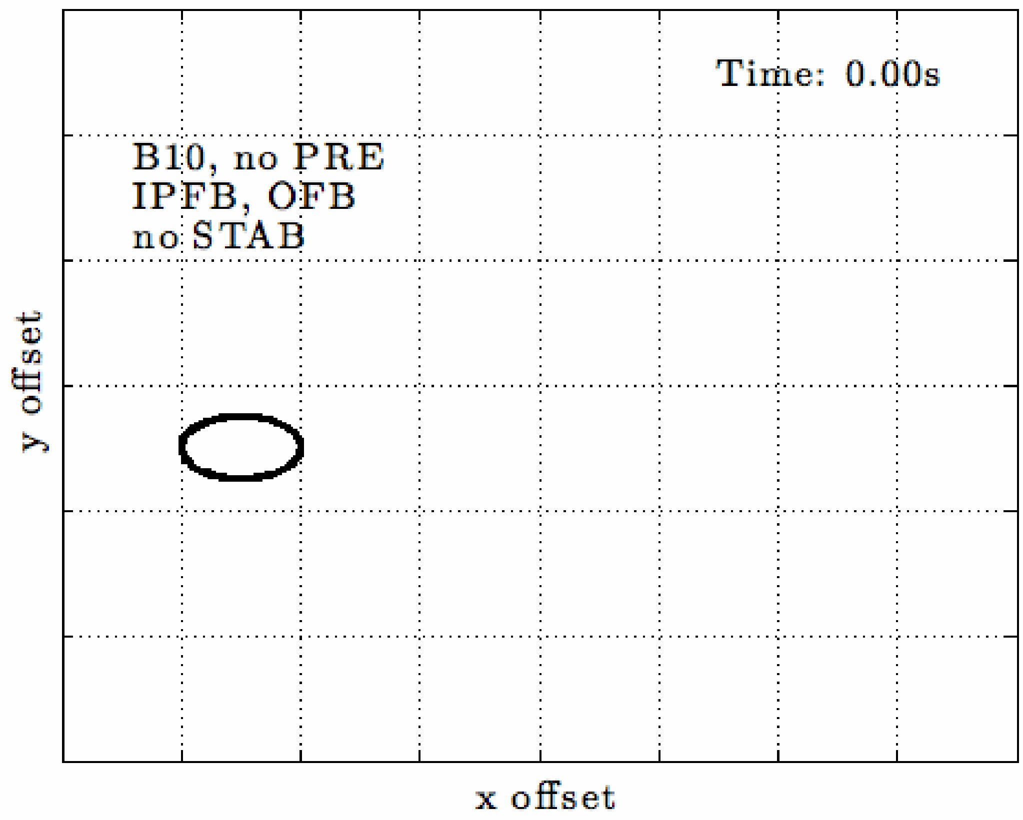

J. Pfingstner

Beams at Collision + Feedback (CLIC)

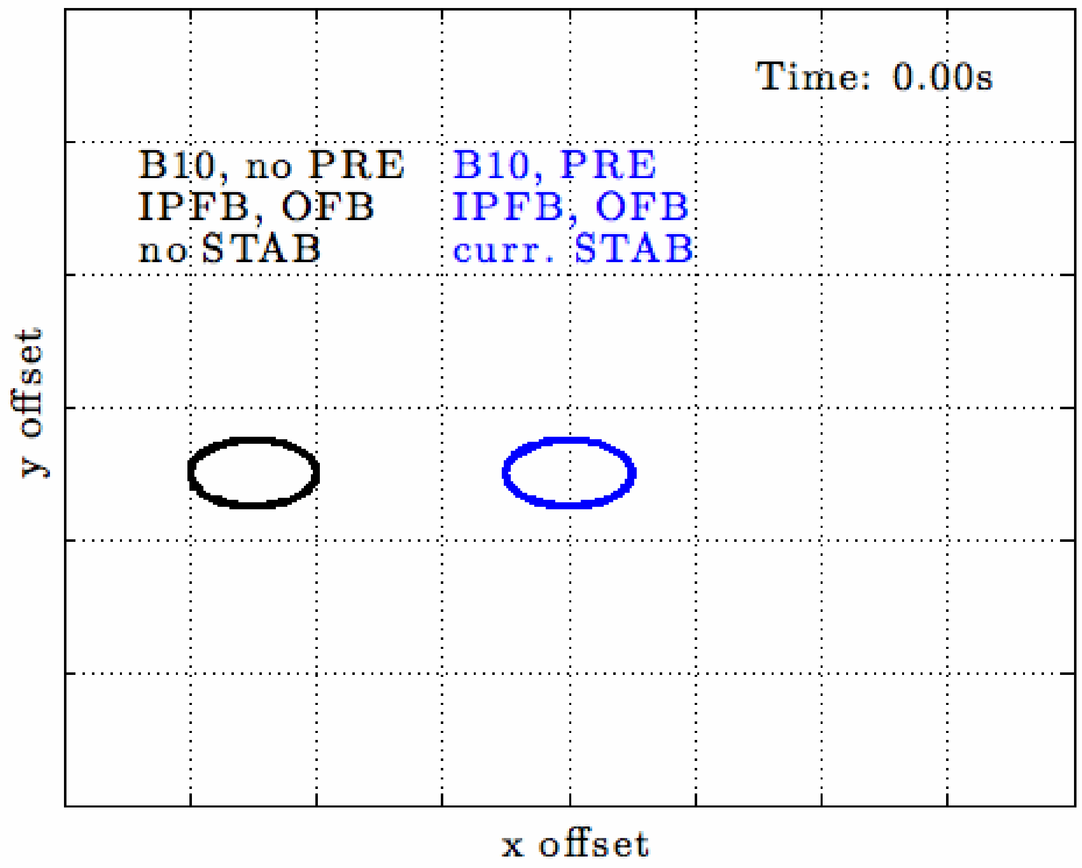

J. Pfingstner

Diffusive Ground Motion: ATL Law

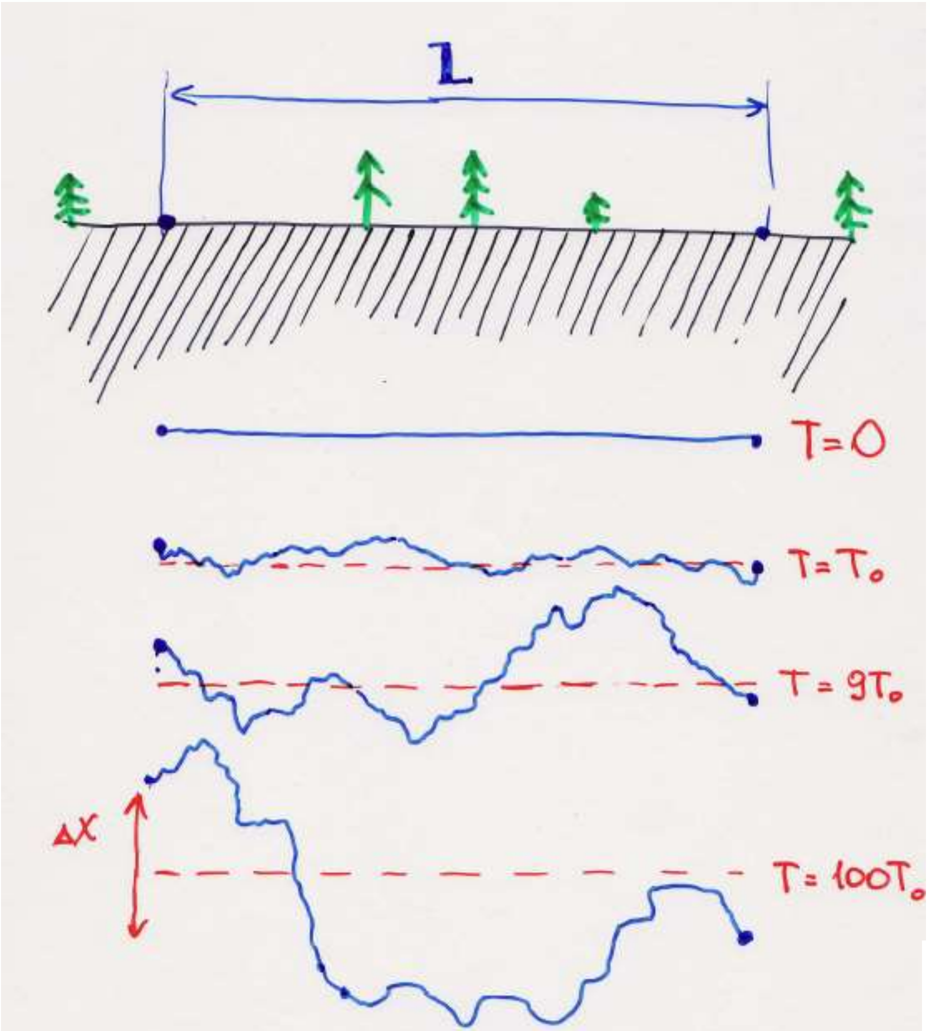

Diffusive ground motion is an indication of fractal dynamics of ground/tunnel elements at the scale of min to years, m to 10's km

Observed essentially at all accelerators

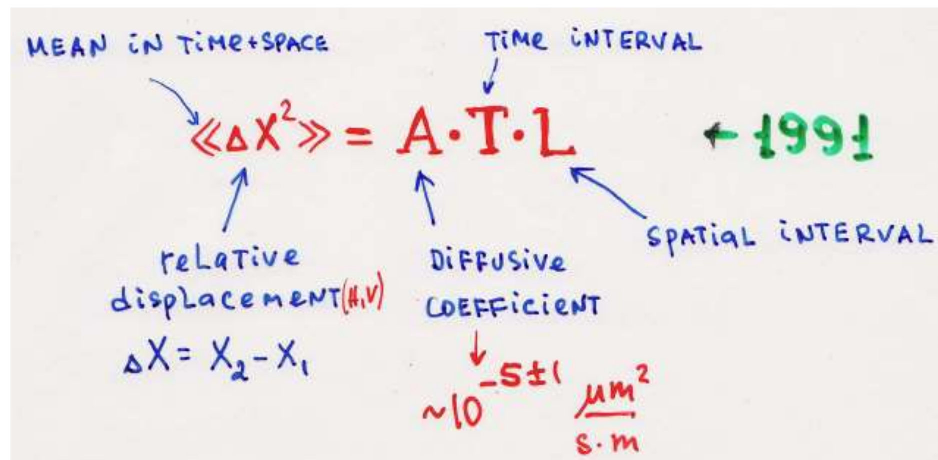

Diffusion coefficient ***A*** is dependent on site geology, depth and tunnel construction technique

In linear colliders – Diffusion of trajectories

ATL diffusion of
quadrupole positions - simulations for ILC
and
X, Y beam trajectories in BPMs along the linac

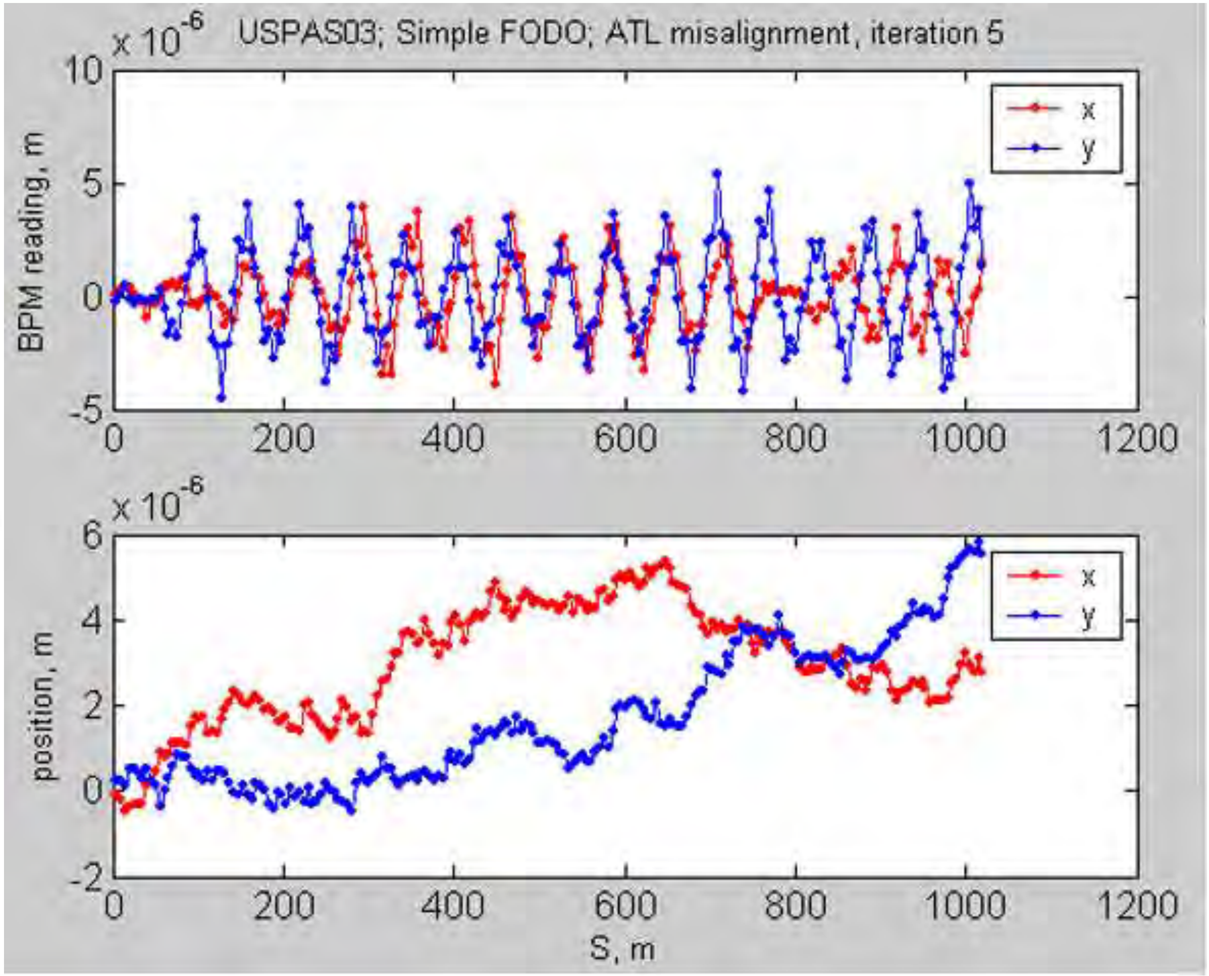

ATL+vibrations require continuous corrections by high resolution feedback systems (BPMs+correctors)

LC: Long-Term Stability and Correction

understanding of ground motion and vibration spectrum important

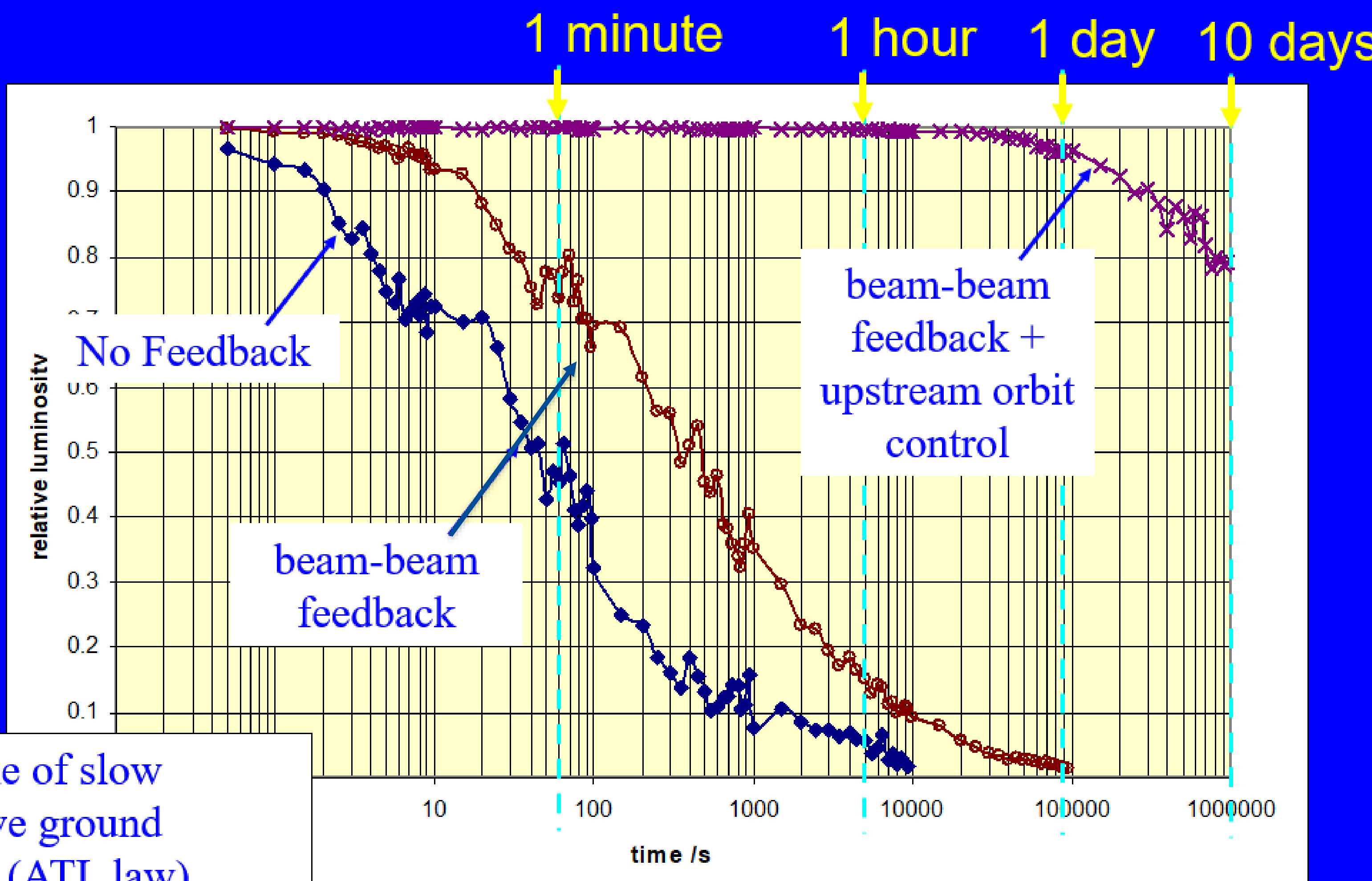

example of slow diffusive ground motion (ATL law)

Muon Colliders:

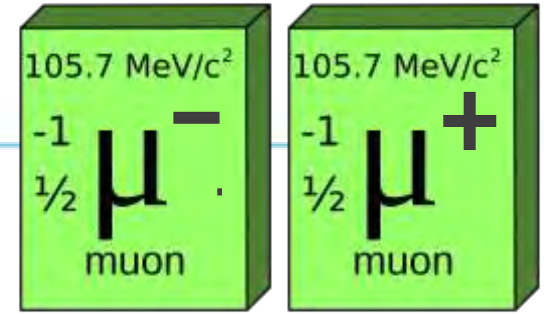

- (Considered by many as) the most viable option for HEP future:
  I. ~ x7 energy reach vs *pp*
  II. *μ*'s do not radiate when bent → acceler'n in rings:
     1. *(Best) power efficiency*
     2. *Smaller(est) footprint*
     3. *Low(est) cost*
  III. Based on traditional accelerator technologies *NC/SC magnets, NC/SC RF*
- (some believe that) 3-10 TeV cme Muon Collider can be designed in ~10-15 yrs and built in 20-25 yrs from now

Protons *(particles of choice for energy frontier till now)*

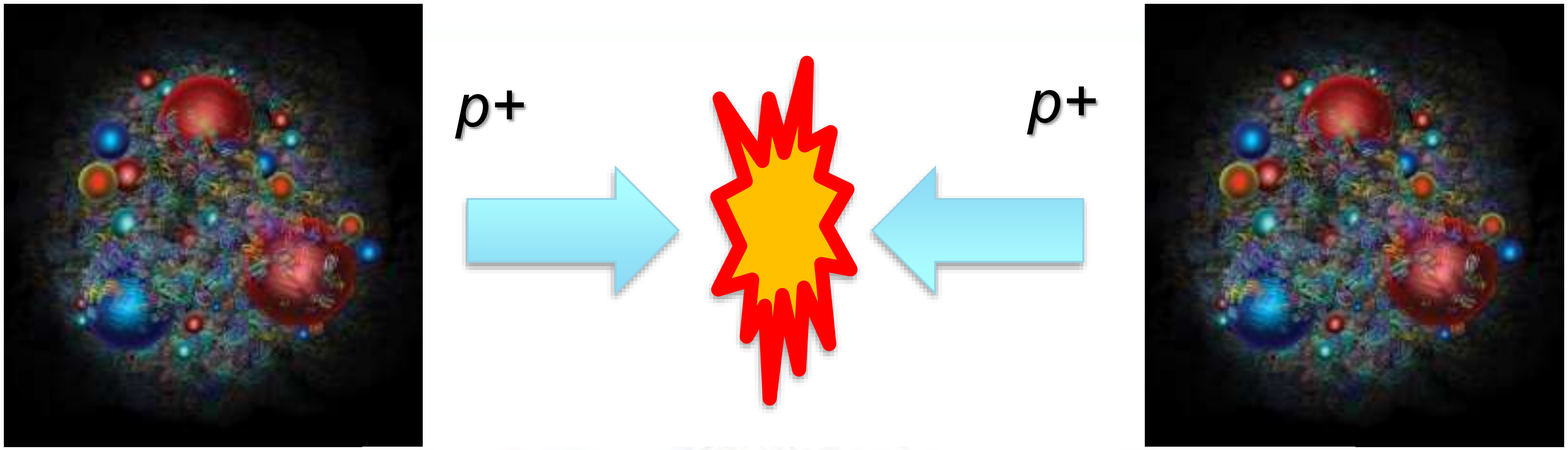

Parton Luminosity Falls OFF with (E/E_{max})

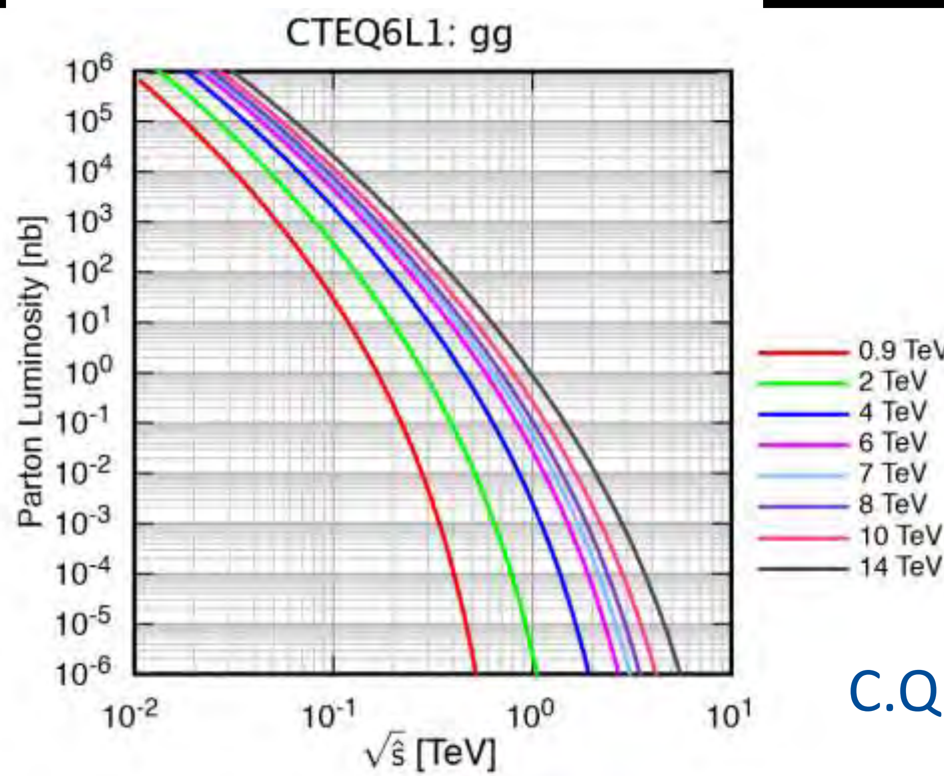

$E_{max}=2E_{beam}$

C.Quigg et al

Muons *(particles of choice for future colliders)*

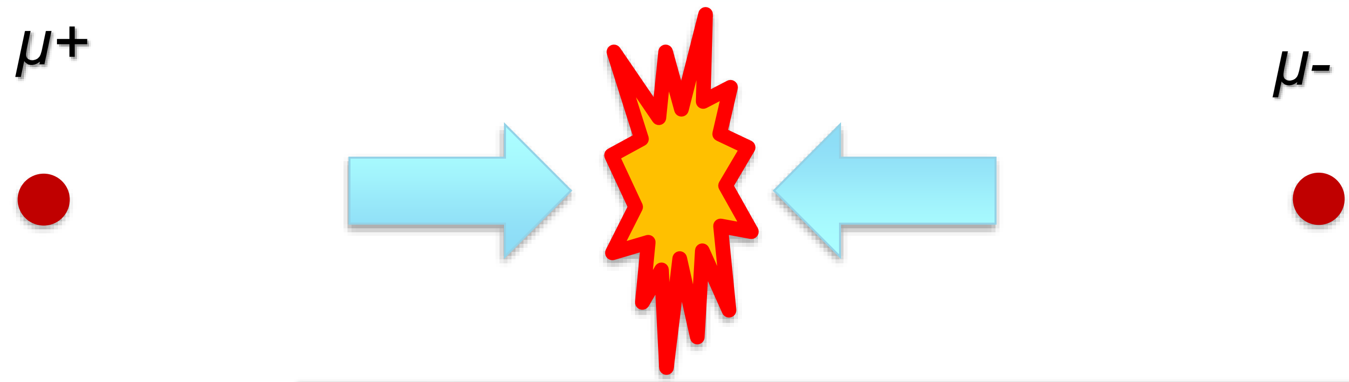

Luminosity Spectrum
vs (E/E_{max})

$E_{max}=2E_{beam}$

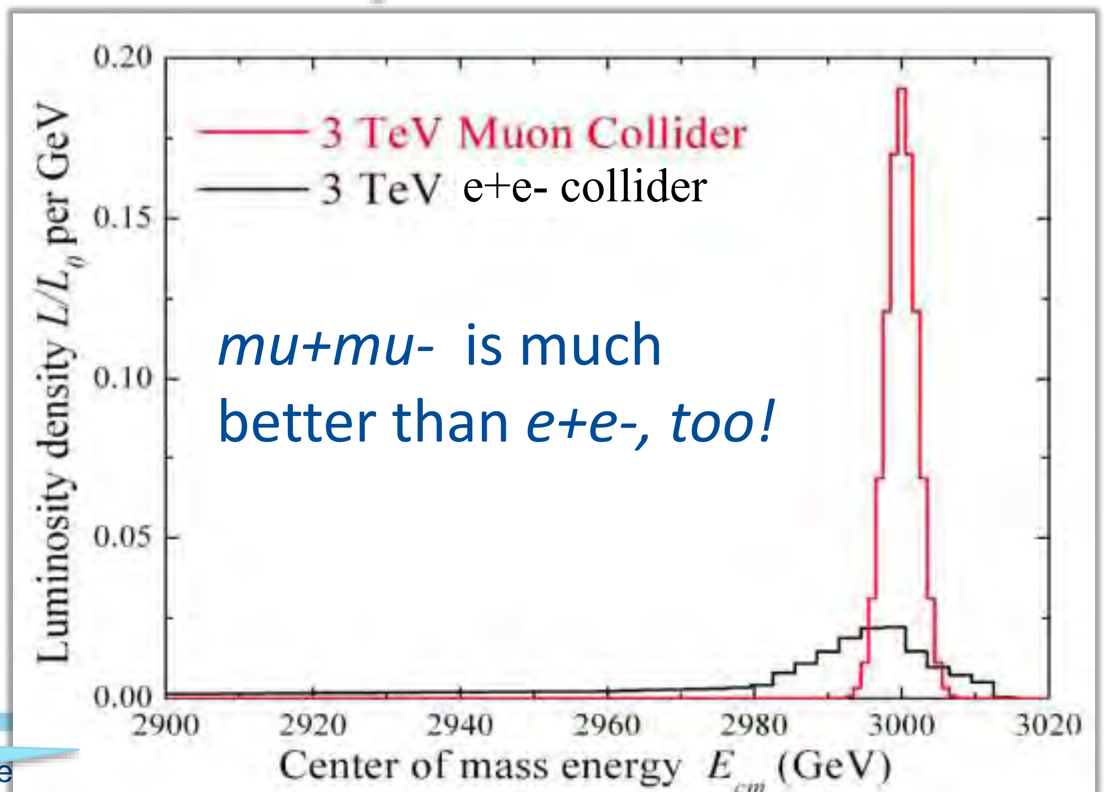

S.Geer, Ann.Rev. (2009)
V.Shiltsev, MPLA (2010)

note the range
dE/E=4%

"equivalent" reach in pp after rescaling for pdf's

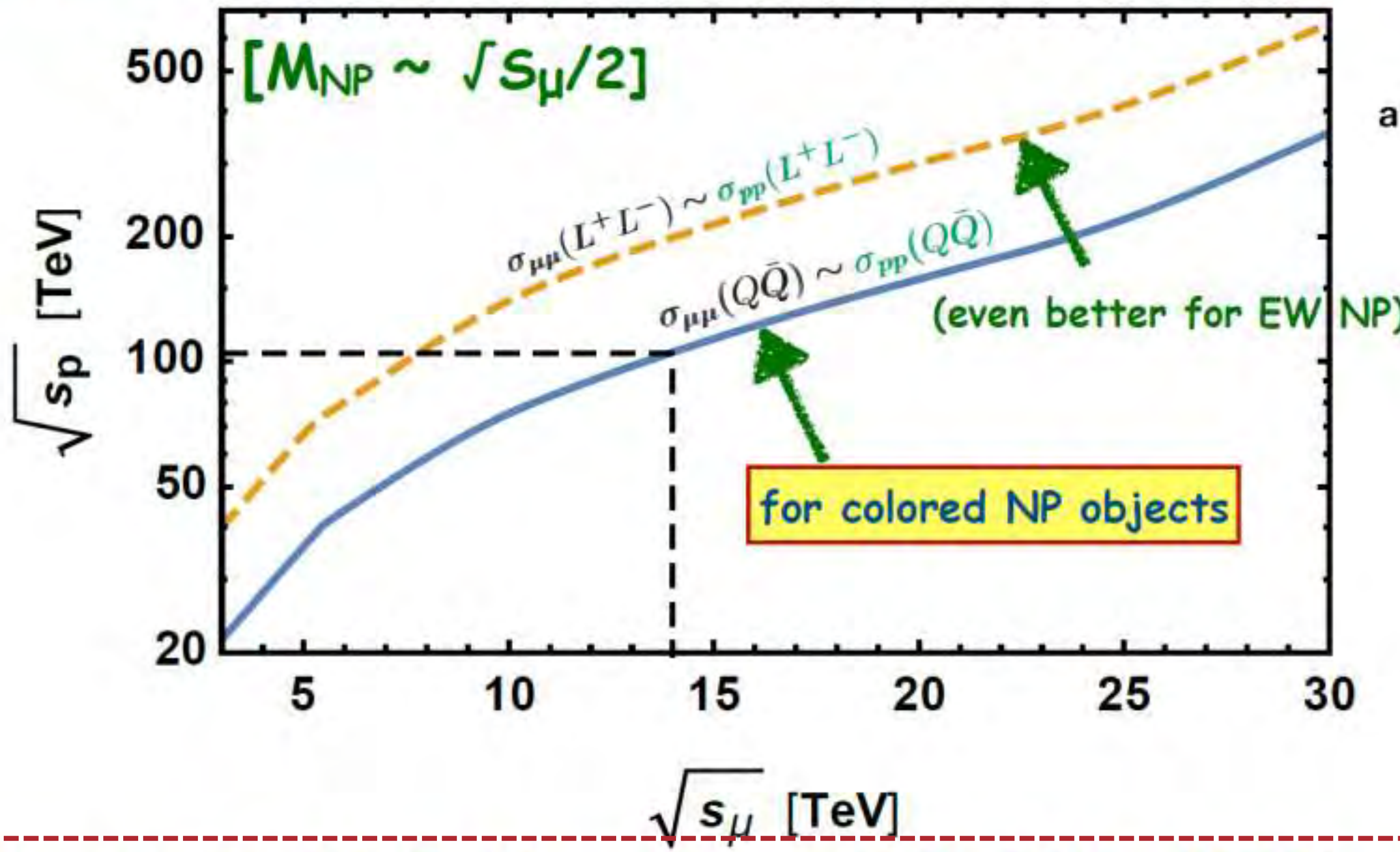

arXiv:1901.06150

* μμ @ 14 TeV → pp @ 100 $(200)_{EW}$ TeV !
* μμ @ 30 TeV → pp @ 350 $(600)_{EW}$ TeV !!

yet unexplored pheno !!!

Comparison of Particle Colliders

To reach higher and higher collision energies, scientists have built and proposed larger and larger machines.

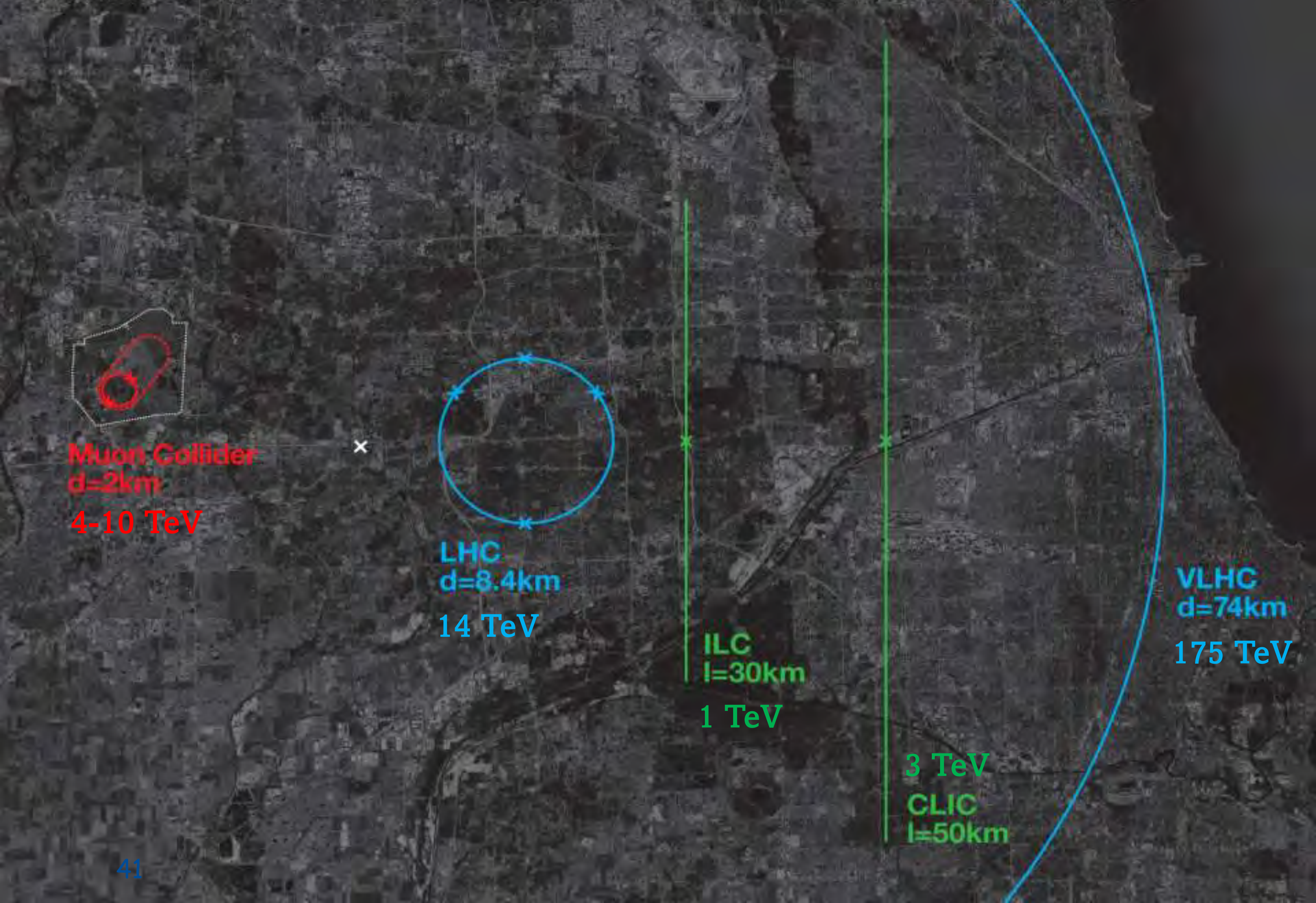

Why the cost is so low ?

Only compared to other energy frontier colliders!!! It's still high ~(1-2) x cost of the LHC

A. (Most important) much less RF

RF is (5-10) times more expensive than magnets per TeV (re-use RF ! multi-turn acceleration)

because muons do not radiate Syncnrotron radition (γ = 1/210 of $e+e$-)

B. (Smaller) size matters

Because of multi-turn acceleration and factor of ~7 c.m. energy advantage vs *pp*

C. (Lower) Power consumption

Effective multi-turn acceleration and SC magnets → same demand as LHC ~1 TWh/yr

because muons do not radiate Syncnrotron radition (γ = 1/210 of $e+e$-)

More Beam Power to increase Lumi

Ratio:

Lumi/Power

for various collider types and energies

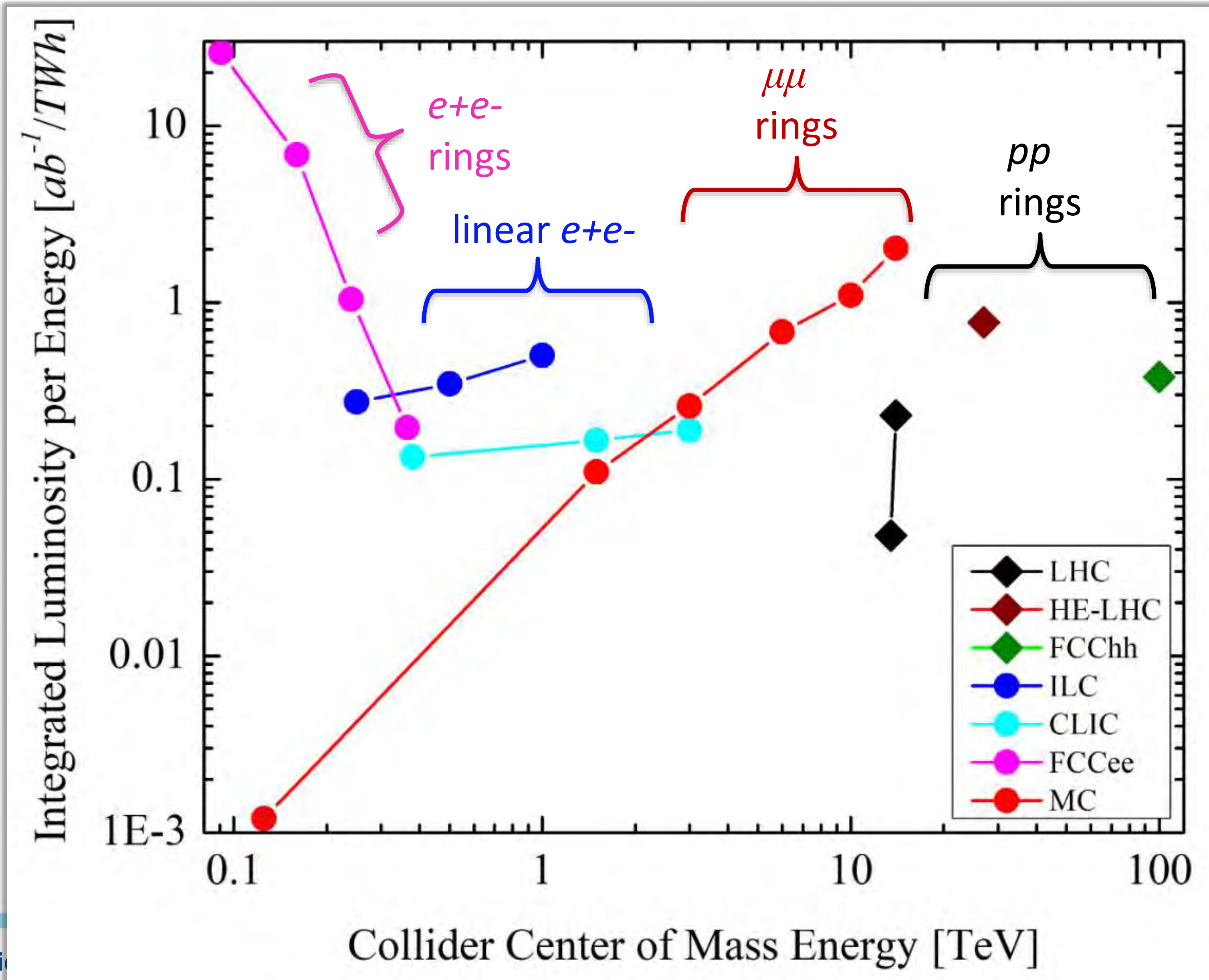

Muon Colliders: Main Challenges

- Muons are not stable particles
  - Muon lifetime at rest (mc^2=0.105 GeV) is 2.2 microseconds
  - Muon lifetime at 5 TeV (collider $\gamma \approx 50000$) is 100 milliseconds
  - Muon can be made available only as secondary or tertrially particle products of reactions like
    - *p*(beam)+*p*(target)→ K,π → μ
    - e+e- → μ+μ-
    - γ + Ze → μ+μ-
- That usually results in large emittance (large angular spread) muon beams and requires deep cooling for **high Luminosity**
- Therefore, major challenges for High Luminosity MC are:
  - Muon production
  - Fast muon cooling
  - Fast muon acceleration
  - Neutrino flux hazard

Luminosity Goal

arXiv:1901.06150

Collecting 100 events might be sufficient to discover new particles with easily identifiable decay products, such as Stops and Top Partners related with Naturalness. An instantaneous luminosity of $2 \cdot 10^{33}\mathrm{cm}^{-2}\mathrm{s}^{-1}$, at 10 TeV, would be sufficient to probe these particles up to the collider reach. Ten thousands events would instead be needed to aim at percent-level measurements of electroweak SM processes at high invariant mass, allowing to probe hundreds of TeV New Physics scales indirectly as previously mentioned. In this case the luminosity requirement becomes:

$$L \gtrsim \frac{5\,\mathrm{years}}{\mathrm{time}} \left(\frac{\sqrt{s_\mu}}{10\,\mathrm{TeV}} \right)^2 2 \cdot 10^{35}\mathrm{cm}^{-2}\mathrm{s}^{-1}$$

i.e., about 1-2 ab^{-1} per year

Average Luminosity of Muon Collider

NB: each muon makes ~300B[T] turns in a ring with average field B

$$\langle \mathcal{L} \rangle = f_0 \gamma^2 \frac{c\tau_0}{2C} \frac{n_\mathrm{b} N^2}{4\pi\varepsilon_\mathrm{n}\beta^*} \mathcal{F} = B P_\mathrm{b} \frac{N r_0}{4\pi\varepsilon_\mathrm{n}} \frac{\gamma}{\beta^*} \left(\frac{c\tau_0 \mathcal{F}}{8\pi e} \right)$$

scales with B, the total beam power P_b, and the beam brightness (the third factor above is the beam-beam ξ)

The beta-function at the two IPs scales as $\beta^* \sim 1/\gamma$ within certain range of energies, giving overall scaling **Lumi ~ γ^2** with other limiting parameters fixed. The main challenges to luminosity achievement with decaying particles are related to production and fast cooling and acceleration of $O(10^{12})$ muons per bunch without emittance degradation.

(Explanatory to Previous slide)

$$\Delta \int \mathcal{L} \approx \sum_{i=0}^{\infty} \frac{\left(N_0 e^{-i\Delta t/\gamma\tau}\right)^2}{4\pi\sigma_x\sigma_y} \leftarrow \sum_{i=0}^{\infty} \left(N_0 e^{-i\Delta t/\gamma\tau}\right)^2 \propto N_0^2 B$$

$$\Delta \int \mathcal{L} \propto \frac{BN_0^2}{4\pi\epsilon\beta/\gamma}$$

$$\beta \approx \sigma_z \qquad \frac{\sigma_E}{E} = \text{const}$$

$$\beta \propto \frac{1}{\gamma} \qquad \sigma_E\sigma_z = \text{const}$$

$$\sigma_z \propto \frac{1}{\gamma}$$

Note: this might be limited by technology

$$\Delta \int \mathcal{L} \propto B\frac{N_0^2\gamma^2}{\epsilon}$$

$$\mathcal{L} \propto B\frac{N_0}{\epsilon}\gamma P_{beam}$$

Muon Collider Parameter Table

under development by the *International Muon Collider Collaboration*

Target integrated luminosities

$\sqrt{s}$	$\int \mathcal{L}dt$
3 TeV	$1\ \mathrm{ab}^{-1}$
10 TeV	$10\ \mathrm{ab}^{-1}$
14 TeV	$20\ \mathrm{ab}^{-1}$

Reasonably conservative

- each point in 5 years with tentative target parameters
- FCC-hh to operate for 25 years
- Aim to have two detectors
- But might need some operational margins

Note: focus on 3 and 10 TeV
Have to define staging strategy

Tentative target parameters, scaled from MAP parameters

Parameter	Unit	3 TeV	10 TeV	14 TeV
L	$10^{34}\ \mathrm{cm}^{-2}\mathrm{s}^{-1}$	1.8	20	40
N	10^{12}	2.2	1.8	1.8
f_r	Hz	5	5	5
P_{beam}	MW	5.3	14.4	20
C	km	4.5	10	14
<B>	T	7	10.5	10.5
ε_L	MeV m	7.5	7.5	7.5
σ_E / E	%	0.1	0.1	0.1
σ_z	mm	5	1.5	1.07
β	mm	5	1.5	1.07
ε	µm	25	25	25
$\sigma_{x,y}$	µm	3.0	0.9	0.63

Snowmass process to give feedback on this

O(14 TeV) Muon Collider Sub-Systems (approx. to scale)

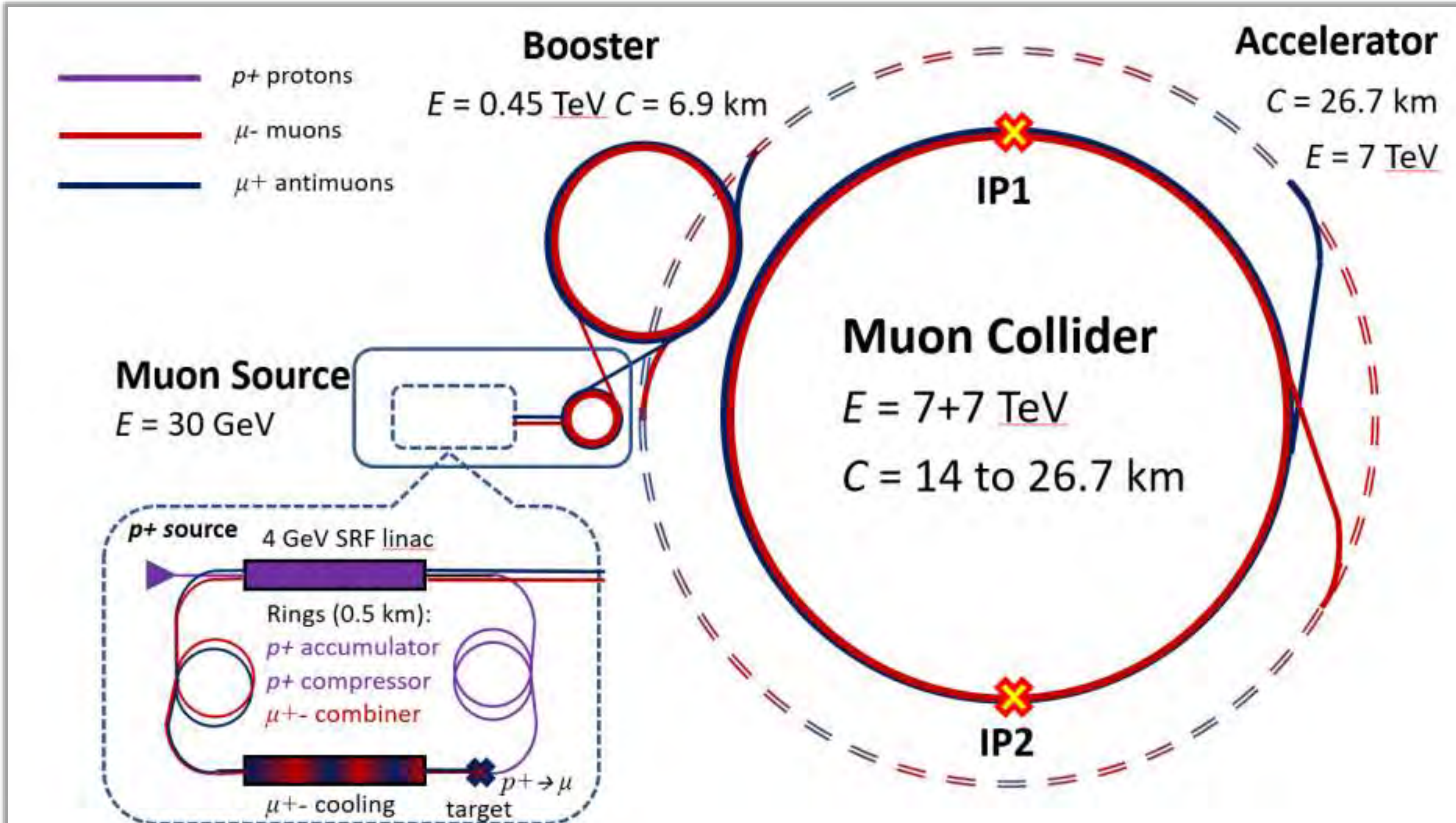

Muon Collider Subsystems

- (i) a high power proton driver (SRF 4 GeV 2-4 MW *H-* linac);
- (ii) pre-target accumulation and compressor rings, in which high-intensity 1-3 ns long proton bunches are formed;
- (iii) a liquid mercury target for converting the proton beam into a tertiary muon beam with energy of about 200 MeV;
- (iv) a multi-stage ionization cooling section that reduces the transverse and longitudinal emittances and, thereby, creates a low emittance beam;
- (v) a multistage acceleration (initial and main) system --- the latter employing a series recirculating rapid cycling synchrotrons (RCS) to accelerate muons in a modest number of turns up to 3-7 TeV using high gradient superconducting RF cavities;
- (vi) about 8.5 km diameter collider ring located some 100 m underground, where counter-propagating muon beams are stored and collide over the roughly 1000--2000 turns corresponding to the muon lifetime.

**** From the point of beam physics, complexity of a Muon Collider is closer to that of the Tevatron (higher) than to that of the LHC (lower)***

Muon Production: 1-4 MW proton driver needed

Protons → Target → Pions → Muons

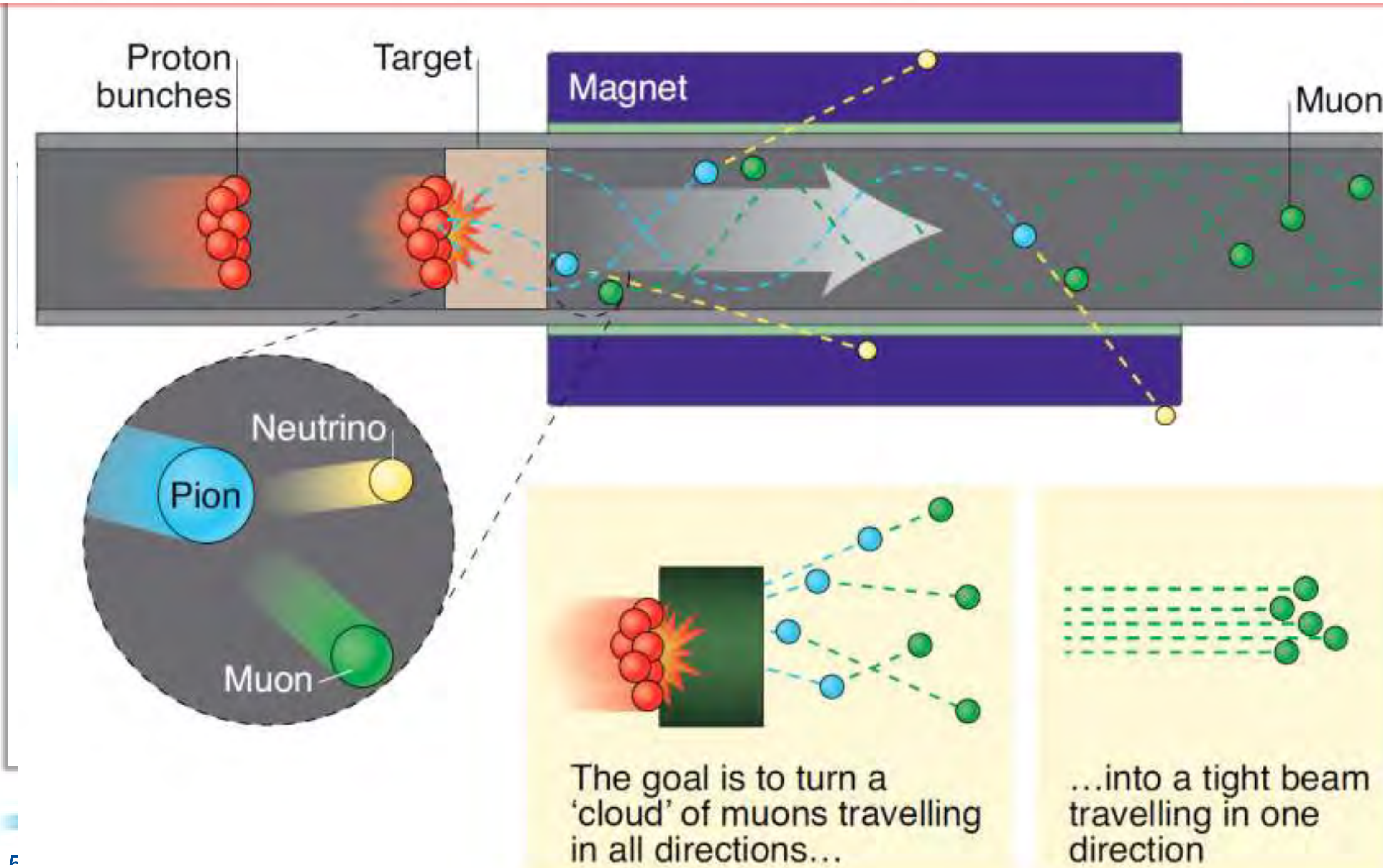

MERIT Experiment – Demo of 4-8 MW Proton Targetry

- At CERN PS
- 1e13 protons 24 GeV (115kJ/pulse)
- Liquid Mercury target 20 m/s
- 15 T Solenoid

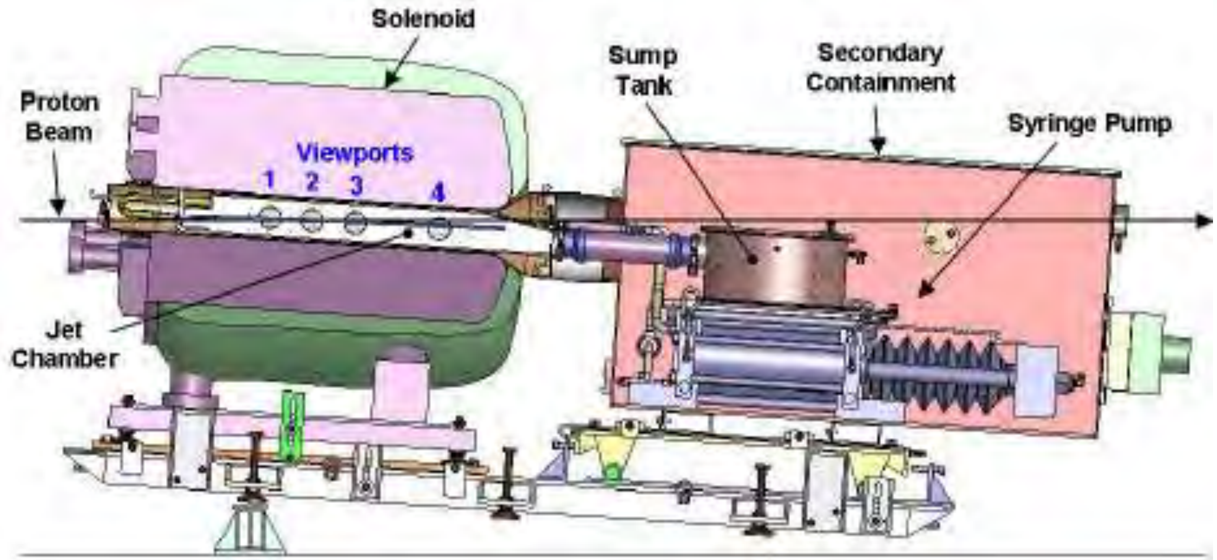

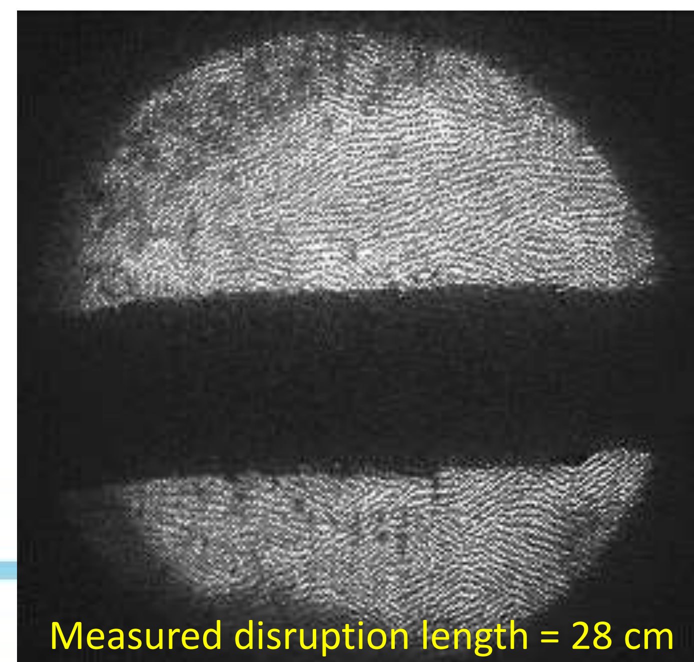

The Need for Muon Cooling

$$\mathcal{L} = f_{\text{coll}} \frac{N_1 N_2}{4\pi\sigma_x^*\sigma_y^*}$$

Muon Phase Space After Target

vs What's Needed for Collider

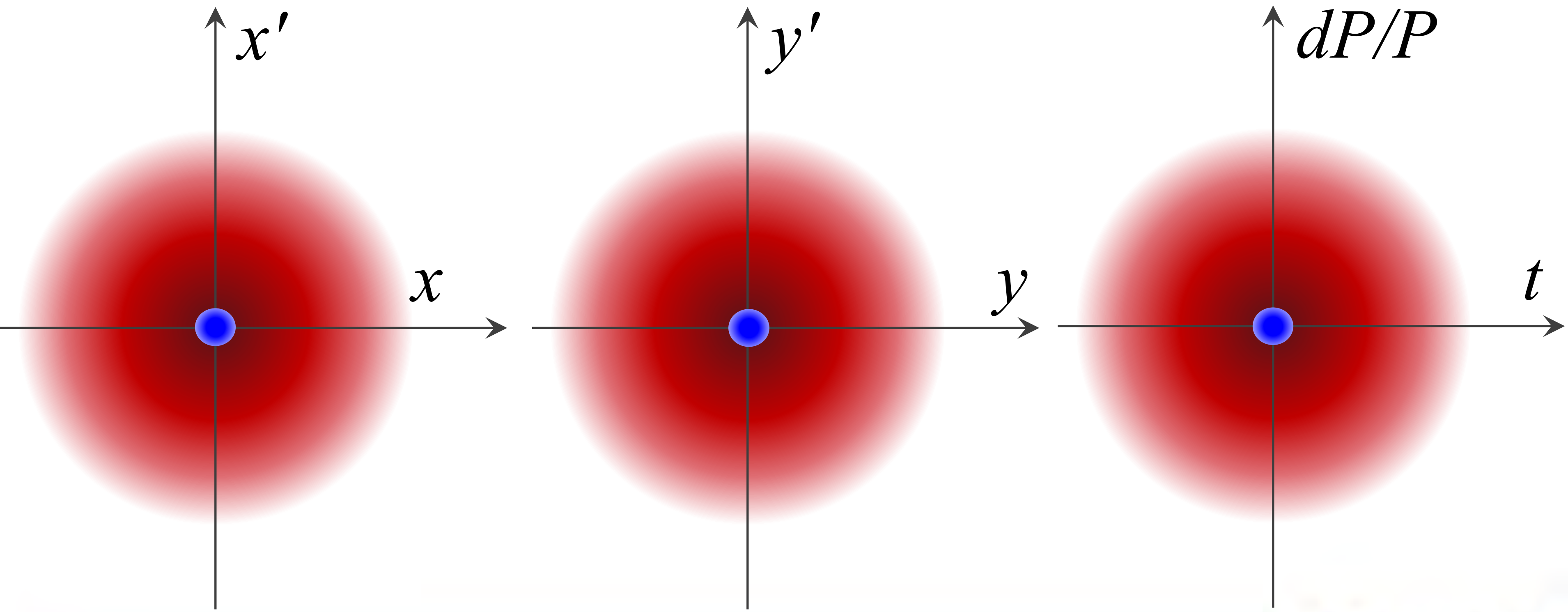

Need "6D-Cooling"

Fermilab

Fast Cooling of Muon Beams

- The desired 6D emittance for a MC is 5-6 orders of magnitude less from the emittance of the beam at the target
- How that can be done before muons decay? → ionization cooling: ionization loss ***along momentum*** followed by RF acceleration (***restore energy***) along longitudinal axis only (like in the Synchr Rad damping)

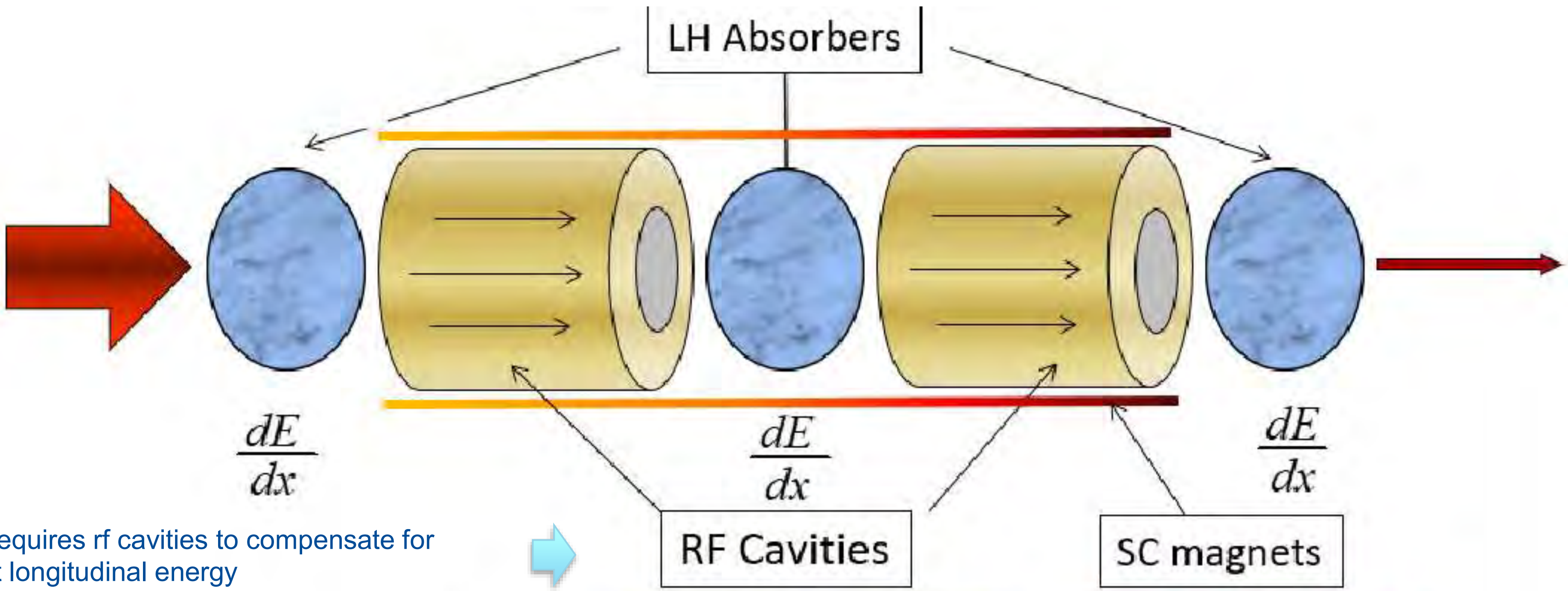

- Requires rf cavities to compensate for lost longitudinal energy
- Use strong B-fields to confine beams

$$\frac{d\epsilon_N}{ds} \approx \underbrace{-\frac{1}{\beta^2}\left\langle\frac{dE_\mu}{ds}\right\rangle\frac{\epsilon_N}{E_\mu}}_{\text{Cooling}} + \underbrace{\frac{\beta_\perp(0.014GeV)^2}{2\beta^3 E_\mu m_\mu X_0}}_{\text{Heating}}$$

Equation:

$$\frac{d\epsilon_n}{ds} = -\frac{dE_\mu}{ds}\,\frac{\epsilon_n}{E_\mu} + \frac{\beta_\perp (0.014)^2}{2\, E_\mu m_\mu\, L_R}$$

- (1st) Cooling term ~ (dE/ds) – larger the better
- (2nd) Heating/ scattering term ~ beta-function at the absorber and *1/radiation length* of the material (a low-Z preferred, *Liquid Hydrogen, Li, LiH, Be*)
- Eneregy of muons

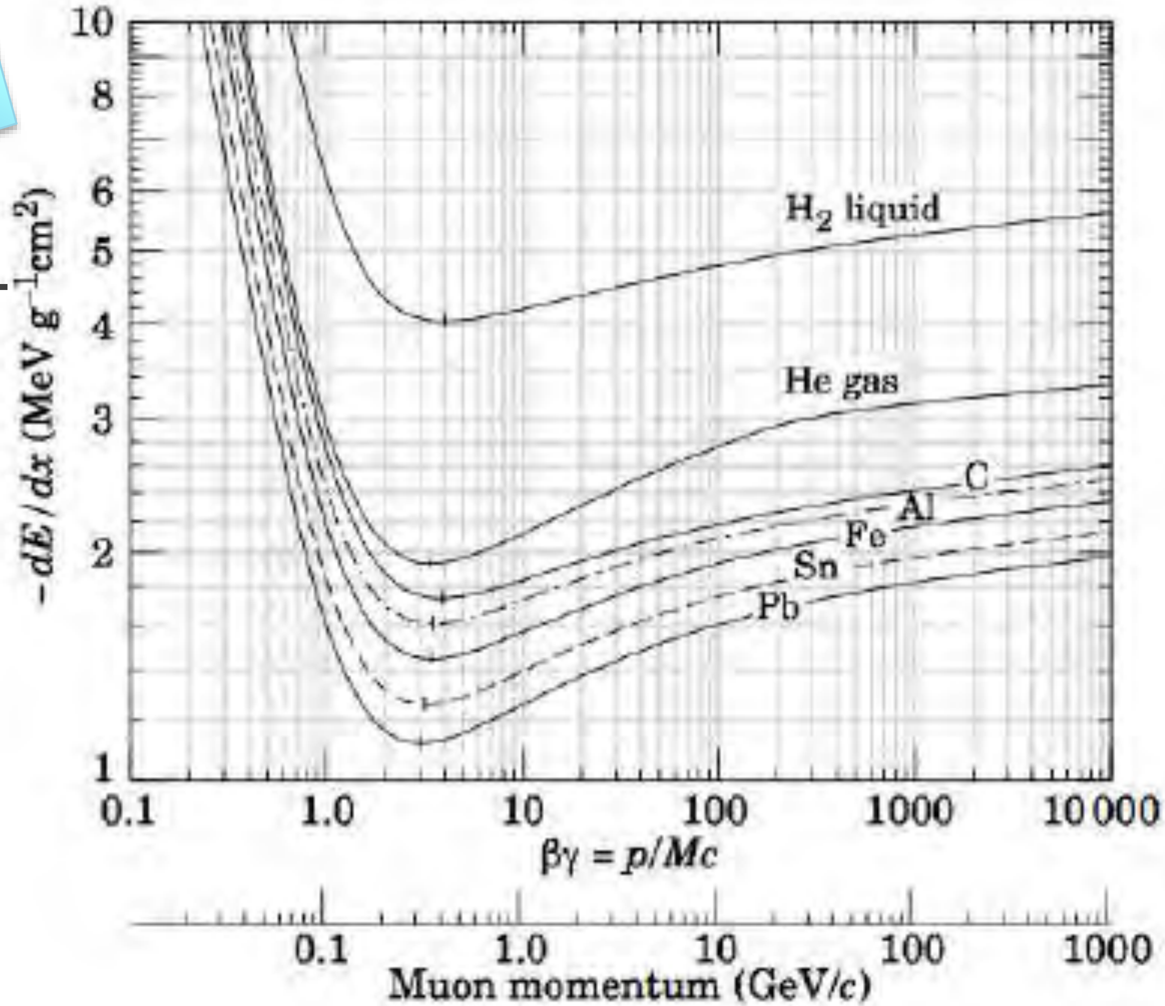

Longitudinal DoF: rms E spread

cooling term

fluctuations of ionization energy losses

$$\frac{d(\Delta E)^2}{ds} = -2\,\frac{d\left(\frac{dE_\mu}{ds}\right)}{dE_\mu} < (\Delta E_\mu)^2 > + \frac{d(\Delta E_\mu)^2_{straggling}}{ds}$$

- Cooling requires that d(dEμ/ds)/dEμ > 0. But at energies below about 200 MeV, the energy loss function for muons, dEμ/ds, is decreasing with energy and there is thus heating of the beam. Above 400 MeV the energy loss function increases gently, thus giving some cooling, though not sufficient for fast cooling application (see previous slide).
- The "struggling" term

$$\frac{d(\Delta E_\mu)^2_{straggling}}{ds} = 4\pi\,(r_e m_e c^2)^2\,N_o\,\frac{Z}{A}\,\rho\gamma^2\left(1-\frac{\beta^2}{2}\right)$$

increases as γ^2, and the cooling system size scales as γ → cooling at low energies is desired.

- Energy spread can also be reduced by artificially increasing d(dEμ/ds)/dEμ by placing a transverse variation in absorber density or thickness at a location where position is energy dependent, i.e. where there is dispersion (= emittance exchange long→ transverse)

Fermilab

MICE: Muon Ionization Cooling Experiment = 1 "cell"

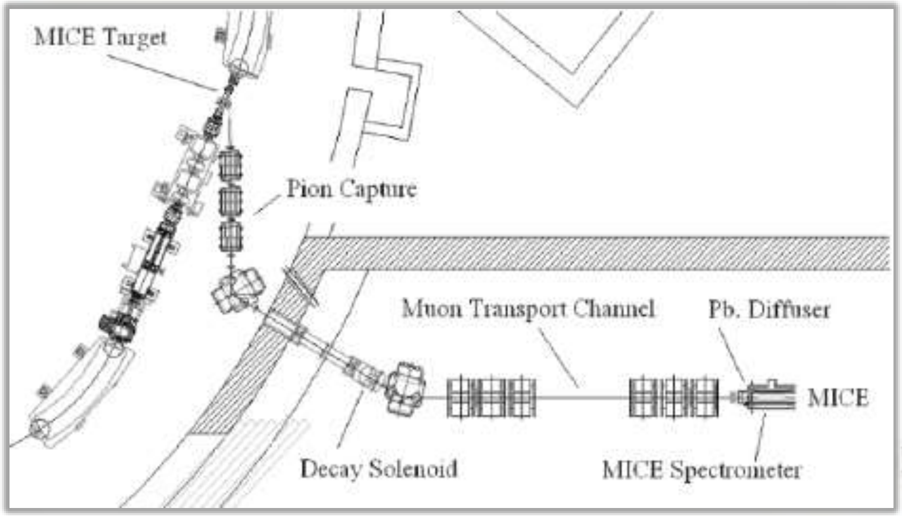

ISIS 800 MeV proton synchrotron @ RAL (UK)

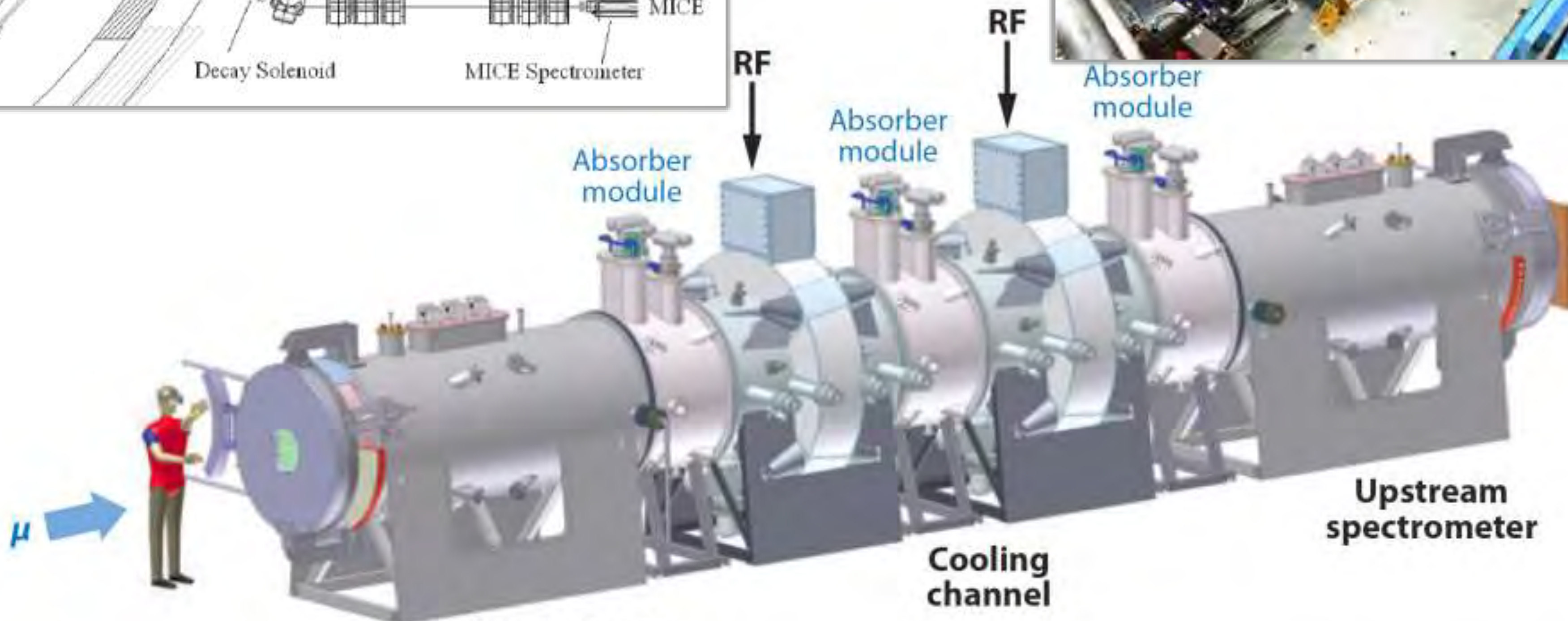

- with muons @ ~140 MeV/c
- each muon individually measured

MICE(2)

Nature **578**, 53–59(2020)

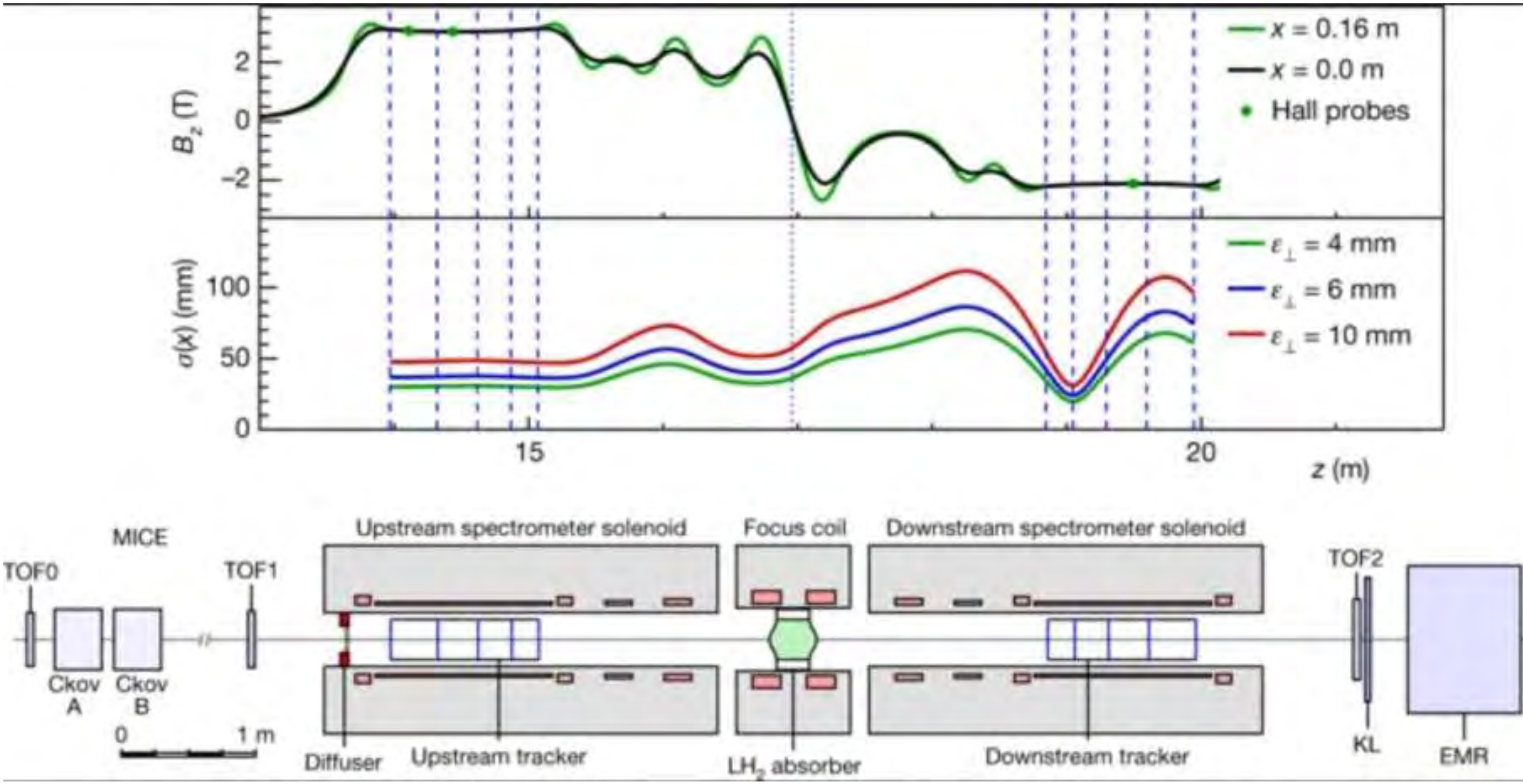

MICE(3)

Nature **578**, 53–59(2020)

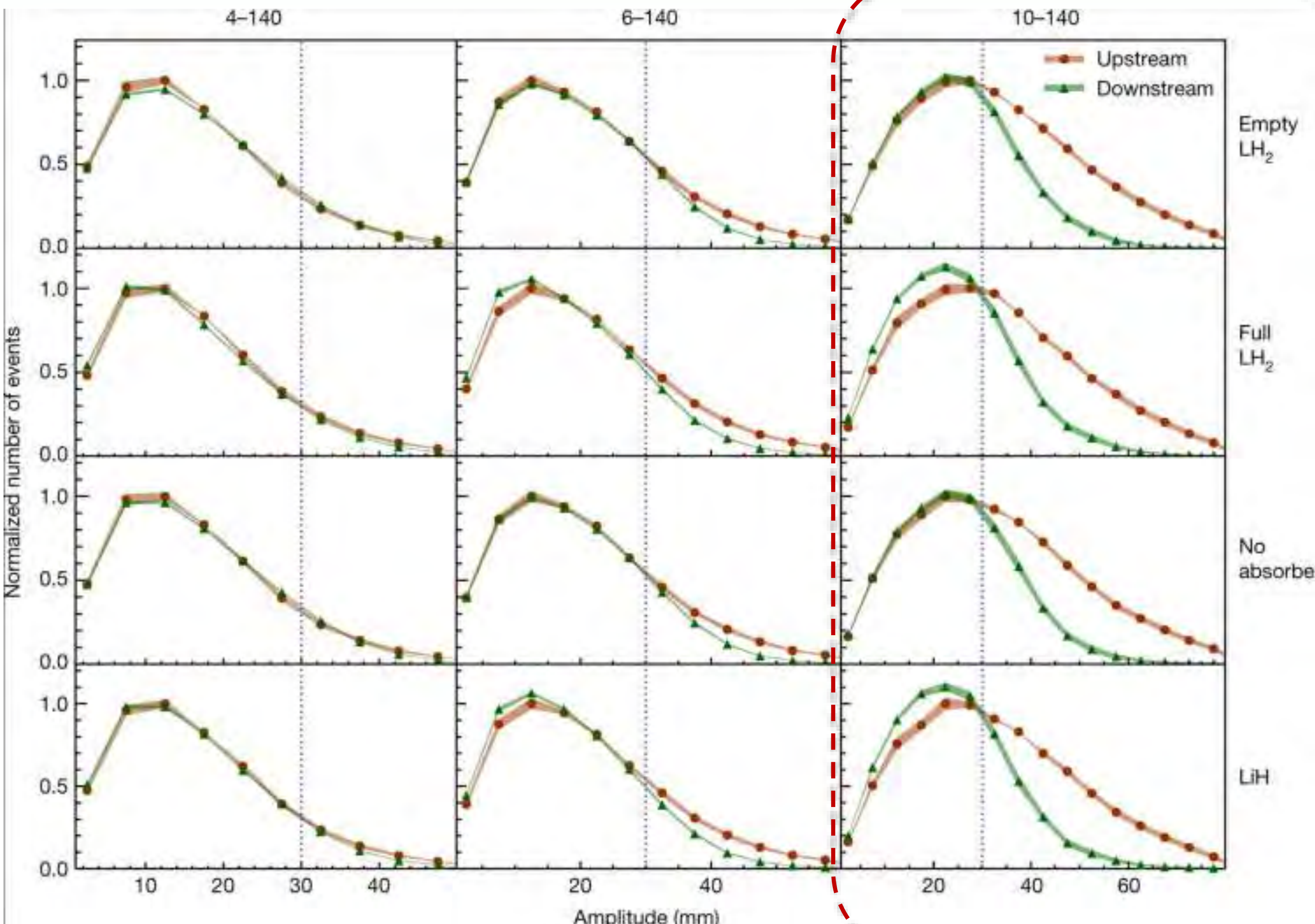

“Nothing”

“Good”

“Nothing”

“Good”

6D Ionization Cooling

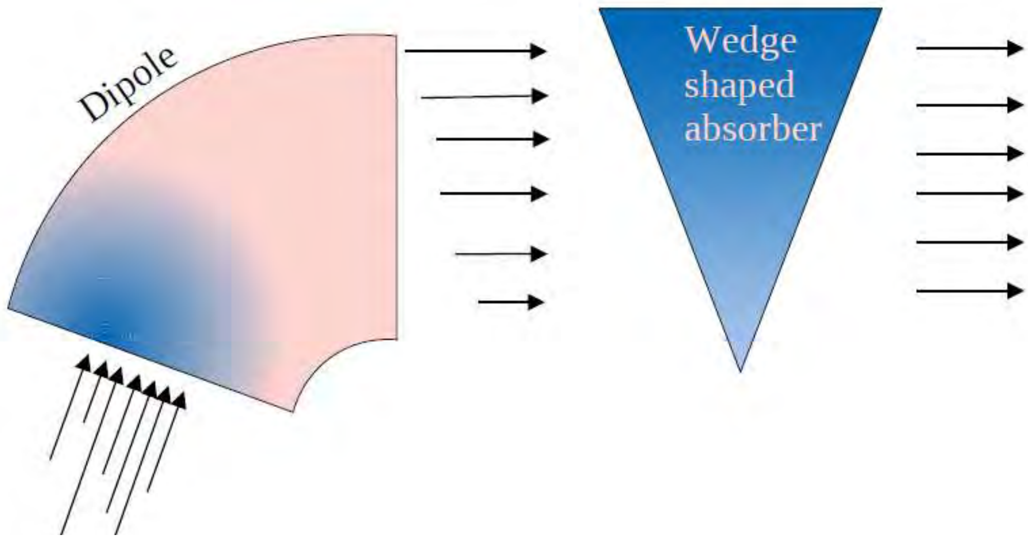

- Initial beam is narrow with some momentum spread
  - Low transverse emittance and high longitudinal emittance
- Beam follows curved trajectory in dipole
  - Higher momentum particles have higher radius trajectory
  - Beam leaves wider with energy-position correlation
- Beam goes through wedge shaped absorber
  - Beam leaves wider without energy-position correlation
  - High transverse emittance and low longitudinal emittance
- (Do transverse 4D cooling… and repeat the cycle)

Need 6D Cooling (x,y, energy spread)

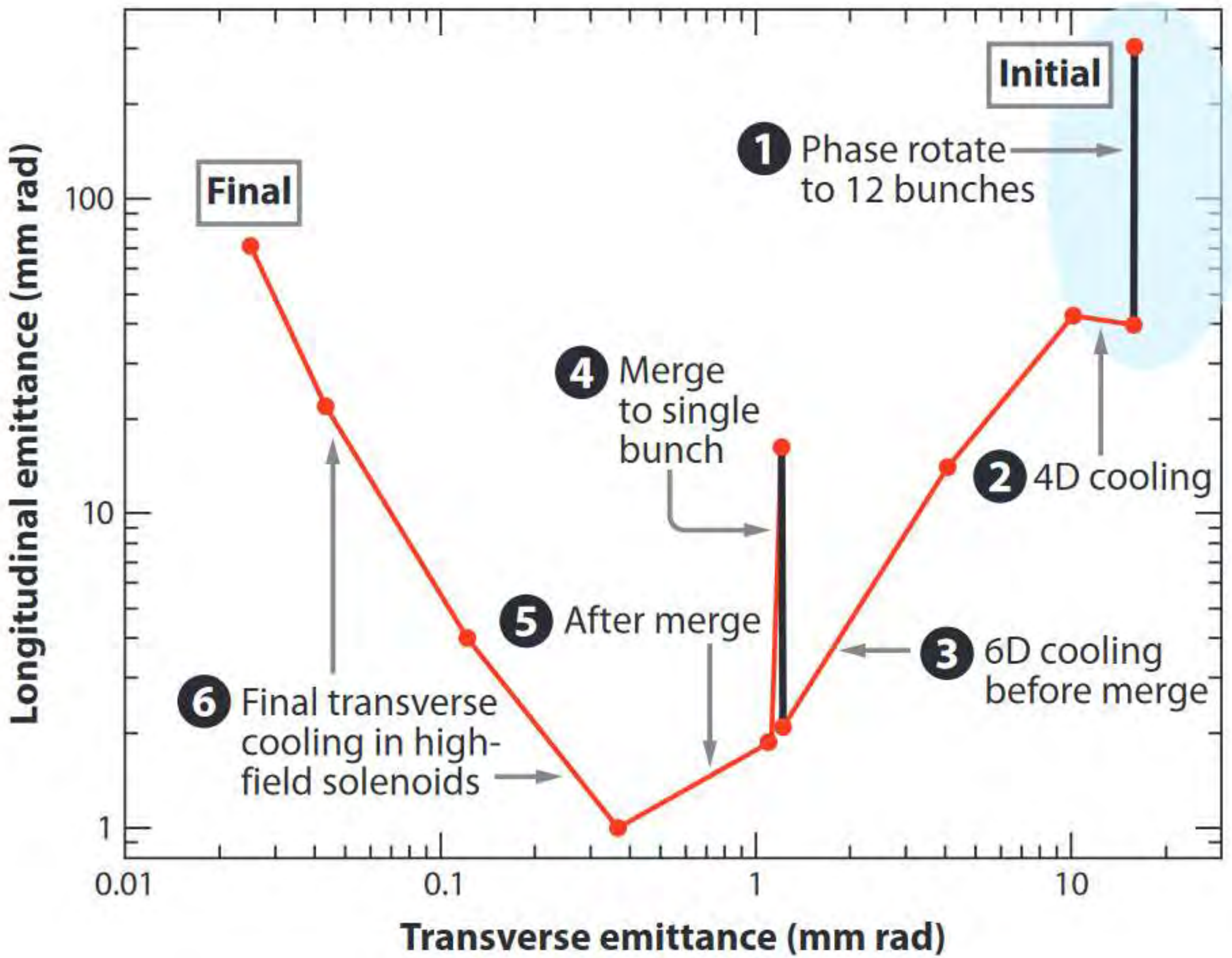

Rectilinear Ionization Cooling Channel

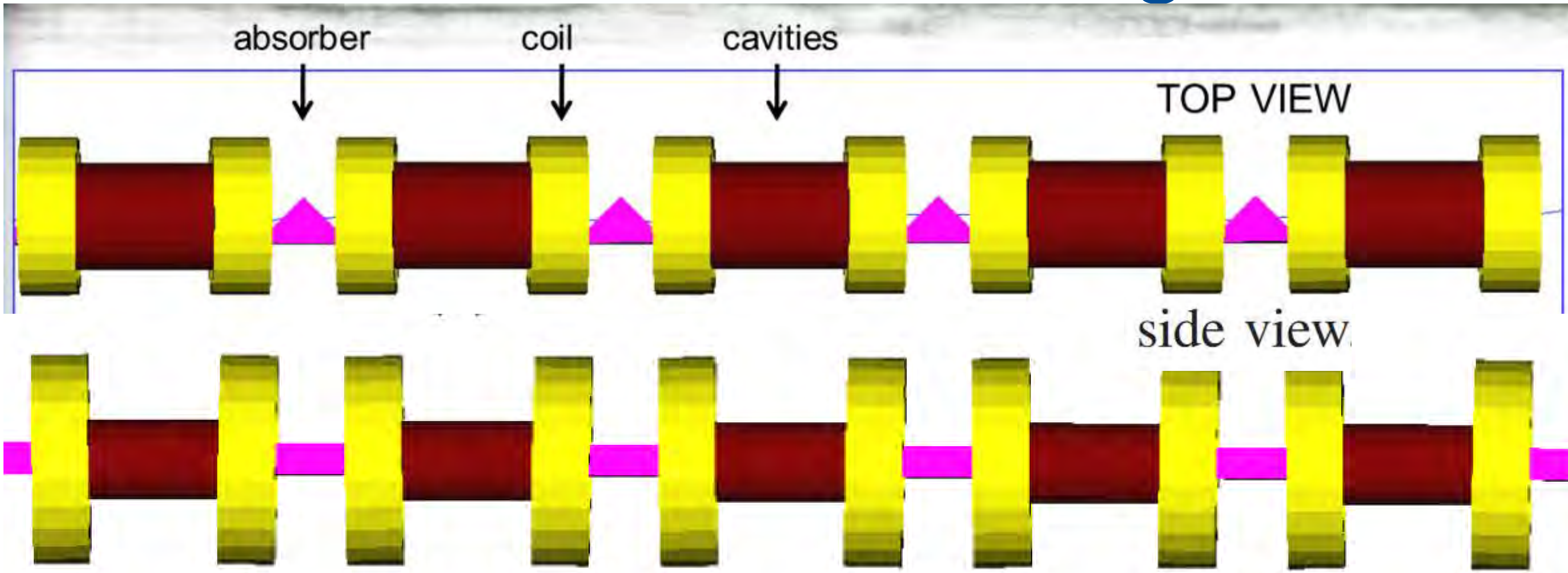

6D emittance reduction by 5 orders of magnitude (between point 2 to 5).
Length ~ 900 m

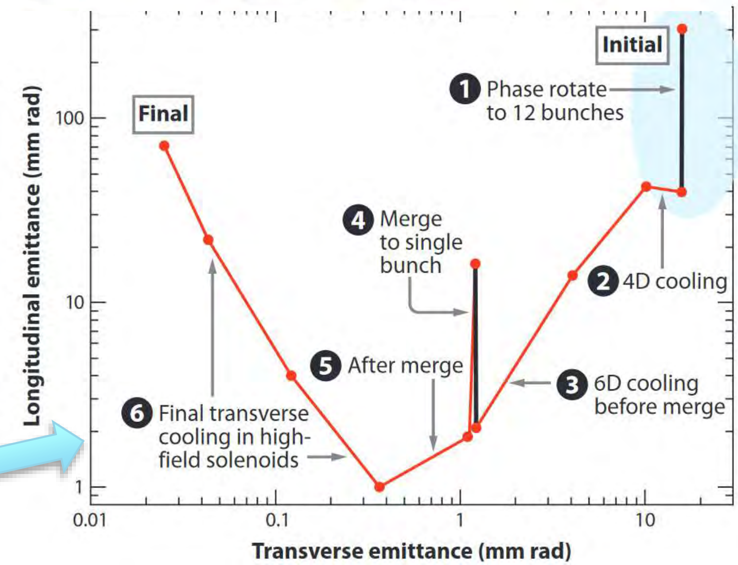

Final cooling section design requires ~30 T solenoids (point 5 to 6)

Acceleration and Collider Ring ~75% of the MC Cost

Options (high→ low cost):

- Linac (very costly!)
- Recirculating linear accelerator (RLA)
- Fixed field alternating gradient (FFA)
- Pulsed synchrotrons

~14T Large Aperture Collider Magnets

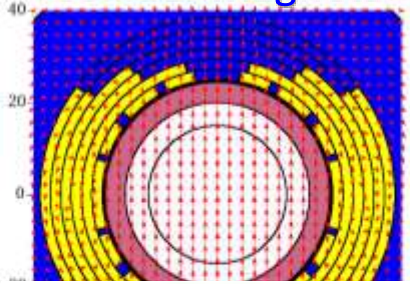

Alexahin *et al* 2018 *JINST* **13** P11002

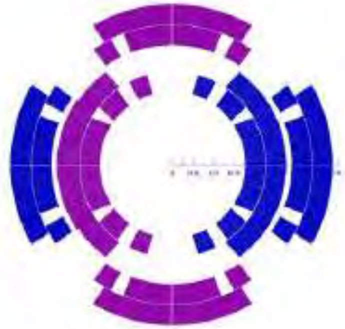

Dipole/Quad

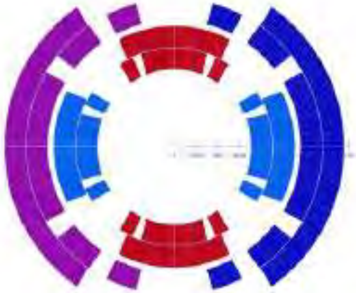

Quad/Dipole

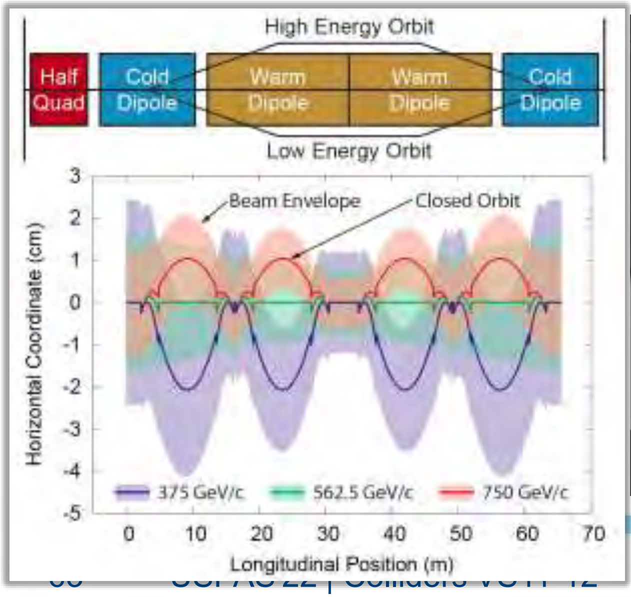

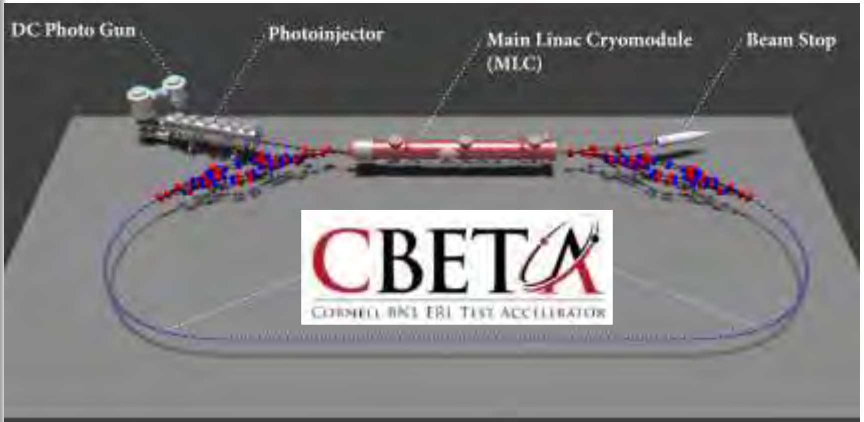

CBETA FFA at Cornell/BNL arXiv1706.04245

The Idea of Pulsed Muon RCS

- Rapid cycling synchrotron (RCS)
  - Potentially larger acceleration range at affordable cost
  - Could use combination of static superconducting and ramping normal-conducting or HTS magnets
  - But have to deal with energy in fast pulsing magnets

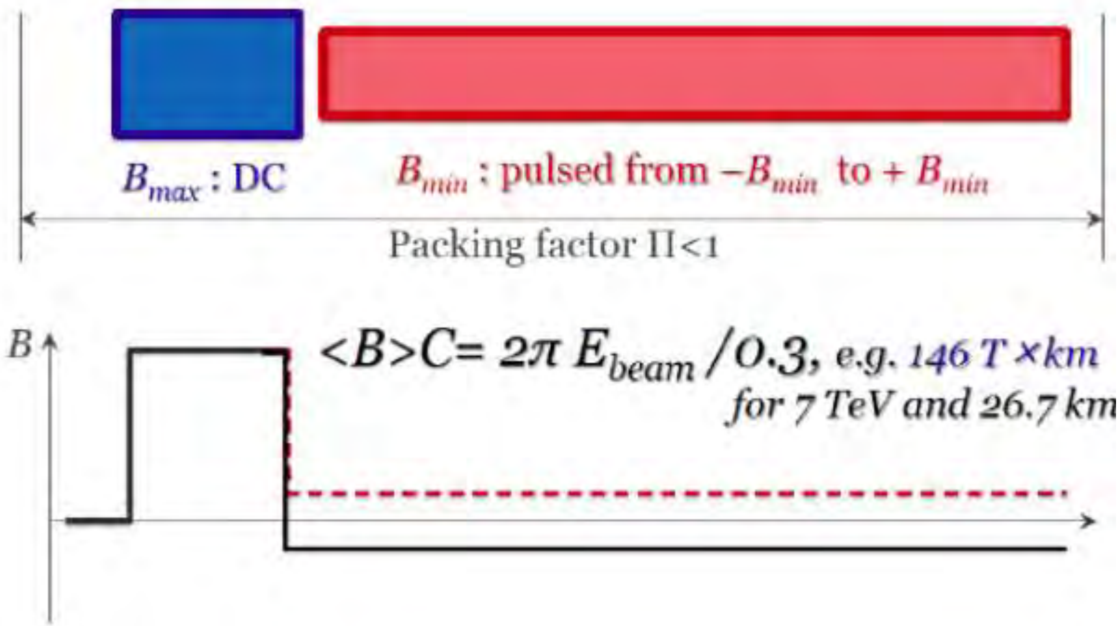

- Of course, circumference of the RCS will be larger than that of collider as AVERAGE max B-field in RCS < AVERAGE (static) B-field collider ring

FNAL-Site filler MC

➢Largest

Radius is ~2.65 km

- ~16.5 km Circumference
  - ~2/3 LHC

RCS accelerator

If B_{ave}= 3 T → E_{μ}= 2.4 TeV

(B_{max} = 8T, B_{pulse} =±2T)

Doubled ?

B_{ave}= 6.3 T → E_{μ}= 5 TeV

(B_{max} = 16T, B_{pulse} =±4T)

10 TeV collider

Collider Ring ~10 km

B_{ave} = 10 T τ_{μ} = 0.104 s

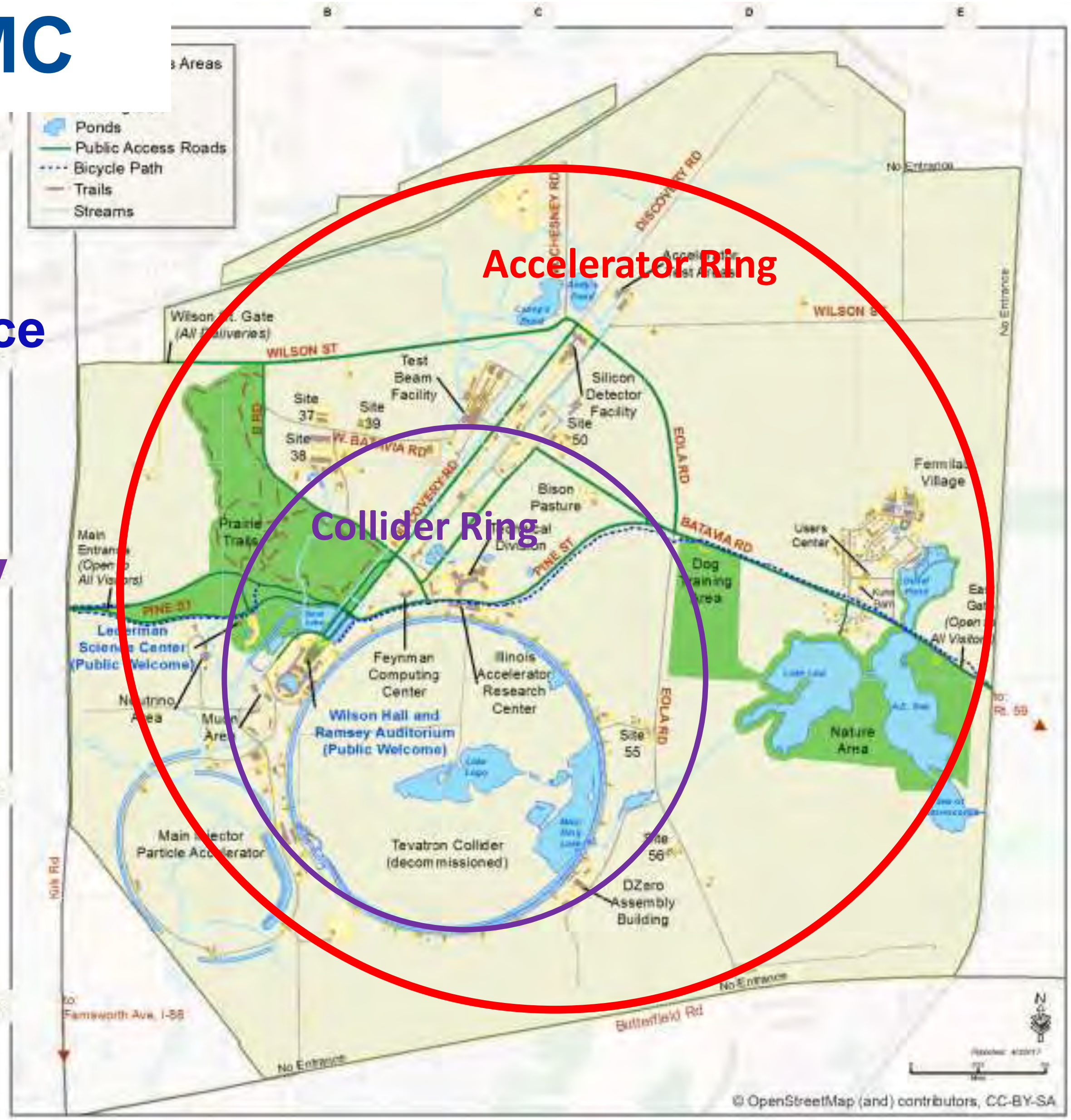

$$R=\frac{B\rho}{B}=\frac{P(GeV/c)}{0.3B(T)}m=\frac{P(TeV/c)}{0.3B(T)}km$$

Need pulsed magnets dB/dt ~500T/s

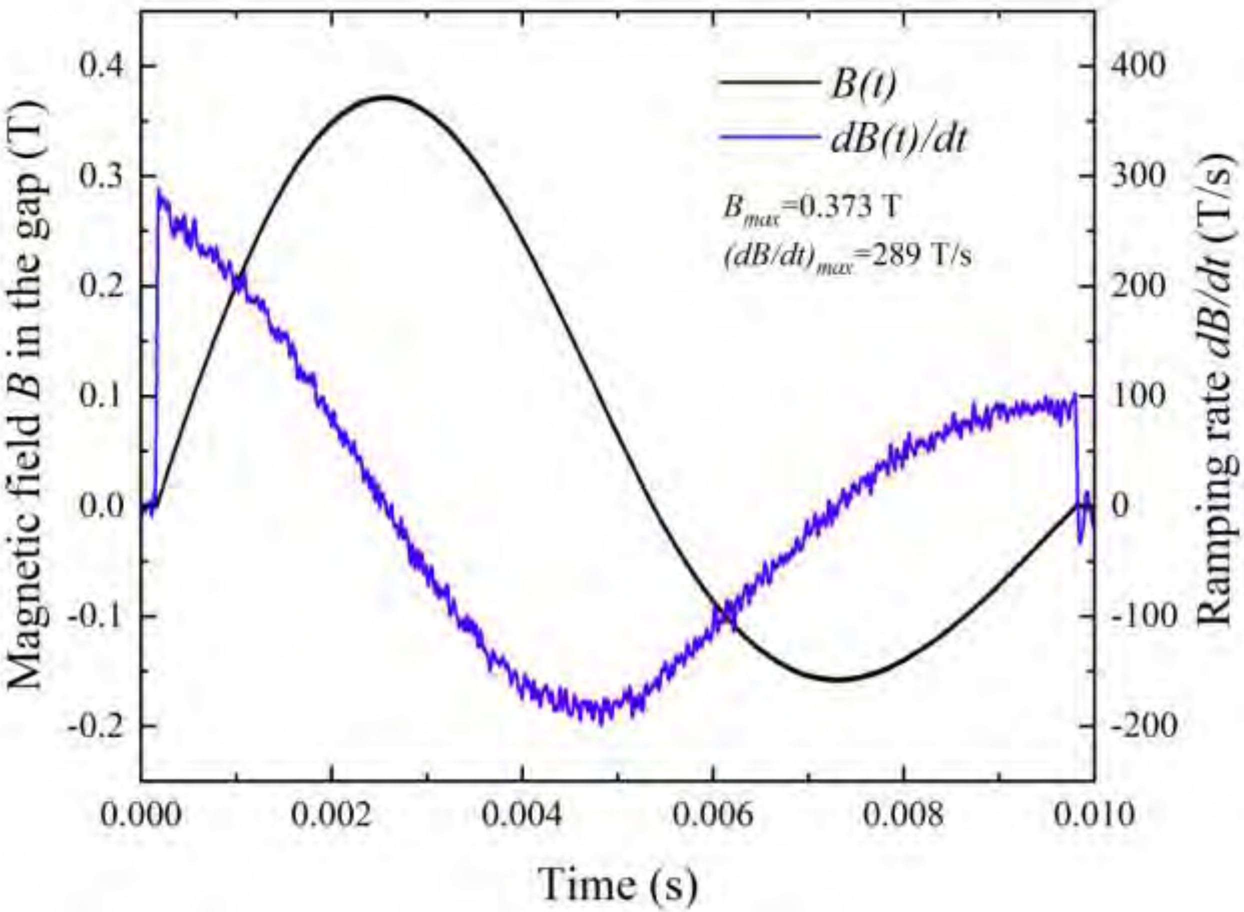

Fermilab, 2021

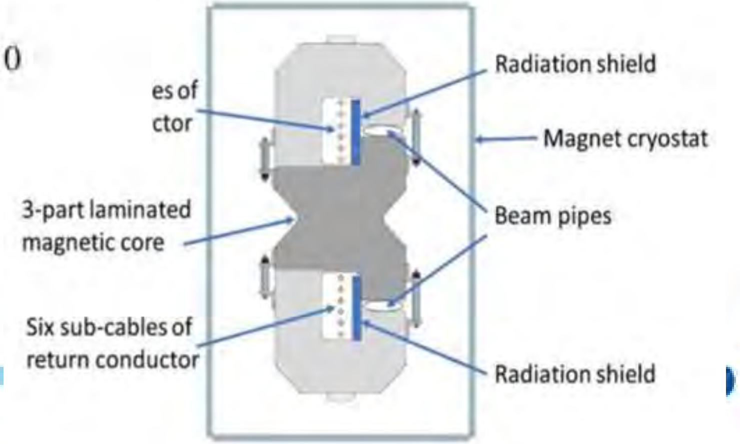

Approach to an economical magnet is to use HTS tape: very low AC losses in superconductor

Neutrino Flux (Muons decay to $e+\nu\,\bar{\nu}$)

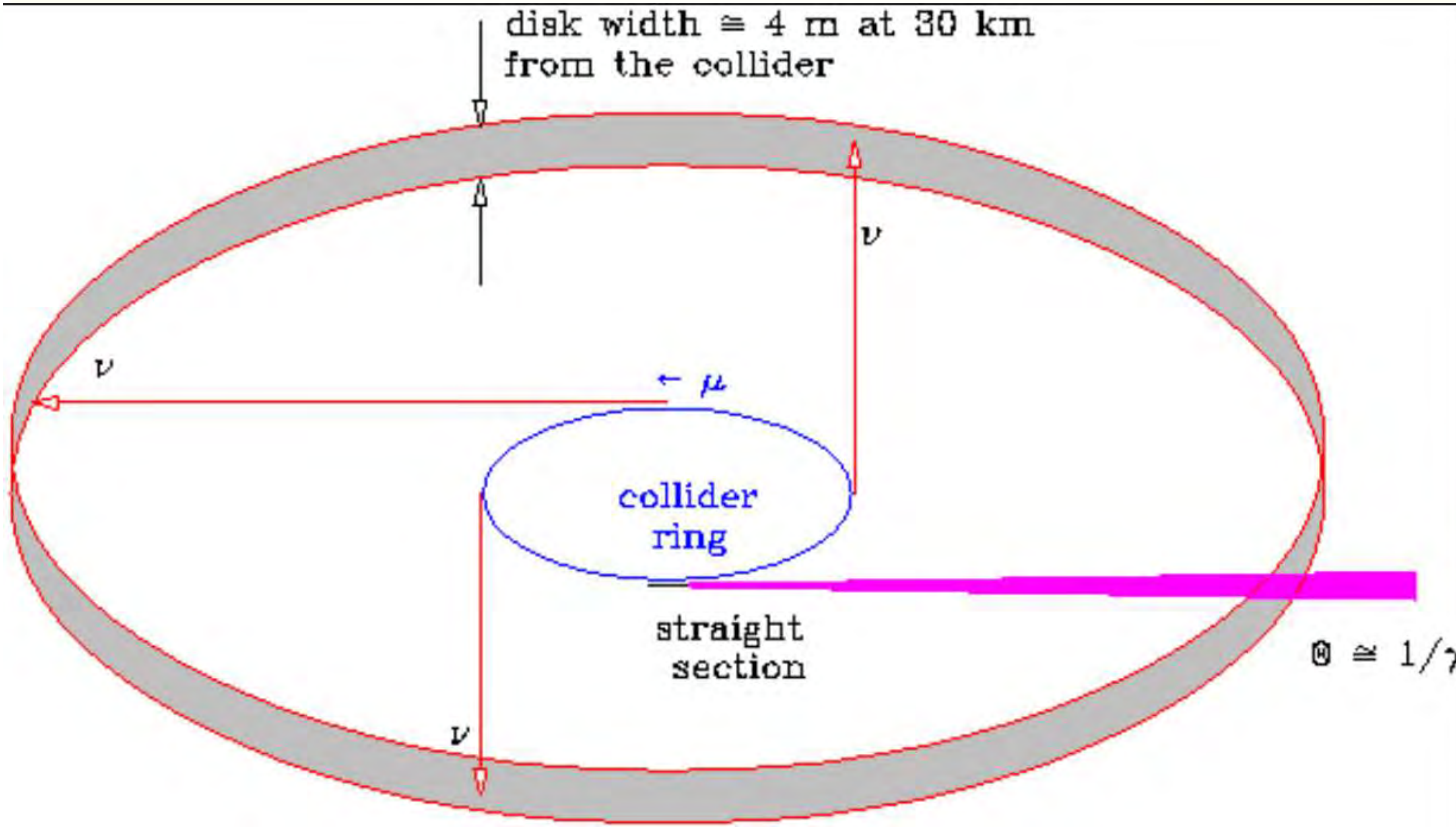

Neutrino Radiation Dose & Control

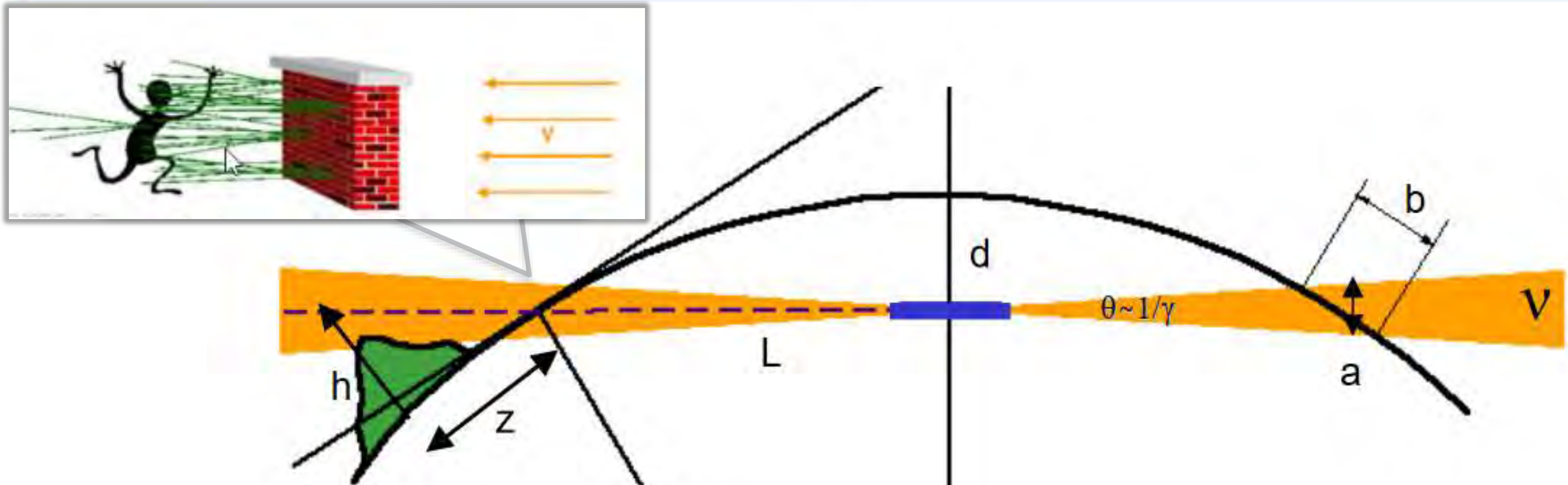

Cone gets narrower with energy
Cross section grows with energy

$$D^{ave}[Sv] = 3.7 \times 10^{-23} \times \frac{N_\mu \times (E_\mu[TeV])^3}{(L[km])^2}.$$

<1 mSv/yr mitigation ideas:

- depth
- few mm vertical collider orbit variation (next slide)
- few cm magnet positions float (next slide)
- less muons… =smaller emittance to keep *L*

Neutrino Radiation Mitigation **Φ~100 possible**

disk width ≅ 4 m at 30 km

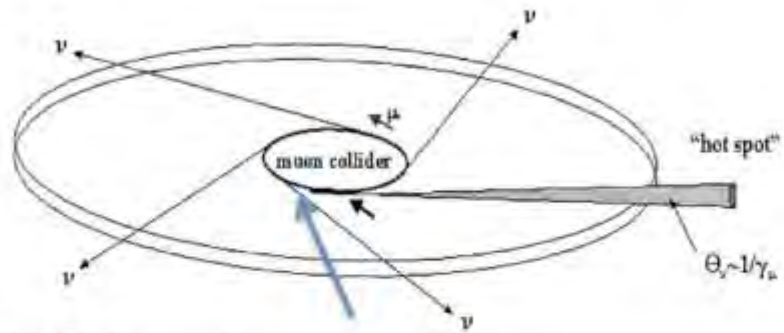

Move collider ring components, e.g. vertical bending with 1% of main field

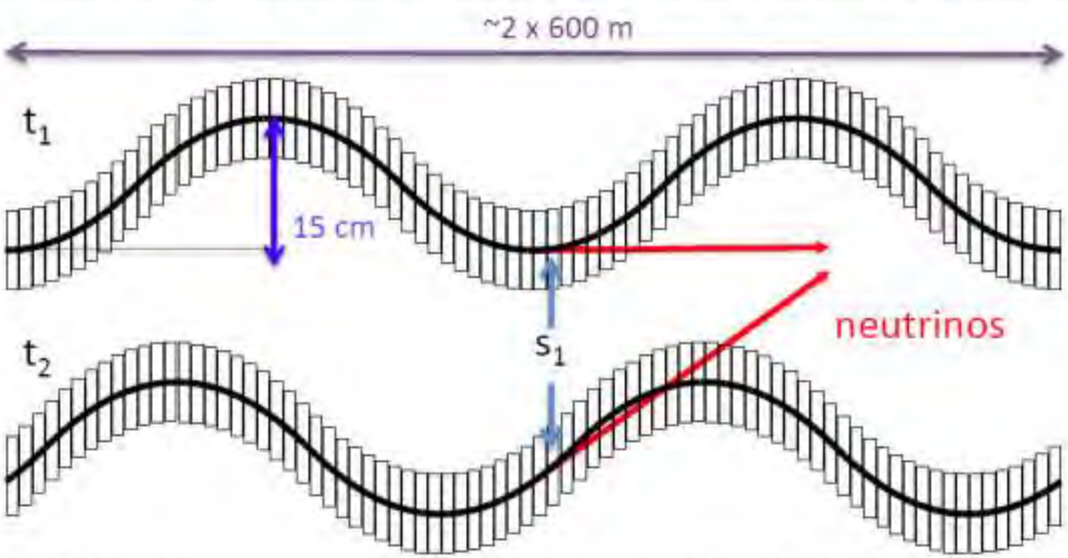

Opening angle ± 1 mradian

O(100) larger than decay cone
⇒ gain O(100) in radiation

In straights, additional improvement in horizontal

Need to study impact on beam and operation, e.g. dispersion control

D. Schulte Muon Collider Radiation 12

Expected Steps Toward a Muon Collider

- MC R&D endorsed by the European Particle Physics Strategy R&D in 2020 and (expected) by the US HEP in 2023
- Plan includes:
  - R&D to be carried out by truly international collaboration incl. US
  - 6D muon cooling demontration test facility design(2025) & construction (2031) & research operation (~3036)
  - Main technology items (12-16 T magnets, fast ramping magnets, 4 MW targets, etc) are all prototyped by ~2037
  - MC technical design (2036) and start of construction (2037-45)
- Significant part of that plan will take place in the US and a Fermilab site-filler collider (6-10 TeV cme max.) is one of most viable alternatives (another one – to re-use CERNaccelerator infrastructure, incl 27 km circumference LHC tunnel, for a 10-14 TeV cme muon collider).

Thanks for Your Attention !

Questions !?

Literature

- V.Shiltsev, F.Zimmermann, Modern and Future Colliders (Rev.Mod.Phys., 2021)

https://journals.aps.org/rmp/abstract/10.1103/RevModPhys.93.015006

Also:

1. Nature Physics MC – K.Long, et al, *Nature Physics* 17, 289–292 (2021)
2. RMP Colliders – V.Shiltsev, F.Zimmermann, *Rev.Mod.Phys.* 93, 015006 (2021)
3. 1998 PhysicsToday – A.Sessler, *Physics Today* 51(3), 48-53 (Mar.1998)
4. 1999 Design – C.Ankenbrandt, *Phys.Rev.ST-Accel.Beams* 2, 081001 (1999)
5. *αβγ* cost model – V.Shiltsev, *JINST* 9 T07002 (2014)
6. Alvin Tollestrup Book – FERMILAB-BOOK-2021-001 (2021)
7. Muon-Proton Collider – V.Shiltsev, *Proc. IEEE PAC'97*, FNAL-Conf-97/114 (1997)
8. MC and Neutrino Factory - S.Geer, Annu. *Rev. Nucl. Part. Sci*. 59:347–65 (2009)
9. Tevatron - S.Holmes, V.Shiltsev, *Annu. Rev. Nucl. Part. Sci.* 63:435-465 (2013)
10. Muon Colliders - R.B. Palmer, *Rev. Accel. Sci. Tech.* 7, 137–159 (2014)
11. 14 TeV MC in LHC tunnel - D. Neuffer and V. Shiltsev, *JINST* 13, T10003 (2018)
12. USMAP - M. Boscolo, J.-P. Delahaye, M. Palmer, *Rev.Accel.Sci.Tech.* 10, 189 (2019)
13. 2020 European Strategy https://cds.cern.ch/record/2721370/files/CERN-ESU-015-2020%20Update%20European%20Strategy.pdf
14. JINST Special Issue on Muon Accelerators https://iopscience.iop.org/journal/1748-0221/page/extraproc46
15. Muon Collider Collaboration https://muoncollider.web.cern.ch/

U.S. Particle Accelerator School
Education in Beam Physics and Accelerator Technology

Fermilab

Managed by Fermi Research Alliance, LLC for the U.S. Department of Energy Office of Science

Advanced (Plasma) Colliders
Limits of Colliders

Vladimir Shiltsev, Fermilab

part of the "Colliders" class by V.Lebedev, N.Mokhov and V.Shiltsev

US Particle Accelerator School, Jan 24 – Feb 4, 2022

Plasma Can Sustain Very High Gradients

$$E_0 = \frac{m_e c \omega_p}{e} \approx 100[\frac{GeV}{m}] \cdot \sqrt{n_0[10^{18} cm^{-3}]}$$

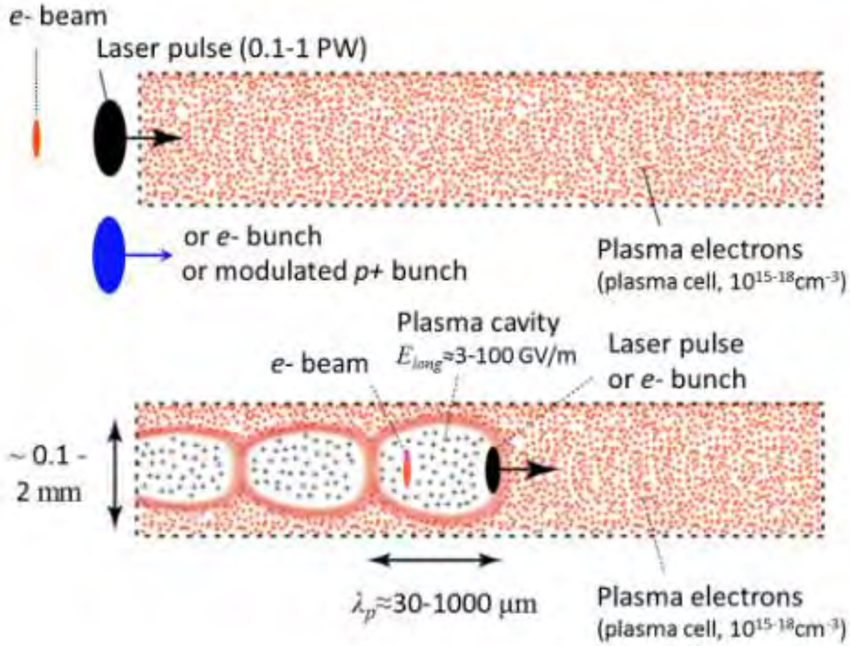

$$\lambda_p = c/\omega_p \approx 1\ \mathrm{mm}\times\sqrt{10^{15}\ \mathrm{cm}^{-3}/n_0}$$

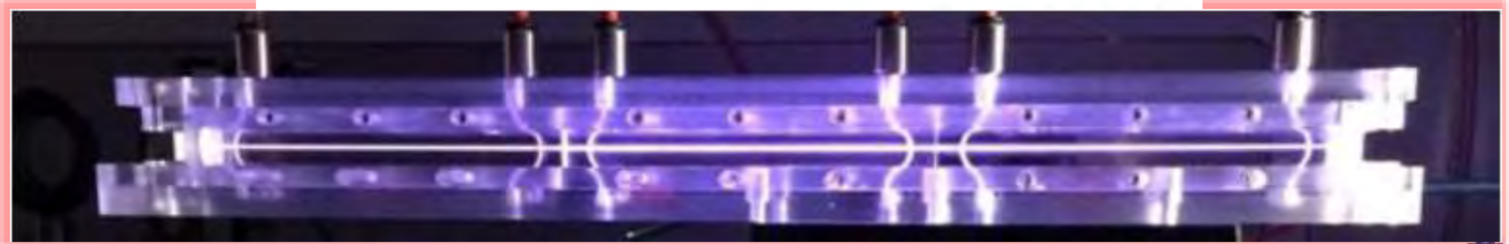

10cm Plasma Cell → 4.3 GeV Accelerator

Plasma Wakefield Accelerators

$$E_0 = \frac{m_e c \omega_p}{e} \approx 100\left[\frac{GeV}{m}\right] \cdot \sqrt{n_0[10^{18} cm^{-3}]}$$

Key facts:

Three ways to excite plasma (drivers)

laser $dE \sim 7.8$ GeV ($3 \cdot 10^{17}$ cm^{-3} 0.2m)

e- bunch $dE \sim 9$ GeV ($\sim 10^{17}$ cm^{-3} 1.3m)

p+ bunch $dE \sim 2$ GeV ($\sim 10^{15}$ cm^{-3} 10m)

Impressive proof-of-principle demos

In principle, feasible for *e*+*e*- collisions

Collider cost and power will greatly depend on the driver technology:

- lasers, super-beams of electrons or protons

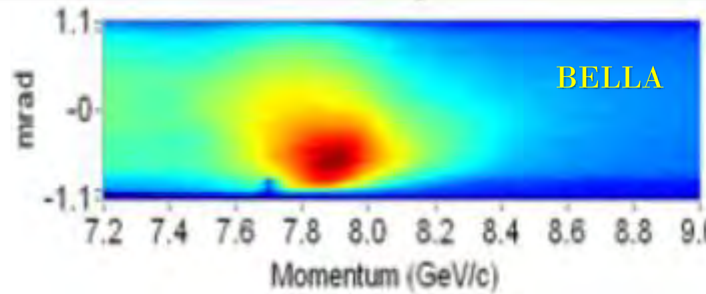

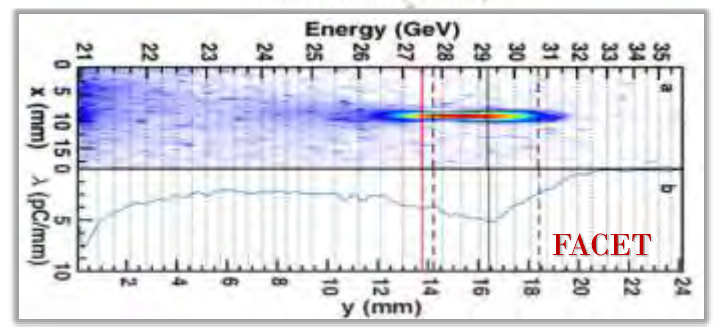

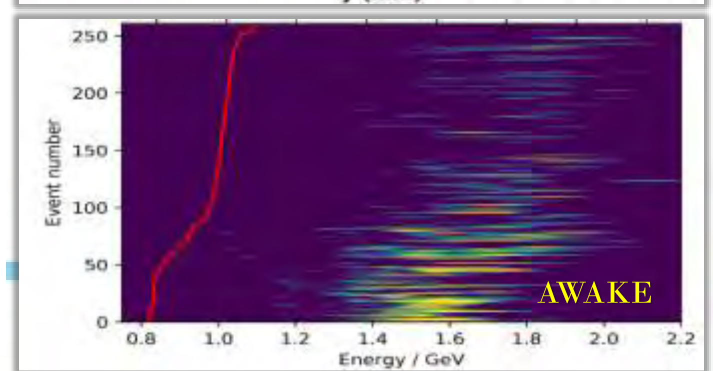

Plasma-based collider: staged plasma accelerators with >1 GV/m geometric gradients (>TeV/km) - Concepts

Beam-driven plasma accelerators (PWFA)

E. Adli et al., arXiv:1308.1145 (2013)

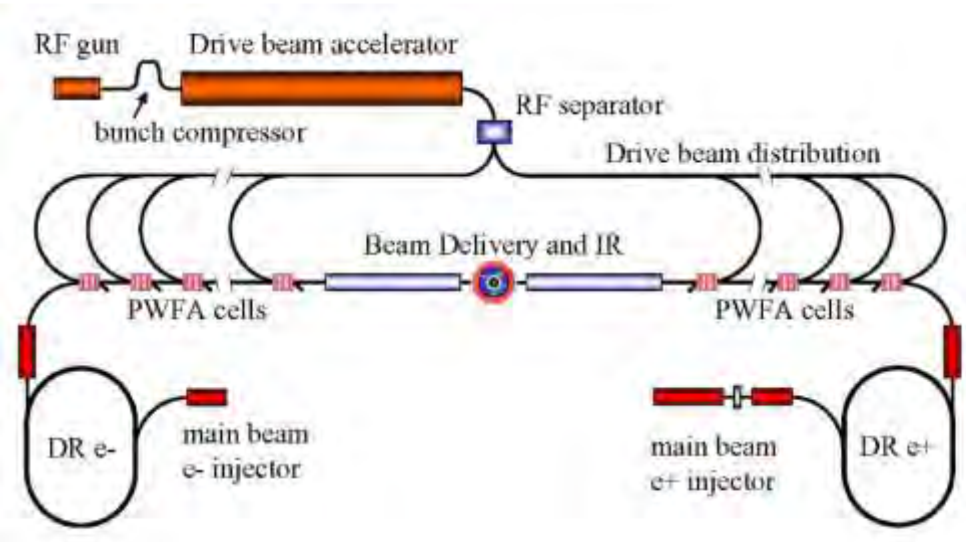

- Operating plasma density: 2×10^{16} cm^{-3}
- 25 GeV/stage
- Geometric gradient: 1 GV/m

Laser-driven plasma accelerators (LWFA)

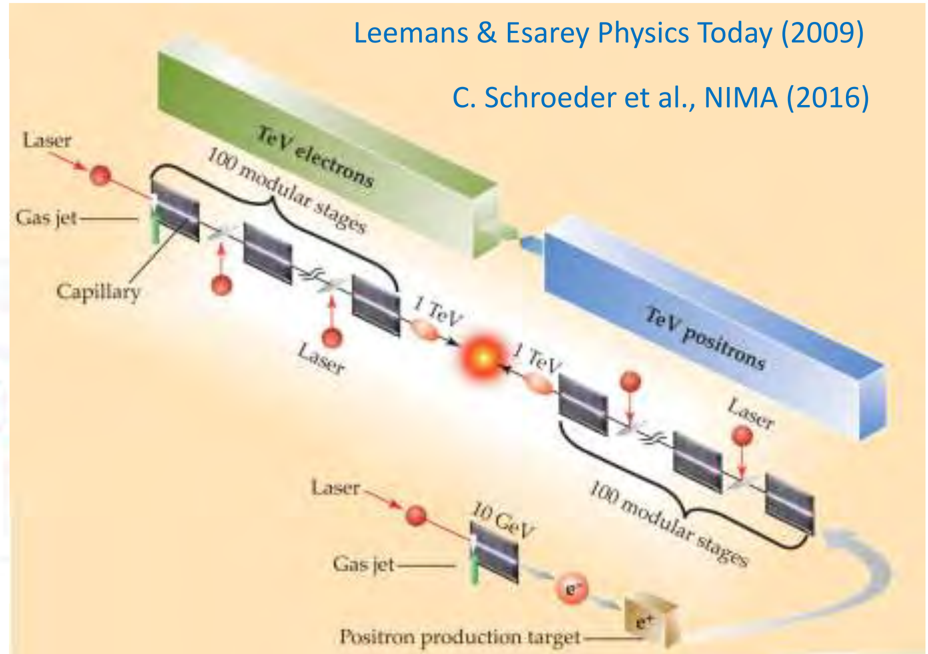

- Operating plasma density: 1×10^{17} cm^{-3}
- 5 GeV/stage
- Geometric gradient: 2.3 GV/m

Why Geometric Gradient is <100 GeV/m ?

Beam-driven plasma accelerators (PWFA) – one cell

E. Adli et al., arXiv:1308.1145 (2013)

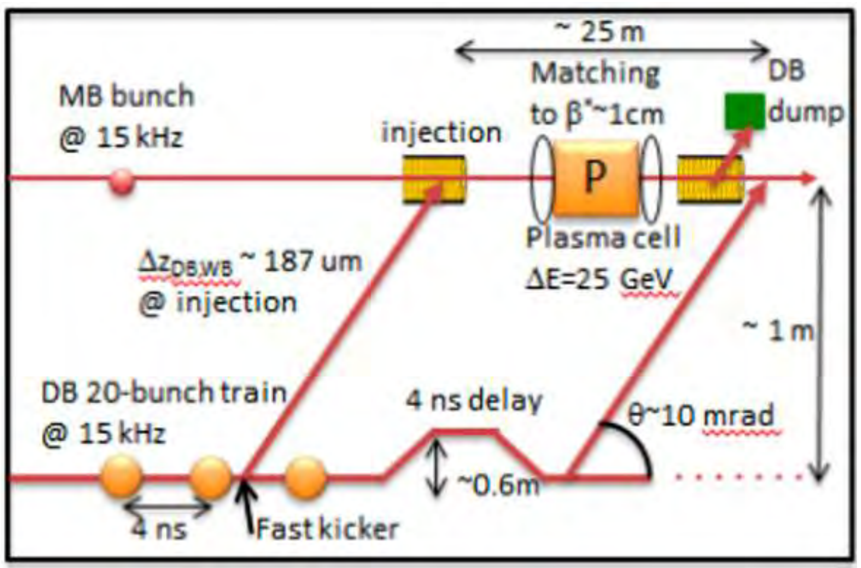

- 25 GeV drive beam needs to be coupled to plasma:
  - Fast kicker, smooth injection optics, delay chicanes, etc → ~22m minimum
- Plasma ~3.3 m (25 GeV)+22 m
- Geometric gradient: 1 GV/m

Laser-driven plasma accelerators (LWFA) – one cell

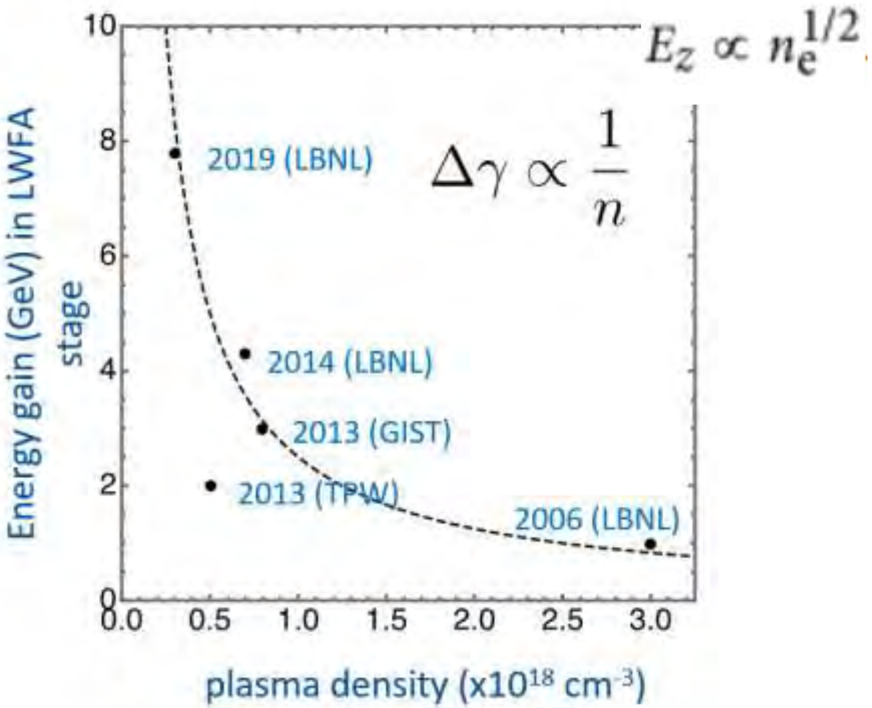

- At higher densities: $L_{deplete} \propto n_e^{-3/2}$
  - laser power gets depleted quickly
  - Dephasing= laser wave speed < c
- So, operate at optimal 10^{17} cm^{-3}
- 5 GeV/ 1 meter + 1 meter for coupling laser optics→2.3GV/m

Length Beam Delivery System (Scaling from CLIC)

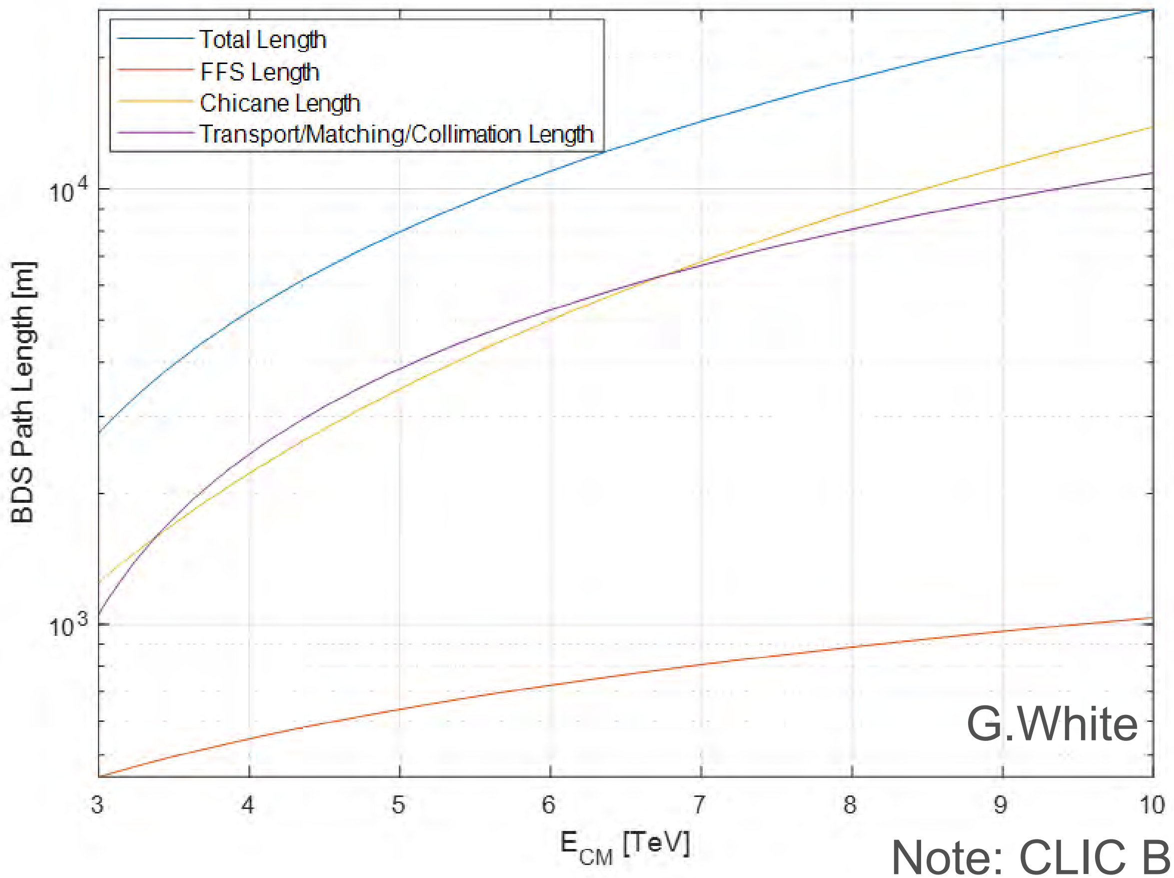

For plasma-based colliders with E_{cme} < 3 TeV the length of the Beam Delivery System dominates the length of the linacs and they become comparable above (6-10) TeV

That makes the average accelerating gradient

E/total length ~0.5 GeV/m

at high energies and much less at lower energies

Note: CLIC BDS accepts dE/E~0.3%

	CLIC E_{cm} = 3 TeV
FFS	**446**
Bending Sections	**1250**
Other	**1054**
Total	**2750**

=> L ~ $E^{7/10}$ (Original Raimondi/Seryi paper)

$\Delta\gamma\epsilon \approx (4 \times 10^{-8} m^2 GeV^{-6}) E^6 \sum_i \frac{L_i}{|\rho_i|^3} \mathcal{H}_i$ (ISR) **=> L ~ E^2**

L ~ E

(for fixed peak Dispersion)

Examples of Advanced LC Main Parameters

Parameter	Symbol [unit]	ILC	CLIC	LPA	PWFA	PWFAx
CMS energy	E_{cm} [GeV]	500	3000	1000	3000	3000
Luminosity	L $[10^{34}cm^{-2}s^{-1}]$	1.8	6	2.0(2.7)	6.3(6.0)	9.0
Lum. in peak	$L_{0.01}$ $[10^{34}cm^{-2}s^{-1}]$	1	2	(0.74)	2.5(3.0)	2.8
Beam power	[MW]	10.5	28	9.6	48	29
Eff. gradient	G [MV/m]	21	80	5000	1000	1000
Particl./bunch	N $[10^9]$	20	3.72	4	10	10
Bunch length	σ_z [μm]	300	44	1	20	20
IP beam size	$\sigma_{x,y}$ [nm/nm]	474/6	40/1	10/10	194/1.1	97/1.1
Emittances	$\varepsilon_{x,y}$ [nm]	10^4/35	660/20	100/100	10^4/35	2500/35
Bunches/train	n_b	1312	312	1	1	1
Bunch dist.	Δz [ns]	554	0.5	66.7×10^3	10^5	1.67×10^5
Rep. rate	f_r [Hz]	5	50	1.5×10^4	10^4	6000

Plasma collider parameters are evolving… Sets for higher energies upto 30 TeV cme also exist

Plasma e+e- Colliders :

- Energy: 0.25, 1, 3, …30 TeV
  - compact (?)… less cost (?)

- Many (most) issues are the same as for any (traditional) linear collider:

$$\mathcal{L} \propto \frac{n_\gamma^{3/2}}{\sqrt{\sigma_z}} \frac{1}{\sigma_y} N n_b f_r$$

  - Power efficiency (CLIC 11%)
  - Small emittances, jitter, etc
  - Few nm focusing, FF stability
  - Beamstrahalung

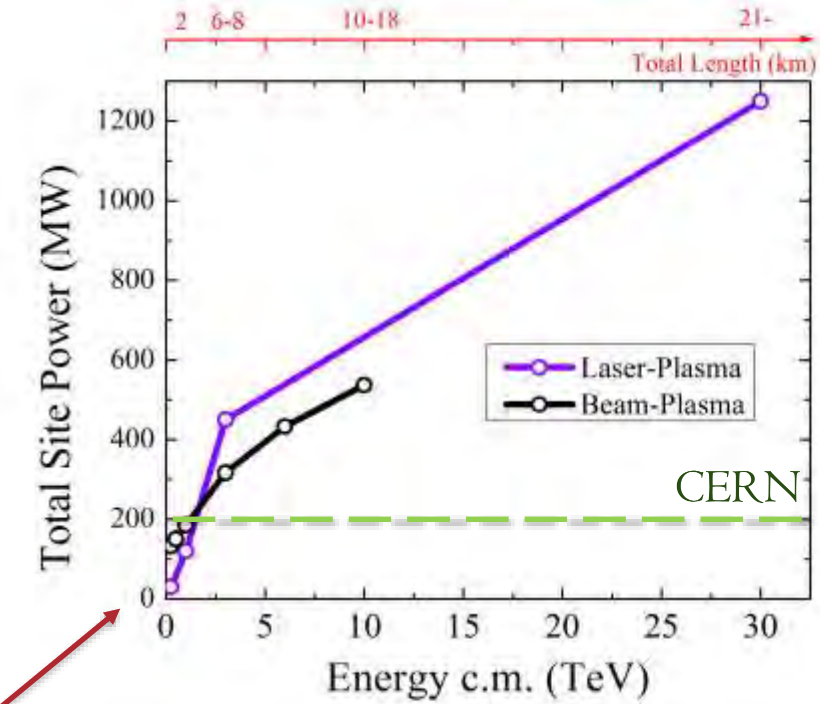

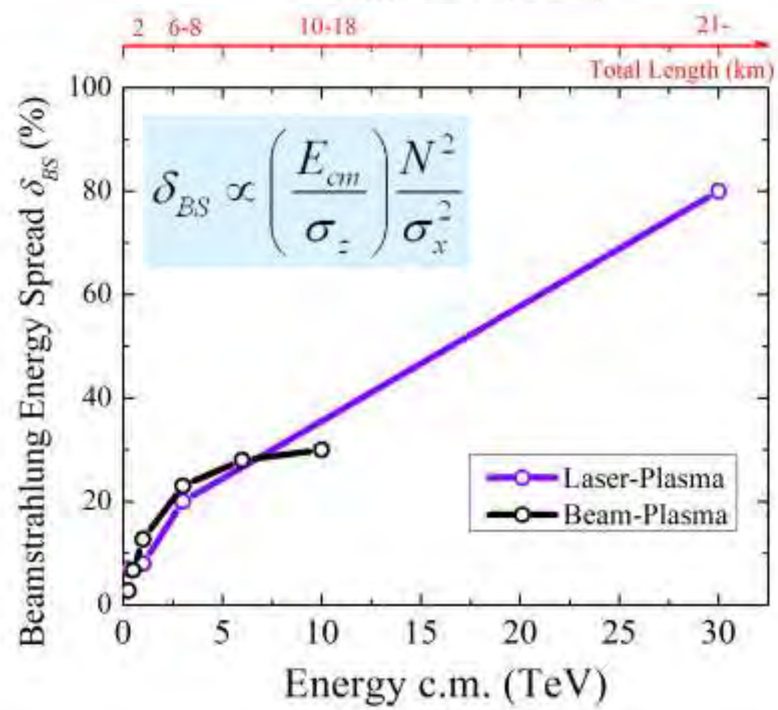

Potential Advantage of Plasma-based Colliders: Beamstrahlung Minimization (due to x100 shorter bunches)

- TeV-scale colliders will operate in high-beamstrahlung regime Y>1

$$\Upsilon = \frac{2}{3}\frac{\hbar\omega_c}{E_0} = \frac{5}{6}\frac{N r_e^2 \gamma}{\alpha(\sigma_x + \sigma_y)\sigma_z}$$

- Beamstrahlung suppressed by using short beams (in limit Y>>1)

Photons/e$^-$: $n_\gamma \approx 3.5\delta_{\mathcal{E}} \propto \mathcal{L}^{1/3}\sigma_z^{1/3}$

e$^+$e$^-$ pairs : $n_{e^+e^-} \propto \sigma_z^2\Upsilon^2\Xi(\Upsilon) \propto \sigma_z^{2/3}\ln(\Upsilon)$

- Shorter beams save power:

Beamstrahlung background

Collider power

$$\frac{\mathcal{L}}{\mathcal{E}_{\rm cm}^2} \propto \frac{n_\gamma^{2/3}\eta P_{\rm wall}}{\sigma_* \sigma_z^{1/2}}$$

Short beams

- Plasma-based accelerations intrinsically produce short (~plasma skin depth) beam (plasma wavelength $\lambda_p = 2\pi c\sqrt{m\varepsilon_0/n_e e^2}$ ~100 um at 1e17 cm^-3 density)

Fermilab

Key R&D challenges for plasma accelerators

- **Energy staging + Beam matching/coupling between stages**
  - Strong focusing forces in plasma: $\beta \sim 0.01$ - 0.1 m
  - Finite energy spread (<1%)
  - >99% transfer efficiency (100 stages → 1/e survive), ~<1% ε growth
- **Resolve positron (e+) acceleration challenge**
  - Proposed configurations (hollow plasma channels, plasma columns) require experimental demos
- **Alignment**
  - Small structures (~10-100 um) place severe (~nm) alignment tolerances
- **Potential plasma-based sources of beam quality degradation**
  - Transverse stability in strongly beam-loaded regime
  - Scattering (with background ions)
  - Betatron radiation in strong plasma focusing fields
- **Laser/Beam driver technology development**
  - Coherent combining of fiber lasers or Tm:YLF lasers (PW/1 sec → PW at 10 kHz)
  - E.g., SLC ~600kW beam → 2x 25 MW SC drive beam linacs (ie ~x40)

Energy Staging : LWFAs

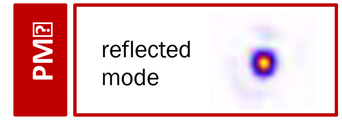

- **Proof-of-principle staging of laser-driven plasma wakefield accelerators (LWFAs) at (BELLA, LBNL)**

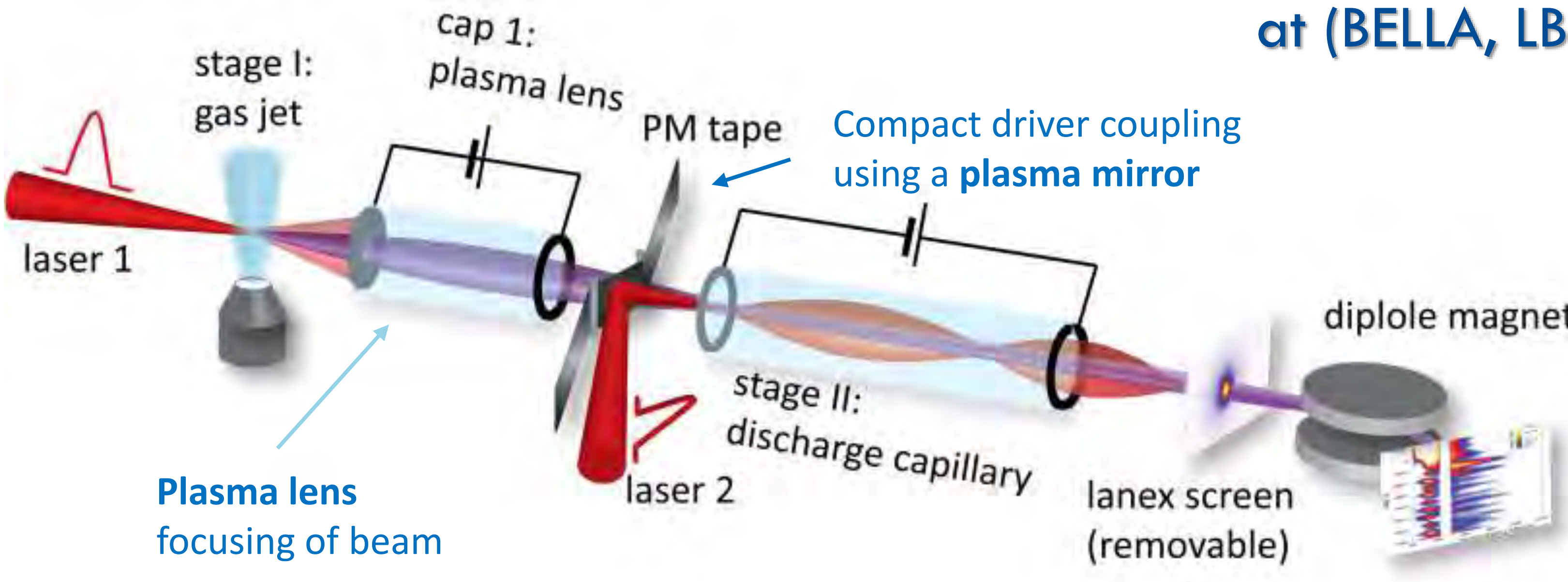

- Proof-of-principle experiment demonstrate 100 MeV energy gain (on top of 120 MeV stage1)
  - Poor capture efficiency, beam-quality preservation
- Multi-GeV (5 GeV + 5 GeV) staging experi-ments are planned at Berkeley Lab (BELLA)
  - *Goal*: near-100% capture efficiency, quality preserve

Steinke et al. Nature (2016)

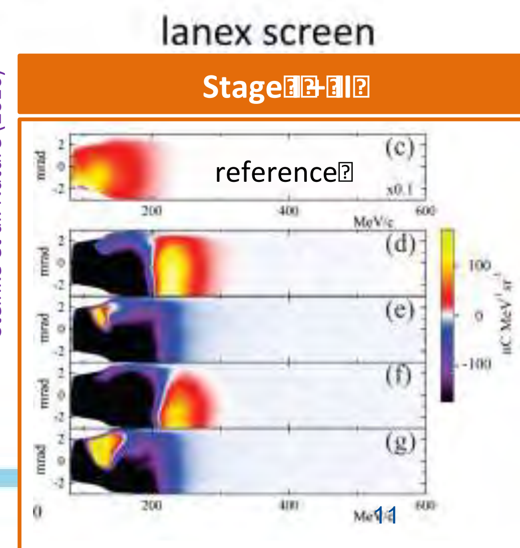

Focusing and Matching and Timing btw Stages

Plasma channel is a strong focusing element!

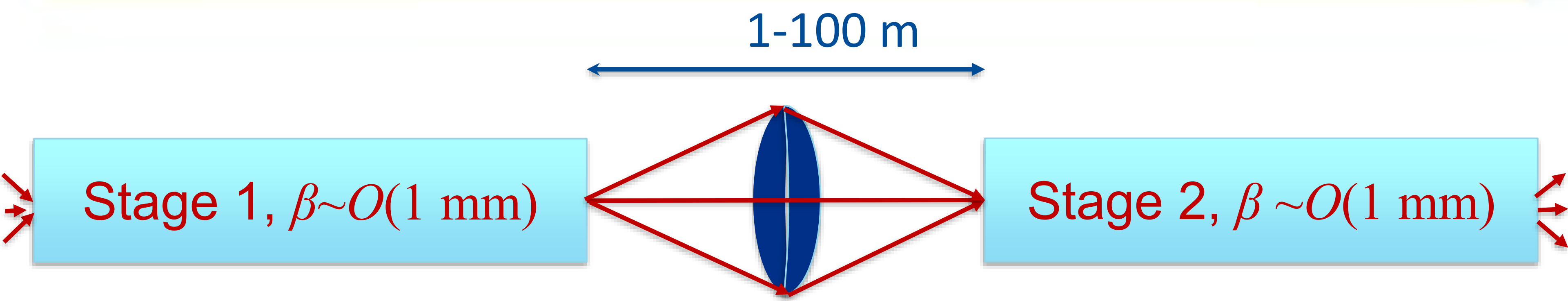

- Longitudinal timing accuracy ~1% of plasma wavelength ~1um
  - 0.5% energy spread at end of linac (100 stages) can be caused by wake field timing jitter 0.3 um
- From small β to large – need short focusing lens (eg plasma lens) as $\beta(s) = \beta(0) + s^2/\beta(0)$
- Stability (shot to shot) and nonlinearities of the optical channel
- Transport channel with few % energy acceptance, minimal β mismatch (<3-10%) and good chromaticity compensation
- NB: main beam focusing optics should be compatible with drive beam/laser pulse optics

Issue: Transverse Tolerances *O*(1 nm)

First order estimate for middle part of cell

Laser or drive beam center defines center of the focusing

$$\sigma_y \approx 42 \text{ nm} \left(\frac{\text{GeV}}{\text{E}} \frac{10^{16} \text{ cm}^{-3}}{\text{n}_0} \right)^{\frac{1}{4}} \sqrt{\frac{\epsilon_\text{y}}{\text{nm}}}$$

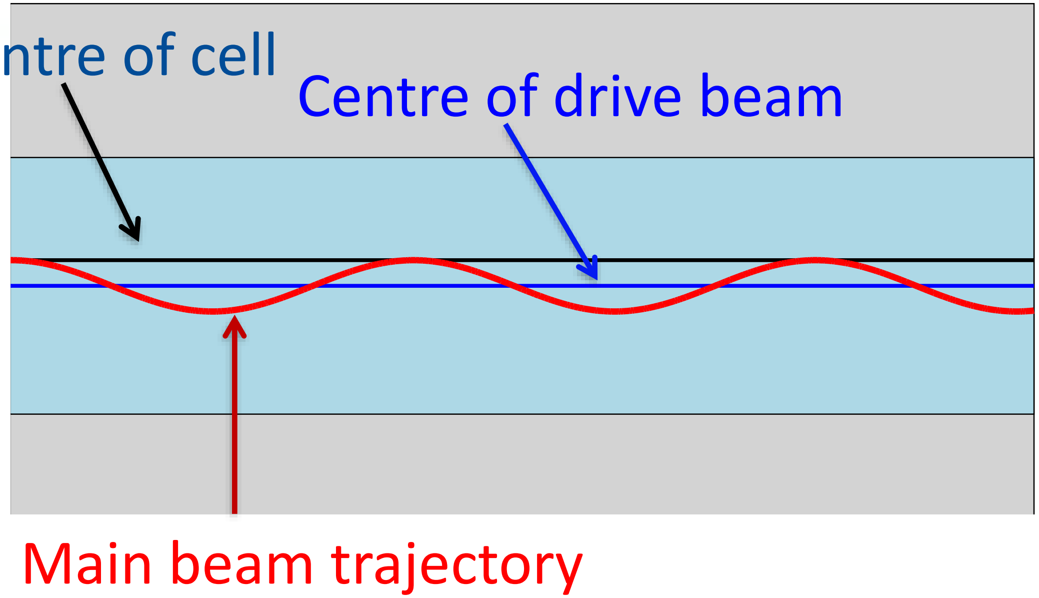

PWFA beam at 1.5TeV has σ_y=O(30 nm) for $n_0=2\text{x}10^{16}\text{cm}^{-3}$

⇒ Beam jitter stability O(1 nm)?

  ⇒ Tough for laser/drive beam

⇒ Static misalignment is also critical

  ⇒ but depends on beam energy spread and tuning methods

Important to understand tolerances correctly

R&D programme essential on transverse alignment and stabilisation

Two possible plasma regimes:

Quasi-linear regime vs "Bubble" (a.k.a blow-out)

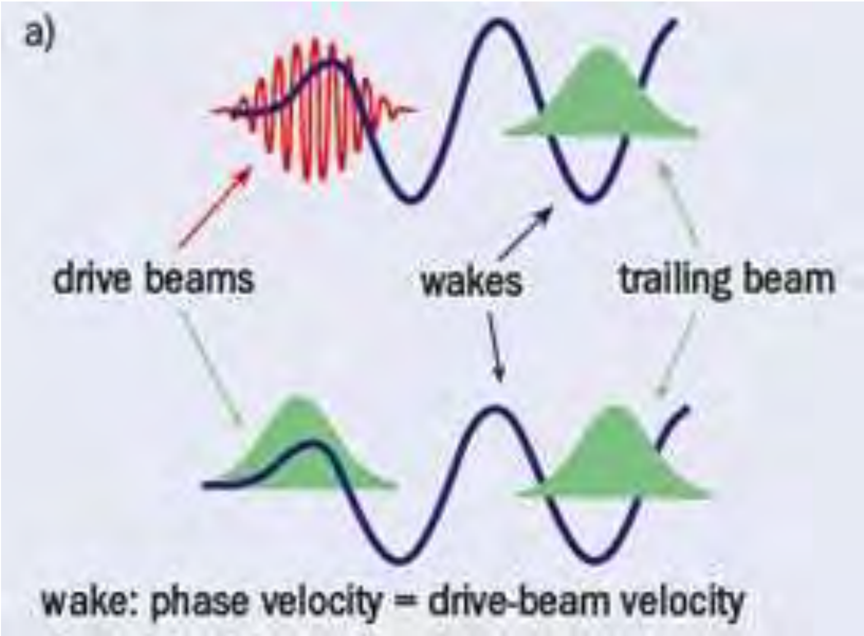

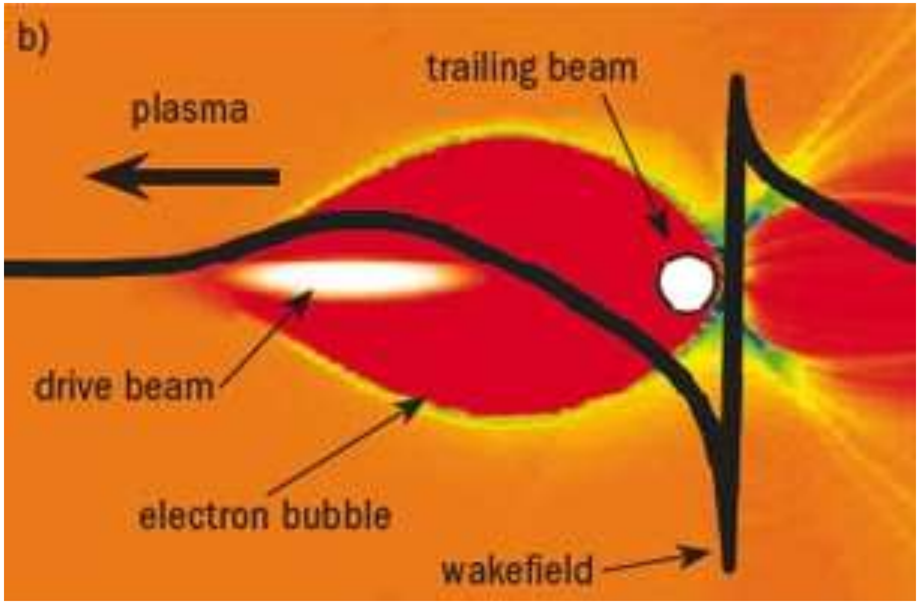

$$\Delta n < n_e$$

suitable for both e- and e+

$$n_e = 0$$

Suitable for e-,
not suitable for e+
(positively charged ions left behind in the bubble defocus positrons)

Issue: acceleration of positrons

- Acceleration of positrons is possible (in principle) in a quasi-linear regime $(\Delta n < n_e)$
  - To avoid plasma pinching by the trailing bunch, it requires low bunch density, $n_b < n_e$. This, in turn, requires weak focusing, especially because of the adiabatic emittance damping during acceleration.
  - Challenging for colliders: Because of weak focusing, Coulomb scattering in plasma (or gas) leads to high emittances (PRST-AB 16, 108001 (2013))
  - Mitigation suggested: a hollow plasma channel (no plasma focusing) to avoid Coulomb scattering. However, weak focusing makes transverse head-tail instability severe.
  - In a regime of dense positron bunches, $n_b > n_e$, the plasma electrons get pulled into the positron bunch and create highly-nonlinear focusing

Quasi-linear regime: linear e+ focusing and acceleration, Independent control of acceleration and focusing

Accelerating field

Plasma density

Focusing field

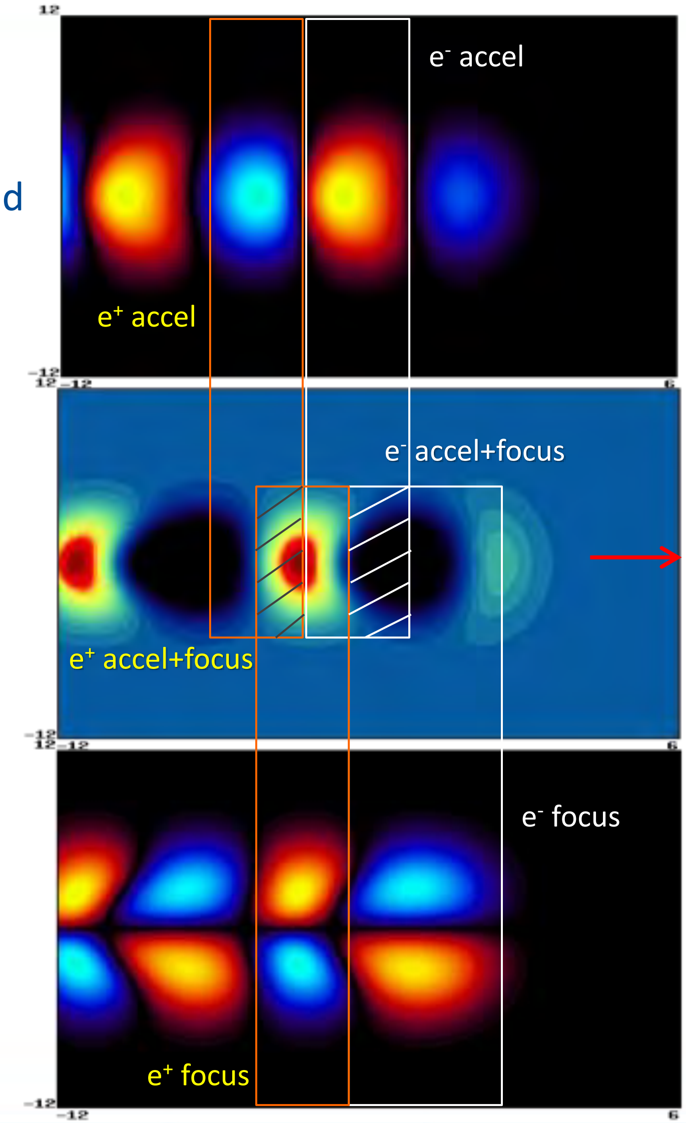

Positron beam quality preservation in highly-nonlinear regime difficult

- Electron focusing determined by background ion density
- Focusing of e+ may take place only at (very peculiar) locations where plasm electrons get back together

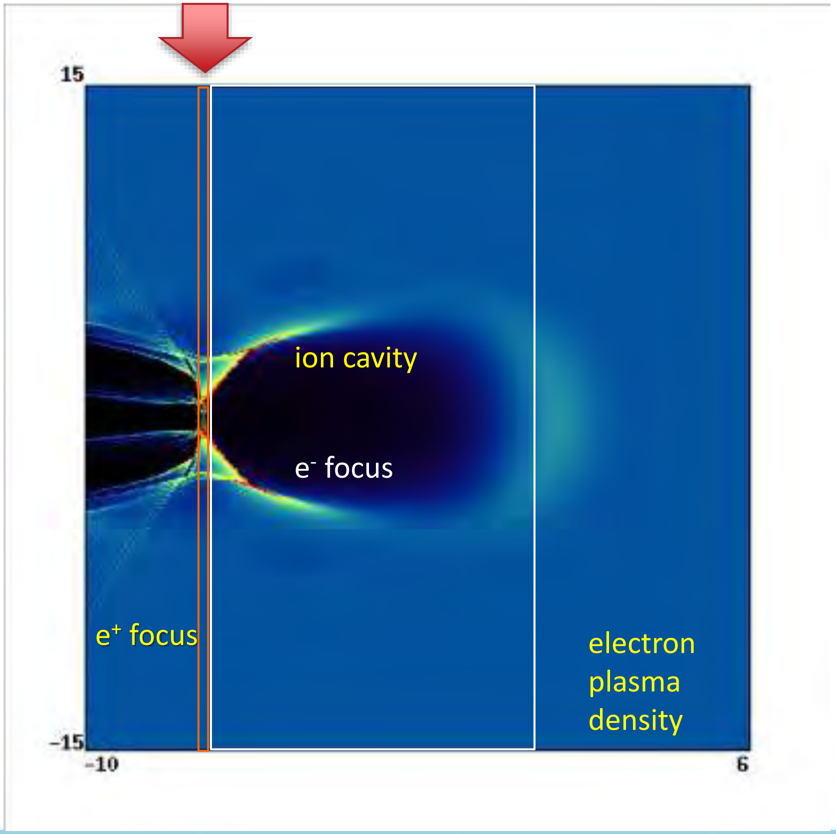

Positron beams accelerated in hollow plasma channel with external focusing

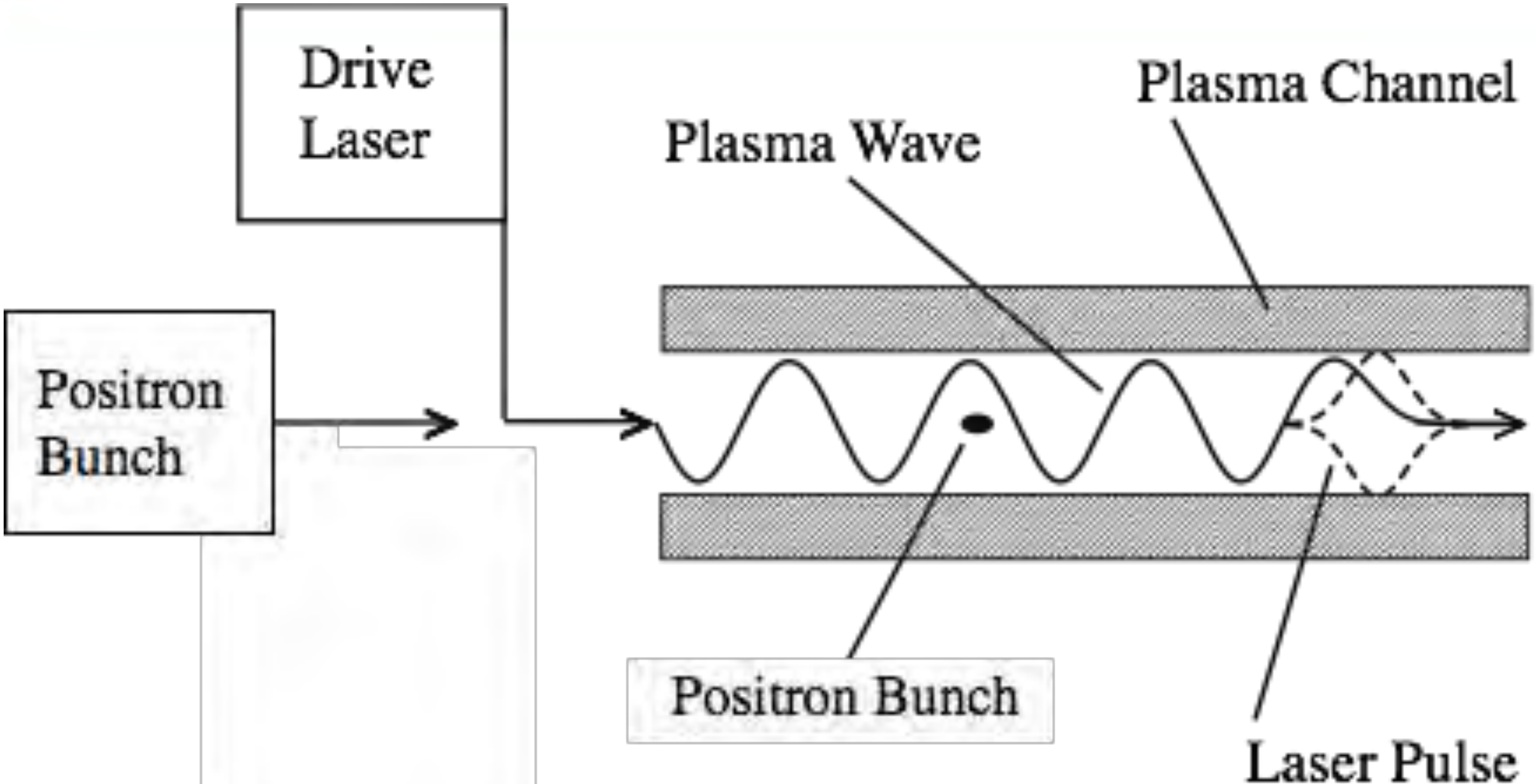

- Provides structure for laser guiding (determined by channel depth not on-axis density)
- Excellent wakefield properties in plasma channel and *independent* control over accelerating and focusing forces
  - Accelerating wakefield transversely uniform
  - Focusing wakefield linear in radial position and uniform longitudinally
- Focusing for positrons provided by external magnets – too weak to control BBU (see below)

Efficient Acceleration in Plasma

- …besides technical issue of heating plasma O(100kW/m)
- The *Q*-factor is very low (for high fields) – must accelerate the bunch within one plasma wavelength of the driver!
- Cannot add energy between bunches, thus a single bunch must absorb as much energy as possible from the wake field

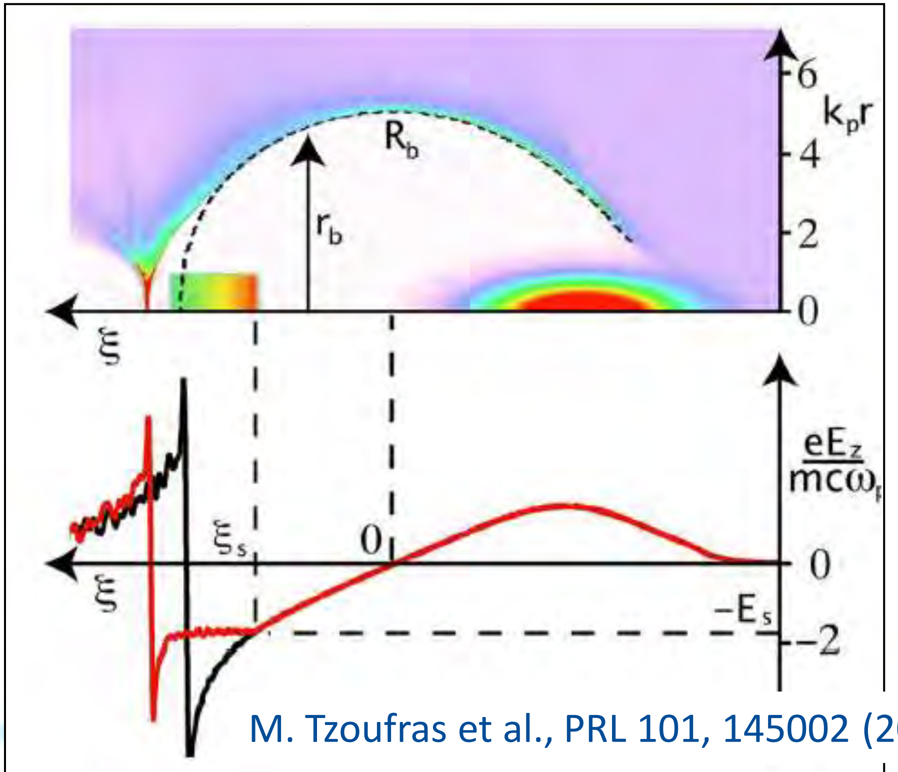

M. Tzoufras et al., PRL 101, 145002 (2(

= strong beamloading (beam distorts accelerating field wave)

- Beam loading is needed for overall acceleration efficiency
- To achieve L ~10^{34}, bunches should have ~10^{10} particles (similar to ILC and CLIC).
- Wakefield is quite nonlinear and longitudinal shaping of the e+e- bunches is needed to keep reasonably small dE/E

On Efficiency of Energy Transfer in a quasi-linear regime

- Shaping of bunch profile can significantly reduce accelerating voltage variations along the bunch
  - Growth of accelerating voltage is compensated by growth of decelerating force along the bunch

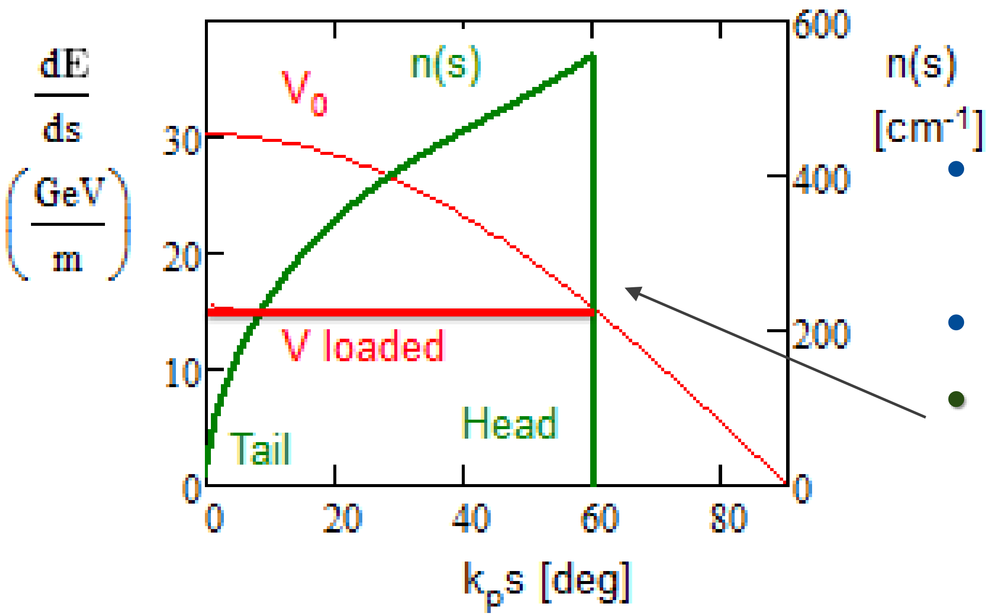

Longitudinal bunch density and loaded accelerating voltage for 50% beam loading

- The total bunch length is (60 deg. for 50% beam loading)
- Zero energy spread
- Creating such shapes (triangular or trapezoid) with required beam brightness is a challenge
- Long bunches are challenging because of IP beamstrahlung

Transverse Beam Break-Up (head-tail instability)

- Transverse wakes act as deflecting force on bunch tail
  - beam position jitter is exponentially amplified

Beam Stability

- Transverse stability of a beam with initial offset of σ_y
  - no energy spread assumed in the beam
  - emittance with respect to the beam axis is shown

$\Rightarrow$ acceptable for ILC (top)

$\Rightarrow$ would be intolerable for CLIC (bottom)

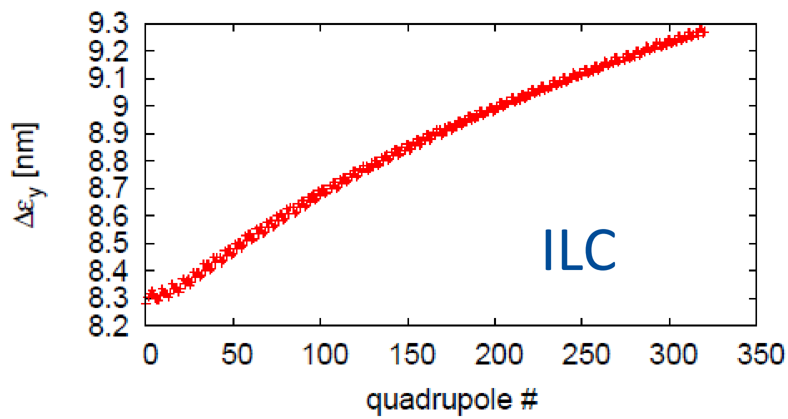

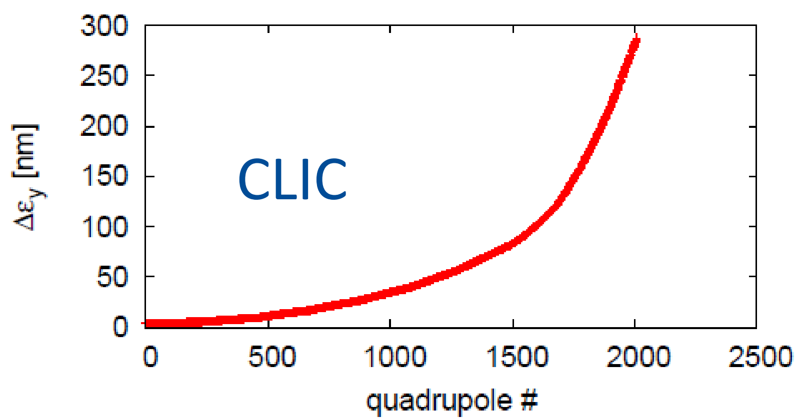

D. Schulte, 6th Linear Collider School 2011, Main Linac Basics 69

Short-range transverse wake

$$W_\perp(z) \sim \frac{Z_0 c z}{a^4}$$

$a \approx 35$ mm (ILC)

$a \approx 3.5$ mm (CLIC)

$a \sim 0.1$ mm (PWFA)

BNS damping needs

$$\left.\frac{\delta p}{p}\right|_{BNS} = \frac{N_w r_0 W_\perp}{4 k_\beta^2 \gamma}$$

Beam breakup in various collider proposals

- ILC
  - Not important; bunch rf phase is selected to compensate for long wake and to minimize the momentum spread
- CLIC
  - Important; bunch rf phase is selected to introduce an energy chirp along the bunch for BNS damping (~0.5% rms). May need to be de-chirped after acceleration to meet final-focus energy acceptance requirements
- PWFA
  - Critical; BNS damping requires large energy chirp (see below). De-chirping and beam transport is very challenging because of plasma stages (small beta-function in plasma ~1 cm). In essence, requires a "final-focus" optics between every stage.

BNS damping is needed → need dE/E

Achieving Beam Stability

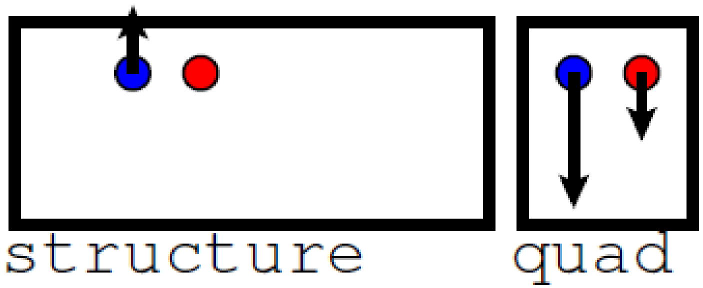

- Transverse wakes act as defocusing force on tail

  ⇒ beam jitter is exponentially amplified

- BNS (Balakin, Novokhatsky, and Smirnov) damping prevents this growth
  - manipulate RF phases to have energy spread
  - take spread out at end

$$\left.\frac{\delta p}{p}\right|_{BNS} = \frac{N_w r_0 W_\perp}{4k_\beta^2 \gamma}$$

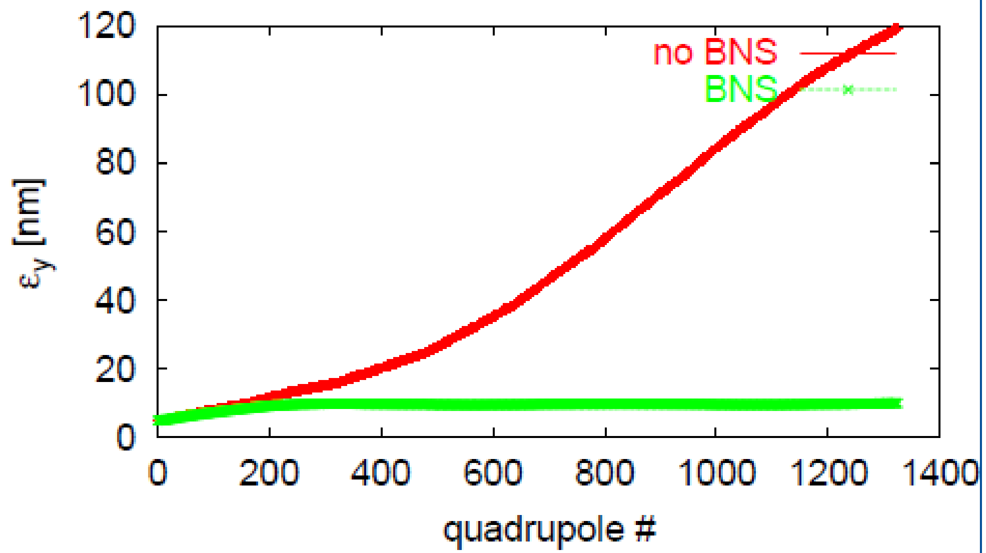

D. Schulte, 6th Linear Collider School 2011, Main Linac Basics 70

BNS Damping in Plasma Accelerators

- Head-to-tail betatron frequency spread effective in suppressing BBU is single stage, but requires large energy spreads:

$$\frac{\Delta\gamma}{\gamma} \approx \frac{I}{I_A}(k_w L_b)\left[\frac{2K_1(k_w r_c)\Omega_1(k_w r_c)}{(k_w r_c)^3 K_2(k_w r_c)}\right] \sim 0.1$$

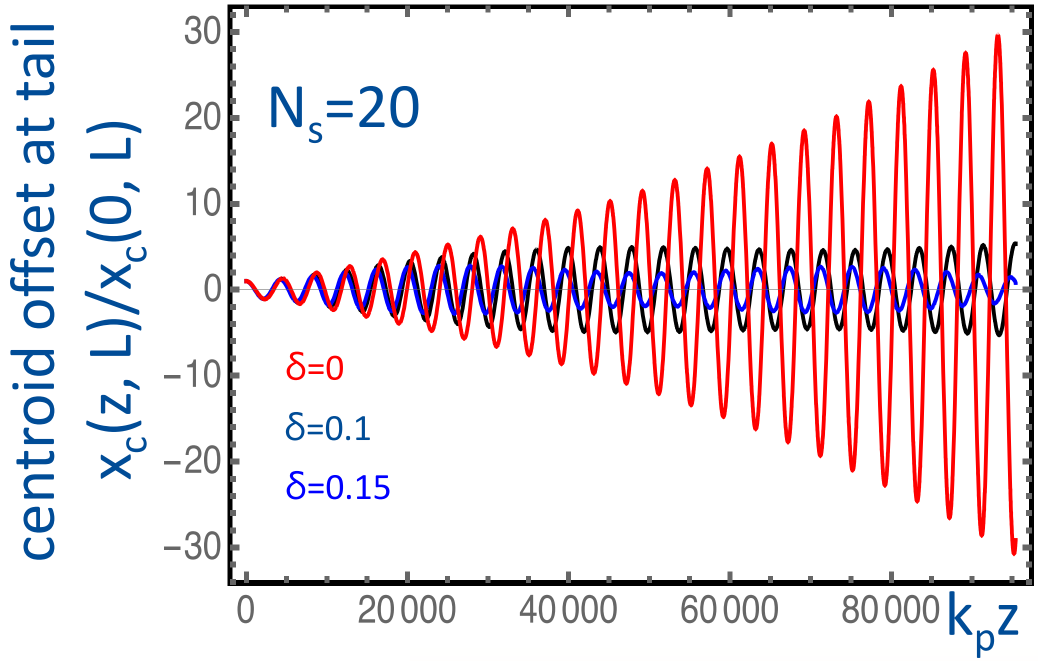

- Linear head-tail energy chirp:

$$\gamma(\zeta) = \gamma_0\left[1 - \delta(\zeta/L_b)\right]$$

Fermilab

Beam Loading and BNS Damping

- Beam loading and the transverse beam stability are closely coupled:
  - higher beam loading requires higher energy spreads along the bunch to keep the bunch transversely stable (by BNS damping).
  - Consequence of Panofsky-Wenzel theorem

$$\left.\frac{\delta p}{p}\right|_{BNS} \geq \left(\frac{P_w}{P_d}\right)^2$$

- In the bubble regime (where focusing forces are the strongest) the transverse bunch stability requires energy spread comparable to beam loading: 50% beam loading requires ~25% energy spread (in a linear BNS theory)

Energy Spread and Final Focus System

Final focus system has limited energy bandwidth

⇒ Need to limit beam energy spread

⇒ In CLIC 0.35% RMS spread

⇒ This is an important limitation for CLIC

Energy stability required for CLIC is O(0.1%)

- Due to limited final focus system acceptance
- Corresponds to 0.2° (=15μm) coherent phase tolerance drive-beam to main-beam
- Challenging task, similar to XFEL goal

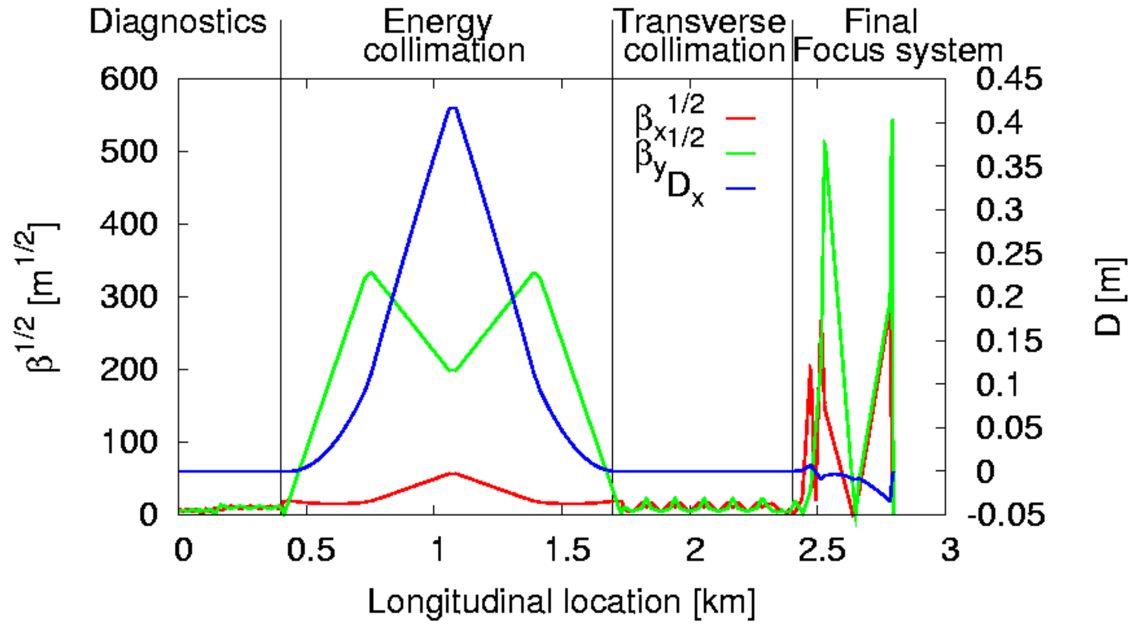

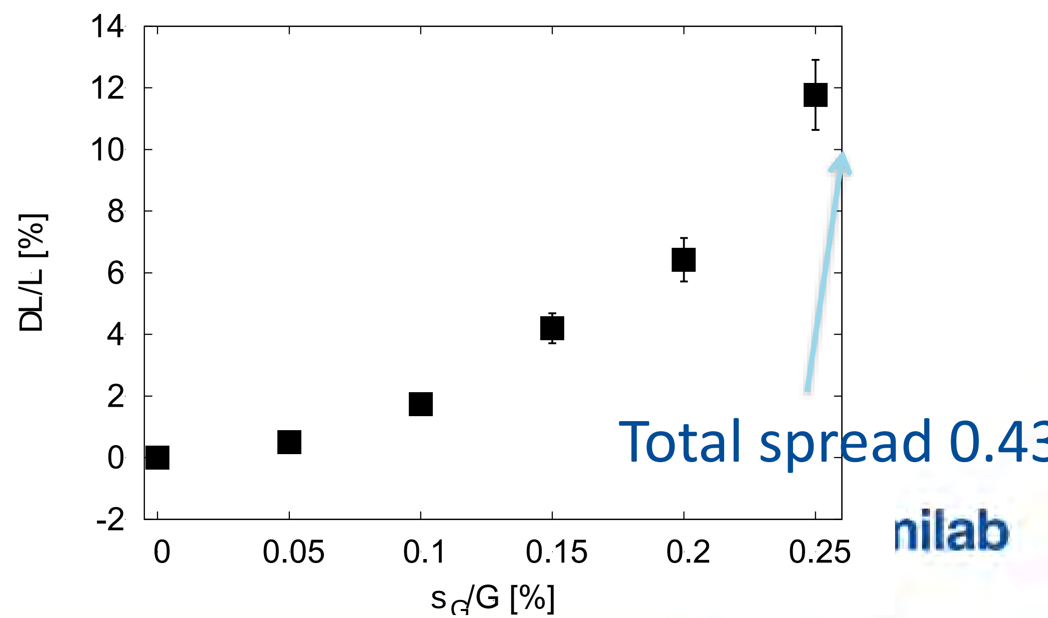

… for completeness:
(more or less) exotic schemes

Variety of Possibilities to Accelerate

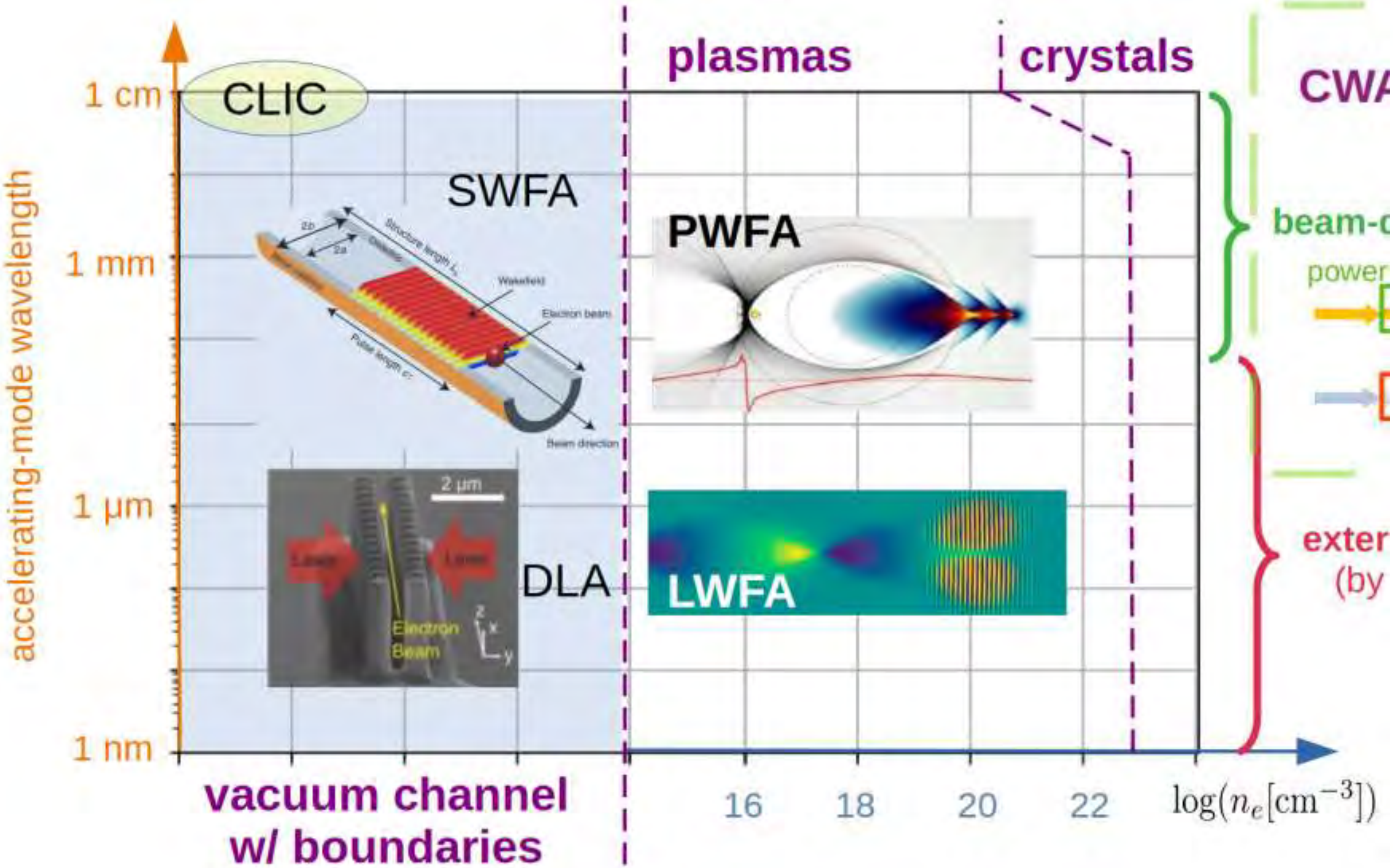

Structure Wakefield Accelerator (SWFA)

Collinear Acceleration

- Single wakefield structure
- No need for RF couplers
- Wide range of RF frequencies
- Easier to explore very high gradients at high frequencies
- Common transport optics for both beams (drive and witness) may create difficulties, especially for staging

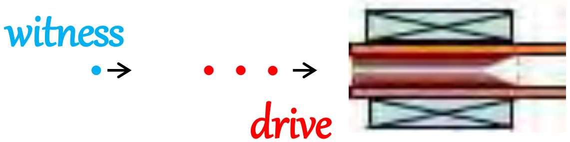

Two Beam Acceleration (TBA)

- Need for RF couplers on both structures
- Short RF pulses require broad bandwidth couplers
- Each structure can be optimized independently
- Independent beamline optics makes staging much simpler

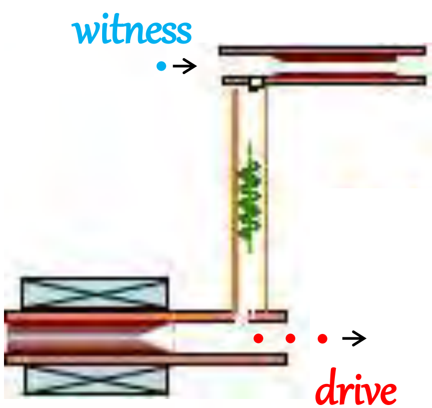

SWFA State-of-the-Art ~1.3 GV/m

Quartz tube : 0.4 ID, 0.53 mm OD
Resonant mode 422 GHz
Excited by 3.2 nC 20 GeV e- bunch
~30x30x30 um

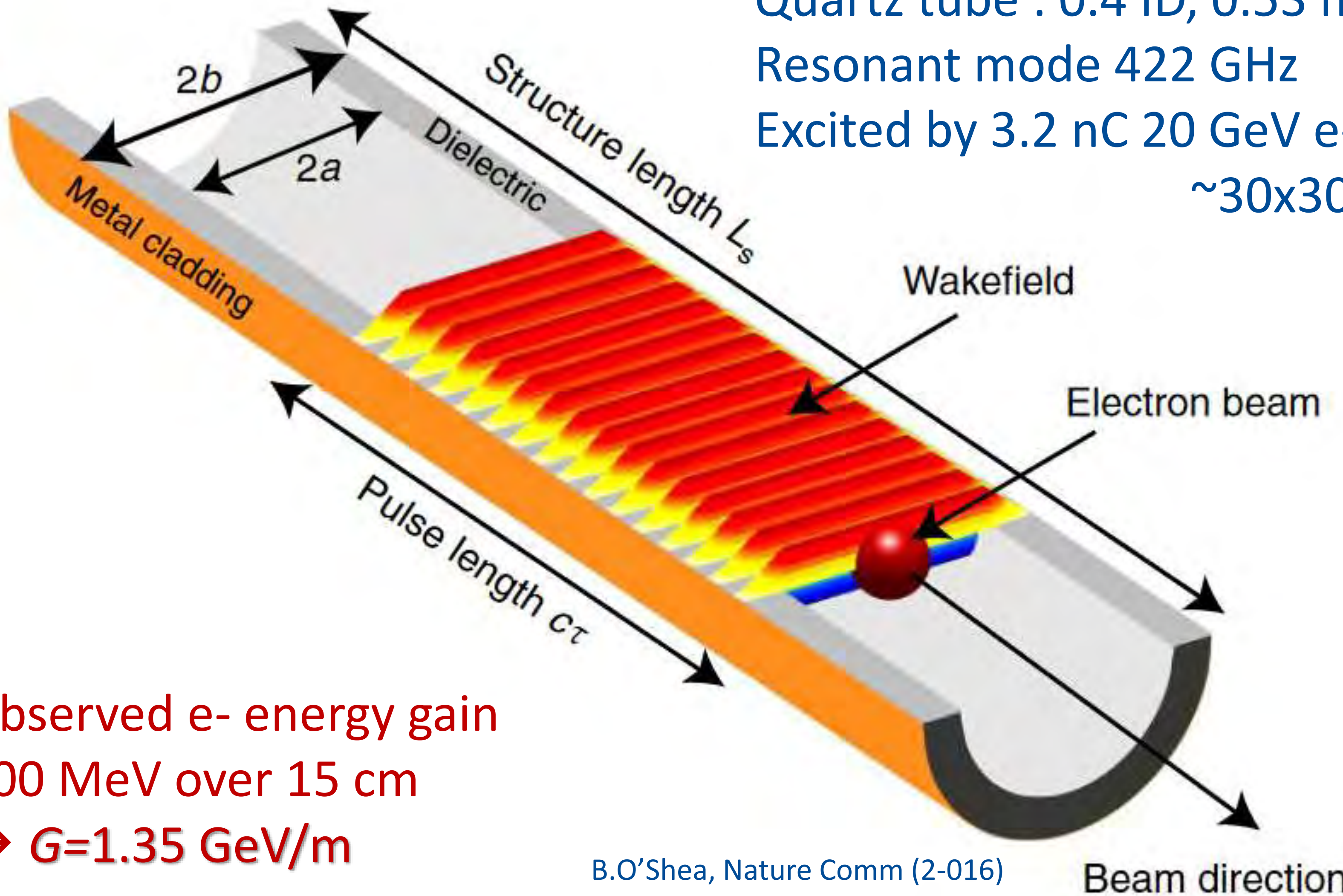

Observed e- energy gain
200 MeV over 15 cm
→ *G*=1.35 GeV/m

B.O'Shea, Nature Comm (2-016)

Tw-beam SWFA: Argonne Flexible Linear Collider

strawman

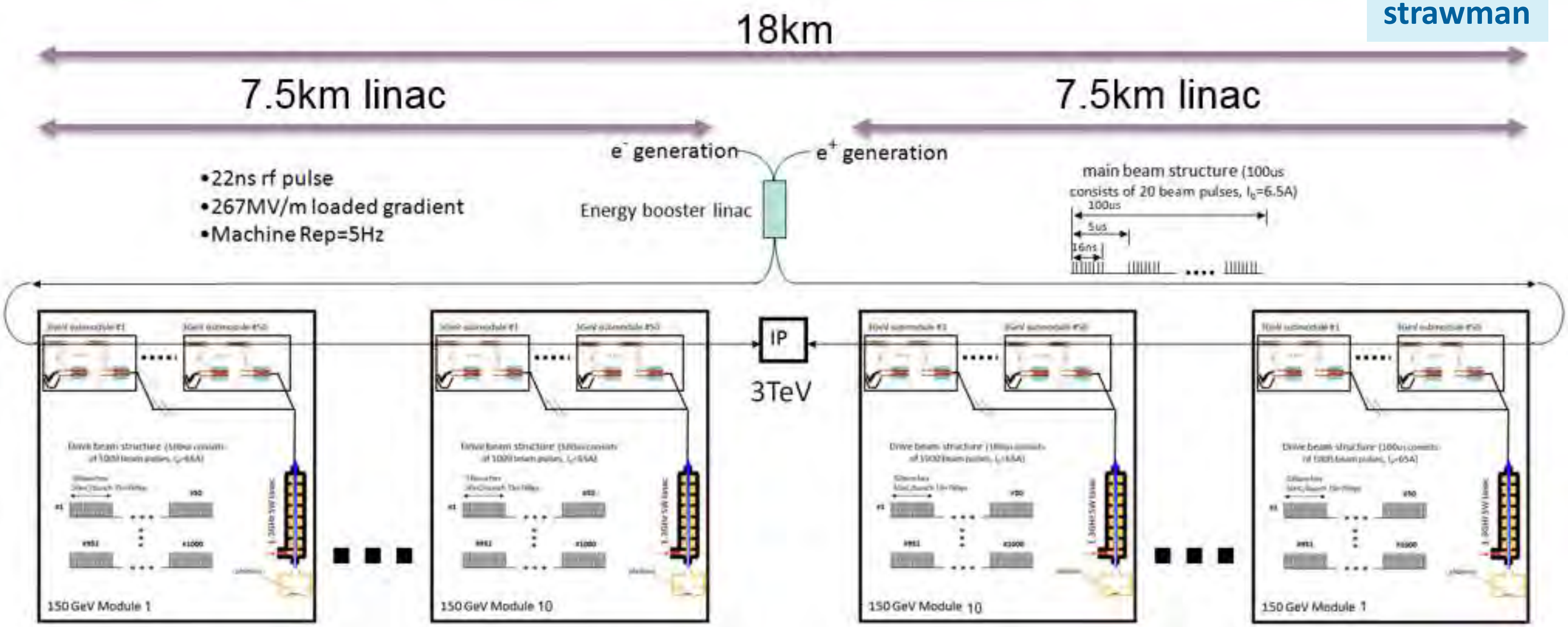

W. Gai, C. Jing, J.G. Power, *JPP* **78**, 339-345 (2012)

- **~300 MV/m loaded accelerating gradient using short RF pulse (~20 ns)**
- **26 GHz normal-conducting dielectric decelerating/accelerating structure**
- **Efficiency under systematic study (7-15% depending on technologies development)**

Dielectric Laser Collider (DLA)

R. J. England et al.

"Accelerator on a Chip"

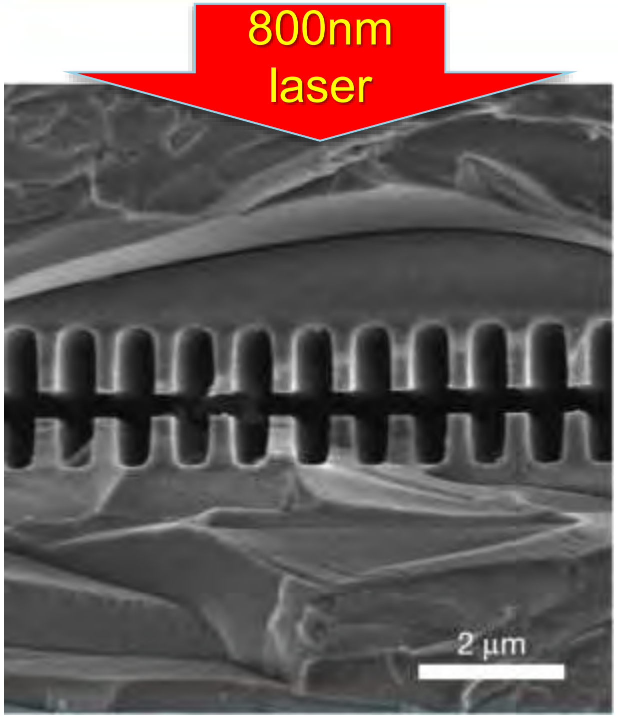

Required lasers are MHz rep rate, low pulse energy, wallplug efficiency ~ 30%

Dielectric materials can withstand upto GV/m fields and kilowatts of average power

Can be mass produced using techniques of the integrated circuit industry.

SEM images of DLA prototypes tested at SLAC

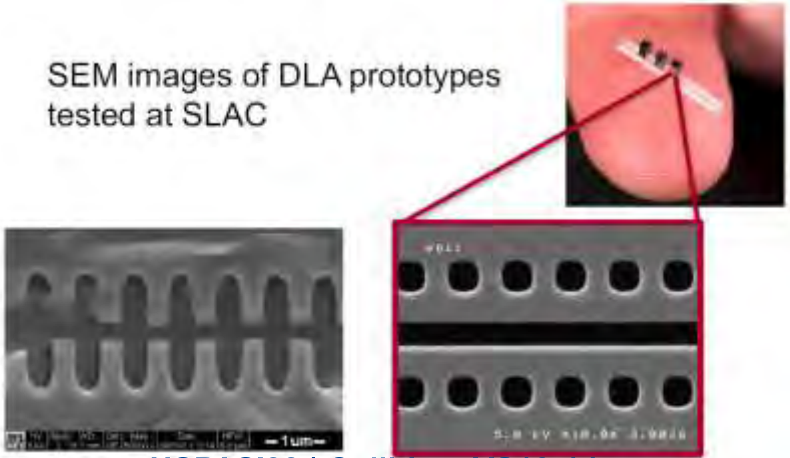

Record 315 keV/0.5mm=0.56GV/m

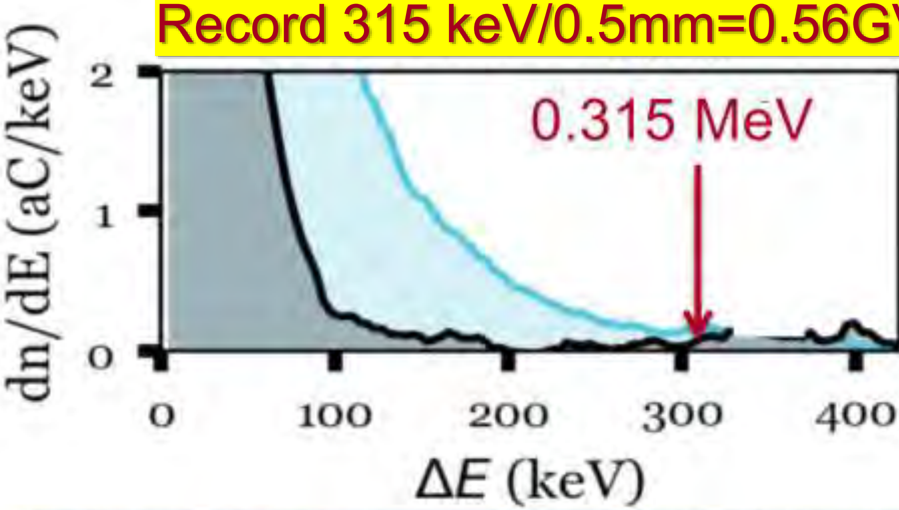

D. Cesar, et al., Optics Express **26** (22), 29216 (2018)

DLA Collider Concept Scheme

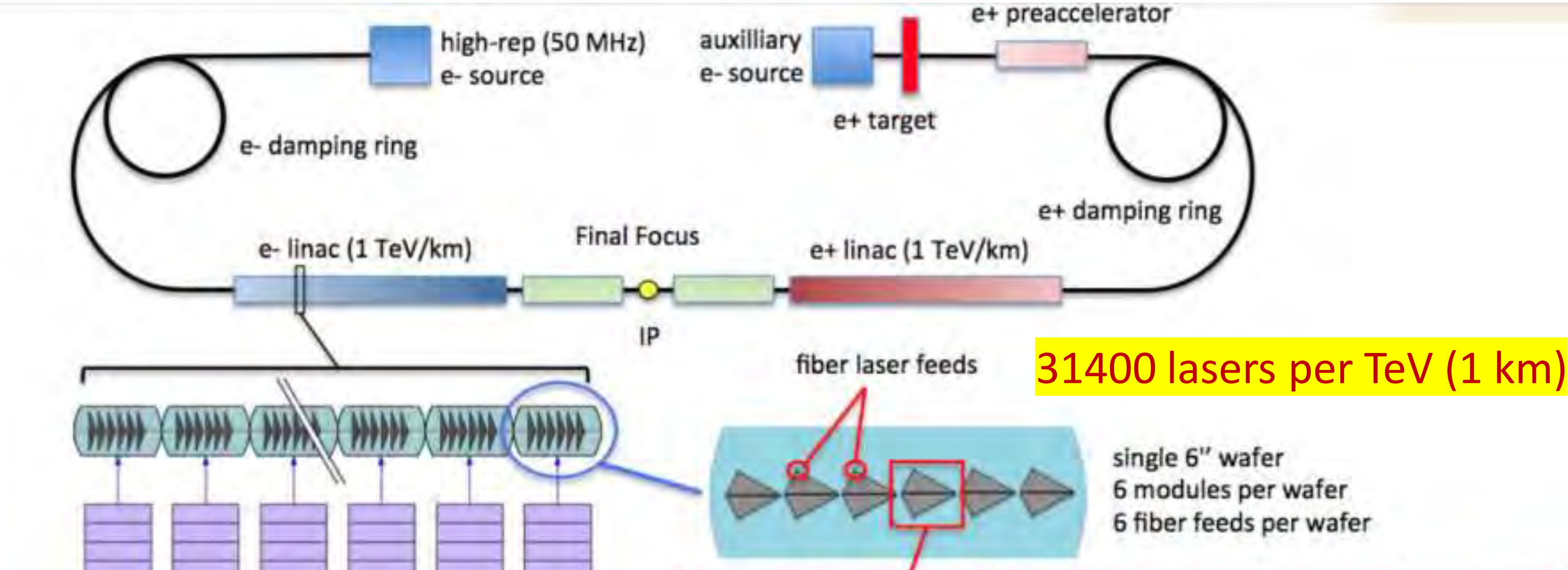

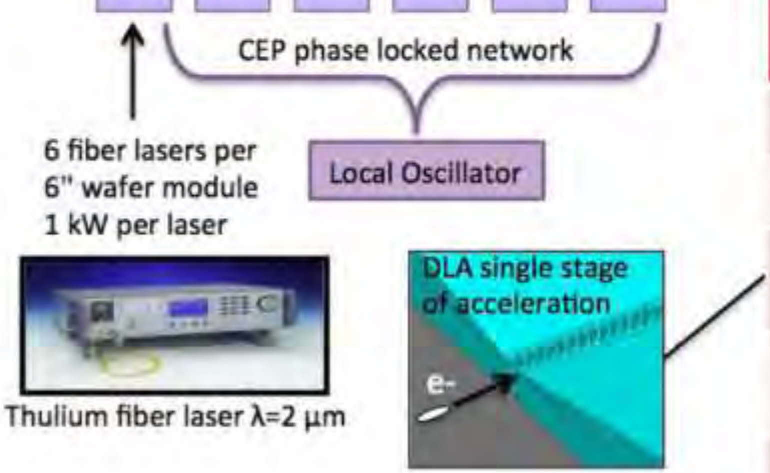

Parameter	Units	CLIC 3 TeV	DLA 3TeV	DLA 250 GeV
Bunch Charge	e	3.7e9	3.0e5	3.8e5
Rep Rate	MHz	5e-5	20	60
Beamstrahlung E-loss	%	**28.1**	**1.0**	**0.6**
Enhanced Luminosity / top 1%	cm-2/s	2.0e34	3.2e34	1.3e34
Wallplug Power	MW	582	374	152

Acceleration in Xtals: Continuous Focusing Channel

works best for muons

Tajima, Cavenago → Chen, Noble → Shiltsev, Corde

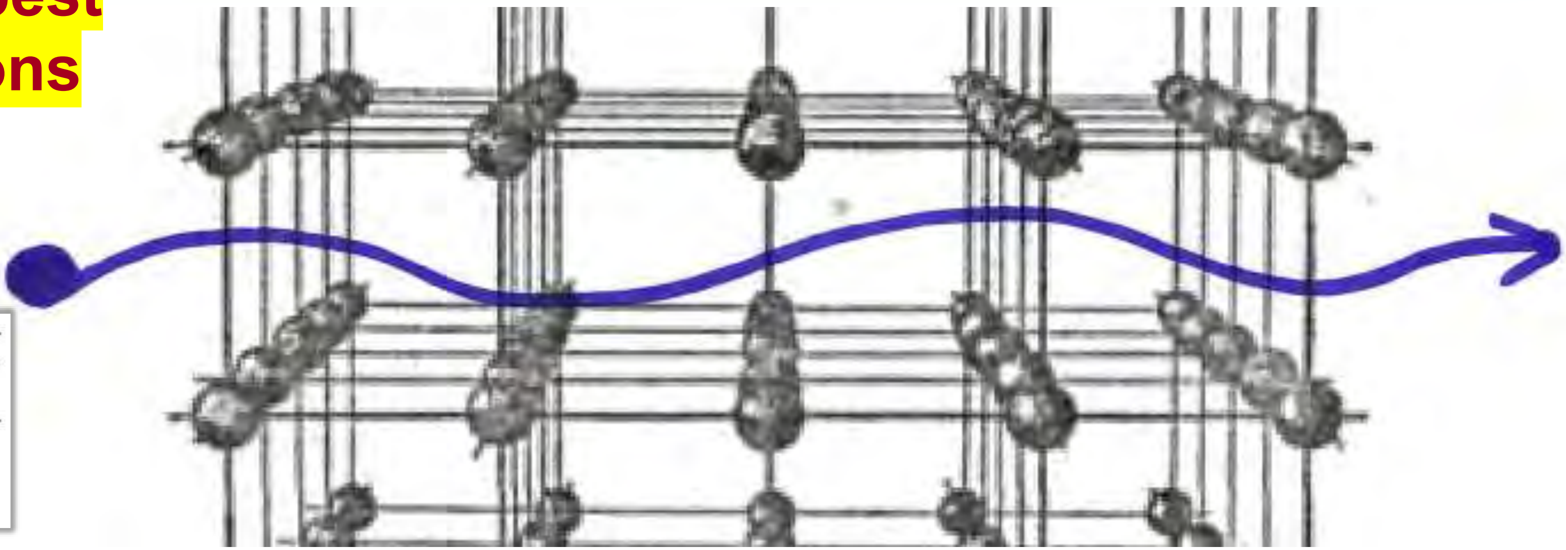

Particle can channel if angle is less than critical

$$\theta_{max} = \sqrt{\frac{2U}{E}}$$

U~20 eV for Si

$$E_0 = \frac{m_e c \omega_p}{e} \approx 100[\frac{GeV}{m}] \cdot \sqrt{n_0[10^{18} cm^{-3}]}$$

10^{22} cm^{-3} → 10 TV/m, λ_p~0.3µm

10^{24} cm^{-3} → 100 TV/m, λ_p~0.03µm

Synchtrotron radiation losses balance energy gain:
0.3TeV for positrons
10 000 TeV for muons (+)
1000 000 TeV for protons

Chen P, Noble R J *AIP Conf. Proc.* **398** 273 (1997)

Wakefield Excitation in Solid Plasmas

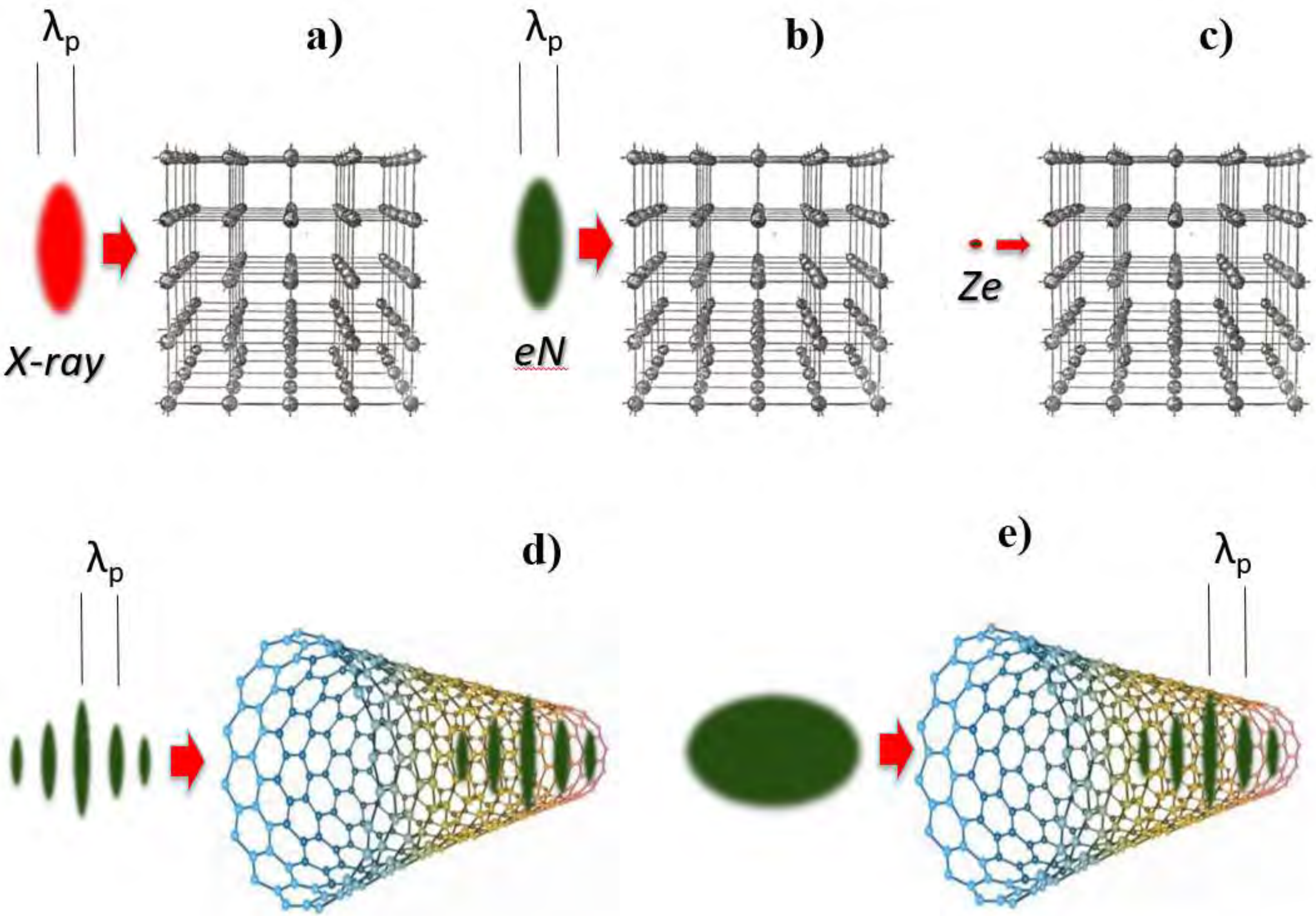

E336 Experiment at FACET-II

Linear $\mu+\mu-$ Crystal X-ray Collider

V.Shiltsev, Physics-Uspekhi 55 (10), 965 (2012)

1 PeV = 1000 TeV

n_{μ} ~1000
n_B ~100
f_{rep} ~10^6
L ~$10^{30\text{-}32}$

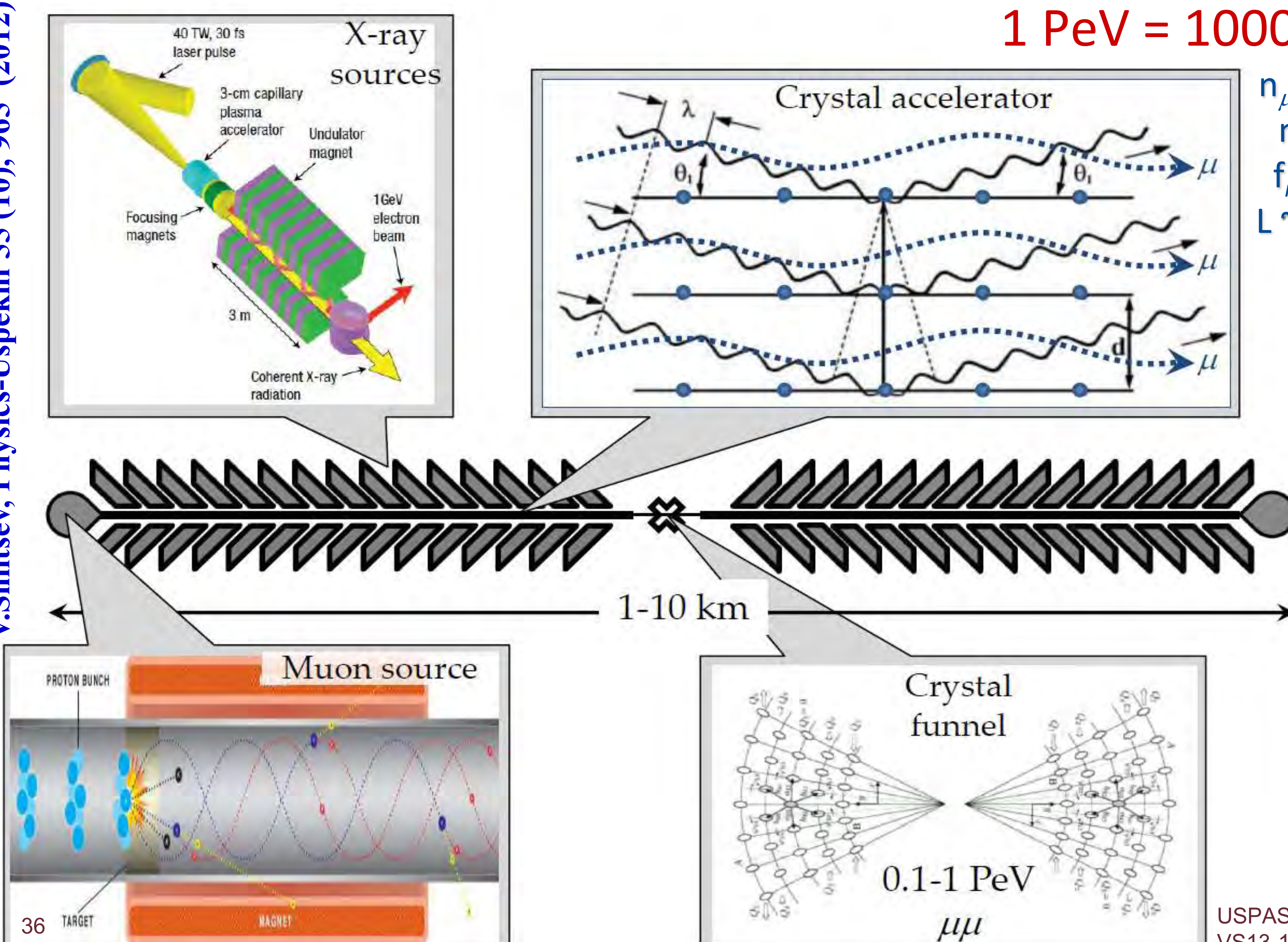

Ultimate Colliders
How would they look like?

Will they look like this?

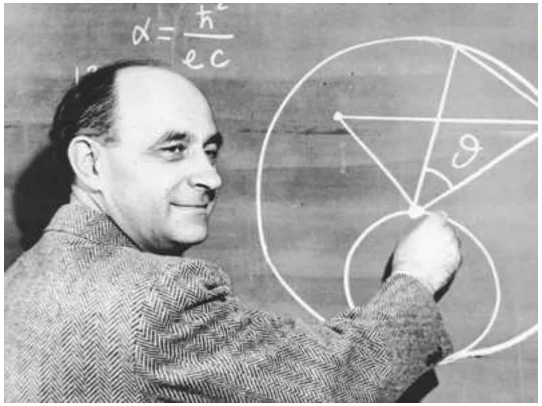

Enrico Fermi

as Enrico Fermi's ultimate accelerator or "globaltron" [46] (see Fig. 6), whose cost would exceed \$20,000B even under a modest estimate of \$0.5B per kilometer of a high-tech accelerator.

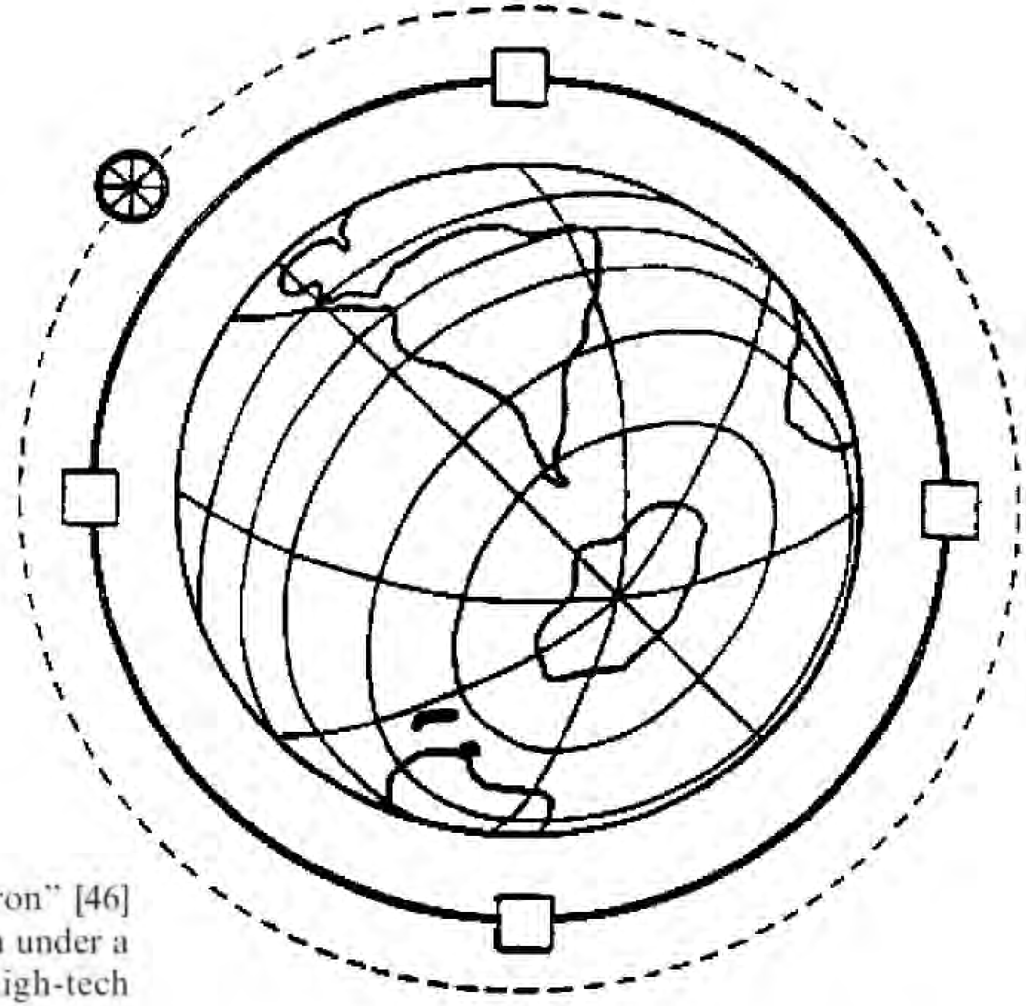

Figure 6. Enrico Fermi's "ultimate accelerator" encircling Earth.

Or like that?

Very large hadron collider on the Moon (CCM), C~11 Mm, $E_{c.m.}$~14 PeV (1000x LHC's), 6x10^5 dipoles with **20 T field**, either ReBCO, requiring ~7-13 k tons rare-earth elements, or IBS, requiring ~a million tons of IBS. **Many of the raw materials required to construct machine, injector complex, detectors, and facilities can potentially be sourced directly on the Moon. 11000-km tunnel a few 10 to 100 m under lunar surface** to avoid lunary day-night temperature variations, cosmic radiation damage, and meteoroid strikes. **Dyson band or belt to continuously collect sun power.** Required: <0.1% sun power incident on Moon surface.

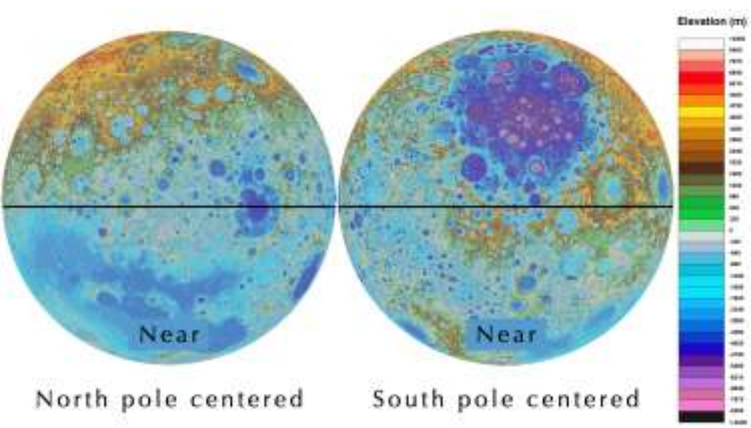

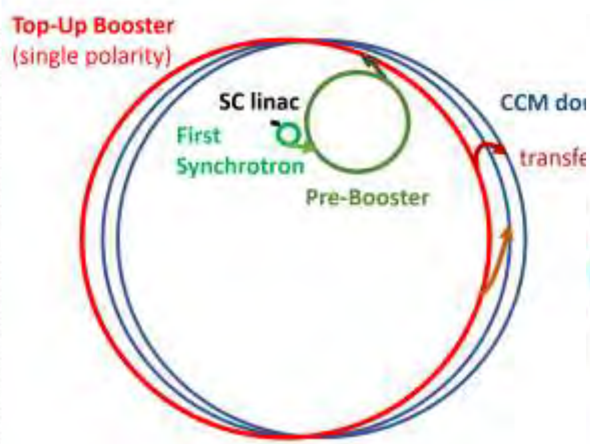

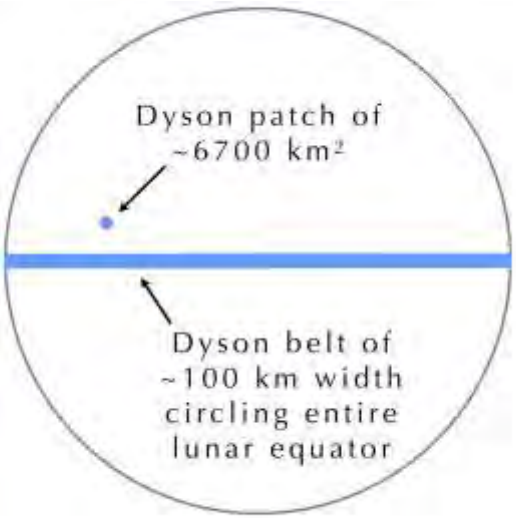

J. Beacham, F. Zimmermann, 2022 *New J. Phys.*, https://doi.org/10.1088/1367-2

Fermilab

In search of uniform approach to discuss far future/ultimate machines

- **BASED ON EXISTING TECHNOLOGIES**
  - **Circular ee**
  - **Linear *ee*/$\gamma\gamma$**
  - **Circular *pp***
  - **Circular $\mu\mu$**
- **BASED ON EMERGING TECHNOLOGIES**
  - **ERL *ee*/$\gamma\gamma$**
  - **Plasma *ee*/$\gamma\gamma$**
  - **Linear $\mu\mu$ / Plasma $\mu\mu$**
- **EXOTIC SCHEMES**
  - **Crystal linear $\mu\mu/\tau\tau$**
  - **Crystal linear $\tau\tau$**
  - **Crystal circular *pp***

"*ELC – Ansatz*"

- We will evaluate possible (ultimate) future colliders on base of
  - Feasibility of ***E***nergy
  - Feasibility of ***L***uminosity
  - Feasibility of ***C***ost
- For each machine type / technology we will start with what is the state-of-the-art now and attempt to make *"1-2-several"* orders of magnitude steps in *Energy*
  - see how if affects *Luminosity*
  - see how it affects *Cost*
- Leave it to others to judge where the lower limit on *L* and upper limit on *C* are… other limits may appear

"ELC – Ansatz" : Choice of Units

- Units of Energy will be ***TeV***
  - *most often cme = 2 x E_beam, sometimes - per beam*
- Units of Luminosity will be ***ab^{-1}/yr***
  - *e.g.,1e35 over 1e7 sec/yr… HL-LHC will have 0.3 ab^{-1}/yr*
  - *factor of ~2 uncertainty in peak lumi / machine availability*
- Units of power(total facility) will be ***TWh/yr***
  - *Eg CERN/LHC ~200MW and 1.1-1.3 TWh/yr*
- Units of Cost will be ***LHCU***
  - *cost of the LHC construction, approx. 10B$ - see below*
  - *for other machines the cost will be estimated using αβγ model with uncertainty O(2) - see below*
  - *the αβγ model needs to be extended for novel approaches*

Limits on *Energy* (1)

- Linear vs Circular

$$\Delta U_{SR} = \frac{90\,\text{keV} \cdot E_e^4(\text{GeV})}{R[\text{m}]}$$

SR loss per turn to be less than the total beam energy (1/2 of cme)

$$\Delta E \leq E/2.$$

Eg for electrons/positrons

That results in

$$E\,[\text{TeV}] \leq (m/m_e)^{4/3}(R/10[\text{km}])^{1/3}$$

Circular does not make sense beyond these c.m.energies

~1 TeV = 0.001 PeV for electrons

~1.2 PeV for muons (~210 m_e)

~25 PeV for protons (~2000m_e)

Limits on *Energy* (2)

- Particles don't survive acceleration
  - *Unstable particles*

$$dN/dt = -N/\gamma\tau_0$$

$$\frac{N}{N_0} \approx \left(\frac{m_\mu c^2}{E}\right)^\kappa, \quad \kappa = (m_\mu c/\tau_0 G)$$

Physics – Uspekhi **55** (10)

for muons $G \gg 3\ \mathrm{MeV\ m^{-1}}$

for τ-leptons $G \gg 0.3\ \mathrm{TeV\ m^{-1}}$

  - *Lossy transport from cell to cell (loss in plasma material, c-t-c efficiency)*

$$\left(1 - \frac{\Delta N}{N}\right)^M \lesssim 1$$

$$M = \frac{E}{\Delta E_{cell}} = \frac{5\,\mathrm{TeV}}{5\,\mathrm{GeV}} = 10^3$$

$$M \cdot \frac{\Delta N}{N} \lesssim 1 \Rightarrow \frac{\Delta N}{N} < 10^{-3}$$

ab

Limits on *Energy* (3)

- Corollary limits
  - *Space/area available*
  - *Power available*
  - *Money available*

For example:

Circumference **100 km** , B<16 T , ***E*<50 TeV**

Circumference **40,000 km**, B=1 T, ***E*<1.3 PeV**

Length **50 km** , G<0.1 GV/m, ***E*<5 TeV**

Length **10 km**, G<1 TV/m, ***E*<10 PeV**

Limits on *Luminosity* (1)

- General Equation $$L = f_0 n_b N^2 / 4\pi\sigma^2$$
  - *rewrite with norm.emm.* $$\mathcal{L} \sim f_0 \cdot n_b \cdot \gamma \cdot \frac{N_b^2}{4\pi\varepsilon_n\beta^*}$$
  - *HEP demand* $$L \propto E^2$$
  - *limits, eg,* ***beam power*** $$P_b = f_0 n_b N \gamma m c^2$$

$$L = P_b^2 / (4\pi\gamma n_b \varepsilon \beta^* m^2 c^4) \propto P_b^2 / E$$

All Colliders: Past, Existing, under Discussion

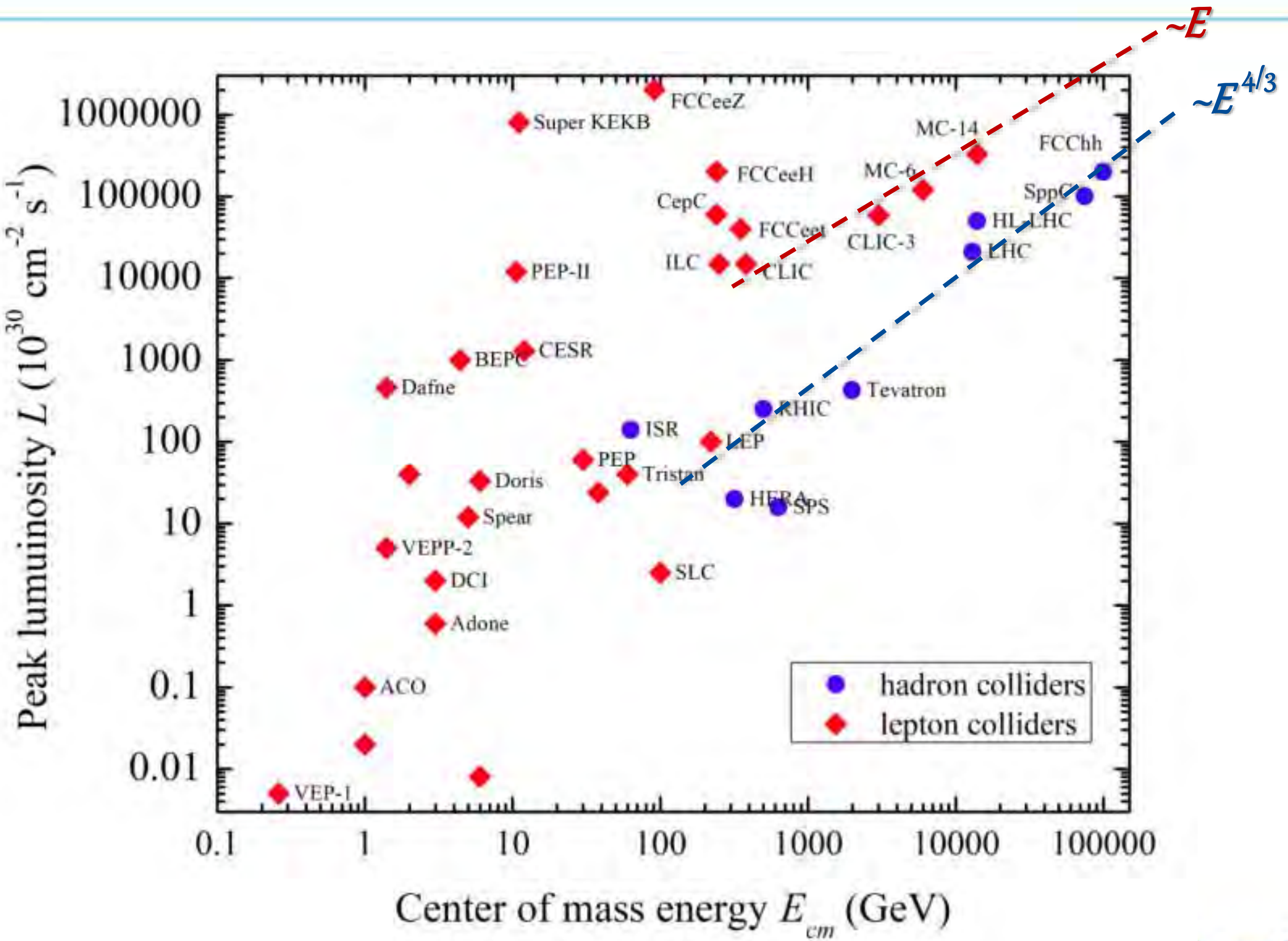

On base of *Shiltsev&Zimmermann, Rev.Mod.Phys.* (2021)

Paradigm Shift looming for > 0.1-1 PeV…

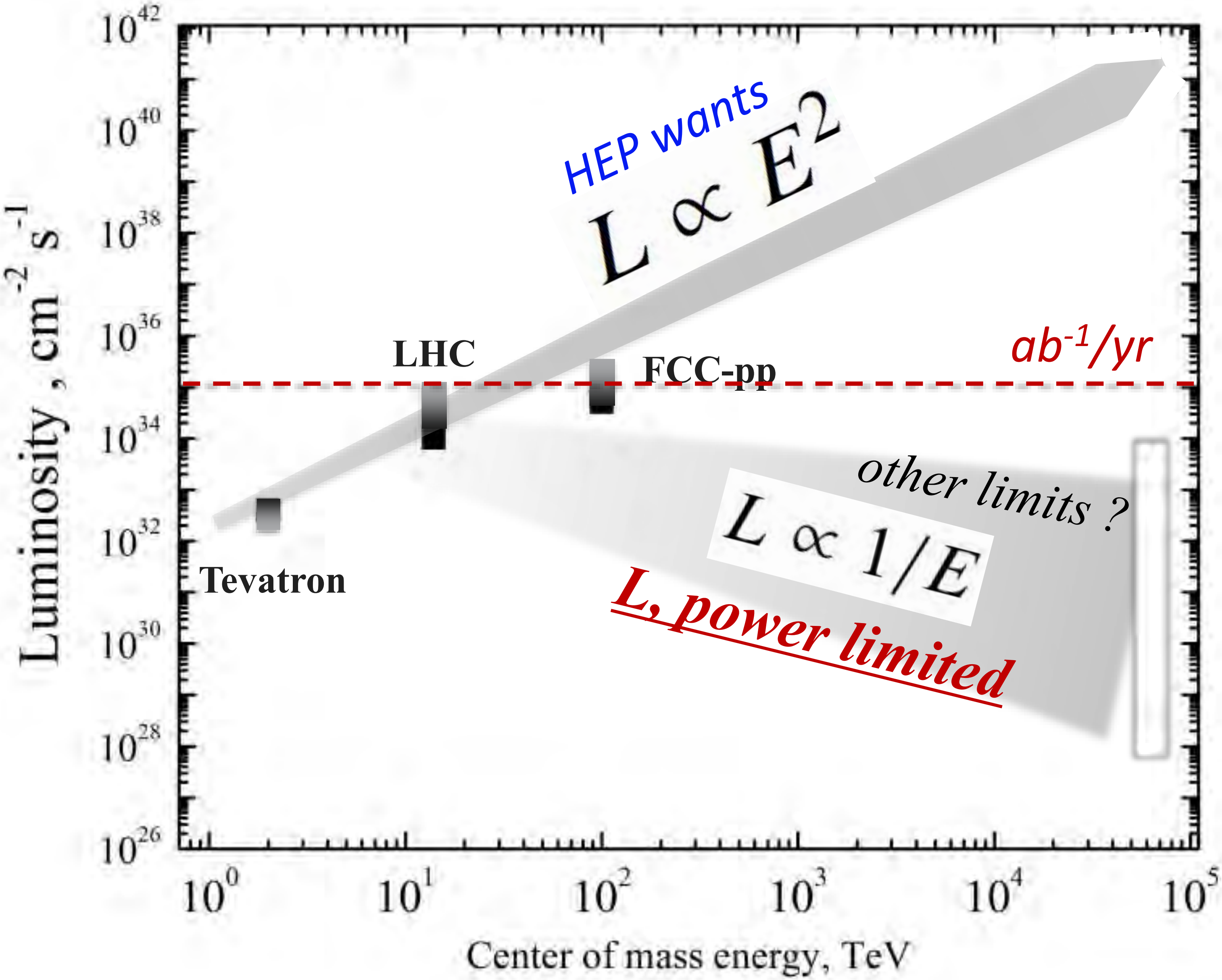

… to be discussed below…

Limits on *Luminosity* (2)

σ_{IP} is limited (e.g. 1Å)

- Another example

$$\mathcal{L} \sim \frac{p^2}{f_0 n_b E^2 \cdot 4\pi\sigma_{IP}^2}$$

  - *beam-beam limit*

$$\xi = \frac{r_p N_p}{4\pi\varepsilon_n}$$

  - *space-charge limit*

$$\Delta Q_{sc} = \frac{r_p N_p}{4\pi\varepsilon_n \beta\gamma^2}$$

  - *beam loading*

$$V_L \sim N_p \cdot \text{impedance}$$

  - *event pile-up*

$$PU \sim \frac{\mathcal{L}}{f_0 n_b}\sigma_{inel}$$

Limits on *Luminosity* (3)

– *particle production* $\frac{dN}{dt}(\mu, e^+)$

– *beamstrahlung* $\delta_E \sim \frac{\gamma^2 N_p}{\sigma_z \sigma_x^2}$

– *synchrotron radiation* $P_{SR} \sim \frac{\gamma^4}{R}$

– *SR/meter* $\sim \frac{\gamma^4}{R^2}$

– *IR rad damage* $\sim PU \cdot E \cdot f_0 \cdot n_b$

– *ν-radiation dose* $D \sim \frac{\dot{N}_p \gamma^3}{R^{\#}}$

– *instabilities* TMCI, RW, e-cloud $N \sim \frac{E}{Z_\perp}$

– *jitter/emittance growth* $\sim \gamma$

Limits on *Cost* (1)

- Cost is set by technology
  - *Accelerator technology*
  - *Civil construction technology*
  - *Power production, delivery and distribution technology*

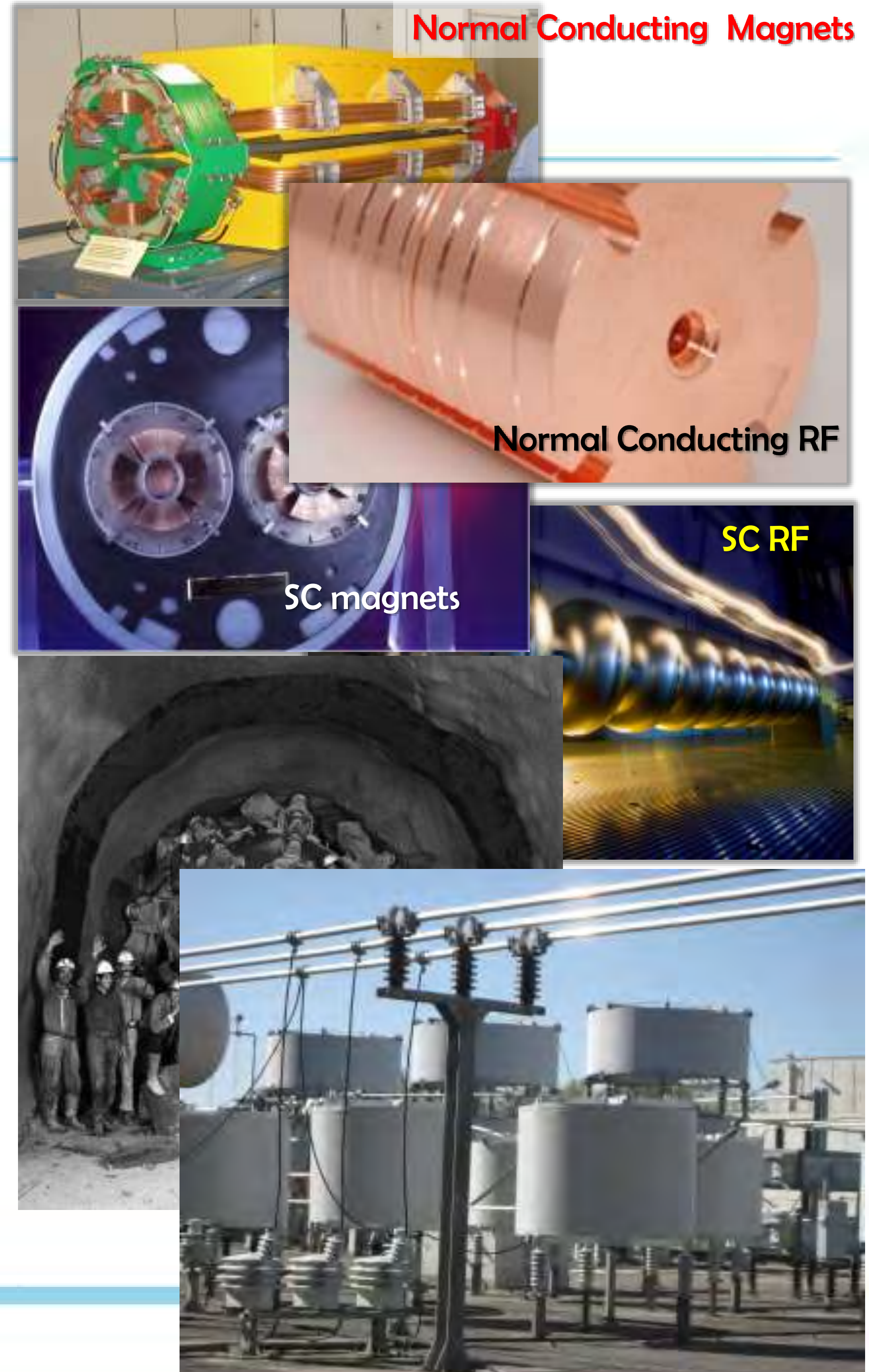

2014 Cost analysis:

2014 JINST 9 T07002

17 "Data Points" - Costs of Big Accelerators:

- Actually built:
  - RHIC, MI, SNS, LHC
- Under construction:
  - XFEL, FAIR, ESS
- Not built but costed:
  - SSC, VLHC, NLC
  - ILC, TESLA, CLIC, Project-X, Beta-Beam, SPL, ν-Factory

Wide range :

- 4 orders in *E*nergy, >1 order in *P*ower, >2 orders in *L*engt
- Almost 2 orders in cost
  - (normalized to US TPC)

	Cost (B$) Year	Energy (TeV)	Accelerator technology	Comments	Length (km)	Site power (MW)	TPC range (Y14 B$)
SSC	11.8 B$ (1993)	40	SC Mag	Estimates changed many times [6–8]	87	~100	19–25
FNAL MI	260M$ (1994)	0.12	NC Mag	"old rules", no OH, existing injector [9]	3.3	~20	0.4–0.54
RHIC	660M$ (1999)	0.5	SC Mag	Tunnel, some infrastructure, injector re-used [10]	3.8	~40	0.8–1.2
TESLA	3.14 B€ (2000)	0.5	SC RF	"European accounting" [11]	39	~130	11–14
VLHC-1	4.1 B$ (2001)	40	SC Mag	"European accounting", existing injector [12]	233	~60	10–18
NLC	~7.5 B$ (2001)	1	NC RF	~6 B$ for 0.5 TeV collider, [13]	30	250	9–15
SNS	1.4 B$ (2006)	0.001	SC RF	[14]	0.4	20	1.6–1.7
LHC	6.5 BCHF (2009)	14	SC Mag	collider only — existing injector, tunnel & infrstr., no OH, R&D [15]	27	~40	7–11
CLIC	7.4–8.3B CHF(2012)	0.5	NC RF	"European accounting" [16]	18	250	12–18
Project X	1.5 B$ (2009)	0.008	SC RF	[17]	0.4	37	1.2–1.8
XFEL	1.2 B€ (2012)	0.014	SC RF	in 2005 prices, "European accounting" [18]	3.4	~10	2.9–4.0
NuFactory	4.7–6.5 B€ (2012)	0.012	NC RF	Mixed accounting, w. contingency [19]	6	~90	7–11
Beta-Beam	1.4–2.3 B€ (2012)	0.1	SC RF	Mixed accounting, w. contingency [19]	9.5	~30	3.7–5.4
SPL	1.2–1.6 B€ (2012)	0.005	SC RF	Mixed accounting, w. contingency [19]	0.6	~70	2.6–4.6
FAIR	1.2 B€ (2012)	0.003-.08	SC Mag	"European accounting" [20], 6 rings, existing injector	~3	~30	1.8–3.0
ILC	7.8 B$ (2013)	0.5	SC RF	"European accounting" [21]	34	230	13–19
ESS	1.84 B€ (2013)	0.0025	SC RF	"European accounting" [22, 23]	0.4	37	2.5–3.8

V.Shiltsev, A phenomenological cost model for high energy particle accelerators

! WARNING !

The ***αβγ*** cost model:

$$\mathrm{Cost(TPC)} = \alpha\, L^{1/2} + \beta\, E^{1/2} + \gamma\, P^{1/2}$$

a) **Is for a "green field" facility !**
b) **US-Accounting !**
c) **There is hidden correlation btw *E* and technology progress**
d) **Pay attention to units**(10 km for *L*, 1 TeV for *E*, 100 MW for *P*)
   – ***α*≈ 2B$/sqrt(L/10 km)**
   – ***β*≈ 10B$/sqrt(E/TeV)** for SC/NC RF
   – ***β*≈ 2B$ /sqrt(E/TeV)** for SC magnets
   – ***β*≈ 1B$ /sqrt(E/TeV)** for NC magnets
   – ***γ*≈ 2B$/sqrt(P/100 MW)**

USE AT YOUR OWN RISK!

Total Cost vs *αβγ-Model* (Log-Log)

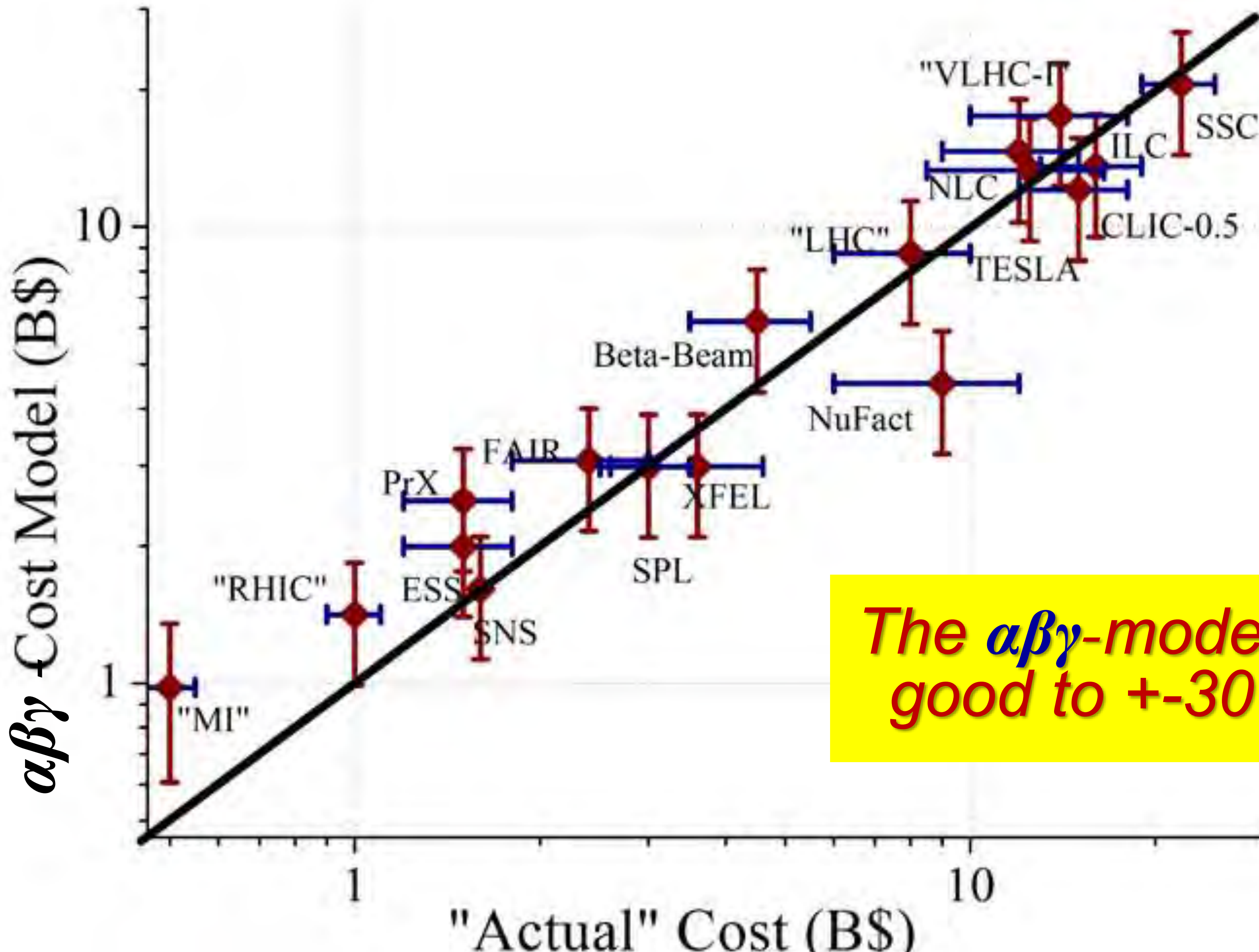

The αβγ-model is good to +-30%

ilab

Illustrations

Comment:

Sqrt-functions are quite accurate over wide range because such dependence well approximates the *"initial cost" – effect* :

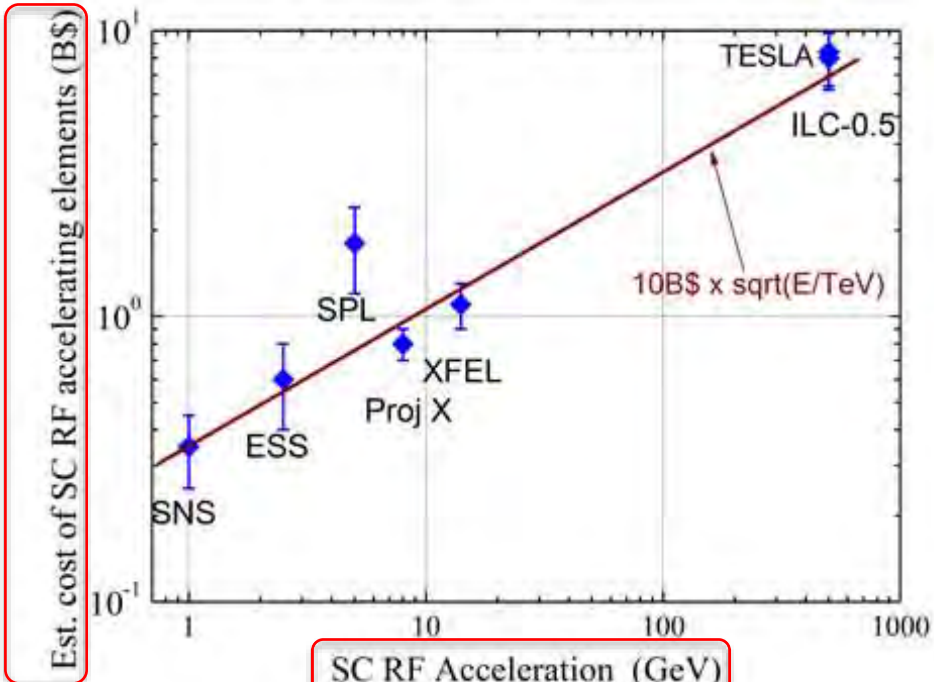

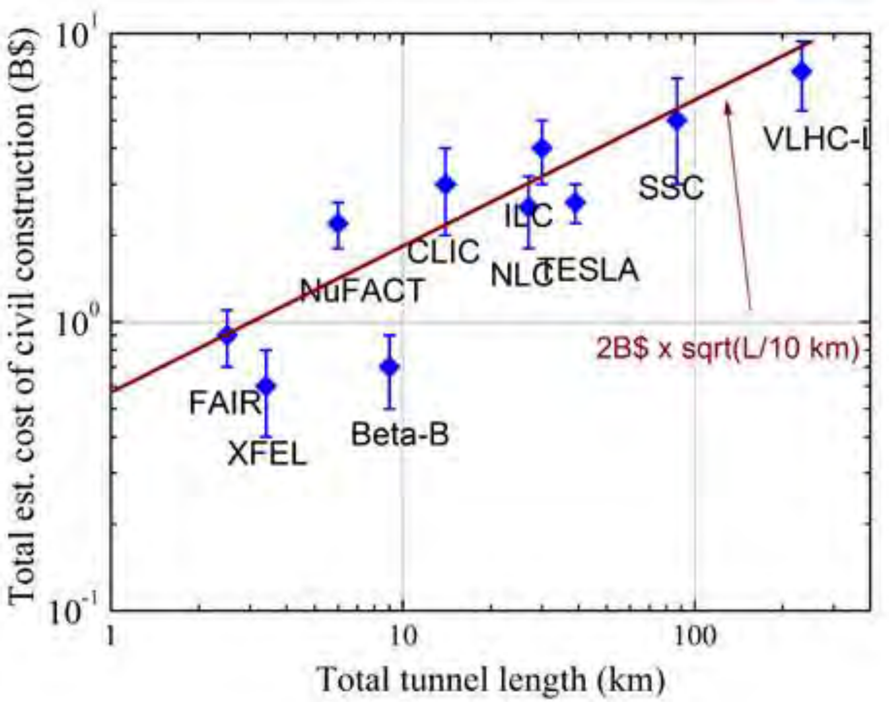

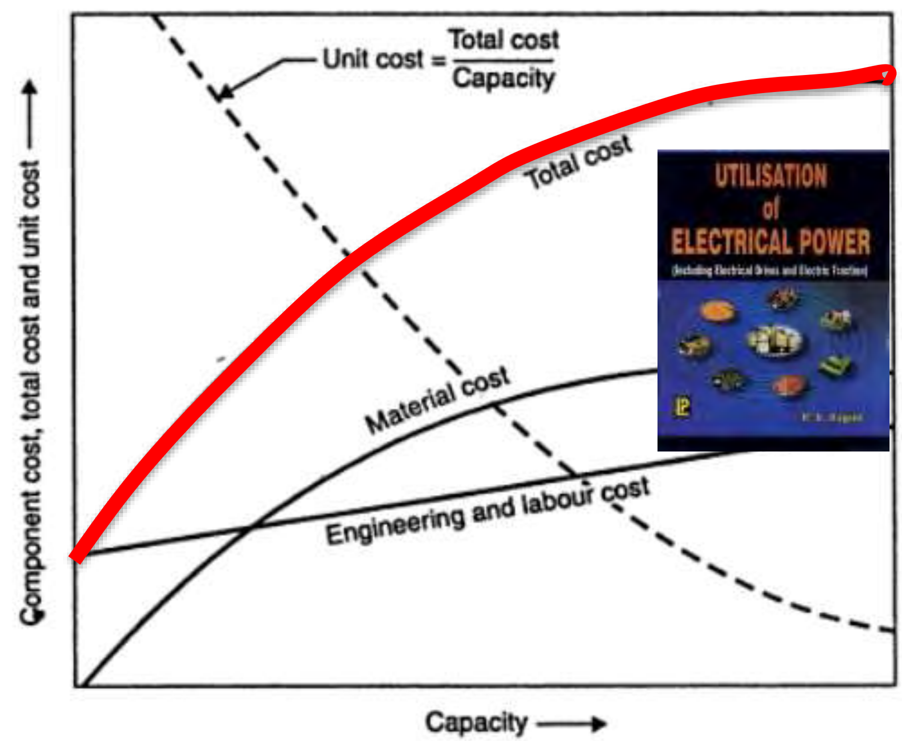

Fig. 9.5. Variation of costs of power plant *versus* its capacity.

Take LHC as an Example:

- ***αβγ* – Model:**
  - 40 km of tunnels
  - 14 TeV c.o.m SC magnets
  - ~150 MW of site power

$$2\sqrt{40/10} = 4$$

$$2\sqrt{14} = 7.5$$

$$2\sqrt{150/100} = 2.5$$

TOTAL PROJECT COST : **14B$ ± 4.5B$**

- **ITF T.Roser talk @ PLUB-II (USD 2021):**
  - existing injector complex **4.6 B$**
  - new accelerator systems **4.06 B$**
  - new infrastructure and civil **2.75 B$**
  - explicit labor **~1.4 B$**

Total: **12.8B$**

Fermilab

“αβγ – Model” : Caveats

- (once again) note three warning signs:
  - *“…+- 30% …green field… US accounting…“*
  - *rounded powers and coefficients, e.g.,* $\sqrt{x} \approx x^{0.4 \ldots 0.6}$
- Analysis was done in 2013:
  - *inflation 7yrs x 3% = 21%*
  - *many more projects have been costed since then, others updated*
- “*Not-yet-built*” machine costs estim’d by proponents
- That’s why:
  - **a) further in-depth analysis is neded/very important**
  - **b) I’ll use LHCU for rough estimates/analysis here**

NB: worlds’ total HEP budget ~3.5-4B$ (0.4 LHCU)

"αβγ – Model" : Notes

- Costs of future technologies are not well known:
  - plasma, lasers, crystals, "magic cheap" magnets, tunnels, HTS, etc
- Costs of civil construction and power systems are driven by larger economy (not by us)… "stable"
- Having injector (~1/3 of cost) → factor of 2 in energy reach
- Also, follows from the model:
  - Cost is weak function of luminosity (see next slide)
    - Also, LHC 10B$, HL-LHC 1B$ with x5 increase in luminosity
    - It's OK to start high *E*, low *L*…CESR, Tevatron increased *L* >100x, LHC >10x
  - Cost is moderate function of length/circumference
  - Cost is strong function of *E*nergy and technology
- Of course, the model does not tell us "what's affordable"
  - but at least allows approximately sort proposals in categories
    - E.g., "Less than LHCU", "1-2 LHCU", "More than 3 LHCU", etc

Example: Muon Colliders
cost(color) vs *E* vs *Lumi*

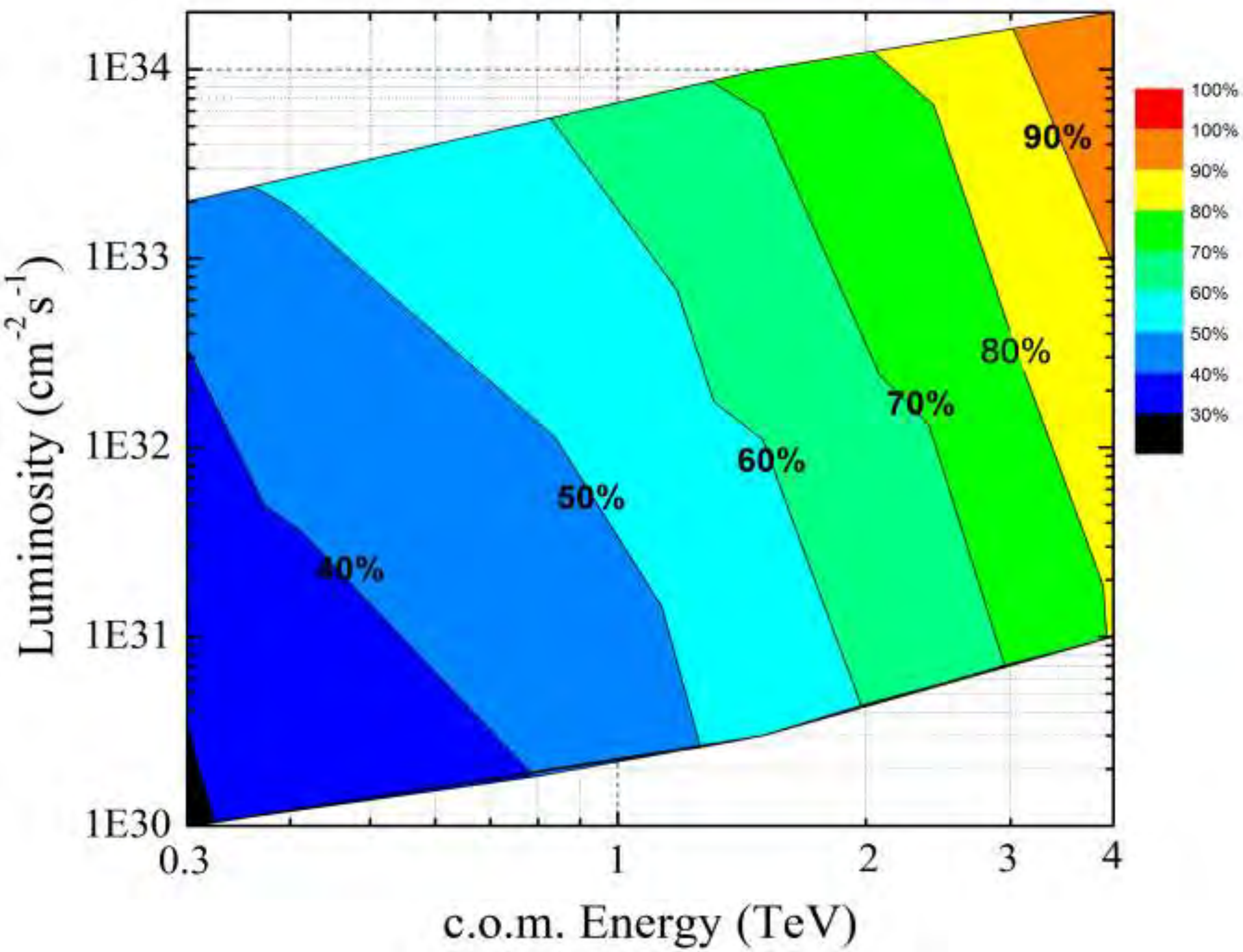

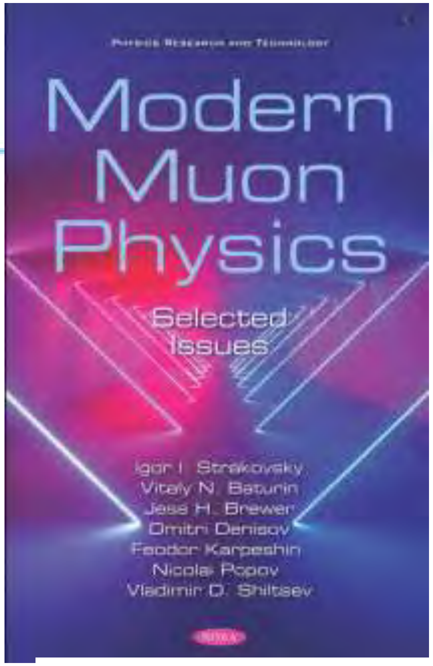

Modern Muon Physics: Selected Issues, I.Strakovsky, et al (Nova, 2020)

Some projects discussed @ *EPPSU'19* and *Snowmass'21*

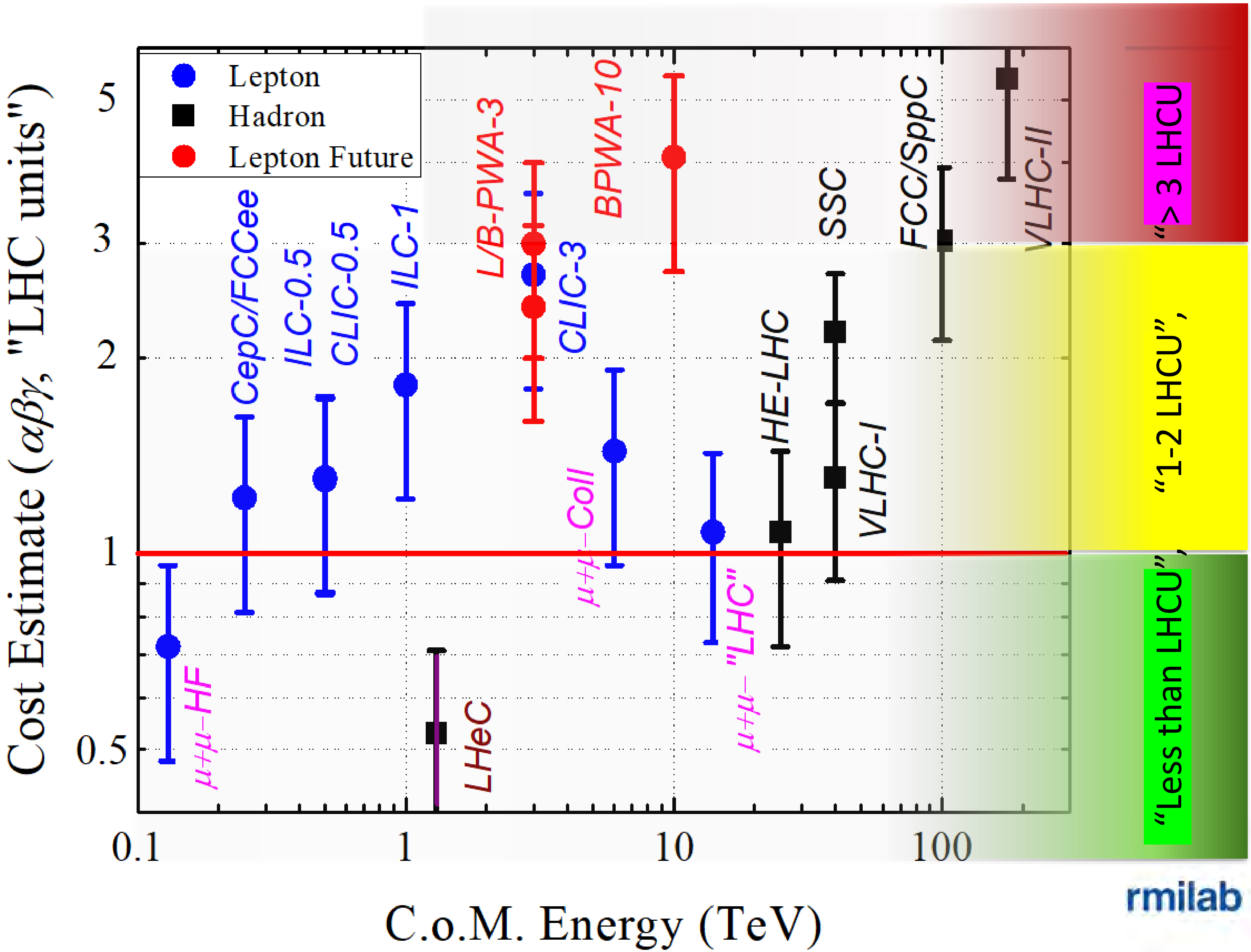

Colliders: Probability to Be Built

~1/ Cost^2 (is it true?)

1/(1 x LHC)^2 = 100%

1/(2 x LHC)^2 = 25%

1/(3 x LHC)^2 = 10%

No-one wants low-class things
→ probability

$$\propto \; C^2/(1+C^\kappa) \qquad \kappa \approx 4-5$$

Energy Ranges and Reference Points : *leptons* vs *hadrons*

About 1:7 in *E* = 1 : sqrt(7) in Cost!

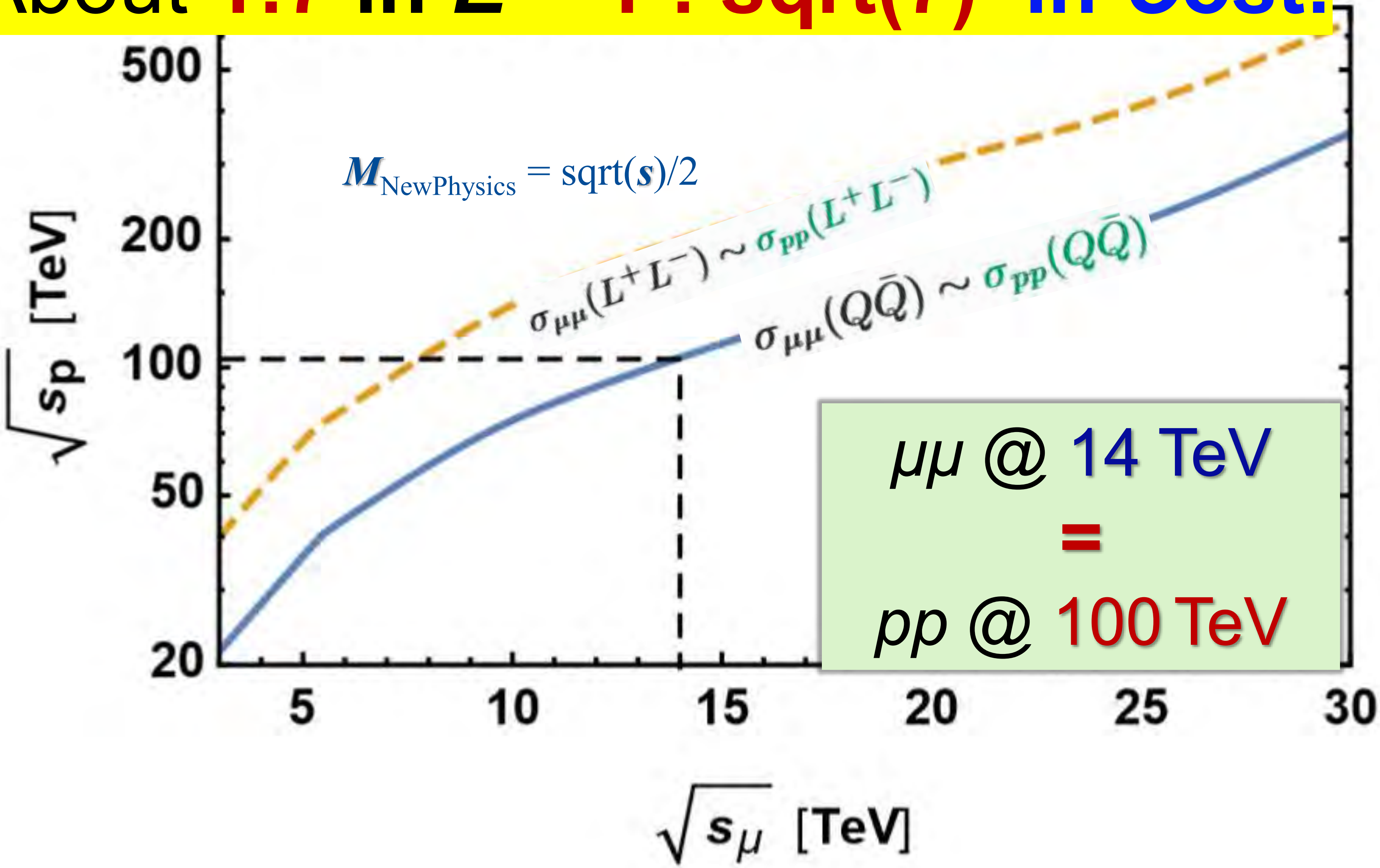

Equivalent reach in *pp* after rescaling for *pdf*'s

Reference Points and (Far) Future

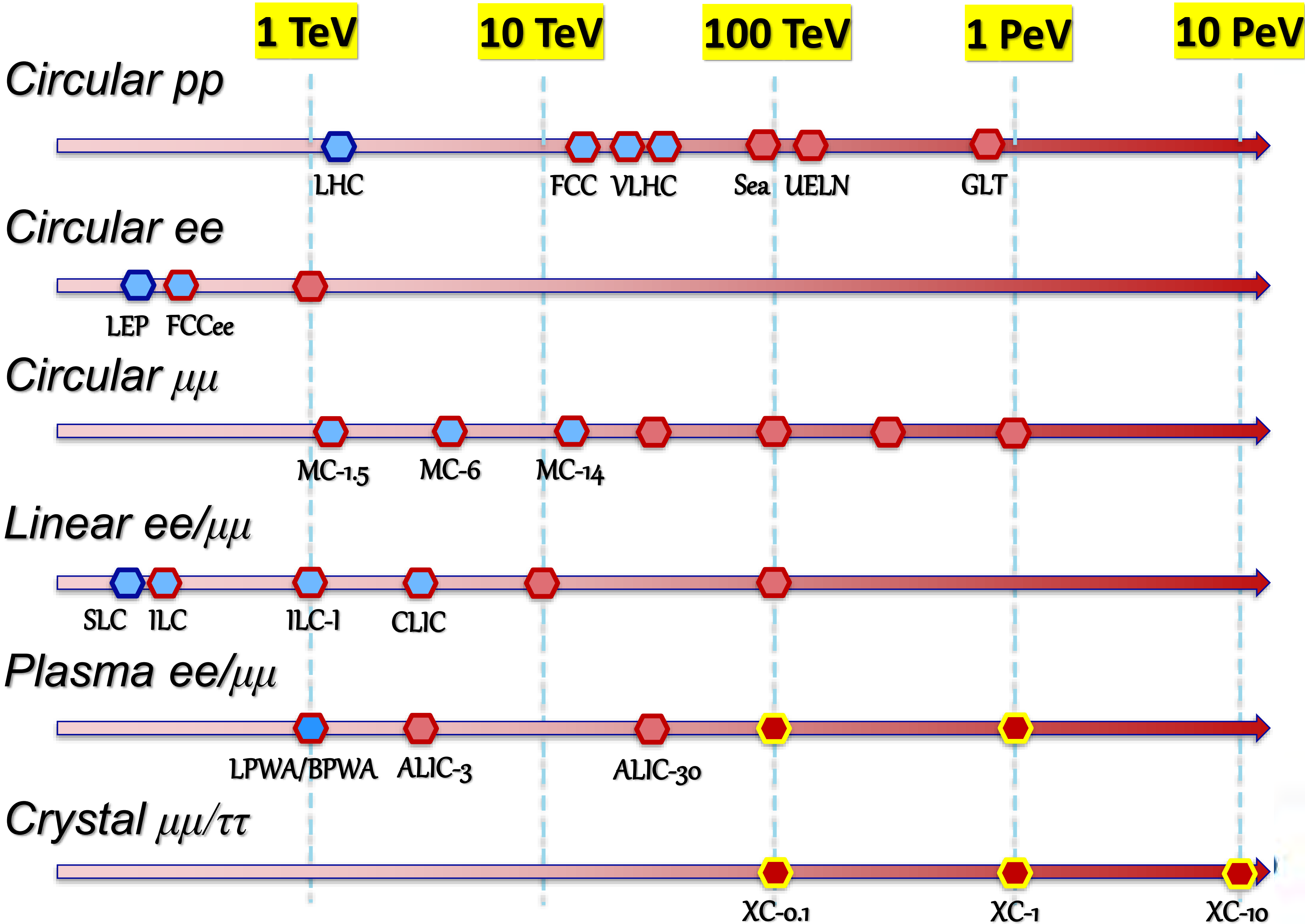

"Social Cost" and Social Limits

- There is probably a limit on cost of ultimate accelerators
  - *how much society (national, regional, global) wants/can afford spending on HEP…slowly varies in time (grows?)*
  - *current estimate for global big collider ~* **2-3 LHCU ?**
  - *Large cost/size → long construction and commissioning time*
- Since recently – awareness of the "carbon footprint"/"ecology" limit for large facilities
  - *current estimate for global big collider ~* **1(2) TWH/yr ?**
  - *disturbed environment (land use, radiation, pollutants, etc)*
- Scarcity of materials
  - *Helium, Nb, W, etc* **?**

Content:

- Part I
  - Ultimate colliders: *Scope and Approach*
  - Ultimate colliders: *ELC-Ansatz, Units*
  - Ultimate colliders: *Limits of E*
  - Ultimate colliders: *Limits of L*
  - Ultimate colliders: *Limits of C*
  - Other considerations: *T*
- **Part II**
  - **Circular *pp* / *ee* / $\mu\mu$**
  - **Linear and Plasma *ee* / $\gamma\gamma$ / $\mu\mu$**
  - **Exotic (crystal) $\mu\mu$ / $\mu\mu$**
- Conclusions / Q&A / Discussion

Circular *pp* Colliders

- Can use Tevatron and LHC as reference points
- Parameter sets exist for SCC, FCC-hh, SppC, VLHC, Eloisatron
- Major advantages:
  - known technology and physics
  - good power efficiency ab^{-1}/TWh
- Major limitations:
  - Size (magnetic field *B*)
  - Power
  - Beam-beam, burn-off, instabilities
  - Synchrotron radiation
  - Cost

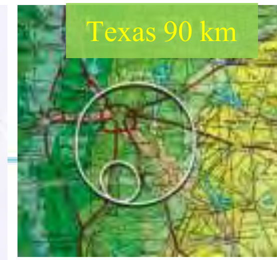

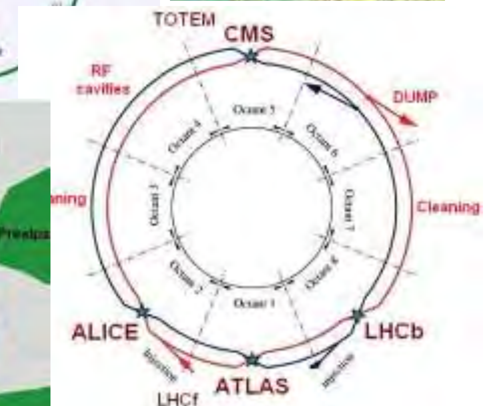

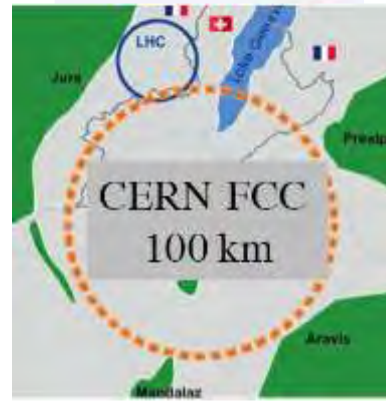

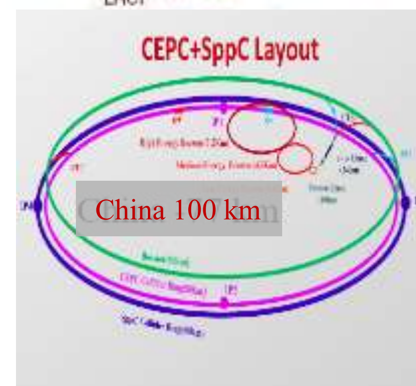

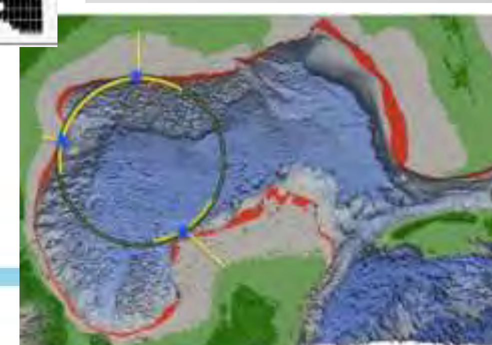

pp Luminosity : Two Main Limits

- #1 Beam-beam limit → $\xi = \frac{r_p N}{4\pi \varepsilon_n}$
- #2 Synchrotron radiation power/meter : $P_{SR} \simeq n_b N_0 \frac{\gamma^4}{R} \cdot f_0$

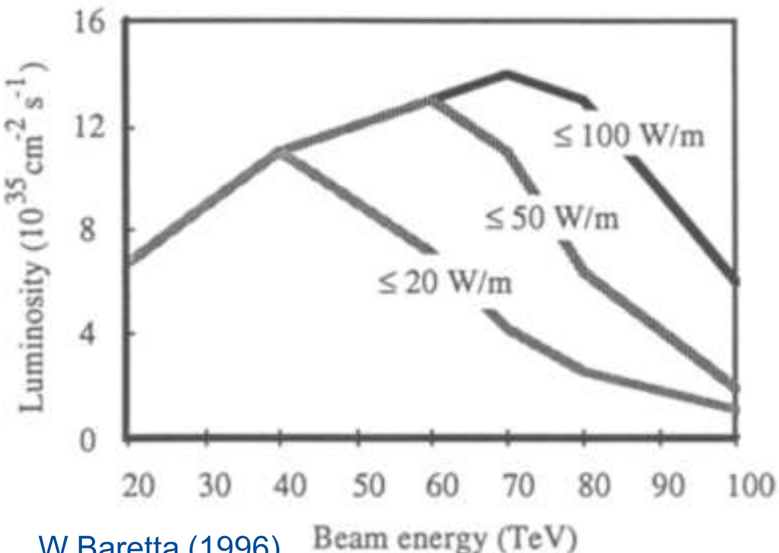

W.Baretta (1996)

Give following Luminosity scaling:

$$L \propto (\xi/\beta^*)(P_{SR}/2\pi R)(R^2/\gamma^3))$$

Other limits

– Pile up

$$PU = \mathcal{L} \cdot \sigma_{in}$$

$$\mathcal{L} = f_0 n_b \frac{PU}{\sigma_{in}} \sim \frac{PU}{\tau_{BB} \cdot \log E}$$

– IR radiation damage

$$Rad = \mathcal{L} \cdot E$$

$$\rightarrow \mathcal{L} \sim \frac{Rad}{E}$$

– Resistive wall instability

$$N_{\mathrm{RW}} \equiv \tau_{\mathrm{RW}} f_0 = \frac{\sqrt{2\pi}(E_{\mathrm{p}}/e)a^3}{I_{\mathrm{B}} Z_0 \langle\beta\rangle} \sqrt{\frac{(1-\Delta\nu)\sigma_{\mathrm{W}}}{cR^3}}.$$

– TMCI

$$N_{\mathrm{thr}} = 1.24 \times 10^{10} \times \sqrt{\frac{\sigma_s}{0.1\ \mathrm{m}} \frac{E}{3\mathrm{TeV}} \frac{\nu_s}{0.005}} \times \left(\frac{a}{0.9\ \mathrm{cm}}\right)^3 \frac{520\ \mathrm{km}}{C} \times \frac{250\ \mathrm{m}}{\langle\beta\rangle}$$

– e-cloud

– Turn around time vs *L*uminosity evolution

Qualitative Cost Dependencies - 100 TeV *pp*

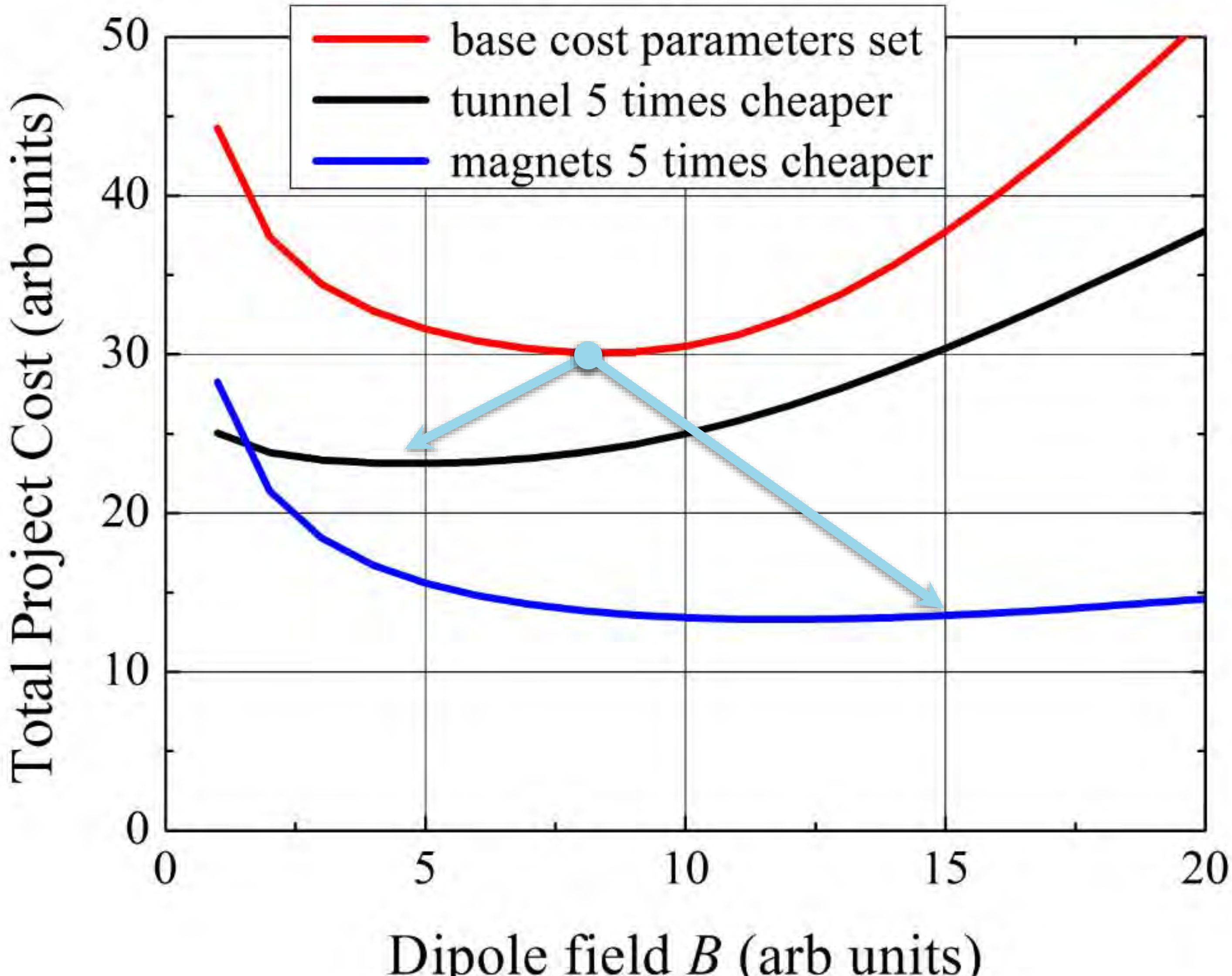

* for illustration purposes only

Fermilab

pp Colliders: *Lumi* and *Cost* vs *Energy*

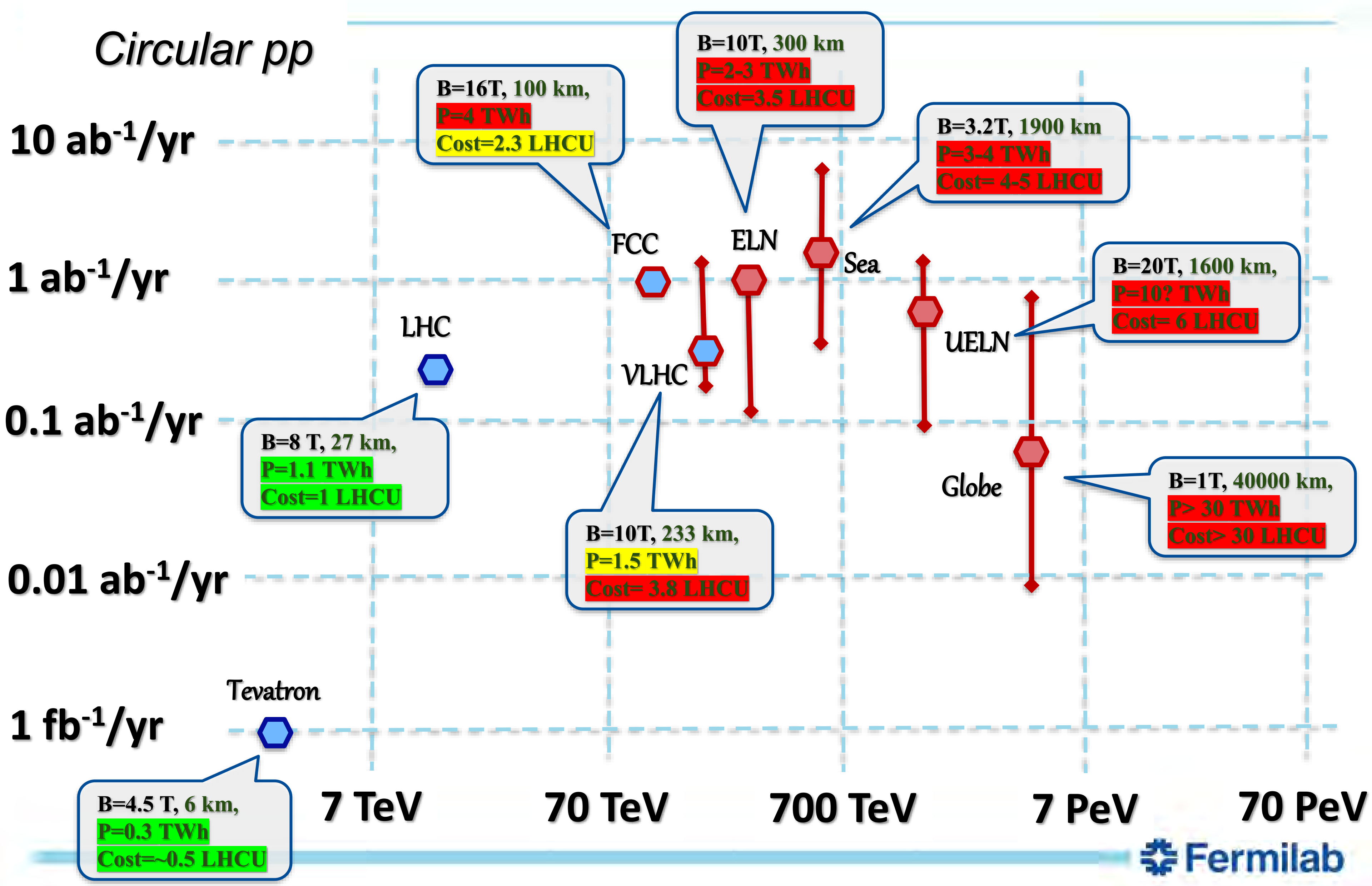

Fermilab

Circular e+e- Colliders

- Let's skip them… **dead end**… SR power

$$L = \frac{3}{16\pi r_e^2 (m_e c^2)} \frac{\xi_y P_T}{\beta_y^*} \rho \gamma^{-3}$$

- E.g. >0.5 TeV cme ring will be
  - Big (>200-300 km?)
  - Low luminosity O(10 fb-1/yr)
  - A lot of RF → expensive **>1.5-2 LHCU**

Circular Muon Colliders

- Parameter sets exist for 1.5, 3, 6, 10, 14 TeV
- Major advantages:
  - factor of x7 in *E*_reach
  - best power efficiency ab^{-1}/TWh
  - Traditional core technologies
- Major limitations:
  - Muon production
  - Muon cooling
  - Neutrino radiation

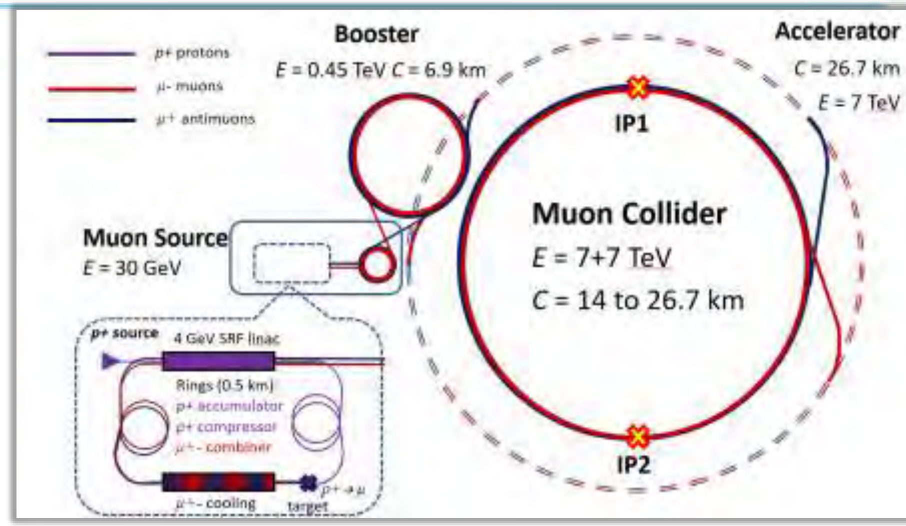

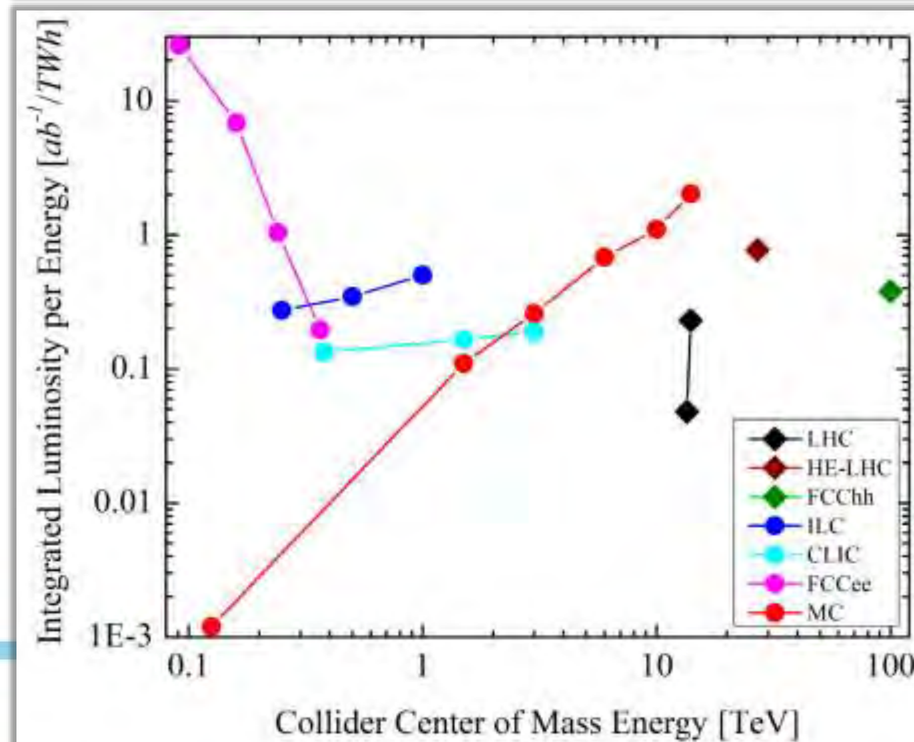

NATURE PHYSICS | www.nature.com/naturephysics

arXiv:2007.15684

Muon colliders to expand frontiers of particle physics

Jan 28, 2021

Muon colliders offer enormous potential for the exploration of the particle physics frontier but are challenging to realize. A new international collaboration is forming to make such a muon collider a reality.

K. R. Long, D. Lucchesi, M. A. Palmer, N. Pastrone, D. Schulte and V. Shiltsev

MC Luminosity

- ***L ~ B*** field

$$L \propto B$$

- Assuming :
  - Enough muons can be produced
  - *L ~ Power x Energy*

$$\dot{N} = N_0 \cdot n_b \cdot f_{rep} \sim 2 \cdot 10^{9} \cdot 5 \sim 10^{12}/s$$

$$\mathcal{L} \sim B \cdot P \cdot \gamma \cdot \frac{N_0}{\varepsilon}$$

$$D \propto (dN/dt)E^3/\Phi$$

  - At some energy, neutrino radiation sets the limit
  - Ultimate lumi depends on suppression factor Φ

$$\text{Power} \sim \frac{D\Phi}{\gamma^2} \leq P_0$$

$$\boxed{L \propto B \frac{D\Phi}{E^2} \frac{N}{4\pi\epsilon_n\beta^*}}$$

Neutrino Radiation Mitigation Φ~100 possible

disk width ≅ 4 m at 30 km

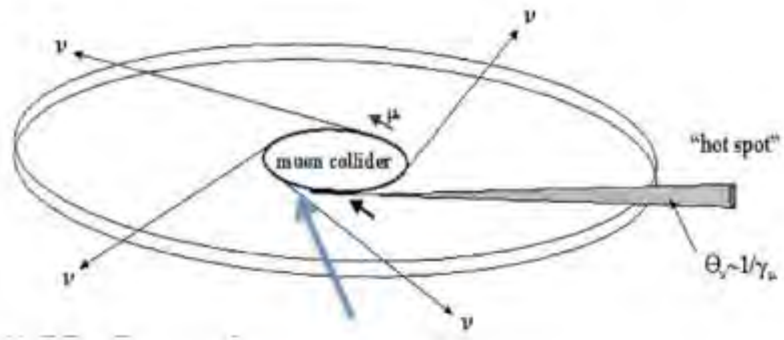

Move collider ring components, e.g. vertical bending with 1% of main field

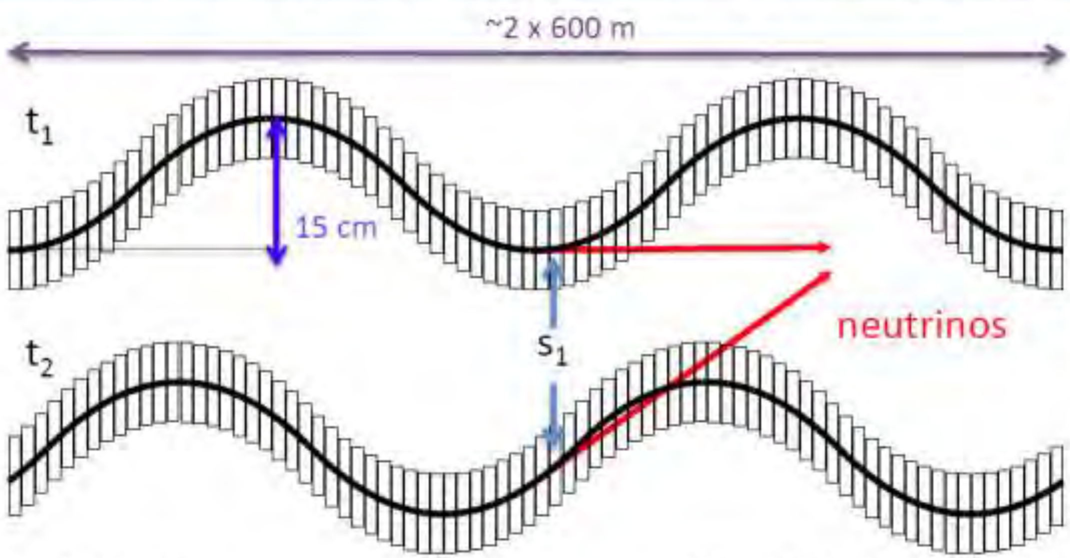

Opening angle ± 1 mradian

O(100) larger than decay cone
⇒ gain O(100) in radiation

In straights, additional improvement in horizontal

Need to study impact on beam and operation, e.g. dispersion control

Muon Collidets: *Lumi* and *Cost* vs *Energy*

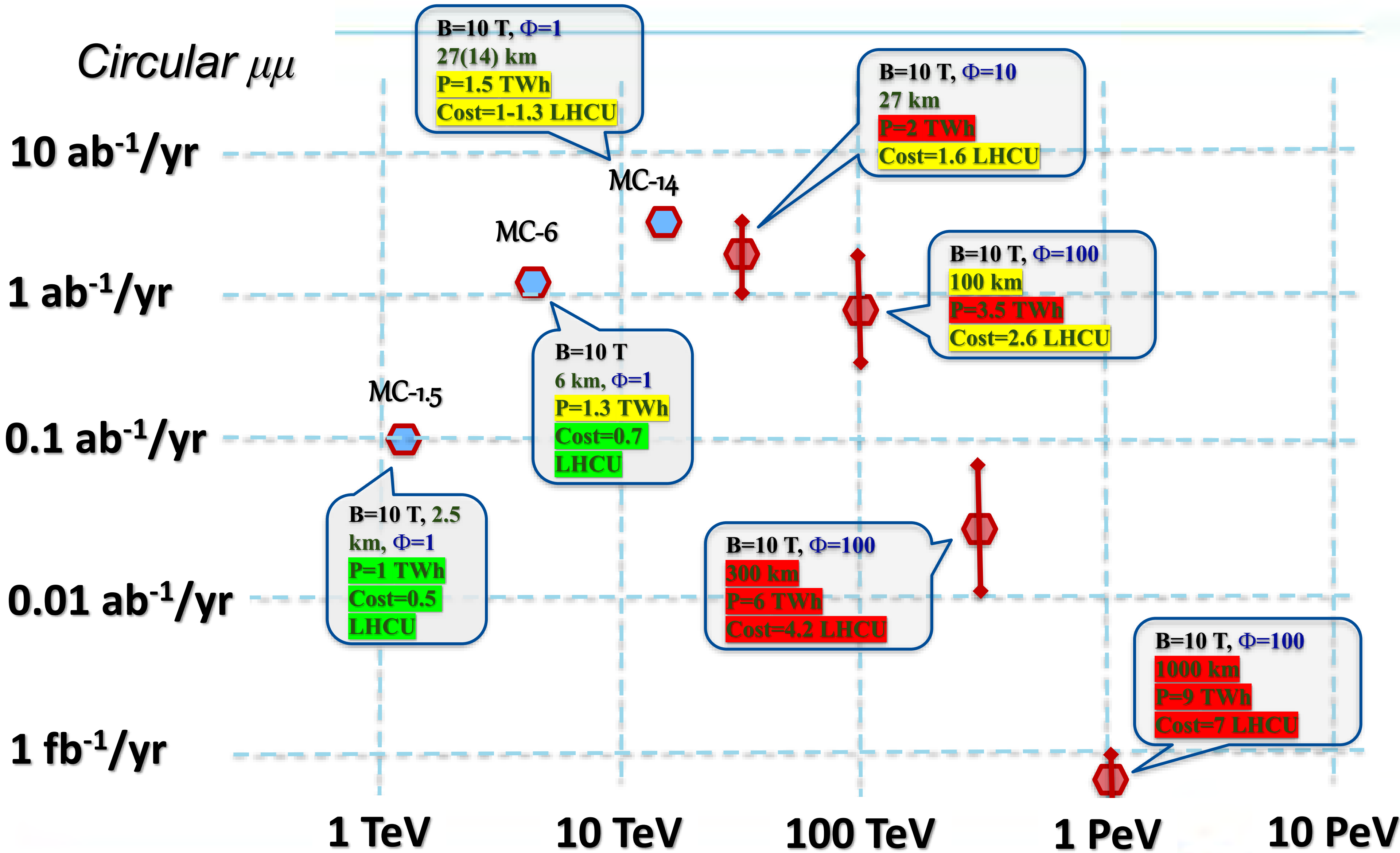

Fermilab

Linear *lepton* Colliders

- Mostly *e+e-/e-e-/γγ*
  - Muons possible, but μ-sources are expensive (and limited prod'n *dN/dt*)
  - Protons possible, but lose factor of 7 in effective cme energy reach in *hh*
  - *NC RF, SC RF, plasma, wakefields*
- Major advantages:
  - No SR losses
  - RF acceleration well developed
- Major limitations:
  - *L* scales with power, jitter/size and beamstrahlung
  - plasma/wakefield acceleration is not fully matured yet (many unknowns - energy staging, *e+*, power, cost, etc)

$$\boxed{E_b = eGL}$$

$$\mathcal{L} = (N_e n_b f_r)\left(\frac{1}{\sigma_y^*}\right)\left(\frac{N_e}{\sigma_x^*}\right)\frac{H_D}{4\pi}$$

$$\eta \equiv P_b / P_{\text{wall}}$$

$$N_e n_b f_r = \eta P_{\text{wall}} / eE_{\text{c.m.e.}}$$

$$L \propto \frac{\eta_{\text{linac}} P_{wall}}{E} \frac{N_\gamma}{\sigma_y}$$

(luminosity spectrum) $N_\gamma \simeq \frac{2\alpha r_e N}{\sigma_x}$

ee/γγ or μμ Linear Collider Luminosity

see detail analysis in eg D.Schulte, *Rev.Accel.Sci.Tech.* 9 (2016): 209-233.

- Other considerations :
  - Positron production and acceleration in plasma
    - Can be solved by switching to *ee/γγ*
  - Beamstrahlung
    - Can be solved by ultrashort bunches or switching to *ee/γγ* or μμ
      (see M.Peskin @ PLUB-II and Swapan C. talk today)
  - Instabilities in RF structures or plasma
  - Jitter/emittance control
    - Problems grow with more elements and smaller beams at IP → limit at 1A

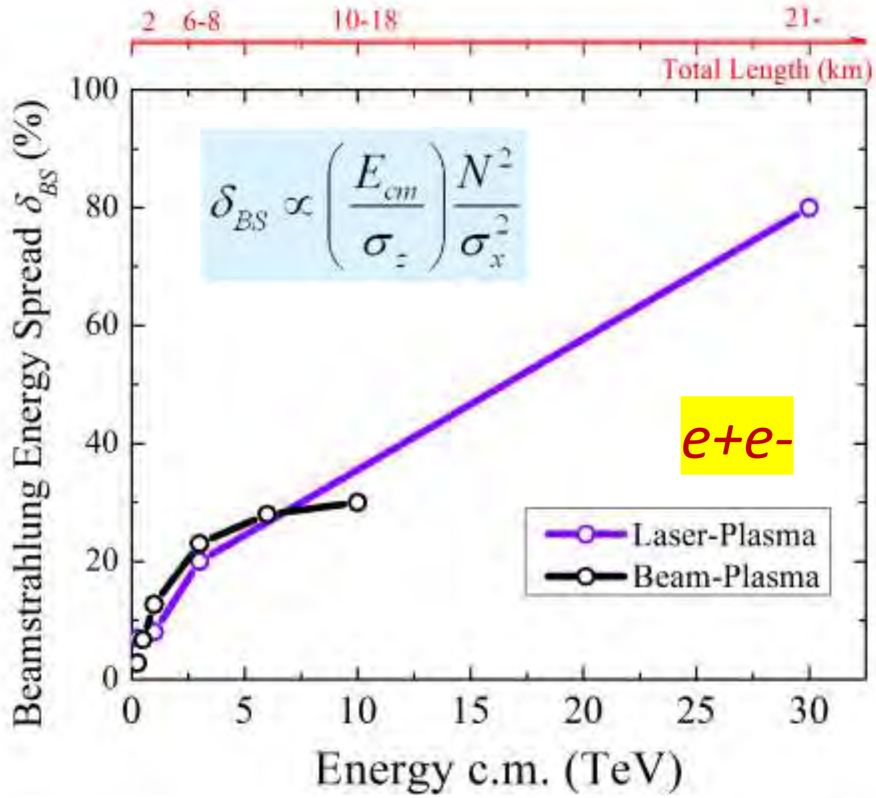

$$\delta_B \approx \frac{24}{3\sqrt{3}\pi^{3/2}} \frac{r_e^3 \gamma N_b^2}{\sigma_z(\sigma_x^* + \sigma_y^*)^2} \approx \frac{24}{3\sqrt{3}\pi^{3/2}} \frac{r_e^3 \gamma N_b^2}{\sigma_z \sigma_x^{*2}}$$

$$\mathcal{L} \propto \frac{n_\gamma^{3/2}}{\sqrt{\sigma_z}} \frac{1}{\sigma_y} N n_b f_r.$$

(T.Raubenheimer, PRSTAB 2000)

Linear RF and Plasma: *Lumi* and *Cost* vs *Energy*

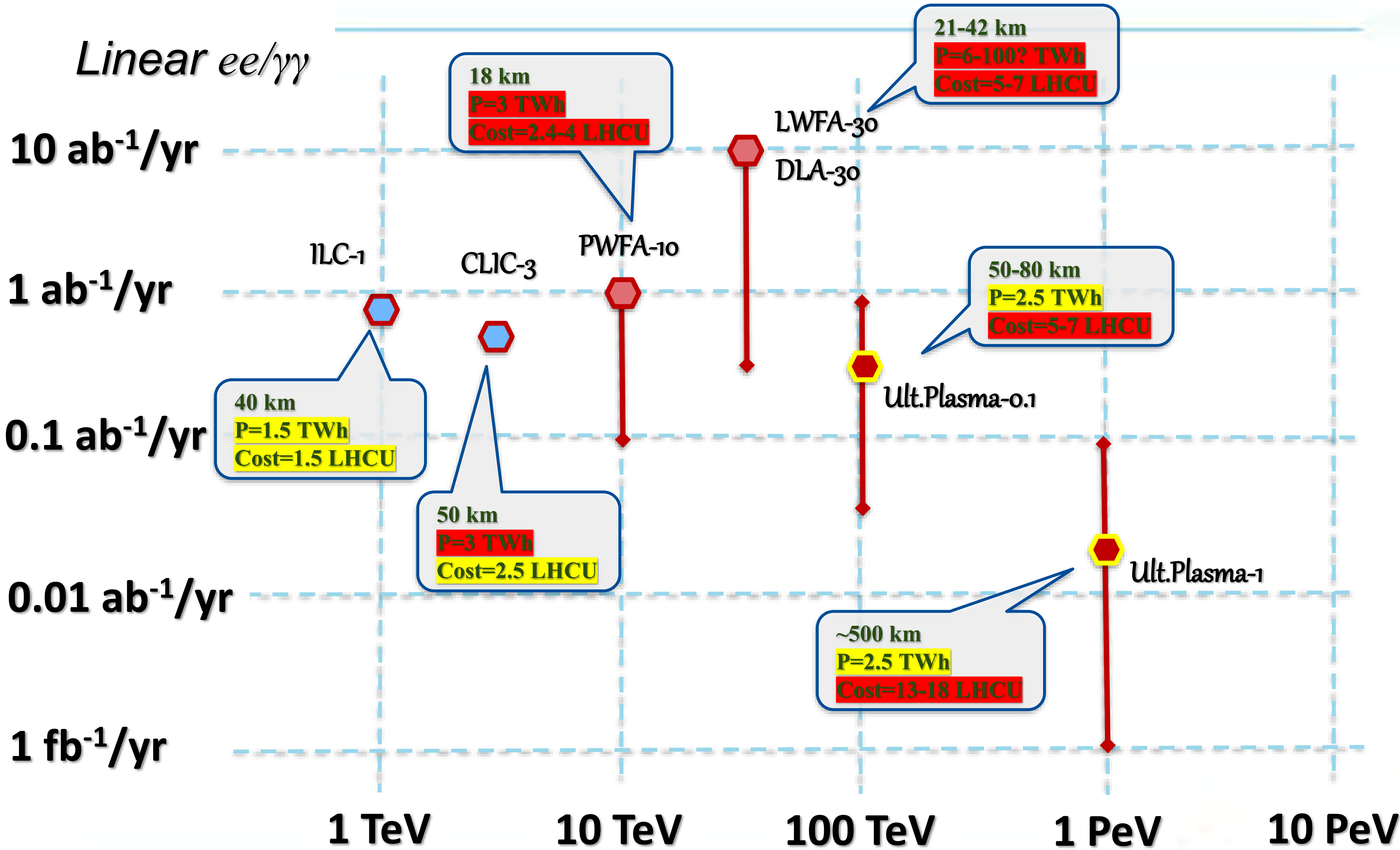

Exotic Colliders

$$E\,[\mathrm{GV/m}] \approx 100\sqrt{n_0\,[10^{18}\,\mathrm{cm}^{-3}]}$$

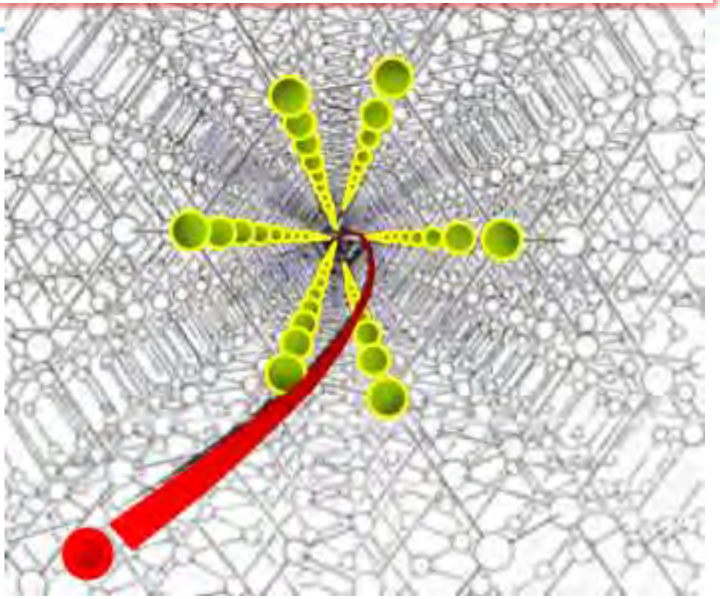

- Acceleration in structured media, eg CNTs or crystals (***only muons!!!***)
- Major advantages:
  - solid density → 1-10 TV/m gradients
  - continuous focusing and acceleration (no cells, one long channel, particles get strongly cooled *betatron radiation*)
  - small size promises low cost
- Major limitations:
  - "blue sky", *O*(10) papers, plans for proof-of-principle experiment *E336* @FACET-II (S.Corde, T.Tajima, et al)
  - how to drive Xtals? lasers, beams?
  - Cost is unknown, power is unknown, luminosity - (how low?)

Acceleration in Xtals book (T.Tajima, et al 2020)

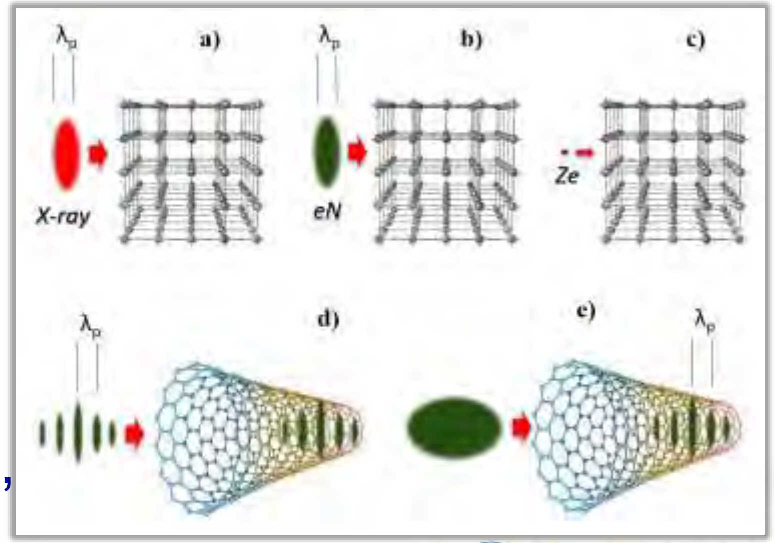

Fig. 2. Possible ways to excite plasma wakefields in crystals or/and nanostructures: (a) by short X-ray laser pulses; (b) by short high density bunches of charged particles; (c) by heavy high-Z ions; (d) by modulated high current beams; (d) by longer bunches experiencing self modulation instability in the media.

Exotic Colliders: Line of Thinking

E_{cm} Size is limited <10 km → calls for the highest gradients → crystals → muons

$$L = f\frac{N_1 N_2}{A}$$

Luminosity calls for more particles in the smallest beam size

$$A \sim 1\ \text{Å}^2 = 10^{-16}\,\text{cm}^{-2}$$

This is the smallest beam size at IP

$$P = f n_{ch} \cdot NE$$

The power is limited <10MW → ***N*** is small at high ***E*** → *low* ***L***

XC Luminosity

$$L = f N^2 / A$$

- Considerations :
  - Muons/bunch < Xtal electrons excited

    $$100\lambda_p \times \lambda_p^2$$
    $$N_0 \sim 10^3$$
  - Employ many channels

    $$n_{ch} \sim 100$$
    gain a factor of n_{ch}
  - Limit beam power O(10MW)

    $$P = f n_{ch} N E$$
    $$f = 10^6 \text{ Hz}$$
  - Combine *n_channels* to gain ***L*** via *crystal funnel* (? Is it possible)

$$L\,[\mathrm{sm}^{-2}\,\mathrm{s}^{-1}] \approx 4 \times 10^{33\text{–}35} \, \frac{P^2\,[\mathrm{MW}]}{E^2\,[\mathrm{TeV}]\, f n_{ch} [10^8\ \mathrm{Hz}]}$$

Xtal Collider

n~10^{22} cm^{-3}, **10 TeV/m** → 1 PeV = 1000 TeV

n_μ ~1000, n_B ~100, f_{rep} ~10^6 L ~$10^{30\text{-}32}$

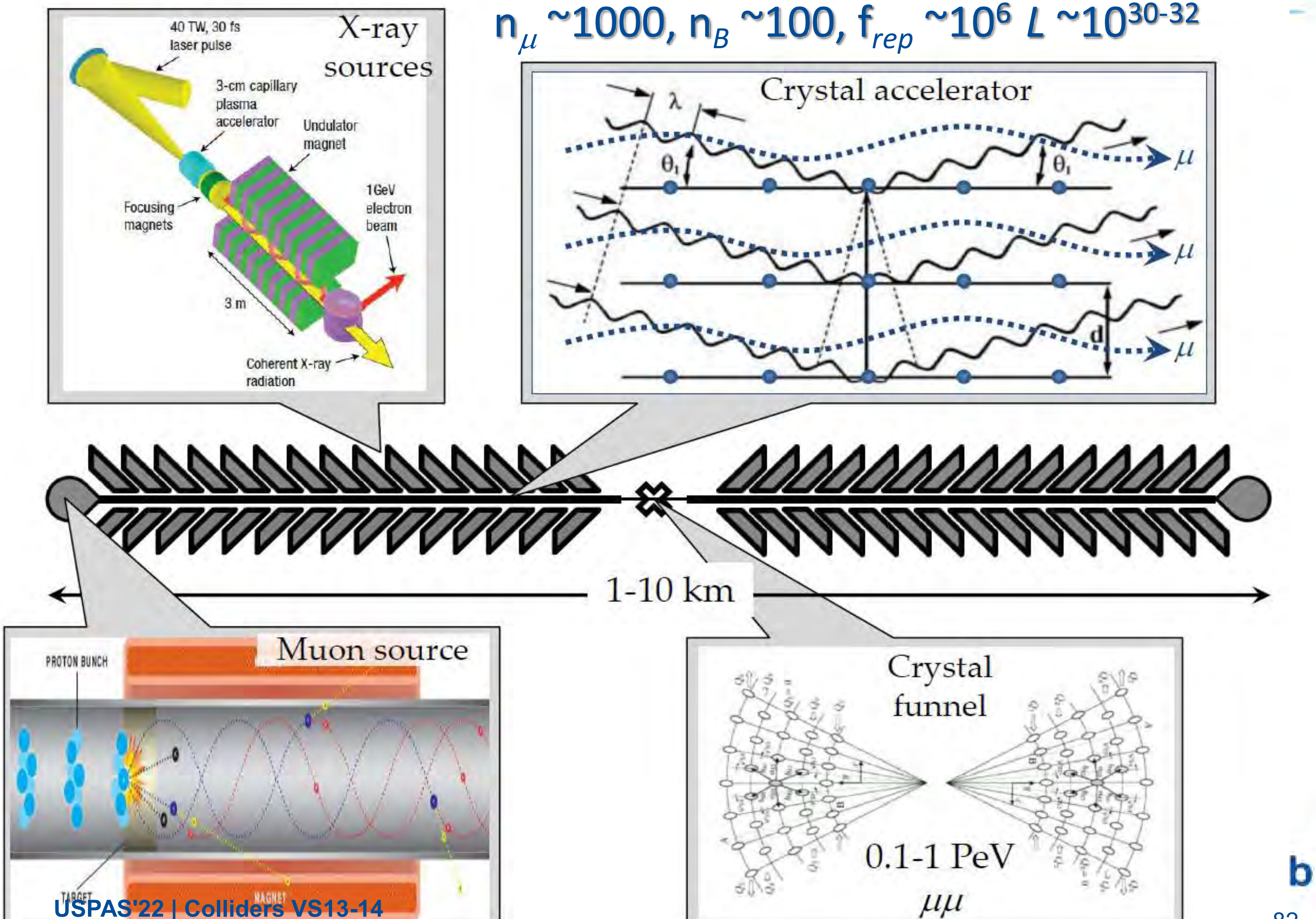

V.Shiltsev, Phys. Uspekhy 55 965 (2012)

Xtal Colliders: *Lumi* and *Cost* vs *Energy*

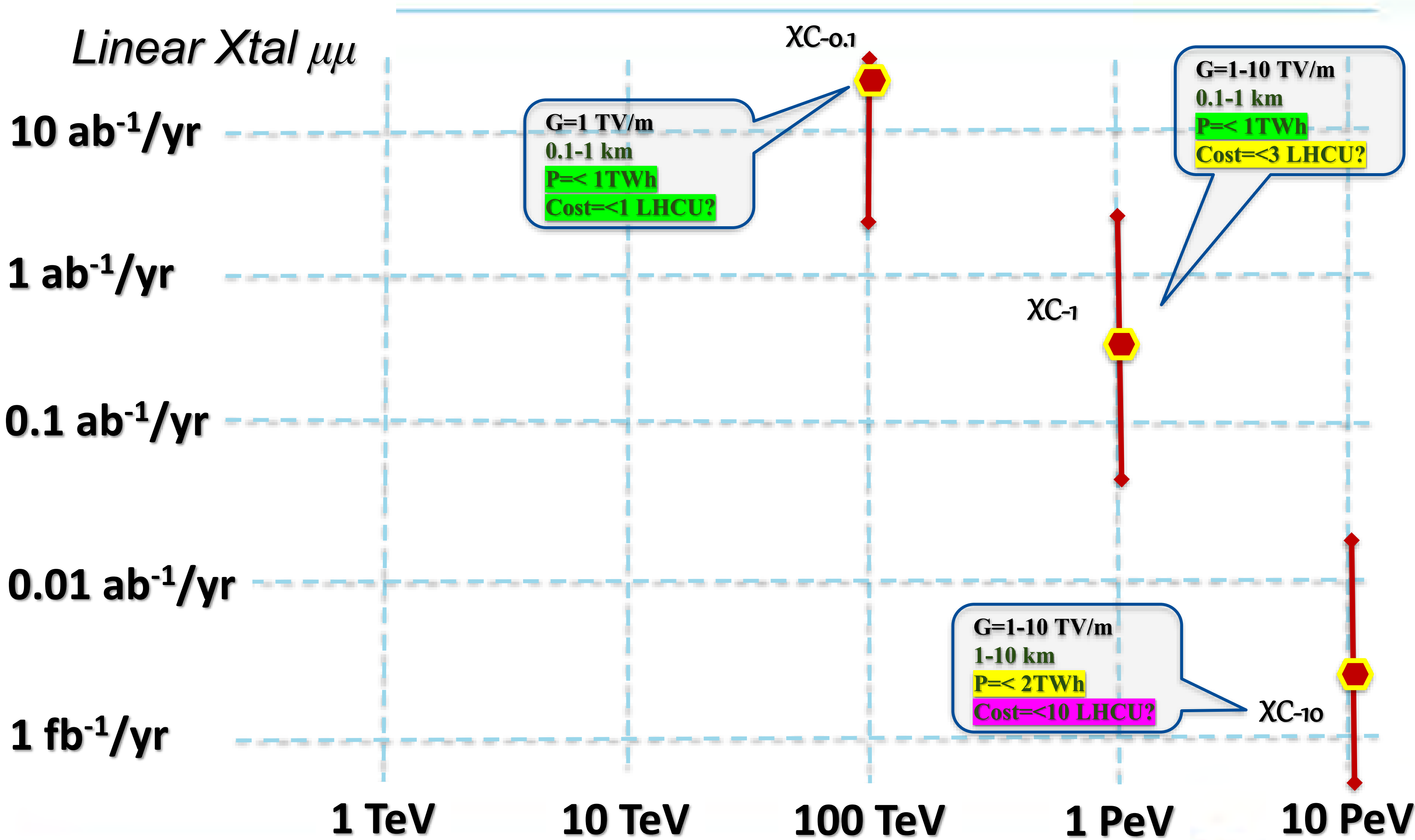

Main Conclusions:

- **For ultimate high energy colliders:**
  - **Major thrust is *Energy***
  - **Major concern/limit *is Cost***
  - **Main focus is *Luminosity* and *Power***
- **Cost:**
  - **Critically dependent on core acceleration technology**
  - **Existing injectors and infrastructure greatly help**
- **High *E*nergy means low *L*uminosity :**
  - **Don’t expect more than 0.1-1 ab^{-1}/yr at 30TeV-1 PeV**
  - **Assume *P*ower limited to 1-3 TWh/yr**

Main Conclusions (2):

- **For considered collider types:**
  - **Circular *pp* – limit is close or below 100 TeV (14 TeV cm)**
  - **Circular ee – limit is ~0.4-0.5 TeV**
  - **Circular $\mu\mu$ – limit is between 30 and 100 TeV**
  - **Linear RF ee/$\gamma\gamma$ – limit is between 3 and 10 TeV**

    Plasma ee/$\gamma\gamma$
  - **Exotic crystal $\mu\mu$ – promise of 0.1-1 PeV, low *L*uminosity**
- **Muons are particles of the future**

Fermilab

Thanks for Your Attention !

Questions !?

Acknowledgements

Author (VS) greatly appreciates input from and very helpful discussion on the subjects of this lecture series with many colleagues. Some material (tables, slides, illustrations) were borrowed from various presentations and/or publications by F. Zimmermann, V. Lebedev, N.Mokhov, M. Palmer, D. Schulte, A. Zlobin, S.Stapnes, E.Nanni, W.Herr, N.Walker, A.Seryi, C.Schroeder, M.Hogan, W.Fischer, A.Yamomoto, K.Oide, V.Livinenko, J.Gao, J.Tang, V.Telnov, M.Pivi, D.Stratakis, K.Yonehara, T.Roser, S.Gourlay, T. Raubenheimer, and many others.

(Some) References:

1. *αβγ* model – V.Shiltsev, *JINST* 9 T07002 (2014).
2. RMP Colliders – V.Shiltsev, F.Zimmermann, *Rev.Mod.Phys.* (2021); see also arxiv
3. NatPhys MC – K.Long, et al, *Nature Physics* (2021), see also arxiv
4. Eloisatron – W.Barletta, in *AIP Conference Proceedings*, vol. 351, no. 1, pp. 56-67(1996).
5. Xtal collider – V.Shiltsev, *Physics Uspekhi*, v.55 (10), p.1033 (2012)
6. F.Zimmermann – *NIMA* 909 (2018): 33-37; see also ARIES Workshops summary
7. T.Raubenheimer - Phys. Rev. ST Accel. Beams 3, 121002 (2000)
8. D.Schulte Plasma Colliders – *Rev.Accel.Sci.Tech.* 9 (2016): 209-233.
9. Granada ALEGRO – Input to *EPPSU*, #007a (Granada, 2019)
10. *Modern Muon Physics: Selected Issues*, I.Strakovsky, et al (Nova, 2020)
11. 2019 Crystal Workshop - eds. T.Tajima et al *Beam Acceleration in Crystals and Nanostructures* (World Scientific, 2020)
12. *CPT*-theorem – V.Shiltsev *Mod. Phys. Lett. A*, vol. 26, No. 11 (2011) pp. 761-772
13. Cheap magnets – V.Kashikhin, Fermilab beams-doc-8948 (2021)

Happy Class USPAS'22 Colliders

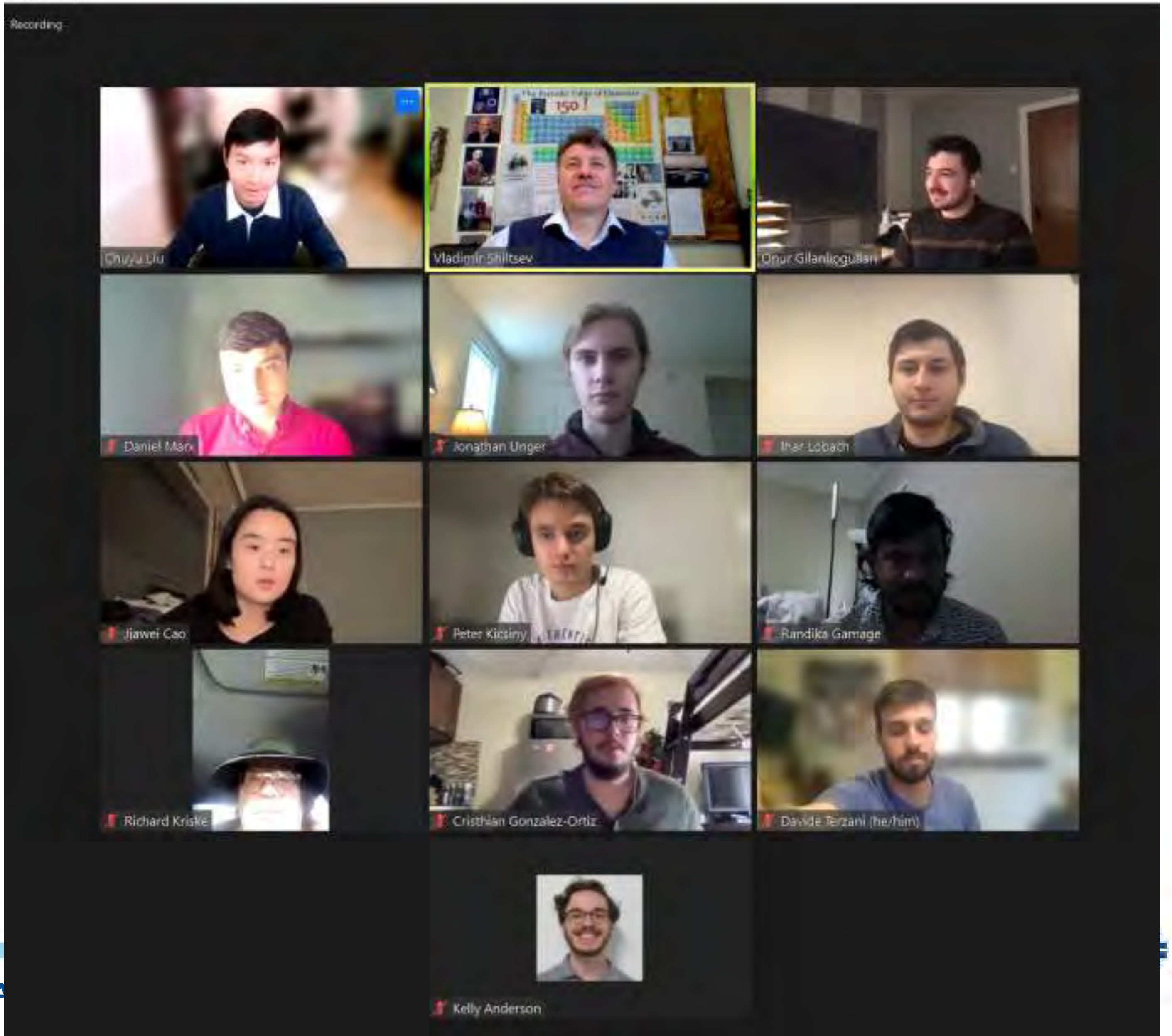

Fermilab

Lectures 1&2: Linear Optics

Valeri Lebedev
JINR & Fermilab

US Particle Accelerator School
February 2022

Objectives

- Design of linear optics is a very important step in the design of an accelerator
- It determines all major parameters and properties
- In majority of cases the optics design does not require accounting of coupling between different degrees of freedom
  - And coupling can be considered in the perturbation theory
- However, in the recent years, machines, where different degrees of freedom are strongly coupled, were considered
  - Examples: Electron and Ionization cooling (including both linear and the ring-based machines), Optical stochastic cooling
- In this lecture we consider basics of linear optics for the coupled and uncoupled optics
  - We shortly refresh uncoupled optics
  - Then, having some experience, we consider x-y coupled optics

Uncoupled Betatron Motion

Equations for Uncoupled Motion

- Linearized equation of motion

$$x'' + \left(K_x^{\ 2} + k\right)x = 0$$

where: $K_x(s) \equiv K_x = eB_y(s)/Pc$, $k(s) \equiv k = eG(s)/Pc$

- In Hamiltonian form

$$\begin{cases} \dfrac{dx}{ds} = \dfrac{\partial H}{dp} \\ \dfrac{dp}{ds} = -\dfrac{\partial H}{dx} \end{cases} \quad \text{with} \quad H = \frac{p^2}{2} + \left(K_x^{\ 2} + k\right)\frac{x^2}{2}$$

- General solution of 2-nd order linear equation

$$x(s) = C(s)x(0) + S(s)\theta(0)\,, \quad \theta(s) \equiv dx/ds$$

where C(s) and S(s) two linear independent solutions

We can rewrite it in matrix form

$$\begin{bmatrix} x(s) \\ \theta(s) \end{bmatrix} = \begin{bmatrix} M_{11}(s) & M_{12}(s) \\ M_{21}(s) & M_{22}(s) \end{bmatrix} \begin{bmatrix} x(0) \\ \theta(0) \end{bmatrix} \quad \text{or} \quad \boxed{\mathbf{x}(s) = \mathbf{M}(s)\mathbf{x}(0)}$$

Conservation of the Phase Space Volume

Jacobian does not depend on time

$$\frac{d}{ds}\left(\frac{\partial(p,q)}{\partial(p_0,q_0)}\right)=\frac{d}{ds}\left(\begin{vmatrix}\frac{\partial}{\partial p_0}\left(p_0+\frac{dp}{ds}ds\right) & \frac{\partial}{\partial p_0}\left(x_0+\frac{dx}{ds}ds\right)\\ \frac{\partial}{\partial x_0}\left(p_0+\frac{dp}{ds}ds\right) & \frac{\partial}{\partial x_0}\left(x_0+\frac{dx}{ds}ds\right)\end{vmatrix}\right)=\frac{d}{ds}\left(\begin{vmatrix}1-\frac{\partial^2 H}{\partial s\partial p}ds & \frac{\partial^2 H}{\partial p^2}ds\\ \frac{\partial^2 H}{\partial^2 x}ds & 1+\frac{\partial^2 H}{\partial x\partial p}ds\end{vmatrix}\right)=0$$

where we used
$$\begin{cases}\dfrac{dx}{ds}=\dfrac{\partial H}{dp}\\[2ex] \dfrac{dp}{ds}=-\dfrac{\partial H}{dx}\end{cases}$$

⇨ The phase space volume is conserved in the course of motion and, consequently, $|\mathbf{M}|=1$

- The conservation of the phase space volume is also justified for multidimensional motion.
  It is called **Liouville theorem**

Betatron Motion in a Ring

- Arbitrary turn-by-turn betatron motion at a given place may be presented through eigen-vectors

$$\mathbf{x}_n = \mathrm{Re}\left(\Lambda_1{}^n\left(A_1\mathbf{v}_1\right) + \Lambda_2{}^n\left(A_2\mathbf{v}_2\right)\right) \quad \text{where} \quad \mathbf{M}\mathbf{v}_k = \Lambda_k\mathbf{v}_k\ , \quad k = 1, 2$$

  - ♦ Stable betatron motion requires $|\Lambda_k| = 1$ => $\Lambda_2 = \Lambda_1{}^*$ (since real ***M***)
  - ♦ Introduce betatron frequencies so that $\Lambda_{1,2} = e^{\pm i\mu}$

    Corresponding betatron tune (fractional part): $Q = \mu / 2\pi$

- Description of betatron motion for the entire ring
  - ♦ The eigen-vector $\mathbf{v}(s) = \mathbf{M}(0,s)\mathbf{v}$ is the eigen-vector for the total ring transfer matrix for coordinate ***s***.
  - ♦ Then we normalize the eigen-vectors so that

    $\mathbf{v}(s) = \mathbf{M}(0,s)\mathbf{v}(0)e^{-\mu(s)}$

    and require $\mathrm{Im}(\mathrm{v}_{1'}(s)) = 0$ and $\mathbf{v}^+(s)\mathbf{S}\mathbf{v}(s) = -2i$, where $\mathbf{S} = \begin{bmatrix} 0 & 1 \\ -1 & 0 \end{bmatrix}$

    Then we can describe the entire ring betatron motion

$$\boxed{\mathbf{x}(s) = \sqrt{2I}\,\mathrm{Re}\left(e^{i(\psi-\mu(s))}\mathbf{v}\right)}$$

where the action ***I*** and the betatron phase ψ determine initial part. pos.

The Eigen-vector Parameterization

- Parametrize the eigen-vector

$$\mathbf{v} \equiv \mathbf{v}(s) = \begin{bmatrix} \sqrt{\beta(s)} \\ -\dfrac{i+\alpha(s)}{\sqrt{\beta(s)}} \end{bmatrix}$$

  - $\mathrm{Im}(\mathrm{v}_{1}(s)) = 0$
  - The eigen-vectors are orthogonal and correctly normalized

$$\begin{cases} \mathbf{v}^{+}\mathbf{S}\mathbf{v} = \begin{bmatrix} \sqrt{\beta(s)} & \dfrac{i-\alpha(s)}{\sqrt{\beta(s)}} \end{bmatrix} \begin{bmatrix} 0 & 1 \\ -1 & 0 \end{bmatrix} \begin{bmatrix} \sqrt{\beta(s)} \\ -\dfrac{i+\alpha(s)}{\sqrt{\beta(s)}} \end{bmatrix} = -2i \\ \mathbf{v}^{T}\mathbf{S}\mathbf{v} = 0 = 0 \quad \text{or} \quad \mathbf{v}_2^{+}\mathbf{S}\mathbf{v}_1 = 0 \end{cases}$$

Courant-Snider Invariant

The betatron amplitude (maximum particle displacement) $=\sqrt{2I\beta}$

The maximum angle $=\sqrt{\dfrac{2I}{\beta}\left(1+\alpha^2\right)}$

The maximum angle for x=0 is achieved when

$$\sqrt{2I}\,\mathrm{Re}\left(\begin{bmatrix}\sqrt{\beta(s)}\\ -\dfrac{i+\alpha(s)}{\sqrt{\beta(s)}}\end{bmatrix}e^{i\pi/2}\right)=\sqrt{2I}\,\mathrm{Re}\left(\begin{bmatrix}i\\ \dfrac{1-i\alpha(s)}{\sqrt{\beta(s)}}\end{bmatrix}\right)$$

⇨ Local angular spread: $\theta_m=\sqrt{\dfrac{2I}{\beta}}$

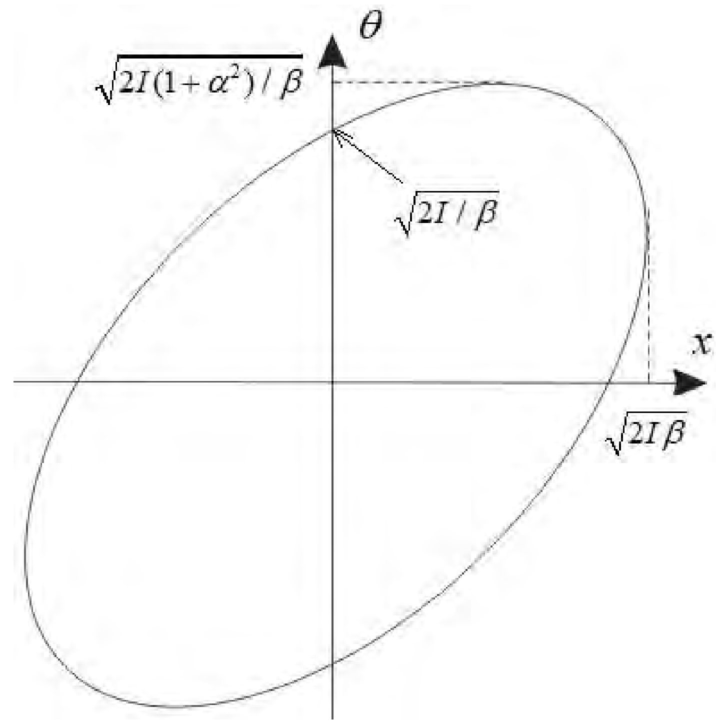

- Finding action from the known x and θ

$$\mathbf{v}^{+}\mathbf{S}\left[\mathbf{x}=\sqrt{2I}\left(\frac{e^{i\psi}\mathbf{v}+CC}{2}\right)\right]\xrightarrow[condition]{orthogonality}\mathbf{v}^{+}\mathbf{S}\mathbf{x}=-i\sqrt{2I}\to I=\frac{1}{2}\left|\mathbf{v}^{+}\mathbf{S}\mathbf{x}\right|^2$$

- Courant-Snyder invariant

Remember that: $\mathbf{S}=\begin{bmatrix}0 & 1\\ -1 & 0\end{bmatrix}$

$$\boxed{2I=\left|\mathbf{v}^{+}\mathbf{S}\mathbf{x}\right|^2=\beta\theta^2+2\alpha x\theta+\frac{1+\alpha^2}{\beta}x^2}$$

Computation of Machine Optics

Software for Computation of machine optics

- There are many computer codes allowing one to compute beam optics
- I mention 3 of them
  1. MAD -> MAD-8 -> MADX - supported by CERN
     https://mad.web.cern.ch/mad/
  2. Elegant - supported by ANL
     https://www.aps.anl.gov/Accelerator-Operations-Physics/Software#elegant
  3. OptiMX - supported by Fermilab
     https://home.fnal.gov/~ostiguy/OptiM/ (temporary link because of Fermilab security:
     https://www.dropbox.com/s/56l4nctnwegf7w7/OptimX64-20210526-setup.exe?dl=0)
- In this course we will be using OptiM
  - Interactive, GUI driven, easy to learn
  - Operates on major computer platforms: Windows, Unix, MAC
  - Free installation, Easy to install
  - Online help (documentation)
- Input file consists of:
  - Math header
  - Main body starting from keyword OptiM. It includes: (1) beam parameters, (2) element sequence, (3) parameters of elements, (4) service blocks

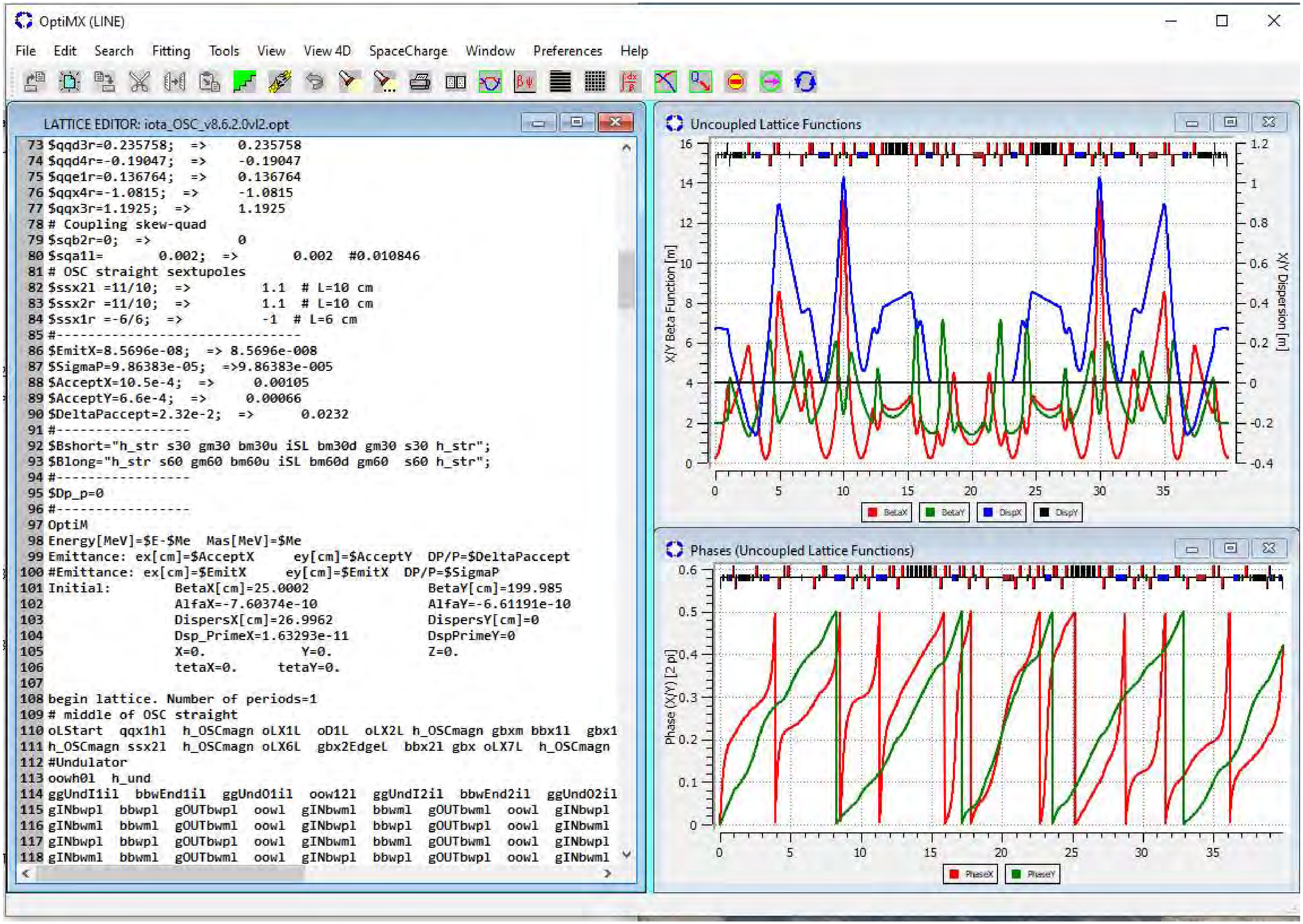

Computations can be done in a ring and beam line modes

X-Y Coupled Betatron Motion

Equations for X-Y Coupled Motion

- Linearized equations of motion

$$\begin{cases} x'' + \left(K_x^{\,2} + k\right)x + \left(N - \dfrac{1}{2}R'\right)y - Ry' = 0 \\ y'' + \left(K_y^{\,2} - k\right)y + \left(N + \dfrac{1}{2}R'\right)x + Rx' = 0 \end{cases}$$

where: $K_{x,y}(s) \equiv K_{x,y} = eB_{y,x}(s)/Pc$, $k(s) \equiv k = eG(s)/Pc$, $N = eG_s/Pc$, $R = eB_s/Pc$

- In Hamiltonian

$$H = \frac{p_x^{\,2} + p_y^{\,2}}{2} + \left(K_x^{\,2} + k + \frac{R^2}{4}\right)\frac{x^2}{2} + \left(K_y^{\,2} - k + \frac{R^2}{4}\right)\frac{y^2}{2} + Nxy + \frac{R}{2}\left(yp_x - xp_y\right)$$

the corresponding canonical momenta are: $\begin{cases} p_x = x' - \dfrac{R}{2}y \\ p_y = y' + \dfrac{R}{2}x \end{cases}$

In matrix form: $\hat{\mathbf{x}} = \mathbf{R}\mathbf{x}$

$$\hat{\mathbf{x}} \equiv \begin{bmatrix} x \\ p_x \\ y \\ p_y \end{bmatrix} \quad , \quad \mathbf{x} \equiv \begin{bmatrix} x \\ \theta_x \\ y \\ \theta_y \end{bmatrix} \quad , \quad \mathbf{R} = \begin{bmatrix} 1 & 0 & 0 & 0 \\ 0 & 1 & -R/2 & 0 \\ 0 & 0 & 1 & 0 \\ R/2 & 0 & 0 & 1 \end{bmatrix}$$

Matrix Form of Equations for X-Y Coupled Motion

$$H = \frac{1}{2}\hat{\mathbf{x}}^T \mathbf{H}\hat{\mathbf{x}}$$ where

$$\mathbf{H} = \begin{bmatrix} K_x^{\,2} + k + \frac{R^2}{4} & 0 & N & -R/2 \\ 0 & 1 & R/2 & 0 \\ N & R/2 & K_y^{\,2} - k + \frac{R^2}{4} & 0 \\ -R/2 & 0 & 0 & 1 \end{bmatrix}$$

Then the motion equations are

$$\boxed{\frac{d\hat{\mathbf{x}}}{ds} = \mathbf{U}\mathbf{H}\hat{\mathbf{x}}}$$

$$\mathbf{U} = \begin{bmatrix} 0 & 1 & 0 & 0 \\ -1 & 0 & 0 & 0 \\ 0 & 0 & 0 & 1 \\ 0 & 0 & -1 & 0 \end{bmatrix}$$

- Properties of matrix $\mathbf{U}$ (called unit symplectic matrix)
  $\mathbf{U}^T\mathbf{U} = \mathbf{I}$ and $\mathbf{U}\mathbf{U} = -\mathbf{I}$, where $\mathbf{I}$ is the identity matrix
- Similar to the single dimensional motion we introduce 4-dimensional transfer matrix, $\hat{\mathbf{x}} = \hat{\mathbf{M}}(0,s)\hat{\mathbf{x}}_0$, for the 2-dimensional motion
  The cap here and below denotes that we consider the transfer matrix which uses canonical momenta instead of angles

Motion Symplecticity

$$\boxed{\frac{d\hat{\mathbf{x}}}{ds} = \mathbf{U}\mathbf{H}\hat{\mathbf{x}}}$$

- Lagrange invariant

$$\frac{d}{ds}\left(\hat{\mathbf{x}}_1{}^T \mathbf{U}\hat{\mathbf{x}}_2\right) = \frac{d\hat{\mathbf{x}}_1{}^T}{ds}\mathbf{U}\hat{\mathbf{x}}_2 + \hat{\mathbf{x}}_1{}^T\mathbf{U}\frac{d\hat{\mathbf{x}}_2}{ds} = \hat{\mathbf{x}}_1{}^T\mathbf{H}^T\mathbf{U}^T\mathbf{U}\hat{\mathbf{x}}_2 + \hat{\mathbf{x}}_1{}^T\mathbf{U}\mathbf{U}\mathbf{H}\hat{\mathbf{x}}_2 = 0$$

$\Rightarrow$ $\hat{\mathbf{x}}_1{}^T\mathbf{U}\hat{\mathbf{x}}_2 = \text{const}$

- Motion symplecticity

  Substituting $\hat{\mathbf{x}} = \hat{\mathbf{M}}\hat{\mathbf{x}}_0$ into above equation one obtains

$$\hat{\mathbf{x}}_1{}^T\mathbf{U}\hat{\mathbf{x}}_2 = \hat{\mathbf{x}}_1{}^T\hat{\mathbf{M}}(0,s)^T\mathbf{U}\hat{\mathbf{M}}(0,s)\hat{\mathbf{x}}_2 = \text{const}$$

  As the above equation is satisfied for any $\hat{\mathbf{x}}_1$ and $\hat{\mathbf{x}}_2$ it yields

$$\boxed{\hat{\mathbf{M}}^T\mathbf{U}\hat{\mathbf{M}} = \mathbf{U}}$$

  This property is called symplecticity and matrix $\hat{\mathbf{M}}$ symplectic

- $\hat{\mathbf{M}}(0,s)^T\mathbf{U}\hat{\mathbf{M}}(0,s)$ is antisymmetric

  $\Rightarrow$ Only six $((n^2-n)/2 = 6)$ of these equations are independent

  Thus out of 16 matrix elements of matrix **M** the motion symplecticity leaves only 10 elements linearly independent

Symplecticity of Eigen-Vectors

$$\hat{\mathbf{M}}\hat{\mathbf{v}}_k = \lambda_k \hat{\mathbf{v}}_k \ , \quad k = 1,..,4$$

- For any two eigen-vectors the symplecticity yields the identity

$$0 = \lambda_j \hat{\mathbf{v}}_j^T \mathbf{U}\left(\hat{\mathbf{M}}\hat{\mathbf{v}}_i - \lambda_i \hat{\mathbf{v}}_i\right) = \left(\hat{\mathbf{M}}\hat{\mathbf{v}}_j\right)^T \mathbf{U}\hat{\mathbf{M}}\hat{\mathbf{v}}_i - \lambda_j \hat{\mathbf{v}}_j^T \mathbf{U}\lambda_i \hat{\mathbf{v}}_i = \left(1 - \lambda_j \lambda_i\right)\hat{\mathbf{v}}_j^T \mathbf{U}\hat{\mathbf{v}}_i$$

where we substituted: $\left(\hat{\mathbf{M}}\hat{\mathbf{v}}_j\right)^T \mathbf{U}\hat{\mathbf{M}}\hat{\mathbf{v}}_i = \hat{\mathbf{v}}_i^T \hat{\mathbf{M}}^T \mathbf{U}\hat{\mathbf{M}}\hat{\mathbf{v}}_i = \hat{\mathbf{v}}_i^T \mathbf{U}\hat{\mathbf{v}}_i$

It determines that the eigen-values always appear in two reciprocal pairs, and, consequently, the four eigen-values split into two complex conjugate pairs: λ_1, λ_1^* and λ_2, λ_2^*

For $\lambda_1 \neq \lambda_2$ (non-degenerate case) we obtain the orthogonality condition

$$\hat{\mathbf{v}}_1^+ \mathbf{U}\hat{\mathbf{v}}_1 \neq 0 \ ,$$

$$\hat{\mathbf{v}}_2^+ \mathbf{U}\hat{\mathbf{v}}_2 \neq 0 \ ,$$

$$\hat{\mathbf{v}}_i^+ \mathbf{U}\hat{\mathbf{v}}_j = 0 \qquad \text{if } i \neq j,$$

$$\hat{\mathbf{v}}_i^T \mathbf{U}\hat{\mathbf{v}}_j = 0 \ ,$$

Normalizing eigen-vectors we obtain:

$$\hat{\mathbf{v}}_1^+ \mathbf{U}\hat{\mathbf{v}}_1 = -2i \quad , \quad \hat{\mathbf{v}}_2^+ \mathbf{U}\hat{\mathbf{v}}_2 = -2i \quad ,$$

$$\hat{\mathbf{v}}_1^T \mathbf{U}\hat{\mathbf{v}}_1 = 0 \quad , \quad \hat{\mathbf{v}}_2^T \mathbf{U}\hat{\mathbf{v}}_2 = 0 \quad ,$$

$$\hat{\mathbf{v}}_2^T \mathbf{U}\hat{\mathbf{v}}_1 = 0 \quad , \quad \hat{\mathbf{v}}_2^+ \mathbf{U}\hat{\mathbf{v}}_1 = 0 \quad .$$

Out of 2 complex conjugated vectors we choose one which satisfies the normalization condition. Normalization of CC vector has different sign.

Parameterization of Eigen-vectors

- Betatron motion is described similar to 1D case:

$$\hat{\mathbf{x}}(s) == \mathrm{Re}\left(\sqrt{2I_1}\hat{\mathbf{v}}_1(s)e^{-i(\psi_1+\mu_1(s))} + \sqrt{2I_2}\hat{\mathbf{v}}_2(s)e^{-i(\psi_2+\mu_2(s))}\right)$$

- There are 2 popular parameterizations: Edwards-Teng and Mais-Ripken
  - Here we shortly consider the extended Mais-Ripken

$$\hat{\mathbf{v}}_1 = \begin{bmatrix} \sqrt{\beta_{1x}} \\ -\dfrac{i(1-u)+\alpha_{1x}}{\sqrt{\beta_{1x}}} \\ \sqrt{\beta_{1y}}\, e^{i\nu_1} \\ -\dfrac{iu+\alpha_{1y}}{\sqrt{\beta_{1y}}} e^{i\nu_1} \end{bmatrix} \qquad \hat{\mathbf{v}}_2 = \begin{bmatrix} \sqrt{\beta_{2x}}\, e^{i\nu_2} \\ -\dfrac{iu+\alpha_{2x}}{\sqrt{\beta_{2x}}} e^{i\nu_2} \\ \sqrt{\beta_{2y}} \\ -\dfrac{i(1-u)+\alpha_{2y}}{\sqrt{\beta_{2y}}} \end{bmatrix}$$

- The betatron motion is described by 10 linearly independent functions: 4 β-functions, 4 α-functions, and 2 betatron phase advances
- Symplecticity allows one to compute functions u, ν_1 & ν_2 from known α's & β's. However, there are 4 solutions for their values and additional information is required to find α's and β's. In practice, first, we find the eigen-vectors from known transfer matrix, and, then unique solutions for all 4D-Twiss functions

4D Ellipsoid in the Phase Space

$$\hat{\mathbf{x}} = \mathrm{Re}\left(A_1 e^{-i\psi_1}\hat{\mathbf{v}}_1 + A_2 e^{-i\psi_2}\hat{\mathbf{v}}_2\right) = A_1\left(\hat{\mathbf{v}}_1{}'\cos\psi_1 + \hat{\mathbf{v}}_1{}''\sin\psi_1\right) + A_2\left(\hat{\mathbf{v}}_2{}'\cos\psi_2 + \hat{\mathbf{v}}_2{}''\sin\psi_2\right)$$

- Rewrite it in matrix form

$\boxed{\hat{\mathbf{x}} = \hat{\mathbf{V}}\mathbf{A}\boldsymbol{\xi}_A}$ where $\hat{\mathbf{V}} = \left[\hat{\mathbf{v}}_1{}', -\hat{\mathbf{v}}_1{}'', \hat{\mathbf{v}}_2{}', -\hat{\mathbf{v}}_2{}''\right]$ $\quad \mathbf{A} = \begin{bmatrix} A_1 & 0 & 0 & 0 \\ 0 & A_1 & 0 & 0 \\ 0 & 0 & A_2 & 0 \\ 0 & 0 & 0 & A_2 \end{bmatrix}$ $\quad \boldsymbol{\xi}_A = \begin{bmatrix} \cos\psi_1 \\ -\sin\psi_1 \\ \cos\psi_2 \\ -\sin\psi_2 \end{bmatrix}$

- To obtain a 4D ellipsoid which includes all particles we need to account that the mode amplitudes are interdependent. To account it we put:

$$\boldsymbol{\xi} = \begin{bmatrix} \cos\psi_1 \cos\psi_3 \\ -\sin\psi_1 \cos\psi_3 \\ \cos\psi_2 \sin\psi_3 \\ -\sin\psi_2 \sin\psi_3 \end{bmatrix}$$

so that vector ξ stays at 3D surface with unit radius, i. e. $(\boldsymbol{\xi},\boldsymbol{\xi}) = 1$

  - Substituting x in this equation we obtain: $\hat{\mathbf{x}}^T\left(\left(\hat{\mathbf{V}}\mathbf{A}\right)^{-1}\right)^T\left(\hat{\mathbf{V}}\mathbf{A}\right)^{-1}\hat{\mathbf{x}} = 1$
  - Matrix symplecticity yields $\hat{\mathbf{V}}^{-1} = \mathbf{U}^T\hat{\mathbf{V}}^T\mathbf{U}$ using this equation we finally obtain: $\boxed{\hat{\mathbf{x}}^T\hat{\boldsymbol{\Xi}}\hat{\mathbf{x}} = 1, \quad \hat{\boldsymbol{\Xi}} = \mathbf{U}\hat{\mathbf{V}}\hat{\boldsymbol{\Xi}}'\hat{\mathbf{V}}^T\mathbf{U}^T, \quad \hat{\boldsymbol{\Xi}}' = \mathbf{A}^{-1}\mathbf{A}^{-1}}$

1D and 2D Emittances

- We define the beam emittance as a product of the ellipsoid semi-axes (omitting the factor $\pi^2/2$ correcting for the real 4D volume of the ellipsoid):
$$\varepsilon_{4D} = \frac{1}{\sqrt{\hat{\Xi}'_{11}\hat{\Xi}'_{22}\hat{\Xi}'_{33}\hat{\Xi}'_{44}}} = \frac{1}{\sqrt{\det(\hat{\mathbf{\Xi}}')}}$$
- Consequently:
$$\varepsilon_1\varepsilon_2 = \varepsilon_{4D}\ , \qquad \hat{\mathbf{\Xi}}' = \begin{bmatrix} 1/\varepsilon_1 & 0 & 0 & 0 \\ 0 & 1/\varepsilon_1 & 0 & 0 \\ 0 & 0 & 1/\varepsilon_2 & 0 \\ 0 & 0 & 0 & 1/\varepsilon_2 \end{bmatrix}$$
- Gaussian distribution: $f(\hat{\mathbf{x}}) = \dfrac{1}{4\pi^2\varepsilon_1\varepsilon_2}\exp\left(-\dfrac{1}{2}\hat{\mathbf{x}}^T\hat{\mathbf{\Xi}}\hat{\mathbf{x}}\right)$
- Second order moments
$$\hat{\Sigma}_{ij} \equiv \overline{\hat{x}_i\hat{x}_j} = \int \hat{x}_i\hat{x}_j f(\hat{\mathbf{x}})d\hat{x}^4 = \frac{1}{4\pi^2\varepsilon_1\varepsilon_2}\int \hat{x}_i\hat{x}_j \exp\left(-\frac{1}{2}\hat{\mathbf{x}}^T\hat{\mathbf{\Xi}}\hat{\mathbf{x}}\right)d\hat{x}^4$$
To carry out the integration we use a transform $\hat{\mathbf{y}} = \hat{\mathbf{V}}^{-1}\hat{\mathbf{x}}$. It reduces matrix to the diagonal form. => $\hat{\mathbf{\Sigma}} = \hat{\mathbf{V}}\hat{\mathbf{\Xi}}'^{-1}\hat{\mathbf{V}}^T = \hat{\mathbf{\Xi}}^{-1}$

General Remarks

- ε_1 and ε_2 are the motion invariants – they are conserved
- In practical applications the longitudinal magnetic field at boundaries of elements is zero. Consequently, the difference between variables with and without caps disappears.

OptiMX 4D Calculations

- 4D Twiss parameters for Tevatron near B0 (CDF detector)

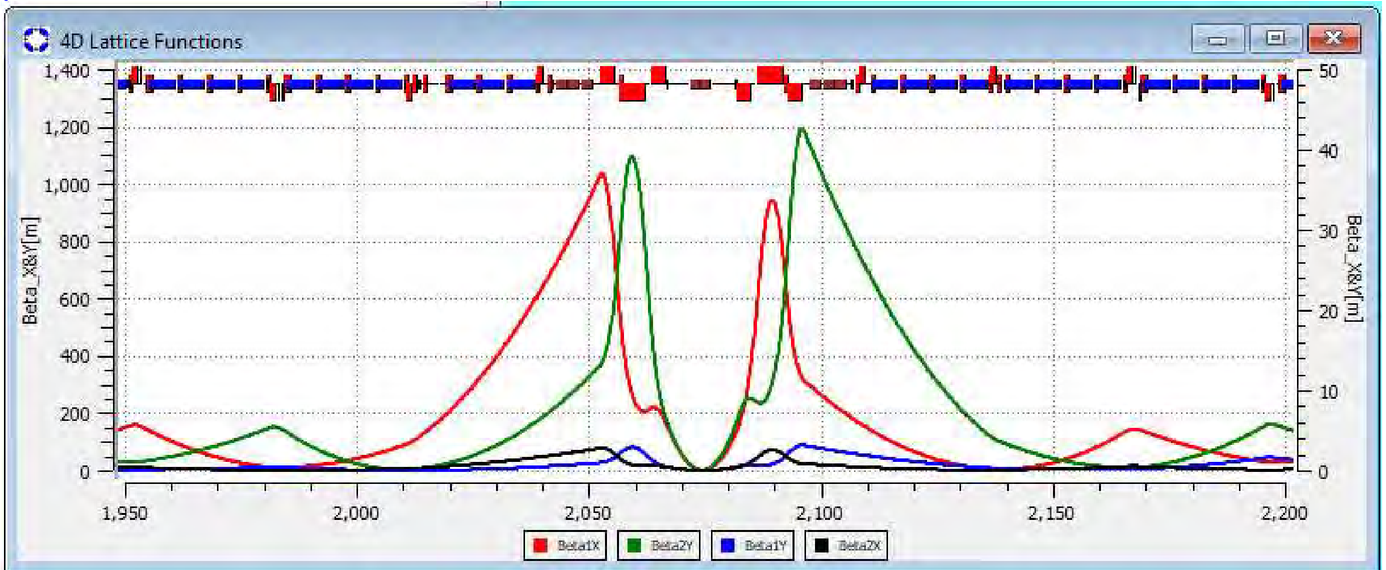

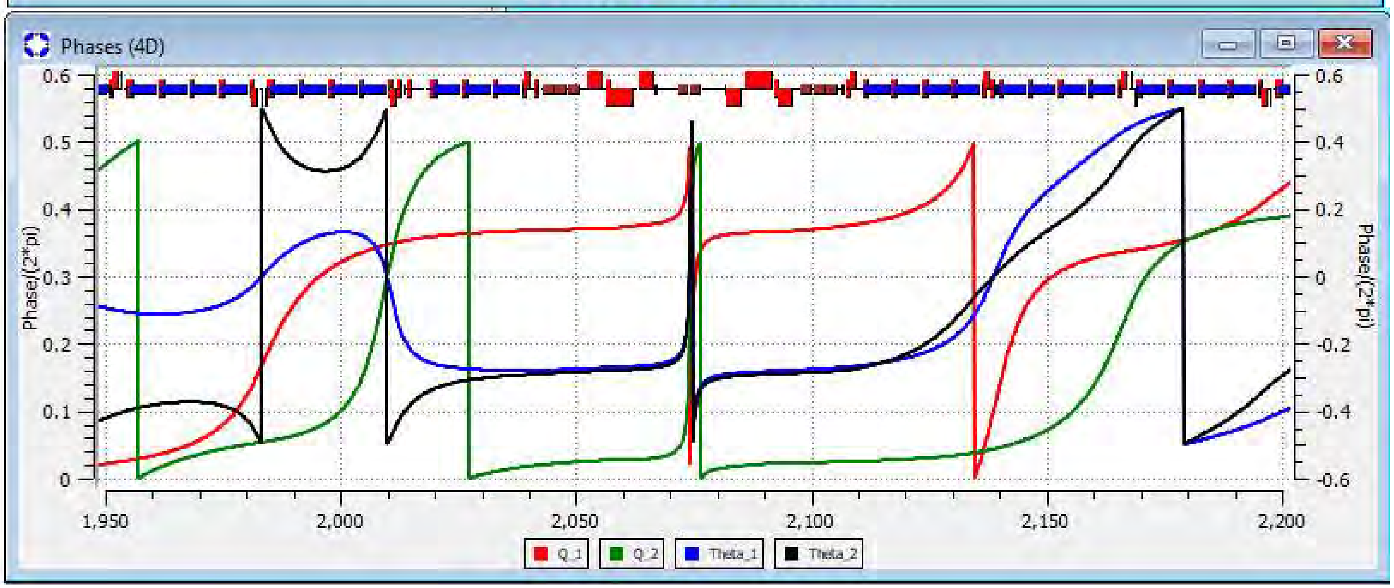

Perturbed Betatron Motion

- To simplify equations, we transit to new variables

$$x=\frac{X}{\sqrt{\beta}}\,,\quad p=\beta\frac{d}{ds}\frac{X}{\sqrt{\beta}}=\beta\left(\frac{1}{\sqrt{\beta}}\frac{dX}{ds}-\frac{X}{2\beta^{3/2}}\frac{d\beta}{ds}\right)=\sqrt{\beta}\theta+\alpha\frac{X}{\sqrt{\beta}}\,,\quad \frac{d\mu}{ds}=\frac{1}{\beta}$$

- In the new variables the motion description is greatly simplified

$$\frac{d^2X}{d\mu^2}=-X\,,\quad \mathbf{M}=\begin{bmatrix}\cos\mu & \sin\mu\\ -\sin\mu & \cos\mu\end{bmatrix}$$

Consequently, the unperturbed solution is characterized by $\beta=1,\alpha=1$

- Choose perturbed initial particle coordinates as following:

$$\mathbf{X}_0=\sqrt{\varepsilon}\,\mathrm{Re}\left(\begin{bmatrix}\sqrt{\hat\beta}\\ -\dfrac{i+\hat\alpha}{\sqrt{\hat\beta}}\end{bmatrix}e^{i\psi}\right)$$

⇨ Dependence of beam size on μ is

$$A(s)=\sqrt{\varepsilon}\,\mathrm{Re}\left(\left(\sqrt{\hat\beta}\cos\mu-\frac{i+\hat\alpha}{\sqrt{\hat\beta}}\sin\mu\right)e^{i\psi}\right)_{\max\limits_{\psi}}=\sqrt{\varepsilon\left(\left(\sqrt{\hat\beta}\cos\mu-\frac{\hat\alpha}{\sqrt{\hat\beta}}\sin\mu\right)^2+\left(\frac{\sin\mu}{\sqrt{\hat\beta}}\right)^2\right)}$$

$$A(s)=\sqrt{\varepsilon\left(c^2\hat\beta+s^2\left(\frac{1+\hat\alpha^2}{\hat\beta}\right)-2\hat\alpha cs\right)}=\sqrt{\varepsilon\left(\frac{1+\cos(2\mu)}{2}\hat\beta+\frac{1-\cos(2\mu)}{2}\left(\frac{1+\hat\alpha^2}{\hat\beta}\right)-\hat\alpha\sin(2\mu)\right)}$$

Perturbed Betatron Motion (2)

- The beam size oscillates at the double betatron frequency

$$\boxed{A(s)=\sqrt{\frac{\varepsilon}{2}\left(\left(\hat{\beta}+\frac{1+\hat{\alpha}^2}{\hat{\beta}}\right)+\left(\hat{\beta}-\frac{1+\hat{\alpha}^2}{\hat{\beta}}\right)\cos(2\mu)-2\hat{\alpha}\sin(2\mu)\right)}}$$

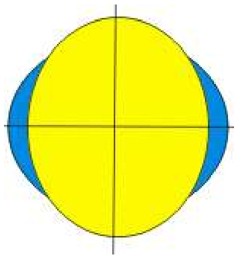

Consequently, the perturbed beta-function oscillates at the double betatron frequency as well.

What is missed in the Lecture?

- Not all calculations are shown in detail
- Edwards-Teng parameterization
- How to find eigen-vectors from matrices Σ an Ξ and vice versa
- How to express a transfer matrix from known Twiss parameters or eigen vectors and betatron phase advances

- These details are not required to follow other lectures

- Look for details in:
  - V. A. Lebedev (Fermilab), S. A. Bogacz (Jefferson Lab), "Betatron motion with coupling of horizontal and vertical degrees of freedom", https://arxiv.org/abs/1207.5526
  - or "Accelerator Physics at the Tevatron Collider", edited by V. Lebedev and V. Shiltsev, Springer, 2014.

Problems

1. Prove that if **v** is the eigen-vector for matrix **M** corresponding to the one turn matrix starting at s=0 (point 1) then the vector $\mathbf{M}_{12}\,\mathbf{v}$ will be the eigen vector of the transfer matrix corresponding to the point 2. Here $\mathbf{M}_{12}$ is the transfer matrix from point 1 to point 2.
2. Find 2D analog of Courant-Snyder invariant
3. Prove that matrix $\hat{\mathbf{V}} = \left[\hat{\mathbf{v}}_1{}', -\hat{\mathbf{v}}_1{}'', \hat{\mathbf{v}}_2{}', -\hat{\mathbf{v}}_2{}''\right]$ is symplectic
4. Fill missed calculations in computation $\hat{\mathbf{\Sigma}} = \hat{\mathbf{V}}\hat{\mathbf{\Xi}}'^{-1}\hat{\mathbf{V}}^T = \hat{\mathbf{\Xi}}^{-1}$
5. Prove that for a symplectic matrix, defined by the following equation $\hat{\mathbf{M}}^T\mathbf{U}\hat{\mathbf{M}} = \mathbf{U}$, its determinant is $\left|\hat{\mathbf{M}}\right| = 1$, $\hat{\mathbf{M}}^{-1} = \mathbf{U}^T\hat{\mathbf{M}}^T\mathbf{U}$ and the matrix also satisfies to $\hat{\mathbf{M}}\mathbf{U}\hat{\mathbf{M}}^T = \mathbf{U}$.

Lectures 3&4: Longitudinal Motion and IR Focusing Limitations

Valeri Lebedev
JINR & Fermilab

US Particle Accelerator School
February 2022

U.S. DEPARTMENT OF ENERGY

Objectives

- Beam acceleration and bunching are based on the dependence of particle revolution frequency on its energy
- Longitudinal OSC and CEC use dependence of particle longitudinal displacement on particle momentum
  while transverse OSC and CEC use dependence of particle longitudinal displacement on particle betatron motion
- In this lecture we consider
  - basics of linear optics for longitudinal degree of freedom
  - longitudinal motion in a harmonic RF
  - the perturbation theory for symplectic motion
  - and limitations on beam focusing in the design of interaction region

S-X Coupled Motion

Transfer Matrix for X-S Coupled Motion

- Parameterization of transfer matrix in the absence of RF

$$\mathbf{x}_2 = \mathbf{M}\mathbf{x}_1 \quad , \quad \mathbf{M} = \begin{bmatrix} M_{11} & M_{12} & 0 & M_{16} \\ M_{21} & M_{22} & 0 & M_{26} \\ M_{51} & M_{52} & 1 & M_{56} \\ 0 & 0 & 0 & 1 \end{bmatrix}, \quad \mathbf{x} \equiv \begin{bmatrix} x \\ \theta_x \\ s \\ \theta_s \end{bmatrix}, \quad \theta_s = \frac{\Delta p}{p}$$

Longitudinal displacements are counted relative to the reference particle

- Elements M_{16} and M_{26} are directly related to dispersion

$$\begin{bmatrix} D_2 \\ D_2' \\ \dots \\ 1 \end{bmatrix}^T = \begin{bmatrix} M_{11} & M_{12} & 0 & M_{16} \\ M_{21} & M_{22} & 0 & M_{26} \\ M_{51} & M_{52} & 1 & M_{56} \\ 0 & 0 & 0 & 1 \end{bmatrix} \begin{bmatrix} D_1 \\ D_1' \\ \dots \\ 1 \end{bmatrix}, \quad \begin{cases} D_2 = M_{11}D_1 + M_{12}D_1' + M_{16} \\ D_2' = M_{21}D_1 + M_{22}D_1' + M_{26} \end{cases} \xrightarrow[\substack{D_2=D_1 \\ D_2'=D_1'}]{\text{For ring}} \begin{cases} M_{16} = D(1-M_{11}) - D'M_{12} \\ M_{26} = -M_{21}D + D'(1-M_{22}) \end{cases}$$

- Elements M_{51} and M_{52} are bound to others by symplecticity condition

$$\hat{\mathbf{M}}^T\mathbf{U}\hat{\mathbf{M}} = \mathbf{U} \;\Rightarrow\; \begin{cases} M_{51} = M_{21}M_{16} - M_{11}M_{26} \\ M_{52} = M_{22}M_{16} - M_{12}M_{26} \end{cases} \xrightarrow[\substack{D_2=D_1 \\ D_2'=D_1'}]{\text{For ring}} \begin{cases} M_{51} = DM_{21} + D'\left(1-M_{11}\right) \\ M_{52} = -D(1-M_{22}) - D'M_{12} \end{cases}$$

where we accounted that $M_{11}M_{22} - M_{12}M_{21} = 1$

- i.e. for a ring without RF M_{16}, M_{26}, M_{51} and M_{52} can be expressed through dispersion and its derivative. M_{56} is independent on other elements

Equations of Longitudinal Motion (no acceleration)

- Orbit lengthening

$$\begin{bmatrix} \dots \\ \dots \\ \Delta s \\ \dots \end{bmatrix}^T = \begin{bmatrix} M_{11} & M_{12} & 0 & M_{16} \\ M_{21} & M_{22} & 0 & M_{26} \\ M_{51} & M_{52} & 1 & M_{56} \\ 0 & 0 & 0 & 1 \end{bmatrix} \begin{bmatrix} D \\ D' \\ \dots \\ 1 \end{bmatrix} \frac{\Delta p}{p} \quad \Rightarrow \quad \Delta s = \left(M_{51} D + M_{52} D' + M_{56} \right) \frac{\Delta p}{p} = \alpha C \frac{\Delta p}{p}$$

- Momentum compaction: $\dfrac{\Delta C}{C} = \alpha \dfrac{\Delta p}{p}, \quad \alpha = \dfrac{M_{51} D + M_{52} D' + M_{56}}{C}$

- Slip-factor: $\dfrac{\Delta T}{T} = \dfrac{\Delta C}{C} - \dfrac{\Delta \mathrm{v}}{\mathrm{v}} = \eta \dfrac{\Delta p}{p} \xrightarrow[\frac{\Delta C}{C} = \alpha \frac{\Delta p}{p}]{\frac{\Delta \mathrm{v}}{\mathrm{v}} = \frac{1}{\gamma^2} \frac{\Delta p}{p}} \left(\alpha - \dfrac{1}{\gamma^2} \right) \dfrac{\Delta p}{p} \quad \Rightarrow \quad \eta = \alpha - \dfrac{1}{\gamma^2}$

- Equations for the longitudinal motion

$$\begin{cases} \dfrac{d\varphi}{dt} = q \omega_0 \eta \dfrac{\Delta p}{p} \\ \dfrac{d}{dt} \dfrac{\Delta p}{p} = \dfrac{1}{\beta^2} \dfrac{d}{dt} \dfrac{\Delta E}{E} = -\dfrac{1}{\beta^2 E} e V_0 \dfrac{\omega_0}{2\pi} \sin \varphi \end{cases} \quad \Rightarrow \quad \frac{d^2 \varphi}{dt^2} = -\Omega_s{}^2 \sin \varphi, \quad \Omega_s = \omega_0 \sqrt{\frac{e V_0 q \eta}{2\pi m c^2 \beta^2 \gamma}}$$

Effect of Deceleration due to SR on Longit. Motion

- Motion equation: $\dfrac{d^2\varphi}{dt^2} = -\Omega_s^{\,2}\left(\sin\varphi + \sin\varphi_0\right), \quad \sin\varphi_0 = \dfrac{V_{SR}}{V_0}$
- Its solution

$$\xrightarrow[\frac{d^2\varphi}{dt^2}=\frac{d\varphi}{dt}\frac{d}{d\varphi}\frac{d\varphi}{dt}=p\frac{dp}{d\varphi}]{d\varphi/dt=p} \quad \frac{d}{d\varphi}\left(\frac{p^2}{2}\right) = -\Omega_s^{\,2}\left(\sin\varphi + \sin\varphi_0\right) \Rightarrow \frac{p^2}{2} = \Omega_s^{\,2}\left(\cos\varphi + \varphi\sin\varphi_0\right) + C$$

Introduce Hamiltonian and the potential energy

$$H = \frac{p^2}{2} + U(\varphi), \quad U(\varphi) = -\Omega_s^{\,2}\left(\cos\varphi + \varphi\sin\varphi_0\right)$$

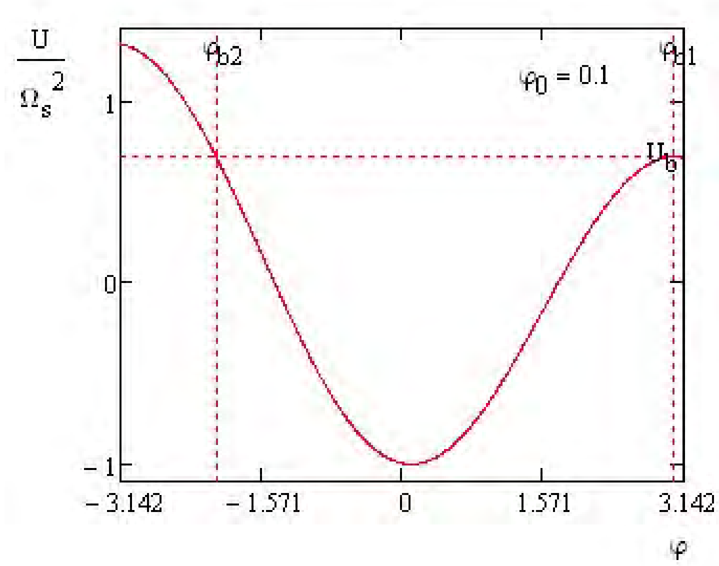

- Separatrix boundaries

$$\sin\varphi_{b1} = \sin\varphi_0 \Rightarrow \varphi_{b1} = \pi - \varphi_0$$

$$\Rightarrow \quad C = \Omega_s^{\,2}\left(\cos\varphi_0 - \varphi_0\sin\varphi_0\right)$$

- For small φ_0 the transcendent equation for finding the second boundary can be using perturbation theory
- Accounting of acceleration one needs to account vortex electric field due to changing magnetic field!!! -> conservation of the phase space

Particle Migration due to Scattering out & in RF Bucket

- In the above consideration we neglected damping due to SR
- In its absence a particle which was knocked out of the RF bucket will never drift back
- Particles which have energy above the bucket separatrix will be decelerated, and then they will penetrate to lower energy through the gap between two RF buckets and will continue deceleration to the momentum acceptance

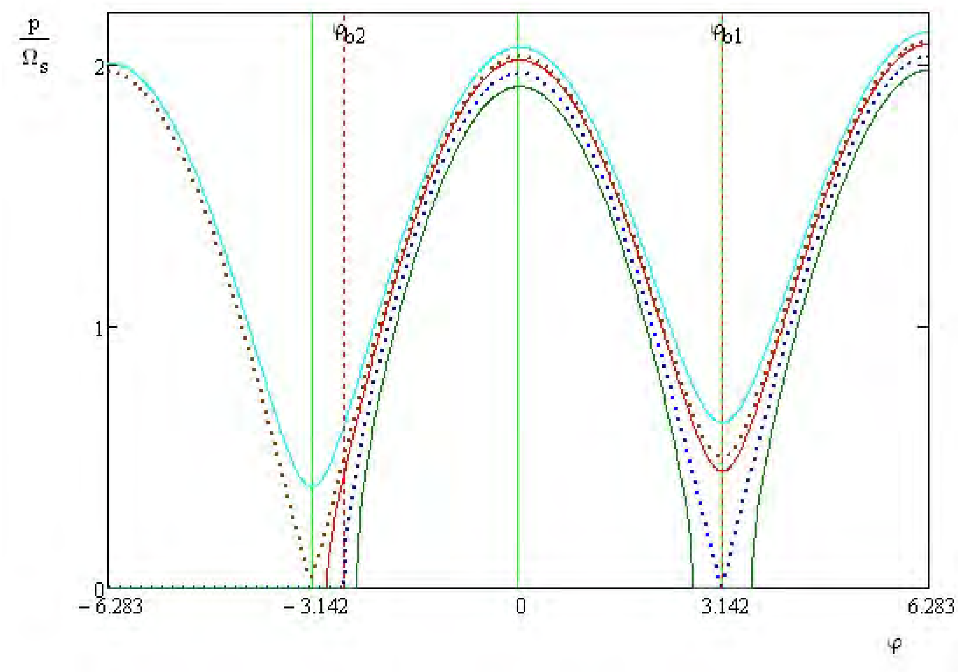

- Probability of a particle to be accepted back to the bucket is inversely proportional to the ratio of damping time to the synchrotron period.
- For a proton collider it is very big number.
- Consequently, the probability to drift to another bucket after Touschek scattering is strongly suppressed

Perturbation Theory for Symplectic Motion

Perturbation Theory

- The symplecticity enables to build an effective perturbation theory for the case of coupled motion.
- For the perturbed motion one can write: $\left(\mathbf{I}+\Delta\mathbf{M}\right)\mathbf{M}\tilde{\mathbf{v}}_j=\left(\lambda_j+\Delta\lambda_j\right)\tilde{\mathbf{v}}_j$
  - $\mathbf{M}$ – symplectic
  - transfer matrix, $\left(\mathbf{I}+\Delta\mathbf{M}\right)\mathbf{M}$, is not required to be symplectic
- Express the eigenvectors of perturbed motion as a sum of the unperturbed ones $\tilde{\mathbf{v}}_j=\mathbf{v}_j+\sum_{i=1}^{4}\varepsilon_{ij}\mathbf{v}_i\,,\quad \varepsilon_{ij}<<1\,,$
  - without limitation of generality one can consider that $\varepsilon_{ii}=0$ for every i.
  - Substituting and using properties of eigen-vectors one obtains

$$\left(\mathbf{I}+\Delta\mathbf{M}\right)\mathbf{M}\left(\mathbf{v}_j+\sum_{i=1}^{4}\varepsilon_{ij}\mathbf{v}_i\right)=\left(\lambda_j+\Delta\lambda_j\right)\left(\mathbf{v}_j+\sum_{i=1}^{4}\varepsilon_{ij}\mathbf{v}_i\right)$$

Dropping 2nd order terms: $\mathbf{M}\mathbf{v}_j+\Delta\mathbf{M}\mathbf{M}\mathbf{v}_j+\mathbf{M}\sum_{i=1}^{4}\varepsilon_{ij}\mathbf{v}_i\simeq\lambda_j\mathbf{v}_j+\Delta\lambda_j\mathbf{v}_j+\lambda_j\sum_{i=1}^{4}\varepsilon_{ij}\mathbf{v}_i$

$$\Delta\mathbf{M}\mathbf{M}\mathbf{v}_j+\sum_{i=1}^{4}\lambda_i\varepsilon_{ij}\mathbf{v}_i\simeq\Delta\lambda_j\mathbf{v}_j+\lambda_j\sum_{i=1}^{4}\varepsilon_{ij}\mathbf{v}_i \;\Rightarrow\; \sum_{i=1}^{4}\left(\lambda_i-\lambda_j\right)\varepsilon_{ij}\mathbf{v}_i\simeq\left(\Delta\lambda_j\mathbf{I}-\Delta\mathbf{M}\mathbf{M}\right)\mathbf{v}_j$$

Perturbation Theory (2)

- introducing matrix $\mathbf{V}_p = \left[\mathbf{v}_1 \quad \mathbf{v}_1^* \quad \mathbf{v}_2 \quad \mathbf{v}_2^* \right]$ we rewrite it as 2 matrix eq.

$$\sum_{i=1}^{4} \left(\lambda_j - \lambda_i \right) \varepsilon_{ij} \mathbf{v}_i + \Delta\lambda_j \mathbf{v}_j = \mathbf{\Delta M M v}_j \quad \Rightarrow \quad \mathbf{V}_p \begin{bmatrix} 1 & 0 & 0 & 0 \\ 0 & \lambda_1 - \lambda_1^* & 0 & 0 \\ 0 & 0 & \lambda_1 - \lambda_2 & 0 \\ 0 & 0 & 0 & \lambda_1 - \lambda_2^* \end{bmatrix} \begin{bmatrix} \Delta\lambda_1 \\ \varepsilon_{21} \\ \varepsilon_{31} \\ \varepsilon_{41} \end{bmatrix} = \mathbf{\Delta M M v}_1 ,$$

$$\mathbf{V}_p \begin{bmatrix} \lambda_2 - \lambda_1 & 0 & 0 & 0 \\ 0 & \lambda_2 - \lambda_1^* & 0 & 0 \\ 0 & 0 & 1 & 0 \\ 0 & 0 & 0 & \lambda_2 - \lambda_2^* \end{bmatrix} \begin{bmatrix} \varepsilon_{12} \\ \varepsilon_{22} \\ \Delta\lambda_2 \\ \varepsilon_{42} \end{bmatrix} = \mathbf{\Delta M M v}_2 .$$

- Matrix $\mathbf{V}_p$ is built from symplectic vectors and its inverse is:

$$\mathbf{V}_p^{-1} = -\frac{1}{2i} \mathbf{U V}_p^T \mathbf{U}$$

$$\Rightarrow \quad \begin{bmatrix} \Delta\lambda_1 \\ \left(\lambda_1 - \lambda_1^* \right) \varepsilon_{21} \\ \left(\lambda_1 - \lambda_2 \right) \varepsilon_{31} \\ \left(\lambda_1 - \lambda_2^* \right) \varepsilon_{41} \end{bmatrix} = -\frac{1}{2i} \mathbf{U V}_p^T \mathbf{U \Delta M M v}_1 \quad \Rightarrow \quad \begin{cases} \Delta\lambda_1 = -\dfrac{\lambda_1}{2i} \ \mathbf{v}_1^+ \mathbf{U \Delta M v}_1 \\ \Delta\lambda_2 = -\dfrac{\lambda_2}{2i} \ \mathbf{v}_2^+ \mathbf{U \Delta M v}_2 \end{cases}$$

Perturbation Theory (3)

- Account relationship between eigenvalue corrections and tune shifts

$$\Delta Q_n = i/(4\pi)\left(\Delta\lambda_n/\lambda_n\right)$$

- That finally yields

$$\boxed{\begin{cases} \Delta Q_1 = -\dfrac{1}{4\pi}\mathbf{v}_1^{\;+}\mathbf{U}\,\boldsymbol{\Delta}\mathbf{M}\,\mathbf{v}_1 \\ \Delta Q_2 = -\dfrac{1}{4\pi}\mathbf{v}_2^{\;+}\mathbf{U}\,\boldsymbol{\Delta}\mathbf{M}\,\mathbf{v}_2 \end{cases}}$$

Linear Tune Shifts in Strongly Coupled Lattice

- Let us find tune shifts in strongly coupled lattice for a general case local focusing perturbation.
- Corresponding addition to Hamiltonian: $\Phi_x x^2 + 2\Phi_s xy + \Phi_y y^2$

$$\Rightarrow \quad \mathbf{\Delta M} = \begin{bmatrix} 0 & 0 & 0 & 0 \\ -\Phi_x & 0 & -\Phi_s & 0 \\ 0 & 0 & 0 & 0 \\ -\Phi_s & 0 & -\Phi_y & 0 \end{bmatrix}$$

- Substitution $\Delta\mathbf{M}$ to the tune shift equation and using the eigen-vector parameterization yields:

$$\Delta Q_1 = \frac{1}{4\pi}\left(\Phi_x \beta_{1x} + 2\Phi_s \sqrt{\beta_{1x}\beta_{1y}}\cos\nu_1 + \Phi_y \beta_{1y}\right),$$

$$\Delta Q_2 = \frac{1}{4\pi}\left(\Phi_x \beta_{2x} + 2\Phi_s \sqrt{\beta_{2x}\beta_{2y}}\cos\nu_2 + \Phi_y \beta_{2y}\right).$$

Limitations on the Focusing of Interaction Region Quads

Collider Type Optics

- High luminosity -> small beta in IP $\beta(s)=\beta^* + \dfrac{s^2}{\beta^*}$
- Detector requires long drift => very large β-function in IR quads

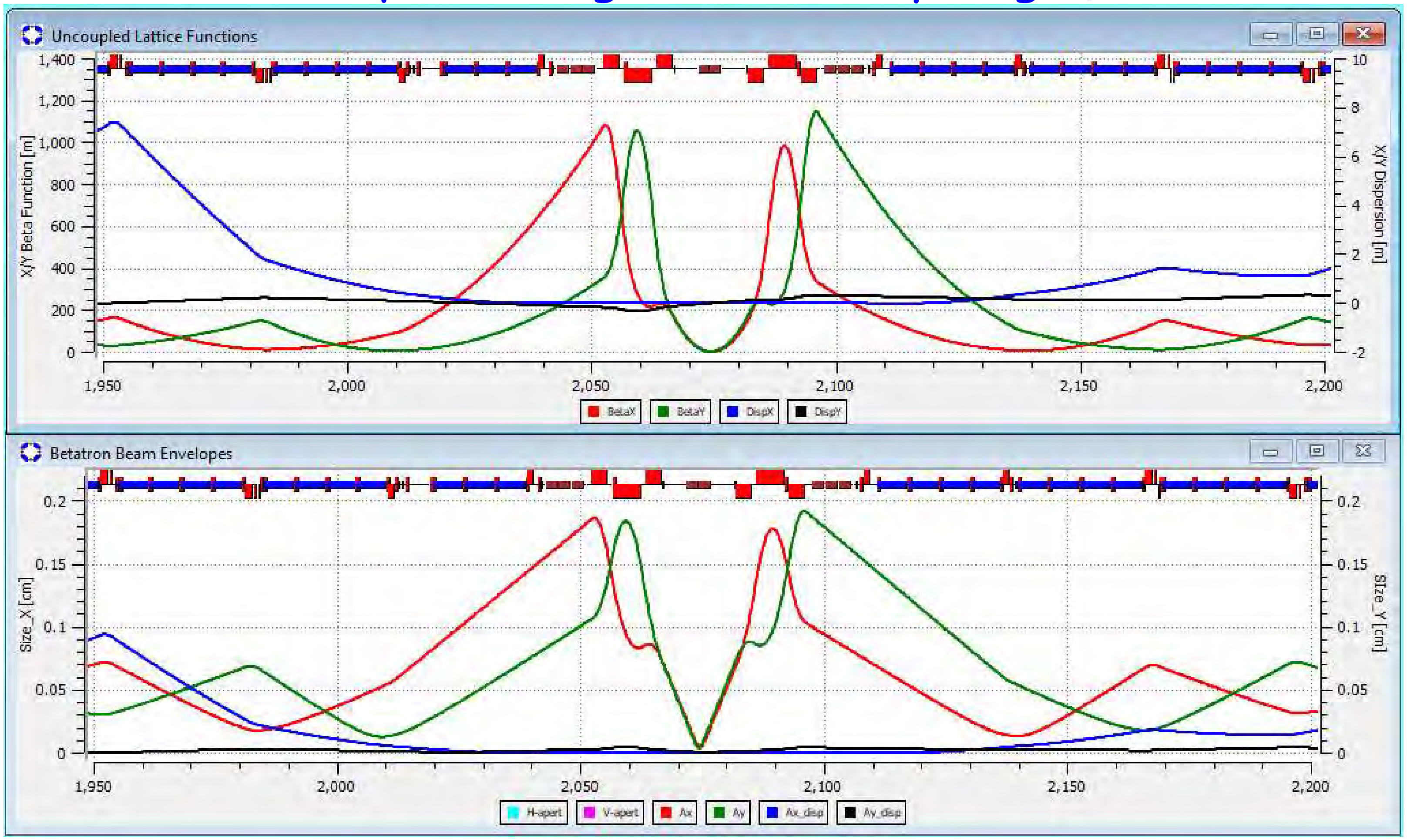

- Therefore, the IR quads introduce major limitation on ring focusing

Changes of Tune and β-function at Perturbation Location

- Consider a lattice with one local perturbation =>

$$M=\begin{bmatrix}1 & 0\\ -\Phi/2 & 1\end{bmatrix}\begin{bmatrix}c & s\beta\\ -s/\beta & c\end{bmatrix}\begin{bmatrix}1 & 0\\ -\Phi/2 & 1\end{bmatrix}=\begin{bmatrix}c-\Phi\beta s/2 & \beta s\\ -\Phi c-\left(1-\Phi^2\beta^2/4\right)s/\beta & c-\Phi\beta s/2\end{bmatrix}$$

On other hand: $M=\begin{bmatrix}c' & s'\beta'\\ -s'/\beta' & c'\end{bmatrix},\quad c'=\cos(\mu_0+\Delta\mu)\,,\quad s'=\sin(\mu_0+\Delta\mu)$

- Equalizing we obtain

$$\cos(\mu_0+\Delta\mu)=\cos\mu_0-\frac{\Phi\beta\sin\mu_0}{2},\quad \beta'=\frac{\beta}{\sqrt{1+\Phi\beta/\tan\mu_0-(\Phi\beta/2)^2}}$$

- For $\Phi > 0$ the stability is not lost above the half-integer resonance

It is used in KEKB

- Stability is lost when

$$\cos\mu_0-\frac{\Phi\beta\sin\mu_0}{2}=1\quad\Rightarrow$$

$$\Phi\beta=2\frac{\cos\mu_0-1}{\sin\mu_0}=-2\frac{2\sin^2(\mu_0/2)}{2\sin(\mu_0/2)\cos(\mu_0/2)}$$

i.e. the stop-band width

$$\boxed{\Phi\beta=-2\tan\left(\frac{\mu_0}{2}\right)}$$

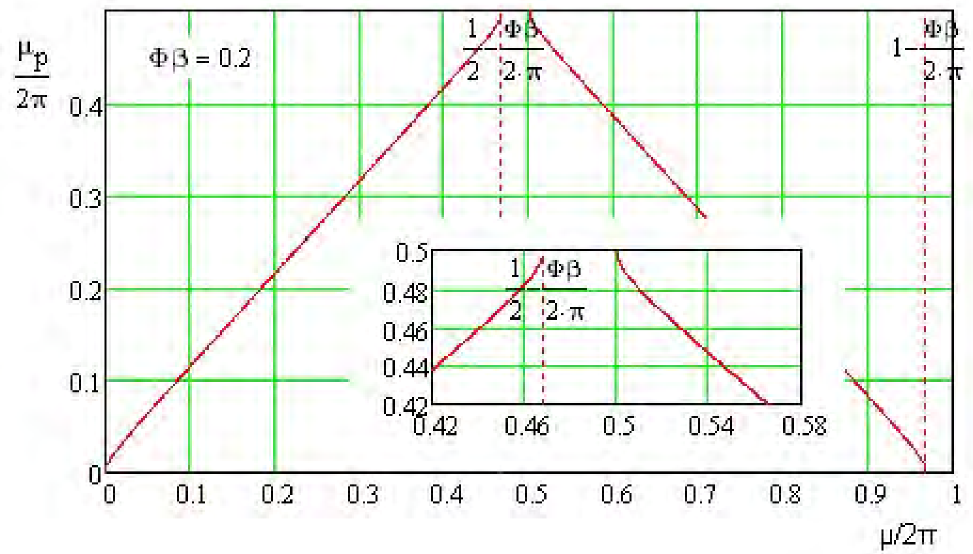

Changes of Tune and β-function in Linear Approximation

- In linear approximation

$$\boxed{\Delta\mu = \frac{1}{2}\Phi\beta} \qquad \frac{\beta'}{\beta} = 1 + \frac{\Phi\beta}{\tan\mu_0}$$

- Let's find the β-function perturbation for the rest of the ring

$$\hat{\beta}(\mu) \equiv \frac{\beta'}{\beta} = 1 + \Delta\beta\cos 2\mu$$

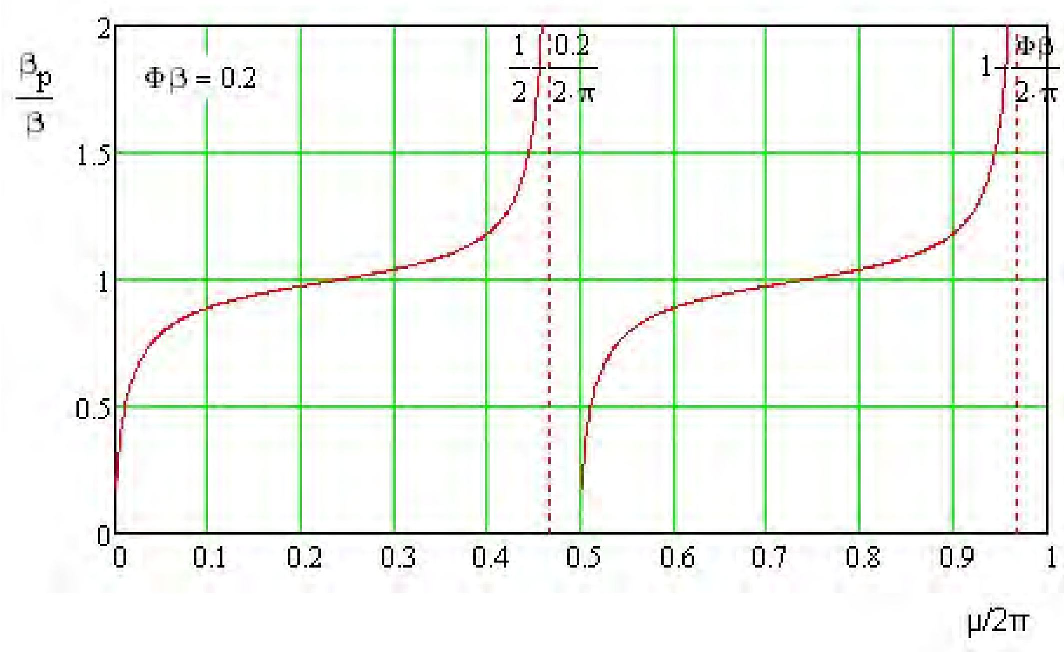

- Account that there is discontinuity at the perturbation location

$$\hat{\beta}(\mu) \equiv \frac{\beta'}{\beta} = 1 + \Delta\beta\cos(\mu_0 - 2\mu) \quad \Rightarrow \quad \hat{\beta}(0) = 1 + \Delta\beta\cos(\mu_0)$$

$$\hat{\beta}(\mu) = 1 + \frac{\Phi\beta}{\tan\mu_0}\frac{\cos(\mu_0 - 2\mu)}{\cos\mu_0}$$

$$\boxed{\hat{\beta}(\mu) = 1 + \frac{\Phi\beta}{\sin\mu_0}\cos(\mu_0 - 2\mu)}$$

Tune and β-function Chromaticities

- Change in momentum changes focusing $\Phi \equiv \frac{1}{F} = \frac{eGL}{pc}$ => $\frac{\Delta\Phi}{\Phi} \equiv -\frac{\Delta p}{p}$
- Chromaticity for point-like single perturbation

$$\Delta\nu = \frac{\Delta\mu}{2\pi} = \frac{1}{2\pi}\left(\frac{1}{2}\Delta\Phi\beta\right) = -\frac{\Phi\beta}{4\pi}\frac{\Delta p}{p}$$

- Summing for all perturbation sources we have: $\boxed{\xi \equiv p\frac{d\nu}{dp} = -\frac{1}{4\pi}\sum_k \Phi_p \beta_k}$
- Estimate for Tevatron collider

$$\xi = -\frac{1}{4\pi}\sum_k \Phi_p \beta_k \xrightarrow[\beta = L^2/\beta^*,\, 2\,\mathrm{IP\,quads}]{\Phi = 1/F = 1/L} -\frac{1}{4\pi}2\frac{1}{L}\frac{L^2}{\beta^*} = -\frac{1}{2\pi}\frac{L}{\beta^*} \xrightarrow{\text{Tevatron}} -\frac{1}{2\pi}\frac{30m}{30cm} \approx -15$$

Contribution of 2 IPs exceeds the ring natural chromaticity of ~20

- What can be more important is the chromaticity of β-functions
- For single quad: $\left.\frac{\Delta\beta}{\beta}\right|_{\max} = \frac{2\Delta\mu}{\sin\mu_0} = \frac{2\xi}{\sin\mu_0}\frac{\Delta p}{p}$

=> chromatic β: $\left. p\frac{d}{dp}\left(\frac{\Delta\beta}{\beta}\right)\right|_{\max} = \frac{2\xi}{\sin\mu_0} \xrightarrow{\mathit{Tevatron}} \approx \frac{2\cdot 7.5}{0.2} = 75$

- The chromaticity of β-functions is closely related to the 2nd order chromaticity. Affects beam-beam. Has to be suppressed.

Correction Tune and β-function Chromaticities

- Sextupoles are used for the correction: $B = \frac{1}{2} S x^2 \quad \Rightarrow \quad G_S\left(x_0\right) = S x_0$

$$\Delta\nu = \frac{\Delta\Phi\beta}{4\pi} = -\frac{1}{4\pi}\sum_k \beta_k \frac{eSL}{pc}\left(D\frac{\Delta p}{p}\right)$$

$$\Rightarrow \qquad \boxed{\xi = -\frac{e}{4\pi pc}\sum_k \beta_k D_k \left(SL\right)_k}$$

- Location of F and D sextupoles near F and D quads enables chromaticity correction for both planes
- For correction of chromatic β-function sextupoles located at "right" phases are used

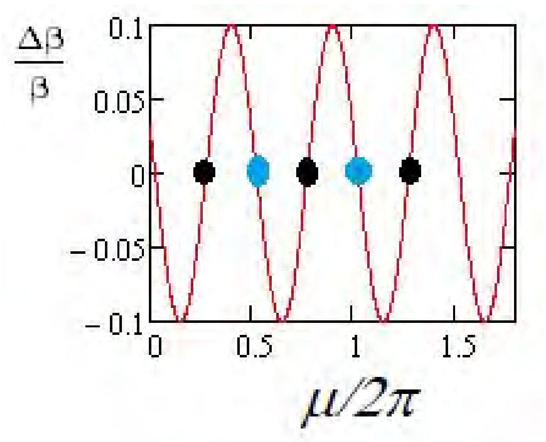

Correction Tune and β-function Chromaticities at Tevatron

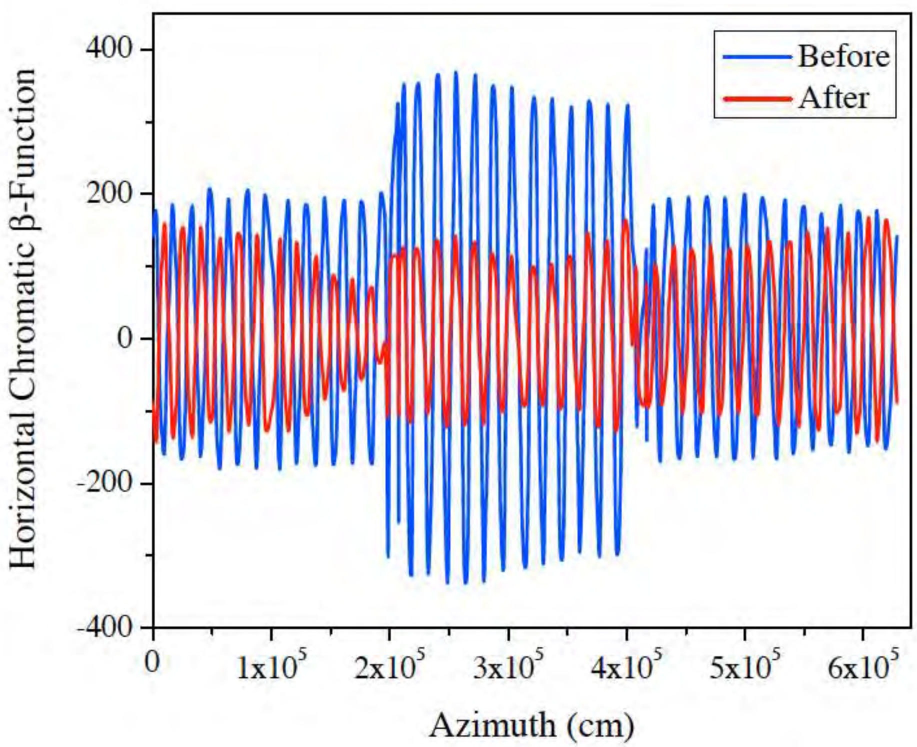

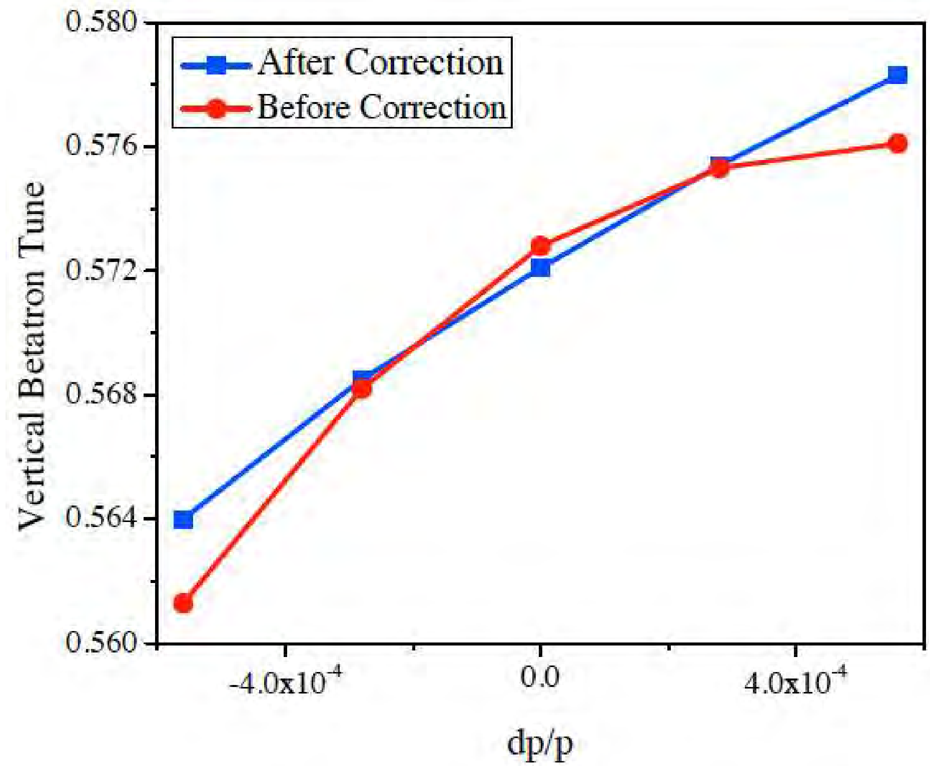

Horizontal chromatic beta-function at the injection energy. Blue line is for the original sextupole configuration, red - for the proposed correction

Dependence of the vertical betatron tune on particle momentum in the collider mode.

How OptiMX Computes Betatron Tune Shifts

- All nonlinearities are described by zero length multipoles
- The closed orbit can be excited by dipole correctors
- In Reference Orbit mode program finds new CO by iterations with accounting all non-linearities. Then it builds new lattice where feeddown from high order multipoles are accounted.
  - Consequently, in linear optics calculations all corrections to optics are correctly accounted.
- In View4D|Chromaticity this procedure is produced automatically on a number of momentum offsets. That yields dependence of mode tunes on momentum

  ⇨Linear and non-linear chromaticities

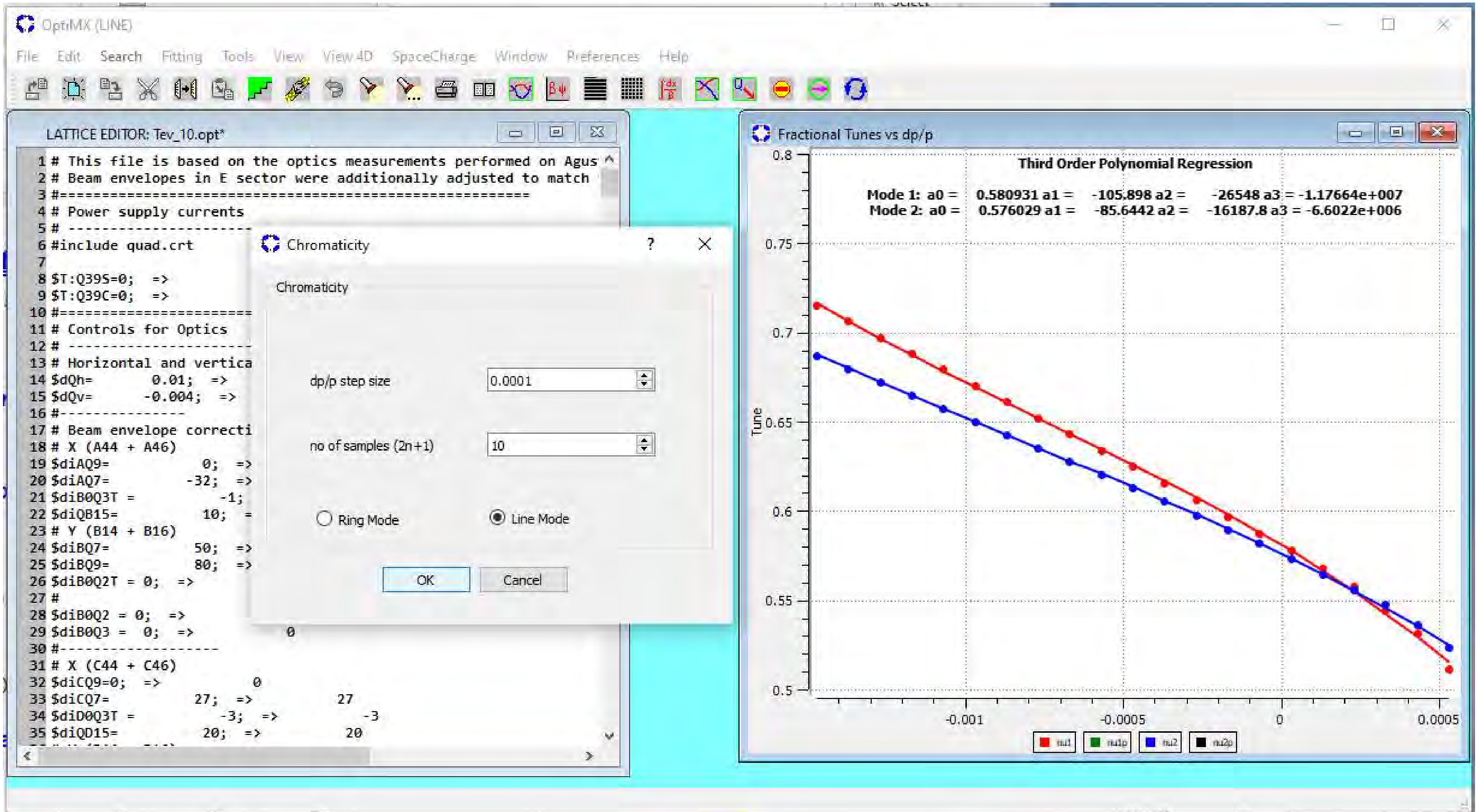
OptiMX (LINE)
File Edit Search Fitting Tools View View 4D SpaceCharge Window Preferences Help
LATTICE EDITOR: Tev_10.opt*
1 # This file is based on the optics measurements performed on Agus
2 # Beam envelopes in E sector were additionally adjusted to match
3 #===
4 # Power supply currents
5 # ----------------------
6 #include quad.crt
7
8 $T:Q39S=0; =>
9 $T:Q39C=0; =>
10 #======================
11 # Controls for Optics
12 # ----------------------
13 # Horizontal and vertica
14 $dQh= 0.01; =>
15 $dQv= -0.004; =>
16 #---------------
17 # Beam envelope correcti
18 # X (A44 + A46)
19 $diAQ9= 0; =>
20 $diAQ7= -32; =>
21 $diB0Q3T = -1;
22 $diQB15= 10; =
23 # Y (B14 + B16)
24 $diBQ7= 50; =>
25 $diBQ9= 80; =>
26 $diB0Q2T = 0; =>
27 #
28 $diB0Q2 = 0; =>
29 $diB0Q3 = 0; => 0
30 #-------------------
31 # X (C44 + C46)
32 $diCQ9=0; => 0
33 $diCQ7= 27; => 27
34 $diD0Q3T = -3; => -3
35 $diQD15= 20; => 20
Chromaticity
Chromaticity
dp/p step size 0.0001
no of samples (2n+1) 10
Ring Mode
Line Mode
OK
Cancel
Fractional Tunes vs dp/p
Third Order Polynomial Regression
Mode 1: a0 = 0.580931 a1 = -105.898 a2 = -26548 a3 = -1.17664e+007
Mode 2: a0 = 0.576029 a1 = -85.6442 a2 = -16187.8 a3 = -6.6022e+006
Tune
0.8
0.75
0.7
0.65
0.6
0.55
0.5
-0.001
-0.0005
0
0.0005
nu1
nu1p
nu2
nu2p

References

- “Accelerator Physics at the Tevatron Collider”, edited by V. Lebedev and V. Shiltsev, Springer, 2014.

Problems

1. Using symplecticity condition prove that for the 4x4 matrix written through 2x2 matrices as $\begin{bmatrix} P & p \\ q & Q \end{bmatrix}$ the following is correct:
   $\det(P)+\det(p)=\det(Q)+\det(q)=1$ and $\det(P)=\det(Q), \det(p)=\det(q)$
2. Using software for analytical computations prove that for a ring without RF
   $$\begin{cases} M_{16}=D(1-M_{11})-D'M_{12} \\ M_{26}=-M_{21}D+D'(1-M_{22}) \end{cases} \quad \begin{cases} M_{51}=DM_{21}+D'\left(1-M_{11}\right) \\ M_{52}=-D(1-M_{22})-D'M_{12} \end{cases}$$
3. Prove that for matrix built from symplectic eigen-vectors, $\mathbf{V}_p=\left[\mathbf{v}_1 \quad \mathbf{v}_1^* \quad \mathbf{v}_2 \quad \mathbf{v}_2^*\right]$, the following is correct:
   $$\mathbf{V}_p^{-1}=-\frac{1}{2i}\mathbf{U}\mathbf{V}_p^{\,T}\mathbf{U}$$
4. Restore missed calculations in computation of tune shifts in strongly coupled optics
   $$\Delta Q_1=\frac{1}{4\pi}\left(\Phi_x\beta_{1x}+2\Phi_s\sqrt{\beta_{1x}\beta_{1y}}\cos\nu_1+\Phi_y\beta_{1y}\right),$$
   $$\Delta Q_2=\frac{1}{4\pi}\left(\Phi_x\beta_{2x}+2\Phi_s\sqrt{\beta_{2x}\beta_{2y}}\cos\nu_2+\Phi_y\beta_{2y}\right).$$

Lectures 5&6: Non-Linearity in Quad Focusing and Optics Measurements

Valeri Lebedev
JINR & Fermilab

US Particle Accelerator School
February 2022

U.S. DEPARTMENT OF ENERGY

Fermilab

Objectives

- Large value of β-function in IR quadrupoles greatly increases effects of their non-linear fields
- Optics correction based on accurate optics measurements is extremely important for maximizing collider luminosity
- In this lecture we consider
  - aberrations in quadrupole focusing
  - and methods of linear optics measurements

Intrinsic Nonlinearity in Quadrupole Focusing

Magnetic Field of a Quadrupole

- Magnetic field
  - If there are no currents in the aria the magnetic field can be described by scalar potential: $B = -\nabla \varphi$
  - For quadrupole, in the first approximation, we can write:

$$\varphi = -G(s)xy + \frac{x^3 y + xy^3}{12}\frac{d^2 G}{ds^2} + \ldots$$

$$\Delta\varphi = -\frac{d^2 G}{ds^2}xy + xy\frac{d^2 G}{ds^2} + \frac{x^3 y + xy^3}{12}\frac{d^4 G}{ds^2} + \ldots = \frac{x^3 y + xy^3}{12}\frac{d^4 G}{ds^4} + \ldots \approx 0$$

$$\Rightarrow \quad \begin{bmatrix} B_x \\ B_y \\ B_z \end{bmatrix} = G(s)\begin{bmatrix} y \\ x \\ 0 \end{bmatrix} + \frac{1}{12}\begin{bmatrix} -G_{ss}\left(3x^2 y + y^3\right) \\ -G_{ss}\left(x^3 + 3xy^2\right) \\ 12 G_s xy \end{bmatrix} + \ldots, \quad G_s \equiv \frac{dG}{ds}, \quad G_{ss} \equiv \frac{d^2 G}{ds^2}$$

Equations of Motion

- Equations of motion

$$\frac{d}{dt}\begin{bmatrix} p_x \\ p_y \end{bmatrix} = \frac{e}{c}\begin{bmatrix} \mathrm{v}_y B_z - \mathrm{v}_z B_y \\ \mathrm{v}_z B_x - \mathrm{v}_x B_z \end{bmatrix}$$

Transit from t to z:

$$\frac{d}{dt}\begin{bmatrix} p_x \\ p_y \end{bmatrix} = p_0 \mathrm{v}_z \frac{d}{dz}\begin{bmatrix} \dfrac{dx}{ds} \\ \dfrac{dy}{ds} \end{bmatrix} = p_0 \mathrm{v}_z \frac{d}{dz}\begin{bmatrix} \dfrac{1}{\sqrt{1+(dx/dz)^2+(dy/dz)^2}}\dfrac{dx}{dz} \\ \dfrac{1}{\sqrt{1+(dx/dz)^2+(dy/dz)^2}}\dfrac{dy}{dz} \end{bmatrix}$$

- Finally, we obtain

$$\frac{d}{dz}\left(\frac{1}{\sqrt{1+\theta_x{}^2+\theta_y{}^2}}\begin{bmatrix} dx/dz \\ dy/dz \end{bmatrix}\right) = \frac{1}{\sqrt{1-\theta_x{}^2-\theta_y{}^2}}\frac{e}{p_0 \mathrm{v}_0 c}\begin{bmatrix} \theta_y B_z - \theta_z B_y \\ \theta_z B_x - \theta_x B_z \end{bmatrix}, \quad \theta_x \equiv \frac{dx}{dz}, \quad \theta_y \equiv \frac{dy}{dz}$$

Equations of Motion in the Quadrupole Body

- $B_z = 0$ in the body

  ⇨

$$\frac{d}{dt}\begin{bmatrix} p_x \\ p_y \end{bmatrix} = \frac{e}{c}\begin{bmatrix} -\mathrm{v}_z B_y \\ \mathrm{v}_z B_x \end{bmatrix} \Rightarrow \frac{d}{dz}\begin{bmatrix} p_0\left(dx/ds\right) \\ p_0\left(dy/ds\right) \end{bmatrix} = \frac{e}{c}\begin{bmatrix} -B_y \\ B_x \end{bmatrix}$$

$$\Rightarrow \frac{d}{dz}\left(\frac{dz}{ds}\frac{d}{dz}\begin{bmatrix} x \\ y \end{bmatrix}\right) = \frac{eG}{cp_0}\begin{bmatrix} -x \\ y \end{bmatrix}$$

$$\Rightarrow \frac{d}{dz}\left(\left(1+\left(\frac{dx}{dz}\right)^2+\left(\frac{dy}{dz}\right)^2\right)^{-1/2}\frac{d}{dz}\begin{bmatrix} x \\ y \end{bmatrix}\right) = k_0\begin{bmatrix} -x \\ y \end{bmatrix}$$

where we accounted that p_0 is not changed in magnetic field

- ♦ Not quite linear motion!!!

Edge Focusing in a Quadrupole

- Length of quad edge is short. => We can neglect other aberrations

$$\frac{d^2}{dz^2}\begin{bmatrix} x \\ y \end{bmatrix} = \frac{e}{p_0 v_0 c}\begin{bmatrix} -B_y + \theta_y B_z \\ B_x - \theta_x B_z \end{bmatrix} = k\begin{bmatrix} -x \\ y \end{bmatrix} + \frac{k_{ss}}{12}\begin{bmatrix} x^3 + 3xy^2 \\ -\left(3x^2 y + y^3\right) \end{bmatrix} + k_s xy\begin{bmatrix} \theta_y \\ -\theta_x \end{bmatrix}$$

where $k = \dfrac{eG}{p_0 v_0 c},\ k_s = \dfrac{dk}{dz},\ k_{ss} = \dfrac{d^2 k}{dz^2}$

- The angular kick from the edge

$$\delta\theta_x \equiv \Delta\left(\frac{dx}{ds}\right) = \frac{1}{12}\int k_{ss}\left(x^3 + 3xy^2\right)dz + \int k_s xy \frac{dy}{dz} dz\ , \quad x(z) \equiv x,\ y(z) \equiv y$$

- We approximate edge focusing at quad entrance $k(z) = k_0 \Theta(z),\ k_s = k_0 \delta(z)$, and trajectory $x(z) = x + \theta_x z,\ y(z) = y + \theta_y z$. Then

$$\delta\theta_x = -\frac{1}{12}\int k_s \frac{d}{dz}\left(\left(x + \theta_x z\right)^3 + 3\left(x + \theta_x z\right)\left(y + \theta_y z\right)^2\right)dz + \int k_s xy\theta_y dz$$

$$= -\frac{k_0}{12}\int \delta(z)\left(3\left(x + \theta_x z\right)^2 \theta_x + 3\theta_x\left(y + \theta_y z\right)^2 + 6\left(x + \theta_x z\right)\left(y + \theta_y z\right)\theta_y - 12xy\theta_y\right)dz$$

$$= -\frac{k_0}{12}\left(3x^2\theta_x + 3\theta_x y^2 + 6xy\theta_y - 12xy\theta_y\right) = \frac{k_0}{4}\left(2xy\theta_y - \left(x^2 + y^2\right)\theta_x\right)$$

The sign of expression is changed at the quad exit

Edge Focusing for a thin Quadrupole

- Angular kick from the input edge (from prev. slide)

$$\delta\theta_x = \frac{k_0}{4}\left(2xy\theta_y - \left(x^2+y^2\right)\theta_x\right)$$

- Assume that input and output coordinates coincide then

$$\Delta\theta_x = -k_0 L_q x = -\frac{x}{F_x}$$

$$\delta\theta_x = \frac{k_0}{4}\left(2xy\theta_{1y} - \left(x^2+y^2\right)\theta_{1x}\right) - \frac{k_0}{4}\left(2xy\theta_{2y} - \left(x^2+y^2\right)\theta_{2x}\right)$$

- Accounting that $\theta_{2x} - \theta_{1x} = -\dfrac{x}{F_x}, \quad \theta_{2y} - \theta_{1y} = \dfrac{x}{F_x}$ we obtain

$$\delta\theta_x = -\frac{k_0}{4}\left(2xy\frac{y}{F_x} + \left(x^2+y^2\right)\frac{x}{F_x}\right) = -\frac{k_0}{4F_x}\left(x^3+3xy^2\right)$$

$$\boxed{\frac{\delta F_x}{F_x} = \frac{\delta\theta_x}{\Delta\theta_x} = \frac{x^2+3y^2}{4F_x L_q}}$$

- Note that this cannot be easy compensated by octupoles

$$\Delta\theta_x \propto G_o\left(x^3 - 3xy^2\right) \quad \text{scalar potential} \quad \varphi \propto \frac{G_o}{12}\left(x^4 - 6x^2y^2 + y^4\right)$$

Simulations of Edge Focusing for Thin Quadrupole

- In simulations in addition to the angle change we need additional to account for a coordinate change

$$\frac{d^2}{dz^2}\begin{bmatrix} x \\ y \end{bmatrix} = \frac{e}{p_0 v_0 c}\begin{bmatrix} -B_y + \theta_y B_z \\ B_x - \theta_x B_z \end{bmatrix} = k\begin{bmatrix} -x \\ y \end{bmatrix} + \frac{k_{ss}}{12}\begin{bmatrix} x^3 + 3xy^2 \\ -\left(3x^2 y + y^3\right) \end{bmatrix} + k_s xy\begin{bmatrix} \theta_y \\ -\theta_x \end{bmatrix}$$

$$\delta x = \int_{-\infty}^{\infty} dz \int_{-\infty}^{z} \left(\frac{k_{ss}}{12}\left(x^3 + 3xy^2\right) + k_s xy \frac{dy}{dz} \right) dz'$$

⇨

$$= \int_{-\infty}^{\infty} dz \left(\frac{k_s}{12}\left(x^3 + 3xy^2\right) + \int_{-\infty}^{z} \left(k_s xy \frac{dy}{dz} - \frac{k_s}{12}\frac{d}{dz'}\left(x^3 + 3xy^2\right) \right) dz' \right)$$

- Only first 2 terms make non-zero contribution =>

$$\boxed{\delta x = \frac{k_0}{12}\left(x^3 + 3xy^2\right)}$$

Recollect that

$$\boxed{\delta\theta_x = \frac{k_0}{4}\left(2xy\theta_y - \left(x^2 + y^2\right)\theta_x\right)}$$

- MADX and OptiMX account this non-linear correction in their tracking routines

Simple Estimates for IR quads

- Comparison with non-linearity coming from the quad body
  - For the body (B_z=0) in the 1st order

$$\frac{d}{dz}\left(\frac{1}{\sqrt{1+\theta_x^2+\theta_y^2}}\frac{d}{dz}\begin{bmatrix} x \\ y \end{bmatrix}\right) = k_0 \begin{bmatrix} -x \\ y \end{bmatrix} \quad \Rightarrow \quad \Delta\theta_x = -k_0 \int \sqrt{1+\theta_x^2+\theta_y^2}\, x(z)dz \approx \left(1+\frac{\overline{\theta_\perp^2}}{2}\right)\Delta\theta_{x0}$$

For IR quad: $\Delta\theta_{x0} = \sqrt{\varepsilon/\beta^*}$, $\overline{\Delta\theta_\perp^2} \approx \varepsilon/(2\beta^*)$ => $\dfrac{\Delta F}{F} \approx \dfrac{\varepsilon}{2\beta^*}(1)$

  - For edge focusing

$$\frac{\delta F}{F} \approx \frac{x^2}{FL_q} = \frac{\left(F\sqrt{\varepsilon/\beta^*}\right)^2}{FL_q} = \frac{\varepsilon}{\beta^*}\left(\frac{F}{L_q}\right)$$

- As one can see the aberrations of the IR quads due to edge focusing exceed the body aberrations by ~2F/Lq or by ~10 times
- The tune shift due to edge focusing (one quad):

$$\Delta\nu = \frac{1}{4\pi}\delta\Phi\beta \xrightarrow{\delta\Phi\approx x^2/(4F^2L_q)} \frac{1}{4\pi}\frac{x^2}{4F^2L_q}\beta \xrightarrow{\beta=F^2/\beta^*} \frac{x^2}{16\pi\beta^* L_q}$$

For x=8 cm, β^*=10 cm, L_q=80 cm => $\Delta\nu \sim 1.5\cdot 10^{-3}$ (per quad)

Optics Measurements

Why do we need optics measurements?

- Linear optics measurements play an important role for improvement of collider performance.
- Accurate knowledge of the rings and transfer lines optics results in
  - significant reduction of the emittance growth for beam transfers
  - increases the acceptances of the rings and transfer lines
  - reduction of the beam loss at transfers and other operations
- A number of methods and software tools were developed to streamline the process of data acquisition, processing and analysis.
  - Differential orbits
  - LOCO (Linear Optics from Closed Orbit) (uses SVD)
  - Dipole kicks
  - The AC dipole (adiabatic excitation near betatron sideband)
- What makes accurate optics measurements difficult
  - Difference in differential response of BPMs
  - Inaccuracy of calibrations of dipole correctors
  - Rolls of BPMs and correctors
  - Getting accurate data for transfer lines takes much longer time and typically has much smaller accuracy

Differential Orbits

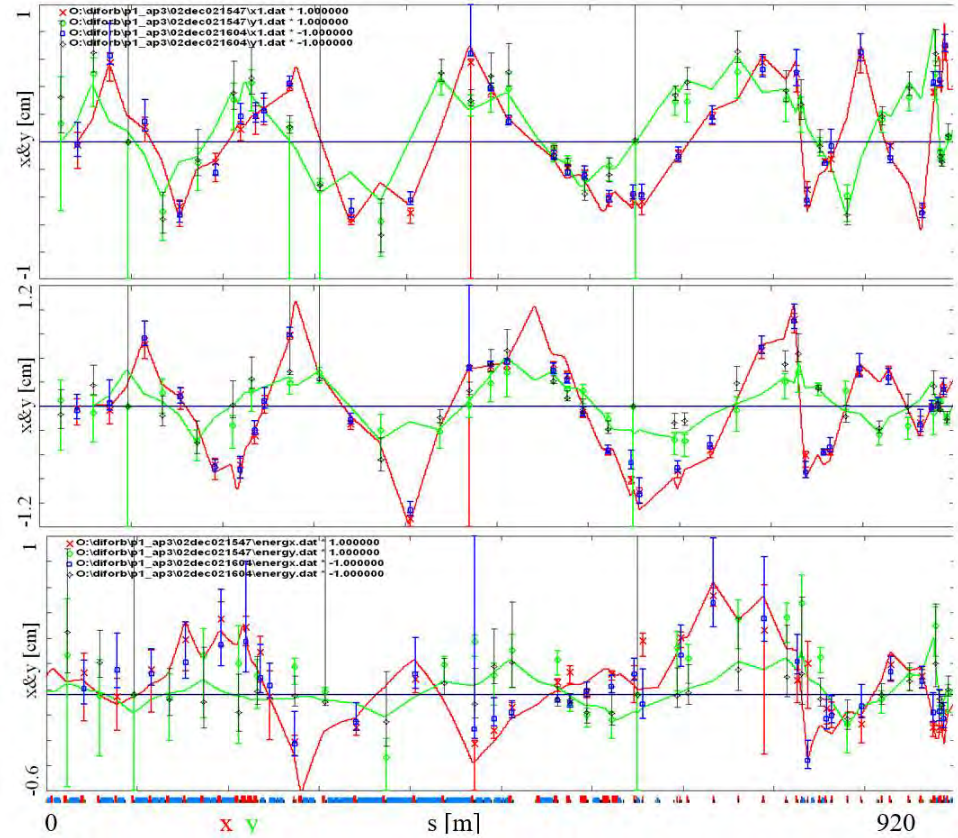

- In minimal configuration one uses:
  - All BPMs
  - Excites differential orbits with 4 correctors (2 in each plane) and beam energy change
  - Each plane correctors are shifted in betatron phase by ~90° (45-135°)
- Optics model has pseudo-quadrupoles which values are adjusted to match measurements and the model
- Typically, analysis is done manually due to an absence of redundancy in data
  - BPMs with large differential response are less trustable due to unknown differential response
  - Measurements with energy change are extremely helpful to get to a trustable result
- Measured optics is corrected & new measurements are done to verify

Optics Match at Transfers

- Typically, optics correction accuracy in a transfer line is not sufficient to prevent the emittance growth at transfers and additional correction is required
- Effective method is based on the turn-by-turn beam size measurements
  - Two possibilities
    - Ionization profile monitor
    - Quad BPM (tried by many but to my knowledge never was used as a regular means for optics correction)
- Effective way to correct the final mismatch is based on orthogonal quads
  - Two F and two D quads installed at locations with large difference in x and y β-functions
  - Each couple is shifted in betatron phase by $(45+n\cdot 90)^o$

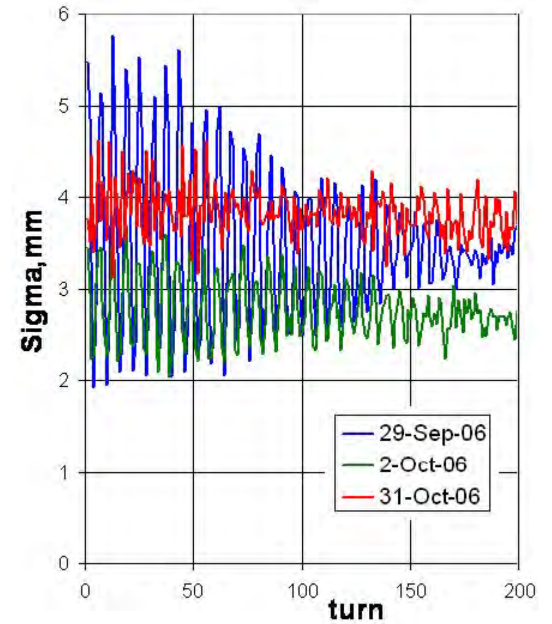

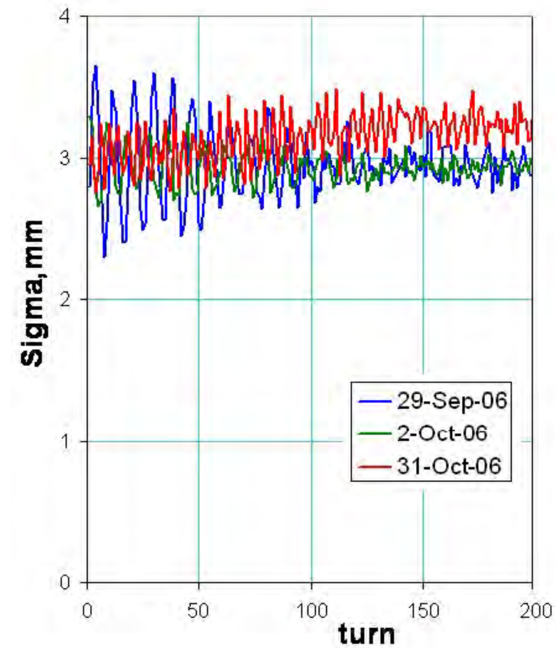

LOCO (Linear Optics from Closed Orbit)

- The data analysis for differential orbit measurements described above was tedious and the results still were not sufficiently accurate
- This can be addressed by LOCO
  - LOCO is an extension of differential orbit method to many correctors
- A usage of very large number of dipole correctors (ideally all of them) delivers redundancy enabling to resolve degeneracy in the solution
- Typically, the unknown values include:
  - Differential responses of BPMs
  - Corrections to kick values of correctors
  - Rolls of BPMs and correctors
  - Values of pseudo-quads and skew-quads
- Single Value Decomposition (SVD) algorithm was used to find unknowns

LOCO at Tevatron

- For Tevatron an acquisition of the full response matrix required approximately 2 hours of beam time. However, it was determined that a good quality fit could be obtained with a smaller data set, and in normal operations the response matrix was measured using 60 correctors, which took less than one hour.
- The dispersion measurement was done by scanning the RF frequency, measuring orbit at five points and fitting a straight line at each BPM. It resulted in an improvement of measurement accuracy
- Typically, the SVD cutoff was ~1
- Significant improvement was achieved after upgrade of BPMs
  - Smaller noise, more uniform differential responese

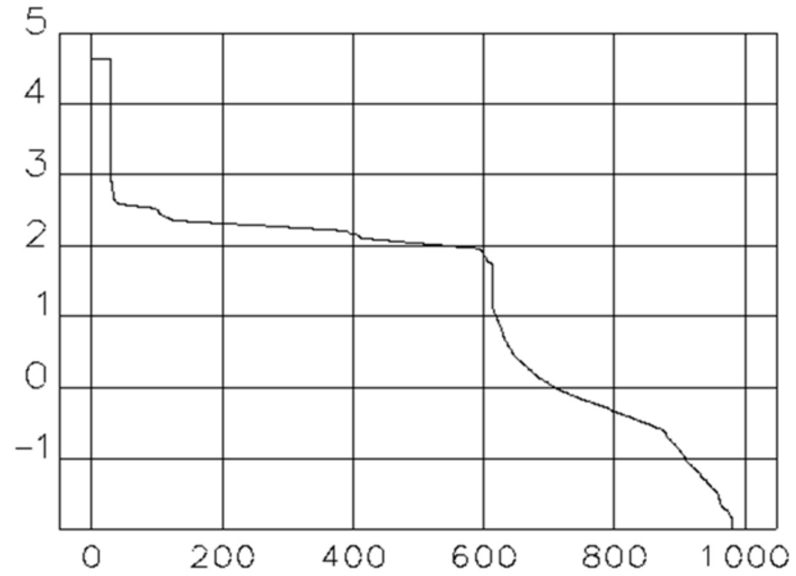

Singular values (logarithmic scale) of the Tevatron response matrix derivative

LOCO at Tevatron (2)

Relative quadrupole errors in final focus

Name	Gradient Error (10^{-3})
B0Q3	-11.18
B0Q2	-1.87
B0Q3D	-0.09
B0Q3F	-0.47
D0Q3	-9.49
D0Q2	-0.83
D0Q3F	0.24
D0Q3F	-1.84

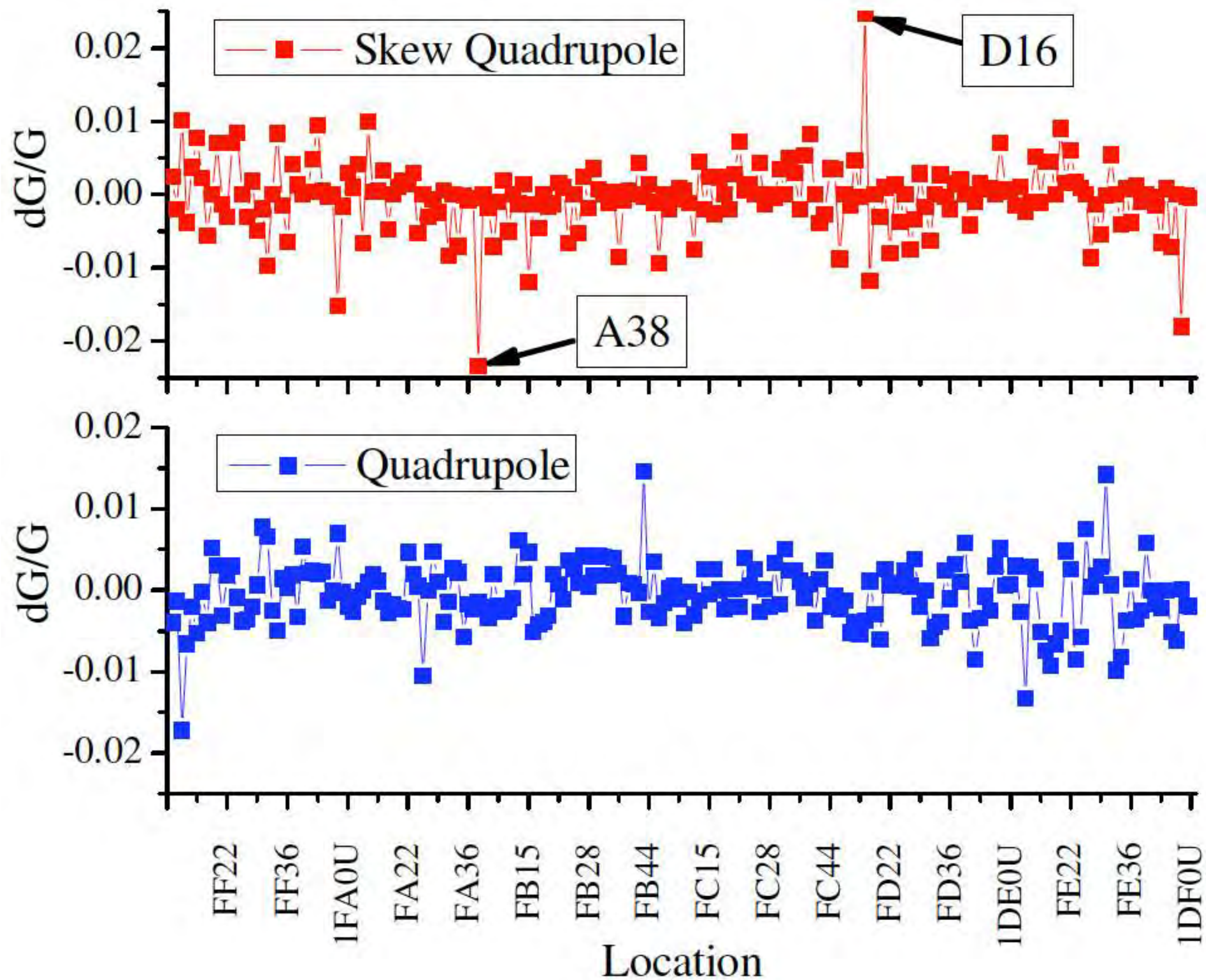

Measured relative quadrupole and skew-quadrupole errors

Dipole Kicks

- If BPMs can measure the turn-by-turn data then optics measurements can be performed with dipole kicks
- There are 6 independent signals present in each BPM turn-by-turn data. They are: sin and cos parts of 2 betatron and synchrotron mode
- The independent component analysis enables to find the form of each signal and their amplitudes at each BPM
  - ⇨ Beta-functions and betatron phase advances at each BPM

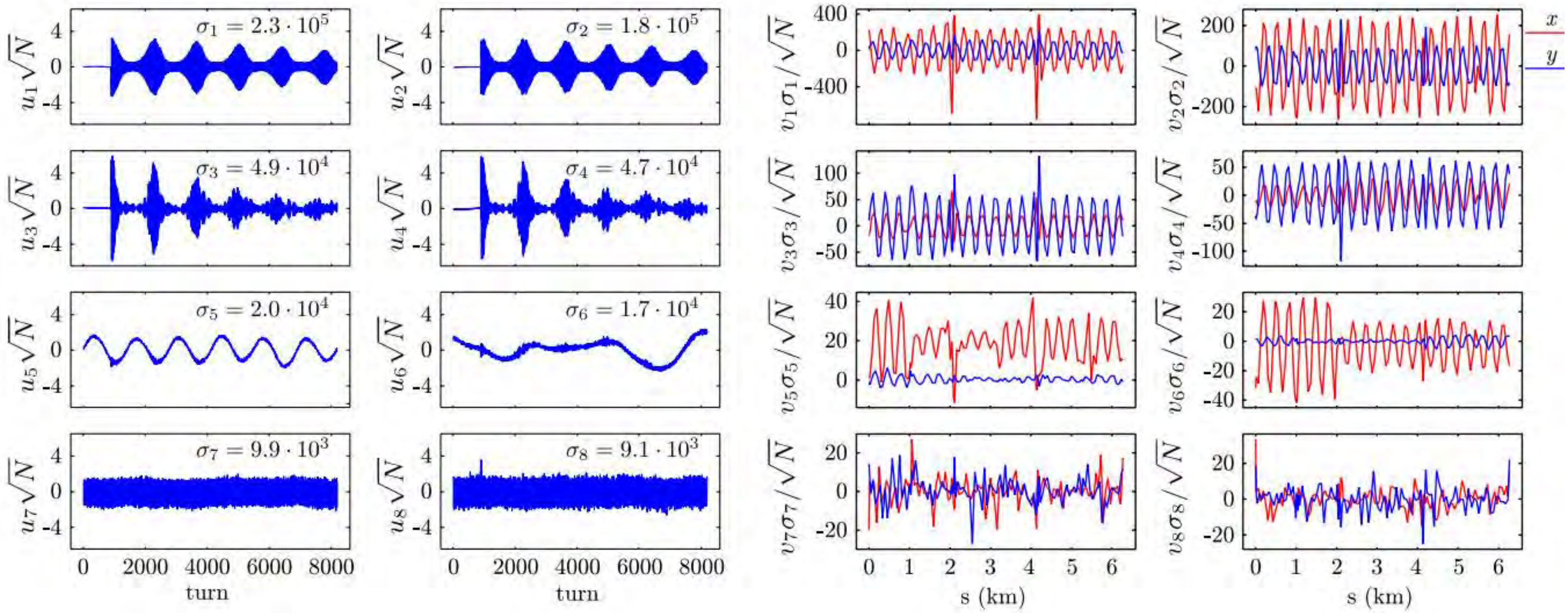

Temporal (left) and spatial (right) modes of MIA corresponding to the largest eight singular values

The AC Dipole (Adiabatic Excitation near Betatron Sideband)

- The measurements with dipole kick have a problem:
  - Each kick increases the beam emittance making the beam unusable after a few kicks
- The way to overcame this problem is to excite the betatron motion with adiabatic excitation of transverse beam motion near a betatron sideband
  - This is the way how the optics measurements are done at the LHC
- A successful usage of this measurement requires high accuracy BPMs with turn-by-turn capabilities
  - Sophisticated algorithms for data processing were used to measure beta-functions to ~1% at the LHC

Requirements for the Betatron Match at Transfers

- Express particle position at ring through eigen-vectors of the ring

$$\mathbf{x} = \frac{1}{2}\left(\sqrt{2\varepsilon_1}e^{i\psi_1}\mathbf{v}_1' + \sqrt{2\varepsilon_2}e^{i\psi_2}\mathbf{v}_2' + CC\right)$$

- Using symplectic orthogonality

$$\mathbf{v}_1'^{+}\mathbf{U}\mathbf{x} = \frac{1}{2}\left(\sqrt{2\varepsilon_1}e^{i\psi_1}\mathbf{v}_1'^{+}\mathbf{U}\mathbf{v}_1' + \sqrt{2\varepsilon_2}e^{i\psi_2}\mathbf{v}_1'^{+}\mathbf{U}\mathbf{v}_2 + \mathbf{v}_1'^{+}\mathbf{U}(CC)\right) = -i\sqrt{2\varepsilon_1}e^{i\psi_1}$$

$\Rightarrow$ $\varepsilon_1' = \frac{1}{2}\mathbf{x}^{+}\mathbf{U}^{+}\mathbf{v}_1'\mathbf{v}_1'^{+}\mathbf{U}\mathbf{x}$, $\varepsilon_2' = \frac{1}{2}\mathbf{x}^{+}\mathbf{U}^{+}\mathbf{v}_2'\mathbf{v}_2'^{+}\mathbf{U}\mathbf{x}$

- Now we need to average over all particles

$$\varepsilon_1' = \frac{1}{2}\int \mathbf{x}^{+}\mathbf{U}^{+}\mathbf{v}_1'\mathbf{v}_1'^{+}\mathbf{U}\mathbf{x}\left(\frac{1}{4\pi^2\varepsilon_1\varepsilon_2}\exp\left(-\frac{1}{2}\hat{\mathbf{x}}^T\hat{\boldsymbol{\Xi}}\hat{\mathbf{x}}\right)\right)d^4x \xrightarrow{\hat{\mathbf{y}}=\hat{\mathbf{V}}^{-1}\hat{\mathbf{x}}} \frac{1}{8\pi^2\varepsilon_1\varepsilon_2}\int \hat{\mathbf{y}}^{+}\hat{\mathbf{V}}^T\mathbf{U}^{+}\mathbf{v}_1'\mathbf{v}_1'^{+}\mathbf{U}\hat{\mathbf{V}}\hat{\mathbf{y}}\exp\left(-\frac{\hat{\mathbf{y}}^T\hat{\mathbf{V}}^T\hat{\boldsymbol{\Xi}}\hat{\mathbf{V}}\hat{\mathbf{y}}}{2}\right)d^4y$$

Account that: $\hat{\boldsymbol{\Xi}}_d \equiv diag(\varepsilon_1^{-1},\varepsilon_1^{-1},\varepsilon_2^{-1},\varepsilon_2^{-1},) = \hat{\mathbf{V}}^T\hat{\boldsymbol{\Xi}}\hat{\mathbf{V}}$

$\Rightarrow$

$$\varepsilon_1' = \frac{1}{8\pi^2\varepsilon_1\varepsilon_2}\int \hat{\mathbf{y}}^{+}\hat{\mathbf{V}}^T\mathbf{U}^{+}\mathbf{v}_1'\mathbf{v}_1'^{+}\mathbf{U}\hat{\mathbf{V}}\hat{\mathbf{y}}\exp\left(-\frac{\hat{\mathbf{y}}^T\hat{\boldsymbol{\Xi}}_d\hat{\mathbf{y}}}{2}\right)d^4y$$

$$= \frac{\left(\hat{\mathbf{V}}^T\mathbf{U}^{+}\mathbf{v}_1'\mathbf{v}_1'^{+}\mathbf{U}\hat{\mathbf{V}}\right)_{ij}}{8\pi^2\varepsilon_1\varepsilon_2}\int \hat{y}_j\hat{y}_i\exp\left(-\frac{y_1^2+y_2^2}{2\varepsilon_1}--\frac{y_3^2+y_4^2}{2\varepsilon_2}\right)d^4y = \frac{1}{2}\left(\hat{\mathbf{V}}^T\mathbf{U}^{+}\mathbf{v}_1'\mathbf{v}_1'^{+}\mathbf{U}\hat{\mathbf{V}}\right)_{ij}\left(diag(\varepsilon_1,\varepsilon_1,\varepsilon_2,\varepsilon_2)\right)_{ij}$$

Requirements for the Betatron Match (2)

$$\varepsilon_1' = \frac{1}{2}\left(\hat{\mathbf{V}}^T \mathbf{U}^+ \mathbf{v}_1' \mathbf{v}_1'^+ \mathbf{U}\hat{\mathbf{V}}\right)_{ij} \left(diag(\varepsilon_1, \varepsilon_1, \varepsilon_2, \varepsilon_2)\right)_{ij}$$

- For single dimensional measurement we have:

$$\mathbf{v} = \begin{bmatrix} \sqrt{\beta'} \\ -\frac{i+\alpha'}{\sqrt{\beta'}} \end{bmatrix}, \quad \mathbf{V} = \begin{bmatrix} \sqrt{\beta} & 0 \\ -\frac{\alpha}{\sqrt{\beta}} & \frac{1}{\sqrt{\beta}} \end{bmatrix}$$

- Substituting and performing calculations one obtains

$$\boxed{\varepsilon' = \frac{\varepsilon}{2}\left(\frac{\beta}{\beta'}\left[1+\alpha'^2\right] + \frac{\beta'}{\beta}\left[1+\alpha^2\right] - 2\alpha\alpha'\right)}$$

where β and α are the β- and α-functions for the incoming beam, and β' and α' are the β- and α-functions of circulating beam

- For small variations

$$\frac{\delta\varepsilon}{\varepsilon} \propto \frac{1}{2}\left(\frac{\delta\beta}{\beta}\right)^2$$

References

1. G.E. Lee-Whiting, “Third order aberrations of a magnetic quadrupole lens”, NIM-83, pp. 232-244
2. Etienne Forest, “Beam Dynamics - 1st Edition”, - Routledge Book, 1998
3. V. Sajaev, L. Emery, in Proceeding of EPAC’02, (Paris, France, 2002) 742
4. A. V. Petrenko, A. A. Valishev, and V. A. Lebedev, “Model-independent analysis of the Fermilab Tevatron turn-by-turn beam position monitor measurements”, Phys. Rev. ST Accel. Beams 14, 092801
5. T. Persson, et.al. “LHC optics commissioning: A journey towards 1% optics control”, Phys. Rev. Acc. and Beams 20, 061002 (2017)

Problems

1. Find equations describing transition through quad edge for the vertical degree of freedom
2. Obtain an expression for the emittance increase at transfers between two rings due to betatron and dispersion mismatches. First – no coupling, second - arbitrary x-y coupling and both dispersions (the answer in matrix form is sufficient for the latter)
3. Explain shape of temporal modes in Tevatron optics measurements with dipole kicks
4. *AC* dipole optics measurements use a point-like excitation of betatron motion. In normalized coordinates the beam equation of motion is:

$$\frac{dx^2}{d\tau^2} \equiv \left(\frac{\partial}{\partial \tau} + \frac{\partial}{\partial \mu}\right)\left(\frac{\partial}{\partial \tau} + \frac{\partial}{\partial \mu}\right) x + x = f_0 e^{i\omega t} \delta(\mu) \,, \quad \omega \approx 1$$

   Find dependence of beam position on time and position (μ).

Lectures 7&8 Emittance Growth due to Noise in RF and Magnets

Valeri Lebedev
JINR & Fermilab

US Particle Accelerator School
February 2022

Objectives

- In a collider the beam should stay for a long time
  ⇨ The growth rates for beam emittances and bunch length should be sufficiently small
- In a properly built machine the IBS typically dominates
- However, the RF noise, if not properly addressed, may result in unacceptably large longitudinal emittance growth
  - Proton bunches are long
    - Therefore, both the phase and amplitude noises are important
  - Additional complication originates from non-linearity of potential well. It is important for hadron beams which, typically, take large fraction of RF well.
- Similar to the longitudinal degree of freedom, noise in bending magnetic field and $\perp$ dampers leads to transverse emittance growth
  - Proton colliders have larger circumference => small revolution frequency => more susceptible to noise due to its fast growth with frequency decrease

Longitudinal Emittance Growth due to RF Noise

Equations of Longitudinal Motion

- In the absence of perturbations

$$\frac{d^2\varphi}{dt^2}+\Omega_s{}^2\sin\varphi=0\,,\quad \Omega_s{}^2=\frac{eV_0\eta q}{2\pi mc^2\gamma\beta^2}$$

- Fluctuations of RF phase and amplitude result in

$$\frac{d^2\varphi}{dt^2}+\Omega_s{}^2\left(1+\frac{\delta V(t)}{V_0}\right)\sin\left(\varphi-\psi(t)\right)=0\quad\xrightarrow[u(t)\equiv\delta V(t)/V_0]{\text{exp}ending}\quad\frac{d^2\varphi}{dt^2}+\Omega_s{}^2\sin\varphi=-\Omega_s{}^2\left(\sin(\varphi)u(t)+\cos(\varphi)\psi(t)\right)$$

- First, we consider the small amplitude (i.e.) linear motion and RF phase fluctuations. Then

$$\frac{d^2\varphi}{dt^2}+\Omega_s{}^2\varphi=-\Omega_s{}^2\psi(t)$$

The solution is well-known

$$\varphi(t)=-\Omega_s\int_0^t\psi(t')\sin\left(\Omega_s(t-t')\right)dt'$$

The rms particle deviation is

$$\overline{\varphi^2(t)}=\Omega_s{}^2\int_0^t\int_0^t\overline{\psi(t_1)\psi(t_2)}\sin\left(\Omega_s(t-t_1)\right)\sin\left(\Omega_s(t-t_2)\right)dt_1dt_2$$

Spectral Density and Correlation Function

- Correlation function

$$K(\tau)=\overline{\psi(t)\psi(t+\tau)} \quad \Rightarrow \quad K(t_1-t_2)=\overline{\psi(t_1)\psi(t_2)}$$

- Wiener-Khinchin theorem

$$\boxed{K(\tau)=\int_{-\infty}^{\infty}P(\omega)e^{i\omega\tau}d\omega\,, \quad P(\omega)=\frac{1}{2\pi}\int_{-\infty}^{\infty}K(\tau)e^{-i\omega\tau}dt}$$

$$\overline{\psi(t_1)\psi(t_2)}=K(t_1-t_2) \quad \Rightarrow \quad \overline{\psi^2}=K(0)=\int_{-\infty}^{\infty}P(\omega)d\omega$$

- Particle motion under random phase fluctuations

$$\overline{\varphi^2(t)}=\Omega_s{}^2\int_0^t\int_0^t\overline{\psi(t_1)\psi(t_2)}\sin\left(\Omega_s(t-t_1)\right)\sin\left(\Omega_s(t-t_2)\right)dt_1dt_2$$

$$=\Omega_s{}^2\int_0^t\int_0^t K_\psi(t_1-t_2)\sin\left(\Omega_s(t-t_1)\right)\sin\left(\Omega_s(t-t_2)\right)dt_1dt_2$$

Computation of integral

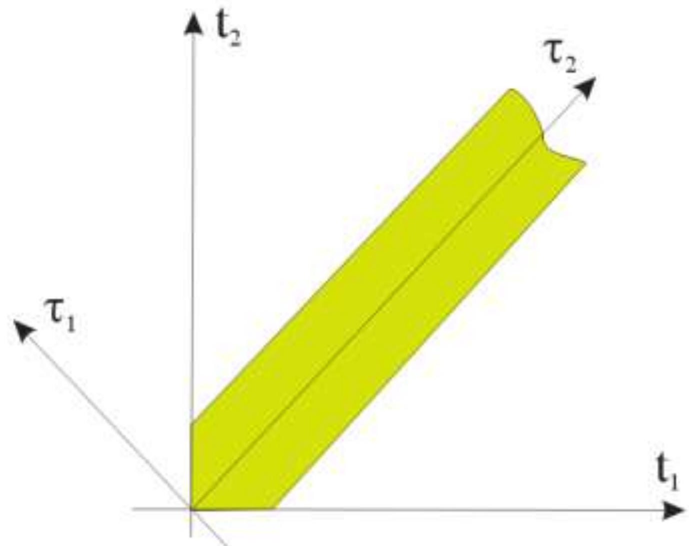

Make substitution $\begin{cases} \tau_1 = t_1 - t_2 \\ \tau_2 = t_1 + t_2 \end{cases} \qquad \begin{cases} t_1 = (\tau_1 + \tau_2)/2 \\ t_2 = (\tau_2 - \tau_1)/2 \end{cases}$

Corresponding Jacobian is:

$$\frac{\partial(t_1,t_2)}{\partial(\tau_1,\tau_2)} = \begin{bmatrix} 1/2 & 1/2 \\ -1/2 & 1/2 \end{bmatrix} = \frac{1}{2}$$

Then we have

$$\overline{\varphi^2(t)} = \Omega_s^{\,2} \int_0^t \int_0^t \overline{\psi(t_1)\psi(t_2)} \sin\left(\Omega_s (t-t_1)\right) \sin\left(\Omega_s (t-t_2)\right) dt_1 dt_2$$

$$= \Omega_s^{\,2} \int_0^t \int_0^t K_\psi(t_1-t_2) \left[\frac{\cos\left(\Omega_s (t_1-t_2)\right) + \cos\left(\Omega_s (2t-t_1-t_2)\right)}{2} \right] \left(\frac{1}{2}\right) dt_1 dt_2$$

$$\approx \frac{\Omega_s^{\,2}}{4} \int_{-\infty}^{\infty} d\tau_1 \int_0^{2t} K_\psi(\tau_1) \left[\cos\left(\Omega_s \tau_1\right) + \cos\left(\Omega_s (2t-\tau_2)\right)\right] d\tau_1 d\tau_2 \xrightarrow[\textit{oscillating term}]{\textit{drop fast}}$$

$$\approx \frac{\Omega_s^{\,2}}{2} t \int_{-\infty}^{\infty} K_\psi(\tau) \cos\left(\Omega_s \tau\right) d\tau$$

Recollecting connection between the correlation function and the spectral density we finally obtain: $\boxed{\dfrac{d}{dt}\overline{\varphi^2(t)} = \pi \Omega_s^{\,2} P_\psi(\Omega_s)}$

Bunch Lengthening due to Amplitude Noise

- Equation of motion for the small amplitude RF voltage fluctuations:

$$\frac{d^2\varphi}{dt^2} + \Omega_s{}^2\varphi = -\Omega_s{}^2\varphi u(t)$$

In perturbation theory we replace φ in RH side by $\varphi_0 \sin(\Omega_s t)$

$$\Rightarrow \quad \overline{\varphi^2(t)} \approx \Omega_s{}^2\varphi_0{}^2 \int_0^t \int_0^t \overline{u(t_1)u(t_2)} \sin(\Omega_s t_1) \sin(\Omega_s t_2) \sin(\Omega_s(t-t_1)) \sin(\Omega_s(t-t_2))\, dt_1 dt_2$$

Acting similar to the case of phase noise, accounting that $K_u(t_1 - t_2) = \overline{u(t_1)u(t_2)}$ and dropping fast oscillating terms we obtain

$$\overline{\varphi^2(t)} \approx \frac{\Omega_s{}^2}{4} t\varphi_0{}^2 \int_{-\infty}^{\infty} K_u(\tau)\cos(2\Omega_s\tau)\, d\tau$$

Accounting also $\overline{\varphi^2(t)} = \varphi_0{}^2/2$ we finally obtain

$$\boxed{\frac{d}{dt}\overline{\varphi^2(t)} = \pi\Omega_s{}^2\,\overline{\varphi^2(t)}\,P_u(2\Omega_s)}$$

Practical Estimate

- Let's consider Tevatron: $f_s = \Omega_s / 2\pi$ = 35 Hz, initial bunch length 30 cm and RF bucket length of 5.65 m (53.1 MHz)
- Require the bunch lengthening 10% after in 10 hours

$$\varphi_{fin} = \sqrt{\varphi_0^{\ 2} + T \frac{d}{dt}\overline{\varphi^2}} \approx \varphi_0 + \frac{T}{2\varphi_0}\frac{d}{dt}\overline{\varphi^2}$$

⇨ $$\Rightarrow \frac{d}{dt}\overline{\varphi^2} = \frac{\varphi_{fin} - \varphi_0}{\varphi_0 T} 2\varphi_0^{\ 2} = \frac{0.05}{10 \cdot 3600} 2 \left(2\pi \frac{35}{565} \right)^2 = 6.5 \cdot 10^{-7} \frac{\text{rad}^2}{\text{s}}$$

⇨ Corresponding spectral densities

⇨ $$P_\psi = 4.3 \cdot 10^{-12} \text{s}^{-1} , \quad P_u = 3.8 \cdot 10^{-11} \text{s}^{-1}$$

⇨ Corresponding rms fluctuations for the white noise in 100 Hz band

⇨ $$\sqrt{\overline{\psi^2}} = \sqrt{4\pi P_\psi \Delta f} = 7.3 \cdot 10^{-5} \text{rad} , \quad \sqrt{\overline{u^2}} = \sqrt{4\pi P_{u\psi} \Delta f} = 2.2 \cdot 10^{-4} \text{rad}$$

⇨ 4π accounts transition from "physical" to "technical" definition of spectral density

Action-Phase Variables

$$H=\frac{\hat{p}^2}{2}+U(\varphi)\xrightarrow{\text{Single harmonic RF}}\frac{\hat{p}^2}{2}+2\Omega_s^{\,2}\left(\sin\frac{\varphi}{2}\right)^2$$

$$I=\frac{1}{2\pi}\oint\hat{p}\,d\varphi\,,\qquad \frac{dH}{dI}=\omega\,,\qquad \phi=\omega t$$

- For single harmonic RF

$$I=\frac{2\sqrt{2}\Omega_s}{\pi}\int_0^{\varphi_{\max}}\sqrt{\cos\varphi-\cos\varphi_{\max}}\,d\varphi\,,\quad H=2\Omega_s^{\,2}\left(\sin\frac{\varphi_{\max}}{2}\right)^2$$

$$T=\frac{4}{\sqrt{2}\Omega_s}\int_0^{\varphi_{\max}}\frac{d\varphi}{\sqrt{\cos\varphi-\cos\varphi_{\max}}}\,,\quad \omega=\frac{2\pi}{T}$$

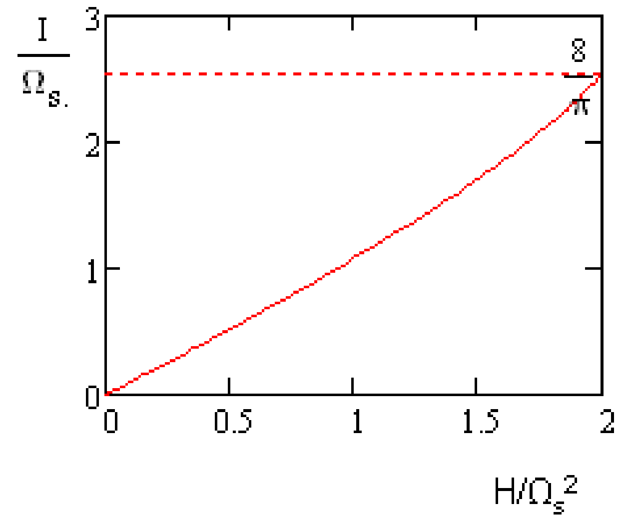

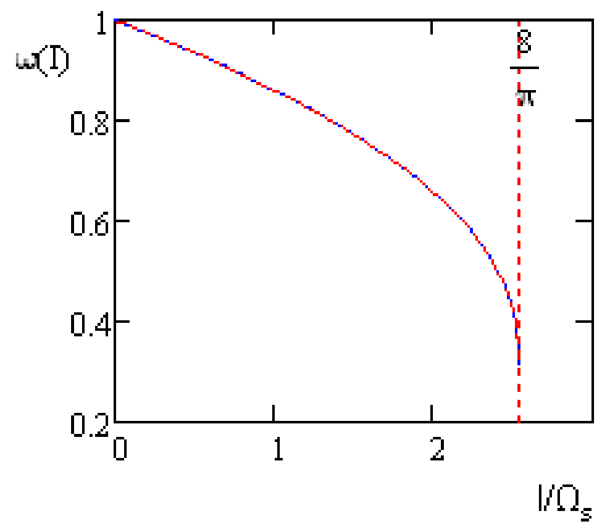

Fokker-Planck Equation

- Introduce the diffusion equation in the following form:

$$\boxed{\frac{\partial f}{\partial t}=\frac{1}{2}\frac{\partial}{\partial I}\left(\frac{D(I)}{\omega(I)}I\frac{\partial f}{\partial I}\right)}$$

- Changes in average action

$$\frac{d\overline{I}}{dt}=\int_0^\infty I\frac{\partial f}{\partial t}dI=\frac{1}{2}\int_0^\infty I\frac{\partial}{\partial I}\left(\frac{D(I)}{\omega(I)}I\frac{\partial f}{\partial I}\right)dI=-\frac{1}{2}\int_0^\infty \frac{D(I)}{\omega(I)}I\frac{\partial f}{\partial I}dI=\frac{1}{2}\int_0^\infty f\frac{d}{dI}\left(I\frac{D(I)}{\omega(I)}\right)fdI$$

$$\xrightarrow{f(I)=\delta(I-I_0)}\frac{1}{2}\left(\frac{D(I)}{\omega(I)}+I\frac{d}{dI}\left(\frac{D(I)}{\omega(I)}\right)\right)\Rightarrow\frac{d\overline{H}}{dt}=\frac{1}{2}\left(D(I)+I\omega(I)\frac{d}{dI}\left(\frac{D(I)}{\omega(I)}\right)\right)$$

<u>For linear RF</u>: $\dfrac{d\overline{H}}{dt}=\dfrac{1}{2}D\Rightarrow\quad\dfrac{d}{dt}\overline{p^2}=\dfrac{1}{2}D$

1/2 accounts reduction of momentum growth in linear oscillator

Finally for linear RF: $\boxed{D(I)=\pi\Omega_s{}^3\left(2\Omega_s P_\varphi(\Omega_s)+P_u(2\Omega_s)I\right)}$

- Widening of the distribution in the action space

$$\frac{d}{dt}\overline{\delta I^2}\equiv\frac{d}{dt}\overline{(I-I_0)^2}=\frac{1}{2}\int_0^\infty(I-I_0)^2\frac{\partial}{\partial I}\left(\frac{D(I)}{\omega(I)}I\frac{\partial f}{\partial I}\right)dI=-\int_0^\infty(I-I_0)\frac{D(I)}{\omega(I)}I\frac{\partial f}{\partial I}dI$$

$$=\int_0^\infty f\frac{d}{dI}\left((I-I_0)I\frac{D(I)}{\omega(I)}\right)fdI\xrightarrow{f(I)=\delta(I-I_0)}\int_0^\infty\delta(I-I_0)I\frac{D(I)}{\omega(I)}dI=I_0\frac{D(I_0)}{\omega(I_0)}$$

Diffusion in Harmonic RF

- Motion non-linearity couples the diffusion to higher harmonics of synchrotron frequency [*]

$$D_\varphi = \sum_{n=1}^{\infty} P_\varphi(n\omega) C_{\varphi n}(I) \ , \quad C_{\varphi n}(I) = \frac{\omega \Omega_s^{\ 4}}{\pi I} \left| \oint d\phi \cos\phi \exp\left(in\omega t(\phi)\right) \right|^2 ,$$

$$D_u = \sum_{n=1}^{\infty} P_u(n\omega) C_{un}(I) , \quad C_{un}(I) = \frac{\omega \Omega_s^{\ 4}}{\pi I} \left| \oint \frac{d\phi}{2\pi} \sin\phi \exp\left(in\omega t(\phi)\right) \right|^2 .$$

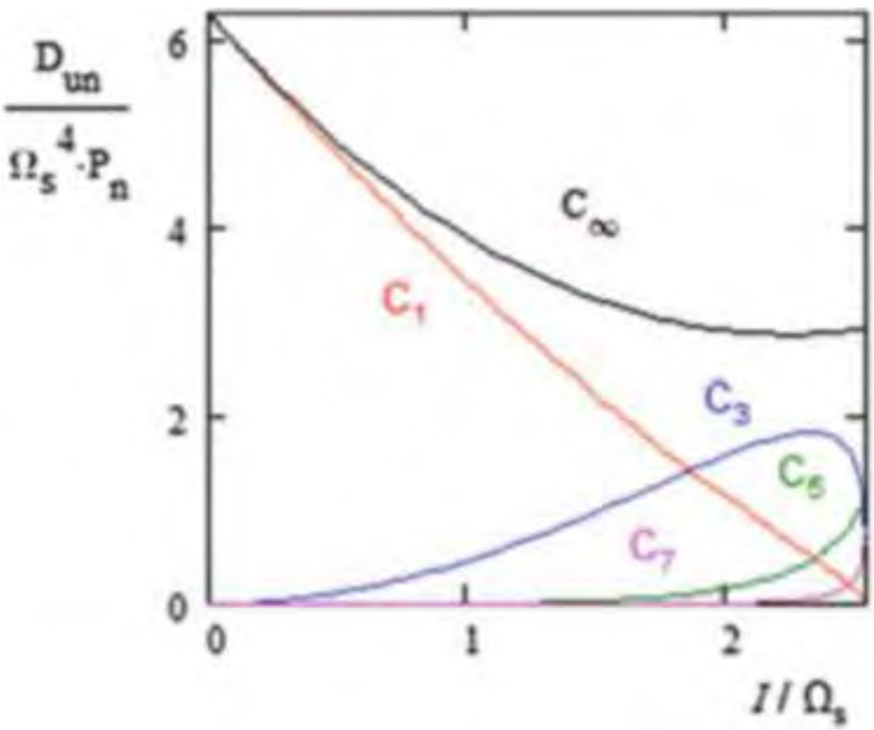

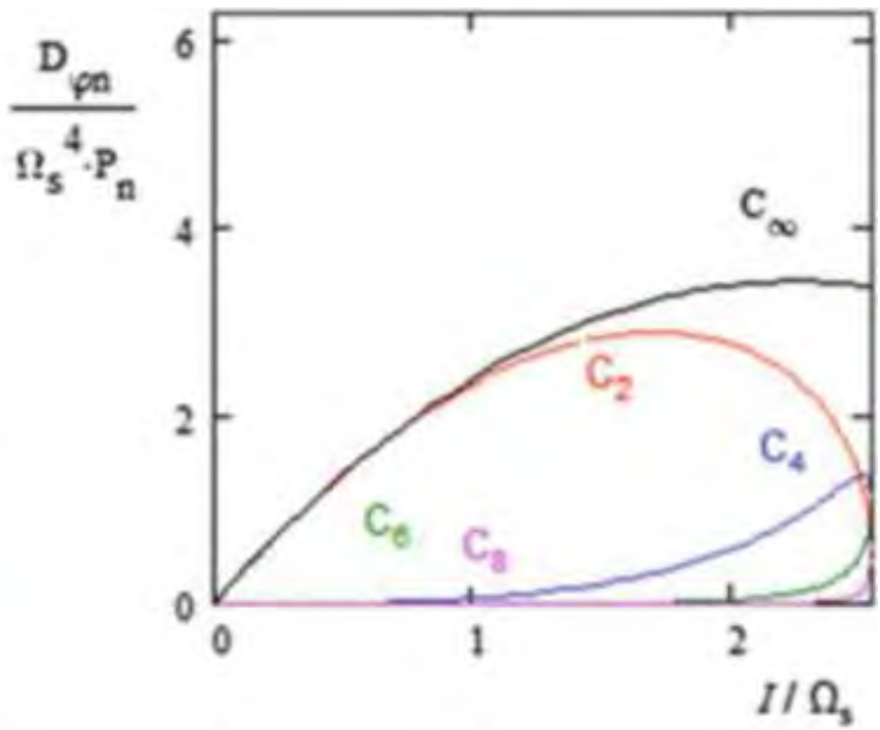

[*]"Accelerator Physics at the Tevatron Collider", edited by V. Lebedev and V. Shiltsev, Springer, 2014.

Final Remarks to the RF noise

- To prevent longitudinal emittance growth a hadron collider requires high quality RF, both in the RF phase and the RF amplitude
- Modern high quality RF generators are well within these requirements for the master oscillator
  - Microphonics in RF cavities as well as noise in power amplifiers may excite RF noise to unacceptable level
    - To address this problem in the Tevatron Run II the phase feedback was used. It stabilized the RF phase relative to the master oscillator
  - As will be seen in the second half of the lecture the longitudinal damper may be helpful to reduce effect of phase noise
    - However, it will require very small noise in detecting synchrotron motion
- Noise in the bending magnetic field at synchrotron frequency harmonics works the same way as RF

Transverse Emittance Growth due to Noise in Magnets and its Suppression by Transverse Damper

*Equations of Motion and their Solution**

- In difference to synchrotron tune the betatron tunes are large. That completely changes beam response to a perturbation
- First, we consider one point-like dipole perturbation
- To simplify equations, we transit to new variables

$$x=\frac{X}{\sqrt{\beta}}\,,\quad p=\beta\frac{d}{ds}\frac{X}{\sqrt{\beta}}=\beta\left(\frac{1}{\sqrt{\beta}}\frac{dX}{ds}-\frac{X}{2\beta^{3/2}}\frac{d\beta}{ds}\right)=\sqrt{\beta}\theta+\alpha\frac{X}{\sqrt{\beta}}$$

- In new variables particle position after N turns is:

$$x_N=x_0\cos\left(\mu N+\psi_0\right)+\sum_{n=0}^{N-1}\Delta p_n\sin\left(\mu\left(N-n\right)\right),\quad \Delta p_n=\sqrt{\beta}\theta_n$$

- Further we imply that: $\Delta p_n=p(nT)\,,\quad \overline{p(t_1)p(t_2)}=K_p\left(t_1-t_2\right),\ K_p\left(\tau\right)=\int_{-\infty}^{\infty}P_p(\omega)e^{i\omega\tau}d\omega$
- Then

$$\overline{x_N{}^2}=x_0{}^2\cos^2\left(\mu N+\psi_0\right)+\sum_{n,m=0}^{N-1}\overline{\Delta p_n\Delta p_m}\sin\left(\mu\left(N-n\right)\right)\sin\left(\mu\left(N-m\right)\right)$$

$$=x_0{}^2\cos^2\left(\mu N+\psi_0\right)+\sum_{n,m=0}^{N-1}K\left(T(n-m)\right)\sin\left(\mu\left(N-n\right)\right)\sin\left(\mu\left(N-m\right)\right)$$

* V. Lebedev, et.al. “EMITTANCE GROWTH DUE TO NOISE AND ITS SUPPRESSION WITH THE FEEDBACK SYSTEM IN LARGE HADRON COLLIDERS”, Particle Accelerators, 1994, Vol. 44, pp. 147-164; http://cds.cern.ch/record/248620/files/p147.pdf

Equations of Motion and their Solution (2)

- Express the correlation function through the spectral density

$$\overline{x_N{}^2} = x_0{}^2 \cos^2\left(\mu N + \psi_0\right) + \int_{-\infty}^{\infty} d\omega \sum_{n,m=0}^{N-1} P(\omega) e^{i\omega T(n-m)} \sin\left(\mu\left(N-n\right)\right)\sin\left(\mu\left(N-m\right)\right)$$

- Perform summation

$$\Sigma = \sum_{n,m=0}^{N-1} e^{i\omega T(n-m)} \sin\left(\mu\left(N-n\right)\right)\sin\left(\mu\left(N-m\right)\right) = \frac{1}{4}\sum_{n,m=0}^{N-1} e^{i\omega T(n-m)}\left(e^{i\mu(N-n)} - e^{-i\mu(N-n)}\right)\left(e^{-i\mu(N-m)} - e^{i\mu(N-m)}\right)$$

$$= \frac{1}{4}\sum_{n,m=0}^{N-1} e^{i\omega T(n-m)}\left(e^{i\mu(m-n)} + e^{-i\mu(m-n)} - e^{i\mu(2N-n-m)} - e^{-i\mu(2N-n-m)}\right) \xrightarrow[\textit{drop last 2 terms}]{N\to\infty}$$

$$= \frac{1}{4}\left(\left|\sum_{n=0}^{N-1} e^{i(\omega T-\mu)n}\right|^2 + \left|\sum_{n=0}^{N-1} e^{i(\omega T+\mu)n}\right|^2\right) = \frac{1}{4}\left(\left|\frac{1-e^{i(\omega T-\mu)N}}{1-e^{i(\omega T-\mu)}}\right|^2 + \left|\frac{1-e^{i(\omega T+\mu)N}}{1-e^{i(\omega T+\mu)}}\right|^2\right)$$

$$= \frac{1}{4}\left(\frac{\sin^2\left((\omega T-\mu)N/2\right)}{\sin^2\left((\omega T-\mu)/2\right)} + \frac{\sin^2\left((\omega T+\mu)N/2\right)}{\sin^2\left((\omega T+\mu)/2\right)}\right)$$

- Account that: $\dfrac{\sin^2(\xi/2N)}{\sin^2(\xi/2)} \xrightarrow{N\to\infty} 2\pi N \displaystyle\sum_{n=-\infty}^{\infty} \delta(\xi - 2\pi n)$

$\Rightarrow$ $$\Sigma = \frac{2\pi N}{4}\left(\sum_{n=-\infty}^{\infty} \delta((\omega T-\mu) - 2\pi n) + \sum_{n=-\infty}^{\infty} \delta((\omega T+\mu) - 2\pi n)\right)$$

Transverse Emittance Growth due to Noise

- Combining we obtain

$$\overline{x_N^{\,2}} = x_0^{\,2}\cos^2\left(\mu N+\psi_0\right)+\int_{-\infty}^{\infty} d\omega \sum_{n,m=0}^{N-1} P_p(\omega)e^{i\omega T(n-m)}\sin\left(\mu\left(N-n\right)\right)\sin\left(\mu\left(N-m\right)\right)$$

$$= x_0^{\,2}\cos^2\left(\mu N+\psi_0\right)+\frac{\pi N}{2}\int_{-\infty}^{\infty} P_p(\omega)d\omega\left(\sum_{n=-\infty}^{\infty}\delta((\omega T-\mu)-2\pi n)+\sum_{n=-\infty}^{\infty}\delta((\omega T+\mu)-2\pi n)\right)$$

$$= x_0^{\,2}\cos^2\left(\mu N+\psi_0\right)+\frac{\pi N}{2T}\sum_{n=-\infty}^{\infty}\left(P_p\left(\frac{2\pi n+\mu}{T}\right)+P_p\left(\frac{2\pi n-\mu}{T}\right)\right)$$

Returning to initial variables and accounting that $\mu = 2\pi\nu \;\&\; \omega_0 = 2\pi / T$

$$\overline{X_N^{\,2}} = X_0^{\,2}\cos^2\left(\mu N+\psi_0\right)+\frac{N\omega_0\beta^2}{4}\sum_{n=-\infty}^{\infty}\left(P_\theta\left(\omega_0\left(n+\nu\right)\right)+P_\theta\left(\omega_0\left(\nu-n\right)\right)\right)$$

Averaging over all particles and accounting that both terms make equal contribution we finally obtain

$$\varepsilon_N = \frac{1}{\beta}\left[\overline{X_N^{\,2}}\right]_{\substack{all\\part}} = \varepsilon_N + \frac{N\omega_0\beta}{2}\sum_{n=-\infty}^{\infty}P_\theta\left(\frac{2\pi n-\mu}{T}\right)$$

- If all sources of perturbation are statistically independent the for the entire ring we obtain

$$\boxed{\frac{d\varepsilon}{dn} = \frac{\omega_0}{2}\sum_{k}^{\substack{all\\sorces}}\beta_k\sum_{n=-\infty}^{\infty}P_{\theta k}\left(\frac{2\pi n-\mu}{T}\right)}$$

Transverse Emittance Growth due to White Noise

- For the white noise in the band $\Delta f >> n_{max}\omega_0/2\pi$, n_{max} >> 1

$$\overline{\theta^2} = \int_{-n_{max}\omega_0}^{n_{max}\omega_0} P_\theta(\omega)\,d\omega = \omega_0 \sum_{n=-n_{max}}^{n_{max}} P_\theta(\omega_0 n) \approx \omega_0 \sum_{n=-n_{max}}^{n_{max}} P_\theta\left(\omega_0 (n+\nu)\right)$$

Accounting this we obtain

$$\varepsilon_N = \varepsilon_0 + \frac{N\omega_0\beta}{2} \sum_{n=-\infty}^{\infty} P_\theta\left(\frac{2\pi n-\mu}{T}\right) = \varepsilon_0 + \frac{1}{2}\beta\overline{\theta^2}N$$

which we could obtain immediately

Suppression of Emittance Growth by Damper

- If in the above consideration all particles have the same betatron tune actual emittance of the beam does not increase. Only the beam centroid oscillations grow
- Therefore, a transverse damper suppresses the emittance growth
- In real world, and in a collider in particular, different particles have different betatron tunes and therefore beam decoheres with typical decoherence time ~1000 turns.
  - Therefore, to prevent the emittance growth the damper should damp the beam faster than it decoheres.
- Steps in our calculations
  - Consider damping of the entire beam.
  - Make a transition from matrix formalism to ODE
  - Find solution for a single kick of the entire beam
  - Find solution for a single particle
  - Obtain equation for the emittance growth

Entire Beam Damping

- Turn-by-turn transformation referenced to the pickup location

$$\mathbf{x}_{n+1} = \mathbf{M}_{kp}\left(\mathbf{M}_{pk}\mathbf{x}_n + \mathbf{G}\sum_{k=0}^{K-1} A_k \mathbf{x}_{n-k}\right), \qquad \mathbf{G} = \begin{bmatrix} 0 & 0 \\ g & 0 \end{bmatrix}$$

- Consider the simplest one turn model with μ_{pk}=90 deg.

$$\mathbf{x}_{n+1} = \begin{bmatrix} c & s \\ -s & c \end{bmatrix}\left(\begin{bmatrix} 0 & 1 \\ -1 & 0 \end{bmatrix}\mathbf{x}_n + \begin{bmatrix} 0 & 0 \\ g & 0 \end{bmatrix}\mathbf{x}_n\right) = \begin{bmatrix} c(1-g) & s \\ -s(1-g) & c \end{bmatrix}\mathbf{x}_n , \quad c = \cos\mu,\ s = \sin\mu$$

- Solution

$$\left\| \begin{bmatrix} c(1-g) - \Lambda & s \\ -s(1-g) & c - \Lambda \end{bmatrix} \right\| = 0$$

$$\Rightarrow \quad \Lambda_{1,2} = c\left(1 - \frac{g}{2}\right) \pm \sqrt{c^2\left(1 - \frac{g}{2}\right)^2 - (1-g)}$$

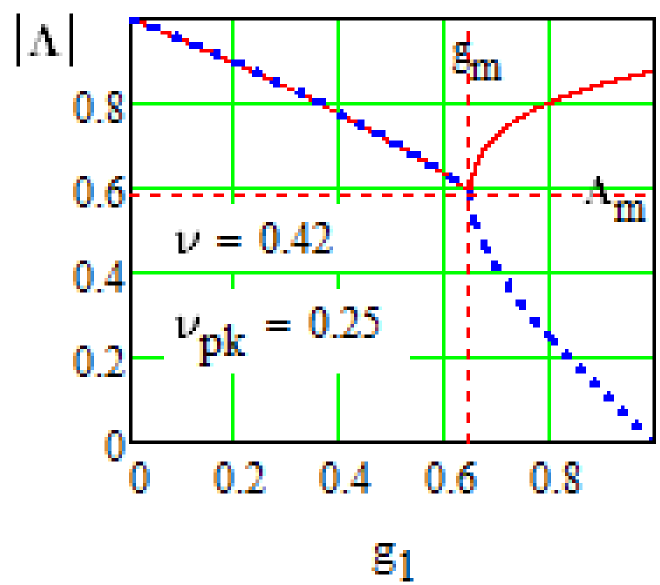

- For small gain: $\Lambda_{1,2} = \left(1 - \dfrac{g}{2}\right)e^{\pm i\mu}$
- Optimal gain decreases with number of turns, K, as $\approx 1/K$

Transition from Matrix Formalism to ODE

$$\Lambda_{1,2} = \left(1 - \frac{g}{2}\right) e^{\pm i\mu} \approx e^{\pm i\mu - g/2} \Rightarrow \mathbf{x}_n = \mathbf{x}_0 e^{(i\mu - g/2)n} \quad \Rightarrow \quad \mathbf{x}(t) = \mathbf{x}(0) e^{(i\mu - g/2)t/T}, \quad \mathbf{x} = x + ip$$

- For small g we can use ODE for description of motion

$$\mathbf{x}_n = \mathbf{x}_0 e^{(i\mu - g/2)n} \quad \Rightarrow \quad \mathbf{x}(t) = \mathbf{x}(0) e^{(i\mu - g/2)t/T}, \quad \mathbf{x} = x + ip$$

$$\Rightarrow \quad \boxed{\frac{d^2x}{d\theta^2} + \frac{g}{\mu}\frac{dx}{d\theta} + x = 0, \quad \theta \in [0, \mu]}$$

- The solution is

$$x(\theta) \approx e^{-g\theta/2\mu}\left(x(0)\cos\theta + p(0)\sin\theta\right), \quad g/2\mu \ll 1$$

Solution for a Single kick of the Entire Beam

$$\bar{x} \approx \left(\Delta x \cos\theta + \Delta p \sin\theta\right) e^{-g\theta/2\mu}$$

$$\bar{p} \approx \left(-\Delta x \sin\theta + \Delta p \cos\theta\right) e^{-g\theta/2\mu}$$

where we assume that the decoherence time is much longer than the damping time

Damping of a Single Particle

- Single particle does not produce sufficient signal to affect the damper => no damping
  - Particle with $\Delta\nu=0$ and $x_0=\Delta x$ is damped together with the beam

$$\frac{d^2x}{d\theta^2}+\left(1+\frac{\Delta\nu}{\nu}\right)^2 x=-\frac{g}{\mu}e^{-g\theta/2\mu}\left(-\Delta x\sin\theta+\cos\theta\,\Delta p\right)$$

- The general solution for initial conditions $x=x_0+\Delta x,\ p=p_0+\Delta p$:

$$x=\left(x_0+\Delta x\right)\cos\left(\nu_p\theta\right)+\left(p_0+\Delta p\right)\sin\left(\nu_p\theta\right)-\frac{1}{\nu_p}\int_0^\theta\left(\frac{g}{\mu}e^{-g\theta'/2\mu}\left(-\Delta x\sin\theta'+\cos\theta'\,\Delta p\right)\right)\sin\left(\nu_p\left(\theta-\theta'\right)\right)d\theta'$$

where we accounted $\varphi(t)=\frac{1}{\Omega_s}\int_0^t f(t')\sin\left(\Omega_s(t-t')\right)dt'$ for $\frac{d^2\varphi}{dt^2}+\Omega_s{}^2\varphi=f(t)$, and $\nu_p=1+\frac{\Delta\nu}{\nu}$

- Lengthy integration in the limit of large θ (see below) yields:

$$x=\left(x_0+\frac{2\mu\left(\nu_p-1\right)}{g}\Delta x\right)\cos\left(\nu_p\theta\right)+\left(p_0-\frac{2\mu\left(\nu_p-1\right)}{g}\Delta p\right)\cos\left(\nu_p\theta\right)$$

- Thus detuning results in its single particle emittance increase

$$\delta\varepsilon=\frac{\delta p^2+\delta x^2}{2}=\left(\frac{4\pi\Delta\nu}{g}\right)^2\frac{\Delta x^2+\Delta p^2}{2}=\left(\frac{4\pi\Delta\nu}{g}\right)^2\Delta\varepsilon \quad => \quad \boxed{\frac{d\varepsilon}{dt}=\frac{16\pi^2\overline{\Delta\nu^2}}{g^2}\left(\frac{d\varepsilon}{dt}\right)_0}$$

where we accounted that $\left(\nu_p-1\right)\mu=2\pi\Delta\nu$

Computation of Integrals

- Consider only term with Δx (term with Δp done similarly, same result)

$$I=\cos\left(\nu_p\theta\right)+\frac{g}{\nu_p\mu}\int_0^{\theta}e^{-g\theta'/2\mu}\sin\theta'\sin\left(\nu_p\left(\theta-\theta'\right)\right)d\theta'$$

$$=\cos\left(\nu_p\theta\right)+\frac{g}{\nu_p\mu}\left(\sin\left(\nu_p\theta\right)\int_0^{\theta}e^{-g\theta'/2\mu}\sin\theta'\cos\left(\nu_p\theta'\right)d\theta'-\cos\left(\nu_p\theta\right)\int_0^{\theta}e^{-g\theta'/2\mu}\sin\theta'\sin\left(\nu_p\theta'\right)d\theta'\right)$$

  - Account that: $2\sin x\cos y=\sin(x+y)+\sin(x-y),\quad 2\sin x\sin y=\cos(x-y)-\cos(x+y)$

    and drop fast oscillating terms

$$I=\cos\left(\nu_p\theta\right)-\frac{g}{\nu_p\mu}\left(\sin\left(\nu_p\theta\right)\int_0^{\theta}e^{-g\theta'/2\mu}\sin\left((\nu_p-1)\theta'\right)d\theta'+\cos\left(\nu_p\theta\right)\int_0^{\theta}e^{-g\theta'/2\mu}\cos\left((\nu_p-1)\theta'\right)d\theta'\right)$$

  - In the limit of large θ

$$I=\cos\left(\nu_p\theta\right)-\frac{g}{\nu_p\mu}\left(\frac{\sin\left(\nu_p\theta\right)}{2i}\left(\frac{1}{1-e^{-g/2\mu+i\left(\nu_p-1\right)}}-CC\right)+\frac{\cos\left(\nu_p\theta\right)}{2}\left(\frac{1}{1-e^{-g/2\mu+i\left(\nu_p-1\right)}}+CC\right)\right)$$

$$\xrightarrow[\nu_p-1\ll 1]{g/2\mu\ll 1}\cos\left(\nu_p\theta\right)-\frac{g}{\nu_p\mu}\left(\frac{\sin\left(\nu_p\theta\right)}{2i}\left(\frac{1}{-\left(-g/2\mu+i\left(\nu_p-1\right)\right)}-CC\right)+\frac{\cos\left(\nu_p\theta\right)}{2}\left(\frac{1}{\left(-g/2\mu+i\left(\nu_p-1\right)\right)}+CC\right)\right)$$

$$=\cos\left(\nu_p\theta\right)-\frac{1}{\nu_p}\left(\frac{2\mu g(\nu_p-1)\sin\left(\nu_p\theta\right)+g^2\cos\left(\nu_p\theta\right)}{g^2+4\mu^2(\nu_p-1)^2}\right)\xrightarrow[\nu_p-1\ll 1]{g\ll\mu(\nu_p-1)}\frac{2\mu(\nu_p-1)}{g}\sin\left(\nu_p\theta\right)$$

Suppression of Emittance Growth by Damper

- In the above calculations we assumed that $g \gg \Delta\nu$. Otherwise the problem would be much more complicated because we would need to account the beam decoherence in computation of damper response.
- Therefore, the obtained answer

$$\frac{d\varepsilon}{dt} = \frac{16\pi^2 \overline{\Delta\nu^2}}{g^2} \left(\frac{d\varepsilon}{dt} \right)_0$$

  is justified for $g \gg \Delta\nu$.
- For practical estimates, since there is no suppression for small g, we use an interpolation

$$\boxed{\frac{d\varepsilon}{dt} = \frac{16\pi^2 \overline{\Delta\nu^2}}{g^2 + 16\pi^2 \overline{\Delta\nu^2}} \left(\frac{d\varepsilon}{dt} \right)_0}$$

References

1. V. Lebedev, et.al. "Emittance growth due to noise and its suppression with feedback system in large hadron colliders", SSCL-Preprint-188, (1993); https://inis.iaea.org/collection/NCLCollectionStore/_Public/26/066/26066808.pdf
2. "Accelerator Physics at the Tevatron Collider", edited by V. Lebedev and V. Shiltsev, Springer, 2014.

Problems

1. Prove that $\varphi(t)=\frac{1}{\Omega_s}\int_0^t f(t')\sin\left(\Omega_s(t-t')\right)dt'$ is the solution of the following equation

   $\frac{d^2\varphi}{dt^2}+\Omega_s{}^2\varphi=f(t)$ with zero initial coordinates
2. Rewrite equations of longitudinal motion for low frequency noise in bending magnets which can drive the longitudinal emittance growth. Make estimates for the LHC and Tevatron
3. Prove that $\frac{\sin^2(\xi/2N)}{\sin^2\left(\xi/2\right)}\xrightarrow{N\to\infty}2\pi N\sum_{n=-\infty}^{\infty}\delta(\xi-2\pi n)$
4. Find the rms tune spread due to head-on beam-beam effects in round beams. Estimate corresponding decoherence time. Assume round beams of the same rms sizes and $\beta_x=\beta_y$.
5. Estimate acceptable value of white noise in the LHC dipole in the absence of emittance growth suppression by transverse damper. Assume noise in different dipoles independent. Compute corresponding spectral density assuming 5 kHz band.
6. Extend the equation for the emittance growth suppression by damper so that in addition to external noise it would include the damper noise.

Lectures 9&10
Intrabeam Scattering

Valeri Lebedev
JINR & Fermilab

US Particle Accelerator School
February 2022

U.S. DEPARTMENT OF ENERGY

Fermilab

Objectives

- In a "properly built machine" the IBS typically represents the main source of emittance growth, both $\perp$ & $||$
  - Coulomb scattering cross-section diverges
  - In a beam this divergence is limited by other particle screening or size
- Conventionally, multiple and single particle scattering in a storage ring are considered to be independent. Such an approach is simple and often yields sufficiently accurate results.
  - Multiple scattering is described by Fokker-Planck equation
    - Landau collision integral
  - Single scattering – Touschek effect (important for very different T's)
- However, there is a class of problems where such approach is not adequate; and single & multiple scatterings should to be considered together.
  - It is described by integrodifferential equation for particle distribution function, which correctly treats particle Coulomb scattering
- In this lecture we consider an evolution of particle distribution due to multiple intrabeam scattering: first in plasma then in a beam

Diffusion and Friction Force in Plasma

Multiple Scattering in Plasma

- Landau collision integral

$$\frac{df}{dt} = -2\pi n r_0^2 c^4 L_c \frac{\partial}{\partial \mathrm{v}_i} \int \left(f \frac{\partial f'}{\partial \mathrm{v}'_j} - f' \frac{\partial f}{\partial \mathrm{v}_j} \right) \frac{(\mathbf{v}-\mathbf{v}')^2 \delta_{ij} - (\mathrm{v}_i - \mathrm{v}'_i)(\mathrm{v}_j - \mathrm{v}'_j)}{|\mathbf{v}-\mathbf{v}'|^3} d^3\mathrm{v}'$$

$$\Rightarrow \quad \frac{df}{dt} = -\frac{\partial}{\partial p_i}(F_i f) + \frac{1}{2}\frac{\partial}{\partial p_i}\left(D_{ij} \frac{\partial f}{\partial p_j} \right), \quad \begin{cases} F_i(\mathrm{v}) = -\dfrac{4\pi n e^4 L_c}{m} \displaystyle\int f(\mathrm{v}') \frac{u_i}{|\mathbf{u}|^3} d^3\mathrm{v}' , \\ D_{ij}(\mathrm{v}) = 4\pi n e^4 L_c \displaystyle\int f(\mathrm{v}') \frac{u^2 \delta_{ij} - u_i u_j}{|\mathbf{u}|^3} d^3\mathrm{v}' , \end{cases} \quad \mathbf{u} = \mathbf{v} - \mathbf{v}'$$

where $L_c = \ln(\rho_{\max} / \rho_{\min})$, $\rho_{\min} = r_0 c^2 / \overline{\mathrm{v}^2}$, $\rho_{\max} = \sqrt{\overline{\mathrm{v}^2} / 4\pi n r_0 c^2}$, $r_0 = \dfrac{e^2}{mc}$, $\overline{\mathrm{v}^2} = \sigma_{\mathrm{v}x}^2 + \sigma_{\mathrm{vy}}^2 + \sigma_{\mathrm{vz}}^2$, $\int f(\mathbf{v}) d^3\mathrm{v} = 1$

and we accounted: $\dfrac{\partial u}{\partial u_i} = \dfrac{u_i}{u}$, $\dfrac{\partial}{\partial u_i}\left(\dfrac{u^2\delta_{ij} - u_i u_j}{u^3} \right) = -2\dfrac{u_i}{u^3}$, $\dfrac{\partial}{\partial \mathrm{v}'_i}\left(\dfrac{u^2\delta_{ij} - u_i u_j}{u^3} \right) = 2\dfrac{u_i}{u^3}$

- Conditions of applicability: $L_c = \ln(\rho_{\max} / \rho_{\min}) \gg 1$, or $T \gg e^2 n^{1/3}$
  - Plasma theory – a perturbation theory where we can neglect interaction of more than 2 particles
  - Lenard-Balescu equations bind low and higher order distributions

Friction and Diffusion

$$\frac{df}{dt} = -\frac{\partial}{\partial p_i}\left(F_i f\right) + \frac{1}{2}\frac{\partial}{\partial p_i}\left(D_{ij}\frac{\partial f}{\partial p_j}\right)$$

- Let's consider a single particle deceleration

  ⇨ $f = \delta\left(\mathbf{p} - \mathbf{p}_0\right)$, but D and F fixed

$$\frac{d}{dt}\overline{\delta p_i} \equiv \frac{d}{dt}\left(\overline{(p_i - p_{0i})}\right) = \int (p_i - p_{0i})\frac{\partial}{\partial p_l}\left(-F_l f + D_{kl}\frac{\partial f}{\partial p_k}\right)\mathrm{d}p^3$$

$$= -\int \delta_{il}\left(-F_l f + D_{kl}\frac{\partial f}{\partial p_k}\right)\mathrm{d}p^3 = F_i(\mathbf{p}_0) - \int D_{ki}\frac{\partial f}{\partial p_k}\mathrm{d}p^3 = F_i(\mathbf{p}_0) + \int f\frac{\partial D_{ki}}{\partial p_k}\mathrm{d}p^3 = F_i(\mathbf{p}_0) + \left.\frac{\partial D_{ki}}{\partial p_k}\right|_{\mathbf{p}=\mathbf{p}_0}$$

  i.e. the gradient in diffusion adds to deceleration:

  For Gaussian distribution it doubles the "force"

$$\boxed{\frac{d}{dt}\overline{\delta p_i} = F_i(\mathbf{p}_0) + \left.\frac{\partial D_{ki}}{\partial \mathrm{v}_k}\right|_{\mathbf{p}=\mathbf{p}_0}}$$

- Let's consider a single particle diffusion

$$\frac{d}{dt}\overline{\delta p_i \delta p_j} = \int\left((p_i - p_{0i})(p_j - p_{0j})\right)\frac{\partial}{\partial p_l}\left(-F_l f + D_{kl}\frac{\partial f}{\partial p_k}\right)dp^3 = \int\frac{\partial}{\partial p_l}\left((p_i - p_{0i})(p_j - p_{0j})\right)\left(F_l f - D_{kl}\frac{\partial f}{\partial p_k}\right)dp^3$$

$$= \int\left(\delta_{il}(p_j - p_{0j}) + \delta_{jl}(p_i - p_{0i})\right)\left(F_l f - D_{kl}\frac{\partial f}{\partial p_k}\right)dp^3$$

$$= \int\left((p_j - p_{0j})F_i + (p_i - p_{0i})F_j\right)f dp^3 - \int\left((p_j - p_{0j})\delta_{il} + (p_i - p_{0i})\right)\delta_{jl}D_{kl}\frac{\partial f}{\partial p_k}dp^3$$

$$\xrightarrow{1^{\text{st}}\text{ term}=0}\int f\delta_{jl}\frac{\partial}{\partial p_k}\left[\left((p_j - p_{0j})\delta_{il} + (p_i - p_{0i})\right)D_{kl}\right]dp^3 = 2\int fD_{ij}dp^3$$

$$\boxed{\frac{d}{dt}\overline{\delta p_i \delta p_j} = 2\left.D_{ij}\right|_{\mathbf{p}=\mathbf{p}_0}}$$

Temperature Exchange in Plasma

- Consider 3 temperature Gaussian distribution

$$f=\frac{1}{(2\pi)^{3/2}\sigma_{vx}\sigma_{vy}\sigma_{vz}}\exp\left(-\frac{1}{2}\left(\frac{v_x^2}{\sigma_{vx}^2}+\frac{v_y^2}{\sigma_{vy}^2}+\frac{v_z^2}{\sigma_{vz}^2}\right)\right)$$

- Then the rate of rms velocity is

$$\frac{d}{dt}\overline{v_i v_j}=-\frac{2\pi e^4 nL_c}{m^2}\int v_i v_j\frac{\partial}{\partial v_k}\left(\left(f\frac{\partial f'}{\partial v'_l}-f'\frac{\partial f}{\partial v_l}\right)\frac{u^2\delta_{kl}-u_k u_l}{u^3}\right)dv'^3\,dv^3$$

$$\xrightarrow{\partial f/\partial v_j=-\left(v_j/\sigma_j^2\right)f}=-\frac{2\pi e^4 nL_c}{m^2}\int v_i v_j\frac{\partial}{\partial v_k}\left(-ff'\left(\frac{v'_l}{\sigma_l^2}-\frac{v_l}{\sigma_l^2}\right)\frac{u^2\delta_{kl}-u_k u_l}{u^3}\right)dv'^3\,dv^3$$

$$=-\frac{2\pi e^4 nL_c}{m^2}\int v_i v_j\frac{\partial}{\partial v_k}\left(ff'\frac{u_l}{\sigma_l^2}\frac{u^2\delta_{kl}-u_k u_l}{u^3}\right)dv'^3\,dv^3$$

$$=\frac{2\pi e^4 nL_c}{m^2}\int ff'\left(\delta_{ki}v_j+\delta_{kj}v_i\right)\frac{u_l}{\sigma_l^2}\frac{u^2\delta_{kl}-u_k u_l}{u^3}dv'^3\,dv^3$$

- The Tensor is diagonal. Let's consider *x*-plane.

$$\Rightarrow\quad\frac{d}{dt}\overline{v_x^2}=\frac{4\pi e^4 nL_c}{m^2}\int\frac{v_x u_x}{u^3}ff'\left(\frac{u^2}{\sigma_x^2}-\left(\frac{u_x^2}{\sigma_x^2}+\frac{u_y^2}{\sigma_y^2}+\frac{u_z^2}{\sigma_z^2}\right)\right)dv'^3\,dv^3$$

Temperature Exchange in Plasma (2)

- Substituting the distribution

$$\frac{d}{dt}\overline{\mathrm{v}_x{}^2}=\frac{4\pi e^4 nL_c}{(2\pi)^3\sigma_x{}^2\sigma_y{}^2\sigma_z{}^2 m^2}\int\frac{\mathrm{v}_x u_x}{u^3}\left(\frac{u^2}{\sigma_x{}^2}-\left(\frac{u_x{}^2}{\sigma_x{}^2}+\frac{u_y{}^2}{\sigma_y{}^2}+\frac{u_z{}^2}{\sigma_z{}^2}\right)\right)\exp\left(-\frac{\mathrm{v}_x{}^2+\mathrm{v}_x'^2}{2\sigma_x{}^2}-\frac{\mathrm{v}_y{}^2+\mathrm{v}_y'^2}{2\sigma_y{}^2}-\frac{\mathrm{v}_z{}^2+\mathrm{v}_z'^2}{2\sigma_z{}^2}\right)d\mathrm{v}'^3\,d\mathrm{v}^3$$

- Make transition to

$\mathbf{u}=\mathbf{v}-\mathbf{v}'$, $\quad\mathbf{w}=\mathbf{v}+\mathbf{v}'$, => $\mathbf{v}=\dfrac{\mathbf{u}+\mathbf{w}}{2},\mathbf{v}'=\dfrac{\mathbf{w}-\mathbf{u}}{2}$,

$$\frac{\partial\left(\mathrm{v}_x,\mathrm{v}_y,\mathrm{v}_z,\mathrm{v}_x',\mathrm{v}_y',\mathrm{v}_z'\right)}{\partial\left(u_x,u_y,u_z,w_x,w_y,w_z,\right)}=\begin{vmatrix}1/2&0&0&1/2&0&0\\0&1/2&0&0&1/2&0\\0&0&1/2&0&0&1/2\\-1/2&0&0&1/2&0&0\\0&-1/2&0&0&1/2&0\\0&0&-1/2&0&0&1/2\end{vmatrix}=1/8$$

$$\frac{d}{dt}\overline{\mathrm{v}_x{}^2}=\frac{4\pi e^4 nL_c}{8(2\pi)^3\sigma_x{}^2\sigma_y{}^2\sigma_z{}^2 m^2}\int\frac{(u_x+w_x)u_x}{2u^3}\left(\frac{u^2}{\sigma_x{}^2}-\left(\frac{u_x{}^2}{\sigma_x{}^2}+\frac{u_y{}^2}{\sigma_y{}^2}+\frac{u_z{}^2}{\sigma_z{}^2}\right)\right)\exp\left(-\frac{u_x{}^2+w_x{}^2}{4\sigma_x{}^2}-\frac{u_y{}^2+w_y{}^2}{4\sigma_y{}^2}-\frac{u_z{}^2+w_z{}^2}{4\sigma_z{}^2}\right)dw^3du^3$$

- Computing integral over w yields $2\sqrt{\pi}\sigma_i$ for each integration. =>

$$\frac{d}{dt}\overline{\mathrm{v}_x{}^2}=\frac{e^4 nL_c}{4\sqrt{\pi}\sigma_x\sigma_y\sigma_z m^2}\int\frac{u_x{}^2}{u^3}\left(\frac{u^2}{\sigma_x{}^2}-\left(\frac{u_x{}^2}{\sigma_x{}^2}+\frac{u_y{}^2}{\sigma_y{}^2}+\frac{u_z{}^2}{\sigma_z{}^2}\right)\right)\exp\left(-\frac{u_x{}^2}{4\sigma_x{}^2}-\frac{u_y{}^2}{4\sigma_y{}^2}-\frac{u_z{}^2}{4\sigma_z{}^2}\right)du^3$$

Temperature Exchange in Plasma (3)

- To compute integrals we use the identity: $\dfrac{1}{\theta^3} = \dfrac{1}{4\sqrt{\pi}}\int_0^\infty \sqrt{\lambda}\, e^{-\lambda\theta^2/4} d\lambda$

$$\frac{d}{dt}\overline{\mathrm{v}_x^{\,2}} = \frac{e^4 n L_c}{4\sqrt{\pi}\sigma_x\sigma_y\sigma_z m^2}\int_0^\infty \frac{\sqrt{\lambda}}{4\sqrt{\pi}} d\lambda \int \left(\frac{u^2}{\sigma_x^{\,2}} - \left(\frac{u_x^{\,2}}{\sigma_x^{\,2}} + \frac{u_y^{\,2}}{\sigma_y^{\,2}} + \frac{u_z^{\,2}}{\sigma_z^{\,2}}\right)\right) u_x^{\,2}\, \mathrm{e}^{-\frac{u_x^{\,2}+u_y^{\,2}+u_z^{\,2}}{4}\lambda}\, \mathrm{e}^{-\frac{u_x^{\,2}}{4\sigma_x^{\,2}}-\frac{u_y^{\,2}}{4\sigma_y^{\,2}}-\frac{u_z^{\,2}}{4\sigma_z^{\,2}}}\, d^3u$$

$$\Rightarrow \quad = \frac{e^4 n L_c}{4\sqrt{\pi}\sigma_x\sigma_y\sigma_z m^2}\int_0^\infty \frac{\sqrt{\lambda}}{4\sqrt{\pi}} d\lambda \int \left(\frac{u_y^{\,2}+u_z^{\,2}}{\sigma_x^{\,2}} - \frac{u_y^{\,2}}{\sigma_y^{\,2}} - \frac{u_z^{\,2}}{\sigma_z^{\,2}}\right) u_x^{\,2}\, \mathrm{e}^{-\frac{u_x^{\,2}+u_y^{\,2}+u_z^{\,2}}{4}\lambda}\, \mathrm{e}^{-\frac{u_x^{\,2}}{4\sigma_x^{\,2}}-\frac{u_y^{\,2}}{4\sigma_y^{\,2}}-\frac{u_z^{\,2}}{4\sigma_z^{\,2}}}\, d^3u$$

- Straightforward integration yields:

$$\frac{d}{dt}\overline{\mathrm{v}_x^{\,2}} = \frac{2\sqrt{\pi}e^4 n L_c}{\sigma_x\sigma_y\sigma_z m^2}\int_0^\infty \left(\frac{\left(\frac{1}{\sigma_x^{\,2}} - \frac{1}{\sigma_y^{\,2}}\right)}{\lambda + \frac{1}{\sigma_y^{\,2}}} + \frac{\left(\frac{1}{\sigma_x^{\,2}} - \frac{1}{\sigma_z^{\,2}}\right)}{\lambda + \frac{1}{\sigma_z^{\,2}}}\right) \frac{\sqrt{\lambda}\, d\lambda}{\left(\lambda + \frac{1}{\sigma_x^{\,2}}\right)^{3/2}\sqrt{\lambda + \frac{1}{\sigma_y^{\,2}}}\sqrt{\lambda + \frac{1}{\sigma_z^{\,2}}}}$$

- Finally, we rewrite:

$$\boxed{\frac{d}{dt}\overline{\mathrm{v}_x^{\,2}} = \frac{(2\pi)^{3/2} e^4 n L_c}{\sqrt{\sigma_x^{\,2}+\sigma_y^{\,2}+\sigma_z^{\,2}}\, m^2}\psi(\sigma_x,\sigma_y,\sigma_z)}$$

$$\boxed{\psi(\sigma_x,\sigma_y,\sigma_z) = \frac{\sqrt{\sigma_x^{\,2}+\sigma_y^{\,2}+\sigma_z^{\,2}}}{\sqrt{2\pi}\sigma_x\sigma_y\sigma_z}\int_0^\infty \left(\frac{\left(\frac{1}{\sigma_x^{\,2}} - \frac{1}{\sigma_y^{\,2}}\right)}{\lambda + \frac{1}{\sigma_y^{\,2}}} + \frac{\left(\frac{1}{\sigma_x^{\,2}} - \frac{1}{\sigma_z^{\,2}}\right)}{\lambda + \frac{1}{\sigma_z^{\,2}}}\right) \frac{\sqrt{\lambda}\, d\lambda}{\left(\lambda + \frac{1}{\sigma_x^{\,2}}\right)^{3/2}\sqrt{\lambda + \frac{1}{\sigma_y^{\,2}}}\sqrt{\lambda + \frac{1}{\sigma_z^{\,2}}}}}$$

Properties of Function $\psi(x,y,z)$

- Function $\psi(x,y,z)$ can be reduced to the sum off symmetric elliptic integrals

$$\psi\left(x,y,z\right)=\frac{\sqrt{2}r}{3\pi}\left(y^2\,\mathrm{R_D}\left(z^2,x^2,y^2\right)+z^2\,\mathrm{R_D}\left(x^2,y^2,z^2\right)-2x^2\,\mathrm{R_D}\left(y^2,z^2,x^2\right)\right)$$

where: $$\mathrm{R_D}\left(x,y,z\right)=\frac{3}{2}\int_0^\infty\frac{dt}{\sqrt{\left(t+x\right)\left(t+y\right)\left(t+z\right)^3}}\,,\quad r=\sqrt{x^2+y^2+z^2}$$

see algorithm for fast computation of $\psi(x,y,z)$ in Appendix to the lecture

- $\psi(x,y,z)$ depends on the ratios of its variables but not on r.
- $\psi(x,y,z)$ is symmetric relative to the variables y and z, and is normalized so that $\psi(0,1,1) = 1$.
- The energy conservation requires: $\psi(x,y,z)+\psi(y,z,x)+\psi(z,x,y)=0$

  ⇨ $\psi(1,0,1) = \psi(1,1,0) = -1/2$
- The thermal equilibrium corresponds to $\psi(1,1,1) = 0$.
- The function $\psi(0,y,z)$ can be approximated with ~0.5% accuracy by:

$$\psi\left(0,y,z\right)\simeq1+\frac{\sqrt{2}}{\pi}\ln\left(\frac{y^2+z^2}{2yz}\right)-0.055\left(\frac{y^2-z^2}{y^2+z^2}\right)^2$$

Properties of Function $\psi(x,y,z)$

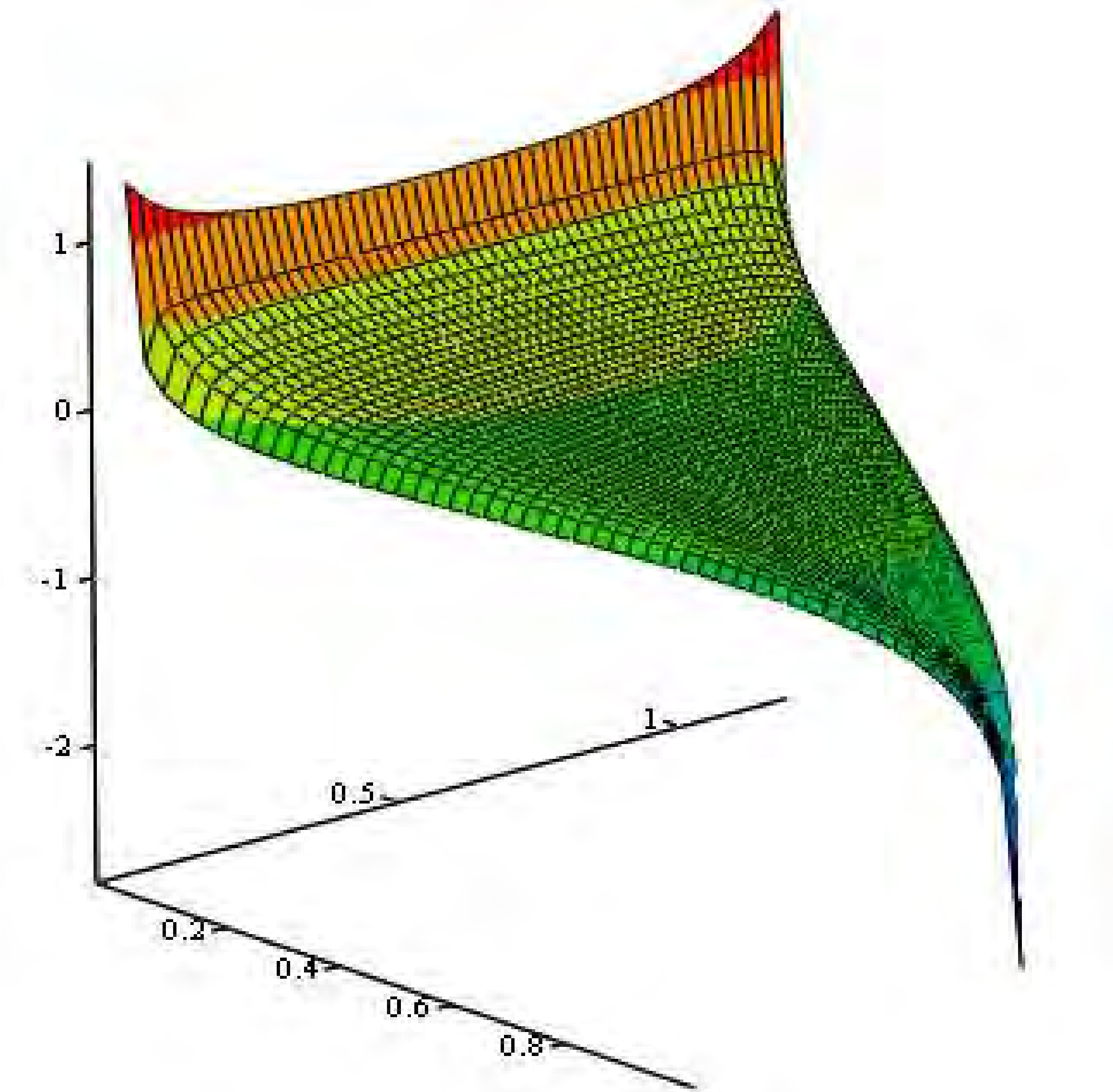

Function $\psi(0,y,z)$

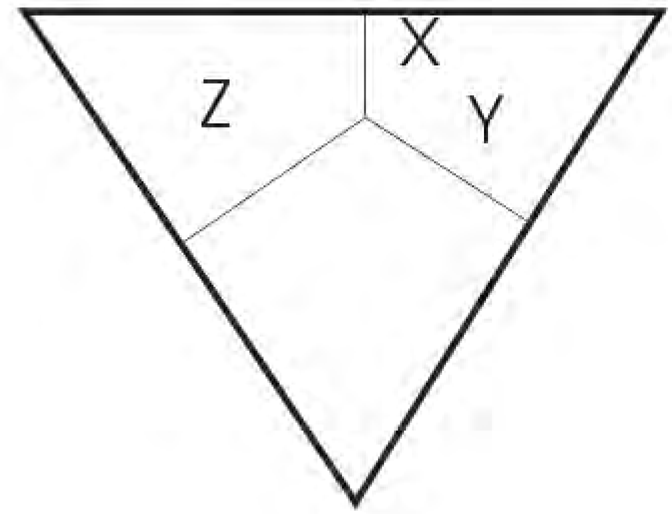

Boersch Effect

- In the course of the beam electrostatic acceleration its longitudinal temperature decreases as 1/E
  - Energy conservation yields || temperature in the beam frame

$$\begin{cases} E \\ E+T \end{cases} \xrightarrow[\textit{velosities}]{\textit{Corresponding}} \begin{cases} \mathrm{v}_0 = \sqrt{2E/m} \\ \mathrm{v}_0 + \Delta\mathrm{v} = \sqrt{2(E+T)/m} = \sqrt{\dfrac{2E}{m}}\left(1+\dfrac{T}{2E}\right) \end{cases} \Rightarrow \begin{cases} \Delta\mathrm{v} = \sqrt{\dfrac{1}{2Em}}T \\ T' = \dfrac{m\Delta\mathrm{v}^2}{2} = \dfrac{T^2}{4E} \end{cases}$$

  - Transverse temperature does not change much
    - For long transport the beam size can be stabilized by accompanying magnetic field

⇨ $T_{||} \ll T_{\perp}$

- IBS results in the energy transfer from ⊥ to || degree of freedom:

$$\boxed{\frac{d}{dt}\overline{\mathrm{v}_z^{\,2}} = \frac{(2\pi)^{3/2} e^4 n L_c}{\sqrt{\sigma_x^{\,2}+\sigma_y^{\,2}+\sigma_z^{\,2}}\,m^2}\psi(\sigma_z,\sigma_y,\sigma_y) \xrightarrow[\sigma_z^{\,2}\ll\sigma_\perp^{\,2}\Rightarrow\sigma_z^{\,2}=0]{\sigma_x^{\,2}=\sigma_y^{\,2}=\overline{\mathrm{v}_\perp^{\,2}}} \frac{d}{dt}\overline{\mathrm{v}_{||}^{\,2}} = \frac{2\pi\sqrt{\pi}e^4 n L_c}{m\sqrt{\overline{\mathrm{v}_\perp^{\,2}}}}}$$

Suppression of IBS by Strong Magnetic field

- Longitudinal-longitudinal relaxation set longitudinal temperature to

$$T_{\parallel} \approx \frac{T_c^{\,2}}{2W} + 1.9 e^2 n_e^{\,-1/3}$$

  after quarter of plasma period
- When $r_L \le n_e^{\,-1/3}$ magnetic field strongly suppresses IBS

INFLUENCE ON THE SIGN OF AN ION CHARGE ON FRICTION FORCE AT ELECTRON COOLING

N.S. Dikansky, N.Kh. Kot, V.I. Kudelainen, V.A. Lebedev, V.V. Parkhomchuk, A.A. Seriy, A.N. Skrinsky, B.N. Sukhina, V.D. Shiltsev

Institute of Nuclear Physics, 630090 Novosibirsk, USSR

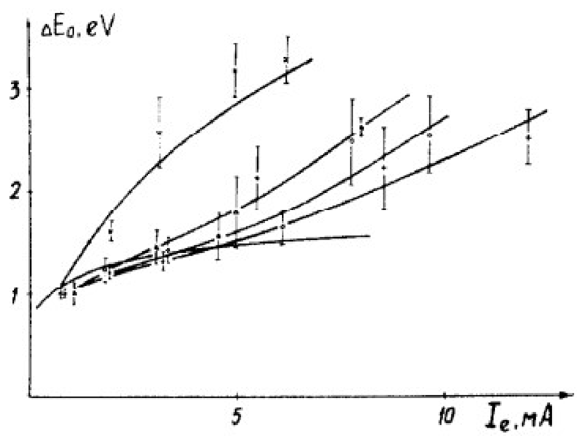

Fig. 6. The energy width ΔE_0 vs the electron current for different magnetic fields: 4(+), 3(o), 2(Δ) and 1 kGs (×), for positive and negative ions the values of ΔE_0 coincide accurate within the measurements. The dotted curve corresponds to expression $\Delta E_0 = \sqrt{32 W e^2 n^{1/3}}$.

Intrabeam Scattering in a Storage Ring

RMS Velocities in Smooth Lattice Approximation

$$\beta_x = \frac{R_0}{\nu_x}, \quad \beta_y = \frac{R_0}{\nu_y}, \quad D = \frac{R_0}{\nu_x^{\,3}}, \quad \alpha = \frac{1}{\nu_x^{\,2}}$$

- RMS velocities and angles
  - Trivial in vert. plane $\theta_y = \sqrt{\varepsilon_y / \beta_y}\,, \quad \mathrm{v}_y = \theta_y \beta\gamma c$
  - Radial and horizontal planes are coupled

$$f \propto \exp\left(-\frac{1}{2}\left(\frac{\left(x - D\theta_s\right)^2}{\varepsilon_x \beta_x} + \frac{\beta_x}{\varepsilon_x}\theta_x^{\,2} + \frac{\theta_s^{\,2}}{\sigma_p^{\,2}}\right)\right)$$

For Gaussian distribution temperatures across the beam do not depend on location. Therefore, it is sufficient to see in the beam center

$$f \propto \exp\left(-\frac{1}{2}\left(\left(\frac{D^2}{\varepsilon_x \beta_x} + \frac{1}{\sigma_p^{\,2}}\right)\theta_s^{\,2} + \frac{\beta_x}{\varepsilon_x}\theta_x^{\,2}\right)\right) = \exp\left(-\frac{\theta_x^{\,2}}{2\sigma_{\theta x}^{\,2}} - \frac{\theta_s^{\,2}}{2\sigma_{\theta s}^{\,2}}\right)$$

where $\sigma_{\theta x} = \sqrt{\dfrac{\varepsilon_x}{\beta_x}}\,, \quad \sigma_{\theta s} = \sqrt{\dfrac{\varepsilon_x \beta_x}{\varepsilon_x \beta_x + D^2 \sigma_p^{\,2}}}\,\sigma_p$

  - In the beam frame: $\sigma_{\mathrm{v}x} = \gamma\beta c\sqrt{\dfrac{\varepsilon_x}{\beta_x}}\,, \quad \sigma_{\mathrm{v}s} = \beta c\sqrt{\dfrac{\varepsilon_x \beta_x}{\varepsilon_x \beta_x + D^2 \sigma_p^{\,2}}}\,\sigma_p$

Thermal Equilibrium in Smooth Lattice Approximation

- Thermal equilibrium implies

$$\sigma_{vx} = \sigma_{vs} \Rightarrow \gamma\sqrt{\frac{\varepsilon_x}{\beta_x}} = \sqrt{\frac{\varepsilon_x\beta_x}{\varepsilon_x\beta_x + D^2\sigma_p{}^2}}\sigma_p \Rightarrow \gamma^2\left(\varepsilon_x\beta_x + D^2\sigma_p{}^2\right) = \beta_x{}^2\sigma_p{}^2$$

⇨ Momentum spread in equilibrium: $\boxed{\sigma_p = \gamma\sqrt{\frac{\varepsilon_x\beta_x}{\beta_x{}^2 - \gamma^2 D^2}}}$

- Denominator equal to zero at

$$\beta_x = \gamma_{tr} D \Rightarrow \frac{R_0}{\nu_x{}^2} = \gamma_{tr}\frac{R_0}{\nu_x{}^3} \Rightarrow \gamma_{tr} = \nu_x \xrightarrow{\alpha=1/\nu_x{}^2} \gamma_{tr} = \frac{1}{\sqrt{\alpha}}$$

i.e. at the transition energy
=> Equilibrium is impossible above transition

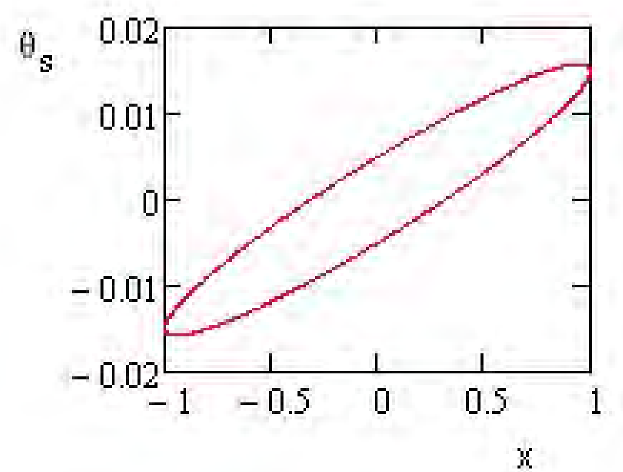

- In other words, the longitudinal particle mass changes its sign at the transition what makes the thermal equilibrium impossible above transition

IBS in Smooth Lattice Approximation

- In plasma: $\frac{d}{dt}\overline{\mathrm{v}_x^{\ 2}} = \frac{(2\pi)^{3/2} e^4 n L_c}{m^2\sqrt{\overline{\mathrm{v}_x^{\ 2}}+\overline{\mathrm{v}_y^{\ 2}}+\overline{\mathrm{v}_z^{\ 2}}}}\psi\left(\sqrt{\overline{\mathrm{v}_x^{\ 2}}},\sqrt{\overline{\mathrm{v}_y^{\ 2}}},\sqrt{\overline{\mathrm{v}_z^{\ 2}}}\right)$
- In the beam we need
  - to substitute velocity spreads in the beam frame

$$\sigma_{\mathrm{v}x} = \gamma\beta c\sqrt{\frac{\varepsilon_x}{\beta_x}}\ , \quad \sigma_{\mathrm{v}y} = \gamma\beta c\sqrt{\frac{\varepsilon_y}{\beta_y}}\ , \quad \sigma_{\mathrm{v}s} = \beta c\sqrt{\frac{\varepsilon_x\beta_x}{\varepsilon_x\beta_x + D^2\sigma_p^{\ 2}}}\sigma_p$$

  - average across the beam volume. For continues beam

$$n = \left(\frac{1}{\sqrt{2}}\right)^2 \frac{N}{2\pi\sigma_x\sigma_y C\gamma}$$

  - make transition to the lab frame and divide by 2 for oscillatory degrees of freedom

$$\frac{dp_\perp}{dt} = \frac{dp_\perp}{\gamma dt_{bf}} = \frac{1}{\gamma}\frac{d\mathrm{v}_\perp}{dt_{bf}}\ , \qquad \frac{dp_\parallel}{dt} = \frac{\gamma dp_\parallel}{\gamma dt_{bf}} = m\frac{d\mathrm{v}_\parallel}{dt_{bf}}$$

  - We also need to account that the longitudinal kicks contribute to the transverse emittance growth

$$\frac{d}{dt}\overline{\delta a_x^{\ 2}} = \beta_x\frac{d\varepsilon_x}{dt} = D^2\frac{d}{dt}\frac{\overline{\delta p^2}}{p^2} \Rightarrow \frac{d\varepsilon_x}{dt} = \frac{D^2}{\beta_x}\frac{d}{dt}\frac{\overline{\delta p^2}}{p^2}$$

IBS in Smooth Lattice Approximation (2)

- Performing the previous slide actions, one obtains the emittance growth rates for continuous beam:

$$\frac{d}{dt}\begin{bmatrix} \varepsilon_x \\ \varepsilon_y \\ \sigma_p{}^2 \end{bmatrix} = \frac{\sqrt{\pi}}{2\sqrt{2}}\frac{e^4 N L_c}{M^2 c^3 \sigma_x \sigma_y C \beta^3 \gamma^5 \sqrt{\theta_x{}^2+\theta_y{}^2+\theta_p{}^2}}\begin{bmatrix} \beta_x \psi\left(\theta_x,\theta_y,\theta_p\right)+\gamma^2 \dfrac{D^2}{\beta_x}\psi\left(\theta_p,\theta_x,\theta_y\right) \\ \beta_y \psi\left(\theta_y,\theta_x,\theta_p\right) \\ 2\gamma^2 \psi\left(\theta_p,\theta_x,\theta_y\right) \end{bmatrix}$$

where

$$\sigma_x=\sqrt{\varepsilon_x\beta_x+D^2\sigma_p{}^2}\ ,\quad \sigma_y=\sqrt{\varepsilon_y\beta_y}\ ,\quad \theta_x=\sqrt{\frac{\varepsilon_x}{\beta_x}}\ ,\quad \theta_y=\sqrt{\frac{\varepsilon_y}{\beta_y}}\ ,\quad \theta_p=\sqrt{\frac{\varepsilon_x\beta_x}{\varepsilon_x\beta_x+D^2\sigma_p{}^2}}\frac{\sigma_p}{\gamma}\equiv\frac{\sqrt{\varepsilon_x\beta_x}}{\sigma_x}\frac{\sigma_p}{\gamma}$$

- For the bunched beam with linear RF one needs to replace

$$\frac{1}{C}\to\frac{1}{\sqrt{2}}\frac{1}{\sqrt{2\pi}\sigma_s}$$

and $2\gamma^2\to\gamma^2$ in the bottom row of the matrix (because the energy is equally divided between potential and kinetic energies)

IBS in Relativistic Hadron Colliders

- At present energies the proton beam is non-relativistic in the beam frame. It enables to consider considered above non-relativistic collisions and greatly simplifies formulas
- For ultra-relativistic beam one can neglect the longitudinal velocity (in the beam frame) and set it to zero.
- In the absence of coupling the vertical emittance growth is suppressed as $(\nu_x/\gamma)^2$ and is negligible in comparison to the horizontal emittance growth
- Then in the smooth lattice approximation we have

$$\frac{d}{dt}\begin{bmatrix} \varepsilon_x \\ \varepsilon_y \\ {\sigma_p}^2 \end{bmatrix} = \frac{1}{4\sqrt{2}} \frac{e^4 N L_c \psi\left(0, \theta_x, \theta_y\right)}{M^2 c^3 \sigma_x \sigma_y \sigma_s \beta^3 \gamma^3 \sqrt{{\theta_x}^2 + {\theta_y}^2}} \begin{bmatrix} \dfrac{D^2}{\beta_x} \\ 0 \\ 1 \end{bmatrix}$$

  - ♦ As one can see both x and s planes are heated due to scattering from transverse planes to the longitudinal plane

IBS in Relativistic Hadron Colliders (2)

- It is straightforward to account for the actual beta-functions
- In this case we need to accurately account the hor. emittance heating only from || kicks

$$\begin{cases} x = D\theta_s \\ \theta_x = D'\theta_s \end{cases} \quad \Rightarrow \quad \Delta\varepsilon = \frac{x^2}{\beta_x}\left(1+\alpha_x{}^2\right) + 2\alpha_x x\theta + \beta_x\theta_x{}^2 = \left(\frac{D^2}{\beta_x}\left(1+\alpha_x{}^2\right) + 2\alpha_x DD' + \beta_x D'^2\right)\theta_s{}^2$$

$$\Rightarrow \quad \frac{d\varepsilon}{dt} = A_x \frac{d}{dt}\sigma_p{}^2 , \quad A_x = \frac{D^2}{\beta_x}\left(1+\alpha_x{}^2\right) + 2\alpha_x DD' + \beta_x D'^2 = \frac{D^2 + \left(D\alpha_x + D'\beta_x\right)^2}{\beta_x}$$

- Finally averaging over machine circumference, we obtain

$$\boxed{\frac{d}{dt}\begin{bmatrix} \varepsilon_x \\ \varepsilon_y \\ \sigma_p{}^2 \end{bmatrix} = \frac{1}{4\sqrt{2}} \frac{e^4 N}{M^2 c^3 \sigma_s \beta^3 \gamma^3} \left\langle \frac{\psi\left(0,\theta_x,\theta_y\right)}{\sigma_x\sigma_y\sqrt{\theta_x{}^2 + \theta_y{}^2}} \begin{bmatrix} A \\ 0 \\ 1 \end{bmatrix} \right\rangle_s}$$

where $\sigma_x = \sqrt{\varepsilon_x\beta_x + D^2\sigma_p{}^2}$, $\sigma_y = \sqrt{\varepsilon_y\beta_y}$, $\theta_x = \sqrt{\frac{\varepsilon_x}{\beta_x}\left(1 + \frac{\sigma_p{}^2\left(\beta_x D_x' + \alpha_x D_x\right)^2}{\sigma_x{}^2}\right)}$, $\theta_y = \sqrt{\frac{\varepsilon_y}{\beta_y}}$

and we can approximately write that

$$\psi\left(0,y,z\right) \simeq 1 + \frac{\sqrt{2}}{\pi}\ln\left(\frac{y^2+z^2}{2yz}\right) - 0.055\left(\frac{y^2-z^2}{y^2+z^2}\right)^2$$

IBS and Transverse Noise

- Noise in the magnetic field made significant contribution to the emittance growth

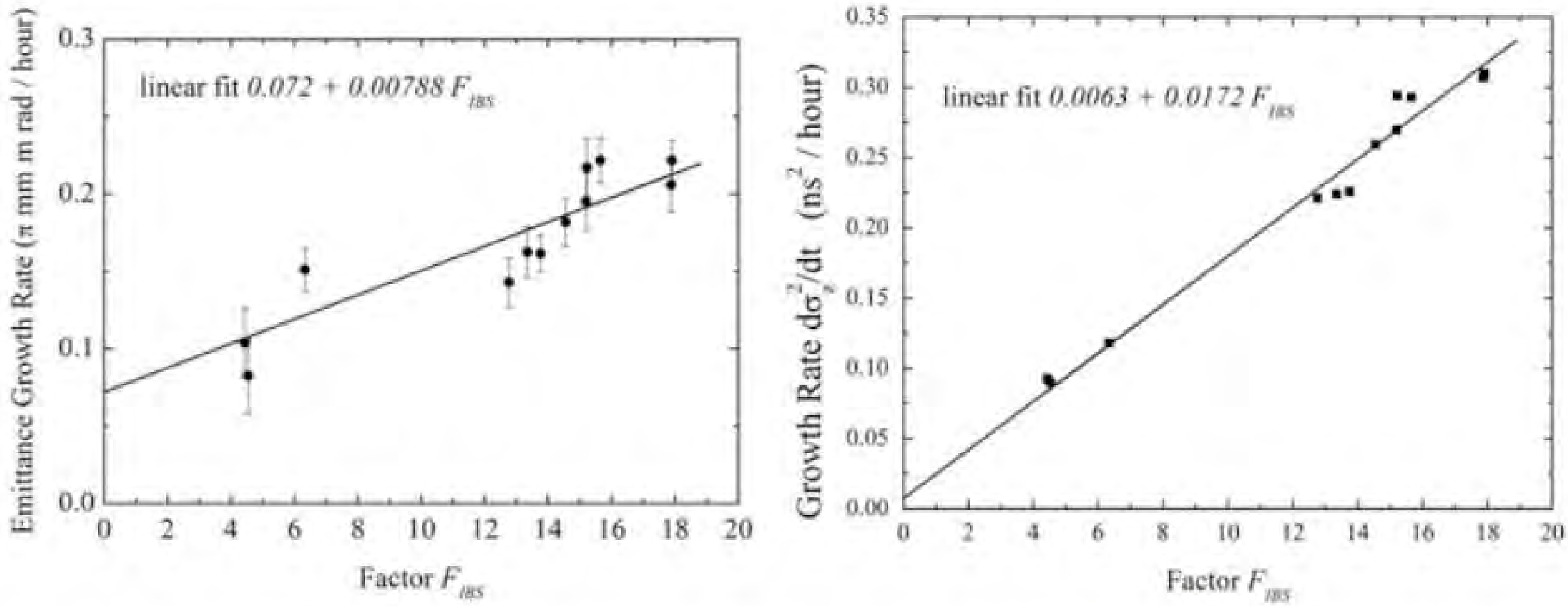

Fig. 6.12 Vertical emittance growth rates (rms, norm.) of proton bunches vs the IBS factor F_{IBS} (*left*); the rms bunch length growth rates vs the IBS factor F_{IBS} (*right*) [20]

- Measurements at injection energy showed that magnetic noise is smaller than then scattering at the residual gas. It is not right at the top energy (150->1000 GeV). $d\varepsilon/dt_{gas} \propto 1/\gamma^2, \quad d\varepsilon/dt_{noise} \propto 1/\gamma^0$

Reading

- Lenard-Balescu equations bind low and higher order distributions. Details can be found in any good plasma textbook.

References

1. "Accelerator Physics at the Tevatron Collider", edited by V. Lebedev and V. Shiltsev, Springer, 2014.
2. S. Nagaitsev, Phys. Rev. ST Accel. Beams 8, 064403 (2005).
3. H. Boersch, Z. Phys. 139, 115 (1954)

Problems

1. Prove that for gaussian distribution with equal temperatures for all degrees of freedom the Landau collision integral in plasma yields $df/dt=0$.
2. Electron beam with 2 mm diameter, energy 500 V and the beam current of 5 mA passes distance of 2 mm. Find rms energy spread at the exit. Weak magnetic field keeps the transverse beam size constant, but does not affect on the intrabeam scattering.
3. Prove that for ultra-relativistic beam the vertical emittance growth is suppressed as $(\nu_x/\gamma)^2$ relative to the horizontal emittance growth. Use the smooth lattice approximation.
4. Prove that the rms local horizontal angular spread in the beam is

$$\theta_x = \sqrt{\frac{\varepsilon_x}{\beta_x}\left(1+\frac{\sigma_p{}^2\left(\beta_x D_x' + \alpha_x D_x\right)^2}{\sigma_x{}^2}\right)}$$

Appendix: Algorithm for fast computation of symmetric elliptic integral

$C1 := \frac{3}{14}$ $\quad C2 := \frac{1}{6}$ $\quad C3 := \frac{9}{22}$ $\quad C4 := \frac{3}{26}$ $\quad C5 := \frac{9}{88}$ $\quad C6 := \frac{9}{52}$

$ERRTOL := 0.05$

$R_D(x,y,z) :=$

```
xt ← x
yt ← y
zt ← z
delx ← 1
dely ← 1
delz ← 1
sum ← 0.0
fac ← 1.0
while max(|delx|, |dely|, |delz|) > ERRTOL
    sqrtx ← √xt
    sqrty ← √yt
    sqrtz ← √zt
    alamb ← sqrtx·(sqrty + sqrtz) + sqrty·sqrtz
    sum ← sum + fac / (sqrtz·(zt + alamb))
    fac ← 0.25·fac
    xt ← 0.25·(xt + alamb)
    yt ← 0.25·(yt + alamb)
    zt ← 0.25·(zt + alamb)
    ave ← 0.2·(xt + yt + 3.0·zt)
    delx ← (ave − xt) / ave
    dely ← (ave − yt) / ave
    delz ← (ave − zt) / ave
ea ← delx·dely
eb ← delz·delz
ec ← ea − eb
ed ← ea − 6.0·eb
ee ← ed + ec + ec
return 3.0·sum + fac·(1.0 + ed·(−C1 + C5·ed − C6·delz·ee) + delz·[C2·ee + delz·(−C3·ec + delz·C4·ea)]) / (ave·√ave)
```

Lectures 12-14: High Energy Cooling

Valeri Lebedev
JINR & Fermilab

US Particle Accelerator School
February 2022

Objectives

- Presently, there are two major methods of the cooling the electron cooling and stochastic cooling.
- The stochastic cooling can be additionally separated on (1) the microwave stochastic cooling, (1) the optical stochastic cooling (OSC) and (3) the coherent electron cooling (CEC).
  - OSC and CEC are essentially extensions of microwave stochastic cooling operating in 1-10 GHz frequency range to the optical frequencies corresponding to 30-300 THz frequency range.
    - The OSC uses undulators as a pickup and a kicker, and an optical amplifier for signal amplification,
    - while the CEC uses an electron beam for all these functions.
- In these 3 lectures we consider electron and stochastic cooling mostly concentrating on cooling of high energy heavy particles (protons or ions) in the high energy colliders. Further in all equations we assume protons – the most challenging case.
- In the next lecture we consider the stochastic cooling at optical wavelengths

Electron cooling

- Invented in 1966 by A. M. Budker
  - In the beam frame - heavy particles come into equilibrium with electron gas
- Tested experimentally in BINP, Novosibirsk, in 1974-79 at NAP-M
  - 35 keV electron beam (65 MeV protons)
  - Magnetized electron cooling

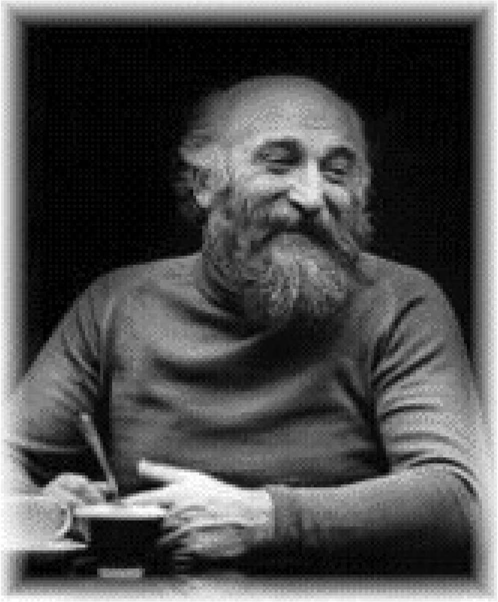

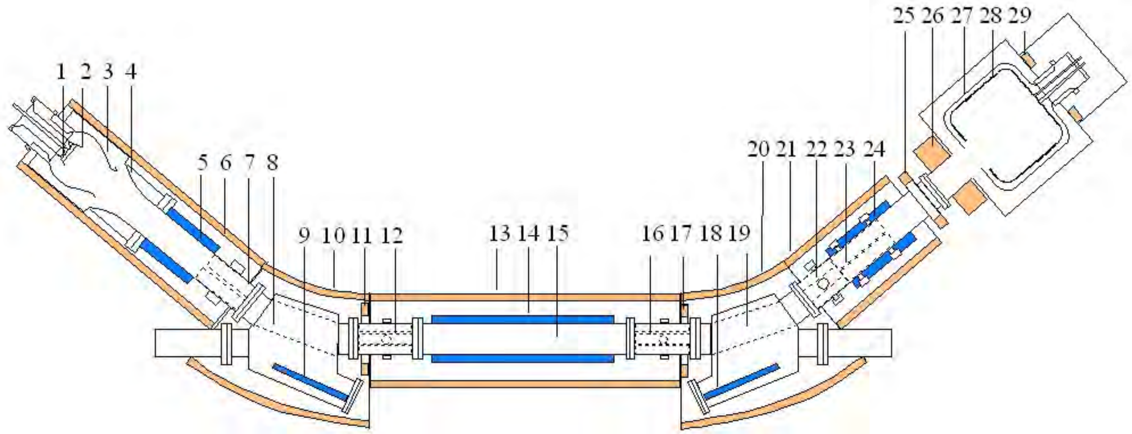

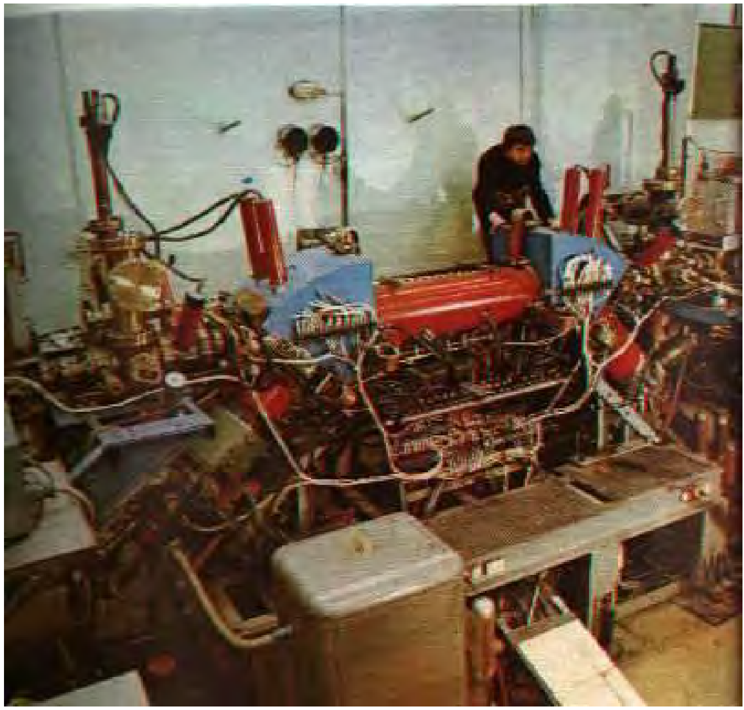

- Many installations since then, up to 300 kV electron beam (GSI, Darmstadt)
- FNAL 4.3 MeV cooler – next step in technology

Electron Cooling at FNAL (1)

- Fermilab made next step in the electron cooling technology
- Main Parameters
  - 4.34 MeV pelletron
  - 0.5 A DC electron beam with radius of about 4 mm
  - Magnetic field in the cooling section - 100 G
  - Interaction length – 20 m (out of 3319 m of Recycler circumference)

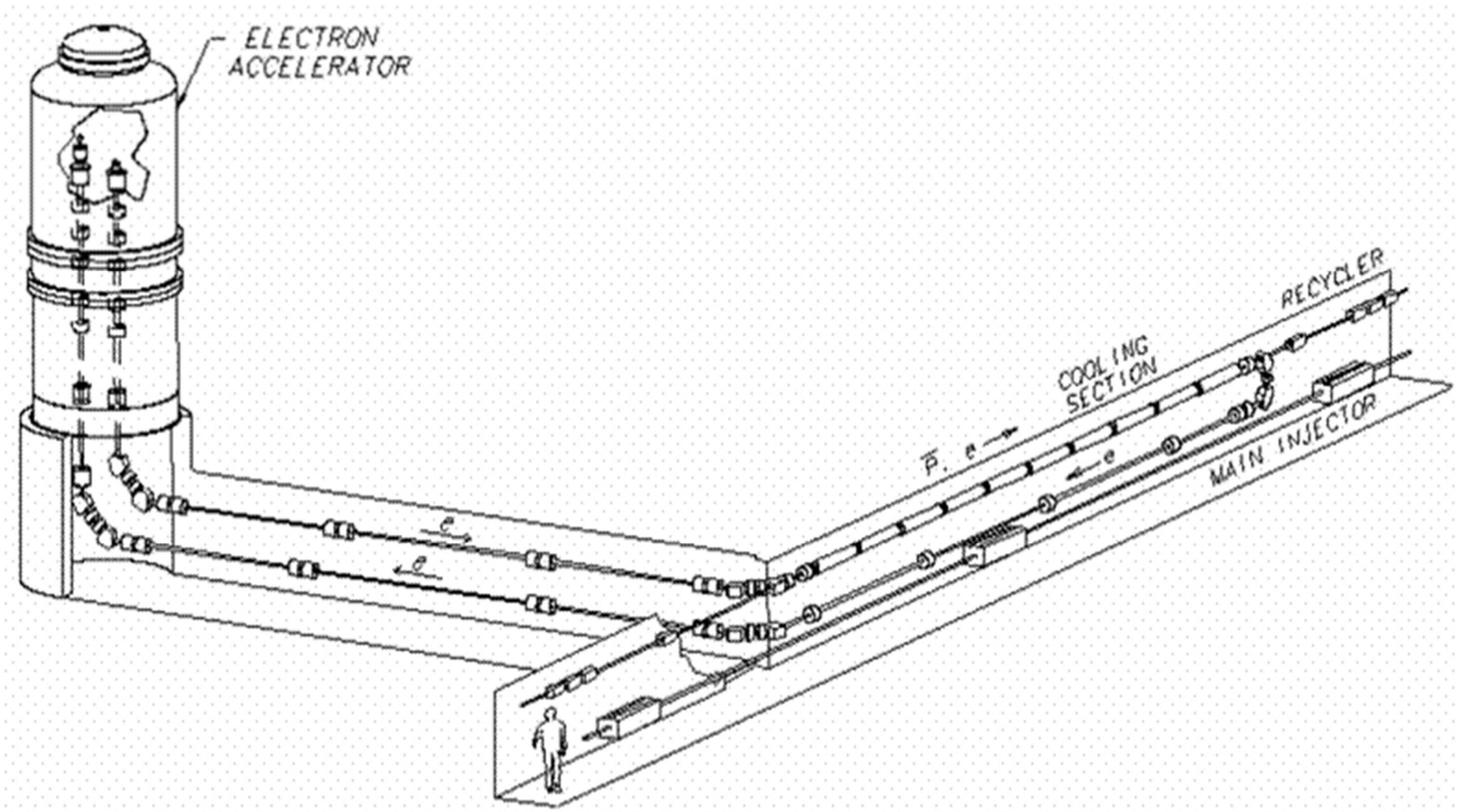

Stochastic Cooling

- Invented in 1969 by Simon van der Meer
- Naïve transverse cooling model
  - 90 deg. between pickup and kicker

    $\delta\theta = -g\theta$
  - Averaging over betatron oscillations yields

    $$\delta\overline{\theta^2} = -\frac{1}{2}2g\overline{\theta^2} \equiv -g\overline{\theta^2}$$
  - Adding noise of other particles yields

    $$\delta\overline{\theta^2} = -g\overline{\theta^2} + N_{sample}g^2\overline{\theta^2} \equiv -\left(g - N_{sample}g^2\right)\overline{\theta^2}$$
  - That yields

$$\boxed{\delta\overline{\theta^2} = -\frac{1}{2}g_{opt}\overline{\theta^2} \quad , \quad g_{opt} = \frac{1}{2N_{sample}} \quad , \quad N_{sample} \approx N\frac{f_0}{W}}$$

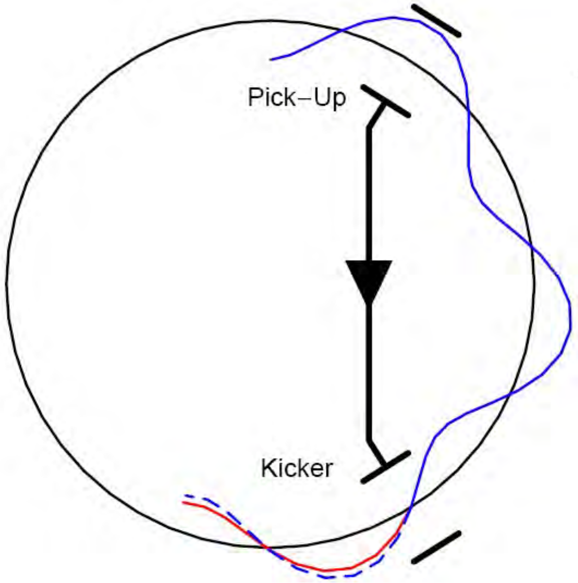

- In accurate analytical theory the cooling process is described by Fokker-Planck equation
  - The theory is built on the same principle as plasma theory – which is a perturbation theory (large number of particles in the Debye sphere versus large number of particles in the sample

Requirements for Cooling in Collision Mode

- Cooling time is typically set by IBS.
  - 20-40 minutes for ep collider for 275 GeV protons
- Cooling acceptances
  - Good beam lifetime in the presence of beam-beam effects requires cooling range to be > 5 - 6 σ.
- Overcooling in the bunch center has to be avoided
  - Overcooling greatly amplifies beam-beam effects
  - Ideally the cooling force should be proportional to particle amplitudes

Historical Remarks

- Maximum beam energy achieved in electron cooling with 8 GeV protons was demonstrated in Fermilab in the course of Tevatron Run II (2001 -2011).
  - This energy is well below required for most of modern proton colliders. There are few ideas how energy increase can be accomplished but no definite plans to demonstrate it in experiment
- The stochastic cooling was absolutely essential for stacking and cooling antiprotons in SPPS (CERN) and Tevatron (Fermilab).
  - Up to 2021, the stochastic cooling has been only operating at the microwave frequencies ($f < 8$ GHz).
  - BNL demonstrated SC of bunched heavy ions at RHIC
- First cooling at optical frequencies – the OSC - was demonstrated in Fermilab with electrons in 2021.
  - Passive OSC for now
  - A usage of electrons greatly decreased the cost of the experiment but still enabled us to study the physics in detail

Electron versus Stochastic Cooling

- The electron and stochastic cooling are based on completely different principles.
- The electron cooling is dissipative in its principle of operation and therefore the Liouville theorem is not applicable. That enables direct reduction of the beam phase space.
- The stochastic cooling is a "Hamiltonian" process which formally does not violate the Liouville theorem and cooling happens due to the phase space mapping so that phase space volumes containing particles are moved to the beam center while the rest mostly moves out. That makes stochastic colling rates strongly dependent on the beam particle density.
- Each method has its own domain where it achieves a superior efficiency. The electron cooling is preferred at a smaller energy and momentum spread, and its efficiency weakly depends on the particle density in the cooled beam. While the stochastic cooling is preferred at a higher energy, but its efficiency reduces fast with increase of particle phase density.

Electron Cooling

Cooling Force in non-magnetized Cooling

$$\mathbf{F}(\mathbf{v}) = \frac{4\pi n_e e^4 L_c}{m_e} \int f(\mathbf{v}') \frac{\mathbf{v}-\mathbf{v}'}{\left|\mathbf{v}-\mathbf{v}'\right|^3} d\mathbf{v}'^3 = \frac{4\pi n_e e^4 L_c}{m_e} \nabla_{\mathrm{v}} \left(\int \frac{f(\mathbf{v}')}{\left|\mathbf{v}-\mathbf{v}'\right|} d\mathbf{v}'^3 \right)$$

Coulomb logarithm

$$L_c = \ln\left(\frac{r_{\max}}{r_{\min}}\right), \quad r_{\min} \approx \frac{2e^2}{m_e \mathrm{v}_{eff}^{\ 2}}, \quad r_{\max} \approx \frac{\mathrm{v}_{eff}}{\omega_p}, \quad \mathrm{v}_{eff} = \max\left(|\mathbf{v}|, \overline{\mathrm{v}}_e\right),$$

The term with $dD_{ij}/d\mathrm{v}_j$ is im m_p/m_e times smaller and can be neglected

- By-Gaussian distribution of electrons in velocity

$$f(\mathbf{v}_\perp, \mathrm{v}_{||}) = \frac{1}{(2\pi)^{3/2} \sigma_{\mathrm{v}||} \sigma_{\mathrm{v}\perp}^{\ 2}} \exp\left(-\frac{\mathrm{v}_{||}^{\ 2}}{2\sigma_{\mathrm{v}||}^{\ 2}} - \frac{\mathbf{v}_\perp^{\ 2}}{2\sigma_{\mathrm{v}\perp}^{\ 2}} \right), \quad \mathrm{v}_{||} \ll \mathrm{v}_\perp$$

- Similar to the IBS, the following formula $\dfrac{1}{\theta} = \dfrac{1}{\sqrt{\pi}} \displaystyle\int_0^\infty e^{-\lambda^2\theta^2} d\lambda$

enables to reduce the cooling force to single dimensional integral

$$\mathbf{F}(\mathbf{v}) = \frac{4\pi n_e e^4 L_c}{m_e} \nabla_{\mathrm{v}} \left(\frac{2}{\sqrt{\pi}} \int_0^\infty \frac{\exp\left(-\dfrac{\mathrm{v}_{||}^{\ 2} t^2}{1+2\sigma_{\mathrm{v}||}^{\ 2} t^2} - \dfrac{\mathbf{v}_\perp^{\ 2} t^2}{1+2\sigma_{\mathrm{v}\perp}^{\ 2} t^2} \right)}{\sqrt{\left(1+2\sigma_{\mathrm{v}||}^{\ 2} t^2\right)\left(1+2\sigma_{\mathrm{v}\perp}^{\ 2} t^2\right)^2}} dt \right)$$

Cooling Force

- For T_{beam}=0 the cooling force is

$$\mathbf{F}(\mathbf{v}) = \frac{4\pi n_e e^4 L_c}{m_e}\frac{\mathbf{v}}{\mathbf{v}^3}$$

- The force saturates at velocity where the plasma perturbation theory stops to work:

$$\rho_{\min} \approx \rho_{\max} \quad \text{or} \quad e^2 n^{1/3} \approx m\mathrm{v}^2/2$$

$$\Rightarrow F_{\max} \approx e^2 n^{2/3}$$

The velocity, where the maximum is achieved, is orders of magnitude smaller than rms velocity in the proton beam

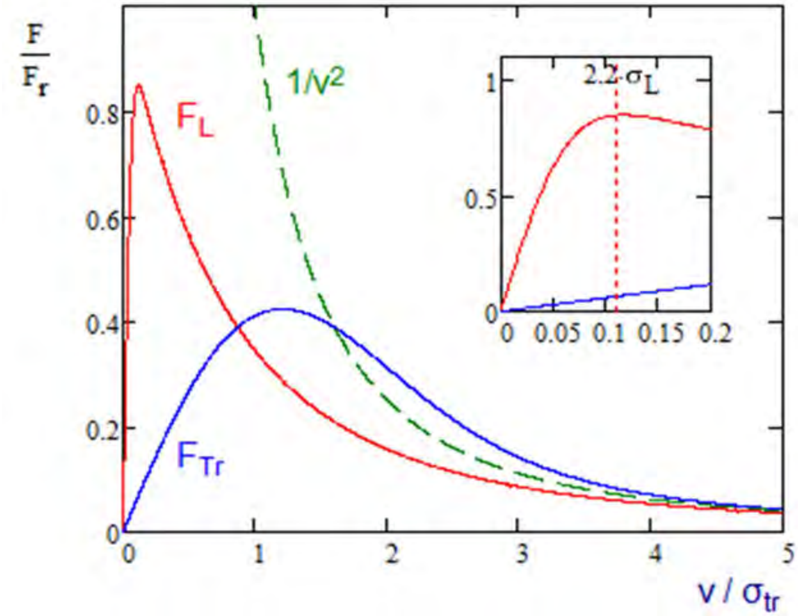

|| ($F_{||}(\mathrm{v}_{||}, \mathrm{v}_{\perp}=0)$) and $\perp$ ($F_{\perp}(\mathrm{v}_{||}=0, \mathrm{v}_{\perp})$) cooling forces on particle velocity; $F_r = 4\pi n_e e^4 L_c / (m_e \sigma_{\mathrm{v}\perp}{}^2)$, $\sigma_{\mathrm{v}||} = \sigma_{\mathrm{v}\perp}/20$.

- For electrostatic acceleration temperatures are:

$$T_\perp \approx T_{cathotde}\ , \quad T_{||} \approx T_{cathotde}{}^2/W + 2e^2 n^{1/3} \ll T_\perp$$

- Strong accompanying magnetic field freezes out $T_\perp$ (magnetized cooling)
  - That greatly increases cooling force at small velocities. However, it is not helpful for collider cooling where T_{proton_beam} is much larger
  - It only makes overcooling in the distribution center

Cooling Rates for Highly Relativistic El. Cooling

- For practical applications

$$\lambda_{\parallel} \approx \frac{4\sqrt{2\pi} n_e r_e r_p L_c}{\gamma^4 \beta^4 \left(\Theta_{\perp} + 1.083\Theta_{\parallel}/\gamma\right)^{3/2} \sqrt{\Theta_{\perp}\Theta_{\parallel}}} L_{cs} f_0 \ ,$$

$$\lambda_{\perp} \approx \frac{\pi\sqrt{2\pi} n_e r_e r_p L_c}{\gamma^5 \beta^4 \Theta_{\perp}^{\ 2} \left(\Theta_{\perp} + \sqrt{2}\Theta_{\parallel}/\gamma\right)} L_{cs} f_0 \ ,$$

$$\frac{\Theta_{\parallel}}{\gamma\Theta_{\perp}} \le 2 .$$

$$\Theta_{\parallel} = \sqrt{\theta_{\parallel e}^{\ 2} + \theta_{\parallel p}^{\ 2}} \ ,$$

$$\Theta_{\perp} = \sqrt{\theta_{\perp e}^{\ 2} + \theta_{\perp p}^{\ 2}} \ ,$$

- Beam power grows fast with beam energy. For fixed $L_{cs} f_0$ one has

$$P = mc^2(\gamma - 1) \cdot \pi r_{eb}^{\ 2} e n_e c\beta \xrightarrow[r_{eb}^{\ 2} \propto 1/\gamma]{\varepsilon_n = const} \propto \gamma\gamma^5 \frac{1}{\gamma} = \gamma^5$$

  - For the 275 GeV proton beam one needs ~100 A electron beam current. It corresponds ~10 GW reactive beam power
- Typical rms angles in proton beam is ~10 - 20 μrad for 275 GeV
  - The straightness of magnetic field should be better – the extremely challenging problem

Possible Implementation of HE Electron Cooling

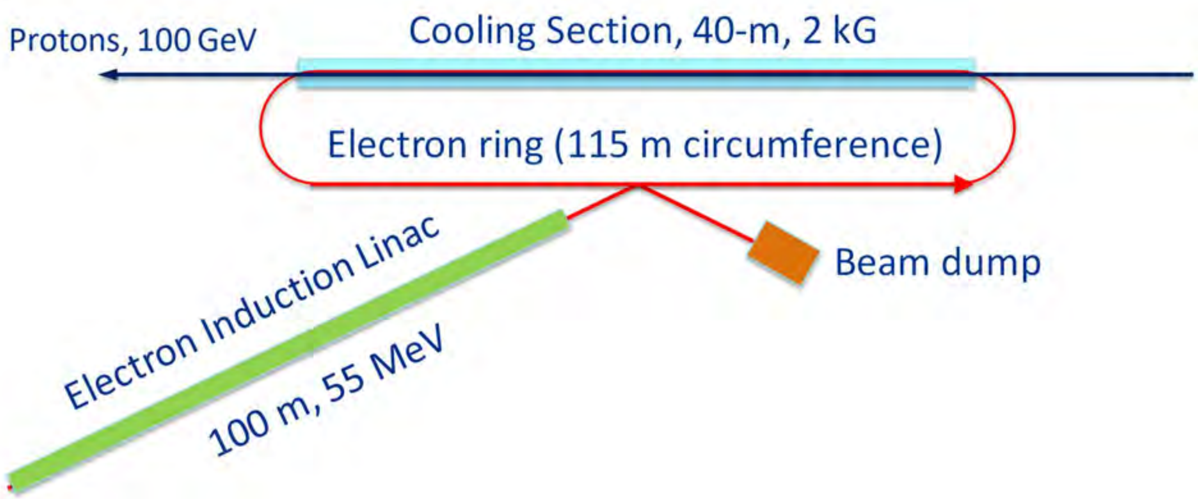

- Acceleration beam in induction linac with subsequent beam recirculation for ~10,000 turns (limited by IBS in e-beam). P~1 MW
  - The number of turns is limited by IBS in the electron beam
- Derbenev's transform is used to optimally match proton and electron velocities in the cooling section
  - Fully coupled ring optics
  - Electron gun cathode emersed in long. magnetic field to create rotational modes
- Major challenges: (1) space charge in electron beam, (2) beam stability (CSR impedances), (3) emittance growth due to interaction with proton bunches (suppressed by integer number of electron rotations in the cooling section)

Derbenev's Adapter (Transform)

- Transformation of rotational betatron modes to flat uncoupled beam
  - Achieved by system of skew-quads making 90° difference in betatron phase advances for 2 planes (directed along quad planes)

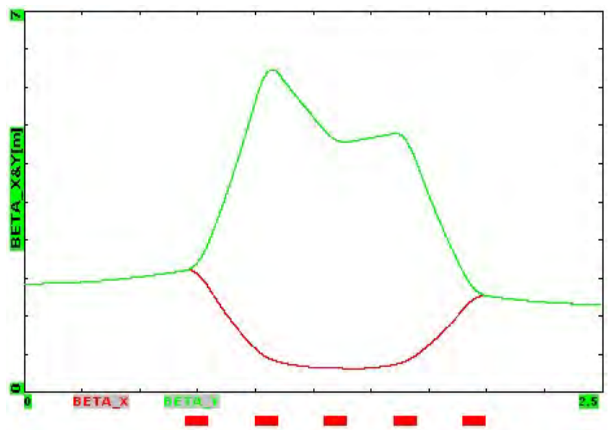

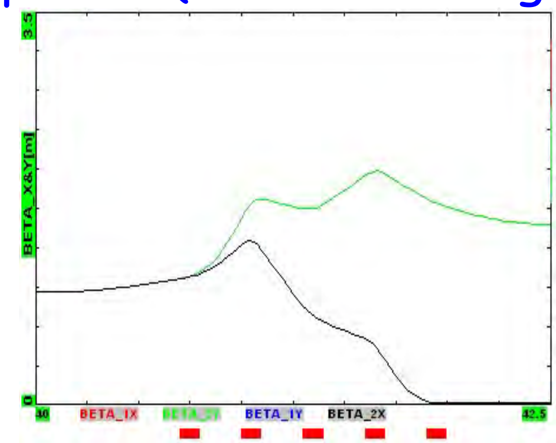

$$\begin{bmatrix} \sqrt{\beta} \\ -\dfrac{i/2+\alpha}{\sqrt{\beta}} \\ \sqrt{\beta_{1y}}\,e^{i\pi/2} \\ -\dfrac{i/2+\alpha}{\sqrt{\beta}}\,e^{i\pi/2} \end{bmatrix} \rightarrow \begin{bmatrix} \sqrt{\beta} \\ -\dfrac{i/2+\alpha}{\sqrt{\beta}} \\ \sqrt{\beta_{1y}} \\ -\dfrac{i/2+\alpha}{\sqrt{\beta}} \end{bmatrix}$$

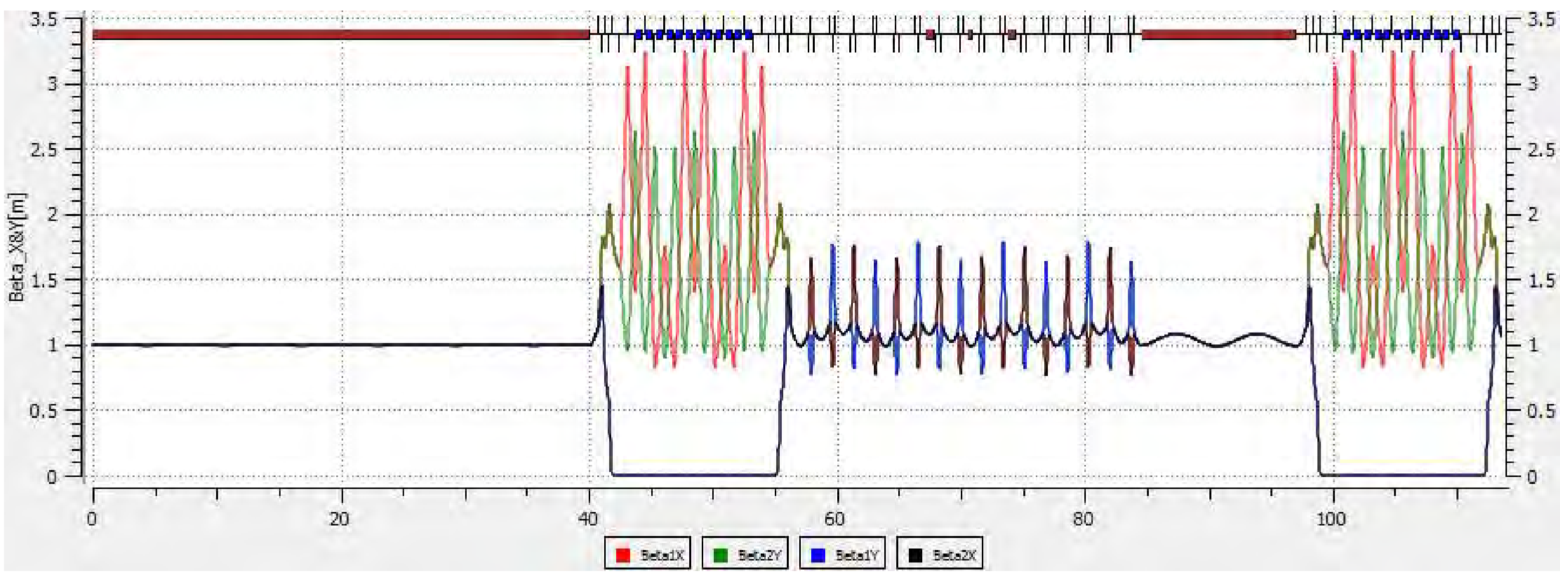

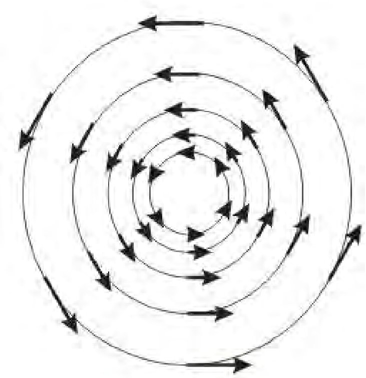

Why Do We Need Derbenev's Adapter

- In the absence of magnetic field x and y norm. emittances are equal and are conserved in further beam motion/manipulations; $\varepsilon_{4n}=\varepsilon_{xn}\varepsilon_{yn}$
- Introduction of magnetic field enables controlled redistribution of mode emittances; $\varepsilon_{4n}=\varepsilon_{xn}\varepsilon_{yn}$

$$\varepsilon_{1n,2n} = \frac{\sqrt{\varepsilon_{4n}}}{\sqrt{1+\Phi_r^{\,2}\beta_0^{\,2}} \pm \Phi_r \beta_0}$$

where $\beta_0 = a_e^{\,2} / (\varepsilon_n / \beta\gamma)$ is the effective beta-function, a_e is the electron beam radius in the cooling section, β and γ are the relativistic factors, B_0 is the magnetic field in the cooling solenoid, and $\Phi_r = eB_0 / (2\gamma\beta m_e c^2)$ is its focusing strength.

⇨ independent control of the beam size and transverse angles

⇨ It enables to avoid large β-functions which makes beam optics more stable

- There was recently published a paper suggesting electron cooling for ep-collider without magnetic field in the cooling section
  - For the suggested parameters the interaction with proton beam space charge destroys the electron beam emittance at a fraction of cooling section length

Discussion on High Energy Electron Cooling

- Cooling at proton energies above ~20 GeV cannot be done as a classical electron cooling with electrostatic acceleration
- That leaves the following possibilities (or their combination):
  - Acceleration in the energy recovery SC linac
    - Bunching of electrons reduces current in comparison with DC beam
    - Small number of turns in a ring was also considered to additionally reduce linac current (problem with frequent injection & extraction)
  - Acceleration in energy recovery linac with beam storage in a ring for long time. Fast cooling of electrons to prevent IBS (Possibilities: SR cooling with wigglers, OSC)
  - Acceleration in induction linac with beam circulation in a ring for many turns
- Only last proposal was elaborated in some details
    - Still there are not answered questions (chromaticity of Derbenev adapter)
- All choices are extremely challenging and require both theoretical and experimental studies

Stochastic Cooling

Methods of Longitudinal (Microwave) Stochastic Cooling

- Palmer cooling
  - Diff. pickup signal is proportional to particle momentum. It is measured by pickup at high dispersion location
  - Example: FNAL Accumulator
- Filter cooling
  - Signal proportional to particle momentum is obtained as difference of particle signals for two successive turns (notch filter)

$$U(t)=u(t)-u\left(t-T_0\left(1+\eta\frac{\Delta p}{p}\right)+T_0\right)\approx\frac{du}{dt}T_0\eta\frac{\Delta p}{p}$$

  - Examples: FNAL Debuncher and Recycler
- Transient time cooling
  - No signal treatment
  - The same expression for kick as for FC
  - Larger diffusion => less effective than FC
  - Examples: OSC, CEC

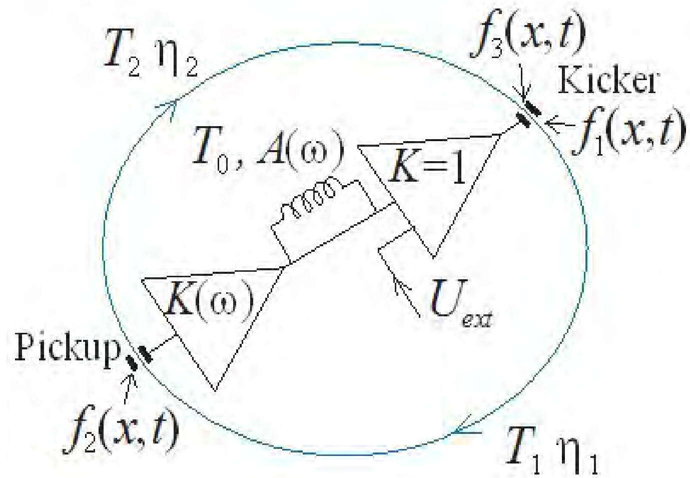

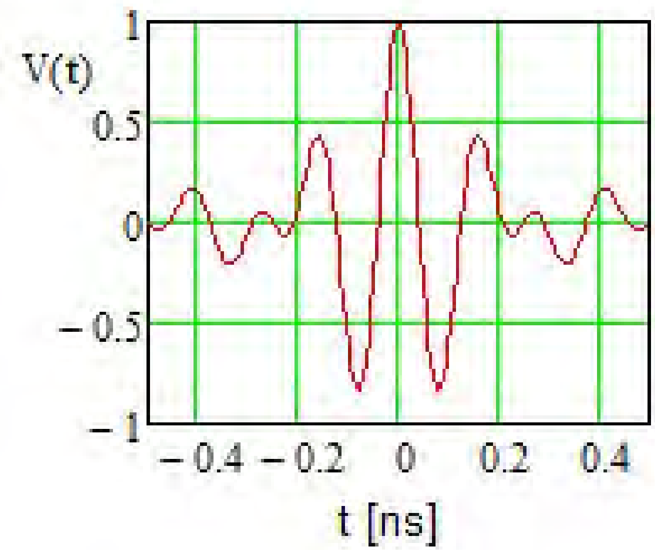

particle in a system with constant gain in 4-8 GHz band

Before we start: Basics of Stochastic Cooling Theory

- SC theory is closely related to the plasma perturbation theory
  - Similar to the Vlasov equation with Landau collision term

$$\frac{\partial \psi}{\partial t}+\mathrm{v}_i\frac{\partial \psi}{\partial x_i}+\frac{\partial}{\partial p_i}\left(eE_i\psi\right)=\frac{1}{2}\frac{\partial}{\partial p_i}\left(F_i(x)\psi+D_{ij}(x)\frac{\partial \psi}{\partial p_j}\right)$$

    - No coherent motion (otherwise too large power)

      $\Rightarrow$ only $\partial\psi/\partial t$ is left in the left-hand side
  - Friction -> Cooling force
  - Diffusion due to collisions -> Diffusion due to particle interaction through cooling system
    - Diffusion coefficient is proportional to the spectral density of Schottky noise (slow process => non-resonant terms are negligible)
      - At betatron sidebands for $\perp$ cooling
      - At revolution harmonics for || cooling
  - Signal suppression due to particle interaction through cooling system
    - Reduces both Cooling Force and Diffusion
  - In most practical cases one can neglect cross-plane diffusion (D_{ij}=0, $i\neq j$)

Schottky Noise

Fourier transform: applicable if $f(t)\xrightarrow{t\to\pm\infty}0$

$$f_\omega=\frac{1}{2\pi}\int_{-\infty}^{\infty} f(t)e^{-i\omega t}dt \Leftrightarrow f(t)=\int_{-\infty}^{\infty} f_\omega e^{i\omega t}d\omega\ ,$$

$$\int_{-\infty}^{\infty} e^{i\omega t}d\omega=2\pi\delta(t)\ \Rightarrow\ \int_{-\infty}^{\infty}\left|f(t)\right|^2dt=\int_{-\infty}^{\infty}dt\int_{-\infty}^{\infty}\int_{-\infty}^{\infty}d\omega d\omega' f_\omega f_{\omega'}{}^* e^{i(\omega-\omega')t}=2\pi\int_{-\infty}^{\infty}\left|f_\omega\right|^2d\omega$$

Spectral density of random noise: $f(t)$ is not zero at $t\to\pm\infty$ => divergence of FT

$$\overline{f_\omega f_{\omega'}{}^*}=P(\omega)\delta(\omega-\omega')\ \Rightarrow$$

$$K(\tau)\equiv\overline{f(t)f^*(t-\tau)}=\frac{1}{T}\int_{-T/2}^{T/2}f(t)f^*(t-\tau)dt=\frac{1}{T}\int_{-T/2}^{T/2}\left(\int_{-\infty}^{\infty}\int_{-\infty}^{\infty}d\omega d\omega' f_\omega f_{\omega'}{}^* e^{i\omega(t-(t-\tau))}\right)dt$$

$$=\frac{1}{T}\int_{-T/2}^{T/2}dt\left(\int_{-\infty}^{\infty}\int_{-\infty}^{\infty}d\omega d\omega' P(\omega)\delta(\omega-\omega')e^{i\omega\tau}\right)=\frac{1}{T}\int_{-T/2}^{T/2}\left(\int_{-\infty}^{\infty}e^{i\omega\tau}P(\omega)d\omega\right)dt=\int_{-\infty}^{\infty}P(\omega)e^{i\omega\tau}d\omega$$

Schottky noise of random pulses: $U(t)=\sum_n u(t-t_n)$

$$\overline{U^2}=\frac{1}{T}\int_{-T/2}^{T/2}dt\sum_{n,m}u(t-t_n)u^*(t-t_m)=\frac{1}{T}\int_{-T/2}^{T/2}dt\left(\int_{-\infty}^{\infty}\int_{-\infty}^{\infty}d\omega d\omega'\sum_{n,m}u_\omega u_{\omega'}\overline{e^{i(\omega(t-t_n)-\omega'(t-t_n))}}\right)\xrightarrow{\overline{e^{i(\omega(t-t_n)-\omega'(t-t_m))}}=\delta_{nm}e^{i(\omega-\omega')(t-t_n)}}$$

$$\int_{-\infty}^{\infty}\int_{-\infty}^{\infty}u_\omega u_{\omega'}d\omega d\omega'\frac{1}{T}\int_{-T/2}^{T/2}dt\sum_n e^{i(\omega-\omega')(t-t_n)}=\dot{n}\int_{-\infty}^{\infty}\int_{-\infty}^{\infty}u_\omega u_{\omega'}d\omega d\omega'\int_{-\infty}^{\infty}dte^{i(\omega-\omega')t}=2\pi\dot{n}\int_{-\infty}^{\infty}\left|u_\omega\right|^2d\omega$$

$\boxed{P(\omega)=2\pi\dot{n}\left|u_\omega\right|^2}$. For el. current $u(t)=e\delta(t)$ => $P_I(\omega)=\dfrac{e^2\dot{n}}{2\pi}=\dfrac{eI}{2\pi}$ => $\boxed{\overline{\Delta I^2}=2eI\Delta f}$

Schottky Noise in Circulating Beam

$$u(t) = e\delta(t) \;\Rightarrow\; u(t) = e\sum_{k=-\infty}^{\infty}\delta(t-kT) \quad \& \quad u_\omega = \frac{1}{T}e\sum_{k=-\infty}^{\infty}\delta\left(\omega - \frac{2\pi}{T}k\right)$$

$$P_I(\omega) = \frac{eI}{2\pi} \;\Rightarrow\; \boxed{P(\omega) = \frac{eI}{2\pi}\sum_{n=-\infty}^{\infty}\frac{\psi_0\left(x(\omega/n)\right)}{\left|n\eta\left(x(\omega/n)\right)\right|}} \qquad \eta(x) = -\frac{1}{\omega}\frac{d\omega}{dx}, \quad x = \frac{\Delta p}{p}, \quad \int\psi_0(x)\,dx = 1$$

- This equation correctly describes noise even if Schottky bands overlap

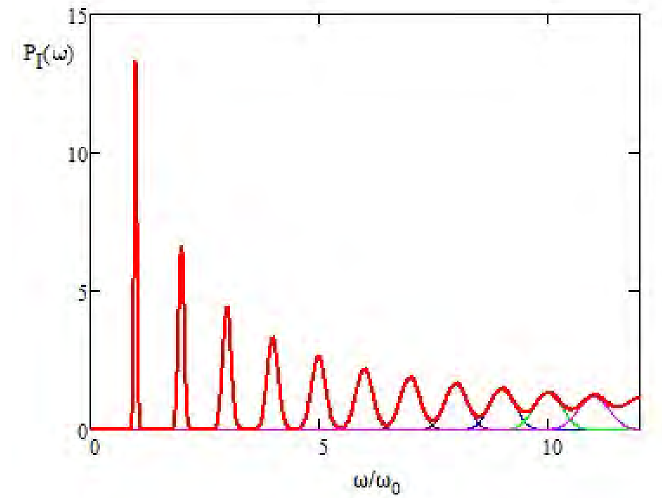

- In vicinity of *n*-th harmonic for constant η one obtains:

$$\boxed{P_I(\Delta\omega_n) \equiv P_I(\omega - n\omega_0) = \frac{eI}{2\pi}\frac{1}{|k\eta|}\psi_0\left(\frac{\Delta\omega_n}{n\omega_0\eta}\right)}$$

- Compute integral around one harmonic: (accounting negative frequency will double it)

$$\overline{\Delta I_n{}^2} = \overline{\Delta I_{-n}{}^2} = \int P_I(\Delta\omega_n)d\Delta\omega_n = \int\frac{eI}{2\pi}\frac{1}{|n\eta|}\psi_0\left(\frac{\Delta\omega_n}{n\omega_0\eta}\right)d\Delta\omega_n = \frac{eI\omega_0}{2\pi} \quad \text{compare to} \quad \overline{\Delta I^2} = 2eI\Delta f$$

  - *i.e.* integral around each harmonic does not depend on *n* and the relative current fluctuations at n-th harmonic are: $\sqrt{\frac{\overline{\Delta I_n{}^2}}{I_0{}^2}} = \sqrt{\frac{e\omega_0}{2\pi I}} = \frac{1}{\sqrt{N}}$
  - Schottky bands overlap when: $\omega_0 \approx n_{th}\omega_0\eta\frac{\Delta p}{p} \Rightarrow n_{th} \approx \frac{1}{\eta\,\Delta p/p}$

Effect of Random Noise on Oscillator

Noise spectral density and correlation function

$$\overline{f(t)f(t+\tau)} \equiv K(\tau) = \int_{-\infty}^{\infty} P(\omega)e^{i\omega\tau}d\omega, \quad K(\tau) = K(-\tau) \quad \Rightarrow \quad P(\omega) = P(-\omega) \ge 0$$

Growth of particle amplitude due to noise

- Equation of motion $\boxed{\ddot{x} + \omega_0{}^2 x = f(t)}$
- Solution: $x(t) = \dfrac{1}{\omega_0}\displaystyle\int_0^t f(t')\sin\left(\omega_0(t-t')\right)dt'$
- Growth of RMS amplitude with time

$$\overline{x(t)^2} = \frac{1}{\omega_0{}^2}\int_0^t dt'\int_0^t dt''\,\overline{f(t')f(t'')}\sin\left(\omega_0(t-t')\right)\sin\left(\omega_0(t-t'')\right) \quad \Rightarrow \quad \boxed{\overline{x(t)^2} = \frac{2\pi t}{\omega_0{}^2}P(\omega_0)}$$

Growth of particle amplitude due to kicker noise in a ring

- Only resonance harmonics contributes to $d\varepsilon/dt$
  - 1/2 in $d\varepsilon_\perp/dt$ due to oscillatory motion

$$\boxed{\begin{array}{ll} \dfrac{d}{dt}\overline{\Delta \mathrm{E}^2} = \dfrac{\omega_0{}^2}{2\pi}\displaystyle\sum_{n=-\infty}^{\infty} P_{\mathrm{E}}(\omega_0 n)\,, & \overline{\delta \mathrm{E}^2} = \displaystyle\int_{-\infty}^{\infty} P_{\mathrm{E}}(\omega)d\omega \\ \dfrac{d\varepsilon_\perp}{dt} \equiv \dfrac{1}{\beta}\dfrac{d}{dt}\overline{x(t)^2} = \dfrac{\beta\omega_0{}^2}{4\pi}\displaystyle\sum_{n=-\infty}^{\infty} P_\theta(\omega_0(\nu+n))\,, & \overline{\theta^2} = \displaystyle\int_{-\infty}^{\infty} P_\theta(\omega)d\omega \end{array}}$$

Signal Suppression in Longitudinal Cooling

- Denote: $x \equiv \Delta p / p$
- No particle interaction

  => evolution of particle distribution:

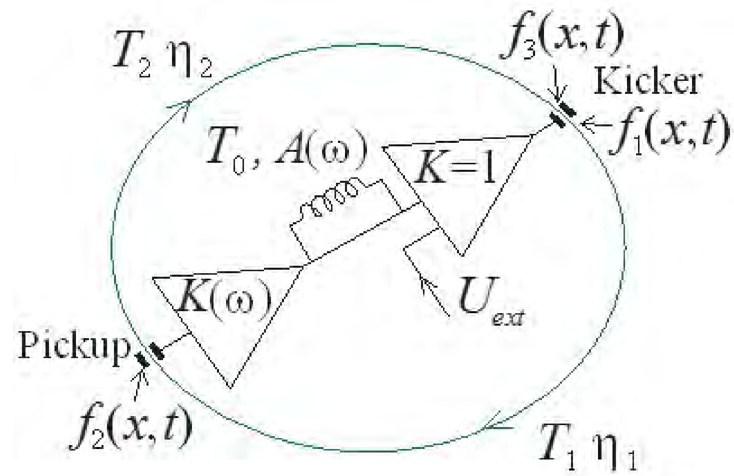

$$\begin{cases} \psi f_2(x,t) = \psi_1(x, t - T_1(x)) \\ \psi_3(x,t) = \psi_2(x, t - T_2(x)) \\ \psi_1(x,t) = \psi_3(x - \delta p(t)/p_0,\ t) \end{cases}$$

where
$$\begin{cases} T_1(x) = T_{10} + T_0\eta_1 x + \ldots \\ T_2(x) = T_{20} + T_0\eta_2 x + \ldots \\ T(x) = T_0(1 + \eta x + \ldots) \end{cases}$$

$\eta = \alpha - 1/\gamma^2$ is the slip-factor, and we call η_1 and η_2 the partial slip-factors

- Expending the last Eq. => $\tilde{\psi}_1(x,t) = \tilde{\psi}_3(x,t) - \dfrac{\delta p(t)}{p_0}\dfrac{d\psi_0(x)}{dx}$

  and performing Fourier transform

$$\begin{cases} \tilde{\psi}_{2\omega}(x) = \tilde{\psi}_{1\omega}(x)\exp(-i\omega T_1(x)) \\ \tilde{\psi}_{3\omega}(x) = \tilde{\psi}_{2\omega}(x)\exp(-i\omega T_2(x)) \\ \tilde{\psi}_{1\omega}(x) = \tilde{\psi}_{3\omega}(x) - (df_0(x)/dx)(\delta p_\omega / p_0) \end{cases}$$

$$\Rightarrow \tilde{\psi}_{2\omega}(x)e^{i\omega T_1(x)} = \tilde{\psi}_{2\omega}(x)e^{-i\omega T_2(x)} - \frac{d\psi_0(x)}{dx}\frac{\delta p_\omega}{p_0}$$

Signal Suppression in Longitudinal Cooling (2)

- Introduce Longitudinal Cooling Gain (most general case)

$$\frac{\delta p_\omega}{p_0} = \frac{\Delta p_{ext\omega}}{p_0} + \int e^{-i\omega T_{20}} \left[1 - A(\omega) e^{-i\omega T_0} \right] G(x,\omega) \tilde{\psi}_{2\omega}(x) dx$$

A(ω)=0 – Palmer cooling, A(ω)=1 – filter cooling

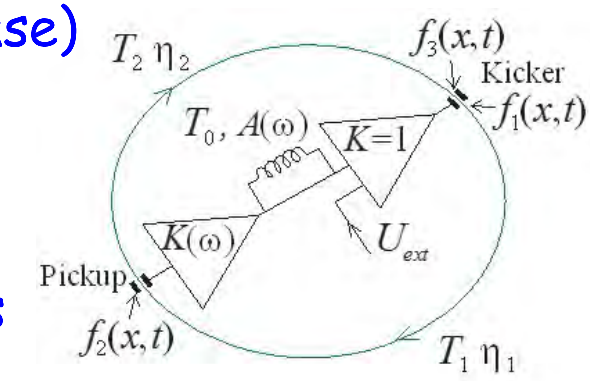

- On other hand, pickup signal at frequency ω depends on hor. particle coordinate ($X = D\Delta p / p \equiv Dx$)

$$U_{pickup\,\omega} = I_0 \int Z_p(x,\omega) \psi_{2\omega}(x,\omega) dx \xrightarrow[Z_{ampl}=50\Omega]{\delta E_{kicker\omega} = eU_{kicker\omega}\left(Z_k(\omega)/Z_{ampl}\right)} \boxed{G(x,\omega) = \frac{eI_0 Z_p(x,\omega) Z_k(\omega)}{\gamma\beta^2 mc^2 Z_{ampl}} K(\omega)}$$

- Combining we obtain Eq. for $\tilde{f}_{2\omega}(x)$

$$\tilde{\psi}_{2\omega}(x)\left[e^{i\omega T_1(x)} - e^{-i\omega T_2(x)}\right] + \frac{d\psi_0(x)}{dx}\left[\frac{\Delta p_{ext\omega}}{p_0} + e^{-i\omega T_{20}}\left[1 - A(\omega)e^{-i\omega T_0}\right]\int dx' \tilde{\psi}_{2\omega}(x') G(x',\omega)\right] = 0$$

- Solving we obtain pickup signal excited by external perturbation

$$\boxed{S_\omega \equiv \int dx' \tilde{\psi}_{2\omega}(x') G(x',\omega) = -\frac{1}{\varepsilon(\omega)} \frac{\Delta p_{ext\omega}}{p_0} \int_{\delta \to 0_+} \frac{d\psi_0(x)}{dx} \frac{G(x',\omega) e^{i\omega T_2(x)}}{e^{i\omega T(x)} - (1-\delta)} dx}$$

$$\varepsilon(\omega) = 1 + \left(1 - A(\omega)e^{-i\omega T_0}\right) \int_{\delta \to 0_+} \frac{d\psi_0(x)}{dx} \frac{G(x,\omega) e^{i\omega(T_2(x) - T_2(0))}}{e^{i\omega T(x)} - (1-\delta)} dx$$

$$\boxed{\xrightarrow[\text{overlap}]{\text{Far away from band}} \varepsilon(\omega) = 1 + \left(1 - A(n\omega_0)e^{2\pi i n\eta y}\right) \frac{1}{2\pi i n\eta} \int_{\delta \to 0_+} \frac{d\psi_0(x)}{dx} \frac{G(x, n\omega_0)}{x - y - i\delta\,\mathrm{sign}(n\eta)} dx\,, \quad \omega = n\omega_0(1 - \eta y)}$$

Discussion: Signal Suppression in Long. Cooling

- For cooling of fixed number of particles, signal suppression is negligible (*i.e.* $\varepsilon \approx 1$) at the beginning and becomes important with cooling
  - Simplified formula can be used
- For particle accumulation the signal suppression is negligible at the process beginning and becomes important at full intensity if system operates near or at band overlap
  - Exact formula has to be used

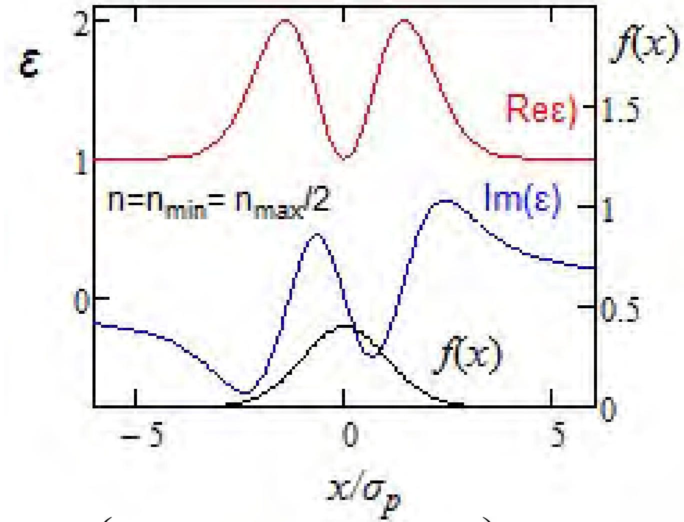

- Palmer cooling: $G(x,\omega) = -G_n' x$ - near n^{th} harmonic

$$\varepsilon(y) = 1 - \frac{G_n'}{2\pi i n\eta} \int_{\delta\to 0_+} \frac{d\psi_0(x)}{dx} \frac{x dx}{x - y - i\delta\,\mathrm{sign}(n\eta)} = 1 - \frac{G_n'}{2\pi i n\eta} \int_{\delta\to 0_+} \frac{d\psi_0(x)}{dx}\left(1 + \frac{y}{x - y - i\delta\,\mathrm{sign}(n\eta)}\right)dx$$

$$\boxed{\varepsilon(y) = 1 + i\frac{G_n'}{2\pi n\eta} y \int_{\delta\to 0_+} \frac{d\psi_0(x)}{dx} \frac{dx}{x - y - i\delta\,\mathrm{sign}(n\eta)}}$$ where $y = \Delta\omega_n / (\eta n \omega_0)$

- Filter cooling: $G(x,\omega) = -iG(n\omega_0) = -iG_n$ - near n-th harmonic

$$\left(1 - A(n\omega_0)e^{2\pi i n\eta y}\right) \xrightarrow[2\pi i n\eta y \ll 1]{A(n\omega_0)=1} -2\pi i n\eta\, y \quad \Rightarrow \quad \boxed{\varepsilon(y) = 1 + iG_n y \int_{\delta\to 0_+} \frac{d\psi_0(x)}{dx} \frac{dx}{x - y - i\delta\,\mathrm{sign}(n\eta)}}$$

- For constant gain: suppression is decreased with harmonic number as ~1/n for Palmer cooling, and stays the same in Filter cooling

Theory of Longitudinal Stochastic Cooling

Cooling force

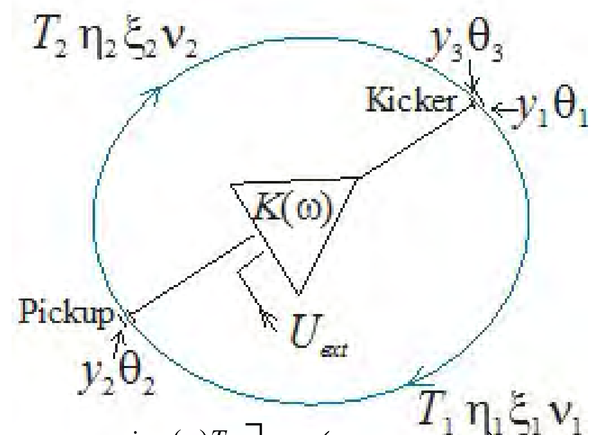

- The gain was introduced as

$$\frac{\delta p_\omega}{p_0} = \frac{\Delta p_{ext\omega}}{p_0} + \int e^{-i\omega T_2(0)} \left[1 - A(\omega) e^{-i\omega T_0}\right] G(x,\omega)\tilde{\psi}_{2\omega}(x)dx$$

For single particle: $\psi(x,t) = \delta(x - x_0)\dfrac{e}{T(x)} \sum_{n=-\infty}^{\infty} \delta(t - t_0 - nT(x))$

summing for all harmonics yields: $\dfrac{\delta p}{p_0} = \sum_n e^{i\omega_n(x)(T_2(x)-T_{20})} \left[1 - A(\omega_n(x)) e^{-i\omega_n(x)T_0}\right] G(x,\omega_n(x))$

⇨ Cooling force $F(x) \equiv \dfrac{dx}{dt} = \dfrac{1}{T_0}\sum_{n=-\infty}^{\infty} \dfrac{G_1(x,\omega_n(x))}{\varepsilon(\omega_n(x))}\left(1 - A(\omega_n(x)) e^{-i\omega_n(x)T_0}\right) e^{i\omega_n(x)(T_2(x)-T_{20})}$

where we additionally accounted for signal suppression

Diffusion

- To obtain diffusion one needs
  - find noise spectral density at the pickup
  - Multiply by the transfer function (responses of pickup and kicker, & amplifier gain)
  - account for signal suppression
  - find effect of kicker noise on particle motion

Equations Describing Longitudinal Stochastic Cooling

- Finally we can write

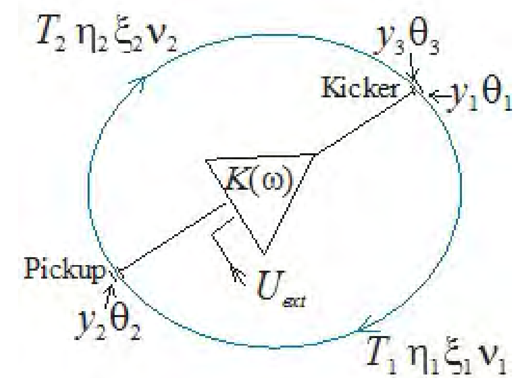

$$\frac{\partial \psi}{\partial t}+\frac{\partial}{\partial x}\left(F(x)\psi\right)=\frac{1}{2}\frac{\partial}{\partial x}\left(D(x)\frac{\partial \psi}{\partial x}\right)$$

$\psi(x)$ is the distribution function, $x \equiv \Delta p / p$

$$F(x)\equiv\frac{dx}{dt}=\frac{1}{T_0}\sum_{n=-\infty}^{\infty}\frac{G(x,\omega_n)}{\varepsilon(\omega_n)}\left(1-A(\omega_n)e^{-i\omega_n T_0}\right)e^{i\omega_n T_0\eta_2 x}, \qquad \omega_n=n\omega_0(1-\eta x)$$

$$D(x)=\frac{N}{T_0}\sum_{n=-\infty}^{\infty}\left|G(x,\omega_n)\right|^2\left|\left(1-A(\omega_n)e^{-i\omega_n T_0}\right)\right|^2\begin{cases}\dfrac{\psi(x)}{|n\eta|\left|\varepsilon(\omega_n)\right|^2}, & \text{no band overlap}\\ 1, & \text{complete band overlap}\end{cases}$$

$$\varepsilon(\omega)=1+\left(1-A(\omega)e^{-i\omega T_0}\right)N\int_{\delta\to 0_+}\frac{d\psi(x)}{dx}\frac{G(x,\omega)e^{i\omega T_0\eta_2 x}}{e^{i\omega T_0(1+\eta x)}-(1-\delta)}dx$$

- Amplifier noise is not accounted (insignificant in most of real systems)
- Note: the theory is built on the same principle as plasma theory - which is a perturbation theory (large number of particles in the Debye sphere versus large number of particles in the sample)

Equations Describing Transverse Stochastic Cooling

- Fokker-Planck equation in the action-phase variables describes transverse cooling in the case of linear transverse motion

$$\frac{\partial \psi}{\partial t} + \lambda_\perp(x)\frac{\partial}{\partial I}\left(I\psi\right) = D_\perp(x)\frac{\partial}{\partial I}\left(I\frac{\partial \psi}{\partial I}\right) \xrightarrow{\times I \text{ \& Integrating}} \frac{\partial \overline{I(x,t)}}{\partial t} - \lambda_\perp(x)\overline{I(x,t)} = D_\perp(x)$$

$\lambda(x)$ and $D(x)$ do not depend on I

$\psi(x,I)$ is the distribution function, $\psi_\parallel(x) = \int \psi(x,I)dI$

$$\lambda_\perp(x) = \frac{1}{T_0}\sum_{n=-\infty}^{\infty}\mathrm{Re}\left(\frac{G_\perp\left(\omega_{n\perp}(x)\right)}{i\varepsilon_\perp\left(\omega_{n\perp}(x)\right)}e^{i\omega_n\left(T_2(x)-T_{20}\right)-2\pi i\nu_2(x)}\right) ,$$

$$\omega_{n\perp}(x) = \frac{2\pi n}{T(x)} - \nu(x) \approx \omega_0\left(n(1-\eta x)-(\nu+\xi x)\right) .$$

$$D_\perp(x) = \sum_{n=-\infty}^{\infty}\frac{1}{\left|\varepsilon_\perp(\omega_{n\perp}(x))\right|^2}\left(\frac{\pi\beta_k}{2T_0^{\,2}}\left(\frac{e\left|Z_{k\perp}\left(\omega_{n\perp}(x)\right)\right|}{mc^2\beta^2\gamma Z_{ampl}}\right)^2 P_{\perp U}\left(\omega_{n\perp}(x)\right) + \left|G_\perp(\omega_{n\perp}(x))\right|^2\frac{\overline{I(x)}N\psi_\parallel(x)}{2T_0\left|\nu'(x)+\eta(x)n\right|}\right)$$

$$\varepsilon_\perp(\omega) = 1 - \frac{G_\perp(\omega)N}{2}\int_{\delta\to 0_+}\frac{\left[e^{-i\omega T(x)}\sin\left(2\pi\nu_2(x)\right)+\sin\left(2\pi\nu_1(x)\right)\right]e^{i\omega\left(T_2(x)-T_{20}\right)}}{\cos\left(\omega T(x)\right)-\cos\left(2\pi\nu(x)\right)+i\delta\sin\left(\omega T(x)\right)}\psi_\parallel(x)dx$$

- Amplifier noise is referenced to the pickup output
    - Negligible in most of real systems

Cooling Force and Cooling Range for Palmer Cooling

- Palmer cooling: $G(x,\omega) = -xG'(\omega); \quad A(\omega) = 0$

$$F(x) = -\frac{1}{T_0}\sum_{n=-\infty}^{\infty} G'(n\omega_0)e^{i\omega_n T_0 \eta_2 x}$$

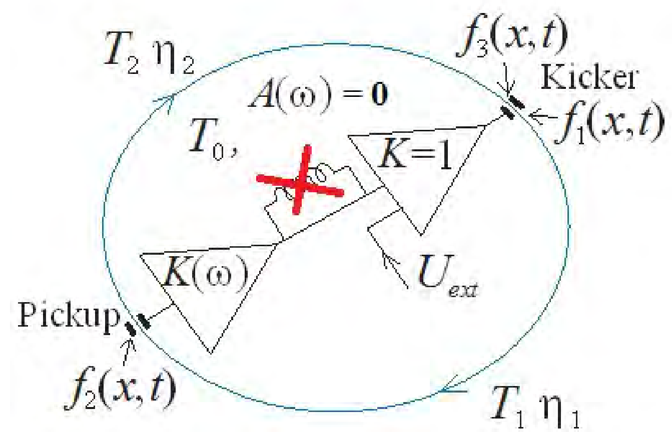

- P-K partial slip factor: $\Delta t = T_0\eta_2 x \equiv T_0\eta_2\dfrac{\Delta p}{p}$

- For a rectangular band with perfect phasing ($G'(\omega) = G', \omega\in[\omega_{\min},\omega_{\max}]; \quad \mathrm{Im}(G') = 0$)

$$F(x) = -\frac{2G'x}{T_0}(n_{\max} - n_{\min})\Im(x)$$

  - The cooling range: $x_{\max} = \dfrac{1}{2(n_{\max}+n_{\min})\eta_2}$

$$\Im(x) = \frac{\sin(2\pi n_{\max}\eta_2 x) - \sin(2\pi n_{\min}\eta_2 x)}{2\pi(n_{\max}-n_{\min})\eta_2 x}$$

- Cooling range ≡ "Bad mixing"?
  - Good lifetime requires the cooling range >4σ
- η_2 can be controlled by machine optics and cooling range can be ∞

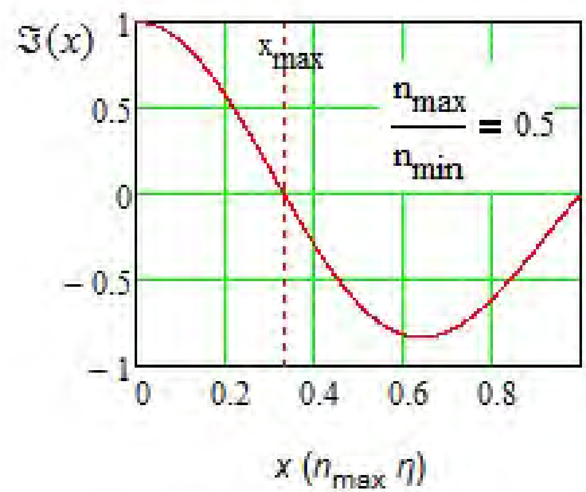

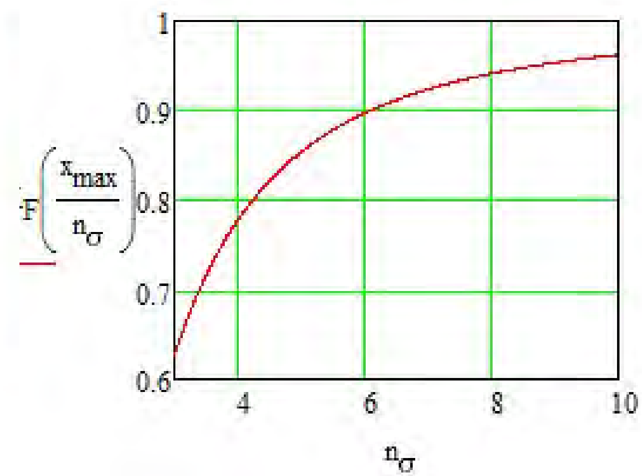

Form-factor of cooling rate reduction ($K_F(\sigma)$) for Gaussian distribution as function of $n_\sigma = x_{max}/\sigma$

Cooling Force and Range for Transient Time Cooling

- Transient time cooling is the only method which can work at optical frequencies
  - FC requires notch filter
- Transient time cooling:

$$G(x,\omega_n) = -iG_F(\omega); \quad A(\omega) = 0$$

$$F(x) = \frac{1}{T_0}\sum_{n=-\infty}^{\infty} iG_F(n\omega_0)e^{2\pi i n \eta_2 x}$$

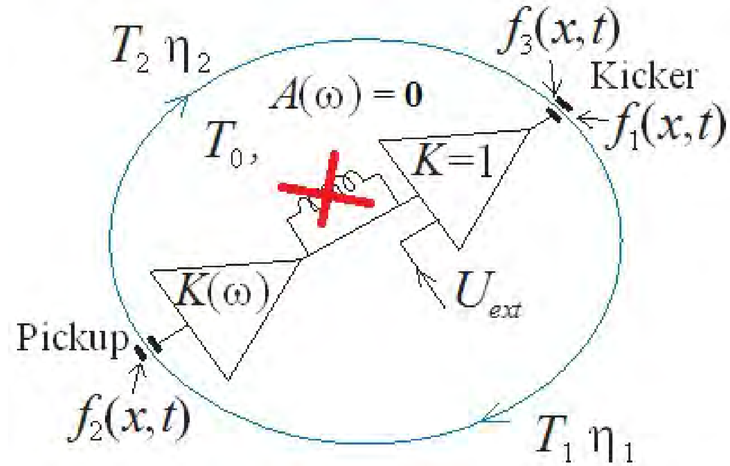

- For a rectangular band

$(G_F(\omega) = G_0, \omega \in [\omega_{min}, \omega_{max}])$

$$F(x) = \frac{2G_0}{T_0}\frac{\sin(\pi\eta_2(n_{max}-n_{min})x)}{\pi\eta_2 x}\sin(\pi\eta_2(n_{max}+n_{min})x)$$

  - The cooling range: $x_{max} = \dfrac{1}{\eta_2(n_{max}+n_{min})}$
    - Does not depend on η
    - And is determined by η_2

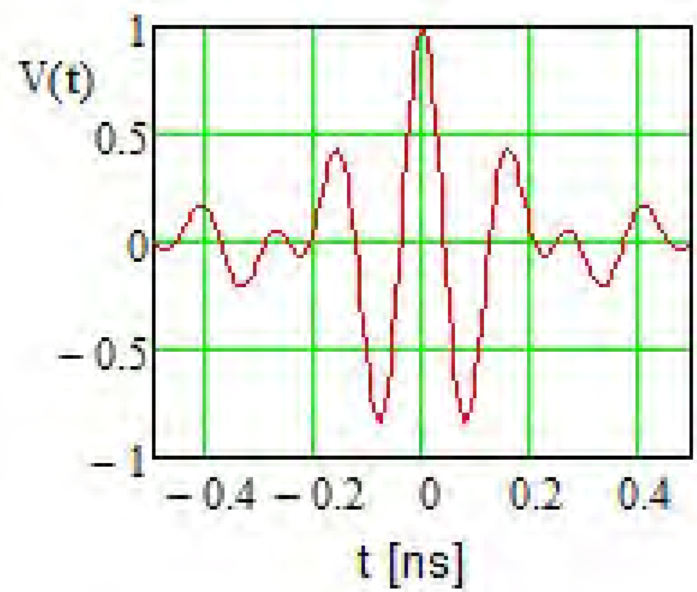

Optimal Gain and Maximum Damping Rate

- Optimum depends on particle distribution, technical and other limitations

$$\int x^2 dx\left(\frac{\partial\psi}{\partial t}+\frac{\partial}{\partial x}\big(F(x)\psi\big)=\frac{1}{2}\frac{\partial}{\partial x}\left(D(x)\frac{\partial\psi}{\partial x}\right)\right) \quad\rightarrow\quad \frac{d\overline{x^2}}{dt}=-2\frac{G}{G_{ref}}\overline{F}+\left(\frac{G}{G_{ref}}\right)^2\overline{D}$$

where $\overline{F}=-\int xF(x)\psi(x)dx\,,\quad \overline{D}=\int\psi(x)\frac{d}{dx}\big(xD(x)\big)dx$

Differentiating over G yields optimal gain => optimal damping

$$\left.\frac{d\overline{x^2}}{dt}\right|_{\max}=\frac{\overline{F}^2}{\overline{D}} \quad\Rightarrow\quad \left.\frac{d\overline{x^2}}{dt}\right|_{\max}=\frac{\left(\int dx\,x\psi(x)\frac{1}{T_0}\sum_{n=-\infty}^{\infty}\frac{G(x,\omega_n)}{\varepsilon(\omega_n)}\left(1-A(\omega_n)e^{-i\omega_n T_0}\right)e^{i\omega_n T_2\eta_2 x}\right)^2}{\int dx\,\psi(x)\frac{d}{dx}\left(\frac{N}{T_0}\sum_{n=-\infty}^{\infty}\left|G(x,\omega_n)\right|^2\left|\left(1-A(\omega_n)e^{-i\omega_n T_0}\right)\right|^2\frac{\psi(x)}{|n\eta|\left|\varepsilon(\omega_n)\right|^2}\right)}$$

  - Signal suppression (1/ε) affects both diffusion and cooling force and can be neglected

- For major fraction of particles

$$\left.\frac{d\overline{x^2}}{dt}\right|_{\max}\propto\frac{\left(\sum_{n=0}^{\infty}\mathrm{Re}\big(G(\omega_n)\big)\right)^2}{\sum_{n=0}^{\infty}\left|G(\omega_n)/n\right|}$$

Replacing summation by integration we introduce the effective bandwidth

$$\boxed{W_{eff}=\sqrt{\frac{\left(\int_0^{\infty}\mathrm{Re}\big(G(f)\big)df\right)^2}{\int_0^{\infty}\left|G(f)\right|^2 df/f}}}$$

Optimal Damping Rate for Transient Cooling

- Small amp. oscillations, Gaussian distribution, continuous beam & Rectangular band
  - Cooling range: $x_{\max} \approx \dfrac{1}{\eta_2 \left(n_{\max} + n_{\min} \right)}$
  - Diffusion is much larger than for filter cooling
    - Noncompetitive to the filter cooling in the case of non-overlapped bands
      - at optimum: $\lambda_{TTC} \approx \lambda_{FC} \left(\dfrac{\eta_2}{\eta} \right)^2$
    - For completely overlapped bands
      - Diffusion does not depend on momentum deviation and momentum spread: $D = 2NG_0{}^2W$
      - signal suppression is negligible

$$\boxed{\lambda_{opt} \approx \frac{2\pi^2 W}{N n_\sigma{}^2}} \qquad W = \frac{n_{\max} - n_{\min}}{T_0}, \quad n_\sigma = \frac{x_{\max}}{\sigma_p}.$$

Back to Signal Suppression

Filter Cooling

- For $G_n \approx const\ , n \in [n_{\min}, n_{\max}]$ the effective gain is proportional to n
  $\Rightarrow$ signal suppression does not depend on n

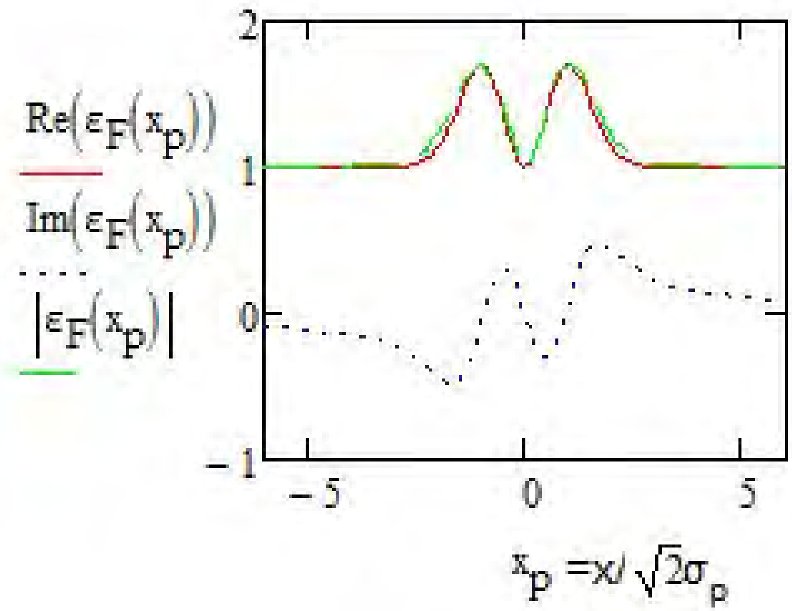

- Cooling force: $F_n \approx \mathrm{Re}\left(F_{n0}(x) / \varepsilon_n(\mathrm{x})\right)$
- Diffusion: $D_n \approx D_{n0}(x) / \left|\varepsilon_n(\mathrm{x})\right|^2$
- Damping rate:

$$\left.\frac{d\overline{x^2}}{dt}\right|_{\max} = \frac{\left\langle \sum_{n=-\infty}^{\infty} \frac{G(n\omega_0)}{\varepsilon_n(x)} \left(1-e^{-2\pi i n \eta_2 x}\right) e^{2\pi i n \eta_2 x} \right\rangle_x^2}{\left\langle x\psi(x) \sum_{n=-\infty}^{\infty} \left|\frac{G(n\omega_0)}{\varepsilon_n(x)}\right|^2 \frac{\left|1-e^{-2\pi i n \eta_2 x}\right|^2}{|n|} \right\rangle_x}$$

  - Numerical computation with signal suppression at optimal gain and for rectangular band yields only a few % correction

Palmer cooling and Transient time cooling

- Qualitatively - similar picture
- Signal suppression is reduced when bands start to overlap
  - negligible for completely overlapped bands

Causality in Stochastic Cooling

- Causality binds the real and imaginary parts of system response
- The same as for the medium permeability, the Kramers-Kronig relations bind the real and imaginary parts of the gain for an amplifier
- It is true for any system where causality works
  - But there is no causality limitations in a stochastic cooling system
    - Changing delay in the cable we can deliver signal earlier than particle will arrive

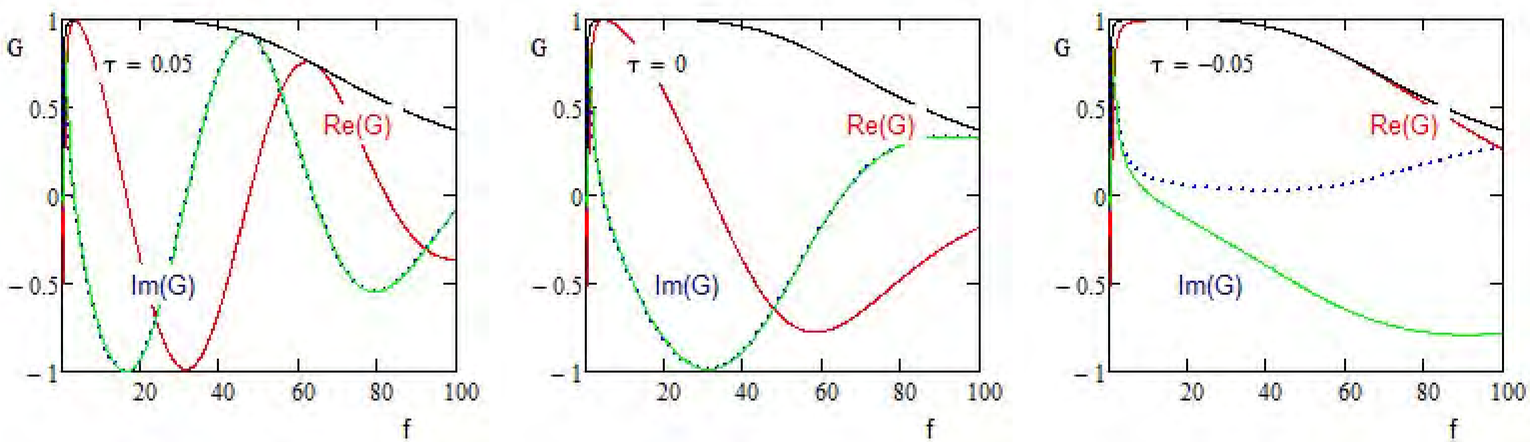

Real and imaginary parts of system response for LPF*HPF*Delay (4th order Bessel filters)

Negative delay makes a flat phase response but breaks Kramers-Kronig relationship

$$G''(\omega) = \frac{1}{\pi} \int_{-\infty}^{\infty} \frac{G'(x)}{x-\omega} dx$$

Typical Stochastic Cooling Block Diagram

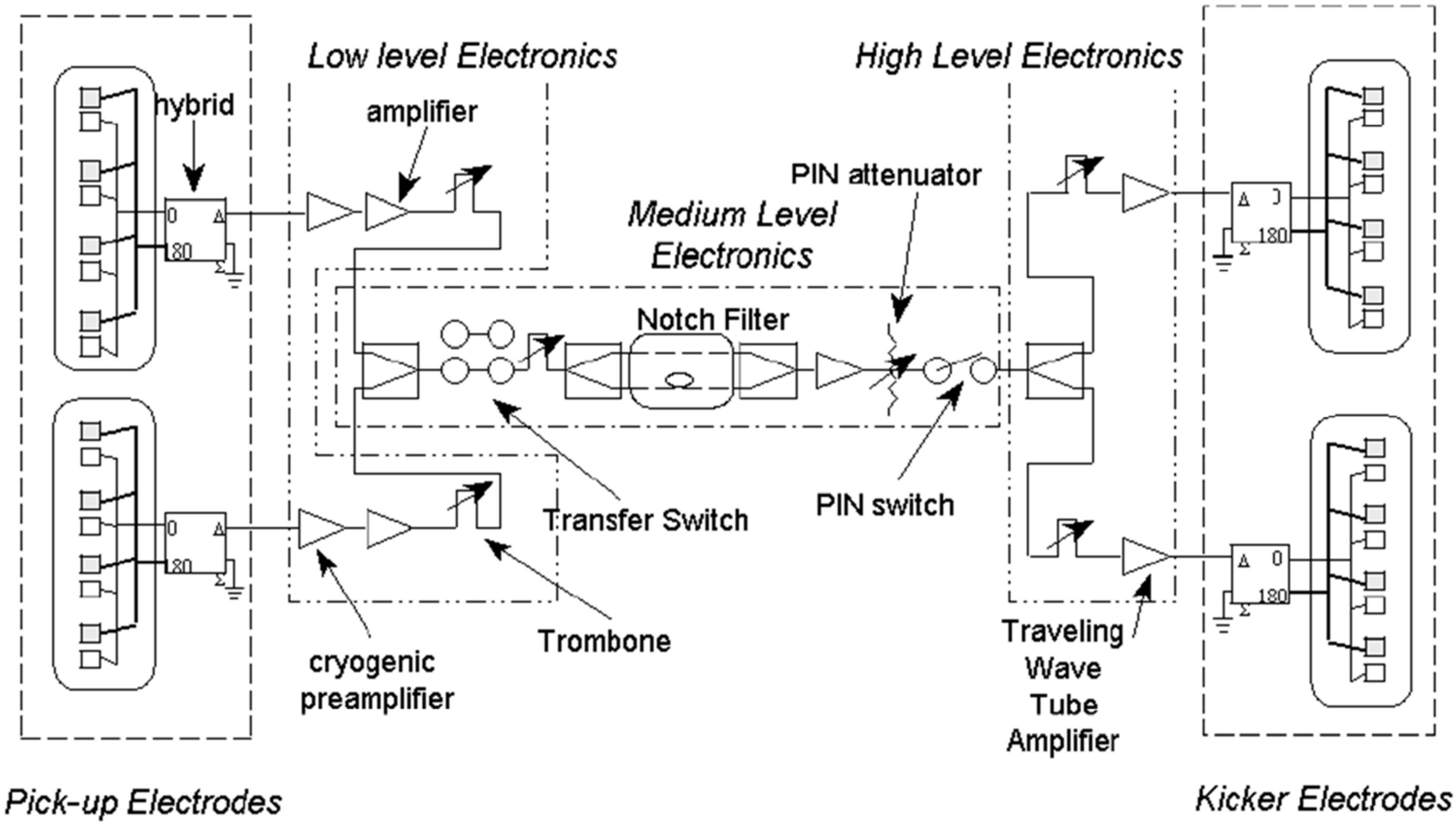

Lectures 15-16: OSC & CEC

Valeri Lebedev
JINR & Fermilab

US Particle Accelerator School
February 2022

Bunched Beam Stochastic Cooling

Schottky Noise of Bunched Beam

$$P(\omega)=\frac{e^2}{T_0^{\,2}}\left[\sum_{k,l}\sum_{n=-\infty}^{\infty}\left\langle z_{0_k} z_{0_l}^{\;*}\right\rangle\delta\left(\omega-n\omega_0\right)+\sum_{k}\sum_{n=-\infty}^{\infty}\sum_{\substack{m=-\infty\\ m\neq 0}}^{\infty}\left\langle\left|z_{m_k}\right|^2\right\rangle\delta\left(\omega-\omega_{nm}\right)\right]\quad,\quad \omega_{nm}=n\omega_0+m\omega_{s_k}\,.$$

$$z_{nm}=\frac{1}{T_s}\int_{-T_s/2}^{T_s/2}\exp\left(-i\frac{\omega_{nm}z(t)}{\beta c}\right)\mathrm{e}^{-im\omega_s t}\,dt.$$

where k enumerates particles

- For linear RF $z_{nm}=e^{-i\pi m/2}J_m\left(\pi\kappa_b n\right)$, $\kappa_b = L_b/2\pi R_0$

- Number of synchrotron lines around n-th harmonic grows $\propto n$
  - ⇨ Even very small tune spread will result in synchrotron band overlap for large m
- For large n the shape of the spectrum corresponds to the actual particle distribution on the momentum (see the proof in "Accelerator Physics At Tevatron Collider")
- For Gaussian distribution the coherent term exponentially decays with increase of n and disappears for sufficiently large frequencies.

Optimal Cooling Rate of TT cooling of Bunched Beam

- For complete band overlap the diffusion does not depend on rel. momentum (x) but is position dependent

  $\Rightarrow$ for Gaussian distribution

$$D(s) = \frac{2N_b}{T_0} \frac{Ce^{-s^2/2\sigma_s^2}}{\sqrt{2\pi}\sigma_s} \sum_{n=-\infty}^{\infty} \left| G(n\omega_0) \right|^2$$

$\Rightarrow$

$$\overline{D} = \int_{-\infty}^{\infty} \frac{e^{-s^2/2\sigma_s^2}}{\sqrt{2\pi}\sigma_s} D(s)ds$$

- For rectangular band

$$\boxed{\lambda_{opt} \approx \frac{2\pi^2 W}{N n_\sigma^{\ 2}} \frac{\sqrt{\pi}\sigma_s}{C}} \qquad W = \frac{n_{\max} - n_{\min}}{T_0}, \quad n_\sigma = \frac{x_{\max}}{\sigma_p}.$$

- Bandwidth for Gaussian band: $W = 2\sqrt{\pi}\sigma_f$ $\quad \left(G(\omega) = G_0 \exp\left(-\omega^2 / 2\left(2\pi\sigma_f\right)^2 \right) \right)$

Optical Stochastic Cooling

Optical Stochastic Cooling

- Suggested by Zolotorev, Zholents and Mikhailichenko (1994)
- OSC obeys the same principles as the microwave stochastic cooling, but exploits the superior bandwidth of optical amplifiers ~ 10^{14} Hz
- Pickup and kicker must work in the optical range and support the same bandwidth as the amplifier
  - Microwave pickups cannot be scaled to μm
    - Distance to the beam is 10^3-10^4 λ
  - Undulators were suggested: both for pickup & kicker

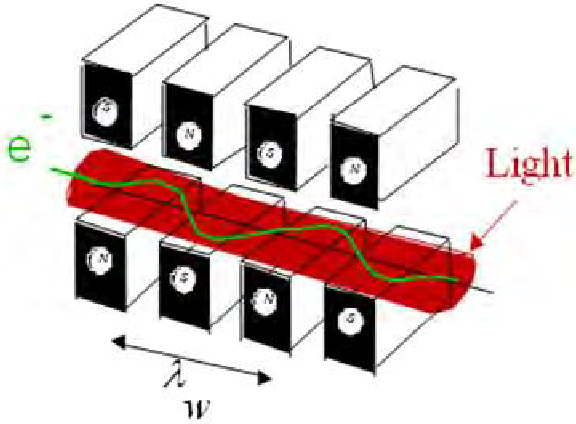

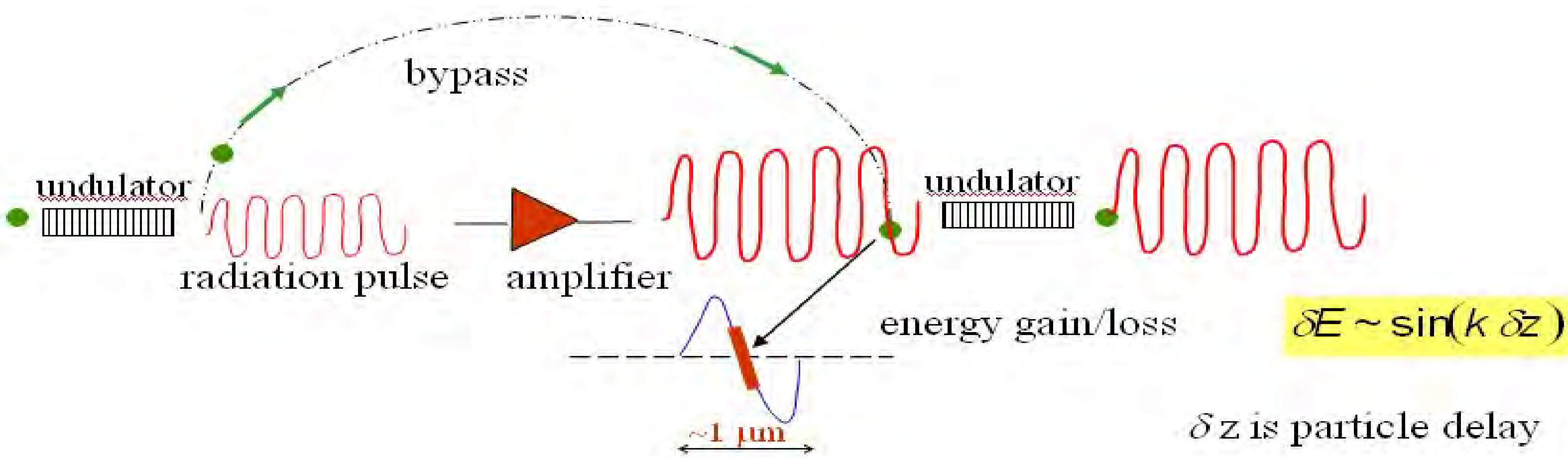

- ⊥ cooling is due to coupling between different degrees of freedom

Optical Stochastic Cooling

- OSC was experimentally tested at FNAL at IOTA (summer 2021)
  - 100 MeV electrons in 40 m ring
  - Multipurpose ring (Integrable optics, high space charge, OSC, …)
    - reasonably small price for OSC
- Cooling of hadrons requires a beyond "state of art" optical amplifier
  - Power?
  - Small signal delay?
  - Large duty-factor: 0.01 - 0.1

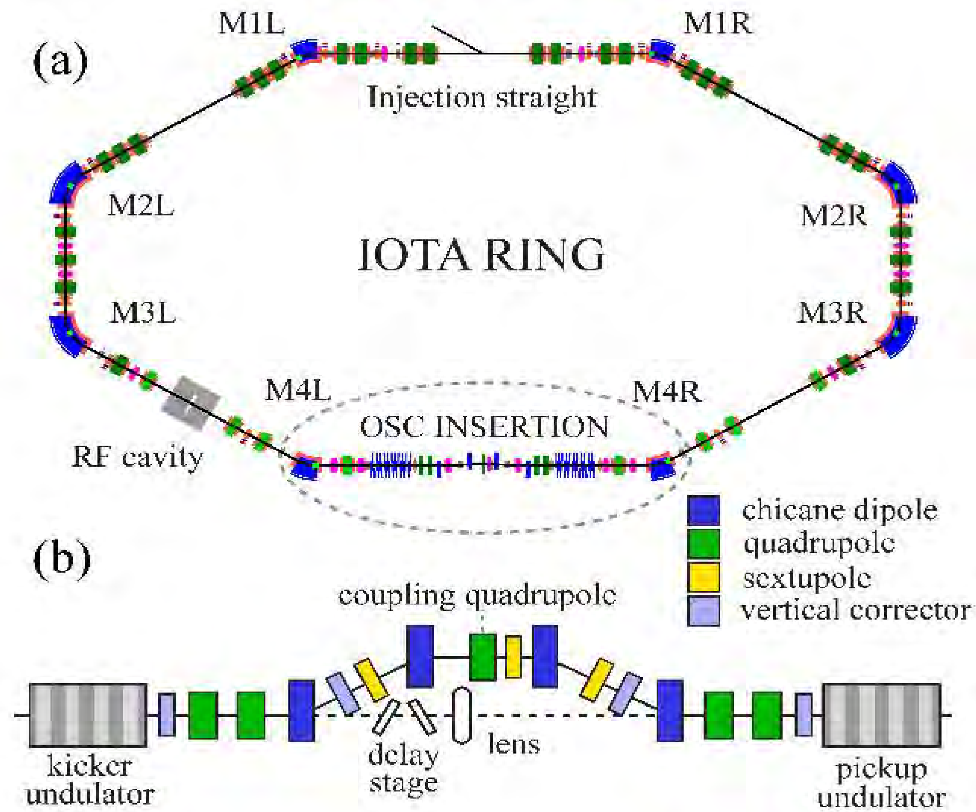

Schematic of the IOTA OSC system. a, Schematic of the IOTA ring and the location of the OSC insertion. **b,** Diagram of the OSC insertion including the undulators, chicane and light optics.

Amplifier	λ [nm]	Δf/f	D.F.
Ti-Sapphaire	800	0.2	CW
Dye	300-900	0.2	CW
Parametric	350-1500	0.2	~10^{-6} @10 W

Basics of OSC - Damping Rates

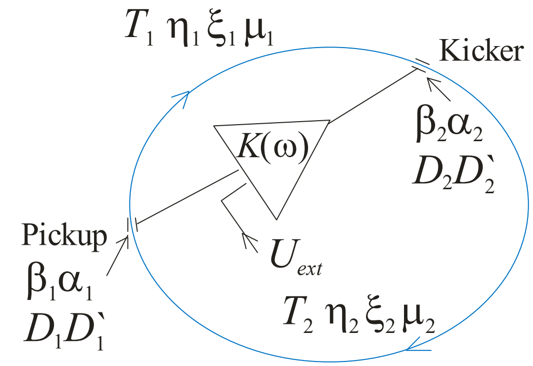

M^{pk} - pickup-to-kicker matrix

M^{kp} - kicker-to-pickup matrix

M = M^{pk}M^{kp} – ring matrix

- Pickup-to-Kicker Transfer Matrix
  - Vertical plane is uncoupled and we omit it

$$\mathbf{M}^{pk}=\begin{bmatrix} M_{11} & M_{12} & 0 & M_{16} \\ M_{21} & M_{22} & 0 & M_{26} \\ M_{51} & M_{52} & 1 & M_{56} \\ 0 & 0 & 0 & 1 \end{bmatrix},\quad \mathbf{x}=\begin{bmatrix} x \\ \theta_x \\ s \\ \Delta p/p \end{bmatrix}$$

- Partial slip factor (pickup-to-kicker) describes a longitudinal particle displacement in the course of synchrotron motion

$$\tilde{M}_{56}=M_{51}D_1+M_{52}D_1'+M_{56}$$

- Linearized longitudinal kick in pickup wiggler

$$\frac{\delta p}{p}=k\xi_0\,\Delta s=k\xi_0\left(M_{51}x_1+M_{52}\theta_{x1}+M_{56}\frac{\Delta p}{p}\right)$$

- Cooling rates (per turn)

$$\boxed{\begin{aligned}\lambda_x &= \frac{k\xi_0}{2}\left(M_{56}-\tilde{M}_{56}\right)\\ \lambda_s &= \frac{k\xi_0}{2}\tilde{M}_{56}\end{aligned}}\quad \Leftrightarrow \quad \boxed{\lambda_x+\lambda_s=\frac{k\xi_0}{2}M_{56}^{pk}}$$

Basics of OSC - Cooling Range

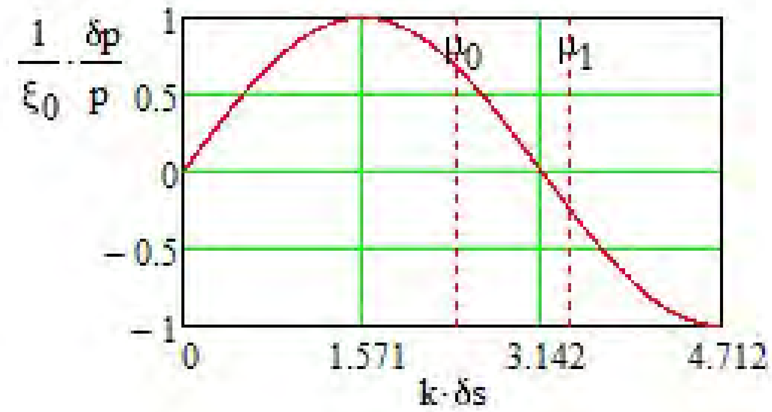

- Cooling force depends on Δs nonlinearly

$$\frac{\delta p}{p} = k\xi_0 \Delta s \quad \Rightarrow \quad \frac{\delta p}{p} = \xi_0 \sin\left(k\delta s\right)$$

where $k\delta s = a_x \sin(\psi_x) + a_p \sin(\psi_p)$

and a_x & a_p are the amplitudes of longitudinal displacements in cooling chicane due to ⊥ and L motions measured in units of laser phase

- Averaging yields the form-factors for damping rates

$$\boxed{\begin{aligned} &\lambda_{s,x}(a_x,a_p) = F_{s,x}(a_x,a_p)\lambda_{s,x} \\ &F_x(a_x,a_p) = \frac{2}{a_x} \mathrm{J}_0(a_p)\mathrm{J}_1(a_x) \\ &F_p(a_x,a_p) = \frac{2}{a_p} \mathrm{J}_0(a_x)\mathrm{J}_1(a_p) \end{aligned}}$$

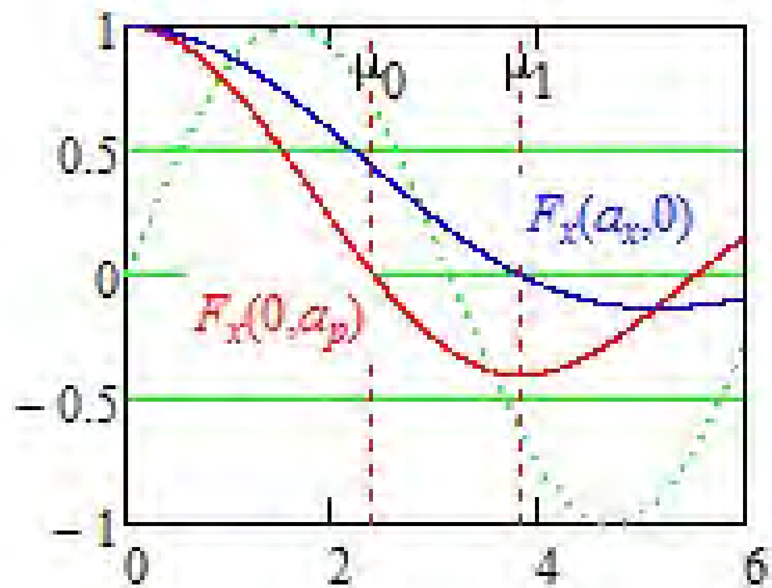

- Damping requires both lengthening amplitudes (a_x and a_p) to be smaller than $\mu_0 \approx 2.405$

Linear Sample Lengthening on the Travel through Chicane

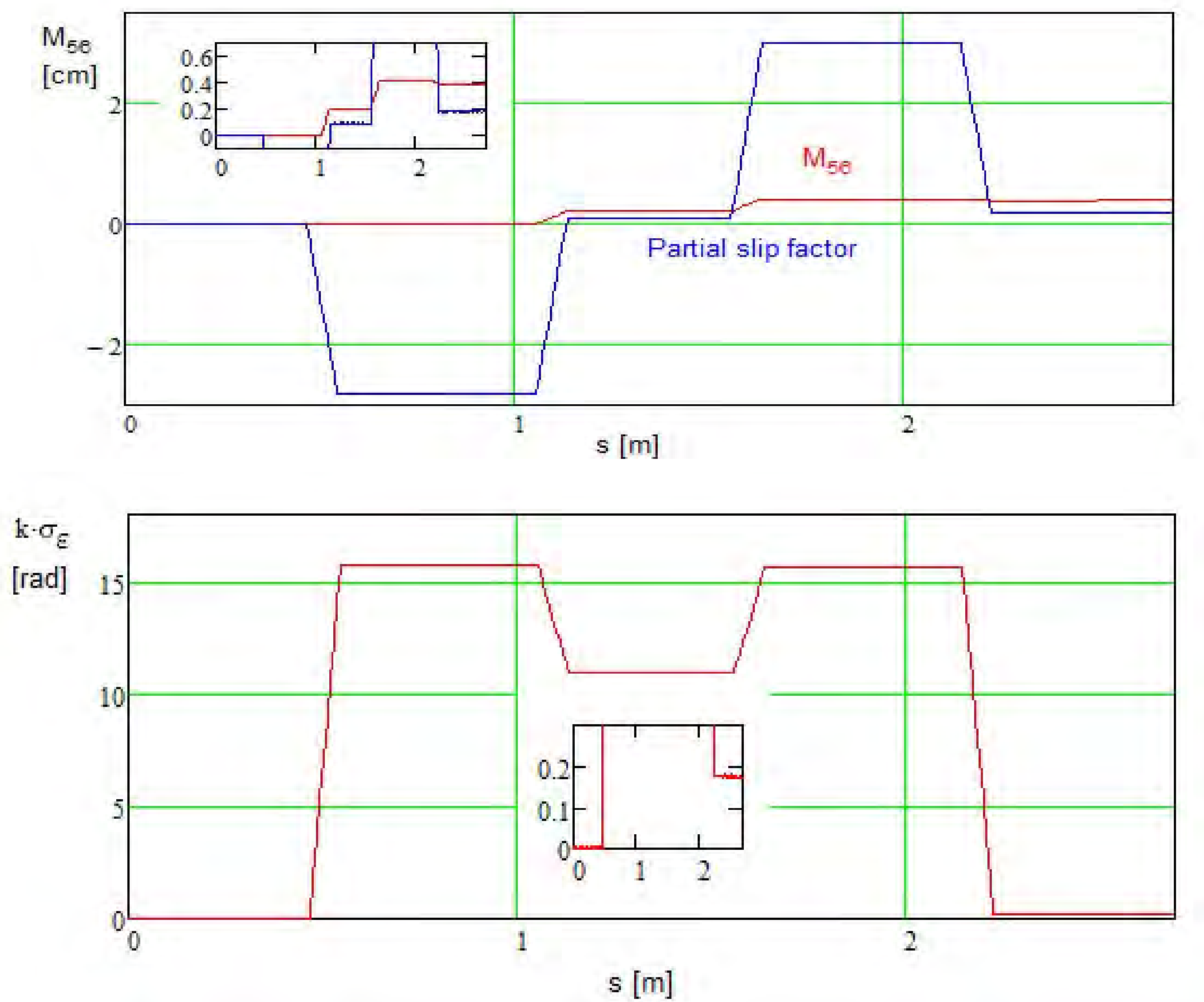

- Very large sample lengthening on the travel through chicane
- High accuracy of dipole field is required to prevent uncontrolled lengthening,
  $\Delta(BL)/(BL)_{dipole}<10^{-3}$

Sample lengthening due to momentum spread (top) and due to betatron motion (bottom, H. emittance for x-y coupled case)

Compensation of Non Linear Sample Lengthening

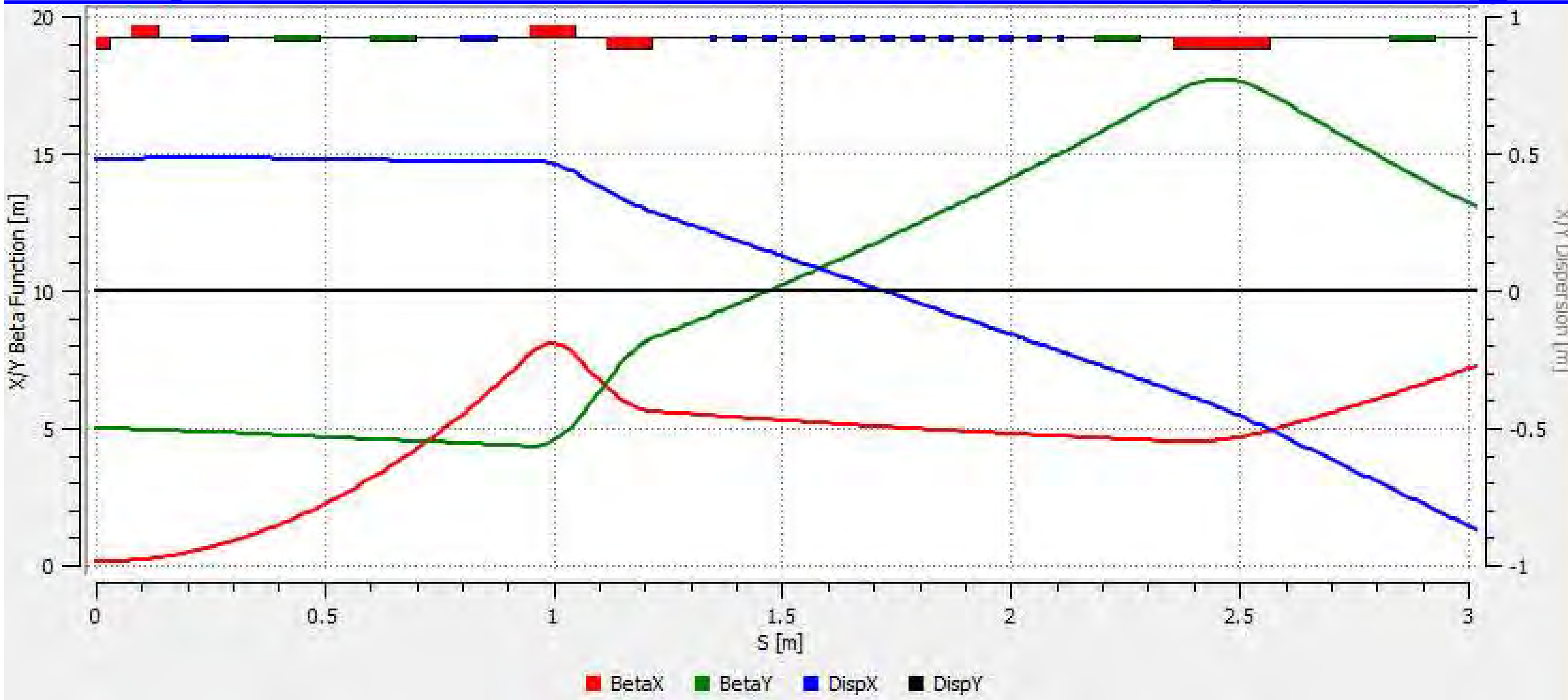

- Nonlinear lengthening
  - It mainly comes from the betatron angles, $\Delta L_{x,y} = \int \left(\theta_{x,y}{}^2 / 2 \right) ds$, and is larger for horizontal plane
  - It is large and has to be compensated
- Compensation is achieved by two pairs of sextupoles located between dipoles of each dipole pair of the chicane (marked by green boxes)
  - Strengths of sextupoles are large: SdL_y=-7.5 kG/cm, SdL_x=1.37 kG/cm. It results in considerable limitation of the dynamic aperture.

Compensation of Non Linear Sample Lengthening

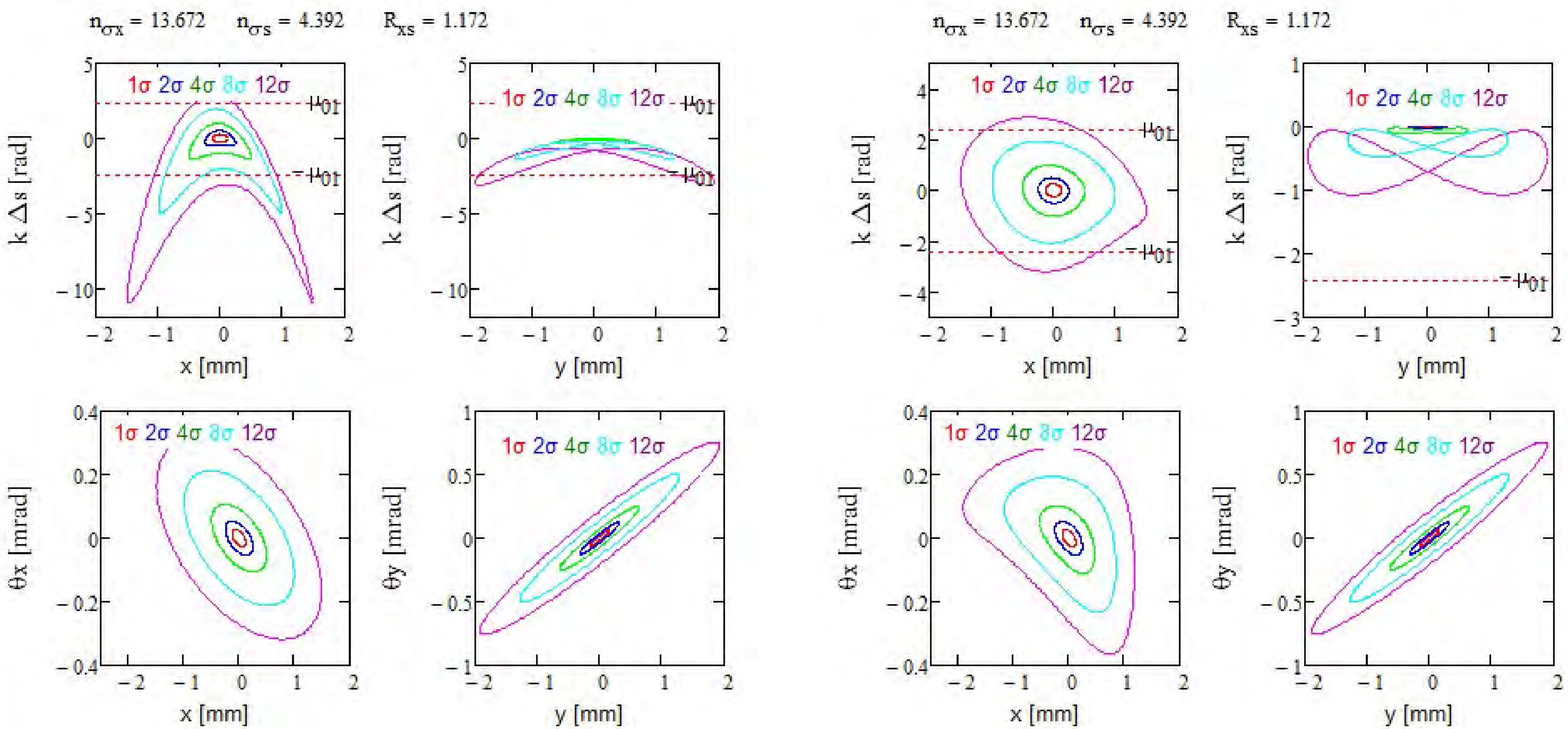

Phase space distortion for the cases of uncompensated (left) and compensated (right) sample lengthening (reference emittance is equal to the horizontal emittance of x-y uncoupled case)

Dependence of Cooling Efficiency on Undulator Parameter

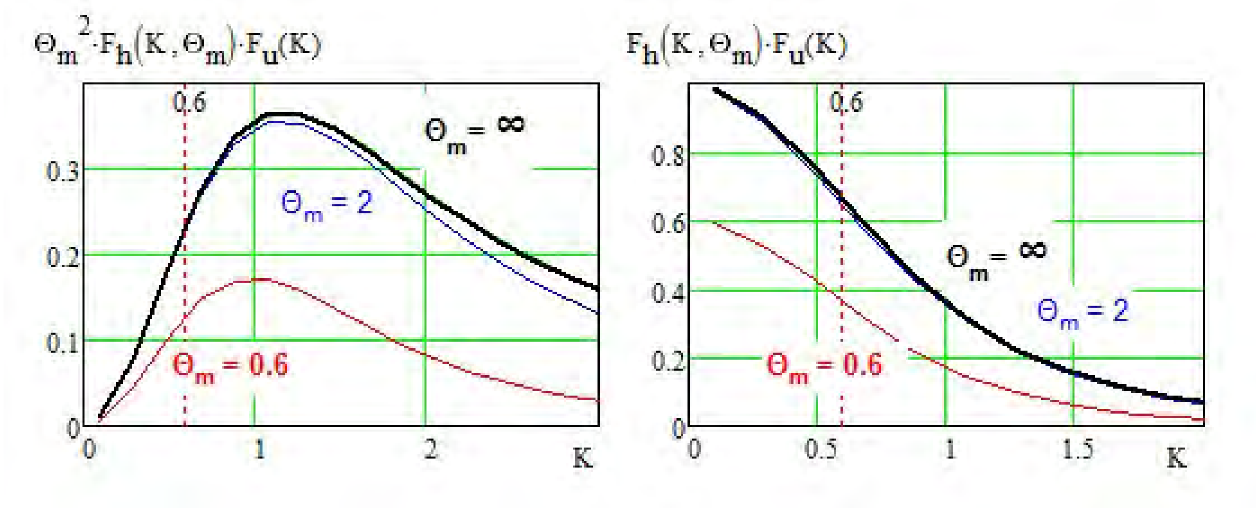

- Particle motion in undulator becomes comparable to the size of the focused radiation
  - It reduces cooling efficiency
- An increase of the undulator parameter also increases undulator magnetic field and, consequently, the equilibrium emittance and undulator focusing
- Chosen undulator parameter K=1.038 corresponds to the 7 period undulator with B_0=1 kG. It results in moderate increase of equilibrium emittance of ~5%.

The Depth of Field for Focusing of Radiation

- Two possibilities
  - Four lens system with complete suppression of depth of field

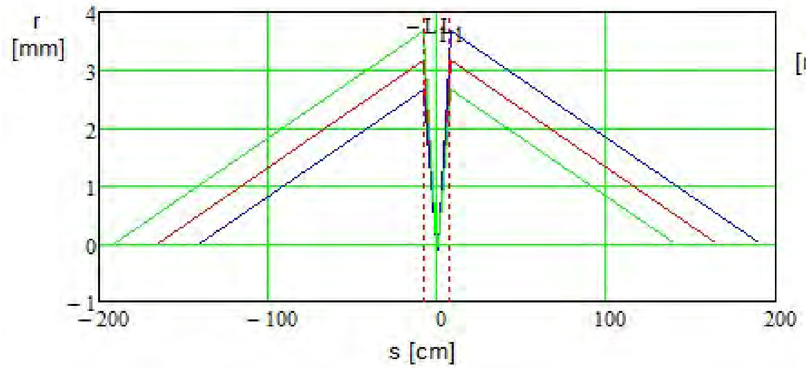

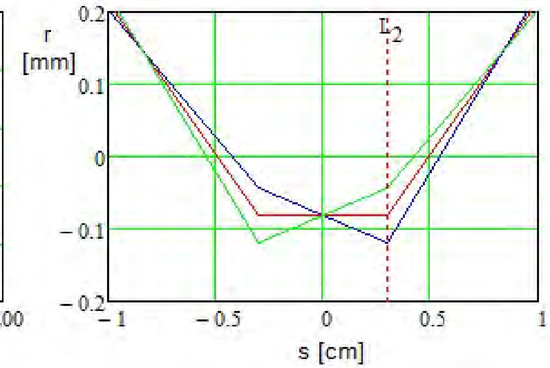

$$\begin{pmatrix} 1 & L_1 \\ 0 & 1 \end{pmatrix} \cdot \begin{pmatrix} 1 & 0 \\ -\frac{1}{F_1} & 1 \end{pmatrix} \cdot \begin{pmatrix} 1 & L_2 \\ 0 & 1 \end{pmatrix} \cdot \begin{pmatrix} 1 & 0 \\ -\frac{1}{F_2} & 1 \end{pmatrix} \cdot \begin{pmatrix} 1 & L_2 \\ 0 & 1 \end{pmatrix} \cdot \begin{pmatrix} 1 & 0 \\ -\frac{1}{F_1} & 1 \end{pmatrix} \cdot \begin{pmatrix} 1 & L_1 \\ 0 & 1 \end{pmatrix} = p \cdot \begin{pmatrix} 1 & 0 \\ 0 & 1 \end{pmatrix}$$

$L_2 := 33$ cm $\quad L_1 := L_{tot} - L_2 = 140$ cm $\quad F_1 := L_2 = 33$ cm $\quad F_2 := \dfrac{L_2^{\,2}}{2 \cdot (L_2 - L_1)} = -5.089$ cm

- Lenses are manufactured from barium fluoride
  - Antireflection coating protects from humidity damage
- Excellent material with very small second order dispersion

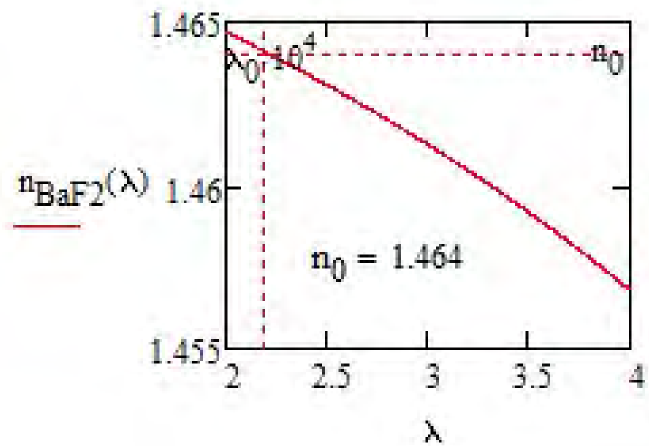

First Order Dispersion Effects in Optical Lenses

- The first order dispersion, $dn/d\lambda$, results in 1.5% difference between phase and group velocities in the lens material
  - It has to be accounted in the total lens thickness
  - Significant separation of radiation of the first and higher harmonics

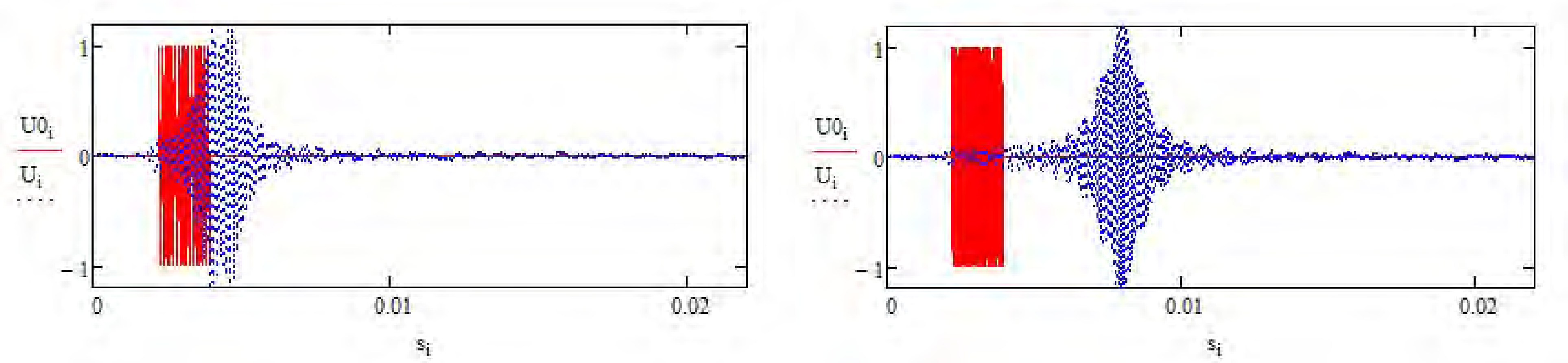

Overlap of radiation for the second and third harmonics of undulator radiation

- Dependence of focusing strength on wave length makes reasonably small reduction of the damping rates
  - Accurate numbers will be obtained soon

Second Order Dispersion Effects in Optical Lenses

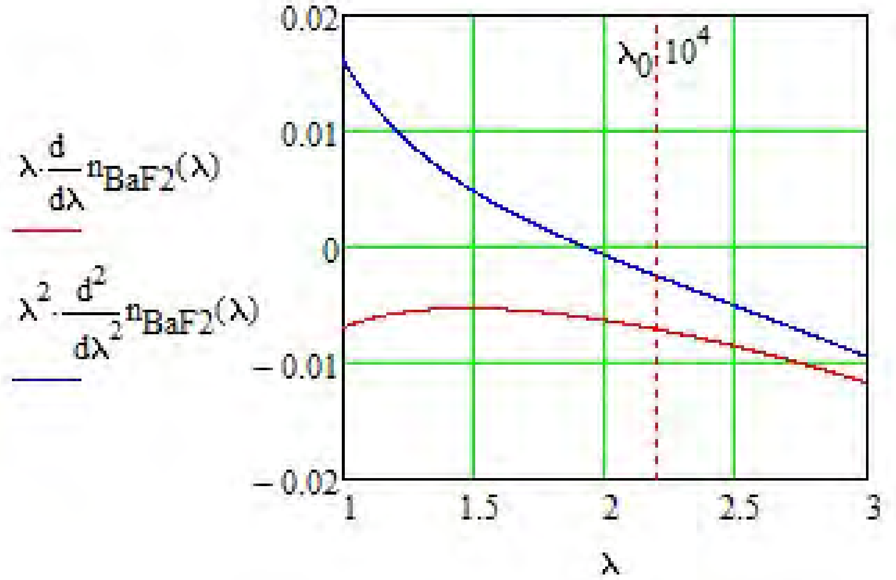

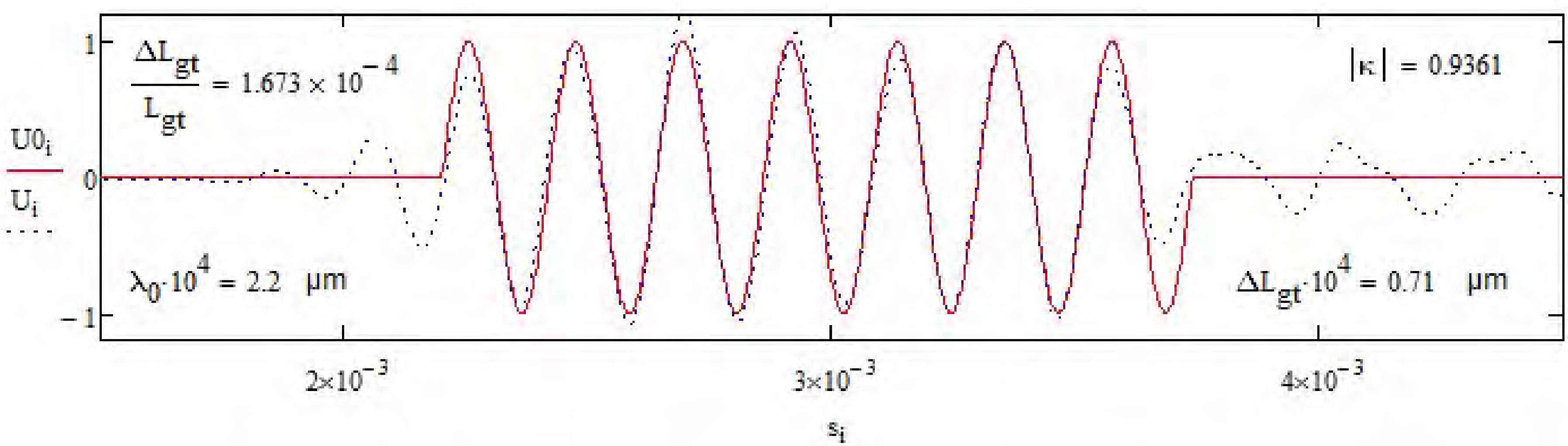

The second order dispersion, $d^2n/d\lambda^2$, results in lengthening of the light packet and, consequently, 6% loss of cooling rates

Effect of Beams Overlap on Cooling Rates

- Transfer matrix for the light is equal to the negative identity matrix
- Transfer matrices for particles are close to the negative identity matrix. It compensates separation of light and particles due to betatron motion

Bandwidth of Optical Stochastic Cooling

- In the absence of dispersion in the lenses and OA the bandwidth is determined by
  - Number of wiggles in the undulators

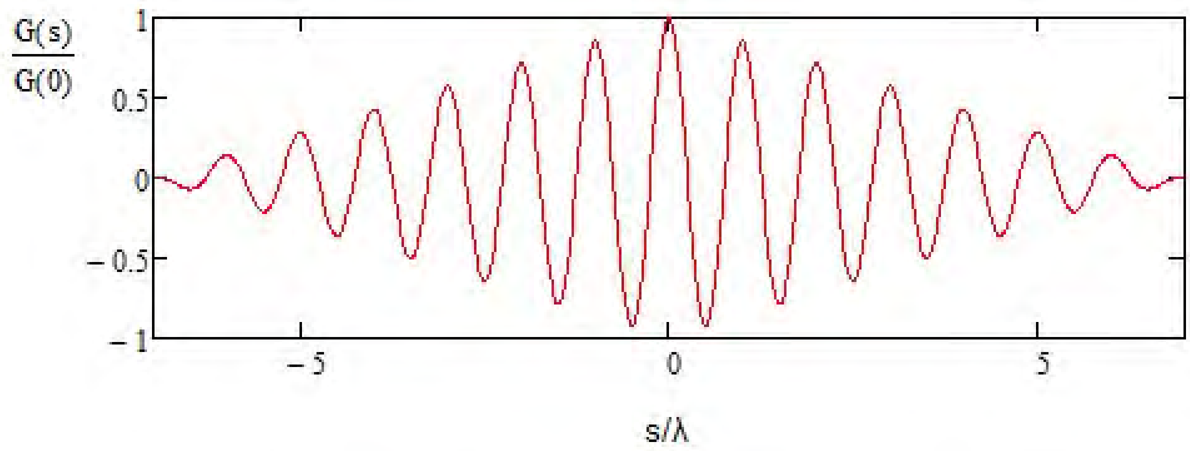

- Radiation focused back to the kicker wiggler has "correct" freq. for resonant particle interaction
  - ⇨ frequency dependence of SR θ does not directly affect the bandwidth
- It is desirable to have the bandwidth of optical amplifier larger than the bandwidth of radiation (both forward and at the aperture of optical system)
- Total rms bandwidth for Fermilab OSC test is ~3% (~10% effective);

Can Parametric Optical Amplifier help?

- POA looks as a good choice
  - Large amplification & small delay
- However there are problems
  - typical duty factor <~10^{-5}
  - Amplification duration (pump length) ~30 fs (10 μm)
    - 100 μJ*50 MHz=5 kW
  - Looks to be impossible to obtain reasonable duty factor (1-10%) with reasonable pumping power

$$\lambda_{opt} = \frac{2\pi^3 \sigma_f}{n_\sigma^{\;2}} \frac{\sigma_s}{N_p C} \frac{\sigma_g}{\sigma_s}$$

We will lose orders of magnitude in the damping rate due to small gain length, σ_g

OSC in IOTA

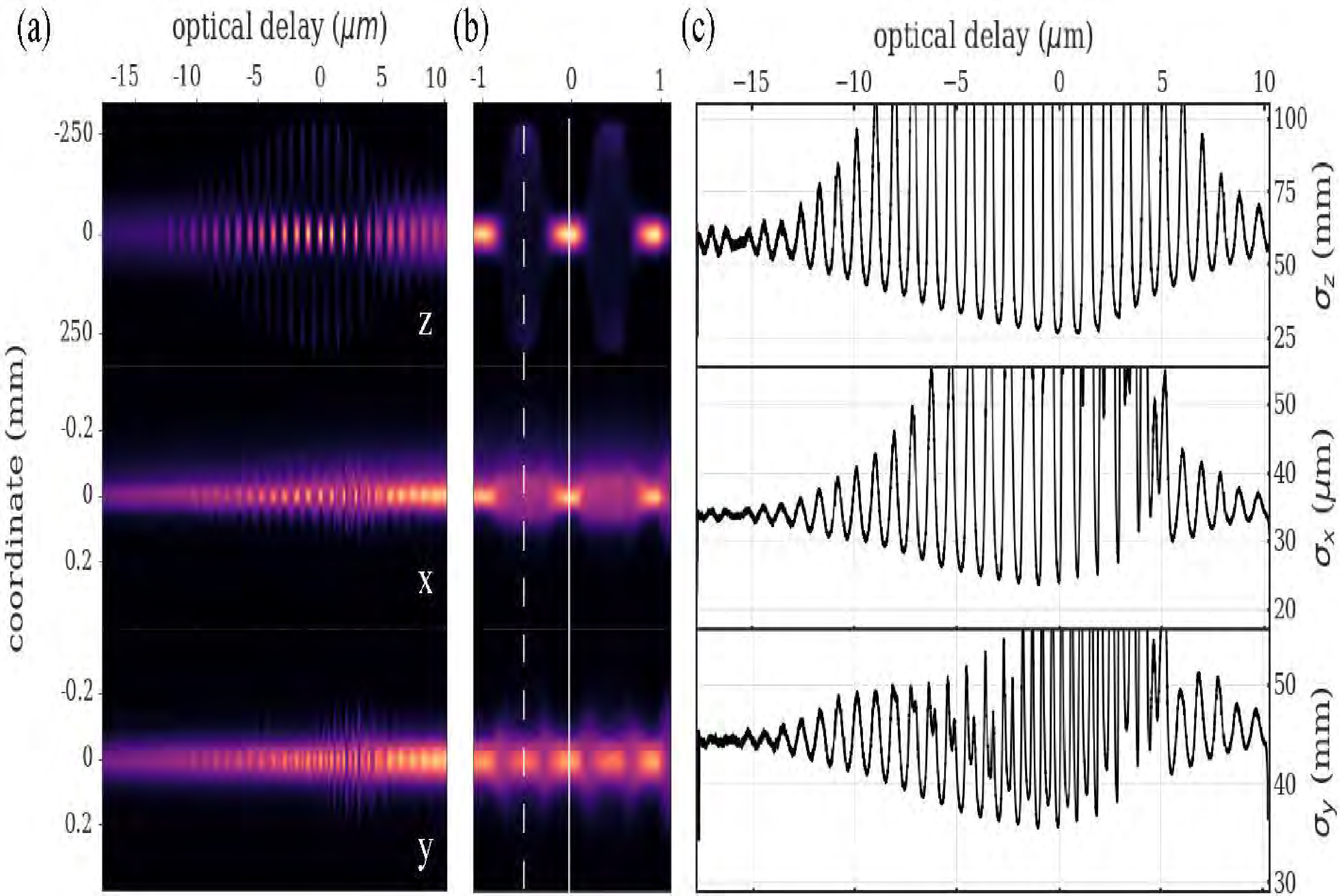

|Projected beam distributions for a delay scan in the 3D OSC configuration. a,

OSC in IOTA

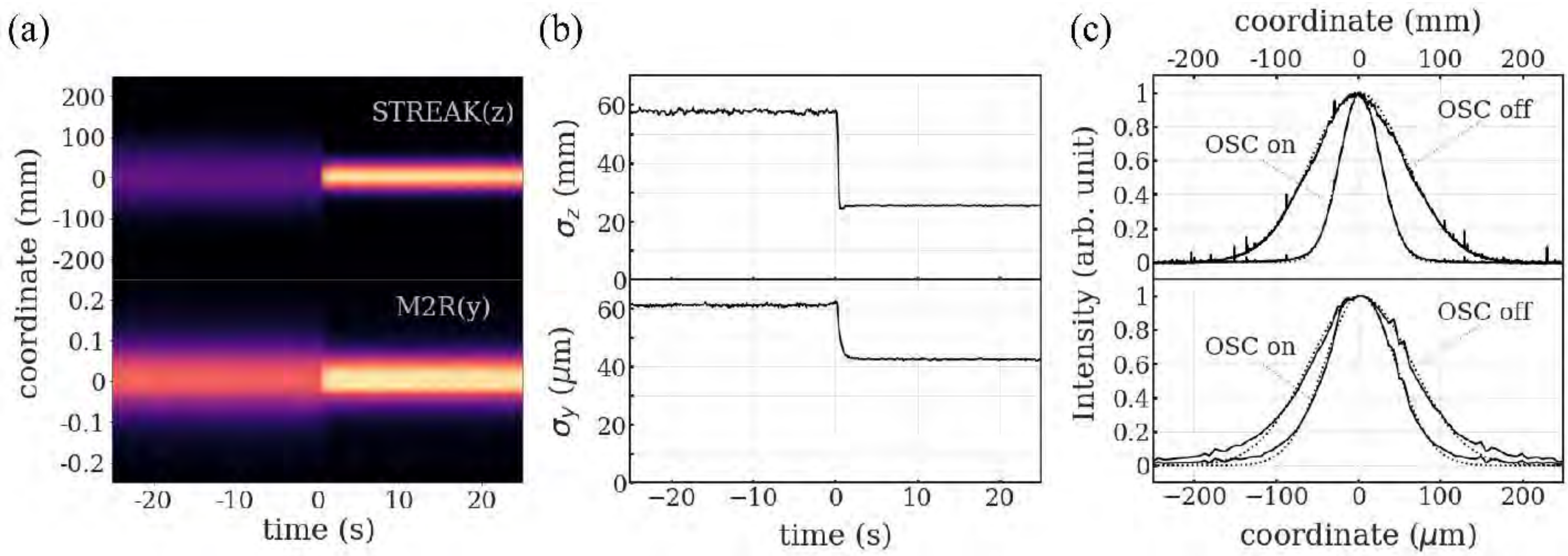

Fast toggle of the OSC system

- The non-Gaussian tails in the transverse distribution appear due to scattering on the residual gas
- Very small electron beam current (~1 μA) reduces the IBS. Multiple IBS reduces the difference in the beam size with cooling on and off. Touschek does not create considerable tails.

Coherent Electron Cooling

- Idea proposed by Derbenev in 1980
- First realistic proposal by Derbenev and Litvinenko in 2007

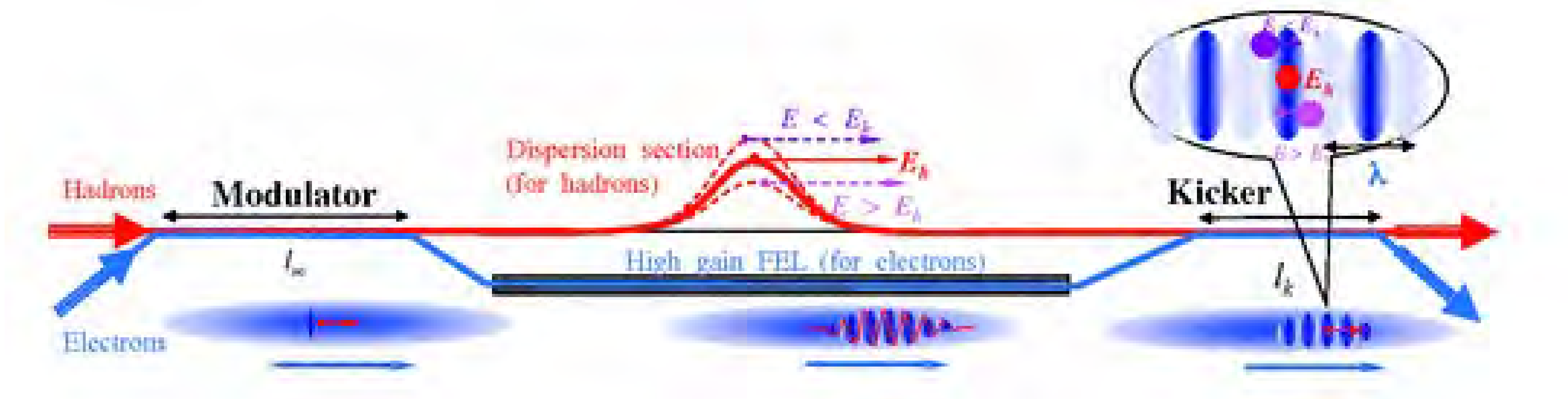

  - Based on the amplification in FEL
    - Gain in frequency by ~10^4 relative to microwave SC
    - Loss ~100 due to bandwidth: 50% -> 0.5%
    - Loss due to short length of FEL electron bunch ~100
- Two proposals address the bandwidth problem (0.5%->~50%).
  They use: (1) plasma cascade instability, and
  (2) micro-bunching in a chicane (first observed in SLAC SASE FEL
- Major problems with CEC
  - Saturation of amplifier $\Delta n/n$ ~1/2
  - Noise in electron beam

Problems

1. Using electrostatic analogy find the maximum longitudinal force in electron cooling for pan cake distribution ($\sigma_{vx}=\sigma_{vy}$, $\sigma_{vz}=0$). Assume that the transverse velocity of a proton is equal to zero and non-magnetized electron cooling.
2. In the shortwave approximation ($k\sigma_{tr}$>>1) find the maximum cooling force in the coherent electron cooling. Assume Gaussian beam in the transverse direction with equal rms transverse sizes, and neglect plasma oscillations.

- Prove the rate-sum theorem. Let the revolution symplectic matrix $\mathbf{M}$ be perturbed: $\mathbf{M}=(\mathbf{I}+\mathbf{P})\mathbf{M}_0$, where the perturbation $\mathbf{P}$ is small, but not necessarily symplectic. Then in the first order of perturbation theory, the complex tune shifts are: $\Delta\mu_l/(2\pi)=-(4\pi)^{-1}\,\mathbf{v}_l^{\dagger}\mathbf{U}\,\mathbf{P}\,\mathbf{v}_l$ and the sum of all growth rates is independent on the eigenvectors so that $\mathrm{Im}\left(\sum_l \Delta\mu_1\right)=\mathrm{Tr}(\mathbf{P})/2$. Here l changes from 1 to the number of degrees of freedom (3 - for 3-dimensional motion).

Machine Protection Concepts

Part 1 (NVM4)

Nikolai Mokhov, Fermilab

USPAS Colliders

February 3, 2022

Outline

Part 1:

- Beam Stored Energy
- Protection of Beam, Experiment and Machine
- Machine Protection System (MPS) Landscape
- Collimation and Active Protection
- Tevatron MPS Concepts and 2003 Beam Accident

Part 2:

- LHC 2008 Incident
- MPS Strategy and Design Guidelines
- LHC MPS Performance
- MPS in the HL-LHC Era and Beyond

Beam Stored Energy

- Example: FCC parameters
- >8 GJ kinetic energy per beam
  - **Airbus A380 at 720 km/h**
  - 24 times larger than in LHC at 14 TeV
  - Can melt 12 tons of copper
  - Or drill a 300 m long hole
  - ⇒ Machine protection

- Also *small* loss is important
  - *e.g.* beam-gas scattering, non-linear dynamics
  - Can quench arc magnets
  - Background for the experiments
  - Activation of the machine
  - ⇒ Collimation system

Beam loss of ~10^{-4} = 1 MJ

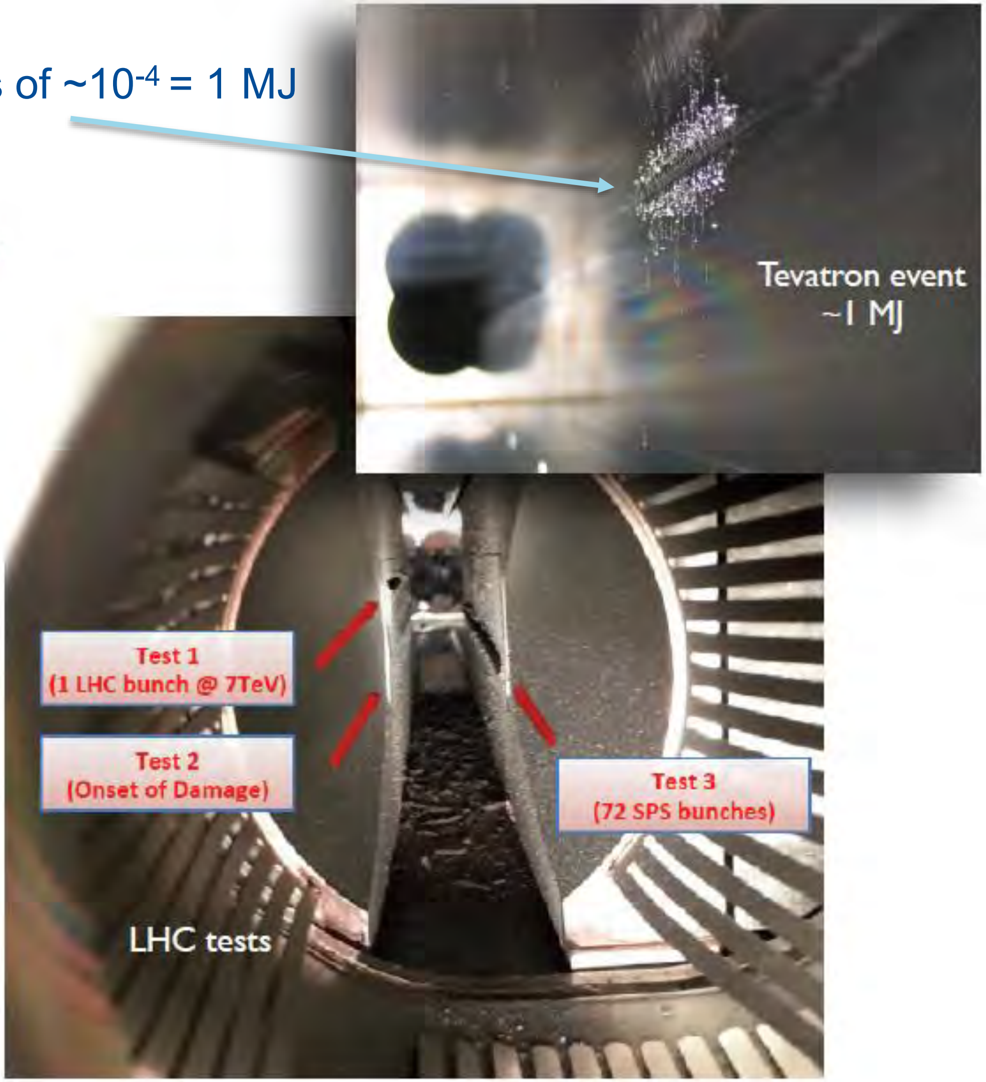

Protection of Beam, Experiment and Machine

$p\bar{p}$ colliders ($Sp\bar{p}S$ & Tevatron)

1. Protect the beam: ~10^{-5} useful antiprotons per proton on target, takes many hours to produce them & setup collisions $\rightarrow$ no unintentional beam aborts
2. Protect the experiments: backgrounds and the most expensive near beam detector components
3. Protect the machine components (superconducting magnets, collimators, beam diagnostics etc.) from uncontrolled beam loss

pp colliders (LHC & beyond)

1. Protect the machine components (superconducting magnets, collimators, beam diagnostics etc.) from uncontrolled beam loss
2. Protect the experiments: backgrounds and the most expensive near beam detector components
3. Protect the beam: minimize beam aborts to maximize the integrated luminosity

Hazard, Risk and Protection at Accelerators

Hazard: a situation that poses a level of threat to the accelerator. It is dormant or potential, it turns to **incident** or **accident** once a hazard becomes "active".

Accident quantification: Risk = Consequences × Probability

Consequences of a failure (in Euro, downtime, radiation dose to people or environment, reputation) in hardware systems or uncontrolled beam loss.

The higher the **Risk**, the more **protection** is needed:

- Protection of people during operation (highest priority) – keep them away from the accelerator when beam is running (access system), taking care also of electrical, pressure, oxygen deficiency and other hazards.
- Protection of the environment.
- Protection of accelerator and experiment equipment.

Motivation for Protection Systems

1. All technical systems cause some downtime
2. A protection system will always contribute to downtime
3. If the risk is low, it might be better to operate without or with a reduced protection system (see the Tevatron example)
4. If the risk is significant, protection systems is mandatory
5. If the downtime due to expected damage is larger than the downtime due to the protection system, such system is mandatory
6. The investment required for repair in case of damage needs to be considered

R. Schmidt

Tevatron 1.96-TeV $p\bar{p}$ Collider Magnet Quenches

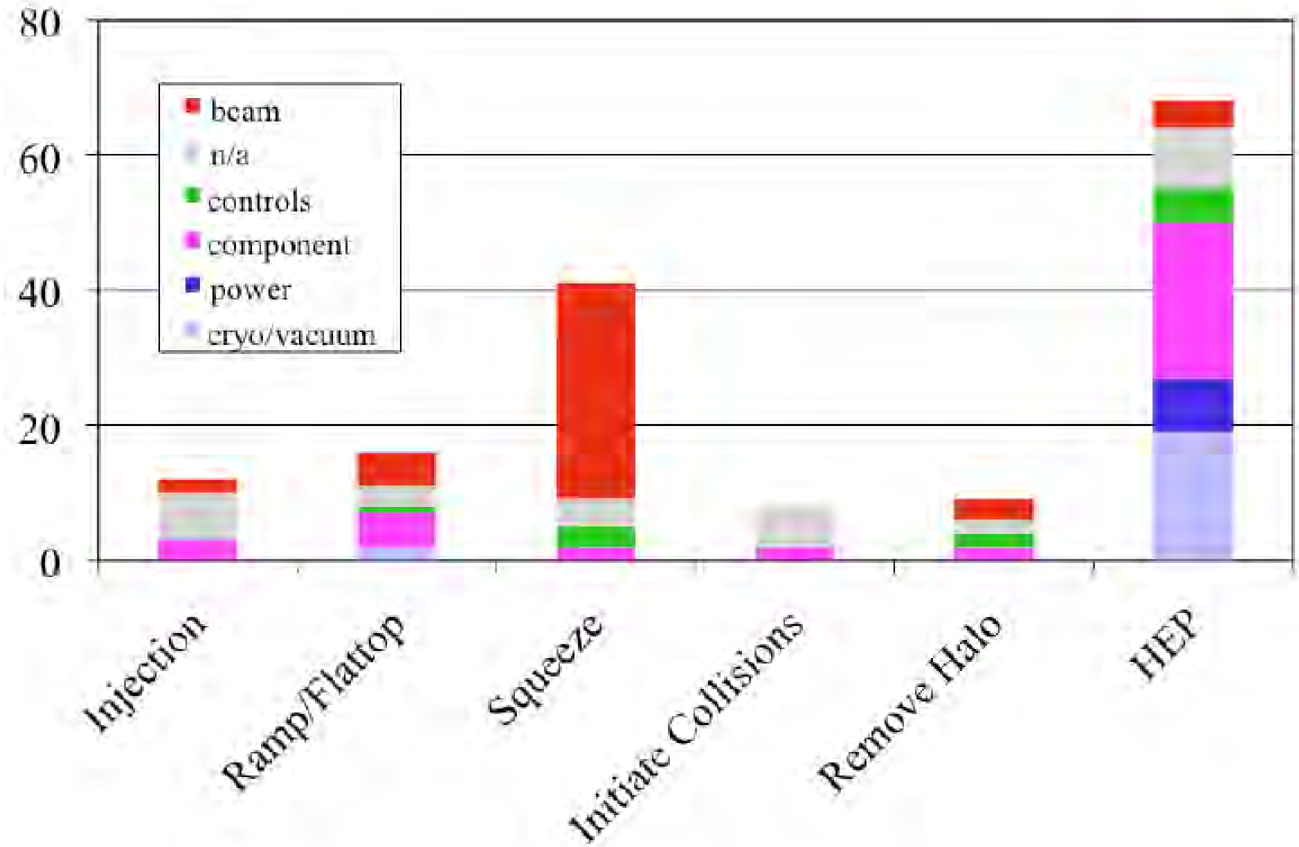

Characterization of Tevatron magnet quenches between October 2007 and March 2011. Out of 154 total, 32 were during low-beta squeeze (3 to 4% luminosity loss), 5 during acceleration, 3 during halo removal and 4 at HEP collisions. Cryo recovery at HEP was 3 hours. D. Still & A. Valishev

Machine Protection System (MPS)

- If something goes wrong, the beam energy has to be safely deposited (aborting the beam to an external absorber)
- If something goes wrong, the energy stored in each of the magnet has to be safely discharged (1232 superconducting dipole magnets in LHC)
- Obviously, if something goes wrong, injection has to be stopped

Beam Loss Timescale: Specs for MPS at LHC

- Single-pass (ns to μs)
  - ➢ Beam transfer lines (injection, extraction, beam abort, fixed target experiments)
  - ➢ Kicker magnet failures (injection, extraction, special kickers – diagnostics)
  - ➢ Accidental local (~200 ns, 60 m)
- Very fast (ms) transient
  - ➢ 10 turns or so in LHC
  - ➢ Large number of possible failures in technical systems (e.g., magnet powering)
- Fast (10 ms to sec)
  - ➢ Large number of possible failures in technical systems
- Slow (many sec)
  - ➢ Beam-gas scattering, non-linear dynamics, experiment cross-talk
  - ➢ Tails from collimators (collimation inefficiency)

Beam Collimation: 0.5 MW to 5 TW at LHC

- Beam cleaning (halo scraping): reduction of slow loss (beam-gas scattering, non-linear dynamics etc.) to minimize radiation loads to superconducting and warm magnets, detector backgrounds and mitigate radiological issues

- Passive protection of machine and detector components against irregular fast losses and failures; always needed in case of MPS failures and if the MPS response time is two long

Specified 7 TeV maximum allowed beam losses:

- Slow: 0.1% of beam per s for 10 s **0.5 MW**
- Transient: 5×10^{-5} of beam in ~10 turns (~1 ms) **20 MW**
- Accidental: up to 1 MJ in 200 ns into 0.2 mm^2 **5 TW**

Stored energy at max beam energy: LHC 362 MJ, FCC > 8 GJ

Multi-Stage Beam Collimation

Built for the first time at the Tevatron Collider in 1995. Built and installed at the LHC complex in 2008; now 110 movable collimators, with amazingly high performance

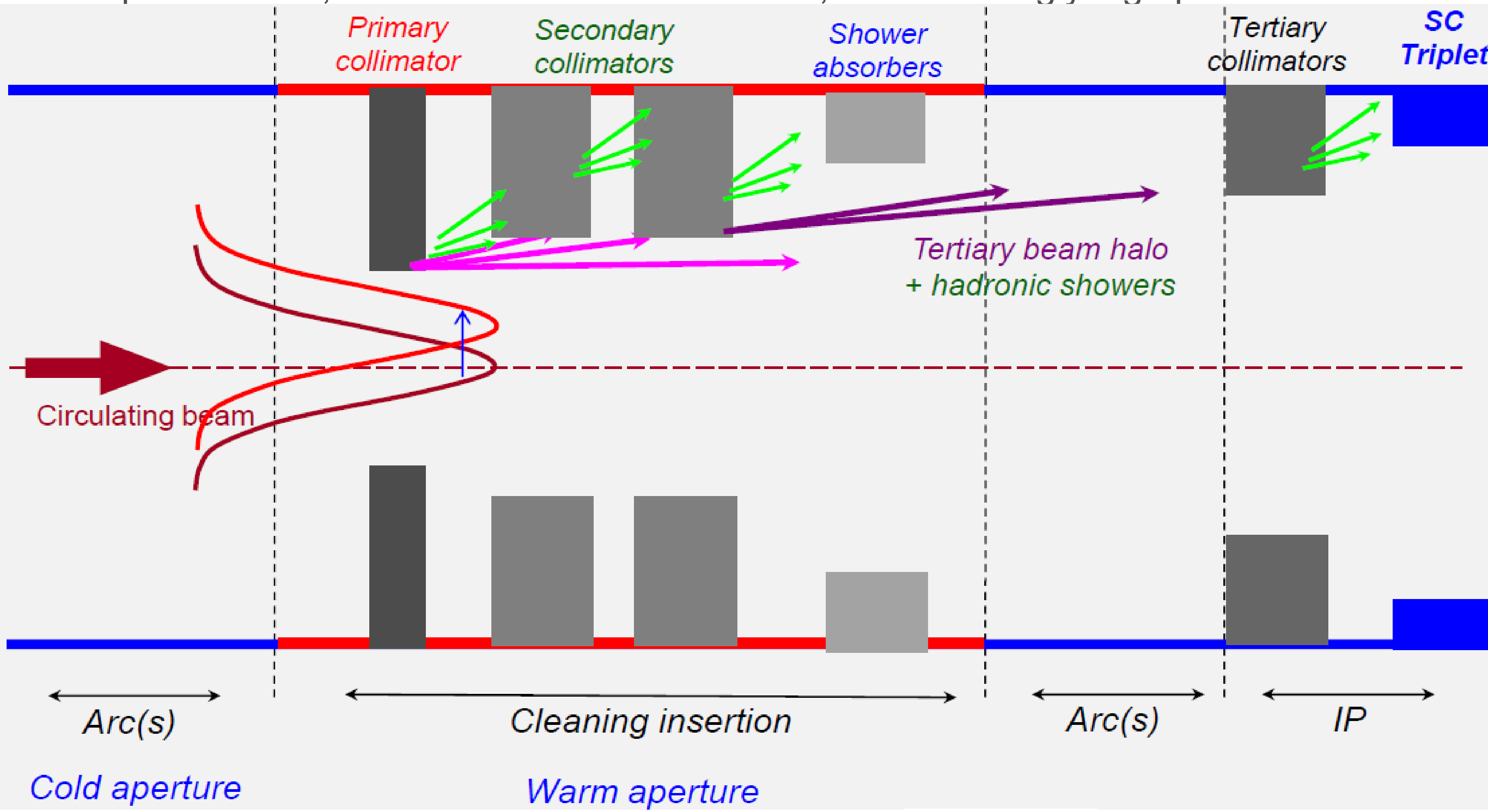

Active Protection

- A system is monitored, the monitor delivers some values (e.g. beam loss monitors measuring beam losses)
- The acceptable range of values is predefined (e.g. maximum beam losses within a time interval)
- If a value is out of the predefined range (e.g., after an equipment failure): take action (dump the circulating beam, stop injection, *etc*)
- The information has to travel from the monitor to the activator (extraction system, injection inhibit) ➔ interlock system
- There is some **reaction time required for the response** (depending on the system this can range between some ns and many seconds)

R. Schmidt

Transient Beam Loss Handling at the Tevatron

- Early days of Tevatron fixed target
  - ➢ Protect against any possible quench
  - ➢ Unnecessary abort wastes a single beam pulse
- Early days of Collider (6×6 , 900 GeV, ~2E12)
  - ➢ Tevatron can survive a quench
  - ➢ An abort turns off collider for ~ 1 day
  - ➢ A quench is no worse than an abort
- Run II Intensities(36×36, 980 GeV, ~1E13)
  - ➢ There is enough beam to damage Tevatron again
  - ➢ Improve protection of Tevatron components
  - ➢ Do not cause unnecessary down time

Beam Abort System at the Tevatron

- Abort Inputs
  - QPM (Quench Protection Monitor controlling superconducting state of the magnets)
  - Beam Loss Monitors (masked during stores)
  - Power supplies (etc.)
- Abort Loop
  - Hardware fail-safe loop
  - Can abort beam within a couple revolutions (40 μs)
  - Aborts synchronized to single beam abort gap

Beam-Induced Accident at the Tevatron in 2003

There were 24 cryogenic refrigerator houses for the Fermilab Tevatron ring. One house cryogenically kept about 40 superconducting magnets. On December 5, 2003, the Tevatron suffered a 16 house quench (**2/3** of the 6-km ring) during the end of a proton-antiproton colliding beam store.

That followed by the damage of **2 collimators** used for halo reduction at the CDF and DØ interaction points. In addition, two cryogenic spool pieces with **3 correction elements** were also damaged as a result of helium evaporation and pressure rise during the quench, requiring **10 days of Tevatron downtime** for repairs.


C18 spool

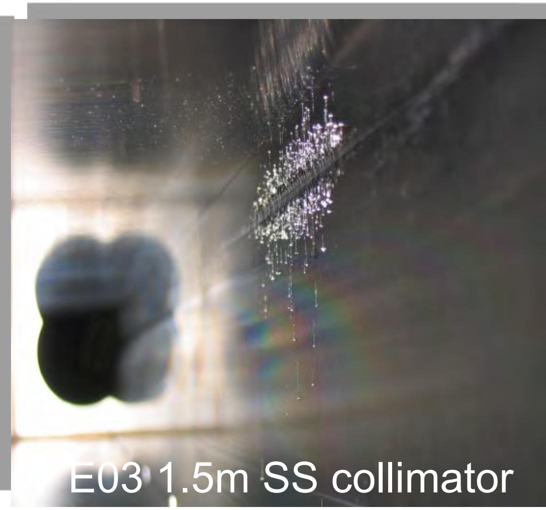
E03 1.5m SS collimator

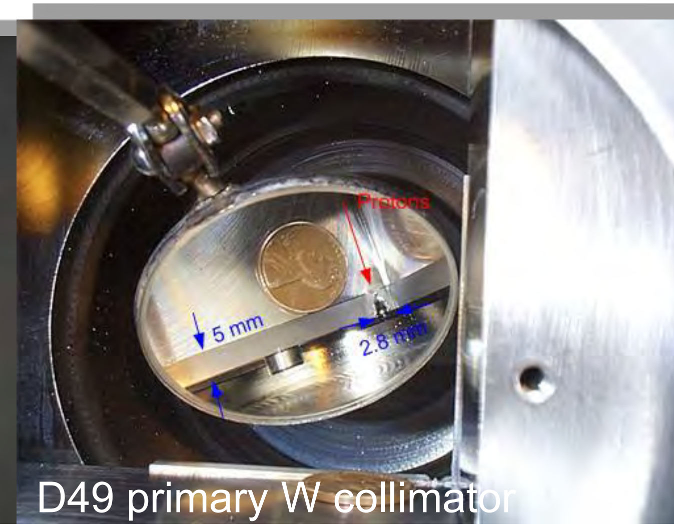

D49 primary W collimator

Sequence of Events

The large quench was found to be initially caused by a CDF Roman Pot reinserting itself quickly back into the beam after it had been issued retract commands.

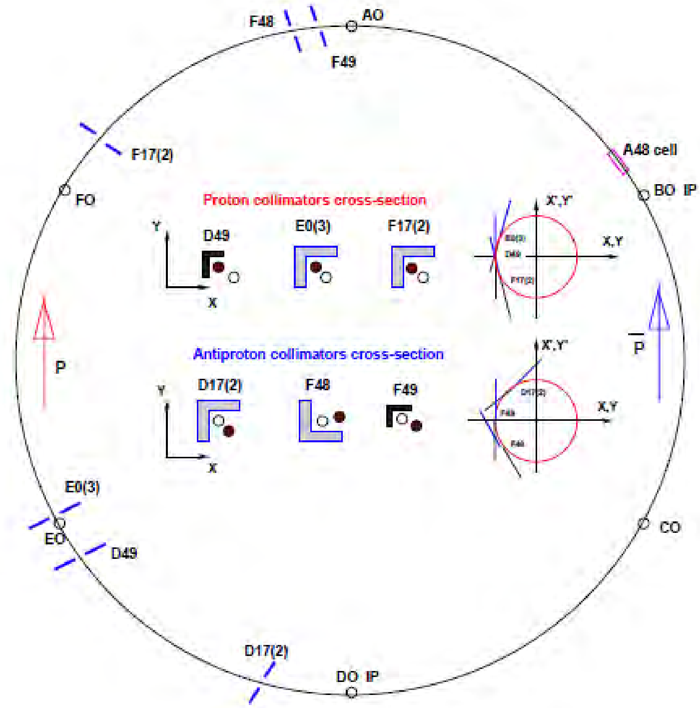

- Losses generated quickly and quench A48U
- Field in 5 dipoles starts decaying (500 A/sec)
- Orbit moves everywhere
- Beam moves through D49 primary collimator, E11 spool piece, and E03 Collimator.
- Protons are extinguished in E03 collimator in about several turns
- QPM detects quench in A48
- Abort kickers fire
- This all occurs within 16 msec

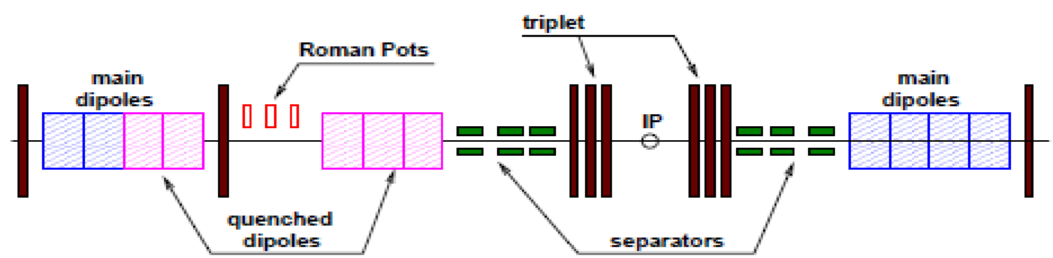

Modelling of Tungsten Collimator Ablation

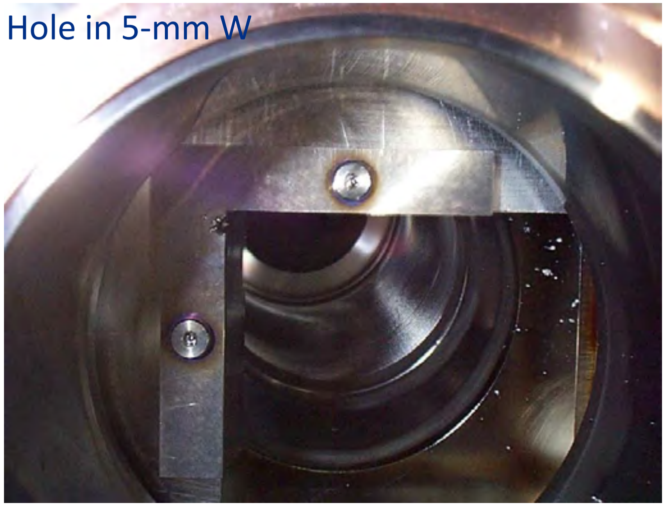

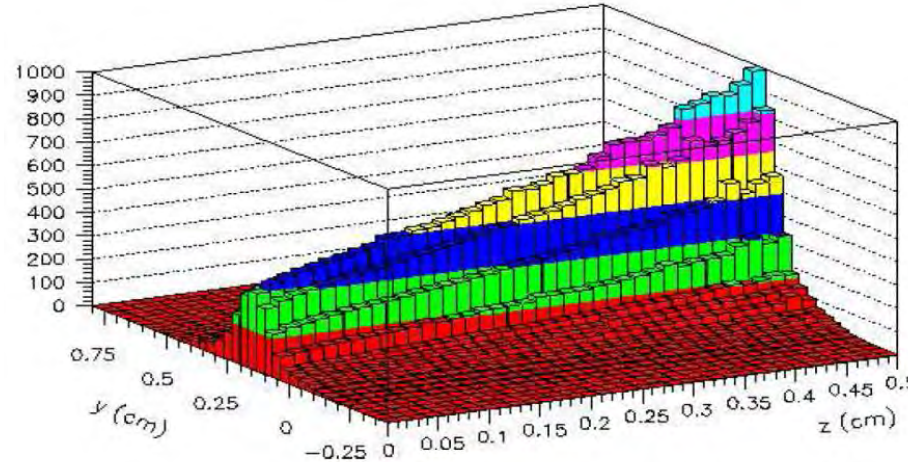

Detailed modelling of dynamics of beam loss (STRUCT), energy deposition (MARS14) as high as 1 kJ/g, and time evolution over 1.6 ms of the tungsten collimator ablation (FRONTIER), explained what happened

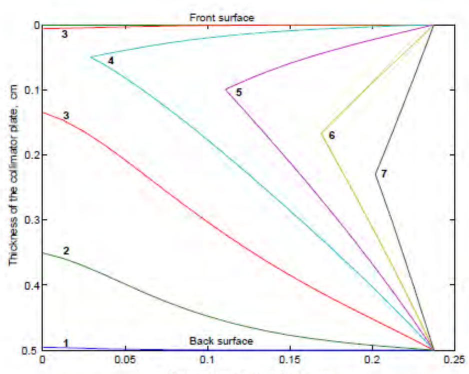

Figure 7: Evolution of the front and back surfaces of the collimator plate at $t = 0.4_{[1]} - 1.6_{[7]}\ ms$ with Δt=0.2 ms.

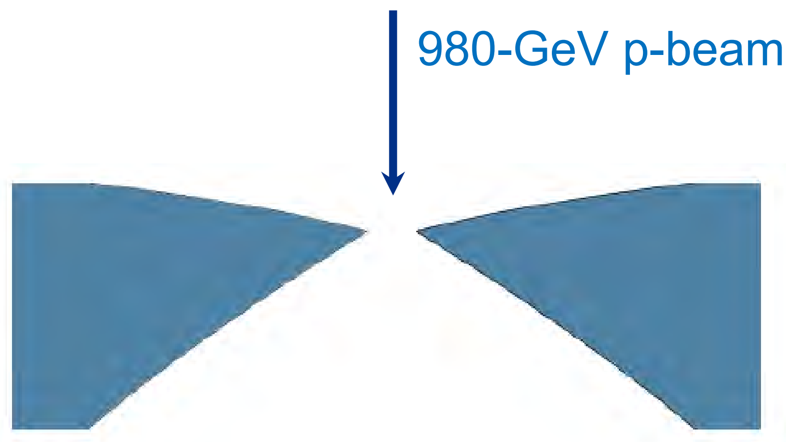

What Has Been Done after the Accident (1)

- **Roman Pots:** the controllers have been fixed, drivers changed and hard stops installed
- **AC Power in Kicker Room:** reconfigured so the kicker and the CAMAC Abort controls are on a separate feed from the sub-station
- **Timing Generator**: the CAMAC abort system now generates an abort pulse – phase locked to the abort gap – if the accelerator timing system clock is lost
- **Multi-House Quench**: implantation of a new fast detection buffer inside the Quench Protection Monitor system (QPM) that samples quench data at 5kHz (instead of the original 60 Hz) and determines a quench and pull the abort in 2 msec instead of 16 msec before the change

What Has Been Done after the Accident (2)

- **BLM System:** upgrade
- **Vacuum System Failures:** it took 200 ms for the abort to be generated in the old system. A new chassis that monitor the voltages going to the valves have been designed, built and installed. If the voltage is removed, this generates an abort command in ~7 ms. It was verified this works appropriately. Twenty four crates have been installed during the shutdown
- **Controls:** The beam abort loop was comprised of a loop of C200 family modules (one in each sector) that provides a permit (antifire) signal for the kickers. Each upstream module was input into the next downstream module. Modifications have been made to ensure the startup state for the masks. The timer circuitry was also modified
- **Correctors:** checked and confirmed that these are OK

Brand New Example: PIP-II MPS Concept

PIP-II is the Fermilab 800 MeV superconducting Linac project

The main goal of the MPS is to protect the machine from beam induced damage; thereby inhibiting the beam in case of excessive beam loss, equipment failures, or operator request. In achieving that objective, the system will also provide the following features:

- Manage beam intensity and permit limits of MPS designated devices while providing post-mortem data to the control system.
- Provide a comprehensive overview of the machine state and readiness status to subsystems and the broader complex.
- Provide a global synchronization trigger for beam related system fault analysis.
- Provide linac beam status to the accelerator complex control system.
- Provide high availability and fail-safe operation where possible.
- Manage and display MPS alarms.
- The MPS is not a personnel safety system.

Machine Protection Concepts
Part 2 (NVM5)

Nikolai Mokhov, Fermilab

USPAS, Colliders

February 3, 2022

Outline

Part 1:

- Beam Stored Energy
- Protection of Beam, Experiment and Machine
- Machine Protection System (MPS) Landscape
- Collimation and Active Protection
- Tevatron MPS Concepts and 2003 Beam Accident

Part 2:

- LHC 2008 Incident
- MPS Strategy and Design Guidelines
- LHC MPS Performance
- MPS in the HL-LHC Era and Beyond

LHC Incident of September 19, 2008

The most serious machine incident

- Last commissioning step of one out of the 8 main dipole electrical circuit in sector 34 : ramp to 9.3kA (5.5 TeV).
- At 8.7kA an electrical fault developed in the **dipole bus bar** located in the interconnection between quadrupole Q24.R3 and the neighboring dipole.

  Later correlated to a local resistance of ~220 nΩ – nominal value 0.35 nΩ.

- An electrical arc developed which punctured the helium enclosure.

  Secondary arcs developed along the arc.

  Around 400 MJ from a total of 600 MJ stored in the circuit were dissipated in the cold-mass and in electrical arcs.

- Large amounts of Helium were released into the insulating vacuum.

  In total 6 tons of He were released.

This incident involved magnet powering, but no beam!

J. Wenninger

Release of 600 MJ at LHC

The Helium pressure wave damaged ~600 m of LHC, polluting the beam vacuum over more than 2 km.

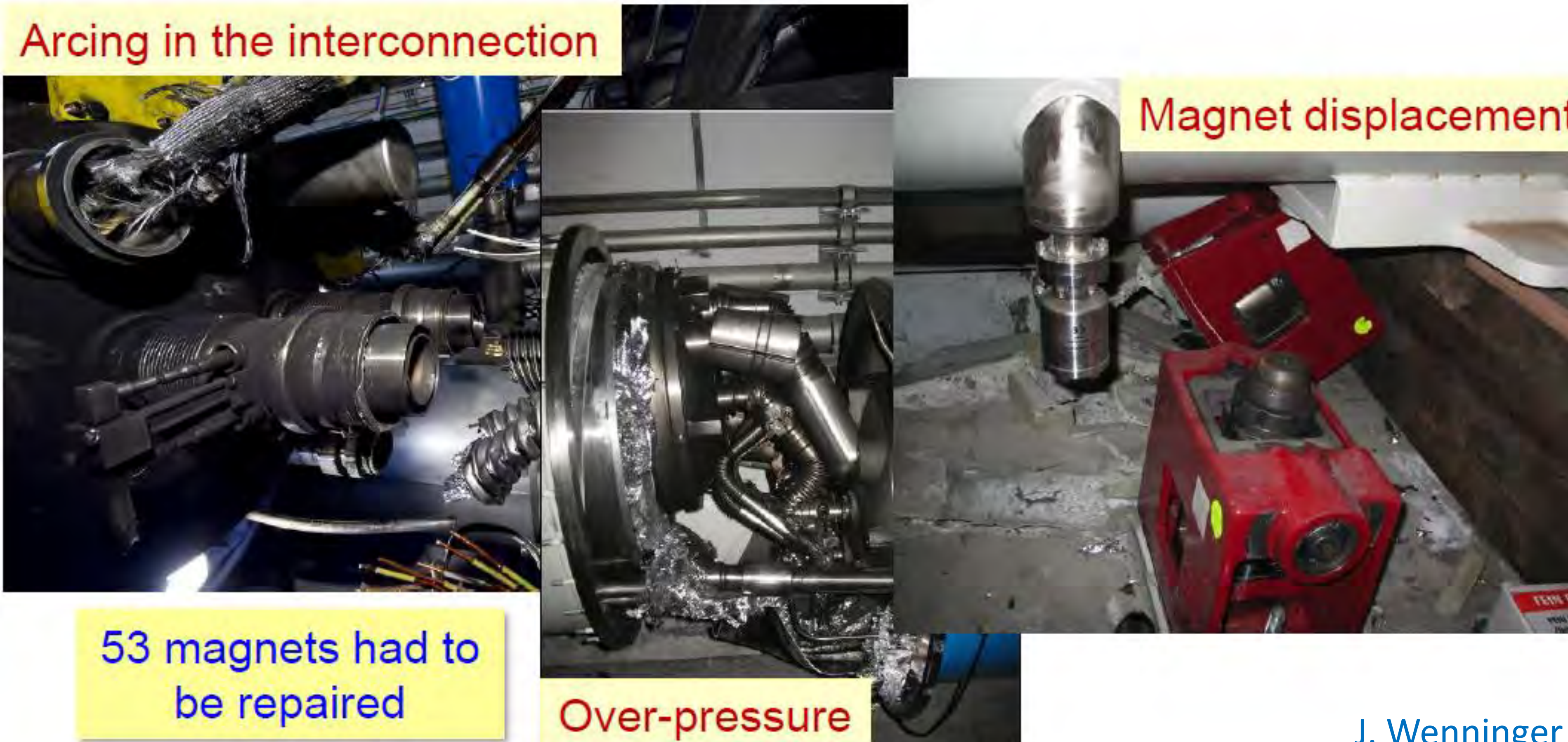

53 magnets had to be repaired

J. Wenninger

Consequences

- Machine down for more than 1 year for repair and re-commissioning
- Major upgrades to protection system of the magnets (surveillance of the busbar stabilizer)
- Major upgrades to pressure release and magnet anchoring
- Limitation of the machine energy to 3.5 TeV instead of 7 TeV
- Almost 2-year long shutdown (2013-2014) to repair all magnet interconnections
- **Bonus:** commissioning and early operation in “easier” conditions 3.5–4 TeV *vs* 7 TeV, lower fields, increased quench-resistance; ➔ no beam-induced quench in Run 1 (2010-2013) with stored energy up to 70 times above previous state-of-the art

J. Wenninger

Launching MPS Design

1. Identify hazards: what failures can have a direct impact on beam parameters and cause loss of particles on aperture
2. Classify the failures in different categories
3. Estimate the risk for each failure (or for categories of failures)
4. Work out the worst case failures
5. Identify how to prevent the failures or mitigate the consequences
6. Design systems for machine protection (e.g., 3600 BLMs around LHC plus much more)

R. Schmidt

Classification of Failures

- Type of the Failure
  - Hardware: power converter trip, magnet quench, AC distribution (thunderstorm etc.), object in beam pipe, vacuum leak, RF trip, kicker misfire etc.
  - Controls: wrong data, wrong magnet current function, trigger problem, timing system, feedback failure etc.
  - Operational: chromaticity/tune/orbit wrong values
  - Beam instabilities: e-clouds or too high beam/bunch current
  - Objects in the beampipe: movable devices, RF fingers, gas above nominal pressure, some beam instrumentation, Roman Pots

- Parameters of the Failure
  - Time constant of beam loss
  - Location of beam loss (normally, in the predefined places)
  - Probability for the failure
  - Damage potential

R. Schmidt

Protection at Injection to LHC

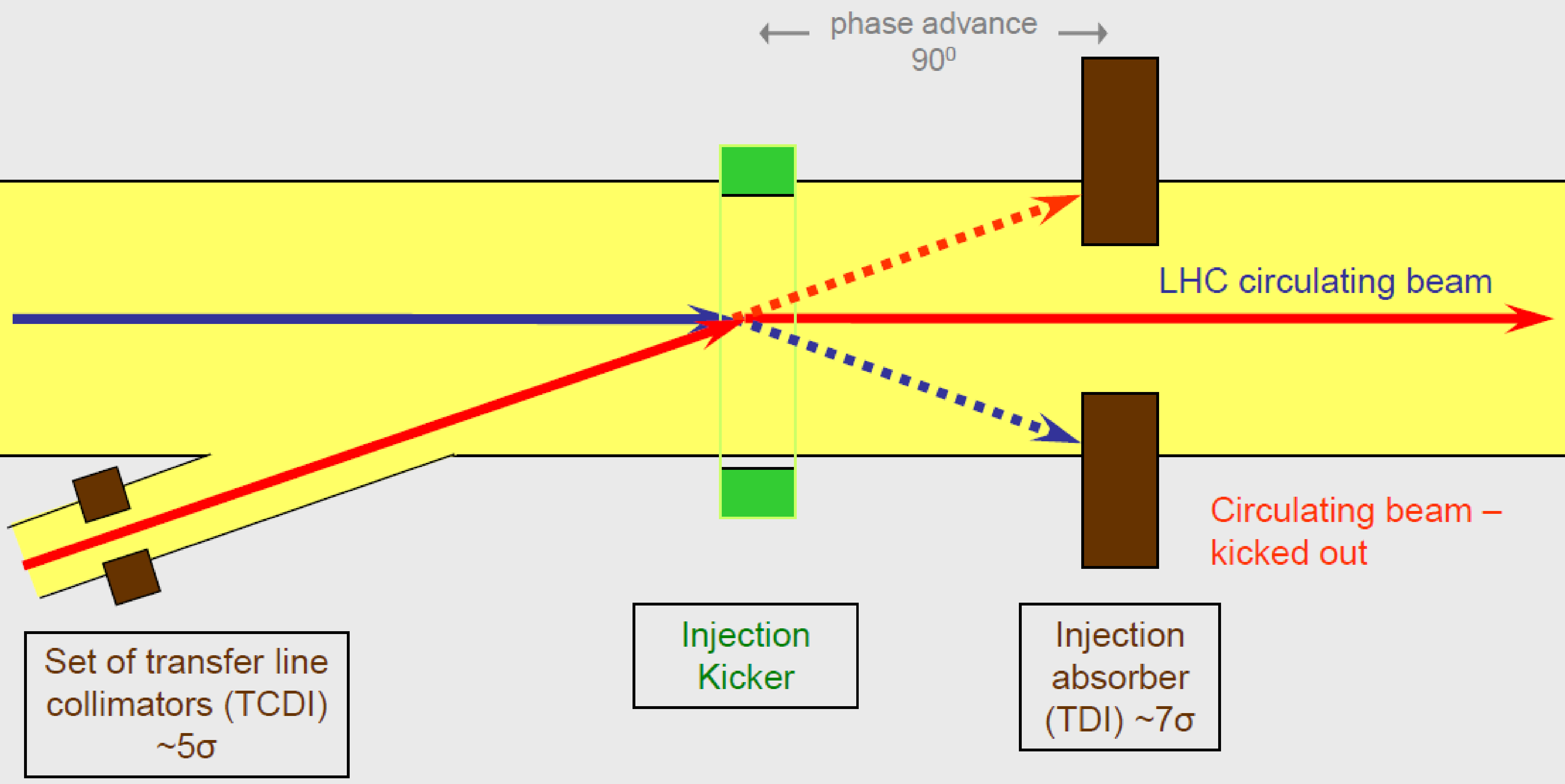

Beam absorbers take beam in case of kicker misfiring on circulating beam

LHC Beam Abort System

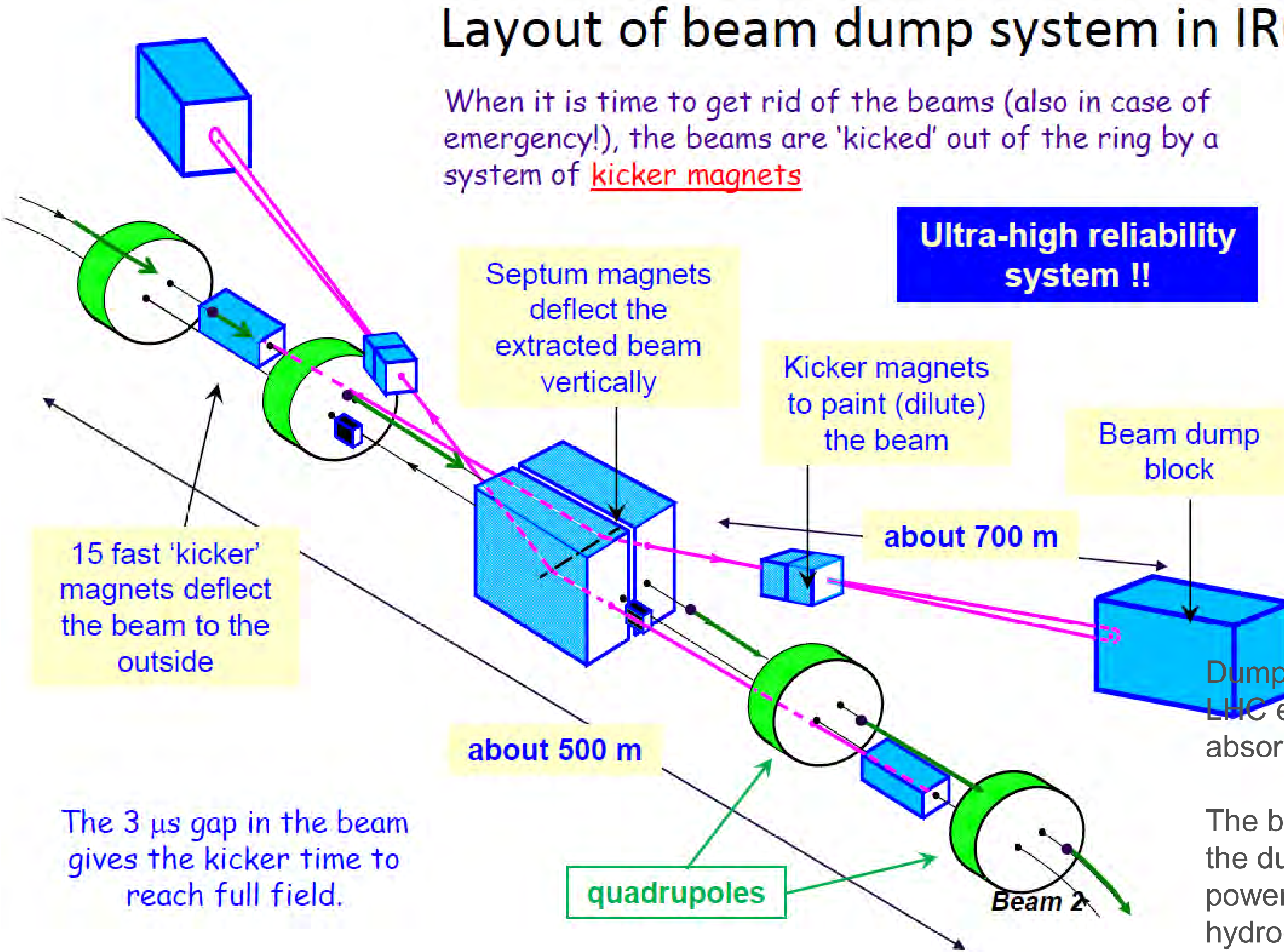

Dump block is the only LHC element capable of absorbing the full beam.

The beam is swept over the dump face to lower power density, otherwise hydrodynamic tunneling.

LHC Strategy for Machine Protection

• Definition of aperture by collimators.	**Beam Cleaning System**
• Early detection of equipment failures generates dump request, possibly before beam is affected.	**Powering Interlocks** **Fast Magnet Current change Monitor**
• Active monitoring of the beams detects abnormal beam conditions and generates beam dump requests down to a single machine turn.	**Beam Loss Monitors** Other Beam Monitors
• Reliable operation of beam dumping system for dump requests or internal faults, safely extracting beams onto the external dump blocks.	**Beam Dumping System**
• Reliable transmission of beam dump requests to beam dumping system. Active signal required for operation, absence of signal is considered as beam dump request and injection inhibit.	**Beam Interlock System**
• Passive protection by beam absorbers and collimators for specific failure cases.	**Collimator and Beam Absorbers**

R. Schmidt

Machine Interlock Systems at LHC

- Beam Interlock: Ensures beam extraction into the beam dump blocks when one of the MP systems detects a failure
- Powering Interlock: Ensures communication between systems involved in powering superconducting magnets (magnet protection, power converters, cryogenics, controls)
- Normal-Conducting Magnet Interlock: Ensures magnet protection in case of overheating and communication between systems involved in magnet powering
- Machine interlocks are strictly separated from interlock for personnel safety

Fermilab Machine Control and Safety Mechanisms

Administrative Controls

- Policies
- Procedures
- Signs
- Machine operators

Machine Protection Systems

- Beam permit system (BPS)
  - Beam alarms
  - Loss monitor inputs
  - Power supply monitoring
  - Vacuum valve positions
  - RF systems
  - Safety system (it provides input to BPS for monitoring purposes, but will terminate the beam directly and independently of all other systems)
  - Control system software monitoring
- Elements of the accelerator control system

FRCM-2018

Fermilab Machine Controls (MC)

- MC are systems that are used to limit accidental beam losses. They may prevent a beam loss from occurring, may prevent subsequent beam losses from occurring, or may include monitoring secondary effects from significant beam losses, such as loss of vacuum, that then potentially result in actions that prevent further beam losses from occurring.

- While all of these machine controls are capable of terminating beam operations upon discovery of an excessive beam loss, the laboratory recognizes well that they all have failure modes and do not meet the level of rigor designed into to the Safety System.

- Administrative controls are obviously subject to well-known human performance factors that can lead to failures. Likewise, <u>the automated machine protection systems, unlike the redundant Safety System items, are single output devices</u>. Inputs to the MPS can be "masked" (i.e., taken off line) during beam tuning and troubleshooting activities and thus have the potential to not be "unmasked" when normal operations resume.

FRCM-2018

LHC MPS Flow

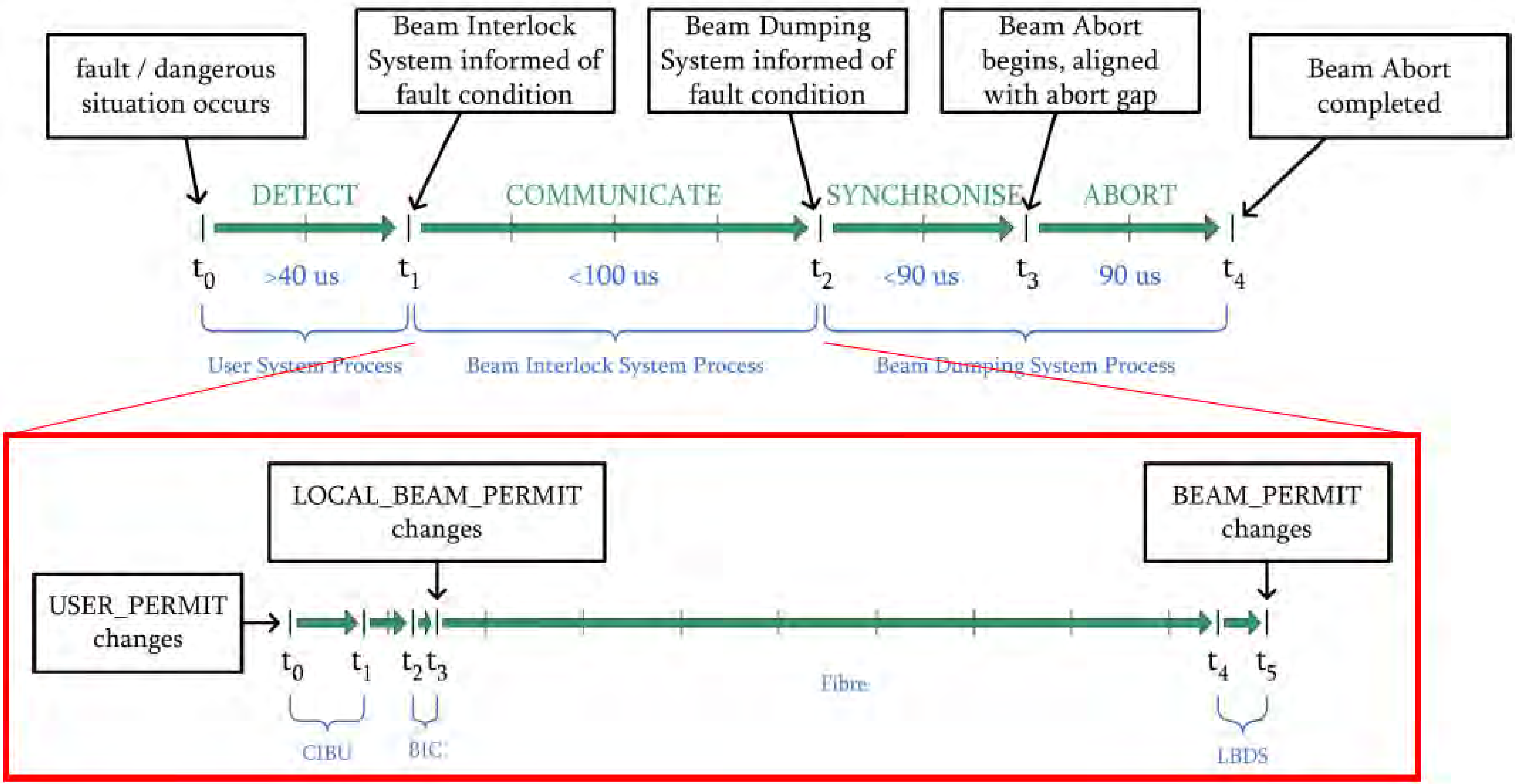

CIBU=Controls-Interlocks-Beam-User BIC=Beam Interlock Controller LBDS=LHC Beam Dumping System

R. Schmidt

Design Guidelines for MPS

- Fail-safety: detect internal faults, remote testing, stop operation if MPS off
- Redundant critical equipment
- No remote changes of most critical parameters
- Quantify safety, availability, reliability to predict failure rate
- Managing interlocks (e.g., their masking for beam setup)
- Test-benching of electronics
- Documentation for MPS design, installation, maintenance and operation is mandatory
- During commissioning, test accurate execution of each protection function
- Establish requirements for the test interval of each function
- Keep in mind that most failures (at LHC) are due to power supplies, mechanical parts and connectors

LHC MPS Topics in 2015

- ❑ Electronics of quench detection: radiation induced failures.
  - o *No safety, repair during TS2.*
- ❑ TDI absorber failures > 400 deg.
  - o *Limit on no. injected bunches.*
- ❑ BLM threshold changes
  - o *Weigh unnecessary UFO dumps vs protection.*
- ❑ Issues with interlock BPMs
- ❑ Beam dump block N2 pressure.
  - o *Discovered a weakness in the surveillance of the dump*.

Efficient and fast reactions, mitigations were put in place
No problems during the intensity ramp up of the LHC in 2015

Chamonix 2016 Summary

LHC MPS Dumps

Beam dump causes 2015 versus 2012
above injection

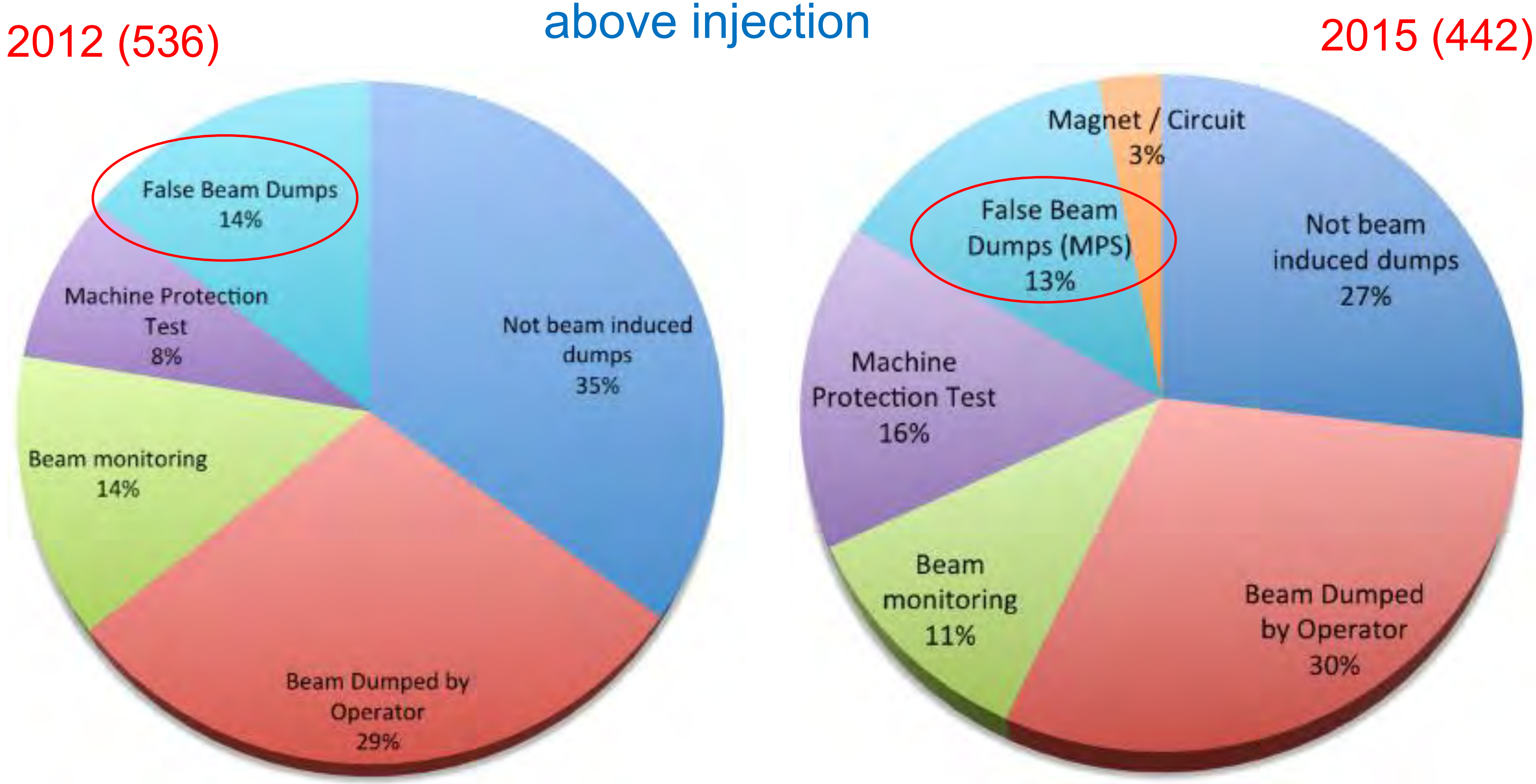

- False beam Dumps by Machine Protection Systems stable (LBDS, PIC, BLM, BIC, SIS, QPS, FMCM): 14 % in 2012 ➔ 13 % in 2015: OK

Chamonix 2016 Summary

LHC Collimation in 2015: Faster than Ever

- ❑ Thanks to experience and automation, the collimation setup and validation time was reduced by more than a **factor 4** since 2010.
- ❑ In 2015, 80% of the collimators were aligned with BLMs, 20% with BPMs.

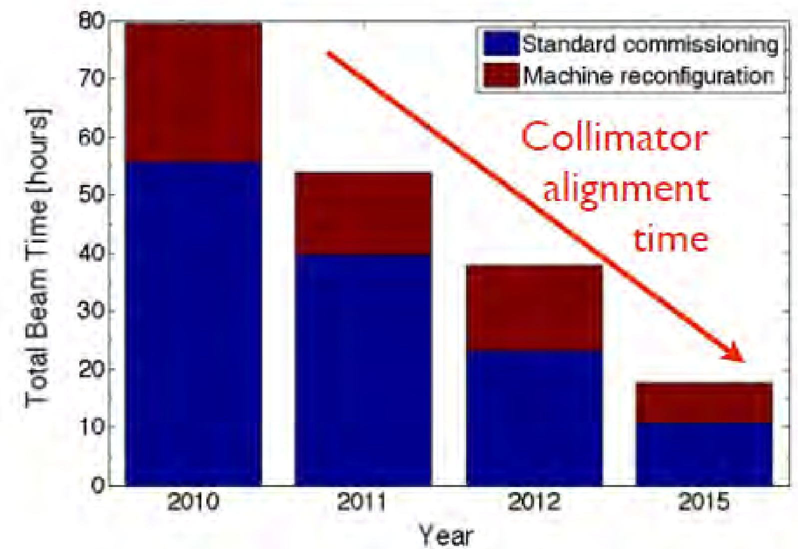

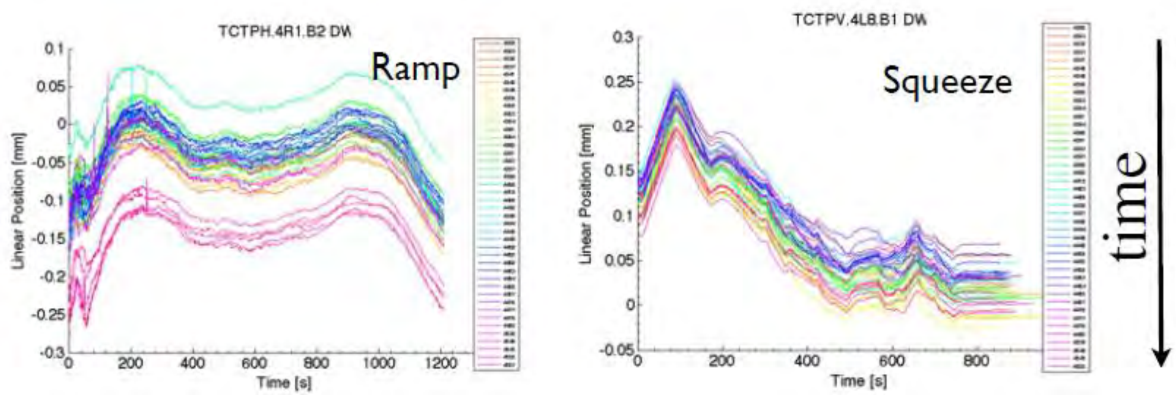

- ❑ Systematic orbit offsets in the collimators during the cycle (ramp, squeeze) will be corrected in 2016…
- ❑ Preparing to interlock the beam position in collimators at lowest β^*.

Chamonix 2016 Summary

Protection Devices in the LIU & HL-LHC Project

Protection devices in the whole accelerator chain will be upgraded for beams with higher intensity and brightness. Main examples:

- **SPS internal dump** will be replaced with a re-designed version with improved shielding and vacuum performance
- **TCDI collimators** in the SPS-to-LHC transfer lines will be replaced with longer and more robust devices
- **TDI injection dumps** will be replaced with re-designed versions featuring better impedance, cooling and vacuum
- A large fraction of **LHC collimators** will be replaced with low-impedance ones; collimation still needs more work for the HL-LHC era

Chamonix 2017 Summary

Beam Halo Depletion in the HL-LHC Era

1. Active halo control would allow **controlling diffusion speed** and **distributing losses** over time. **Overpopulated tails** (33 MJ outside 3.5 σ) combined with **fast failures** (e.g. by crab cavities) can cause high **losses into aperture** / collimation system.
Halo control via **e-lens** might be necessary to **mitigate fast failures and loss spikes**.

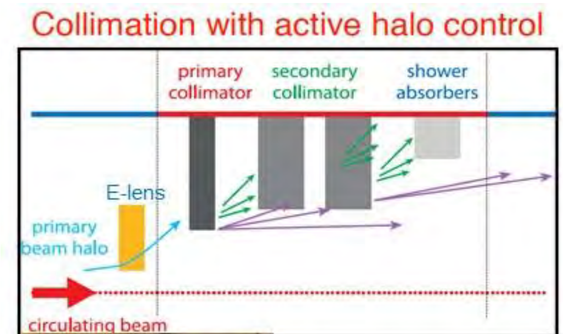

2. Low impedance secondary collimators (CFC) stabilize HL-LHC beams → **Prototype** collimators (MoGr, MoGr + TiN, MoGr + Mo) are being **installed** in LHC to **measure impedance** effects.

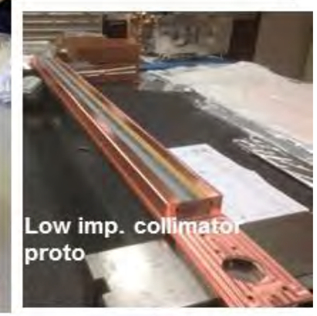

3. Reduction of phase advance (dump kickers to tertiary) or use of **more robust jaw material** allow for **tighter collimator settings** → nearly recover β^*=15 cm

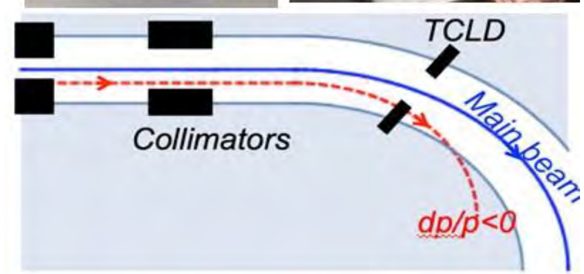

4. **Implementing BPM buttons** in **all new collimators**: reduction of setup time
5. In IP7 dispersion suppressor, installation of **TCLD + 11 T dipoles** during LS2 will provide factor 3-4 margin (baseline) for protons.

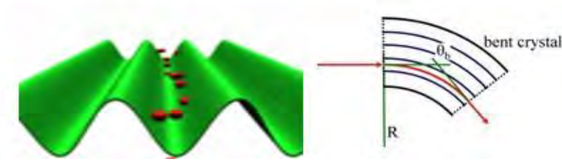

Chamonix 2017 Summary

Towards FCC

- Slow beam losses: decrease collimation cleaning inefficiency (to ≈ < 10^{-6})
- Fast losses: new ideas on MPS to protect a single magnet and magnet strings:
  dT/dt ≈ 1000…2000 (K/s), $\tau_{(300\ K)}$ ≈ 0.15…0.3 (s), E/l ≈ 1MJ/m

$$\left.\begin{aligned} E/l &\propto B^2 \\ A_{coil} &\propto \left(\frac{B}{J}\right)^n \end{aligned}\right\} \longrightarrow e \approx \frac{E/l}{A_{coil}} \propto J^n B^{2-n}$$

In the range of typical magnet designs considered n≈1.5

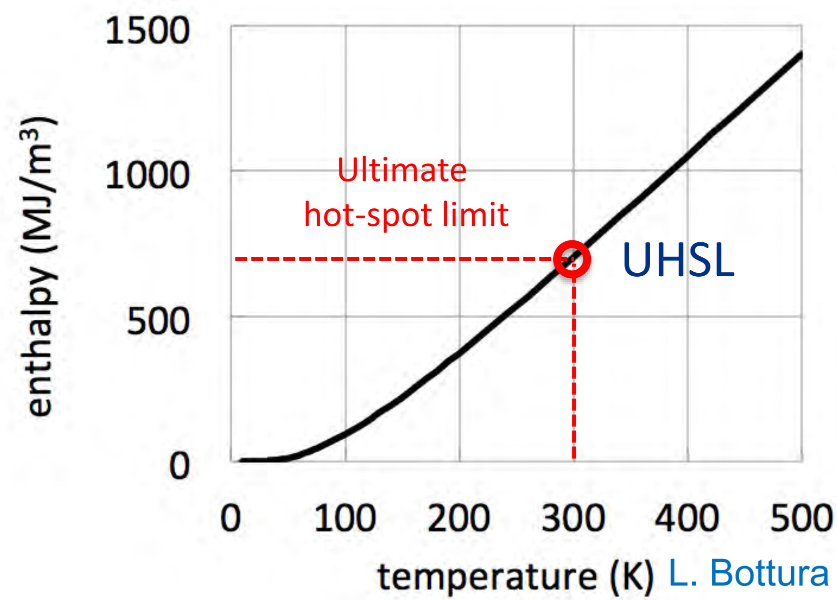

L. Bottura

Typical energy densities e:

LHC MB(8.33T) ≈ 50 MJ/m^3
LHC MBH(11T) ≈ 85 MJ/m^3
FRESCA2(13T) ≈ 100 MJ/m^3

FCC MB(16T) ≈ 200 MJ/m^3

50 < 200 MJ/m^3 < UHSL

Managed by Fermi Research Alliance, LLC for the U.S. Department of Energy Office of Science

Neutrino Flux around Muon Colliders and 7 Ways to Mitigate it (NVM6)

Nikolai Mokhov, Fermilab

USPAS, Colliders

February 3, 2022

Tentative Muon Collider Parameters

Parameter	Symbol	unit			
Centre-of-mass energy	E_{cm}	TeV	3	10	14
Luminosity	$\mathcal{L}$	$10^{34}\mathrm{cm}^{-2}\mathrm{s}$	1.8	20	40
Collider circumference	C_{coll}	km	4.5	10	14
Average field	$\langle B \rangle$	T	7	10.5	10.5
Muons/bunch	N	10^{12}	2.2	1.8	1.8
Repetition rate	f_r	Hz	5	5	5
Beam power	P_{coll}	MW	5.3	14.4	20
Longitudinal emittance	ϵ_L	MeVm	7.5	7.5	7.5
Transverse emittance	ϵ	μm	25	25	25
IP bunch length	σ_z	mm	5	1.5	1.07
IP betafunction	β	mm	5	1.5	1.07
IP beam size	σ	μm	3	0.9	0.63

Neutrino Flux at a Distance from Collider Ring (1)

Intense highly collimated neutrino beams, created from muon decays in the ring and various straight sections of high-energy $\mu^+\mu^-$ colliders (MC), can cause – to the surprise of many - radiation problems even at very large distances from the machine.

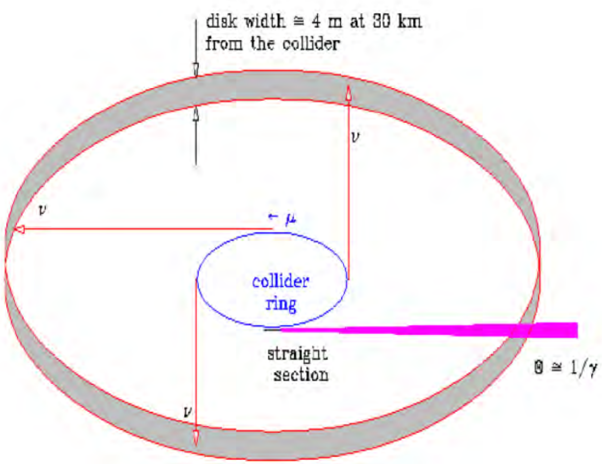

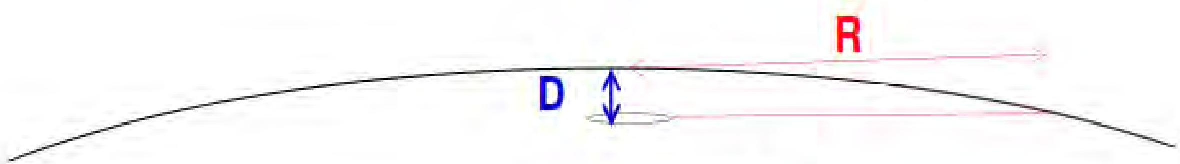

$$R = \sqrt{2R_{earth}D}$$

The more energetic decay neutrinos emanate radially outward from the collider ring at angles with respect to the muon direction of order

$$\theta_\nu = 1/\gamma_\mu = m_\mu/E_\mu \simeq 10^{-4}/E_\mu[\mathrm{TeV}]$$

Neutrino Flux at a Distance from Collider Ring (2)

Neutrino flux and dose per neutrino at a given location from muon colliders (MC) grow with muon energy – keeping all other MC parameters the same - roughly as $\boldsymbol{E_\mu^3}$ due to (each responsible for a factor of E_μ):

1. Increase with energy of the neutrino cross section
2. Grows of total energy deposited
3. Collimation of the decay neutrinos

This will impact strongly siting issues and cost of a high energy muon collider and needs to be taken seriously in evaluating long-term averaged neutrino flux and resulting dose.

Developed by NM & AVG in 1996 a weighted neutrino interaction generator for the MARS Monte Carlo code permitted detailed simulations of the interactions with matter of neutrinos and of their progeny in and around MC capable to modeling neutrinos in the energy range from 10 MeV to 10 TeV.

Neutrino-Interaction Model in MARS15 (1)

The model serves to represent energy and angle of the particles emanating from a simulated interaction. These particles, along with the showers initiated by them, are then further processed by the MARS code which calculates, e.g., energy deposition, absorbed and effective dose as a function of location in a user specified geometry model. Effective dose – caused by charged particles from neutrino interactions - is calculated with particle- and energy-dependent quality factors taken into account. Muon and electron neutrinos and their antiparticles are included and distinguished throughout, which are represented in the decays from MC in roughly equal amounts. The MARS model identifies charged and neutral current deep inelastic neutrino and antineutrino interactions with nuclei as the dominant channels forming the main contributions to the dose from neutrino interactions. For the first channel (first row in the Table), total cross-sections σ in cm^2 are assumed to be $6.7\times 10^{-39}\, E_\nu$ per nucleon with E in GeV for neutrino and a half of that for antineutrino. The differential cross section is

$$\frac{d\sigma}{dx\,dy} = \frac{G^2 x s}{2\pi}\left(Q(x) + (1-y)^2\,\overline{Q}(x)\right)$$

where $x=-q^2/2M\nu$ with q the momentum transfer, M the nucleon mass and ν the energy loss of the neutrino in the lab, $y=\nu/E_\nu$, G is the Fermi coupling constant, s is the total energy in the center of mass, and $Q(x)$ represents quark (antiquark) momentum distributions inside the nucleon.

Neutrino-Interaction Model in MARS15 (2)

For the neutral current deep inelastic neutrino and antineutrino interactions with nuclei (second row in the Table), total cross-sections σ in cm^2 are taken as 2.2×10^{-39} E_ν per nucleon with E in GeV for neutrino and 1.35×10^{-39} E_ν for antineutrino. The differential cross section is built similarly to that as for the charged current deep inelastic neutrino and antineutrino interactions.

Besides that, the model accurately describes neutrino-nucleon elastic and quasi-elastic scattering (rows 3-5), interactions with atomic electrons (rows 6-7) and coherent elastic scattering (row 8 in the Table). In latter, a Pauli formfactor of quark – topological fluctuation of QCD vacuum - is included (as a weight) to discourage small $|q^2|$ insufficient to liberate a nucleon or promote the nucleus to an excited state.

Table 1: *Neutrino Interactions*

$\nu_\mu N$	$\rightarrow$	$\mu^+ X$	$\overline{\nu}_\mu N$	$\rightarrow$	$\mu^- X$	Charged current deep inelastic
$\nu_\mu N$	$\rightarrow$	$\nu_\mu X$	$\overline{\nu}_\mu N$	$\rightarrow$	$\overline{\nu}_\mu X$	Neutral current deep inelastic
$\nu_\mu p$	$\rightarrow$	$\mu^+ n$	$\overline{\nu}_\mu n$	$\rightarrow$	$\mu^- p$	Elastic and quasi-elastic scattering
$\nu_\mu p$	$\rightarrow$	$\nu_\mu p$	$\overline{\nu}_\mu p$	$\rightarrow$	$\overline{\nu}_\mu p$	Elastic and quasi-elastic scattering
$\nu_\mu n$	$\rightarrow$	$\nu_\mu n$	$\overline{\nu}_\mu n$	$\rightarrow$	$\overline{\nu}_\mu n$	Elastic and quasi-elastic scattering
$\nu_\mu e^-$	$\rightarrow$	$\nu_\mu e^-$	$\overline{\nu}_\mu e^-$	$\rightarrow$	$\overline{\nu}_\mu e^-$	*Neutrino-electron* – almost negligible
$\nu_\mu e^-$	$\rightarrow$	$\nu_e \mu^-$				
$\nu_\mu A$	$\rightarrow$	$\nu_\mu A$	$\overline{\nu}_\mu A$	$\rightarrow$	$\overline{\nu}_\mu A$	Coherent elastic scattering

"Neutrino" Dose around Muon Colliders

Extremely low interaction and scattering probabilities mean that neutrinos travel essentially in a straight line and survive over enormous distances. Much like neutrons and gammas, neutrinos by themselves cause little or no biological damage but instead create charged particles which in turn deposit their energy in tissue to be interpreted as dose "due to neutrinos".

"Neutrino" dose is by charged particles generated by neutrinos upstream a human.

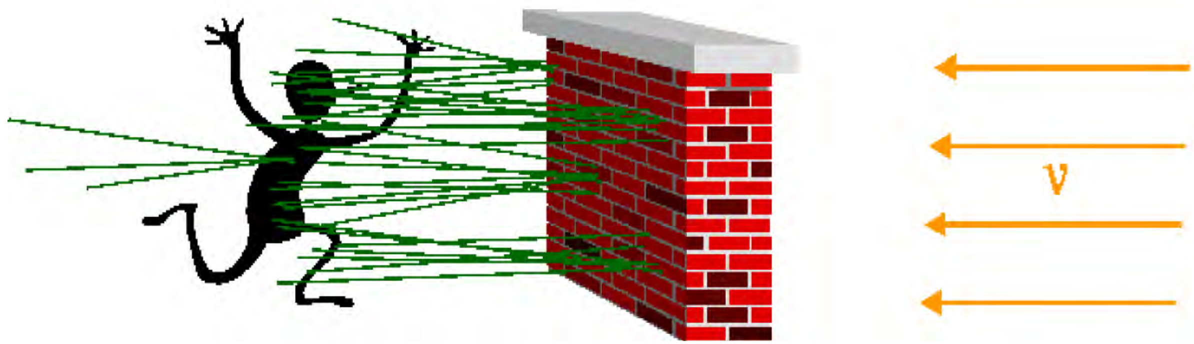

Therefore:

- Small effect for anyone above ground or/and above ground building
- Noticeable effect inside a basement swimming pool
- Unacceptably high effect, e.g., for a person lying in a basement room for extended period

Dose to a Human Body *vs* Neutrino Energy

- Total whole-body effective dose in a bare seated person (**non-equilibrium**) and in one embedded in infinite soil (**equilibrium**).
- The whole-body dose is a factor of 2 lower than the maximum dose, because a neutrino flux footprint could be smaller than typical human directions.
- The equilibrium dose is achieved after 3-4 m of soil or concrete at all neutrino energies considered here.
- Instead of providing shielding, the presence of soil/concrete upstream enhances the dose by a factor of 1000 in the TeV region as compared to the case with no shielding.

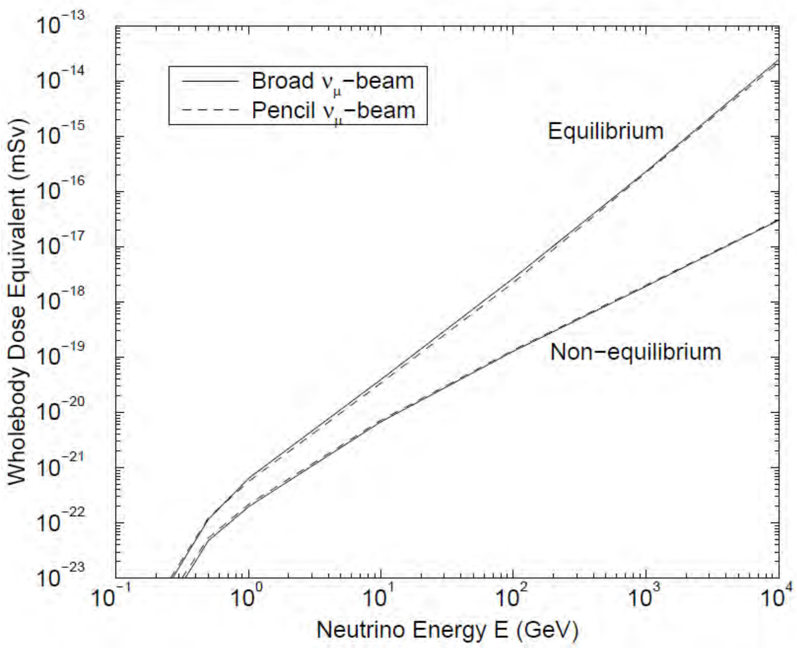

<u>Annual off-site limits:</u>

DOE 1 mSv = 100 mrem
FNAL 0.1 mSv = 10 mrem
Europe 0.01 mSv = 1 mrem

Neutrino-Induced Dose *vs* Upstream Material

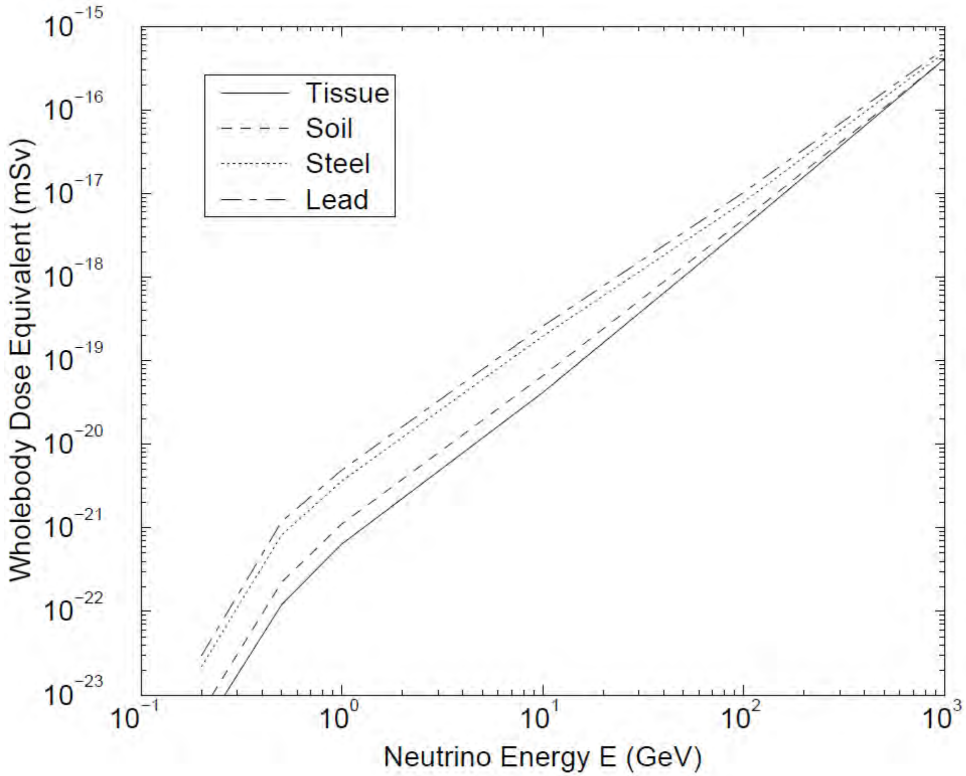

Whole-body dose in a 60-cm long tissue equivalent phantom embedded in infinite materials *vs* neutrino energy for a broad ν_μ-beam. Dose after a high-Z shielding is up to a factor of ten higher than that for a low-Z shielding at low neutrino energies, while the values converge in the TeV energy range.

At low energy, a larger fraction of the dose is delivered by (high quality factor) low energy neutrons whereas at high energy the electromagnetic component (with quality factor essentially unity) dominates.

Maximum Equilibrium Dose *vs* Distance in Soil

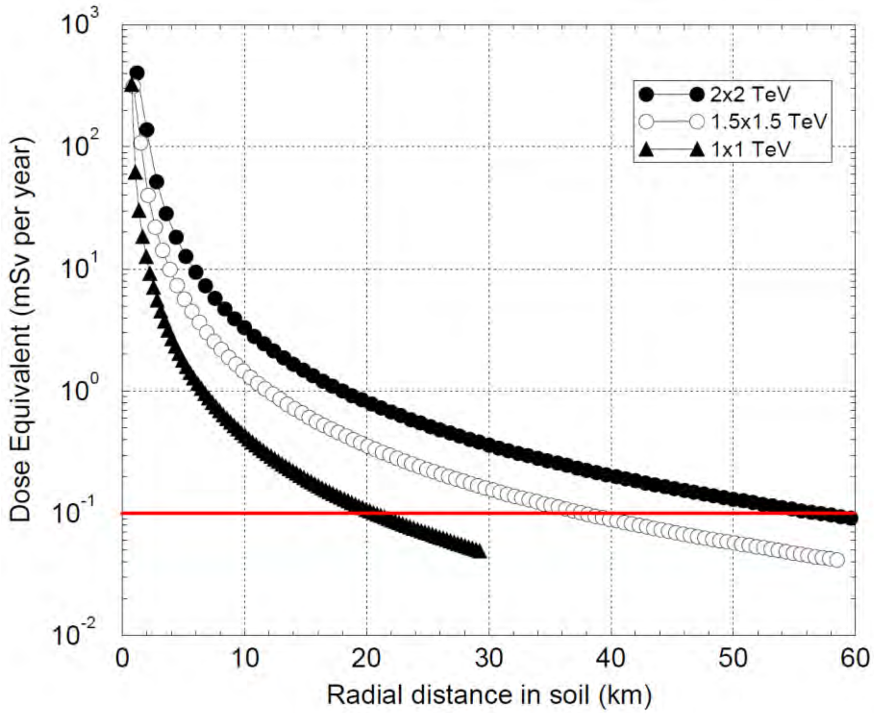

Around the 2, 3 and 4 TeV MC rings in the orbit plane with 1.2×10^{21} decays per year *vs* distance in soil from the ring center

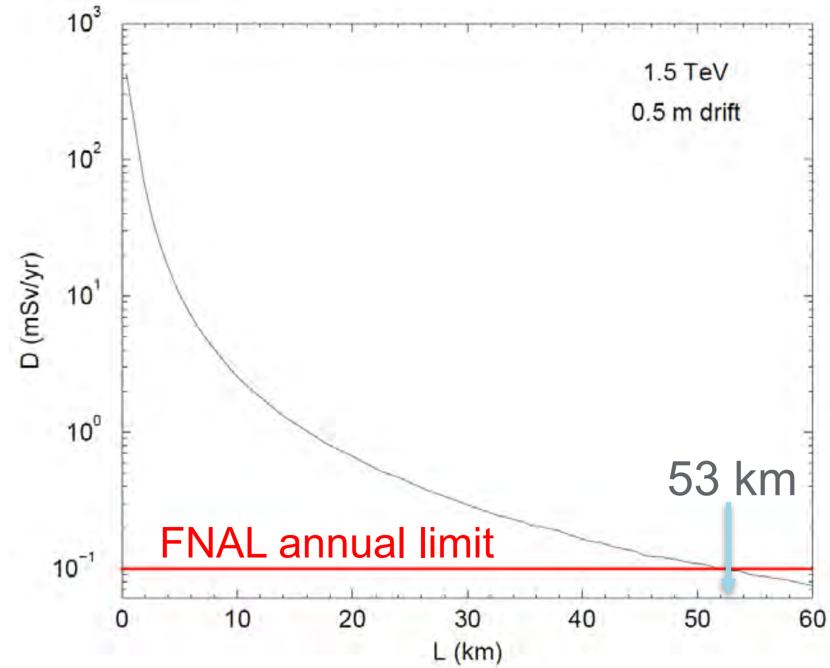

1.5-TeV muon beam with 2.6×10^{16} decays/yr in a 0.5-m drift *vs* distance in soil downstream the drift.

Contribution from field-free regions (drifts, straight sections, etc.) becomes a serious one at high-energy muon colliders even with very short regions: at E_μ = 10 TeV, 0.1-m drift and 10^{16} decays/yr $\longrightarrow$ L=380 km

Seven Ways to Mitigate Neutrino Flux around Muon Colliders

Mitigation (1): Place Collider Deep Underground

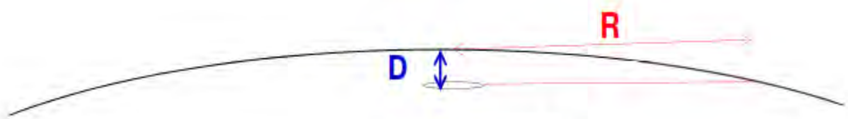

$$R = \sqrt{2R_{earth}D}$$

	$\sqrt{s}$ (TeV)	0.5	1	2	3	4
	$N \times 10^{21}$	0.2	0.2	1.2	1.2	1.2
1 mSv	R (km)	0.4	1.1	6.5	12	18
	D (m)	≤ 1	≤ 1	3.3	11	25
0.1 mSv	R (km)	1.2	3.2	21	37	57
	D (m)	≤ 1	≤ 1	34	107	254

0.01 mSv/yr -> *D*=300 m for 3TeV case

- Assuming suppressed contribution from field-free regions
- The Earth's curvature prevents this from being a generic solution
- There is also the regulatory question whether delivering an off-site dose above the limit at any depth underground or height above it is permissible

MARS-calculated depth *D* to reduce ν-induced long-term maximum dose at surface (at radial distance *R* from collider ring center) to DOE and Fermilab annual off-site limits at N decays/yr.

Note that simplified expressions derived by B. King in 1996-1998 give noticeably more conservative results compared to those from MARS full Monte Carlo. For example, for the 3-TeV case, depth to stay within 0.01 mSv/yr 1% of the DOE limit is 300 m (MARS) compared to the analytical 500 m (Ankenbrandt et al, 1999).

Mitigation (2): Isolated Site for multi-TeV MC

- Desert
- Mountain region
- Remote island

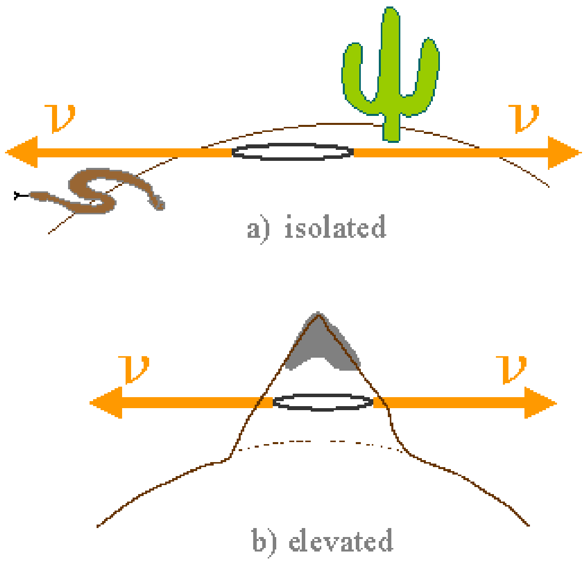

Mitigation (3): Minimize Field-Free Regions

- Presence of a field of even a fraction of 1 T is enough to reduce the dose to a below-limit level
- The application of such a field over all RF and other components seems possible
- Straight sections could be shortened by using continuous combined function magnets

Mitigation (4-5): Beam Wobbling or/and Magnet Movers

4. Fast beam wobbling by systematic time-varying vertical wave field in the ring to disperse the strongly-directed neutrino flux (proposed by NM & CJJ at PAC1997 and studied in great details by NM&AVG in 2000)
5. Alternatively, large-stroke high-resolution magnet movers (proposed in 2021 at CERN)

MARS15

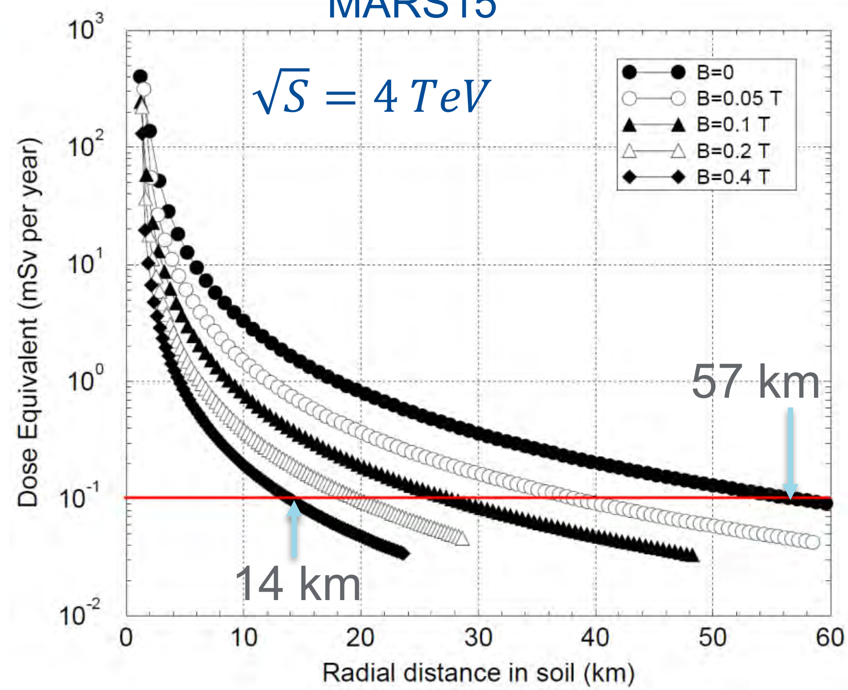

Fermilab

Mitigation (6-7): Reduce Muon Beam Intensity

6. Better cooling, *e.g.*, optical stochastic cooling, might reduce the emittances by several orders of magnitude, thus greatly reducing the muon beam currents

7. The focusing strength could be increased by the use of plasma or other exotic focusing method at IP

Managed by Fermi Research Alliance, LLC for the U.S. Department of Energy Office of Science

Simulation of Particle-Material Interactions: Advanced Implementation in the Monte-Carlo Codes NVM3(2)

Nikolai Mokhov, Fermilab

USPAS, Colliders

February 3, 2022

MARS15 (mars.fnal.gov)

- MARS15 is a set of **Fortran 77 and C++** programs for Monte-Carlo simulations of coupled hadronic and electromagnetic cascades, with heavy ion, muon and neutrino production and interaction. It covers a wide energy range: 1 keV to 100 TeV for muons, hadrons, heavy ions and electromagnetic showers; and 10^{-5} eV to 100 TeV for neutrons.

- Nuclear interactions as well as practically all other strong, weak and electromagnetic interactions in the entire energy range can be simulated either inclusively or exclusively – i.e, in a biased mode or in a fully or partially analogue mode.

- Nuclide production, decay, transmutation and calculation of the activity distribution is done with the built-in DeTra code.

- MARS15 uses ENDF/B-VIII.0(2018) nuclear data to handle interactions of neutrons with energies below 14 MeV and derive the NRT/Stoller/Nordlund DPA x-sections below 200 MeV. The elemental distributions are automatically unpacked into isotope distributions for both user-defined and those from the 172 built-in materials.

MARS15: Other Features

- A tagging module allows one to tag the origin of a given signal for source term or sensitivity analyses. Several variance reduction techniques, such as weight windows, particle splitting, and Russian roulette are possible.

- Six ways to describe geometry are offered, with a basic solid body representation and a ROOT-based powerful engine among them.

- ***The powerful capabilities of MARS15 for simulation in accelerator environment*** with the MARS-MAD Beamline Builder (**MMBLB**) working in concert with an accelerator tracking code (since almost 20 years ago) and with a recent active merge with MADX-PTC for a convenient creation of accelerator models and multi-turn tracking and cascade simulation in accelerator and beamline lattices.

- MARS15 is routinely used in concert with ANSYS for iterative studies of thermo-mechanical problems and can be interfaced to a hydrodynamic code to study phase transition and "**hydrodynamic tunneling**" – first done at SSC for a 20-TeV proton beam in 1993.

Geometry Description and ROOT-based Beamline Builder

1. User-generated via MARS extended geometry input files
2. User-generated ROOT files
3. GDML files (two-way exchange with Geant4 teams)
4. G4beamline's BruitDeFond can generate MARS's input files MARS.INP, GEOM.INP and FIELD.INP
5. STEP files from project CAD models used to generate ROOT geometry modules
6. Lattice and beamline components such as dipole and quadrupole magnets, correctors, accelerating cavities, cryomodules and tunnel with all the details available on geometry, materials and electromagnetic fields by means of the advanced ROOT-based Beamline Builder

MARS15 Simple GEOM.INP Example

```
Extended Demo  05/17/06
OPT
box-1      1 0 2   0.  -5.   5.  10.  10. 15. 1 4 3
cyl-1a    -2 1 7   0.   0.   0.   0.   5. 20.
cyl-1a    -2 1 1   0.   0.   0.   5.  10. 20. 4 2
ball-a     3 0 8   0.  25. 20.   0.   5.
ball-b     3 0 3   0.  25. 20.   5.  10. 3
cone-in   -4 0 0   0. -30.  30.   0.   3.  0.  6. 20.
cone-out  -4 0 4   0. -30.  30.   3.   5.  6. 12. 20. 2 2
th         5 0 6   0. 0. 35. 5. 3. 55. 0. 20. 60. 0. -5. 65.
ell-tub1  -6 2 6   0.   0.   0.   8.   3.  0.  40.
ell-tub2  -6 2 5   0.   0.   0.   8.   3.  3.  40.
TR1  0.  -15. 75. -20.
TR2  0.   30. 70.  20. 90.
stop
```

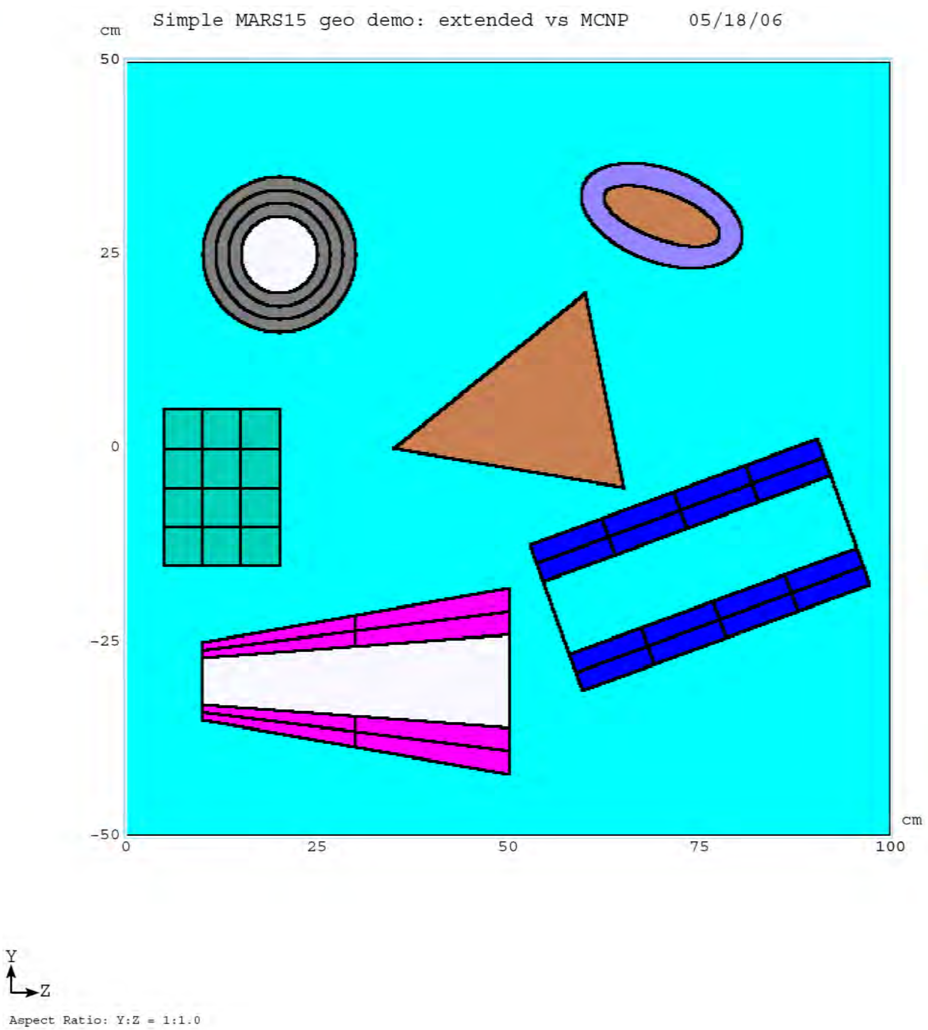

Comparing MARS and MCNP Geo Descriptions

```
 Extended & MCNP Demo  05/17/06
/home/mokhov/restricted/mars15/dat
INDX 3=F 5=T 16=T
CTRL 1
NEVT 50
ENRG 10.
ZSEC 100.
RSEC 50. 101=7
NMAT 7
MATR 'NBS2' 'SCI' 'CONC' 'MRBL' 'CAST' 'S316' 'AIR'
NHBK 1
STOP
*MCNP START
1  7  -0.00129    2 -1   (-26:27:25)   8 17 (-19:21:23) imp:n,p=1
2  2  -0.7903     -2    -3   -6           imp:n,p=1
3  2  -0.7903     -2    3 -4   -6         imp:n,p=1
4  2  -0.7903     -2    4 -5   -6         imp:n,p=1
5  2  -0.7903     -2    5     -6          imp:n,p=1
6  2  -0.7903     -2    -3   6 -7         imp:n,p=1
7  2  -0.7903     -2    3 -4   6 -7       imp:n,p=1
8  2  -0.7903     -2    4 -5   6 -7       imp:n,p=1
9  2  -0.7903     -2    5     6 -7        imp:n,p=1
10  2  -0.7903    -2    -3   7            imp:n,p=1
11  2  -0.7903    -2    3 -4   7          imp:n,p=1
12  2  -0.7903    -2    4 -5   7          imp:n,p=1
13  2  -0.7903    -2    5     7           imp:n,p=1
14  7  -0.00129   -8    -9                imp:n,p=1
15  1  -7.0       -8  9 -10    -11        imp:n,p=1
16  1  -7.0       -8  9 -10   11 -12      imp:n,p=1
17  1  -7.0       -8  9 -10   12 -13      imp:n,p=1
18  1  -7.0       -8  9 -10   13          imp:n,p=1
19  1  -7.0       -8 10       -11         imp:n,p=1
20  1  -7.0       -8 10      11 -12       imp:n,p=1
21  1  -7.0       -8 10      12 -13       imp:n,p=1
22  1  -7.0       -8 10      13           imp:n,p=1
23  0             -14                     imp:n,p=1
24  3  -2.35      14 -15                  imp:n,p=1
25  3  -2.35      15 -16                  imp:n,p=1
26  3  -2.35      16 -17                  imp:n,p=1
27  0             -18   19 -21            imp:n,p=1
28  4  -2.7       18 -22   19 -20         imp:n,p=1
29  4  -2.7       18 -22   20 -21         imp:n,p=1
30  4  -2.7       22 -23   19 -20         imp:n,p=1
31  4  -2.7       22 -23   20 -21         imp:n,p=1
32  6  -7.92         -24   26 -27         imp:n,p=1
33  5  -7.31      24 -25   26 -27         imp:n,p=1
34  0        1                            imp:n,p=0
1   rcc   0 0 0   0 0 100   50
2   rpp   -10 10   -15 5   5 20
3   py  -10
4   py   -5
5   py    0
6   pz   10
7   pz   15
8  1  rcc   0 0 -20   0 0 40   10
9  1  cz    5
10 1  cz    7.5
11 1  pz  -10
12 1  pz    0
13 1  pz   10
14   s    0 25 20   5
15   s    0 25 20   6.667
16   s    0 25 20   8.333
17   s    0 25 20   10
18   k/z   0 -30 -30   .005625
19   pz    10
20   pz    30
21   pz    50
22   k/z   0 -30 -22     .015625
23   k/z   0 -30 -18.57   .030626
24 2 sq    0  64  9   0 0 0  -576   0 0 0
25 2 sq    0 121 36   0 0 0 -4356   0 0 0
26   px  -40
27   px   40
mode n p

m1   2004 -.02   29000 -.38   13027 -.2    41093 -.280522    50000 -.119478  $  NBS2
m2   1001 -.13314  6000 -.86651  7014 -.00016  8016 -.00019          $  SCI
m3   1001 -.006   6000 -.030   8016 -.500   11023 -.010 13027 -0.03 &  $  Conc
   14000 -.200  19000 -.010  20000 -.200   26000.42c -.014
m4  20000 -.400431 6000 -.120005 8016 -.479564                    $  MRBL
m5   6000 -.0365  14000 -.025   25055 -.0018   26000.42c -.9347  29000 -.002 $ CAST
m6  24000 -.17    25055 -.02   26000.42c -.655 28000  -.12  14000 -.01   42000 -.025 $ S316
m7   7014  .78443  8016  .21076 18000.42c 4.671E-3 6000 1.39E-4 gas=1     $  Air
vol  1 33r
*MCNP END
```

G4beamline's BruitDeFond Can Generate MARS's Input Files

BruitDeFond

BeamMaker

MARS.INP
GEOM.INP
FIELD.INP

BeamMaker.txt

MARS15

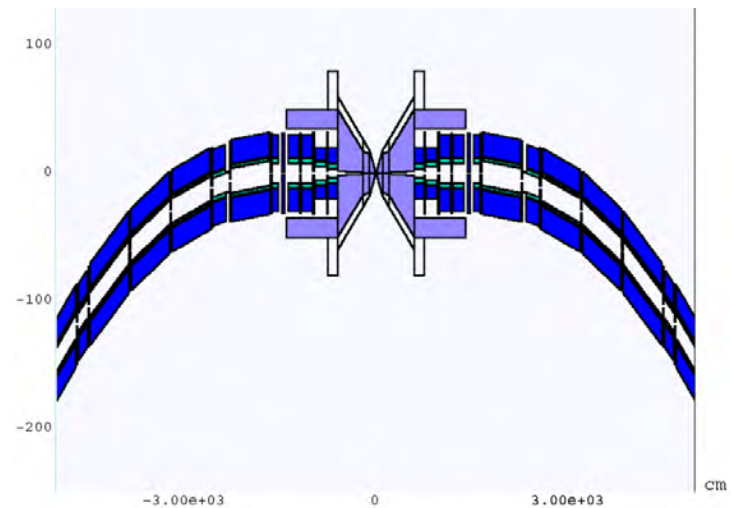

•*BruitDeFond* can generate MARS.INP and GEOM.INP files.
•The *extended* geometry is description is used.
•The field is described by the FIELD.INP file which is read by the MARS user subroutine "field" that we wrote.
•We use the same BeamMaker.txt file for the MARS input.

MARS15 Models

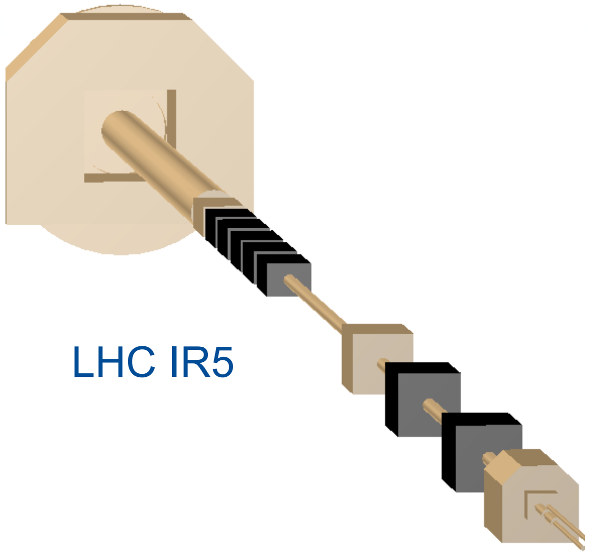

LHC IR5

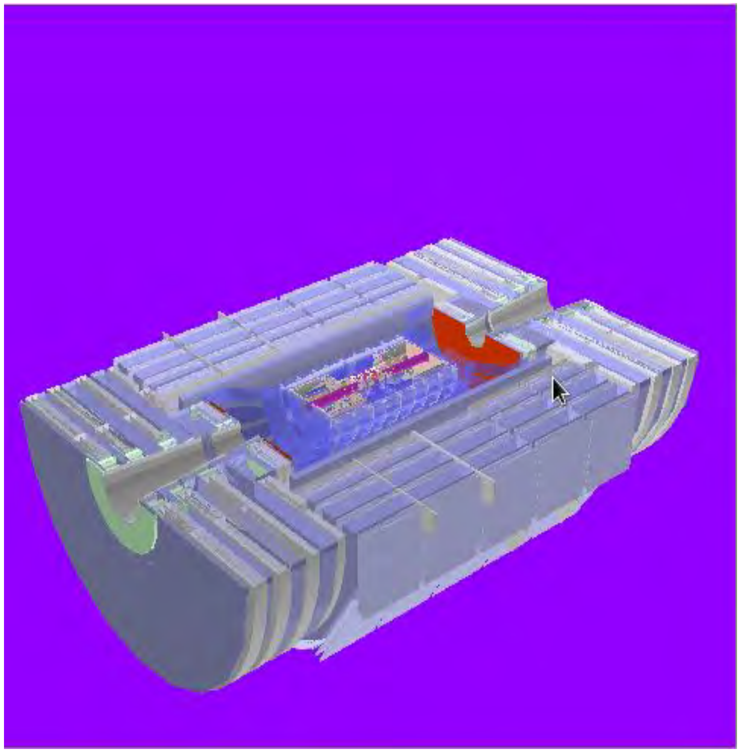

LHC CMS detector

Fermilab Booster by ROOT-based BeamlineBuilder

MARS15 Model of the Higgs Factory Muon Collider

300-m $\mu^+\mu^-$ Collider

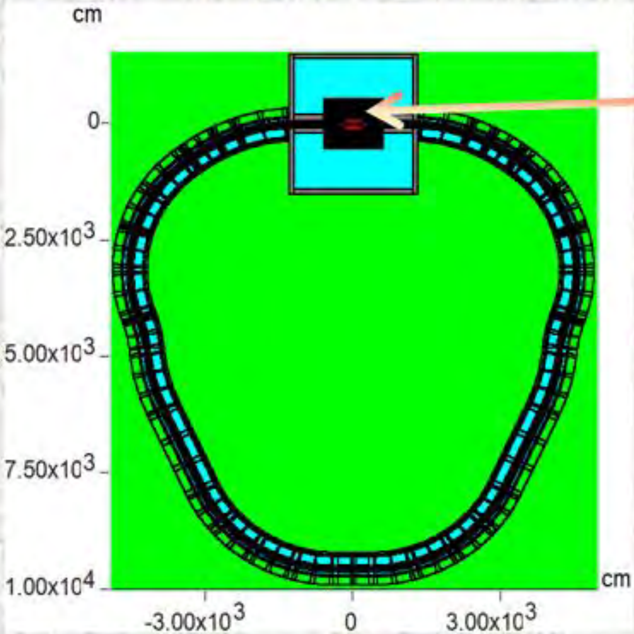

SiD-like detector with CMS upgrade-type tracker

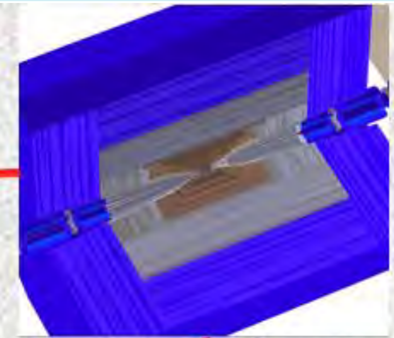

HFMC

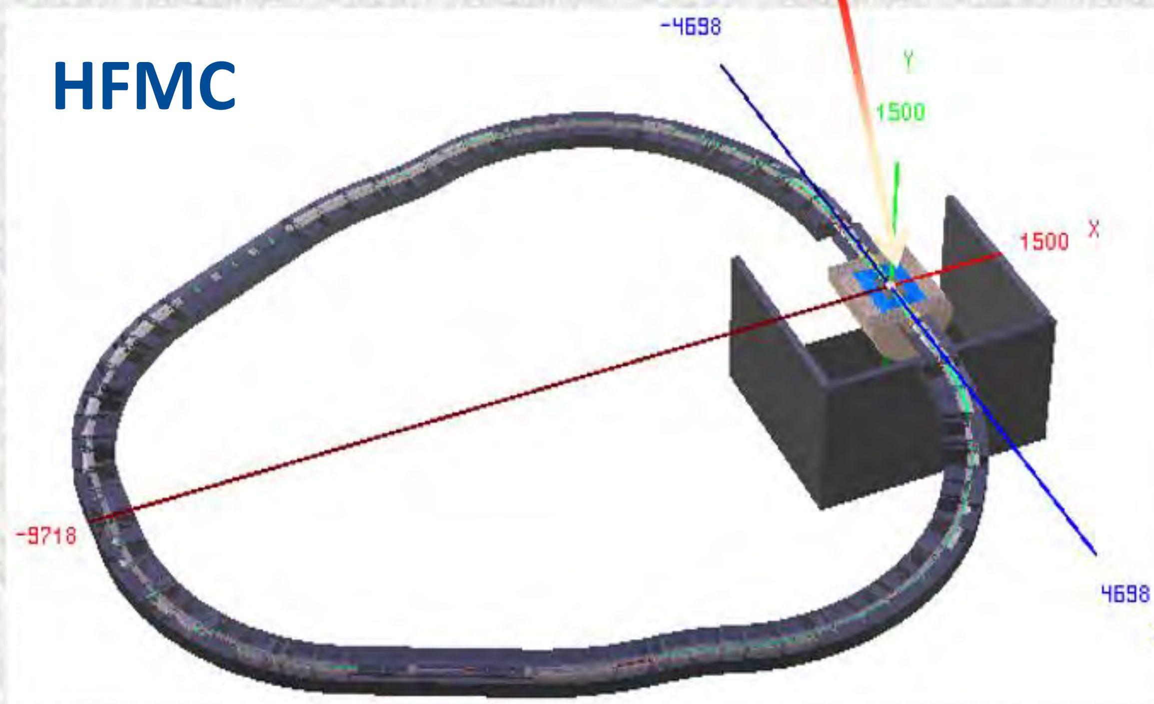

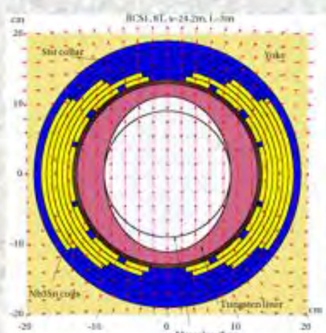

8-T SC dipole

HFMC: Protection of SC magnets and Detector

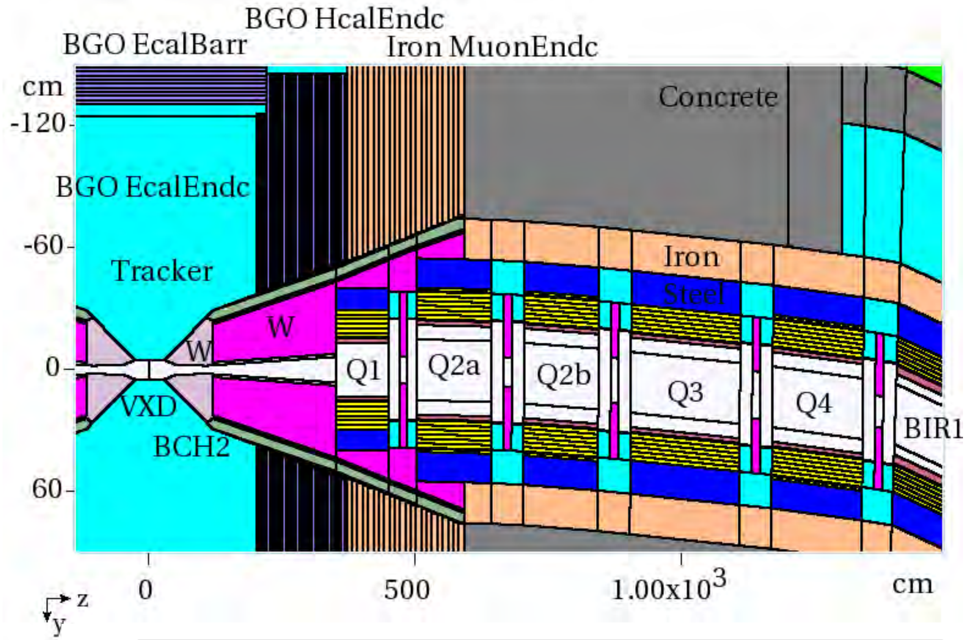

MARS15 model of the HFMC Machine-Detector Interface with a sophisticated tungsten nozzle near IP, collimators in interconnect regions and liners inside SC magnets – all resulted in reduction of detector backgrounds to the design limits.

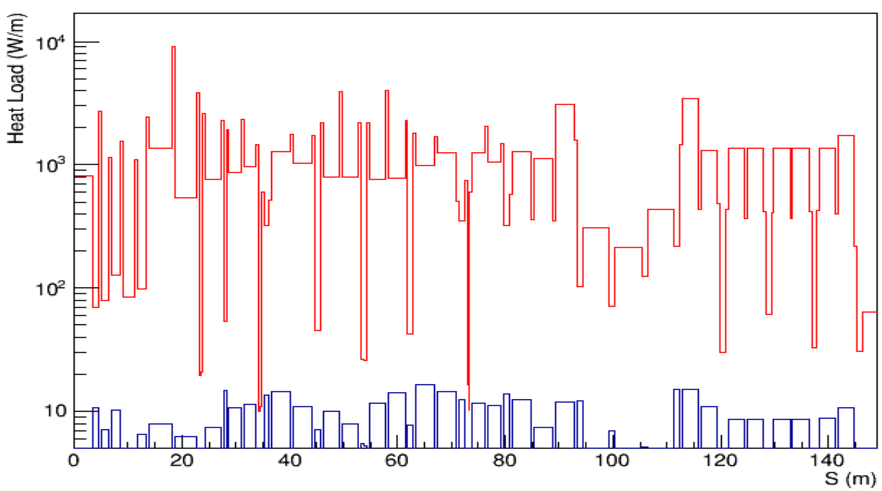

Collimators in interconnect regions and liners inside magnets in the ring have resulted in x100 reduction of dynamic heat loads in the magnet superconducting coils.

MMBLB Model: J-PARC 3-GeV Ring

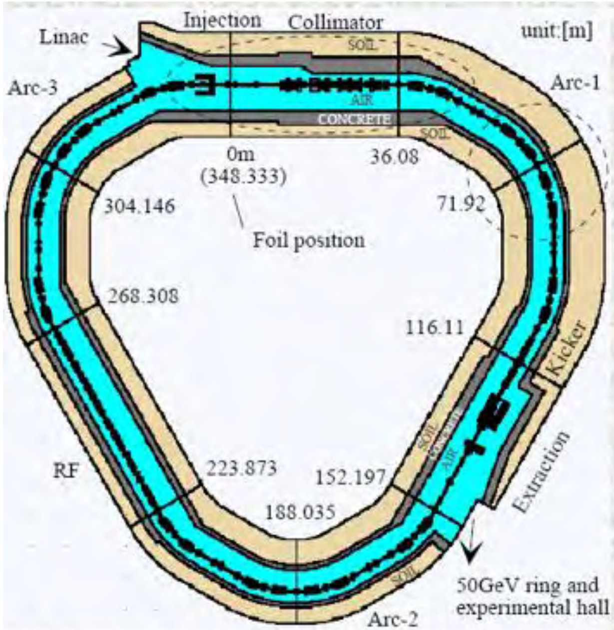

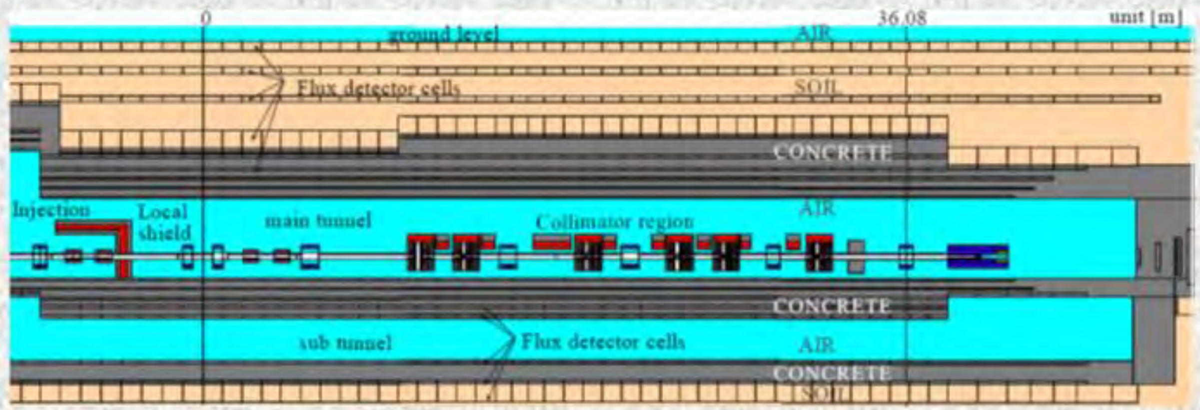

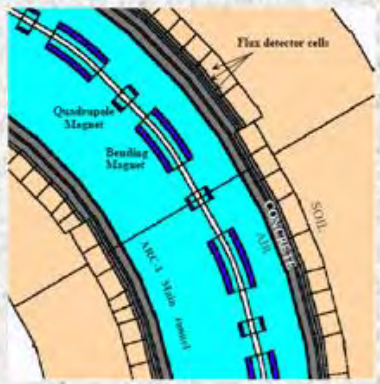

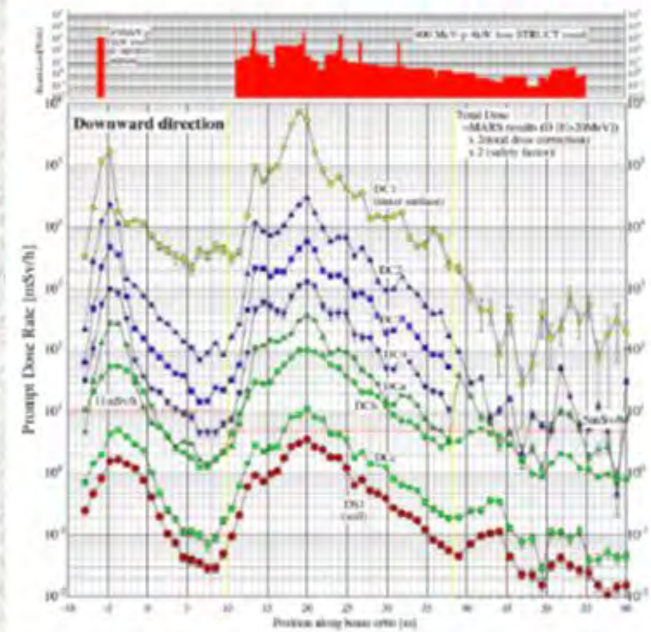

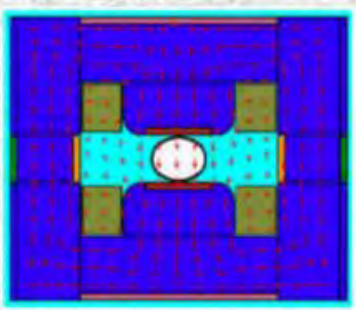

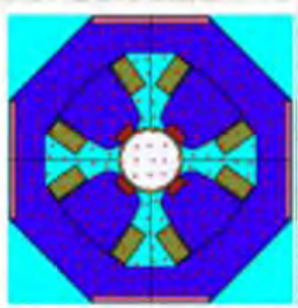

Fermilab

MCNP6 (mcnp.lanl.gov)

MCNP6 is the latest version of the Monte Carlo N-Particle transport (MCNP) family of particle interaction and transport codes (**Fortran-90**) and features comprehensive and detailed descriptions of the related physical processes. It transports 37 different particle types, including ions and electromagnetic particles. The neutron interaction and transport modules use standard evaluated data libraries mixed with physics models where such libraries are not available. ***Considered by many as the industry standard for simulation in reactor, medical, space and low- and medium-energy accelerator applications.***

The transport is continuous in energy. MCNP6 contains one of the most powerful implementations of variance reduction techniques. Spherical mesh weight windows can be created by a generator in order to focus the simulation time on certain spatial regions of interest. In addition, a more generalized phase space biasing is also possible through energy- and time-dependent weight windows. Other biasing options include pulse-height tallies with variance reduction and criticality source convergence acceleration.

MCNP6 Models

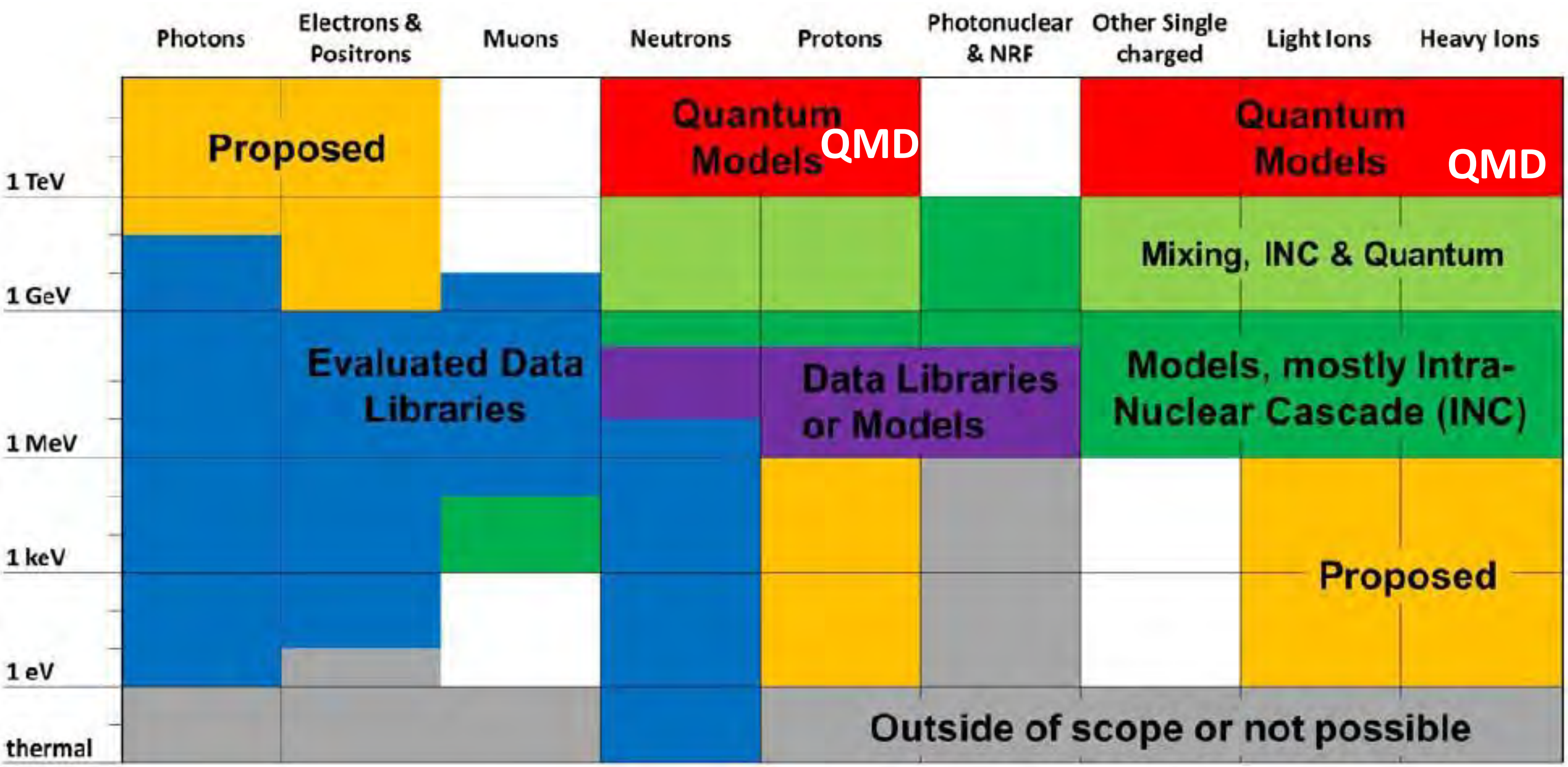

MCNP6 Geometry, B-Field and Tests

- Geometry options: traditional surface-based, voxel lattice, constructive solid and unstructured mesh
- Magnetic fields: (1) Constant dipole, square-edge quadrupole and quadrupole with a fringe-field kick – all in low-density materials, such as air; (2) COSY maps only in vacuum and specific to one particle type; both are rather limited compared to four other codes with the arbitrary EM field capability in arbitrary geometry/materials
- **Unique feature:** MCNP6 is considered risk level two software (death is risk level one), i.e. is treated as if failure of the software could result in temporary injury or illness to workers or the public. Therefore, a set of hundreds automated verification, validation and regression tests. Latter is detecting unintended changes to the code and installation testing.
- Super-precise simulation of EMS at 1 eV to 100 GeV

MCNP6: Super-Precise Simulation of EMS

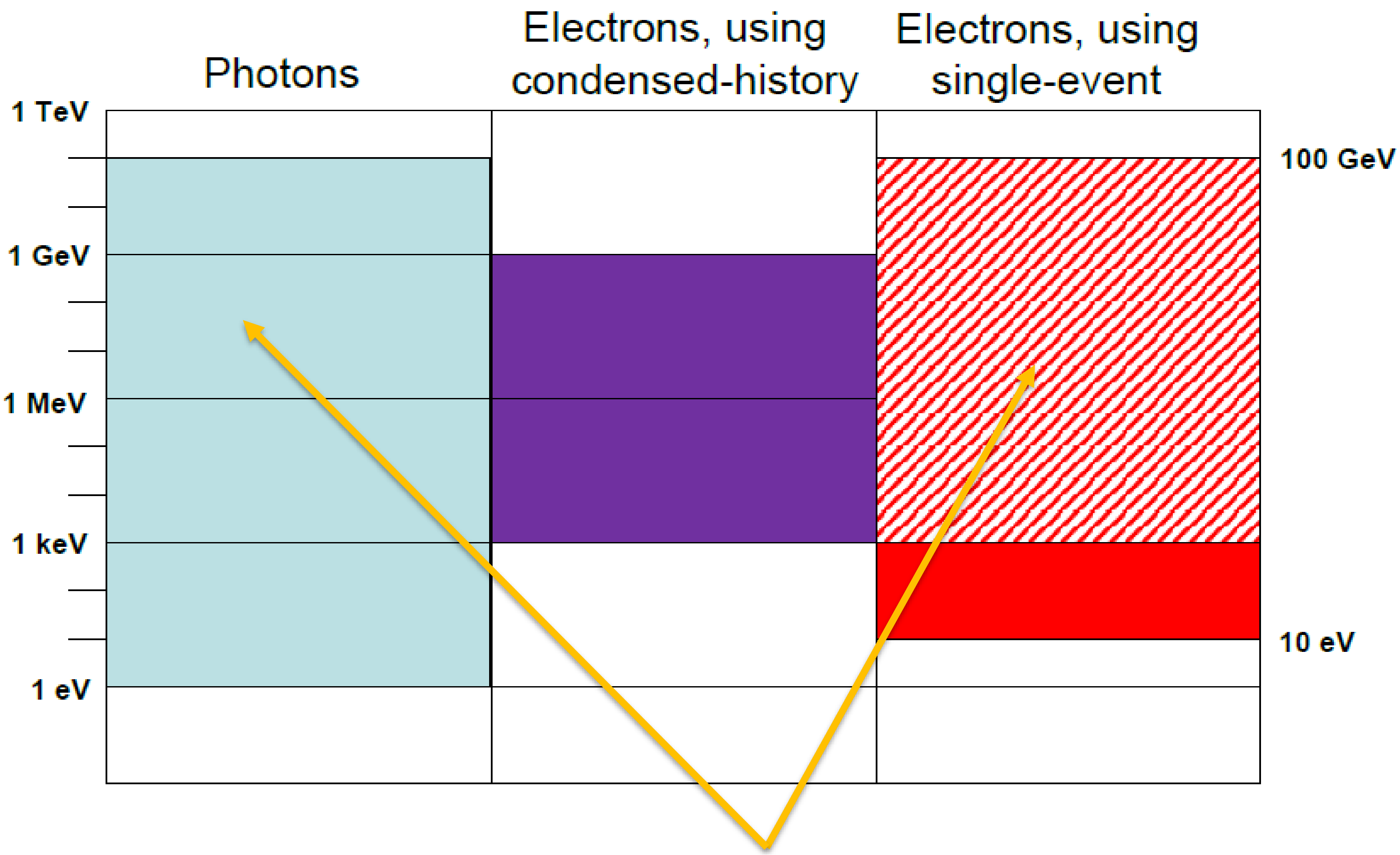

Can be very CPU-time consuming

PHITS (phits.jaea.go.jp)

PHITS is the Particle and Heavy-Ion Transport code System (**Fortran 77**). ***It was among the first general-purpose codes to simulate the transport and interactions of heavy ions in a wide energy range***, from 10 MeV/nucleon to 100 GeV/nucleon. It is based on the high-energy hadron transport code NMTC/JAM that was extended to heavy ions.

The transport of low-energy neutrons employs cross sections from evaluated nuclear data libraries such as ENDF and JENDL below 20 MeV. Electromagnetic interactions are simulated based on the EGS5 code in the energy range between 1 keV and 100 MeV for electrons and positrons and between 1 keV and 100 GeV for photons. Several variance reduction techniques, including weight windows and region importance biasing, are available. An accurate calculation of DPA supported by dedicated experiments with medium-energy protons.

PHITS Models

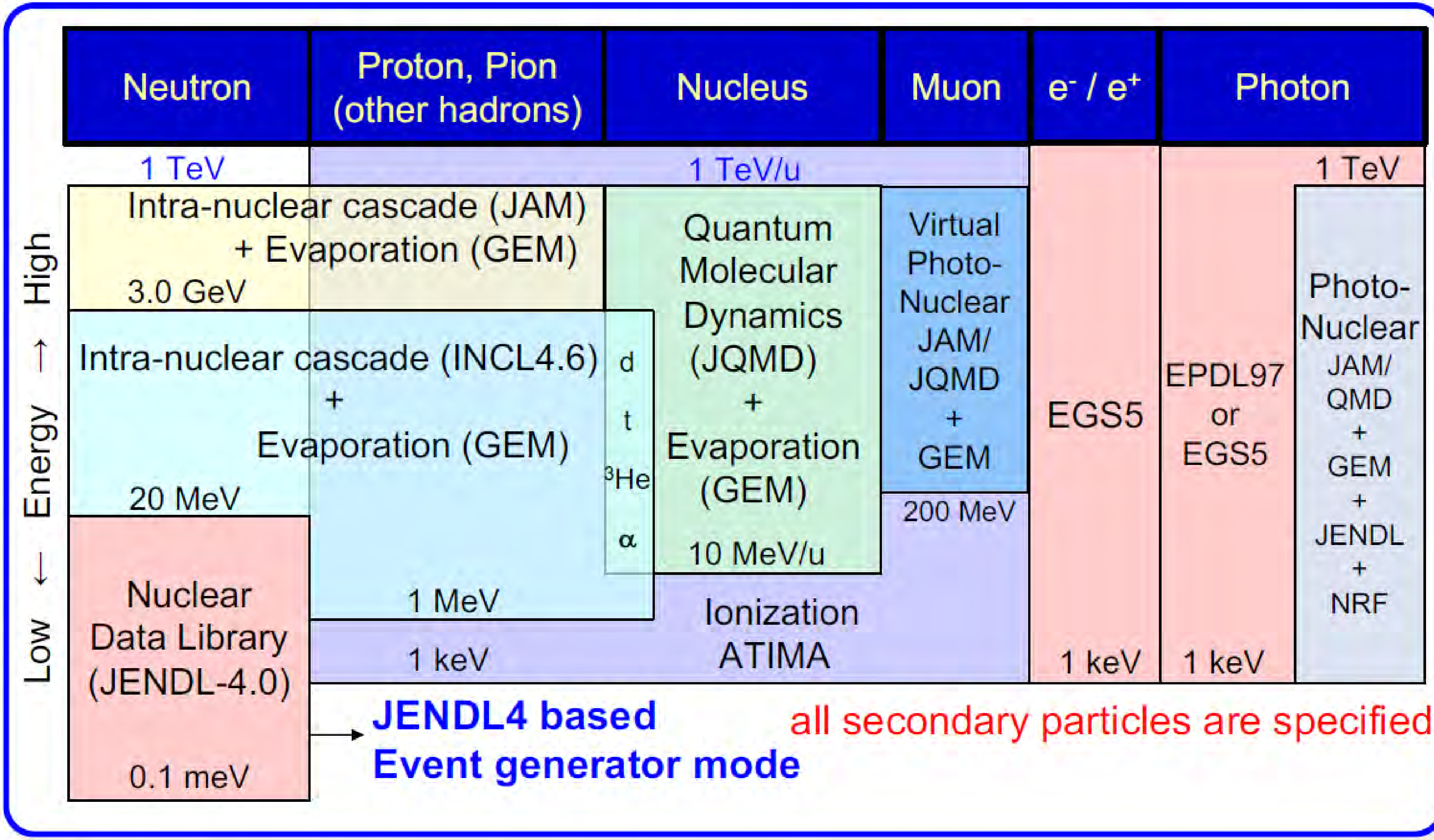

PHITS Geometry, Fields, Nuclides & Tallying

- The geometrical configuration of a simulation is set with general geometry (GG) in a manner similar to MCNP. The interactive solid modeler Simple-Geo (FLUKA) can be used for generating the geometries written in PHITS-readable GG format.
- Computer-aided Design (CAD)-based geometries can be incorporated into PHITS by converting CAD data into tetrahedral-mesh geometries. In addition, CAD geometries can be directly converted into the PHITS-readable GG format by using SuperMC.

  - Electromagnetic fields and gravity can be considered in transport simulation of all particles.
  - The time evolution of radioactivity is estimated by built-in DCHAIN-SP module.
  - An example of tallying is shown

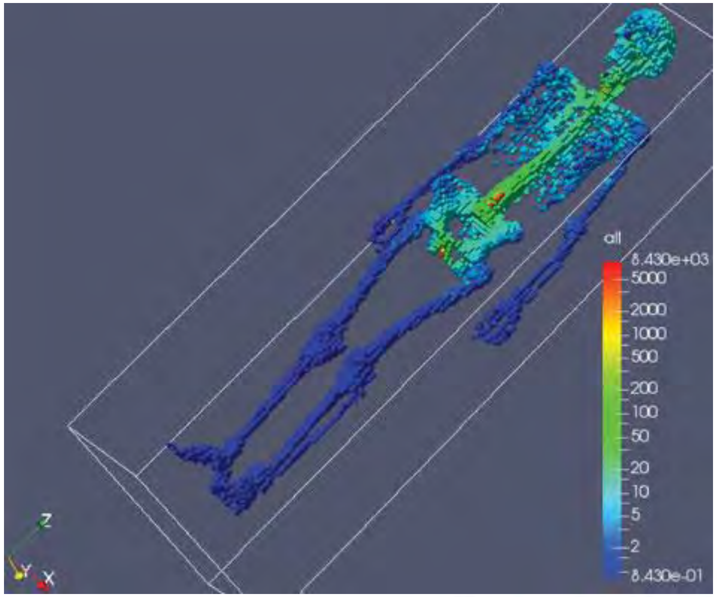

MARS15-MADX-PTC Integration (1)

In accelerator simulations, one provides – one way or another - a cross-talk between an accelerator tracking code and a code (MARS, FLUKA) for particle-matter interactions

On the accelerator side, we used for more than two decades a home-made STRUCT code working in concert with MARS. Recently, we have successfully switched to MADX-PTC for accelerator tracking

MARS15-MADX-PTC Integration (2)

Basic integration outline:

1. A library containing functions and C++ classes which interfaces MARS with MADX is now packed with the MARS15 distribution. The library allows to

- Create a 3-D TGeo ROOT geometry model for the sequence described in a MADX-PTC input file. Alignment of elements is performed by means of the MAD-X survey table.
- Define transformation for each point in the phase space used in the PTC module to the phase space used in MARS15 and vice-versa.
- Inject particles transported by MARS15 to MADX-PTC module using a formulated acceptance for the accelerator code model.
- For particles transported in PTC, perform check of boundary crossing against the ROOT geometry in MARS15; the particle is forwarded to the MARS15 stack.

MARS15-MADX-PTC Integration (3)

2. The original PTC code was modified in order to

- Allow a particle to start from the upstream end of an arbitrary element in the sequence. Originally, it always started from S=0.
- Check the aperture crossing against the MARS15 geometry not only at the entrance and exit of the element, but also all along a curved track (e.g., in dipoles).

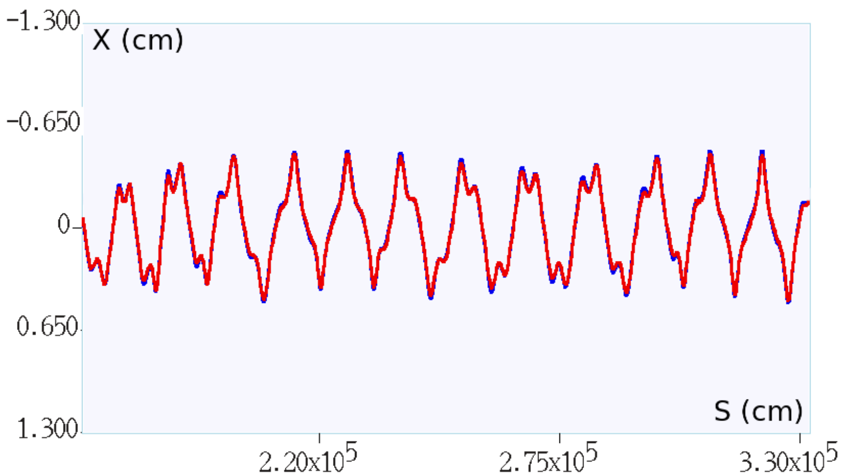

Beam orbits in the Fermilab 8-GeV Recycler calculated with MAD-X PTC module (blue) and MARS15 native stepper (red)

Examples: Fermilab Recycler and ILC

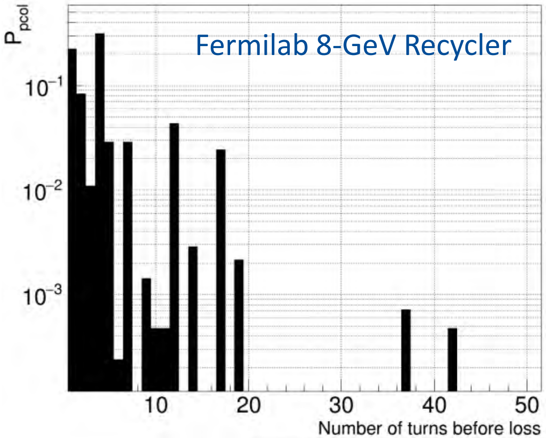

Probability to be lost for beam halo protons passed through the primary collimator vs #turns

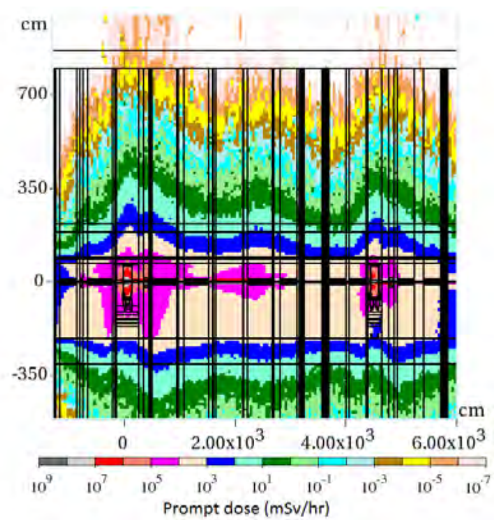

Prompt dose in collimation region

MARS15 SRF model

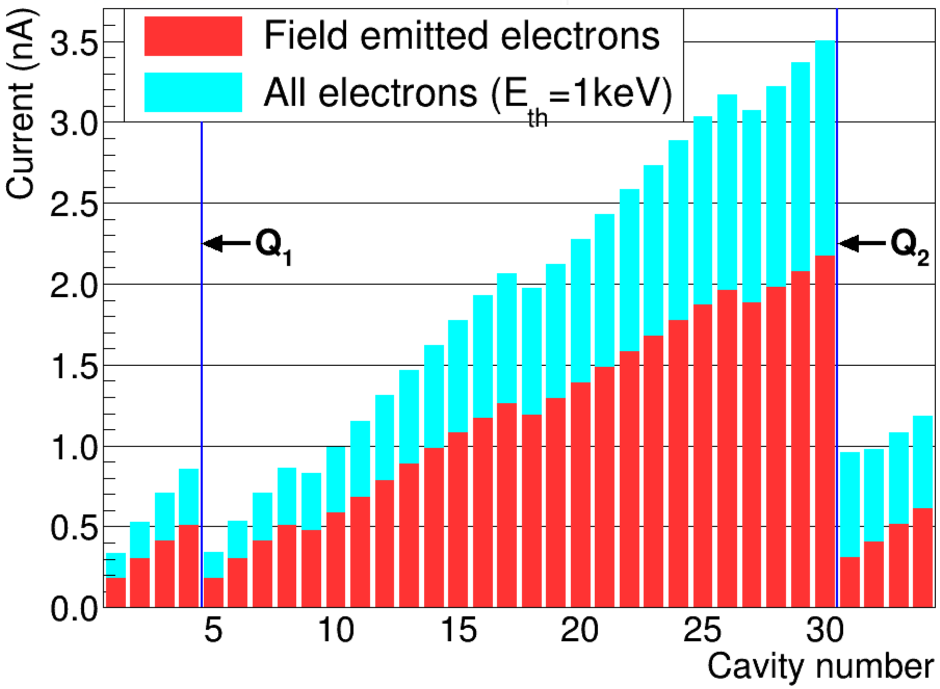

Dark current electrons and EMS electrons in ILC aperture with their loss responsible for radiation load to components and radiation field in ILC tunnel

MARS15 Platform, Compilers, ROOT and MPI

- Linux ≥ gcc-4.8 on 64 bit architectures; our compiler policy: use the latest stable release, e.g., currently, gcc-8.2, which is ideal for modern c++ codes
- C++11 standard
- gsl-2.4 or 2.5
- ROOT-6.14
- ISO standard Fortran ⇔ C interface
- Many-core jobs (standard for decade); 10^2 to 10^5 cores routinely; improved submission scripts and built-in averaging
- Genuine MPI mode in MARS15(2018) is now used more and more often; to eliminate discovered scalability bottleneck, common physics data (x-sections etc.) are accessed via a shared memory window (MPI-3 feature)

Multithreading and Multi-Core Approaches

Multithreading is usually found in multitasking operating system. Multithreading is a widespread programming and execution model that allows multiple threads to exist within the context of one process. These threads share the process's resources, but are able to execute independently

Nowadays, multithreading is a common techniques used by particle-matter interaction codes in CPU-hungry applications. It is applied to one process to enable parallel execution on a multiprocessing system

Multithreading is a user-friendly alternative to a **multiple-core failproof approach** (used, for example, in MARS for decades) with thousands independent jobs on a cluster submitted with a user-created script and with results averaged at a post-processing stage

Flow Chart of Multithreading

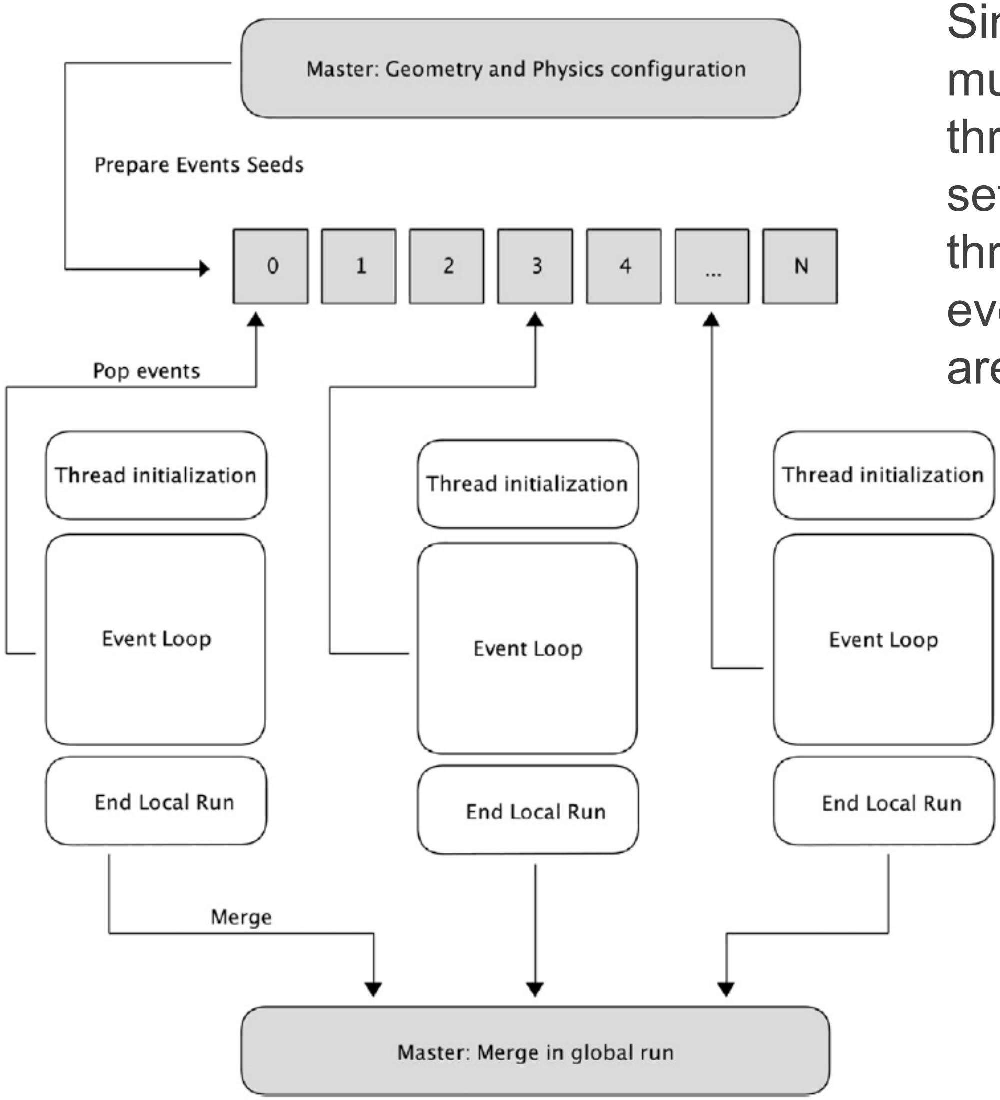

Simplified description of a GEANT4 multithreaded application: the master thread prepares geometry and physics setups for the simulation, and the worker threads compete for the next (group of) events to be simulated; otherwise they are independent.

LBNF Beamline: Schematic & MARS Model

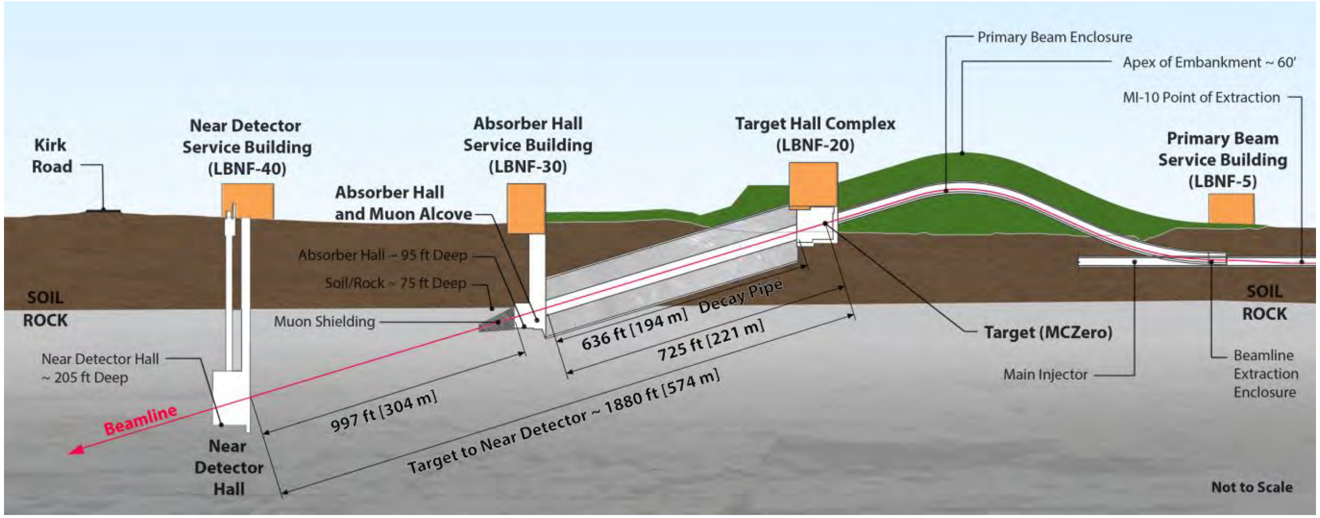

- LBNF and DUNE
- Neutrinos from 60 to 120 GeV proton beam
- **1.2 MW from day one**; upgradeable to 2.4 MW
- **Near detector** to characterize the beam
- Massive underground LAr TP Chambers
- **4 x 17 kton** (fiducial mass of more than 40 kton)

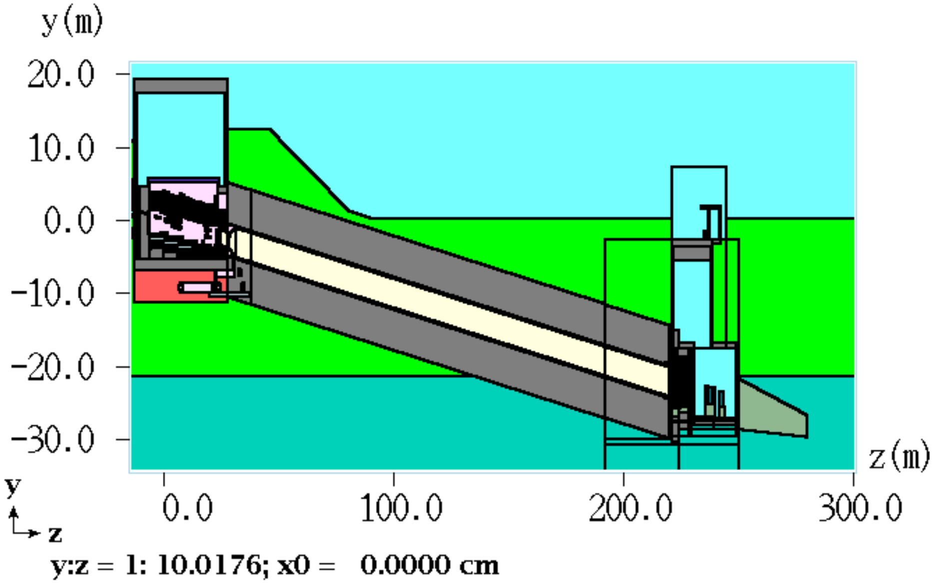

Target Station (TS): CAD & MARS15 Models

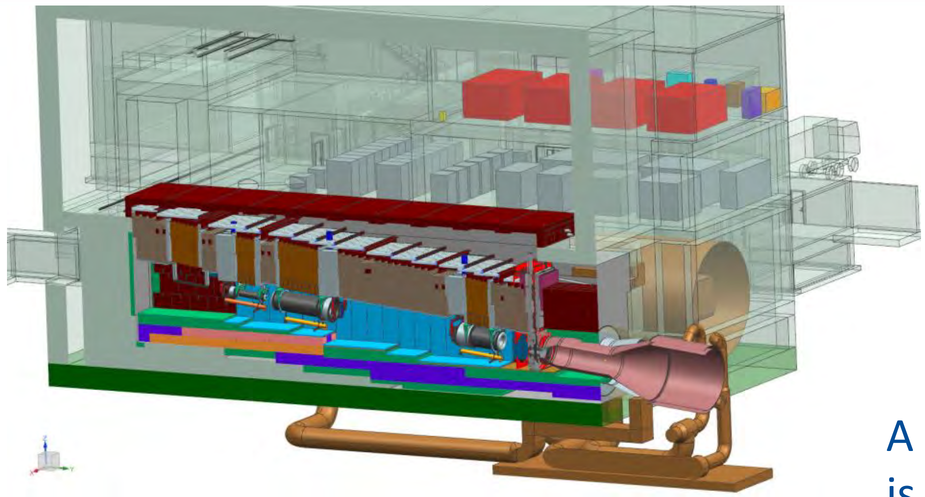

A replaceable target design is still in a preliminary stage

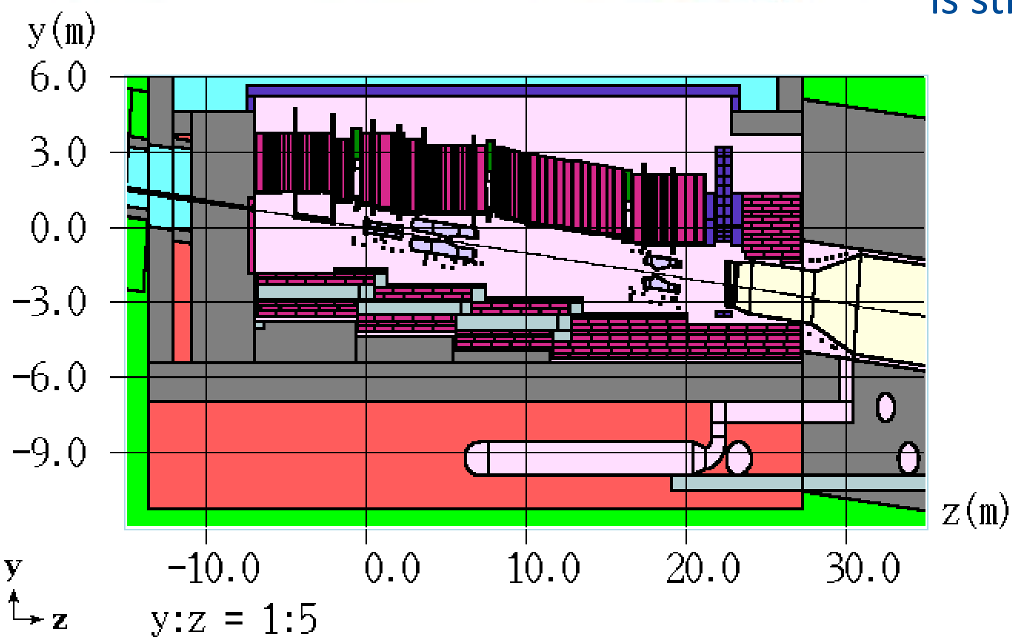

Details of the LBNF-MARS TS Model

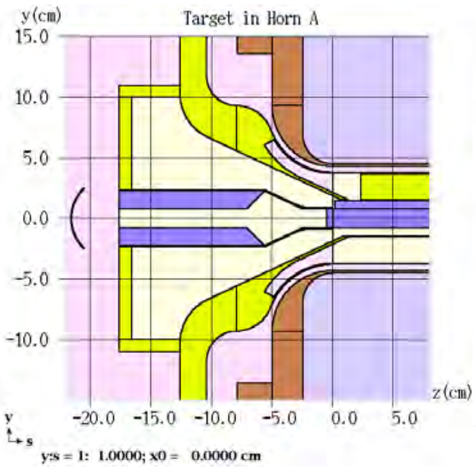

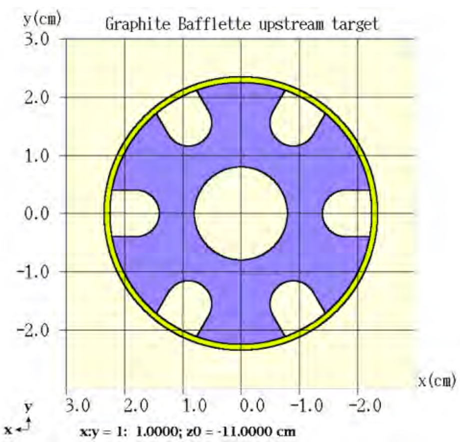

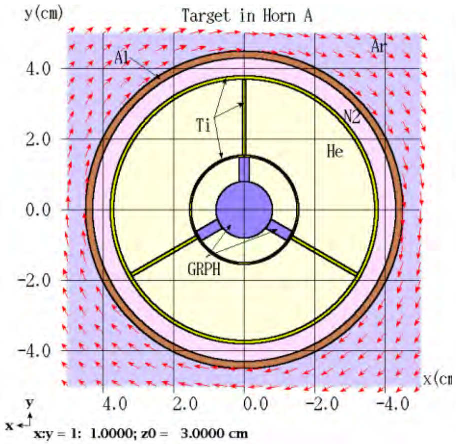

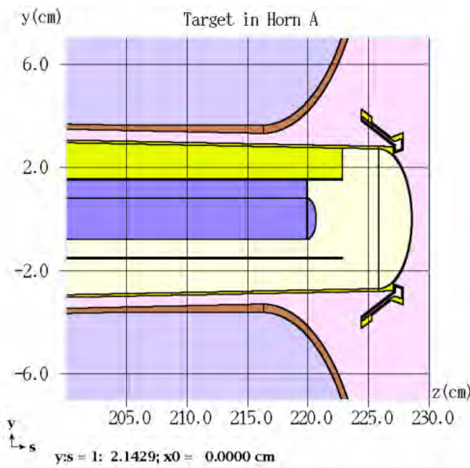

Horns A, B and C

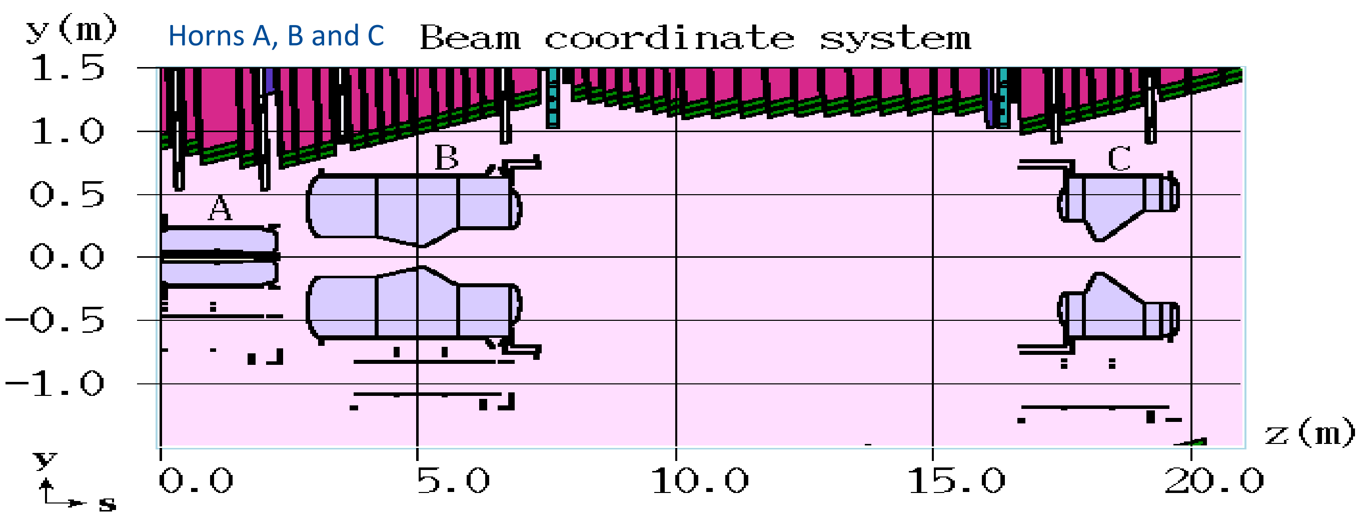

Upstream of DK pipe

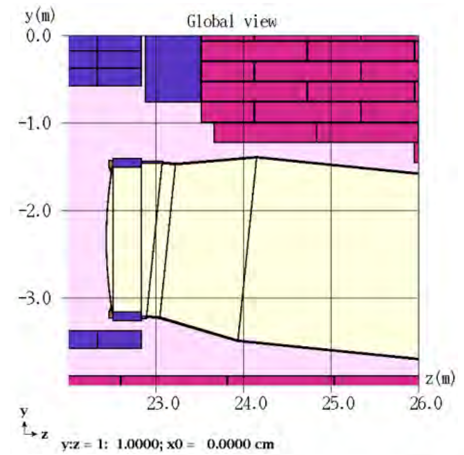

Hadron Absorber Complex: EDEP & Prompt Dose

No-target beam accident (σ=2.4mm)

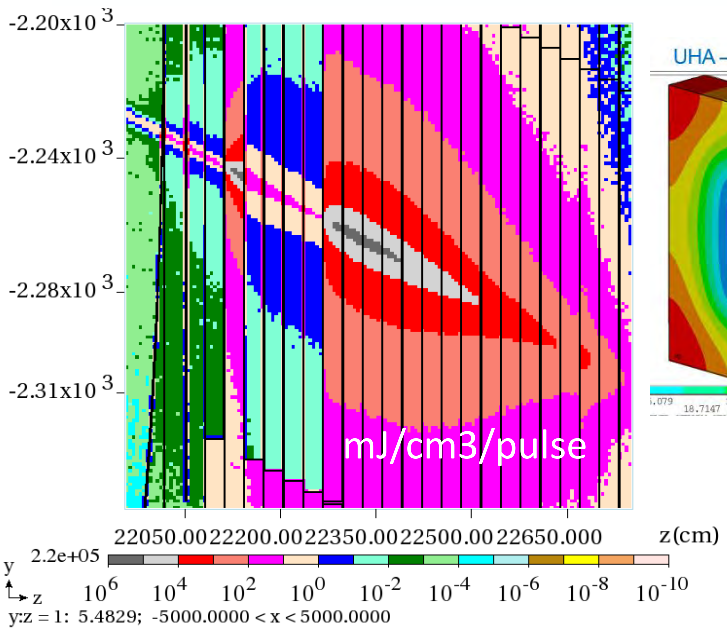

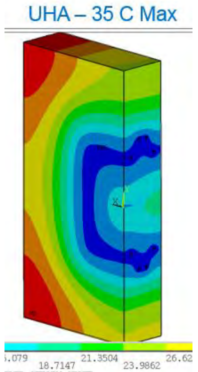

Temperature and stresses below the limits

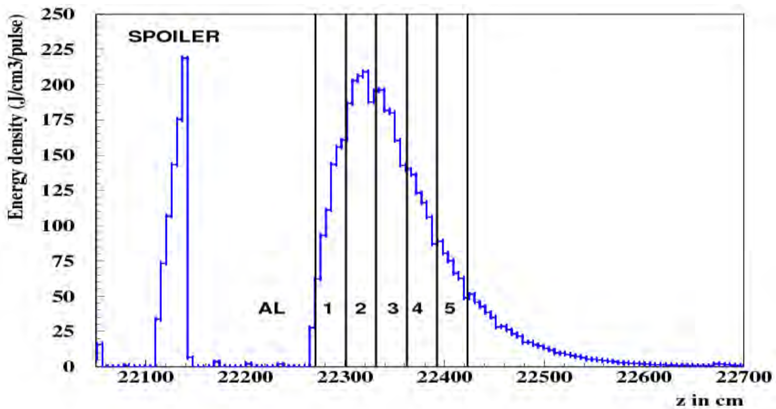

2.4-MW normal operation (σ=1.7mm)

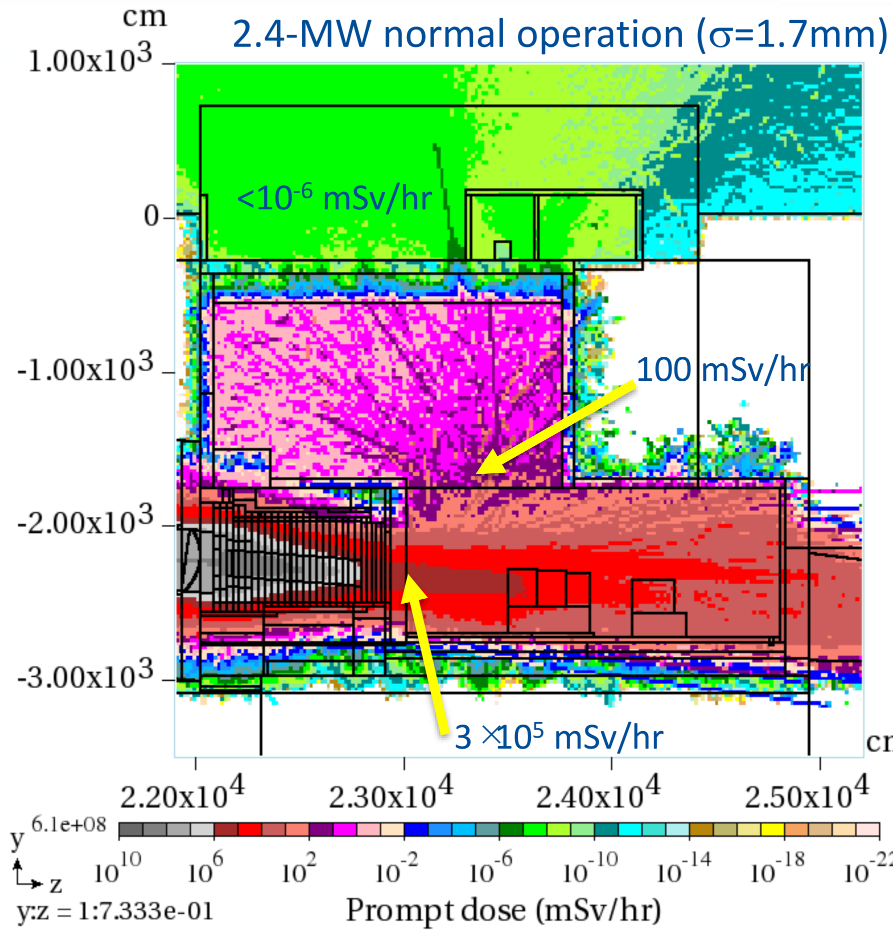

Carefully designed shielding guarantees prompt and residual dose, air and cooling water activation as well as radiation load on ground water to be below the administrative limits with corresponding safety margins

Neutrino Fluxes at Far Detector (1300 km)

Thorough search and elimination of differences in MARS15LBNF and G4LBNF models were performed on the optimized ν-flux: geometry, materials, magnetic fields etc.

ν-fluxes at the Far Detector calculated with MARS15 and Geant4 now agree within 10%. The code related uncertainties were reduced to the differences in the event generators, especially for K^- and K^0 mesons (need data!)

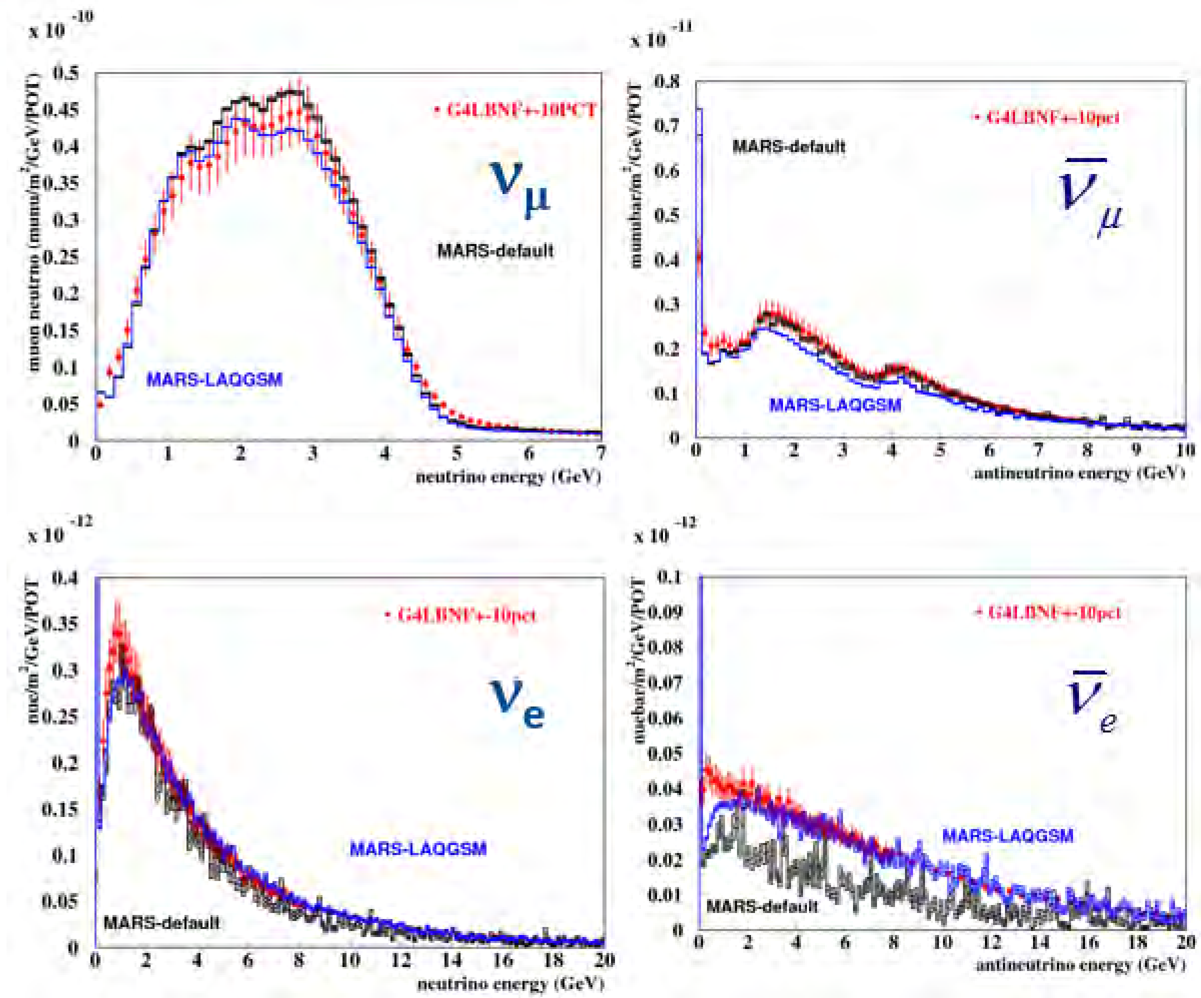

Particle–Matter Interactions in Accelerator Applications (NVM1-short)

Nikolai Mokhov, Fermilab

USPAS, Colliders

February 2, 2022

Introduction

The consequences of controlled and uncontrolled impacts of high-intensity or/and high-power or/and high-energy beams on components of accelerators, beamlines, target stations, beam collimators, absorbers, detectors, shielding, and environment can range from minor to catastrophic.

Strong, weak, electromagnetic and even gravitational forces (neutron oscillation and neutron TOF experiments) govern high-energy beam interactions with complex components in presence of electromagnetic fields → simulations are only possible with a few well-established Monte-Carlo codes (no analytic or simplified approaches are used these days).

Predictive power and reliability of particle transport simulation tools and physics models in the multi-TeV region should be well-understood and justified to allow for viable designs of future colliders with a minimal risk and a reasonable safety margin.

Interactions of Fast Particles with Matter

Electromagnetic interactions, decays of unstable particles and strong inelastic and elastic nuclear interactions all affect the passage of high-energy particles through matter. At high energies the characteristic feature of the phenomenon is creation of hadronic cascades and electromagnetic showers (EMS) in matter due to multi-particle production in electromagnetic and strong nuclear interactions.

Because of consecutive multiplication, the interaction avalanche rapidly accrues, passes the maximum and then dies as a result of energy dissipation between the cascade particles and due to ionization energy loss. Energetic particles are concentrated around the projectile axis forming the shower core. Neutral particles (mainly neutrons) and photons dominate with a cascade development when energy drops below a few hundred MeV.

Scales of Cascades and Particle Propagation

The length scale in hadronic cascades is a nuclear interaction length λ_I (16.8 cm in iron) while in EMS it is a radiation length X_0 (1.76 cm in iron). The hadronic cascade longitudinal dimension is (5-10) λ_I, while in EMS it is (10-30) X_0. It grows logarithmically with primary energy in both cases. Transversely, the effective radius of hadronic cascade is about λ_I, while for EMS it is about $2r_M$, where r_M is a Moliere radius R_M = 0.0265 X_0 (Z+1.2). Low-energy neutrons coupled to photons propagate much larger distance in matter around cascade core, both longitudinally and transversely, until they dissipate their energy in a region of a fraction of an electronvolt.

Muons - created predominantly in pion and kaon decays during the cascade development – can travel hundreds and thousands of meters in matter along the cascade axis. Neutrinos – usual muon partners in such decays – propagate even farther, hundreds and thousands of kilometers, until they exit the Earth’s surface.

Materials Under Irradiation

Depending on material, level of energy deposition density and its time structure, one can face a variety of effects in materials under impact of directly particle beams or radiation induced by them.

Component damage (lifetime):

- Thermal shocks and quasi-instantaneous damage
- Insulation property deterioration due to dose buildup
- Radiation damage to inorganic materials due to atomic displacements and helium production

Operational (performance):

- Superconducting magnet quench
- Single-event upset and other soft errors in electronics
- Detector performance deterioration
- Radioactivation, prompt dose and impact on environment

Hydrodynamics in Solid Materials

Pulses with EDD >15 kJ/g: hydrodynamic regime.
First done for the 300-μs, 400-MJ, 20-TeV proton beams for the SSC graphite beam dump, steel collimators and tunnel-surrounding Austin Chalk by SSC-LANL Collaboration (D. Wilson, …, N. Mokhov, PAC93, p. 3090). Combining MARS ED calculations at each time step for a fresh material state and MESA/SPHINX hydrodynamics codes.

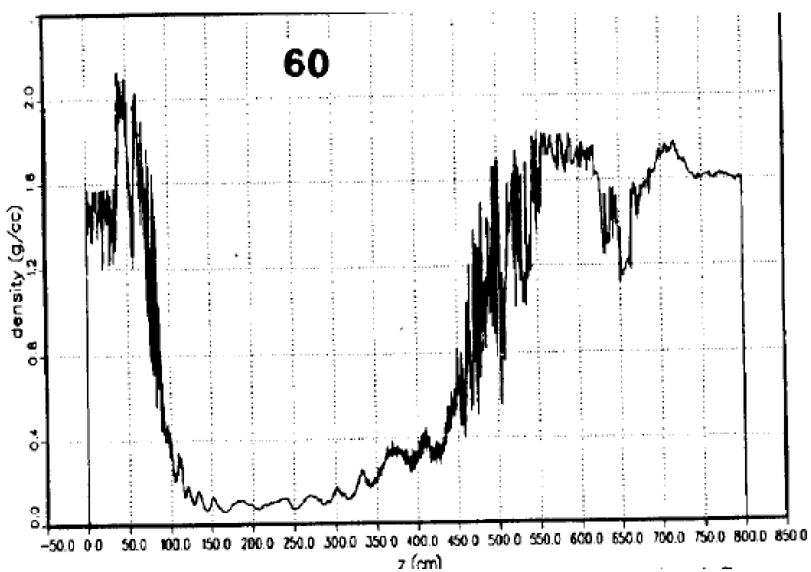

The hole was drilled at the 7 cm/μs penetration rate. Shown is axial density of graphite beam dump in 60 μs after the spill start

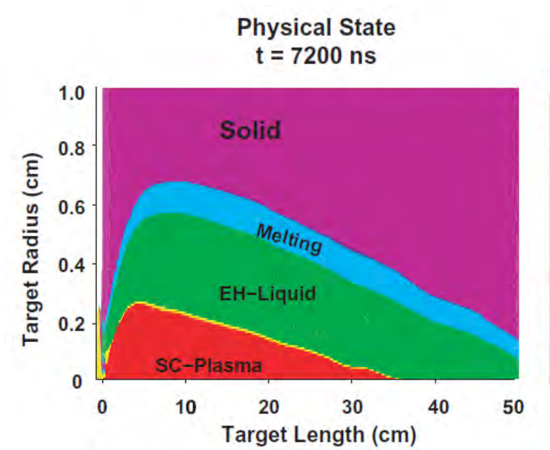

Later, studies by N. Tahir et al with FLUKA+BIG2 codes for SPS & LHC

These days we use MARS+FRONTIER

Thermal Shock

Short pulses with energy deposition density EDD in the range from 200 J/g (W), 600 J/g (Cu), ~1 kJ/g (Ni, Inconel) to ~15 kJ/g: thermal shocks resulting in fast ablation and slower structural changes.

FNAL pbar production target under 120-GeV p-beam (3e12 ppp, σ ~ 0.2 mm)

MARS simulations explained target damage, reduction of pbar yield and justified better target materials

Tevatron Tungsten Collimator Ablation

Hole in 5-mm W

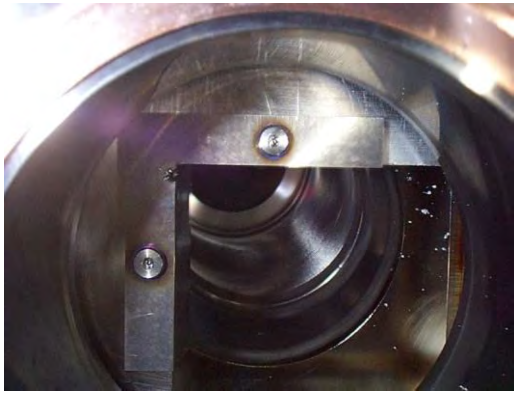

25-cm groove in SS

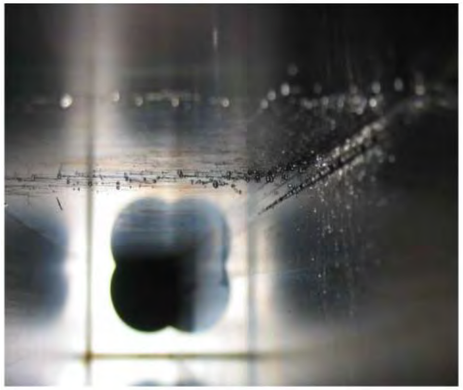

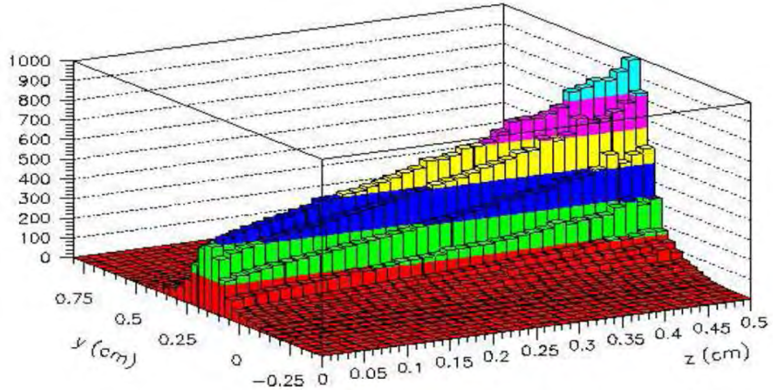

Detailed modeling of dynamics of beam loss (STRUCT), energy deposition (MARS15) as high as 1 kJ/g, and time evolution over 1.6 ms of the tungsten collimator ablation, fully explained what happened

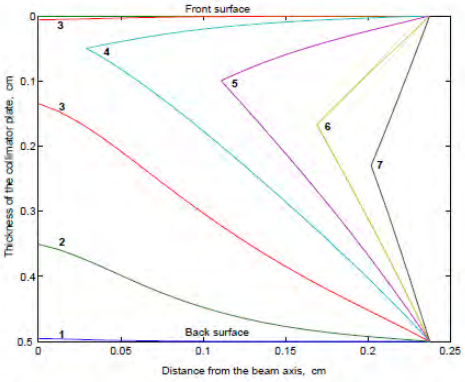

Figure 7: Evolution of the front and back surfaces of the collimator plate at $t = 0.4_{[1]} - 1.6_{[7]}\ ms$ with Δt=0.2 ms.

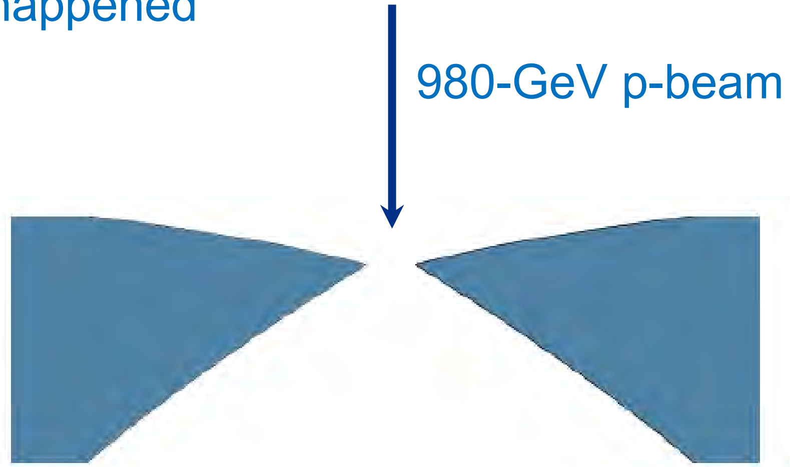

LAQGSM *vs* HARP-CDP Data at 8 GeV/c

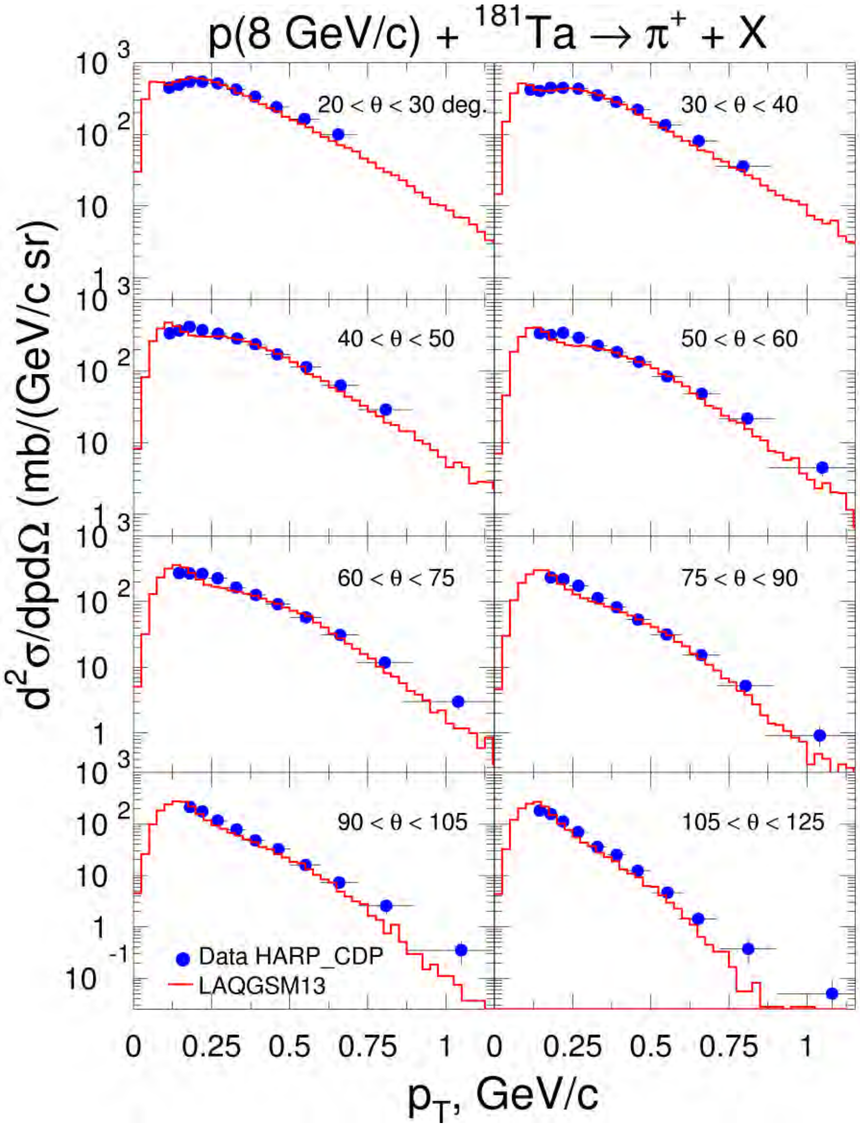

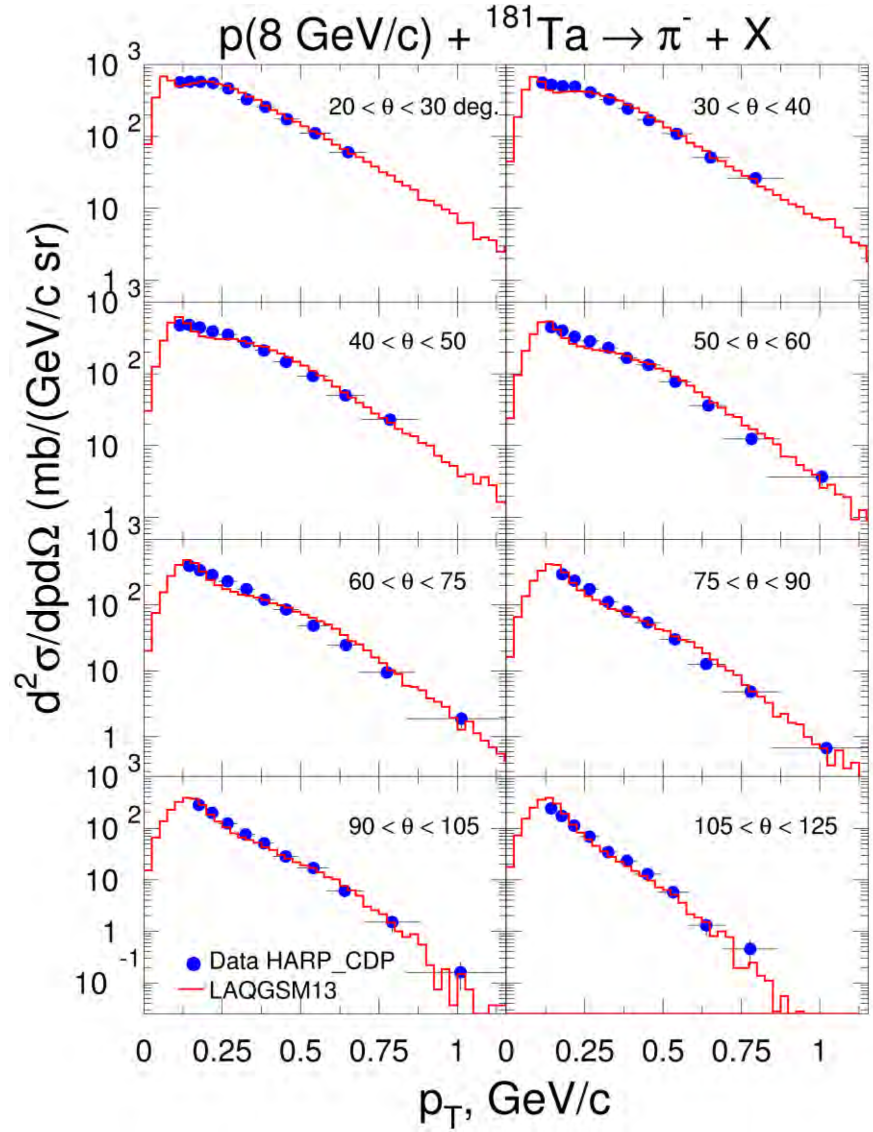

Kaon Production: LAQGSM *vs* Data

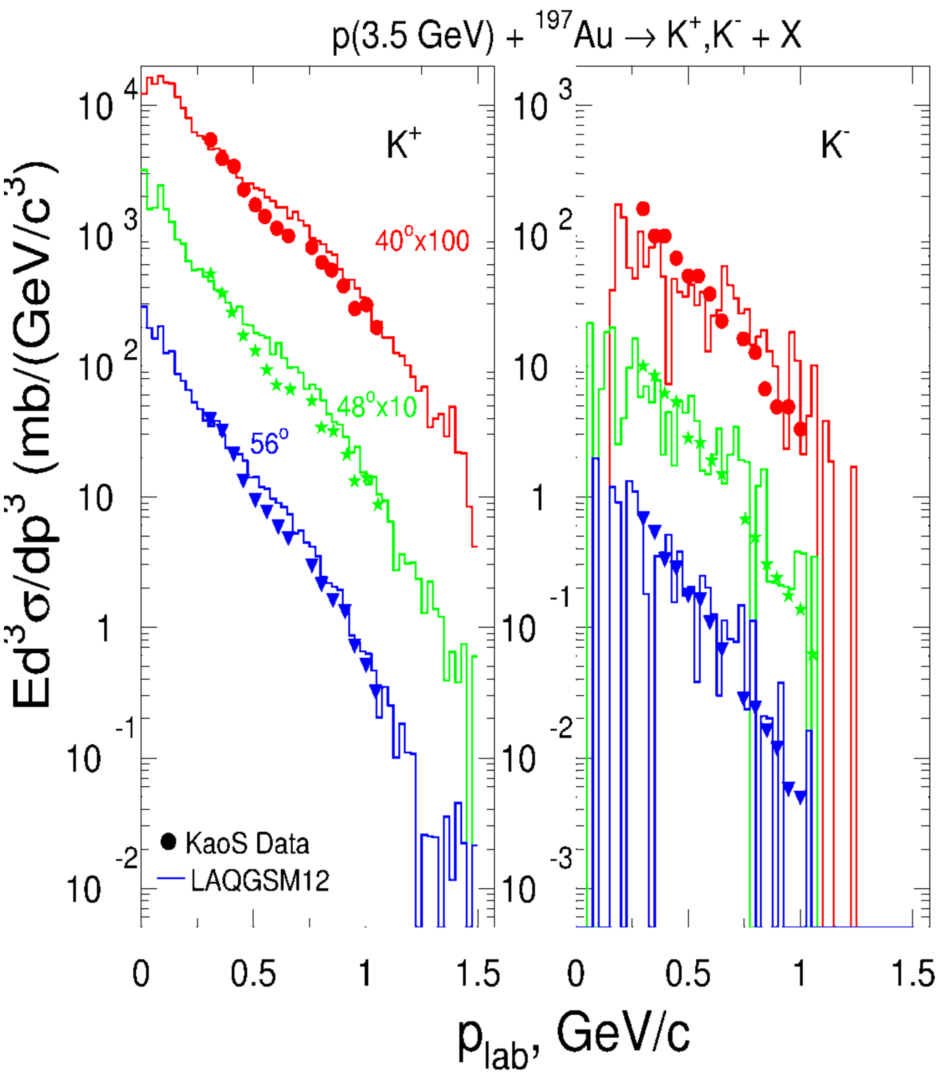

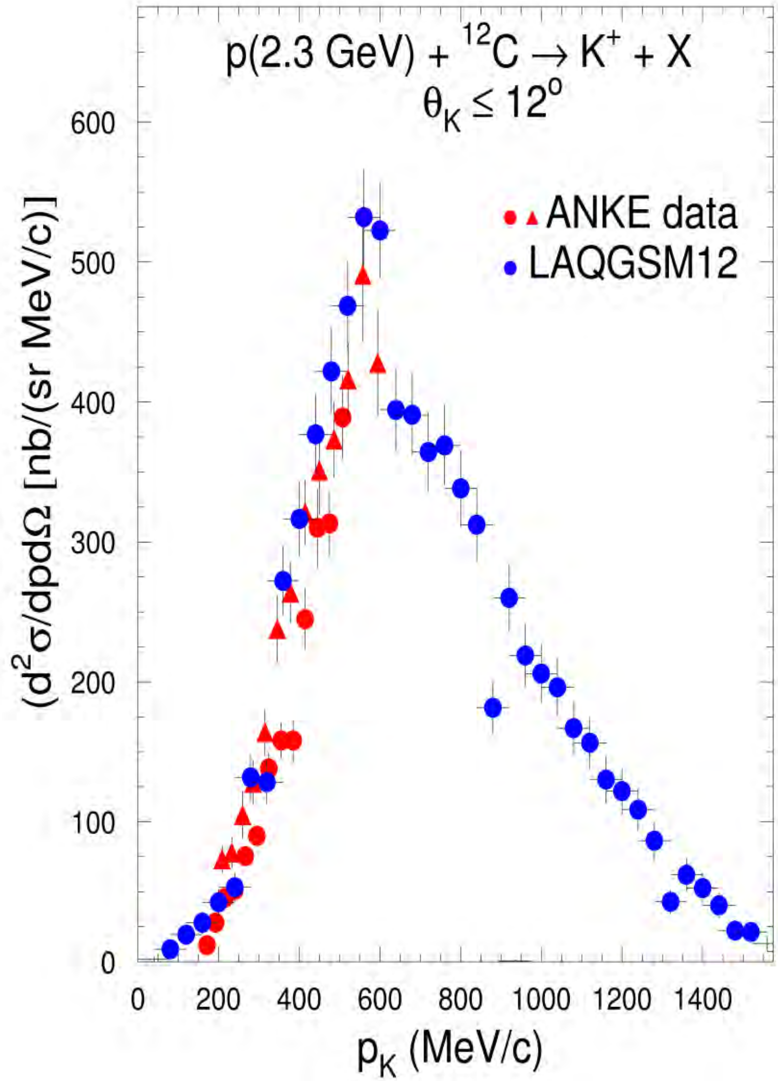

FLUKA Nucleon Production *vs* Data at 80 & 400 MeV

80 MeV p + ^{90}Zr $\rightarrow$ p + X

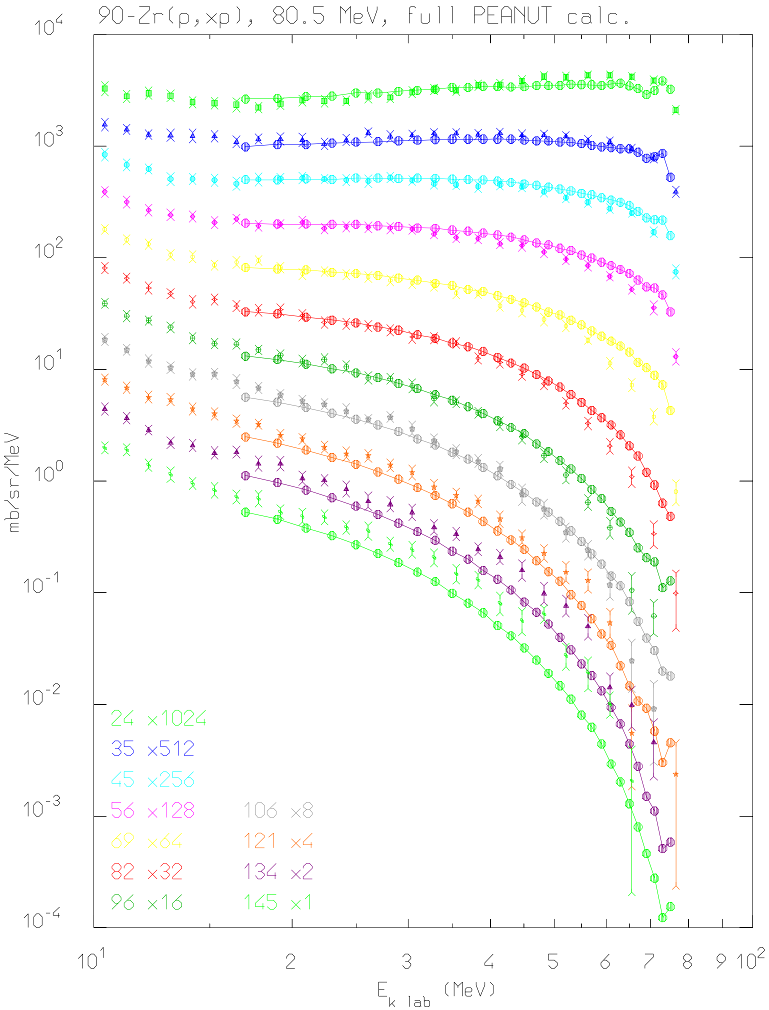

Thick target

Neutrons from 400 MeV α on carbon

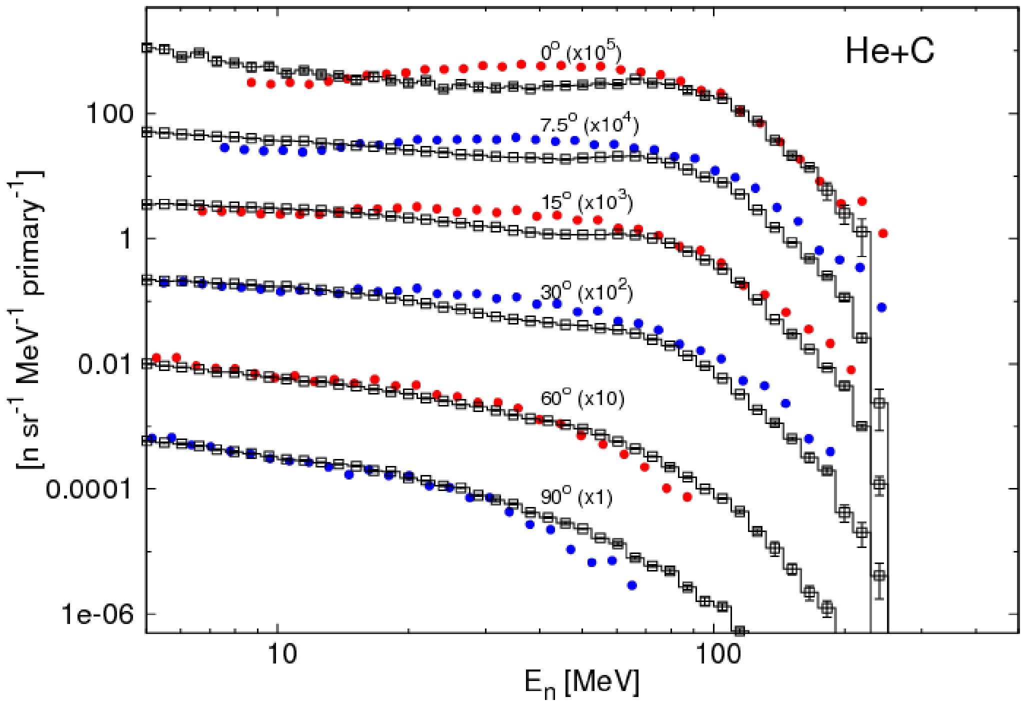

DPMJET III and FLUKA's EMD *vs* LHC Data

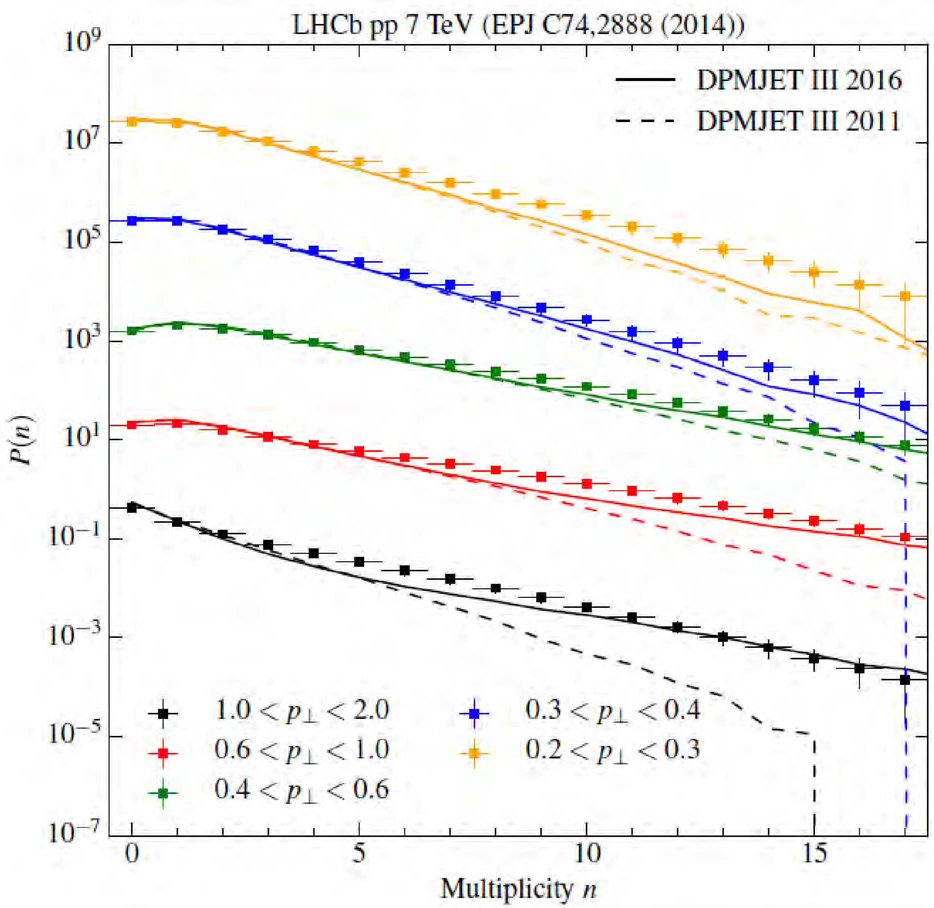

Charged particle multiplicity in pp-collisions at $\sqrt{s}$ = 7 TeV integrated over η = 2 - 4.5 as measured by LHCb (symbols) and simulated with DPMJET-III

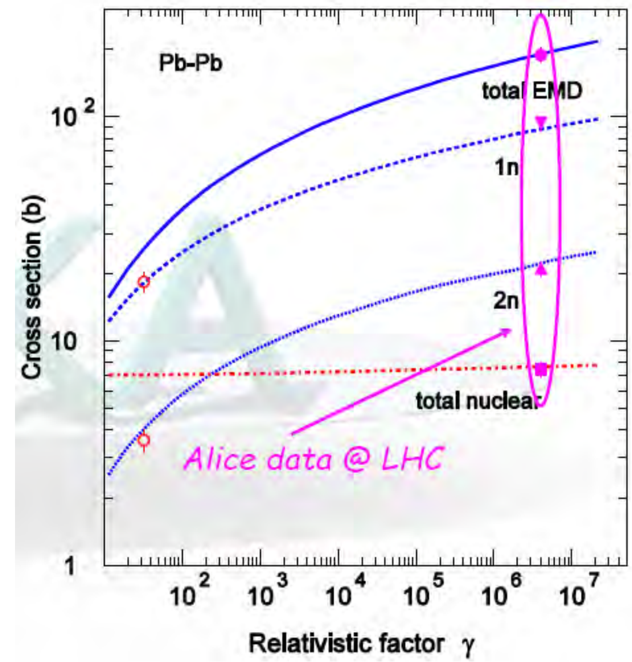

Electromagnetic dissociation (EMD) and nuclear x-sections in Pb-Pb collisions: FLUKA *vs* ALICE data. EMD = very peripheral nuclear interactions thru time-dependent EM field caused by moving nuclei. 1n – one-phonon GDR (high-frequency collective excitation of atomic nuclei, 2n – DGDR (double-phonon giant dipole resonance)

Courtesy A. Ferrari & A. Fedynitch

Nuclides from FLUKA & MARS15 Event Generators

FLUKA: 1 GeV/A ^{208}Pb + p

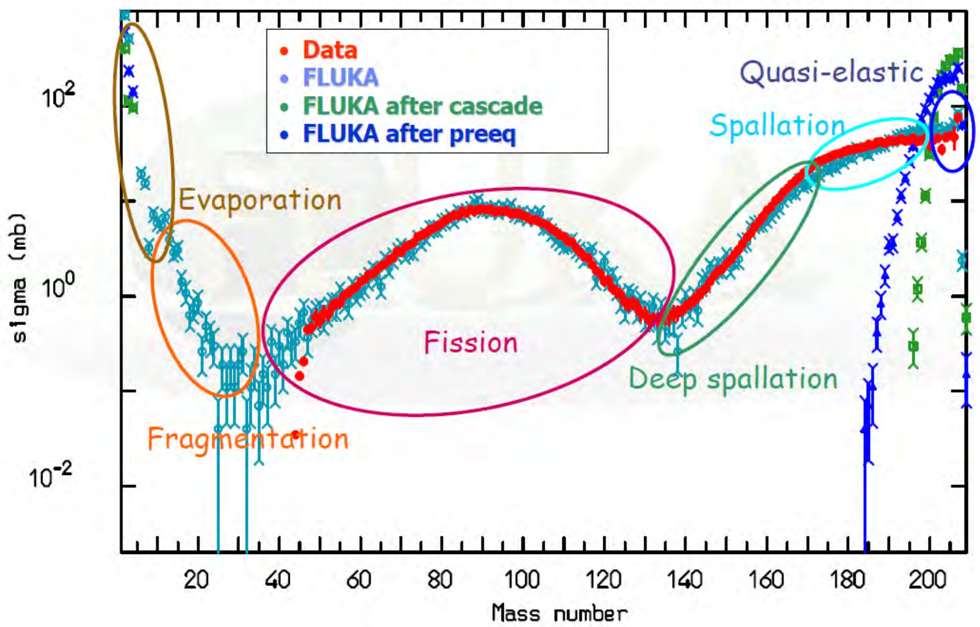

MARS-LAQGSM

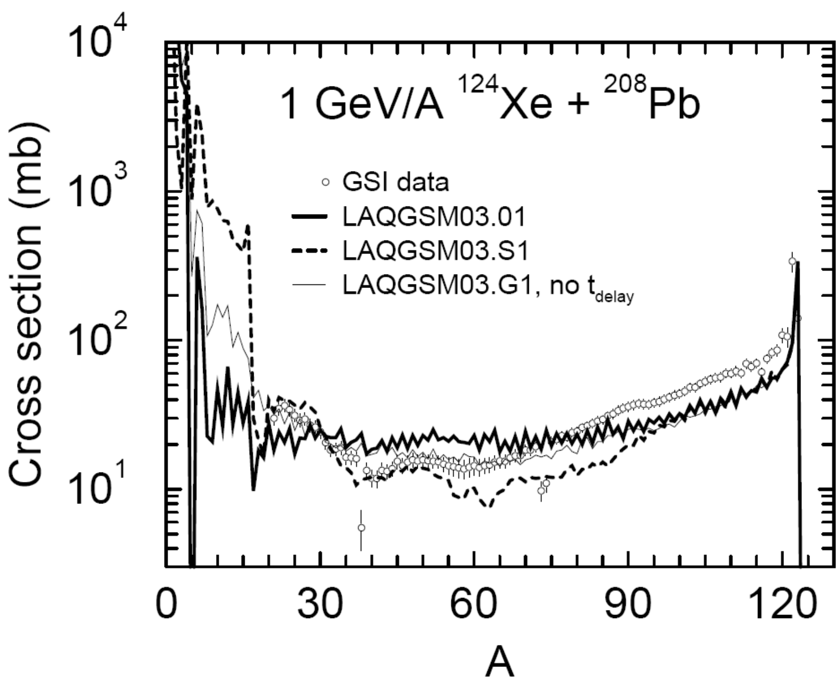

Ionization and Radiative Energy Loss dE/dx

Continuous-slowing-down-approximation (CSDA)

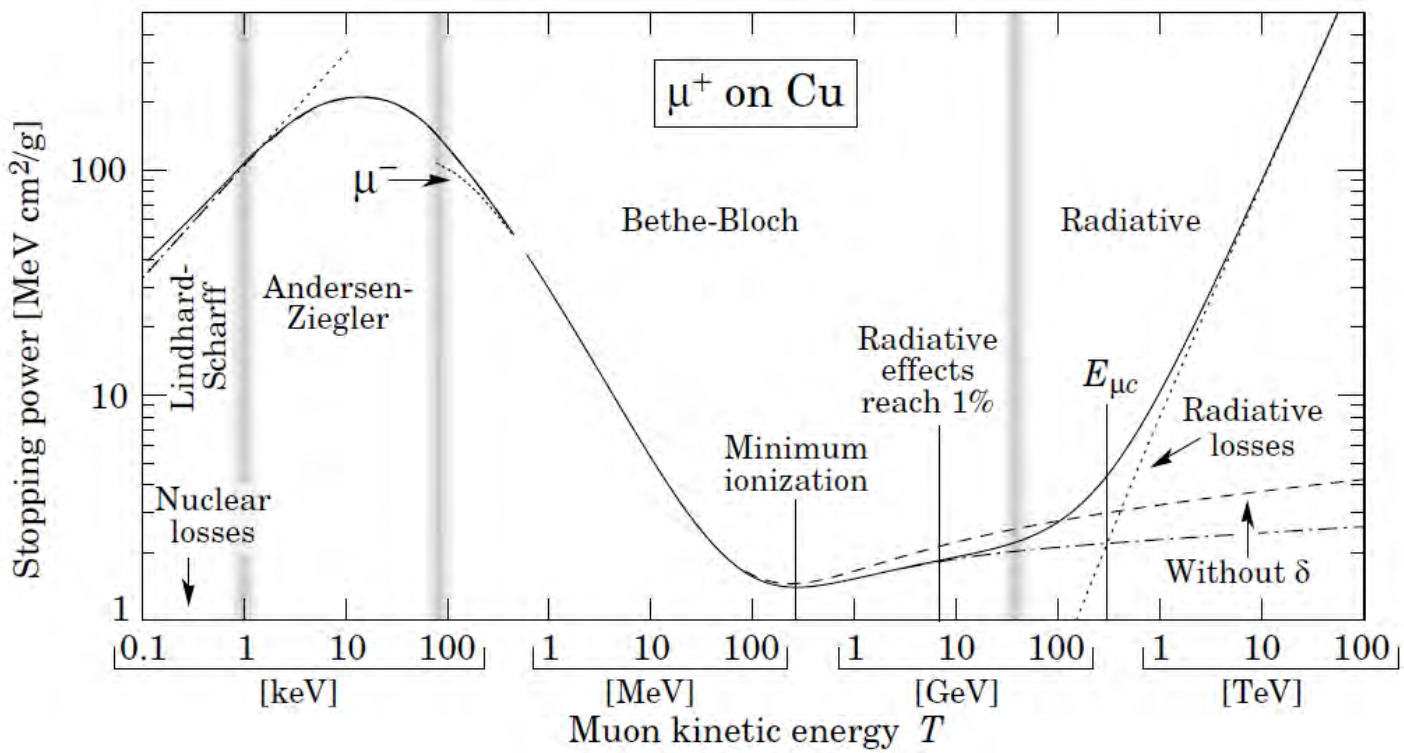

Mean stopping power for charged particles: (-dE/dx) = a (E) + b (E)E, where a (E) is the electronic stopping power, and b (E) is due to radiative processes – bremsstrahlung, pair production and photonuclear interactions; both a (E) and b (E) are slowly varying functions of E at high energies

Mean Ionization Stopping Power dE/dx

$$-\frac{1}{\rho}\frac{dE}{dx} = 4\pi N_A r_e^2 m_e c^2 z^2 \frac{Z}{A}\frac{1}{\beta^2} L(\beta)$$

$$L(\beta) = L_0(\beta) + \sum_i \Delta L_i$$

$$L_0(\beta) = \ln\left(\frac{2m_e c^2 \beta^2 \gamma^2}{I}\right) - \beta^2 - \frac{\delta}{2}$$

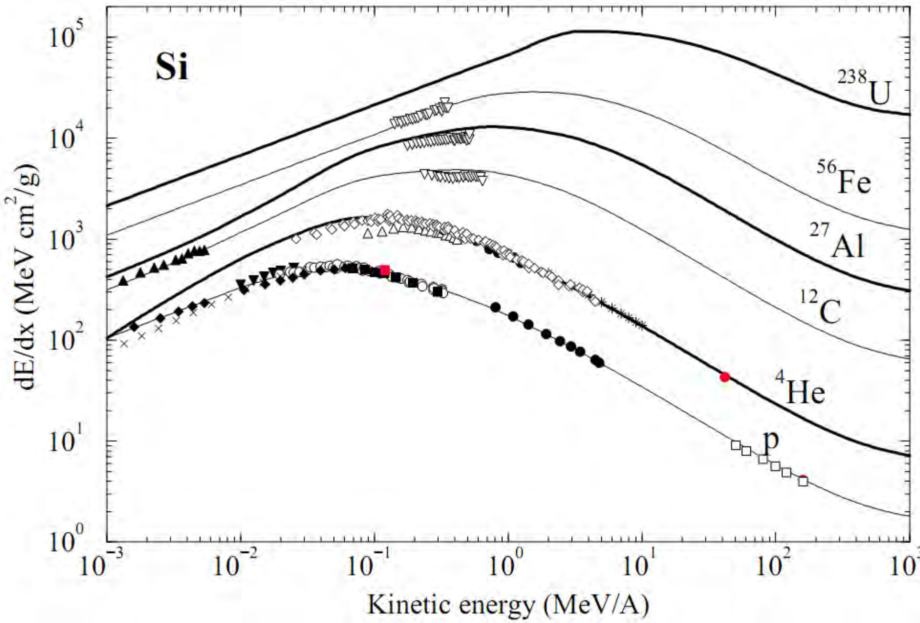

ΔLi: (i) **Lindhard-Sørensen** correction (exact solution to the Dirac equation; terms higher than z^2)

(ii) **Barkas** correction (target polarization effects due to low-energy distant collisions)

(iii) **shell** correction

Projectile **effective charge** comes separately as a multiplicative factor that takes into account electron capture at low projectile energies (e.g., z_{eff} ~ 20 for 1-MeV/A ^{238}U in Al, instead of bare charge of 92)

dE/dx: Mixtures and Heavy Ions

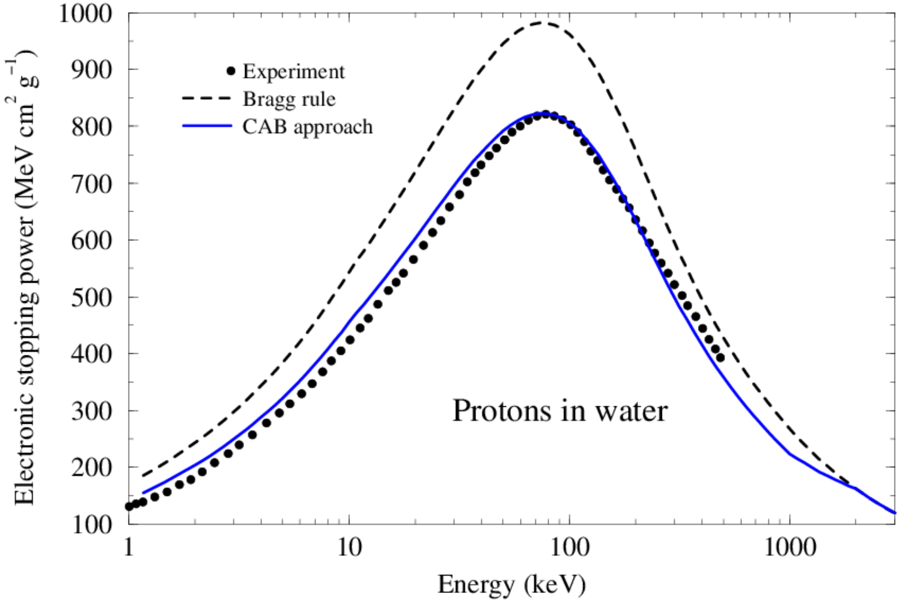

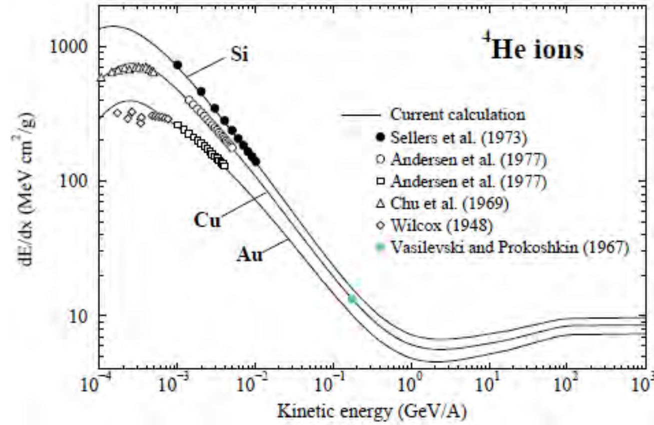

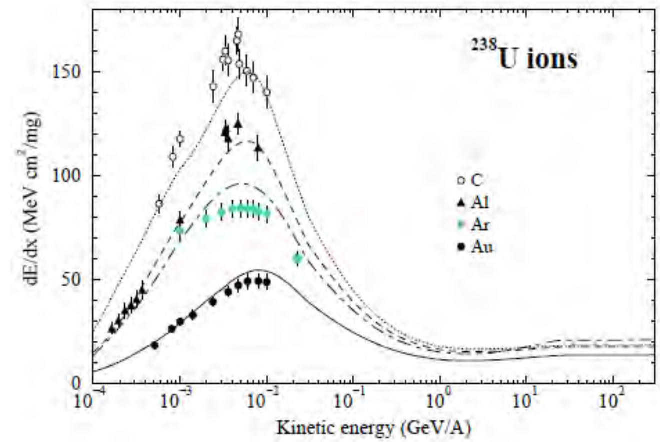

Stopping power of ions in compounds usually is described according to Bragg's rule. At low energies and for low-Z materials the difference between measured and predicted dE/dx can be as large as 20%. The "cores-and-bonds" (CAB) method in MARS15 takes into account chemical bonds fitted to experiment for various compounds

Energy Loss and Energy Deposition Modeling

1. The CSDA dE/dx is widely used in quick estimations of energy loss by particle beams and in simplified simulations of energy loss and energy deposition along the charged particle tracks in hadronic and electromagnetic cascades.
2. In a more sophisticated approach used these days in several codes, precise modeling of knock-on electron production with energy-angle correlations taken into account is done for electronic losses.

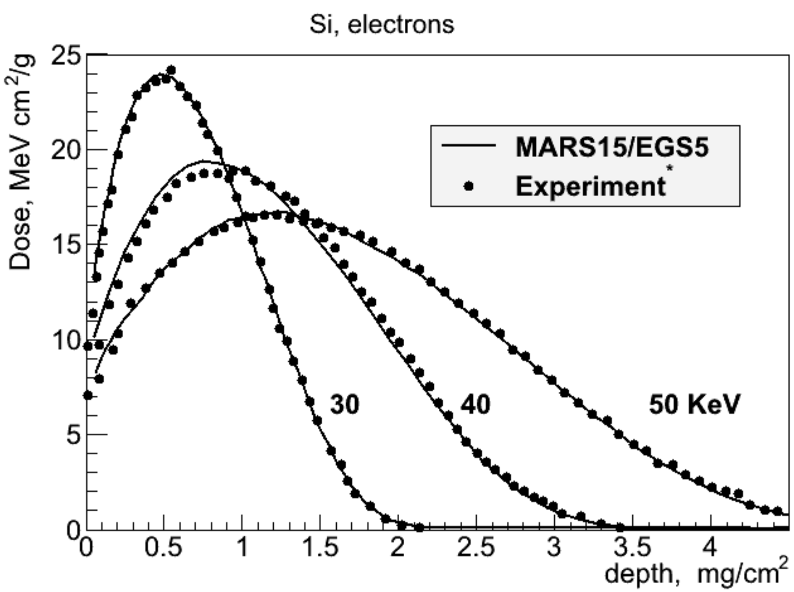

3. Radiative processes – bremsstrahlung, pair production and inelastic nuclear interactions (via virtual photon) – for muons and high-energy hadrons - are modelled exclusively using pointwise x-sections.

Items (2) and (3) allow precise calculation of 3D energy deposition maps induced by high energy cascades.

Stopped Muons in Uranium: exp *vs* MARS15

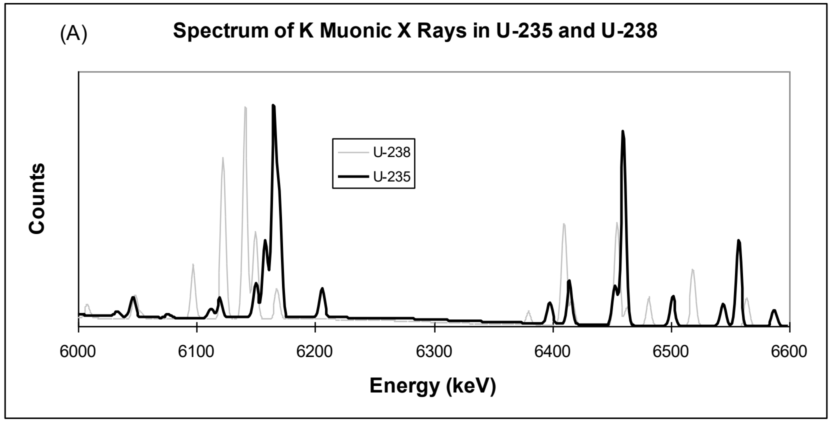

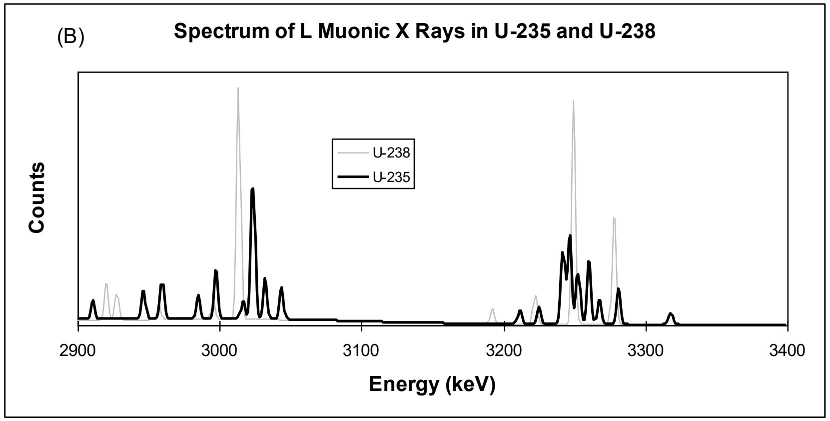

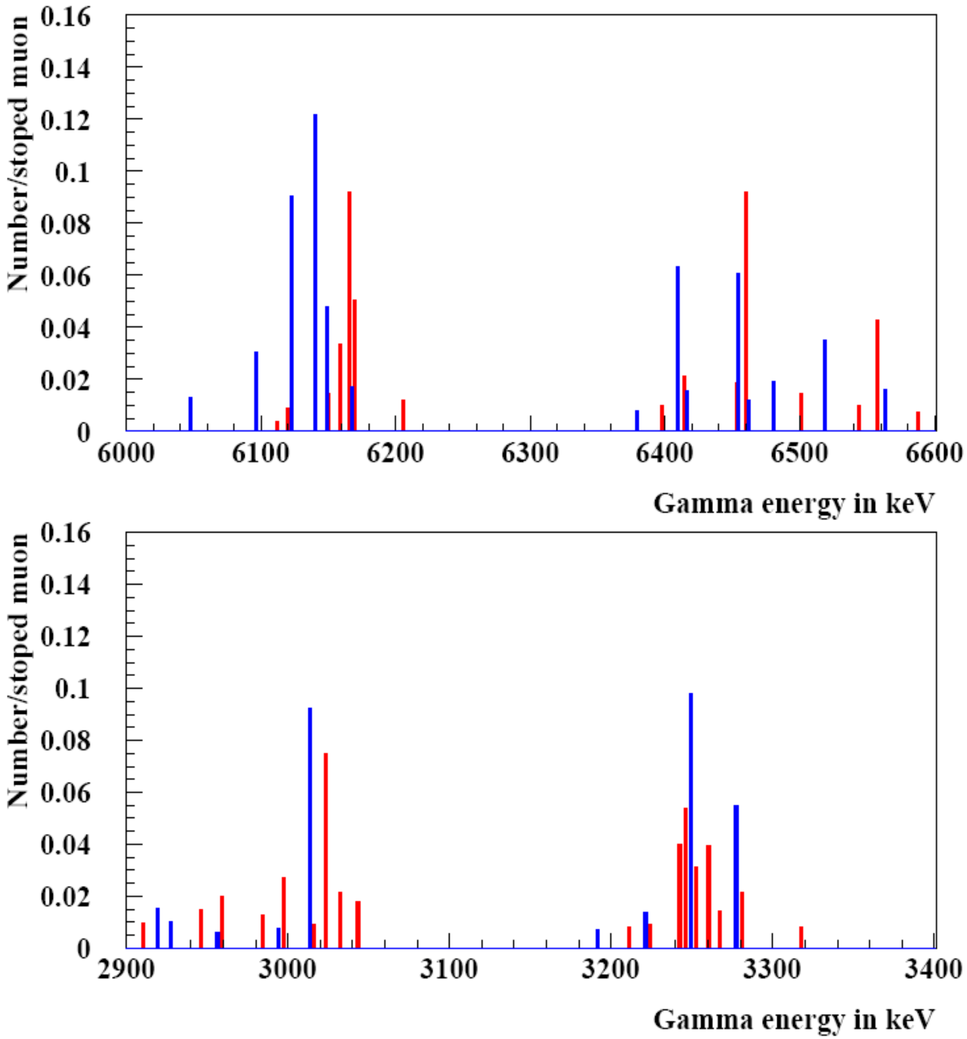

X-rays at muon stop. Red - U^{235}. Blue - U^{238}.

Simulation from experimental data on μ^- cascade in U^{238} and U^{235}

Checking at ports of entry…

Interaction of Particles with Organic Materials

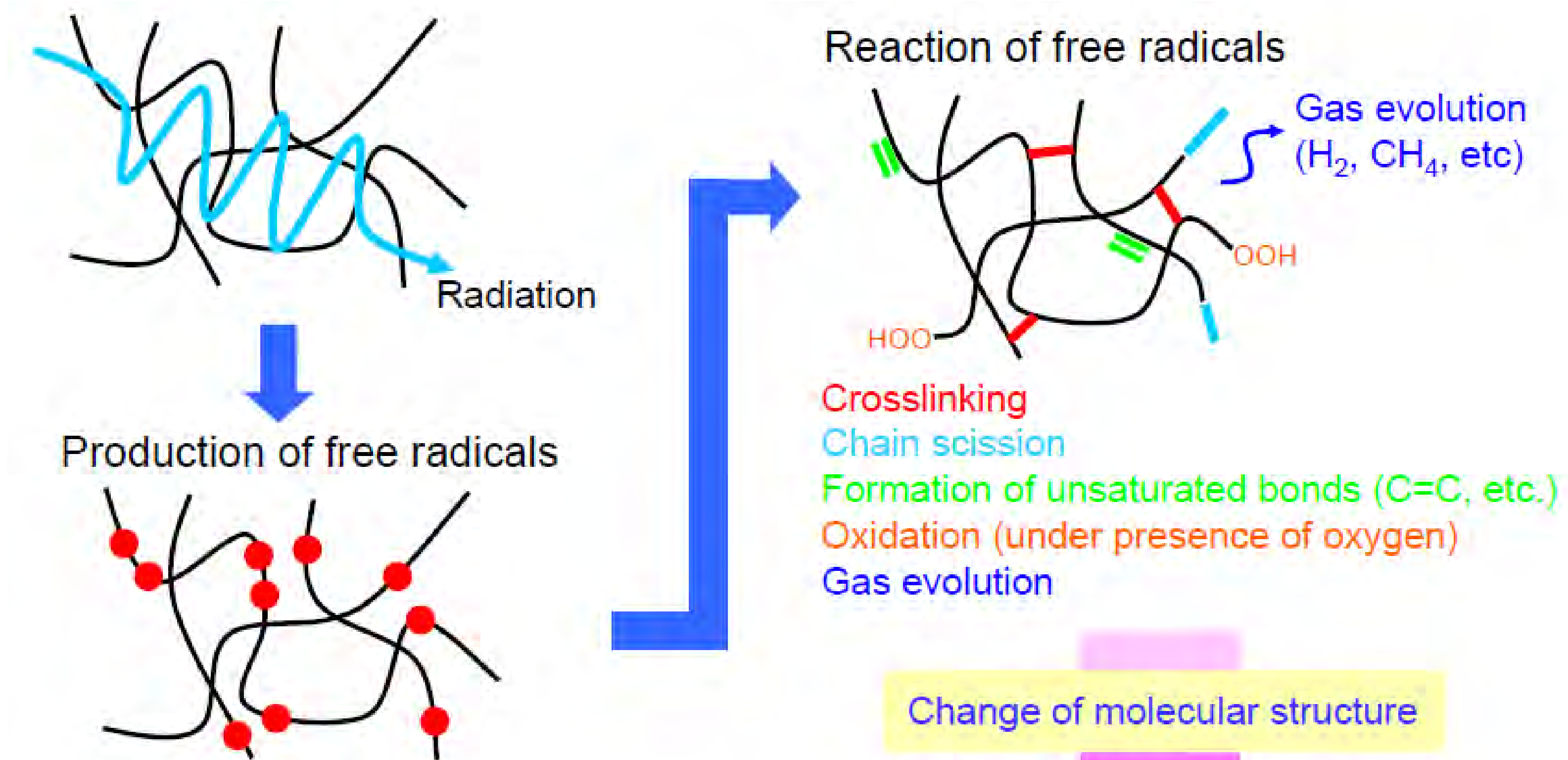

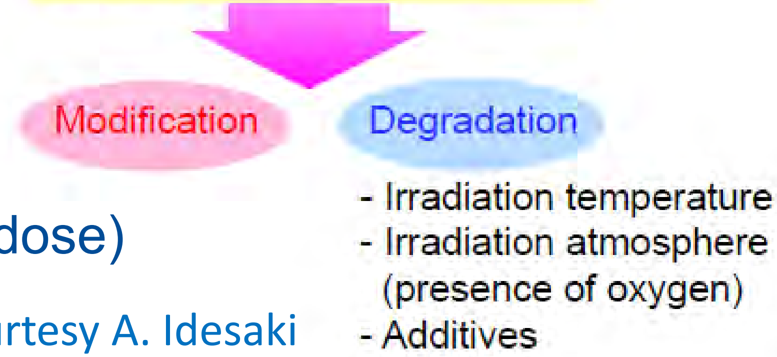

For given insulator and irradiation conditions radiation damage is proportional to energy deposition (dose)

Courtesy A. Idesaki

Beam-Induced Effects in Organic Materials

Contrary to the MeV type accelerators with their insulators made mostly of ceramics or glasses, the majority of insulators in high-energy accelerator equipment are made of organic materials: epoxy, G11, polymers etc. Apart from electronics and optical devices, the organic materials are the ones most sensitive to radiation. Radiation test findings:

- Degradation is enhanced at high temperatures.
- Radiation oxidation in presence of oxygen accelerates degradation.
- Radiation oxidation is promoted in the case of low dose rate.
- Additives can improve radiation resistance. For example, 1% by weight of antioxidant in polyethylene can prolong its lifetime 5 to 10 times.

Beam-Induced Effects in Inorganic Materials

- The dominant mechanism of structural damage of inorganic materials is displacement of atoms from their equilibrium position in a crystalline lattice due to irradiation with formation of interstitial atoms and vacancies in the lattice. Resulting deterioration of material critical properties is characterized – in the most universal way - as a function of **displacements per target atom (DPA).** DPA is a strong function of projectile type, energy and charge as well as material properties including its temperature.

- At accelerators, radiation damage to structural materials is amplified by **increased hydrogen and helium gas production** for high-energy beams. In the Spallation Neutron Source (SNS) type beam windows, the ratio of He/atom to DPA is about 500 of that in fission reactors. These gases can lead to grain boundary embrittlement and accelerated swelling.

Atomic Displacement Cross-Section and NIEL

- Atomic displacement cross section

$$\sigma_d = \sum_r \int_{E_d}^{T_r^{\max}} \frac{d\sigma(E, Z_t, A_t, Z_r, A_r)}{dT_r} N_d(T_r, Z_t, A_t, Z_r, A_r)\, dT_r$$

- N_d – number of stable defects produced, E_d –displacement threshold, $d\sigma/dT_r$ - recoil fragment energy (T_r) distribution

- Non-ionizing energy loss (NIEL)

$$\frac{dE}{dx}_{ni} = N \sum_r \int_{E_d}^{T_r^{\max}} \frac{d\sigma(E, Z_t, A_t, Z_r, A_r)}{dT_r} T_d(T_r, Z_t, A_t, Z_r, A_r)\, dT_r$$

N – number of atoms per unit volume

T_d - damage energy=total energy lost in non-ionizing process (atomic motion)

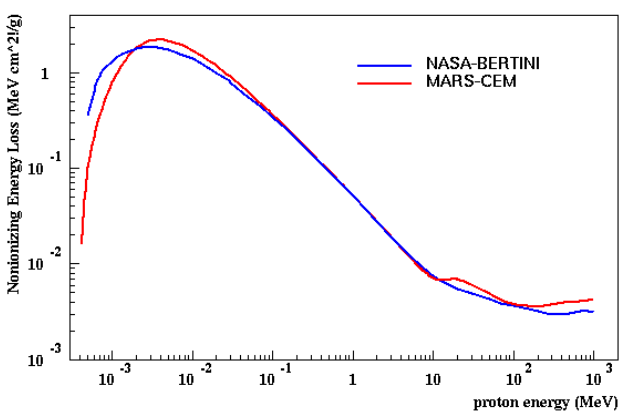

NRT “Standard” Model to Calculate a Number of Frenkel Pairs and Damage Energy

M.J. Norgett, M.T. Robinson, I.M. Torrens Nucl. Eng. Des 33, 50 (1975)

$$N_d = \frac{0.8}{2E_d} T_d$$

$$T_d = \frac{T_r}{1 + k(Z_t, A_t, Z_r, A_r)\, g(T_r, Z_t, A_t, Z_r, A_r)}$$

T_r, Z_r, A_r - recoil fragment energy=primary knock-on (PKA) energy, charge and atomic mass

Z_t, A_t - charge and atomic mass of irradiated material

Nuclear physics (T_r, T_d) + solid state physics (N_d)

NRT-DPA is successfully applied to correlate data from many studies involving direct comparison from different irradiation environments

Efficiency Function: Stoller MD Parametrization

Corrections to NRT to account for atom recombination in elastic cascading. Database based on MD simulations. Its parametrization, efficiency function $\xi(T)=N_D/N_{NRT}$, is used for several years in MARS15 (=1 if >1.

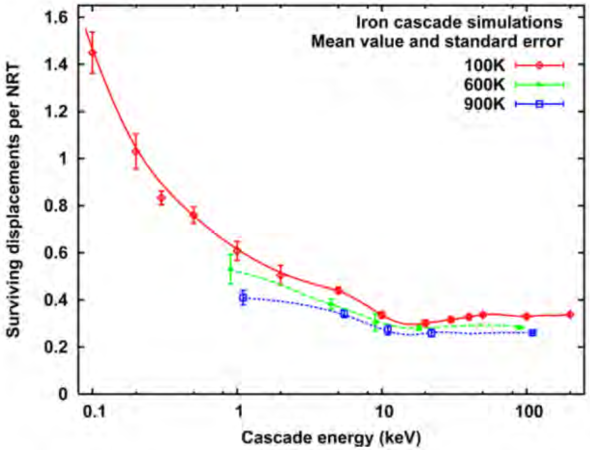

Also, Nordlund's concept (athermal recombination-corrected DPA, in MARS15 since 2016):

$$N_d = \begin{cases} 0 & T_d < E_d \\ 1 & E_d < T_d < 2.5E_d \\ \dfrac{T_d}{2.5E_d}\xi(T_d) & 2.5E_d < T_d \end{cases}$$

with efficiency function

$$\xi(T) = 0.214 + 0.786 \times (2.5E_d / T)^{0.541}$$

Proton & Neutron DPA on Copper: MARS15 *vs* Data

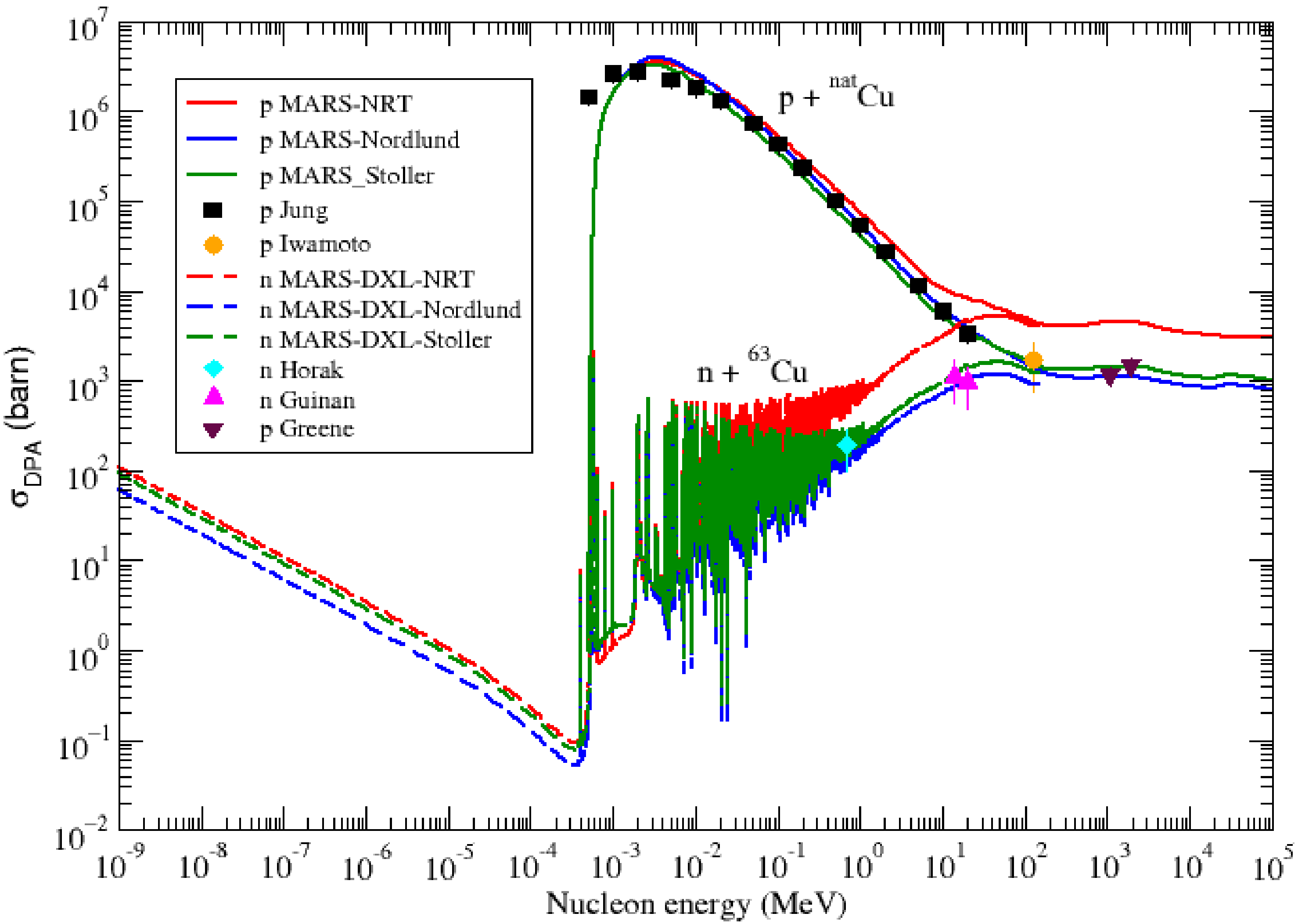

Accumulated Beam-Induced Effects in Silicon Detectors and Electronics

- **Surface damage**: ionization in SiO_2 layer and at Si-SiO_2 interface

- **Bulk damage**: conventional DPA mechanism, implemented in simulation codes as a **1-MeV (Si) equivalent neutron fluence**

$$\Phi_{\mathrm{eq}}^{1\mathrm{MeV}} = \int dE \, \frac{D(E)}{95\mathrm{MeV mb}} \Phi(E)$$

where D(E) is a displacement damage function of any particle for a given energy E, normalized to the one for 1-MeV neutrons (= 95 MeV mb)

Beam-Induced Soft Errors in Silicon Electronics

<u>Single-Event Upset (SEU):</u> a change of state caused by one single ionizing particle (ions, electrons, photons...) striking a sensitive node in a micro-electronic device, such as in a microprocessor, semiconductor memory, or power transistors.

The state change is a result of the free charge created by ionization in or close to an important node of a logic element (e.g. memory "bit").

The error in device output or operation caused as a result of the strike is called an SEU or a soft error.

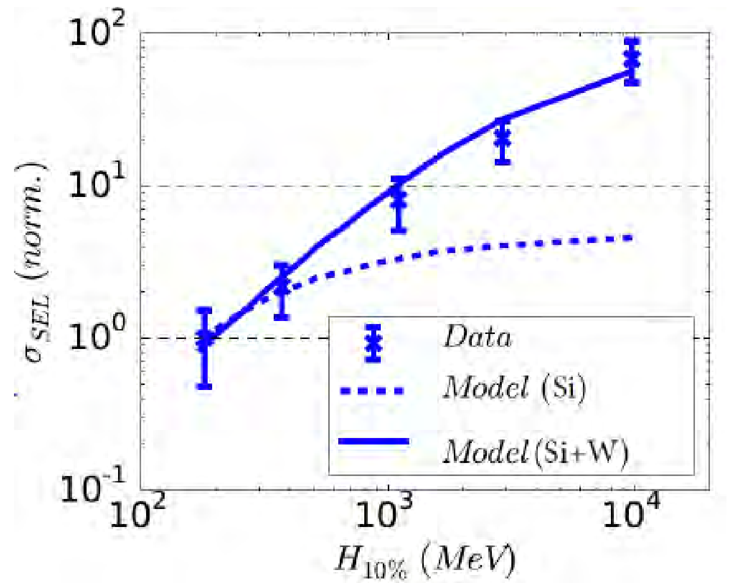

Courtesy A. Ferrari & R. Garcia Alia

CHARM data *vs* FLUKA model with and w/o heavy materials as a function of spectral hardness (energy above which 10% of the spectrum remains)

Coherent Beam Interactions with Crystals

- Extremely high interplanar electric fields (a few GV/cm) from screened nuclei allow bending of high-energy beams with a few mm thick crystals. Interplanar spacing ~ 2Å
- Applications: beam extraction, collimation and focusing
- Demonstrated at IHEP U-70, Tevatron, SPS and LHC. Considered for collimation at HL-LHC
- Drastically reduced nuclear interaction rates & energy loss; crystals are heat and radiation resistant
- But setting crystals up at high energies is more challenging compared to a conventional amorphous scatterer

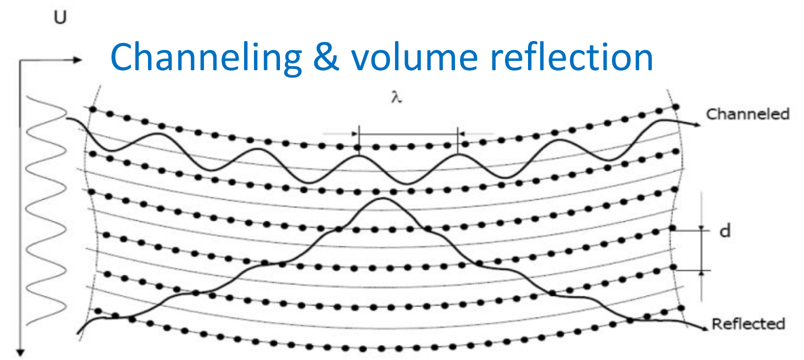

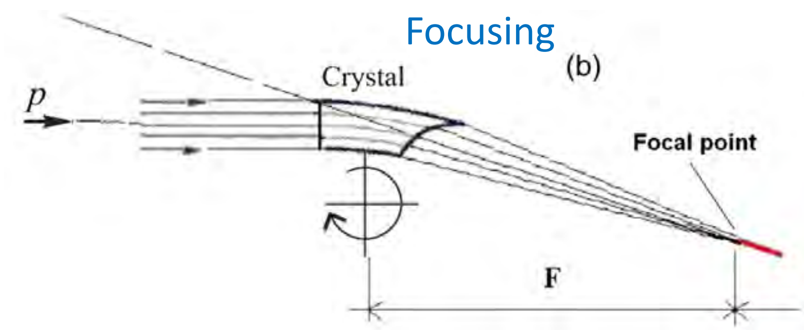

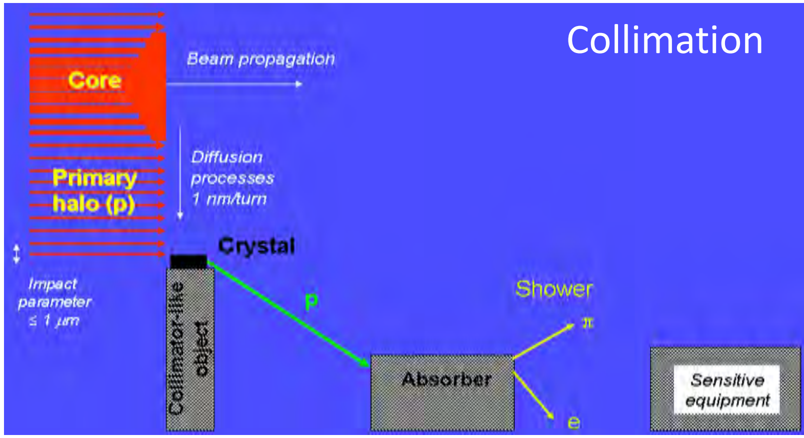

Managed by Fermi Research Alliance, LLC for the U.S. Department of Energy Office of Science

Simulation of Particle-Material Interactions: Advanced Implementation in the Monte-Carlo Codes NVM2(1)

Nikolai Mokhov, Fermilab

USPAS, Colliders

February 2, 2022

Outline

- Magnetic and Electric Fields
- Atomic Displacements (DPA) and Radiation Damage
- Five General-Purpose Particle Interaction and Transport Codes: FLUKA, GEANT4, MARS15, MCNP6 and PHITS
- MARS15-MADX-PTC Integration
- Compilers, ROOT, MPI
- Multithreading and Multi-Core Approaches
- LBNF/DUNE Application Example

Tracking in Magnetic and Electric Fields

The ***charged particle*** pathlength x is usually subdivided into **steps** $\boldsymbol{s}$ to account for quasi-continuous effects as ionization energy loss and multiple Coulomb scattering (MCS). If a magnetic field $\boldsymbol{B}$ is present, the particle will further change its direction upon passing the step $\boldsymbol{s}$. If an electric field $\boldsymbol{E}$ is present, the particle can in addition change its energy. These effects are governed by the Lorentz force $\boldsymbol{F} = q[\boldsymbol{E} + \boldsymbol{v} \times \boldsymbol{B}]$, where q and $\boldsymbol{v}$ are particle electric charge and velocity vector.

If the step $\boldsymbol{s}$ is already small enough – due to ionization loss and MCS constraints – one can neglect the variations of $\boldsymbol{B}$ and $\boldsymbol{E}$ on the step. Then, the new direction $\boldsymbol{\Omega}$ of the particle after the step is accurately derived from the equation of helical motion in a constant field. Otherwise – especially in complex geometry and field configurations - it is found by solving a high-order Runge-Kutta equation. The particle energy gain or loss in an electric field is calculated from the field component co-linear with the particle direction of motion and – in a case of a RF cavity – taking into account the distribution of the full $\boldsymbol{E}$ phase.

Atomic Displacements (DPA) in MARS15

- Atomic displacement cross-section σ_{DPA} is a reference way to characterize the radiation damage induced by neutrons and charged particles in crystalline materials. To evaluate a number of displaced atoms, Norget, Torrens and Robinson proposed in 1975 a standard (so-called, NRT-DPA), which has been widely used since. DPA is the left side of Eq. (3) while $D = \Sigma_{DPA}$ in the right side of Eq. (3) of the first lecture.
- Energy of recoil fragments and new charge particles in (elastic and inelastic) nuclear interactions is used to calculate atomic displacement cross sections σ_{DPA} for the NRT model – w/o or with Nordlund/Stoller damage efficiency $\xi(T)$ – for a number of stable defects
- Atomic screening parameters are calculated using the Hartree-Fock form-factors and recently suggested corrections to the Born approximation
- NJOY2016+ENDF/B-VIII.0(2018) is used to generate an NRT/Nordlund/Stoller database for 490 nuclides for neutrons from 10^{-5} eV to 200 MeV; DPA in neutron-nuclear interactions above 200 MeV are treated the same way as described in the second bullet

Fermilab

NRT "Standard" Model to Calculate a Number of Frenkel Pairs and Damage Energy

M.J. Norgett, M.T. Robinson, I.M. Torrens Nucl. Eng. Des 33, 50 (1975)

$$N_d = \frac{0.8}{2E_d} T_d$$

$$T_d = \frac{T_r}{1 + k(Z_t, A_t, Z_r, A_r) g(T_r, Z_t, A_t, Z_r, A_r)}$$

T_r, Z_r, A_r - recoil fragment energy=primary knock-on (PKA) energy, charge and atomic mass

Z_t, A_t - charge and atomic mass of irradiated material

Nuclear physics (T_r, T_d) + solid state physics (N_d)

NRT-DPA is successfully applied to correlate data from many studies involving direct comparison from different irradiation environments

Fermilab

Efficiency Function (1): Stoller MD Parametrization

Corrections to NRT to account for atom recombination in elastic cascading. Database based on MD simulations. Its parametrization, efficiency function $\xi(T)=N_D/N_{NRT}$, is used for several years in MARS15 (=1 if >1, since 2016).

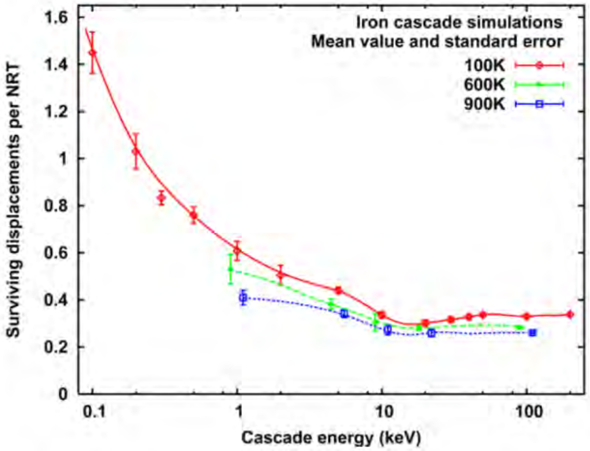

<u>Temperature dependence.</u> The calculations of Stoller (J. Nucl.Mater. 276 (2000) 22) for iron at 100-900K show some temperature dependence of the number of stable defects. At the same time the comparison of displacement cross-sections for p+Fe calculated using Stoller defect generation efficiency with the displacement cross-sections derived by Jung (J. Nucl. Mater. 117 (1983) 70) from low temperature experiments shows very good agreement.

Efficiency Function (2): Nordlund ARC-DPA

Nordlund's the ARC-DPA concept (athermal recombination-corrected DPA, in MARS15 since 2016):

"The recombination process does not require any thermally activated defect migration (atom motion is caused primarily by the high kinetic energy introduced by the recoil atom), this recombination is called "athermal" (i.e. it would also happen if the ambient temperature of the sample would be 0 K)."

"**<u>The arc-dpa concept allows empirical validation against frozen defects at cryogenic temperature</u>** (whereas NRT is an unobservable quantity)."

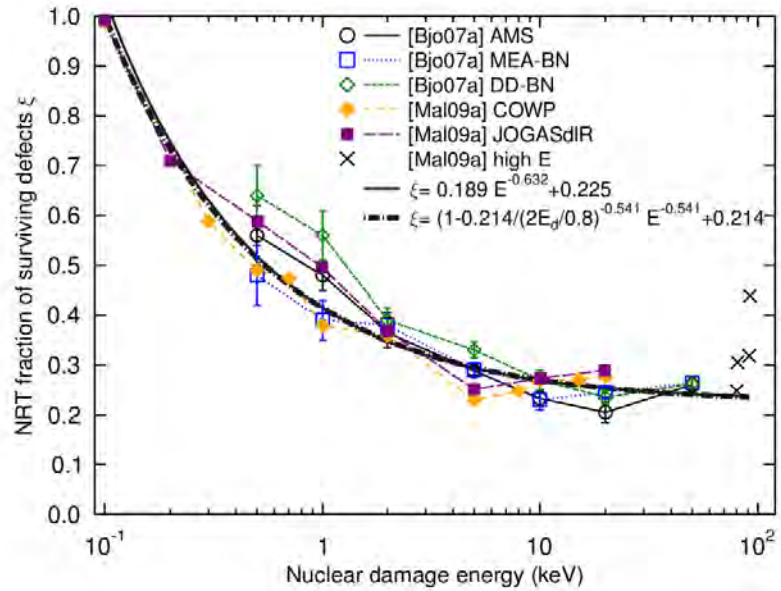

Modified NRT

$$N_d = \begin{cases} 0 & T_d < E_d \\ 1 & E_d < T_d < 2.5E_d \\ \dfrac{T_d}{2.5E_d}\xi(T_d) & 2.5E_d < T_d \end{cases}$$

with efficiency function

$$\xi(T) = 0.214 + 0.786 \times (2.5E_d / T)^{0.541}$$

Experimental Data Relevant to DPA Analysis

Jung et al, Greene et al and Iwamoto measured electrical resistivity change due to protons, electrons, light ions, fast and low-energy neutrons at low temperatures and low doses. It is connected to displacement cross section σ_d

$$\Delta\rho_d(\Phi, E) = \Phi \ \sigma_d(E)\rho_F$$

ρ_F is a resistivity per unit concentration of Frenkel defects. This constant cannot be accurately calculated and is determined from measurements. Jung and Greene groups choose different ρ_F (μΩm/u.c.) for the same material

	Jung	Greene	Iwamoto
Cu	2.5 ± 0.3	2	2 ± 1
W	27 ± 6	14	-

Konobeev, Broeders and Fisher (IOTA) note that Greene's choice for W seems questionable taking into account later analysis

Proton and Neutron DPA Verification

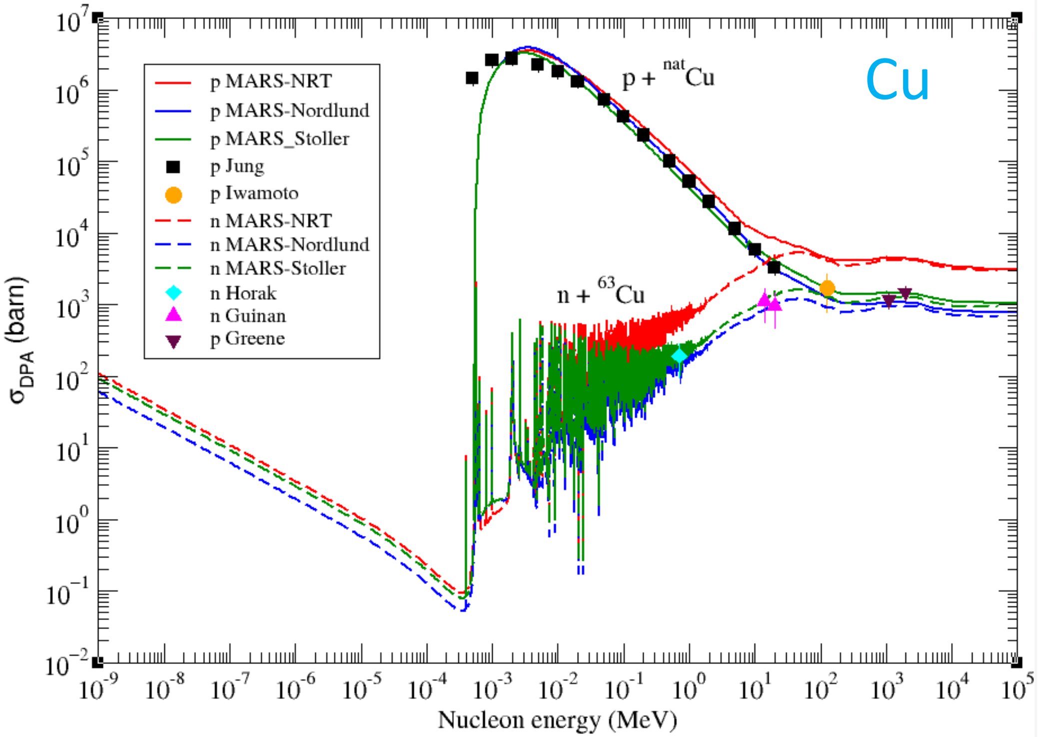

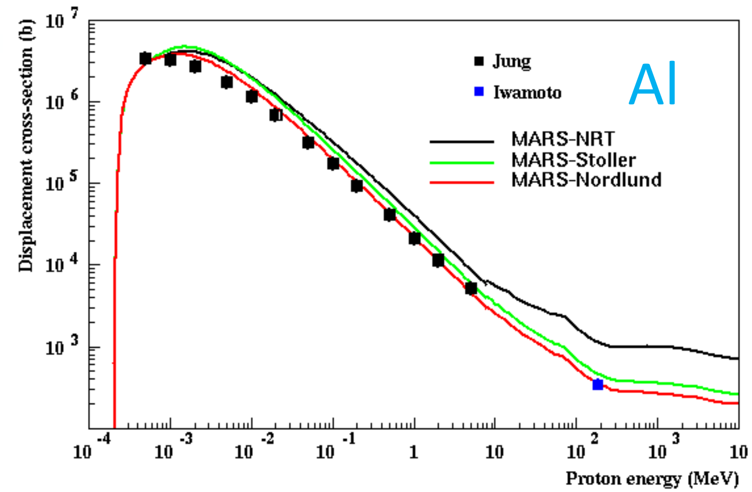

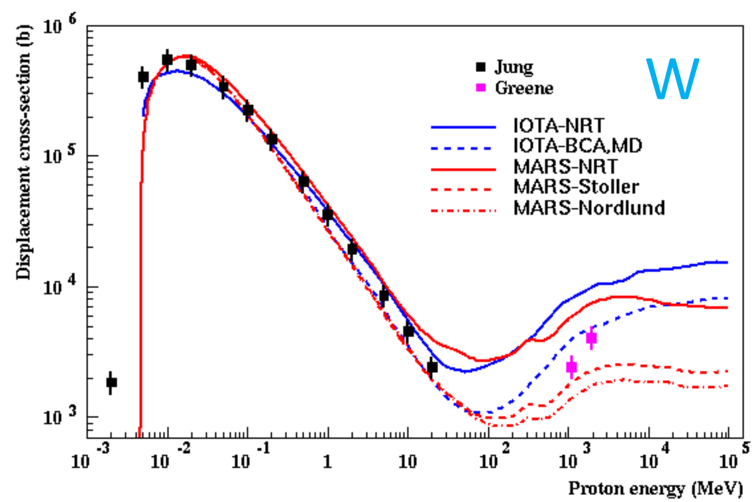

Fermilab

DPA in FLUKA

Charged particles and heavy ions

- During transport: The restricted non-ionizing energy loss
- Below threshold: The integrated nuclear stopping power with Lindhard partition
- At elastic and inelastic interactions: The is transported and treated as "below threshold"

Neutrons

- High energy E>20 MeV: treat recoils after interaction as a "normal" charged particle/ion
- Low energy E≤20 MeV (group-wise): NIEL from NJOY
- Low energy E≤20 MeV (point-wise): treat recoil (if created) as a "normal" charged particle/ion

DPA at High-Z BLIP: FLUKA *vs* MARS15

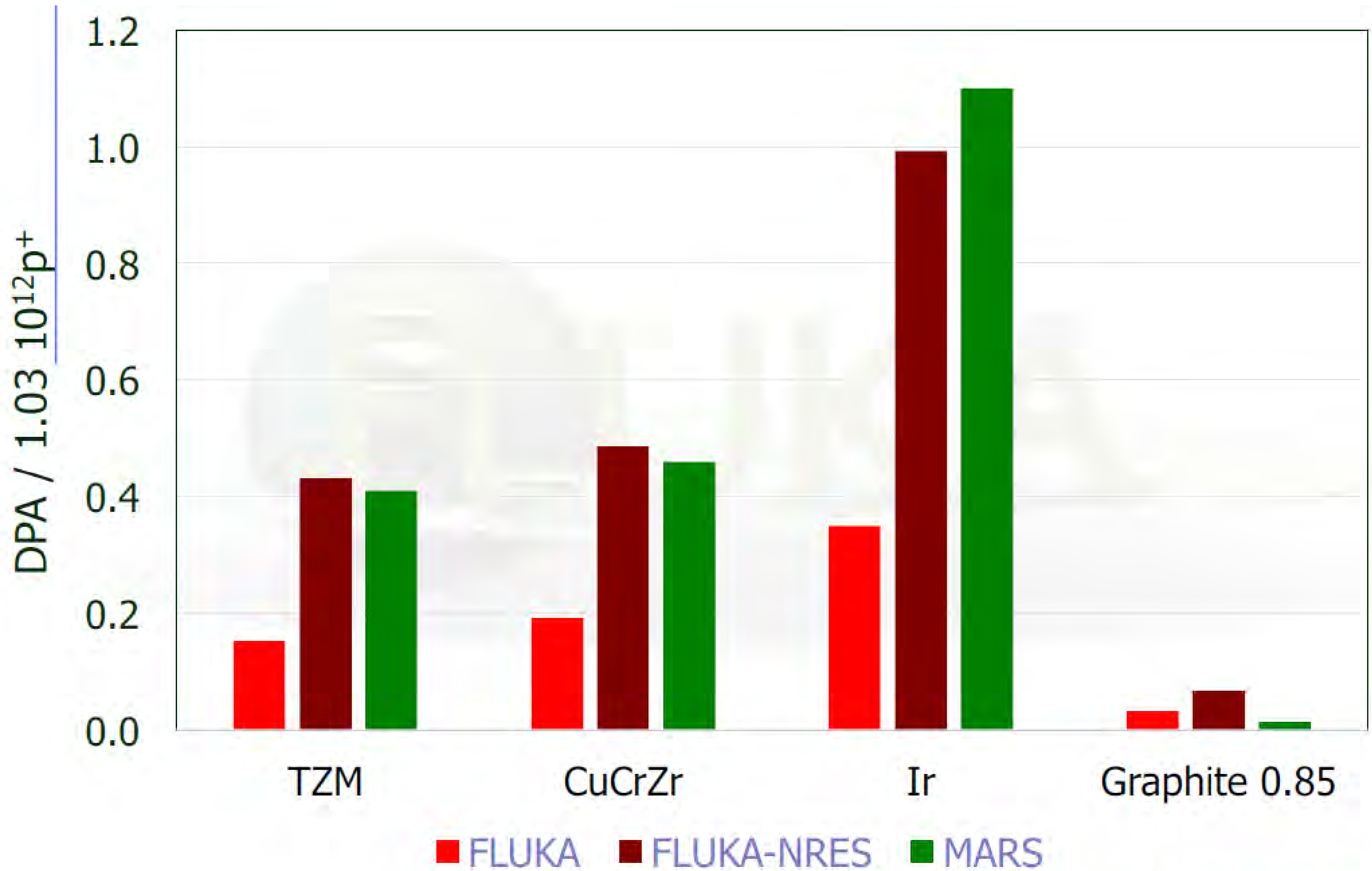

Note: NRT model of MARS

Code Benchmarking Definition

- **Debugging:** The code should calculate what is supposed to calculate
- **Validation:** Results should agree with established (or analytic) result for the specific case
- **Inter-comparison:** Two codes should agree if the model is the same
- **Verification:** The code should agree with (reliable) measurements

Hydrodynamic Tunneling in Solid Materials

Pulses with EDD >15 kJ/g: hydrodynamic regime.
First done for the 300-μs, 400-MJ, 20-TeV proton beams for the SSC graphite beam dump, steel collimators and tunnel-surrounding Austin Chalk by SSC-LANL Collaboration (D. Wilson, …, N. Mokhov, PAC93, p. 3090). Combining MARS ED calculations at each time step for a fresh material state and MESA/SPHINX hydrodynamics codes.

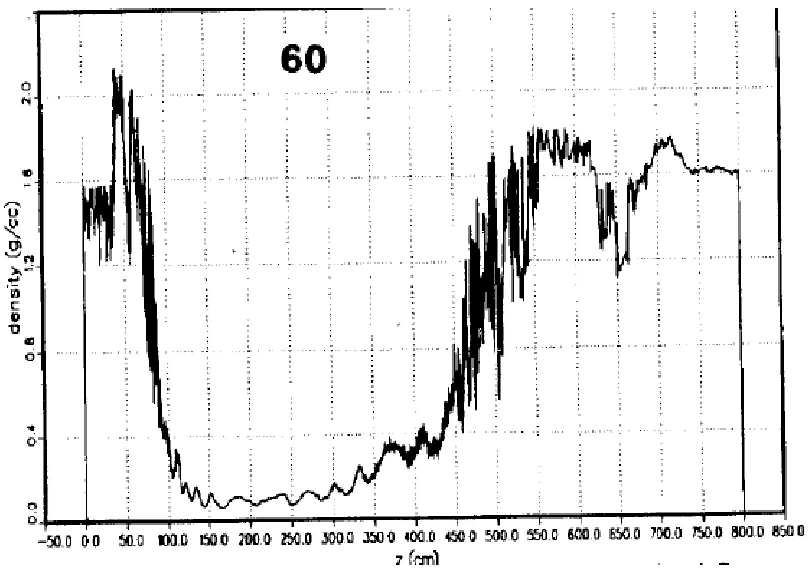

The hole was drilled at the 7 cm/μs penetration rate. Shown is axial density of graphite beam dump in 60 μs after the spill start

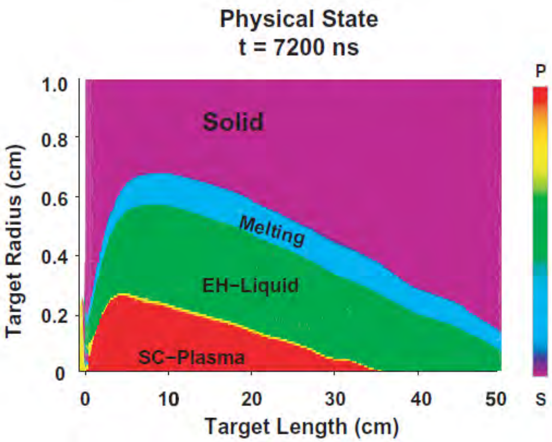

Later, studies by N. Tahir et al with FLUKA+BIG2 codes for SPS & LHC

These days we use MARS+FRONTIER

Example of Simulation Code Applications (true for the codes considered here)

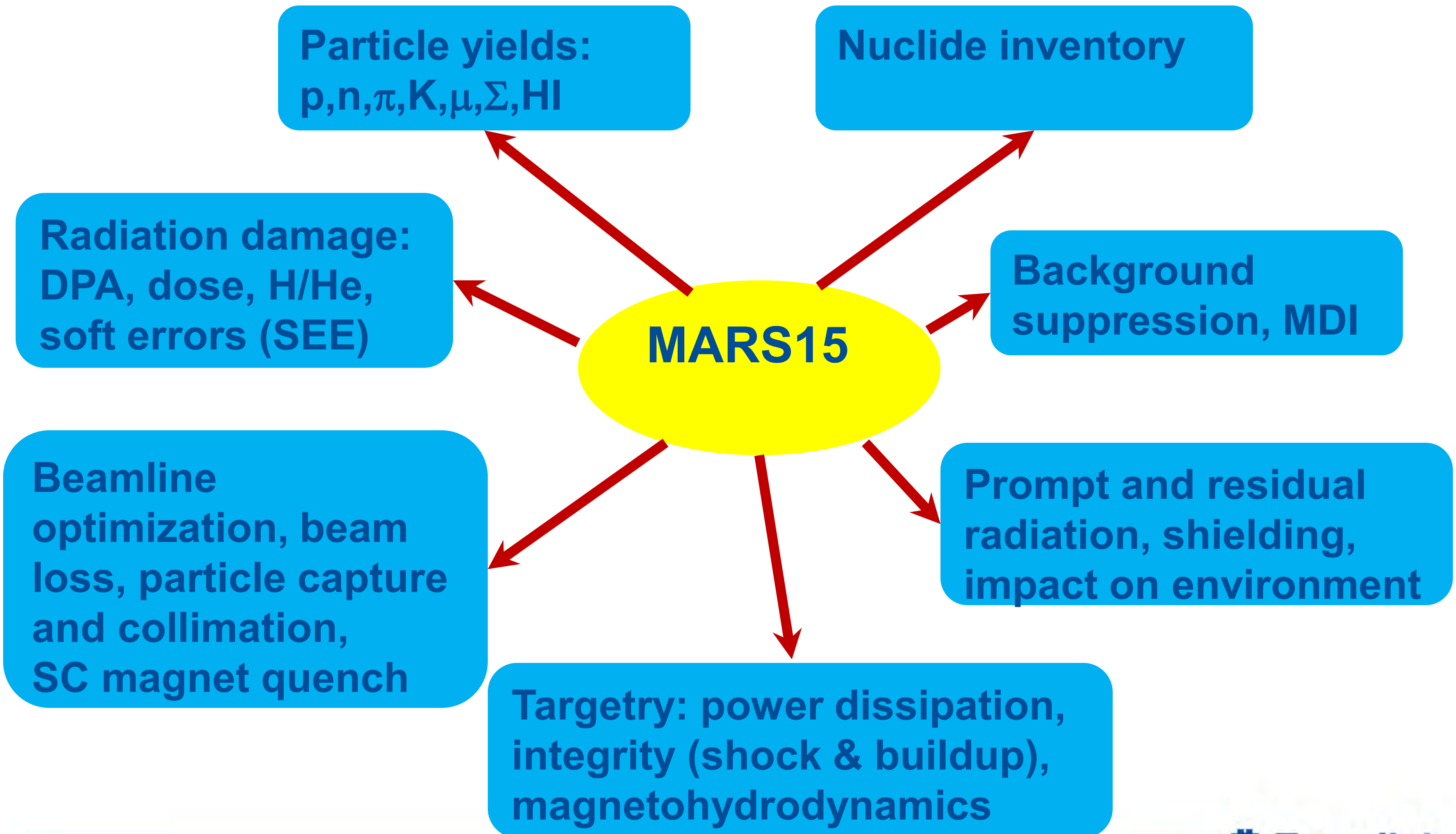

Five Codes Widely Used Around the Globe

The use of **general-purpose particle interaction and transport Monte Carlo codes** is nowadays the most accurate and efficient choice for assessing impact and consequences of particle-matter interactions at accelerators. Due to the vast spread of such codes to all areas of particle physics and the associated extensive benchmarking with experimental data, **the modeling has reached an unprecedented accuracy**.

Furthermore, most of these codes allow the user to simulate all aspects of a high energy particle cascade in one and the same run: from the first interaction of a primary beam (of up to TeV energies) over the transport and re-interactions (hadronic and electromagnetic) of the produced secondaries, to detailed nuclear fragmentation, the calculation of radioactive decays, secondary electromagnetic showers, muon and neutrino generation and their interaction with surroundings.

A brief account of these codes – taken from Review of Particle Physics, Phys. Rev. **D98, 030001 (2018**) and extended with principal features and examples – is given in the following slides for

FLUKA, GEANT4, MARS15, MCNP6 and PHITS

FLUKA (www.fluka.org)

FLUKA is a general-purpose particle interaction and transport (**Fortran 77**) code. It comprises all features needed for radiation protection, such as detailed hadronic and nuclear interaction models up to 10 PeV, full coupling between hadronic and electromagnetic processes and numerous variance reduction options. The latter include weight windows, region importance biasing, and leading particle, interaction, and decay length biasing (among others).

The capabilities of FLUKA are very good for studies of induced radioactivity, especially with regard to nuclide production, decay, and transport of residual radiation (cite from RPP). In particular, particle cascades by prompt and residual radiation are simulated in parallel based on the microscopic models for nuclide production and a solution of the Bateman equations for activity build-up and decay. **FLUKA is de facto the official code in numerous LHC and other applications at CERN.**

FLUKA’s Features (1)

The highest priority in the design and development of FLUKA has always been the implementation and improvement of sound and modern physical models. Microscopic models are adopted whenever possible, consistency among all the reaction steps and/or reaction types is ensured, conservation laws are enforced at each step, results are checked against experimental data at single interaction level.

As a result, final predictions are obtained with a minimal set of free parameters fixed for all energy/target/projectile combinations. Therefore results in complex cases, as well as properties and scaling laws, arise naturally from the underlying physical models, predictivity is provided where no experimental data are directly available, and correlations within interactions and among shower components are preserved.

FLUKA's Features (2)

FLUKA can handle very complex geometries, using an improved version of the well-known Combinatorial Geometry (CG) package. The FLUKA CG has been designed to track correctly also charged particles (even in the presence of magnetic or electric fields). Various visualisation and debugging tools are also available.

Similar to the MARS15 code, FLUKA has a double capability to be used in a biased mode as well as a fully analogue code. That means that while it can be used to predict fluctuations, signal coincidences and other correlated events, a wide choice of statistical techniques are also available to investigate punch-through or other rare events in connection with attenuations by many orders of magnitude.

FLUKA Geometry Modeling (1)

NEED FOR DETAILED MODELS OF ACCELERATOR COMPONENTS WITH ASSOCIATED SCORING

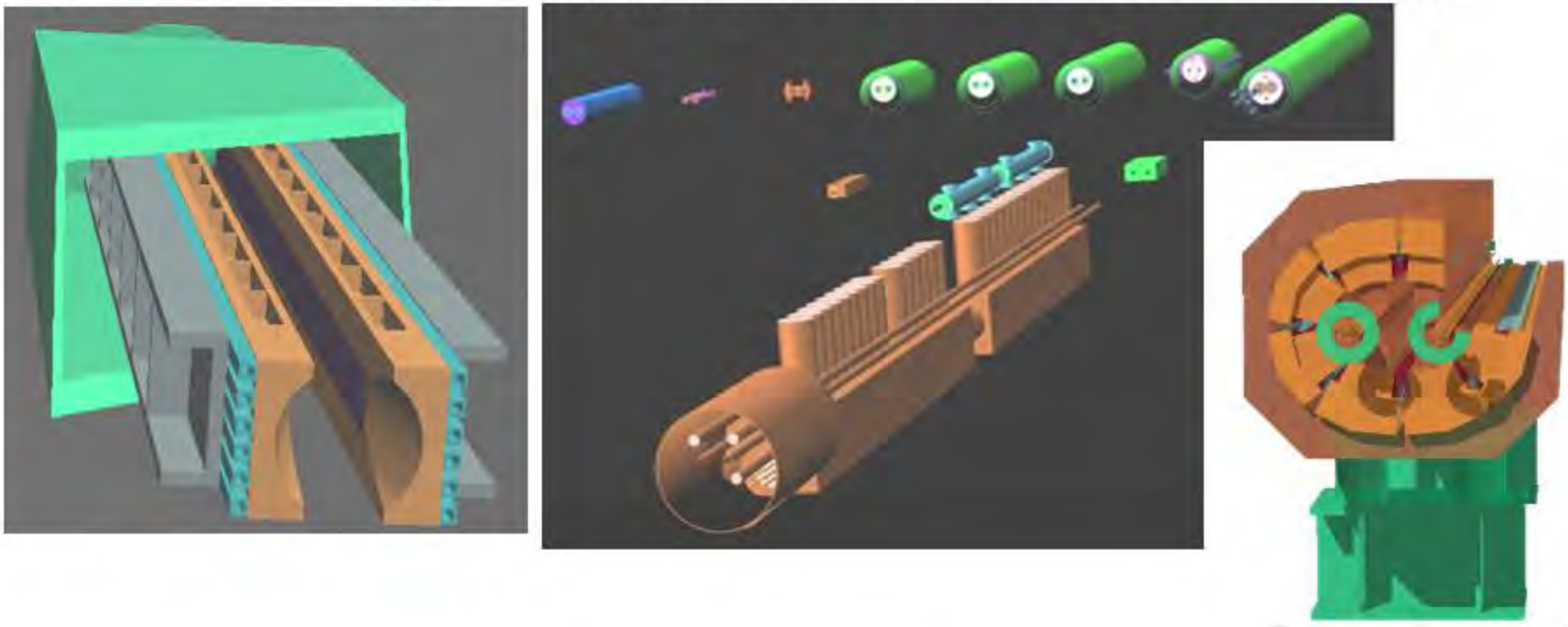

ELEMENT SEQUENCE AND RESPECTIVE MAGNETIC STRENGTHS
IN THE MACHINE OPTICS (TWISS) FILES

F. Cerutti

FLUKA Geometry Modeling (2)

Profiting from roto-translation directives and replication (lattice) capabilities, the AUTOMATIC CONSTRUCTION OF COMPLEX BEAM LINES, including collimator settings and element displacement (BLMs), is achievable

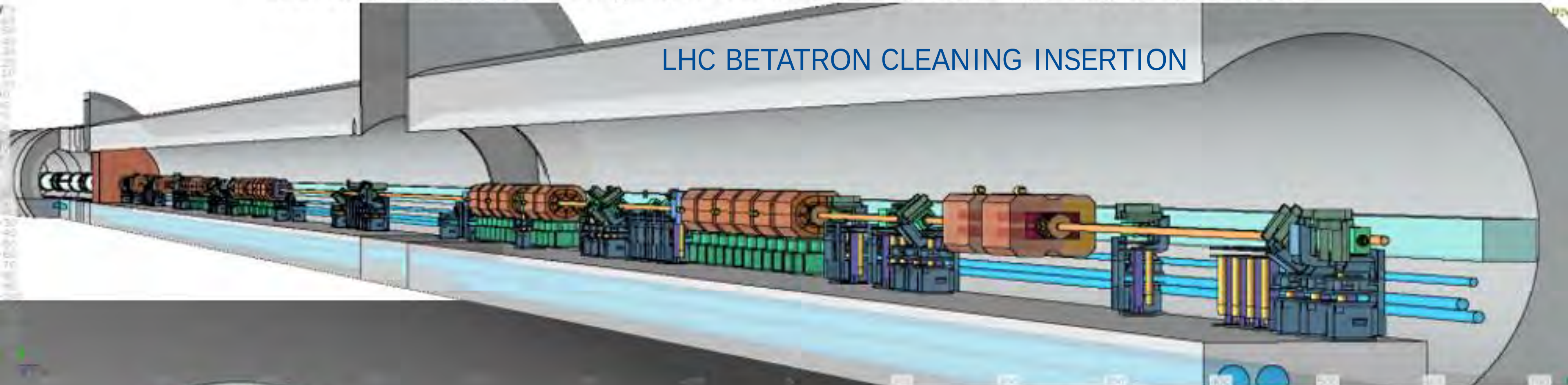

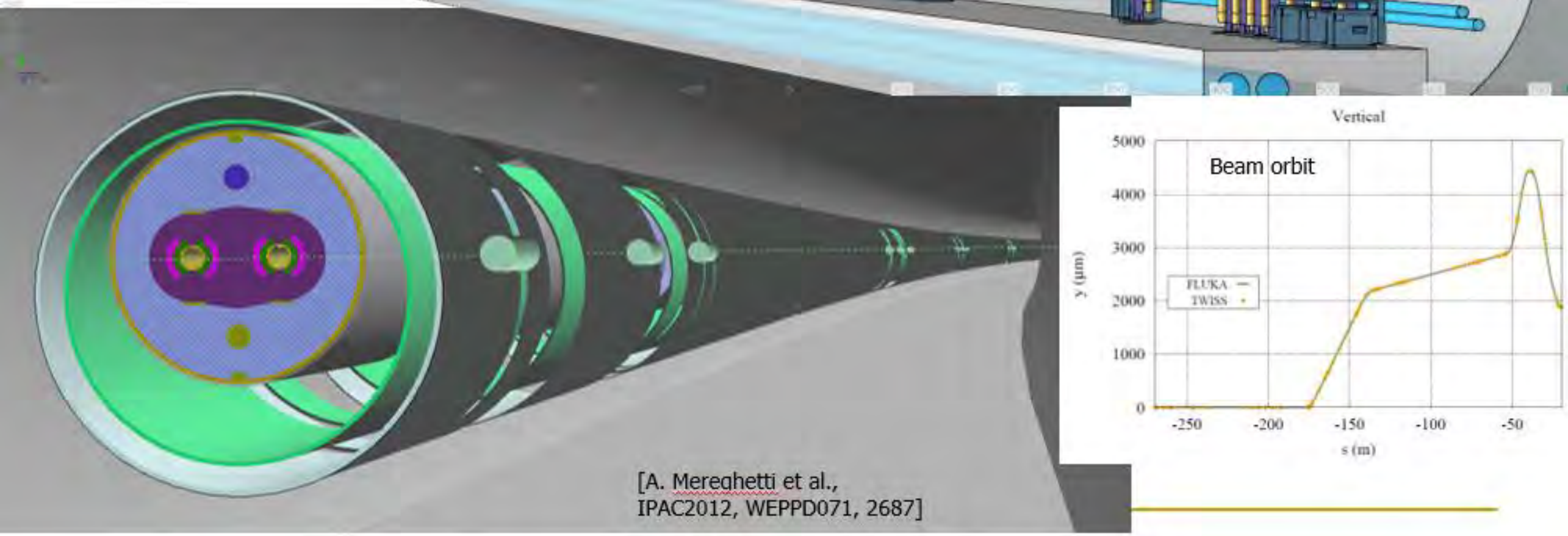

[A. Mereghetti et al., IPAC2012, WEPPD071, 2687]

FLUKA Geometry Modeling (3)

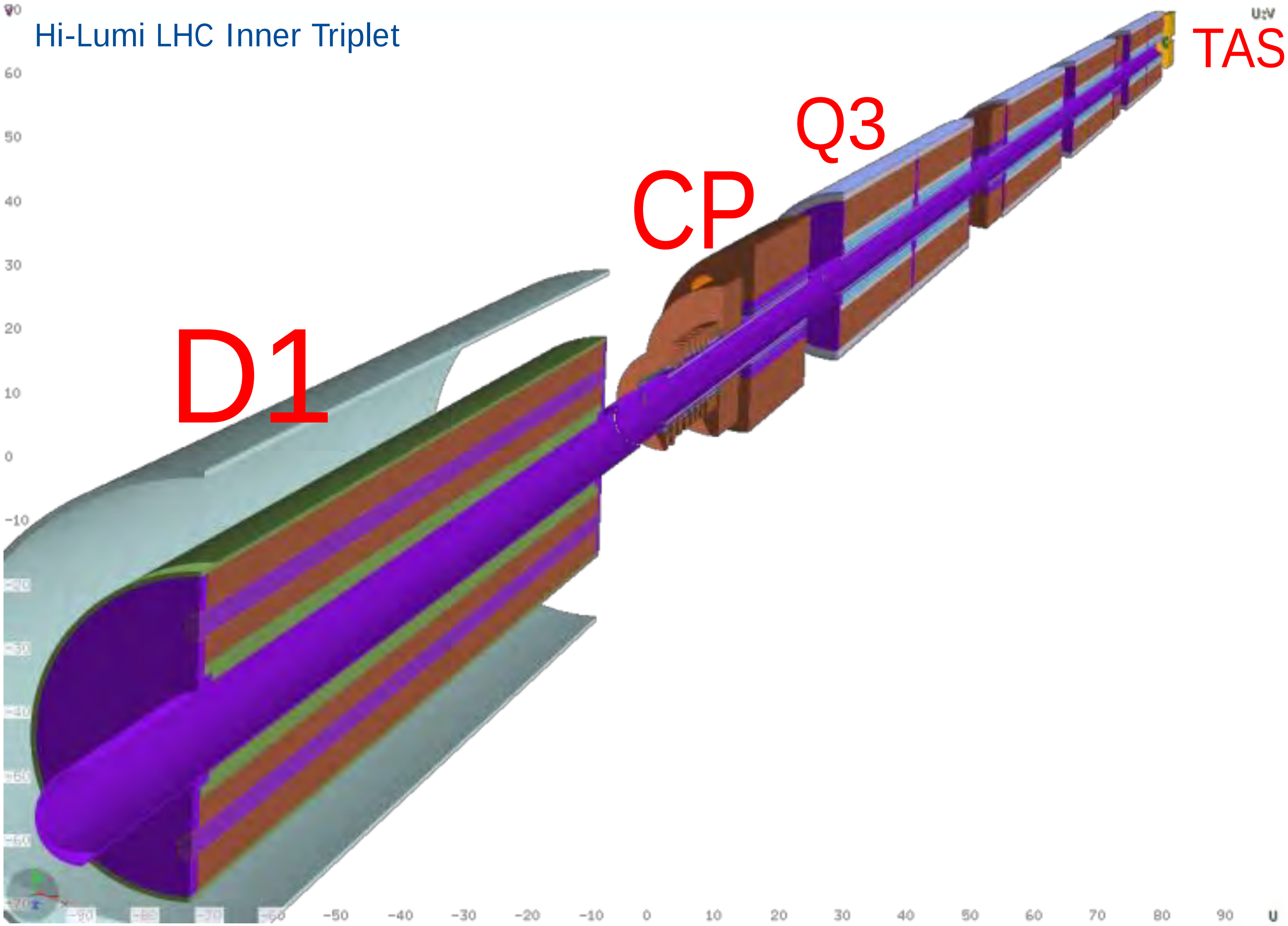

F. Cerutti

GEANT4 (geant4.cern.ch)

GEANT4 is an **object-oriented toolkit** consisting of a kernel that provides the framework for particle transport, including tracking, geometry description, material specifications, management of events and interfaces to external graphics systems. The kernel also provides interfaces to physics processes. It allows the user to freely select the physics models that best serve the particular application needs. Implementations of interaction models exist over an extended range of energies, from optical photons and thermal neutrons to high-energy interactions required for the simulation of accelerator and cosmic ray experiments.

G4 is the industry standard for HEP detector simulation. To facilitate the use of variance reduction techniques, general-purpose biasing methods such as importance biasing, weight windows, and a weight cut-off method have been introduced directly into the toolkit. Other variance reduction methods, such as leading particle biasing for hadronic processes, come with the respective physics packages.

GEANT4 Physics Models

A comprehensive set of the well-established models comprises GEANT's physics lists for users to chose from. Substantial efforts were and still are put by the GEANT4 team on validation and verification of electro-magnetic physics in the code and hadronic physics loosely defined to cover any reaction which can produce hadrons in final state: purely hadronic interactions, lepton- and gamma-induced nuclear reactions, and radioactive decay.

Models and x-sections are provided which span an energy range from sub-eV to TeV. Following the toolkit philosophy, more than one model or process is usually offered in any given energy range in order to provide alternative approaches for different applications.

GEANT4's performance was noticeably improved after several international benchmarking campaigns over last 15 years.

GEANT4 Geometry

There are several ways to build a geometry model in GEANT4. The standard one is to write a C++ code that contains all the definitions, material, dependence, position and hierarchy assignments, and arranges all these in the model. The shapes or geometrical primitives can be taken from a comprehensive library built in the toolkit. Fragments of the model can be imported and exported from external files according to two different formats: GDML or plain ASCII text (next slide).

GEANT4 provides internal modules which allow the interpretation and conversion of these formats to and from the internal geometry representation, without the need for C++ programming for the implementation of the various detector description setups.

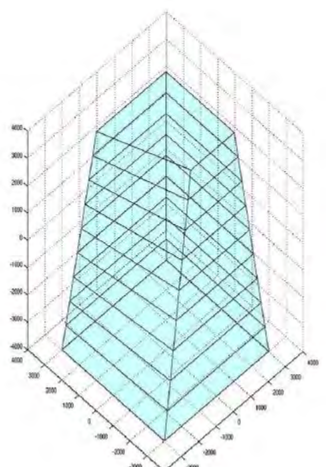

Trapezoid

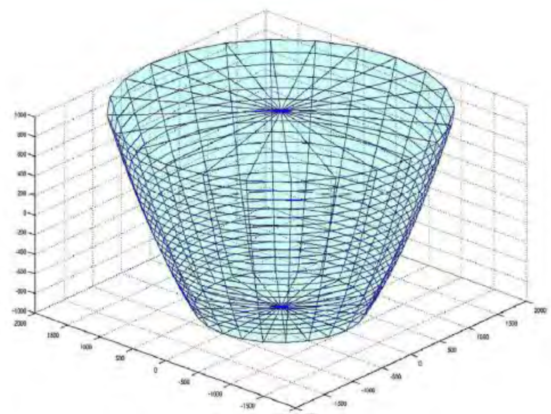

Parabolic solid

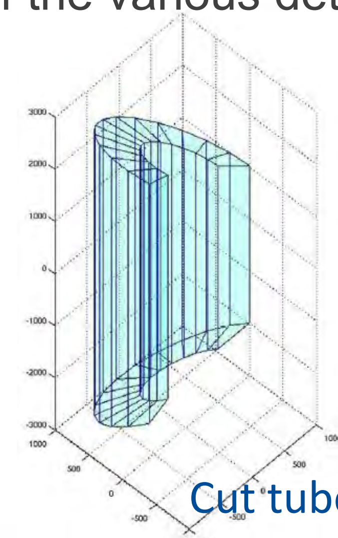

Cut tube

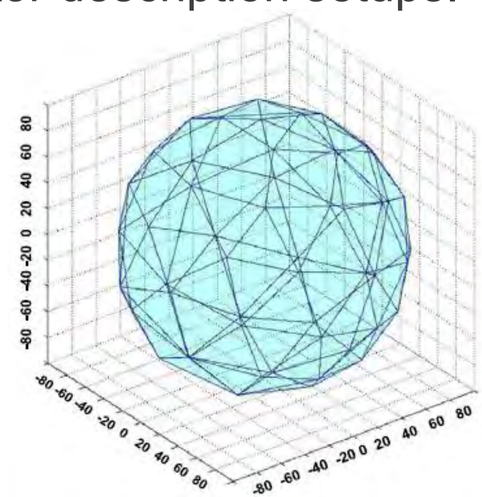

Sphere

GEANT4: Example of Geometry ASCII Text Format

```
// Define a parameter for later use
:P DIMZ 5.

// Define materials
:ELEM Hydrogen H 1. 1.
:ELEM Oxygen O 8 16.
:ELEM Nitrogen N 7 14.
:MIXT Air 1.214E-03 2
   Nitrogen 0.75
   Oxygen 0.25

// Define rotation matrix
:ROTM R00 0. 0. 0. // unit matrix

// Define volumes and place them
:VOLU world BOX 30. 30. 30. Air

:VOLU "my tube" TUBE 0. 10. $DIMZ*4 G4_WATER
:PLACE "my tube" 1 world R00 0. 0. $DIMZ

:VOLU sphere ORB 5. G4_AIR
:PLACE sphere 1 "my tube" R00 0. 1. 10.
```

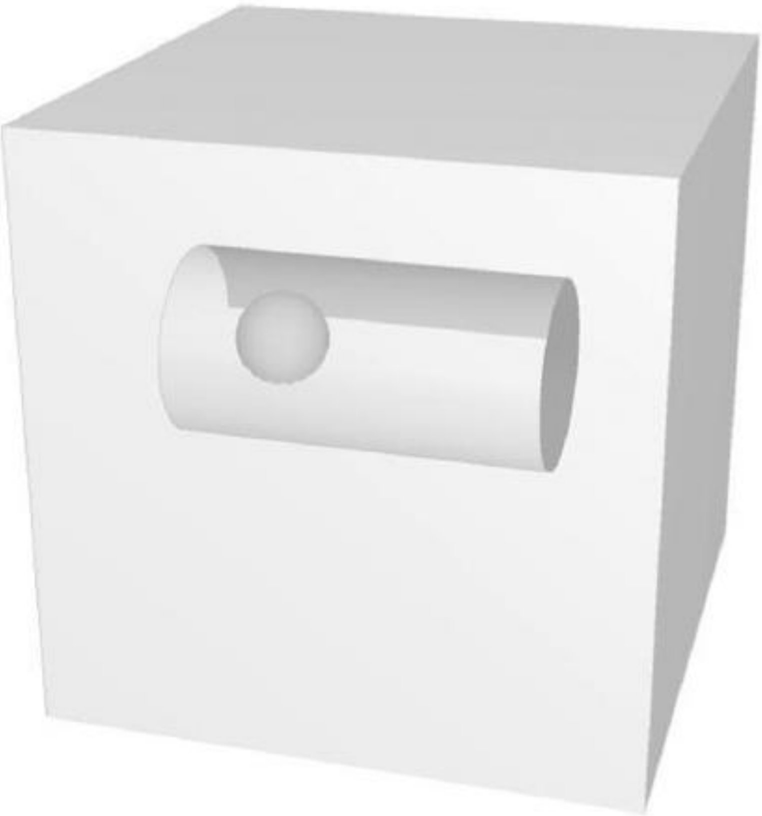

GEANT4: OpenGL Viewer Wrapped in Qt

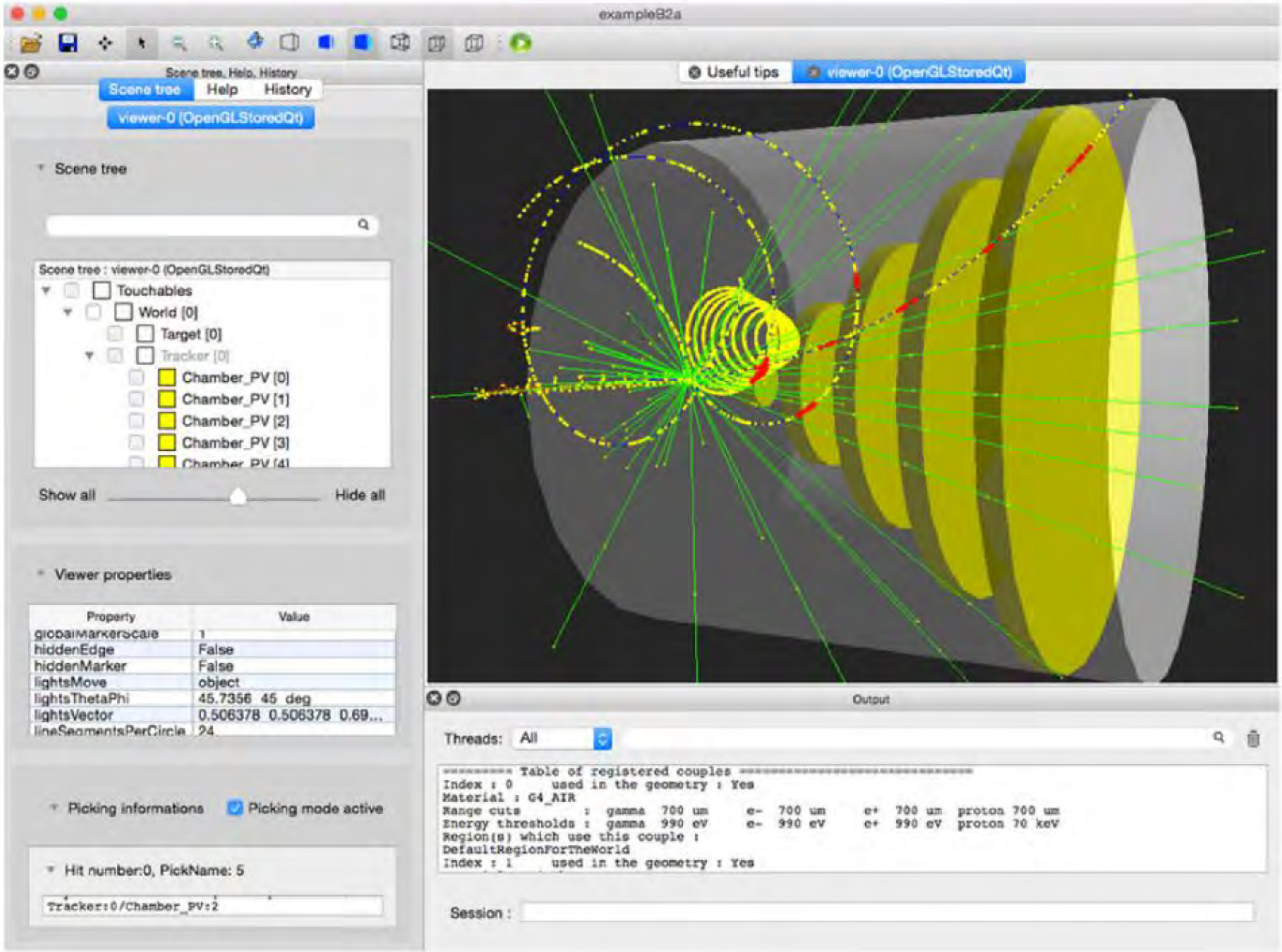

Fermilab

GEANT4: Open Inventor Extended Viewer

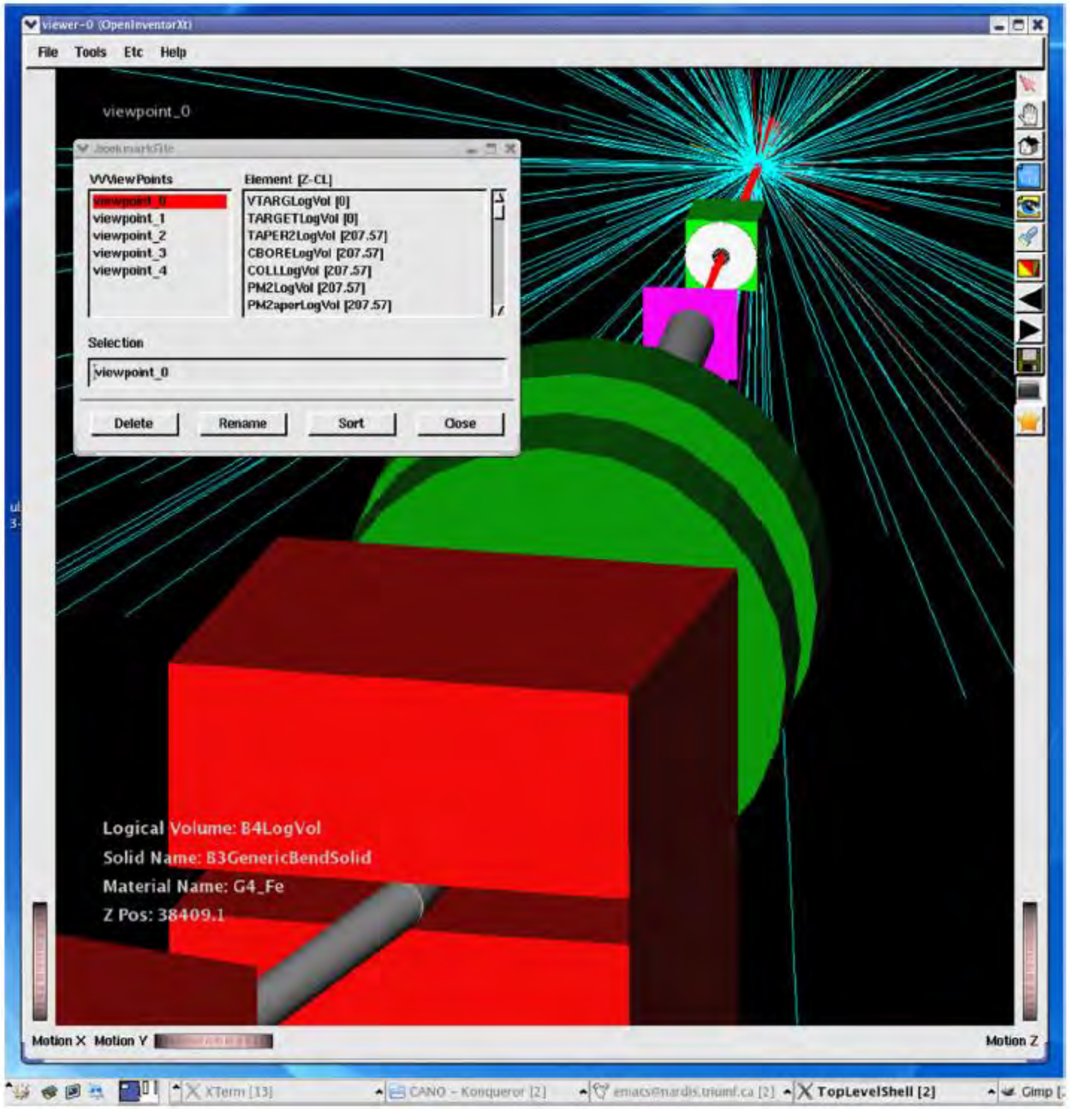

USPAS'2022 "Colliders" Class (V.Lebedev, N.Mokhov, V.Shiltsev, asst. C.Liu)

Examination Questions Problems

Set #1

1. 50 TeV muons are injected in the FCChh magnetic system: estimate a) time and number of turns for muon intensity decay 1/e times; b) synchrotron radiation loss of muon energy per turn ; c) max muon current allowed for same SR power per meter as FCChh and 1 Hz muon booster rep rate; d) average total power ***IE*** in two muon beams corresponding to such current. (FCChh parameter can be found in lecture *VS9-10*, slide *#50*)

2. Channeling in crystals occurs only of entering particle's angle is less than *a critical angle* (acceptance angle). What is that angle for 100 GeV muons? What is corresponding normalized phase space area (admittance) for a single crystal channel? Compare with emittances required for traditional multi-TeV muon colliders. (see eg lecture *VS13-14*, slide *#34*)

3. Assume for simplicity a damping ring of a linear e+e- collider with a uniform dipole field of 1 kG. What percentage of the ring circumference will need to be filled with high field superconducting wigglers to reduce the synchrotron radiation damping time by a factor of 10? (see eg lecture *VS5-6*, slides *#30 and 36*)

4. Find maximum energy transfer in coherent electron cooling with the kicker length of 20 m, and following electron beam parameters: rms transverse size - 1 mm, rms longitudinal size - 20 mm, number of particles per bunch 10^{10}, the electron beam energy – 150 MeV, and characteristic wave length of the perturbation 0.5 μm.

5. Introduce and estimate a value which would characterize a chromaticity of Derbenev's adapter. At which momentum spread the chromaticity of the adapter starts to affect its performance is the ratio of mode emittances is equal to 1000.

6. In the smooth lattice approximation, estimate the equilibrium emittances and momentum spread for 150 MeV round electron storage ring with IBS taken into account. The ring parameters are: energy 100 MeV, circumference – 20 m, betatron frequencies – 5, RF harmonic – 4, RF voltage – 5 kV.

7. What are the main functions of collider Machine Protection Systems?

USPAS'2022 "Colliders" Class (V.Lebedev, N.Mokhov, V.Shiltsev, asst. C.Liu)

Examination Questions Problems

Set #2

1. NICA collider ring rigidity $\boldsymbol{B\rho}$ = 45 Tm. Calculate a) maximum kinetic energy of protons; b) maximum kinetic energy (GeV per nucleon) of gold nuclei $^{197}Au^{+79}$.

2. Muons get accelerated from 1 GeV to 1 and 7 TeV. What is the required average accelerating gradient $\boldsymbol{G}$ to have 50% muons survived? 90%? 99%?

3. Estimate possible accelerating gradient and plasma wavelength in the ionized air at atmospheric pressure and room temperature (see eg lecture *VS13-14*, slide *#2*)

4. Find the bunch population and the bunch frequency where the multipacting of electrons due to space charge of the proton beam achieves its maximum. Assume that the electron energy, where the peak of secondary emission achieves its maximum is equal to 100 eV. Also assume that the secondary electrons have energies close to zero, zero length of proton bunch, and vacuum chamber radius of 3 cm.

5. Find maximum energy transfer in relativistic electron cooler with the following parameters: length – 100 m, electron energy – 150 MeV, electron beam radius - 1 mm, beam current - 100 A, energy spread – 10^{-4}.

6. In IOTA OSC the cooling chicane delays the beam by 0.65 mm. Estimate the required accuracy of the relative stabilization of the ring and chicane magnetic fields. The basic wave-length of OSC is 0.95 μm.

7. What are the main deleterious effects of beam loss on a collider lattice components and beam loss induced backgrounds on a collider detector performance?

8. What are the main deleterious effects of beam loss on collider components and beam-induced backgrounds on a collider detector performance?

USPAS'2022 "Colliders" Class (V.Lebedev, N.Mokhov, V.Shiltsev, asst. C.Liu)

Examination Questions Problems

Set #3

1. Diffusive ground motion follows $\boldsymbol{\Delta Y^2_{rms}=ATL}$ with A=10^{-6} (μm)^2/m/s (ATL law). Estimate corresponding rms beam orbit distortions after 1 day and 1 year a) in the positron linac of the C^3 Higgs factory collider ; b) in the arcs of FCChh collider (see eg lectures *VS11-12*, slide *#34 and 16,* FCChh in lectures *VS9-10*, slide *#50*).

2. If the head-on beam-beam tune shift for round Gaussian beams with rms size $\boldsymbol{\sigma}$ is equal to $\boldsymbol{\xi}$, what is scaling of the horizontal beam-beam tuneshift for beams separated horizontally by $\boldsymbol{d_x}$? What is vertical tuneshift scaling for the same (horizontal) separation? (see some useful info in lectures *VS3-4*, slides *#10, 37, 43*).)

3. LEP e+ and e- beam are separated by 10 microns at the IP during the luminosity scan. Estimate corresponding beam orbit distortion in the arcs of LEP (see eg lecture *VS3-4*, slides *#12 and 19*).

4. Estimate how much the longitudinal damper with gain of 0.05 suppresses the longitudinal emittance growth due to RF phase noise. RF frequency - 53 MHz, rms bunch length – 35 cm.

5. In the absence of cooling the beam transverse emittances grow as $(d\varepsilon/dt)_0$. In the smooth lattice approximation estimate transverse equilibrium emittances if only longitudinal cooling is present and transverse degrees of freedom are cooled due to IBS (sympathetic cooling). Assume an absence of longitudinal diffusion, and smooth lattice approximation.

6. RF cavity is located at the place with dispersion - D, β-function – β and their derivatives equal to zero. Assuming linear RF find how the betatron and synchrotron tunes will be changed relative to the case of zero dispersion.

7. What is the principle of a two-stage collimation system? What are requirements on collimator and collimation system parameters (lateral and longitudinal positions of primary, secondary and tertiary collimators)?